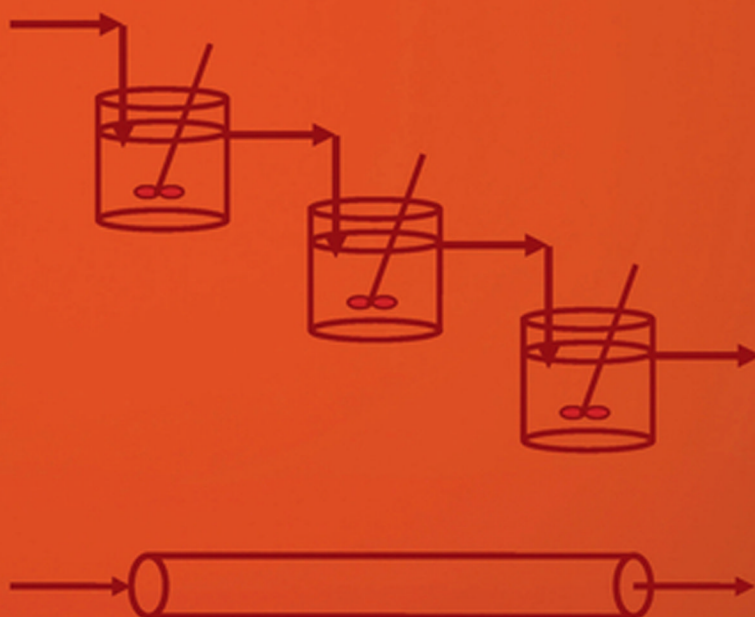


# Introduction to Chemical Engineering Kinetics & Reactor Design

*Second Edition*

Charles G. Hill, Jr.

Thatcher W. Root



WILEY

**Uploaded by:**

## **Ebooks Chemical Engineering**

<https://www.facebook.com/pages/Ebooks-Chemical-Engineering/238197077030>

For More Books, softwares & tutorials Related to Chemical Engineering  
Join Us

@facebook: <https://www.facebook.com/pages/Ebooks-Chemical-Engineering/238197077030>

@facebook: <https://www.facebook.com/AllAboutChemcalEngineering>

@facebook: <https://www.facebook.com/groups/10436265147/>

**ADMIN:**

**I.W**

**<< If you like this Book, than support the author and BuY it >>**



# **Introduction to Chemical Engineering Kinetics and Reactor Design**



# Introduction to Chemical Engineering Kinetics and Reactor Design

Second Edition

**Charles G. Hill, Jr.  
Thatcher W. Root**

*Professors of Chemical and Biological Engineering  
University of Wisconsin – Madison*

WILEY

Copyright © 2014 by John Wiley & Sons, Inc. All rights reserved.

Published by John Wiley & Sons, Inc., Hoboken, New Jersey.  
Published simultaneously in Canada.

No part of this publication may be reproduced, stored in a retrieval system, or transmitted in any form or by any means, electronic, mechanical, photocopying, recording, scanning, or otherwise, except as permitted under Section 107 or 108 of the 1976 United States Copyright Act, without either the prior written permission of the Publisher, or authorization through payment of the appropriate per-copy fee to the Copyright Clearance Center, Inc., 222 Rosewood Drive, Danvers, MA 01923, (978) 750-8400, fax (978) 750-4470, or on the web at [www.copyright.com](http://www.copyright.com). Requests to the Publisher for permission should be addressed to the Permissions Department, John Wiley & Sons, Inc., 111 River Street, Hoboken, NJ 07030, (201) 748-6011, fax (201) 748-6008, or online at <http://www.wiley.com/go/permission>.

**Limit of Liability/Disclaimer of Warranty:** While the publisher and author have used their best efforts in preparing this book, they make no representations or warranties with respect to the accuracy or completeness of the contents of this book and specifically disclaim any implied warranties of merchantability or fitness for a particular purpose. No warranty may be created or extended by sales representatives or written sales materials. The advice and strategies contained herein may not be suitable for your situation. You should consult with a professional where appropriate. Neither the publisher nor author shall be liable for any loss of profit or any other commercial damages, including but not limited to special, incidental, consequential, or other damages.

For general information on our other products and services or for technical support, please contact our Customer Care Department within the United States at (800) 762-2974, outside the United States at (317) 572-3993 or fax (317) 572-4002.

Wiley also publishes its books in a variety of electronic formats. Some content that appears in print may not be available in electronic formats. For more information about Wiley products, visit our web site at [www.wiley.com](http://www.wiley.com).

***Library of Congress Cataloging-in-Publication Data:***

Hill, Charles G., 1937-

Introduction to chemical engineering kinetics & reactor design / Charles G. Hill, Jr.,  
Thatcher W. Root, professors of chemical and biological engineering, University of Wisconsin,  
Madison. – Second edition.

pages cm

Includes bibliographical references and index.

ISBN 978-1-118-36825-1 (cloth)

1. Chemical kinetics. 2. Chemical reactors—Design and construction. I. Root, Thatcher W.  
1957- II. Title. III. Title: Introduction to chemical engineering kinetics and reactor design.

QD502.H54 2014

660'.2832—dc23

2013023526

Printed in the United States of America

10 9 8 7 6 5 4 3 2 1

# Contents

---

<b>Preface</b>	<b>ix</b>
<b>Preface to the First Edition</b>	<b>xi</b>
<b>1. Stoichiometric Coefficients and Reaction Progress Variables</b>	<b>1</b>
1.0 Introduction	1
1.1 Basic Stoichiometric Concepts	2
Literature Citation	3
<b>2. Thermodynamics of Chemical Reactions</b>	<b>4</b>
2.0 Introduction	4
2.1 Chemical Potentials and Standard States	4
2.2 Energy Effects Associated with Chemical Reactions	5
2.3 Sources of Thermochemical Data	7
2.4 The Equilibrium Constant and its Relation to $\Delta G^0$	7
2.5 Effects of Temperature and Pressure Changes on the Equilibrium Constant	8
2.6 Determination of Equilibrium Compositions	9
2.7 Effects of Reaction Conditions on Equilibrium Yields	11
2.8 Heterogeneous Reactions	12
2.9 Equilibrium Treatment of Simultaneous Reactions	12
2.10 Supplementary Reading References	15
Literature Citations	15
Problems	15
<b>3. Basic Concepts in Chemical Kinetics: Determination of the Reaction Rate Expression</b>	<b>22</b>
3.0 Introduction	22
3.1 Mathematical Characterization of Simple Reaction Systems	25
3.2 Experimental Aspects of Kinetic Studies	29
3.3 Techniques for the Interpretation of Kinetic Data	34
Literature Citations	53
Problems	54
<b>4. Basic Concepts in Chemical Kinetics: Molecular Interpretations of Kinetic Phenomena</b>	<b>72</b>
4.0 Introduction	72
4.1 Reaction Mechanisms	73
4.2 Chain Reactions	83
4.3 Molecular Theories of Chemical Kinetics	93
Literature Citations	103
Problems	104
<b>5. Chemical Systems Involving Multiple Reactions</b>	<b>117</b>
5.0 Introduction	117
5.1 Reversible Reactions	117
5.2 Parallel or Competitive Reactions	125
5.3 Series or Consecutive Reactions: Irreversible Series Reactions	133
5.4 Complex Reactions	137
Literature Citations	142
Problems	142
<b>6. Elements of Heterogeneous Catalysis</b>	<b>152</b>
6.0 Introduction	152
6.1 Adsorption Phenomena	153
6.2 Adsorption Isotherms	156

6.3	Reaction Rate Expressions for Heterogeneous Catalytic Reactions	160	6.4	Reactor Design for Autocatalytic Reactions	290
6.4	Physical Characterization of Heterogeneous Catalysts	170		Literature Citations	294
6.5	Catalyst Preparation, Fabrication, and Activation	174	6.6	Problems	294
6.6	Poisoning and Deactivation of Catalysts	177			
	Literature Citations	178			
	Problems	179			
<b>7.</b>	<b>Liquid Phase Reactions</b>	<b>189</b>			
7.0	Introduction	189	10.0	Introduction	305
7.1	Electrostatic Effects in Liquid Solution	191	10.1	The Energy Balance as Applied to Chemical Reactors	305
7.2	Pressure Effects on Reactions in Liquid Solution	192	10.2	The Ideal Well-Stirred Batch Reactor	307
7.3	Homogeneous Catalysis in Liquid Solution	193	10.3	The Ideal Continuous Flow Stirred-Tank Reactor	311
7.4	Correlation Methods for Kinetic Data: Linear Free Energy Relations	202	10.4	Temperature and Energy Considerations in Tubular Reactors	314
	Literature Citations	207	10.5	Autothermal Operation of Reactors	317
	Problems	207	10.6	Stable Operating Conditions in Stirred Tank Reactors	320
			10.7	Selection of Optimum Reactor Temperature Profiles: Thermodynamic and Selectivity Considerations	324
				Literature Citations	327
				Problems	328
<b>8.</b>	<b>Basic Concepts in Reactor Design and Ideal Reactor Models</b>	<b>216</b>			
8.0	Introduction	216	<b>11.</b>	<b>Deviations from Ideal Flow Conditions</b>	<b>337</b>
8.1	Design Analysis for Batch Reactors	225	11.0	Introduction	337
8.2	Design of Tubular Reactors	228	11.1	Residence Time Distribution Functions, $F(t)$ and $dF(t)$	337
8.3	Continuous Flow Stirred-Tank Reactors	234	11.2	Conversion Levels in Nonideal Flow Reactors	352
8.4	Reactor Networks Composed of Combinations of Ideal Continuous Flow Stirred-Tank Reactors and Plug Flow Reactors	254	11.3	General Comments and Rules of Thumb	358
8.5	Summary of Fundamental Design Relations: Comparison of Isothermal Stirred-Tank and Plug Flow Reactors	256		Literature Citations	359
8.6	Semibatch or Semiflow Reactors	256		Problems	359
	Literature Citations	259			
	Problems	259			
<b>9.</b>	<b>Selectivity and Optimization Considerations in the Design of Isothermal Reactors</b>	<b>273</b>			
9.0	Introduction	273	<b>12.</b>	<b>Reactor Design for Heterogeneous Catalytic Reactions</b>	<b>371</b>
9.1	Competitive (Parallel) Reactions	274	12.0	Introduction	371
9.2	Consecutive (Series) Reactions: $A \xrightarrow{k_1} B \xrightarrow{k_2} C \xrightarrow{k_3} D$	278	12.1	Commercially Significant Types of Heterogeneous Catalytic Reactors	371
9.3	Competitive Consecutive Reactions	283	12.2	Mass Transport Processes within Porous Catalysts	376
			12.3	Diffusion and Reaction in Porous Catalysts	380
			12.4	Mass Transfer Between the Bulk Fluid and External Surfaces of Solid Catalysts	386

12.5	Heat Transfer Between the Bulk Fluid and External Surfaces of Solid Catalysts	413	13.3	Commercial Scale Applications of Bioreactors in Chemical and Environmental Engineering	495
12.6	Global Reaction Rates	416	Literature Citations	516	
12.7	Design of Fixed Bed Reactors	418	Problems	517	
12.8	Design of Fluidized Bed Catalytic Reactors	437			
	Literature Citations	439			
	Problems	441			
<b>13.</b>	<b>Basic and Applied Aspects of Biochemical Transformations and Bioreactors</b>	<b>451</b>	<b>Appendix A. Fugacity Coefficient Chart</b>	<b>527</b>	
13.0	Introduction	451	<b>Appendix B. Nomenclature</b>	<b>528</b>	
13.1	Growth Cycles of Microorganisms: Batch Operation of Bioreactors	452	<b>Appendix C. Supplementary References</b>	<b>535</b>	
13.2	Principles and Special Considerations for Bioreactor Design	472	<b>Author Index</b>	<b>537</b>	
			<b>Subject Index</b>	<b>545</b>	



# Preface

---

More than three decades have elapsed since the publication of the first edition of this book in 1977. Although the basic principles on which the exposition in the body of the text is based remain unchanged, there have been noteworthy advances in the tools employed by practicing engineers in solving problems associated with the design of chemical reactors. Some of these tools need to be present in the knowledge base of chemical engineers engaged in studies of the principles of chemical kinetics and reactor design—the need for preparation of a second edition is thus evident. It has been primarily the pressure of other professional responsibilities, rather than a lack of interest on the part of the principal author, which has been responsible for the time elapsed between editions. Only since Professor Hill's retirement was precipitated by complications from surgery have sufficiently large blocks of time become available to permit a concerted effort to prepare the manuscript for the second edition.

Both the major thrust of the book as an introductory textbook focusing on chemical kinetics and reactor design, and the pedagogical approach involving applications of the laws of conservation of mass and energy to increasingly difficult situations remain at heart the same as the exposition in the first edition. The major changes in the second edition involve a multitude of new problems based on articles in the relevant literature that are designed to provide stimulating challenges to the development of a solid understanding of this material. Both students and instructors will benefit from scrutiny of the problems with a view to determining which problems are most germane to developing the problem-solving skills of the students in those areas that are most relevant to the particular topics emphasized by the instructor. Practicing engineers engaged in self study will also find the large array of problems useful in assessing their own command of the particular topic areas of immediate interest. We believe that it is only when one can apply to challenging new situations the basic principles in an area that he or she has been studying that

one truly comprehends the subject matter. Hence one of the distinctive features of both the first and second editions is the inclusion of a large number of practical problems encompassing a wide range of situations featuring actual chemical compounds and interpretation of actual data from the literature, rather than problems involving nebulous species A, B, C, and so on, and hypothetical rate constants which are commonly found in most undergraduate textbooks. Roughly 75% of the problems are new, and these new problems were often designed to take advantage of advances in both the relevant computer software (i.e., spreadsheets, equation solvers, MathCad, Matlab, etc.) and the degree of computer literacy expected of students matriculating in chemical engineering programs. We believe that regardless of whether the reader is a student, a teaching assistant or instructor, or a practicing engineer, he or she will find many of the problems in the text to be both intellectually challenging and excellent vehicles for sharpening one's professional skills in the areas of chemical kinetics, catalysis, and chemical reactor design.

Even though the International System of units (SI) is used extensively in the text and the associated problems, we do not apologize for the fact that we do not employ this system of units to the exclusion of others. One powerful tool that chemical engineers have employed for more than a century is the use of empirical correlations of data obtained from equipment carrying out one or more traditional unit operation(s). Often these empirical correlations are based on dimensional analysis of the process and involve use of physical properties, thermochemical properties, transport properties, transfer coefficients, and so on, that may or may not be readily available from the literature in SI units. The ability of practicing chemical engineers to make the necessary conversion of units correctly has long been a hallmark of the profession. Especially in the area of chemical kinetics and heterogeneous catalytic reactor design, students must be able to convert units properly to be successful in their efforts to utilize these empirical correlations.

The senior author has always enjoyed teaching the undergraduate course in chemical kinetics and reactor design and has regarded the positive feedback he received from students during his 40+ years as a teacher of this subject as a generous return on investments of his time preparing new problems, giving and updating lectures, counseling individual students, and preparing the manuscripts for both the first and second editions of this book. It is always a pleasure to learn of the successes achieved by former students, both undergraduate and graduate. Although individual students are responsible for the efforts leading to their own success, I have been pleased to note that five students who were in my undergraduate course in kinetics have gone on to base their research careers in kinetics and catalysis at leading departments of chemical engineering and have served as chairs of said departments. At least I did nothing to turn off their interest in this aspect of chemical engineering.

This preface would be incomplete if I did not acknowledge the invaluable contributions of some 30 to 40 teaching assistants and undergraduate paper graders who worked with me in teaching this course. They often pointed out ambiguities in problem statements, missing data, or other difficulties associated with individual problem statements. I am grateful for their contributions but am reluctant to name them for fear of not properly acknowledging others whose contributions occurred decades ago.

We also need to acknowledge the invaluable assistance of several members of the department staff in providing assistance when problems with computers exceeded our abilities to diagnose and correct computer related difficulties. Todd Ninman and Mary Heimbecker were particularly helpful in this respect. Many undergraduates addressed Professor Hill's needs for help in generating accurate versions of the numerous equations in the book. They removed one of the major impediments to generating enthusiasm for the Sisyphean task of reducing ideas to a finished manuscript. At various points along the path to a finished manuscript we sought and received assistance from our colleagues on the UW faculty and staff, both inside and outside the department. The occasions were numerous and we much appreciate their cooperation. During the final stages of preparing the manuscript for

the second edition, Jody Hoesly of the University of Wisconsin's Wendt Engineering Library was an wonderful resource in helping Professor Hill to locate and chase down the holders of the copyrights or viable alternatives for materials appearing in the first edition that were also needed in the second edition. She was an invaluable guide in helping us fulfill our responsibilities under copyright law.

Professor Hill also wishes to acknowledge the inspiration of the late Professor Robert C. Reid of MIT as a role model for how a faculty member should interact with students and research assistants. He is also grateful for the technique that Bob taught him of requiring participants in a course to read an article in the relevant literature and to prepare a problem (with the associated solution) based on an article that applies to material learned in this class. Typically, the assignment was made in the last week or two of the course. Professor Hill has used this assignment for decades as a vehicle for both demonstrating to students not only how much they have learned in the class as they prepare for the final exam, but also that they can read and comprehend much of the literature focusing on kinetics and reactor design. Often, the problems posed by students are trivial or impossibly difficult, but the benefit for the instructor is that the students identify for future generations of students not only interesting articles, but articles that are sufficiently relevant to the course that they may merit review with the idea that a senior instructor may use the article as the basis for challenging and stimulating problems at an appropriate pedagogical level. Such problems form the basis for many of the problems in the text that utilize techniques or data taken directly from the literature.

Professor Root is pleased to help rejuvenate this book for use by future classes of students seeking to improve their knowledge and understanding of this very important aspect of chemical engineering. Professor Hill hopes that readers enjoy the subject area as much as he has in more than four decades of studying and teaching this material.

*Madison, Wisconsin  
June 1, 2013*

CHARLES G. HILL, JR.  
THATCHER W. ROOT

# Preface to the First Edition

---

One feature that distinguishes the education of the chemical engineer from that of other engineers is an exposure to the basic concepts of chemical reaction kinetics and chemical reactor design. This textbook provides a judicious introductory level overview of these subjects. Emphasis is placed on the aspects of chemical kinetics and material and energy balances that form the foundation for the practice of reactor design.

The text is designed as a teaching instrument. It can be used to introduce the novice to chemical kinetics and reactor design and to guide him/her until he/she understands the fundamentals well enough to read both articles in the literature and more advanced texts with understanding. Because the chemical engineer who practices reactor design must have more than a nodding acquaintance with the chemical aspects of reaction kinetics, a significant portion of this textbook is devoted to this subject. The modern chemical process industry, which has played a significant role in the development of our technology-based society, has evolved because the engineer has been able to commercialize the laboratory discoveries of the scientist. To carry out the necessary scale-up procedures safely and economically, the reactor designer must have a sound knowledge of the chemistry involved. Modern introductory courses in physical chemistry usually do not provide the breadth or the in-depth treatment of reaction kinetics that is required by the chemical engineer who is faced with a reactor design problem. More advanced courses in kinetics that are taught by physical chemists naturally reflect the research interests of the individuals involved; they do not stress the transmittal of that information which is most useful to individuals engaged in the practice of reactor design. Seldom is significant attention paid to the subject of heterogeneous catalysis and to the key role that catalytic processes play in the industrial world.

Chapters 3 to 7 treat the aspects of chemical kinetics that are important to the education of a well-read chemical engineer. To stress further the chemical problems involved

and to provide links to the real world, I have attempted where possible to use actual chemical reactions and kinetic parameters in the many illustrative examples and problems. However, to retain as much generality as possible, the presentations of basic concepts and the derivations of fundamental equations are couched in terms of the anonymous chemical species A, B, C, U, V, etc. Where it is appropriate, the specific chemical reactions used in the illustrations are reformulated in these terms to indicate the manner in which the generalized relations are employed.

Chapters 8 to 12 provide an introduction to chemical reactor design. We start with the concept of idealized reactors with specified mixing characteristics operating isothermally and then introduce complications such as the use of combinations of reactors, implications of multiple reactions, temperature and energy effects, residence time effects, and heat and mass transfer limitations that are often involved when heterogeneous catalysts are employed. Emphasis is placed on the fact that chemical reactor design represents a straightforward application of the bread and butter tools of the chemical engineer - the material balance and the energy balance. The fundamental design equations in the second half of the text are algebraic descendants of the generalized material balance equation

$$\text{rate of input} = \text{rate of output} + \text{rate of accumulation} \\ + \text{rate of disappearance by reaction} \quad (P.1)$$

In the case of nonisothermal systems one must write equations of this form for both for energy and for the chemical species of interest, and then solve the resultant equations simultaneously to characterize the effluent composition and the thermal effects associated with operation of the reactor. Although the material and energy balance equations are not coupled when no temperature changes occur in the reactor, the design engineer still must solve the energy balance equation to ensure that sufficient capacity for energy transfer is provided so that the reactor will

indeed operate isothermally. The text stresses that the design process merely involves an extension of concepts learned previously. The application of these concepts in the design process involves equations that differ somewhat in mathematical form from the algebraic equations normally encountered in the introductory material and energy balance course, but the underlying principles are unchanged. The illustrations involved in the reactor design portion of the text are again based where possible on real chemical examples and actual kinetic data. I believe that the basic concepts underlying the subject of chemical kinetics and reactor design as developed in this text may readily be rephrased or applied in computer language. However, my pedagogical preference is to present material relevant to computer-aided reactor design only after the students have been thoroughly exposed to the fundamental concepts of this subject and mastered their use in attacking simple reactor design problems. I believe that full exposure to the subject of computer-aided reactor design should be deferred to intermediate courses in reactor design (and to more advanced texts), but this text focuses on providing a rational foundation for such courses while deliberately avoiding any discussion of the (forever-evolving) details of the software currently used to solve problems of interest in computer-aided design.

The notes that form the basis for the bulk of this textbook have been used for several years in the undergraduate course in chemical kinetics and reactor design at the University of Wisconsin. In this course, emphasis is placed on Chapters 3 to 6 and 8 to 12, omitting detailed class discussions of many of the mathematical derivations. My colleagues and I stress the necessity for developing a "seat of the pants" feeling for the phenomena involved as well as an ability to analyze quantitative problems in terms of the design framework developed in the text.

The material on catalysis and heterogeneous reactions in Chapters 6 and 12 is a useful framework for an intermediate level course in catalysis and chemical reactor design. In such a course emphasis is placed on developing the student's ability to critically analyze actual kinetic data obtained from the literature in order to acquaint him/her with many of the traps into which the unwary may fall. Some of the problems in Chapter 12 have evolved from a course of this type.

Most of the illustrative examples and problems in the text are based on actual data from the kinetics literature. However, in many cases, rate constants, heats of reaction, activation energies, and other parameters have been converted to SI units from various other systems. To be able to utilize the vast literature of kinetics for reactor design purposes, one must develop a facility for making appropriate transformations of parameters from one system of units to another. Consequently, I have chosen not to employ SI units exclusively in this text.

Like other authors of textbooks for undergraduates, I owe major debts to the instructors who first introduced me to this subject matter and to the authors and researchers whose publications have contributed to my understanding of the subject. As a student, I benefited from instruction by R. C. Reid, C. N. Satterfield, and I. Amdur and from exposure to the texts of Walas, Frost and Pearson, and Benson. Some of the material in Chapter 6 has been adapted with permission from the course notes of Professor C. N. Satterfield of MIT, whose direct and indirect influence on my thinking is further evident in some of the data interpretation problems in Chapters 6 and 12. As an instructor I have found the texts by Levenspiel and Smith to be particularly useful at the undergraduate level; the books by Denbigh, Laidler, Hinshelwood, Aris, and Kramers and Westerterp have also helped to shape my views of chemical kinetics and reactor design. I have tried to use the best ideas of these individuals and the approaches that I have found particularly useful in the classroom in the synthesis of this textbook. A major attraction of this subject is that there are many alternative ways of viewing the subject. Without an exposure to several viewpoints, one cannot begin to grasp the subject in its entirety. Only after such exposure, bombardment by the probing questions of one's students, and much contemplation can one begin to synthesize an individual philosophy of kinetics. To the humanist it may seem a misnomer to talk in terms of a philosophical approach to kinetics, but to the individuals who have taken kinetics courses at different schools or even in different departments and to the individuals who have read widely in the kinetics literature, it is evident that several such approaches do exist and that specialists in the area do have individual philosophies that characterize their approach to the subject.

The stimulating environment provided by the students and staff of the Chemical Engineering Department at the University of Wisconsin has provided much of the necessary encouragement and motivation for writing this textbook. The Department has long been a fertile environment for research and textbook writing in the area of chemical kinetics and reactor design. The text by O. A. Hougen and K. M. Watson represents a classic pioneering effort to establish a rational approach to the subject from the viewpoint of the chemical engineer. Through the years these individuals and several members of our current staff have contributed significantly to the evolution of the subject. I am indebted to my colleagues, W. E. Stewart, S. H. Langer, C. C. Watson, R. A. Grieger, S. L. Cooper, and T. W. Chapman, who have used earlier versions of this textbook as class notes or commented thereon, to my benefit. All errors are, of course, my own responsibility.

I am grateful to the graduate students who have served as my teaching assistants and who have brought to my attention various ambiguities in the text or problem statements.

These include J. F. Welch, A. Yu, R. Krug, E. Guertin, A. Kozinski, G. Estes, J. Coca, R. Safford, R. Harrison, J. Yurchak, G. Schrader, A. Parker, T. Kumar, and A. Spence. I also thank the students on whom I have tried out my ideas. Their response to the subject matter has provided much of the motivation for this textbook.

Since drafts of this text were used as course notes, the secretarial staff of the department, which includes D. Peterson, C. Sherven, M. Sullivan, and M. Carr, deserves my warmest thanks for typing this material. I am also very

appreciative of my (former) wife's efforts in typing the final draft of this manuscript and in correcting the galley proofs. Vivian Kehane, Jacqueline Lachmann, and Peter Klein of Wiley were particularly helpful in transforming my manuscript into this text.

My (former) wife and my children were at times neglected during the preparation of this book; for their cooperation and inspiration I am particularly grateful.

*Madison, Wisconsin*

CHARLES G. HILL, JR.



# Chapter 1

---

## Stoichiometric Coefficients and Reaction Progress Variables

### 1.0 INTRODUCTION

In the absence of chemical reactions, Earth would be a barren planet. No life of any sort would exist. Even if we were to exempt the fundamental reactions involved in life processes from our proscription on chemical reactions, our lives would be extremely different from what they are today. There would be no fire for warmth and cooking, no iron and steel with which to fashion even the crudest implements, no synthetic fibers for making clothing or bedding, no combustion engines to power our vehicles, and no pharmaceutical products to treat our health problems.

One feature that distinguishes the chemical engineer from other types of engineers is the ability to analyze systems in which chemical reactions are occurring and to apply the results of his or her analysis in a manner that benefits society. Consequently, chemical engineers must be well acquainted with the fundamentals of chemical reaction kinetics and the manner in which they are applied in reactor design. In this book we provide a systematic introduction to these subjects. Three fundamental types of equations are employed in the development of the subject: material balances, energy balances, and rate expressions.

*Chemical kinetics* is the branch of physical chemistry that deals with quantitative studies of the rates at which chemical processes occur, the factors on which these rates depend, and the molecular acts involved in reaction processes. A description of a reaction in terms of its constituent molecular acts is known as the *mechanism* of the reaction. Physical and organic chemists are interested in chemical kinetics primarily for the light that it sheds on molecular properties. From interpretations of macroscopic kinetic data in terms of molecular mechanisms, they can gain insight into the nature of reacting systems, the processes by which chemical bonds are made and broken, and the structure of the resulting product. Although chemical engineers find the concept of a reaction mechanism

useful in the correlation, interpolation, and extrapolation of rate data, they are more concerned with applications of chemical kinetics in the development of profitable manufacturing processes.

Chemical engineers have traditionally approached kinetics studies with the goal of describing the behavior of reacting systems in terms of macroscopically observable quantities such as temperature, pressure, composition, and Reynolds number. This empirical approach has been very fruitful in that it has permitted chemical reactor technology to develop to the point that it can be employed in the manufacture of an amazing array of products that enhance our quality of life.

The dynamic viewpoint of chemical kinetics focuses on variations in chemical composition with either time in a batch reactor or position in a continuous flow reactor. This situation may be contrasted with the essentially static perspective of thermodynamics. A *kinetic system* is a system in which there is unidirectional movement toward thermodynamic equilibrium. The chemical composition of a closed system in which a reaction is occurring evolves as time elapses. A system that is in thermodynamic equilibrium, on the other hand, undergoes no net change with time. The thermodynamicist is interested only in the initial and final states of the system and is not concerned with the time required for the transition or the molecular processes involved therein; the chemical kineticist is concerned primarily with these issues.

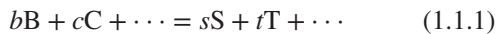
In principle, one can treat the thermodynamics of chemical reactions on a kinetic basis by recognizing that the equilibrium condition corresponds to the situation in which the rates of the forward and reverse reactions are identical. In this sense kinetics is the more fundamental science. Nonetheless, thermodynamics provides much vital information to the kineticist and to the reactor designer. In particular, the first step in determining the economic feasibility of producing a given material from a specified

feedstock should be a determination of the product yield at equilibrium at the conditions of the reactor outlet. Since this composition represents the goal toward which the kinetic process is moving, it places an upper limit on the product yield that may be obtained. Chemical engineers must also employ thermodynamics to determine heat transfer requirements for proposed reactor configurations.

## 1.1 BASIC STOICHIOMETRIC CONCEPTS

### 1.1.1 Stoichiometric Coefficients

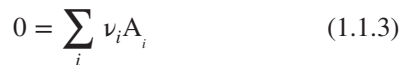
An arbitrary chemical reaction may be written as



where  $b$ ,  $c$ ,  $s$ , and  $t$  are the stoichiometric coefficients of the species B, C, S, and T, respectively. We define generalized stoichiometric coefficients ( $\nu_i$ ) for reaction (1.1.1) by rewriting it in the following manner:

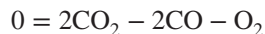


where  $\nu_B = -b$ ,  $\nu_C = -c$ ,  $\nu_S = s$ , and  $\nu_T = t$ . The generalized stoichiometric coefficients are defined as positive quantities for the products of the reaction and as negative quantities for the reactants. The coefficients of species that are neither produced nor consumed by the indicated reaction are taken to be zero. Equation (1.1.2) has been written in transposed form with the zero first to emphasize the use of this sign convention, even though this transposition is rarely used in practice. One may further generalize equation (1.1.2) by rewriting it as

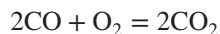


where the sum is taken over all components  $A_i$  present in the system.

There are many equivalent ways of writing the stoichiometric equation for a reaction. For example, one could write the oxidation of carbon monoxide in our notation as

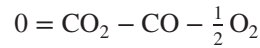


instead of the more conventional form, which has the reactants on the left side and the products on the right side:



This second form is preferred, provided that one keeps in mind the proper sign convention for the stoichiometric coefficients. For the example above,  $\nu_{CO} = -2$ ,  $\nu_{O_2} = -1$ , and  $\nu_{CO_2} = 2$ .

Alternatively, this reaction may be written as



The choice is a matter of personal convenience. The essential point is that the ratios of the stoichiometric coefficients are unique for a specific reaction. In terms of the two forms of the chemical equation above,

$$\frac{\nu_{CO}}{\nu_{O_2}} = \frac{-2}{-1} = \frac{-1}{-1/2} = 2$$

Because the reaction stoichiometry can be expressed in various ways, one must always write down a stoichiometric equation for the reaction under study during the initial stages of the analysis and base subsequent calculations on this reference equation. If a consistent set of stoichiometric coefficients is used throughout the calculations, the results can be readily understood and utilized by other workers in the field.

### 1.1.2 Reaction Progress Variables

To measure the progress of a reaction along a particular pathway, it is necessary to define a parameter that provides a measure of the degree of conversion of the reactants. For this purpose it is convenient to use the concept of the *extent* or degree of *advancement* of a reaction. This concept has its origins in the thermodynamic literature, dating back to the work of de Donder (1). Consider a *closed system*, one in which there is no exchange of matter between the system and its surroundings, where a single chemical reaction may occur according to equation (1.1.3). Initially, there are  $n_{i0}$  moles of constituent  $A_i$  present in the system. At some later time there are  $n_i$  moles of species  $A_i$  present. At this time the molar extent of reaction ( $\xi$ ) is defined as

$$\xi = \frac{n_i - n_{i0}}{\nu_i} \quad (1.1.4)$$

This equation is valid for all species  $A_i$ , a fact that is a consequence of the law of definite proportions. The molar extent of reaction  $\xi$  is a time-dependent extensive variable that is measured in moles. It is a useful measure of the progress of the reaction because it is not tied to any particular species  $A_i$ . Changes in the mole numbers of two species  $i$  and  $j$  can be related to one another by eliminating  $\xi$  between two expressions that may be derived using equation (1.1.4):

$$n_j = n_{j0} + \frac{\nu_j}{\nu_i} (n_i - n_{i0}) \quad (1.1.5)$$

If more than one chemical reaction is possible, an extent may be defined for each reaction. If  $\xi_k$  is the extent of the  $k$ th reaction, and  $\nu_{ki}$  is the stoichiometric coefficient

of species  $i$  in reaction  $k$ , the total change in the number of moles of species  $A_i$  as a consequence of  $r$  reactions is

$$n_i - n_{i0} = \sum_{k=1}^{k=r} \nu_{ki} \xi_k \quad (1.1.6)$$

Another advantage of using the concept of extent is that it permits a unique specification of the rate of a given reaction. This point is discussed in Section 3.0. The major drawbacks of the concept are that the extent is defined for a closed system and that it is an extensive variable. Consequently, the extent is proportional to the mass of the system being investigated.

The fraction conversion  $f$  is an intensive measure of the progress of a reaction. It is a variable that is simply related to the extent of reaction. The fraction conversion of a reactant  $A_i$  in a closed system in which only a single reaction is occurring is given by

$$f = \frac{n_{i0} - n_i}{n_{i0}} = 1 - \frac{n_i}{n_{i0}} \quad (1.1.7)$$

The variable  $f$  depends on the particular species chosen as a reference substance. In general, the initial mole numbers of the reactants do not constitute simple stoichiometric ratios, and the number of moles of product that may be formed is limited by the amount of one of the reactants present in the system. If the extent of reaction is not limited by thermodynamic equilibrium constraints, this limiting reagent is the one that determines the maximum possible value of the extent of reaction ( $\xi_{\max}$ ). We should refer our fractional conversions to this stoichiometrically limiting reactant if  $f$  is to lie between zero and unity. Consequently, the treatment used in subsequent chapters will *define fractional conversions in terms of the limiting reactant*. In analyzing conventional batch reactors in which only a single reaction is occurring, one may employ either the concept of fraction conversion or the concept of extent of reaction. A batch reactor is a closed system, a system for which there is no transport of matter across the boundaries between the system and its surroundings. When multiple reactions take place in a batch reactor, it is more convenient to employ the extent concept. However, for open systems such as continuous flow reactors, the fraction conversion of the limiting reagent is more useful in conducting the

analysis, sometimes in conjunction with the concept of reaction yield, as described in Chapter 9. An *open system* is one whose analysis requires consideration of the transport of matter across the boundaries between the system and its surroundings.

One can relate the extent of reaction to the fraction conversion by solving equations (1.1.4) and (1.1.7) for the number of moles of the limiting reagent  $n_{\text{lim}}$  and equating the resulting expressions:

$$n_{\text{lim}} = n_{\text{lim},0} + \nu_{\text{lim}} \xi = n_{\text{lim},0} (1 - f) \quad (1.1.8)$$

or

$$\xi = -\frac{f n_{\text{lim},0}}{\nu_{\text{lim}}} \quad (1.1.9)$$

The maximum extent of an irreversible reaction ( $\xi_{\max,\text{irr}}$ ) can be obtained by setting  $f$  in equation (1.1.9) equal to 1. However, for reversible reactions, the maximum extent of reaction is limited by the position of chemical equilibrium. For these situations, equation (1.1.9) becomes

$$\xi_e = -\frac{f_e n_{\text{lim},0}}{\nu_{\text{lim}}} \quad (1.1.10)$$

where  $f_e$  and  $\xi_e$  are the conversion and extent of reaction at equilibrium, respectively.  $\xi_e$  will always be less than  $\xi_{\max,\text{irr}}$ . However, in many cases  $\xi_e$  is approximately equal to  $\xi_{\max,\text{irr}}$ . In these cases the equilibrium for the reaction highly favors formation of the products, and only an *extremely small* quantity of the limiting reagent remains in the system at equilibrium. We classify these reactions as *irreversible*. When the extent of reaction at equilibrium differs measurably from  $\xi_{\max}$ , we classify the reaction involved as *reversible*. From a thermodynamic point of view, all reactions are reversible. However, to simplify the analysis, when one is analyzing a reacting system, it is often convenient to neglect the reverse reaction. For “irreversible” reactions, one then arrives at a result that is an extremely good approximation to the correct answer.

## LITERATURE CITATION

1. DE DONDER, T., *Leçons de thermodynamique et de chimie-physique*, Gauthier-Villars, Paris 1920.

# Chapter 2

---

## Thermodynamics of Chemical Reactions

### 2.0 INTRODUCTION

The science of chemical kinetics is concerned primarily with chemical changes and the energy and mass fluxes associated therewith. Thermodynamics, on the other hand, is focused on equilibrium systems—systems that are undergoing *no net change* with time. In this chapter we remind the reader of the key thermodynamic principles with which he or she should be familiar. Emphasis is placed on calculations of equilibrium extents of reaction and enthalpy changes accompanying chemical reactions.

Of primary consideration in any discussion of chemical reaction equilibria are the constraints on the system in question. If calculations of equilibrium compositions are to be in accord with experimental observations, one must include in his or her analysis all reactions that occur at appreciable rates relative to the time frame involved. Such calculations are useful in that the equilibrium conversion provides a standard against which the actual performance of a reactor may be compared. For example, if the equilibrium yield of a particular reaction under specified conditions is 75% and the yield observed from a reactor operating under these conditions is only 30%, one can presumably obtain major improvements in the process yield by appropriate manipulation of the reaction conditions. On the other hand, if the process yield is close to 75%, potential improvements in yield would be minimal unless there are opportunities for making major changes in process conditions that have significant effects on the equilibrium yield. Additional efforts aimed at improving the process yield may not be fruitful if such changes cannot be made. Without a knowledge of the equilibrium yield, one might be tempted to look for catalysts giving higher yields when, in fact, the present catalyst provides a sufficiently rapid approach to equilibrium for the temperature, pressure, and feed composition specified.

The basic criterion for the establishment of equilibrium with respect to reaction  $k$  is that

$$\Delta G_k = \sum_i \nu_{ki} \mu_i = 0 \quad (2.0.1)$$

where  $\Delta G_k$  is the change in the Gibbs free energy associated with reaction  $k$ ,  $\mu_i$  the chemical potential of species  $i$  in the reaction mixture, and  $\nu_{ki}$  the stoichiometric coefficient of species  $i$  in the  $k$ th reaction. If  $r$  reactions may occur in the system and equilibrium is established with respect to each of these reactions, thermodynamics requires that

$$\sum_i \nu_{ki} \mu_i = 0 \quad \text{for } k = 1, 2, \dots, r \quad (2.0.2)$$

These equations are equivalent to a requirement that at equilibrium the Gibbs free-energy change ( $\Delta G$ ) be zero for every reaction.

### 2.1 CHEMICAL POTENTIALS AND STANDARD STATES

The activity  $a_i$  of species  $i$  is related to its chemical potential by

$$\mu_i = \mu_i^0 + RT \ln a_i \quad (2.1.1)$$

where  $R$  is the gas constant,  $T$  the absolute temperature, and  $\mu_i^0$  the standard chemical potential of species  $i$  in a reference state where its activity is taken as unity.

The choice of the standard state is largely arbitrary and is based primarily on experimental convenience and reproducibility. The temperature of the standard state is the same as that of the system under investigation. In some cases, the standard state may represent a hypothetical condition that cannot be achieved experimentally, but that is susceptible

**Table 2.1** Standard States for Chemical Potential Calculations (for use in studies of chemical reaction equilibria)

State of aggregation	Standard state
Gas	Pure gas at unit fugacity (for an ideal gas the fugacity is unity at a pressure of 1 bar; this approximation is valid for most real gases)
Liquid	Pure liquid in the most stable form at 1 bar
Solid	Pure solid in the most stable form at 1 bar

to calculations giving reproducible results. Although different standard states may be chosen for various species, *throughout any set of calculations, to minimize possibilities for error it is important that the standard state of a particular component be kept the same*. Certain choices of standard states have found such widespread use that they have achieved the status of recognized conventions. In particular, those included in Table 2.1 are used in calculations dealing with chemical reaction equilibria. In all cases the temperature is the same as that of the reaction mixture.

Once the standard states for the various species have been established, one can proceed to calculate a number of standard energy changes for processes involving a change from reactants, all in their respective standard states, to products, all in their respective standard states. For example, the standard Gibbs free energy change ( $\Delta G^0$ ) for a single reaction is

$$\Delta G^0 = \sum_i \nu_i \mu_i^0 \quad (2.1.2)$$

where the superscript zero emphasizes the fact that this is a process involving standard states for both the final and initial conditions of the system. In a similar manner, one can determine standard enthalpy ( $\Delta H^0$ ) and standard entropy changes ( $\Delta S^0$ ) for this process.

## 2.2 ENERGY EFFECTS ASSOCIATED WITH CHEMICAL REACTIONS

Because chemical reactions involve the formation, destruction, or rearrangement of chemical bonds, they are invariably accompanied by changes in the enthalpy and Gibbs free energy of the system. The enthalpy change on reaction provides information that is necessary for any engineering analysis of the system in terms of the first law of thermodynamics. Standard enthalpy changes are also useful in determining the effect of temperature on the equilibrium constant for the reaction and thus on the reaction yield. Gibbs free energy changes are useful in determining

whether or not chemical equilibrium exists in the system being studied and in determining how changes in process variables can influence the yield of the reaction.

In chemical kinetics there are two types of processes for which one is typically interested in changes in these energy functions:

1. A chemical process whereby stoichiometric quantities of reactants, each in its standard state, are completely converted to stoichiometric amounts of products, each in its standard state, under conditions such that the initial temperature of the reactants is equal to the final temperature of the products.
2. An actual chemical process as it might occur under either equilibrium or nonequilibrium conditions in a chemical reactor.

One must be very careful not to confuse actual energy effects with those that are associated with the process whose initial and final states are the standard states of the reactants and products, respectively.

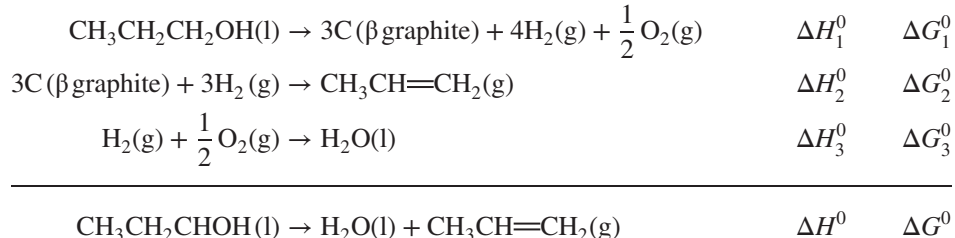
To have a consistent basis for comparing different reactions and to permit the tabulation of thermochemical data for various reaction systems, it is convenient to define enthalpy and Gibbs free energy changes for standard reaction conditions. These conditions involve the use of stoichiometric amounts of the various reactants (each in its standard state at some temperature  $T$ ). The reaction proceeds by some unspecified path to end up with complete conversion of reactants to the various products (each in its standard state at the same temperature  $T$ ).

The enthalpy and Gibbs free energy changes for a standard reaction are denoted by the symbols  $\Delta H^0$  and  $\Delta G^0$ , where the superscript zero is used to signify that a “standard” reaction is involved. Use of these symbols is restricted to the case where the extent of reaction is 1 mol for the reaction as written with a specific set of stoichiometric coefficients. The remaining discussion in this chapter refers to this basis.

Because  $G$  and  $H$  are state functions, changes in these quantities are independent of whether the reaction takes place in one or in several steps. Consequently, it is possible to tabulate data for relatively few reactions and use these data in the calculation of  $\Delta G^0$  and  $\Delta H^0$  for other reactions. In particular, one tabulates data for the standard reactions that involve the formation of a compound from its elements. One may then consider a reaction involving several compounds as being an appropriate algebraic sum of a number of elementary reactions, each of which involves the formation of a single compound. The dehydration of *n*-propanol,



may be considered as the algebraic sum of the following series of reactions:



For the overall reaction,

$$\Delta H^0 = \Delta H_1^0 + \Delta H_2^0 + \Delta H_3^0 \quad (2.2.1)$$

$$\Delta G^0 = \Delta G_1^0 + \Delta G_2^0 + \Delta G_3^0 \quad (2.2.2)$$

However, each of the individual reactions involves the formation of a compound from its elements or the decomposition of a compound into those elements. The standard enthalpy change of a reaction that involves the formation of a compound from its elements is referred to as the *enthalpy* (or heat) of formation of that compound and is denoted by the symbol  $\Delta H_f^0$ . Thus, for the dehydration of *n*-propanol,

$$\Delta H_{\text{overall}}^0 = -\Delta H_f^0 \text{ propanol} + \Delta H_f^0 \text{ water} + \Delta H_f^0 \text{ propylene} \quad (2.2.3)$$

and

$$\Delta G_{\text{overall}}^0 = -\Delta G_f^0 \text{ propanol} + \Delta G_f^0 \text{ water} + \Delta G_f^0 \text{ propylene} \quad (2.2.4)$$

where  $\Delta G_{f,i}^0$  refers to the standard Gibbs free energy of formation of the indicated compound *i*.

This example illustrates the principle that values of  $\Delta G^0$  and  $\Delta H^0$  may be calculated from values of the enthalpies and Gibbs free energies of formation of the products and reactants. In more general form,

$$\Delta H^0 = \sum_i \nu_i \Delta H_{f,i}^0 \quad (2.2.5)$$

$$\Delta G^0 = \sum_i \nu_i \Delta G_{f,i}^0 \quad (2.2.6)$$

When an element enters into a reaction, its standard Gibbs free energy and standard enthalpy of formation are taken as zero if its state of aggregation is identical to that selected as the basis for the determination of the standard Gibbs free energy and enthalpy of formation of its compounds. If  $\Delta H^0$  is negative, the reaction is said to be *exothermic*; if  $\Delta H^0$  is positive, the reaction is said to be *endothermic*.

It is not necessary to tabulate values of  $\Delta G^0$  or  $\Delta H^0$  for all conceivable reactions. It is sufficient to tabulate values of these parameters only for the reactions that involve the formation of a compound from its elements. The problem of data compilation is further simplified by the fact that it is unnecessary to record  $\Delta G_f^0$  and  $\Delta H_f^0$  at all temperatures, because of the relations that exist between these quantities and other thermodynamic properties of the reactants and

products. The convention that is most commonly accepted in engineering practice today is to report values of standard enthalpies of formation and Gibbs free energies of formation at 25°C (298.16 K), although 0 K is sometimes used as the reference state. The problem of calculating a value for  $\Delta G^0$  or  $\Delta H^0$  at temperature *T* thus reduces to one of determining values of  $\Delta G^0$  and  $\Delta H^0$  at 25°C or 0 K and then adjusting the value obtained to take into account the effects of temperature on the property in question. The appropriate techniques for carrying out these adjustments are indicated below.

For temperatures in K, the effect of temperature on  $\Delta H^0$  is given by

$$\Delta H_T^0 = \Delta H_{298.16}^0 + \int_{298.16 \text{ K}}^T \left( \sum_i \nu_i C_{p,i}^0 \right) dT \quad (2.2.7)$$

where  $C_{p,i}^0$  is the constant pressure heat capacity of species *i* in its standard state.

In many cases the magnitude of the last term on the right side of equation (2.2.7) is very small compared to  $\Delta H_{298.16}^0$ . However, if one is to be able to evaluate the standard heat of reaction properly at some temperature other than 298.16 K, one must know the constant pressure heat capacities of the reactants and the products as functions of temperature as well as the standard heat of reaction at 298.16 K. Data of this type and techniques for estimating these properties are contained in the references in Section 2.3.

The most useful expression for describing the variation of standard Gibbs free energy changes with the *absolute* temperature is

$$\left[ \frac{\partial(\Delta G^0/T)}{\partial T} \right]_P = -\frac{\Delta H^0}{T^2} \quad (2.2.8)$$

In Section 2.5 we shall see that the equilibrium constant for a chemical reaction is simply related to  $\Delta G^0/T$  and that equation (2.2.8) is useful in determining how equilibrium constants vary with temperature. If one desires to obtain an expression for  $\Delta G^0$  itself as a function of temperature, equation (2.2.7) may be integrated to give  $\Delta H^0$  as a function of temperature. This relation may then be used with equation (2.2.8) to arrive at the desired relation.

The effects of pressure on  $\Delta G^0$  and  $\Delta H^0$  depend on the choice of standard states employed. When the standard state of each component of the reaction system is taken at 1 bar whether the species in question is a gas, liquid, or solid, the values of  $\Delta G^0$  and  $\Delta H^0$  refer to a process that starts and ends at 1 bar. For this choice of standard states, the *values of  $\Delta G^0$  and  $\Delta H^0$  are independent of the pressure at which the reaction is actually carried out*. It is important to note in this connection that we are calculating the enthalpy change for a hypothetical process, not for the process as it actually occurs in nature. The choice of standard states at a pressure (or fugacity) of 1 bar is the convention that is customarily adopted in the analysis of chemical reaction equilibria.

For cases where the standard-state pressure for the various species is chosen as that of the system under investigation, changes in this variable will alter the values of  $\Delta G^0$  and  $\Delta H^0$ . In such cases a thermodynamic analysis indicates that

$$\Delta H_P^0 = \Delta H_{1\text{bar}}^0 + \sum_i \nu_i \int_1^P \left[ V_i - T \left( \frac{\partial V_i}{\partial T} \right)_P \right] dP \quad (2.2.9)$$

where  $V_i$  is the molal volume of component  $i$  in its standard state and where each integral is evaluated for the species in question along an isothermal path between 1 bar and the final pressure  $P$ . The term in brackets represents the variation of the enthalpy of a component with pressure at constant temperature  $(\partial H / \partial P)_T$ .

It should be emphasized that the choice of standard states implied by equation (2.2.9) is *not* that which is used conventionally in the analysis of chemically reacting systems. Furthermore, *in the vast majority of cases the summation term on the right side of this equation is very small compared to the magnitude of  $\Delta H_{1\text{bar}}^0$  and, indeed, is usually considerably smaller than the uncertainty in this term*.

The Gibbs free energy analog of equation (2.2.9) is

$$\Delta G_P^0 = \Delta G_{1\text{bar}}^0 + \sum_i \nu_i \int_1^P V_i dP \quad (2.2.10)$$

where the integral is again evaluated along an isothermal path. For cases where the species involved is a condensed phase,  $V_i$  will be a very small quantity and the contribution of this species to the summation will be quite small unless the system pressure is extremely high. For ideal gases, the integral may be evaluated directly as  $RT \ln P$ . For nonideal gases the integral is equal to  $RT \ln f_i^0$ , where  $f_i^0$  is the fugacity of pure species  $i$  at pressure  $P$ .

## 2.3 SOURCES OF THERMOCHEMICAL DATA

There are a large number of scientific handbooks and textbooks that contain thermochemical data. In addition, many

websites serve as sources of such data. Some useful supplementary references are listed below.

1. NIST (National Institutes of Standards and Technology) Scientific and Technical Databases (<http://www.nist.gov/srd/thermo.htm>), most notably the NIST Chemistry WebBook (2005), which contains an extensive collection of thermochemical data for over 7000 organic and small inorganic compounds.
2. D. R. LIDE and H. V. KEHIAIAN (Eds.), *CRC Handbook of Thermo-physical and Thermochemical Data*, CRC Press, Boca Raton, FL, 1994.
3. M. BINNEWIES and E. MILKE (Eds.), *Thermochemical Data of Elements and Compounds*, 2nd rev. ed., Wiley-VCH, Weinheim, Germany, 2002.
4. W. M. HAYNES (Ed.), *CRC Handbook of Chemistry and Physics*, 92nd ed., CRC Press, Boca Raton, FL, 2011.
5. J. B. PEDLEY, R. D. NAYLOR, and S. P. KIRBY, *Thermochemical Data of Organic Compounds*, 2nd ed., Chapman & Hall, New York, 1986.
6. J. D. COX and G. PILCHER, *Thermochemistry of Organic and Organometallic Compounds*, Academic Press, New York, 1970.
7. D. R. STULL, E. F. WESTRUM, and G. C. SINKE, *The Chemical Thermodynamics of Organic Compounds*, Wiley, New York, 1969.
8. D. W. GREEN and R. H. PERRY (Eds.), *Perry's Chemical Engineers' Handbook*, 8th ed., McGraw-Hill, New York, 2008.

If thermochemical data are not available, the following references are useful to describe techniques for estimating thermochemical properties from a knowledge of the molecular structures of the compounds of interest.

1. B. E. POLING, J. M. PRAUSNITZ, and J. O'CONNELL, *The Properties of Gases and Liquids*, 5th rev. ed., McGraw-Hill, New York, 2000.
2. N. COHEN and S. W. BENSON, Estimation of Heats of Formation of Organic Compounds by Additivity Methods, *Chem. Rev.*, **93**, 2419–2438 (1993).

## 2.4 THE EQUILIBRIUM CONSTANT AND ITS RELATION TO $\Delta G^0$

The basic criterion for equilibrium with respect to a given chemical reaction is that the Gibbs free energy change associated with the progress of the reaction be zero:

$$\Delta G = \sum_i \nu_i \mu_i = 0 \quad (2.4.1)$$

where the  $\mu_i$  are the chemical potentials of the various species in the equilibrium mixture. The *standard* Gibbs free energy change for a reaction refers to the process wherein stoichiometric quantities of reactants, each in its standard state of unit activity, at some arbitrary temperature  $T$  are completely converted to products, each in its standard state of unit activity at this same temperature. In general, the standard Gibbs free energy change,  $\Delta G^0$ , is nonzero and is given by

$$\Delta G^0 = \sum_i \nu_i \mu_i^0 \quad (2.4.2)$$

where the  $\mu_i^0$  are the chemical potentials of the various species in their standard states at the temperature of the reaction mixture.

Subtraction of equation (2.4.2) from (2.4.1) gives

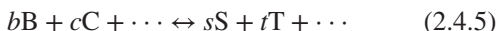
$$\Delta G - \Delta G^0 = \sum_i \nu_i (\mu_i - \mu_i^0) \quad (2.4.3)$$

This equation may be rewritten in terms of the activities of the various species by making use of equation (2.1.1):

$$\Delta G - \Delta G^0 = RT \sum_i [\nu_i \ln a_i] = RT \ln \left( \prod_i a_i^{\nu_i} \right) \quad (2.4.4)$$

where  $\prod_i$  denotes a product over  $i$  species of the term that follows.

For a general reaction of the form



the equations above lead to

$$\Delta G - \Delta G^0 = RT \ln \left( \frac{a_S^s a_T^t \dots}{a_B^b a_C^c \dots} \right) \quad (2.4.6)$$

For a system at equilibrium,  $\Delta G = 0$ , so

$$\Delta G^0 = -RT \ln \left( \frac{a_S^s a_T^t \dots}{a_B^b a_C^c \dots} \right) = -RT \ln K_a \quad (2.4.7)$$

where the equilibrium constant for the reaction ( $K_a$ ) at temperature  $T$  is defined as the  $\ln$  term. The subscript  $a$  in the symbol  $K_a$  has been used to emphasize that an equilibrium constant is written properly as a product of the activities raised to appropriate powers. Thus, in general,

$$K_a = \prod_i a_i^{\nu_i} = e^{-\Delta G^0/RT} \quad (2.4.8)$$

Inspection of equation (2.4.8) indicates that the equilibrium constant for a reaction is determined by the absolute temperature and the standard Gibbs free energy change ( $\Delta G^0$ ) for the process. The latter quantity depends, in turn, on temperature, the definitions of the standard states of the various components, and the stoichiometric coefficients of these species. Consequently, in assigning a numerical value to an equilibrium constant, one must be careful to specify all three of these quantities to give meaning to this value. Once one has thus specified the point of reference, this value may be used to calculate the equilibrium composition of the mixture in the manner described in Sections 2.6 to 2.9.

## 2.5 EFFECTS OF TEMPERATURE AND PRESSURE CHANGES ON THE EQUILIBRIUM CONSTANT

Equilibrium constants are very sensitive to temperature changes. A quantitative description of the influence of

temperature changes is readily obtained by combining equations (2.2.8) and (2.4.7):

$$\left[ \frac{\partial (-\Delta G^0/T)}{\partial T} \right]_P = \left( \frac{R \partial \ln K_a}{\partial T} \right)_P = \frac{\Delta H^0}{T^2} \quad (2.5.1)$$

or

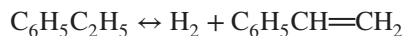
$$\left( \frac{\partial \ln K_a}{\partial T} \right)_P = \frac{\Delta H^0}{RT^2} \quad (2.5.2)$$

and

$$\left[ \frac{\partial \ln K_a}{\partial (1/T)} \right]_P = -\frac{\Delta H^0}{R} \quad (2.5.3)$$

For cases where  $\Delta H^0$  is essentially independent of temperature, plots of data in the form  $\ln K_a$  versus  $1/T$  are linear with a slope equal to  $-\Delta H^0/R$ . Such plots are often referred to as *van't Hoff plots*. For cases where the heat capacity term in equation (2.2.7) is appreciable, this equation must be substituted into either equation (2.5.2) or (2.5.3) to determine the temperature dependence of the equilibrium constant. For exothermic reactions ( $\Delta H^0$  is negative), the equilibrium constant decreases with increasing temperature, whereas for endothermic reactions the equilibrium constant increases with increasing temperature.

Figure 2.1 contains van't Hoff plots for three industrially significant reactions. The mathematical models used to correlate the data incorporate the dependence of  $\Delta H^0$  on the absolute temperature. The quasi-linearity of the two plots for exothermic reactions (those with positive slopes) attests to the fact that the dominant term in equation (2.2.7) is the standard enthalpy change at temperature  $T$  and that the heat capacity term may frequently be neglected over fairly wide temperature ranges. In terms of this simplifying assumption, one in essence regards the standard enthalpy change as a constant that can be determined from the slope of a best-fit line through experimental data plotted in the form of equation (2.2.8). The fact that  $\Delta G^0 = \Delta H^0 - T \Delta S^0$  implies that the intercept corresponding to a reciprocal absolute temperature of zero for such lines is equal to  $\Delta S^0/R$ . The plot in Figure 2.1 that has a negative slope is characteristic of many dehydrogenation reactions. Such slopes identify the reaction as endothermic. In this case the stoichiometry of the reaction is



For cases in which the standard states of the reactants and products are chosen as 1 bar, the value of  $\Delta G^0$  is independent of pressure. Consequently, equation (2.4.7) indicates that  $K_a$  is also pressure independent for this choice of standard states. This convention is the one normally encountered in engineering practice. For the *unconventional* choice of standard states discussed in Section 2.2,

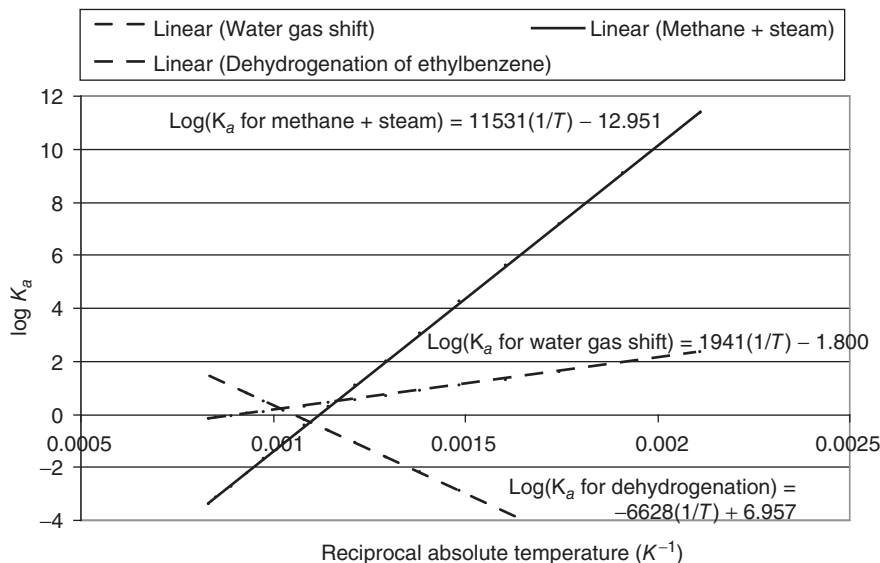


**Figure 2.1** Dependence of equilibrium constants on absolute temperature plotted using coordinates suggested by the van't Hoff relation. The plots for exothermic reactions (water gas shift and methane + steam) have positive slopes. The reaction of methane with steam is  $\text{CH}_4 + \text{H}_2\text{O} \leftrightarrow \text{CO} + 3\text{H}_2$ , and the stoichiometry of the water gas shift is  $\text{CO} + \text{H}_2\text{O} \leftrightarrow \text{CO}_2 + \text{H}_2$ . The plot with a negative slope corresponds to the endothermic dehydrogenation of ethylbenzene to form styrene (1). Because we have plotted the logarithms of the equilibrium constants rather than using natural logarithms, the slopes of these plots correspond to  $-\Delta H^\circ/2.303R$  and the intercepts to  $\Delta S^\circ/2.303R$ . [These plots are based on correlating equations contained in Appendixes 6 and 7 of M. V. Twigg (Ed.), *Catalyst Handbook*, 2nd ed., Wolfe Publishing, London, 1989.]

equations (2.4.7) and (2.2.10) may be combined to give the effect of pressure on  $K_a$ :

$$\left( \frac{\partial \ln K_a}{\partial P} \right)_T = -\frac{\sum_i \nu_i V_i^0}{RT} \quad (2.5.4)$$

where the  $V_i^0$  are the standard-state molar volumes of the reactants and products. However, use of this choice of standard states is extremely rare in engineering practice.

## 2.6 DETERMINATION OF EQUILIBRIUM COMPOSITIONS

The basic equation from which one calculates the composition of an equilibrium mixture is equation (2.4.7). Application of this relation to the chemical reaction defined by equation (2.4.5) gives

$$\Delta G^\circ = -RT \ln K_a = -RT \ln \left( \frac{a_S^s a_T^t}{a_B^b a_C^c} \right) \quad (2.6.1)$$

In a system that involves gaseous components, one normally chooses as the standard state the pure component gases, each at unit fugacity (essentially, 1 bar). The activity of a gaseous species B is then given by

$$a_B = \frac{\hat{f}_B}{f_{B,SS}} = \frac{\hat{f}_B}{1} = \hat{f}_B \quad (2.6.2)$$

where  $\hat{f}_B$  is the fugacity of species B as it exists in the equilibrium reaction mixture and  $f_{B,SS}$  is the fugacity of species B in its standard state.

The fugacity of species B in an ideal solution of gases is given by the *Lewis and Randall rule*,

$$\hat{f}_B = y_B f_B^0 \quad (2.6.3)$$

where  $y_B$  is the mole fraction B in the gaseous phase and  $f_B^0$  is the fugacity of pure component B evaluated at the temperature and total pressure ( $P$ ) of the reaction mixture. Alternatively,

$$\hat{f}_B = y_B \left( \frac{f}{P} \right)_B P \quad (2.6.4)$$

where  $(f/P)_B$  is the fugacity coefficient for pure component B at the temperature and total pressure of the system.

If all of the species involved in the reaction are gases, combining equations (2.6.1), (2.6.2), and (2.6.4) gives

$$K_a = \frac{y_S^s y_T^t}{y_B^b y_C^c} \frac{(f/P)_S^s (f/P)_T^t}{(f/P)_B^b (f/P)_C^c} P^{s+t-b-c} \quad (2.6.5)$$

The first term on the right is assigned the symbol  $K_y$ , while the second term is assigned the symbol  $K_{f/P}$ . The quantity  $K_{f/P}$  is constant for a given temperature and pressure. However, unlike the equilibrium constant  $K_a$ , the term  $K_{f/P}$  is affected by changes in the system pressure as well as by changes in temperature. The product of  $K_y$  and  $P^{s+t-b-c}$  is assigned the symbol  $K_P$ :

$$K_P \equiv K_y P^{s+t-b-c} = \frac{(y_S P)^s (y_T P)^t}{(y_B P)^b (y_C P)^c} = \frac{P_S^s P_T^t}{P_B^b P_C^c} \quad (2.6.6)$$

because each term in parentheses is a component partial pressure. Thus,

$$K_a = K_{f/P} K_P \quad (2.6.7)$$

For cases where the gases behave ideally, the fugacity coefficients may be taken as unity and the term  $K_P$  equated to  $K_a$ . At higher pressures, where the gases are no longer ideal, the  $K_{f/P}$  term may differ appreciably from unity and have a significant effect on the equilibrium composition. The corresponding states plot of fugacity coefficients contained in Appendix A may be used to estimate  $K_{f/P}$ .

In a system containing an inert gas  $I$  in the amount of  $n_I$  moles, the mole fraction of reactant gas B is given by

$$y_B = \frac{n_B}{n_B + n_C + \dots + n_S + n_T + \dots + n_I} \quad (2.6.8)$$

where the  $n_i$  refer to the mole numbers of reactant and product species. Combination of equations (2.6.5) to (2.6.7) and defining equations similar to equation (2.6.8) for the various mole fractions gives

$$K_a = K_{f/P} \left( \frac{n_S n_T}{n_B n_C} \right) \times \left( \frac{P}{n_B + n_C + \dots + n_S + n_T + \dots + n_I} \right)^{s+t-b-c} \quad (2.6.9)$$

This equation is extremely useful for calculating the equilibrium composition of the reaction mixture. The mole numbers of the various species at equilibrium may be related to their values at time zero using the extent of reaction. When these relations are substituted into equation (2.6.9), one obtains a single equation in a single unknown, the equilibrium extent of reaction. This technique is utilized in Illustration 2.1. If more than one independent reaction is occurring in a given system, one requires as many equations of the form of equation (2.6.9) as there are independent reactions. These equations are then written in terms of the various extents of reaction to obtain a set of independent equations equal to the number of unknowns. Such a system is considered in Illustration 2.2.

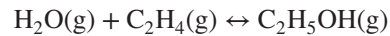
## ILLUSTRATION 2.1 Calculation of Equilibrium Yield for a Chemical Reaction

### Problem

Calculate the equilibrium composition of a mixture of the following species:

$N_2$	15.0 mol%
$H_2O$	60.0 mol%
$C_2H_4$	25.0 mol%

The mixture is maintained at a constant temperature of 527 K and a constant pressure of 264.2 bar. Assume that the only significant chemical reaction is



The standard state of each species is taken as the pure material at unit fugacity. Use only the following critical properties, thermochemical data, and a fugacity coefficient chart.

Compound	$T_C$ (K)	$P_C$ (bar)
$H_2O(g)$	647.3	218.2
$C_2H_4(g)$	283.1	50.5
$C_2H_5OH(g)$	516.3	63.0

Compound	$\Delta G_{f/298.16}^0$ (kJ/mol)	$\Delta H_{f/298.16}^0$ (kJ/mol)
$H_2O(g)$	-228.705	-241.942
$C_2H_4(g)$	68.156	52.308
$C_2H_5OH(g)$	-168.696	-235.421

### Solution

The basis is 100 mol of initial gas. To calculate the equilibrium composition, one must know the equilibrium constant for the reaction at 527 K. From the values of  $\Delta G_{f,i}^0$  and  $\Delta H_{f,i}^0$  at 298.16 K and equations (2.2.5) and (2.2.6):

$$\begin{aligned} \Delta G_{298}^0 &= (1)(-168.696) + (-1)(68.156) \\ &\quad + (-1)(-228.705) = -8.147 \text{ kJ/mol} \\ \Delta H_{298}^0 &= (1)(-235.421) + (-1)(52.308) \\ &\quad + (-1)(-241.942) = -45.787 \text{ kJ/mol} \end{aligned}$$

The equilibrium constant at 298.16 K may be determined from equation (2.4.7):

$$\Delta G^0 = -RT \ln K_a$$

or

$$\ln K_a = -\frac{-8147}{8.31(298.16)} = 3.29$$

The equilibrium constant at 527 K may be determined using equation (2.5.3):

$$\left[ \frac{\partial \ln K_a}{\partial (1/T)} \right]_P = -\frac{\Delta H^0}{R}$$

If one assumes that  $\Delta H^0$  is independent of temperature, this equation may be integrated to obtain

$$\ln K_{a,2} - \ln K_{a,1} = \frac{\Delta H^0}{R} \left( \frac{1}{T_1} - \frac{1}{T_2} \right)$$

For our case,

$$\ln K_{a,2} - 3.29 = \frac{-45,787}{8.31} \left( \frac{1}{298.16} - \frac{1}{527} \right) = -8.02$$

or

$$K_{a,2} = 8.83 \times 10^{-3} \text{ at } 527 \text{ K}$$

Because the standard states are the pure materials at unit fugacity, equation (2.6.5) may be rewritten as

$$K_a = \frac{y_{C_2H_5OH}}{y_{H_2O}y_{C_2H_4}} \frac{(f/P)_{C_2H_5OH}}{(f/P)_{H_2O}(f/P)_{C_2H_4}} \frac{1}{P} \quad (\text{A})$$

The fugacity coefficients ( $f/P$ ) for the various species may be determined from a corresponding states chart if one knows the reduced temperature and pressure corresponding to the species in question. Therefore:

Species	Reduced temperature,	Reduced pressure,	$f/P$
	527 K	264.2 atm	
$H_2O(g)$	$527/647.3 = 0.814$	$264.2/218.2 = 1.211$	0.190
$C_2H_4(g)$	$527/283.1 = 1.862$	$264.2/50.5 = 5.232$	0.885
$C_2H_5OH(g)$	$527/516.3 = 1.021$	$264.2/63.0 = 4.194$	0.280

From the stoichiometry of the reaction it is possible to determine the mole numbers of the various species in terms of the extent of reaction and their initial mole numbers:

$$n_i = n_{i,0} + \nu_i \xi$$

Species	Initial moles	Moles at extent $\xi$
$N_2$	15.0	15.0
$H_2O$	60.0	$60.0 - \xi$
$C_2H_4$	25.0	$25.0 - \xi$
$C_2H_5OH$	0.0	$0.0 + \xi$
Total	100.0	$100.0 - \xi$

The various mole fractions are readily determined from this table. Note that the upper limit on  $\xi$  is 25.0. Substitution of numerical values and expressions for the various mole fractions into equation (A) gives

$$8.83 \times 10^{-3} = \left[ \frac{\frac{\xi}{100.0 - \xi}}{\left( \frac{60.0 - \xi}{100.0 - \xi} \right) \left( \frac{25.0 - \xi}{100.0 - \xi} \right)} \right] \times \left\{ \left[ \frac{0.280}{0.190(0.885)} \right] \frac{1}{264.2} \right\}$$

or

$$\begin{aligned} & \frac{\xi(100.0 - \xi)}{(60.0 - \xi)(25.0 - \xi)} \\ &= 8.83 \times 10^{-3} (264.2) \left[ \frac{0.190(0.885)}{0.280} \right] = 1.404 \end{aligned}$$

This equation is quadratic in  $\xi$ . The solution is  $\xi = 10.9$ . On the basis of 100 mol of starting material, the equilibrium composition is then as follows:

Species	Mole numbers	Mole percentages
$N_2$	15.0	16.83
$H_2O$	49.1	55.11
$C_2H_4$	14.1	15.82
$C_2H_5OH$	10.9	12.23
Total	89.1	99.99

## 2.7 EFFECTS OF REACTION CONDITIONS ON EQUILIBRIUM YIELDS

Equation (2.6.9) is an extremely useful relation for determining the effects of changes in process parameters on the equilibrium yield of a specific product in a system in which only a single gas-phase reaction is important. Rearrangement of this equation gives

$$\frac{n_S^s n_T^t}{n_B^b n_C^c} = \frac{K_a}{K_{f/P}} \left( \frac{n_B + n_C + \dots + n_S + n_T + \dots + n_I}{P} \right)^{s+t-b-c} \quad (2.7.1)$$

Any change that increases the right side of equation (2.7.1) will increase the ratio of products to reactants in the equilibrium mixture and thus correspond to increased conversions.

### 2.7.1 Effects of Temperature Changes

The temperature affects the equilibrium yield primarily through its influence on the equilibrium constant  $K_a$ . From equation (2.5.2) it follows that for exothermic reactions the equilibrium conversion decreases as the temperature increases. The equilibrium yield increases with increasing temperature for endothermic reactions. Temperature changes also affect the value of  $K_{f/P}$ . The changes in this term, however, are generally very small compared to those in  $K_a$ .

### 2.7.2 Effects of Total Pressure

The equilibrium constant  $K_a$  is independent of pressure for those cases where the standard states are taken as the pure components at 1 bar. This situation was used as the basis for deriving equation (2.6.9). The effects of pressure changes then appear in the terms  $K_{f/P}$  and  $P^{s+t-b-c}$ . For reactions that produce a change in the total number of gaseous species in the system, the term that has the largest effect on the equilibrium yield of products is  $P^{s+t-b-c}$ . Thus, if a reaction

produces a decrease in the total number of gaseous components, the equilibrium yield is increased by an increase in pressure. If an increase in the total number of gaseous moles accompanies the reaction, the equilibrium yield decreases as the pressure increases.

The influence of moderate changes in pressure on  $K_{f/P}$  is normally negligible. However, for situations in which there is no change in the total number of gaseous moles during the reaction, this term is the only one by which pressure changes can affect the equilibrium yield. To determine the effect of major changes in pressure on the equilibrium yield, one should calculate the value of  $K_{f/P}$  using generalized fugacity coefficient charts for the system and conditions of interest.

### 2.7.3 Effect of Addition of Inert Gases

The only term in equation (2.7.1) that is influenced by the addition of inert gases is  $n_1$ . Thus, for reactions in which there is no change in the total number of gaseous moles, addition of inerts has no effect on the equilibrium yield. For cases where there is a change, the effect produced by addition of inert gases is in the same direction as that which would be produced by a pressure decrease.

### 2.7.4 Effect of Addition of Catalysts

The equilibrium constant and equilibrium yield are independent of whether or not a catalyst is present. If the catalyst does not remove any of the passive restraints that have been placed on the system by opening up the possibility of additional reactions, the equilibrium yield will not be affected by the presence of this material.

### 2.7.5 Effect of Excess Reactants

If nonstoichiometric amounts of reactants are present in the initial system, the presence of excess reactants tends to increase the equilibrium fractional conversion of the limiting reagent above that which would be obtained with stoichiometric ratios of the reactants.

## 2.8 HETEROGENEOUS REACTIONS

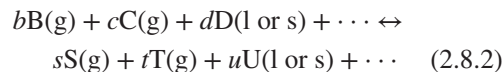
The fundamental fact on which the analysis of heterogeneous reactions is based is that when a component is present as a pure liquid or as a pure solid, its activity may be taken as unity, provided that the pressure on the system is not extremely high. For very high pressures, the effects

of pressure on the activities of pure solids or liquids may be determined using the *Poynting correction factor*:

$$\ln \left( \frac{a_{P=P}}{a_{P=1\text{bar}}} \right) = \frac{\int_1^P V dP}{RT} \quad (2.8.1)$$

where  $V$  is the molar volume of the condensed phase. The activity ratio is essentially unity at moderate pressures.

If we now return to our generalized reaction (2.4.5) and add to our gaseous components B, C, S, and T a pure liquid or solid reactant D and a pure liquid or solid product U with stoichiometric coefficients  $d$  and  $u$ , respectively, the reaction may be written as



The equilibrium constant for this reaction is

$$K_a = \frac{a_{\text{S}}^s a_{\text{T}}^t a_{\text{U}}^u \dots}{a_{\text{B}}^b a_{\text{C}}^c a_{\text{D}}^d \dots} \quad (2.8.3)$$

When the standard states for the solid and liquid species correspond to the pure species at a pressure of 1 bar or at a low equilibrium vapor pressure of the condensed phase, the activities of the pure species at equilibrium are taken as unity at all moderate pressures. Consequently, the gas-phase composition at equilibrium will not be affected by the amount of solid or liquid present. At very high pressures, equation (2.8.1) must be used to calculate these activities. When solid or liquid solutions are present, the activities of the components of these solutions are no longer unity even at moderate pressures. In this case, to determine the equilibrium composition of the system, one needs data on the activity coefficients of the various species and the solution composition.

## 2.9 EQUILIBRIUM TREATMENT OF SIMULTANEOUS REACTIONS

The treatment of chemical reaction equilibria outlined above can be generalized to cover the situation where multiple reactions occur simultaneously. In principle one can take all conceivable reactions into account in computing the composition of a gas mixture at equilibrium. However, because of kinetic limitations on the rate of approach of certain reactions to equilibrium, one can treat many systems as if equilibrium is achieved in some reactions but not in others. In many cases, reactions that are thermodynamically possible do not, in fact, occur at appreciable rates.

In practice, additional simplifications occur because at equilibrium many of the possible reactions either occur

to a negligible extent, or else proceed substantially to completion. One criterion for determining if either of these conditions prevails is to examine the magnitude of the equilibrium constant in question. If it is many orders of magnitude greater than unity, the reaction may be said to go to completion. If it is orders of magnitude less than unity, the reaction may be assumed to occur to a negligible extent. In either event, the number of chemical species that must be considered is reduced and the analysis is thereby simplified. After the simplifications are made, there may remain a group of reactions whose equilibrium constants are neither extremely small nor very large, indicating that appreciable amounts of both products and reactants are present at equilibrium. All of these reactions must be considered in calculating the equilibrium composition.

To arrive at a consistent set of relationships from which complex reaction equilibria may be determined, one must develop the same number of independent equations as there are unknowns. The following treatment indicates the Gauss–Jordan method of arriving at a set of chemical reactions that are independent (2).

If  $R$  reactions occur simultaneously within a system composed of  $S$  species, one has  $R$  stoichiometric equations of the form

$$\sum_{i=1}^S \nu_{ki} A_i = 0 \quad k = 1, 2, \dots, R \quad (2.9.1)$$

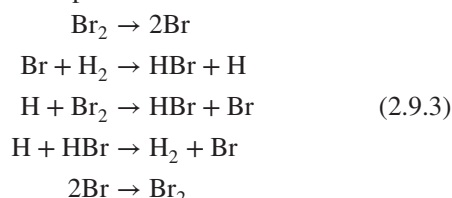
where  $\nu_{ki}$  is the stoichiometric coefficient of species  $i$  in reaction  $k$ .

Because the same reaction may be written with different stoichiometric coefficients, the importance of the coefficients lies in the fact that the ratios of the coefficients of two species must be identical, no matter how the reaction is written. Thus, the stoichiometric coefficients of a reaction are given only up to a constant multiplier  $\lambda$ . The equation

$$\sum_{i=1}^S \lambda \nu_{ki} A_i = 0 \quad k = 1, 2, \dots, R \quad (2.9.2)$$

has the same meaning as equation (2.9.1), provided that  $\lambda$  is nonzero.

If three or more reactions can be written for a given system, one must test to see if any is a multiple of one of the others and if any is a linear combination of two or more others. We will use a set of elementary reactions representing a mechanism for the reaction between  $H_2$  and  $Br_2$  as a vehicle for indicating how one may determine which of a set of reactions are independent.



If we define

$$A_1 = Br_2 \quad A_2 = Br \quad A_3 = H_2 \quad A_4 = H \quad A_5 = HBr \quad (2.9.4)$$

the reactions in (2.9.3) may be rewritten as

$$\begin{array}{rccccc} -A_1 & +2A_2 & & & & = 0 \\ & -A_2 & -A_3 & +A_4 & +A_5 & = 0 \\ -A_1 & +A_2 & & -A_4 & +A_5 & = 0 \\ & & A_2 & +A_3 & -A_4 & -A_5 & = 0 \\ A_1 & -2A_2 & & & & = 0 \end{array} \quad (2.9.5)$$

To test for independence, form the matrix of the stoichiometric coefficients of the foregoing reactions with  $\nu_{ki}$  in the  $k$ th row and the  $i$ th column.

$$\begin{array}{cccccc} -1 & 2 & 0 & 0 & 0 & \\ 0 & -1 & -1 & 1 & 1 & \\ -1 & 1 & 0 & -1 & 1 & \\ 0 & 1 & 1 & -1 & -1 & \\ 1 & -2 & 0 & 0 & 0 & \end{array} \quad (2.9.6)$$

Next, take the first row with a nonzero element in the first column and divide through by the leading element. If  $\nu_{k1} \neq 0$ , this will give a new first row of

$$1 \quad \frac{\nu_{12}}{\nu_{11}} \quad \frac{\nu_{13}}{\nu_{11}} \quad \dots \quad \frac{\nu_{1S}}{\nu_{11}} \quad (2.9.7)$$

This new row may now be used to make all other elements of the first column zero by subtracting  $\nu_{ki}$  times the new first row from the corresponding element in the  $k$ th row. The row that results is

$$0 \quad \left( \nu_{k2} - \nu_{k1} \frac{\nu_{12}}{\nu_{11}} \right) \quad \left( \nu_{k3} - \nu_{k1} \frac{\nu_{13}}{\nu_{11}} \right) \quad \dots \quad \left( \nu_{kS} - \nu_{k1} \frac{\nu_{1S}}{\nu_{11}} \right) \quad (2.9.8)$$

In the present example the revised coefficient matrix becomes

$$\begin{array}{ccccc} 1 & -2 & 0 & 0 & 0 \\ 0 & -1 & -1 & 1 & 1 \\ 0 & -1 & 0 & -1 & 1 \\ 0 & 1 & 1 & -1 & -1 \\ 0 & 0 & 0 & 0 & 0 \end{array} \quad (2.9.9)$$

The next step is to ignore the first row and the first column of this matrix and repeat the reduction above on the resulting reduced matrix containing  $R - 1$  rows. Thus, matrix (2.9.9) becomes

$$\begin{array}{ccccc} 1 & -2 & 0 & 0 & 0 \\ 0 & 1 & 1 & -1 & -1 \\ 0 & 0 & 1 & -2 & 0 \\ 0 & 0 & 0 & 0 & 0 \\ 0 & 0 & 0 & 0 & 0 \end{array} \quad (2.9.10)$$

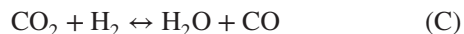
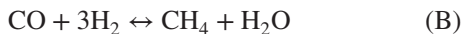
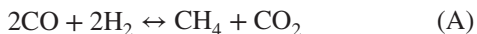
This procedure may be repeated as often as necessary until one has 1's down the diagonal as far as possible and 0's beneath them. In the present case we have reached this point. If this had not been the case, the next step would have been to ignore the first two rows and columns and to repeat the operations above on the resulting array. The number of independent reactions is then equal to the number of 1's on the diagonal.

Once the number of independent reactions has been determined, an independent subset can be chosen for use in subsequent calculations.

## ILLUSTRATION 2.2 Determination of Equilibrium Compositions in the Presence of Simultaneous Reactions

This material has been adapted from Strickland-Constable (3), with permission.

Consider a system that consists initially of 1 mol of CO and 3 mol of H<sub>2</sub> at 1000 K. The system pressure is 25 bar. The following reactions are to be considered:



When the equilibrium constants for reactions (A) and (B) are expressed in terms of the partial pressures of the various species (in bar), the equilibrium constants for these reactions have the following values:

$$K_{P,\text{A}} = 0.046 \quad K_{P,\text{B}} = 0.034 \quad K_{P,\text{C}} = ?$$

Determine the equilibrium composition of the mixture.

### Solution

The first step in the analysis is to determine if the chemical equations (A) to (C) are independent by applying the test described above. When one does this, one finds that only two of the reactions are independent. We will choose the first two for use in subsequent calculations. Let the variables  $\xi_A$  and  $\xi_B$  represent the equilibrium extents of reactions A and B, respectively. A mole table indicating the mole numbers of the various species present at equilibrium may be prepared using the following form of equation (1.1.6):

$$n_1 = n_{i0} + \nu_{Ai}\xi_A + \nu_{Bi}\xi_B$$

Species	Initial mole number	Equilibrium mole number
CO	1	$1 - 2\xi_A - \xi_B$
H <sub>2</sub>	3	$3 - 2\xi_A - 3\xi_B$
CH <sub>4</sub>	0	$\xi_A + \xi_B$
CO <sub>2</sub>	0	$\xi_A$
H <sub>2</sub> O	0	$\xi_B$
Total	4	$4 - 2\xi_A - 2\xi_B$

The fact that none of the mole numbers can ever be negative places maximum values of  $\frac{1}{2}$  on  $\xi_A$  and 1 on  $\xi_B$ .

The values of  $K_P$  for reactions A and B are given by

$$K_{P,\text{A}} = \frac{P_{\text{CH}_4}P_{\text{CO}_2}}{P_{\text{CO}}^2P_{\text{H}_2}^2} = \frac{y_{\text{CH}_4}y_{\text{CO}_2}}{y_{\text{CO}}^2y_{\text{H}_2}^2 P^2}$$

$$K_{P,\text{B}} = \frac{P_{\text{CH}_4}P_{\text{H}_2\text{O}}}{P_{\text{CO}}P_{\text{H}_2}^3} = \frac{y_{\text{CH}_4}y_{\text{H}_2\text{O}}}{y_{\text{CO}}y_{\text{H}_2}^3 P^2}$$

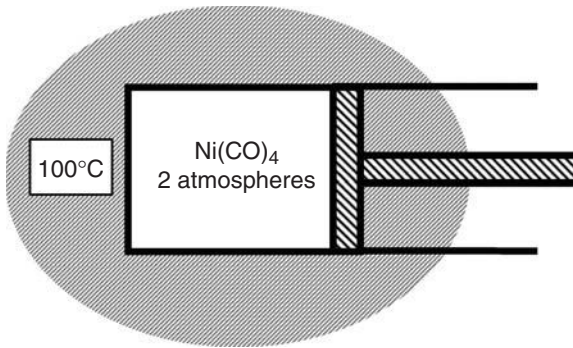
The mole fractions of the various species may be expressed in terms of  $\xi_A$  and  $\xi_B$ , so that the above relations for  $K_P$  become

$$\begin{aligned} K_{P,\text{A}} &= \frac{\left(\frac{\xi_A + \xi_B}{4 - 2\xi_A - 2\xi_B}\right) \left(\frac{\xi_A}{4 - 2\xi_A - 2\xi_B}\right)}{\left(\frac{1 - 2\xi_A - \xi_B}{4 - 2\xi_A - 2\xi_B}\right)^2 \left(\frac{3 - 2\xi_A - 3\xi_B}{4 - 2\xi_A - 2\xi_B}\right)^2 P^2} \\ &= \frac{(\xi_A + \xi_B)\xi_A(4 - 2\xi_A - 2\xi_B)^2}{(1 - 2\xi_B - \xi_B)^2(3 - 2\xi_A - 3\xi_B)^2 P^2} \\ K_{P,\text{B}} &= \frac{\left(\frac{\xi_A + \xi_B}{4 - 2\xi_A - 2\xi_B}\right) \left(\frac{\xi_B}{4 - 2\xi_A - 2\xi_B}\right)}{\frac{1 - 2\xi_A - \xi_B}{4 - 2\xi_A - 2\xi_B} \left(\frac{3 - 2\xi_A - 3\xi_B}{4 - 2\xi_A - 2\xi_B}\right)^3 P^2} \\ &= \frac{(\xi_A + \xi_B)\xi_B(4 - 2\xi_A - 2\xi_B)^2}{(1 - 2\xi_A - \xi_B)(3 - 2\xi_A - 3\xi_B)^3 P^2} \end{aligned}$$

Substitution of numerical values for  $P$ ,  $K_{P,\text{A}}$ , and  $K_{P,\text{B}}$  gives two equations in two unknowns.

The resulting equations can be solved only by numerical techniques. In this case, a simple graphical approach can be employed in which one plots  $\xi_A$  versus  $\xi_B$  for each equation and notes the point of intersection. Values of  $\xi_A = 0.128$  and  $\xi_B = 0.593$  are consistent with these equations. Thus, at equilibrium,

Species	Mole number	Mole fraction
CO	0.151	0.059
H <sub>2</sub>	0.965	0.377
CH <sub>4</sub>	0.721	0.282
CO <sub>2</sub>	0.128	0.050
H <sub>2</sub> O	0.593	0.232
Total	2.558	1.000



## 2.10 SUPPLEMENTARY READING REFERENCES

The following texts contain informative discussions of the thermodynamics of chemical reaction equilibria; they can be recommended without implying criticism of others that are not mentioned.

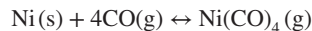
1. H. C. VAN NESS, J. M. SMITH, and M. M. ABBOTT, *Introduction to Chemical Engineering Thermodynamics*, 7th ed., McGraw-Hill, New York, 2004.
2. J. W. TESTER and M. MODELL, *Thermodynamics and Its Applications*, 3rd ed., Prentice Hall, Englewood Cliffs, NJ, 1996.
3. S. I. SANDLER, *Chemical, Biochemical, and Engineering Thermodynamics*, 4th ed., Wiley, New York, 2006.
4. J. R. ELLIOT and C. T. LIRA, *Introductory Chemical Engineering Thermodynamics*, Prentice Hall, Upper Saddle River, NJ, 1999.

## LITERATURE CITATIONS

1. TISCAREÑO-LECHUGA, F., Ph.D. thesis, Department of Chemical Engineering, University of Wisconsin-Madison, p. 53, 1992.
2. ARIS, R., *Introduction to the Analysis of Chemical Reactors*, Prentice-Hall, Englewood Cliffs, NJ, 1965.
3. STRICKLAND-CONSTABLE, R. F., Chemical Thermodynamics, in H. W. CREMER and S. B. WATKINS (Eds.), *Chemical Engineering Practice*, Vol. 8, Butterworth, London, 1965.

## PROBLEMS

- 2.1** Consider the equilibrium between solid nickel, carbon monoxide, and nickel tetracarbonyl:



For the reaction as written, the standard Gibbs free-energy change at 100°C is 1292 cal/mol when the following standard states are used:

Ni(s) pure crystalline solid at 100°C under its own vapor pressure

CO(g) pure gas at 100°C, unit fugacity

Ni(CO)<sub>4</sub>(g) pure gas at 100°C, unit fugacity

- (a)** If a vessel is initially charged with pure Ni(CO)<sub>4</sub> and maintained at a temperature of 100°C by immersion in a container of boiling water, what fraction of the Ni(CO)<sub>4</sub> will decompose if the total pressure in the vessel is maintained constant at 2 atm?

The vapor pressure of pure nickel at 100°C is  $1.23 \times 10^{-46}$  atm. For purposes of this problem you may assume that the gaseous mixture behaves as an ideal gas. State explicitly any other assumptions that you make.

- (b)** What pressure would be necessary to cause 95% of the Ni(CO)<sub>4</sub> to decompose? Assume that all other conditions are the same as in part (a).
- 2.2** C. D. Chang, J. C. W. Kuo, W. H. Lang, S. M. Jacob, J. J. Wise, and A. J. Silvestri [*Ind. Eng. Chem. Process Des. Dev.*, **17**, 255–260 (1978)] studied the dehydration of methanol to dimethyl ether as part of a process for production of gasoline from methanol ( $2\text{CH}_3\text{OH} \leftrightarrow \text{H}_2\text{O} + \text{CH}_3\text{OCH}_3$ ). Use enthalpy of formation and Gibbs free energy of formation data to prepare a plot of the fraction of the methanol fed to the dehydration reactor that is converted to dimethyl ether versus the effluent temperature of the gas. Consider operation with an effluent pressure of 200 psia and temperatures from 500 to 760°F. As first approximations, you may neglect the variation of the standard heat of reaction with temperature, and you may consider the gas mixture as ideal.
- (a)** What conclusions can you draw concerning thermodynamic constraints on this reaction if high yields are desired? What are the implications of your conclusion with respect to the kinetics of this reaction?
- (b)** Does thermodynamics favor operation at high or low pressures? What might be the advantages of operating at 200 psia rather than at approximately 1 atm or 2000 psia?

- 2.3** The SO<sub>3</sub> used in the manufacture of sulfuric acid is obtained by the oxidation of SO<sub>2</sub> in the presence of an appropriate catalyst:

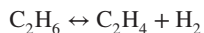


If one starts with a feed of the composition shown below, determine the temperature at which the fluid must leave the reactor if the equilibrium effluent composition corresponds to 95% conversion of the SO<sub>2</sub> fed to the reactor.

Species	Feed composition (mol%)
O <sub>2</sub>	13.0
N <sub>2</sub>	79.0
SO <sub>2</sub>	8.0

The effluent pressure is 2 atm. At 600°C the standard Gibbs free-energy change for standard states of unit fugacity is known to be  $-3995$  cal/mol for the reaction as written above. For the temperature range of interest, the standard heat of reaction may be taken as a constant equal to  $-22,650$  cal/mol.

- 2.4** One of the members of your research group, Stu Dent, claims to have developed a new cracking catalyst that can be used to convert pure ethane to ethylene and hydrogen in high yields:



Stu claims that when the temperature and absolute pressure of the effluent stream are 1000 K and 10.0 atm, respectively, the conversion of ethane is 95%. If one takes the standard states of these three materials as the pure gases at 298 K and unit fugacity, the following thermodynamic data are applicable for  $T$  in kelvin.

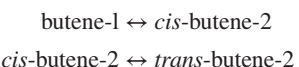
Species	$\Delta G_{f,298}^0$ (cal/mol)	$\Delta H_{f,298}^0$ (cal/mol)	$C_p$ [cal/(mol·K)]
$\text{C}_2\text{H}_6$	-7,860	-20,236	$2.3 + 0.02T$
$\text{C}_2\text{H}_4$	16,282	12,500	$2.8 + 0.03T$
$\text{H}_2$	0	0	$6.9 + 0.004T$

$\Delta G_{f,298}^0$  and  $\Delta H_{f,298}^0$  are the standard Gibbs free energy of formation and the standard enthalpy of formation of the compounds from their elements at 298 K, respectively. You may assume that the heat capacity relations are valid over the range 250 to 1500 K.

- (a) Perform as rigorous a thermodynamic analysis of Stu's claim as you can using the information supplied. That is, determine if Stu's claim of 95% conversion is possible, assuming that no other reactions occur.
- (b) If 95% conversion is not possible, how must the effluent conditions be changed to obtain this yield? That is, (1) if the effluent temperature remains at 1000 K, what must the effluent pressure be; and (2) if the effluent pressure remains at 10 atm, what must the effluent temperature be?

- 2.5** As a thermodynamicist working at the Lower Slobbovian Research Institute, you have been asked to determine the standard Gibbs free energy of formation and the standard enthalpy of formation of the compounds *cis*-butene-2 and *trans*-butene-2. Your boss has informed you that the standard enthalpy of formation of butene-1 is 1.172 kJ/mol and the corresponding standard Gibbs free energy of formation is 72.10 kJ/mol, where the standard state is taken as the pure component at 25°C and 101.3 kPa.

Your associate, Kem Injuneer, has been testing a new catalyst for selective butene isomerization reactions. He says that the only reactions that occur to any appreciable extent over this material are:



He has reported the following sets of data from his system as being appropriate for equilibrium conditions:

*Run I:*

Reactor pressure	53.33 kPa
Reactor temperature	25°C
Gas composition (mol %):	
butene-1	3.0
<i>cis</i> -butene-2	21.9
<i>trans</i> -butene-2	75.1

*Run II:*

Reactor pressure	101.3 kPa
Reactor temperature	127°C
Gas composition (mol %):	
butene-1	8.1
<i>cis</i> -butene-2	28.8
<i>trans</i> -butene-2	63.1

Kem maintains that you now have enough data to determine the values of  $\Delta G_f^0$  and  $\Delta H_f^0$  for the two isomers of butene-2 at 25°C. Proceed to evaluate these quantities. State specifically what assumptions you must make in your analysis and comment on their validity. Use *only* the data given above.

- 2.6** In the presence of an appropriate catalyst, carbon monoxide and hydrogen will react to form alcohols. Consider the following two reactions:



Determine the equilibrium composition that is achieved at 300 bar and 700 K when the initial mole ratio of hydrogen to carbon monoxide is 2. You may use standard enthalpy and Gibbs free energy of formation data. For purposes of this problem you should not neglect the variation of the standard heat of reaction with temperature. You may assume ideal solution behavior but not ideal gas behavior. You may also use a generalized fugacity coefficient chart based on the principle of corresponding states as well as the heat capacity data listed below.

R. C. Reid, J. M. Prausnitz, and B. E. Poling (*The Properties of Gases and Liquids*, 4th ed., McGraw-Hill, New York, 1987, App. A) indicate that if the heat capacities at constant pressure for gases are written as a power series in the absolute temperature,

$$C_p = A + BT + CT^2 + DT^3$$

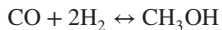
**Table P2.6**

Species	A	B	C	D
CO	30.87	-0.01285	$2.789 \times 10^{-5}$	$-1.272 \times 10^{-8}$
$\text{H}_2$	27.14	0.009274	$-1.381 \times 10^{-5}$	$7.645 \times 10^{-9}$
$\text{CH}_3\text{OH}$	21.15	0.07092	$2.587 \times 10^{-5}$	$-2.852 \times 10^{-8}$
$\text{C}_2\text{H}_5\text{OH}$	9.014	0.2141	$-8.39 \times 10^{-5}$	$1.373 \times 10^{-9}$
$\text{H}_2\text{O}$	32.24	0.00192	$1.055 \times 10^{-5}$	$-3.596 \times 10^{-9}$

with  $C_p$  in J/(mol·K) and  $T$  in kelvin, the coefficients shown in Table P2.6 may be employed.

You should note that when employing corresponding-states correlations of  $PVT$  and thermodynamic properties, it is appropriate to employ pseudocritical values for hydrogen.

**2.7** Consider the following reaction of synthesis gas,



in a packed-bed reactor. The reactor is well insulated and may be assumed to operate at steady state. The feed enters the catalyst bed at 275°C and the effluent leaves at 429°C. The reaction takes place at 300 atm. Unfortunately, the analytical chromatograph has suffered a short, so you do not know the effluent composition. You do know that the feed consists of a mixture of CO and H<sub>2</sub> in the mole ratio 1 : 2. The flow rate through the reactor is sufficiently low that you believe that reaction equilibrium is achieved. The standard heat of reaction is given by

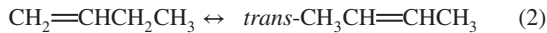
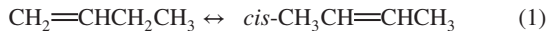
$$\Delta H^0 = -17,539 - 18.19T + 0.0141T^2$$

for  $T$  in K and  $\Delta H^0$  in cal/g-mol. You may ignore the variation of enthalpy with pressure. For purposes of this problem you may employ the following heat capacity values as being independent of temperature and pressure:

$$\begin{aligned} C_{p_{\text{H}_2}} &= C_{p_{\text{CO}}} = 7.0 \text{ cal}/(\text{mol}\cdot\text{K}) \\ C_{p_{\text{CH}_3\text{OH}}} &= 21.0 \text{ cal}/(\text{mol}\cdot\text{K}) \end{aligned}$$

- (a)** What are your best estimates of the effluent composition and the equilibrium constant  $K_a$  for this reaction? Use only the information above, the assumption of ideal solution behavior, and the fact that the fugacity coefficients ( $f/P$ ) for CO, H<sub>2</sub>, and CH<sub>3</sub>OH at the temperature and total pressure in question are 1.178, 1.068, and 0.762, respectively. Calculate  $K_a$  relative to standard states of unit fugacity for all species. Clearly state any other assumptions that you make.
- (b)** *Note:* You may not use the information contained in part (b) to solve part (a). Results of a previous study indicate that at 390°C and 300 atm, the standard Gibbs free energy of reaction relative to standard states of unit fugacity is 14,700 cal/mol. Are the results you obtain in part (a) reasonably consistent with this value? For your calculations you may neglect the variation of  $\Delta H^0$  with temperature over the range 390 to 429°C by employing an average value (i.e., evaluate  $\Delta H^0$  at 410°C and presume it to be a constant).

**2.8** Consider the following reactions of butene-1:



These reactions take place over a new catalyst which you have been studying in the laboratory. Other side reactions may be neglected.

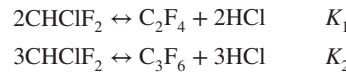
The following data on standard Gibbs free energies and enthalpies of formation are available for use in your analysis.

The standard states are taken as the pure components as ideal gases at 25°C and 1 bar.

	$\Delta G_f^0$ (kJ/mol)	$\Delta H_f^0$ (kJ/mol)
Butene-1	71.34	-0.126
<i>cis</i> -Butene-2	65.90	-6.99
<i>trans</i> -Butene-2	63.01	-11.18
Ethylene	68.16	52.34

- (a)** If 0.05 mol of pure butene-1 is placed in a reactor containing the aforementioned catalyst at 25°C, calculate the equilibrium composition of the mixture (in mole fractions) corresponding to the three reactions above if the total pressure on the system is 2 bar.
- (b)** Will the equilibrium constant for reaction (3) at 25°C and 10 atm be greater than, less than, or equal to that calculated as part of your solution to part (a)? Explain your reasoning.
- (c)** Determine the equilibrium constants for these three reactions at 127°C and 2 bar absolute pressure. Comment on the directions that the mole fractions of the various species will be expected to move (increase or decrease) if the reactor is operated at 127°C. State *explicitly* all assumptions that you make.

- 2.9** P. B. Chinoy and P. D. Sunavala [*Ind. Eng. Chem. Res.*, **26**, 1340 (1987)] studied the kinetics and thermodynamics of the manufacture of C<sub>2</sub>F<sub>4</sub>, the monomer for the production of Teflon, via pyrolysis of CHClF<sub>2</sub>. A thermodynamic analysis of this reaction as it occurs in the presence of steam as a diluent or thermal moderator must take into account the following equilibria:



The first reaction is the desired reaction; the second reaction is that responsible for formation of the primary by-product.

Standard enthalpies and Gibbs free energies of formation, as well as heat capacity data, are tabulated below. Use these data to demonstrate your ability to calculate values of the equilibrium constants for these reactions at temperatures of 700 and 900°C.

Compound	Thermochemical Data	
	$\Delta G_f^0$ at 298 K (kcal/mol)	$\Delta H_f^0$ at 298 K (kcal/mol)
C <sub>2</sub> F <sub>4</sub>	-149.10	-157.40
CHClF <sub>2</sub>	-112.47	-119.90
C <sub>3</sub> F <sub>6</sub>	-240.64	-257.80
HCl	-22.78	-22.06

The standard states of aggregation for the indicated compounds are the pure materials at the temperature of interest and unit fugacity.

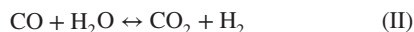
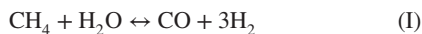
If the heat capacities (at constant pressure) are expressed as a linear function of the absolute temperature in K, (i.e.,

$C_p = a + bT$ ), the following parameter values are approximate for use for  $C_p$  in cal/(mol·K):

Compound	$a$	$10^2 b$
$\text{C}_2\text{F}_4$	6.929	5.439
$\text{CHClF}_2$	4.132	3.865
$\text{C}_3\text{F}_6$	1.172	9.920
HCl	6.700	0.084

You may assume that the gases behave ideally, but you should *not* assume that the standard heats of reaction are independent of temperature.

- 2.10** In the steam reforming of methane, the primary reactions of interest are



If the feed mole ratio of water to methane is  $X$ , and if equilibrium is achieved at reactor effluent conditions of 1073 K and 200 psia, determine the composition of the effluent gas for values of  $X$  from 1 to 10. Prepare plots of the extents of reactions (I) and (II), as well as plots of the fractions of the original  $\text{CH}_4$  that are converted to CO and  $\text{CO}_2$  versus  $X$ .

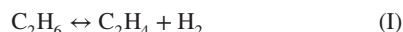
The text by A. M. Mearns (*Chemical Engineering Process Analysis*, Oliver & Boyd, Edinburgh, 1973, p. 96) indicates that at 1073 K,  $K_1 = 1.644 \times 10^2$  and  $K_{\text{II}} = 1.015$  for standard states of unit fugacity. Ideal gas behavior may be assumed.

What are the engineering implications of the trends observed in the plots you have prepared?

- 2.11** A company has a large ethane ( $\text{C}_2\text{H}_6$ ) stream available and has demands for both ethylene ( $\text{C}_2\text{H}_4$ ) and acetylene ( $\text{C}_2\text{H}_2$ ). Because the demands for these two chemicals vary seasonally, the company proposes to build a single plant operating at atmospheric pressure to produce either material.

The particular mix of products that is obtained will depend on the temperature at which the reactor is operated. Determine the equilibrium compositions corresponding to operation at 1 atm and temperatures of 1000, 1500, and 2000 K. Comment on your results.

Assume that only the following reactions occur:



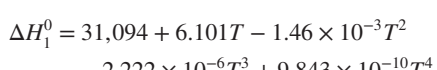
The corresponding standard Gibbs free energies of reaction are

$$\Delta G_{\text{I},298}^0 = 24,142 \text{ cal/mol}$$

$$\Delta G_{\text{II},298}^0 = 57,860 \text{ cal/mol}$$

$$\Delta G_{\text{III},298}^0 = 33,718 \text{ cal/mol}$$

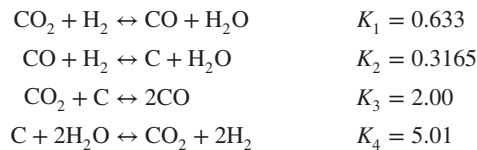
Standard enthalpies of reaction in cal/mol for  $T$  in K:



$$\begin{aligned} \Delta H_2^0 &= 69,936 + 18.082T - 0.010T^2 - 6.617 \times 10^{-7}T^3 + 1.236 \times 10^{-9}T^4 \\ \Delta H_3^0 &= 38,842 + 11.981T - 8.546 \times 10^{-3}T^2 + 1.561 \times 10^{-6}T^3 + 2.517 \times 10^{-10}T^4 \end{aligned}$$

Do not neglect the variation of the standard heat of reaction with temperature.

- 2.12** Consider the task of reforming a mixture containing 40% v/v  $\text{CO}_2$ , 40%  $\text{H}_2$ , and 20%  $\text{N}_2$  by passing it through a packed-bed reactor containing an active catalyst. The reactor operates in a manner such that the effluent leaves at 1000 K. The composition of the effluent stream depends on the pressure at the exit of the reactor. Equilibrium is achieved within the reactor for the following reactions:

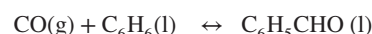


- (a) Over what range of pressures will carbon deposit on the catalyst if only the four reactions indicated above occur?  
 (b) At what operating pressure will 25% of the  $\text{CO}_2$  fed to the reactor be deposited as carbon in the packed bed?

The equilibrium constants are based on a standard state of unit fugacity for the gaseous species and on a standard state corresponding to the pure solid for carbon.

Note that you may calculate a first approximation to the pressure at which 25% of the carbon deposits by assuming that all fugacity coefficients are unity. Then improve the accuracy of your answer by using the first and subsequent approximations of the pressure to determine values of the fugacity coefficients.

- 2.13** It might be possible to produce benzaldehyde by the following reaction:



R. R. Wenner (*Thermochemical Calculations*, McGraw-Hill, New York, 1941) provided the following absolute entropy and thermochemical data for this reaction:

Species	Absolute entropy at 298 K (cal/mol·K)	Standard heat of formation at 298 K (cal/mol)
CO (g)	47.32	-26,390
$\text{C}_6\text{H}_6$ (l)	41.9	12,390
$\text{C}_6\text{H}_5\text{CHO(l)}$	49.4	-21,860

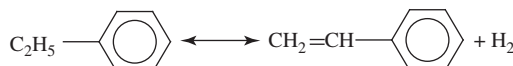
Assume that benzaldehyde and benzene are completely miscible under the conditions of interest, that the solution formed is ideal, that carbon monoxide is insoluble in the liquid phase, and that the liquids are incompressible. The standard states for benzene and benzaldehyde are the pure liquids at 25°C. The standard state for the gas is unit fugacity.

Additional thermophysical data:

Species	Temperature (°C)	Vapor pressure (bar)	Molar volume (cm <sup>3</sup> /mol)
C <sub>6</sub> H <sub>6</sub> (l)	25	0.125	89.5
C <sub>6</sub> H <sub>5</sub> CHO(l)	25	0.001	102

Calculate the amount of benzaldehyde formed at 25°C and 100 bar if 1 mol of liquid benzene and 2 mol of gaseous CO are fed to the reactor. Should one operate at higher or lower pressure at 100°C if one desires to obtain the same yield? The fugacity coefficient for gaseous CO at 25°C and 100 bar is 0.965. State explicitly and justify any additional approximations that you make.

- 2.14** Dehydrogenation of ethylbenzene to form styrene is being studied in an adiabatic tubular reactor packed with a catalyst:



The feed to the reactor consists of a 9 : 1 mole ratio of steam to ethylbenzene at a temperature of 875 K. The steam is present both to reduce the temperature drop that would accompany this endothermic reaction and to minimize carbon deposition on the catalyst. The reactor is sufficiently long that the effluent stream is in equilibrium. If the effluent pressure is 2 atm, determine if the following experimental results reported by your technician are internally consistent.

Effluent temperature	825 K
Effluent composition (mol%)	
H <sub>2</sub> O	83.33
C <sub>2</sub> H <sub>5</sub> C <sub>6</sub> H <sub>5</sub>	1.85
H <sub>2</sub>	7.41
C <sub>2</sub> H <sub>3</sub> C <sub>6</sub> H <sub>5</sub>	7.41

Be as quantitative as possible in your analysis.

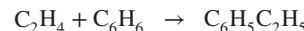
Relevant data from handbooks includes standard heats and Gibbs free energies of formation as ideal gases at 25°C (kJ/mol):

Species	$\Delta H_f^0$	$\Delta G_f^0$
H <sub>2</sub> O	-242.0	-228.8
C <sub>2</sub> H <sub>5</sub> C <sub>6</sub> H <sub>5</sub>	29.8	130.7
C <sub>2</sub> H <sub>3</sub> C <sub>6</sub> H <sub>5</sub>	147.5	213.9

Over the temperature range indicated, the following values of the mean heat capacity ( $C_p$ ) may be considered appropriate for use:

Species	Average $C_p$ [J/mol·K]	
	For 825 to 875 K	For 298.16 to 825 K
H <sub>2</sub> O	39.3	36.1
H <sub>2</sub>	29.7	29.3
C <sub>2</sub> H <sub>5</sub> C <sub>6</sub> H <sub>5</sub>	290.0	219.0
C <sub>2</sub> H <sub>3</sub> C <sub>6</sub> H <sub>5</sub>	266.0	203.0

- 2.15** Ethylbenzene can be formed via the reaction of ethylene and benzene:



Buck E. Badger and a colleague, Sue Dent, are conducting a series of tests of a new catalyst for this reaction. They are employing a well-insulated tubular reactor to which equal molal quantities of benzene and ethylene are being fed at a temperature of 127°C. The activity of the catalyst contained in the reactor is believed to be sufficiently high that at steady state the gases leaving the reactor at 4 atm will be in chemical equilibrium.

A chromatographic analysis of the effluent stream indicates that the composition of the effluent gases in mole fractions is

Benzene	0.045
Ethylene	0.045
Ethylbenzene	0.910

The chromatograph is believed to be reliable and has given accurate results in the past.

A recently installed thermocouple indicates that the temperature of the effluent is 415°C. Buck and Sue have asked you to employ your knowledge of thermodynamics to conduct a quantitative assessment of whether or not the experimental data are consistent with the working hypothesis that the effluent stream is in chemical equilibrium. You may use the thermochemical information presented below as well as any other type of information that is appropriate.

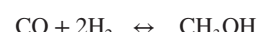
The standard enthalpy change for the reaction above at 25°C is -105.5 kJ/mol. Mean heat capacities of the various gases in the temperature range of interest are:

$$C_p, \text{ benzene} = 125 \text{ J/(mol·K)}$$

$$C_p, \text{ ethylene} = 76 \text{ J/(mol·K)}$$

$$C_p, \text{ ethylbenzene} = 189.4 \text{ J/(mol·K)}$$

- 2.16** Methanol may be synthesized from hydrogen and carbon monoxide in the presence of an appropriate catalyst:



If one has a feed stream containing these gases in stoichiometric proportions (H<sub>2</sub>/CO = 2) at 200 atm and 275°C, determine the effluent composition from the reactor (a) if it operates isothermally and equilibrium is achieved, and (b) if it operates adiabatically and equilibrium is achieved. (Also determine the temperature of the effluent.)

Pertinent data are as follows:

1.  $\Delta H^0 = -17,530 - 18.19T + 0.0141T^2$  for  $\Delta H^0$  in cal/g-mol and  $T$  in K.

2. Molal heat capacities at constant pressure:

H <sub>2</sub> :	$C_p = 6.65 + 0.00070T$
CO:	$C_p = 6.89 + 0.00038T$
CH <sub>3</sub> OH:	$C_p = 2.0 + 0.03T$

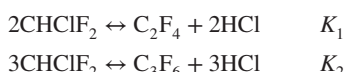
for  $C_p$  in cal/(g-mol·K).

3. Equilibrium constant expressed in terms of fugacities:

$$\log_{10} K_a = \frac{3835}{T} - 9.150 \log_{10} T + 3.08 \times 10^{-3} T + 13.20$$

4. Note that in part (b) a trial-and-error solution is required.  
(Hint: The effluent temperature will be close to 700 K.)

- 2.17** P. B. Chinoy and P. D. Sunavala [*Ind. Eng. Chem. Res.*, **26**, 1340 (1987)] studied the kinetics and thermodynamics of the manufacture of  $C_2F_4$ , the monomer for the production of Teflon via pyrolysis of  $CHClF_2$ . A thermodynamic analysis of this reaction as it occurs in the presence of steam as a diluent/thermal moderator must take into account the following equilibria:



These researchers have indicated the following values of the equilibrium constants ( $K_p$ ) (for pressures in atm):

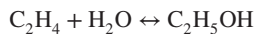
	700°C	900°C
$K_{p1}$	0.3353	23.3120
$K_{p2}$	0.03960	1.6810

Use these constants to determine the equilibrium yields and conversions obtained at these temperatures when the total pressure in the system is 1.2 atm. Consider both the case in which water is supplied at a 2 : 1 mole ratio with  $CHClF_2$  and the case in which the feed consists solely of  $CHClF_2$ . (There are thus four sets of conditions for which you are to calculate yields and conversions.)

1. Temperature = 700°C;  $H_2O/CHClF_2 = 0.0$ .
2. Temperature = 700°C;  $H_2O/CHClF_2 = 2.0$ .
3. Temperature = 900°C;  $H_2O/CHClF_2 = 0.0$ .
4. Temperature = 900°C;  $H_2O/CHClF_2 = 2.0$ .

The standard states of aggregation for the compounds indicated are the pure materials at the indicated temperatures and unit fugacity. Comment on the effects of temperature and diluent on the yield of the desired product.

- 2.18** Consider the reaction of ethylene and water to form ethanol:



If the reaction takes place at 254°C and 100 atm, determine the compositions of the liquid and vapor phases that coexist at equilibrium. You may assume that the reactants are present initially in equimolar quantities.

- (a) Calculate these compositions (mole fractions) based on  $K_a = 7.43 \times 10^{-3}$  for  $\Delta G^0$  referred to standard states of unit fugacity at 254°C for each species.
- (b) Calculate these compositions based on  $K_a = 6.00 \times 10^{-3}$  for  $\Delta G^0$  referred to a standard state of unit fugacity at 254°C for ethylene, and standard states of the pure liquids at 254°C for both water and ethanol.

In both parts (a) and (b) you may assume ideal solution behavior, but not ideal gas behavior. The Poynting

correction factor may be taken as unity. You may also employ the data tabulated below.

Species	$C_2H_4$	$H_2O$	$C_2H_5OH$
Vapor pressure at 254°C (atm)	$\infty$	42	76
$f/P$ at 254°C and total pressure	0.94	0.71	0.49
$f/P$ at 254°C and vapor pressure	—	0.86	0.59

- 2.19** The reaction between ethylene (E) and benzene (B) to form ethylbenzene (EB) is being studied in a tubular reactor packed with solid catalyst pellets. The reactor is operating adiabatically at steady state:



If the residence time is sufficiently long that the leaving gases are in equilibrium, determine the effluent temperature and composition for the case where the feed consists of 60 mol% benzene and 40 mol% ethylene at 500°C. The exit gases leave at a pressure of 4 atm. The data follow.

	Ethylene	Benzene	Ethylbenzene
Standard Gibbs free energy of formation at 25°C (kcal/mol)	16.282	30.989	31.208
Standard heat of combustion to gaseous $H_2O$ and $CO_2$ at 25 °C (kcal/mol)	-316.195	-757.52	-1048.53
Mean heat capacity ( $C_p$ ) over the temperature range of interest [cal/(mol·°C)]	20.5	45.9	68.3

Standard states are taken as the gases at unit fugacity. Ideal gas behavior may be assumed. Do not use any thermochemical data other than those given above. Remember to allow for the variation in the heat of reaction with temperature.

What would be the potential advantages and disadvantages of increasing the operating pressure to 8 atm or to 40 atm? You may again assume ideal gas behavior to determine effluent compositions and temperatures for these cases.

- 2.20** This problem is adapted from M. Modell and R. C. Reid, *Thermodynamics and Its Applications*, Prentice-Hall, Englewood Cliffs, NJ, 1974, with permission.

A dimerization reaction of type  $2A \leftrightarrow B$  is being studied in a continuous flow reactor at 200°C and 10.13 MPa. The reactor is sufficiently large that equilibrium is achieved at the exit to link the reactor to a low-pressure (101.3 kPa) thermal

conductivity meter. As the gas sample passes at steady state through this cracked sampling valve, it undergoes a decrease in temperature to 100°C. The conductivity reading corresponds to gas-phase mole fractions of A and B of 0.55 and 0.45, respectively. Determine the relationship between the composition of gases leaving the reactor at 200°C and 10.13 MPa and the composition corresponding to the reading of the conductivity cell. In particular, you should use the experimental data and the thermochemical properties listed below to:

- (a) Calculate the high pressure effluent composition corresponding to the measured composition of the sample at low pressure.

- (b) Assess whether or not the low-pressure gas sample is at, far from, or near chemical reaction equilibrium. (Provide quantitative evidence to support your position.)

At 200°C the standard enthalpy of reaction is 29.31 kJ/mol of species B formed. The heat capacities at constant pressure for species B and A are 58.62 and 29.31 J/(mol.K), respectively. Over the pressure and temperature range of interest, these heat capacities are independent of both temperature and pressure. The gaseous mixture may be treated as an ideal gas at all temperatures, pressures, and compositions. There are no heat losses from the sampling line or across the sampling valve.

## Basic Concepts in Chemical Kinetics: Determination of the Reaction Rate Expression

### 3.0 INTRODUCTION

Key concepts employed by chemists and chemical engineers in the acquisition, analysis, and interpretation of kinetic data are presented in this chapter. The focus is on determination of empirical rate expressions that can subsequently be utilized in the design of chemical reactors. To begin, we find it convenient to approach the concept of reaction rate by considering a closed isothermal constant pressure homogeneous system of uniform composition in which a single chemical reaction is taking place. In such a system the rate of the chemical reaction ( $r$ ) is defined as

$$r = \frac{1}{V} \frac{d\xi}{dt} \quad (3.0.1)$$

where  $V$  is the system volume,  $\xi$  the extent of reaction, and  $t$  is time. Several facts about this definition should be noted.

1. The rate is defined as an intensive variable. Note that the reciprocal of the system volume is outside the derivative term. This consideration is important in treating variable volume systems.
2. The definition is independent of any particular reactant or product species.
3. Because the reaction rate almost invariably changes with time, it is necessary to use the time derivative to express the instantaneous rate of reaction.

Many sets of units may be used to measure reaction rates. Because the extent of reaction is expressed in terms of moles, the reaction rate has the units of moles transformed per unit time per unit volume. The majority of the data reported in the literature are expressed in some

form of the metric system of units [e.g., mol/(L · s) or molecules/(cm<sup>3</sup> · s)].

Changes in the mole numbers  $n_i$  of the various species involved in a reaction are related to the extent of reaction by equation (1.1.4):

$$\xi = \frac{n_i - n_{i0}}{\nu_i} \quad (3.0.2)$$

Differentiation of this equation with respect to time and substitution in equation (3.0.1) gives

$$r = \frac{1}{\nu_i} \frac{1}{V} \frac{dn_i}{dt} \quad (3.0.3)$$

If one defines the rate of *increase* of the moles of species  $i$  as

$$r_i = \frac{1}{V} \frac{dn_i}{dt} \quad (3.0.4)$$

then

$$r_i = \nu_i r \quad (3.0.5)$$

Because the  $\nu_i$  are positive for products and negative for reactants, and because the reaction rate  $r$  is intrinsically positive, the various  $r_i$  will have the same sign as the corresponding  $\nu_i$ , and  $dn_i/dt$  will have the appropriate sign (i.e., positive for products and negative for reactants).

In the analysis of engineering systems, one frequently encounters systems whose properties vary from point to point within the system. Just as it is possible to define local temperatures, pressures, concentrations, and so on, it is possible to generalize equations (3.0.1) and (3.0.4) to define local reaction rates.

In constant volume systems it is convenient to employ the extent per unit volume:

$$\xi^* = \frac{\xi}{V} \quad (3.0.6)$$

and to identify the rate for such systems by using a subscript  $V$  on the symbol for the rate:

$$r_V = \frac{1}{V} \frac{d\xi}{dt} = \frac{d\xi^*}{dt} \quad (3.0.7)$$

In terms of molar concentrations,  $C_i = n_i/V$ , and equation (3.0.3) becomes

$$r_V = \frac{1}{v_i} \frac{dC_i}{dt} = \frac{r_{i,V}}{v_i} \quad (3.0.8)$$

The rate of reaction at constant volume is thus proportional to the time derivative of the molar concentration. However, it *should be emphasized that in general the rate of reaction is not equal to the time derivative of a concentration*. Moreover, omission of the  $1/v_i$  term frequently leads to errors in the analysis and use of kinetic data. When one substitutes the product of concentration and volume for  $n_i$  in equation (3.0.3), the essential difference between equations (3.0.3) and (3.0.8) becomes obvious:

$$r = \frac{1}{v_i} \frac{1}{V} \frac{d}{dt}(C_i V) = \frac{1}{v_i} \frac{dC_i}{dt} + \frac{C_i}{v_i V} \frac{dV}{dt} \quad (3.0.9)$$

In variable volume systems the  $dV/dt$  term is significant. Although equation (3.0.9) is a valid expression arrived at by legitimate mathematical operations, its use in the analysis of rate data is extremely limited because of the awkward nature of the equations to which it leads. Equation (3.0.1) is much easier to use.

Many reactions take place in heterogeneous systems rather than in a single homogeneous phase. These reactions often occur at the interface between the two phases. In such cases it is appropriate to define the reaction rate in terms of the interfacial area ( $S$ ) available for reaction.

$$r'' = \frac{1}{S} \frac{d\xi}{dt} \quad (3.0.10)$$

The double-prime superscript is used to emphasize the basis of unit surface area. In many cases, however, the interfacial area is not known, particularly when one is dealing with reactions involving more than a single fluid phase or solids. Consequently, the following definitions of the reaction rate are sometimes useful when dealing with solid catalysts:

$$r_m = \frac{1}{W} \frac{d\xi}{dt} \quad (3.0.11)$$

$$r''' = \frac{1}{V'} \frac{d\xi}{dt} \quad (3.0.12)$$

where  $W$  and  $V'$  are the weight and volume of the solid particles dispersed in a fluid phase. The subscript and superscript emphasize the definition employed. The choice of the definition of the rate to be used in any given situation is governed by convenience in use. The various forms of the definition are interrelated, and chemical engineers should be capable of switching from one form to another without excessive difficulty.

Many process variables can affect the rate at which reactants are converted to products. The conversion rate should be considered as a phenomenological property of the reaction system under the operating conditions specified. The nature of the dependence of a reaction rate on macroscopic or laboratory variables cannot be completely determined on an *a priori* basis. On the contrary, recourse to experimental data on the reaction of interest and on the relative rates of the physical and chemical processes involved is almost always necessary. Among the variables that can influence the reaction rate are the system temperature, pressure, and composition, the properties of a catalyst that may be present, and the system parameters that govern the various physical transport processes (i.e., the flow conditions, degree of mixing, and the heat and mass transfer parameters of the system). Since several of these variables may change from location to location within the reactor under consideration, knowledge of the relationships between these variables and the conversion rate is needed if one is to be able to integrate the appropriate material balance equations over the reactor volume. It is important to note that in many situations of practical engineering importance, *the rate of reaction observed is not identical with the intrinsic chemical reaction rate evaluated using the bulk fluid properties*. The rate observed in the laboratory reflects the effects of both chemical and physical rate processes. The intrinsic rate may be thought of as the conversion rate that would exist if all physical rate processes occurred at infinitely fast rates.

Situations in which both physical (e.g., mass transfer, diffusion, or heat transfer) and chemical rate processes influence the conversion rate are discussed in Chapter 12; the present chapter is concerned only with those situations for which the effects of physical rate processes are unimportant. This approach permits us to focus our concern on the variables that influence intrinsic chemical reaction rates (i.e., temperature, pressure, composition, and the presence or absence of catalysts in the system).

In reaction rate studies one's goal is a phenomenological description of a system in terms of a limited number of empirical constants. Such descriptions permit one to predict the time-dependent behavior of similar systems. In these studies the usual procedure is to try to isolate the effects of the different variables and to investigate each independently. For example, one encloses the reacting system in a thermostat to maintain it at a constant temperature.

Several generalizations can be made about the variables that influence reaction rates. Those that follow are in large measure adapted from Boudart's text (1).

1. The rate of a chemical reaction depends on the temperature, pressure, and composition of the system under investigation.
2. Certain species that do not appear in the stoichiometric equation for the reaction under study can markedly affect the reaction rate, even when they are present in only trace amounts. These materials are known as *catalysts* or *inhibitors*, depending on whether they increase or decrease the reaction rate.
3. At a constant temperature, the rate of reaction generally decreases monotonically with time or extent of reaction.
4. If one considers reactions that occur in systems that are far removed from equilibrium, the rate expressions can generally be written in the form

$$r = k\phi(C_i) \quad (3.0.13)$$

where  $\phi(C_i)$  is a function that depends on the concentrations ( $C_i$ ) of the various species present in the system (reactants, products, catalysts, and inhibitors). This function  $\phi(C_i)$  may also depend on the temperature. The coefficient  $k$  is called the *reaction rate constant*. It usually does not depend on the composition of the system and is consequently independent of time in an isothermal system.

5. The rate constant  $k$  generally varies with the absolute temperature  $T$  of the system according to the *law proposed by Arrhenius*:

$$k = Ae^{-E/RT} \quad (3.0.14)$$

where  $E$  is the apparent activation energy of the reaction,  $R$  the gas constant, and  $A$  the preexponential factor, sometimes called the *frequency factor*, which is usually assumed to be independent of temperature.

6. Very often the function  $\phi(C_i)$  in equation (3.0.13) is temperature independent and, to a high degree of approximation, can be written as

$$\phi(C_i) = \prod_i C_i^{\beta_i} \quad (3.0.15)$$

where the product  $\prod_i$  is taken over all components of the system. The exponents  $\beta_i$  are the *orders of the reaction with respect to each of the  $i$  species* present in the system. The algebraic sum of the exponents is called the *total order* or *overall order* of the reaction.

7. If one considers a system in which both forward and reverse reactions are important, the net rate of reaction

can generally be expressed as the difference between the rate in the forward direction  $\vec{r}$  and that in the reverse direction  $\overleftarrow{r}$ :

$$r = \vec{r} - \overleftarrow{r} \quad (3.0.16)$$

The rates of both the forward and reverse reactions can often be described by expressions of the form of equation (3.0.13).

### 3.0.1 Reaction Orders

The manner in which the reaction rate varies with the concentrations of the reactants and products is indicated by stating the order of the reaction. If equation (3.0.15) is written in more explicit form as

$$r = kC_A^{\beta_A} C_B^{\beta_B} C_C^{\beta_C} \dots \quad (3.0.17)$$

the reaction is said to be of  $\beta_A$ th order with respect to A,  $\beta_B$ th order with respect to B, and so on. The overall order of the reaction ( $m$ ) is simply

$$m = \beta_A + \beta_B + \beta_C + \dots \quad (3.0.18)$$

These exponents  $\beta_i$  may be small integers, fractions, or decimal values, and they may take on both positive and negative values as well as the value zero. In many cases these exponents are independent of temperature. In other cases where the experimental data have been forced to fit expressions of the form of equation (3.0.17), the exponents may vary with temperature. In these instances the correlation observed should be applied only in the restricted temperature interval for which data are available.

It must be emphasized that, in general, the individual orders of the reaction ( $\beta_i$ ) are *not necessarily related* to the corresponding stoichiometric coefficients  $v_i$ . *The individual  $\beta_i$  values are quantities that must be determined experimentally.* It is also important to recognize that by no means can all reactions be said to have an order. For example, the gas-phase reaction of  $H_2$  and  $Br_2$  to form  $HBr$  has a rate expression of the following form:

$$r = \frac{k(H_2)(Br_2)^{1/2}}{1 + [k'(HBr)/(Br_2)]} \quad (3.0.19)$$

where  $k$  and  $k'$  are constants at a given temperature and where the molecular species contained in parentheses refer to the concentrations of these species. This rate expression is discussed in more detail in Section 4.2.1.

When one reactant is present in very large excess, the amount of this material that can be consumed by reaction is negligible compared to the total amount present. Under these circumstances, its concentration may be regarded as remaining essentially constant throughout the course of the reaction, and the product of the reaction rate constant and

the concentration of this species raised to the appropriate order will also be constant. This product is then an apparent or empirical pseudo rate constant, and a corresponding pseudo reaction order can be determined from the resulting simplified form of the rate expression.

### 3.0.2 The Reaction Rate Constant

The term *reaction rate constant* is actually a misnomer, because  $k$  may vary with temperature, the solvent for the reaction, and the concentrations of any catalysts that may be present in the reaction system. The term is in universal use, however, because it implies that the parameter  $k$  is independent of the concentrations of reactant and product species.

The reaction rate is properly defined in terms of the time derivative of the extent of reaction [equation (3.0.1)]. One *must* define  $k$  in a similar fashion to ensure uniqueness. Definitions of  $k$  in terms of the various  $r_i$  would lead to rate constants that would differ by the ratios of their stoichiometric coefficients. The units of the rate constant will vary depending on the overall order of the reaction. These units are those of a rate divided by an  $m$ th power of concentration (where  $m$  is the overall order of the rate law). Thus, from examination of equations (3.0.17) and (3.0.18),

$$(k) = \frac{(r)}{(C)^m} = \frac{\text{mol}/(\text{volume} \cdot \text{time})}{(\text{mol}/\text{volume})^m} \quad (3.0.20)$$

or

$$(k) = \text{time}^{-1}(\text{mol}/\text{volume})^{-m+1} \quad (3.0.21)$$

For a first-order reaction, the units of  $k$  are  $\text{time}^{-1}$ ; for the second-order case, typical units are  $\text{m}^3/(\text{mol} \cdot \text{s})$ .

## 3.1 MATHEMATICAL CHARACTERIZATION OF SIMPLE REACTION SYSTEMS

Although the reaction rate function can take on a variety of mathematical forms and the reaction orders that one observes in the laboratory are not necessarily positive integers, a surprisingly large number of reactions have an overall order that is a positive integer. In this section we treat the mathematical forms that the integrated rate expression will take for several simple cases. The discussion is restricted to *irreversible reactions* carried out *isothermally*. The resulting equations provide a useful framework for subsequent analysis of the experimental results obtained in batch reactors. We start by treating constant-volume systems that lead to closed-form solutions and then proceed to the complications present in variable-volume systems. We have chosen to place a “V” to the right of certain equation numbers in this section to emphasize to the reader

that these equations are not general but are restricted to constant volume systems. The use of  $\xi^*$ , the extent of reaction per unit volume in a constant volume system, will also emphasize this restriction.

### 3.1.1 Mathematical Characterization of Simple Constant Volume Reaction Systems

#### 3.1.1.1 First-Order Reactions in Constant Volume Systems

For a first-order reaction the rate is proportional to the first power of the concentration of one of the reacting substances:

$$r = kC_A \quad (3.1.1)$$

For a constant volume system,

$$C_A = C_{A0} + \nu_A \xi^* \quad (3.1.2) V$$

Combination of this equation with equations (3.0.7) and (3.1.1) gives

$$\frac{d\xi^*}{dt} = k(C_{A0} + \nu_A \xi^*) \quad (3.1.3) V$$

Separation of variables and integration recognizing that  $\xi^* = 0$  at  $t = 0$  gives

$$\frac{1}{\nu_A} \ln\left(\frac{C_{A0} + \nu_A \xi^*}{C_{A0}}\right) = kt \quad (3.1.4) V$$

Thus,

$$\xi^* = \frac{C_{A0}}{\nu_A} (e^{\nu_A kt} - 1) \quad (3.1.5) V$$

The species concentrations at various times can now be determined from the reaction stoichiometry:

$$C_i = C_{i0} + \nu_i \xi^* = C_{i0} + \frac{\nu_i}{\nu_A} C_{A0} (e^{\nu_A kt} - 1) \quad (3.1.6) V$$

If one is interested in the time dependence of the concentration of species A and if the stoichiometric coefficient of A is equal to  $-1$ , this relation becomes

$$C_A = C_{A0} e^{-kt} \quad (3.1.7) V$$

or

$$\ln\left(\frac{C_A}{C_{A0}}\right) = -kt \quad (3.1.8) V$$

In graphical form, the preceding two equations imply that for first-order reactions, plots of  $\ln C_A$  versus time will be linear with a slope equal to  $-k$  and an intercept equal to  $\ln C_{A0}$ . Because this type of plot is linear, it is frequently used in testing experimental data to ascertain if a reaction obeys a first-order rate law.

A great many reactions follow first-order kinetics or pseudo first-order kinetics over certain ranges of experimental conditions. Among these are many pyrolysis reactions, the cracking of butane, the decomposition of nitrogen pentoxide ( $\text{N}_2\text{O}_5$ ), and radioactive decay processes.

### 3.1.1.2 Second-Order Reactions in Constant Volume Systems

There are two primary classes of second-order reactions. For the first the rate is proportional to the square of the concentration of a single reacting species; for the second the rate is proportional to the product of the concentrations of two different species.

$$\text{Class I: } r = kC_A^2 \quad (3.1.9)$$

$$\text{Class II: } r = kC_A C_B \quad (3.1.10)$$

For class I second-order rate expressions, combination of equations (3.0.7), (3.1.2), and (3.1.9) gives

$$\frac{d\xi^*}{dt} = k(C_{A0} + \nu_A \xi^*)^2 \quad (3.1.11) \text{ V}$$

Integration of this equation subject to the initial condition that  $\xi^* = 0$  at  $t = 0$  gives

$$-\frac{1}{\nu_A} \left( \frac{1}{C_{A0} + \nu_A \xi^*} - \frac{1}{C_{A0}} \right) = kt \quad (3.1.12) \text{ V}$$

or

$$\frac{1}{C_A} - \frac{1}{C_{A0}} = -\nu_A kt \quad (3.1.13) \text{ V}$$

The concentrations of the various species can then be determined by solving equation (3.1.12) for  $\xi^*$  and employing basic stoichiometric relations:

$$C_i = C_{i0} + \nu_i \xi^* = C_{i0} + \frac{\nu_i k C_{A0}^2 t}{1 - \nu_A k C_{A0} t} \quad (3.1.14) \text{ V}$$

If  $\nu_A$  is equal to  $-1$ , equation (3.1.13) becomes

$$\frac{1}{C_A} - \frac{1}{C_{A0}} = kt \quad (3.1.15) \text{ V}$$

In testing experimental data to see if they are consistent with this type of rate expression, one often plots  $1/C_A$  versus  $t$ . If the data fall on a straight line, the rate expression is of the form of equation (3.1.9), and the slope and intercept of the line are equal to  $-\nu_A k$  and  $1/C_{A0}$ , respectively.

Many second-order reactions follow class I rate expressions. Among these are the gas-phase thermal decomposition of hydrogen iodide ( $2\text{HI} \rightarrow \text{H}_2 + \text{I}_2$ ), dimerization of cyclopentadiene ( $2\text{C}_5\text{H}_6 \rightarrow \text{C}_{10}\text{H}_{12}$ ), and the gas-phase thermal decomposition of nitrogen dioxide ( $2\text{NO}_2 \rightarrow 2\text{NO} + \text{O}_2$ ).

For class II second-order rate expressions of the form of equation (3.1.10), the rate can be expressed in terms of the extent of reaction per unit volume as

$$r_v = \frac{d\xi^*}{dt} = k(C_{A0} + \nu_A \xi^*)(C_{B0} + \nu_B \xi^*) \quad (3.1.16) \text{ V}$$

When the stoichiometric coefficients of species A and B are identical and when one starts with equal concentrations of these species, the class II rate expression will collapse to the class I form because, under these conditions, one can always say that  $C_A = C_B$ . Separation of variables and integration of equation (3.1.16) leads to the following relation:

$$\ln \left[ \frac{(C_{B0} + \nu_B \xi^*) (C_{A0})}{(C_{A0} + \nu_A \xi^*) (C_{B0})} \right] = (C_{A0} \nu_B - C_{B0} \nu_A) kt \quad (3.1.17) \text{ V}$$

or

$$\xi^* = \frac{C_{A0} \{1 - \exp[(C_{A0} \nu_B - C_{B0} \nu_A) kt]\}}{\nu_A \exp[(C_{A0} \nu_B - C_{B0} \nu_A) kt] - \nu_B (C_{A0}/C_{B0})} \quad (3.1.18) \text{ V}$$

Because two of the terms in the left-hand term in equation (3.1.17) are the residual reactant concentrations at time  $t$  or extent per unit volume  $\xi^*$ , it is often useful to rewrite this equation as

$$\ln \left( \frac{C_B}{C_A} \frac{C_{A0}}{C_{B0}} \right) = (C_{A0} \nu_B - C_{B0} \nu_A) kt \quad (3.1.19) \text{ V}$$

or

$$\ln \left( \frac{C_B}{C_A} \right) + \ln \left( \frac{C_{A0}}{C_{B0}} \right) = (C_{A0} \nu_B - C_{B0} \nu_A) kt \quad (3.1.20) \text{ V}$$

These equations are convenient for use in determining if experimental rate data follow class II second-order kinetics in that they predict a linear relationship between  $\ln(C_B/C_A)$  and time. The  $y$  intercept is  $\ln(C_{B0}/C_{A0})$  and the slope is equal to  $(C_{A0} \nu_B - C_{B0} \nu_A)k$ .

Class II second-order rate expressions are one of the forms most commonly encountered in the laboratory. They include the gas phase reaction of molecular hydrogen and iodine ( $\text{H}_2 + \text{I}_2 \rightarrow 2\text{HI}$ ), the reactions of free radicals with molecules (e.g.,  $\text{H} + \text{Br}_2 \rightarrow \text{HBr} + \text{Br}$ ), and the hydrolysis of organic esters in nonaqueous media.

### 3.1.1.3 Third-Order Reactions in Constant Volume Systems

Third-order reactions can be classified into three primary types, according to the general definition:

$$\text{Class I: } r = kC_A^3 \quad (3.1.21)$$

$$\text{Class II: } r = kC_A^2 C_B \quad (3.1.22)$$

$$\text{Class III: } r = kC_A C_B C_Q \quad (3.1.23)$$

If one employs reactants in precisely stoichiometric proportions, the class II and class III rate expressions will reduce to the mathematical form of the class I rate function. Because the mathematical principles employed in deriving the relations between the extent of reaction per unit volume (or the concentrations of the various species) and time are similar to those used in Sections 3.1.1.1 and 3.1.1.2, we list only the most interesting results for third-order reactions.

*Class I third-order rate expression:*

$$\frac{1}{C_A^2} - \frac{1}{C_{A0}^2} = -2\nu_A kt \quad (3.1.24) \text{ V}$$

and

$$\xi^* = \frac{C_{A0}}{\nu_A} \left( \frac{1}{\sqrt{1 - 2\nu_A k C_{A0}^2 t}} - 1 \right) \quad (3.1.25) \text{ V}$$

*Class II third-order rate expression:*

$$\begin{aligned} \frac{1}{C_A} - \frac{1}{C_{A0}} + \frac{1}{C_{A0} - C_{B0}(\nu_A/\nu_B)} \ln \left( \frac{C_B C_{A0}}{C_A C_{B0}} \right) \\ = (C_{A0} \nu_B - C_{B0} \nu_A) kt \end{aligned} \quad (3.1.26) \text{ V}$$

In this case one obtains an expression for  $\xi^*$  that cannot be manipulated to yield a simple algebraic form. However, if the concentration of one species is known as a function of time, the concentrations of all other species may be determined from the definition of the extent of reaction per unit volume, that is,

$$\xi^* = \frac{C_i - C_{i0}}{\nu_i} = \frac{C_j - C_{j0}}{\nu_j} \quad (3.1.27) \text{ V}$$

Hence,

$$C_j = C_{j0} + \frac{\nu_j}{\nu_i} (C_i - C_{i0}) \quad (3.1.28) \text{ V}$$

*Class III third-order rate expression:*

$$\begin{aligned} & \nu_A (\nu_Q C_{B0} - \nu_B C_{Q0}) \ln \left( \frac{C_A}{C_{A0}} \right) \\ & + \nu_B (\nu_A C_{Q0} - \nu_Q C_{A0}) \ln \left( \frac{C_B}{C_{B0}} \right) \\ & + \nu_Q (\nu_B C_{A0} - \nu_A C_{B0}) \ln \left( \frac{C_Q}{C_{Q0}} \right) \\ = & kt (\nu_A C_{B0} - \nu_B C_{A0}) (\nu_A C_{Q0} - \nu_Q C_{A0}) \times \\ & (\nu_Q C_{B0} - \nu_B C_{Q0}) \end{aligned} \quad (3.1.29) \text{ V}$$

This equation has extremely limited utility and is presented more as a subject of academic interest than of practical instruction.

Gas-phase third-order reactions are rarely encountered in engineering practice. Perhaps the best-known examples

of third-order reactions are atomic recombination reactions in the presence of a third body in the gas phase and the reactions of nitric oxide with chlorine and oxygen:  $(2\text{NO} + \text{Cl}_2 \rightarrow 2\text{NOCl}; 2\text{NO} + \text{O}_2 \rightarrow 2\text{NO}_2)$ .

### 3.1.1.4 Fractional and Other Order Reactions in Constant Volume Systems

In chemical kinetics, one frequently encounters reactions whose orders are not integers. Consider a reaction involving only a single reactant A whose rate expression is of the form

$$\frac{d\xi^*}{dt} = k C_A^n = k(C_{A0} + \nu_A \xi^*)^n \quad (3.1.30) \text{ V}$$

Systems composed of stoichiometric proportions of reactants also have rate expressions that will often degenerate to the form above. Except for the case where  $n$  is unity, equation (3.1.30) can be integrated to give

$$\frac{1}{(C_{A0} + \nu_A \xi^*)^{n-1}} - \frac{1}{C_{A0}^{n-1}} = (1-n)\nu_A kt \quad (3.1.31) \text{ V}$$

or

$$\frac{1}{C_A^{n-1}} - \frac{1}{C_{A0}^{n-1}} = (1-n)\nu_A kt \quad (3.1.32) \text{ V}$$

Among the reactions whose orders are not integers are the pyrolysis of acetaldehyde ( $n = \frac{3}{2}$ ) and the formation of phosgene from CO and Cl<sub>2</sub>  $\left[ r = k(\text{Cl}_2)^{\frac{3}{2}}(\text{CO}) \right]$ .

### 3.1.2 Mathematical Characterization of Simple Variable Volume Reaction Systems

From the viewpoint of an engineer who must design commercial reactors to carry out gaseous reactions involving changes in the total number of moles present in the system, it is important to recognize that such reactions may be accompanied by changes in the specific volume of the system, especially if the reaction takes place in a continuous flow tubular reactor operating at substantially constant pressure. For gas phase reactions in which there is a significant difference in the number of moles of reactants and products, one must employ the basic definition of the reaction rate given by equation (3.0.1):

$$r = \frac{1}{V} \frac{d\xi}{dt} \quad (3.0.1)$$

Unfortunately, when one combines this relation with the rate expressions for various reaction orders, the situation is entirely different from that which prevails in the constant-volume case. One cannot develop explicit closed-form expressions for the extent of reaction as a function of

time for all the cases treated in Section 3.1.1. The most useful case for which one can develop such a solution is a first-order reaction. Since

$$C_A = \frac{n_A}{V} = \frac{n_{A0} + \nu_A \xi}{V} \quad (3.1.33)$$

the first-order rate expression becomes

$$\frac{1}{V} \frac{d\xi}{dt} = k \frac{n_{A0} + \nu_A \xi}{V} \quad (3.1.34)$$

Solution of this equation subject to the condition that  $\xi = 0$  at  $t = 0$  gives

$$\nu_A k t = \ln\left(\frac{n_{A0} + \nu_A \xi}{n_{A0}}\right) = \ln\left(\frac{n_A}{n_{A0}}\right) \quad (3.1.35)$$

or

$$\xi = \left(\frac{n_{A0}}{\nu_A}\right) (e^{\nu_A k t} - 1) \quad (3.1.36)$$

For reaction orders other than unity, one must treat the various reactions on an individual basis and be able to express the total volume of the mixture as a function of the composition, temperature, and pressure of the system. If one is interested in gas-phase reactions that occur at constant pressure and temperature, one can say that

$$V = V(n_1, n_2, \dots) \equiv V(n_j) \quad (3.1.37)$$

If the functional form of this relation is known (e.g., if one is dealing with a gaseous system that behaves ideally or whose equation of state is known), this relationship can be combined with equation (3.0.1) and the rate expression to obtain a differential equation, which can then be integrated numerically or in explicit form. Consider a generalized rate expression of the form

$$r = k \prod_i C_i^{\beta_i} = k C_1^{\beta_1} C_2^{\beta_2} C_3^{\beta_3} \dots \quad (3.1.38)$$

where  $i$  represents the number of species of interest.

Combination of this relation with equation (3.0.1) leads to

$$\frac{1}{V(n_j)} \frac{d\xi}{dt} = k \prod_i \left[ \frac{n_i}{V(n_j)} \right]^{\beta_i} \quad (3.1.39)$$

The various mole numbers at any time ( $n_j$ ) can be expressed in terms of the extent of reaction and the initial mole numbers. If the functional form of  $V$  is known (i.e., one has an equation of state), one obtains a differential equation that can be integrated even if it is necessary to resort to numerical methods to do so.

In the analysis of experimental rate data taken in variable volume systems, it is possible to develop another expression for the rate of formation of species  $i$  that

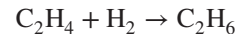
is more convenient to use than equation (3.1.39). This alternative approach has been popularized by Levenspiel (2). It involves the use of fraction conversion rather than extent of reaction or concentration as a primary variable and is applicable only to systems in which the volume varies linearly with the fraction conversion:

$$V = V_0(1 + \delta_A f_A) \quad (3.1.40)$$

The fraction conversion is based on the limiting reagent, in this case assumed to be species A. The parameter  $\delta_A$  is the fraction change in the volume of a closed reacting system between zero conversion and complete conversion. As such, it may take on both positive and negative values as well as the value zero. Hence,

$$\delta_A = \frac{V(\text{at } f_A = 1) - V(\text{at } f_A = 0)}{V(\text{at } f_A = 0)} \quad (3.1.41)$$

The parameter  $\delta_A$  takes into account not only the stoichiometry of the reaction, but also the presence of inert, the use of nonstoichiometric quantities of reactants, and the presence of one or more of the reaction products in the original system. To illustrate this point, consider as an example the isothermal gas phase hydrogenation of ethylene:



taking place at constant pressure under conditions such that deviations from the ideal gas law are negligible. The total volume of the system is then given by

$$V = n_{\text{total}} \frac{RT}{P} \quad (3.1.42)$$

Thus

$$\delta_A = \frac{[n_{\text{total}}(\text{at } f_A = 1) - n_{\text{total}}(\text{at } f_A = 0)](RT/P)}{n_{\text{total}}(\text{at } f_A = 0)(RT/P)} = \frac{n_{\text{total}}(\text{at } f_A = 1) - n_{\text{total}}(\text{at } f_A = 0)}{n_{\text{total}}(\text{at } f_A = 0)} \quad (3.1.43)$$

If one starts with a mixture consisting of 2 mol of hydrogen, 4 mol of ethylene, and 3 mol of inert gases, the following mole table may be created.

	Moles	
	At $f_A = 0$	At $f_A = 1$
$\text{H}_2$	2	0
$\text{C}_2\text{H}_4$	4	2
$\text{C}_2\text{H}_6$	0	2
Inerts	3	3
Total	9	7

In this case hydrogen is the limiting reagent and equation (3.1.43) gives

$$\delta_A = \frac{7 - 9}{9} = -\frac{2}{9}$$

If 2 mol of ethane was also present in the original mixture, the value of  $\delta_A$  becomes  $-2/11$ . The reader should verify this point.

If one is dealing with a gaseous system in which deviations from ideality are negligible, one may also take variations in the absolute temperature and the absolute pressure into account by a slight modification of equations (3.1.40) and (3.1.41). In such situations,

$$V = V_0(1 + \delta_A f_A) \frac{T}{T_0} \frac{P_0}{P} \quad (3.1.44)$$

with

$$\delta_A = \frac{V_{f_A=1, T=T_0, P=P_0} - V_{f_A=0, T=T_0, P=P_0}}{V_{f_A=0, T=T_0, P=P_0}} \quad (3.1.45)$$

where the temperature  $T$  and pressure  $P$  correspond to a given fraction conversion  $f_A$ . To determine the concentration of the limiting reagent at a given fraction conversion, one need only note that

$$n_A = n_{A0}(1 - f_A) \quad (3.1.46)$$

and that at constant temperature and pressure,

$$C_A = \frac{n_A}{V} = \frac{n_{A0}(1 - f_A)}{V_0(1 + \delta_A f_A)} = C_{A0} \left( \frac{1 - f_A}{1 + \delta_A f_A} \right) \quad (3.1.47)$$

The concentrations of the other species present in the reaction mixture may be found by using the concept of extent of reaction. From equation (1.1.9),

$$\xi = \frac{-n_{A0}f_A}{\nu_A} \quad (3.1.48)$$

Thus,

$$n_i = n_{i0} + \nu_i \xi = n_{i0} - \frac{\nu_i n_{A0} f_A}{\nu_A} \quad (3.1.49)$$

The concentration of species  $i$  is then given by

$$C_i = \frac{n_i}{V} = \frac{n_{i0} - (\nu_i/\nu_A)n_{A0}f_A}{V_0(1 + \delta_A f_A)} \quad (3.1.50)$$

Equations (3.1.47) and (3.1.50) express the relations between gas phase concentrations and the fraction conversion for variable volume systems that satisfy the linearity assumption of equation (3.1.40). This assumption is a reasonably unrestrictive one that is valid for all practical purposes in isothermal constant pressure systems in which one need not be concerned with consecutive reactions. The assumption is also valid for many nonisothermal condensed phase systems. For nonisothermal or variable pressure *gaseous systems*, a modification of the form of equation (3.1.44) is more appropriate for use.

To develop expressions for the reaction rate in variable-volume systems, one need only return to the fundamental definition of the reaction rate (3.0.1) and combine this relation with equations (3.1.40) and (3.1.48):

$$r = \frac{1}{V} \frac{d\xi}{dt} = \frac{1}{V_0(1 + \delta_A f_A)} \left( -\frac{n_{A0}}{\nu_A} \frac{df_A}{dt} \right) = -\left( \frac{C_{A0}}{1 + \delta_A f_A} \right) \frac{1}{\nu_A} \frac{df_A}{dt} \quad (3.1.51)$$

For variable-volume systems, equation (3.1.51) is much simpler in form and easier to use than equation (3.0.9):

$$r = \frac{1}{\nu_i} \frac{dC_i}{dt} + \frac{C_i}{\nu_i V} \frac{dV}{dt} \quad (3.0.9)$$

The  $\delta_A$  concept will prove to be particularly useful in the design of tubular reactors for gas-phase reactions.

## 3.2 EXPERIMENTAL ASPECTS OF KINETIC STUDIES

The chief significance of reaction rate expressions is that they provide a useful framework for the interpretation and evaluation of experimental kinetic data. In this section we indicate how a chemical engineer can interpret laboratory scale kinetic data in terms of such expressions. Emphasis is placed on the problems involved in the evaluation and interpretation of kinetic data, especially data obtained using a constant volume batch reactor.

One should be very careful to distinguish between the problem of determining the reaction rate expression and the problem of determining the mechanism of this reaction. The latter involves determination of the exact sequence of molecular processes involved in the reaction. It is by far the more difficult problem. From the viewpoint of a chemical engineer, who is interested in the design of commercial-scale reactors, a knowledge of the reaction mechanism is useful but not essential. Such individuals are more concerned with the problem of determining reaction rate expressions for use in design calculations. Since the rate expression must be determined experimentally, we now turn our attention to some of the points to be considered in obtaining kinetic data.

### 3.2.1 Preliminary Questions to Be Answered in Experimental Kinetics Studies

Because the proper design of chemical reactors requires a knowledge of the reaction rate expression for the system under consideration, it is essential that chemical engineers understand thoroughly the methods by which these empirical functions are determined. One should be

extremely careful in experimental work to obtain a valid rate expression by taking appropriate precautions in the laboratory and in the interpretation of the data. Since many kinetic data in the literature are in error in one important respect or another, and since many experienced chemists and chemical engineers have erred in carrying out kinetics experiments, it is crucial for the beginning student to be aware of some of the potential pitfalls. The sections that follow treat several aspects of kinetics experimentation that must be considered if one is to obtain meaningful data. The discussion extends the analysis by Bunnett (3) described in *Technique of Organic Chemistry*.

### 3.2.1.1 Is the Reaction Under Study Properly Identified?

It may seem ridiculous to ask the experimenter whether the reaction whose kinetics are being studied is actually the reaction that he or she thinks it is. Nonetheless, the literature contains many examples of the incorrect identification of reactions. One cannot always reason that the products of a reaction are the corresponding analogs of a well-characterized reaction. Even though the reaction under investigation may be reported in textbooks, isolation and identification of the products should be carried out *with the products of the reaction run under the conditions of the rate measurement*. Errors exist in the literature, and one may have components present in his or her system that may promote side reactions and/or inhibit the reaction that one thinks is being studied.

### 3.2.1.2 Are Side Reactions Important? What Is the Stoichiometry of the Reaction?

When a mixture of various species is present in a reaction vessel, one often has to worry about the possibility that several reactions, not just a single reaction, may occur. If one is trying to study one particular reaction, side reactions may complicate both chemical analysis of the reaction mixture and mathematical analysis of the raw data. The stoichiometry of the reaction involved and the relative importance of the side reactions must be determined by qualitative and quantitative analyses of the products of the reaction at various times. If one is to observe the growth and decay of intermediate products in consecutive reactions, measurements must be made on the reaction system before the reaction goes to completion.

### 3.2.1.3 Are the Conditions of the Experiment Properly Specified?

All kineticists should recognize the importance in experimental work of using pure materials, of controlling and measuring temperatures accurately, and of recording

times properly. Nonetheless, it is common for individuals to “save time” by using reactants or solvents that are not properly purified. The first tendency of the chemist involved in experimental kinetics work might well be to say that one should purify the reagents and solvents as much as possible. On the other hand, the first tendency of a practicing engineer would be to use a minimum of purification procedures, particularly if the ultimate goal is to design a commercial-scale reactor that will use a relatively impure feedstock. In practice, what one does is to accept reagents and solvents at a certain degree of purification as being conditionally satisfactory subject to the reservation that preliminary experiments might indicate the need for further purification. These preliminary experiments may also indicate that the chemical engineer will have to allow for purification of the feedstock in the design of the corresponding commercial scale facility.

The reason for stressing the importance of working with relatively pure reagents and solvents is that the rates of many reactions are extremely sensitive to the presence of trace impurities in the reaction system. If there is reason to suspect the presence of these effects, a series of systematic experiments may be carried out to explore the question by seeing how the reaction rate is affected by the intentional addition of particular impurities. In many cases, lack of reproducibility between experiments may be an indication that trace impurity effects are present.

Temperature control for most reactions in solution can be provided by immersion of the reactor in a liquid constant temperature bath that can be controlled to  $\pm 0.1^\circ\text{C}$  or better, depending on the degree of control desired. For gas phase reactions, particularly those that occur at high temperatures, the reactor can be immersed in a fluidized sand bath. The fact that these thermostatted baths can be held at a constant temperature for prolonged periods of time may lead to such a sense of complacency on the part of the experimenter that he or she fails to record the temperature at periodic intervals. One of the laws of experimental work (“If anything can go wrong, it will.”) dictates that the investigator adhere to a strict timetable for recording the system temperature. When kinetic data from different laboratories disagree, the failure to calibrate temperatures properly is often at fault. Consequently, it is wise to periodically calibrate the device used to record the bath temperature.

Although some precautions must be observed in timing a reaction, the direct measurement of time seldom affects the accuracy of a rate determination. The time required for sampling, for initiating, or for quenching a reaction is likely to introduce larger uncertainties in the rate measurement than is inherent in the performance of a good timer. One generally determines the value of the reaction rate constant by plotting some function of the instantaneous concentrations versus time and determining the slope of the straight

line that results. Since this slope is determined by differences between the time points and not by their absolute values, it is not essential in most cases to know these absolute values of time. However, a word of caution is appropriate when one is concerned with the analysis of consecutive reactions. In such cases, knowledge of the true zero of time is required (see Section 5.3).

### 3.2.1.4 Does the Analytical Method Properly Represent the Extent of Reaction?

One should test the analytical procedure by analyzing mixtures of known compositions that are similar to those expected for samples from the reaction vessel. Even if this test gives an excellent check, one must still face the possibility that the primary reaction under investigation may be accompanied by unexpected side reactions that consume reactants or produce products in such a way as to distort the meaning of the analytical results. One general approach that provides a measure of protection against being misled by analytical information is to follow the progress of a reaction by two or more different and independent analytical methods. Where possible, each of these methods should involve analysis for a different species.

### 3.2.1.5 Is the Experiment Planned Properly to Provide Significant Data?

One cannot measure a reaction rate directly. One is restricted to measurements of the concentrations of various species or of a physical property of the system as a function of time. Thus, one must plan the experiments so as to obtain significant differences in the quantities that are observed in the laboratory. In a properly planned experiment the kineticist chooses experimental techniques that provide differences between successive samples that are much larger than the expected uncertainty in the measurement. This procedure permits the kineticist to derive a meaningful rate expression from the original measurements.

One decision that the kineticist must make in planning experiments is the number of observations to be made during a run and the times at which these observations are to be made. One usually tries to work up the data in a form such that a plot of some function of the concentrations in the reaction vessel versus time gives a straight line, or such that it is readily amenable to conventional methods of statistical analysis. In the former case the rate constant is obtained using the slope of the straight line. The question then becomes: How many points does it take to establish the linearity and slope of the line? Two points are adequate to determine a straight line, but they are not sufficient to establish linearity of data. Any number of curved lines could be drawn through two points. Various functional

forms  $\phi(C_i)$  corresponding to different reaction orders could be used as the ordinate in these plots, and one could not distinguish between them on the basis of two experimental points. The straight line joining these points will not give any indication of whether or not other experimental points would lie on the same straight line. Moreover, this approach to determining a rate constant cannot reveal any of the experimental defects or complications that are often called to one's attention by curved or scattered plots. If one has three or four completely accurate points, an adequate test of the linearity of the assumed concentration function could be made. However, one cannot be sure whether departures from linearity are the result of scatter of the data, of a slowly curving function, or of some combination of these circumstances. When one recognizes further that one or two points in a set of data may be in error as a result of an experimental mishap and that these points may deviate substantially from the line established by the rest of the data, one comes to the conclusion that it is desirable to have at least eight to 10 data points per run, including points at low, intermediate, and high conversions. Such numbers are usually adequate to allow curvature to be distinguished from linearity, even when one needs to reject one or two points because of scatter of the data. We should note further that even though it is possible to employ a variety of standard statistical methods for purposes of fitting various mathematical models (rate expressions) to experimental data, it is nonetheless useful in interpreting the results to employ plots of the data in assessing the quality of the fit, determining outlying points, and evaluating what additional experiments might be most informative.

### 3.2.1.6 Are the Data Reproducible?

If experimental results are to be accepted as meaningful by the scientific community, they must be capable of being reproduced by investigators in other laboratories as well as by the original investigator. Individuals should assure this reproducibility by replicating the experiment.

There are several sources of irreproducibility in kinetics experimentation, but two of the most common are individual error and unsuspected contamination of the materials or reaction vessel used in the experiments. A person may use the wrong reagent, record an instrument reading improperly, make a manipulative error in the use of the apparatus, or plot a point incorrectly on a graph. Any of these mistakes can lead to an erroneous rate constant. The probability of repeating the same error in two successive *independent* experiments is small. Consequently, every effort should be made to make sure that the runs are truly independent, by starting with fresh samples, weighing these out individually, and so on. Since trace impurity effects also have a tendency to be time-variable, it is wise to check for reproducibility, not only between runs over

short time spans but also between runs performed weeks or months apart.

It is commendable experimental procedure to repeat each run in duplicate and to be satisfied if the two results agree, but this is expensive in terms of the labor costs involved. Moreover, precise replication of each trial is not always necessary. For example, if one is studying the effect on the reaction rate of a variable such as temperature or reactant concentration, a series of experiments in which the parameter under investigation is varied systematically may be planned. If a plot of the results versus this parameter yields a smooth curve, one generally assumes that the reproducibility of the data is satisfactory.

In addition to worrying about the reproducibility of the data, one should also take care to ensure that the calculations are reproducible in an independent calculation by a colleague. The literature contains numerous values of mis-calculated rate constants. One has the usual problem of conversion of units and the problem of conversion from natural logarithms to common logarithms. Thus, even though one's raw data might be highly accurate, the results calculated may be off by a large multiple. If a colleague uses the raw data, determines the rate constant for a particular experimental run with reference only to first principles, and obtains the same rate constant as that of the original investigator, one has a good indication that a systematic error in calculations has not been made.

## 3.2.2 Experimental Techniques and Apparatus

To determine reaction rate constants and reaction orders, individuals must determine reactant or product concentrations at known times and control the environmental conditions (i.e., temperature, homogeneity, pH, etc.) during the course of the reaction. The experimental techniques that have been used in kinetics studies to accomplish these measurements are many and varied, and an extensive treatment of these techniques is far beyond the intended scope of this book. It is nonetheless instructive to consider some experimental techniques that are in general use. More detailed treatments of the subject may be found in the literature.

### 3.2.2.1 General Reactor Types

In planning experiments the chemist is most apt to think in terms of closed systems and has traditionally used some form of batch reactor. The chemical engineer, on the other hand, is accustomed to dealing with open systems and the eventual design of large scale continuous processes. Consequently, the chemical engineer will often choose some form of flow reactor for laboratory scale investigations. The discussion in this chapter is restricted to batch reactors, but the relations developed in Chapter 8 may be used to analyze kinetic data obtained using continuous flow reactors.

### 3.2.2.2 Methods of Following the Course of a Reaction

A general direct method of measuring the *rate* of a reaction does not exist. One can only determine the amount of one or more product or reactant species present at a certain time in the system under observation. If the composition of the system is known at a particular time, it is sufficient to know the amount of a single species involved in the reaction as a function of time in order to be able to establish the complete system composition at any other time. This statement is true of any system whose reaction can be characterized by a single reaction progress variable,  $\xi$  or  $f_A$ . In practice, it is always wise where possible to analyze occasionally for one or more other species, to check for unexpected errors, losses of material, or the presence of side reactions.

In more complex cases when several reactions are occurring simultaneously in the system under observation, calculations of the composition of the system as a function of time will require knowledge of a number of independent composition variables equal to the number of independent chemical equations used to characterize the reactions involved. In principle, one can use any of the many tools and methods of the analytical chemist in carrying out these determinations. In practice, analytical methods are chosen on the basis of their specificity, accuracy, ease of use, and rapidity of measurement. For purposes of discussion, these methods may be classified into two groups: physical and chemical. Regardless of the method chosen, however, it must meet the following criteria:

1. It must not disturb the system under investigation by affecting the kinetic processes occurring therein.
2. The measurement should be representative of the system at the time it is made or at the time the sample analyzed was taken.
3. The method must provide a true measure of the extent of reaction.

In the choice of an analytical technique for following the course of a reaction, it is important to recognize that no aspect of the measurement should affect the kinetic processes occurring in the system. For example, use of electrical conductivity measurements for monitoring the progress of a reaction in liquid solution should not involve the use of platinized electrodes if this reaction is catalyzed by platinum.

Perhaps the most obvious method of studying reaction rates is to withdraw samples from the system periodically and subject them to chemical analysis. When the sample is withdrawn, however, one is immediately faced with a problem. The reaction may continue to proceed in the sample. Since the analysis will require a certain amount of time, regardless of the technique used, it is evident that if one is

to obtain a true measurement of the system composition at the time the sample was taken, the reaction must somehow be quenched or extinguished at the moment the sample is taken. The quenching process may involve rapid cooling to effectively stop the reaction, or it may consist of elimination of one of the reactants. In the latter case, the concentration of a reactant may be reduced rapidly by precipitation or by fast quantitative reaction with another material that is added to the sample. This material may then be back-titrated. For example, reactions between iodine and various reducing agents can be quenched by addition of a suitably buffered arsenite solution.

It is useful at this point to consider briefly the relative merits of chemical and physical methods for monitoring the course of a reaction. A *chemical* method involves removal of a portion of the reacting system, quenching the reaction occurring within the sample, and subsequent analysis of the system composition. This analysis may be carried out using conventional wet chemistry techniques, a spectroscopic method, or any of a variety of other analytical techniques. The essence of the chemical method, however, lies in the fact that it requires removal of a sample from the reacting system. Chemical methods give absolute values of the concentrations of the various species present in the reaction mixture. However, it should be stressed that even the most *precise* of these methods has an *accuracy* that is no better than the *accuracy* of the standard analytical procedure that was used to calibrate the method. Another disadvantage inherent in the use of chemical methods is that the sampling procedure involved does not provide a *continuous* record of the progress of the reaction. It is impossible to study very fast reactions using these methods.

*Physical methods* involve measurements of an appropriate physical property of the system while the reaction proceeds. The measurements are usually made in the actual reaction vessel (*in situ*) so that the necessity for sampling with the possibility of attendant errors is eliminated. With physical methods it is usually possible to obtain an essentially continuous record of the values of the property being measured. These values can then be transformed into a continuous record of reactant and product concentrations. It is usually easier to accumulate much more data on a given reaction system with such methods than is possible with chemical methods. There are certain limitations on physical methods, however. There must be substantial differences in the contributions of the reactants and products to the value of the particular physical property used to monitor the progress of the reaction. Thus, one would not use pressure measurements to follow the course of a reaction that does not involve a change in the total number of moles in the gas phase.

It is always wise to calibrate physical methods of analysis using mixtures of known composition under

conditions that approximate as closely as practicable those prevailing in the reaction system. This procedure is recommended because side reactions can introduce large errors and because some unforeseen complication may invalidate the results obtained with the technique. For example, in spectrophotometric studies of reaction kinetics, the absorbance that one measures can be grossly distorted by the presence of small amounts of highly colored absorbing impurities or by-products. For this reason, when one uses indirect physical methods in kinetic studies, it is essential to verify the stoichiometry of the reaction to ensure that the products of the reaction and their relative mole numbers are known with certainty. For the same reason it is recommended that more than one physical method of analysis be used in detailed kinetic studies.

In principle, any physical property that varies during the course of the reaction can be used to follow the course of the reaction. In practice, one chooses methods that use physical properties that are simple exact functions of the system composition. The most useful relationship is that the property is an additive function of the contributions of the different species and that each of these contributions is a linear function of the concentration of the species involved. This physical situation implies that there will be a linear dependence of the property in question on the extent of reaction. As examples of physical properties that obey this relationship, one may cite the electrical conductivity of dilute solutions, optical density or absorbance at a particular wavelength, the total pressure of gaseous systems under nearly ideal conditions, and the rotation of polarized light. In sufficiently dilute solutions, other physical properties behave in the desired manner to a fairly high degree of approximation. More complex relationships than the linear one can be utilized, but in such cases it is all the more imperative that the experimentalist carefully prepare calibration curves relating the property being measured to the extent of reaction or species concentrations.

### 3.2.2.3 Use of Physical Methods to Monitor Reaction Rates

In this section some physical property measurements of general utility are discussed. One of the oldest and most useful techniques for studying the kinetics of gas phase reactions involves measurements of the total pressure in an *isothermal constant volume reactor*. This technique is limited to homogeneous gas phase reactions that involve a change in the total number of gaseous molecules present in the reaction vessel (e.g., hydrogenation of propylene):



Pressure measurements can be accomplished by a number of different types of devices without disturbing the system being observed. Another type of reaction system that can be monitored by pressure measurements is one in which one of the products can be quantitatively removed by a solid or liquid reagent that does not otherwise affect the reaction. For example, acids formed by reactions in the gas phase can be removed by absorption in basic solutions. From knowledge of the reaction stoichiometry and measurements of the total pressure as a function of time, one can determine the corresponding extents of reaction and partial pressures or concentrations of the various reactant and product species. An example of how pressure measurements can be used to determine a reaction rate expression is provided in Illustration 3.3.

The various forms of spectroscopy find widespread application in studies of reaction kinetics. They are usually well suited for application to *in situ* studies of the characteristics of the reaction mixture. The absorption by a reacting system of electromagnetic radiation (i.e., light, microwaves, radio-frequency waves, etc.) is a highly specific property of the system composition, the frequency of the incident radiation, and the dimensions of the reaction vessel. Both the magnitude of the absorption coefficient and the wavelengths at which absorption maxima occur are characteristic of the absorbing compound and, to a lesser extent, its physical state. By appropriate choice of the wavelength of the incident radiation, one is able to take advantage of the remarkable specificity of the various forms of spectroscopy to monitor the progress of a wide variety of reactions. Among the various forms of spectroscopy that can be used in *in situ* kinetic studies are visible, ultraviolet, infrared, microwave, nuclear magnetic resonance, and electron spin resonance spectroscopies. For treatments of the limitations and uses of spectroscopic techniques, consult treatises on analytical chemistry.

In addition to spectrophotometric or spectroscopic measurements, there are a number of other optical measurements that can be used to monitor the course of various reactions. Among the optical properties that can be used for these studies are optical rotation, refractive indices, fluorescence, and colorimetry. There also are several electrical measurements that may be used for analysis of solutions under *in situ* conditions. Among the properties that may be measured are dielectric constants, electrical conductivity or resistivity, and the redox potential of solutions. These properties are easily measured with instrumentation that is readily interfaced to a computer for data acquisition and manipulation for analysis. However, most of these techniques should be used only after careful calibration and do not give better than 1% accuracy without unusual care in the experimental work.

### 3.3 TECHNIQUES FOR THE INTERPRETATION OF KINETIC DATA

In Section 3.1 the mathematical expressions that result from integration of various reaction rate functions were discussed in some detail. Our present problem is the converse of that considered earlier (i.e., given data on the concentration of a reactant or product as a function of time, how does one proceed to determine the reaction rate expression?).

Determination of the rate expression normally involves a two-step procedure. First, the concentration dependence is determined at a fixed temperature. Then the temperature dependence of the rate constants is evaluated to obtain a complete reaction rate expression. The form of this temperature dependence is given by equation (3.0.14), so our present problem reduces to that of determining the form of the concentration dependence and the value of the rate constant at the temperature of the experiment.

Unfortunately, there is no completely general method of determining the reaction rate expression or even of determining the order of a reaction. Usually, one employs an iterative trial-and-error procedure based on intelligent guesses and past experience with similar systems. Very often the stoichiometry of the reaction and knowledge of whether the reaction is “reversible” or “irreversible” will suggest a form of the rate equation to try first. If this initial guess (hypothesis) is incorrect, the investigator may then try other forms that are suggested either by assumptions about the mechanism of the reaction or by the nature of the discrepancies between the data and the mathematical model employed in a previous trial. Each reaction presents a unique problem, and success in fitting a reaction rate expression to the experimental data depends on the ingenuity of the individual investigator.

The discussion that follows is largely confined to irreversible reactions with simple rate expressions of the form of equation (3.0.17), but the methods developed are more generally applicable. We have chosen this approach to keep the discussion as simple as possible and to present the material in a manner that avoids the introduction of more complex rate expressions. Most of the methods presented below are applicable regardless of the mathematical form of the rate expression, and they may readily be extended to cover the rate expressions that will be encountered in Chapters 6, 7 and 13.

The techniques used to determine reaction rate expressions may be classified into three general categories:

1. Integral methods based on integration of the reaction rate expression. In these approaches one customarily analyzes the data by plotting some function of the reactant concentrations or the extent of reaction versus time using coordinates that would yield a straight line if the

hypothesis concerning the mathematical form of the rate expression is correct.

2. Differential methods based on differentiation of experimental concentration versus time data to obtain an approximation to the actual rate of reaction. In these approaches one analyzes the data by postulating various functional relations between the rate of reaction and the concentrations of the various species in the reaction mixture and tests these hypotheses using appropriate plots of the data.
3. Methods based on simplification of the reaction rate expression. In these approaches one uses stoichiometric ratios of the reactants or a vast excess of one or more of the reactants in order to permit a partial evaluation of the form of the rate expression. These methods may be used in conjunction with either a differential or an integral analysis of the experimental data.

Discussions of each of these general categories follow.

### 3.3.1 Differential Methods for the Treatment of Rate Data

In experimental kinetics studies one measures (directly or indirectly) the concentration of one or more of the reactant and/or product species as a function of time. If these concentrations are plotted against time, smooth curves should be obtained. For reactions occurring at constant volume in a batch reactor, the rate may be obtained by graphical or numerical differentiation of these data. For kinetics trials involving variable volume batch reactors or continuous flow reactors, additional mathematical manipulations of the data are usually necessary. For example, from a knowledge of the concentration of one of the reactants or products at some time  $t$ , the initial composition of the system, and the reaction stoichiometry (from which  $\delta_A$  may be determined), it is possible to use equation (3.1.47) or (3.1.50) to determine the fraction conversion of the limiting reagent at this time. Equation (3.1.51) may then be used to determine the reaction rate corresponding to this conversion:

$$r = \left( \frac{-C_{A0}}{1 + \delta_A f_A} \right) \frac{1}{\nu_A} \frac{df_A}{dt} \quad (3.1.51)$$

Thus, for both variable and constant volume batch reactors, one can manipulate concentration versus time data to obtain values of the reaction rate as a function of time or as a function of the concentrations of the various species present in the reaction mixture. The task then becomes one of fitting these data to a reaction rate expression of the form of equation (3.0.13).

Since data are almost invariably taken under isothermal conditions to eliminate the temperature dependence of reaction rate constants, one is concerned primarily with determining the concentration dependence of the rate expression  $\phi(C_i)$  and the rate constant at the temperature in question. Next we consider two differential methods that can be used in the analysis of rate data.

#### 3.3.1.1 Differentiation of Data Obtained in the Course of a Single Experimental Run

If one has experimental results in the form of concentration versus time data, the following general differential procedure may be used to determine  $\phi(C_i)$  and the rate constant at the temperature in question:

1. Set forth a hypothesis as to the form of the concentration dependent portion of the rate function,  $\phi(C_i)$ .
2. From the experimental concentration versus time data, determine reaction rates corresponding to various times.
3. At the selected times, prepare a table listing the reaction rate and the concentrations of the various species present in the reaction mixture. Calculate  $\phi(C_i)$  at each of these points.
4. Prepare a plot of the reaction rate versus  $\phi(C_i)$ . If the plot is linear and passes through the origin, the form of  $\phi(C_i)$  is consistent with the experimental data. Consequently, insofar as the accuracy of the data is concerned, the form of the rate expression is satisfactory for subsequent use in design calculations. The slope of this straight line equals the reaction rate constant. If the plot is not linear or does not pass through the origin, one must return to step 1, hypothesize a different mathematical form for the concentration dependence of the rate expression, and iterate until a satisfactory form is obtained.

In its application to studies of specific reactions, this general procedure may take on a variety of forms that are minor modifications of that outlined above. One useful modification does not require an explicit assumption of the form of  $\phi(C_i)$ , including numerical values of the orders of the reaction with respect to the various species, but merely an assumption that the rate expression is of the form

$$r = k\phi(C_i) = kC_A^{\beta_A} C_B^{\beta_B} C_C^{\beta_C} \dots \quad (3.3.1)$$

The reaction rate  $r$  and the various  $C_i$  may be determined from the experimental data. Taking the logarithms of both sides of this equation yields

$$\log r = \log k + \beta_A \log C_A + \beta_B \log C_B + \beta_C \log C_C + \dots \quad (3.3.2)$$

This relation may be fit to the data by the *method of least squares* to determine the values of the constants  $\log k$ ,  $\beta_A$ ,  $\beta_B$ , and so on, that provide the best statistical fit of this mathematical model. A qualitative assessment of the goodness of fit may be ascertained from visual examination of a figure containing plots of both the data and the values of  $\phi(C_i)$  calculated using the parameter values that give the best fit to the data. Scrutiny of a plot of the reaction rate versus the function  $\phi(C_i)$  then permits one to address the question of whether or not the mathematical model meets the criteria of the general method outlined above. Quantitative assessments of the ability of the model to fit the data may be made using one of a variety of commercially available statistical software packages.

A second common modification of the general method is that which ensues when one uses stoichiometric ratios of the reactants. This approach is valid only when the rate expression is of the form of equation (3.3.1) with the  $\beta_i$  for all species other than reactants taken as zero.

From the use of a stoichiometric feed ratio,

$$\frac{n_{A0}}{\nu_A} = \frac{n_{B0}}{\nu_B} = \frac{n_{C0}}{\nu_C} \quad (3.3.3)$$

From the definition of the extent of reaction,

$$\xi = \frac{n_A - n_{A0}}{\nu_A} \quad \xi = \frac{n_B - n_{B0}}{\nu_B} \quad \xi = \frac{n_C - n_{C0}}{\nu_C} \quad (3.3.4)$$

Scrutiny of equations (3.3.3) and (3.3.4) reveals that when the feed consists of stoichiometric proportions of reactants, one can state that at all times

$$\frac{n_A}{\nu_A} = \frac{n_B}{\nu_B} = \frac{n_C}{\nu_C} \quad (3.3.5)$$

Alternatively,

$$\frac{C_A}{\nu_A} = \frac{C_B}{\nu_B} = \frac{C_C}{\nu_C} = \frac{C_i}{\nu_i} \quad (3.3.6)$$

because all species occupy the same volume. Consequently, for trials involving stoichiometric proportions of reactants, equation (3.3.1) may be written as

$$r = k \prod_{\text{reactants}} C_i^{\beta_i} = \left[ k \left( \frac{C_A}{\nu_A} \right)^{\sum \beta_i} \right] \left[ \prod_{\text{reactants}} (\nu_i)^{\beta_i} \right] = k' C_A^m \quad (3.3.7)$$

where we have defined a new rate constant  $k'$  to include the effect of the stoichiometric coefficients and have replaced the overall order of the reaction ( $\sum_{\text{reactants}} \beta_i$ ) by  $m$ . If one now takes the logarithm of both sides of this expression, the result is

$$\log r = \log k' + m \log C_A \quad (3.3.8)$$

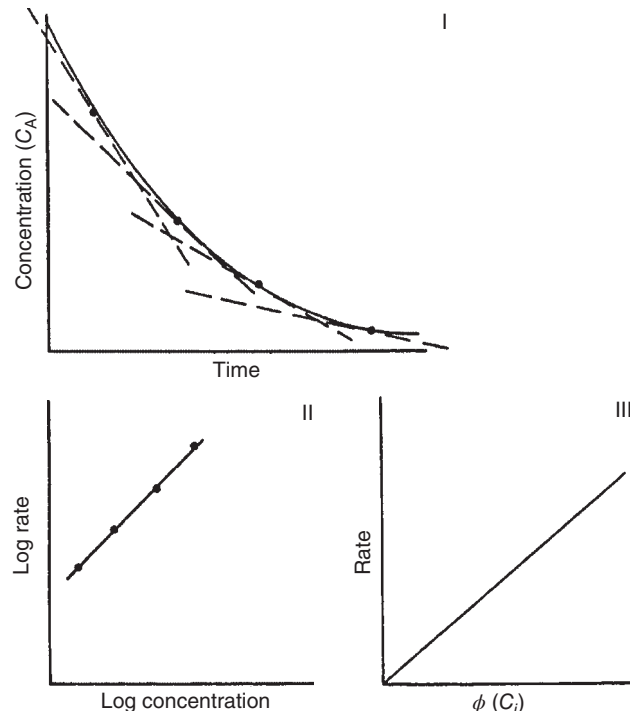


**Figure 3.1** Schematic representation of the application of the differential method of data analysis.

The constants  $k'$  and  $m$  may be determined from a log-log plot of the rate versus  $C_A$ . This procedure leads to a value for the overall order of the reaction. Experiments involving nonstoichiometric ratios of reactants can then be used to determine the orders of the reaction with respect to each individual species. This differential procedure is illustrated schematically in Figure 3.1. Panel I indicates how the rate may be determined from concentration versus time data in a constant-volume system; panel II illustrates the method just described; and panel III represents the application of our general differential method to this system.

It is always preferable to use as much of the data as possible to determine the reaction rate expression. This principle often implies that one should use some sort of graphical procedure to analyze the data. Visual inspection of such plots may indicate that certain points are seriously in error and should not be weighted heavily in the determination of the reaction rate expression. The consistency and precision of the data can also be evaluated visually by observing the deviation of the data points from a smooth curve (ideally, their deviations from a straight line).

Illustration 3.1 involves use of the differential method for the analysis of kinetic data. It also exemplifies some of the problems one has in attempting to utilize a differential approach in the analysis of rate data.

### ILLUSTRATION 3.1 Use of a Differential Method to Determine a Pseudo Reaction Rate Expression for the Iodine-Catalyzed Bromination of *m*-Xylene

Neyens (4) studied the bromination of *meta*-xylene at 17°C. The reaction was carried out by introducing small quantities of bromine into a xylene solution containing very small (catalytic) amounts of iodine and following the rate of disappearance of bromine by titrating samples removed from the liquid to determine their bromine content. Since the concentrations of xylene and catalyst remain essentially unchanged during the course of the reaction, one can assume that the rate expression is of the form

$$r = kC_{\text{Br}_2}^m = -\frac{dC_{\text{Br}_2}}{dt} \quad (\text{A})$$

where  $k$  is a pseudo *m*th-order rate constant that will depend on the concentration of iodine. Use a differential method to determine the order of the reaction and the rate constant.

#### Solution

Two differential approaches to the analysis of the data in Table I3.1-1 will be presented. The first of these is based on the similarity of equation (A) to equation (3.3.7). The second is the general approach outlined earlier. In logarithmic form, equation (A) becomes

$$\log \left( -\frac{dC_{\text{Br}_2}}{dt} \right) = \log k + m \log C_{\text{Br}_2} \quad (\text{B})$$

The term on the left side of equation (B) may be determined from the data (Table I3.1-1) in several ways. The bromine concentration may be plotted as a function of time and the slopes of the curve at various times determined graphically. Alternatively, any of several methods of numerical differentiation may be employed. The simplest of these is used in Table I3.1-2, where  $dC/dt$  at the midpoint of the time interval is approximated by  $\Delta C/\Delta t$  for the entire time interval. Mean bromine concentrations corresponding to each derivative are also tabulated for future use, together with these concentrations raised to the 1.5 power.

Figure I3.1-1 is a plot of reaction rate versus mean bromine concentration using logarithmic coordinates. The slope of this plot ( $m$ ) is 1.54, or approximately 1.5. Neyens concluded that the order of the reactin in bromine was  $(\frac{3}{2})$ . The rate constant can be determined from the value of the rate corresponding to a bromine concentration of 1 mol/L. Thus,  $k = 1.0 \times 10^{-1} \text{ (L/mol)}^{1/2} \text{ min}^{-1}$ . The value reported by Neyens was  $0.91 \times 10^{-1}$  based on the use of an integral method for analysis of the data. However, slight shifts in the slope of the straight line in Figure I3.1-1

Table I3.1-1 Data

Time, $t$ (min)	Concentration of bromine, $C$ (mol/L)	Time, $t$ (min)	Concentration of bromine, $C$ (mol/L)
0.0	0.3335	19.60	0.1429
2.25	0.2965	27.00	0.1160
4.50	0.2660	30.00	0.1053
6.33	0.2450	38.00	0.0830
8.00	0.2255	41.00	0.0767
10.25	0.2050	45.00	0.0705
12.00	0.1910	47.00	0.0678
13.50	0.1794	57.00	0.0553
15.60	0.1632	63.00	0.0482
17.85	0.1500		

Table I3.1-2 Data Workup

Time, $t$ (min)	Concentration of bromine, $C$ (mol/L)	$-\frac{\Delta C}{\Delta t} \times 10^3$	$\bar{C}$ (mol/L)	$\bar{C}^{1.5}$ (mol/L) <sup>1.5</sup>
0.00	0.3335	16.44	0.3150	0.1762
2.25	0.2965	13.56	0.2812	0.1491
4.50	0.2660	11.48	0.2555	0.1291
6.33	0.2450	11.68	0.2353	0.1141
8.00	0.2255	9.11	0.2153	0.0999
10.25	0.2050	8.00	0.1980	0.0881
12.00	0.1910	7.73	0.1852	0.0797
13.50	0.1794	7.71	0.1713	0.0709
15.60	0.1632	5.87	0.1566	0.0620
17.85	0.1500	4.06	0.1465	0.0561
19.60	0.1429	3.64	0.1295	0.0466
27.00	0.1160	3.23	0.1107	0.0369
30.00	0.1053	2.79	0.0942	0.0289
38.00	0.0830	2.10	0.0799	0.0226
41.00	0.0767	1.55	0.0736	0.0200
45.00	0.0705	1.35	0.0692	0.0182
47.00	0.0678	1.25	0.0615	0.0153
57.00	0.0553	1.18	0.0518	0.0118
63.00	0.0482			

could bring about rather large changes in the intercept at  $C = 1 \text{ mol/L}$ . Inspection of this figure indicates that the fit of the straight line to the data is not nearly as good as one might like. One frequently encounters problems of this type in attempting to use differential methods for the analysis of data taken in a batch reactor. Some of the scatter in the data points might be removed if one prepared

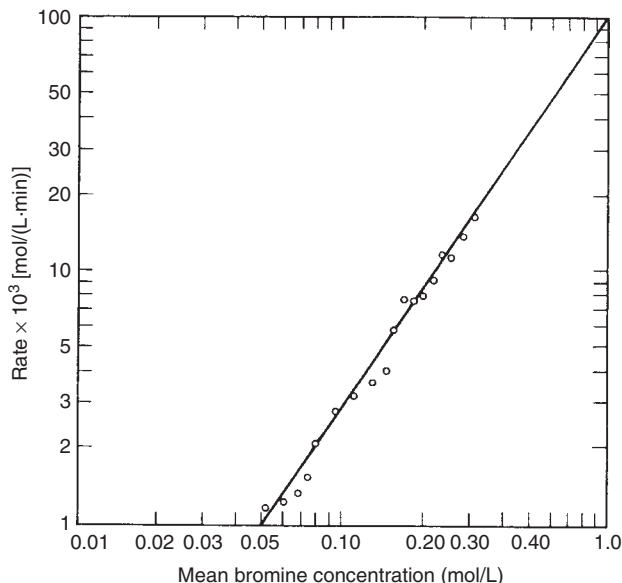


**Figure I3.1-1** Log-log plot of reaction rate versus bromine concentration.

a concentration versus time plot and determined the slope graphically.

The second method that will be used for the solution of this problem is the general procedure outlined at the beginning of this section.

1. Assume that the concentration dependent portion of the rate function  $\phi(C_i)$  is equal to  $C_{Br_2}^{1.5}$ .
2. From the experimental concentration vs time data, determine the reaction rate at various times (see Table I3.1-2).
3. Calculate values of  $C_{Br_2}^{1.5}$  at those times for which the reaction rate has been determined (see Table I3.1-2).
4. Plot the reaction rate versus  $C_{Br_2}^{1.5}$ , as shown in Figure I3.1-2. The plot is reasonably linear and passes through the origin.
5. If one plots the rate versus either  $C_{Br_2}^2$  or  $C_{Br_2}$ , these plots show marked curvature, particularly at the points corresponding to high conversions of bromine (low concentrations of bromine). One plot is concave and the other is convex. From the quasi-linear relationship that exists for the 1.5-order case, one may conclude that this order provides a good fit to the data. Again, however, one should note the fact that there is appreciable scatter in the data when one attempts to apply this method.

The value of the pseudo-reaction rate constant determined from the slope of the straight line in Figure I3.1-2 is  $9.2 \times 10^{-2} (L/mol)^{1/2}/min$ . This number is consistent with the value reported by Neyens ( $9.1 \times 10^{-2}$ ).

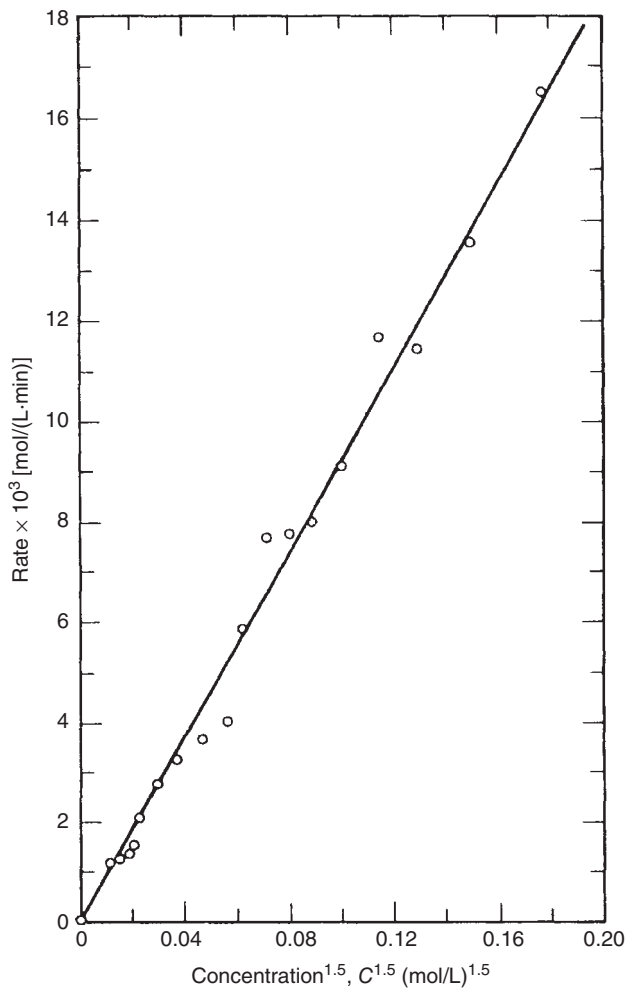


**Figure I3.1-2** Plot used to test for 1.5-order rate expression.

### 3.3.1.2 Initial Rate Measurements

Another differential method that is useful in the determination of rate expressions is the initial rate approach. This method involves a series of rate measurements at different initial reactant concentrations but restricted to very small conversions of the limiting reagent (5 to 10% or less). This technique differs from those discussed previously in that lower conversions are used and each rate measurement involves a new experiment.

In an initial rate study, one focuses on the conditions that prevail at the start of the reaction. Since the concentrations of the various species do not undergo large changes during this period (varying by 10% at the most), one may characterize these concentrations by initial or average values that can then be substituted directly into the trial rate expression. One may determine the values of the reaction rate corresponding to zero time by measuring the initial slopes of concentration versus time curves in constant-volume systems or by measuring the initial

slope of a fraction conversion versus time curve and using equation (3.1.51) to calculate the initial reaction rate. Numerical calculations could also be used. In either event, for each run one obtains a value of the initial reaction rate,  $r_0$ , at a specific mixture composition.

If the reaction rate expression is of the form

$$r_0 = k C_{A0}^{\beta_A} C_{B0}^{\beta_B} C_{C0}^{\beta_C} = k \prod_i C_{i0}^{\beta_i} \quad (3.3.9)$$

one may determine the order of the reaction with respect to an individual component (e.g., A) by making rate measurements at two different initial concentrations of this species while holding all other concentrations constant between the two trials. If we denote the two rates observed by  $r_0$  and  $r'_0$  and the corresponding initial concentrations by  $C_{A0}$  and  $C'_{A0}$ , equation (3.3.9) may be written for these runs as

$$r_0 = (k C_{B0}^{\beta_B} C_{C0}^{\beta_C} \cdots) C_{A0}^{\beta_A} \quad (3.3.10)$$

and

$$r'_0 = (k C_{B0}^{\beta_B} C_{C0}^{\beta_C} \cdots) (C'_{A0})^{\beta_A} \quad (3.3.11)$$

Division of equation (3.3.10) by (3.3.11) and solution of the resulting expression for  $\beta_A$  gives

$$\beta_A = \frac{\log(r_0/r'_0)}{\log(C_{A0}/C'_{A0})} \quad (3.3.12)$$

By varying the initial concentration of each component of the reaction mixture in turn, one can determine the order of the reaction with respect to each species. Once these orders have been established, equation (3.3.9) may be used to determine the reaction rate constant.

If one has initial rate data available at several different concentrations of species A and at the same initial concentrations of all other species, a more accurate value of  $\beta_A$  may be determined from a log-log plot of the data in the form of equation (3.3.10). In many cases, orders determined in this fashion will not be simple integers or half-integers. When this is the case, one should note that the values of  $\beta_i$  that fit the data may not have mechanistic significance. Instead, they merely provide exponents for a reasonable mathematical approximation to the true rate expression, which itself may be a much more complex mathematical function.

One advantage of the initial rate method is that complex rate functions that may be extremely difficult to integrate can be handled in a convenient manner. Moreover, if one uses initial reaction rates, the reverse reactions can be neglected and attention can be focused solely on the reaction rate expression for the forward reaction. More complex rate functions may be tested by the choice of appropriate

coordinates for plotting the initial rate data. For example, the validity of a rate expression of the form

$$r_0 = \frac{k C_{A0}}{1 + k' C_{A0}} \quad (3.3.13)$$

can be assessed by plotting the reciprocal of the initial rate versus the reciprocal of the initial concentration of species A. If the data are consistent with this rate law, such a plot would be linear with an intercept equal to  $k'/k$  and a slope equal to  $1/k$ :

$$\frac{1}{r_0} = \frac{1}{k C_{A0}} + \frac{k'}{k} \quad (3.3.14)$$

### 3.3.2 Integral Methods for the Treatment of Rate Data

When integral methods are used in data analysis, measured concentrations are used in tests of proposed mathematical formulations of the reaction rate function. One hypothesizes a form of the reaction rate expression on the basis of the reaction stoichiometry and assumptions concerning its mechanism. The assumed expression is then integrated to give a relation between the composition of the reaction mixture and time. A number of such relations were developed in Section 3.1. In the present section we indicate how experimental data are tested for consistency with these relations. Several methods based on integration of the reaction rate expression are considered.

#### 3.3.2.1 A General Integral Method for the Analysis of Kinetic Data: Graphical Procedure

The general integral technique for the determination of reaction rate expressions consists of the following trial-and-error procedure.

1. Set forth a hypothesis as to the mathematical form of the reaction rate function:

$$\frac{1}{V} \frac{d\xi}{dt} = k \phi(C_i) \quad (3.3.15)$$

2. Separate variables and integrate:

$$t = \int_0^{\xi} \frac{d\xi}{V k \phi(C_i)} \quad (3.3.16)$$

To evaluate this integral it is necessary to express all terms on the right in terms of a single variable. For isothermal systems  $k$  is a constant, and this equation can be written as

$$kt = \int_0^{\xi} \frac{d\xi}{V \phi(C_i)} \quad (3.3.17)$$

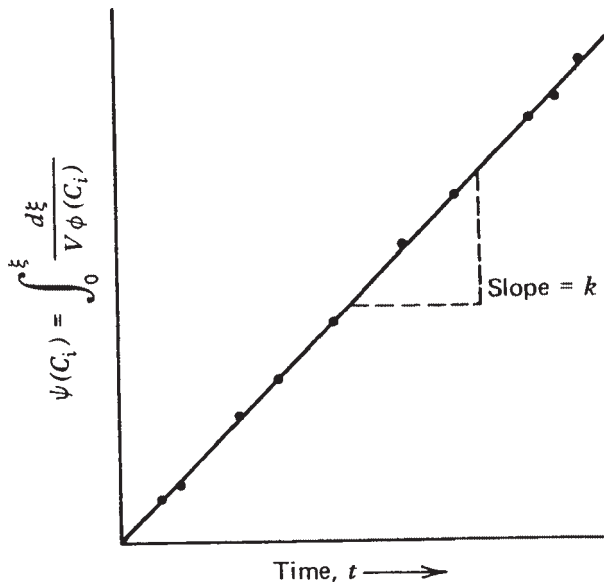


**Figure 3.2** Test of the fit of a reaction rate expression to kinetic data by the integral method of data analysis.

Since our present goal is the determination of  $\phi(C_i)$ , we will restrict the subsequent discussion to isothermal systems. If the integral is represented by  $\psi(C_i)$ ,

$$kt = \psi(C_i) \quad (3.3.18)$$

- From experimentally determined values of the various concentrations, or from the value of a single measured concentration and the reaction stoichiometry, calculate the value of  $\psi(C_i)$  at the times corresponding to these measurements. In some cases it may be necessary to resort to graphical integration to determine  $\psi(C_i)$ .
- Plot the calculated values of  $\psi(C_i)$  versus  $t$  as shown in Figure 3.2. If the data yield a satisfactory straight line passing through the origin, the reaction rate expression assumed in step 1 is said to be consistent with the data and may be accepted as a basis for subsequent work in the same temperature-concentration regime of operation. The slope of this line is equal to the reaction rate constant  $k$ . If the data do not fall on a satisfactory straight line, one must iterate as necessary by returning to step 1 and assuming a new mathematical form of the rate expression until the most recent assumption yields agreement between the proposed mathematical model and the data. This agreement may be reflected in the form of an acceptable straight line or in an otherwise acceptable response to a standard statistical test of the ability of the model to fit the data.

Simple modifications of the above procedure are often employed to reduce the numerical calculations required. For example, the value of  $\psi(C_i)$  corresponding to a class II

second-order rate expression is

$$kt = \psi(C_i) = \frac{1}{C_{A0}\nu_B - C_{B0}\nu_A} \ln \left( \frac{C_{A0}C_B}{C_{B0}C_A} \right) \quad (3.3.19)$$

A plot of this function versus time should be linear in time with a slope equal to the rate constant  $k$ . However, it is often more convenient to rearrange this equation as

$$\ln \left( \frac{C_B}{C_A} \right) = \ln \left( \frac{C_{B0}}{C_{A0}} \right) + (C_{A0}\nu_B - C_{B0}\nu_A)kt \quad (3.3.20)$$

and plot the left side versus time. One still requires the data plot to be linear, but the restriction that the line pass through the origin is modified so that the  $y$  intercept at time zero becomes  $\ln(C_{B0}/C_{A0})$ .

The graphical approach to the analysis of kinetic data has several advantages. The best straight line through the experimental points can often be found by inspection (i.e., by moving a transparent straightedge until it appears to fit the data with a minimum of deviation). Since errors in the concentration measurements are usually much greater than those in the time measurements, in estimating the best straight line through a series of points one should think of the residuals as parallel to the concentration axis (i.e., vertical), not as perpendicular to the line. The graphical method readily shows trends and deviations from linear behavior. Scattered points that are obviously in error can easily be recognized and eliminated from further consideration. In those rare cases where the accuracy of the data exceeds that obtained in plotting on a reasonable scale, one should use the numerical methods described in Section 3.3.2.2.

Since the integral method described above is based on the premise that some rate expression exists that will lead to a value of  $\psi(C_i)$  that is linear in time, deviations from linearity (e.g., curvature) indicate that further evaluation or interpretation of the rate data is necessary. Many mathematical functions are roughly linear over sufficiently small ranges of variables. To provide a challenging test of the linearity of the data, one should perform at least one experimental run in which data are taken at 80%, 90%, or higher conversions of the limiting reagent.

Perhaps the most discouraging type of deviation from linearity is random scatter of the data points. Such results indicate that something is seriously wrong with the experiment. The method of analysis may be at fault or the reaction may not be following the expected stoichiometry. Side reactions may be interfering with the analytical procedures used to follow the progress of the reaction, or they may render invalid the mathematical analysis employed. When such plots are obtained, it is wise to reevaluate the entire experimental procedure and the method used to evaluate the data before carrying out additional experiments.

Another form of deviation from linearity that is often encountered in plots of  $\psi(C_i)$  versus time is curvature of the data, as shown in Figure 3.3. If the order assumed is greater

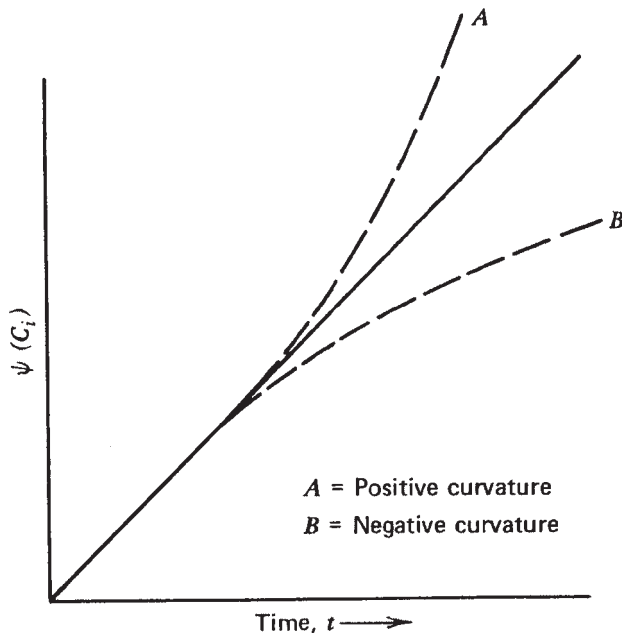


**Figure 3.3** Observation of curvature in tests of proposed rate expressions.

than the true order of the reaction, upward curvature will be observed. If the assumed order is less than the true order, downward curvature will result.

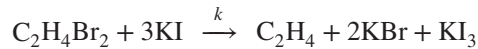
In some cases one attempts to cause a simplification of the rate expression by using stoichiometric ratios of reactants. For example, a mixed second-order rate expression ( $r = kC_A C_B$ ) becomes a class I second-order rate expression ( $r = kC_A^2$ ) if stoichiometric proportions of A and B are used. If, by mistake, a nonstoichiometric mixture is used, positive or negative deviations can be observed, depending on which species is present in excess.

If a reaction is reversible and if one has assumed a rate function that does not take the reverse reaction into account, one observes a downward curvature. As equilibrium is approached, the slope of this curve approaches zero. Another cause of curvature is a change in temperature during the course of the experiment. An increase in temperature causes an increase in the reaction rate, leading to an upward curvature. Bennett (3) discussed a number of other sources of curvature, including changes in pH and ionic strength, impurity effects, autocatalysis, and side reactions.

Illustrations 3.2 and 3.3 are examples of the use of the graphical integral method for the analysis of kinetic data.

### ILLUSTRATION 3.2 Use of a Graphical Integral Method for Determining the Rate Constant for a Class II Second-Order Reaction

R. T. Dillon (5) studied the reaction between ethylene bromide and potassium iodide in 99% methanol.



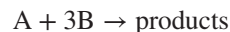
Given the data that follow, determine the second-order reaction rate constant.

Temperature	59.72°C
Initial KI concentration	0.1531 kmol/m <sup>3</sup>
Initial $C_2H_4Br_2$ concentration	0.02864 kmol/m <sup>3</sup>

Time, t (ks)	Fraction dibromide reacted
29.7	0.2863
40.5	0.3630
47.7	0.4099
55.8	0.4572
62.1	0.4890
72.9	0.5396
83.7	0.5795

### Solution

The stoichiometry of the reaction is of the form



As a starting point, we assume that the rate expression is of the form

$$\frac{d\xi^*}{dt} = kC_A C_B \quad (\text{A})$$

The instantaneous concentrations  $C_A$  and  $C_B$  can be expressed in terms of the initial values and the extent of reaction per unit volume:

$$C_A = C_{A0} - \xi^* \quad C_B = C_{B0} - 3\xi^*$$

Thus,

$$\frac{d\xi^*}{dt} = k(C_{A0} - \xi^*)(C_{B0} - 3\xi^*)$$

Separation of variables and integration give

$$\begin{aligned} kt &= \int_0^{\xi^*} \frac{d\xi^*}{(C_{A0} - \xi^*)(C_{B0} - 3\xi^*)} \\ &= \frac{1}{(C_{B0} - 3C_{A0})} \ln \left[ \frac{(C_{B0} - 3\xi^*) C_{A0}}{(C_{A0} - \xi^*) C_{B0}} \right] \end{aligned} \quad (\text{B})$$

The stoichiometry of the reaction indicates that for the trial of interest the limiting reagent is the dibromide (species A). The fraction reacted ( $f_A$ ) is given by

$$f_A = \left( \frac{\xi^*}{C_{A0}} \right) \quad (\text{C})$$

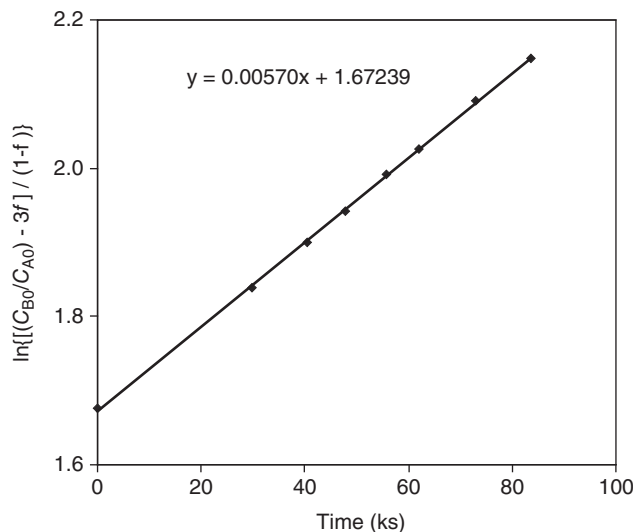


Figure I3.2 Plot for determination of rate constant.

Elimination of  $\xi^*$  between equations (B) and (C) gives

$$kt = \frac{1}{(C_{B0} - 3C_{A0})} \ln \left\{ \left[ \frac{(C_{B0}/C_{A0}) - 3f}{1-f} \right] \left( \frac{C_{A0}}{C_{B0}} \right) \right\} \quad (\text{D})$$

If the reaction is second order, it is evident from equation (D) that a plot of  $\ln \{[(C_{B0}/C_{A0}) - 3f]/(1-f)\}$  versus time should be linear with a slope equal to  $(C_{B0} - 3C_{A0})k$ . The results of the calculations necessary to determine the logarithmic term are given in Table I3.2.

$$\frac{C_{B0}}{C_{A0}} = \frac{0.1531}{0.02864} = 5.3457$$

A regression analysis was carried out using the plotting wizard and the Linest function associated with an Excel spreadsheet (see Figure I3.2). The linearity of the plot indicates that the data are consistent with the assumed rate expression and that

$$(C_{B0} - 3C_{A0})k = (5.70 \pm 0.04) \times 10^{-3} \text{ ks}^{-1}$$

Table I3.2

Time, $t$ (ks)	$f$	$1-f$	$\frac{C_{B0}}{C_{A0}} - 3f$	$\ln \left[ \frac{(C_{B0}/C_{A0}) - 3f}{1-f} \right]$
0.0	0.0000	1.0000	5.3457	1.6763
29.7	0.2863	0.7137	4.4868	1.8384
40.5	0.3630	0.6370	4.2567	1.8995
47.7	0.4099	0.5901	4.1160	1.9423
55.8	0.4572	0.5428	3.9741	1.9908
62.1	0.4890	0.5110	3.8787	2.0269
72.9	0.5396	0.4604	3.7269	2.0912
83.7	0.5795	0.4205	3.6072	2.1492

Thus,

$$k = \frac{5.70 \times 10^{-3}}{0.0672} = 8.48 \times 10^{-2} \text{ m}^3/(\text{kmol} \cdot \text{ks})$$

In more conventional units this value is  $0.305 \text{ L}/(\text{mol} \cdot \text{h})$ , a value that is comparable to the value of  $0.300 \text{ L}/(\text{mol} \cdot \text{h})$  reported by Dillon.

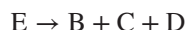
Use of modern spreadsheets such as Excel facilitates the solution of problems of this type, preparation of appropriate plots of the data for visualization, and regression analyses to generate model parameters and the uncertainties associated therewith. The parameter  $(C_{B0} - 3C_{A0})k$  was obtained using the linear trendline and Linest capabilities of Excel.

### ILLUSTRATION 3.3 Use of the Graphical Integral Method to Determine the Rate Expression for a Gas Phase Chemical Reaction Monitored Using the Total Pressure of the System

Hinshelwood and Askey (6) investigated the gas-phase decomposition of dimethyl ether:



or



The following data were recorded in an isothermal ( $552^\circ\text{C}$ ) constant-volume reactor.

Time, $t$ (s)	Total pressure (torr)
0	420
57	584
85	662
114	743
145	815
182	891
219	954
261	1013
299	1054

Use a graphical integral method to determine the order of the reaction and the reaction rate constant.

### Solution

As an initial hypothesis assume that the reaction follows first-order kinetics. The integrated form of the reaction rate expression is then given by equation (3.1.8):

$$\ln \left( \frac{C_E}{C_{E0}} \right) = -kt \quad (\text{A})$$

At the temperature and pressures of this experiment, ideal gas behavior may be assumed. Thus,

$$C_E = \frac{P_E}{RT} = y_E \frac{\pi}{RT} \quad (B)$$

where  $\pi$  is the total pressure in the system. Combination of equations (A) and (B) gives

$$\ln \left( \frac{y_E \pi}{\pi_0} \right) = -kt \quad (C)$$

If the mole fraction ether (E) can be expressed in terms of the total pressure of the system, it can be used in conjunction with equation (C) to obtain an integral equation against which the data can be tested. To develop this relation, it is helpful to prepare a mole table.

Time, $t$	0	$t$	$\infty$
Species	Mole number		
$\text{CH}_3\text{OCH}_3$	$n_0$	$n_0 - \xi$	0
$\text{CH}_4$	0	$\xi$	$\xi_\infty = n_0$
$\text{H}_2$	0	$\xi$	$\xi_\infty = n_0$
CO	0	$\xi$	$\xi_\infty = n_0$
Total moles	$n_0$	$n_0 + 2\xi$	$3n_0$
Pressure	$\pi_0$	$\pi$	$\pi_\infty = 3\pi_0$

From this table and the ideal gas law, it is evident that

$$\frac{\pi - \pi_0}{\pi_\infty - \pi_0} = \frac{[(n_0 + 2\xi) - n_0](RT/V)}{(3n_0 - n_0)(RT/V)} = \frac{2\xi}{2n_0}$$

or

$$\frac{\xi}{n_0} = \frac{\pi - \pi_0}{3\pi_0 - \pi_0} = \frac{1}{2} \left( \frac{\pi}{\pi_0} - 1 \right) \quad (D)$$

The mole fraction ether at time  $t$  is given by

$$y_E = \frac{n_0 - \xi}{n_0 + 2\xi} = \frac{1 - (\xi/n_0)}{1 + 2(\xi/n_0)} \quad (E)$$

Combination of equations (D) and (E) gives

$$y_E = \frac{1 - \frac{1}{2}[(\pi/\pi_0) - 1]}{1 + [(\pi/\pi_0) - 1]} = \frac{\frac{3}{2} - \frac{1}{2}(\pi/\pi_0)}{\pi/\pi_0} = \frac{3\pi_0 - \pi}{2\pi}$$

Substitution of this relation in equation (C) gives

$$\ln \left( \frac{3\pi_0 - \pi}{2\pi_0} \right) = -kt$$

This equation is one against which the data can be tested to see if the assumption of first-order kinetics is appropriate. The data are worked up below and plotted on semi-logarithmic coordinates in Figure I3.3.

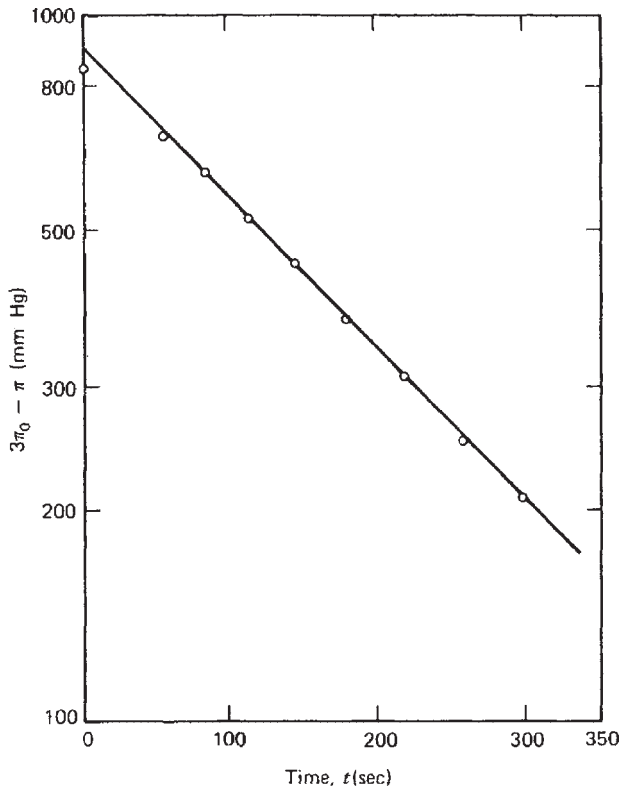


Figure I3.3 Graphical test of data.

Time, $t$ (s)	Pressure (mmHg)	$[3\pi_0 - \pi]$ (mmHg)
0	420	840
57	584	676
85	662	598
114	743	517
145	815	445
182	891	369
219	954	306
261	1013	247
299	1054	206

The linearity of the plot indicates that a first-order rate expression provides an excellent fit of the data. The reaction rate constant may be determined from the slope of this plot.

$$k = \frac{d\ln(3\pi_0 - \pi)}{dt} = 4.81 \times 10^{-3} \text{ s}^{-1}$$

Use of the LINEST function in Excel to ascertain the uncertainty in  $k$  indicates that

$$k = (4.81 \pm 0.08) \times 10^{-3} \text{ s}^{-1}$$

### 3.3.2.2 Integral Methods for the Analysis of Kinetic Data: Numerical Procedures

Although the graphical procedures discussed in Section 3.3.2.1 are perhaps the most practical and useful of the simple methods for determining rate constants, a number of simple numerical procedures exist for accomplishing this task. Some of these procedures are of doubtful utility, whereas others are widely used because they are embodiments of techniques for the statistical analysis of experimental data. All of these procedures are based on the calculation of  $k$  from the integrated form of a reaction rate expression such as equations (3.1.8), (3.1.15), and (3.1.19). For a detailed evaluation of the various averaging procedures that can be employed in the calculation of  $k$ , see the works of Livingston (7) and Margerison (8). They have been used as the basis for the present discussion. Regardless of the averaging procedure employed, it is good practice to arrange the computed values of  $k$  in order of increasing time or to plot  $k$  versus time so that systematic trends may be observed. Such trends indicate significant departures from the rate law assumed.

The long- and short-interval methods are simple computational procedures that the budding kineticist might be tempted to use. They avoid the subjective weighting of the various experimental points that is inherent in any graphical method, but they have the common disadvantage of weighting the points in arbitrary, illogical fashion.

The *long-interval method* involves the calculation of  $k$  using the *initial* values of reactant concentrations successively with each of the other values of the measured concentrations and times: If there are  $n + 1$  measurements of the concentrations of interest (including the initial value), the procedure yields  $n$  values of  $k$ . The “average” value of  $k$  is then taken to be the arithmetic average of these computed values:

$$\bar{k} = \frac{1}{n} \sum_{i=1}^{i=n} k_{0,i} \quad (3.3.21)$$

where  $k_{0,i}$  is the value of the rate constant computed using the concentration value determined at time  $t_i$ . For a class I second-order reaction ( $\nu_A = -1$ ) taking place in a constant volume system, the several values of the rate constant may be determined using equation (3.1.15):

$$\begin{aligned} k_{0,1} &= \frac{1}{t_1} \left( \frac{1}{C_{A1}} - \frac{1}{C_{A0}} \right) \\ k_{0,2} &= \frac{1}{t_2} \left( \frac{1}{C_{A2}} - \frac{1}{C_{A0}} \right) \\ k_{0,i} &= \frac{1}{t_i} \left( \frac{1}{C_{Ai}} - \frac{1}{C_{A0}} \right) \end{aligned} \quad (3.3.22)$$

The arithmetic mean of these values is

$$\bar{k} = \frac{1}{n} \sum_{i=1}^{i=n} \frac{1}{t_i C_{Ai}} - \frac{1}{n C_{A0}} \sum_{i=1}^{i=n} \frac{1}{t_i} \quad (3.3.23)$$

This method assigns a much greater weight to the initial starting point than to any succeeding data point. Moreover, as the time interval increases, the contribution of the corresponding concentration term to the average rate constant becomes smaller and smaller, so that  $k$  is essentially determined by the early concentration observations and the heavily overweighted starting value. It is reasonable to employ this method of computation only in cases where the initial concentration is known much more accurately than any of the succeeding values. This condition is achieved in practice when the initial reaction mixture can be made up exactly, the time of mixing is short compared to the interval between experimental data points, and the analytical determinations of  $C_{Ai}$  are relatively inaccurate. More often the standard deviation of  $C_{A0}$  is approximately equal to those of the  $C_{Ai}$ .

In the *short-interval method*, one computes a value of the rate constant  $k_{i-1,i}$  for each successive pair of data points. The arithmetic average of the rate constants computed in this manner is assumed to be a representative value of the rate constant. However, it can be shown that *when the time interval between experimental observations is constant, the short-interval method for computing  $k$  is equivalent to rejecting all but the first and last measurements!* The intermediate observations might just as well not have been made. When the time intervals are approximately but not exactly equal, the result is not much different. The greatest weights are placed on the initial and final measurements (which in practice are often the least accurate), and relatively small, varying weights are placed on the others.

If one does not desire to employ elaborate statistical methods for determining a rate constant, there is one good, simple method for determining  $k$  that depends on careful planning of the experimental work. To begin, one makes a series of  $n + 1$  measurements of the concentrations of interest at times  $0, t_1, 2t_1, 3t_1, nt_1$ . The total time interval ( $nt_1$ ) should be less than the time for 50% conversion of the limiting reagent ( $\tau_{1/2}$ ). After a known period of time  $\Delta$  that is as large as or larger than  $\tau_{1/2}$ , one makes a second series of  $n + 1$  measurements of the concentrations at times that differ by the constant increment  $t_1$ .

One then proceeds to calculate a value of the rate constant for each pair of points separated by a time  $\Delta$  [i.e., a value is calculated from the points corresponding to (0 and  $\Delta$ ),  $t_1$  and  $(\Delta + t_1)$ ,  $2t_1$  and  $(\Delta + 2t_1)$ , etc.]. The arithmetic mean of these values is a good representative value of the rate constant. In this technique each data point is used once and only once, and the probable errors of the quantities that are averaged are all of comparable magnitude. For

in the first-order case it is apparent from equation (3.1.8) that the average value of the rate constant is given by

$$\bar{k} = \frac{1}{(n+1)\Delta} \sum_{i=0}^{i=n} \ln \left( \frac{C_{Ai}}{C'_{Ai}} \right) \quad (3.3.24)$$

where  $C_{Ai}$  and  $C'_{Ai}$  are the concentrations of the species of interest at times  $t_1$  and  $\Delta + it_1$ , respectively.

This approach can be used with other simple rate expressions to determine a representative value of the reaction rate constant. Moreover, the experimental plan on which this technique is based will provide data over such a range of fraction conversions that it is readily adapted to various graphical techniques. Illustration 3.4 indicates how this approach is used to determine a reaction rate constant.

One may also use the methods of the statistician to determine average rate constants (e.g., the standard unweighted least-squares procedure). The unweighted least-squares analysis is based on the assumption that the best value of the rate constant  $k$  is the one that minimizes the sum of the squares of the residuals. In the general case one should regard the zero time point as an adjustable constant to avoid undue weighting of the initial point. An analysis of this type gives the following expressions for first- and second-order rate constants:

First-order rate law:

$$\bar{k} = \frac{\sum (t_i \ln C_{Ai}) - [(\sum t_i) (\sum \ln C_{Ai}) / n]}{[(\sum t_i^2) / n] - \sum t_i^2} \quad (3.3.25)$$

Class I, second-order rate law:

$$\bar{k} = \frac{\sum (t_i / C_{Ai}) - (1/n) (\sum 1/C_{Ai}) (\sum t_i)}{\sum (t_i^2) - (1/n) (\sum t_i)^2} \quad (3.3.26)$$

These expressions apply to constant volume systems in which  $\nu_A = -1$ . The sums are taken from  $i = 1$  to  $i = n$ . Although use of these equations is somewhat laborious for hand calculations, they are easily handled by even the simplest types of computers using spreadsheets.

Although the unweighted least squares method of data analysis is commonly used for the determination of reaction rate constants, it *does not* yield the *best possible* value for  $k$ . There are two principal reasons for this failure.

1. All points are assigned equal weights.
2. Functions of the measured concentrations must be used in the equations defining the residuals.

Statisticians have developed general calculation procedures that avoid these difficulties. Many software libraries contain programs that perform the necessary statistical calculations and relieve the engineer of this burden. For

discussions of the use of weighted least squares methods for the analysis of kinetic data, see Margerison's review (8) on the treatment of experimental data and the treatments of Kittrell et al. (9) and Peterson (10).

### 3.3.2.3 Integral Methods for the Analysis of Kinetic Data: Fractional Life Methods

The time necessary for a given fraction of a limiting reagent to react will depend on the initial concentrations of the reactants in a manner that is determined by the rate expression for the reaction. This fact is the basis for the development of the fractional life method (in particular, the half-life method) for the analysis of kinetic data. The half-life, or half-period, of a reaction is the time necessary for one-half of the original reactant to disappear. In constant-volume systems it is also the time necessary for the concentration of the limiting reagent to decline to one-half of its original value.

The fractional life approach is most useful as a means of obtaining a preliminary estimate of the reaction order. It is not recommended for the accurate determination of rate constants. Moreover, it cannot be used for systems that do not obey  $n$ th-order rate expressions.

If one combines the definition of the reaction rate in variable volume systems with a general  $n$ th-order rate expression, one finds that the time necessary to achieve a specified fraction conversion is given by

$$t_f = \int_0^{\xi} \frac{d\xi}{V k C_A^n} = \int_0^{f_A} \frac{n_{A0} df_A}{-\nu_A V k C_A^n} \quad (3.3.27)$$

or, using equations (3.1.40) and (3.1.47),

$$t_f = \frac{1}{C_{A0}^{n-1}} \int_0^{f_A} \frac{(1 + \delta_A f_A)^{n-1} df_A}{-k \nu_A (1 - f_A)^n} \quad (3.3.28)$$

This relation indicates that for all values of  $n$ ,  $k$ ,  $\nu_A$ , and  $\delta_A$ , the fractional life is inversely proportional to the initial concentration raised to the  $(n-1)$ th power. A given fractional life is independent of initial concentration for first-order reactions. It increases with  $C_{A0}$  for  $n$  less than 1, and it decreases with  $C_{A0}$  for  $n$  greater than 1.

For constant volume conditions,  $\delta_A = 0$  and

$$t_f = \frac{1}{\nu_A (1 - n) k C_{A0}^{n-1}} \left[ \frac{1}{(1 - f)^{n-1}} - 1 \right] \quad (3.3.29) V$$

with

$$t_{1/2} = \frac{2^{n-1} - 1}{\nu_A k C_{A0}^{n-1} (1 - n)} \quad \text{when } n \neq 1 \quad (3.3.30) V$$

For first-order reactions,

$$t_f = \frac{\ln(1-f)}{k\nu_A} \quad (3.3.31) \text{ V}$$

with

$$t_{1/2} = \frac{\ln 2}{k} \quad \text{for } \nu_A = -1 \quad (3.3.32) \text{ V}$$

Equations (3.3.28) and (3.3.29) indicate that plots of  $\log t_f$  versus  $\log C_{A0}$  are linear and that reaction orders may be determined from the slopes of such plots (slope =  $1 - n$ ). For constant-volume systems there is another method based on equations (3.3.29) and (3.3.31) by which one can obtain preliminary estimates of the reaction order. From the data from a single experimental run or from different runs using the same initial composition, one may determine the times necessary to achieve two different fraction conversions. The ratio of these times ( $t_{f1}$  and  $t_{f2}$ ) is given by

$$\frac{t_{f1}}{t_{f2}} = \frac{[1/(1-f_1)^{n-1}] - 1}{[1/(1-f_2)^{n-1}] - 1} \quad \text{for } n \neq 1 \quad (3.3.33) \text{ V}$$

and

$$\frac{t_{f1}}{t_{f2}} = \frac{\ln(1-f_1)}{\ln(1-f_2)} \quad \text{for } n = 1 \quad (3.3.34) \text{ V}$$

The value of this ratio is characteristic of the reaction order. Partial reaction times for various rate expressions of the form  $r = kC_A^n$  are presented in Table 3.1, together with some useful ratios of reaction times. By using ratios of the

partial reaction times based on experimental data, one is able to obtain a quick estimate of the reaction order with minimum effort. Once this estimate is in hand, one may proceed to use a more exact method of determining the reaction rate parameters.

### 3.3.2.4 Integral Methods for the Analysis of Kinetic Data: Guggenheim's Method for First-Order Reactions

Guggenheim (11) developed a special method that is useful in obtaining the rate constant *for a first-order reaction* when an accurate value of the initial reactant concentration is not available. It requires a series of readings of the parameter being used to follow the progress of the reaction at times  $t_1$ ,  $t_2$ ,  $t_3$ , etc. and at times  $t_1 + \Delta$ ,  $t_2 + \Delta$ ,  $t_3 + \Delta$ , etc. The time increment  $\Delta$  should be comparable in magnitude to the half-life of the reaction. If we denote the extents of reaction at times  $t_1$  and  $t_1 + \Delta$  by  $\xi_1$  and  $\xi'_1$ , respectively, equation (3.1.36) indicates that

$$\xi_1 = \frac{n_{A0}}{\nu_A} (e^{\nu_A k t_1} - 1) \quad (3.3.35)$$

and

$$\xi'_1 = \frac{n_{A0}}{\nu_A} (e^{\nu_A k (t_1 + \Delta)} - 1) \quad (3.3.36)$$

where  $n_{A0}$  need not be known. Subtraction of equation (3.3.36) from (3.3.35) gives

$$\xi_1 - \xi'_1 = \frac{n_{A0}}{\nu_A} e^{\nu_A k t_1} (1 - e^{\nu_A k \Delta}) \quad (3.3.37)$$

**Table 3.1** Fractional Life Relationships for Constant Volume Systems

Partial reaction time	Reaction order $n$				
	0	1	2	3	$n$
$t_{1/4}$	$-\frac{1}{4} \frac{C_{A0}}{\nu_A k}$	$\frac{\ln(4/3)}{k}$	$-\frac{1}{3} \frac{1}{\nu_A k C_{A0}}$	$-\frac{7}{18} \frac{1}{\nu_A k C_{A0}^2}$	$\frac{(4/3)^{n-1} - 1}{(1-n)\nu_A k C_{A0}^{n-1}}$
$t_{1/3}$	$-\frac{1}{3} \frac{C_{A0}}{\nu_A k}$	$\frac{\ln(3/2)}{k}$	$-\frac{1}{2} \frac{1}{\nu_A k C_{A0}}$	$-\frac{5}{8} \frac{1}{\nu_A k C_{A0}^2}$	$\frac{(3/2)^{n-1} - 1}{(1-n)\nu_A k C_{A0}^{n-1}}$
$t_{1/2}$	$-\frac{1}{2} \frac{C_{A0}}{\nu_A k}$	$\frac{\ln 2}{k}$	$-\frac{1}{\nu_A k C_{A0}}$	$-\frac{3}{2} \frac{1}{\nu_A k C_{A0}^2}$	$\frac{2^{n-1} - 1}{(1-n)\nu_A k C_{A0}^{n-1}}$
$t_f$	$-f \frac{C_{A0}}{\nu_A k}$	$-\frac{\ln(1-f)}{k}$	$-\frac{f/(1-f)}{\nu_A k C_{A0}}$	$-\frac{(2f-f^2)}{2(1-f)^2 \nu_A k C_{A0}^2}$	$\frac{[1/(1-f)]^{n-1} - 1}{(1-n)\nu_A k C_{A0}^{n-1}}$
$\frac{t_{1/2}}{t_{1/4}}$	2.000	2.409	3.000	3.857	$\frac{2^{n-1} - 1}{(4/3)^{n-1} - 1}$
$\frac{t_{1/2}}{t_{1/3}}$	1.500	1.709	2.000	2.400	$\frac{2^{n-1} - 1}{(3/2)^{n-1} - 1}$
$\frac{t_f'}{t_f''}$	$\frac{f'}{f''}$	$\frac{\ln(1-f')}{\ln(1-f'')}$	$\left(\frac{f'}{1-f'}\right) \left(\frac{1-f''}{f''}\right)$	$\frac{f'(2-f')(1-f'')^2}{(1-f')^2 f''(2-f'')}$	$\frac{[1/(1-f')]^{n-1} - 1}{[1/(1-f'')]^{n-1} - 1}$

Rearrangement of this equation yields the logarithmic form

$$\ln(\xi_1 - \xi'_1) - \nu_A k t_1 = \ln \left[ \frac{n_{A0}}{\nu_A} (1 - e^{\nu_A k \Delta}) \right] \quad (3.3.38)$$

Similar equations are valid at times  $t_2, t_3$ , etc. In all cases, however, the right side of these equations will be a constant, because the time increment  $\Delta$  is a constant. Thus, at time  $t_i$ ,

$$\ln(\xi_i - \xi'_i) = \nu_A k t_i + \text{constant} \quad (3.3.39)$$

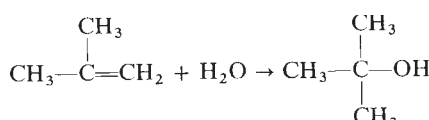
For a reaction that obeys a first-order rate expression a plot of  $\ln(\xi_i - \xi'_i)$  versus  $t$  will thus give a straight line with a slope equal to  $\nu_A k$ .

This technique is readily adaptable for use with the generalized additive physical approach discussed in Section 3.3.3.2. It is applicable to systems that can be characterized by “apparent” first-order rate constants. These systems include not only irreversible reactions that are either truly first-order or pseudo first-order, but also reaction networks consisting solely of competitive (parallel) irreversible first-order reactions. In addition, reversible reactions that are first-order in both the forward and reverse directions can be analyzed using the generalized Guggenheim approach. The technique provides an example of the advantages that can be obtained by careful planning of kinetics experiments instead of allowing the experimental design to be dictated entirely by laboratory convention and/or experimental convenience.

Guggenheim’s technique has been extended to other order reactions (12, 13), but the final expressions are somewhat cumbersome.

### ILLUSTRATION 3.4 Use of Guggenheim’s Method and a Numerical Integral Procedure to Determine the Rate Constant for the Hydration of Isobutene in Hydrochloric Acid Solution

Ciapetta and Kilpatrick (14) used a dilatometric technique to investigate the kinetics of the hydration of isobutene in perchloric acid solution at 25°C:



The dilatometer readings ( $h$ ) below are given in arbitrary units and are arranged in pairs taken at a fixed interval of

2 h. They are related to the extent of reaction by

$$\frac{\xi}{\xi_\infty} = \frac{h - h_0}{h_\infty - h_0}$$

1. Use Guggenheim’s method to determine the pseudo first-order rate constant.
2. Given the additional fact that the reading at “infinite” time is 12.16, use a numerical averaging procedure to determine the reaction rate constant.

The initial concentrations (in mol/L) are  $\text{HClO}_4 = 0.3974$  and  $\text{C}_4\text{H}_8 = 0.00483$ .

Time, $t$ (min)	Dilatometer reading at time $t$	Dilatometer reading at time $t + 2$ h
0	18.84	13.50
10	17.91	13.35
20	17.19	13.19
30	16.56	13.05
40	16.00	12.94
50	15.53	12.84
60	15.13	12.75
70	14.76	12.69

### Solution

Equation (3.3.39) indicates that the natural logarithm of the difference in extents of reactions at times  $t$  and  $t + \Delta$  should be linear in  $t$ . The difference between the extents of reaction at times  $t$  and  $t + \Delta$  is

$$\xi - \xi' = \frac{h - h'}{h_\infty - h_0} \xi_\infty \quad (\text{A})$$

Combination of equations (A) and (3.3.39) gives

$$\ln(h - h') = \nu_A k t + \ln \left( \frac{h_\infty - h_0}{\xi_\infty} \right) + \text{constant}$$

If one notes that for this reaction  $\nu_A = -1$ , and that the quantity  $\ln((h_\infty - h_0)/\xi_\infty)$  is itself a constant,

$$\ln(h - h') = -kt + \text{a new constant} \quad (\text{B})$$

Note that  $k$  can be determined from the slope of a plot of the left side of equation (B) versus time and that this plot can be prepared without a knowledge of the dilatometer readings at times zero and infinity. The data are worked up below and plotted in Figure I3.4 using semi-logarithmic coordinates.

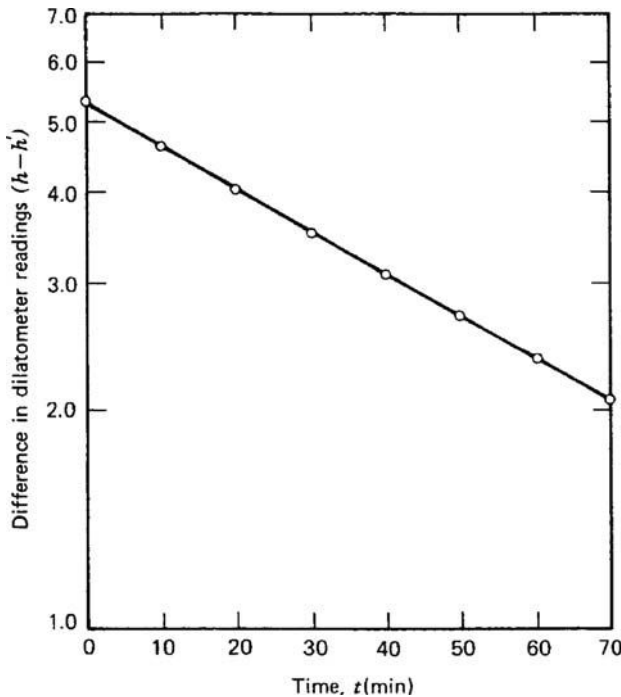


**Figure I3.4** Use of a semi-logarithmic Guggenheim plot to determine a first-order rate constant.

Time, $t$ (min)	$h - h'$
0	5.34
10	4.56
20	4.00
30	3.51
40	3.06
50	2.69
60	2.38
70	2.07

From the slope of the plot,

$$k = \frac{\ln(5.26/2.06)}{70} = 1.34 \times 10^{-2} \text{ min}^{-1}$$

This value compares favorably with the literature value of  $1.32 \times 10^{-2} \text{ min}^{-1}$ , which is based on much more data.

The half-life of this reaction is given by

$$t_{1/2} = \frac{0.693}{k} = \frac{0.693}{1.34 \times 10^{-2}} = 51.7 \text{ min}$$

The time  $\Delta$  between readings (2 h) is thus greater than the reaction half-life, and the numerical averaging procedure leading to equation (3.3.24) could be used for an analysis of these data if an estimate of the reading at infinite time can be obtained. To manipulate this equation to a form that can make use of the available data, one can note that:

$$1. \frac{C_{Ai}}{C'_{Ai}} = \frac{C_{A0} - \xi^*}{C_{A0} - \xi^{*'}} = \frac{1 - (\xi^*/C_{A0})}{1 - (\xi^{*'}/C_{A0})}$$

$$2. \frac{h - h_0}{h_\infty - h_0} = \frac{\xi}{\xi_\infty} = \frac{\xi^*}{\xi_\infty^*} = \frac{\xi^*}{C_{A0}}$$

$$3. 1 - \frac{\xi^*}{C_{A0}} = \frac{h_\infty - h}{h_\infty - h_0}$$

$$4. \frac{C_{Ai}}{C'_{Ai}} = \frac{h_\infty - h}{h_\infty - h'} \text{ (from 1 and 3)}$$

Thus, the average value of the reaction rate constant can be calculated numerically from

$$\bar{k} = \frac{1}{(n+1)\Delta} \sum_{i=0}^{i=n} \ln \left( \frac{h_\infty - h_i}{h_\infty - h'_i} \right)$$

where  $n$  is the number of pairs of data points. Numerical calculations indicate that

$$\bar{k} = \frac{1}{(7+1)(120)}(12.768) = 1.33 \times 10^{-2} \text{ min}^{-1}$$

This value is consistent with that obtained above.

### 3.3.3 Techniques for the Analysis of Reaction Rate Data That Are Suitable for Use with Either Integral or Differential Methods

#### 3.3.3.1 Use of Excess Concentrations: The Isolation Method

The method of isolation for elucidating the form of the reaction rate expression is based on the simplifications that occur when the concentration of one or more of the reactants appearing in the rate expression is much greater than that called for by the stoichiometry of the reaction.

Consider a power law rate expression

$$r = k C_A^{\beta_A} C_B^{\beta_B} C_C^{\beta_C} \quad (3.3.40)$$

If one now plans an experiment such that  $C_{B0} \gg C_{A0}$  and  $C_{C0} \gg C_{A0}$ , the only concentration that will change appreciably during the course of the experiment is that of species A. This situation implies that the above power law will simplify to the following form:

$$r = k' C_A^{\beta_A} \quad (3.3.41)$$

where

$$k' = k C_{B0}^{\beta_B} C_{C0}^{\beta_C} \quad (3.3.42)$$

We thus have a pseudo  $\beta_A$ th-order reaction and an effective rate constant  $k'$ . The methods discussed in Sections 3.3.1 and 3.3.2 may now be used to determine  $k'$  and  $\beta_A$ . It should be noted that this technique should

always be used in conjunction with other methods of determining the rate expression, because it forces the data to fit equation (3.3.40) when, in fact, the rate expression may be more complex. If one observes that the exponents  $\beta_i$  are nonintegers that vary continuously with temperature or pressure, this is an indication that the rate expression is more complex than equation (3.3.40).

### 3.3.3.2 Use of Physical Property Measurements to Determine the Extent of Reaction

The most useful physical properties for use in kinetics studies are those that are an additive function of the contributions of the various constituents, the contribution of each species being a linear function of its concentration. Total pressure, absorbance, optical rotation, and the electrical conductivity of dilute solutions are all properties of this type. In this section we indicate how such physical property measurements may be easily related to the extent of reaction per unit volume.

Consider some physical property  $\lambda$  that reflects the contributions of the various species present in the reaction mixture:

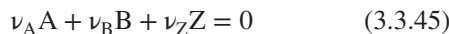
$$\lambda = \sum_i \lambda_i \quad (3.3.43)$$

where  $\lambda$  is the experimentally measured quantity and  $\lambda_i$  is the contribution of the  $i$ th species. Furthermore, for the derivation presented below, it is necessary that the contribution of a species be a linear function of the concentration of that species:

$$\lambda_i = g_i + h_i C_i \quad (3.3.44)$$

where  $g_i$  and  $h_i$  are constants characteristic of species  $i$ . The constants  $g_i$  are normally zero, but can have any value.

If one now considers the general reaction



the concentrations of the various species at time  $t$  may be expressed in terms of the extent of reaction per unit volume  $\xi^*$ :

$$C_i = C_{i0} + \nu_i \xi^* \quad (3.3.46)$$

The experimental variable  $\lambda$  may now be written as

$$\lambda = \lambda_M + \lambda_A + \lambda_B + \lambda_Z \quad (3.3.47)$$

where  $\lambda_M$  includes the contribution of the solvent or medium in which the reaction is carried out as well as the contributions of any inert species that are present. It also includes any contributions arising from the reaction vessel

itself. Combination of equations (3.3.44) and (3.3.47) gives

$$\lambda = \lambda_M + g_A + h_A C_A + g_B + h_B C_B + g_Z + h_Z C_Z \quad (3.3.48)$$

If the initial property value is denoted by  $\lambda_0$ ,

$$\lambda_0 = \lambda_M + g_A + h_A C_{A0} + g_B + h_B C_{B0} + g_Z + h_Z C_{Z0} \quad (3.3.49)$$

the change in the value of the property  $\lambda$  between time zero and time  $t$  is given by

$$\lambda - \lambda_0 = h_A (C_A - C_{A0}) + h_B (C_B - C_{B0}) + h_Z (C_Z - C_{Z0}) \quad (3.3.50)$$

Combination of equations (3.3.46) and (3.3.50) gives

$$\lambda - \lambda_0 = h_A \nu_A \xi^* + h_B \nu_B \xi^* + h_Z \nu_Z \xi^* = \xi^* \sum_i (h_i \nu_i) \quad (3.3.51)$$

As equation (3.3.51) indicates, the change in  $\lambda$  is directly proportional to the extent of reaction per unit volume. Similarly, the change in  $\lambda$  between times zero and infinity is given by

$$\lambda_\infty - \lambda_0 = \xi_\infty^* \sum_i (h_i \nu_i) \quad (3.3.52)$$

The ratio of the extent of reaction at time  $t$  to that at equilibrium is then

$$\frac{\xi^*}{\xi_\infty^*} = \frac{\lambda - \lambda_0}{\lambda_\infty - \lambda_0} \quad (3.3.53)$$

Equation (3.3.53) is an extremely useful relation that is applicable to a very large number of physical properties. If the reaction is reversible, the value of  $\xi_\infty^*$  can easily be determined using the expression for the equilibrium constant in terms of reactant and product concentrations. If the reaction is irreversible,  $\xi_\infty^*$  may be determined from the initial concentration of the limiting reagent:

$$\xi_\infty^* = -\frac{C_{\text{lim},0}}{\nu_{\text{lim}}} \quad (3.3.54)$$

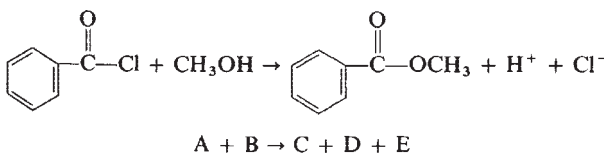
The concentrations of the various species present in the reaction mixture can be determined by combining equations (3.3.53) and (3.3.46):

$$C_i = C_{i0} + \nu_i \xi_\infty^* \left( \frac{\lambda - \lambda_0}{\lambda_\infty - \lambda_0} \right) \quad (3.3.55)$$

These concentrations may be used in the various integral and differential methods for the analysis of kinetic data that have been described in previous sections. An example of the use of this approach is given in Illustration 3.5.

### ILLUSTRATION 3.5 Use of Conductivity Measurements in Conjunction with the Graphical Integral Method for the Analysis of Reaction Rate Data

Biordi (15) employed conductivity measurements to monitor the progress of the methanolysis of benzoyl chloride at 25°C in methanol solution:



Under the conditions of the experiment, it is known that the reaction may be considered to be irreversible. From the data that follow, determine the order of the reaction with respect to benzoyl chloride and the apparent rate constant.

Time, $t$ (s)	Solution conductivity $\times 10^4 (\Omega^{-1}/\text{cm})$
0	Negligible
27	0.352
48	0.656
55	0.732
62	0.813
70	0.900
79	0.969
86	1.07
93	1.12
100	1.21
105	1.26
114	1.33
120	1.40
:	:
10,800	3.50

### Solution

Because a vast excess of methanol (the solvent) was used, the concentration of methanol was essentially invariant, and it is appropriate to assume a rate expression of the form  $r = k' C_A^{\beta_A}$ . Since the conductivity of the solution is a property that is an additive function of contributions that are linear in concentration, the generalized physical property approach may be used:

$$\frac{\kappa - \kappa_0}{\kappa_\infty - \kappa_0} = \frac{\xi^*}{\xi_\infty^*} = \frac{\xi}{C_{A0}} \quad (\text{A})$$

where  $\kappa_\infty$  is taken to be the conductivity reading at 10,800 s. The integrated form of the rate law for a first-order reaction is given by equation (3.1.4):

$$-kt = \ln \left( \frac{C_{A0} - \xi^*}{C_{A0}} \right) = \ln \left( 1 - \frac{\xi^*}{C_{A0}} \right) \quad (\text{B})$$

Combination of equations (A) and (B) gives

$$-kt = \ln \left( 1 - \frac{\kappa - \kappa_0}{\kappa_\infty - \kappa_0} \right) = \ln \left( \frac{\kappa_\infty - \kappa}{\kappa_\infty - \kappa_0} \right)$$

or

$$\ln(\kappa_\infty - \kappa) = \ln(\kappa_\infty - \kappa_0) - kt \quad (\text{C})$$

If a plot of the left side of equation (C) versus time is linear, the reaction is first-order and the slope of this plot is equal to  $(-k)$ . A plot of the data in this form indicates that the reaction is indeed first-order with respect to benzoyl chloride. The slope of the line corresponds to a pseudo first-order rate constant of  $(4.24 \pm 0.041) \times 10^{-3} \text{ s}^{-1}$ .

#### 3.3.3.3 Tests for the Goodness of Fit of a Mathematical Model to Experimental Rate Data

When fitting a mathematical model to a particular set of data, practicing engineers usually also seek to obtain a statistical measure of the goodness of fit. Sometimes it is necessary to decide which of several rate laws best fits a data set, whereas at other times the engineer desires to ascertain the confidence intervals or uncertainties associated with the kinetic parameters obtained from the fit of a specific model to the data. Standard computer tools for fitting data usually have built-in functions with options that provide statistical analysis or have special tool kits for advanced data interpretation. One simple measure of the quality of the fit is the coefficient of determination, or  $r^2$  value. Although this coefficient is very useful for epidemiological studies and other applications inquiring as to whether a relationship exists between the observed result and any of several possible causal variables, use of the  $r^2$  value is not recommended for the evaluation of kinetic data when one fully expects the rate to vary with reactant concentrations. By contrast, the primary goal of the practicing engineer is to fit a particular mathematical model to the data rather than to establish the existence of a correlation. In particular, it is difficult to use the  $r^2$  value to obtain a meaningful comparison of the quality of fit provided by linearized forms of different rate laws based on integral methods of data analysis because the associated nonlinear transformations change the weighting of the underlying data and make it more difficult to assess the uncertainties associated with the kinetic parameters.

Instead, when fitting a linear function to the linearized form of an integrated rate expression one should use

engineering software that reports the least-squares best-fit slope and intercept, together with the standard errors in both of these parameters. In a spreadsheet such as Excel, the LINEST function can generate a  $2 \times 2$  array of slope, intercept, and the standard errors in the slope and intercept. Engineering software containing nonlinear solver capability typically contains options to report standard errors in fitted parameters. These standard errors may be used to determine the relative accuracy of the fitted parameters for comparison of the quality of fit for different underlying models. When a linearized model predicts a line through the origin and a fit of data with a model of the form  $y = mx + b$  gives a nonzero intercept, the standard error can be used to determine if the intercept of the best fit to the data includes the origin within its uncertainty. The standard error can also be combined with Student's *t*-distribution to determine confidence intervals at the 95% level. In Matlab, the Statistics Toolbox is one of several options for regression analysis that include commands for confidence intervals on the resulting fit parameters. Other engineering software packages contain similar features. Different user communities have their own standards for how to report confidence intervals or the quality of the fit of a model to data. Interested readers should explore statistics textbooks to learn about related concepts that are useful for more advanced applications.

### 3.3.4 Determination of the Activation Energy

In this section we focus on the problem of determining the temperature dependence of the reaction rate expression (i.e., the activation energy of the reaction). Virtually all rate constants may be written in Arrhenius form:

$$k = Ae^{-E/RT} \quad (3.3.56)$$

where  $E$  is the activation energy,  $A$  the frequency (or pre-exponential) factor for the reaction,  $R$  the gas constant, and  $T$  the absolute temperature. The variation of  $k$  with temperature may be determined by differentiating the logarithmic form of this equation:

$$\frac{d \ln k}{dT} = \frac{E}{RT^2} \quad (3.3.57)$$

Because virtually all known activation energies are positive quantities, this relation indicates that the reaction rate constant will almost always increase with temperature. A useful alternative form of this relation is

$$\frac{d \ln k}{d(1/T)} = -\frac{E}{R} \quad (3.3.58)$$

If one has data on the reaction rate constant at several temperatures, this equation provides the basis for the most

commonly used method for determining the activation energy of a reaction. If  $E$  is temperature invariant, a plot of  $\ln k$  versus the reciprocal of the absolute temperature should be linear with slope  $-E/R$ . Alternatively, if the rate constants are plotted as  $\log k$  versus  $1/T$ , the corresponding slope is  $[-E/(2.303R)]$ . A typical plot is shown in Figure 3.4 for the reaction  $\text{H}_2 + \text{I}_2 \rightarrow 2\text{HI}$ . The slope corresponds to an activation energy of 44.3 kcal/mol.

A somewhat less accurate method for determining the activation energy involves integration of equation (3.3.58) over the interval between two data points, assuming that  $E$  is constant:

$$\ln \left( \frac{k_2}{k_1} \right) = -\frac{E}{R} \left( \frac{1}{T_2} - \frac{1}{T_1} \right) \quad (3.3.59)$$

When more than two data points are available, the graphical method is much better to use than common averaging techniques. It gives one a visual picture of the fit of the data to equation (3.3.58). If one has several data points and estimates of the uncertainty in each point, a weighted least-squares fit of the data would then be appropriate.

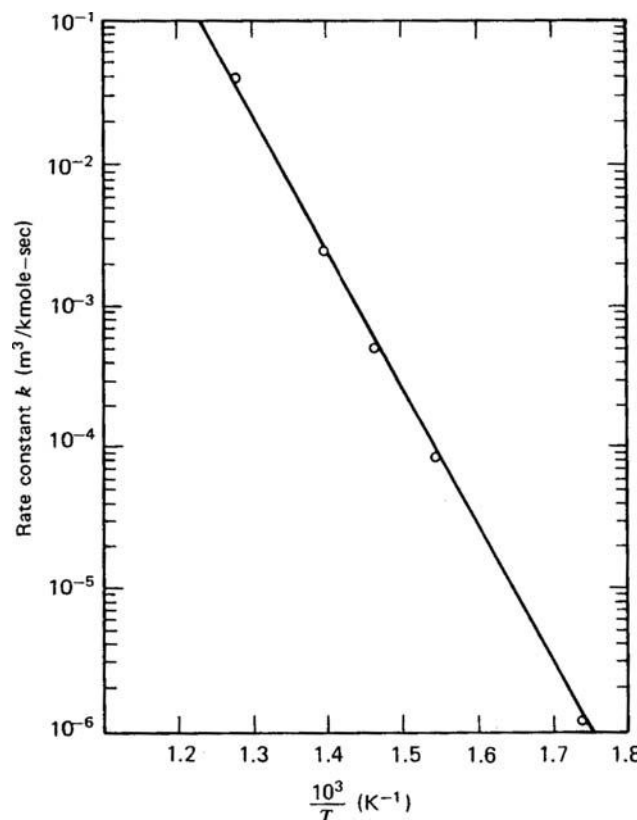


**Figure 3.4** Arrhenius plot of the rate constant for the reaction  $\text{H}_2 + \text{I}_2 \rightarrow 2\text{HI}$  (16).

### 3.3.5 Precision of Rate Measurements for Simple Irreversible Reactions

To obtain a feeling for the major sources of uncertainty and error in the calculation of reaction rate constants, it is useful to consider the nature of the errors in the measurement of these parameters.

#### 3.3.5.1 Precision/Uncertainties Associated with Reaction Rate Constants

A reaction rate constant can be calculated from the integrated form of a kinetic expression if one has data on the state of the system at two or more different times. This statement assumes that sufficient measurements have been made to establish the functional form of the reaction rate expression. Once the equation for the reaction rate constant has been determined, standard techniques for error analysis may be used to evaluate the error expected in the reaction rate constant.

For a dependent variable  $y = f(x_1, x_2, x_3, \dots, x_m)$  which is a known function of the  $m$  independent variables  $x_1, x_2, x_3, \dots, x_m$ , the expected relative error in  $y$  resulting from the relative errors in  $x_1, x_2, x_3, \dots, x_m$  is given by

$$\left(\frac{\Delta y}{y}\right)^2 = \sum_{i=1}^m \left[ \left( \frac{\partial \ln f}{\partial \ln x_i} \right)^2 \left( \frac{\Delta x_i}{x_i} \right)^2 \right] \quad (3.3.60)$$

Equation (3.1.32) applies to a constant-volume system that follows  $n$ th-order kinetics. If we take  $\nu_A = -1$ , it can be rewritten as

$$k = \frac{C_{A1}^{n-1} - C_{A2}^{n-1}}{(n-1)(t_2 - t_1)C_{A2}^{n-1}C_{A1}^{n-1}} \quad (3.3.61)$$

where  $C_{A2}$  and  $C_{A1}$  are the concentrations of A present at times  $t_2$  and  $t_1$ , respectively, and where  $n \neq 1$ .

If one assumes that the errors in the four quantities  $t_1$ ,  $t_2$ ,  $C_{A1}$ , and  $C_{A2}$  are independent and that  $n$  is a known constant, the random error expected in the rate constant  $\Delta k$  may be expressed as follows:

$$\begin{aligned} \left(\frac{\Delta k}{k}\right)^2 &= \left( \frac{\partial \ln k}{\partial \ln t_1} \right)^2 \left( \frac{\Delta t_1}{t_1} \right)^2 + \left( \frac{\partial \ln k}{\partial \ln t_2} \right)^2 \left( \frac{\Delta t_2}{t_2} \right)^2 \\ &+ \left( \frac{\partial \ln k}{\partial \ln C_{A1}} \right)^2 \left( \frac{\Delta C_{A1}}{C_{A1}} \right)^2 \\ &+ \left( \frac{\partial \ln k}{\partial \ln C_{A2}} \right)^2 \left( \frac{\Delta C_{A2}}{C_{A2}} \right)^2 \end{aligned} \quad (3.3.62)$$

or

$$\begin{aligned} \left(\frac{\Delta k}{k}\right)^2 &= \left( \frac{\Delta t_1}{t_2 - t_1} \right)^2 + \left( \frac{\Delta t_2}{t_2 - t_1} \right)^2 \\ &+ \left[ \frac{(n-1)C_{A2}^{n-1}}{C_{A1}^{n-1} - C_{A2}^{n-1}} \right]^2 \left( \frac{\Delta C_{A1}}{C_{A1}} \right)^2 \\ &+ \left[ \frac{(1-n)C_{A1}^{n-1}}{C_{A1}^{n-1} - C_{A2}^{n-1}} \right]^2 \left( \frac{\Delta C_{A2}}{C_{A2}} \right)^2 \end{aligned} \quad (3.3.63)$$

For the case where  $n = 1$ , the corresponding equation is

$$\begin{aligned} \left(\frac{\Delta k}{k}\right)^2 &= \left( \frac{\Delta t_1}{t_2 - t_1} \right)^2 + \left( \frac{\Delta t_2}{t_2 - t_1} \right)^2 \\ &+ \left[ \frac{1}{\ln(C_{A1}/C_{A2})} \right]^2 \left( \frac{\Delta C_{A1}}{C_{A1}} \right)^2 \\ &+ \left[ \frac{1}{\ln(C_{A1}/C_{A2})} \right]^2 \left( \frac{\Delta C_{A2}}{C_{A2}} \right)^2 \end{aligned} \quad (3.3.64)$$

To illustrate the use of equation (3.3.63) for estimating the relative uncertainty in the reaction rate constant, consider an example where  $n = 2$ ,  $t_2 - t_1 = 100$  s, the uncertainty in each time measurement ( $\Delta t_1$  and  $\Delta t_2$ ) is 1 s,  $C_{A2} = 0.9C_{A1}$  (10% reaction), and the relative uncertainty in each concentration measurement is 0.01 (1%). Substitution of these values into equation (3.3.60) gives

$$\begin{aligned} \left(\frac{\Delta k}{k}\right)^2 &= \left( \frac{1}{100} \right)^2 + \left( \frac{1}{100} \right)^2 + \left( \frac{0.9}{1-0.9} \right)^2 (0.01)^2 \\ &+ \left( \frac{1}{1-0.9} \right)^2 (0.01)^2 \\ &= 10^{-4} + 10^{-4} + 81 \times 10^{-4} + 100 \times 10^{-4} \\ &= 183 \times 10^{-4} \end{aligned}$$

Thus, the relative uncertainty in the rate constant is

$$\frac{\Delta k}{k} = (183 \times 10^{-4})^{1/2} = \pm 13.7 \times 10^{-2} = \pm 0.137$$

Inspection of the various contributions to the uncertainty in the rate constant indicated above reveals that the major sources of error are the concentration measurements. Attempts to improve the accuracy of the rate constant should focus on trying to improve the accuracy of the concentration measurements (17). Figure 3.5 contains useful information concerning the converse of the problem we have just considered (i.e., what precision in analytical capability is required to measure  $k$  to a given degree of accuracy). The uncertainties are about the same for orders of reaction from zero to 4 and are primarily dependent on the extent of reaction occurring between the two points chosen. Inspection of this figure illustrates the dilemma the kineticist faces in planning experiments. To measure  $k$

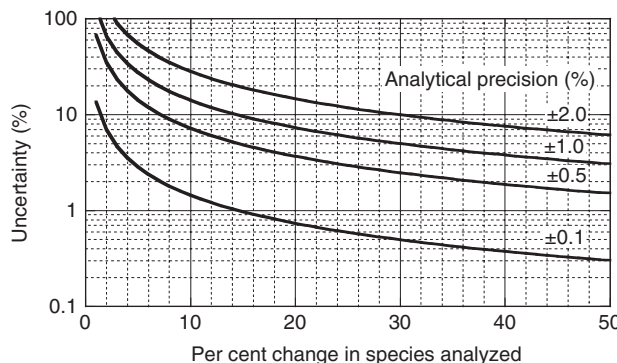


**Figure 3.5** Dependence of uncertainty in calculated rate constant on the percentage change in the concentration of the species for which one analyzes and the precision of the chemical analysis. (Figure courtesy of Professor F. Tiscareño of the Instituto Tecnológico de Celaya, Mexico. Used with permission.)

to within 1% uncertainty, he or she must be able to analyze for his or her reactants with a precision of approximately 0.1% at a conversion level of approximately 15%. If higher precision in  $k$  is desired, much higher analytical precision in the concentration measurements must be obtained and higher degrees of conversion must be used.

The situation is changed significantly if it is possible to monitor the appearance of products instead of the disappearance of reactants. The mathematics of the situation leads one to the general principle that whenever possible, it is advantageous to monitor the products during the initial stages and the reactants during the final stages of the reaction.

### 3.3.5.2 Precision of Activation Energy Measurements

The activation energy of a reaction can be determined from knowledge of the reaction rate constants for at least two different temperatures. The Arrhenius relation may be written in the form

$$E = \frac{RT_1 T_2}{T_2 - T_1} \ln \left( \frac{k_2}{k_1} \right) \quad (3.3.65)$$

If the errors in each of the experimental quantities  $k_1$ ,  $k_2$ ,  $T_1$ , and  $T_2$  are random, the relative error in the Arrhenius activation energy is given by

$$\begin{aligned} \left( \frac{\Delta E}{E} \right)^2 &= \left( \frac{T_2}{T_2 - T_1} \right)^2 \left( \frac{\Delta T_1}{T_1} \right)^2 \\ &+ \left( \frac{T_1}{T_2 - T_1} \right)^2 \left( \frac{\Delta T_2}{T_2} \right)^2 \\ &+ \left[ \frac{1}{\ln(k_2/k_1)} \right]^2 \left[ \left( \frac{\Delta k_1}{k_1} \right)^2 + \left( \frac{\Delta k_2}{k_2} \right)^2 \right] \end{aligned} \quad (3.3.66)$$

From this equation it can be seen that the relative error in the activation energy is strongly dependent on the size of the temperature interval chosen. Decreases in the size of the temperature interval greatly increase the uncertainty in  $E$  because they not only increase the contributions of the first two terms but also simultaneously increase the contribution of the last term, since the term  $\ln(k_2/k_1)$  in the denominator approaches zero as  $k_2$  approaches  $k_1$ .

To measure  $E$  over a 10°C temperature interval to within  $\pm 0.5\%$ , one generally requires temperature uncertainties of less than  $\pm 0.03^\circ\text{C}$  and rate constant uncertainties of 0.3%. Inspection of the curves in Figure 3.5 indicates that the latter requirement will necessitate analytical precision of  $\pm 0.1\%$  over an extended range of concentration changes. These numbers indicate the difficulty that one faces in obtaining precise measurements of the activation energy and why it is so difficult to observe the variation of  $E$  with temperature.

At room temperature the relative uncertainty in measuring  $E$  over 10°C temperature intervals is generally about  $\pm 5\%$  for gas phase reactions and about  $\pm 3\%$  for liquid phase reactions.

## LITERATURE CITATIONS

- BOUDART, M., *Kinetics of Chemical Processes*, Chap. I, Prentice-Hall, Englewood Cliffs, NJ, 1968.
- LEVENSPIEL, O., *Chemical Reaction Engineering*, 2nd ed., Wiley, New York, 1972.
- BUNNELL, J. F., *The Interpretation of Rate Data*, in *Investigation of Rates and Mechanisms of Reactions*, Vol. VIII, Part I, of *Technique of Organic Chemistry*, S. L. FREISS, E. S. LEWIS, and A. WEISSBERGER (Eds.), Interscience, New York, 1961.
- NEYENS, A., unpublished results cited on page 88 of J. C. JUNGERS, J. C. BALACEANU, F. COUSSEMAN, F. ESCHARD, A. GIRAUD, M. HELLIN, P. LE PRINCE, and G. E. LIMIDO, *Cinétique Chimique Appliquée*, Société des Éditions Technip, Paris, 1958, Table VII, p. 88.
- DILLON, R. T., *J. Am. Chem. Soc.*, **54**, 952 (1932).
- HINSHELWOOD, C. N., and ASKEY, P. J., *Proc. R. Soc. London*, **A115**, 215 (1927).
- LIVINGSTON, R., Evaluation and Interpretation of Rate Data, in *Investigation of Rates and Mechanisms of Reactions*, Vol. VIII, Part I, of *Technique of Organic Chemistry*, S. L. FREISS, E. S. LEWIS, and A. WEISSBERGER, (Eds.), Interscience, New York, 1961.
- MARGERISON, D., The Treatment of Experimental Data, in *The Practice of Kinetics*, Vol. I of *Comprehensive Chemical Kinetics*, C. H. BAMFORD and C. F. H. TIPPER (Eds.), Elsevier, New York, 1969.
- KITTRILL, J. R., MEZAKI, R., and WATSON, C. C., *Ind. Eng. Chem.*, **58**, 50 (1966).
- PETERSON, T. I., *Chem. Eng. Sci.*, **17**, 203, (1962).
- GUGGENHEIM, E. A., *Phil. Mag.*, **1**, 538 (1926).
- ROSEVEARE, W. E., *J. Am. Chem. Soc.*, **53**, 1651 (1931).
- STURTEVANT, J. M., *J. Am. Chem. Soc.*, **59**, 699 (1937).
- CIAPETTA, F. G., and KILPATRICK, M., *J. Am. Chem. Soc.*, **70**, 641 (1948).
- BIORDI, J. C., *J. Chem. Eng. Data*, **15**, 166 (1970).
- MOELWYN-HUGHES, E. A., *Physical Chemistry*, p. 1109, Pergamon Press, New York, 1957.

17. BENSON, S. W., *The Foundations of Chemical Kinetics*, McGraw-Hill, New York, 1960.

## PROBLEMS

- 3.1** A.P. Gavriliv, V.F. Kochubei, and F.B. Moin [*Kinet. Catal.*, **16**, 978 (1976)] investigated the kinetics of the gas-phase reaction between HI and O<sub>2</sub> over the temperature range 100 to 200°C.



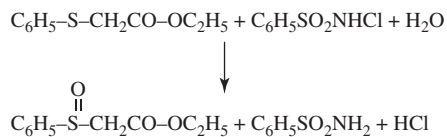
The following initial rate data are typical of this reaction.

rate × 10 <sup>5</sup> [mole/(cm <sup>3</sup> · s)]	C <sub>HI</sub> × 10 <sup>3</sup> (mol/cm <sup>3</sup> )	C <sub>O<sub>2</sub></sub> × 10 <sup>3</sup> (mol/cm <sup>3</sup> )
2.49	1.49	1.50
3.44	1.49	2.03
4.54	1.49	2.74
5.23	1.49	3.18
1.12	2.48	0.368
1.67	3.70	0.368
2.75	6.74	0.368
4.11	10.00	0.368

- (a) Determine the order of the reaction with respect to each reactant and the reaction rate constant. The orders may be assumed to be integers or half-integers.
- (b) The following initial rate data were also reported for systems of constant initial composition. What is the activation energy of this reaction?

Temperature (K)	Rate × 10 <sup>12</sup> [mol/(cm <sup>3</sup> · s)]
373	1.25
393	4.70
413	12.0
433	30.3
453	86.4
473	210

- 3.2** R. Gurumurthy, K. Sathiyaranayanan, and M. Gopalakrishnan [*Int. J. Chem. Kinet.*, **24**, 953 (1992)] studied the oxidation of several phenylmercaptoacetates (A) by chloramine-B (B) in aqueous ethanol media.



The following data are typical of this reaction at 30°C and a pH of ca. 6.5. Determine the order of the reaction with respect to each reactant (other than water) and the reaction rate constant.

Rate × 10 <sup>4</sup> (M/s)	C <sub>A</sub> × 10 <sup>2</sup> (M)	C <sub>B</sub> × 10 <sup>4</sup> (M)
0.5767	1.0	10.00
1.2788	1.5	10.00
2.3162	2.0	10.00
5.2434	3.0	10.00
9.4088	4.0	10.00
14.5155	5.0	10.00
20.4126	6.0	10.00
28.0147	7.0	10.00
37.2256	8.0	10.00
2.3624	2.0	2.00
2.3224	2.0	5.00
2.2840	2.0	7.50
2.2916	2.0	11.25
2.2944	2.0	15.00
2.2824	2.0	17.50
2.2796	2.0	20.00

- 3.3** A. M. Davis and W. H. Corcoran [*Ind. Eng. Chem.*, **11**, 431 (1972)] studied the reaction between nitrogen dioxide and acetaldehyde in the gas phase. The initial rate data in Table P3.3 were obtained at ambient temperature (22°C) and atmospheric pressure in a constant volume batch reactor.

**Table P3.3**

Trial	Nitrogen dioxide concentration × 10 <sup>4</sup> (mol/m <sup>3</sup> )	Acetaldehyde concentration (mol/m <sup>3</sup> )	Rate × 10 <sup>8</sup> [mol/(m <sup>3</sup> · s)]
1	8.49	4.04	2.895
2	8.21	2.65	1.919
3	12.47	6.88	7.198
4	9.78	6.70	5.650
5	10.71	1.93	1.798
6	8.01	7.98	5.451
7	10.08	1.24	1.099
8	6.77	2.80	1.662
9	6.62	7.06	4.010
10	6.98	7.97	4.739
11	8.44	4.19	3.089
12	6.33	4.36	2.439
13	7.51	4.70	3.101
14	9.41	3.09	2.444
15	7.80	5.68	3.862
16	6.91	5.92	3.418
17	12.81	6.56	7.274
21	9.19	5.18	4.068
22	7.82	5.50	3.660
24	8.37	6.20	4.479
25	9.71	4.27	3.471
26	7.20	4.64	2.870
27	6.61	2.22	1.265
28	11.44	5.58	5.586

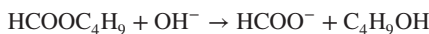
**Table P3.4**

Concentration of butylformate $\times 10^4$ (mol/cm <sup>3</sup> )	Concentration of hydroxide ion $\times 10^4$ (mol/cm <sup>3</sup> )	Temperature (K)	Rate $\times 10^7$ [mol/(cm <sup>3</sup> · s)]
6.5	5	298	4.88
5.5	5	298	3.98
3.3	5	298	2.13
1.7	5	298	0.95
0.63	5	298	0.28
0.43	5	298	0.18
3.3	8	298	3.08
3.3	6.5	298	2.62
3.3	3.5	298	1.61
3.3	2	298	1.04
3.3	1	298	0.61
3.3	5	308	2.98
3.3	5	318	4.08
3.3	5	328	5.49
3.3	5	338	7.24
3.3	5	348	9.41
3.3	5	358	12.04

What is the order of the reaction with respect to each reactant?

What is the rate constant?

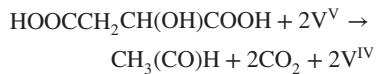
- 3.4** B. K. Abdalla [J. Chem. Tech. Biotechnol. **65**, 335–342 (1996)] studied the kinetics of the hydrolysis of *n*-butylformate using a rising-drop technique. In this experiment, small drops consisting of the ester dissolved in toluene rise under the influence of gravity through a vertical column containing an aqueous solution of NaOH. The entire system is maintained at a constant temperature. The overall stoichiometry of the reaction can be written as



The reaction may be regarded as irreversible.

The data in Table P3.4 are typical of those reported by Abdalla. Use these data to determine the orders of the reaction with respect to the concentrations of the ester and hydroxide ions, the value of the rate constant at 298 K, the activation energy for the reaction and the preexponential factor. You may assume that the rate expression can be written in the general *n*th-order form, but you may not assume that the orders are integers.

- 3.5** M. Ziglio and K. Takashima [Int. J. Chem. Kinet., **27**, 1055–1064 (1995)] studied the oxidation of malic acid by vanadium (V) in aqueous sulfuric acid:



- (a)** These researchers conducted a series of experiments in which a large excess of either malic acid or vanadium was present to force the rate expression to degenerate to a

**Table P3.5**

Run	HMA (M)	$\text{V}^{\text{V}}(\text{M})$	$\text{H}^+(\text{M})$	Initial rate $\times 10^5$ (M/s)
1	0.50	0.01	1.0	3.78
2	0.75	0.01	1.0	5.85
3	1.00	0.01	1.0	7.43
4	1.25	0.01	1.0	9.60
5	1.50	0.01	1.0	11.97
6	1.00	0.005	1.0	3.38
7	1.00	0.015	1.0	11.88
8	1.00	0.020	1.0	17.54
9	1.00	0.025	1.0	23.30
10	1.00	0.01	0.50	3.95
11	1.00	0.01	0.75	5.82
12	1.00	0.01	1.25	9.05
13	1.00	0.01	1.50	11.90

simpler mathematical form. The entries in Table P3.5 are representative of this reaction at 30°C in aqueous sulfuric acid solutions whose ionic strength is 2 M.

If one assumes a rate expression of the general power law form, determine the orders of the reaction with respect to the concentrations of  $\text{V}^{\text{V}}$ , malic acid, and hydrogen ions. When the plots of the data indicate that the orders are within 0.1 of an integer or half-integer, you may round your value to the integer or half-integer indicated. What is the corresponding value of the rate constant at this temperature and ionic strength?

- (b)** These investigators also conducted a second series of experiments to determine the temperature dependence of the rate. For reaction at an ionic strength of 2 M, they reported the following values of pseudo first-order rate constants.

Temperature (°C)	Rate constant $\times 10^3$ (s <sup>-1</sup> )	
	HMA = 1.0 M	HMA = 0.5 M
20	4.25	1.89
25	5.66	2.81
30	7.43	3.52
35	10.31	5.39
40	13.25	7.21

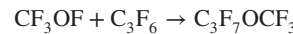
Determine the activation energy for this reaction.

- 3.6** M. dos Santos Afonso and H. J. Schumacher [Int. J. Chem. Kinet., **16**, 103–115 (1984)] studied the kinetics of the gas phase reaction between  $\text{CF}_3\text{OF}$  and  $\text{C}_3\text{F}_6$  at 20°C in a constant volume reactor. They suggest that the rate expression for this reaction is of the form

$$r = k_1(\text{CF}_3\text{OF})(\text{C}_3\text{F}_6) + k_2(\text{CF}_3\text{OF})^{1.5}(\text{C}_3\text{F}_6)^{0.5}$$

where the second term dominates when the concentration of  $\text{CF}_3\text{OF}$  is much greater than that of  $\text{C}_3\text{F}_6$ .

The stoichiometry of the reaction is



although minor amounts of by-products are also formed.

- (a) For the data reported here, perform a graphical test of the data to see if the indicated rate expression provides a good fit of the data. The values of the time derivative of the total pressure were reported by these researchers for run 38. You may assume that these values are accurate estimates of this derivative. If a reasonable linear plot of the data is obtained, determine the values for  $k_1$  and  $k_2$  that correspond to the situation in which the concentrations of the various species are represented by partial pressures. Be careful to employ the proper units!

Time (min)	$-\Delta P$ (total) (torr)	$-(dP/dt)$ (torr/min)
0.00	0.00	
4.00	4.9	1.30
7.25	8.6	1.18
11.50	13.0	1.06
17.33	18.3	0.94
23.92	23.3	0.82
31.42	28.4	0.70
43.50	35.1	0.57
56.16	40.9	0.46
75.25	46.4	0.36
92.83	51.6	0.28
110.83	55.1	0.22
147.83	60.4	0.16
201.66	65.6	0.10
281.16	69.8	0.065

The initial partial pressures of  $\text{CF}_3\text{OF}$  and  $\text{C}_3\text{F}_6$  are 79.0 and 223.4 torr, respectively. Note that the rate expression can also be written as

$$\frac{dP_A}{dt} = k_1^*(P_A)(P_B) + k_2^*(P_A)^{1.5}(P_B)^{0.5}$$

where A and B refer to  $\text{CF}_3\text{OF}$  and  $\text{C}_3\text{F}_6$ , respectively.

- (b) Suggest an experiment that could be used in an integral test of the data to assess the accuracy of the value of the sum of  $k_1$  and  $k_2$  determined in part (a). How would you plot the data in this case, and what combination of rate constants could be determined from the slope and/or intercept of this plot?

- 3.7 S. Mittal, V. Sharma, and K. Banerji {*Int. J. Chem. Kinet.*, **18**, 689–699 (1986)} studied the oxidation of propanol with *N*-chloroethylcarbamate in acid solution:



- (a) The following data are characteristic of this reaction at 30°C. Determine the integers that characterize the orders of this reaction with respect to each of the reactants and the reaction rate constant. You may assume that the rate expression is of the form  $r = k P^p C^c$  where P refers to propanol and C to *N*-chloroethylcarbamate.

Propanol (M)	<i>N</i> -Chloroethyl- carbamate $\times 10^3$ (M)	Rate $\times 10^8$ (M/s)
0.5	2.0	2.66
0.5	5.0	6.15
0.5	7.5	9.45
0.5	10.5	12.60
0.5	12.5	15.40
0.5	15.0	17.85
0.1	5.0	1.25
0.2	5.0	2.46
0.3	5.0	3.78
0.7	5.0	8.65
0.9	5.0	11.30

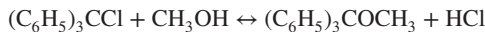
- (b) Analyze the following values of the rate constant to determine the activation energy and frequency factor.

Temperature (°C)	Rate constant $\times 10^5$ (consistent units for time in seconds)
25	1.66
30	[from part (A)]
35	3.55
40	5.11
45	7.27

- 3.8 A. Chakma and A. Meisen [*Can. J. Chem. Eng.*, **75**, 861–871 (1997)] studied the kinetics of the liquid phase degradation of methyl diethanolamine (A) at 18°C at elevated pressures in an autoclave. Test the following data to ascertain whether they are consistent with zero-, first-, or second-order kinetics. Prepare plots of the data using coordinates that should yield straight lines if the presumed rate expression is correct. Report the value of the rate constant corresponding to the proper value of the order of the reaction. Comment on the shapes of the plots.

Time (h)	MDEA (mol/L)
0	4.28
4	4.10
6	4.10
10	3.80
18	3.52
24	3.30
30	3.03
34	2.92
44	2.65
48	2.50
54	2.45
58	2.35
64	2.20
72	2.10
100	1.65
120	1.41

- 3.9** C. G. Swain [J. Am. Chem. Soc., **70**, 1119 (1948)] studied the reaction between triphenylmethyl chloride and methanol in benzene solution:



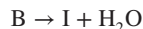
The hydrochloric acid was removed by reaction with pyridine, with subsequent precipitation of pyridine hydrochloride. This procedure prevents the reverse reaction from occurring to any significant extent.

The kinetic data correspond to initial concentrations of triphenylmethyl chloride and methanol of 0.106 and 0.054 kmol/m<sup>3</sup>, respectively, and a temperature of 25°C. The remainder of the solution is comprised of benzene and pyridine.

Time (ks)	(C <sub>6</sub> H <sub>5</sub> ) <sub>3</sub> COCH <sub>3</sub> (kmol/m <sup>3</sup> )
10.44	0.0110
26.64	0.0207
69.00	0.0318
86.40	0.0334
90.60	0.0345
99.60	0.0354
187.20	0.0416

This reaction is known from other experiments to be second-order in methanol. Determine if this reaction is zero- or first-order in triphenylmethyl chloride. Prepare appropriate plots of the data to test each of these proposed forms of the rate law. What are the value of the rate constant and the associated units?

- 3.10** L. C. Abella, P. A. D. Gaspillo, M. Maeda, and S. Gato [Int. J. Chem. Kinet., **31**, 855–859 (1999)] studied the dehydration of *tert*-butanol in the presence of ion-exchange resins. The stoichiometry of this reaction is



where B is *tert*-butanol and I is isobutylene. The reaction can be regarded as irreversible because the product isobutylene is rapidly vaporized at the temperature of interest.

- (a) The following data are characteristic of this reaction at 338 K.

Time (h)	Butanol (M)
0.00	1.00
0.25	0.94
0.50	0.90
0.70	0.86
1.10	0.80
1.50	0.72
1.90	0.66
2.50	0.59
3.00	0.55
4.00	0.43
5.10	0.35
6.00	0.28

Proceed to work up these data in forms such that linear plots should result if the assumed order of the reaction is correct. Prepare plots of the data to test for reaction orders of 0, 0.5, 1.0, and 2.0. What are the order of the reaction and the corresponding value of the rate constant?

- (b) The following data pertain to the temperature dependence of the rate constant corrected for the inhibitory effect of water.

Temperature (°C)	<i>k</i> (in consistent units)
51	0.0088
56	0.0167
66	0.0900
71	0.2153
78	0.4356

Determine the activation energy and the preexponential factor for this reaction. Because the tabulated values of the rate constant correspond to values corrected for the inhibitory effect of water, the value of the rate constant determined in part (a) will not be consistent with the data for part (b).

- 3.11** Isopropylmethylphosphonofluoridate is a highly toxic ester that is a chemical warfare agent. In an effort to characterize the potential for munitions containing this material to degrade during storage, J. R. Bard, L. W. Daasch, and H. Klapper [J. Chem. Eng. Data, **15**, 134 (1970)] utilized NMR measurements to monitor the kinetics of the reaction between isopropylmethylphosphonofluoridate (A) and hydrogen chloride (B):



Analyze the “adjusted” data tabulated below to ascertain whether they are consistent with either of the following rate expressions:

$$r = k(A)^2(B)$$

$$r = k(A)(B)^2$$

Time (h)	C <sub>A</sub> (mol/kg solution)
0.0	6.0
2.1	5.6
4.2	5.3
21.4	4.4
23.7	4.2
27.2	4.1
69.8	3.4
74.8	3.3
141.8	2.8
167.2	2.7
180.5	2.7
189.7	2.6

Use an integral method of data analysis and report the value of the rate constant for the rate expression that provides a suitable fit of the data. The reaction was carried out isothermally at 25°C with an initial HCl concentration of 4.50 mol/kg solution.

- 3.12** D. J. McCracken and P. F. Dickson [*Ind. Eng. Chem., Process Des. Dev.*, **6**, 286 (1967)] studied the esterification of cyclohexanol (B) with acetic acid (A) in the presence of sulfuric acid:

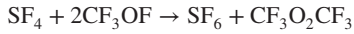


Their results indicate that at 40°C for conversions of less than 70%, the reaction may be regarded as irreversible. Two of their trials conducted using 0.75 mL of H<sub>2</sub>SO<sub>4</sub> in 150 mL of dioxane are of particular interest.

Trial I:		Trial II:	
Initially, A <sub>0</sub> = B <sub>0</sub> = 2.5 M		Initially, B <sub>0</sub> = 8.0 M, A <sub>0</sub> = 1 M	
Time (h)	B (M)	Time (h)	A (M)
2.0	2.070	0.5	0.885
2.5	1.980	0.75	0.847
3.0	1.915	1.25	0.769
3.5	1.860	2.0	0.671
4.0	1.800	2.5	0.625
4.5	1.736	3.5	0.544
5.0	1.692	4.25	0.500
5.5	1.635	5.0	0.463
6.0	1.593		
7.0	1.520		
8.0	1.460		

Determine the orders of the reaction with respect to species A and B, as well as the corresponding value of the rate constant for the forward reaction. The individual orders will be integers. The apparent rate constants may vary between runs, although the orders will not.

- 3.13** A. C. Gonzalez and H. J. Schumacher [*Int. J. Chem. Kinet.*, **17**, 43 (1985)] studied the kinetics of the gas-phase reaction between sulfur tetrafluoride and trifluoromethylhypofluorite in a constant volume reactor. The primary reaction is



although small amounts of CF<sub>3</sub>OSF<sub>5</sub> are also formed. The tabulated data are characteristic of the reaction at 186.5°C and

Time (min)	P <sub>SF<sub>4</sub></sub> (torr)	P <sub>CF<sub>3</sub>OF</sub> (torr)
0	186.5	53.2
4.5	182.2	45.3
12.5	176.4	34.6
20.5	172.0	26.5
30.0	168.1	19.3
51.0	162.8	9.6
81.5	159.5	3.5
∞	157.6	0

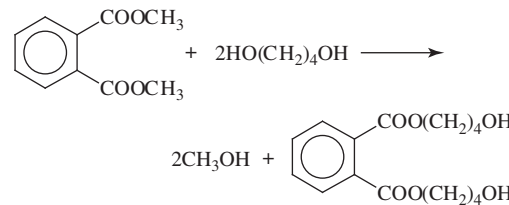
initial partial pressures of 186.5 and 53.2 torr for SF<sub>4</sub> and CF<sub>3</sub>OF, respectively.

- (a) Use these data to perform a graphical test of the data to ascertain whether or not the rate expression for this reaction is first-order in SF<sub>4</sub> and first-order in CF<sub>3</sub>OF (second-order overall). If these data are consistent with the mixed second-order form, also determine the reaction rate constant at this temperature.
- (b) The following additional data are available for the rate constant (in consistent units for time in seconds and concentrations in mol/L).

Temperature (°C)	Rate constant
142.2	5.66 × 10 <sup>-3</sup>
156.5	11.2 × 10 <sup>-3</sup>
164.5	17.6 × 10 <sup>-3</sup>
186.5	From part (a)

What is the activation energy for this reaction?

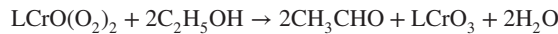
- 3.14** Consider the catalytic transesterification of the dimethyl esters of phthalic acid (A) by butanediol (B):



The data below correspond to an initial mole ratio of diol of 4 : 1. If the reaction is irreversible, determine the orders of the reaction with respect to species A and B. You may assume that these orders are integers or zero. Work up the data in a form that should be linear if the proposed rate expression is correct. Note that you need not know the absolute values of the initial reactant concentrations to determine the reaction order. You need only know their ratio. Test the following rate expressions: (1) first-order in A; (2) first-order in both A and B; (3) first-order in A and second-order in B.

Time (ks)	C <sub>A</sub> /C <sub>A0</sub>
0	1.00
1.5	0.61
3.0	0.43
4.5	0.29
6.0	0.22
7.5	0.16
9.0	0.12
10.5	0.09

- 3.15** M. F. Mousavi, H. Firouzabadi, and M. Shamsipur [*Int. J. Chem. Kinet.*, **26**, 497 (1994)] studied the kinetics of the oxidation of ethanol by 3,4-lutidine chromium(VI) peroxide.



where L is the lutidine moiety. In the presence of a large excess of ethanol, the rate expression becomes pseudo first-order in the peroxide. The following data are characteristic of the reaction as it occurs in the presence of a 3,4-lutidine chromium peroxide concentration of  $8.9 \times 10^{-4}$  M.

Temperature (°C)	Ethanol (M)	Pseudo-first-order rate constant (min <sup>-1</sup> )
35	0.12	0.0101
35	0.34	0.0164
35	0.68	0.0247
35	1.37	0.0353
32.5	1.37	0.0254
30.0	1.37	0.0172
25.0	1.37	0.0100

(a) Determine the order of the reaction with respect to ethanol and the values of the true rate constant corresponding to each of the temperatures indicated.

(b) Determine the corresponding values of the activation energy and the preexponential factor.

- 3.16 C. N. Hinshelwood and R. E. Burk [*Proc. Roy. Soc.*, **106A**, 284, (1924)] studied the thermal decomposition of nitrous oxide. Consider the following “adjusted” data at 1030 K.

Initial pressure of N <sub>2</sub> O (torr)	Half-life (s)
82.5	860
139	470
296	255
360	212

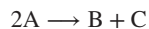
(a) Determine the order of the reaction and the reaction rate constant.

(b) The following additional data were reported at the temperatures indicated.

Temperature (K)	Initial pressure (torr)	Half-life (s)
1085	345	53
1030	360	212
967	294	1520

What is the activation energy for the reaction?

- 3.17 The data that follow are typical of the liquid-phase decomposition of an organometallic vanadium compound. The stoichiometry of this irreversible reaction is of the form

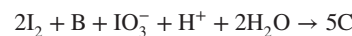


The solution is prepared in a manner such that a weight of material corresponding to 0.75 mol of reactant A is dissolved in 1 L of solution. However, it is thought that some of this material has decomposed during storage, so that the initial

concentration of species A is uncertain. Furthermore, the analytical data for the samples taken at 10 and 20 h are suspect because of a malfunction of the spectrometer employed for the analyses. Test these data to ascertain whether or not they are consistent with a rate expression that is  $3/2$ -order in species A. Prepare an appropriate plot of the data to perform this test. If this rate expression is consistent with the data, what is the value of the rate constant?

Time (h)	C <sub>B</sub> (M)
10	0.080
20	0.140
30	0.175
40	0.201
50	0.222
60	0.239
70	0.254
80	0.266
90	0.278
100	0.285
110	0.294
120	0.300

- 3.18 S. D. Furrow [*Int. J. Chem. Kinet.*, **14**, 927–932 (1982)] studied the kinetics of the hydroxy iodination of 2-butenoic acid (B) in aqueous solution:



where C is CH<sub>3</sub>CH(OH)CHCOOH.

(a) Furrow used absorbance measurements to monitor the concentration of I<sub>2</sub> as a function of time for an experiment in which the initial concentrations of I<sub>2</sub>, B, IO<sub>3</sub><sup>-</sup>, and H<sup>+</sup> were  $1.98 \times 10^{-4}$ , 0.10, 0.025, and 0.10 M, respectively. If the rate expression is of the form

$$r = k(I_2)^m(B)^n(IO_3^-)^p(H^+)^q$$

Time (s)	I <sub>2</sub> × 10 <sup>4</sup> (M)
0	1.98
35	1.94
96	1.84
232	1.68
339	1.56
588	1.28
824	1.06
1060	0.856
1290	0.650
1530	0.479
1760	0.350
2000	0.250
2250	0.145
2500	0.063
2750	0.017

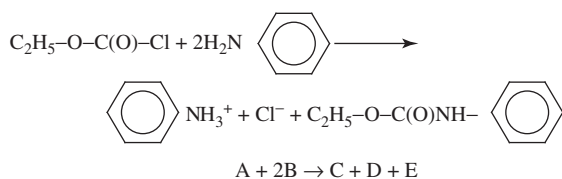
where the various orders are either integers or half-integers, use the following data to determine the order of this reaction with respect to  $I_2$  and the corresponding value of the pseudo-*m*th-order rate constant. What assumptions must be made to arrive at numerical values of these parameters?

- (b) From analyses of the type conducted to determine the order of the reaction with respect to  $I_2$ , Furrow reported the values of the pseudo-*m*th-order rate constant ( $k_{\text{pseudo}}$ ) tabulated below.

$\text{IO}_3^-$ (M)	B (M)	$\text{H}^+$ (M)	$k_{\text{pseudo}}$ $\times 10^5$
0.0250	0.025	0.0985	0.442
0.0250	0.005	0.0985	0.203
0.0250	0.10	0.0493	0.458
0.0250	0.10	0.0197	0.175
0.00625	0.10	0.0985	0.375
0.0500	0.10	0.0985	1.46

What are the orders of the reaction with respect to  $\text{IO}_3^-$ , B, and  $\text{H}^+$ ? Note that the values tabulated above may not be consistent with your answer to part (a) because of Furrow's failure to employ the modern convention for the definition of the reaction rate.

- 3.19 G. Ostrogovich, C. Csunderlik, and R. Bacaloglu (*J. Chem. Soc.* **B1971**, 18) used electrical conductivity measurements to monitor the progress of the reaction between ethyl chloroformate and aniline in acetone solution at 25°C.

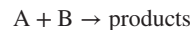


They reported the results tabulated here for the dependence of the concentration of the quaternary ammonium salt on time.

Time (s)	$C_{\text{C}} \times 10^2$ (M)
0	0.000
30	0.070
60	0.140
90	0.210
120	0.280
150	0.335
180	0.400
210	0.440
240	0.485
300	0.555
360	0.625
420	0.680
480	0.740
540	0.790
600	0.835

Initial concentrations of ethyl chloroformate and aniline were  $1.396 \times 10^{-2}$  and  $4.605 \times 10^{-2}$  M, respectively. Are the data below consistent with a rate expression of the mixed second-order form ( $r = kC_{\text{A}}C_{\text{B}}$ )? If so, what is the rate constant?

- 3.20 S. Wang and G. L. Foutch [*Chem. Eng. Sci.*, **46**, 2373 (1991)] studied the kinetics of solid-phase peptide synthesis reactions. The stoichiometry of the reactions of interest can be written as



where A is a symmetrical amino acid anhydride, B a resin-supported peptide containing amino acids, and the products are a resin-supported peptide containing ( $N + 1$ ) acids, water, and an amino acid. The initial concentration of peptide reactive sites is 0.015 M. The initial mole ratio of the symmetrical anhydride to the peptide reactive sites is 1.5 : 1. It has been suggested that the rate expression is of the mixed second-order form

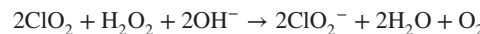
$$r = kC_{\text{A}}C_{\text{B}}$$

Perform a graphical test to determine if this rate expression is consistent with the following data for the attachment of phenylalanine at position 2 in the synthesis of [Tyr]bradykinin.

Time (s)	Fraction conversion	
	at 14°C	at 26°C
0	0	0
20	0.431	0.552
30	0.573	0.652
40	0.662	0.750
50	0.718	0.795
60	0.751	0.835
80	0.825	0.886

If the second-order rate expression indicated is consistent with the data, calculate the rate constant at each temperature and the associated activation energy.

- 3.21 The reaction between chlorine dioxide and hydrogen peroxide is of interest in bleaching wood pulp for the manufacture of paper. Y. Ni and X. Wang [*Can. J. Chem. Eng.*, **75**, 31–35 (1996)] reported the data in Table P3.21 for the reaction



If the rate expression for this reaction is of the general power law form, use these data to determine the orders of the reaction with respect to each of the three reactants, the rate constants at these temperatures, and the activation energy of the reaction. The orders are all integers.

The data were obtained using different buffer solutions so that the pH for a specific trial remained constant.

**Table P3.21**

Run A:			Run B:			Run C:		
$[H_2O_2] = 16.86 \text{ mmol/L}$			$[H_2O_2] = 16.36 \text{ mmol/L}$			$[H_2O_2] = 16.27 \text{ mmol/L}$		
$T = 10^\circ\text{C}$			$T = 25^\circ\text{C}$			$T = 25^\circ\text{C}$		
$pH = 5.07$			$pH = 5.05$			$pH = 3.60$		
Time (min)	$[ClO_2]$ (mmol/L)		Time (min)	$[ClO_2]$ (mmol/L)		Time (min)	$[ClO_2]$ (mmol/L)	
0	0.750		0	0.843		0	0.798	
2.5	0.683		2	0.702		35	0.730	
5	0.646		6	0.530		40	0.705	
7.5	0.620		10	0.372		50	0.684	
10	0.571		15	0.254		55	0.681	
15	0.494		20	0.162		60	0.674	
20	0.443		25	0.110		75	0.643	
24	0.398		34	0.059		90	0.618	
60	0.185					120	0.560	

Run D:			Run E:			Run F:		
$[H_2O_2] = 16.23 \text{ mmol/L}$			$[H_2O_2] = 15.86 \text{ mmol/L}$			$[H_2O_2] = 15.92 \text{ mmol/L}$		
$T = 40^\circ\text{C}$			$T = 25^\circ\text{C}$			$T = 40^\circ\text{C}$		
$pH = 3.86$			$pH = 3.63$			$pH = 3.85$		
Time (min)	$[ClO_2]$ (mmol/L)		Time (min)	$[ClO_2]$ (mmol/L)		Time (min)	$[ClO_2]$ (mmol/L)	
0	1.151		0	0.828		0	0.828	
20	0.864		15	0.803		10	0.772	
30	0.744		25	0.788		15	0.741	
40	0.646		30	0.784		20	0.710	
50	0.572		35	0.777		25	0.692	
60	0.491		40	0.773		30	0.664	
70	0.424		45	0.768		40	0.615	
80	0.370		50	0.759		45	0.598	
90	0.300		80	0.724		50	0.580	
						55	0.558	
						70	0.508	
						80	0.468	

- 3.22** M. Santos Alfonso and H. J. Schumacher [*Int. J. Kinet.*, **16**, 103 (1984)] studied the kinetics of the gas-phase reaction between hexafluoropropene and trifluormethylhypofluorite at  $75^\circ\text{C}$ :



They have reported that the reaction is  $(\frac{3}{2})$ -order in  $CF_3OF$  and  $(\frac{1}{2})$ -order in  $C_3F_6$ .

Consider the case where this reaction is carried out isothermally at a constant pressure of 800 torr in a variable volume batch reactor. At the temperature of interest, the value of the rate constant is  $1.30 \text{ M}^{-1}/\text{s}$ . The initial mixture consists of equal moles of  $C_3F_6$  and  $CF_3OF$ . Determine the time necessary for the concentration of  $C_3F_6$  to decrease to

50% of its original value. You may assume that these gases obey the ideal gas law.

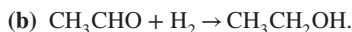
- 3.23** When one makes use of the assumption that the volume of a system is linear in the fraction conversion

$$V = V_0(1 + \delta f)$$

the parameter  $\delta$  is based on the limiting reagent. Calculate  $\delta$  for the following gaseous reactions and the feed concentrations given. I refers to the concentration of inert in the feed stream.

- (a)**  $C_2H_5OH \rightarrow H_2O + C_2H_4$ .  
Initial concentration ratios:

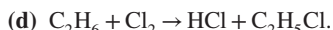
$$C_2H_5OH : H_2O : C_2H_4 = 1 : 0.5 : 2$$



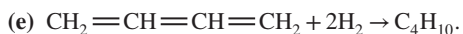
Initial concentration ratios:



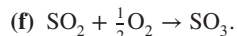
Initial concentration ratios:



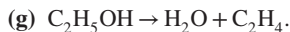
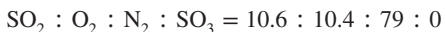
Initial concentration ratios:



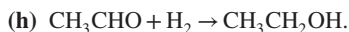
Initial concentration ratios:



Initial concentration ratios:



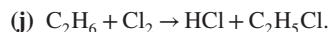
Initial concentration ratios:



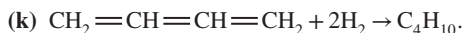
Initial concentration ratios:



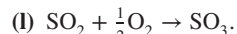
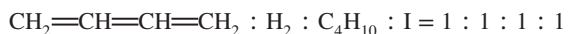
Initial concentration ratios:



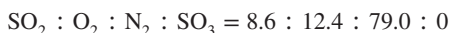
Initial concentration ratios:



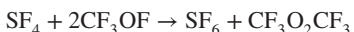
Initial concentration ratios:



Initial concentration ratios:



- 3.24** A. C. Gonzalez and H. J. Schumacher [*Int. J. Kinet.*, **17**, 43 (1985)] studied the kinetics of the gas phase reaction between sulfur tetrafluoride and trifluoromethyl hypofluorite in a constant volume reactor. The primary reaction is



The following data are characteristic of the primary reaction at 186.5°C and initial partial pressures of 186.5 and 53.2 torr for  $\text{SF}_4$  and  $\text{CF}_3\text{OF}$ , respectively.

Time (min)	$P_{\text{SF}_4}$ (torr)	$P_{\text{CF}_3\text{OF}}$ (torr)
0	186.5	53.2
4.5	182.2	45.3
12.5	176.4	34.6
20.5	172.0	26.5
30.0	168.1	19.3
51.0	162.8	9.6
81.5	159.5	3.5
$\infty$	157.6	0

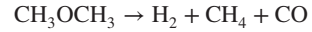
(a) Use these data to determine the orders of the reaction with respect to  $\text{SF}_4$  and  $\text{CF}_3\text{OF}$  and the reaction rate constant at this temperature. You may assume that these orders are both nonzero and are both positive integers.

(b) The following additional data are available for the rate constant for this reaction (in consistent units for time in seconds and concentrations in molarity):

Temperature (°C)	Rate constant
142.2	$5.66 \times 10^{-3}$
156.5	$11.2 \times 10^{-3}$
164.5	$17.6 \times 10^{-3}$
186.5	From part (a)

Determine the activation energy and the frequency factor.

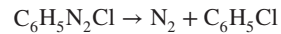
- 3.25** The gas-phase thermal decomposition of methyl ether at 504°C can be represented by a stoichiometric equation of the form



Assuming that this reaction is first-order in methyl ether, determine the reaction rate constant at this temperature if the time necessary for the total pressure in a constant volume reactor to increase from 600 torr to 1000 torr is 921 s. You may assume that only methyl ether is present initially and that the reaction may be treated as if it is irreversible.

If this reaction is now carried out in a batch reactor designed to operate at constant pressure, determine the time necessary for the concentration of methyl ether to decrease from its initial value to half of that value. The reaction takes place at 504°C in a vessel in which the initial pressure of methyl ether is now 1200 torr. Again, the initial contents of the reaction vessel consist of pure methyl ether.

- 3.26** J. C. Cain and F. Nicoll [*J. Chem. Soc.*, **81**, 1412 (1902)] have monitored the kinetics of the irreversible decomposition of 10 g of the chloride of diazobenzene in aqueous solution by measuring the volume of gaseous nitrogen released.

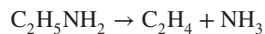


The following data are characteristic of this reaction at 20°C.

Time (min)	Volume of N <sub>2</sub> (mL)
118	9.7
192	16.2
270	21.5
355	26.3
482	32.0
629	37.8
918	46.4
992	47.9
1,070	49.3
1,155	50.7
1,282	51.4
1,429	53.8
10,000	60.0

Determine whether or not this reaction obeys first-order kinetics. Start with the differential equation for the rate expression and derive the integrated form that you use to test the data. If this reaction is first-order, what is the corresponding value of the rate constant?

- 3.27** In their textbook, M. Diaz Peña and A. Roig Muntaner (*Química Física*, Vol. II, pp. 1060–1061, Editorial Alhambra, Madrid, 1976) presented data for the pyrolysis of ethylamine at 500°C in a constant volume reactor.



The progress of this gas phase reaction was monitored using total pressure measurements to obtain the following data.

Time (min)	Pressure (torr)
0	55
1	60
2	64
4	72
8	84
10	89
20	102
30	107
40	108.5
420	110

Determine the order of the reaction and the rate constant at this temperature.

- 3.28** G. Chuchani, R. M. Dominguez, and A. Rotinov [*Int. J. Chem. Kinet.*, **23**, 779–783 (1991)] studied the kinetics of the thermal pyrolysis of 2-bromopropionic acid:



These investigators reported that in the presence of toluene, which serves to inhibit (suppress) free-radical reactions, the reaction obeys a first-order rate expression.

- (a)** At 320°C, the rate constant is  $3.37 \times 10^{-4} \text{ s}^{-1}$ . If this reaction is carried out at 320°C using 106 torr of 2-bromopropionic acid and 268.5 torr of toluene inhibitor as the starting materials, how long does it take for the total pressure to reach 500 torr? You may assume that the mixture behaves as an ideal gas.

The activation energy for this reaction is 180.3 kJ/mol. If the same partial pressures of toluene and 2-bromopropionic acid are used at 339.6°C, how long does it now take for the total pressure to reach 500 torr?

- 3.29** M. dos Santos Alfonso and H. J. Schumacher [*Int. J. Chem. Kinet.*, **16**, 103 (1984)] studied the reaction between hexafluoropropene and trifluoromethylhypofluorite. The stoichiometry is as follows:



They reported that for appropriate reaction conditions the reaction is 1.5-order in CF<sub>3</sub>OF and 0.5-order in C<sub>3</sub>F<sub>6</sub>.

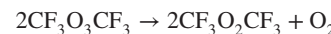
Because integration of the corresponding differential equation is complex, in posing a problem to his students, Professor Dino Saurio has used the results of dos Santos Alfonso and Schumacher to generate a table of total pressure versus time for a situation in which a large excess of one of the reactants is present. In particular, he has generated the values expected at 75°C for a system in which the initial partial pressures of CF<sub>3</sub>OF and C<sub>3</sub>F<sub>6</sub> are 20.0 and 400.0 torr, respectively. To make the problem a bit more realistic, he also introduced a bit of noise in the tabular entries.

Use an analysis based on the generalized physical properties relation to determine whether or not the following values are consistent with the rate expression reported. Use a graphical approach to determine the corresponding value of the reaction rate constant.

Time (s)	Total pressure (torr)
0	420.0
10	418.8
20	418.3
40	416.5
60	414.8
80	413.6
100	412.5
200	408.5
300	406.2
400	404.9

Remember to recognize that the use of a large excess of one reactant causes the rate expression to degenerate to a simpler mathematical form.

- 3.30** J. Czarnowski and H. J. Schumacher [*Int. J. Chem. Kinet.*, **24**, 639 (1981)] studied the thermal decomposition of bis(trifluoromethyl)trioxide at temperatures between 59.8 and 90.3°C.



For reaction at 80.4°C, the data consist of total pressure measurements as a function of time. This irreversible gas-phase reaction takes place in a constant volume reactor.

Time (min)	Pressure (torr)
0	206.8
5.2	216.4
8.0	221.4
14.2	231.3
21.7	241.5
29.4	250.8
39.75	261.3
51.4	270.7
66.6	280.3
74.4	284.3
104.5	295.3
151.6	303.6
270.8	309.4
$\infty$	310.2

- (a) Determine the order of the reaction with respect to  $\text{CF}_3\text{O}_3\text{CF}_3$  and the value of the rate constant at this temperature. The initial charge to the reactor consists solely of  $\text{CF}_3\text{O}_3\text{CF}_3$ .
- (b) The following rate constants were determined at the temperatures indicated. Use these data and the value for the rate constant determined in part (a) to prepare an Arrhenius plot and determine the activation energy and preexponential factor for the rate constant.

Temperature (°C)	Rate constant $\times 10^{-4}$
59.8	0.1035
69.8	0.398
90.3	5.01

The values of the rate constant are expressed in terms of consistent units with time in seconds and concentrations in moles per liter.

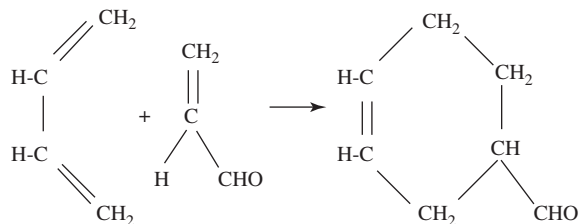
- 3.31 J. Czarnowski and H. J. Schumacher [*Int. J. Chem. Kinet.*, **11**, 613 (1979)] studied the kinetics and mechanism of the gas-phase decomposition of bispentafluorosulfurtrioxide  $\text{SF}_5\text{OOOSF}_5$ . In the presence of sufficiently high oxygen pressures, the stoichiometry of this irreversible reaction is



The progress of the reaction was monitored via pressure measurements. The data that follow are typical of reaction at 9.8°C for a system in which the initial partial pressures of  $\text{SF}_5\text{O}_3\text{SF}_5$  and  $\text{O}_2$  are 49.2 and 214.2 torr, respectively. Determine the form of the rate expression that best fits these data and the numerical value of the rate constant.

Time (min)	Pressure (torr)
0	263.4
11.4	264.9
27.8	266.8
56.7	269.6
119.1	274.6
149.2	276.6
176.4	278.1
296.4	282.7
386.6	284.7
10,000	288.0

- 3.32 Combine and extend the concept of the generalized physical properties approach and Guggenheim's method to the case of an irreversible second-order reaction. Use your analysis to solve the following problem. Note that the data are recorded at time  $t$  and at time  $t + \Delta$  with  $\Delta = 1500$  s, and that stoichiometric quantities of reactants are used in the experiment in question. You may find it useful to group your time terms such that they appear in the form  $(t + \Delta)\lambda^* - t\lambda$ , where  $\lambda^*$  is the value of the property measured at  $t^* = t + \Delta$  and  $\lambda$  is the value measured at time  $t$ . Consider the Diels–Alder reaction between acrolein and butadiene.

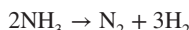


Time (s)	Total pressure (torr)
60	727
120	712
180	700
240	690
300	679
360	669
420	660
480	651
1560	558
1620	554
1680	550
1740	548
1800	544
1860	542
1920	538
1980	536

In shorthand notation this reaction can be written  $\text{A} + \text{B} \rightarrow \text{C}$ . If this irreversible reaction takes place isothermally

(300°C) in the gas phase in a constant volume reactor, determine whether or not the data are consistent with a rate expression of the form  $r = kC_A C_B$  and the value of the rate constant. Initially, the reaction mixture contains equal molar quantities of species A and B, together with an unknown concentration of an inert species (i.e., the quantity of the Diels–Adler adduct, which forms as the gas mixture is heated to 300°C).

- 3.33** C. N. Hinshelwood and R. E. Burk [*J. Chem. Soc.*, **127**, 1105 (1925)] studied the decomposition of ammonia into its elements over a heated platinum filament at 1138°C. The reaction stoichiometry is



Initially, 200 torr of NH<sub>3</sub> was present in the reaction vessel. The following data are representative of the kinetics of the reaction. The reaction occurs in a constant volume system.

Time (s)	Total pressure (torr)
0	200
10	228
60	254
120	268
240	289
360	300
720	330

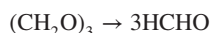
It has been postulated that the rate expression is of the form

$$r = kP_{\text{NH}_3}/P_{\text{H}_2}$$

where the partial pressures of ammonia ( $P_{\text{NH}_3}$ ) and hydrogen ( $P_{\text{H}_2}$ ) are expressed in consistent units. The effect of the reverse reaction may be neglected.

- (a) Determine the manner in which these data should be plotted so that a straight line will result if the form of the postulated rate expression is correct. Use an integrated form of the rate expression in determining the requisite functional form.
- (b) Work up the data in tabular form and prepare a plot using the coordinates determined in part (a).
- (c) Are the data consistent with the rate expression postulated?
- (d) If the data are consistent, what is the corresponding value of the rate constant?

- 3.34** H. K. Aldridge, X. Liu, M. C. Lin, and C. F. Melius [*Int. J. Chem. Kinet.*, **23**, 947–956 (1991)] studied the irreversible gas phase decomposition of 1,3,5-trioxane to formaldehyde at temperatures between 250 and 330°C:



The reaction takes place isothermally in a constant volume reactor. FTIR measurements were used to monitor the progress of the reaction of 0.225% v/v trioxane in argon at several pressures. The data that follow are typical of

this reaction at 315°C and a total pressure of 800 torr. The indicated absorbance values correspond to a wavenumber of 1174.5 cm<sup>-1</sup>, where the major species contributing to the absorbance is trioxane.

Time (s)	Absorbance
0	0.378
150	0.310
300	0.217
450	0.168
600	0.135
750	0.107
900	0.084
1050	0.068
1200	0.053
∞	0.013

- (a) If the order of this reaction with respect to the trioxane is an integer (0, 1, 2, or 3), use an integral method of data analysis to determine the order of the reaction ( $n$ ) and the value of the reaction rate constant.
- (b) The following values of the rate constant have also been reported (for time in seconds and concentration units in mol/L). Unfortunately, these data are not entirely consistent with those reported in part (a). Determine the activation energy for this reaction.

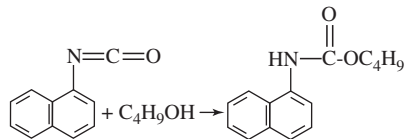
Temperature (°C)	$k$ (in consistent units)
250	$4.17 \times 10^{-6}$
270	$1.94 \times 10^{-5}$
290	$1.04 \times 10^{-4}$
330	$2.18 \times 10^{-3}$

- (c) Experimentally, it is observed that when the total pressure becomes sufficiently low, the apparent  $n$ th-order rate constant decreases and the apparent order of the reaction increases. Explain this observation. [Hint: Consider the Lindemann theory for unimolecular reactions (Section 4.3.1.3)].

- 3.35** P. Neeb, A. Kolloff, S. Koch, and G. K. Moorgat [*Int. J. Chem. Kinet.*, **30**, 769–776 (1998)] used infrared absorbance measurements to monitor the irreversible reaction of ozone with methacrylic acid at room temperature. Use the Guggenheim method and a generalized physical properties analysis to determine if the following data are consistent with a rate expression that is pseudo first-order in methacrylic acid. These data were recorded at room temperature for a very dilute gas phase system containing a large excess of ozone. The reaction occurs isothermally at constant volume. If the data are consistent with a pseudo-first-order rate law, what is the corresponding value of the rate constant?

Time (s)	Absorbance
50	0.01551
100	0.01432
150	0.01268
200	0.01127
250	0.01037
300	0.00938
550	0/00547
600	0/00518
650	0.00451
700	0.00401
750	0.00375
800	0.00331

- 3.36** The data that follow are characteristic of the reaction of *n*-butanol with  $\alpha$ -naphthyl isocyanate:



This irreversible reaction takes place at 25°C in an isothermal reactor with the alcohol acting as solvent (initial concentration  $\sim$ 10.9 mol/L). The absorbance of the solution at 226 nm can be used to monitor the progress of the reaction. It is anticipated that for the indicated conditions the reaction will be pseudo first-order in the isocyanate. Are the data here consistent with this hypothesis? If so, what is the pseudo first-order rate constant? In your analysis you may wish to note that the half-life of the reaction is somewhat in excess of 200 s and that the data are recorded at evenly spaced time increments.

Time (s)	Absorbance
100	0.441
200	0.325
300	0.243
400	0.179
500	0.133
600	0.100
700	0.076
800	0.058
900	0/045
1000	0.036

- 3.37** A. Komlosi, G. Porta, and G. Stedman [*Int. J. Chem. Kinet.*, **27**, 911–917 (1995)] studied the autocatalytic oxidation of the hydrated form of formaldehyde by nitric acid:



The progress of the reaction was monitored via absorbance measurements. The data that follow are characteristic of this irreversible reaction at 20°C. The following rate expression

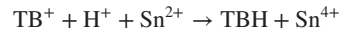
has been proposed to explain these data when  $\text{HNO}_3$  is present in large excess:

$$r = k[\text{H}_2\text{C}(\text{OH})_2][\text{HNO}_2]$$

For the conditions of interest the initial concentrations of  $\text{HNO}_3$ ,  $\text{H}_2\text{C}(\text{OH})_2$ , and  $\text{HNO}_2$  are 7.5, 0.140, and 0.004 mol/dm<sup>3</sup>, respectively. Are the data here consistent with the rate expression proposed? If so, what is the value of the rate constant?

Time (min)	Absorbance
0.0	0.050
5.0	0.078
7.5	0.135
10.0	0.241
12.5	0.425
15.0	0.589
17.5	0.690
20.0	0.735
22.5	0.759
25.0	0.770
$\infty$	0.780

- 3.38** S. B. Jonnalagadda and M. Dumba [*Int. J. Chem. Kinet.*, **25**, 745–753 (1993)] reported that the reaction between toluidine blue  $\text{TB}^+$  and stannous ions in acid solution is characterized by the following stoichiometry:



where TBH refers to protonated toluidine white. The corresponding rate expression is

$$r = k(\text{TB}^+)^{\frac{1}{2}}(\text{H}^+)(\text{Sn}^{2+})^{\frac{3}{2}}$$

Absorbance data were used to monitor the progress of the reaction at 25°C in a system composed initially of  $2.4 \times 10^{-3}$  M  $\text{Sn}^{2+}$ ,  $4.0 \times 10^{-5}$  M  $\text{TB}^+$ , and 0.12 M  $\text{H}^+$ . Use the following data to ascertain whether the order of the reaction in toluidine blue is correct. If it is correct, determine the value of the rate constant at this temperature.

Time (min)	Absorbance
0	0.951
4	0.767
8	0.612
12	0.474
16	0.343
20	0.239
24	0.161
28	0.083
1000	0.015

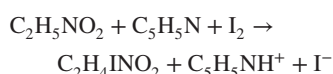
- 3.39** C. S. Marvel, J. Dec, and H. G. Cooke, Jr. [J. Am. Chem. Soc., **62**, 3499 (1940)] employed optical rotation measurements to study the kinetics of polymerization of vinyl-1-phenylbutyrate. In dioxane solution the specific rotation angle represents a linear combination of contributions from the monomer proper and those of the polymerized monomer units. The contribution of the polymerized units can be viewed as independent of chain length. The reaction takes place in a constant-volume system and may be viewed as irreversible. The stoichiometry of the reaction may be viewed as  $A + P_n \rightarrow P_{n+1}$ , where A represents the monomer and  $P_i$  the polymer. The following data are characteristic of this reaction.

Time (min)	Optical rotation	Time (min)	Optical rotation
45	-2.68	345	-3.41
105	-2.90	405	-3.48
165	-3.08	465	-3.53
225	-3.22	525	-3.57

The data point corresponding to time zero has not been given. It may be viewed as suspect because of concerns about the possible presence of an induction period. (The reaction is thought to proceed by a chain reaction mechanism.) Because the reaction was still proceeding at a time of 525 min, this reading may not be employed as an infinite time value.

- (a) Consider the possibility of using a combination of the generalized physical properties approach to data analysis and Guggenheim's method for first-order reactions to assess whether or not these data are consistent with a first-order rate expression. Note that the data can be viewed as two sets taken 300 min apart. Use the Guggenheim approach to derive an expression relating the optical rotation measurements at times  $t$  and  $(t + 300)$  min to time and other appropriate parameters of the system. Assume that the reaction is first-order in the monomer. Be sure to define all the parameters you employ. This expression must not contain any derivatives.
- (b) Use the expression derived in part (a) to work up the data and prepare an appropriate plot to test the validity of the hypothesis of first-order kinetics. Are the data consistent with first-order kinetics? If so, what is the value of the rate constant?

- 3.40** A. A. Frost and R. G. Pearson (*Kinetics and Mechanism*, 2nd ed., Wiley, New York, 1961) suggested that resistance measurements can be employed to monitor the following reaction in a water-alcohol solution of the reactants:



The initial concentrations of nitroethane, pyridine, and iodine were 100, 100, and  $4.5 \text{ mol/l m}^3$ , respectively.

Time (s)	Resistance ( $\Omega$ )
0	2503
300	2295
600	2125
900	1980
1200	1850
1500	1738
1800	1639
$\infty$	1470

Determine the apparent order of reaction and the apparent rate constant in suitable units.

*Hints:*

1. The resistance is inversely proportional to the conductance of the solution. The latter is an additive property of the contributions of the various species in the solution.
2. The order of the reaction in  $\text{I}_2$  is either 0, 1, or 2. Note that the concentrations of nitroethane and pyridine are much greater than that of iodine.
3. Demonstrate that the extent of reaction at time  $t$  relative to the extent at time infinity is related to the resistance measurements by

$$\frac{\xi^*}{\xi_{\infty}^*} = \left( \frac{R - R_0}{R_{\infty} - R_0} \right) \left( \frac{R_{\infty}}{R} \right)$$

- 3.41** Z. Pan, H. Y. Feng, and J. M. Smith [AIChE J., **31**, 721 (1985)] studied the rate of pyrolysis of Colorado shale oil via thermogravimetric analysis in which the weight loss of a sample held at a constant temperature was measured as a function of time. The feedstock contains kerogen, a complex substance whose average molecular weight is about 3000 and whose approximate empirical formula can be written as  $\text{C}_{200}\text{H}_{300}\text{SN}_5\text{O}_{11}$ . At temperatures above 623 K this material begins to decompose and partially vaporize to yield an array of products which, when cooled to room temperature, consist of gas, oil, and residual carbon. The pertinent reactions are irreversible and can be expressed as

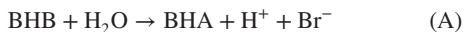


Use the thermogravimetric data that follow to determine if this reaction obeys first-order kinetics and the value of the rate constant at 673 K. Very small particles were employed to eliminate potential mass and heat transfer limitations on the reaction rate. The zero of time is taken as the start of the constant-temperature period, but some reaction has taken place during heating from room temperature to 673 K. Hence, the amount of kerogen present at time zero is not known. Employ a variation of the Guggenheim approach to solve this problem.

Time (s)	Mass of sample (mg)
0	5.10
240	4.93
480	4.77
720	4.64
960	4.52
1200	4.41
2400	4.04
2640	3.99
2880	3.94
3120	3.90
3360	3.87
3600	3.84

**3.42** NMR is an analytical technique that can be utilized in studies of chemical reactions. The chemical shift parameter may be used as a measure of the relative proportions of different species that are present in solution. These shifts are measured relative to a standard reference sample.

Benzhydryl bromide (BHB) undergoes solvolysis in aqueous dioxane to produce benzhydryl alcohol (BHA) and hydrogen bromide:



The rate of formation of hydrogen ions can be determined by observing the chemical shift for the water molecules in the solution. Since the rate of protonation is very rapid compared to a typical NMR time scale, the chemical shift observed ( $\delta$ ) may be said to be a linear combination of the contributions of the protonated water molecules and the unprotonated water molecules. That is,

$$\delta = \delta_{\text{H}_2\text{O}} X_{\text{H}_2\text{O}} + \delta_{\text{H}_3\text{O}^+} X_{\text{H}_3\text{O}^+}$$

where  $\delta_{\text{H}_2\text{O}}$  is the chemical shift that would be observed in the absence of unprotonated species,  $\delta_{\text{H}_3\text{O}^+}$  the chemical shift that would be observed if all species were protonated,  $X_{\text{H}_2\text{O}}$  the fraction of the water molecules that are not protonated, and  $X_{\text{H}_3\text{O}^+}$  the fraction of the water molecules that are protonated. It may be assumed that all the protons formed by reaction immediately react to form protonated water molecules. The following chemical shifts [taken from an article by I. Horman and M. J. Strauss, *J. Chem. Educ.*, **46**, 114 (1969)] were observed as a function of time.

Time (s)	Chemical shift, $\delta$
240	40.1
480	27.0
720	19.3
960	14.8
1200	12.3
1440	10.9
1680	10.1
$\infty$	9.0

(a) If reaction (A) may be considered as an irreversible reaction, what is the order of this reaction with respect to BHB?

(b) The initial concentration of BHB is 360 mol/m<sup>3</sup>. The water is present in sufficient excess that its concentration may be considered to be essentially constant. What is the reaction rate constant?

**3.43** A. V. Tuumlets [*Kinet. and Catal.*, **5**, 71 (1964)] studied the kinetics of the reaction of ethyl magnesium bromide with pinacolin. He used a calorimetric technique to monitor the progress of the reaction. The overall temperature increase of the reaction mixture was less than a degree. Hence, one does not need to worry about the dependence of the rate constant on temperature. Mixture temperatures were determined with a sensitive potentiometer. The data that follow have been corrected to allow for heat losses from the system (i.e., adiabatic operation of the batch reactor may be assumed). The reaction was carried out in diethyl ether solution using initial concentrations of C<sub>2</sub>H<sub>5</sub>Mg Br and pinacolin of 0.403 and 0.01 mol/L, respectively. The stoichiometry of the reaction may be represented as



Changes in the potentiometer reading may be assumed to be proportional to the temperature change in the reaction mixture. Determine the order of the reaction with respect to pinacolin and the apparent rate constant. Use two methods of analysis:

- (a) An approach based on the generalized physical properties relation that employs the reading at infinite time.
- (b) An approach combining the generalized physical properties relation with Guggenheim's method. Discuss the relative merits of these approaches.

Time (s)	Potentiometer reading
10	65.0
20	94.5
30	107.6
40	113.8
50	116.2
60	117.5
70	118.1
80	118.3
280	118.5

Unfortunately, the potentiometer reading at time zero is not known with sufficient accuracy that it could be used with confidence in your analysis.

**3.44** A. F. Rizvi and C. H. Tong [*J. Food Sci.*, **62**, 1, 1997] studied the effects of thermal processing on the texture of foods. Kinetic parameters can provide valuable insight to understanding and predicting the changes that occur from thermal processing. In addition, information on reaction

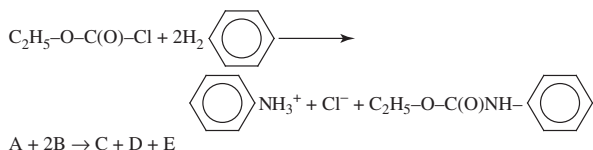
kinetics is needed to optimize the product quality. The firmness of potatoes was measured at various times during a 103°C processing cycle, and the results follow.

Time (min)	Firmness (MPa)
0.0	100.00
0.9	61.00
1.8	37.60
2.2	28.83
2.6	22.00
3.0	17.13
3.6	12.25
4.0	9.81
5.1	5.91
6.0	4.45
600	2.50

Time (s)	Conductance $\times 10^6$ ( $\Omega^{-1}$ )
0	7.9
30	9.8
60	11.4
90	13.3
120	14.9
150	16.2
180	17.8
240	20.0
300	21.8
360	23.2
420	24.9
480	26.3
540	27.6
600	28.8
18,000	42.8

- (a) If one assumes that the firmness values obey the generalized physical properties relation, determine the order of the reaction that results in a loss of firmness. In addition, determine a value for the product  $kC_{A0}^{n-1}$  which is characteristic of the reaction at 103°C.
- (b) For processing at 90 and 120°C, the corresponding values of  $kC_{A0}^{n-1}$  were 0.21 and 2.2  $\text{min}^{-1}$ , respectively. Use these data and the value determined in part (a) to determine the activation energy of the reaction and the product  $AC_{A0}^{n-1}$ , where  $A$  is the Arrhenius frequency factor.
- (c) If one takes into account the extent of reaction that takes place as the potatoes cool to room temperature, the firmness value at which cooling should begin is 10 MPa. At what time after initiation of processing should the cooling cycle be initiated if processing takes place at 103°C? To assess the sensitivity of product quality to changes in the cooking time, calculate the times corresponding to firmness values of 12 and 8, values that would place the product quality outside acceptable limits.

- 3.45 G. Ostrogovich, C. Csunderlik, and R. Bacaloglu [*J. Chem. Soc. B*, **1971**, 18–22] used electrical conductivity measurements to monitor the progress of the reaction between ethyl chloroformate and aniline in acetone solution at 25°C.



They reported the results tabulated here for measurements of the conductance of the solution versus time. Initial concentrations of ethyl chloroformate and aniline were  $1.396 \times 10^{-2}$  and  $4.605 \times 10^{-2}$  M, respectively. Are the data consistent with a rate expression of mixed second-order form ( $r = kC_A C_B$ )? If so, what is the rate constant?

- 3.46 C. Cristallini, A. Villani, L. Lazzeri, G. Ciardelli, and A. S. Rubino [*Polym. Int.*, **48**, 63–68 (1999)] used dilatometry to monitor the kinetics of the homopolymerization of sodium acrylate in aqueous solution. A cathetometer was employed to generate the data tabulated here. The data correspond to reaction at 50°C and an initiator concentration of 10 mM.

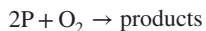
Time (min)	Height of meniscus (cm)
0	0.304
5	0.515
10	0.726
15	0.887
20	1.063
25	1.178
30	1.307
35	1.418
40	1.513
45	1.593
50	1.680
1440	3.617

(The meniscus separates the liquid and air phases in the capillary tube.)

It has been suggested that this reaction is either first- or second-order in sodium acrylate. Determine whether or not the data are consistent with either of these rate expressions. What is the value of the rate constant for the rate expression that best fits the data? The initial concentration of sodium acrylate is 0.4 M.

- 3.47 C. J. Doona and K. Kustin [*Int. J. Chem. Kinet.*, **25**, (1993), 239] studied the kinetics of the reaction of 1,2,3-trihydroxybenzene (pyrogallol) and oxygen in phosphate buffer by monitoring the concentration of dissolved oxygen with a polarographic oxygen electrode. Alkaline solutions of pyrogallol (P) readily absorb oxygen and can be used to strip

oxygen from gas streams. The stoichiometry of this reaction is of the form

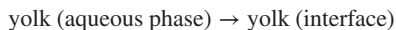


Doona and Kustin reported the data that follow for reaction at pH 10.2 and a temperature of 25°C. The initial concentration of pyrogallol ( $1.3 \times 10^{-2}$  M) is believed to be substantially greater than the initial concentration of oxygen. Unfortunately, the authors do not indicate the initial concentration of oxygen.

Analysis of the data suffers from the additional complication that the initial stage of the reaction is characterized by a “dead” period associated with the characteristic response time of the electrode. During this period, one cannot obtain meaningful data. Nonetheless, the data reported here are believed to be sufficiently accurate to permit one to obtain meaningful values of an apparent pseudo first-order rate constant. Use a variation of the Guggenheim method to determine (1) whether or not the indicated order of the reaction is indeed appropriate for use and (2) the corresponding numerical value of the rate constant. You may assume that the millivolt output of polarographic electrode is proportional to the concentration of dissolved dioxygen present at any time.

Time (s)	Electrode output (mV)
20	1750
30	985
40	600
50	370
60	225
70	151
80	102
90	88
100	83
110	79
120	75
130	65
140	57
150	50

- 3.48** K. Taiwo, H. Karbstein, and H. Schubert [*J. Food Process Eng.*, **20**, 1–16 (1997)] studied the influence of temperature on the kinetics of adsorption of a variety of food emulsifiers at oil–water interfaces. They used interfacial tension measurements to monitor the rate at which egg yolk present at 10 times its critical micelle concentration was transferred to a water–soybean oil interface. The rates of these processes are important in assessing the potential stability of oil-in-water emulsions of the type found in salad dressings and mayonnaise. The interfacial tension can be viewed as a property that reflects the contributions of the various species present at the interface, being an additive function of these contributions. Each individual contribution is proportional to the quantity of the material in question located at the interface between the oil and the water. The “reaction” of interest can be regarded as

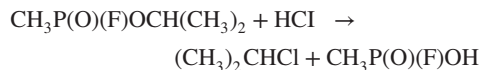


(a) Test these data to determine if they are consistent with either first- or second-order kinetics and determine the corresponding rate constant.

(b) Data obtained at other temperatures indicate that the apparent activation energy for this process is roughly 1.4 kcal/mol. Comment.

Time (s)	Interfacial tension at 25°C (mN/m)
0	19.5
500	9
1,000	6.1
1,500	4.3
2,000	3.3
2,500	2.9
3,000	2.7
3,500	2.6
10,000	2.5

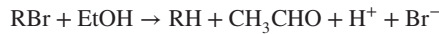
- 3.49** J. R. Bard, L. W. Daasch, and H. Klapper [*J. Chem. Eng. Data*, **15**, 134 (1970)] utilized NMR measurements to monitor the kinetics of the reaction between the highly toxic phosphorus ester isopropylmethylphosphonofluoride (A) and hydrogen chloride (B).



It has been suggested that this liquid phase reaction is second-order in HCl and first-order in A. Use an integral method of data analysis to determine if the data below are consistent with the proposed rate expression. If the data are consistent, what is the third-order rate constant at 25°C? The chemical shift is a property that is an additive function of the contributions of the various species.  $C_{A0} = 6.0 \text{ mol/kg}$  solution and  $C_{B0} = 4.4 \text{ mol/kg}$  solution.

Time (h)	Chemical shift (Hz)
0.0	361
2.1	380
4.2	405
21.4	485
23.7	498
27.2	508
69.8	568
74.8	574
141.8	616
167.2	625
189.7	633
$\infty$	730

- 3.50** Sue Dent is studying the catalytic reduction of bromomethylbarbituric acid (RBr) in ethanol solution at room temperature.



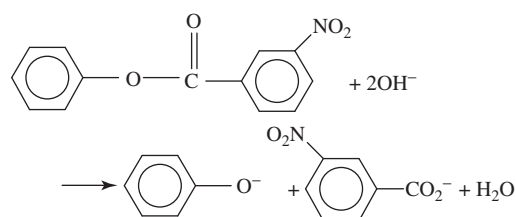
She has employed resistance measurements to monitor the progress of this reaction. Her exposure to reaction kinetics leads her to suggest that it would be appropriate to assume that the presence of a large excess of ethanol will lead to a rate expression that is pseudo-*n*th-order in RBr. Sue knows that it is often convenient to obtain data at time intervals separated by a constant time increment and has taken these precautions. She also knows that when monitoring the progress of a reaction via physical property measurements, one requires measurements at times zero and infinity. Unfortunately, her measurements at these times are invalid because of an equipment malfunction. She is perplexed and wonders if she will have to repeat the experiment.

Professor Simon Legree “suggests” that the fact that Sue was careful to time her measurements appropriately when the equipment was working properly should permit her to determine whether or not the reaction obeys first-order kinetics. If such kinetics are obeyed, Sue would not have to repeat the experiment.

- (a) Derive an expression that combines elements of the generalized physical properties approach and Guggenheim’s method to ascertain whether a first-order rate law is appropriate for use. You may start with either the differential or the integrated form of a first-order rate law.
- (b) Use this expression to prepare an appropriate plot to ascertain whether the data are consistent with pseudo first-order kinetics. If they are, determine the rate constant.

Time (min)	Resistance ( $\Omega$ )
2	1630
3	1380
4	1200
5	1080
6	980
7	911
8	854
9	808
10	765
11	728
12	695
13	670

- 3.51** Combine and extend the concept of the generalized physical properties approach and Guggenheim’s method to the case of an irreversible second-order reaction. Use your analysis to solve a problem adapted from one composed by J. W. Moore and R. G. Pearson (*Kinetics and Mechanisms*, 3rd ed., p. 78, Wiley, New York, 1981). Note that most of the data were recorded at time  $t$  and at time  $t + 110$  s and that stoichiometric quantities of reactants were used in the experiment. You may find it useful to group your time terms such that they appear in the form  $(t + \Delta) \lambda' - t \lambda$ , where  $\lambda'$  is the measured property at time  $t' = t + \Delta$  and  $\lambda$  is the measured property at time  $t$ . S. W. Tobey [*J. Chem. Educ.*, **39**, 473 (1962)] studied the rate of hydrolysis of phenyl-*m*-nitrobenzoate in a 50% aqueous dioxane solution at 25°C.



The resistance of the solution was monitored as a function of time. The initial concentrations of  $\text{OH}^-$  and phenyl-*m*-nitrobenzoate were  $6.275 \times 10^{-3}$  M and  $3.138 \times 10^{-3}$  M, respectively. The reaction is first-order in each reactant. Determine the second-order rate constant.

Time (s)	Resistance ( $\Omega$ )	Time (s)	Resistance ( $\Omega$ )
25	734	130	960
30	753	140	970
40	786	150	980
50	815	160	990
60	841	170	998
70	864	180	1006
80	884	190	1013
90	902	200	1021
100	919	230	1040
125	954	260	1055

# Chapter 4

---

## Basic Concepts in Chemical Kinetics: Molecular Interpretations of Kinetic Phenomena

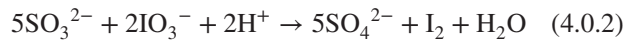
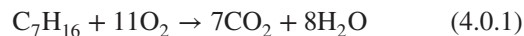
### 4.0 INTRODUCTION

In this chapter we treat the descriptions of the molecular events that lead to the kinetic phenomena that one observes in the laboratory. These events are referred to as the *mechanism* of the reaction. We begin with definitions of the various terms that are basic to the concept of reaction mechanisms, indicate how elementary events may be combined to yield a description that is consistent with observed macroscopic phenomena, and discuss some of the techniques that may be used to elucidate the mechanism of a reaction. Finally, two basic molecular theories of chemical kinetics are discussed: the kinetic theory of gases and transition-state theory. The determination of a reaction mechanism is a much more complex problem than that of obtaining an accurate rate expression, and the well-educated chemical engineer should have a knowledge of and an appreciation for some of the techniques used in such studies.

There are at least two levels of sophistication at which one may approach the problem of providing a molecular description of the phenomena that occur during the course of a chemical reaction. At the first level the sequence of molecular events is described in terms of the number and type of molecules and molecular fragments that come together and react in the various steps. The second level of description contains all of the elements of the first but goes beyond it to treat the geometric and electronic configurations of the various species during the different stages of the reaction sequence. For this book, the first level of description is adequate. The second level is more appropriate for study in courses involving physical organic chemistry or advanced physical chemistry.

The mechanism of a reaction is a hypothetical construct. It is a provisional statement based on available experimental data, representing a suggestion as to the sequence of molecular events that occur in proceeding from reactants to products. It does not necessarily represent the actual events that occur during the reaction process, but *it must be consistent with the available experimental facts*. Often, there will be more than one mechanism that is consistent with these facts. The problem of designing an experiment that will eliminate one or more of the competing mechanisms is a challenging problem for the kineticist. In some cases it is an impossible task.

Implicit in the use of the term *sequence of molecular events* is the idea that the chemical transformation that one observes in the laboratory is not the result of a single molecular process but is the end result of a number of such processes. If one considers reactions such as



it should be evident from a purely statistical viewpoint that there is virtually zero probability that the number of molecular species involved in these reactions would simultaneously be in spatial and electronic configurations such that more than a few chemical bonds could be broken and/or made in a single step. These equations merely describe the stoichiometry that is observed in the laboratory. Nonetheless, they do reflect the conversion of reactant molecules into product molecules. It is quite plausible to assume that the events that occur on a molecular level are encounters at which atomic rearrangements occur and that the reaction observed may be interpreted as the sum total of the changes that occur during a number of such encounters.

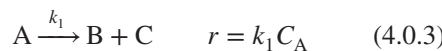
This assumption is the foundation on which all studies of reaction mechanisms are based. The major justifications for its use lie in the tremendous success it has had in providing a molecular interpretation of kinetic phenomena and the fact that it has been possible to experimentally observe some of the intermediates postulated in sequences of elementary reactions.

Each elemental process contributing to the overall mechanism is itself an irreducible chemical reaction. The elementary reactions may also be referred to as simple reactions, mechanistic reactions, or reaction steps. The superposition in time of elementary reactions leads to the reaction observed experimentally. Since each step in the mechanism is itself a chemical reaction and is written as such, the equation representing an elemental process looks the same as an equation that represents the stoichiometry of a chemical reaction. The mechanistic equation, however, has an entirely different meaning than the stoichiometric equation. It is only from the context of their use that the reader knows which type of equation is being used, and the beginning kineticist must be sure to distinguish between their meanings in his or her thinking.

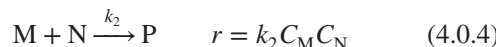
The number of chemical species involved in a single elementary reaction is referred to as the *molecularity* of that reaction. Molecularity is a theoretical concept, whereas stoichiometry and order are empirical in nature. They can be determined experimentally. A simple reaction is referred to as *uni-*, *bi-*, or *termolecular* if one, two, or three species, respectively, participate as reactants. The majority of known elementary steps are bimolecular, with the balance being unimolecular and termolecular.

Because an elementary reaction occurs on a molecular level exactly as it is written, its rate expression can be determined by inspection. A unimolecular reaction is a first-order process, bimolecular reactions are second-order, and termolecular processes are third-order. However, the converse statement is not true. Second-order rate expressions are not necessarily the result of an elementary bimolecular reaction. While a stoichiometric chemical equation remains valid when multiplied by an arbitrary factor, a mechanistic equation loses its meaning when multiplied by an arbitrary factor. Whereas stoichiometric coefficients and reaction orders may be integers or nonintegers, the molecularity of a reaction is always an integer. The following examples indicate the types of rate expressions associated with various molecularities.

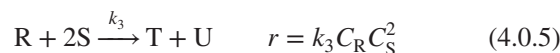
Unimolecular:



Bimolecular:



Termolecular:



Note that for the last reaction the stoichiometric coefficients require that

$$r_S = -2k_3 C_R C_S^2 \quad (4.0.6)$$

Each elementary reaction must fulfill the following criteria:

1. On a molecular scale the reaction occurs exactly as written.
2. The simple reaction should break or form as few bonds as possible. Normally, only one bond is made and/or broken. Occasionally, two bonds are broken and two new ones formed in a four-center reaction. Only very rarely do more complex processes occur.
3. The simple reaction must be feasible with respect to bond energies, atomic geometry, and allowed electron shifts.

In all but the simplest cases, the mechanism of a reaction consists of a number of steps, some of which involve reacting species that do not appear in the overall stoichiometric equation for the reaction. Some of these *intermediate species* are stable molecules that can be isolated in the laboratory. Others are highly reactive species that can be observed only by using sophisticated experimental techniques. These reaction intermediates are sometimes referred to as *active centers*.

Among the various intermediate species that may participate in a reaction sequence are stable molecules, ions, free atoms, free radicals, carbonium ions, molecular and ionic complexes, and tautomeric or excited forms of stable molecules. If the intermediate is, indeed, a stable substance, then its presence can be detected by any of the standard techniques of chemical analysis, provided that the intermediate can be isolated (i.e., prevented from participation in the processes that would normally follow its formation). If isolation is impossible, then the techniques available for the study of stable intermediates are the same as those for the study of highly reactive species. The review by Wayne (1) and the text by Zuman and Patel (2) contain useful discussions of a multiplicity of experimental techniques that are of interest to researchers focusing on the kinetics and mechanisms of reactions.

## 4.1 REACTION MECHANISMS

At first glance the problem of “finding the mechanism” of a reaction may appear to a beginning student as an exercise in modern alchemy. Nonetheless, there are certain basic principles underlying the reasoning that intervenes

between experimental work and postulation of a set of molecular events that give rise to the chemical reaction being investigated. In this section we discuss the nature of the problem, the means by which one derives a rate expression from a proposed sequence of reactions, and some techniques that are useful in the elucidation of reaction mechanisms.

### 4.1.1 The Nature of the Problem

Postulation of a reaction mechanism involves inductive rather than deductive thinking. Even though the kinetics researcher may present the ideas and experiments that lead to a proposed mechanism in a logical orderly manner, the thought processes leading to these results involve elements of experience, intuition, luck, knowledge, and guesswork.

A person who has started work on a kinetics research project will usually have some preconceived ideas about the mechanism of the reaction being investigated and will usually know the major products of the reaction before starting any kinetics experiments. From a literature search the kineticist often has knowledge of experimental rate expressions and proposed mechanisms for similar reactions. As the kineticist proceeds with the experimental work and determines the complete product distribution, the order of the reaction, and the effects of temperature, pressure, solvent, and so on, on the reaction rate, his or her ideas relative to the mechanism will evolve into a coherent and logical picture. Along the path, however, the preliminary ideas may be shuffled, added to, discarded, broadened, or refurbished before they can be manipulated into a logical sequence of events that is consistent with all of the available facts. Each mechanism study evolves in its own fashion as the investigator designs experiments to test provisional mechanisms that have been postulated on the basis of earlier experiments. These experiments constitute a more or less systematic attempt to make mechanistic order and sense out of what may appear to the uninitiated observer to be a random collection of experimental facts. By the time the experimental research is completed and the results are ready for publication, the investigator will have resolved his or her ideas about the mechanism into a coherent picture that can be presented in a systematic and rational manner. Since this end result is all that is published for the judgment of the scientific community, the uninitiated observer obtains the false impression that the research work itself was actually carried out in this systematic and rational fashion. In the actual program there may have been many false starts and erroneous ideas that had to be overcome before arriving at the final result. To a fellow kineticist, however, the investigator's systematic and logical rendering of the experimental facts is an efficient means of communicating the results of the research.

The problem of determining the mechanism of a chemical reaction is one of the most interesting and challenging intellectual and experimental problems that a chemical engineer or chemist is likely to encounter. Even for relatively simple mechanisms, it is occasionally difficult to determine from the assumptions about the elementary reactions just what the exact form of the predicted dependence of the rate on reactant concentrations should be. In many cases the algebra becomes intractable and, without an a priori knowledge of the magnitudes of various terms, it may be difficult or even impossible for the theoretician to make simplifications that will permit these predictions to be made. Many chemical reactions are believed to have mechanisms involving a large number of elementary steps [e.g., the mechanism of the reaction between  $H_2$  and  $O_2$  contains at least 26 steps (3)], and it becomes an extremely formidable task to manipulate the corresponding mathematical relations to predict the dependence of the rate on the concentrations of stable molecules. How much more formidable is the problem that our investigator must tackle—that of deriving such a mechanism consistent with all available experimental data!

Because the problem of deriving a rate expression from a postulated set of elementary reactions is simpler than that of determining the mechanism of a reaction, and because experimental rate expressions provide one of the most useful tests of reaction mechanisms, we now consider this problem.

### 4.1.2 Basic Assumptions Involved in the Derivation of a Rate Expression from a Proposed Reaction Mechanism

The mechanism of a chemical reaction is a microscopic description of the reaction in terms of its constituent elementary reactions. The fundamental principle from which one starts is that the rate of an elementary reaction is proportional to the frequency of collisions indicated by the stoichiometric/mechanistic equation for the reaction (i.e., to the product of the concentrations indicated by the molecularity of the elementary reaction). In addition, one usually bases the analysis on one or more of the following simplifications to make the mathematics amenable to closed-form solution.

First, one often finds it convenient to *neglect reverse reactions* (i.e., the reaction is considered to be “irreversible”). This assumption will be valid during the initial stages of any reaction, since the number of product molecules available to serve as reactants for the reverse reaction will be small during this period. If the equilibrium constant for the reaction is very large, this assumption will also be valid for intermediate and later stages of the reaction.

Second, it may be convenient to assume that one elementary reaction in the sequence occurs at a much slower rate than any of the others. The overall rate of conversion of reactants to products may be calculated correctly on the assumption that this step governs the entire process. The concept of a *rate-limiting step* is discussed in more detail below.

Third, it is often useful to assume that the concentration of one or more of the intermediate species is not changing very rapidly with time (i.e., that one has a *quasi-stationary-state* situation). This approximation is also known as the *Bodenstein steady-state approximation* for intermediates. It implies that the rates of production and consumption of intermediate species are nearly equal. This approximation is particularly good when the intermediates are highly reactive.

Fourth, one often finds it convenient to assume that one or more reactions is in a *quasi-equilibrium condition* (i.e., the forward and reverse rates of this reaction are much greater than those of the other reactions in the sequence). The net effect is that these other reactions do not produce large perturbations of the first reaction from equilibrium.

In the sequence of elementary reactions making up the overall reaction, there often is one step that is very much slower than all the subsequent steps leading to reaction products. In these cases the rate of product formation may depend on the rates of all the steps preceding the last slow step, but will not depend on the rates of any of the subsequent more rapid steps. This last slow step has been termed the *rate-controlling*, *rate-limiting*, or *rate-determining step* by various authors.

In a mechanism consisting of several consecutive elementary reaction steps, fragments of the initial reactant pass through a number of intermediate stages, finally ending up in the products of the reaction. The total time necessary to produce a molecule of product is simply the sum of the discrete times necessary to pass through each individual stage of the overall reaction. Where a reversible reaction step is involved, the net time for that step is necessarily increased by the “feedback” of intermediate accompanying that step. The mean reaction time ( $t_{\text{mean}}$ ) is thus

$$t_{\text{mean}} = t_1 + t_2 + t_3 + \cdots + t_n \quad (4.1.1)$$

where the  $t_i$  represent *effective times necessary on the average* to accomplish each step.

The overall reaction rate  $r$  may be defined as the reciprocal of this mean reaction time:

$$r = \frac{1}{t_{\text{mean}}} \quad (4.1.2)$$

Thus,

$$r = \frac{1}{t_1 + t_2 + t_3 + \cdots + t_n} \quad (4.1.3)$$

The rates of each individual step are given by analogs of equation (4.1.2). Thus,

$$r = \frac{1}{1/r_1 + 1/r_2 + 1/r_3 + \cdots + 1/r_n} \quad (4.1.4)$$

If one of the terms (say,  $t_{\text{RLS}}$ ) in the denominator of equation (4.1.3) is very much larger than any of the others, the right side of this equation can be approximated as

$$r = \frac{1}{t_{\text{RLS}}} = r_{\text{RLS}} \quad (4.1.5)$$

where the subscript RLS refers to the rate-limiting step.

If some of the processes prior to the rate-limiting step are characterized by times comparable to that of the rate-determining step, equation (4.1.4) may be rewritten as

$$r = \frac{1}{1/r_1 + 1/r_2 + 1/r_3 + \cdots + 1/r_{\text{RLS}}} \quad (4.1.6)$$

where terms corresponding to events beyond the last slow step in the process have been dropped. Kinetic events preceding the *last* slow step can influence the overall reaction rate, but subsequent steps cannot.

### 4.1.3 Preliminary Criteria for Testing a Proposed Reaction Mechanism: Stoichiometry and Derivation of a Rate Expression for the Mechanism

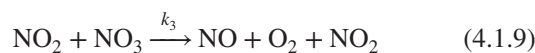
There are two crucial criteria with which a proposed mechanism must be consistent.

1. The net effect of the elementary reactions must correspond to the stoichiometry of the overall reaction and must explain the formation of all observed products.
2. The mechanism must yield a rate expression consistent with that observed experimentally.

For relatively simple reaction mechanisms, the net or overall effect of the elementary reactions can be determined by adding them together. For example, the stoichiometric equation for the decomposition of nitrogen pentoxide is



A mechanism that might be proposed to explain this reaction is

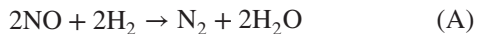


If one multiplies equation (4.1.8) by 2 and adds the result to equations (4.1.9) and (4.1.10), one obtains equation (4.1.7).

For mechanisms that are more complex, the task of showing that the net effect of the elementary reactions is the stoichiometric equation may be a difficult problem in algebra whose solution will not contribute significantly to an understanding of the reaction mechanism. Even though it may be a fruitless task to find the exact linear combination of elementary reactions that gives quantitative agreement with the product distribution observed, it is nonetheless imperative that the mechanism qualitatively imply the reaction stoichiometry. Let us now consider a number of examples that illustrate the techniques used in deriving an overall rate expression from a set of mechanistic equations.

### ILLUSTRATION 4.1 Demonstration That Two Proposed Mechanisms Can Lead to the Same Rate Expression

The stoichiometry of the reaction of nitric oxide with hydrogen is

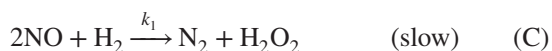


The overall rate expression is third order:

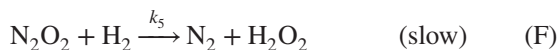
$$r_{\text{N}_2} = k[\text{NO}]^2[\text{H}_2] \quad (\text{B})$$

Two different mechanisms have been proposed for this reaction.

*Mechanism A:*



*Mechanism B:*



Show that these two mechanisms are each consistent with both the rate expression observed and the stoichiometry of the reaction.

### Solution

First consider mechanism A. Addition of reactions (C) and (D) gives reaction (A), so the stoichiometry of the mechanism is consistent. Reaction (C) is the rate-limiting step; hence, the overall reaction rate is given by

$$r_{\text{N}_2} = k_1[\text{NO}]^2[\text{H}_2] \quad (\text{H})$$

This rate expression is consistent with the kinetics observed, so this combination of a slow termolecular step with a rapid bimolecular step is a plausible mechanism based on the information we have been given.

Now consider mechanism B. Addition of reactions (E), (F), and (G) again yields equation (A). Thus, the stoichiometry is consistent. The second step in the mechanism is the rate-controlling step. Thus,

$$r_{\text{N}_2} = k_5[\text{N}_2\text{O}_2][\text{H}_2] \quad (\text{I})$$

This expression contains the concentration of an intermediate species ( $\text{N}_2\text{O}_2$ ). This species may be eliminated by recognizing that reaction (E) is essentially at equilibrium. Hence,

$$k_3[\text{NO}]^2 = k_4[\text{N}_2\text{O}_2] \quad (\text{J})$$

The concentration of the intermediate is given by

$$[\text{N}_2\text{O}_2] = \frac{k_3}{k_4}[\text{NO}]^2 = K_E[\text{NO}]^2 \quad (\text{K})$$

where  $K_E$  is an equilibrium constant for reaction (E). Substitution of this expression for the  $\text{N}_2\text{O}_2$  concentration in equation (I) gives

$$r_{\text{N}_2} = \frac{k_3 k_5}{k_4}[\text{NO}]^2[\text{H}_2] = k_5 K_E[\text{NO}]^2[\text{H}_2] \quad (\text{L})$$

These equations are consistent with the kinetics observed if we identify  $k$  as

$$k = \frac{k_3 k_5}{k_4} = k_5 K_E \quad (\text{M})$$

Thus, mechanism B, which consists solely of bimolecular and unimolecular steps, is also consistent with the information that we have been given. This mechanism is somewhat simpler than the first in that it does not require a termolecular step.

This illustration points out that the fact that a mechanism gives rise to the experimentally observed rate expression is by no means an indication that the mechanism is a unique solution to the problem being studied. We may disqualify a mechanism from further consideration on the grounds that it is inconsistent with the kinetics observed, but consistency merely implies that we are at liberty to continue our search for other mechanisms that are consistent and attempt to use some of the techniques discussed in Section 4.1.5 to discriminate between the consistent mechanisms. It is also entirely possible that more than one mechanism may be applicable to a single overall reaction and that parallel paths for the reaction exist. Indeed, many catalysts are believed to function by providing alternative routes for a reaction. In the case of parallel reaction paths, each mechanism proceeds

independently, but the vast majority of the reaction will occur via the path associated with the fastest rate.

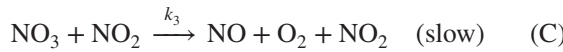
## ILLUSTRATION 4.2 Use of Steady-State and Pseudo-Equilibrium Approximations for Intermediate Concentrations

The thermal decomposition of nitrogen pentoxide to oxygen and nitrogen dioxide



is a classic reaction in kinetics because it was the first gas phase first-order reaction to be reported (4).

Analysis of reports by a number of investigators indicates that the following mechanism appears to give the best agreement with the available experimental facts.



In reaction (C) the  $\text{NO}_2$  itself does not react but plays the role of a collision partner that may effect the decomposition of  $\text{NO}_3$ . The  $\text{NO}_2$  and  $\text{NO}_3$  species may react via the two paths indicated by the rate constants  $k_2$  and  $k_3$ . The first of these reactions is believed to have a very small activation energy; the second reaction is endothermic and consequently will have an appreciable activation energy. On the basis of this reasoning, Ogg (5) postulated that  $k_3$  is much less than  $k_2$  and that reaction (C) is the rate-controlling step in the decomposition. Reaction (D), which we have included, differs from the final step postulated by Ogg. Derive an expression for the overall reaction rate based on the mechanism above.

### Solution

The rate of the overall reaction is given by either of the following expressions:

$$r = \frac{-d[\text{N}_2\text{O}_5]}{2dt} = \frac{d[\text{O}_2]}{dt} \quad (\text{E})$$

The second is more useful for our purposes, because oxygen is produced in only one step of the mechanism and that step is the rate-controlling step. Thus,

$$r = r_{\text{RLS}} = k_3[\text{NO}_3][\text{NO}_2] \quad (\text{F})$$

Equation (F) contains the concentration of an intermediate ( $\text{NO}_3$ ) that does not appear in the overall stoichiometric

equation. This term may be eliminated by means of the Bodenstein steady-state approximation:

$$\begin{aligned} \frac{d[\text{NO}_3]}{dt} &= k_1[\text{N}_2\text{O}_5] - k_2[\text{NO}_2][\text{NO}_3] \\ &- k_3[\text{NO}_3][\text{NO}_2] - k_4[\text{NO}][\text{NO}_3] \approx 0 \end{aligned} \quad (\text{G})$$

Thus,

$$[\text{NO}_3]_{\text{SS}} = \frac{k_1[\text{N}_2\text{O}_5]}{k_2[\text{NO}_2] + k_3[\text{NO}_2] + k_4[\text{NO}]} \quad (\text{H})$$

The subscript SS refers to a steady-state value.

Equation (H) also involves the concentration of a reaction intermediate  $[\text{NO}]$ . If we make the steady-state approximation for this species,

$$\frac{d[\text{NO}]}{dt} = k_3[\text{NO}_2][\text{NO}_3] - k_4[\text{NO}][\text{NO}_3] \approx 0 \quad (\text{I})$$

or

$$[\text{NO}]_{\text{SS}} = \frac{k_3}{k_4}[\text{NO}_2] \quad (\text{J})$$

Combination of equations (H) and (J) gives

$$[\text{NO}_3]_{\text{SS}} = \frac{k_1[\text{N}_2\text{O}_5]}{k_2[\text{NO}_2] + 2k_3[\text{NO}_2]} \quad (\text{K})$$

This relation may now be substituted into equation (F) to obtain an expression for the overall rate of reaction that contains only the concentrations of species that appear in the stoichiometric equation:

$$r = \frac{k_1 k_3 [\text{N}_2\text{O}_5]}{k_2 + 2k_3} \quad (\text{L})$$

This relation is consistent with the first-order rate expression that is observed experimentally.

Instead of using the steady-state approximation in the manipulation of the individual rate expressions, one may arrive at the same result by assuming that a pseudo-equilibrium condition is established with respect to reaction (B) and that reaction (C) continues to be the rate-limiting step. From the pseudo-equilibrium condition,

$$[\text{NO}_3]_{\text{PE}} = \frac{k_1}{k_2} \frac{[\text{N}_2\text{O}_5]}{[\text{NO}_2]} \quad (\text{M})$$

where the subscript PE is used to indicate the pseudo-equilibrium concentration.

As above,

$$r = r_{\text{RLS}} = k_3[\text{NO}_3][\text{NO}_2] \quad (\text{N})$$

Combination of equations (M) and (N) gives

$$r = \frac{k_1 k_3}{k_2} [\text{N}_2\text{O}_5] \quad (\text{O})$$

This expression is the same as that obtained by the steady-state approach if one makes the assumption that  $k_2 \gg k_3$ .

Illustration 4.2 indicates how one employs the assumptions that are frequently made in the derivation of a reaction rate expression from a proposed mechanism. Additional examples involving the use of these assumptions are presented in conjunction with the discussion of chain reactions in Section 4.2.

#### 4.1.4 From Stoichiometry and Rate Expression to Mechanism

To the uninitiated student, the task of postulating a suitable mechanism for a complex chemical reaction often seems to be an exercise in extrasensory perception. Even students who have had some exposure to kinetics often cannot understand how the kineticist can write down a series of elementary reactions and claim that the mechanism is reasonable. Nonetheless, there is a set of guidelines within which the kineticist works in postulating a mechanism. Since these working principles are known to experienced kineticists, they are able to make implicit chemical judgments so automatically that they often cannot see the problem from a student's viewpoint. These principles are seldom stated explicitly in the literature, but the authors have elected to use the extensive collection of Edwards et al. (6) as a useful point of departure in providing guidelines that permit a kineticist to judge the reasonableness of a proposed mechanism. Often, they will permit the elimination of a proposed sequence of reactions as being unreasonable in the light of available experimental data.

**Guideline 1.** *The most fundamental basis for mechanistic speculation is a complete analysis of the reaction products.* It is important to obtain a complete quantitative and qualitative analysis for *all* products of the reaction. Inasmuch as many chemical reactions give a complex array of products, the relative proportions of which change as the time of reaction increases, it is very useful to carry out a complete analysis for the shortest possible reaction time and for successively longer periods. In this manner one can differentiate between primary products formed directly from the reactants and secondary products formed by subsequent reaction of the primary products. Such analyses can give valuable clues as to the identity of reaction intermediates.

**Guideline 2.** *The atomic and electronic structure of the reactants and products may provide important clues as to the nature of possible intermediate species.* The degree of atomic and electronic rearrangement that takes place will often indicate which portions of the reactant molecules participate in the reaction act and which would be involved in elementary reactions leading to the formation of reaction intermediates. The structural arrangement of atoms in the

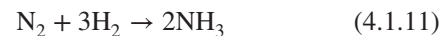
molecules that react must correspond at the instant of reaction to interatomic distances appropriate for the formation of new species.

**Guideline 3.** *All of the elementary reactions involved in a mechanistic sequence must be feasible with respect to bond energies.* Compared to the average density of molecular energies in a reacting mixture, the energies required to break interatomic bonds in a molecule are quite large. Because of this, elementary reactions will normally involve relatively simple acts in which few bonds are involved. Complicated rearrangements consisting of a series of concerted motions must be viewed with skepticism in the absence of strong supporting evidence. Bond energy considerations also lead to the conclusion that highly endothermic elementary reactions will be slow processes because of the large activation energies normally associated with these reactions.

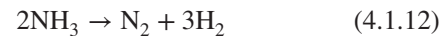
**Guideline 4.** *A number of elementary reactions sufficient to provide a complete path for the formation of all observed products must be employed.*

**Guideline 5.** *All of the intermediates produced by the elementary reactions must be consumed by other elementary reactions so that there will be no net production of intermediate species.*

**Guideline 6.** *The great majority of known elementary steps are bimolecular, the remainder being unimolecular or termolecular.* Any reaction for which the stoichiometric coefficients of the reactants add up to four or more must involve a multiplicity of steps. For example, the ammonia synthesis reaction is known to occur by a number of steps rather than as



**Guideline 7.** *A mechanism postulated for a reaction in the forward direction must also hold for the reverse reaction.* This guideline is a consequence of the principle of microscopic reversibility (see Section 4.1.5.4). Three corollaries of this guideline should also be kept in mind when postulating a reaction mechanism. First, the rate-limiting step for the reverse reaction must be the same as that for the forward reaction. Second, the reverse reaction cannot have a molecularity greater than 3, just as the forward reaction is so limited. Consequently, the ammonia decomposition reaction



cannot occur as a simple bimolecular process. Third, if the reaction rate expression for the forward reaction consists of two or more independent terms corresponding to parallel reaction paths, there will be the same number of independent terms in the rate expression for the reverse reaction. At equilibrium not only is the total rate of the forward reaction

equal to the total rate of the reverse reaction, but the forward rate by each path is equal to the reverse rate for that particular path.

**Guideline 8.** *Transitory intermediates (highly reactive species) do not react preferentially with one another to the exclusion of their reaction with stable species.* The concentration of these intermediates is usually so low that the number of encounters that an intermediate may undergo with other intermediates will be very small compared to the number of encounters it will undergo with stable molecules.

**Guideline 9.** *When the overall order of a reaction is greater than 3, the mechanism probably has one or more equilibria yielding intermediates prior to the rate-determining step.*

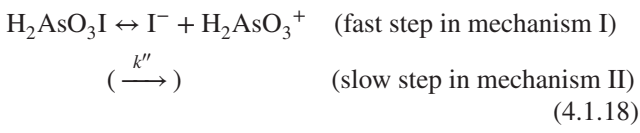
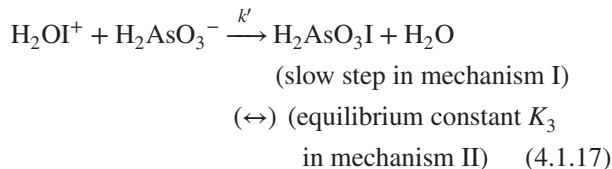
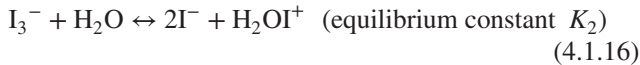
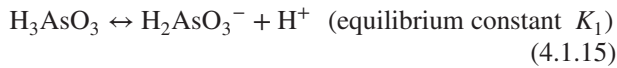
**Guideline 10.** *Inverse (negative) orders arise from rapid equilibria prior to the rate-determining step.* To illustrate this point, consider the oxidation of arsenious acid in an aqueous solution:



The rate expression observed experimentally is

$$r = \frac{k[\text{H}_3\text{AsO}_3][\text{I}_3^-]}{[\text{I}^-]^2[\text{H}^+]} \quad (4.1.14)$$

Two mechanisms that have been proposed are based on the following sequence of elementary reactions:



For the first mechanism the overall reaction rate may be taken to be that of the rate-limiting step:

$$r = k'[\text{H}_2\text{OI}^+][\text{H}_2\text{AsO}_3^-] \quad (4.1.20)$$

With the use of the equilibrium steps (4.1.15) and (4.1.16), this expression may be converted to a form consistent with the experimental rate expression:

$$r = k'K_1K_2 \frac{[\text{I}_3^-][\text{H}_2\text{O}][\text{H}_3\text{AsO}_3]}{[\text{I}^-]^2[\text{H}^+]} \quad (4.1.21)$$

because the solvent concentration  $[\text{H}_2\text{O}]$  is just another constant.

For the second mechanism, equation (4.1.18) is the rate-controlling step, and the arrows in parentheses indicate the assumptions made regarding the reversibility of reactions (4.1.17) and (4.1.18). The overall reaction rate is now that of the rate-limiting step:

$$r = k''[\text{H}_2\text{AsO}_3\text{I}] \quad (4.1.22)$$

With the use of the equilibrium expressions for the first three reactions, equation (4.1.22) may be converted to the form

$$r = k''K_1K_2K_3 \frac{[\text{H}_3\text{AsO}_3][\text{I}_3^-]}{[\text{H}^+][\text{I}^-]^2} \quad (4.1.23)$$

This rate law is also consistent with the experimental rate expression.

In both cases the negative reaction orders arise from equilibria that are established prior to the rate-controlling step. The reader should note that a final rate expression depends only on equilibria that are established by elementary reactions *prior* to the rate-determining step. Subsequent equilibria [e.g., (4.1.19)] do not influence its form.

**Guideline 11.** *Whenever a rate law contains noninteger orders, there are intermediates present in the reaction sequence.* Observation of a fractional order in an empirical rate expression for a homogeneous reaction is often an indication that an important part of the mechanism is the splitting of a molecule into free radicals or ions.

**Guideline 12.** If the magnitude of the stoichiometric coefficient of a reactant exceeds the order of the reaction with respect to that species, there are one or more intermediates and reactions after the rate-determining step. Before applying this rule, one must write the stoichiometric equation for the reaction in a form such that all coefficients are integers (see Illustrations 4.1 and 4.2).

**Guideline 13.** *If the order of a reaction with respect to one or more species increases as the concentration of that species increases, this is an indication that the reaction may be proceeding by two or more parallel paths.* Liebhafsky and Mohammed (7) reported that for the reaction between hydrogen peroxide and iodide ion, the order with respect to hydrogen ion increases from zero to 1 as the pH is decreased.

$$r = k_1[\text{H}_2\text{O}_2][\text{I}^-] + k_2[\text{H}_2\text{O}_2][\text{H}^+][\text{I}^-] \quad (4.1.24)$$

Such expressions are typical of many acid and base catalyzed reactions (see Section 7.3.1).

**Guideline 14.** *If there is a decrease in the order of a reaction with respect to a particular substance as the concentration of that species increases, the dominant form of that species in solution may be undergoing a change*

brought about by the change in concentration. A decrease in reaction order with respect to hydrogen ion concentration with increasing acidity has frequently been observed for reactions involving weak acids.

The guidelines enumerated above are by no means complete, but they do provide a starting point for the beginning student. Further details are available in publications by Edwards et al. (6) and King (8).

### 4.1.5 Additional Methods and Principles Used in Investigations of Reaction Mechanisms

Although reaction rate expressions and reaction stoichiometry are the experimental data most often used as a basis for the postulation of reaction mechanisms, many other experimental techniques can contribute to the elucidation of these molecular processes. The conscientious investigator of reaction mechanisms will draw on a wide variety of experimental and theoretical methods in his or her research program in an attempt to obtain information about the elementary reactions taking place in the system of interest. Some useful techniques are described below. The information that they supply may provide a basis for choice between two or more alternative mechanisms, or it may provide additional circumstantial evidence that a proposed mechanism is indeed correct.

#### 4.1.5.1 Studies of Reaction Intermediates

In recent decades the most fruitful progress in experimental studies of reaction mechanisms has come about through the development of instrumental techniques for detecting and identifying the trace amounts of active intermediates produced in complex reaction systems. Such studies place a mechanism on a much firmer basis than exists in those cases where the identities of intermediates can only be surmised.

A stable species that is suspected to act as an intermediate in a complex chemical reaction can often be added to a reaction mixture and its effects observed. If the appropriate products are formed *at a rate no less than that of the “uninterrupted” or “original” reaction*, this is strong evidence that the reaction proceeds through the intermediate that has been added. This evidence is, however, not unequivocal. Similarly, the failure of other presumed intermediates to give the correct products under appropriate reaction conditions will cause a kineticist to revise his or her ideas concerning the mechanism of the reaction being investigated. For example, the Clemmensen reduction of carbonyl  $[-(CO)-]$  groups to methylene  $[-(CH_2)-]$  groups, using zinc amalgam and hydrochloric acid, cannot proceed through the corresponding carbinol  $[-CH(OH)-]$  because the carbinols themselves are not

generally reduced by the same combination of reactants (9).

For detailed treatments of the experimental methods used in studies of reaction intermediates, consult the work of Wayne (1), Zuman and Patel (2), Melville and Gowenlock (10), Anderson (11), Friess et al. (12), Lewis (13), and Hammes (14).

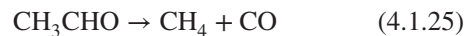
#### 4.1.5.2 Isotopic Substitution Techniques

If one can discover where the various portions of reactant molecules end up in the product molecules, a great deal of insight into the mechanism of the reaction can be gained. By isotopically labeling a functional group or atom in a molecule and examining the distribution (or lack thereof) of the tagged species after reaction, it is possible to determine which bonds are broken and formed. In studies with radioactive and stable isotopes it is generally assumed that the kinetic behavior of a labeled atom is essentially the same as that of an unlabeled atom. The important exceptions are studies involving deuterium and tritium.

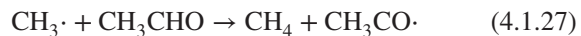
There are three basic types of mechanistic information that are derived from isotopic experiments.

1. A knowledge of which bonds are broken and thus give rise to intramolecular or intermolecular rearrangements
2. A knowledge of whether the reaction proceeds in an isolated molecule or requires the participation of more than one molecule
3. A knowledge of which products are the precursors of others

As an example, consider the thermal and photochemical decomposition of acetaldehyde:



One proposed mechanism involves an intramolecular rearrangement, while a second involves a free-radical chain mechanism composed of the following sequence of elementary reactions:



where reactions (4.1.27) and (4.1.28) occur many, many times for each time that reaction (4.1.26) occurs. If one uses a mixture of  $CH_3CHO$  and  $CD_3CDO$  to study this reaction, the first mechanism predicts that only  $CD_4$  and  $CH_4$  will be formed, while the second predicts that a mixture of  $CD_4$ ,  $CH_4$ ,  $CH_3D$ , and  $CD_3H$  will be formed. The fact that the statistically expected distribution of the latter methane species was observed experimentally (15–17) is taken as evidence that the major path for this reaction is the chain reaction sequence.

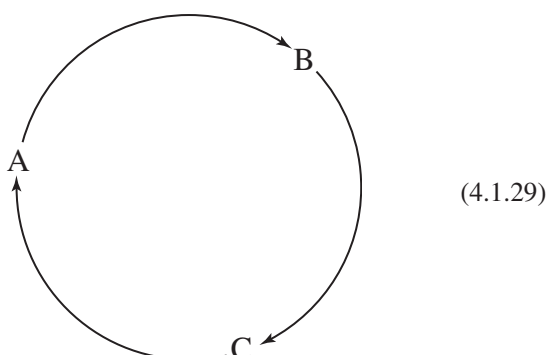
### 4.1.5.3 Stereochemical Methods

Many organic reactions involve reactants that can exist in stereoisomeric forms. If an optically active reactant yields a product that is capable of exhibiting optical activity but does not exhibit such activity, it is usually assumed that the reaction must involve an intermediate that is not optically active (e.g., a carbonium ion intermediate). If it can be determined that the configuration of an optically active product differs from or is similar to that of the optically active reactant, one gains information about whether there is an *inversion of configuration*. Retention of configuration might imply a two-step process, the first step turning the molecule “inside out,” and the second step turning it “outside in” again. It could also mean that none of the bonds of the optically active carbon atom are broken in the reaction.

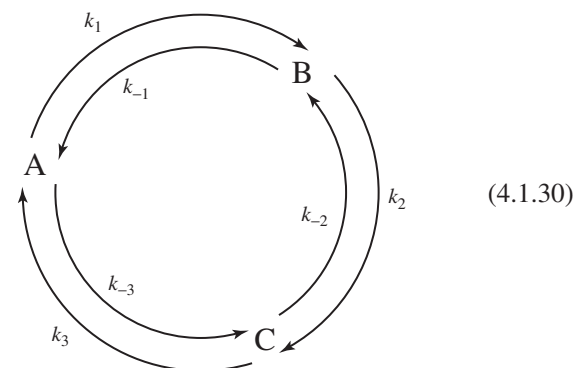
### 4.1.5.4 The Principle of Microscopic Reversibility

The principle of microscopic reversibility is based on statistical mechanical arguments and was first formulated by Tolman (18) in 1924: *In a system at equilibrium, any molecular process and the reverse of that process occur on the average at the same rate.*

The most significant consequence of this principle for kineticists is that if in a system at equilibrium there is a flow of reacting molecules along a particular reaction path, there must be an equal flow in the opposite direction. This principle implies that the reaction path established as most probable for the forward direction must also be the most probable path for the reverse reaction. This consequence is also known as the principle of *detailed balancing* of chemical reactions. Its relationship to the principle of microscopic reversibility has been discussed by Denbigh (19). If we consider a substance that can exist in three intraconvertible isomeric forms, A, B, and C (e.g., *trans*-butene-2, *cis*-butene-2, and butene-1), there is more than one independent reaction that occurs at equilibrium. The conditions for thermodynamic equilibrium would be satisfied if there were a steady unidirectional flow at the molecular level around the cycle



such that the concentration of each species remains constant. However, this flow would not be in accord with the principle of microscopic reversibility. If this principle were not applicable, the concentrations of the various species would show oscillations if one started with a nonequilibrium system and allowed it to approach equilibrium. Several attempts have been made to observe oscillatory phenomena of this type, but they have not led to definitive results. One concludes that each of the reactions should be balanced individually.



The requirement of detailed balancing has implications with regard to the relationships that must exist between reaction rate constants and equilibrium constants. It requires that at equilibrium each reaction must be balanced in the forward and reverse directions; that is,

$$k_1[A] = k_{-1}[B] \quad (4.1.31)$$

$$k_2[B] = k_{-2}[C] \quad (4.1.32)$$

$$k_3[C] = k_{-3}[A] \quad (4.1.33)$$

or

$$\frac{[A]}{[B]} = \frac{k_{-1}}{k_1} = K_{-1} \quad (4.1.34)$$

$$\frac{[C]}{[B]} = \frac{k_2}{k_{-2}} = K_2 \quad (4.1.35)$$

$$\frac{[A]}{[C]} = \frac{k_3}{k_{-3}} = K_3 \quad (4.1.36)$$

where the various  $K_i$  are equilibrium constants. However, equations (4.1.34) to (4.1.36) also indicate that

$$\frac{[A]}{[C]} = \frac{k_{-1}}{k_1} \frac{k_{-2}}{k_2} = \frac{k_3}{k_{-3}} \quad \text{or} \quad \frac{K_{-1}}{K_2} = K_3 \quad (4.1.37)$$

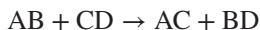
The principle of detailed balancing provides an automatic check on the self-consistency of postulated reaction mechanisms when equilibrium can be approached from both sides.

#### 4.1.5.5 Activation Energy Considerations

Activation energy considerations can provide a basis for eliminating certain elementary reactions from a sequence of proposed reactions. Unfortunately, the necessary activation energy data are seldom available, and one must estimate these parameters by empirical rules and generalizations that are of doubtful reliability.

Activation energies for bimolecular reactions have been correlated with bond energy data by use of the *Hirschfelder rules* (20).

1. For a simple displacement reaction involving atoms or radicals, such as  $A + BC \rightarrow AB + C$ , where the reaction is written in the exothermic direction, the activation energy is 5.5% of the dissociation energy of the bond that is broken. For the reverse endothermic reaction, the standard energy change of reaction must be added to this quantity to obtain the activation energy.
2. For an exchange reaction such as



where the reaction is again written in the exothermic direction, the activation energy is 28% of the sum of the AB and CD bond strengths. For the reverse endothermic reaction, the activation energy is the sum of the standard energy change for the reaction and the activation energy for the exothermic reaction.

Semenov (21) suggested that for *exothermic* abstraction and addition reactions of atoms and small radicals, the following relation is useful:

$$E = 11.5 - 0.25q \quad (4.1.38)$$

where  $q$  is the heat *evolved* in the reaction expressed in kilocalories and  $E$  is also expressed in kilocalories. For the *endothermic* case,

$$E = 11.5 + 0.75q$$

These rules provide only very crude estimates of activation energies and are not sufficiently sensitive to show differences in a series of related reactions.

Other semi-theoretical approaches to the problem of predicting reaction activation energies exist (22–24). For our purposes, however, it is sufficient to recognize that “ballpark” estimates are the best one can expect. Such estimates are often adequate for purposes of differentiating between alternative mechanisms on the basis of a comparison of predicted and actual activation energies.

#### 4.1.5.6 Families of Reactions

Research in chemical kinetics can be influenced in several ways by similarities in reactivity among compounds having similar chemical structures. Consequently, one of the first steps in a kinetics investigation should be a careful study of the published literature on related reactions. Although one may occasionally be led astray by tentative conclusions drawn from a survey of the literature, the possibility of achieving large savings in time and laboratory effort is so much more likely that it should be considered a must. Such a survey furnishes a large bank of tested ideas and hypotheses about elementary reactions on which the investigator may draw for inspiration and stimulation. They provide a framework against which one can orient and test ideas about the mechanism of a specific reaction.

The fact that compounds having similar chemical structures often react in similar ways implies that they follow corresponding mechanisms in proceeding from reactants to products. One must have a very sound basis in experimental fact to be able to defend successfully a proposed reaction mechanism that contains elementary reactions that represent a major departure from those accepted by the scientific community as being a proper mechanistic interpretation of related reactions. On occasion such departures are necessary, and they themselves may provide the key to an improved understanding of the common family of related reactions.

#### 4.1.5.7 Occam's Razor: A Rule of Simplicity

Another principle occasionally used as a basis for choice between two alternative mechanisms is the rule of simplicity that is derived from a more general philosophical principle known as *Occam's razor*. The kineticist resorts to this rule when all of the experimental and theoretical information that has been brought to bear on the problem of determining the mechanism of a reaction leaves two (or more) mechanisms, both consistent with the facts. In this case one assumes that nature prefers the simple to the complex and that the reaction follows the simplest path. In many cases a serious question may exist as to which mechanism is simpler, but in others, the investigator may decide that one mechanism is more likely because it involves only bimolecular steps and no termolecular processes, or because it involves a smaller change in chemical structure than does an alternative mechanism. Complicated atomic rearrangements that occur in a single step are regarded with suspicion, and simpler stepwise processes are generally considered more probable.

Occam's razor states that “multiplicity ought not to be posited without necessity.” This principle is named for the fourteenth-century philosopher William Ockham (William of Occam), who was famous for his hardheaded

approach to problem solving. He believed in shaving away all extraneous details—hence the term *Occam's razor*. In essence his axiom states that when there are several possible solutions to a problem, the right one is probably the most obvious. Therefore, one should not postulate or accept mechanisms that are more complex than necessary to explain all observed experimental facts.

## 4.2 CHAIN REACTIONS

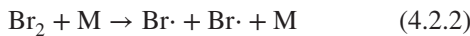
The reaction mechanisms treated thus far have involved the conversion of reactants to products by a sequence of elementary reactions proceeding in simple stepwise fashion. Once these sequences have been completed, all of the reaction intermediates have disappeared and only stable product molecules remain. These types of reaction are classified as *open sequence reactions* because they always proceed in stagewise fashion with no closed reaction cycles wherein a product of one elementary reaction is fed back to react with another species in an earlier elementary reaction. (Reversible reactions are, however, permitted in open sequence mechanisms.) In this section we deal with *closed sequence* or *chain reaction mechanisms* in which one of the reaction intermediates is regenerated during one stage of the reaction and is fed back to an earlier stage to react with other species so that a closed loop or cycle results. The intermediate species are thus periodically renewed by reaction, and the final products are the result of a cyclic repetition of the intervening processes. Because chain reactions play such an important role in systems of practical industrial significance, it is important that the chemical engineer understand their basic nature. Failure to comprehend the implications of chain reaction processes can lead to *hazardous explosions*.

To illustrate the nature of chain reactions, we consider a classic example: the formation of hydrogen bromide from molecular hydrogen and bromine in a homogeneous gas-phase reaction:



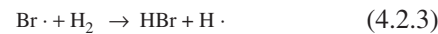
This stoichiometric equation does not give any indication of the complex nature of the mechanism by which this reaction proceeds.

In certain highly energetic collisions with any molecule M in the system, a bromine molecule may be dissociated in a homolytic split of the bond joining two bromine atoms:



The collision must be sufficiently energetic that enough energy is available to break the chemical bond linking the two bromine atoms. This type of reaction is called an *initiation* reaction because it generates a species that can serve as

a *chain carrier* or *active center* in the following sequence of elementary reactions.



and so on.

Equations (4.2.3) and (4.2.4) are the elementary reactions responsible for product formation. Each involves the formation of a chain carrying species [H· for (4.2.3) and Br· for (4.2.4)] that propagates the reaction. Addition of these two relations gives the stoichiometric equation for this reaction. These two relations constitute a single closed sequence in the cycle of events making up the chain reaction. They are referred to as *propagation reactions* because they generate product species that maintain the continuity of the chain.

The chain carriers need not all react with reactant molecules in chain propagation reactions. Some will disappear in *termination reactions* that do not involve the formation of species capable of maintaining the chain; for example,



where M represents a third body or molecule capable of soaking up and carrying away the energy released by the formation of a Br–Br bond.

Bond energy considerations indicate that the initiation reaction, (4.2.2), should be quite slow because its activation energy must be quite high (at least equal to the energy required to dissociate the Br–Br bond). If one were dealing with an open sequence reaction mechanism, such a step would imply that the overall reaction rate would also be low because in these cases the overall reaction becomes approximately equal to that of the rate-limiting step. In the case of a chain reaction, on the other hand, the overall reaction rate is usually much faster because the propagation steps occur *many* times for each time that an initiation step occurs.

The *chain length* of a reaction is defined as the average number of cycles in which a chain-carrying species participates from the time that it is first formed until the time that it is destroyed in a termination reaction. Depending on the relative rates of the propagation and termination steps, a chain may involve only a few links or it may be extremely long. For example, a chain length of  $10^6$  has been determined for the gas-phase chain reaction between hydrogen and chlorine. Chain length represents a statistical concept; some cycles will terminate before, and others after, the average number of propagation steps. This fact leads to a distribution of molecular weights in the polymers formed by

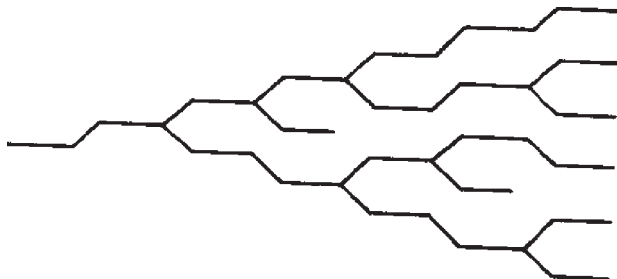
chain reactions. In terms of quantities that can be determined in the laboratory, we find it convenient to define the chain length ( $L$ ) by the ratio

$$L = \frac{\text{rate of disappearance of reactants}}{\text{rate of chain carrier formation by initiation}} \quad (4.2.8)$$

For the hydrogen–bromine reaction, each of the elementary propagation reactions leads to the formation of a single chain carrier. This type of reaction is said to be a *straight* or *linear chain reaction*. Some mechanisms involve elementary propagation reactions in which more than a single chain carrier is formed by the reaction. This type of reaction is known as a *branching reaction*. Examples of such reactions are



Both of these reactions involve the production of two active centers where there was only one before. When reactions of this type occur to a significant extent, the total number of active centers present in the system can increase very rapidly because a multiplication effect sets in as the chains propagate. The growth of chain carriers in a branched chain reaction is pictured as



When chain termination processes are operative such that they destroy chain carriers at a rate that makes the average net production of chain carriers unity, one has a situation corresponding to a nuclear power reactor generating energy at steady-state conditions. The effect of the destruction processes is to cause the chain branching process to degenerate to a straight-chain process. On the other hand, as the sketch indicates, there can be a multiplication of chain carriers. In physical terms this can lead to the chemical analog of a nuclear explosion (see Section 4.2.5).

## 4.2.1 The Reaction between Hydrogen and Bromine: $\text{H}_2 + \text{Br}_2 \rightarrow 2\text{HBr}$

In 1906, Bodenstein and Lind (25) investigated the gas-phase homogeneous reaction between molecular bromine and molecular hydrogen at pressures in the neighborhood of

1 atm. They fitted their experimental data with a rate expression of the form

$$\frac{d[\text{HBr}]}{dt} = \frac{k[\text{H}_2][\text{Br}_2]^{1/2}}{1 + k'([\text{HBr}]/[\text{Br}_2])} \quad (4.2.10)$$

where  $k'$  is a constant independent of temperature and where  $k$  follows the normal Arrhenius form for a reaction rate constant that has an activation energy of 40.2 kcal/mol.

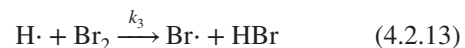
In 1919, Christiansen (26), Herzfeld (27), and Polanyi (28) all suggested the same mechanism for this reaction. The key factor leading to their success was recognition that hydrogen atoms and bromine atoms could serve alternately as chain carriers and thus propagate the reaction. By using a steady-state approximation for the concentrations of these species, these scientists were able to derive rate expressions that were consistent with that observed experimentally.

Their original mechanism consists of the following elementary reactions:

Initiation:



Propagation:



Termination:



Other reactions need not be considered on the basis of the arguments presented below. Reaction (4.2.14) is the reverse of reaction (4.2.12) and is responsible for the inhibition of the reaction by HBr. Steps (4.2.12) to (4.2.14) all produce one chain carrier to replace the chain carrier destroyed by the reaction. The sharp-eyed observer may have noted that the initiation and termination reactions proposed by these three people differ slightly from those discussed previously. The reasons for this are dealt with later.

From these equations, the overall rate of formation of HBr is given by

$$\frac{d[\text{HBr}]}{dt} = k_2[\text{Br}][\text{H}_2] + k_3[\text{H}][\text{Br}_2] - k_4[\text{H}][\text{HBr}] \quad (4.2.16)$$

As it stands, this expression is awkward and inconvenient to test because it contains the concentrations of bromine and hydrogen atoms, parameters that are not easily measured. In principle these quantities could be eliminated by solving this equation simultaneously with the differential equations for each of these species:

$$\frac{d[\text{H}]}{dt} = k_2[\text{Br}][\text{H}_2] - k_3[\text{H}][\text{Br}_2] - k_4[\text{H}][\text{HBr}] \quad (4.2.17)$$

$$\frac{d[\text{Br}]}{dt} = 2k_1[\text{Br}_2] - k_2[\text{Br}][\text{H}_2] + k_3[\text{H}][\text{Br}_2] + k_4[\text{H}][\text{HBr}] - 2k_5[\text{Br}]^2 \quad (4.2.18)$$

However, the complete solution of these three simultaneous differential equations is difficult to obtain and is no more instructive than the approximate solution that can be obtained by means of the steady-state approximation for intermediates. If one sets the time derivatives in equations (4.2.17) and (4.2.18) equal to zero and adds these equations, their sum is

$$2k_1[\text{Br}_2] - 2k_5[\text{Br}]^2 = 0 \quad (4.2.19)$$

This relation expresses the fact that under steady-state conditions, the rate of the initiation reaction is equal to the rate of the termination reaction, and the steady-state bromine atom concentration is equal to that which would arise from the equilibrium  $\text{Br}_2 \leftrightarrow 2\text{Br}\cdot$ ; that is,

$$[\text{Br}]_{\text{SS}} = \left( \frac{k_1}{k_5} [\text{Br}_2] \right)^{1/2} \quad (4.2.20)$$

Equation (4.2.20) may be combined with the steady-state form of either equation (4.2.17) or (4.2.18) to give

$$k_2 \left( \frac{k_1}{k_5} [\text{Br}_2] \right)^{1/2} [\text{H}_2] - (k_3[\text{Br}_2] + k_4[\text{HBr}])[\text{H}] = 0 \quad (4.2.21)$$

which, in turn, may be solved for the steady-state concentration of atomic hydrogen:

$$[\text{H}]_{\text{SS}} = \frac{k_2(k_1/k_5)^{1/2}[\text{Br}_2]^{1/2}[\text{H}_2]}{k_3[\text{Br}_2] + k_4[\text{HBr}]} \quad (4.2.22)$$

Equations (4.2.20) and (4.2.22) may be combined with equation (4.2.16) in straightforward algebraic manipulation to yield an expression for the overall rate of formation of HBr:

$$\frac{d[\text{HBr}]}{dt} = \frac{2k_2(k_1/k_5)^{1/2}[\text{H}_2][\text{Br}_2]^{1/2}}{1 + (k_4/k_3)\{[\text{HBr}]/[\text{Br}_2]\}} \quad (4.2.23)$$

Equation (4.2.23) has the same form as the empirical rate expression (4.2.10) and will agree with it quantitatively if

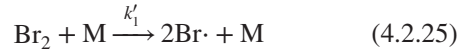
$$k = 2k_2 \left( \frac{k_1}{k_5} \right)^{1/2} \quad \text{and} \quad k' = \frac{k_4}{k_3} \quad (4.2.24)$$

Recognition that the kinetics of this reaction could be explained on the basis of the chain reaction mechanism presented above was one of the major breakthroughs in the evolution of the theory of chemical reaction mechanisms. Since the mechanism was first published, modifications in the initiation and termination steps have been required as additional experimental facts have been established by subsequent investigators. It is enlightening to consider these

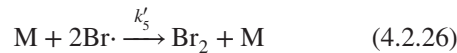
modifications and the rationale underlying the omission of certain elementary reactions from the mechanism.

Because the steady-state assumption leads to the equilibrium relation for the bromine atom concentration (4.2.20), it does not matter what mechanism is assumed to be responsible for establishing this equilibrium. Alternative elementary reactions for the initiation and termination processes, which give rise to the same equilibrium relationship, would also be consistent with the rate expression observed for HBr formation. For example, the following reactions give rise to the same equilibrium:

Initiation:



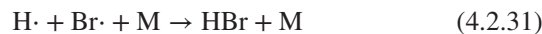
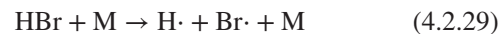
Termination:



where M is a third body. It represents any available molecule that is capable of supplying to bromine molecules the energy necessary for dissociation of the Br-Br bond and of carrying away enough energy in the termolecular reaction so that the Br-Br bond does not dissociate immediately.

If equations (4.2.25) and (4.2.26) are substituted for equations (4.2.11) and (4.2.15), respectively, in the mechanism described above, the net effect is to replace  $k_1$  by  $k'_1[\text{M}]$  and  $k_5$  by  $k'_5[\text{M}]$  everywhere that they appear. Since these quantities appear as a ratio in the final rate expression, the third-body concentration will drop out and  $k_1/k_5$  becomes identical to  $k'_1/k'_5$ . The necessity for the use of the third-body concentration thus is not obvious in kinetic studies of the thermal reaction. However, from studies of photochemical reaction between hydrogen and bromine, there is strong evidence that the termination reaction is termolecular. This fact and others based on studies of various atomic recombination reactions imply that the "correct" initiation and termination reactions are not reactions (4.2.11) and (4.2.15) but reactions (4.2.25) and (4.2.26).

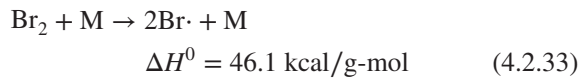
The next step in analysis of the mechanism is to indicate why we have limited the number of elementary reactions in the mechanism to five. To one uninitiated in the task of dealing with reaction mechanisms, it is difficult to see why elementary reactions such as



were rejected. We shall see that these reactions may be eliminated from consideration through the use of some of the concepts of probability and the bond energy requirements outlined previously. If any of these reactions were important, the rate expression for the revised mechanism would have a different mathematical form than that of the empirical rate expression.

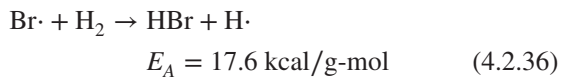
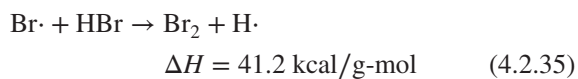
Equation (4.2.27) may be rejected even if it provides a parallel path competitive with the mechanism described above because its presence would require a second-order term in the experimental reaction rate expression.

The initiation reaction is the dissociation of molecular bromine rather than the dissociation of molecular hydrogen because the energy necessary to dissociate the latter is much greater than that required to dissociate the former. This fact is evident from a consideration of the standard enthalpies of reaction:



Because the activation energy of an endothermic elementary reaction cannot be less than  $\Delta H^0$ , the reaction with the significantly lower activation energy will occur much more frequently, other factors being equal. Similar arguments permit one to eliminate the HBr dissociation reaction from consideration.

The  $\text{Br}\cdot + \text{HBr}$  reaction will be unimportant in competition with the  $\text{Br}\cdot + \text{H}_2$  reaction because energy considerations again dictate that the former will have a much higher activation energy than the latter.



Both reactions are endothermic, but the interaction of bromine atoms with HBr is much more so than the interaction with molecular hydrogen. Consequently, the former reaction will occur much less frequently than the latter.

Equations (4.2.31) and (4.2.32) represent radical recombination reactions that might be considered as alternative termination reactions. Since these reactions and reaction (4.2.26) are radical recombination reactions, they will all have very low activation energies. The relative rates of these processes will then be governed by the collision frequencies and thus the concentrations of the reacting species. The relative concentrations of hydrogen and bromine atoms can be determined from the steady-state form of equation (4.2.17):

$$\frac{[\text{H}]}{[\text{Br}]} = \frac{k_2[\text{H}_2]}{k_3[\text{Br}_2] + k_4[\text{HBr}]} \quad (4.2.37)$$

If we consider this ratio during the initial stages of the reaction when the HBr concentration is extremely low and when the concentrations of hydrogen and bromine are nearly equal, this expression reduces to

$$\frac{[\text{H}]}{[\text{Br}]} \approx \frac{k_2}{k_3} \quad (4.2.38)$$

If the preexponential factors of these rate constants are comparable in magnitude, further simplification is possible.

$$\frac{[\text{H}]}{[\text{Br}]} \approx e^{-(E_2 - E_3)/RT} \quad (4.2.39)$$

If the estimation techniques discussed in Section 4.1.5.5 are employed, one finds that  $E_3$  is equal to 2.5 kcal. From (4.2.36),  $E_2$  is equal to 17.6 kcal. At 540 K the ratio of atomic concentrations is thus of the order of  $10^{-6}$ . Consequently, the reaction between atomic hydrogen and atomic bromine is only one millionth as likely as a reaction between two bromine atoms, and that between two hydrogen atoms is only  $1/10^{12}$  as likely. Although the atomic hydrogen concentration is extremely low under reaction conditions, it has been estimated to be four orders of magnitude greater than that which would be in equilibrium with molecular hydrogen. The excess hydrogen atom concentration over that which would exist at equilibrium is “paid for” by the energy liberated by the reacting mixture. This feature is a general characteristic of chain reactions. Superequilibrium steady-state concentrations of highly reactive intermediates can be produced as a result of the energy released by reaction.

The reaction between hydrogen and bromine illustrates many of the general features of straight-chain reactions. This reaction system has been studied by many investigators, and the body of accumulated experimental data represents as nearly a consistent and complete collection of data as is available for any reaction in the literature.

## 4.2.2 Chain Reaction Mechanisms: General Comments

The essential characteristic of a chain reaction mechanism is the existence of a closed cycle of reactions in which unstable or highly reactive intermediates react in propagation steps with stable reactant molecules or other intermediates and are regenerated by the sequence of reactions that follows. The mathematical methods and approximations used to express the overall rate of reaction in terms of the individual rate constants and the concentrations of stable species are merely extensions of those discussed earlier.

The elementary reactions comprising the chain reaction mechanism are generally classified as initiation, propagation, or termination reactions. In the initiation reaction an active center or chain carrier is formed. Often these are atoms or free radicals, but ionic species or other intermediates can also serve as chain carriers. In the propagation steps the chain carriers interact with the reactant molecules to form product molecules and regenerate themselves so that the chain may continue. The termination steps consist of the various methods by which the chain can be broken.

The key assumption that permits one to proceed from mechanistic equations to an overall rate expression is that the steady-state approximation for intermediates is valid. One is also usually required to make the *long-chain* approximation (i.e., that the by-products resulting from the initiation and termination reactions represent only a very small fraction of the total products). The reaction then will remain stoichiometrically simple to within an approximation that improves with increasing chain length. It is also sometimes necessary to make the additional assumption that at steady state the rate of the initiation process must be equal to the rate at which the various chain-breaking processes are occurring but this constraint may change as conditions in the reactor change during the course of the reaction. Otherwise, the concentration of chain carriers would depend explicitly on time. Often this equality is obvious from the algebraic equations resulting from use of the steady-state approximation. However, when there are two or more alternative termination reactions, the algebraic relations may be so complex that the equality is not apparent.

In any attempt to elucidate the mechanism of a chemical reaction, it is very important to determine at an early stage whether or not a chain reaction is occurring. Consequently, we now note some of the characteristics by which the presence of such mechanisms may be recognized. Not all chain reactions will exhibit all of the characteristics enumerated below, but the presence of several of them should be a strong indication to the investigator that a chain reaction is probably taking place. The absence of any of these criteria should not be regarded as particularly significant.

Some pertinent criteria for recognizing the presence of a chain reaction are:

1. An induction period is present.
2. Extremely large increases or decreases in the reaction rate occur when relatively small amounts of other substances are added to the reaction mixture. These materials may act either as initiators or inhibitors of the reaction, depending on whether they participate in the reaction as initiators or terminators of the chain.
3. Small changes in pressure, temperature, or composition can markedly affect the overall reaction rate or cause an explosion.

4. In gas phase reactions an increase in the surface/volume ratio of the reaction vessel may reduce the reaction rate, while the addition of "inert" gases may increase the reaction rate (see Section 4.2.5).
5. Abnormally high quantum yields may occur in photochemical reactions. Einstein's law of photochemical equivalence is the principle that light is absorbed by molecules in discrete amounts as an individual molecular process (i.e., one molecule absorbs one photon at a time). From optical measurements it is possible to determine quantitatively the number of photons absorbed in the course of a reaction and, from analyses of the product mixture, it is possible to determine the number of molecules that have reacted. The quantum yield is defined as the ratio of the number of molecules reacting to the number of photons absorbed. If this quantity exceeds unity, it provides unambiguous evidence for the existence of secondary processes and thus indicates the presence of unstable intermediates. While yields greater than unity provide evidence for chain reactions, yields less than unity do *not* indicate the absence of a chain reaction. Quantum yields as high as  $10^6$  have been observed in the photochemical reaction between  $\text{H}_2$  and  $\text{Cl}_2$ .
6. Complex rate expressions or fractional reaction orders with respect to individual reactants are often indicative of chain reaction mechanisms. However, other mechanisms composed of many elementary reactions may also give rise to these types of rate expressions, so this criterion should be applied with caution.

Because of the variety of chain reaction mechanisms that exist, it is difficult to develop completely general rate equations for these processes. However, some generalizations with regard to the overall rate expression can be made for certain classes of reactions. Some of these are considered in Section 4.2.3.

Illustration 4.3 indicates the techniques used in the derivation of a reaction rate expression from a chain reaction mechanism.

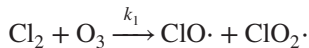
### ILLUSTRATION 4.3 Use of the Bodenstein Steady-State Approximation to Derive a Rate Expression for a Chain Reaction Mechanism

The following rate expression has been determined for the low-temperature chlorine-catalyzed decomposition of ozone:

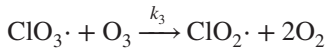
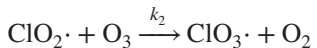
$$\frac{d[\text{O}_3]}{dt} = -k[\text{Cl}_2]^{1/2}[\text{O}_3]^{3/2}$$

The following chain reaction mechanism has been proposed for this reaction.

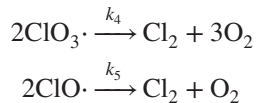
Initiation:



Propagation:



Termination:



What rate expression results from this mechanism? Is this expression consistent with the rate expression determined experimentally?

## Solution

The processes by which ozone will disappear are reactions 1, 2, and 3. We will subsequently make use of the fact that the amount of ozone disappearing via the initiation step will be negligible compared to the amount that is consumed by the propagation steps. The overall rate of disappearance of ozone is given by

$$\frac{d[\text{O}_3]}{dt} = -k_1[\text{Cl}_2][\text{O}_3] - k_2[\text{ClO}_2\cdot][\text{O}_3] - k_3[\text{ClO}_3\cdot][\text{O}_3] \quad (\text{A})$$

This expression contains the concentrations of two intermediate free radicals,  $[\text{ClO}_2\cdot]$  and  $[\text{ClO}_3\cdot]$ . These terms may be eliminated by using the Bodenstein steady-state approximation.

$$\begin{aligned} \frac{d[\text{ClO}_2\cdot]}{dt} &= k_1[\text{Cl}_2][\text{O}_3] - k_2[\text{ClO}_2\cdot][\text{O}_3] \\ &\quad + k_3[\text{ClO}_3\cdot][\text{O}_3] \approx 0 \end{aligned} \quad (\text{B})$$

$$\begin{aligned} \frac{d[\text{ClO}_3\cdot]}{dt} &= k_2[\text{ClO}_2\cdot][\text{O}_3] \\ &\quad - k_3[\text{ClO}_3\cdot][\text{O}_3] - 2k_4[\text{ClO}_3\cdot]^2 \approx 0 \end{aligned} \quad (\text{C})$$

Addition of equations (B) and (C) gives

$$k_1[\text{Cl}_2][\text{O}_3] = 2k_4[\text{ClO}_3\cdot]^2 \quad (\text{D})$$

Thus,

$$[\text{ClO}_3\cdot]_{\text{ss}} = \sqrt{\frac{k_1[\text{Cl}_2][\text{O}_3]}{2k_4}} \quad (\text{E})$$

Substitution of this relation into equation (B) gives

$$k_1[\text{Cl}_2][\text{O}_3] - k_2[\text{ClO}_2\cdot][\text{O}_3] + k_3\sqrt{\frac{k_1[\text{Cl}_2][\text{O}_3]}{2k_4}}[\text{O}_3] = 0 \quad (\text{F})$$

or

$$[\text{ClO}_2\cdot]_{\text{ss}} = \frac{k_1[\text{Cl}_2] + k_3\sqrt{k_1[\text{Cl}_2][\text{O}_3]/2k_4}}{k_2} \quad (\text{G})$$

Substitution of the steady-state concentrations of the two intermediates into the equation for the rate of disappearance of ozone gives

$$\begin{aligned} \frac{d[\text{O}_3]}{dt} &= -k_1[\text{Cl}_2][\text{O}_3] \\ &\quad - k_2\frac{k_1[\text{Cl}_2] + k_3\sqrt{k_1[\text{Cl}_2][\text{O}_3]/2k_4}}{k_2}[\text{O}_3] \\ &\quad - k_3\sqrt{\frac{k_1[\text{Cl}_2][\text{O}_3]}{2k_4}}[\text{O}_3] \end{aligned} \quad (\text{H})$$

or

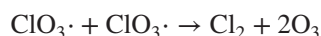
$$\frac{d[\text{O}_3]}{dt} = -2k_1[\text{Cl}_2][\text{O}_3] - 2k_3\sqrt{\frac{k_1[\text{Cl}_2][\text{O}_3]}{2k_4}}[\text{O}_3] \quad (\text{I})$$

The first term in equation (I) refers to ozone consumption via the initiation step. This term is negligible compared to the second. Thus,

$$\frac{d[\text{O}_3]}{dt} = -k_3\sqrt{\frac{2k_1}{k_4}}[\text{Cl}_2]^{1/2}[\text{O}_3]^{3/2}$$

This form is consistent with the experimentally determined rate expression.

Even though this reaction mechanism meets the requirements imposed by experimental rate data and the stoichiometry of the reaction, it is not consistent with all of our principles because the reverse of termination reaction 4 would require a molecularity of 4. Consequently, this reaction may be regarded as suspect. An alternative termination reaction leading to the same rate law might be



Because the propagation steps are the only reactions that significantly affect the concentration of ozone, a mechanism using this equation as a termination step would give a rate expression of the same mathematical form as that described above. It also might be that the second-order reaction of two  $\text{ClO}_3\cdot$  radicals is rapidly followed by several fast steps that are not observable or significant.

### 4.2.3 Rice–Herzfeld Mechanisms

The thermal decomposition reactions of many organic compounds obey relatively simple rate laws. Consequently, it was assumed for many years that they are simple elementary processes. It was not until the middle of the 1930s that it was recognized that free radicals play an essential role in these reactions. Rice and Herzfeld (30) postulated some general principles that are applicable to pyrolysis reactions and have proposed detailed mechanisms for several reactions. They recognized that free-radical chain reaction mechanisms could give rise to simple rate expressions that would be integer- or half-integer-order with respect to the material being pyrolyzed. This fact had not been recognized previously because earlier chain reaction mechanisms had led to rate expressions that were more complicated than those normally associated with organic pyrolysis reactions.

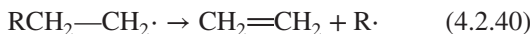
The basic premises on which Rice–Herzfeld mechanisms are based are as follows.

#### Initiation:

1. Free radicals are formed by scission of the weakest bond in the molecule.

#### Propagation:

2. One or both of the radicals formed in the initiation step abstract a hydrogen atom from the parent compound to form a small saturated molecule and a new free radical.
3. The new free radical stabilizes itself by splitting out a simple molecule such as an olefin or CO:

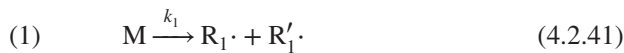


#### Termination:

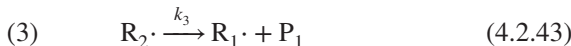
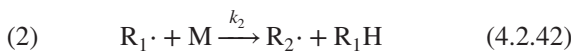
4. The chain is broken by a combination or disproportionation reaction between two radicals.

These basic premises go a long way in correlating and tying together the extraordinary complexity of many pyrolysis reactions. In terms of mechanistic equations, they may be written as follows:

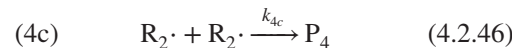
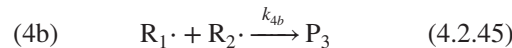
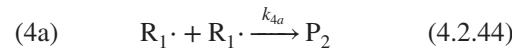
#### Initiation:



#### Propagation:



#### Termination:



The initiation step has been written as a unimolecular reaction. In terms of the Lindemann theory presented in Section 4.3.1.3, this initiation reaction will shift to a bimolecular process at low pressures.

The mechanism above assumes that  $\text{R}_1\cdot$  and  $\text{R}'_1\cdot$  are different radicals and that the latter do not participate in the propagation reactions. In the more general case, the radical  $\text{R}'_1\cdot$  can participate in propagation reactions analogous to reactions (2) and (3). These propagation steps consist of a bimolecular hydrogen abstraction reaction followed by a unimolecular decomposition reaction.

The three possible termination reactions have been written as combination reactions when, in fact, disproportionation reactions may also occur leading to formation of alternative by products of termination reactions. Under a given set of experimental conditions, only one of the three chain-breaking steps (4a), (4b), or (4c) can be expected to be important.

With this general sequence of reactions as a proposed mechanism, we can now use the corresponding rate expressions for the individual steps and our standard assumptions to demonstrate that overall rate expressions with reaction orders of  $\frac{1}{2}$ , 1, and  $\frac{3}{2}$  are associated with the particular chain termination reaction that is most significant. The mathematical form of the overall rate expression reflects the nature of the chain-breaking process. For example, a first-order rate expression results when the termination process involves the dissimilar radicals,  $\text{R}_1\cdot$  and  $\text{R}_2\cdot$ ; that is, when reaction (4b) is the chain-breaking step.

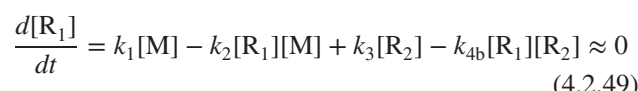
Based on the set of mechanistic equations set forth above, the rate of disappearance of reactant M is given by



For long-chain reactions the amount of reactant undergoing decomposition via the initiation reaction is small compared to that decomposed by the propagation reactions (i.e.,  $k_2[\text{R}_1] \gg k_1$ ). Thus, to a good approximation,



The concentrations of the chain carriers  $\text{R}_1$  and  $\text{R}_2$  may be determined by the use of the stationary-state assumption for each species:



$$\frac{d[R_2]}{dt} = k_2[R_1][M] - k_3[R_2] - k_{4b}[R_1][R_2] \approx 0 \quad (4.2.50)$$

Adding these two equations and rearranging, we find that

$$[R_2] = \frac{k_1[M]}{2k_{4b}[R_1]} \quad (4.2.51)$$

Substitution of this relation into equation (4.2.50) gives

$$k_2[R_1][M] - \frac{k_1k_3[M]}{2k_{4b}[R_1]} - \frac{k_1[M]}{2} = 0 \quad (4.2.52)$$

On the basis of our earlier statement that  $k_2[R_1] \gg k_1$ , the last term is negligible. Therefore,

$$[R_1] = \left( \frac{k_1k_3}{2k_{4b}k_2} \right)^{1/2} \quad (4.2.53)$$

Substitution of relation (4.2.53) into equation (4.2.48) gives

$$\frac{d[M]}{dt} = -\left( \frac{k_1k_2k_3}{2k_{4b}} \right)^{1/2} [M] \quad (4.2.54)$$

which is a first-order rate expression. If each of the individual rate constants is written in the Arrhenius form, the apparent rate constant is given by

$$k = \left( \frac{A_1A_2A_3}{2A_{4b}} \right)^{1/2} e^{-(E_1+E_2+E_3-E_{4b})/2RT} \quad (4.2.55)$$

and it is apparent that the overall activation energy of the reaction is given by

$$E = \frac{E_1 + E_2 + E_3 - E_{4b}}{2} \quad (4.2.56)$$

The average chain length  $L$  is given by the ratio

$$L = \frac{\text{rate of disappearance of reactants}}{\text{rate of initiation process}} = \frac{d[M]/dt}{k_1[M]} \quad (4.2.57)$$

From equations (4.2.54) and (4.2.57) it is evident that

$$L = \left( \frac{k_2k_3}{2k_1k_{4b}} \right)^{1/2} \quad (4.2.58)$$

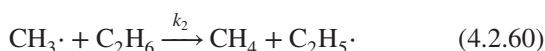
and that the average chain length is independent of the initial concentration of reactants.

The following mechanism has been proposed for the decomposition of ethane into ethylene and hydrogen. The overall rate expression is first-order in ethane.

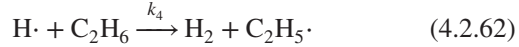
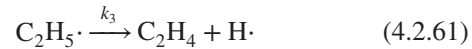
Initiation:



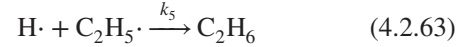
Chain transfer:



Propagation:



Termination:



Because these equations are of the same form as those discussed above, the reader should be able to show that

$$\frac{d[\text{C}_2\text{H}_6]}{dt} = \left( \frac{-k_4k_1}{k_5} \right) \times \left[ \frac{1}{(k_1/2k_3) \pm \sqrt{(k_1/2k_3)^2 + [(k_1k_4) / (k_3k_5)]}} \right] [\text{C}_2\text{H}_6] \quad (4.2.64)$$

which is a first-order rate expression. Physical arguments indicate that  $k_1/k_3$  must be very small compared to unity ( $k_1/k_3 \ll 1$ ). Thus, equation (4.2.64) becomes

$$\frac{d[\text{C}_2\text{H}_6]}{dt} = -\left( \frac{k_1k_3k_4}{k_5} \right)^{1/2} [\text{C}_2\text{H}_6] \quad (4.2.65)$$

A rate expression that is proportional to the square root of the reactant concentration results when the dominant termination step is reaction (4c); that is, when the termination reaction occurs between the two identical radicals that are formed in the bimolecular propagation step and are consumed in the unimolecular propagation step. The generalized Rice–Herzfeld mechanism contained in equations (4.2.41) to (4.2.46) may be employed to derive an overall rate expression for this case. As before, the time rate of change of the reactant concentration is given by

$$\frac{d[M]}{dt} = -k_1[M] - k_2[R_1][M] \quad (4.2.66)$$

The steady-state approximation may be used for each of the chain-carrying species.

$$\frac{d[R_1]}{dt} = k_1[M] - k_2[R_1][M] + k_3[R_2] \approx 0 \quad (4.2.67)$$

$$\frac{d[R_2]}{dt} = k_2[R_1][M] - k_3[R_2] - 2k_{4c}[R_2]^2 \approx 0 \quad (4.2.68)$$

Adding these two equations and rearranging, one finds that

$$[R_2] = \left( \frac{k_1[M]}{2k_{4c}} \right)^{1/2} \quad (4.2.69)$$

Substitution of this result into equation (4.2.67) leads to a relation for  $[R_1]$ :

$$[R_1] = \frac{k_1}{k_2} + \frac{k_3}{k_2} \left( \frac{k_1}{2k_{4c}} \right)^{1/2} \left( \frac{1}{[M]^{1/2}} \right) \quad (4.2.70)$$

Combination of equations (4.2.66) and (4.2.70) gives

$$\frac{d[M]}{dt} = -2k_1[M] - k_3 \left( \frac{k_1}{2k_{4c}} \right)^{1/2} [M]^{1/2} \quad (4.2.71)$$

The first term on the right side of this equation is twice the rate of initiation. Hence, it is negligible compared to the second term and

$$\frac{d[M]}{dt} = -k_3 \left( \frac{k_1}{2k_{4c}} \right)^{1/2} [M]^{1/2} \quad (4.2.72)$$

This result is a half-order rate expression.

For the overall rate expression to be  $(\frac{3}{2})$ -order in reactant for a first-order initiation process, the chain-terminating step must involve a second-order reaction between two of the radicals responsible for the second-order propagation reactions. In terms of our generalized Rice–Herzfeld mechanistic equations, this means that reaction (4a) is the dominant chain-breaking process. One may proceed as above to show that the mechanism leads to a  $(\frac{3}{2})$ -order rate expression.

For Rice–Herzfeld mechanisms the mathematical form of the overall rate expression is strongly influenced by the manner in which the chains are broken. It can also be shown that changing the initiation step from first- to second-order also increases the overall order of the reaction by  $(\frac{1}{2})$  (31). These results are easily obtained from the equations derived previously by substituting  $(k'_1[M])$  for  $k_1$  everywhere that the latter term appears. Since  $k_1$  always appears to the  $(\frac{1}{2})$  power in the final rate expressions, the exponent on M in the existing rate expression must be added to 0.5 to obtain the overall order of the reaction corresponding to the bimolecular initiation step. In like manner, shifts from bimolecular to termolecular termination reactions will decrease the overall order of the reaction by  $(\frac{1}{2})$ .

Although the Rice–Herzfeld mechanisms above lead to simple overall rate expressions, do *not* get the impression that this is always the case. More detailed discussions of these types of reactions may be found in textbooks (32–35) and in the literature.

#### 4.2.4 Inhibitors, Initiators, and Induction Periods

Because the complex decomposition reactions considered in Section 4.2.3 are propagated by a series of elementary steps, it might be expected that they and other chain reaction processes will show an unusual sensitivity to any substance or physical condition that interferes with the propagation of the chain. It is therefore not surprising to find that the rates of such reactions can be markedly reduced either by the presence of trace quantities of certain chemical substances or by changes in the physical condition of the surface of the vessel in which the reaction

is being studied. The latter changes include both variations in the surface/volume ratio of the reactor brought about by adding spun glass or by some other high-surface-area material to the reactor and variations in the nature of the surface itself through the use of Teflon, syrupy phosphoric acid, or other coatings. The reduction in the observed rate associated with the introduction of trace quantities of particular species may occasionally be referred to as negative catalysis, but it is more commonly known as *inhibition*. An additive that slows down a reaction is referred to as an inhibitor.

In the case of chain reactions a mere trace of inhibitor can reduce reaction rates by orders of magnitude. Such inhibitors break the chain, perhaps as a result of a reaction in which a relatively nonreactive free radical is formed. Another manner in which an inhibitor may act is by combining with a catalyst and rendering it inoperative.

Other additives can promote chain reactions by acting as *initiators* of the chain. These compounds are materials that can be more readily dissociated than the primary reactants. For example, benzoyl peroxide has often been used to initiate the polymerization of olefinic monomers because of the ease with which it dissociates.

In many cases complex chain reactions are characterized by an *induction period* (i.e., a period at the beginning of the reaction during which the rate is significantly less than that which subsequently prevails). This period is often caused by the presence of small amounts of inhibitors. After the inhibitors are consumed, the reaction may then proceed at a much faster rate.

#### 4.2.5 Branched-Chain Reactions and Explosions

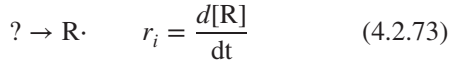
Chain reactions can lead to thermal explosions when the energy liberated by the reaction cannot be transferred to the surroundings at a sufficiently fast rate. An “explosion” may also occur when chain-branching processes cause a rapid increase in the number of chains being propagated. In this section we treat branched-chain reactions that can lead to nonthermal explosions and the physical phenomena that are responsible for both branched-chain and thermal explosions.

A chain-branching reaction is one that leads to an increase in the number of chain carriers present in a reacting system [e.g., (4.2.9)]. When such reactions occur to a significant extent, steady-state conditions are no longer maintained. The reaction proceeds at a very high velocity and, since the associated release of chemical energy is also extremely rapid, the viewer sees this phenomenon as an explosion.

The following generalized mechanism by which branched-chain reactions proceed provides a basis for a

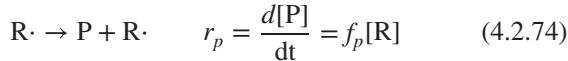
semi-quantitative understanding of explosions resulting from chain branching.<sup>†</sup>

Initiation:

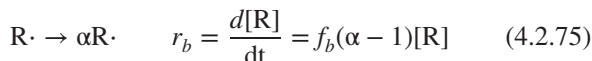


Propagation:

Product formation:

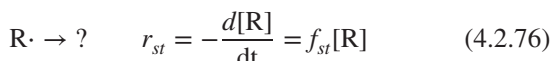


Chain branching:

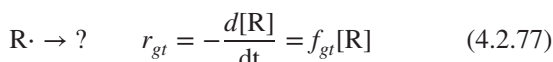


Termination:

Chain breaking at solid surface:



Chain breaking in gas phase:



where R represents the various active centers or free radical chain carriers involved in the reaction, and the question marks signify unknown species. The detailed chemistry of the various steps is thus unspecified. The number of radicals formed in the chain-branching step per radical that reacts is assigned the symbol  $\alpha$ . All of the propagation and termination steps are written as first-order processes, but this is not essential to the argument that follows.

The rate expressions have been written in generalized fashion with the terms  $f_p$ ,  $f_b$ ,  $f_{st}$ , and  $f_{gt}$  containing the reaction rate constants, stoichiometric coefficients, and concentrations of the various stable species present in the reaction mixture. If one also wished to consider bimolecular radical processes, these could also be lumped into the  $f$  parameters.

In terms of the rate expressions above, the Bodenstein steady-state approximation for free-radical intermediates gives

$$r_i + f_b(\alpha - 1)[R] - f_{st}[R] - f_{gt}[R] \approx 0 \quad (4.2.78)$$

Note that this equation does not contain a term corresponding to the straight-chain step in which the primary products are formed. This step does not have any *net* effect on the total concentration of free radicals. Thus,

$$[R] = \frac{r_i}{f_{st} + f_{gt} - f_b(\alpha - 1)} \quad (4.2.79)$$

<sup>†</sup>Adapted from K. J. Laidler, *Chemical Kinetics*, pp. 415–419. Copyright © 1965. Used with permission of McGraw-Hill Book Company.

The overall rate of reaction is therefore

$$r_p = \frac{r_i f_p}{f_{st} + f_{gt} - f_b(\alpha - 1)} \quad (4.2.80)$$

Because the branching parameter  $\alpha$  is greater than unity (often, it is 2), it is conceivable that under certain circumstances the denominator of the overall rate expression could become zero. In principle this would lead to an infinite reaction rate (i.e., an explosion). In reality it becomes very large rather than infinite, since the steady-state approximation will necessarily break down when the radical concentration becomes quite large. Nonetheless, we consider the condition that  $f_b(\alpha - 1)$  is equal to  $f_{st} + f_{gt}$  to be a valid criterion for an explosion limit.

Because there are two positive terms in the denominator of equation (4.2.85) (either of which may be associated with the dominant termination process), this equation leads to two explosion limits. At very low pressures the mean free path of the molecules in the reactor is quite long, and the radical termination processes occur primarily on the surfaces of the reaction vessel. Under these conditions gas-phase collisions leading to chain breaking are relatively infrequent events, and  $f_{st} \gg f_{gt}$ . Steady-state reaction conditions can prevail under these conditions if  $f_{st} + f_{gt} > f_b(\alpha - 1)$ .

As the pressure in the reaction vessel increases, the mean free path of the gaseous molecules will decrease and the ease with which an individual radical species can reach a surface of the vessel will diminish. Surface termination processes will then become increasingly less important (in a relative sense) than chain-branching events. Ultimately, one reaches an intermediate pressure at which the sum of the termination terms  $f_{st} + f_{gt}$  becomes equal to  $f_b(\alpha - 1)$ . At this point an explosion will occur. This point corresponds to the first explosion limit shown in Figure 4.1.

If one now jumps to some higher pressure at which steady-state reaction conditions can again prevail, similar semi-quantitative arguments can be used to explain the phenomenon known as the *second explosion limit*. At these somewhat higher pressures the large majority of the events by which chains are terminated will occur in the gas phase. The higher pressure hinders the diffusion of radicals to the vessel surfaces and provides a number density of gas-phase radicals that is sufficient for radical disproportionation and recombination reactions to become much more significant than surface termination processes.

If the pressure in the reaction vessel is now decreased, the rate at which chains are broken will also decrease because the rates of the disproportionation and combination (termination) reactions will diminish. Eventually, the pressure will decrease to a point at which the rates of the termination processes will become equal to the rate at which the radical concentration is increasing because of

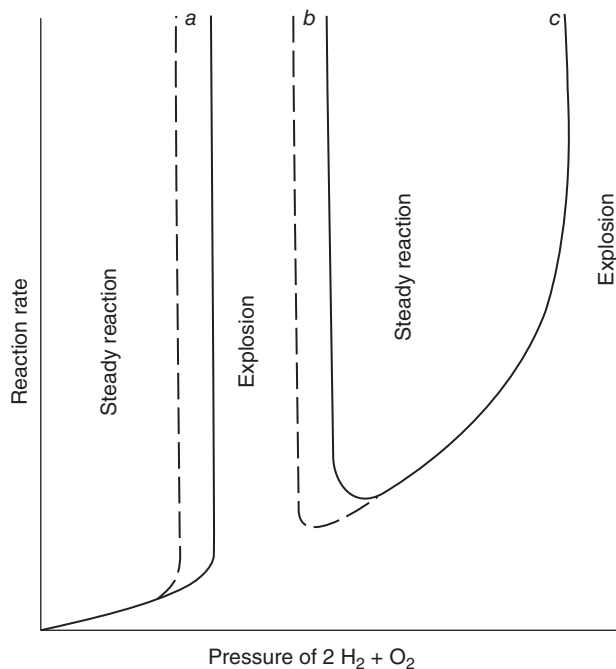


**Figure 4.1** Variation of the rate of reaction in a system containing a 2 : 1 mole ratio of hydrogen to oxygen as a function of the total pressure. First, second, and third explosion limits are labeled *a*, *b*, and *c*, respectively. Displacement of the first and second limits to lower pressures occurs on addition of an inert gas or enlarging the volume of the reactor (dashed lines). (Adapted from J. W. Moore and R. G. Pearson, *Kinetics and Mechanism*, 3rd ed., p. 409. Copyright © 1981 by John Wiley & Sons, Inc.)

the chain-branching process; that is, one again reaches a point at which

$$(f_{gt} + f_{st}) [\text{R}] = f_b(\alpha - 1)[\text{R}] \quad (4.2.81)$$

At this point an explosion will occur corresponding to the second explosion limit in Figure 4.1.

There is a third explosion limit indicated in Figure 4.1 at still higher pressures. This limit is a thermal limit. At these pressures the reaction rate becomes so fast that conditions can no longer remain isothermal. At these pressures the energy liberated by the exothermic chain reaction cannot be transferred to the surroundings at the rate necessary to maintain a constant temperature in the gas phase. As the temperature of the reaction mixture increases, both the rates of the primary propagation reactions and the associated rate at which energy stored in the form of chemical bonds is converted to thermal energy will increase. Thus, one has an accelerating effect of increasing temperature on the rate until an explosion occurs.

It should be evident from this discussion that the first explosion limit will be quite sensitive to the nature of the surface of the reaction vessel and the surface/volume ratio of the reactor. If the surface is coated with a material

that inhibits the surface chain termination process, the first explosion limit will be lowered. Inert foreign gases can also have the effect of lowering the first explosion limit, because they can hinder diffusion to the surface. If materials such as spun glass or large amounts of fine wire are inserted in the reactor, one can effect an increase in the first explosion limit by changing the surface/volume ratio of the system.

#### 4.2.6 Supplementary References

Our discussion of chain reaction processes is necessarily incomplete. For more detailed treatments consult the following references.

1. C. H. BAMFORD and C. F. H. TIPPER (Eds.), *Comprehensive Chemical Kinetics*, Vol. II, *The Theory of Kinetics*, Elsevier, New York, 1969.
2. J. WARNATZ, U. MAAS, and R. W. DIBBLE, *Combustion: Physical and Chemical Fundamentals, Modeling and Simulation, Experiments, Pollutant Formation*, 4th ed., Springer-Verlag, Berlin, 2006.
3. J. F. GRIFFITHS and J. A. BARNARD, *Flame and Combustion*, 3rd ed., Chapman & Hall, London, 1995.
4. G. MOAD and D. H. SOLOMON, *The Chemistry of Free Radical Polymerization*, Pergamon, Press, Oxford, 1995.
5. K. MATYJASZEWSKI and T. P. DAVIS, *Handbook of Radical Polymerization*, Wiley, New York, 2002.

#### 4.2.7 Cautionary Note on Reaction Mechanisms

It is appropriate to conclude our discussion of reaction mechanisms on a note of caution. A mechanism is merely a logical *hypothesis* as to the sequence of molecular events that occur during the course of a chemical reaction. Reaction mechanisms should *not* be regarded as experimental facts. They are plausible explanations of experimental data that are consistent with the data, but that may be subject to revision as new data are obtained. Even if a proposed mechanism gives agreement with all available experimental facts, this is not evidence that the mechanism is unique or that other mechanisms could not give such agreement.

### 4.3 MOLECULAR THEORIES OF CHEMICAL KINETICS

A “complete” theory of reaction kinetics would provide a basis for calculating the rate of an elementary reaction from a knowledge of the properties of the reacting molecules and their concentrations. In terms of the present state of our theoretical knowledge, a complete theory can be regarded as a goal that is far, far down the road. While existing theories are extremely unsatisfactory, chemical engineers must be cognizant of their primary features.

### 4.3.1 Simple Collision Theory

Before a chemical reaction can occur, energy must be available and localized such that it is possible to break and make certain chemical bonds in the reactant molecules. Moreover, the participants in the reaction must be in a spatial configuration such that it is possible for the necessary atomic and electronic rearrangements to occur. The most common means by which such redistributions of energy and changes in geometric configurations can occur are molecular collision processes. In this sense all theories of reaction are collision theories. However, we use this term in a more limited sense. We restrict its use to the theory that links chemical kinetics to the kinetic theory of gases by the use of the theoretical expression for bimolecular collision frequencies.

#### 4.3.1.1 Rates of Bimolecular Reactions

For purposes of chemical reaction kinetics the primary result of the kinetic theory of gases is that the total number of collisions between A molecules and B molecules per unit volume per unit time is given by  $Z_{AB}$ :

$$Z_{AB} = n'_A n'_B \pi \sigma_{AB}^2 \sqrt{\frac{8k_B T}{\pi \mu_{AB}}} \quad (4.3.1)$$

where  $n'_A$  and  $n'_B$  are the number densities of molecules A and B, respectively;  $T$  is the absolute temperature;  $k_B$  is the Boltzmann constant;  $\sigma_{AB}$  is the arithmetic average of the hard-sphere diameters of molecules A and B:

$$\sigma_{AB} = \frac{\sigma_A + \sigma_B}{2} \quad (4.3.2)$$

and  $\mu_{AB}$  is the reduced mass of the system expressed in terms of the molecular masses  $m_A$  and  $m_B$  as

$$\mu_{AB} = \frac{m_A m_B}{m_A + m_B} \quad (4.3.3)$$

If A and B are identical, then  $m_A = m_B = m$ ,  $\mu = m/2$ ,  $\sigma_A = \sigma_B = \sigma_{AB} = \sigma$ , and  $n'_A = n'_B = n$ . To avoid double counting of collisions, one must also introduce an additional factor of  $\frac{1}{2}$  in equation (4.3.1) to obtain an expression for the number of collisions between identical molecules per unit volume per unit time:

$$Z_{AA} = (n')^2 \frac{\pi}{2} \sigma^2 \sqrt{\frac{8k_B T}{\pi(m/2)}} = 2(n')^2 \sigma^2 \sqrt{\frac{\pi k_B T}{m}} \quad (4.3.4)$$

For a typical gas at standard conditions,  $Z_{AA}$  and  $Z_{AB}$  are both of the order of  $10^{28}$  collisions/(cm<sup>3</sup>·s).

Derivations of the expressions above are contained in most texts concerned with the kinetic theory of gases, undergraduate physical chemistry texts or reaction kinetics (see, e.g., 36–39). Different authors may write equations

(4.3.1) and (4.3.4) in slightly different forms because of different assumptions involved in their derivations and the degree of mathematical rigor that they choose to use. They may precede these expressions by some numerical factor that will not differ appreciably from unity. Such differences are insignificant for purposes of chemical kinetics. From a practical viewpoint the uncertainties involved in predicting reaction rates do not justify using anything more complex than the simple hard-sphere model of the kinetic theory.

Bimolecular processes are the primary vehicle by which chemical change occurs. The frequency with which these encounters occur is given by equations (4.3.1) and (4.3.4). However, only an extremely small number of the collisions actually lead to reaction; for predictive purposes one needs to know what fraction of the collisions are effective in that they lead to reaction.

Because chemical reactions involve the making and breaking of chemical bonds with their associated energy effects and geometric requirements, it is not unreasonable to assume that these factors play an important role in determining the probability that a bimolecular collision will lead to chemical reaction. In addition to these factors there are restrictions on bimolecular combination or association reactions and quantum mechanical requirements that can influence this probability.

For complex organic molecules, geometric considerations alone lead one to the conclusion that only a small fraction of bimolecular collisions can lead to reaction. One can represent the fraction of the collisions that have the proper geometric orientation for reaction by a *steric factor* ( $P_s$ ). Except for the very simplest reactions, this factor will be considerably less than unity. On the basis of simple collision theory, it is not possible to make numerical estimates of  $P_s$ , although it may occasionally be possible to make use of one's experience with similar reactions to determine whether  $P_s$  for a given reaction will be large or small. This failure to be able to predict values of  $P_s$  is one of the major weak points of the collision theory, another being that it is also impossible to generate meaningful estimates of the corresponding activation energy on an a priori basis. The inability of the theory to consider the individual geometric shapes of various reactant molecules is responsible for the lack of ability to predict values for  $P_s$ . Since  $P_s$  must be determined empirically, it may be considerably in error because this parameter will contain all of the errors associated with the assumption of hard sphere molecules as well as any quantum mechanical restrictions on the reaction in question.

Of all the factors that determine the effectiveness of a collision, however, the energy requirement is by far the most important. Reaction cannot occur unless sufficient energy is provided and localized so that the appropriate bonds can be broken and new bonds formed. It is reasonable to suppose that there will be a threshold

energy requirement below which these processes cannot occur. It is usually assumed that a collision is effective for reaction purposes only if the relative kinetic energy along the line of collision centers is greater than or equal to this threshold value. Kinetic energy associated with motion perpendicular to this line corresponds to a sideswipe that leads to changes in rotational energy levels but cannot be expected to be effective in promoting reaction.

The principles of the kinetic theory of gases may be used to arrive at an expression for the number of collisions whose relative kinetic energy along the line of centers is greater than  $\epsilon_c$ . The result is the following expression for the number of such collisions per unit volume per unit time:

$$Z'_{AB} = n'_A n'_B \pi \sigma_{AB}^2 \left( \frac{8k_B T}{\pi \mu_{AB}} \right)^{1/2} e^{-\epsilon_c/k_B T} \quad (4.3.5)$$

If this equation is now written in terms of energy per mole instead of per molecule, it becomes

$$Z'_{AB} = n'_A n'_B \pi \sigma_{AB}^2 \left( \frac{8k_B T}{\pi \mu_{AB}} \right)^{1/2} e^{-E_c/RT} \quad (4.3.6)$$

This expression is identical to equation (4.3.1) if we set  $E_c$  equal to zero. Equation (4.3.5) leads to the surprisingly simple result that the fraction of the collisions that will involve at least an energy  $\epsilon_c$  directed along the line of centers is given by  $e^{-\epsilon_c/k_B T}$  or  $e^{-E_c/RT}$ . If the steric factor defined previously is introduced, the rate of reaction between unlike molecules becomes

$$r_{AB} = P_s n'_A n'_B \pi \sigma_{AB}^2 \left( \frac{8k_B T}{\pi \mu_{AB}} \right)^{1/2} e^{-E_c/RT} = k n'_A n'_B \quad (4.3.7)$$

Comparison of this equation with the Arrhenius form of the reaction rate constant reveals a slight difference in the temperature dependence of the rate constant, and this fact must be explained if one is to accept the consistency of the collision theory. Taking the derivative of the natural logarithm of the rate constant in equation (4.3.7) with respect to temperature, one finds that

$$\frac{d \ln k}{dT} = \frac{1}{2T} + \frac{E_c}{RT^2} \quad (4.3.8)$$

while the Arrhenius form is given by equation (3.3.54):

$$\frac{d \ln k}{dT} = \frac{E_A}{RT^2} \quad (4.3.9)$$

Equations (4.3.8) and (4.3.9) can be reconciled only if the experimental activation energy is temperature dependent in such a way as to accommodate the variation in collision frequency with temperature; that is,

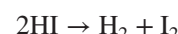
$$E_A = E_c + \frac{RT}{2} \quad (4.3.10)$$

Usually, the last term on the right side of equation (4.3.10) is only a very small fraction of the total. For example, if the activation energy ( $E_A$ ) observed is 10 kcal at 500 K, the  $RT/2$  term is only 0.5 kcal, or 5%. Such discrepancies are usually within the scatter of the data.

Illustration 4.4 indicates how collision frequency calculations are used to obtain a reaction rate expression.

### ILLUSTRATION 4.4 Comparison of Empirical Rate Expression with Collision Frequency Expression

At 700 K the rate expression for the decomposition of HI,



is given by (40)  $r = 1.16 \times 10^{-3} [\text{HI}]^2 \text{ kmol}/(\text{m}^3 \cdot \text{s})$  when  $[\text{HI}]$  is expressed in  $\text{kmol}/\text{m}^3$ . Compare this reaction rate expression with that predicted by the analog of equation (4.3.7), which corresponds to collisions of the type A–A. Given:

Molecular weight of HI = 127.9  $\sigma_{\text{HI}} = 2.0 \times 10^{-10} \text{ m}$

The measured activation energy is 186.1 kJ/mol.

### Solution

On the basis of equation (4.3.4), the A–A analog of equation (4.3.7) is

$$r_{AA} = P_s 2(n'_A)^2 \sigma_A^2 \sqrt{\frac{\pi k_B T}{m_A}} e^{-E_c/RT}$$

From equation (4.3.10), using  $R = 8.31 \text{ J}/(\text{mol} \cdot \text{K})$ ,

$$E_c = 186,100 - \frac{8.31(700)}{2} = 183,200 \text{ J/mol}$$

In SI units,  $M_A = 0.1279 \text{ kg/mol}$ . If  $n'_A$  is measured in molecules/ $\text{m}^3$  and  $r_{AA}$  in molecules/ $\text{m}^3 \cdot \text{s}$ , the expression for  $r_{AA}$  becomes

$$\begin{aligned} r_{AA} &= P_s 2(n'_A)^2 (2.0 \times 10^{-10})^2 \times \\ &\quad \left( \sqrt{\frac{\pi (8.31) 700}{0.1279}} e^{-183,200/[8.31(700)]} \right) \\ &= 6.35 \times 10^{-31} P_s (n'_A)^2 \end{aligned}$$

To convert from number densities of molecules to reactant concentrations in  $\text{kmol}/\text{m}^3$ , one notes that

$$C_A = \frac{n'_A}{1000N_0}$$

where  $N_0$  is Avogadro's number. A similar conversion is necessary to measure  $r_{AA}$  in  $\text{kmol}/(\text{m}^3 \cdot \text{s})$ . In these units,

$$\begin{aligned} r_{AA} &= 6.35 \times 10^{-31} (6.023 \times 10^{23}) \times 10^3 P_s (C_A)^2 \\ &= 3.83 \times 10^{-4} P_s (C_A)^2 \end{aligned}$$

If the steric factor is comparable to unity, the rate calculated is within an order of magnitude of the experimental value of  $1.16 \times 10^{-3} [\text{HI}]^2$ . Authors of other textbooks have reported even better agreement between experimental values of this rate expression and those calculated from collision theory. Changes in the values used for the activation energy of the reaction and the molecular diameter are often sufficient to bring the calculated values into much closer agreement with the experimental values. Since measurements of different properties lead to significant differences in calculated values of hard-sphere molecular diameters, these quantities are not accurately known. Moreover, uncertainties of several percent in reaction activation energies are not at all unusual.

Consideration of a variety of other systems leads to the conclusion that very rarely can one employ the collision theory to predict rate constants that will be comparable in magnitude to experimental values. Although it is not adequate for predictions of reaction rate constants, it nonetheless provides a convenient physical picture of the reaction act and a useful interpretation of the concept of activation energy. The major shortcomings of the theory lie in its failure to relate the steric factor and the activation energy to molecular parameters from which a priori predictions can be made.

### 4.3.1.2 Termolecular Reactions

If one attempts to extend the collision theory from the treatment of bimolecular gas-phase reactions to termolecular processes, the problem of how to define a termolecular collision arises immediately. If such a collision is defined as the simultaneous contact of the spherical surfaces of all three molecules, one must recognize that two hard spheres will be in direct contact only for an extremely short time and that the probability that a third molecule would strike the other two during this period is vanishingly small.

To have a finite probability that termolecular collisions can occur, we must relax our definition of a collision. We will assume that the approach of rigid spheres to within a distance  $\ell$  of one another constitutes a termolecular collision that can lead to reaction if appropriate energy and geometry requirements are met. This approach is often attributed to Tolman (41). The number of ternary collisions per unit volume per unit time between molecules A, B, and C such that A and C are both within a distance  $\ell$  of B is

given by  $Z_{ABC}$ :

$$Z_{ABC} = \left( 8\sqrt{2} \pi^{3/2} \sigma_{AB}^2 \sigma_{BC}^2 \ell \sqrt{k_B T} \right) \times \left( \frac{1}{\sqrt{\mu_{AB}}} + \frac{1}{\sqrt{\mu_{BC}}} \right) n'_A n'_B n'_C \quad (4.3.11)$$

where the symbols correspond to those used previously and  $\ell$  is a somewhat indefinite parameter that should have a value typical of the length of a chemical bond (i.e.,  $\ell \approx 1 \text{\AA}$ ). If one assumes that the same considerations that govern the efficiency of bimolecular collisions are relevant to termolecular processes, the rates of these processes are given by

$$r = Z_{ABC} P_s e^{-E/RT} \quad (4.3.12)$$

One may estimate the relative frequencies of bimolecular and termolecular collisions using equations (4.3.1) and (4.3.11):

$$\frac{Z_{ABC}}{Z_{AB}} = 4\pi \sigma_{BC}^2 \ell \sqrt{\mu_{AB}} \left( \frac{1}{\sqrt{\mu_{AB}}} + \frac{1}{\sqrt{\mu_{BC}}} \right) n'_C \quad (4.3.13)$$

If A, B, and C have similar molecular weights,  $\sigma_{BC}$  is on the order of 2  $\text{\AA}$  or  $(2 \times 10^{-10} \text{ m})$ , and the gas is at atmospheric pressure so that  $n'_C \approx 3 \times 10^{25}$  molecules/ $\text{m}^3$ , then

$$\begin{aligned} \frac{Z_{ABC}}{Z_{AB}} &= O[4\pi(2 \times 10^{-10})^2 (1 \times 10^{-10}) (3 \times 10^{25})] \\ &= O[10^{-3}] \end{aligned} \quad (4.3.14)$$

so that in a gas at standard conditions there are approximately 1000 bimolecular collisions for every termolecular collision.

When the fact that ternary collisions are relatively rare occurrences is combined with the fact that there will probably be severe geometric restrictions on such reactions, one concludes that these reactions must have relatively low activation energies or else their reaction rates would be vanishingly small. This expectation is confirmed by experimental data on such reactions.

Termolecular reactions are very rare. The best known examples are the recombination reactions of small atoms or radicals (e.g.,  $\text{H} \cdot + \text{H} \cdot + \text{M} \rightarrow \text{H}_2 + \text{M}$ ).

### 4.3.1.3 Unimolecular Reactions

Experimental evidence for unimolecular processes posed a dilemma for early kineticists. They observed that several species that appeared to be stable at low temperatures underwent first-order decomposition or isomerization reactions at higher temperatures. For reaction to take place, molecules have to possess sufficient energy to permit the necessary rearrangement of chemical bonds. If this

energy is not supplied in the form of electromagnetic radiation from external sources, the source of this energy can only be molecular collisions. It was difficult for early workers to reconcile the fact that collisions are most frequently bimolecular processes with the fact that the reactions of interest were first-order. In 1922, however, Lindemann (42) resolved this dilemma by showing how collisional processes can give rise to first-order kinetics under certain circumstances. He proposed a mechanism that was supported by several experiments suggested by his hypothesis. His mechanism is the basis for all modern theories of unimolecular reactions, although several important modifications and additions to the theory have been made since 1922.

According to Lindemann's theory, at any given time a small fraction of the reactant molecules possess enough energy distributed among their various degrees of freedom so that it is possible for them to be converted directly to product molecules without receiving additional energy from any other molecules. This process does, however, require localization of sufficient energy in the appropriate vibrational degree of freedom for reaction to occur. This fraction is referred to as *activated* or *energized* molecules. Lindemann assumed that decomposition of the activated molecules is not instantaneous at the moment the energizing collision occurs, but that a certain time is required for the energy to redistribute itself among the different vibrational modes of motion. When the energy in a certain vibrational mode of motion exceeds the bond strength, the associated bond breaks and reaction occurs.

If the stoichiometric equation for a unimolecular reaction is  $A \rightarrow B + C$ , and if the energized molecules are denoted by  $A^*$ , the Lindemann mechanism consists of the following sequence of events.

**1. Activation by collision:**



**2. Deactivation by collision:**



This process is the reverse of the preceding one. It is expected to occur at the first collision of  $A^*$  after it has been formed. The rate constant  $k_2$  will be much greater than  $k_1$  since it is not restricted by the large energy requirement associated with the activation process.

**3. Unimolecular decomposition:**



Because collisional processes occur so rapidly, the concentration of the  $A^*$  molecules builds up to its steady-state

value in a very small fraction of a second and the steady-state approximation for  $A^*$  is appropriate for use.

$$\frac{d[A^*]}{dt} = k_1[A]^2 - k_2[A][A^*] - k_3[A^*] \approx 0 \quad (4.3.18)$$

Thus,

$$A^* = \frac{k_1[A]^2}{k_2[A] + k_3} \quad (4.3.19)$$

The rate of the overall reaction is identical to the rate of formation of B:

$$\frac{d[B]}{dt} = k_3[A^*] = \frac{k_1 k_3 [A]^2}{k_2[A] + k_3} \quad (4.3.20)$$

Analysis of this equation indicates that the rate is neither first-nor second-order with respect to species A. However, there are two limiting cases. At high pressures where  $[A]$  is large, the bimolecular deactivation process is much more rapid than the unimolecular decomposition (i.e.,  $k_2[A][A^*] \gg k_3[A^*]$ ). Under these conditions the second term in the denominator of equation (4.3.20) may be neglected to yield an apparent first-order rate expression:

$$\frac{d[B]}{dt} = \frac{k_1 k_3}{k_2} [A] \quad (4.3.21)$$

However, as the pressure is decreased, one eventually reaches a point at which the rate of the decomposition reaction becomes much larger than the collisional deactivation process, so that  $k_3[A^*] \gg k_2[A][A^*]$ . In this situation the overall rate expression becomes second-order in A:

$$\frac{d[B]}{dt} = k_1[A]^2 \quad (4.3.22)$$

The lifetime of the energized molecule relative to the time between collisions determines the reaction order. If the lifetime is short compared to the time between collisions, virtually all energized molecules will react before they can be deactivated by subsequent collisions. In this case each energizing collision will lead to reaction, and the rate-limiting step in the overall reaction is the rate of activation by collision, a second-order process. On the other hand, if the lifetime of the energized molecule is long compared to the time between collisions, practically all of the energized molecules become deactivated by subsequent collisions without reacting. A quasi-equilibrium situation will exist between the concentrations of energized and "normal" molecules. The concentration of the former will be proportional to that of the latter. Since the reaction rate is proportional to the concentration of energized molecules, it will also be proportional to the concentration of normal molecules (i.e., first-order).

As the system pressure is decreased at constant temperature, the time between collisions will increase, providing greater opportunity for unimolecular decomposition to

occur. Consequently, one expects the reaction rate expression to shift from first- to second-order at low pressures. Experimental observations of this transition and other evidence support Lindemann's theory. It provides a satisfactory qualitative interpretation of unimolecular reactions, but it is not completely satisfactory from a quantitative viewpoint, and certain important modifications have been made in the years since Lindemann set forth this mechanism. The interested reader may wish to consult textbooks that emphasize gas-phase reaction kinetics (e.g., 3, 33, 37–39, 43–51).

One aspect of extensions of the theory is particularly worthy of note. In a bimolecular reaction, the act of bond breaking must occur at the instant of collision. Consequently, the distribution of energy at that instant must be exactly that required for reaction. In a unimolecular reaction, however, the entire time interval between the activating collision and the next collision is available for the energy in the activated molecule to be redistributed and cause bond breaking. This argument retains the “go–no go” concept that reaction will or will not occur, depending on whether or not a minimum energy requirement is met as a result of a collision, but it predicts higher rates than the conventional kinetic theory approach.

Hinshelwood (52) used reasoning based on statistical mechanics to show that the energy probability factor in the kinetic theory expressions ( $e^{-E/RT}$ ) is strictly applicable only to processes for which the energy may be represented in two squared terms. Each translational and rotational degree of freedom of a molecule corresponds to one squared term, and each vibrational degree of freedom corresponds to two squared terms. If one takes into account the energy that may be stored in  $S$  squared terms, the correct probability factor is

$$\int_E^\infty \frac{e^{-E/RT} E^{(S/2)-1} dE}{[(S/2)-1]!(RT)^{S/2}}$$

To a very good approximation when  $S/2$  is an integer and when  $E \gg RT$ , the integral becomes

$$\frac{e^{-E/RT}}{[(S/2)-1]!} \left( \frac{E}{RT} \right)^{(S/2)-1}$$

For the case where  $S = 2$ , this expression reduces to the simple exponential form of Arrhenius. For values of  $S$  greater than 2, it yields a much larger probability of reaction than one would obtain from the normal Arrhenius form. The enhancement may be several orders of magnitude. For example, when  $S = 10$  and  $E/RT = 30$ , the ratio of the probability factor predicted by Hinshelwood's approach to that predicted by the conventional Arrhenius method is  $(30)^4/4! = 3.375 \times 10^4$ . The drawback of the approach is that one cannot accurately predict  $S$  a priori. When one obtains an apparent steric factor in excess of unity, the Hinshelwood approach can often be used in interpretation of the data.

### 4.3.2 Transition State Theory

*Transition state theory* provides a useful framework for correlating kinetic data and for codifying useful generalizations about the dynamic behavior of chemical systems. This theory is also known as the *activated complex theory*, the *theory of absolute reaction rates*, and *Eyring's theory*. In this section we introduce chemical engineers to the terminology, the basic aspects, and the limitations of the theory.

Transition state theory differs from collision theory in that it takes into account the internal structure of reactant molecules. It describes a reaction in terms of movements on a multi-dimensional surface in which the potential energy of the system is depicted as a function of the relative positions of the nuclei constituting the participants in the reaction. The progress of the reaction is characterized in terms of movement along the surface. Although one may envision an infinite number of paths linking the points corresponding to the original reactants and the final products, certain of these paths will require significantly smaller gross energy inputs to surmount the energy barrier for the reaction. The minimum energy requirement is related to the activation energy for the reaction. The atomic configuration corresponding to potential energy values near the top of this minimal barrier is referred to as the *activated complex*. The region in hyperspace corresponding to this configuration is referred to as the *transition state*. Progress along the path corresponding to the series of positions occupied by the system as it moves from reactants to the activated complex and on to the final product is measured in terms of distance along the *reaction coordinate*. If this quantity is used as a measure of the progress of reaction, it is possible to convert the multi-dimensional potential energy diagram into a two-dimensional free-energy diagram, one form of which is shown in Figure 4.2. Such figures emphasize the commonly used analogy in which the reaction and its energy requirements are compared to the movement of a sphere across hilly terrain in the presence of a gravitational field.

In terms of transition state theory, the rate of reaction is controlled by the rate of passage through the region at the top of the energy barrier. This passage may correspond either to movement over the top of the barrier or, in some cases, to quantum mechanical tunneling through the barrier. Several approaches to formulating the reaction rate in terms of such movements have been described, but we will employ the one utilized by Eyring and his co-workers (53–55). Other treatments are presented in numerous texts dealing with kinetics (e.g., 37, 38, 50, 51). The fundamental hypothesis on which Eyring's formulation is based is that an equilibrium exists between an activated complex species and the reactants. This equilibrium determines the number of activated complexes corresponding to specified reactant concentrations, regardless of whether or not an overall chemical equilibrium exists between reactant and

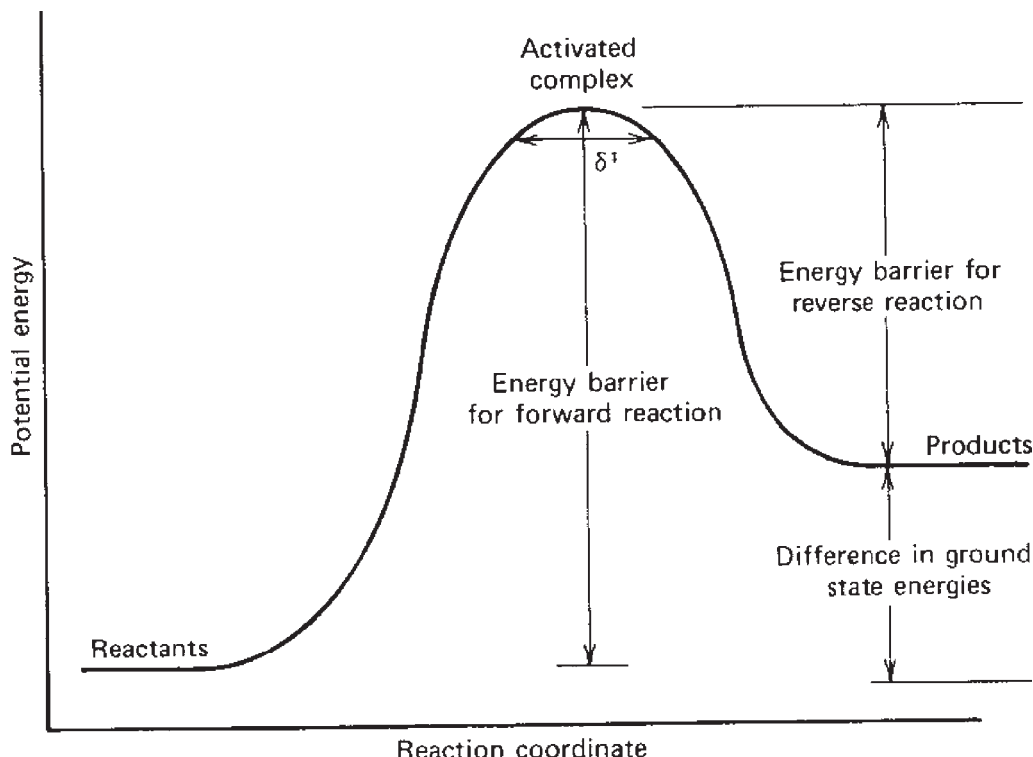


**Figure 4.2** Schematic representation of reaction progress in terms of the reaction coordinate.

product species. This equilibrium hypothesis also permits formulation of the rate expression either in terms of the characteristic partition functions of statistical mechanics or in terms of pseudo thermodynamic parameters.

The task of expressing the energy of a system comprised of a number of nuclei and electrons as a function of their spatial configuration is obviously a complex problem. In fact, it is one that is not amenable to exact solution for even the simplest possible chemical reaction. However, computational chemists have attacked this problem with diligence during the past several decades, and a number of useful approximate methods have been developed. In principle they permit one to generate multi-dimensional potential-energy surfaces linking reactants and products.

Consider a reaction involving three atoms:



In general, three position variables will be needed to specify the potential energy of the reaction system. These may be the X-Y, Y-Z, and X-Z internuclear distances or two internuclear distances and the included angle. Even in this relatively simple case, four dimensions would be required for generation of the potential-energy surface. However, if we restrict our attention to linear configurations of these atoms, it is possible to depict the potential energy surface in three dimensions, as shown in

Figure 4.3. Certain qualitative and semi-quantitative aspects of potential energy surfaces are conveniently illustrated using this figure. The vertical elevation represents the potential energy of the system as a function of the two internuclear distances  $r_{xy}$  and  $r_{yz}$ . Such surfaces may be generated using the techniques of the computational chemist. These surfaces correspond to two valleys linked by a saddle-shaped pass or col. One side of each valley corresponds to a very steep hill, said terrain arising from the strong dependence of the repulsive component of interatomic forces on separation distance. The opposite sides of the valley rise less steeply and eventually lead to a plateau at large values of both internuclear separation distances. The valleys do not join except by way of a pass or saddle point near  $K$  and  $L$ .

If a plane is passed perpendicular to the  $r_{xy}$  axis at a sufficiently large value of this parameter, the cross section of the potential-energy surface one obtains is essentially the potential-energy curve governing formation of the YZ molecule whose constituent atoms exert both attractive and repulsive forces. At smaller values of  $r_{xy}$ , atom X interacts with atoms Y and Z to perturb the shape of the potential function so that the depth of the potential well is less. Point  $J$  is located on the floor of one of the valleys and has a large value for  $r_{xy}$  and a very small value for  $r_{yz}$ . It corresponds to an X atom far removed from a YZ molecule.

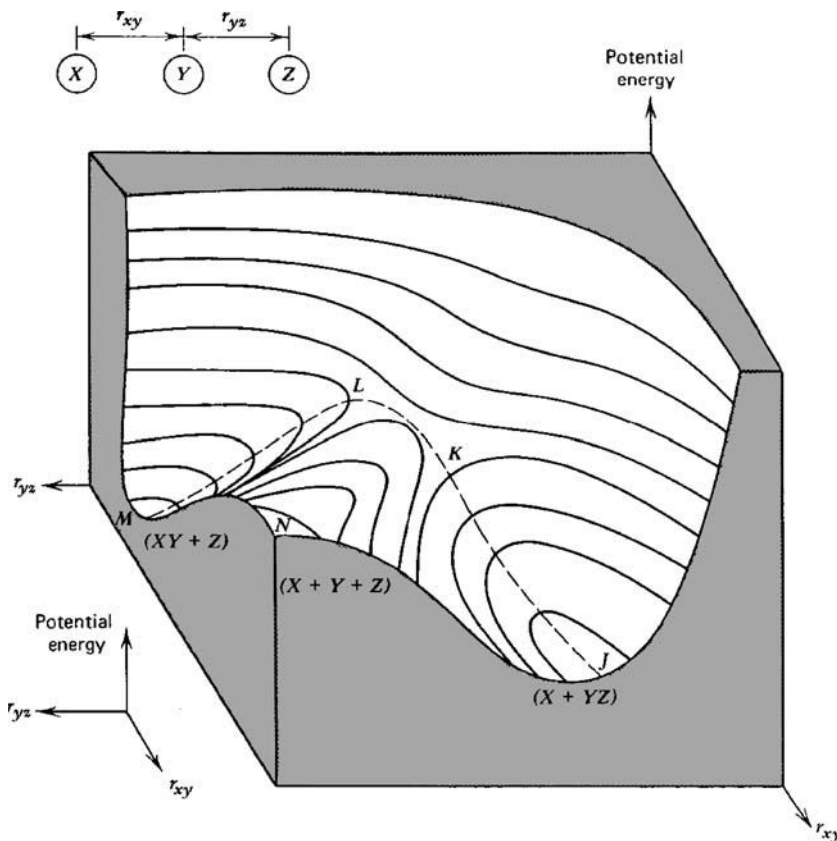


**Figure 4.3** Schematic representation of the potential energy of a system comprised of three atoms in a linear configuration as a function of the internuclear separation distances. The dashed line represents the reaction  $\text{X} + \text{YZ} \rightarrow \text{XY} + \text{Z}$ .

Similarly, it can be shown that a cross section perpendicular to the  $r_{yz}$  axis at large  $r_{yz}$  gives the potential-energy curve characteristic of the formation of XY from its constituent atoms. Point M on the figure corresponds to a Z atom and an XY molecule. At point N both  $r_{xy}$  and  $r_{yz}$  are large, so atoms X, Y, and Z are well separated and no molecules are present. At points K and L both internuclear distances are small, as in a collision between an X atom and a YZ molecule (point K) or between a Z atom and an XY molecule (point L). The region in the neighborhood of these points is referred to as the *transition state*, and the configuration assumed by the atoms in this state is referred to as the *activated complex*. We denote this complex by the symbol  $\text{XYZ}^{\ddagger}$ .

The reaction  $\text{X} + \text{YZ} \rightarrow \text{XY} + \text{Z}$  will correspond to motion from point J in one valley to point M in the second valley. For this reaction to take place with a minimum amount of energy the system will travel along the floor of the first valley, over the col, and down into the second valley. This path is indicated by a dashed line. Energy considerations dictate that the majority of the reaction systems will follow this path. The elevation of the saddle point above the floor of the first valley is thus related to the activation energy for the reaction.

Another common representation of the progress of the system as it moves from reactants to products is that

shown in Figure 4.2. Here the potential energy of the system is plotted versus distance along the dashed line shown in Figure 4.3. This variable is referred to as the *reaction coordinate*. In both figures the energy differences between the transition state and the reactant and product states are related to the activation energies for the forward and reverse reactions, respectively. Energy differences between the reactant and product states are related to the normal thermodynamic energy functions characteristic of the reaction. For exothermic reactions the potential energy of the products lies below that of the reactants, and for endothermic reactions the relative elevations are reversed. Thus, Figure 4.2 indicates an endothermic reaction and Figure 4.3 represents an exothermic reaction.

It is important to recognize that the mechanism indicated by these figures is quite different from one corresponding to an initial complete dissociation of the YZ molecule followed by combination of the X and Y atoms. The latter mechanism corresponds to movement from one valley at J up to the plateau at N and back down to the second valley at M. The activation energy for the latter mechanism would be equal to the energy required to dissociate the YZ molecule. By moving along the valley as in the mechanism indicated by the dashed line in the figure, the system can obviously achieve reaction with significantly lower energy requirements. In physical

terms the process of forming the X–Y bond contributes continuously to the energy requirement for breaking the original Y–Z bond.

For reactions involving more than three atoms, the number of dimensions required to depict the potential-energy surface exceeds human capacity to visualize the surface. Thus, it may be more convenient to consider such reactions as taking place between various moieties that play the same roles as the X, Y, and Z atoms in the discussion above.

The semi-empirical nature of the methods used to construct multi-dimensional potential energy surfaces renders the quantitative validity of the results questionable. Hence, methods for calculation of potential-energy surfaces and the associated activation energies for reaction remain an active area of research.

The development of reaction potential energy surfaces was an essential precursor to formulation of transition state theory. The first calculation of reaction rates in terms of a specific potential-energy surface is attributed to Pelzer and Wigner (56), who studied the reaction between atomic and molecular hydrogen. Eyring and his co-workers (53–55) later developed and extended the basic concepts, leading to codification of the theory, thereby forging the close link between his name and the theory. At about the same time, Evans and Polanyi (57–59) presented a somewhat different formulation of the problem. These and other analyses of the problem lead to very similar conclusions. The chemical engineer should be familiar with these conclusions, even if he or she does not choose to become acquainted with the analytical details of the theory.

In Eyring's formulation of the problem he assumed that an “equilibrium” exists between the activated complex species and the reactant molecules. This equilibrium is said to exist at all times, regardless of whether or not a true chemical equilibrium has been established between the reactants and the products. Although the basic assumption is not unreasonable, neither does it lend itself to simple verification. It does, however, lead to results that are consistent with those obtained by procedures that do not require one to assume equilibrium between reactants and the activated complex.

The reaction rate is then taken to be the product of the frequency at which activated complexes cross the energy barrier and their concentration *at the top of the barrier*. If  $(C^\ddagger)$  represents the concentration of complexes *lying within a region of length  $\delta^\ddagger$*  at the top of the barrier (see Figure 4.2), and if  $\vec{v}^\ddagger$  is the mean velocity at which molecules move from left to right at the top of the barrier, the reaction rate is given by

$$\vec{r} = \frac{(C^\ddagger) \vec{v}^\ddagger}{\delta^\ddagger} \quad (4.3.24)$$

These activated complexes differ from ordinary molecules in that in addition to the three normal translational degrees of freedom, they have a fourth degree of translational freedom corresponding to movement along the reaction coordinate. This degree of freedom replaces one vibrational degree of freedom that would otherwise be observed.

The motion of activated complexes within the transition state may be analyzed in terms of classical or quantum mechanics. In terms of classical physics, motion along the reaction coordinate may be analyzed in terms of a one-dimensional velocity distribution function. In terms of quantum mechanics, motion along the reaction coordinate within the limits of the transition state corresponds to the traditional quantum mechanical problem involving a particle in a box.

Such analyses lead to the conclusions that

$$\vec{v}^\ddagger = \left( \frac{k_B T}{2\pi m^\ddagger} \right)^{1/2} \quad (4.3.25)$$

and

$$(C^\ddagger) = (XYZ^\ddagger) \frac{\delta^\ddagger}{h} (2\pi m^\ddagger k_B T)^{1/2} \quad (4.3.26)$$

where  $m^\ddagger$  is the effective mass of the activated complex,  $h$  is Planck's constant, and  $(XYZ^\ddagger)$  is the total concentration of activated complexes. Combination of equations (4.3.24) to (4.3.26) gives

$$\vec{r} = \frac{k_B T}{h} (XYZ^\ddagger) \quad (4.3.27)$$

Thus, the effective frequency with which activated complexes are transformed into reaction products is  $k_B T/h$ . At 300 K, this group has a value of  $6 \times 10^{12} \text{ s}^{-1}$ , which is comparable in magnitude to normal molecular vibration frequencies.

If one describes the equilibrium between reactants and the activated complex by

$$K^\ddagger = \frac{(XYZ^\ddagger)}{(X)(YZ)} \quad (4.3.28)$$

then

$$\vec{r} = \frac{k_B T}{h} K^\ddagger (X)(YZ) \quad (4.3.29)$$

which is a second-order rate expression. The problem of predicting a rate constant thus reduces to one of evaluating  $K^\ddagger$ . Two basic approaches are used in attacking this problem: one based on statistical mechanics and one based on thermodynamics. From statistical mechanics it is known that for a reaction of the type  $X + YZ \rightarrow XYZ^\ddagger$ , the equilibrium constant is given by

$$K^\ddagger = \frac{Q_{XYZ^\ddagger} e^{-E_0/RT}}{Q_X Q_{YZ}} \quad (4.3.30)$$

where the  $Q$ 's are molecular partition functions for the various species and  $E_0$  is the energy increase accompanying the reaction at absolute zero when 1 mol of activated complex is formed. Combination of equations (4.3.29) and (4.3.30) indicates that the second-order rate constant is given by

$$k = \frac{k_B T}{h} K^\ddagger = \frac{k_B T}{h} \frac{Q_{XYZ^\ddagger} e^{-E_0/RT}}{Q_X Q_{YZ}} \quad (4.3.31)$$

This relation indicates that the rate constant can be determined from a knowledge of the partition functions of the activated complex and the reactant species. For stable molecules or atoms the partition functions can be calculated from experimental data that do not require kinetic measurements. However, they do require that molecular constants such as the vibrational frequencies and moments of inertia be evaluated from spectroscopic data. Evaluation of the partition function for the activated complex  $Q_{XYZ^\ddagger}$  presents a more difficult problem, since the moments of inertia and vibrational frequencies required cannot be determined experimentally. However, theoretical calculations permit one to determine moments of inertia from the various internuclear distances and vibrational frequencies from the curvature of the potential energy surface in directions normal to the reaction coordinate. In practice, one seldom has available a sufficiently accurate potential energy surface for the reaction whose rate constant is to be determined.

Moreover,  $Q_{XYZ^\ddagger}$  is a partition function from which the degree of freedom corresponding to motion along the reaction coordinate has been removed. The contribution of this motion has already been taken into account in the analysis leading to equation (4.3.27). Readers who wish to acquaint themselves with the manner in which partition functions are calculated are encouraged to consult standard texts in physical chemistry and statistical mechanics.

Although equation (4.3.29) refers to a second-order reaction between an atom X and a molecule YZ, the theory is readily generalized to other reaction stoichiometries. An expression characterizing the equilibrium between reactants and the activated complex is used to eliminate the latter from equation (4.3.27), and the desired result is obtained.

Instead of formulating the reaction rate expression in terms of molecular partition functions, it is often convenient to employ an approach utilizing pseudo-thermodynamic functions. From equation (4.3.29), the second-order rate constant is given by

$$k = \frac{k_B T}{h} K^\ddagger \quad (4.3.32)$$

An equilibrium constant is simply related to a standard Gibbs free-energy change, as indicated by equation (2.4.7):

$$\Delta G^\ddagger = -RT \ln K^\ddagger \quad (4.3.33)$$

Hence, the reaction rate constant can be written as

$$k = \frac{k_B T}{h} e^{-\Delta G^\ddagger/RT} \quad (4.3.34)$$

Because the factor  $k_B T/h$  is independent of the nature of the reaction, this approach to transition state theory argues that the Gibbs free energy of activation ( $\Delta G^\ddagger$ ) determines the reaction rate at a given temperature.

The free energy of activation can also be expressed in terms of an entropy ( $\Delta S^\ddagger$ ) and an enthalpy of activation ( $\Delta H^\ddagger$ ) in conventional thermodynamic fashion:

$$\Delta G^\ddagger = \Delta H^\ddagger - T \Delta S^\ddagger \quad (4.3.35)$$

These quantities provide another manner of expressing the rate constant in thermodynamic terms:

$$k = \frac{k_B T}{h} e^{\Delta S^\ddagger/R} e^{-\Delta H^\ddagger/RT} \quad (4.3.36)$$

If  $k$  is expressed in liters per mole per second, the standard state for the free energy, enthalpy, and entropy of activation is 1 mol/L. If the units of  $k$  are cubic centimeters per molecule per second, the corresponding standard-state concentration is 1 molecule/cm<sup>3</sup>. The magnitudes of  $\Delta G^\ddagger$  and  $\Delta S^\ddagger$  reflect changes in the standard state, so it is not useful to say that a particular reaction is characterized by specific numerical values of these parameters unless the standard states associated with them are clearly identified. These standard states are determined automatically by the units chosen to describe the reactant concentrations in the phenomenological rate expressions.

In terms of the collision theory of gases, a bimolecular reaction rate is written as

$$r = P_S Z_{AB} e^{-E/RT} \quad (4.3.37)$$

where  $P_S$  is the steric factor,  $Z_{AB}$  the collision frequency, and  $E$  the activation energy of the reaction. In terms of the thermodynamic formulation of transition-state theory, a bimolecular reaction rate is given by

$$r = \frac{K_B T}{h} e^{\Delta S^\ddagger/R} e^{-\Delta H^\ddagger/RT} (A)(B) \quad (4.3.38)$$

Comparison of these expressions indicates that the entropy of activation is related to the steric factor for the reaction. One may interpret the steric factor in terms of the degree of order of molecular configurations required to bring about the reaction, and this viewpoint is generally regarded as more satisfactory from an intellectual viewpoint than is that which regards  $P_S$  as an a posteriori correction factor necessary to obtain agreement between theory and experiment.

Experimental values of  $\Delta S^\ddagger$  are readily calculated from measured values of reaction rate constants and

activation energies. These experimental values provide significant insight into the nature of the transition state and the structure of the activated complex. Loosely bound complexes have higher entropies than tightly bound ones. A positive entropy of activation implies that the entropy of the complex is greater than that of the reactants. More often there is a decrease in entropy associated with formation of the activated complex. For bimolecular reactions the complex is formed by association of two molecules, and there is a loss of three translational and at least one rotational degree of freedom. Hence,  $\Delta S^\ddagger$  is usually negative and, in some cases, is not too different from the overall entropy change conventionally associated with the reaction. In these cases for reactions of the type  $A + B \rightarrow AB$ , it indicates that the activated complex closely resembles the product molecule in its structure. For a long time such reactions were regarded as abnormal because they had unusually low steric factors. However, transition state theory clearly indicates that these low steric factors are merely a result of the large degree of order (large entropy decrease) necessary to obtain the proper molecular configuration for formation of the activated complex.

The thermodynamic formulation of transition state theory is useful in considerations of reactions in solution when one is examining a particular class of reactions and wants to extrapolate kinetic data obtained for one reactant system to a second system in which the same functional groups are thought to participate (see Section 7.4). For further discussion of the predictive applications of this approach and its limitations, consult the books by Benson (60) and Laidler (61). Laidler's kinetics text (39) and the classic by Glasstone et al. (55) contain additional useful background material.

Although the collision and transition-state theories represent two important methods of attacking the theoretical calculation of reaction rates, they are not the only approaches available. Alternative methods include theories based on nonequilibrium statistical mechanics, stochastic theories, and Monte Carlo simulations of chemical dynamics. Consult the texts by Johnston (46), Laidler (39, 61), and Benson (60) and the review by Wayne (62) for a further introduction to the theoretical aspects of reaction kinetics.

The various theories can provide useful insight into the way in which reactions occur, but we must again emphasize that they must be regarded as inadequate substitutes for experimental rate measurements. Experimental work to determine an accurate reaction rate expression is an essential prerequisite to the reactor design process.

## LITERATURE CITATIONS

1. WAYNE, R. P., The Detection and Estimation of Intermediates, in *Comprehensive Chemical Kinetics*, Vol. I, *The Practice of Kinetics*, C. H. BAMFORD and C. F. H. TIPPER (Eds.), Elsevier, New York, 1969.
2. ZUMAN, P., and PATEL, R. C. *Techniques in Organic Reaction Kinetics*, Krieger Publishing, Malabar, FL, 1992.
3. GARDINER, W. C., Jr., *Rates and Mechanisms of Chemical Reactions*, W.A. Benjamin, New York, 1969.
4. DANIELS, F., and JOHNSTON, E. H., *J. Am. Chem. Soc.*, **43**, 53 (1921).
5. OGG, R. A., *J. Chem. Phys.*, **15**, 337 (1947); **18**, 572 (1950).
6. EDWARDS, J. O., GREENE, E. F., and ROSS, J., *J. Chem. Educ.*, **45**, 381 (1968).
7. LIEBHAFSKY, H. A., and MOHAMMED, A., *J. Am. Chem. Soc.*, **55**, 3977 (1933).
8. KING, E. L., in *Catalysis*, P. H. EMMETT (Ed.), Vol. 2, Part 2, pp. 337–456, Reinhold, New York, 1955.
9. GOULD, E. S., *Mechanism and Structure in Organic Chemistry*, p. 136, Holt, Rinehart and Winston, New York, 1959.
10. MELVILLE, H. W., and GOWENLOCK, B. G., *Experimental Methods in Gas Reactions*, Macmillan, London, 1963.
11. ANDERSON, R. B., *Experimental Methods in Catalytic Research*, Academic Press, New York, 1970.
12. FRIESS, S. L., LEWIS, E. S., and WEISSBERGER, A. (Eds.), *Investigation of Rates and Mechanisms of Reactions*, Vol. VIII, Parts I and II, of *Technique of Organic Chemistry*, 2nd ed., Interscience, New York, 1961, 1963.
13. LEWIS, E. S. (Ed.), *Investigation of Rates and Mechanisms of Reactions*, 3rd ed., Vol. VI, Part I, of *Techniques of Chemistry*, Wiley, New York, 1974.
14. HAMMES, G. G. (Ed.), *Investigation of Rates and Mechanisms of Reactions*, 3rd ed., Vol. VI, Part II of *Techniques of Chemistry*, Wiley, New York, 1974.
15. MORRIS, J. C., *J. Am. Chem. Soc.*, **63**, 2535 (1941); **66**, 584 (1944).
16. ZEMANY, P. D., and BURTON, M., *J. Phys. Colloid Chem.*, **55**, 949 (1951).
17. WALL, L. A., and MOORE, W. J., *J. Phys. Colloid Chem.*, **55**, 965 (1951); *J. Am. Chem. Soc.*, **73**, 2840 (1951).
18. TOLMAN, R. C., *Phys. Rev.*, **23**, 699 (1924); *The Principles of Statistical Mechanics*, p. 163, Clarendon Press, Oxford, 1938.
19. DENBIGH, K. G., *The Thermodynamics of the Steady State*, pp. 31–38, Methuen, London, 1958.
20. HIRSCHFELDER, J., *J. Chem. Phys.*, **9**, 645, (1941).
21. SEMENOV, N. N., *Some Problems in Chemical Kinetics and Reactivity*, M. Boudart (transl.), Vol. I, pp. 29 and 64, Princeton University Press, Princeton, NJ, 1958.
22. BENSON, S. W., *Thermochemical Kinetics, Methods for the Estimation of Thermochemical Data and Rate Parameters*, 2nd ed., Wiley, New York, 1976.
23. SEMENOV, N. N., op. cit., Chap. I.
24. LAIDLER, K. J., *Chemical Kinetics*, Chap. 3, McGraw-Hill, New York, 1965.
25. BODENSTEIN, M., and LIND, S. C., *Z. Phys. Chem.*, **57**, 168 (1907).
26. CHRISTIANSEN, J. A., *K. Dan. Vidensk. Selsk., Mat.-Fys. Medd.*, **1**, 14 (1919).
27. HERZFELD, K. F., *Ann. Phys.*, **59**, 635 (1919).
28. POLANYI, M., *Z. Elektrochem.*, **26**, 50 (1920).
29. JOST, W., and JUNG, G., *Z. Phys. Chem.*, **B3**, 83 (1929).
30. RICE, F. O., and HERZFELD, K. F., *J. Am. Chem. Soc.*, **56**, 284 (1934).
31. GOLDFINGER, P., LETORT, M., and NICIAUSE, M., *Contribution de l'étude de la structure moléculaire*, Victor Henri Commemorative Volume, p. 283, Desoer, Liege, France, 1948.
32. LAIDLER, K. J., op. cit., Chap. 7 and 8.
33. MOORE, J. W., and PEARSON, R. G., *Kinetics and Mechanism*, 3rd ed., Chap. 5, Wiley-Interscience, New York, 1981.
34. BENSON, S. W., op. cit., Chap. XIII.
35. DAINTON, F. S., *Chain Reactions*, Methuen, London, 1956.
36. GUGGENHEIM, E. A., *Elements of the Kinetic Theory of Gases*, Pergamon Press, New York, 1960.

37. MOORE, J. W., and PEARSON, R. G., *Kinetics and Mechanism*, 3rd ed, Wiley, New York, 1981.
38. HOUSTON, P. H., *Chemical Kinetics and Reaction Dynamics*, McGraw-Hill, New York, 2001.
39. LAIDLER, K. J., *Chemical Kinetics*, 3rd ed, Harper & Row, New York, 1987.
40. MOELWYN-HUGHES, E. A., *Physical Chemistry*, p. 1109, Pergamon Press, New York, 1957.
41. TOLMAN, R. C., *Statistical Mechanics*, Chemical Catalog Co., 1927. Cited in Moore and Pearson, op. cit., p. 130.
42. LINDEMANN, F. A., *Trans. Faraday Soc.*, **17**, 598 (1922).
43. BENSON, S. W., op. cit., Chap. 11.
44. FORST, W., *Unimolecular Reactions: A Concise Introduction*, Cambridge University Press, Cambridge, 2003.
45. HOLBROOK, K. A., PILLING, M. J., and ROBERTSON, S. H., *Unimolecular Reactions*, 2nd ed, Wiley, New York, 1996.
46. JOHNSTON, H. S., *Gas Phase Reaction Rate Theory*, Ronald Press, New York, 1966.
47. KONDRATIEV, V. N., *Chemical Kinetics of Gas Reactions*, pp. 283–321, Pergamon Press, Oxford, 1964.
48. BUNKER, D. L., *Theory of Elementary Gas Reaction Rates*, pp. 48–74, Pergamon Press, Oxford, 1960.
49. WAYNE, R. P., op. cit., pp. 256–289.
50. PILLING, J., and SEAKINS, P. W., *Reaction Kinetics*, 2nd ed, Oxford University Press, Oxford, 1995.
51. STEINFELD, J. I., FRANCISCO, J. S., and HASE, W. L., *Chemical Kinetics and Dynamics*, 2nd ed, Prentice Hall, Upper Saddle River, NJ, 1999.
52. HINSHELWOOD, C. N., *The Kinetics of Chemical Change*, Clarendon Press, Oxford, 1940. p. 81.
53. EYRING, H., *J. Chem. Phys.*, **3**, 107 (1935).
54. WYNNE-JONES, W. F. K., and EYRING, H., *J. Chem. Phys.*, **3**, 492 (1935).
55. GLASSTONE, S., LAIDLER, K. J., and EYRING, H., *The Theory of Rate Processes*, McGraw-Hill, New York, 1941.
56. PELZER, H., and WIGNER, E., *Z. Phys. Chem.*, **B15**, 445 (1932).
57. EVANS, M. G., and POLANYI, M., *Trans. Faraday Soc.*, **31**, 875 (1935).
58. EVANS, M. G., and POLANYI, M., *Trans. Faraday Soc.*, **33**, 448 (1937).
59. POLANYI, M., *J. Chem. Soc.*, 1937, 629.
60. BENSON, S. W., *Thermochemical Kinetics*, Wiley, New York, 1968.
61. LAIDLER, K. J., *Theories of Chemical Reaction Rates*, McGraw-Hill, New York, 1969.
62. WAYNE, R. P., in *Comprehensive Chemical Kinetics*, Vol. 2, *The Theory of Kinetics*, C. H. BAMFORD and C. F. H. TIPPER, (Eds.), Elsevier, Amsterdam, 1969.

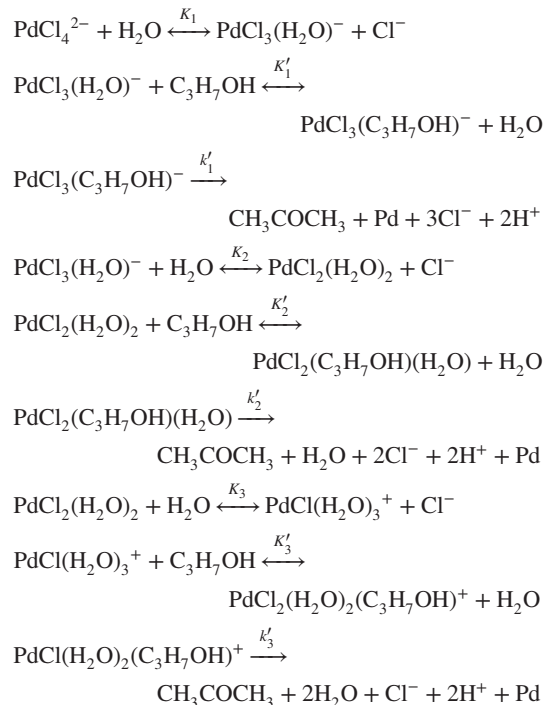
## PROBLEMS

- 4.1** I. V. Kozhevnikov, V. E. Taraban'ko, and K. I. Matveev [*Kinet. Catal.*, **21**, 679 (1980)] have studied the oxidation of isopropanol by palladium chloride in aqueous solution over the temperature range 339 to 369 K. The stoichiometry of the reaction is



- (a) Under the conditions studied,  $\text{PdCl}_2$  exists primarily in the form of the complexes  $\text{PdCl}_4^{2-}$ ,  $\text{PdCl}_3(\text{H}_2\text{O})^-$ ,

$\text{PdCl}_2(\text{H}_2\text{O})_2$ , and  $\text{PdCl}(\text{H}_2\text{O})_3^+$ . The following mechanism has been proposed for this reaction:



(Assume that all equilibrium steps are fast.)

- (b) Derive an expression for the rate of product formation that contains only  $[\text{PdCl}_2]$ ,  $[\text{Cl}^-]$ ,  $[\text{H}^+]$ ,  $[\text{C}_3\text{H}_7\text{OH}]$ , and the rate and equilibrium constants.
- (c) In the region of chloride ion concentrations from 0.1 to 0.7 M, the experimental rate law is of the form

$$\frac{d[\text{CH}_3\text{COCH}_3]}{dt} = k_{\text{exp}}[\text{PdCl}_2][\text{C}_3\text{H}_7\text{OH}]$$

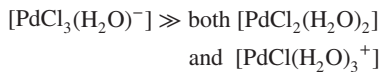
where  $\text{PdCl}_2$  represents the total concentration of palladium fed to the system, regardless of the particular ionic form it takes in solution. The experimental rate law was of the form

$$k_{\text{exp}} = \frac{\alpha}{(\text{Cl} + \beta)}$$

where  $\alpha$  and  $\beta$  are empirical constants. What values of  $\alpha$  and  $\beta$  are consistent with the following data?

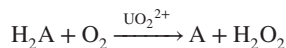
$k \times 10^4$ ( $\text{M}^{-1}/\text{s}$ )	$[\text{Cl}^-]$ (M)
26	0.015
21	0.03
10	0.06
7	0.11
6	0.16
4.5	0.26
3.9	0.35
3.3	0.45
3.0	0.55
2.6	0.63

- (d) How are  $\alpha$  and  $\beta$  related to the rate and equilibrium constants of the proposed mechanism? Note that



- (e) Do any of the steps postulated in the reaction mechanism seem unreasonable in the light of your knowledge of reaction mechanisms? Comment.

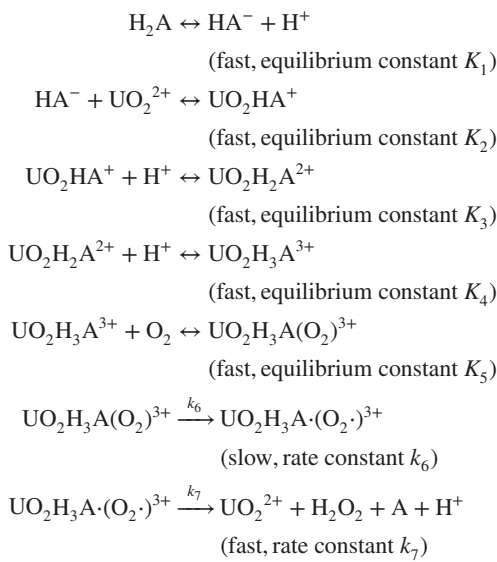
- 4.2 M. M. T. Khan and A. E. Martell [J. Am. Chem. Soc., **91** 4668 (1969)] reported the results of a kinetic study of the uranyl ion-catalyzed oxidation of ascorbic acid. The stoichiometry of this reaction is



and the corresponding rate expression is

$$-\frac{d(\text{H}_2\text{A})}{dt} = k(\text{H}_2\text{A})(\text{H}^+)(\text{O}_2)(\text{UO}_2^{2+})$$

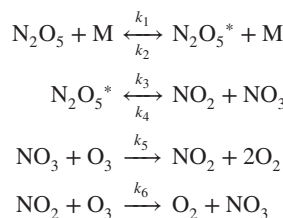
Is the following mechanism consistent with the experimental rate law?



- 4.3 Experimental data for the catalytic decomposition of ozone in the presence of nitrogen pentoxide follow the rate law:

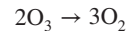
$$r = k(\text{O}_3)^{2/3}(\text{N}_2\text{O}_5)^{2/3}$$

The following mechanism has been proposed as an explanation for these observations.



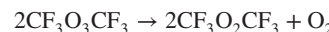
where  $\text{N}_2\text{O}_5^*$  is an excited nitrogen pentoxide molecule and  $\text{M}$  is any molecule.  $\text{NO}_3$  should be treated as an active intermediate. Show whether or not this mechanism is consistent with the experimentally observed rate expression.

Note that the stoichiometry of this reaction is given by

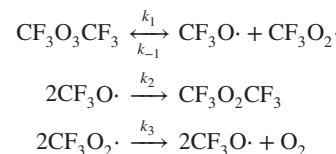


and that there is no net consumption or production of species  $\text{M}$  in any reaction. If the mechanism above is not consistent with the experimental rate law, suggest an alternative mechanism including reactions 1 to 4 and 6 that will be consistent. (Note: It will not be necessary to introduce any chemical species in addition to those used above. Consider only bimolecular reactions.)

- 4.4 J. Czarnowski and H. J. Schumacher [Int. J. Chem. Kinet., **24**, 639 (1981)] studied the thermal decomposition of bis(trifluoromethyl)trioxide at temperatures from 60 to 90°C:



The following mechanism has been proposed to explain the observation that the reaction obeys first-order kinetics:



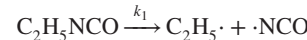
Demonstrate whether or not this mechanism is consistent with the rate expression observed experimentally.

- 4.5 The kinetics and mechanism of the thermal decomposition of ethyl isocyanate,

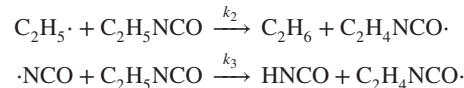


were investigated by P. G. Blake and S. Ijadi-Maghsoodi [Int. J. Chem. Kinet., **15**, 609 (1983)]. The order of the reaction with respect to isocyanate observed experimentally was 1.55. The following chain reaction mechanism has been proposed to explain the observed kinetics:

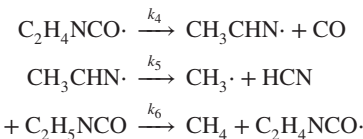
Initiation:



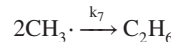
Chain transfer:



Propagation:



Termination:



Derive an expression for the rate of reaction that contains only the rate constants indicated above and the concentrations of stable species (i.e., only those appearing in the stoichiometric equation given above). Under what circumstances is this mechanism consistent with the observed kinetics?

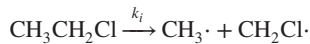
- 4.6** D. J. McCracken and P. F. Dickson [*Ind. Eng. Chem., Process Des. Dev.*, **6**, 286 (1967)] studied the esterification of cyclohexanol (B) with acetic acid (A) in the presence of sulfuric acid:



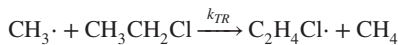
These researchers have indicated that the overall order of this reaction is 3, that the order in acetic acid is 2, and that the order in cyclohexanol is 1. Recognizing that in dioxane solution at 40°C, acetic acid exists primarily as a dimer, propose a set of mechanistic equations that are consistent with the indicated rate expression.

- 4.7** S. W. Benson [*Ind. Eng. Chem.*, **56**, 18 (1964)] discussed the following mechanism for the pyrolysis of ethyl chloride:

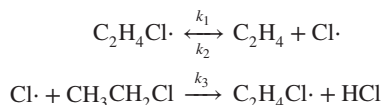
Initiation:



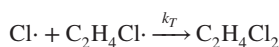
Transfer:



Propagation:



Termination:

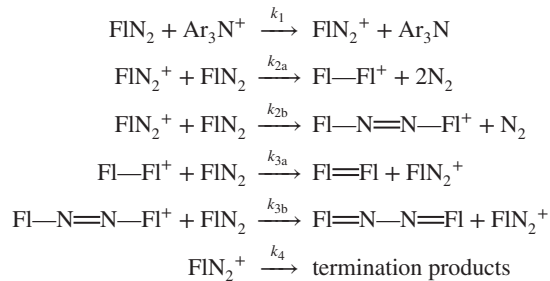


It has been suggested that during the initial stages of the reaction when  $CH_3CH_2Cl \gg C_2H_4$ , this mechanism leads to a rate expression that is first-order in  $CH_3CH_2Cl$  and zero-order in  $C_2H_4$ . Subsequently, when  $CH_3CH_2Cl \ll C_2H_4$ , the mechanism predicts shifts in the orders of the reaction with respect to these species.

- (a) What rate expression does this mechanism predict for the rate of disappearance of  $CH_3CH_2Cl$  when one makes the long-chain approximation?  
 (b) What are the limiting forms of this rate expression?  
 (c) What will be the apparent activation energy of the reaction in terms of the activation energies of the individual steps for the two limiting cases of part (b)?

- 4.8** I. Ahmad [*Int. J. Chem. Kinet.*, **21**, 1095 (1989)] studied the decomposition of 9-diazofluorene ( $FIN_2$ ) by tris(*p*-bromophenyl)aminium hexachloroantimonate (B) in anhydrous acetonitrile. The reaction is reported to be first-order in both  $FIN_2$  and B, second-order overall.

This reaction is thought to proceed via the two parallel routes indicated in the following mechanism:

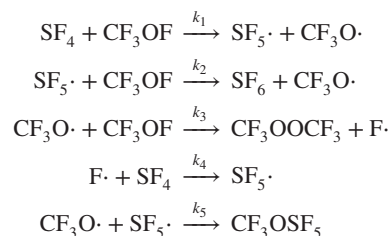


where  $FIN_2$  represents 9-diazofluorene,  $Ar_3N^+$  represents  $(p\text{-BrC}_6\text{H}_4)_3\text{N}^+$ ,  $Fl=Fl$  represents bifluoridylene,  $F=N=N=F$  represents fluorenone azine, and  $FIN_2^+$ ,  $Fl-Fl^+$ , and  $Fl-N=N-Fl^+$  represent postulated intermediates.

- (a) Derive the expression for the rate of consumption of 9-diazofluorene that is associated with this mechanism. Is this expression consistent with the rate expression reported?  
 (b) At 30°C the amounts of  $Fl=Fl$  and  $Fl=N=N=Fl$  in the product mixture are present in the ratio 34.6 : 63.8. Only very small amounts of side products are observed. What does this product distribution imply about the relative values of the various rate constants?  
 (c) A. C. Gonzalez and H. J. Schumacher [*Int. J. Chem. Kinet.*, **17**, 43–53 (1985)] studied the kinetics of the gas-phase reaction between  $SF_4$  and  $CF_3OF$ . This reaction obeys the rate expression

$$r = k(SF_4)(CF_3OF)$$

The following mechanism has been proposed to explain the kinetics of this reaction:



- (a) Is this mechanism consistent with the observation that the products consist primarily of equimolar quantities of  $SF_6$  and  $CF_3OOCF_3$ , together with very small quantities of  $CF_3OSF_5$ ?  
 (b) Determine the rate expression corresponding to these mechanistic equations.  
 (c) Is this rate expression consistent with the experimental results?

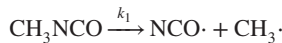
- 4.10** The mechanism below can be regarded as a variation of one proposed by P. G. Blake and S. Ijadi-Maghsoodi [*Int. J. Chem. Kinet.*, **15**, 609–618 (1983)] for the thermal decomposition of methyl isocyanate. Trace quantities of  $CH_4$  and  $HCNO$  are

present in the final products, but the primary product composition is consistent with the stoichiometry

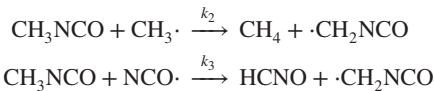


The steps in the mechanism are:

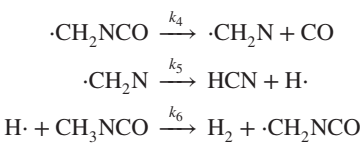
Initiation:



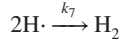
Chain transfer:



Propagation:



Termination:



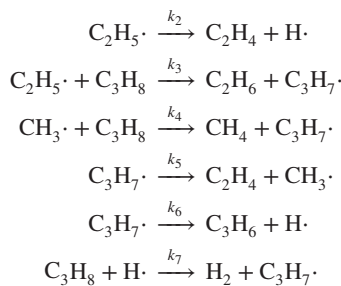
Derive an expression for the rate of disappearance of methyl isocyanate that includes only the indicated rate constants and the concentrations of species appearing in the primary stoichiometric equation. Do not make the long-chain approximation until you have developed the indicated expression. At this point you may simplify this expression as appropriate to determine whether or not this mechanism is consistent with the experimental observation that this reaction is  $(\frac{3}{2})$ -order in  $\text{CH}_3\text{NCO}$ . State explicitly any other assumptions that you make in arriving at your final result.

- 4.11** The following chain reaction mechanism has been suggested for the pyrolysis of propane:

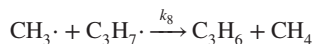
Initiation:



Propagation:



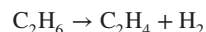
Termination:



Derive expressions for the rates of formation of  $\text{C}_2\text{H}_4$  and  $\text{C}_3\text{H}_6$  and the rate of disappearance of  $\text{C}_3\text{H}_8$ . These expressions are to contain only the rate constants indicated above and

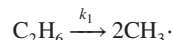
the concentrations of stable species ( $\text{C}_3\text{H}_8$ ,  $\text{C}_3\text{H}_6$ ,  $\text{H}_2$ ,  $\text{CH}_4$ ,  $\text{C}_2\text{H}_4$ , and  $\text{C}_2\text{H}_6$ ).

- 4.12** Pyrolysis of ethane produces a wide variety of products, the relative proportions of which depend on the conditions under which the reaction is carried out. However, the major products are ethylene and hydrogen:

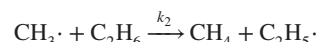


The following chain reaction mechanism may be used to provide a molecular description of the events that occur during the course of this reaction.

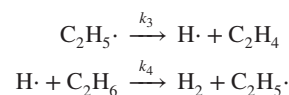
Initiation:



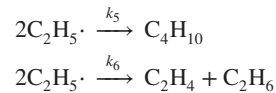
Carrier transfer:



Propagation:

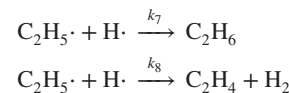


Termination:



- (a)** Is this mechanism consistent with the stoichiometry of this reaction? Derive the rate expression associated with this mechanism.

- (b)** Imagine that the termination reactions indicated above are not the dominant termination processes. Derive the rate expression for a mechanism in which the initiation and propagation steps remain the same, but in which the termination reactions are as follows:

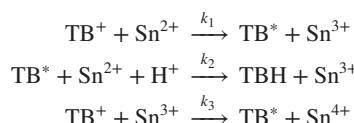


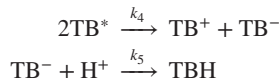
Reactions 5 and 6 do not occur to any significant extent.

- (c)** Indicate how you would proceed to ascertain whether the mechanism of part (a) or that of part (b) is more likely to be correct.

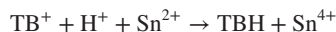
- 4.13** S. B. Jonnalagadda and M. Dumba [Int. J. Chem. Kinet., **25**, 745–753 (1993)] studied the kinetics of the reduction of toluidine blue ( $\text{TB}^+$ ) by stannous ions at low pH.

- (a)** The following chain reaction mechanism has been proposed to explain the observation that the reaction is  $(\frac{3}{2})$ -order in stannous ion and first-order in hydrogen ion:





where  $\text{TB}^+$  refers to toluidine blue,  $\text{TB}^*$  refers to semi-toluidine blue radical,  $\text{TB}^-$  refers to unprotonated leuco toluidine blue, and  $\text{TBH}$  refers to protonated leuco toluidine blue. The stoichiometry of the overall reaction is

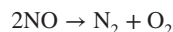


1. Identify the initiation, propagation, and termination reactions.
  2. Derive the rate expression corresponding to this mechanism. This rate expression should contain only the concentrations of toluidine blue, hydrogen ions, and stannous ions, together with appropriate rate constants.
  3. Is the rate expression consistent with the reaction orders noted above?
- (b) In an effort to further assess the validity of the proposed mechanism, these researchers reported the following data at 25°C for a system containing 0.142 M  $\text{H}^+$  and  $1.0 \times 10^{-3}$  M  $\text{Sn}^{2+}$ .

Time (min)	$\text{TB}^+ \times 10^5$ (M)
0	4.00
10	3.39
20	2.78
30	2.27
40	1.77
50	1.37
60	0.97
70	0.72
80	0.42

Determine the order of the reaction with respect to  $\text{TB}^+$  and the value of the rate constant. The order is a half-integer. Is the mechanism above consistent with these data?

- 4.14 R. J. Wu and C. T. Yeh [*Int. J. Chem. Kinet.*, **28**, 89–94 (1996)] studied the thermal decomposition of nitric oxide at elevated temperatures:



In a batch reactor at temperatures below 2000 K, the rate expression that applies to low conversions is

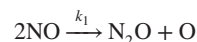
$$r = k(M)^{-0.5}(\text{NO})^2$$

while at high conversions, or when the initial reaction mixture contains a substantial proportion of oxygen, the rate expression is

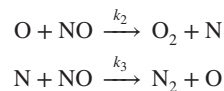
$$r = k'(\text{NO})^{1.5}(\text{O}_2)^{0.5}$$

The following chain reaction mechanism has been proposed to explain the observed kinetics:

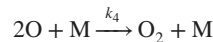
Initiation:



Propagation:

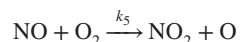


Termination:



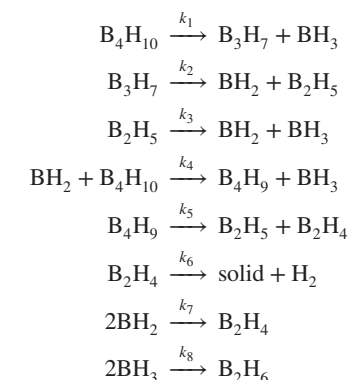
where  $\text{M}$  is any molecule that is capable of the energy transfer necessary to stabilize the oxygen molecule.

Once appreciable amounts of  $\text{O}_2$  are present in the reaction mixture, the initiation reaction that is the primary source of atomic oxygen is no longer the first reaction. Instead, the following reaction begins to dominate the chain initiation process:



Determine whether or not the mechanistic equations above are consistent with the two limiting forms of the rate expression indicated above. If they are consistent, how are the rate constants  $k$  and  $k'$  related to the rate constants for the mechanistic equations? If the values of the activation energies associated with steps 1 to 5 are 272, 161, 1.4, 14, and 198 kJ/mol, respectively, what values of the experimental activation energy are predicted at high and low conversions of NO? Be sure to state explicitly any assumptions that you make.

- 4.15 A. C. Bond and M. L. Pinsky [*J. Am. Chem. Soc.*, **92**, 32 (1970) proposed the following mechanism for the decomposition of tetraborane:



- (a) The stable products of the reaction are  $\text{B}_2\text{H}_6$ ,  $\text{H}_2$ , and the solid. Derive the equation for the rate of disappearance of tetraborane.
- (b) These investigators obtained the data below in an isothermal constant-volume batch reactor operating at 60°C starting with an initial tetraborane pressure of 14.13 kPa.

Time (s)	Tetraborane concentration (mol/m <sup>3</sup> )
0	4.83
1800	3.68
3600	3.38
5400	2.91
7200	2.46
9000	2.18

What is the experimentally observed order of the reaction? The order is equal to  $n/2$ , where  $n = 0, 1, 2, 3$ , or  $4$ . Under what circumstances is the proposed mechanism consistent with the experimentally observed rate expression?

- 4.16** S. Ledakowicz, L. Nowicki, and J. Perkowski [*Int. J. Chem. Kinet.*, **16**, 345–352 (1984)] studied the kinetics of the photochlorination of tetrachloroethylene. The stoichiometry of the reaction is

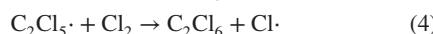
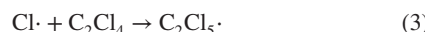


The following free-radical mechanism has been proposed for this reaction:

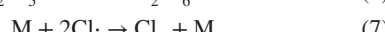
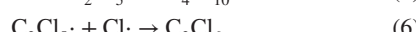
Initiation:



Propagation:



Termination:



where  $\text{M}$  is any third body.

- (a) Derive an expression for the rate of disappearance of molecular chlorine that contains only the various rate constants  $k_i$ , the concentrations of stable species, and the intensity of the incident radiation,  $I$ . Note that the rate of reaction (2) is given by

$$r_2 = k_2 I(\text{Cl}_2)$$

- (b) The experimental data indicate that the rate expression is of the form

$$r = I^a(\text{Cl}_2)^b(\text{C}_2\text{Cl}_4)^c$$

where

$$a = 0.489 \pm 0.003$$

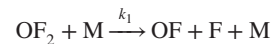
$$b = 0.889 \pm 0.160$$

$$c = 1.040 \pm 0.042$$

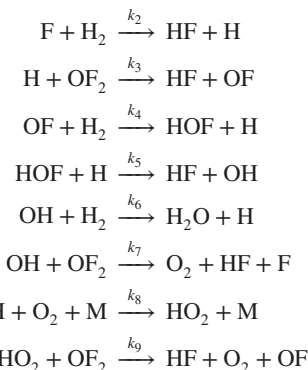
Is the mechanism proposed consistent with the experimental data? Can you draw any conclusions concerning which of the three termination steps predominates?

- 4.17** T. J. Houser [*Int. J. Chem. Kinet.*, **10**, 773 (1998)] proposed the following 10-step mechanism for the reaction between  $\text{OF}_2$  and  $\text{H}_2$  at 1 atm and 160 to 310°C.

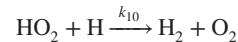
Initiation:



Propagation:



Termination:



To a good approximation the stoichiometry of this reaction can be represented by



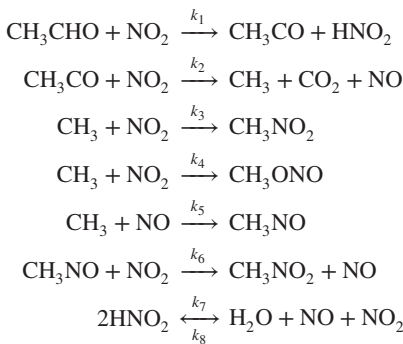
Derive an expression for the rate of disappearance of  $\text{OF}_2$  which contains only the concentrations of stable species ( $\text{OF}_2$ ,  $\text{H}_2$ , HF,  $\text{H}_2\text{O}$ ,  $\text{O}_2$ , and  $\text{M}$ ) and various rate constants. In your derivation you may assume that the long-chain approximation is valid (i.e., that the rates of the propagation reactions are much greater than those of the initiation and termination reactions). However, you should be careful not to make this assumption too soon. Otherwise, some simplifications will not arise in the normal course of the analysis. You may also assume that the rate of reaction 3 is much greater than that of reaction 9, which in turn is much greater than that of reaction 10. (The latter assumptions are necessary so that  $\text{O}_2$  will act as an inhibitor of the reaction, a result that is observed experimentally.)

Does the resulting rate expression agree with the following experimental observations?

1. The rate is strongly dependent on the concentration of  $\text{OF}_2$ .
2. The rate is weakly dependent on the concentration of  $\text{H}_2$ .
3. Oxygen acts as an inhibitor of the reaction.

When the reactants are present in stoichiometric proportions, it is observed that the rate is zero-order in  $\text{H}_2$ , second-order in  $\text{OF}_2$ , and  $(-\frac{1}{2})$ -order in  $\text{O}_2$ . Is the proposed mechanism consistent with these observations?

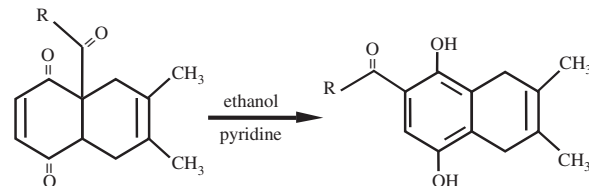
**4.18** A. M. Davis and W. H. Corcoran [*Ind. Eng. Chem. Fundam.*, **11**, 431 (1972)] studied the kinetics and mechanism of the partial oxidation of acetaldehyde by parts-per-million concentrations of  $\text{NO}_2$ . The stoichiometry of this reaction is quite complex and the yields of the various products depend on the reaction conditions. However, one can simplify the mechanism postulated by these researchers so as to focus on the primary reactions. The result of this simplification is the set of mechanistic equations indicated below.



- (a) Derive an expression for the rate of disappearance of  $\text{NO}_2$  that contains only the several rate constants and the concentrations of such stable species as  $\text{CH}_3\text{CHO}$ ,  $\text{NO}_2$ ,  $\text{CH}_3\text{NO}_2$ ,  $\text{CH}_3\text{ONO}$ ,  $\text{H}_2\text{O}$ , and  $\text{NO}$ . You should note that reaction 7/8 is extremely rapid in both the forward and reverse directions and that the equilibrium position for this reaction lies very far to the right.
- (b) The initial rate data tabulated below were reported by these investigators. Is the mechanism above consistent with these data? What is the corresponding numerical value of the reaction rate constant?

Initial rate of consumption of $\text{NO}_2$ , $r_0 \times 10^{11}$ (M/s)	Initial concentration of $\text{NO}_2$ , $C_{\text{A}0} \times 10^7$ (M)	Initial concentration of $\text{CH}_3\text{CHO}$ , $C_{\text{B}0} \times 10^3$ (M)
2.895	8.49	4.04
1.919	8.21	2.65
7.198	12.47	6.88
5.650	9.78	6.70
1.798	10.71	1.93
5.451	8.01	7.98
1.099	10.08	1.24
1.662	6.77	2.80
4.010	6.62	7.06
4.739	6.98	7.97
3.089	8.44	4.19
2.439	6.33	4.36
3.101	7.51	4.70
2.444	9.41	3.09
3.862	7.80	5.68
3.418	6.91	5.92
7.274	12.81	6.56

**4.19** A. M. Dabbagh and R. Al-Hamdan [*Int. J. Chem. Kinet.*, **19**, 49 (1987)] studied the kinetics of the pyridine-catalyzed rearrangements of some benzoquinone adducts in ethanol. These reactions may be regarded as irreversible with the following generalized stoichiometry:



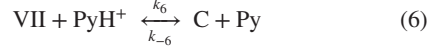
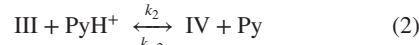
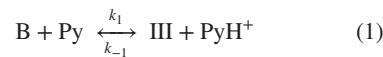
where  $\text{R}$  is an alkyl group or a phenyl group. In shorthand notation, the reaction is of the form  $\text{B} \rightarrow \text{C}$ . The experiments of interest were carried out in 50% v/v ethanolic pyridine with reactant concentrations in the millimolar range.

The progress of the reaction was monitored by absorbance measurements at 368 to 372 nm. Typical data for reaction at 50°C are presented below.

Time (min)	Absorbance
0	0.161
10	0.379
20	0.635
40	0.846
60	0.970
80	1.055
100	1.103
120	1.135
140	1.154
$\infty$	1.176

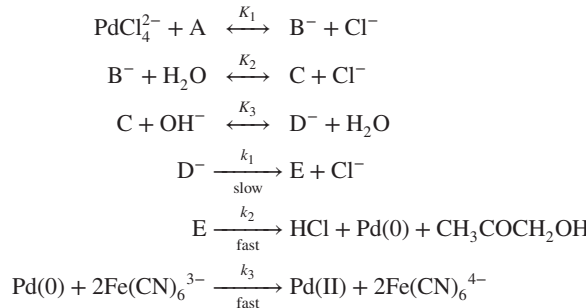
- (a) Determine the rate expression (order and numerical value of the rate constant) for this reaction. You may assume that the order is an integer.

- (b) These researchers proposed the following mechanism for this reaction:



where Py refers to pyridine and the various Roman numerals refer to reaction intermediates. How is the rate constant observed related to the parameters above and the concentration of pyridine? Is this mechanism consistent with the rate expression determined in part (a)?

**4.20** I. Ahmad and C. M. Ashraf [*Int. J. Chem. Kinet.*, **11**, 813 (1979)] studied the kinetics and mechanism of the palladium(II) chloride-catalyzed oxidation of allyl alcohol by potassium hexacyanoferrate(III). These researchers have proposed the following mechanism for this reaction:



where

A is allyl alcohol

B<sup>-</sup> is  $[\text{PdCl}_3\text{CH}_2=\text{CH}-\text{CH}_2\text{OH}]^-$

C is  $[\text{PdCl}_2(\text{H}_2\text{O})\text{CH}_2=\text{CH}-\text{CH}_2\text{OH}]$

D<sup>-</sup> is  $[\text{PdCl}_2(\text{OH})\text{CH}_2=\text{CH}-\text{CH}_2\text{OH}]^-$

E is  $\text{PdClCH}_2-\text{CH}(\text{OH})-\text{CH}_2\text{OH}$

(a) Derive the rate expression associated with this mechanism. Your expression should contain only the concentrations of reactants, products, and other stable species, equilibrium constants, and rate constants.

(b) The experiments indicated below were conducted in an effort to assess the validity of the proposed mechanism. In each case you should prepare a plot that would permit you to determine whether or not the data are consistent with the proposed mechanism. In all experiments the progress of the reaction was monitored by measuring the absorbance of the hexacyanoferrate(III) ion at 410 nm. Because the plots of the concentrations of this ion versus time were all linear for the experimental conditions of interest, these investigators reported their results in the form of pseudo zero-order rate constants.

Series I experiments:  $\text{A} = 13.33 \times 10^{-2}\text{M}$ ;  $\text{PdCl}_2 = 3.28 \times 10^{-5}\text{M}$ ;  $\text{NaOH} = 11.16 \times 10^{-2}\text{M}$ .

$\text{Fe}(\text{CN})_6^{3-} \times 10^3$ (M)	$k_{\text{observed}} \times 10^7$ (M/s)
3.50	2.85
4.00	2.82
4.50	2.86
5.00	2.83
5.50	2.88
6.00	2.86
6.50	2.85

Series II experiments:  $\text{Fe}(\text{CN})_6^{3-} = 4.41 \times 10^{-3}\text{M}$ ;  $\text{PdCl}_2 = 3.28 \times 10^{-5}\text{M}$ ;  $\text{NaOH} = 12.97 \times 10^{-2}\text{M}$ .

A (M)	$k_{\text{observed}} \times 10^7$ (M/s)
0.0735	1.06
0.1471	2.08
0.2206	2.87
0.2941	4.30

Series III experiments:  $\text{A} = 13.33 \times 10^{-2}\text{M}$ ;  $\text{PdCl}_2 = 3.28 \times 10^{-5}\text{M}$ ;  $\text{Fe}(\text{CN})_6^{3-} = 4.41 \times 10^{-3}\text{M}$ .

NaOH (M)	$k_{\text{observed}} \times 10^7$ (M/s)
0.1116	2.81
0.2232	5.83
0.3348	8.56
0.4464	11.53
0.5580	14.35

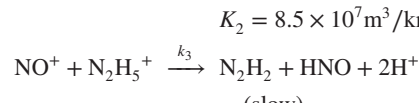
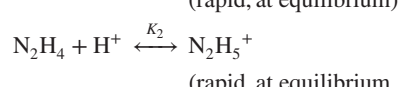
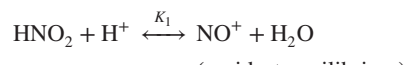
Series IV experiments:

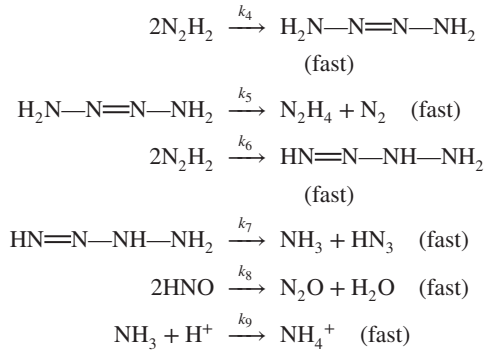
$\text{PdCl}_2 \times 10^5$ (M)	$k_{\text{observed}} \times 10^7$ (M/s)
1.70	1.30
3.30	2.25
5.00	4.15
6.75	5.85
8.00	7.05

Series V experiments:

$\text{Cl}^-(\text{free}) \times 10^3$ (M)	$k_{\text{observed}} \times 10^7$ (M/s)
109.10	0.45
61.65	1.05
51.30	2.50
34.50	5.70
26.54	9.60

**4.21** V. S. Koltunov and V. I. Marchenko [*Kinet. Katal.*, **7**, 224 (1966)] studied the reaction between hydrazine ( $\text{N}_2\text{H}_4$ ) and nitrous acid in aqueous solution. The following mechanism has been proposed for this reaction:





- (a) Derive the expression for the rate of disappearance of nitrous acid implied by this mechanism.
- (b) Under the experimental conditions employed by these investigators, reaction 2 lies very far to the right; i.e.,  $K_2$  and the pH were such that within a time frame that is very short compared to that of the rate measurements, all of the reactant hydrazine is present in ionic form as  $\text{N}_2\text{H}_5^+$ . Test the data tabulated below to determine if the orders of the reaction with respect to  $\text{N}_2\text{H}_5^+$  and with respect to  $\text{HNO}_2$  are each unity. Assume a 1 : 1 stoichiometry in your analysis. [In both runs the pH of the solution was held constant ( $\text{HNO}_3 = 0.1 \text{ kmol/m}^3$ .)]

Time (s)	$(\text{HNO}_2) \times 10^4$ ( $\text{kmol/m}^3$ )	$(\text{N}_2\text{H}_5^+) \times 10^{4a}$ ( $\text{kequiv/m}^3$ )
Run I		
0	2.40	15.00
10	1.17	13.77
20	0.63	13.23
30	0.32	12.92
40	0.18	12.78
50	0.09	12.69
90	0.01	12.61
Run II		
0	2.40	6.00
10	1.13	4.73
15	0.79	4.39
20	0.59	4.19
30	0.32	3.92
40	0.18	3.78

<sup>a</sup>a The analytical procedure employed was such that the entries for  $\text{N}_2\text{H}_5^+$  represent the sums of the  $\text{N}_2\text{H}_4$  and  $\text{N}_2\text{H}_5^+$  species. Since  $K_2$  is so large, the amount of free  $\text{N}_2\text{H}_4$  is only a very small fraction of this sum. These data have been adjusted to account for the proper stoichiometry since some question exists as to the appropriateness of the analysis employed by the original authors.

- (c) Does the proposed mechanism lead to a rate expression that is consistent with the experimental data?
- (d) Runs I and II may have been carried out in solutions of different ionic strengths. What are the corresponding values of the rate constants? Does there appear to be an effect of ionic strength on the observed rate constant? Is this what

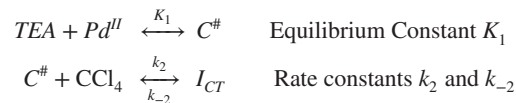
you would expect for a mechanism of the type proposed above?

- 4.22 P. K. Srivasta and S. K. Upadhyay [*Int. J. Chem. Kinet.*, **32** 171–177 (2000)] determined the following rate law for polymerization of methyl methacrylate (MMA) in the presence of  $\text{CCl}_4$ ,  $\text{PdCl}_2$ , and triethanol amine (TEA) in dimethyl sulfoxide solution:

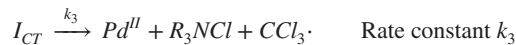
$$r = k[\text{MMA}][\text{CCl}_4]^{0.5}[\text{PdCl}_2]^{0.5}[\text{TEA}]^{0.5}$$

The free-radical mechanism below has been proposed to explain this rate law. Derive the rate expression associated with this mechanism and indicate whether or not it is consistent with the experimental results of Srivasta and Upadhyay.

Initiation:



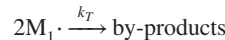
where  $\text{C}^\#$  is an association complex and  $I_{CT}$  is a charge transfer complex.



Propagation:

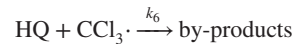


Termination:



As far as the mechanism proposed by these authors is concerned, species  $\text{M}_1 \cdot$  may contain any number of MMA monomer units from one to several thousand, but all such species are presumed to have the same reactivity. Thus from a functional standpoint, we may employ the same rate constant and species label for the multiplicity of mechanistic equations given by reaction 5.

These investigators have also evaluated the effect of adding hydroquinone (HQ) to the reaction mixture. This species can react with the  $\text{CCl}_3 \cdot$  radical to form by-products:



Derive the rate law that results when this step is added to the mechanism.

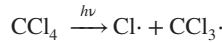
These investigators have also reported the following initial rate data when hydroquinone is present in the system.

Hydroquinone (M)	Rate $\times 10^4$ [mol/(L·s)]
0	2.60
0.018	2.10
0.036	1.50

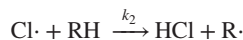
Are the mechanisms above consistent with these data under any circumstances? If so, what statements can you make about the relative rates of the steps involved therein?

- 4.23** M. L. White and R. R. Kuntz [*Int. J. Chem. Kinet.*, **3**, 127 (1971)] studied the gas-phase photolysis of the carbon tetrachloride/cyclohexane system. These researchers have postulated the following chain reaction mechanism to explain their results:

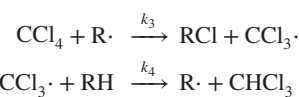
Initiation:



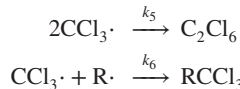
Chain transfer:



Propagation:



Termination:



where RH refers to cyclohexane and R· to a cyclohexyl radical. The rate of the initiation reaction may be taken as  $r_1 = k_1 I(\text{CCl}_4)$  where  $I$  is the intensity of the electromagnetic radiation.

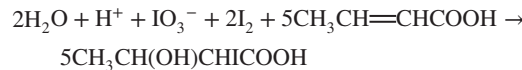
- (a) Derive expressions for the rate of product (RCl) formation for the cases where (1) reaction 5 is the dominant termination step; and (2) reaction 6 is the dominant termination step.
- (b) For the reaction at 132°C and a  $\text{CCl}_4$  concentration of  $1.09 \times 10^{-8}$  M, these researchers reported the following data:

Cyclohexane concentration $\times 10^8$ (M)	Rate of formation of $\text{RCl} \times 10^{15}$ (M/s)	Rate of formation of $\text{C}_2\text{Cl}_6 \times 10^{15}$ (M/s)
0.785	6.25	1.44
1.18	9.12	1.42
1.77	13.5	1.50
1.97	14.1	?
2.36	17.4	1.43
2.36	17.6	?
2.96	21.6	1.53

Is either of the limiting forms of the rate expression associated with cases (1) and (2) consistent with these data? Use the rate data for both  $\text{RCl}$  and  $\text{C}_2\text{Cl}_6$ . [Hint: Derive expressions for the rates of formation of cyclohexyl chloride (RCl) and  $\text{C}_2\text{Cl}_6$ . Which reaction is the primary process for termination of the chain reaction?]

- (c) On the basis of the data indicated, is this a long- or short-chain process? Be as quantitative as possible.

- 4.24** S. D. Furrow [*Int. J. Chem. Kinet.*, **14**, 927–932 (1982)] investigated the kinetics and mechanism of the hydroxy iodination of 2-butenoic acid in aqueous solution. The stoichiometry of this reaction is

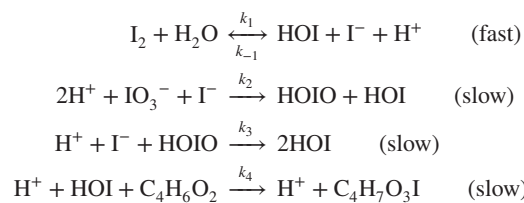


with a rate law at 25°C given by

$$\frac{d[\text{I}_2]}{dt} = k[\text{H}^+]^{0.97}[\text{C}_4\text{H}_6\text{O}_2]^{0.51}[\text{IO}_3^-]^{0.65}[\text{I}_2]^{0.5}$$

where  $\text{C}_4\text{H}_6\text{O}_2$  is 2-butenoic acid.

Furrow has suggested the following mechanism for this reaction:



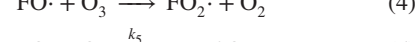
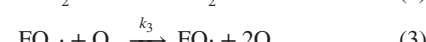
Demonstrate whether or not the rate expression predicted by this mechanism is consistent with that observed experimentally. You may find it convenient to express the rate in terms of the rate of consumption of  $\text{C}_4\text{H}_6\text{O}_2$ . Consider two different approaches. In the first approach make the usual pseudo-steady-state approximation for intermediates, but do not assume that the first reaction is at equilibrium. In the second approach, you may assume that the first reaction is at equilibrium.

If the orders of the reaction predicted by this mechanism are within the anticipated uncertainties in the experimental values, what is the relation between the observed  $k$  and the rate constants associated with the mechanistic equations?

- 4.25** Photochemical reactions of species containing fluorine can lead to the production of atomic fluorine in the upper atmosphere. These fluorine atoms, in turn, can participate in subsequent reactions which bring about the destruction of ozone. Consider the situation in which the rate of production of atomic fluorine by photochemical reactions is given by

$$\left( \frac{d[\text{F}\cdot]}{dt} \right)_{\text{photochemical}} = r_{pc} \quad (1)$$

and the following reactions ensue:



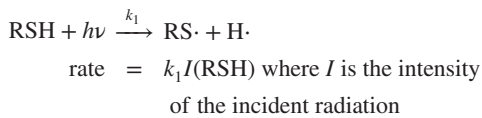
where M is any arbitrary species. Equations (2) to (5) may be regarded as equivalent to a sequence of propagation reactions that constitute the links in a chain reaction mechanism.

- (a) Derive an expression for the rate of disappearance of ozone that contains only the various rate constants, the concentrations of stable species, and  $r_{pc}$ .
- (b) In an effort to elucidate the mechanism by which the FO<sup>·</sup> species react with ozone, Y. Bedzhanyan, E. M. Markin, and Y. M. Gershenson [Kinet. Catal., 33, 601–606 (1992)] used ESR spectroscopy to study the kinetics of elementary reactions of FO<sup>·</sup> radicals. The following data can be employed to determine the net rate of reaction 6 if it is assumed that the rates of propagation reactions 3, 4, and 5 are comparable to one another. Are these data consistent with the bimolecular process proposed for termination of the chain reaction mechanism? If so, what is the value of the rate constant  $k_6$ ?

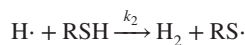
Time (ms)	[FO <sup>·</sup> ] $\times 10^{-14}$ (molecules/cm <sup>3</sup> )
0.00	3.3
2.50	2.9
5.00	2.6
7.50	2.3
10.00	2.0
12.50	1.9
15.00	1.7

- 4.26** The following mechanism has been proposed to explain the kinetics of the radiation curing process for polythio ethers.

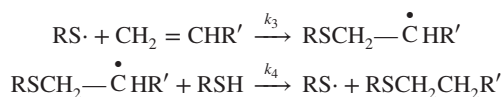
Initiation:



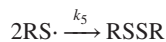
Chain transfer:



Propagation:



Termination:



- (a) In terms of the usual Bodenstein steady-state approximation, derive an expression for the net rate of disappearance of thiol (RSH) in terms of the concentrations of stable species and the various rate constants. Reactions 3 and 4 occur at rates that are much greater than those for the other reactions.

- (b) The following data have been reported for the <sup>60</sup>Co irradiation of an equimolar solution of RSH and CH<sub>2</sub>=CHR' using a constant dose rate.

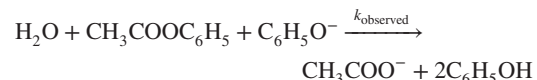
Time, $t$ (s)	Thiol concentration (kmol/m <sup>3</sup> )
0	0.874
300	0.510
600	0.478
900	0.432
1280	0.382
1800	0.343
3710	0.223

Note that the overall stoichiometry of the propagation steps is

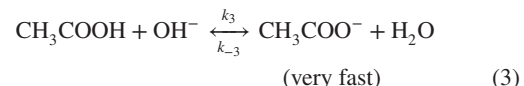
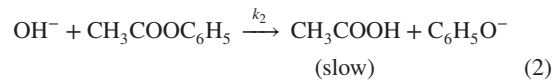
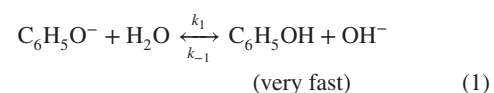


Are these data consistent with the mechanism proposed in part (a)? Note that free-radical reactions are often catalyzed by an induction period at the start of the reaction.

- 4.27** The saponification of the ester phenyl acetate by sodium phenolate in aqueous solution has the following stoichiometry:



The following mechanism has been proposed:



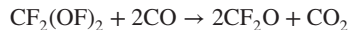
The stoichiometry indicated above can be obtained by summing two times reactions (1), (2), and (3).

- (a) If reaction (2) is the rate-limiting step, what form do you expect the rate equation for the overall reaction to take? Express your answer solely in terms of species appearing in the overall stoichiometric equation.
- (b) Are the following experimental data consistent with this mechanism? If so, what is the experimentally observed rate constant? Note that the initial concentrations of the ester and the phenolate ion are equal to one another.

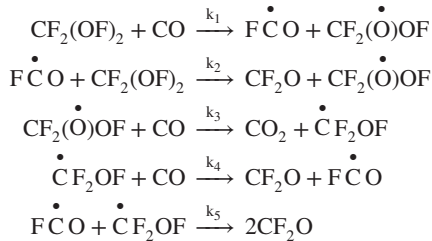
Time (min)	Concentration of ester and phenolate (M)	Concentration of phenol (M)
0	0.02629	0.00742
12	0.02200	
36	0.01830	
72	0.01529	
144	0.01215	
239	0.00999	
344	0.00850	
454	0.00730	

Be very careful to note the appropriate stoichiometric equation for use in your analysis.

- 4.28** A. E. Croce and E. Castellano [*Int. J. Chem. Kinet.*, **14**, 647 (1982)] studied the kinetics of the gas-phase thermal reaction between bis(fluoroxy)difluoromethane  $\text{CF}_2(\text{OF})_2$  and carbon monoxide over the temperature range 110 to 140°C:



They reported that this reaction obeys a mixed second-order rate expression ( $r = k[\text{CO}][\text{CF}_2(\text{OF})_2]$ ). Is the following mechanism consistent with this rate law?



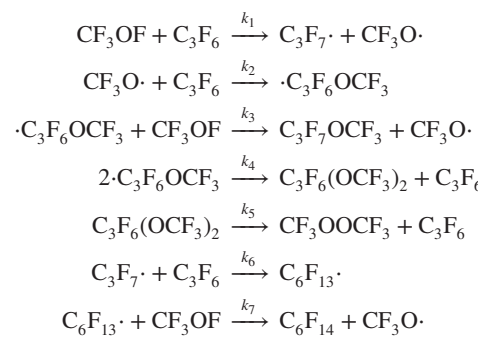
State *explicitly* any assumptions that you make in arriving at your final result. Do not make any more assumptions than are necessary to perform the test for consistency.

- 4.29** M. dos Santos Afonso and H. J. Schumacher [*Int. J. Chem. Kinet.*, **16**, 103–115 (1984)] studied the kinetics and mechanism of the reaction between hexafluoropropene ( $\text{C}_3\text{F}_6$ ) and trifluoromethylhypofluorite ( $\text{CF}_3\text{OF}$ ). The reactions of interest lead to a mixture of the two isomers: 1- $\text{C}_3\text{F}_7\text{OCF}_3$  (68%) and 2- $\text{C}_3\text{F}_7\text{OCF}_3$  (32%). Small traces of  $\text{CF}_3\text{OOCF}_3$  and  $\text{C}_6\text{F}_{14}$  are also present in equimolar proportions in the products. No other product species are present in detectable amounts. The experimental data are consistent with a rate expression of the form

$$\begin{aligned} r &= \frac{-d(\text{C}_3\text{F}_6)}{dt} = \frac{-d(\text{CF}_3\text{OF})}{dt} \\ &= k(\text{C}_3\text{F}_6)(\text{CF}_3\text{OF}) + k^*(\text{C}_3\text{F}_6)^{1/2}(\text{CF}_3\text{OF})^{3/2} \end{aligned}$$

- (a)** One variation of the mechanism proposed by these researchers to explain the observed rate expression consists of the following sequence of elementary

reactions:



Identify the initiation, propagation, and termination steps. Determine the rate expression associated with the set of mechanistic equations above. What is the apparent stoichiometry of this reaction?

- (b)** The following data are typical of this reaction as it occurs at 20°C in a constant volume reactor with initial partial pressures of  $\text{C}_3\text{F}_6$  and  $\text{CF}_3\text{OF}$  of 36.3 and 162.0 torr, respectively.

Time (min)	Total pressure (torr)	$\text{C}_3\text{F}_6$ pressure (torr)	$\text{CF}_3\text{OF}$ pressure (torr)
0.00	198.3	36.3	162.0
2.25	194.8	32.8	158.5
4.58	191.5	29.5	155.2
6.66	188.8	26.8	152.5
10.66	184.1	22.1	147.8
16.75	178.5	16.5	142.2
24.16	172.8	10.8	136.5
34.40	167.5	5.5	131.2
48.06	163.3	1.3	127.0
$\infty$	162.0	0.0	125.7

Use a differential method of data analysis to assess the validity of the proposed rate expression. When appropriate coordinates and scales (linear, log-log, semilog, etc.) are chosen, this method should lead to a linear plot from which  $k$  and  $k^*$  can be determined. What are the values of  $k$  and  $k^*$  at this temperature?

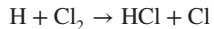
- 4.30** W. H. Rodebush and W. C. Klingshofer [*J. Am. Chem. Soc.*, **55**, 130 (1933)] studied the reaction of atomic chlorine with molecular hydrogen. Chlorine atoms were formed by partial dissociation of molecular chlorine in an electrodeless discharge. A stream of this gas was then mixed with a hydrogen stream and passed through a thermostatted reaction vessel. At the far end of the vessel the reaction was effectively quenched by using a piece of silver foil to catalyze the recombination of chlorine atoms. The products of the reaction were determined by freezing out the  $\text{Cl}_2$  and  $\text{HCl}$  in liquid air traps and titrating samples with standard thiosulfate and alkali, respectively. On the basis of the data and assumptions listed below, determine:

- (a)** The average number of collisions that a chlorine atom undergoes with hydrogen molecules in the reaction vessel.

- (b) The average number of HCl molecules formed per entering chlorine atom.
- (c) The probability that a collision between a chlorine atom and a hydrogen molecule leads to reaction. It may be assumed that each reaction of the type



is followed immediately by a much faster reaction:



The data are as follows, where  $\sigma$  represents the hard-sphere diameter.

$\sigma_{\text{H}_2} = 2.39 \text{ \AA}$	$\sigma_{\text{Cl}} = 2.97 \text{ \AA}$
Hydrogen flow rate	$6.3 \text{ cm}^3(\text{STP})/\text{min}$
Chlorine flow rate (as $\text{Cl}_2$ )	$9.1 \text{ cm}^3(\text{STP})/\text{min}$
Fraction $\text{Cl}_2$ dissociated	11%
Volume of reaction vessel	$10 \text{ cm}^3$
Pressure in vessel	0.340 torr
Temperature in vessel	$0^\circ\text{C}$
Length of run	10 min
Thiosulfate titer of products	$36.5 \text{ cm}^3$ of 0.2 N solution
Alkali titer of products	$9.1 \text{ cm}^3$ of 0.1 N solution

# Chapter 5

---

## Chemical Systems Involving Multiple Reactions

### 5.0 INTRODUCTION

The chemical compositions of many reacting systems can be expressed in terms of a single reaction progress variable. However, a chemical engineer must often consider systems that cannot be adequately described in terms of a single extent of reaction. In this chapter we are concerned with the development of the mathematical relationships that govern the behavior of such systems. We treat reversible reactions, competitive (parallel) reactions, and consecutive reactions, first in terms of the mathematical relations that govern the behavior of such systems and then in terms of the techniques that may be used to relate the kinetic parameters of the system to the phenomena observed in the laboratory.

### 5.1 REVERSIBLE REACTIONS

Reversible reactions are those in which appreciable quantities of *all* reactant and product species coexist at equilibrium. For these reactions the rate that is observed in the laboratory is a reflection of the interaction between the rate at which reactant species are transformed into product molecules and the rate of the reverse transformation. The ultimate composition of the systems in which such reactions occur is dictated not by exhaustion of the limiting reagent but by the constraints imposed by the thermodynamics of the reaction.

#### 5.1.1 Mathematical Characterization of Simple Reversible Reaction Systems

The time dependence of the composition of a system in which a reversible reaction is occurring is governed by the mathematical forms of the rate expressions for the forward

and reverse reactions, the net rate of reaction being the difference between these two quantities:

$$r = \frac{1}{V} \frac{d\xi}{dt} = \vec{r} - \vec{r} \quad (5.1.1)$$

In this section we discuss the mathematical forms of the integrated rate expression for a few simple combinations of the component rate expressions. The discussion is limited to reactions that occur isothermally in constant density systems, because this simplifies the mathematics and permits one to focus on the basic principles involved. Again we place a "V" to the right of certain equation numbers to emphasize that such equations are not general but are restricted to constant volume batch reactors. The use of the extent per unit volume in a constant volume system ( $\xi^*$ ) will also serve to emphasize this restriction. For constant volume systems in which a reversible reaction is occurring,

$$r = \frac{d\xi^*}{dt} = \vec{r} - \vec{r} \quad (5.1.2)V$$

Several forms of the reaction rate expression are considered next.

##### 5.1.1.1 *Opposing First-Order Reactions:* $A \leftrightarrow B$

The simplest case of reversible reactions is that in which the forward and reverse reactions are each first-order. This case may be represented by a rate expression of the form

$$r = k_1 C_A - k_{-1} C_B \quad (5.1.3)$$

Equation (5.1.3) can be rewritten in terms of the extent of reaction per unit volume as

$$\begin{aligned} \frac{d\xi^*}{dt} &= k_1(C_{A0} - \xi^*) - k_{-1}(C_{B0} + \xi^*) \\ &= k_1 C_{A0} - k_{-1} C_{B0} - \xi^*(k_1 + k_{-1}) \end{aligned} \quad (5.1.4)V$$

Separation of variables and integration subject to the initial condition that  $\xi^* = 0$  at  $t = 0$  gives

$$t = - \left( \frac{1}{k_1 + k_{-1}} \right) \times \left\{ \ln \left[ \frac{k_1 C_{A0} - k_{-1} C_{B0} - (k_1 + k_{-1}) \xi^*}{k_1 C_{A0} - k_{-1} C_{B0}} \right] \right\} \quad (5.1.5)V$$

Expressions for the time dependence of reactant and product concentrations may be obtained by solving equation (5.1.5) for  $\xi^*$ :

$$\xi^* = \frac{k_1 C_{A0} - k_{-1} C_{B0}}{k_1 + k_{-1}} (1 - e^{-(k_1 + k_{-1})t}) \quad (5.1.6)V$$

and then using the relations between species concentrations and  $\xi^*$ :

$$C_i = C_{i0} + \nu_i \xi^* \quad (5.1.7)V$$

Equations (5.1.5) and (5.1.7) may be combined to obtain

$$\begin{aligned} -(k_1 + k_{-1})t &= \ln \left[ \frac{k_1 C_A - k_{-1} C_B}{k_1 C_{A0} - k_{-1} C_{B0}} \right] \\ &= \ln \left[ \frac{(k_1/k_{-1}) C_A - C_B}{(k_1/k_{-1}) C_{A0} - C_{B0}} \right] \quad (5.1.8)V \end{aligned}$$

Equations (5.1.5), (5.1.6), and (5.1.8) are alternative methods of characterizing the composition of the system as a function of time. However, for use in the analysis of kinetic data, they require *a priori* knowledge of the ratio of  $k_1$  to  $k_{-1}$ . To determine the individual rate constants, one must either carry out initial rate studies on both the forward and reverse reactions or know the equilibrium constant for the reaction. In the latter connection it is useful to indicate some alternative forms in which the integrated rate expressions may be rewritten using the equilibrium constant, the equilibrium extent of reaction, or equilibrium species concentrations.

From the requirement that the reaction rate must become zero at equilibrium, equation (5.1.4) indicates that the equilibrium extent of reaction per unit volume ( $\xi_e^*$ ) is given by

$$\xi_e^* = \frac{k_1 C_{A0} - k_{-1} C_{B0}}{k_{-1} + k_1} \quad (5.1.9)V$$

One may combine equations (5.1.6) and (5.1.9) to obtain

$$\frac{\xi^*}{\xi_e^*} = 1 - e^{-(k_1 + k_{-1})t} \quad (5.1.10)V$$

or

$$\ln [1 - (\xi^* / \xi_e^*)] = -(k_1 + k_{-1})t \quad (5.1.11)V$$

This expression is useful in analyzing kinetic data using the technique developed in Section 3.3.3.2 for certain types of physical property measurements.

At equilibrium, equation (5.1.3) becomes

$$r_e = k_1 C_{Ae} - k_{-1} C_{Be} = 0 \quad (5.1.12)$$

or

$$\frac{k_1}{k_{-1}} = \frac{C_{Be}}{C_{Ae}} = K \quad (5.1.13)$$

Subtraction of equation (5.1.12) from (5.1.3) gives

$$r = k_1 (C_A - C_{Ae}) - k_{-1} (C_B - C_{Be}) \quad (5.1.14)$$

or

$$\begin{aligned} \frac{d\xi^*}{dt} &= k_1 [(C_{A0} - \xi^*) - (C_{A0} - \xi_e^*)] \\ &\quad - k_{-1} [(C_{B0} + \xi^*) - (C_{B0} + \xi_e^*)] \quad (5.1.15)V \end{aligned}$$

Simplification gives

$$\frac{d\xi^*}{dt} = (k_1 + k_{-1}) (\xi_e^* - \xi^*) \quad (5.1.16)V$$

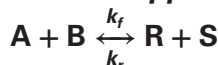
Integration leads to equation (5.1.10). The form of this equation indicates that the reaction may be considered as first-order in the departure from equilibrium, where the effective rate constant is the sum of the rate constants for the forward and reverse reactions.

Equations (5.1.13) and (5.1.8) may be combined to give other forms that are sometimes useful in the analysis of kinetic data:

$$\begin{aligned} -(k_1 + k_{-1})t &= \ln \left[ \frac{KC_A - C_B}{KC_{A0} - C_{B0}} \right] \\ &= \ln \left[ \frac{(C_{Be} C_A / C_{Ae}) - C_B}{(C_{Be} C_{A0} / C_{Ae}) - C_{B0}} \right] \quad (5.1.17)V \end{aligned}$$

In the analysis of kinetic data from reactions believed to be first-order in both directions, the equation that is most suitable for use depends on the pertinent equilibrium data available. Equations (5.1.17) and (5.1.11) are perhaps the most useful, but others may be more appropriate for use in some cases. The integrated forms permit one to determine the sum  $k_1 + k_{-1}$ , while equilibrium data permit one to determine the equilibrium constant  $K = k_1/k_{-1}$ . Such information is sufficient to determine individual values of  $k_1$  and  $k_{-1}$ .

### 5.1.1.2 Opposing Second-Order Reactions:



From a mathematical standpoint the various second-order reversible reactions are quite similar, so we will consider only the most general case—a mixed second-order reaction in which the initial system contains both reactant and product species:

$$r = k_f C_A C_B - k_r C_R C_S \quad (5.1.18)$$

In a constant volume system the rate may be written in terms of the extent per unit volume as

$$\frac{d\xi^*}{dt} = k_f(A_0 - \xi^*)(B_0 - \xi^*) - k_r(R_0 + \xi^*)(S_0 + \xi^*) \quad (5.1.19)V$$

or

$$\frac{d\xi^*}{dt} = (k_f A_0 B_0 - k_r R_0 S_0) - [k_f(A_0 + B_0) + k_r(R_0 + S_0)]\xi^* + (k_f - k_r)\xi^{*2} \quad (5.1.20)V$$

where  $A_0$ ,  $B_0$ ,  $R_0$ , and  $S_0$  refer to the initial concentrations of the various species. As in the preceding section, one may separate variables and integrate to obtain an expression for  $\xi^*$  as a function of time. However, the resulting expression is of extremely limited utility for purposes of analyzing kinetic data.

At equilibrium, equation (5.1.19) becomes

$$r_e = 0 = k_f(A_0 - \xi_e^*)(B_0 - \xi_e^*) - k_r(R_0 + \xi_e^*)(S_0 + \xi_e^*) \quad (5.1.21)V$$

This equation may be rewritten in terms of the equilibrium constant by recognizing that

$$K = \frac{k_f}{k_r} \quad (5.1.22)V$$

$$0 = K(A_0 - \xi_e^*)(B_0 - \xi_e^*) - (R_0 + \xi_e^*)(S_0 + \xi_e^*) \quad (5.1.23)V$$

$\xi_e^*$  is then the root of this quadratic expression that corresponds to physical reality (i.e., it does not give rise to a reactant or product concentration that is negative). The equilibrium concentrations of all species may be evaluated using stoichiometric relations of the form

$$C_{ie} = C_{i0} + \nu_i \xi_e^* \quad (5.1.24)V$$

At any time the concentrations of the various species are given by relations of the form

$$C_i = C_{i0} + \nu_i \xi^* \quad (5.1.25)V$$

Combining equations (5.1.24) and (5.1.25) gives

$$C_i = C_{ie} + \nu_i (\xi^* - \xi_e^*) \quad (5.1.26)V$$

Substitution of expressions of this form into equation (5.1.18) gives

$$\begin{aligned} \frac{d\xi^*}{dt} &= k_f[A_e - (\xi^* - \xi_e^*)][B_e - (\xi^* - \xi_e^*)] \\ &\quad - k_r[R_e + (\xi^* - \xi_e^*)][S_e + (\xi^* - \xi_e^*)] \end{aligned} \quad (5.1.27)V$$

which may be rewritten as

$$\begin{aligned} \frac{d\xi^*}{dt} &= k_f A_e B_e - k_r R_e S_e + (k_f - k_r)(\xi^* - \xi_e^*)^2 \\ &\quad - (\xi^* - \xi_e^*) [k_f (A_e + B_e) + k_r (R_e + S_e)] \end{aligned} \quad (5.1.28)V$$

The length and structure of (5.1.28), the two column format for this book, and the fact that the first two terms on the right represent the net reaction rate at equilibrium (zero) make it convenient to define both a new composite parameter ( $\Omega$ ) as the term in square brackets in (5.1.28) and a new reaction progress variable  $\Psi$  as  $(\xi^* - \xi_e^*)$ , thereby enabling us to write (5.1.28) as

$$\frac{d\Psi}{dt} = 0 + (k_f - k_r)(\Psi)^2 - (\Psi)[\Omega] \quad (5.1.29)V$$

Separation of variables and integration lead to

$$\frac{d\Psi}{\Psi[(k_f - k_r)\Psi - \Omega]} = dt \quad (5.1.30)V$$

The corresponding integral is normally readily available in tables of integrals, appearing as the form

$$\frac{dx}{x(ax + b)} = dt \quad \text{where } a = k_f - k_r \text{ and } b = -\Omega$$

The particular form of the integral is

$$t = \frac{1}{-\Omega} \ln \left[ \frac{\Psi}{(k_f - k_r)\Psi - \Omega} \right] = \frac{1}{\Omega} \ln \left( \frac{(k_f - k_r)\Psi - \Omega}{\Psi} \right) \quad (5.1.31)V$$

$$t = \frac{1}{\Omega} \ln[(k_f - k_r) - (\Omega/\Psi)] \quad (5.1.32)V$$

This form can also be expressed as

$$\begin{aligned} t &= \frac{1}{k_f(A_e + B_e) + k_r(R_e + S_e)} \times \\ &\quad \ln \left[ \frac{\xi^* - \xi_e^*}{(k_f - k_r)(\xi^* - \xi_e^*) - k_f(A_e + B_e) + k_r(R_e + S_e)} \right] \end{aligned} \quad (5.1.33)V$$

From thermochemical data it is possible to evaluate the equilibrium constant and all of the equilibrium concentrations in equation (5.1.33), reducing it to the form

$$\ln \left[ \frac{M_1 (\xi^* - \xi_e^*) + M_2}{\xi^* - \xi_e^*} \right] = [k_f(A_e + B_e) + k_r(R_e + S_e)]t \quad (5.1.34)V$$

where  $M_1$  and  $M_2$  are constants that can be calculated using the equilibrium concentrations.

As before, this equation is not very convenient for use in the interpretation of experimental data unless one knows the forward and reverse rate constants, or at least their ratio. The quantity  $(\xi^* - \xi_e^*)$  is simply related to reactant concentrations by equation (5.1.26), so if the concentration of one reactant is known at various times, it is possible to evaluate the left side at these times. Alternatively, if the data take the form of physical property measurements of the type treated

in Section 3.3.3.2, equation (3.3.50) may be used to relate  $\xi^* - \xi_e^*$  to the property values:

$$\xi^* - \xi_e^* = \xi_e^* \left( \frac{\xi^*}{\xi_e^*} - 1 \right) = \xi_e^* \left( \frac{\lambda - \lambda_0}{\lambda_\infty - \lambda_0} - 1 \right) = \xi_e^* \left( \frac{\lambda - \lambda_\infty}{\lambda_\infty - \lambda_0} \right) \quad (5.1.35)V$$

In either event one should be able to plot the left side of equation (5.1.34) versus time and obtain a straight line with a slope related to the rate constants for the forward and reverse reactions. Equation (5.1.22) gives another relation between these parameters, which permits us to determine each rate constant individually.

### 5.1.1.3 Second-Order Reaction Opposed by First-Order Reaction: $A + B \xrightleftharpoons[k_r]{k_f} R$

For a rate expression of the form

$$r = k_f C_A C_B - k_r C_R \quad (5.1.36)$$

the procedures employed in Sections 5.1.1.1 and 5.1.1.2 lead to the following relation for the time dependence of  $\xi_e^*$ :

$$\begin{aligned} & [k_f(A_e + B_e) + k_r]t \\ &= \ln \left[ \frac{\{K(\xi^* - \xi_e^*) - [K(A_e + B_e) + 1]\}\xi_e^*}{[K\xi_e^* + K(A_e + B_e) + 1](\xi^* - \xi_e^*)} \right] \end{aligned} \quad (5.1.37)V$$

where

$$\xi_e^* = \frac{K(A_0 + B_0) + 1 + \sqrt{\Psi}}{2K} \quad (5.1.38)V$$

and where

$$\Psi = K^2(A_0 - B_0)^2 + 2K(A_0 + B_0 + 2R_0) + 1 \quad (5.1.38a)V$$

From thermodynamic data it is possible to evaluate all quantities pertaining to equilibrium in equation (5.1.37), reducing it to the form

$$[k_f(A_e + B_e) + k_r]t = \ln \left[ \frac{M_1(\xi^* - \xi_e^*) + M_2}{\xi^* - \xi_e^*} \right] \quad (5.1.39)V$$

where  $M_1$  and  $M_2$  are numerical constants. This equation is of the same form as (5.1.34) and may be handled in the manner outlined previously.

## 5.1.2 Determination of Reaction Rate Expressions for Reversible Reactions

The problem of determining the mathematical form of the rate expression for a chemical reaction is one that involves a combination of careful experimental work and sound judgment in the analysis of the data obtained thereby. In many cases the analytical techniques discussed in Section 3.3 are directly applicable to studies of reversible

reactions. In other cases only minor modifications are necessary.

### 5.1.2.1 General Techniques for the Interpretation of Reaction Rate Data for Reversible Reactions

Determination of the mathematical form of a reaction rate expression is generally a two-step procedure. One first determines the dependence of the rate on the concentrations of the various reactant and product species at a fixed temperature and then evaluates the temperature dependence of the various rate constants appearing in the rate expression. For reversible reactions, at least two rate constants will be involved and the Arrhenius relation must be used to analyze data on the temperature dependence of each rate constant individually to determine the influence of temperature changes on the overall reaction rate.

Approaches to the determination of the concentration dependent terms in expressions for reversible reactions are often based on a simplification of the expression to limiting cases. By starting with a mixture containing reactants alone and terminating the study while the reaction system is still very far from equilibrium, one may use an initial rate study to determine the concentration dependence of the rate law for the forward reaction. In similar fashion one may start with mixtures containing only the reaction products and use the initial rates of the reverse reaction to determine the concentration dependence of this part of the rate expression. Additional simplifications in these initial rate studies may arise from the use of stoichiometric ratios of reactants and/or products. At other times the use of a great excess of one or more of the reactants may lead to simplifications. Approaches involving initial rates in which one focuses on one or the other of the two terms comprising the rate expression are the differential methods that are most appropriate for use with reversible reactions. When both terms are significant, one needs a knowledge of the numerical value of the thermodynamic equilibrium constant at the temperature in question in order to be able to employ the general differential approach outlined in Section 3.3.1.

It is also possible to use integral methods to determine the concentration dependence of the reaction rate expression and the associated kinetic parameters. In using such approaches one again requires knowledge of the equilibrium constant for use with one of the integrated forms developed in Section 5.1.1.

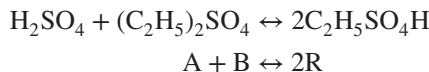
The generalized physical property approach discussed in Section 3.3.3.2 may be used together with one of the differential or integral methods that is appropriate for use with reversible reactions. In this case the extent of reaction per unit volume at time  $t$  is given in terms of equation (3.3.50) as

$$\xi^* = \xi_e^* \left( \frac{\lambda - \lambda_0}{\lambda_\infty - \lambda_0} \right) \quad (5.1.40)V$$

where  $\lambda$ ,  $\lambda_0$ , and  $\lambda_\infty$  are the property measurements at times  $t$ , zero, and infinity, respectively. Illustration 5.1 indicates how one may determine kinetic parameters for a reversible reaction.

### ILLUSTRATION 5.1 Determination of the Rate Law for Reaction of Sulfuric Acid with Diethyl Sulfate

Hellin and Jungers (1) reported the data below for the reaction between stoichiometric quantities of sulfuric acid and diethyl sulfate at 22.9°C:



The initial concentrations of the reactants are each 5.50 kmol/m<sup>3</sup>.

Time (s)	C <sub>2</sub> H <sub>5</sub> SO <sub>4</sub> H (kmol/m <sup>3</sup> )
0	0.00
1,680	0.69
2,880	1.38
4,500	2.24
5,760	2.75
7,620	3.31
9,720	3.81
10,800	4.11
12,720	4.45
16,020	4.86
19,080	5.15
22,740	5.35
24,600	5.42

After 11 days the concentration of C<sub>2</sub>H<sub>5</sub>SO<sub>4</sub>H is equal to approximately 5.80 kmol/m<sup>3</sup>.

Hellin and Jungers determined the following rate expression for this reaction:

$$\begin{aligned} r &= k_f[(\text{C}_2\text{H}_5)_2\text{SO}_4][\text{H}_2\text{SO}_4] - k_r[\text{C}_2\text{H}_5\text{SO}_4\text{H}]^2 \\ &= k_f(\text{A})(\text{B}) - k_r(\text{R})^2 \end{aligned} \quad (\text{A})$$

Is the rate expression proposed consistent with the data above? If so, what are the values of the rate constants at this temperature?

### Solution

Because the rate expression simplifies when stoichiometric quantities of reactants are used, the equations developed earlier in this chapter cannot be applied directly in the solution of this problem. Thus, we will have to derive appropriate relations in the course of our analysis. Each of the

reactant concentrations is given by

$$\text{A} = \text{B} = \text{A}_0 - \xi^*$$

while the concentration of the product is given by

$$\text{R} = 2\xi^*$$

The long-time data may be used to determine the equilibrium concentrations of all species and the equilibrium constant for the reaction:

$$\text{R}_e = 2\xi_e^* = 5.80 \text{ kmol/m}^3$$

Hence,

$$\xi_e^* = 2.90 \text{ kmol/m}^3$$

and

$$\text{A}_e = \text{B}_e = 5.50 - 2.90 = 2.60 \text{ kmol/m}^3$$

The equilibrium constant for this reaction is given by

$$K = \frac{k_f}{k_r} = \frac{\text{R}_e^2}{\text{A}_e \text{B}_e} = \frac{(5.80)^2}{(2.60)^2} = 4.98 \quad (\text{B})$$

Hence,

$$k_f = 4.98k_r \quad (\text{C})$$

Equations of the form of (5.1.26) may now be written for each species:

$$\text{B} = \text{A} = \text{A}_e - (\xi^* - \xi_e^*) \quad \text{R} = \text{R}_e + 2(\xi^* - \xi_e^*) \quad (\text{D})$$

Substitution of these relations into equation (A) gives

$$\frac{d\xi^*}{dt} = k_f[\text{A}_e - (\xi^* - \xi_e^*)]^2 - k_r[\text{R}_e + 2(\xi^* - \xi_e^*)]^2$$

Expansion and use of equation (5.1.30) gives

$$\begin{aligned} \frac{d(\xi^* - \xi_e^*)}{dt} &= k_f\text{A}_e^2 - k_r\text{R}_e^2 - 2k_f\text{A}_e(\xi^* - \xi_e^*) \\ &\quad - 4k_r\text{R}_e(\xi^* - \xi_e^*) + k_f(\xi^* - \xi_e^*)^2 \\ &\quad - 4k_r(\xi^* - \xi_e^*)^2 \end{aligned}$$

The first two terms on the right represent the net rate of reaction at equilibrium, which must be zero. Hence,

$$\begin{aligned} \frac{d(\xi^* - \xi_e^*)}{dt} &= -(2k_f\text{A}_e + 4k_r\text{R}_e)(\xi^* - \xi_e^*) \\ &\quad + (k_f - 4k_r)(\xi^* - \xi_e^*)^2 \end{aligned}$$

Separation of variables and integration give

$$\begin{aligned} t &= \left( \frac{1}{2k_f\text{A}_e + 4k_r\text{R}_e} \right) \times \\ &\quad \left\{ \ln \left[ \frac{(k_f - 4k_r)(\xi^* - \xi_e^*) - (2k_f\text{A}_e + 4k_r\text{R}_e)}{\xi^* - \xi_e^*} \right] \right. \\ &\quad \left. - \ln \left[ \frac{(k_f - 4k_r)(-\xi_e^*) - (2k_f\text{A}_e + 4k_r\text{R}_e)}{-\xi_e^*} \right] \right\} \end{aligned} \quad (\text{E})$$

Combination of equations (B) and (E) and rearrangement gives

$$t = \frac{1}{k_r(2KA_e + 4R_e)} \left\{ \ln \left[ \frac{\xi_e^*}{\xi_e^* - \xi^*} \right] + \ln \left[ \frac{(K-4)(\xi^* - \xi_e^*) - (2KA_e + 4R_e)}{(K-4)(-\xi_e^*) - (2KA_e + 4R_e)} \right] \right\} \quad (F)$$

Now

$$2KA_e + 4R_e = 2(4.98)(2.60) + 4(5.80) \\ = 49.10 \text{ kmol/m}^3$$

Substitution of numerical values into equation (F) gives

$$t = \frac{1}{49.10k_r} \left\{ \ln \left( \frac{2.90}{2.90 - \xi^*} \right) + \ln \left[ \frac{(4.98 - 4)(\xi^* - 2.90) - 49.10}{(4.98 - 4)(-2.90) - 49.10} \right] \right\}$$

or

$$49.1k_r t = \ln \left[ \frac{2.90}{51.94} \left( \frac{51.94 + 0.98\xi^*}{2.90 - \xi^*} \right) \right] \\ = \ln \left[ \frac{1}{18.28} \left( \frac{53.00 + \xi^*}{2.90 - \xi^*} \right) \right]$$

Hence, a plot of  $\ln[(53.00 + \xi^*)/(2.90 - \xi^*)]$  versus time should be linear if the proposed rate expression provides an accurate representation of the experimental results. The data were worked up in this manner and plotted in Figure I5.1. The linearity of the plot indicates that the proposed rate expression is consistent with the data. The slope of the plot is equal to  $1.154 \times 10^{-4} \text{ s}^{-1}$ . Because this value is also equal to  $49.1k_r$  kmol/m<sup>3</sup>,  $k_r = 1.154 \times 10^{-4}/49.1 = 2.35 \times 10^{-6} \text{ m}^3/(\text{kmol}\cdot\text{s})$ . From equation (C),

$$k_f = 4.98(2.35 \times 10^{-6}) = 1.17 \times 10^{-5} \text{ m}^3/(\text{kmol}\cdot\text{s})$$

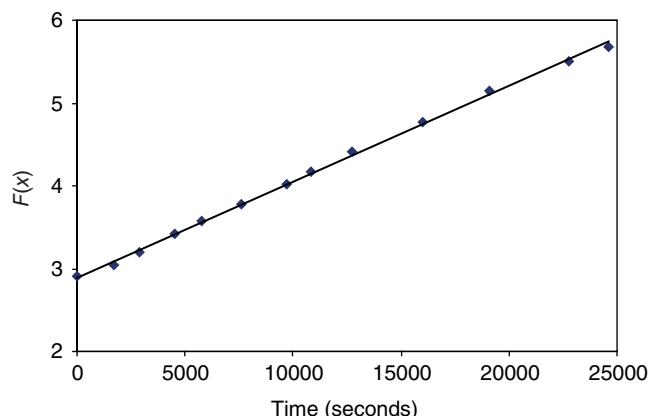


Figure I5.1 Plot of data  $F(x) = \ln[(53.00 + \xi^*)/(2.90 - \xi^*)]$ .

### 5.1.2.2 Use of Relaxation Techniques to Study Rapid Reversible Reactions

If one is interested in the kinetics of reactions that occur at very fast rates, having half-lives on the order of a fraction of a second or less, the methods that we have discussed previously for the determination of reaction rates are no longer applicable. Instead, measurements of the response of an equilibrium system to a perturbation are used to determine its *relaxation time*. The rate at which the system approaches its new equilibrium condition is observed using special electronic techniques. From an analysis of the system behavior and the equilibrium conditions, the form of the reaction rate expression can be determined.

To illustrate how relaxation methods can be used to determine reaction rate constants, let us consider a reaction that is first order in both the forward and reverse directions:



The analysis is very similar to that employed in proceeding from equation (5.1.11) to equation (5.1.16), but the physical situation is somewhat different. The reaction is first allowed to come to equilibrium with  $A_e$  and  $B_e$  representing the equilibrium concentrations of species A and B, and  $\xi_e^*$  the equilibrium extent of reaction per unit volume in a constant volume system. Under these conditions the net rate of reaction is zero:

$$r_e = \left( \frac{d\xi^*}{dt} \right)_e = 0 = k_1 A_e - k_{-1} B_e \quad (5.1.42)V$$

Now suppose that the temperature of the system is suddenly altered slightly so that it is no longer at equilibrium. The net rate of reaction is now given by

$$r = \frac{d\xi^*}{dt} = k_1 A - k_{-1} B \quad (5.1.43)V$$

From equation (5.1.26),

$$A - A_e = -(\xi^* - \xi_e^*) \quad B - B_e = \xi^* - \xi_e^* \quad (5.1.44)V$$

If we denote the deviation from equilibrium conditions by

$$\Delta\xi^* = \xi^* - \xi_e^* \quad (5.1.45)V$$

then

$$A = A_e - \Delta\xi^* \quad B = B_e + \Delta\xi^* \quad (5.1.46)V$$

and

$$\frac{d\xi^*}{dt} = \frac{d\Delta\xi^*}{dt} \quad (5.1.47)V$$

Combination of equations (5.1.43), (5.1.46), and (5.1.47) gives

$$\begin{aligned}\frac{d\Delta\xi^*}{dt} &= k_1(A_e - \Delta\xi^*) - k_{-1}(B_e + \Delta\xi^*) \\ &= k_1A_e - k_{-1}B_e - (k_1 + k_{-1})\Delta\xi^*\end{aligned}\quad (5.1.48)V$$

Combination of equations (5.1.42) and (5.1.48) gives

$$\frac{d\Delta\xi^*}{dt} = -(k_1 + k_{-1})\Delta\xi^* \quad (5.1.49)V$$

Integration subject to the condition that  $\Delta\xi^* = (\Delta\xi^*)_0$  at  $t = 0$  gives

$$\ln\left[\frac{(\Delta\xi^*)_0}{\Delta\xi^*}\right] = (k_1 + k_{-1})t \quad (5.1.50)V$$

The relaxation time ( $t^*$ ) for the chemical reaction is defined as the time corresponding to

$$\ln\left[\frac{(\Delta\xi^*)_0}{\Delta\xi^*}\right] = 1 \quad (5.1.51)V$$

The relaxation time is thus the time at which the distance from equilibrium has been reduced to the fraction  $1/e$  of its initial value. From equation (5.1.50) it is evident that

$$t^* = \frac{1}{k_1 + k_{-1}} \quad (5.1.52)V$$

Consequently, if one can determine the relaxation time of a system experimentally, the sum of the rate constants ( $k_1 + k_{-1}$ ) is known. From the equilibrium constant for the reaction, one can determine the ratio of these rate constants ( $k_1/k_{-1}$ ). Such information is sufficient to determine the individual rate constants  $k_1$  and  $k_{-1}$ .

For certain types of reversible reactions it is necessary to use only slight perturbations from equilibrium so that the differential equations resulting from the analysis are amenable to integration. The theoretical treatment in these cases varies slightly from that presented above and indeed varies slightly with the orders of the forward and reverse reactions. Consider the reaction represented by the following second-order mechanistic equations:



The reaction is assumed to occur in a constant volume system. A relaxation analysis of the type employed for the first-order reaction leads to the following analog of (5.1.49):

$$\begin{aligned}\frac{d\Delta\xi^*}{dt} &= -[k_1(A_e + B_e) + k_{-1}(C_e + D_e)]\Delta\xi^* \\ &\quad + (k_1 - k_{-1})(\Delta\xi^*)^2\end{aligned}\quad (5.1.54)V$$

If the displacement from equilibrium is small, the term involving  $(\Delta\xi^*)^2$  is small compared to the term

involving  $\Delta\xi^*$ . This condition implies that the terms  $A_e + B_e$  and  $C_e + D_e$  are both very much greater in magnitude than  $\Delta\xi^*$ . Under these conditions, equation (5.1.54) becomes

$$\frac{d\Delta\xi^*}{dt} = -[k_1(A_e + B_e) + k_{-1}(C_e + D_e)]\Delta\xi^* \quad (5.1.55)V$$

which, after integration, becomes

$$\ln\left[\frac{(\Delta\xi^*)_0}{\Delta\xi^*}\right] = [k_1(A_e + B_e) + k_{-1}(C_e + D_e)]t \quad (5.1.56)V$$

From the basic definition of the relaxation time, it is evident that

$$t^* = \frac{1}{k_1(A_e + B_e) + k_{-1}(C_e + D_e)} \quad (5.1.57)V$$

As before, the constants  $k_1$  and  $k_{-1}$  can be separated by making use of the fact that  $k_1/k_{-1}$  is the equilibrium constant. Alternatively, the rate constants can be separated by measuring  $t^*$  at various values of  $A_e + B_e$  and  $C_e + D_e$ .

Chemical engineers should be aware of the existence of relaxation techniques for studies of very fast reactions. However, since relaxation time measurements call for sophisticated experimental equipment and techniques, they are seldom made outside basic research laboratories.

### 5.1.3 Thermodynamic Consistency of Rate Expressions

For reversible reactions one normally assumes that the observed rate can be expressed as a difference of two terms, one pertaining to the forward reaction and the other to the reverse reaction. Thermodynamics does not require that the rate expression be restricted to two terms or that one associate individual terms with intrinsic rates for forward and reverse reactions. This section is devoted to a discussion of the limitations that thermodynamics places on reaction rate expressions. The analysis is based on the idea that at equilibrium the net rate of reaction becomes zero, a concept that dates back to the historic studies of Guldberg and Waage (2) on the law of mass action. We consider here only cases for which the net rate expression consists of two terms, one for the forward direction and one for the reverse direction. Cases in which the net rate expression consists of a summation of several terms are usually viewed as corresponding to reactions with two or more parallel paths linking reactants and products. One may associate a pair of terms with each parallel path and use the technique outlined below to determine the thermodynamic restrictions on the form of the concentration dependence within each pair. This type of analysis is based on the principle of detailed balancing discussed in Section 4.1.5.4.

Consider an arbitrary reaction, which we may write in the form



Suppose that under conditions where the concentrations of species R and S are very small, experimental evidence indicates that the expression for the initial reaction rate is of the form

$$r_f = k[A]^\alpha[B]^\beta[R]^\rho[S]^\sigma \quad (5.1.59)$$

where the various orders may be positive, negative, or zero. We would like to know what thermodynamics has to say about permissible forms of the concentration dependence of the reverse reaction. It is logical to expect that the form of the reverse reaction rate will also be a product of powers of concentrations: for example,

$$r_r = k'[A]^\alpha'[B]^\beta'[R]^\rho'[S]^\sigma' \quad (5.1.60)$$

Our problem is that of determining the allowable reaction orders in equation (5.1.60):

The net rate of reaction is given by

$$r = k[A]^\alpha[B]^\beta[R]^\rho[S]^\sigma - k'[A]^\alpha'[B]^\beta'[R]^\rho'[S]^\sigma' \quad (5.1.61)$$

Hence, at equilibrium, one requires that

$$\frac{k}{k'} = [A_e]^{\alpha'-\alpha}[B_e]^{\beta'-\beta}[R_e]^{\rho'-\rho}[S_e]^{\sigma'-\sigma} \quad (5.1.62)$$

where the subscript e's indicate any set of concentrations at which equilibrium exists. The rate constants  $k$  and  $k'$  and thus their ratio are independent of the system composition and depend only on temperature. In an ideal solution, thermodynamics indicates that the equilibrium constant expressed in terms of concentrations ( $K_c$ ) is also a function only of temperature. Consequently, the ratio  $k/k'$  must be a function of  $K_c$ .

$$\frac{k}{k'} = f(K_c) \quad (5.1.63)$$

For equation (5.1.58), the equilibrium constant can be written as

$$K_c = \frac{[R_e]^r[S_e]^s}{[A_e]^a[B_e]^b} \quad (5.1.64)$$

Combining equations (5.1.62) to (5.1.64) gives

$$\begin{aligned} & [A_e]^{\alpha'-\alpha}[B_e]^{\beta'-\beta}[R_e]^{\rho'-\rho}[S_e]^{\sigma'-\sigma} \\ & = f\{[A_e]^{-a}[B_e]^{-b}[R_e]^r[S_e]^s\} \end{aligned} \quad (5.1.65)$$

This equality will be satisfied for all positive values of the concentrations of the various species if the function in question is a power function,

$$\begin{aligned} & [A_e]^{\alpha'-\alpha}[B_e]^{\beta'-\beta}[R_e]^{\rho'-\rho}[S_e]^{\sigma'-\sigma} \\ & = \{[A_e]^{-a}[B_e]^{-b}[R_e]^r[S_e]^s\}^n \end{aligned} \quad (5.1.66)$$

and if  $\alpha' - \alpha$ ,  $\beta' - \beta$ ,  $\rho' - \rho$ , and  $\sigma' - \sigma$  are each the same multiple of the corresponding stoichiometric coefficient (3):

$$\frac{\alpha' - \alpha}{-a} = \frac{\beta' - \beta}{-b} = \frac{\rho' - \rho}{r} = \frac{\sigma' - \sigma}{s} = n \quad (5.1.67)$$

The exponent  $n$  may take on any *positive* value, including fractions. In more general terms for an arbitrary reaction and rate expression, the orders of the forward and reverse reactions must obey the relation

$$n = \frac{\beta'_i - \beta_i}{\nu_i} \quad (5.1.68)$$

where  $\beta_i$  and  $\beta'_i$  are the orders with respect to species  $i$  for the forward reaction and reverse reaction, respectively, and  $\nu_i$  is the generalized stoichiometric coefficient for species  $i$ . Hence, if the concentration dependence is known for one direction, one may choose different values of  $n$  and use equation (5.1.68) to determine the orders of the opposing reaction that are consistent with this value of  $n$ . The resulting rate expressions will then be thermodynamically consistent, and the relation between the rate constants and the equilibrium constant will be given by

$$\frac{k}{k'} = K_c^n \quad (5.1.69)$$

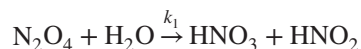
Obviously, if one knows the complete form of the rate expression in one direction and the order of the opposing reaction with respect to one species, this information is sufficient to determine  $n$  uniquely and thus determine the complete form of the rate expression for the opposing reaction. Illustration 5.2 indicates one application of the principle of thermodynamic consistency.

## ILLUSTRATION 5.2 Application of the Principle of Thermodynamic Consistency to an Absorption Process

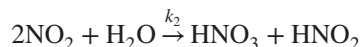
Denbigh and Prince (4) studied the kinetics of the absorption of gaseous  $\text{NO}_2$  in aqueous nitric acid solutions. The following stoichiometric relation governs the process:



They postulated that the rate-limiting molecular processes involved in absorption might be



or



If both of these reactions occur simultaneously in aqueous solution, it would be expected that the absorption rate could be written as

$$r_f = k_1(N_2O_4) + k_2(NO_2)^2 \quad (B)$$

where we have incorporated the water concentration term into the reaction rate constants because a vast excess of water is always present. However, the equilibrium between  $NO_2$  and  $N_2O_4$  is established very rapidly, so the two species concentrations are related by

$$K_1 = \frac{(N_2O_4)}{(NO_2)^2} \quad (C)$$

Hence equation (B) may be written as

$$r_f = k'_f(N_2O_4)$$

where  $k'_f = k_1 + (k_2/K_1)$ . This type of rate expression provides a good correlation of the experimental data for dilute aqueous solutions.

If one assumes that in more concentrated solutions the rate of the forward reaction continues to follow this rate expression, what forms of the reverse rate are thermodynamically consistent in concentrated acid solution? Equilibrium is to be established with respect to equation (A) when written in the  $N_2O_4$  form. It may be assumed that the dependence on the concentrations of  $NO_2$  and  $N_2O_4$  may be lumped together by using equation (C).

## Solution

At equilibrium we require that the net rate of reaction be zero. If we postulate a net rate expression of the general power function form

$$r = k'_f[N_2O_4] - k'_r[N_2O_4]^\alpha[NO]^\beta[HNO_3]^\gamma$$

At equilibrium,

$$\frac{k'_f}{k'_r} = \frac{[N_2O_4]^\alpha[NO]^\beta[HNO_3]^\gamma}{[N_2O_4]} = K^n = \left( \frac{[NO]^1[HNO_3]^2}{[N_2O_4]^{3/2}} \right)^n$$

Thus, thermodynamics requires that

$$\frac{\alpha - 1}{-(3/2)} = \frac{\beta}{1} = \frac{\gamma}{2} = n$$

Thermodynamically consistent forms may be obtained by choosing different positive values of  $n$ .

The following table indicates the reaction orders corresponding to selected arbitrary values of  $n$ .

$n$	$\alpha$	$\beta$	$\gamma$
1	$-(1/2)$	1	2
$(2/3)$	0	$(2/3)$	$(4/3)$
$(1/2)$	$(1/4)$	$(1/2)$	1
0	1	0	0

On the basis of their experimental studies and a search of the literature, Denbigh and Prince indicated that the correct choice of  $n$  is  $(1/2)$ . They found that the data could best be fit using an expression of the form

$$r = k^1[N_2O_4] - C[N_2O_4]^{1/4}[NO]^{1/2}$$

where the constant,  $C$ , depends on the acid concentration ( $HNO_3$ ). (In very concentrated solutions one must worry about the extent of dissociation of  $HNO_3$ , so some difficulties arise in the  $HNO_3$  term.)

In addition to the constraints it imposes on the concentration dependent portions of the rate expression, thermodynamics requires that the activation energies of the forward and reverse reactions be related to the standard enthalpy change accompanying the reaction. In generalized logarithmic form, equation (5.1.69) can be written as

$$\ln k - \ln k' = n \ln K_c \quad (5.1.70)$$

Differentiation with respect to reciprocal absolute temperature and use of the Arrhenius and van't Hoff relations gives

$$E_A - E'_A = n \Delta H^0 \quad (5.1.71)$$

where  $E_A$  and  $E'_A$  are the activation energies for the forward and reverse reactions, respectively, and  $\Delta H^0$  is the standard enthalpy change for the reaction.

## 5.2 PARALLEL OR COMPETITIVE REACTIONS

The term *parallel reactions* describes situations in which reactants can undergo two or more reactions independently and concurrently. These reactions may be reversible or irreversible. They include cases in which one or more species may react through alternative paths to give two or more different product species (simple parallel reactions),



as well as cases where one reactant may not be common to both reactions:



We next consider the kinetic implications of both general classes of parallel reactions.

### 5.2.1 Mathematical Characterization of Parallel Reactions

When dealing with parallel reactions, it is necessary to describe the time dependent behavior of the system in terms of a number of reaction progress variables equal to the number of independent reactions involved. When one tries to integrate the rate expressions to determine the time dependence of the system composition, one finds that in many cases the algebra becomes unmanageable and that closed form solutions cannot be obtained. On the other hand, it is often possible to obtain simple relations between the concentrations of the various species, thereby permitting one to determine the fractions of the original reactants transformed by each of the reactions. The technique of eliminating time as a dependent variable is an invaluable asset in the determination of these relations. It enables one to determine relative values of reaction rate constants while circumventing the necessity to obtain a complete solution to the differential equations that describe the reaction kinetics. We use this technique repeatedly in the sections that follow. We start by describing the mathematical behavior of simple parallel (competitive) reactions and then proceed to a discussion of more complex competitive reactions. Throughout the discussion we restrict our analysis to constant volume systems to simplify the mathematics and focus our attention on the fundamental principles involved.

#### 5.2.1.1 Simple Parallel Reactions

The simplest types of parallel reactions involve the irreversible transformation of a single reactant into two or more product species through reaction paths that have the same dependence on reactant concentrations. The introduction of more than a single reactant species, of reversibility, and of parallel paths that differ in their reaction orders can complicate the analysis considerably. However, under certain conditions, it is still possible to derive useful mathematical relations to characterize the behavior of these systems. A variety of interesting cases are described below.

**5.2.1.1.1 Irreversible First-Order Parallel Reactions** Consider the irreversible decomposition of a reactant A into two sets of products by first-order reactions:



For the first reaction

$$\frac{d\xi_1^*}{dt} = k_1(A_0 - \xi_1^* - \xi_2^*) \quad (5.2.5)V$$

and for the second,

$$\frac{d\xi_2^*}{dt} = k_2(A_0 - \xi_1^* - \xi_2^*) \quad (5.2.6)V$$

where  $\xi_1^*$  and  $\xi_2^*$  are the extents per unit volume of reactions 1 and 2, respectively. These two differential equations are coupled and must be solved simultaneously. In the present case, division of equation (5.2.5) by (5.2.6) gives

$$\frac{d\xi_1^*/dt}{d\xi_2^*/dt} = \frac{d\xi_1^*}{d\xi_2^*} = \frac{k_1}{k_2} \quad (5.2.7)V$$

Integration subject to the constraint that at time zero  $\xi_1^* = \xi_2^* = 0$  gives

$$\xi_1^* = \left(\frac{k_1}{k_2}\right) \xi_2^* \quad (5.2.8)V$$

Combination of equations (5.2.6) and (5.2.8) gives

$$\frac{d\xi_2^*}{dt} = k_2 \left[ A_0 - \left( \frac{k_1}{k_2} + 1 \right) \xi_2^* \right] \quad (5.2.9)V$$

Separation of variables and integration lead to

$$\xi_2^* = \frac{k_2}{k_2 + k_1} A_0 [1 - e^{-(k_1+k_2)t}] \quad (5.2.10)V$$

Combination of equations (5.2.8) and (5.2.10) gives

$$\xi_1^* = \frac{k_1 A_0}{k_2 + k_1} [1 - e^{-(k_1+k_2)t}] \quad (5.2.11)V$$

The concentrations of the various components may now be determined using basic stoichiometric principles:

$$R = R_0 + \nu_R \xi_1^* = R_0 + \frac{k_1 A_0}{k_2 + k_1} \left[ 1 - e^{-(k_1+k_2)t} \right] \quad (5.2.12)V$$

$$T = T_0 + \nu_T \xi_2^* = T_0 + \frac{k_2 A_0}{k_2 + k_1} \left[ 1 - e^{-(k_1+k_2)t} \right] \quad (5.2.13)V$$

$$A = A_0 + \nu_{A1} \xi_1^* + \nu_{A2} \xi_2^* = A_0 \left[ e^{-(k_1+k_2)t} \right] \quad (5.2.14)V$$

The increments in product concentrations are in a constant ratio to one another, independent of time and of the initial reactant concentration:

$$\frac{R - R_0}{T - T_0} = \frac{k_1}{k_2} \quad (5.2.15)V$$

This result is generally applicable to all competitive/parallel reactions in which the alternative paths have the same dependence on reactant concentrations. Also

note that even in cases where the reaction is immeasurably fast, it is still possible to determine relative values of the rate constants by measuring the increments in species concentrations and using equation (5.2.15).

### 5.2.1.1.2 Reversible First-Order Parallel Reactions

In this section we extend the analysis developed in the preceding section to the situation in which the reactions are reversible. Consider the case in which the forward and reverse reactions are all first order, as indicated by the following mechanistic equations:



and



The differential equation governing the first reaction may be written as

$$\begin{aligned} \frac{d\xi_1^*}{dt} &= k_1 (A) - k_{-1}(R) \\ &= k_1[(A_0) - \xi_1^* - \xi_2^*] - k_{-1} [(R_0) + \xi_1^*] \end{aligned} \quad (5.2.18) \text{V}$$

or

$$\frac{d\xi_1^*}{dt} = k_1(A_0) - k_{-1}(R_0) - (k_1 + k_{-1})\xi_1^* - k_1\xi_2^* \quad (5.2.19) \text{V}$$

Similarly,

$$\begin{aligned} \frac{d\xi_2^*}{dt} &= k_2(A) - k_{-2}(S) \\ &= k_2[(A_0) - \xi_1^* - \xi_2^*] - k_{-2}[(S_0) + \xi_2^*] \end{aligned} \quad (5.2.20) \text{V}$$

or

$$\frac{d\xi_2^*}{dt} = k_2(A_0) - k_{-2}(S_0) - k_2\xi_1^* - (k_2 + k_{-2})\xi_2^* \quad (5.2.21) \text{V}$$

Elimination of time as an independent variable between equations (5.2.19) and (5.2.21) gives

$$\frac{d\xi_2^*}{d\xi_1^*} = \frac{k_2(A_0) - k_{-2}(S_0) - k_2\xi_1^* - (k_2 + k_{-2})\xi_2^*}{k_1(A_0) - k_{-1}(R_0) - (k_1 + k_{-1})\xi_1^* - k_1\xi_2^*} \quad (5.2.22) \text{V}$$

which is not a useful result, because this equation is not easily solvable. In this case it is more convenient to rewrite equations (5.2.19) and (5.2.21) in terms of equilibrium concentrations and extents per unit volume. From basic stoichiometric principles,

$$A = A_0 - \xi_1^* - \xi_2^* \quad (5.2.23) \text{V}$$

and

$$A_e = A_0 - \xi_{1e}^* - \xi_{2e}^* \quad (5.2.24) \text{V}$$

where the subscript  $e$  denotes an equilibrium value. These two equations may be combined to give

$$A = A_e - (\xi_1^* - \xi_{1e}^*) - (\xi_2^* - \xi_{2e}^*) = A_e - (\Delta\xi_1^*) - (\Delta\xi_2^*) \quad (5.2.25) \text{V}$$

where  $\Delta\xi_1^*$  and  $\Delta\xi_2^*$  refer to the differences between the extent per unit volume at time  $t$  and the extent at equilibrium for reactions 1 and 2, respectively.

Similarly, it may be shown that

$$R = R_e + \Delta\xi_1^* \quad \text{and} \quad S = S_e + \Delta\xi_2^* \quad (5.2.26) \text{V}$$

Substitution of these relations into equation (5.2.18) gives

$$\begin{aligned} \frac{d\xi_1^*}{dt} &= k_1[(A_e) - \Delta\xi_1^* - \Delta\xi_2^*] - k_{-1}[(R_e) + \Delta\xi_1^*] \\ &= k_1(A_e) - k_{-1}(R_e) - (k_1 + k_{-1}) \Delta\xi_1^* - k_1 \Delta\xi_2^* \end{aligned} \quad (5.2.27) \text{V}$$

Now

$$\frac{d\xi_1^*}{dt} = \frac{d\Delta\xi_1^*}{dt} \quad (5.2.28) \text{V}$$

and at equilibrium,

$$k_1 A_e = k_{-1} R_e \quad (5.2.29) \text{V}$$

Thus,

$$\frac{d\Delta\xi_1^*}{dt} = -(k_1 + k_{-1}) \Delta\xi_1^* - k_1 \Delta\xi_2^* \quad (5.2.30) \text{V}$$

Similarly, it can be shown that

$$\frac{d\Delta\xi_2^*}{dt} = -k_2 \Delta\xi_1^* - (k_2 + k_{-2}) \Delta\xi_2^* \quad (5.2.31) \text{V}$$

Equations (5.2.30) and (5.2.31) are a pair of differential equations that may be solved by differentiating the first with respect to time and eliminating  $\Delta\xi_2^*$  and  $(d\Delta\xi_2^*)/dt$  between the new second-order differential equation and the two original equations in order to arrive at a second-order differential equation with constant coefficients:

$$\begin{aligned} \frac{d^2\Delta\xi_1^*}{dt^2} + (k_1 + k_{-1} + k_2 + k_{-2}) \frac{d\Delta\xi_1^*}{dt} \\ + (k_1 k_{-2} + k_{-1} k_2 + k_{-1} k_{-2}) \Delta\xi_1^* = 0 \end{aligned} \quad (5.2.32) \text{V}$$

The solution contains two exponential terms and may be written as

$$\Delta\xi_1^* = C_1 e^{m_1 t} + C_2 e^{m_2 t} \quad (5.2.33) \text{V}$$

where  $C_1$  and  $C_2$  are integration constants and where  $m_1$  and  $m_2$  are the roots of the quadratic equation

$$m^2 + (k_1 + k_{-1} + k_2 + k_{-2})m + (k_1 k_{-2} + k_{-1} k_2 + k_{-1} k_{-2}) = 0 \quad (5.2.34) \text{V}$$

Both roots will be negative and real.

Now, at  $t = 0$ ,

$$\Delta\xi_1^* = R_0 - R_e \quad \text{and} \quad \Delta\xi_2^* = S_0 - S_e \quad (5.2.35)V$$

These relations may be used to evaluate the constants  $C_1$  and  $C_2$  in equation (5.2.33). The result is

$$C_1 = \frac{1}{m_1 - m_2} [-(R_0 - R_e)(m_2 + k_1 + k_{-1}) - k_1(S_0 - S_e)] \quad (5.2.36)V$$

and

$$C_2 = \frac{1}{m_1 - m_2} [(R_0 - R_e)(m_1 + k_1 + k_{-1}) + k_1(S_0 - S_e)] \quad (5.2.37)V$$

Thus,

$$\Delta\xi_1^* = \frac{(R_e - R_0)[(m_2 + k_1 + k_{-1})e^{m_1 t} - (m_1 + k_1 + k_{-1})e^{m_2 t}]}{m_1 - m_2} + \frac{(S_e - S_0)(k_1 e^{m_1 t} - k_1 e^{m_2 t})}{m_1 - m_2} \quad (5.2.38)V$$

and

$$\begin{aligned} R &= R_e + \Delta\xi_1^* \\ &= R_e + \frac{(R_e - R_0)[(m_2 + k_1 + k_{-1})e^{m_1 t} - (m_1 + k_1 + k_{-1})e^{m_2 t}]}{m_1 - m_2} \\ &\quad + \frac{k_1(S_e - S_0)}{m_1 - m_2} (e^{m_1 t} - e^{m_2 t}) \end{aligned} \quad (5.2.39)V$$

To evaluate  $\Delta\xi_2^*$ , and hence  $S(t)$ , one need only substitute the relation for  $\Delta\xi_1^*$  into equation (5.2.31) and solve the resulting differential equation. The result is

$$\begin{aligned} S &= S_e + \frac{(S_e - S_0) [(m_1 + \sum) e^{m_2 t} - (m_2 + \sum) e^{m_1 t}]}{m_2 - m_1} \\ &\quad + \frac{k_2(R_e - R_0)}{m_2 - m_1} (e^{m_2 t} - e^{m_1 t}) \end{aligned} \quad (5.2.40)V$$

where we have defined  $\sum$  as  $k_2 + k_{-2}$ .

The time dependence of the various species concentrations will depend on the relative magnitudes of the four rate constants. In some cases the curves will involve a simple exponential rise to an asymptote, as is the case for irreversible reactions. In other cases the possibility of overshoot exists, as indicated in Figure 5.1. Whether or not this phenomenon will occur depends on the relative magnitudes of the rate constants and the initial conditions. However, the fact that both roots of equation (5.2.34) must be real requires that there be only one maximum in the curves describing  $R(t)$  or  $S(t)$ .

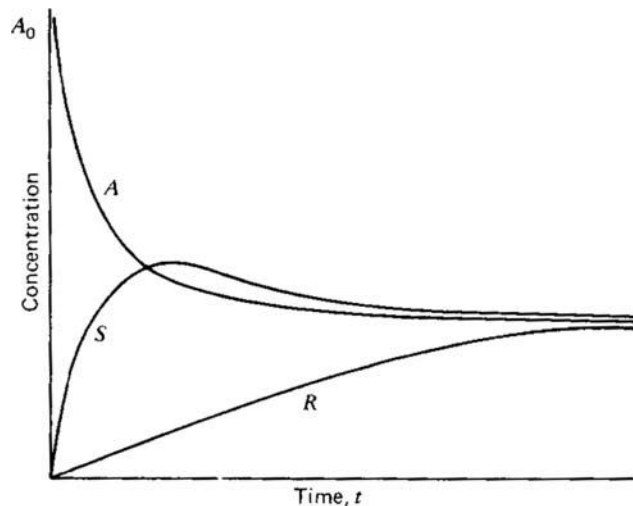
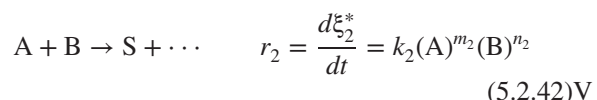
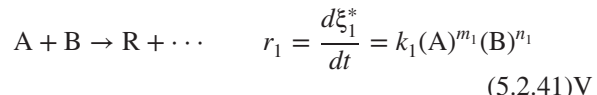


**Figure 5.1** Concentration versus time curves for reversible parallel reactions indicating the possibility of a maximum in the concentration of one product species.

**5.2.1.1.3 Higher Order Irreversible Simple Parallel Reactions** Many simple parallel reactions do not fit the categories discussed in the last two subsections. Of particular interest are the reactions between different chemical species to give two or more different products (e.g., the formation of *ortho*, *meta*, and *para* derivatives of an aromatic compound). This section is devoted to a discussion of the mathematical relations that govern such reactions. Consider the following two stoichiometric equations as representative of this class of reactions:



The form of the solutions that one obtains for reactions of this type is dictated by the relative values of the four reaction orders. For some choices of these orders it is not possible to obtain simple closed form solutions to these rate equations unless one places additional restrictions on the initial composition of the reaction mixture. The three possible cases are discussed below.

**Case I: The Orders with Respect to Each of the Reactants Are Equal ( $m_2 = m_1$  and  $n_2 = n_1$ ).** In this case elimination of time as an independent variable gives

$$\frac{d\xi_1^*}{d\xi_2^*} = \frac{k_1}{k_2} \quad (5.2.43)V$$

which leads to

$$\xi_1^* = \frac{k_1}{k_2} \xi_2^* \quad (5.2.44)V$$

and

$$\frac{R - R_0}{S - S_0} = \frac{k_1}{k_2} \quad (5.2.45)V$$

The fractional yield of product R is given by

$$\frac{R - R_0}{A_0 - A} = \frac{\xi_1^*}{\xi_1^* + \xi_2^*} = \frac{k_1}{k_1 + k_2} \quad (5.2.46)V$$

Similarly,

$$\frac{S - S_0}{A_0 - A} = \frac{k_2}{k_1 + k_2} \quad (5.2.47)V$$

Thus, the fractional yields of the various products are independent of both time and the orders of the reactions. If the increments in the products can be determined (in many cases  $R_0$  and  $S_0$  will be zero), it is possible to evaluate the ratio  $k_1/k_2$ . Moreover, for this case,

$$-\frac{dA}{dt} = (k_1 + k_2)(A)^{m_1}(B)^{n_1} \quad (5.2.48)V$$

and the methods developed in Chapter 3 may be used to evaluate  $m_1$ ,  $n_1$ , and  $(k_1 + k_2)$ . The last result, together with knowledge of the ratio  $k_1/k_2$ , permits one to determine individual values of these parameters.

**Case II: The Orders Are Different with Respect to Each of the Constituents, but the Total Order ( $m + n$ ) of Each Reaction Is the Same.** In this case elimination of time as an independent variable gives

$$\frac{d\xi_1^*}{d\xi_2^*} = \frac{k_1}{k_2} (A)^{m_1 - m_2} (B)^{n_1 - n_2} \quad (5.2.49)V$$

or

$$\frac{d\xi_1^*}{d\xi_2^*} = \frac{k_1}{k_2} (A_0 - \xi_1^* - \xi_2^*)^{m_1 - m_2} (B_0 - \xi_1^* - \xi_2^*)^{n_1 - n_2} \quad (5.2.50)V$$

Only in the case for which  $A_0 = B_0$  is it possible to obtain a closed-form solution to this differential equation. In this particular instance,

$$\frac{d\xi_1^*}{d\xi_2^*} = \frac{k_1}{k_2} \quad (5.2.51)V$$

and the equations involved in the solution become identical with those of case I. In the more general case, the product distribution is influenced strongly by the manner in which the reaction is carried out: in particular, the manner of contacting and the type of reactor used.

**Case III: The Total Order Is Not the Same for Both Reactions.** In this case  $(m_1 + n_1)$  differs from  $m_2 + n_2$  and there are a variety of possible forms that the rate expression may take. We consider only some of the more interesting forms. In this case, elimination of time as an independent variable leads to the same general result as in case II [equation (5.2.50)]. As before, to obtain a closed

form solution to this equation, it is convenient to restrict our consideration to a system in which  $A_0 = B_0$ . In this specific case, equation (5.2.50) becomes

$$\frac{d\xi_1^*}{d\xi_2^*} = \frac{k_1}{k_2} (A_0 - \xi_1^* - \xi_2^*)^{m_1 + n_1 - (m_2 + n_2)} \quad (5.2.52)V$$

The relationship that must exist between  $\xi_1^*$  and  $\xi_2^*$  is obtained most readily by noting that

$$\frac{d(\xi_1^* + \xi_2^*)}{d\xi_2^*} = 1 + \frac{d\xi_1^*}{d\xi_2^*} \quad (5.2.53)V$$

or, using equation (5.2.52),

$$\frac{d(\xi_1^* + \xi_2^*)}{d\xi_2^*} = 1 + \frac{k_1}{k_2} [A_0 - (\xi_1^* + \xi_2^*)]^{m_1 + n_1 - (m_1 + n_2)} \quad (5.2.54)V$$

A closed form solution to this equation exists for all values of  $[(m_1 + n_1) - (m_2 + n_2)]$ . However, the resulting function will depend on this difference. One case that often occurs is that in which the difference is unity. In this case, separation of variables followed by integration leads to

$$\xi_2^* = \frac{k_2}{k_1} \ln \left\{ \frac{1 + (k_1/k_2) A_0}{1 + (k_1/k_2) [A_0 - (\xi_1^* + \xi_2^*)]} \right\} \quad (5.2.55)V$$

To evaluate the relative values of the reaction rate constants, one need only plot  $\xi_1^* + \xi_2^*$  versus  $\xi_2^*$  and take the slope at the origin. From equation (5.2.54) this slope is equal to  $1 + (k_1/k_2)A_0$  when  $(m_1 + n_1) - (m_2 + n_2) = 1$ . From this slope one can thus determine  $k_1/k_2$ . This ratio and the relation between  $\xi_1^*$  and  $\xi_2^*$  given by equation (5.2.55) may be used with either of the original rate expressions (5.2.41) and (5.2.42) to obtain individual values of  $k_1$  and  $k_2$  for specified values of  $m_1 + n_1$  and  $m_2 + n_2$ .

In this subsection we have treated a variety of higher-order simple parallel reactions. Only by the proper choice of initial conditions is it possible to obtain closed form solutions for some of the types of reaction rate expressions that one is likely to encounter in engineering practice. Consequently, in efforts to determine the kinetic parameters characteristic of such systems, one should choose the experimental conditions carefully so as to ensure that potential simplifications will actually occur. These simplifications may arise from the use of stoichiometric ratios of reactants or from the degeneration of reaction rate laws arising from the use of a vast excess of one reactant. Such planning is particularly important in the early stages of research when one has minimal knowledge of the system under study.

### 5.2.1.2 Competitive Parallel Reactions

Some parallel reactions may also involve competitive interactions between different reactant species: for example,



If the kinetic parameters for the upper reaction are denoted by the subscript 1 and those for the lower reaction by the subscript 2, the appropriate rate expressions for constant-volume systems may be written as

$$\frac{d\xi_1^*}{dt} = k_1(A)^{m_1}(B)^{n_1} = k_1(A_0 - \xi_1^* - \xi_2^*)^{m_1}(B_0 - \xi_1^*)^{n_1} \quad (5.2.57)\text{V}$$

and

$$\frac{d\xi_2^*}{dt} = k_2(A)^{m_2}(B')^{n_2} = k_2(A_0 - \xi_1^* - \xi_2^*)^{m_2}(B'_0 - \xi_2^*)^{n_2} \quad (5.2.58)\text{V}$$

The general relation between  $\xi_1^*$  and  $\xi_2^*$  may be determined by eliminating time as an independent variable in the usual fashion:

$$\frac{d\xi_1^*}{d\xi_2^*} = \frac{k_1}{k_2} (A_0 - \xi_1^* - \xi_2^*)^{m_1 - m_2} \frac{(B_0 - \xi_1^*)^{n_1}}{(B'_0 - \xi_2^*)^{n_2}} \quad (5.2.59)\text{V}$$

The complexity of this relation depends on the reaction orders involved. Generally, one finds that it is not easy to arrive at expressions for the time dependence of the various species concentrations. However, it is often possible to obtain relations for the relative extents of reaction that are useful for design purposes. In Chapter 9 we will see the implications of such relations in the selection of reactor type and modes of contacting.

Equation (5.2.59) is greatly simplified when  $m_2 = m_1$  (i.e., when both reactions are the same order with respect to A) because it is then possible to separate variables and integrate each term directly. Reactions of this type are the only ones that we consider in more detail.

In the case for which  $m_2 = m_1$  and for which  $n_1$  and  $n_2$  are both unity, equation (5.2.59) becomes

$$\frac{d\xi_1^*}{d\xi_2^*} = \frac{k_1}{k_2} \left( \frac{B_0 - \xi_1^*}{B'_0 - \xi_2^*} \right) \quad (5.2.60)\text{V}$$

Separation of variables followed by integration gives

$$\ln\left(\frac{B_0 - \xi_1^*}{B_0}\right) = \frac{k_1}{k_2} \ln\left(\frac{B'_0 - \xi_2^*}{B'_0}\right) \quad (5.2.61)\text{V}$$

or

$$\ln\left(\frac{B}{B_0}\right) = \frac{k_1}{k_2} \ln\left(\frac{B'}{B'_0}\right) \quad (5.2.62)\text{V}$$

Thus, from simultaneous measurements of the unreacted fractions of the two competing species, one may readily determine the ratio of the reaction rate constants.

To indicate the types of complications involved in proceeding from this point to equations that indicate the time-dependent behavior of the various species concentrations, it is instructive to consider the following rate expressions:

$$\frac{d\xi_1^*}{dt} = k_1(A)(B) = k_1(A_0 - \xi_1^* - \xi_2^*)(B_0 - \xi_1^*) \quad (5.2.63)\text{V}$$

and

$$\frac{d\xi_2^*}{dt} = k_2(A)(B') = k_2(A_0 - \xi_1^* - \xi_2^*)(B'_0 - \xi_2^*) \quad (5.2.64)\text{V}$$

Now equation (5.2.61) can be rearranged to give the following expression:

$$\xi_2^* = B'_0 \left[ 1 - \left( \frac{B_0 - \xi_1^*}{B_0} \right)^{k_2/k_1} \right] \quad (5.2.65)\text{V}$$

Substitution of this result in equation (5.2.63) gives

$$\frac{d\xi_1^*}{dt} = k_1 \left\{ A_0 - \xi_1^* - B'_0 \left[ 1 - \left( \frac{B_0 - \xi_1^*}{B_0} \right)^{k_2/k_1} \right] \right\} (B_0 - \xi_1^*) \quad (5.2.66)\text{V}$$

In general, this equation must be solved using numerical methods. Once  $\xi_1^*$  has been related to time in such a fashion, equation (5.2.65) maybe used to evaluate  $\xi_2^*$  as a function of time. Basic stoichiometric principles may then be used to determine the corresponding concentrations of the various product and reactant species.

When  $m_1$  equals  $m_2$  and both  $n_1$  and  $n_2$  are 2, equation (5.2.59) can be integrated to obtain

$$\frac{1}{B_0 - \xi_1^*} - \frac{1}{B_0} = \frac{k_1}{k_2} \left( \frac{1}{B'_0 - \xi_2^*} - \frac{1}{B'_0} \right) \quad (5.2.67)\text{V}$$

or

$$\frac{1}{B} - \frac{1}{B_0} = \frac{k_1}{k_2} \left( \frac{1}{B'} - \frac{1}{B'_0} \right) \quad (5.2.68)\text{V}$$

When  $m_1$  equals  $m_2$  and  $n_1$  and  $n_2$  are 1 and 2, respectively, integration of equation (5.2.59) gives

$$\ln\left(\frac{B_0}{B}\right) = \frac{k_1}{k_2} \left( \frac{1}{B'} - \frac{1}{B'_0} \right) \quad (5.2.69)\text{V}$$

Equations (5.2.62), (5.2.68), and (5.2.69) indicate that simultaneous measurements of the concentrations of the competitive species permit one to determine the relative values of the two rate constants using plots appropriate to the rate expressions in question.

### 5.2.2 Techniques for Interpretation of Kinetic Data for Parallel Reactions

In general, an analysis of a system in which noncompetitive parallel reactions are taking place is considerably more difficult than analyses of the type discussed in Chapter 3. In the analysis of competitive parallel reactions, one must deal with the problems of determining reaction orders and rate constants for each of the individual reactions. The chemical engineer must be careful in both planning the experimental work and analyzing the data so as to obtain values of the rate constants that are sufficiently accurate for purposes of reactor design.

The first point to be established in any experimental study is that one is dealing with parallel reactions and not with reactions between the products and the original reactants. One then uses data on the product distribution to determine relative values of the rate constants, employing the relations developed in Section 5.2.1. For simple parallel reactions, one then uses either the differential or integral methods developed in Section 3.3 to analyze the data.

There are few shortcut methods for analyzing simple parallel systems. One useful technique is to use stoichiometric ratios of reactants in the experimental work so that the ratio of the time derivatives of the extents of reaction simplifies where possible. For higher-order irreversible simple parallel reactions represented by equations (5.2.41) and (5.2.42), the degenerate form of the ratio of reaction rates then becomes

$$\frac{d\xi_1^*}{d\xi_2^*} = \frac{k_1}{k_2} [A]^{m_1+n_1-(m_2+n_2)} \quad (5.2.70)V$$

For these conditions the product distribution is time independent when the overall reaction orders are identical. However, when  $(m_1 + n_1) > (m_2 + n_2)$ , the product distribution changes as time proceeds with the ratio of the product formed by reaction 1 to that formed by reaction 2 declining as the reaction proceeds. Conversely, if  $(m_2 + n_2) > (m_1 + n_1)$ , this ratio will increase. Experiments of this type can provide extremely useful clues as to the form of the reaction rate expression and as to the type of experiments that should be performed next. Another technique that is often useful in studies of these systems is the use of a large excess of one reactant so as to cause a degeneration of the concentration dependent term to a simpler form.

In the case of competing parallel reactions, one has the option of studying each reaction independently by varying the composition of the initial reaction mixture. If a chemical species is absent, it obviously cannot react. What is more interesting from the viewpoint of the kineticist is the possibility of using reactions of this type to gain information about complex reaction systems. If one reaction is well

characterized on the basis of previous work and if another reaction is very rapid and not amenable to investigation by conventional techniques, comparative rate studies can be very useful. In such cases it is convenient to "starve" the system with respect to the species for which other reactants compete by providing less than a stoichiometric amount of this species for any of the reactions involved. One lets the competing parallel reactions go to completion and then analyzes the resulting product mixture. Since the equations resulting from the elimination of time as an independent variable are applicable to the final product mixture, compositions of such mixtures can be used to determine relative values of the rate constants of interest.

Relative values of the rate constants are useful in themselves; by measuring such values for the reactions of a series of compounds with the same reactant, one is able to determine the rank order of reactivity within the series. Such determinations are useful in the development of correlations of the effects of substituent groups on the rates of a given class of reactions. By measuring a series of rate constant ratios, one eventually is able to arrive at one reaction that is amenable to investigation by conventional procedures. A study of this reaction provides the key numerical value that permits one to convert the relative rate constants into absolute values for each parameter. Illustrations 5.3 and 5.4 indicate how one utilizes the concepts developed in this section in the determination of kinetic parameters for competitive parallel reactions.

### ILLUSTRATION 5.3 Determination of Relative Rate Constants for Competitive Second-Order Reactions (First-Order in Each Species)

Research (5) indicates that at 25°C reaction of a mixture of benzene (B) and benzyl chloride (C) with nitric acid (A) in acetic anhydride solution yields nitrobenzene (NB) and nitrobenzyl chloride (NC).



Run	Initial HNO <sub>3</sub> (kmol/m <sup>3</sup> )	Final nitrobenzene (kmol/m <sup>3</sup> )	Final nitrobenzyl chloride (kmol/m <sup>3</sup> )
1	0.228	0.172	0.056
2	0.315	0.235	0.080
3	0.343	0.257	0.086
4	0.411	0.307	0.104
5	0.508	0.376	0.132

Data were recorded after very long times so that all the nitric acid present initially was consumed. If the initial concentrations of B and C were each 1 kmole/m<sup>3</sup>, what value of ( $k_2/k_1$ ) fits the data?

### Solution

These reactions are competitive parallel reactions that are each first-order in the competitive species. Equation (5.2.61) is applicable.

$$\ln\left(\frac{B_0 - \xi_1^*}{B_0}\right) = \frac{k_1}{k_2} \ln\left(\frac{C_0 - \xi_2^*}{C_0}\right) \quad (\text{C})$$

As derived originally, equation (5.2.61) is not restricted to use at infinite time (complete reaction), but if one applies it at this time, he or she must be careful that species A is not in stoichiometric excess with respect to either reaction. In such a case, either B or C would be completely consumed at some point, thereby invalidating the analysis.

Rearrangement of equation (C) gives

$$\ln\left(1 - \frac{\xi_1^*}{B_0}\right) = \frac{k_1}{k_2} \ln\left(1 - \frac{\xi_2^*}{C_0}\right) \quad (\text{D})$$

From the reaction stoichiometry  $\xi_1^*$  is numerically equal to the nitrobenzene concentration, and  $\xi_2^*$  is equal to the nitrobenzyl chloride concentration. Since  $B_0$  and  $C_0$  are both unity, equation (D) may be written as

$$\ln(1 - NB) = \frac{k_1}{k_2} \ln(1 - NC) \quad (\text{E})$$

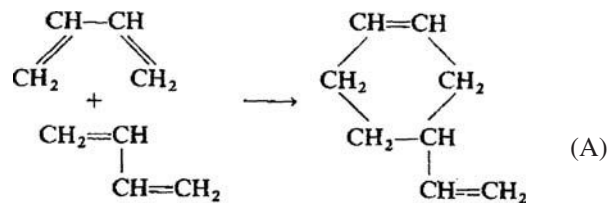
We shall use a numerical averaging procedure based on equation E to evaluate the ratio of rate constants. Thus,

Run	1 - NB	1 - NC	$k_1/k_2$
1	0.828	0.944	3.28
2	0.765	0.920	3.21
3	0.743	0.914	3.30
4	0.693	0.896	3.34
5	0.624	0.868	3.33
Average $3.29 \pm 0.05$			

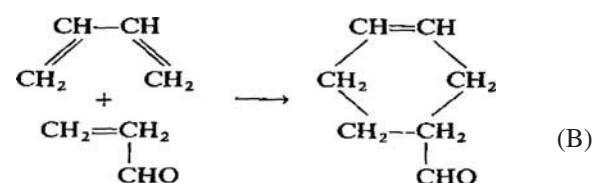
### ILLUSTRATION 5.4 Determination of Rate Constants for Competitive Diels–Alder Reactions

Pannetier and Souchay (6) indicated that when an equimolar gaseous mixture of butadiene and acrolein is allowed to react for 40 min at 330°C and 1 atm, 78.7% of the

initial butadiene and 64.9% of the acrolein have been consumed.



$$2A \rightarrow C \quad r_1 = k_1 C_A^2$$



$$A + B \rightarrow D \quad r_2 = k_2 C_A C_B$$

For the conditions cited, what are the numerical values of the two rate constants?

### Solution

The forms of equations (A) and (B) differ from the competitive parallel reactions considered in Section 5.2.1.2. Thus, it will be necessary to derive appropriate equations for use in the course of our analysis.

From the indicated data and basic stoichiometric principles, one finds that complete reaction leads to:

$$C_A = C_{A0}(1 - 0.787) = C_{A0} - 2\xi_1^* - \xi_2^* \quad (\text{C})$$

and

$$C_B = C_{B0}(1 - 0.649) = C_{B0} - \xi_2^* = C_{A0} - \xi_2^* \quad (\text{D})$$

where we have noted that  $C_{A0} = C_{B0}$ . Hence,

$$\xi_2^* = 0.649C_{A0}$$

and

$$\xi_1^* = \frac{0.787 - 0.649}{2} C_{A0} = 0.069C_{A0}$$

In the present case, elimination of time as an independent variable between equations (A) and (B) gives

$$\frac{d\xi_1^*}{d\xi_2^*} = \frac{k_1 C_A^2}{k_2 C_A C_B} = \frac{k_1 C_A}{k_2 C_B}$$

or, using equations (C) and (D), we have

$$\frac{d\xi_1^*}{d\xi_2^*} = \frac{k_1}{k_2} \left( \frac{C_{A0} - 2\xi_1^* - \xi_2^*}{C_{A0} - \xi_2^*} \right) = \frac{k_1}{k_2} \left( 1 - \frac{2\xi_1^*}{C_{A0} - \xi_2^*} \right)$$

The product distribution thus changes as the reaction proceeds.

Rearrangement and recognition that  $d(C_{A0} - \xi_2^*) = -d\xi_2^*$  gives

$$\frac{d\xi_1^*}{d(C_{A0} - \xi_2^*)} - \frac{2k_1}{k_2} \left( \frac{\xi_1^*}{C_{A0} - \xi_2^*} \right) = -\frac{k_1}{k_2}$$

If we let  $x = C_{A0} - \xi_2^*$  and  $r = k_1/k_2$ ,

$$\frac{d\xi_1^*}{dx} - 2r \frac{\xi_1^*}{x} = -r$$

This first-order linear differential equation may be solved using an integrating factor approach to obtain

$$\xi_1^* = \frac{r}{2r-1} \left[ x - C_{A0} \left( \frac{x}{C_{A0}} \right)^{2r} \right]$$

which can be rewritten as

$$\frac{\xi_1^*}{C_{A0}} = \frac{r}{2r-1} \left[ 1 - \frac{\xi_2^*}{C_{A0}} - \left( 1 - \frac{\xi_2^*}{C_{A0}} \right)^{2r} \right] \quad (\text{E})$$

This transcendental equation must be solved for  $r$  using the numerical values indicated and recognizing that  $0 < r < 1$  for the product distribution cited:

$$0.069 = \frac{r}{2r-1} [1 - 0.649 - (1 - 0.649)^{2r}]$$

The result is  $r = k_1/k_2 = 0.123$ .

To evaluate each of the rate constants individually, it is necessary to obtain another relation between  $k_1$  and  $k_2$ . This evaluation will involve integration of one of the rate expressions. From equations (B) to (D),

$$\frac{d\xi_2^*}{dt} = k_2 (C_{A0} - 2\xi_1^* - \xi_2^*) (C_{A0} - \xi_2^*)$$

Rearrangement and integration give

$$k_2 C_{A0} t = \int_0^{0.649} \frac{d(\xi_2^*/C_{A0})}{[1 - 2(\xi_1^*/C_{A0}) - (\xi_2^*/C_{A0})][1 - (\xi_2^*/C_{A0})]} \quad (\text{F})$$

Equation (E) relates  $\xi_1^*$  and  $\xi_2^*$ , so  $\xi_1^*$  may be evaluated at various values of  $\xi_2^*$  using the value of  $r$  determined above:

$$\begin{aligned} \frac{\xi_1^*}{C_{A0}} &= \left( \frac{0.123}{2(0.123)-1} \right) \left( 1 - \frac{\xi_2^*}{C_{A0}} \right) \left[ 1 - \left( 1 - \frac{\xi_2^*}{C_{A0}} \right)^{2(0.123)-1} \right] \\ &= 0.163 \left( 1 - \frac{\xi_2^*}{C_{A0}} \right) \left[ \left( 1 - \frac{\xi_2^*}{C_{A0}} \right)^{-0.754} - 1 \right] \end{aligned}$$

Using the values of  $\xi_1^*/C_{A0}$  determined from this relation, one can integrate equation (F) numerically. The result is  $k_2 C_{A0} t = 2.37$ .

The initial reactant concentration may be determined from the ideal gas law:

$$C_{A0} = \frac{y_A P}{RT} = \frac{0.5(1)}{0.082(603)} = 1.01 \times 10^{-2} \text{ mol/L}$$

Thus,

$$k_2 = \frac{2.37}{(1.01 \times 10^{-2})40} = 5.86 \text{ L/(mol} \cdot \text{min)}$$

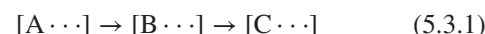
Consequently,

$$k_1 = \left( \frac{k_1}{k_2} \right) k_2 = 0.123(5.86) = 0.72 \text{ L/(mol} \cdot \text{min)}$$

These values of the reaction rate constants differ from those cited by Pannetier and Souchay (6) because these authors treated the two reactions erroneously, as if they were of the simple parallel type instead of as if there were a competition between the acrolein and butadiene molecules for other butadiene molecules.

### 5.3 SERIES OR CONSECUTIVE REACTIONS: IRREVERSIBLE SERIES REACTIONS

The term *series reactions* refers to those reactions in which one or more of the products formed initially undergoes a subsequent reaction to give yet another product. Significant amounts of both the intermediate and final product species will be present during the normal course of the reaction. The general scheme for these reactions may be represented as



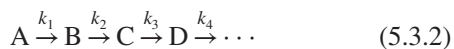
where the quantities in brackets may denote more than one molecular species. Among the many general types of reactions that fall into this category are those leading to mono-, di-, tri-, etc. substituted products, sequential partial oxidation reactions, multiple cracking reactions, and polymerization reactions.

The kinetic implications of series reactions are discussed in this section. We will be concerned only with those cases where the progress of the various stages of the overall transformation is not influenced by either parallel or reverse reactions. The discussion will again be limited to constant-volume systems.

### 5.3.1 Mathematical Characterization of Series Reactions

#### 5.3.1.1 Consecutive First-Order Reactions

The simplest case of series reactions is that in which every reaction in the sequence obeys first-order kinetics. It may be represented in terms of the following sequence of mechanistic equations:



The classic example of “reactions” of this type is a sequence of radioactive decay processes that result in nuclear transformations. The differential equations that govern kinetic systems of this type are most readily solved by working in terms of concentration derivatives. For the first reaction,

$$\frac{dA}{dt} = -k_1 A \quad (5.3.3)V$$

Thus,

$$A = A_0 e^{-k_1 t} \quad (5.3.4)V$$

where  $A_0$  is the initial concentration of reactant A. The concentration of A decreases with time in a fashion that is not influenced by subsequent reactions.

For species B,

$$\frac{dB}{dt} = k_1 A - k_2 B = k_1 A_0 e^{-k_1 t} - k_2 B \quad (5.3.5)V$$

This equation is linear first-order and may be solved in a variety of fashions. One may use an integrating factor approach, Laplace transforms, or rearrange the equation and obtain the sum of the homogeneous and particular solutions. The solution is

$$B = B_0 e^{-k_2 t} + \frac{k_1 A_0}{k_2 - k_1} (e^{-k_1 t} - e^{-k_2 t}) \quad (5.3.6)V$$

The form of the equation for B is dependent on the relative values of the reaction rate constants and the initial concentrations of species A and B. Figure 5.2 indicates the type of behavior to be expected for the case where  $B_0 = 0$ , and Figure 5.3 indicates two modes of behavior for  $B_0 = 0.5A_0$ .

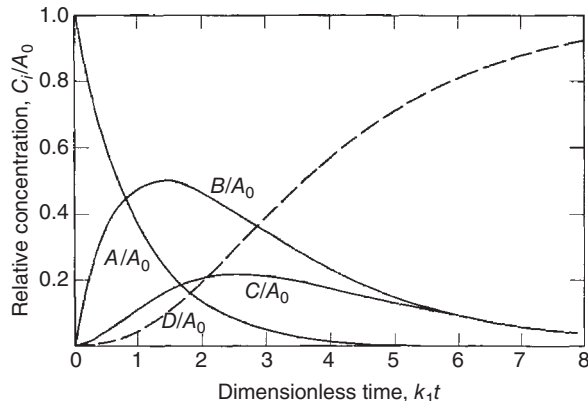


**Figure 5.2** Time dependence of species concentrations for the consecutive reactions  $A \xrightarrow{k_1} B \xrightarrow{k_2} C \xrightarrow{k_3} D$  for  $k_2 = 0.5k_1$  and  $k_3 = 0.9k_1$ .

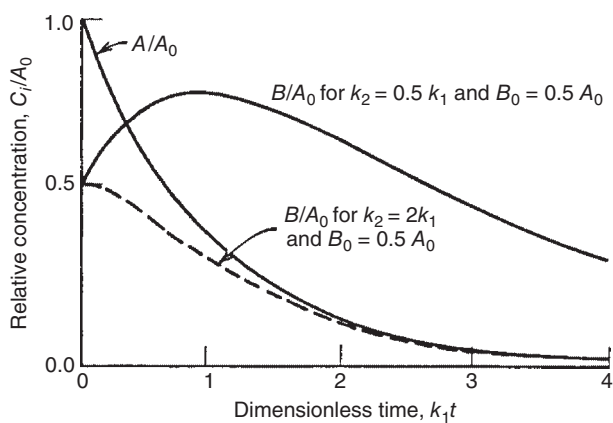


**Figure 5.3** Schematic representation of the time dependence of the concentration of the first intermediate in a series of first-order reactions. The initial intermediate concentration is nonzero.

The time corresponding to a maximum concentration of species B may be found by differentiating the last equation with respect to time and setting the derivative equal to zero. The result is

$$t_{\max} = \frac{1}{k_2 - k_1} \ln \left[ \frac{k_2}{k_1} \left( 1 + \frac{B_0}{A_0} - \frac{k_2 B_0}{k_1 A_0} \right) \right] \quad (5.3.7)V$$

The conditions under which the maximum can exist may be determined by examination of the initial slope. When it is positive, a maximum will occur; if it is negative, there will be no maximum. From equation (5.3.5),

$$\left( \frac{dB}{dt} \right)_0 = k_1 A_0 - k_2 B_0 \quad (5.3.8)V$$

Hence there will be a maximum when  $k_1 A_0 > k_2 B_0$ . When  $k_2 B_0 > k_1 A_0$ , the curve for B starts out with a negative slope and decreases monotonically to zero at infinite time, as shown in Figure 5.3.

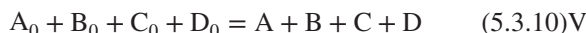
To arrive at an equation for the time dependence of the concentration of species C, one may proceed in a similar fashion. The result is

$$C = \left\{ \begin{array}{l} C_0 e^{-k_3 t} + B_0 \left( \frac{k_2 e^{-k_2 t}}{k_3 - k_2} - \frac{k_2 e^{-k_3 t}}{k_3 - k_2} \right) \\ + A_0 \left[ \frac{k_1 k_2 e^{-k_1 t}}{(k_3 - k_1)(k_2 - k_1)} - \frac{k_1 k_2 e^{-k_2 t}}{(k_3 - k_2)(k_2 - k_1)} \right. \\ \left. + \frac{k_1 k_2 e^{-k_3 t}}{(k_3 - k_2)(k_3 - k_1)} \right] \end{array} \right\} \quad (5.3.9)V$$

Obviously, the curve depicting the time-dependent behavior of the concentration of species C can take on even more forms than that for species B. The shape of the curve is dependent on the initial concentrations of the various species and the three reaction rate constants. Figure 5.2 depicts the time-dependent behavior of species C for the specific case where only species A is present initially.

One may extend this technique to include as many reactions as desired. The irreversibility of the reactions permits one to solve the rate expressions one at a time in recursive fashion. If the first reaction alone is other than first-order, one may still proceed to solve the system of equations in this fashion once the initial equation has been solved to determine  $A(t)$ . However, if any reaction other than the first is not first-order, one must generally resort to numerical methods to obtain a solution.

When one is dealing with a finite series of reactions, it is possible to use stoichiometric principles to determine the concentration of the final species. For example, if only four species (A, B, C, D) are involved in the sequence of equation (5.3.2), then



The concentration of species D at a particular time may then be determined using this relation and the equations for species A, B, and C derived above.

### 5.3.1.2 Consecutive Reactions That Are Other Than First-Order

For consecutive reactions that are not first-order, closed form analytical solutions do not generally exist. This situation is a consequence of the nonlinearity of the set of differential equations involving the time derivatives of the various species concentrations. A few two-member sequences have been analyzed. Unfortunately, the few cases that have been analyzed are seldom encountered in industrial practice. For the most part, one must resort to

approximate methods or to initial conditions that cause a degeneration of the reaction rate expression to a simpler form (e.g., using a stoichiometric ratio of reactants or a large excess of one species). One general technique that is often useful in efforts to analyze the behavior of these systems is the elimination of time as an independent variable.

### 5.3.2 Techniques for the Interpretation of Kinetic Data in the Presence of Series Reactions

The first point that must be established in an experimental study is that one is indeed dealing with a series combination of reactions instead of with some other complex reaction scheme. One technique that is particularly useful in efforts of this type is the introduction of a species that is thought to be a stable intermediate in the reaction sequence. Subsequent changes in the dynamic behavior of the reaction system (or lack thereof) can provide useful information about the character of the reactions involved.

If one monitors the rate of disappearance of the original reactant species, the general differential and integral approaches outlined in Section 3.3 may be used to determine the rate expression for the initial reaction in the sequence. Once this expression is known, one of several other methods for determining either absolute or relative values of the rate constants for subsequent reactions may be used.

If the data are sufficiently accurate, one may use a general differential approach in which the expression for the net rate of formation of a stable intermediate is postulated and tested against experimental data. The difference between the rate of formation by the initial reaction for which the kinetics are known and the actual net rate of formation is tested against the rate expression proposed for the reaction responsible for the destruction of the intermediate. The process involves taking differences in the slopes of two concentration versus time curves (or a simple combination thereof). Since these differences may be very imprecise, this method is often inappropriate for use. In some cases one is able to start with the stable intermediate and determine the rate at which it disappears using conventional methods.

For first-order and pseudo first-order reactions of the series type, several methods exist for determining ratios of rate constants. We next consider a quick estimation technique and then describe a more accurate method for handling systems whose kinetics are represented by equation (5.3.2).

The first approach is based on equation (5.3.7) and makes use of the fact that the time at which the maximum concentration of the intermediate B is reached is a function only of the two rate constants and the initial concentrations.

For the case where no B is present initially, equations (5.3.7) and (5.3.6) can be written as

$$k_1 t_{\max} = \frac{1}{\kappa - 1} \ln \kappa \quad (5.3.11)V$$

and

$$\frac{B_{\max}}{A_0} = \frac{1}{\kappa - 1} (e^{-k_1 t_{\max}} - e^{-k_2 t_{\max}}) \quad (5.3.12)V$$

where

$$\kappa = \frac{k_2}{k_1} \quad (5.3.13)V$$

Combination of these relations and further algebraic manipulation gives

$$\frac{B_{\max}}{A_0} = \kappa^{\kappa/(1-\kappa)} \quad (5.3.14)V$$

This equation indicates that the maximum becomes more pronounced as  $k_2/k_1$  becomes smaller. If  $k_1$  is known and the maximum concentration of the intermediate is measured,  $k_2$  may be determined from this equation. If  $t_{\max}$  is known sufficiently accurately, equation (5.3.14) may be used to determine  $\kappa$  and (5.3.11) to determine  $k_1$ . For meaningful results, this approach requires that one accurately determine the maximum concentration of the intermediate species B and the time at which this maximum is reached.

Swain (7) discussed the general problem of determining rate constants from experimental data of this type and

some of the limitations of numerical curve-fitting procedures. He suggested that a reaction progress variable for two consecutive reactions like (5.3.2) be defined as

$$\delta^* = \frac{B + 2C}{A_0} = \frac{B + 2(A_0 - A - B)}{A_0} \quad (5.3.15)V$$

so that  $50\delta^*$  is a measure of the percentage of the total irreversible reaction that has taken place (i.e.,  $\delta^* = 2$  corresponds to complete conversion to C). Equations (5.3.4), (5.3.6), and (5.3.13) can be manipulated to show that

$$50\delta^* = 50 \left[ 2 + \frac{(2\kappa - 1)e^{-k_1 t}}{1 - \kappa} - \frac{e^{-\kappa k_1 t}}{1 - \kappa} \right] \quad (5.3.16)V$$

If we let  $t_1$  and  $t_2$  represent the times corresponding to reaction progress variables  $\delta_1^*$  and  $\delta_2^*$ , respectively, the time ratio  $t_2/t_1$  for fixed values of  $\delta_1^*$  and  $\delta_2^*$  will depend only on the ratio of rate constants  $\kappa$ . One may readily prepare a table or plot of  $\delta^*$  versus  $k_1 t$  for fixed  $\kappa$  and then cross-plot or cross-tabulate the data to obtain the relation between  $\kappa$  and  $k_1 t$  at a fixed value of  $\delta^*$ . Table 5.1 is of this type. At specified values of  $\delta_1^*$  and  $\delta_2^*$  one may compute the difference  $\log(k_1 t)_2 - \log(k_1 t)_1$ , which is identical to  $\log t_2 - \log t_1$ . One then enters the table using experimental values of  $t_2$  and  $t_1$  and reads off the value of  $\kappa = k_2/k_1$ . One application of this time-ratio method is given in Illustration 5.5.

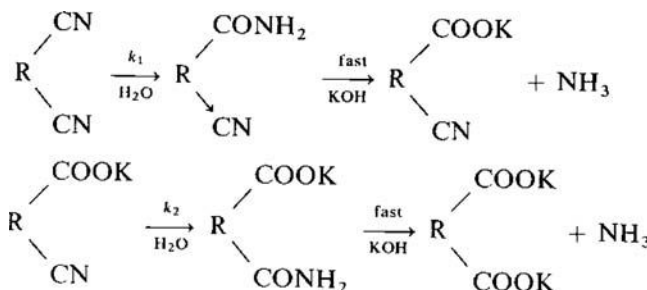
**Table 5.1** Consecutive First-Order Reactions: Time-Percentage Reaction Relations for Various Relative Rate Constants

$\kappa$	$(k_1 t)_{15}$	$(k_1 t)_{35}$	$(k_1 t)_{70}$	$\log(t_{35}/t_{15})$	$\log(t_{70}/t_{15})$	$\log(t_{70}/t_{35})$
100	0.168	0.436	1.21	0.415	0.858	0.443
50	0.172	0.441	1.21	0.407	0.847	0.440
20	0.188	0.457	1.23	0.385	0.815	0.430
10	0.209	0.484	1.26	0.366	0.781	0.415
5	0.236	0.536	1.32	0.356	0.748	0.392
2	0.277	0.664	1.54	0.367	0.745	0.378
1.5	0.289	0.686	1.65	0.376	0.757	0.381
1.1	0.300	0.734	1.80	0.388	0.779	0.391
0.9	0.308	0.766	1.93	0.395	0.796	0.401
0.7	0.315	0.806	2.11	0.409	0.826	0.417
0.5	0.324	0.863	2.41	0.425	0.871	0.446
0.2	0.342	0.999	3.81	0.465	1.047	0.582
0.1	0.349	1.078	6.19	0.490	1.249	0.759
0.05	0.353	1.132	11.10	0.506	1.497	0.991
0.02	0.355	1.173	26.55	0.519	1.874	1.355
0.01	0.356	1.188	52.09	0.524	2.166	1.642

Source: Adapted from J. W. Moore and R. G. Pearson, *Kinetics and Mechanism*, 3rd ed., p. 296, Wiley-Interscience, New York. Copyright © 1981. Used with permission of John Wiley & Sons, Inc.

### ILLUSTRATION 5.5 Determination of Relative Rate Constants Using the Time-Ratio Method

The hydrolysis of 2,7-dicyanonaphthalene has been studied by Kaufler (9):



The kinetics observed are typical of two consecutive first-order reactions. The following data represent the progress of the reaction as reported in Swain's (7) analysis of Kaufler's work.

Percent reaction (508*)	Time, <i>t</i> (h)
15	0.367
35	1.067
70	4.200

Use the time-ratio method to determine  $k_2/k_1$ .

#### Solution

Using the data, one can obtain three time ratios and their logarithms. We evaluate  $\kappa$  using each of these ratios and average the results. From the ratios and Table 5.1:

$$\log\left(\frac{t_{70}}{t_{15}}\right) = 1.0586 \quad \kappa_I = 0.194$$

$$\log\left(\frac{t_{70}}{t_{35}}\right) = 0.5951 \quad \kappa_{II} = 0.193$$

$$\log\left(\frac{t_{35}}{t_{15}}\right) = 0.4635 \quad \kappa_{III} = 0.196$$

The average value of  $k_2/k_1$  is thus 0.194.

## 5.4 COMPLEX REACTIONS

### 5.4.1 General Comments

Many industrially significant reactions do not follow any of the types of rate expressions discussed previously. There are a great number of possible combinations of parallel, series, and reversible reactions that we have not considered

but that may occur in nature in chemical processing operations. Benson (10) has described this situation in an apt fashion: "Kinetic systems when investigated in detail display an anarchistic tendency to become unique laws unto themselves." In this section we turn our attention to these more complex systems.

It is extremely difficult to generalize with regard to systems of complex reactions. Often, it is useful to attempt to simplify the kinetics by using experimental techniques that cause degeneration of the reaction order by using a large excess of one or more reactants or using stoichiometric ratios of reactants. In many cases, however, even these techniques will not effect a simplification in the reaction kinetics. Then one must be content with a numerical approach or qualitative or semi-quantitative descriptions of the system behavior.

We have not treated all the mathematical descriptions of reacting systems that have appeared in the literature. Indeed, such coverage goes far beyond the scope and spirit of this book. For material of this type, consult the kinetics literature.

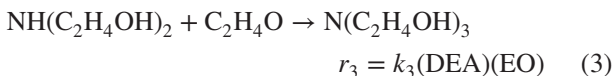
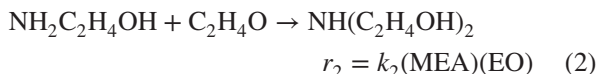
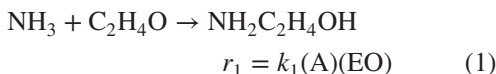
### 5.4.2 Competitive-Consecutive Second-Order Reactions

Competitive-consecutive reactions are combinations of parallel and series reactions that include processes such as multiple halogenation and nitration reactions. For example, when a nitrating mixture of  $\text{HNO}_3$  and  $\text{H}_2\text{SO}_4$  acts on an aromatic compound such as benzene,  $\text{NO}_2$  groups substitute for hydrogen atoms in the ring to form mono-, di-, and tri-substituted nitro compounds.

Since many reactions of this type involve a series of second-order processes, it is instructive to consider (1) how to obtain solutions to the differential equations describing the speciation of the reaction mixture as a function of time for reaction networks of the general competitive-consecutive type if one has available the rate constants for the individual reactions constituting the reaction network, and (2) how one analyzes systems of this sort to determine the kinetic parameters that are necessary for reactor design purposes. Given the rate laws and rate constants for each of the reactions constituting the reaction network, one can employ commercially available engineering software packages (e.g., Matlab) to numerically integrate the corresponding differential equations to obtain the desired speciation as a function of the time of reaction. An example of this class of problems is considered in Illustration 5.6, involving the reactions of ammonia and ethylene oxide in aqueous solution to form mono-, di, and tri-ethanolamines. A useful approach to planning experiments and analyzing the associated data for competitive-consecutive second-order reactions is that of Frost and Schwemer (11–13) discussed in Illustration 5.7.

## ILLUSTRATION 5.6 Evolution of Species Concentrations for Competitive-Consecutive Second-Order Reactions Occurring in a Batch Reactor

Alkanolamines are used in scrubbers to clean streams containing acid gases. Extension of existing applications to new situations involving carbon capture and sequestration of CO<sub>2</sub> for environmental reasons will lead to increased demand for these substances. The reaction of ammonia (A) with ethylene oxide (EO) in aqueous solution produces monoethanolamine (MEA), diethanolamine (DEA), and triethanolamine (TEA). The reactions for stepwise formation of these products are



Viewed from the perspective of ethylene oxide, these reactions are competitive; by contrast, from the perspective of the amines, they are consecutive. Consider a research scale batch reactor operating at 60°C and 20 bar to maintain all species in the liquid phase. Actual production of these commodity products on a large scale would be conducted in flow reactors, as described in Illustration 9.5. The rate laws are of the mixed second-order form (first-order in each reactant), with hypothetical rate constants  $k_1$ ,  $k_2$ , and  $k_3$  equal to 1, 0.4, and 0.1 L·mol<sup>-1</sup> / min, respectively. MEA and DEA are both high-volume chemicals, while TEA is less in demand. The distribution of alkanolamine products obtained under the specified conditions can be influenced by controlling the initial mole ratio of EO to A and the time of reaction.

- Solutions of ammonia and ethylene oxide are prepared independently and heated to the reaction temperature. At time zero the solutions are blended rapidly in a batch reactor to obtain a solution that is 1 M in ammonia and 2.4 M in ethylene oxide. Determine the concentrations of all five reactant and product species present at times from 0 to 15 min when reactions (1) to (3) take place under isothermal conditions.
- What would be the anticipated effects of using a lower mole ratio of ethylene oxide to ammonia (but holding the initial concentration of ammonia at 1 M) in the initial charge to the reactor?

## Solution

(a) Because these reactions take place at constant volume (liquid phase), the progress of these coupled reactions can be tracked using either three extents of reaction per unit volume or three suitable species concentrations. This solution employs the former progress variables. The concentrations of all species are expressed in these terms as follows:

$$A = A_0 - \xi_1^* \quad (A)$$

$$\text{EO} = \text{EO}_0 - \xi_1^* - \xi_2^* - \xi_3^* \quad (B)$$

$$\text{MEA} = \xi_1^* - \xi_2^* \quad (C)$$

$$\text{DEA} = \xi_2^* - \xi_3^* \quad (D)$$

$$\text{TEA} = \xi_3^* \quad (E)$$

The three independent rates of reaction per unit volume are then

$$\frac{d\xi_1^*}{dt} = k_1(\text{A})(\text{EO}) = k_1(A_0 - \xi_1^*)(\text{EO}_0 - \xi_1^* - \xi_2^* - \xi_3^*) \quad (F)$$

$$\frac{d\xi_2^*}{dt} = k_2(\text{MEA})(\text{EO}) = k_2(\xi_1^* - \xi_2^*)(\text{EO}_0 - \xi_1^* - \xi_2^* - \xi_3^*) \quad (G)$$

$$\frac{d\xi_3^*}{dt} = k_3(\text{DEA})(\text{EO}) = k_3(\xi_2^* - \xi_3^*)(\text{EO}_0 - \xi_1^* - \xi_2^* - \xi_3^*) \quad (H)$$

with initial conditions  $\xi_1^* = \xi_2^* = \xi_3^* = 0$  at  $t = 0$ . This system of coupled, nonlinear differential equations may be integrated numerically by any suitable computer routine, such as the *ode15* or *ode23* commands in Matlab. The results for the extents of reaction per unit volume then lead to the plots of the evolution of the concentrations of all reactant and product species shown in Figure I5.6.

Examination of the various plots in Figure I5.6 reveals that the concentration of MEA goes through a maximum (0.54 M) at 0.8 min and that the peak corresponding to this maximum is relatively narrow. By contrast, the peak corresponding to the plot of the concentration of DEA is very broad, with concentrations of this species varying only slightly (near 0.6 M) during the period from 5 to 10 min.

(b) If a lower mole ratio of EO to ammonia were employed in a batch trial, one is still likely to observe a maximum in the concentration of MEA at short times, but the location of the maximum will occur at a longer time and at a higher concentration than that for the base case. The product mixture at times greater than 15 min will contain less TEA than in the base case. As for ethylene oxide and ammonia, their concentrations will each decline less rapidly than in the base case.

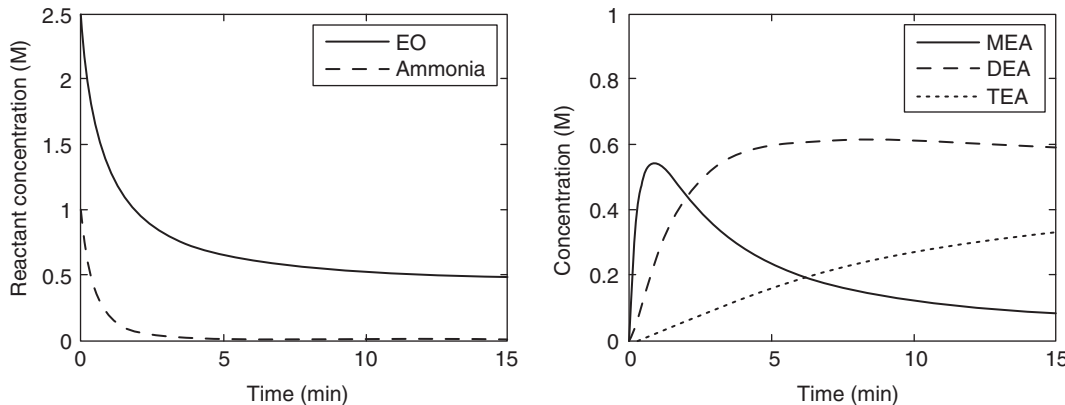


**Figure 15.6** Speciation plots for the competitive-consecutive second-order reactions of ammonia and ethylene oxide in a batch reactor to form mono-, di-, and triethanolamines (MEA, DEA, and TEA).

Now consider the complement of the task described in Illustration 5.6: that of planning, executing, and analyzing data from a series of experiments to arrive at numerical values of kinetic parameters for specified reaction conditions. We can begin by considering the following mechanistic equations:



These reactions may be regarded as parallel with respect to species A and series with respect to species B, C, and D. Only species A and B are present at time zero.

The equations for the time derivatives of certain species concentrations are given by

$$\frac{dA}{dt} = -k_1 BA - k_2 CA \quad (5.4.3)V$$

$$\frac{dB}{dt} = -k_1 BA \quad (5.4.4)V$$

$$\frac{dC}{dt} = k_1 BA - k_2 CA \quad (5.4.5)V$$

By the use of a large excess of A, one may cause these equations to degenerate to pseudo first-order forms. The analysis for these conditions is then equivalent to that presented in Section 5.3.

There are two other limiting forms of these equations that are also of interest. If  $k_1 \gg k_2$ , the first step is very rapid compared to the second, so that it is essentially complete before the second reaction gathers appreciable momentum. The reaction may then be treated as a simple irreversible second-order reaction, with the second step being rate limiting. On the other hand, if  $k_2 \gg k_1$ , the first step controls the reaction so that the kinetics observed are those for a single second-order process. However, the analysis must take into account the fact that in this case 2 mol of species A will react for each mole of B that is consumed.

For the more general case of arbitrary rate constants, the analysis is more complex. Various approximate techniques that are applicable to the analysis of reactions (5.4.1) and (5.4.2) have been described in the literature. Moore and Pearson's text (11) treats some of these. One useful general approach to this problem is that of Frost and Schwemer (12, 13). This approach may be regarded as an extension of the time-ratio method discussed in Section 5.3.2. The analysis is predicated on a specific choice of initial reactant concentrations. One uses equivalent amounts of reactants A and B ( $A_0 = 2B_0$ ) instead of equimolar quantities.

A material balance on species A indicates that

$$A_0 - A = C + 2D \quad (5.4.6)V$$

while a balance on species B gives

$$B_0 = B + C + D \quad (5.4.7)V$$

Elimination of D between equations (5.4.7) and (5.4.6) gives

$$A_0 - A = C + 2(B_0 - B - C) \quad (5.4.8)V$$

or

$$A_0 - 2B_0 = A - 2B - C \quad (5.4.9)V$$

For the specified choice of initial reactant concentrations, equation (5.4.9) requires that

$$C = A - 2B \quad (5.4.10)V$$

With this substitution, equation (5.4.3) becomes

$$\frac{dA}{dt} = (2k_2 - k_1)BA - k_2 A^2 \quad (5.4.11)V$$

Elimination of time as an independent variable between equations (5.4.4) and (5.4.11) gives

$$\frac{dA}{dB} = \left(1 - 2\frac{k_2}{k_1}\right) + \frac{k_2}{k_1} \left(\frac{A}{B}\right) \quad (5.4.12)V$$

This equation may be solved using the substitution

$$A = B\phi \quad (5.4.13)V$$

Hence,

$$\frac{dA}{dB} = \phi + B \frac{d\phi}{dB} = \phi + \frac{d\phi}{d\ln(B)} \quad (5.4.14)V$$

Combination of equations (5.4.12) to (5.4.14) gives

$$\phi + \frac{d\phi}{d\ln(B)} = \left(1 - 2\frac{k_2}{k_1}\right) + \frac{k_2}{k_1}\phi \quad (5.4.15)V$$

Solution of this linear differential equation by separation of variables and subsequent mathematical manipulation leads to

$$\frac{A}{A_0} = \frac{(1-2\kappa)}{2(1-\kappa)} \left(\frac{B}{B_0}\right) + \frac{1}{2(1-\kappa)} \left(\frac{B}{B_0}\right)^\kappa \quad (5.4.16)V$$

where  $\kappa = k_2/k_1$ .

If this result is substituted into equation (5.4.4), one obtains

$$\frac{dB}{dt} = -k_1 B \left[ \frac{(1-2\kappa)}{2(1-\kappa)} \left(\frac{B}{B_0}\right) + \frac{1}{2(1-\kappa)} \left(\frac{B}{B_0}\right)^\kappa \right] A_0 \quad (5.4.17)V$$

This equation may be rewritten in terms of a dimensionless time  $\tau^*$  and a dimensionless concentration for species B if we let

$$\tau^* = k_1 B_0 t \quad \text{and} \quad \beta = \frac{B}{B_0} \quad (5.4.18)V$$

In this case, equation (5.4.17) becomes

$$\frac{d\beta}{d\tau^*} = -\beta \left[ \frac{(1-2\kappa)\beta}{2(1-\kappa)} + \frac{\beta^\kappa}{2(1-\kappa)} \right] \frac{A_0}{B_0} \quad (5.4.19)V$$

Recognition that  $A_0/B_0 = 2$  leads to

$$\frac{d\beta}{d\tau^*} = - \left[ \frac{(1-2\kappa)\beta^2}{1-\kappa} + \frac{\beta^{\kappa+1}}{1-\kappa} \right] \quad (5.4.20)V$$

**Table 5.2**  $\tau^*$  as a Function of  $\kappa$  and  $A/A_0$

$1/\kappa$	$A/A_0 = 0.8$ 20% reaction	$A/A_0 = 0.7$ 30% reaction	$A/A_0 = 0.6$ 40% reaction	$A/A_0 = 0.5$ 50% reaction	$A/A_0 = 0.4$ 60% reaction
2.0	0.2500	0.4286	0.6667	1.000	1.500
3.0	0.2599	0.4564	0.7305	1.133	1.770
4.0	0.2656	0.4741	0.7756	1.239	2.011
5.0	0.2693	0.4865	0.8098	1.327	2.235
6.0	0.2720	0.4957	0.8368	1.404	2.449
7.0	0.2740	0.5028	0.8589	1.471	2.657
8.0	0.2755	0.5085	0.8773	1.531	2.862
9.0	0.2768	0.5131	0.8929	1.586	3.066
10.0	0.2778	0.5170	0.9064	1.637	3.270

*Source:* Adapted from J. W. Moore and R. G. Pearson, *Kinetics and Mechanism*, 3rd ed., p. 302, Wiley-Interscience, New York. Copyright © 1981. Used with permission of John Wiley & Sons, Inc.

Separation of variables followed by integration gives

$$\begin{aligned} \tau^* &= -(1-\kappa) \int_1^\beta \frac{d\beta}{(1-2\kappa)\beta^2 + \beta^{\kappa+1}} \\ &= (1-\kappa) \int_\beta^1 \frac{d\beta}{(1-2\kappa)\beta^2 + \beta^{\kappa+1}} \end{aligned} \quad (5.4.21)V$$

In principle, this integral may be evaluated in closed form for any value of  $\kappa$  that is a rational number (i.e., a ratio of integers). In other cases, numerical integration is necessary. This integral will degenerate to the limiting forms mentioned earlier for  $\kappa$  values of zero and infinity. The integral also simplifies for  $\kappa = \frac{1}{2}$ . If we let  $\alpha = A/A_0$ , the limiting expressions for equations (5.4.16) and (5.4.21) become:

For  $\kappa = 0$ , or ( $k_1 \gg k_2$ ):

$$\tau^* = \int_\beta^1 \frac{d\beta}{\beta^2 + \beta} = \ln\left(\frac{\beta+1}{2\beta}\right) \quad \text{and} \quad \alpha = \frac{\beta+1}{2} \quad (5.4.22)V$$

For  $\kappa = \frac{1}{2}$  or ( $k_1 = 2k_2$ ):

$$\tau^* = \frac{1}{2} \int_\beta^1 \frac{d\beta}{\beta^{3/2}} = \left(\frac{1}{\beta^{1/2}} - 1\right) \quad \text{and} \quad \alpha = \sqrt{\beta} \quad (5.4.23)V$$

For  $\kappa = \infty$  or ( $k_1 \ll k_2$ ):

$$\tau^* = \frac{1}{2} \left(\frac{1}{\beta} - 1\right) \quad \text{and} \quad \alpha = \beta \quad (5.4.24)V$$

Frost and Schwemer (12, 13) developed a time-ratio technique based on equations (5.4.21) and (5.4.16) to facilitate the calculation of second-order rate constants for the class of reactions under consideration. Data for  $A/A_0$  versus  $\tau^*$  at various values of  $\kappa$  are presented in Table 5.2, and time ratios are given in Table 5.3. The latter values may be used to determine  $\kappa$  by using various time ratios from a single kinetic run if one recognizes that  $\tau_1^*/\tau_2^* = t_1/t_2$ . Once

**Table 5.3** Time Ratios as a Function of  $\kappa^a$ 

$1/\kappa$	$t_{60}/t_{20}$	$t_{60}/t_{30}$	$t_{60}/t_{40}$	$t_{60}/t_{50}$	$t_{50}/t_{20}$	$t_{50}/t_{30}$
2.0	6.000	3.500	2.250	1.500	4.000	2.333
3.0	6.812	3.878	2.423	1.562	4.362	2.483
4.0	7.571	4.241	2.592	1.623	4.666	2.614
5.0	8.297	4.593	2.760	1.684	4.928	2.728
6.0	9.003	4.940	2.927	1.745	5.161	2.832
7.0	9.698	5.285	3.094	1.806	5.369	2.925
8.0	10.388	5.629	3.263	1.869	5.558	3.012
9.0	11.078	5.975	3.434	1.933	5.731	3.091
10.0	11.772	6.325	3.607	1.998	5.892	3.166

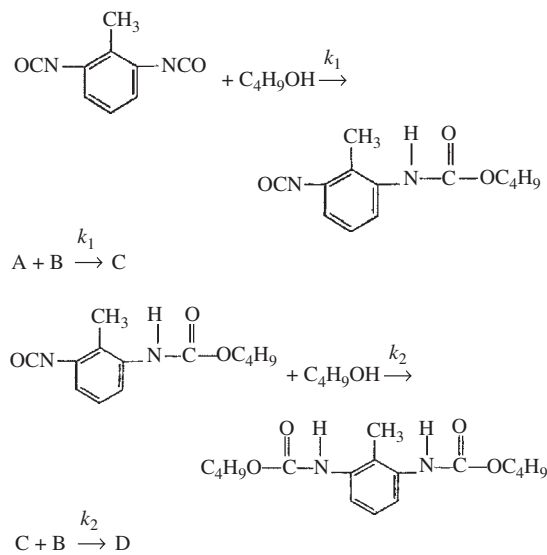
Source: Adapted from J. W. Moore and R. G. Pearson, *Kinetics and Mechanism*, 3rd ed., p. 303. Wiley-Interscience, New York. Copyright © 1981. Used with permission of John Wiley & Sons, Inc.

<sup>a</sup> $(t_{60}/t_{20})$  is the ratio of the time for 60% A reacting to the time for 20% reaction, or where  $A/A_0 = 0.4$  and 0.8, respectively.

$\kappa$  has been determined, Table 5.2 may be used to determine the  $\tau^*$  values at given values of  $A/A_0$  and  $\kappa$ . Equation (5.4.18) may then be used to determine  $k_1$ . This value and the value of  $\kappa$  then may be combined to evaluate  $k_2$ . Illustration 5.7 indicates the application of this technique.

### ILLUSTRATION 5.7 Determination of Reaction Rate Constants for Competitive-Consecutive Second-Order Reactions

Burkus and Eckert (14) studied the kinetics of the triethylamine-catalyzed reaction of 2,6-toluene diisocyanate (A) with 1-butanol (B) in toluene solution. The reactions may be represented as



A titrimetric method was used to follow the progress of the reaction at 39.69°C. On the basis of the data given

below, what are the corresponding values of the reaction rate constants,  $k_1$  and  $k_2$ ?

Initial concentration of 2,6-tolylene diisocyanate	53.2 mol/m <sup>3</sup>
Initial concentration of 1-butanol	106.4 mol/m <sup>3</sup>
Catalyst concentration (triethylamine)	31.3 mol/m <sup>3</sup>
Time (k)	1-Butanol reacted (%)
0.360	20
0.657	30
1.118	40
1.866	50
3.282	60

### Solution

Because *equivalent* amounts of reactants were employed ( $A_0 = 2B_0$ ), the time-ratio method of Frost and Schwemer (11–13) may be used in the solution of this problem. From Table 5.3 the following values of  $1/\kappa$  may be determined at the time ratios indicated.

$$\begin{aligned}
 \frac{t_{60}}{t_{50}} &= \frac{3.282}{1.866} = 1.759 & \frac{1}{\kappa} &= 6.21 \\
 \frac{t_{60}}{t_{40}} &= \frac{3.282}{1.116} = 2.941 & \frac{1}{\kappa} &= 6.08 \\
 \frac{t_{60}}{t_{30}} &= \frac{3.282}{0.657} = 4.995 & \frac{1}{\kappa} &= 6.16 \\
 \frac{t_{60}}{t_{20}} &= \frac{3.282}{0.360} = 9.117 & \frac{1}{\kappa} &= 6.16 \\
 \frac{t_{50}}{t_{30}} &= \frac{1.866}{0.657} = 2.840 & \frac{1}{\kappa} &= 6.09 \\
 \frac{t_{50}}{t_{20}} &= \frac{1.866}{0.360} = 5.183 & \frac{1}{\kappa} &= 6.11 \\
 \text{Average: } \frac{1}{\kappa} &= 6.13
 \end{aligned}$$

The values of  $\kappa$  that correspond to the various conversion levels and  $1/\kappa = 6.13$  may be found in Table 5.2. The rate constant  $k_1$  may then be calculated using equation (5.4.18). Hence,

Conversion (%)	$\tau^*$	$k_1 = \tau^* / (B_0 t)$ [m <sup>3</sup> /(kmol·ks)]
20	0.2722	14.21
30	0.4966	14.21
40	0.8397	14.14
50	1.413	14.23
60	2.476	14.18
Average = 14.19		

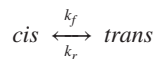
Thus,  $k_2 = \kappa k_1 = 14.19/6.13 = 2.31$  m<sup>3</sup>/(kmol·ks).

## LITERATURE CITATIONS

- HELLIN, M., and JUNGERS, J. C., *Bull. Soc. Chim.*, **1957**, 386 (1957).
- GULDBERG, C. M., WAAGE, P., *Etudes sur les affinités chimiques*, Brøgger and Christie, Christiania, Oslo, Norway, 1867.
- DENBIGH, K. G., *The Principles of Chemical Equilibrium*, 2nd ed., p. 445, Cambridge University Press, Cambridge, 1966.
- DENBIGH, K. G., and PRINCE, A. J., *J. Chem. Soc.*, **1947**, 790 (1947).
- EMANUEL', N. M., and KNORRE, D. G., *Chemical Kinetics: Homogeneous Reactions*, R. Kondor (transl.), p. 215 Wiley, New York, 1973.
- PANNETIER, G., and SOUCHAY, P., *Chemical Kinetics* H. D. Gesser and H. H. Emond (transl.), pp. 177–178, Elsevier, Amsterdam, 1967.
- SWAIN, C. G., *J. Am. Chem. Soc.*, **66**, 1696 (1944).
- MOORE, J. W., and PEARSON, R. G., *Kinetics and Mechanism*, 3rd ed., p. 296, Wiley-Interscience, New York, 1981.
- KAUFLER, F., *Z. Phys. Chem.*, **55**, 502 (1906).
- BENSON, S. W., *Foundations of Chemical Kinetics*, p. 27, McGraw-Hill, New York, 1960.
- MOORE, J. W., and PEARSON, R. G., *op. cit.*, pp. 302–303.
- FROST, A. A., and SCHWEMER, W. C., *J. Am. Chem. Soc.*, **74**, 1268 (1952).
- SCHWEMER, W. C., and FROST, A. A., *J. Am. Chem. Soc.*, **73**, 4541 (1951).
- BURKUS, J., and ECKERT, C. F., *J. Am. Chem. Soc.*, **80**, 5948 (1958).

## PROBLEMS

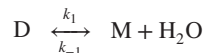
- 5.1** In their textbook, M. Diaz Piña and A. Roig Muntaner (*Química Física*, Vol. II, pp. 1073–1074, Editorial Alhambra, Madrid, 1976) reported the data below for the reversible *cis-trans* isomerization of 1,2-dimethyl cyclopropane. Test these data to ascertain if they are consistent with a rate expression that is first-order in both the forward and reverse directions.



If the data are consistent with the indicated rate expression, determine values for  $k_f$ ,  $k_r$ , and the equilibrium constant for the reaction.

Time (s)	Percent trans
0	100
45	89.2
90	81.2
225	62.3
270	58.2
360	50.7
495	43.5
585	39.9
10,000	30.0

- 5.2** Y. K. Kim and J. D. Hatfield [*J. Chem. Eng. Data*, **30**, 149 (1985)] studied the kinetics of the dehydration of diacetone alcohol (D) to mesityl oxide (M) in aqueous phosphoric acid. This reversible reaction may be written as



It has been suggested that the rate expression for the reaction as written is of the form

$$\frac{d(M)}{dt} = k_1(D) - k_{-1}(M)a_w$$

where  $a_w$  is the activity of water. Similarly, the equilibrium constant for the reaction may be written as

$$K_e = \frac{(M)}{(D)} a_w$$

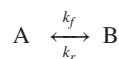
These researchers monitored the progress of the reaction by measuring the absorbance of the solution at 243 nm. The reaction was studied in both directions by adding 5 mL of either D or M to 495 g of phosphoric acid solution. Note that the units to be employed for  $k_{-1}$  are time<sup>-1</sup> because the rate of the reverse reaction becomes pseudo first-order at constant water activity.

The data below correspond to reaction at 39.7°C in an aqueous solution containing 17.2% w/w H<sub>3</sub>PO<sub>4</sub>. The corresponding activity of water is 0.956. The data correspond to an experiment in which the initial reaction mixture contained M but not D.

Time (h)	Absorbance
0.00	1.092
0.25	1.016
0.50	0.940
0.75	0.881
1.00	0.823
1.50	0.720
2.00	0.627
2.50	0.548
3.00	0.481
24.00	0.108

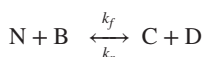
Measurements of the corresponding equilibrium composition indicate that the fraction of the original mesityl oxide that remains unconverted is 0.0869. Use these data to determine if the proposed rate expression provides a good fit of the data. If a good fit is obtained, determine numerical values for  $k_f$ ,  $k_r$ , and  $K_e$ .

- 5.3** Guggenheim's method for the analysis of kinetic data is useful for situations in which the initial concentrations of reactants are not known or are inaccessible. This method is generally regarded as applicable only to cases in which the rate expression obeys first-order or pseudo first-order kinetics. However, it is also possible to extend Guggenheim's analysis to reversible reactions that are first-order (or pseudo first-order) in both the forward and reverse directions. Consider as an example the generic isomerization reaction with mechanistic equations of the form



- (a) Starting with the differential form of the general rate expression for this reaction as it occurs in a constant volume system, which initially contains only species A at an initial concentration  $C_{A0}$ , derive the integrated form of the equation for the extent of reaction per unit volume ( $\xi^*$ ) as a function of time. This equation should contain as parameters only the rate constants  $k_f$  and  $k_r$  and the initial concentration of species A ( $C_{B0} = 0$ ).
- (b) The fundamental premise of the Guggenheim method is that data are available at times  $t_i$  and  $t_{i+\Delta}$ , where  $\Delta$  is a fixed time increment. Use the equation determined in part (a) to obtain an expression involving the difference in the extent of reaction per unit volume at times  $t_i$  and  $t_{i+\Delta}$ . That is, determine how  $\xi_{i+\Delta}^* - \xi_i^*$  will vary with time.
- (c) If optical rotation measurements are used to monitor the progress of this reaction, indicate how one would manipulate the equation derived in part (b) and the data available at times  $t_{i+\Delta}$  and  $t_i$  to generate a plot from which the sum of the rate constants ( $k_f + k_r$ ) can be determined. That is, how can the optical rotation values at times  $i$  and  $i + \Delta$  be used to determine this sum?

- 5.4** J. M. Antelo, F. Arce, J. Franco, M. C. Garcia Lopez, M. Sanchez, and A. Varela [Int. J. Chem. Kinet., **20**, 397–409 (1988)] studied the kinetics of the reaction between *N*-chlorosuccinimide (N) and diethylamine (B) to give succinimide (C) and the corresponding *N*-chloroamine (D):



Absorbance measurements at 262 nm were used to monitor the progress of the reaction.

- (a) The data below are representative of this reaction at a pH of 3.39 and a temperature of 25°C for a series of experiments in which the initial concentrations of species N and C were 0.01 M and the initial concentration of the amine was lower by an order of magnitude, or more. Although

the rate expression for this reaction is believed to be of the form

$$r = k_f(N)(B) - k_r(C)(D)$$

the use of significantly higher concentrations of species N and C will cause the rate expression to simplify to a form that is pseudo first-order in both the forward and reverse directions. Use the generalized physical property relation to demonstrate that the form of the rate expression proposed is consistent with the data. What is the value of the sum of the rate constants for the forward and reverse reactions?

Time (s)	Absorbance for B = 0.001 M	Absorbance for B = 0.0008 M
0	0.3490	0.141
7	0.3620	0.156
15	0.3780	0.183
35	0.3980	0.214
55	0.4120	0.234
70	0.4290	0.259
90	0.4398	0.276
105	0.4530	0.295
125	0.4620	0.309
140	0.4730	0.324
160	0.4800	0.335
175	0.4880	0.348
195	0.4960	0.359
215	0.5020	0.368
2000	0.5500	0.439

- (b) In a second series of experiments, these investigators studied this reaction under conditions such that the concentration of either the amine or succinimide was varied while the other experimental conditions were held constant. In all cases, however, the concentrations of these species were at least an order of magnitude greater than that of the *N*-chloroamine. Data of the type presented here were worked up and analyzed to obtain values of an apparent first-order rate constant,  $k_{\text{exp}}$ . This rate constant is given by

$$k_{\text{exp}} = k_f(B_0) + k_r(C_0)$$

Values of the experimental rate constant are presented below for different initial concentrations of diethylamine and succinimide. Determine whether the assumptions that the forward reaction is first-order in B and that the reverse reaction is first-order in C are consistent with the data. If the rate law proposed is valid, evaluate not only the rate constants  $k_f$  and  $k_r$ , but also the equilibrium constant for the reaction at 298 K.

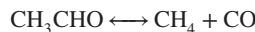
The influence of the reactant and product concentrations on the apparent first-order rate constant at 25°C and pH 3.4 is as follows (the initial concentration of N = 0.001 M):

Diethylamine (M)	Succinimide (M)	$k_{\text{exp}}$ (s <sup>-1</sup> )
0.010	0.010	0.0064
0.014	0.010	0.0082
0.018	0.010	0.0102
0.020	0.010	0.0109
0.022	0.010	0.0108
0.024	0.010	0.0127
0.026	0.010	0.0141
0.030	0.010	0.0154
0.010	0.014	0.0061
0.010	0.018	0.0069
0.010	0.020	0.0073
0.010	0.022	0.0074
0.010	0.024	0.0077
0.010	0.026	0.0078
0.010	0.030	0.0084

- (c) This research group also presented information concerning the temperature dependence of this reaction. Use the following data to determine the activation energies for the forward and reverse reactions as well as the standard enthalpy change for the reaction.

Temperature (°C)	$k_f$ (M <sup>-1</sup> /s)	$k_r$ (M <sup>-1</sup> /s)
17	0.153	0.054
19	0.237	0.065
21	0.262	0.073
22	0.314	0.073
23	0.345	0.088
25	0.453	0.101
27	0.488	0.103
29	0.639	0.141

- 5.5 Under certain conditions, acetaldehyde decomposes into methane and carbon monoxide in a second-order reaction:

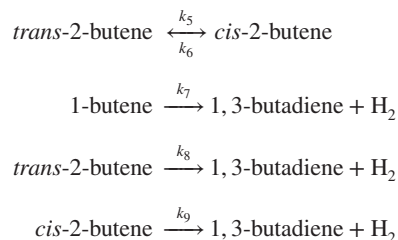
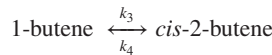
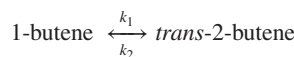


For a constant volume reactor, the rate of the forward reaction is given by

$$\frac{dC_{\text{CH}_3\text{CHO}}}{dt} = -k_f C_{\text{CH}_3\text{CHO}}^2$$

State two possible rate laws for the reverse reaction.

- 5.6 R. A. Ziman, S. G. Garagin, A. D. Berman, and M. I. Yanovskii. [Kinet. Katal., 9, 117 (1968)] studied the kinetics of catalytic oxidative dehydrogenation of various butene isomers to form 1,3-butadiene. Over a Bi–Mo catalyst the following reactions are important.

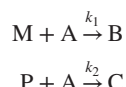


These authors have reported the following values of the reaction rate constants at 396°C in units of inverse seconds.

$k_1$	9.0	$k_6$	13.0
$k_2$	6.0	$k_7$	19.0
$k_3$	11.0	$k_8$	1.0
$k_4$	7.0	$k_9$	3.0

A value of  $k_5$  was not reported because of the large uncertainty in this parameter. Use the principle of microscopic reversibility to determine a value of  $k_5$  at this temperature for this catalyst.

- 5.7 B. Chadhuri, A. A. Patwardham, and M. M. Sharma [Ind. Eng. Chem. Res. 29, 1025 (1990)] studied the catalytic alkylation of *m*-cresol (M) and *p*-cresol (P) with  $\alpha$ -methylstyrene (A). These reactions can be represented in schematic form as



where B represents *p*-cumyl-*m*-cresol, C represents *o*-cumyl-*p*-cresol, and where each of the rate expressions is of mixed second-order form; that is,

$$r_1 = k_1 (M) (A)$$

and

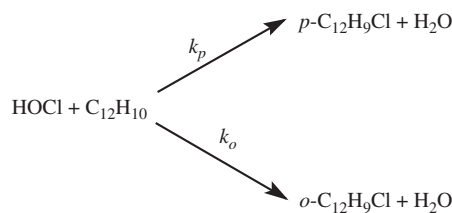
$$r_2 = k_2 (P) (A)$$

These reactions are of interest because of their involvement in a scheme proposed for separation of mixtures of *o*- and *p*-cresols. Consider these reactions as they occur in the liquid phase at 60°C with cumene as the solvent in the presence of an Amberlyst 15 catalyst. For this system at this temperature, the ratio of rate constants ( $k_1/k_2$ ) is 4.8.

- (a) If one starts with an equimolar mixture of species M and P (0.30 M in each species) and adds an amount of the olefin A to bring its concentration to 0.30 M, determine the concentrations of the species A, M, P, B, and C as functions of the fraction of the olefin (A) that has reacted. Express your results in the form of both equations and plots. (Hint: Start by deriving an equation relating the concentration of species M that will be present at a given time to the concentration of species P present at that time. Time itself should not appear as a variable in this equation. Then proceed to derive an equation relating the concentration of species A present at a given time to the concentration of species P at that same time.)
- (b) When 33% of the olefin (A) had reacted, the ratio of B to C in the product mixture was approximately 77 : 23, a

result that supports the hypothesis that these reactions can constitute part of a process for separating the two isomers of cresol. Demonstrate whether or not a selectivity analysis based on the aforementioned reactivity ratio gives a result that is consistent with this value.

- 5.8 E. H. Snider and F. C. Alley [*Environ. Sci. Technol.*, **13**, 1244 (1979)] studied the kinetics of the chlorination of biphenyl in dilute aqueous solution. The conditions employed were representative of those employed in waste treatment facilities. The reactions of interest may be written as



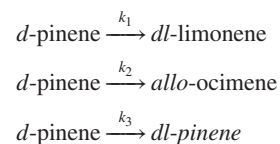
where *o* and *p* refer to the *ortho* and *para* forms of chlorobiphenyl.

The data listed in the table below indicate the amounts of these products formed in 12 hours of reaction at 40°C in buffered aqueous solutions. These authors suggest that the data can be interpreted using the initial rate method, in which it is normally assumed that the reactions are terminated before the consumption of the limiting reagent reaches 10%. Perform an initial rate analysis to determine the orders of these reactions with respect to biphenyl and HOCl. These

[C <sub>12</sub> H <sub>10</sub> ] ( $\mu\text{g/L}$ )	[HOCl] ( $\mu\text{g/L}$ )	<i>o</i> -C <sub>12</sub> H <sub>9</sub> Cl ( $\mu\text{g/L}$ )	<i>p</i> -C <sub>12</sub> H <sub>9</sub> Cl ( $\mu\text{g/L}$ )
3770	17.9	1.2	0.8
3770	38.5	5.7	3.8
3770	54.7	11.0	8.3
3770	74.7	23.0	15.8
3770	90.5	34.3	21.7
3400	247.0	222.0	134.0
2720	247.0	163.0	99.1
2040	247.0	122.0	62.5
1360	247.0	83.4	47.7
680	247.0	42.5	23.8

orders may be rounded to the nearest integer. In addition, determine values of the rate constants  $k_o$  and  $k_p$  and comment on the validity of this approach.

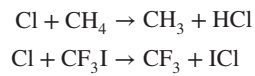
- 5.9 When optically active  $\alpha$ -pinene is heated above 200°C in the liquid phase, it becomes optically inactive. Initially, the reaction processes may be written as



The *allo*-ocimene may undergo subsequent reaction to form  $\alpha$ - and  $\beta$ -pyronene and a dimer of *allo*-ocimene.

R. E. Fugitt and J. E. Hawkins [(*J. Am. Chem. Soc.*, **69**, 319 (1947)] reported the data in Table P5.9 as typical of these reactions at 204.5°C. The data have been modified somewhat for the purposes of this problem. By summing the amounts of dimer,  $\alpha$ - and  $\beta$ -pyronene, and *allo*-ocimene present in the final mixture, one may determine the total amount of *allo*-ocimene formed in the initial reaction. These investigators have postulated that all three of the parallel reactions are first-order. Are the data consistent with this hypothesis? If so, what are the values of the three first-order rate constants?

- 5.10 By international agreement, chlorofluorocarbons are being replaced by environmentally acceptable alternatives that are less harmful with respect to the destruction of ozone in the atmosphere. E. W. Kaiser, T. J. Wallington, and M. D. Hurley [*Int. J. Chem. Kinet.*, **27**, 205–218 (1995)] studied several of the reactions that are thought to be involved in the overall reaction network. Of particular interest is their study of the relative rates at which chlorine atoms react with methane and CF<sub>3</sub>I. The data tabulated below correspond to reaction at 23°C in a batch reactor illuminated with ultraviolet radiation. The reactions of interest are



If the rate constant for the reaction involving methane is  $1.008 \times 10^{-13} \text{ cm}^3/(\text{molecule}\cdot\text{s})$ , prepare an appropriate plot of the data that can be used to obtain an accurate estimate of the rate constant for the reaction involving CF<sub>3</sub>I.

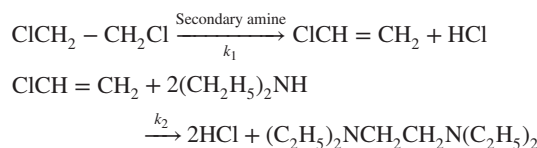
Table P5.9

Time (ks)	% $\alpha$ -pinene unreacted	% $\alpha$ - and $\beta$ -pyronene	% allo-ocimene	% dimer	% d-l-limonene	% racemized
26.4	85.9	0.4	4.1	0.6	8.2	0.8
49.5	74.3	0.8	6.8	1.6	15.6	0.9
72.0	65.1	1.0	7.7	3.4	21.5	1.3
90.0	58.6	1.2	8.4	5.0	25.5	1.3
122.4	48.1	1.6	8.5	8.2	31.9	1.7
183.6	32.1	2.0	8.2	13.5	42.0	2.2
363.6	11.2	2.7	6.9	21.9	54.7	2.6

Sample	$(\text{CH}_4)/(\text{CH}_4)_0$	$(\text{CF}_3\text{I})/(\text{CF}_3\text{I})_0$
1	0.912	0.695
2	0.908	0.690
3	0.863	0.566
4	0.791	0.395
5	0.675	0.212
6	0.665	0.210

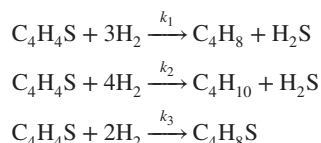
- 5.11** H. Yang and F. C. Thyron [*Int. J. Chem. Kinet.*, **26**, 309–315 (1994)] studied the kinetics of the reaction between 1, 2-dichloroethane (DCE) and diethylamine (DEA). These researchers reported that in this reaction the amine can either function as a base and effect an elimination reaction releasing HCl from DCE, or as a nucleophile in an  $S_N2$  substitution reaction.

When these compounds are allowed to react in dimethylformamide containing  $\text{Na}_2\text{CO}_3$ , the stoichiometries of the reactions of interest can be written as



The HCl is neutralized by the  $\text{Na}_2\text{CO}_3$  as it is formed. Each of the reactions indicated is first-order in both DCE and the secondary amine (second-order overall).

- (a) For reaction at  $71^\circ\text{C}$ , the values of the rate constants  $k_1$  and  $k_2$  are  $14.1 \times 10^{-3}$  and  $20.7 \times 10^{-3} \text{ dm}^3/(\text{mol}\cdot\text{h})$ , respectively. Prepare plots of the concentrations of DCE,  $N, N', N'$ -tetraethylmethylenediamine, and vinyl chloride as functions of time for times up to 15 h. Consider the case for which the initial concentrations of DCE and DEA are 6.07 and  $3.55 \text{ mol}/\text{dm}^3$ , respectively. When is the concentration of  $N, N, N', N'$ -tetraethylmethylenediamine equal to that of DEA?
- (b) Describe an experimental program by which one could proceed to determine values of  $k_1$  and  $k_2$  at a particular temperature. Indicate the type of data that you will generate, the types of plots you will prepare, and the equations you will use.
- 5.12** P. Kieran and C. Kemball [*J. Catal.*, **4**, 394 (1965)] studied the reactions of thiophene ( $\text{C}_4\text{H}_4\text{S}$ ) and hydrogen over a tungsten disulfide catalyst. The reaction network can be simplified to the following form:



On the basis of experiments in which a large excess of hydrogen was employed, these researchers reported that the pseudo orders of reactions 1, 2, and 3 with respect to thiophene were 0, 0, and 1, respectively.

Given the following values of the rate constants, prepare plots of the dimensionless concentrations of thiophene, tetrahydrothiophene, butene, and butane as functions of time for a period corresponding to 50% reaction of the initial thiophene:

$$k_1\text{AW} = 4.86 \times 10^{-7} \text{ mol}/\text{min}$$

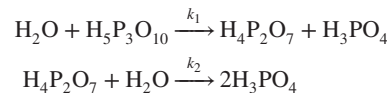
$$k_3\text{AW} = 7.4 \times 10^{-6} \text{ L}/\text{min}$$

where  $A$  is the interfacial surface area per unit mass of catalyst. The indicated numerical values correspond to a given loading of catalyst ( $W$ ) in the reactor.

The concentrations of all species may be made dimensionless using the initial concentration of thiophene. The reaction takes place in a reactor with a volume of  $100 \text{ cm}^3$ . You may assume that only hydrogen and thiophene are present initially and that the initial concentration of thiophene is  $3.6 \times 10^{-4} \text{ M}$ . Remember that in the case of a heterogeneous catalytic reaction, it is appropriate to define a rate as

$$\frac{1}{WA} \frac{d\xi}{dt} = f(\text{temperature, concentrations})$$

- 5.13** E. Prodan and I. L. Shashkova [*Kinet. Catal.*, **24**, 891–894 (1984)] studied the kinetics of the decomposition of tripolyphosphoric acid in aqueous solution. The decomposition involves the following reactions:



In aqueous solution each of these reactions can be regarded as pseudo first-order in the participating acid. The data below are characteristic of reaction at  $40^\circ\text{C}$ .

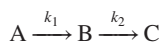
Time (h)	$\text{H}_5\text{P}_3\text{O}_{10}$ (M)	$\text{H}_4\text{P}_2\text{O}_7$ (M)	$\text{H}_3\text{PO}_4$ (M)
0.0	0.165	0.00377	0.00151
0.3	0.141	0.0277	0.0252
0.7	0.124	0.0440	0.0654
1.5	0.095	0.068	0.0805
2.0	0.079	0.075	0.116
2.5	0.069	0.082	0.126
3.0	0.056	0.097	0.136
3.5	0.046	0.102	0.161
5.0	0.028	0.113	0.191
7.0	0.013	0.113	0.231
8.0	0.010	0.116	0.247

- (a) Derive general equations for the concentrations of all acid species for a system in which all three acids are present initially.
- (b) Plot the data in a form such that the rate constant  $k_1$  can be determined via a linear regression analysis.
- (c) Use the value of  $k_1$  determined in part (b) and the equations developed in part (a) to ascertain the value of  $k_2$ . You may use either a nonlinear regression analysis

package or a trial and-error procedure involving spreadsheet calculations to obtain a value of  $k_2$  containing two significant figures. As your first estimate of  $k_2$ , use  $5 \times 10^{-2} \text{ M}^{-1}/\text{h}$ .

- (d) Use the estimates of  $k_1$  and  $k_2$ , together with the values of the initial species concentrations, to generate plots of the concentrations of  $\text{H}_5\text{P}_3\text{O}_{10}$ ,  $\text{H}_4\text{P}_2\text{O}_7$ , and  $\text{H}_3\text{PO}_4$  as functions of time. Include the reported values of species concentrations on these plots. At what time is the concentration of  $\text{H}_4\text{P}_2\text{O}_7$  a maximum?

- 5.14 Decolorization of aqueous solutions of dyes used in the textile industry may be accomplished via the use of ozone. Y.-C. Hsu, J.-T. Chen, H.-C. Yang, and J.-H. Chen [*AIChE J.*, **47**, 169–176 (2001)] investigated the kinetics of the oxidation of C.I. Mordant Black and other dyes in a well-agitated reactor to which a gas containing ozone was fed continuously. Initially, decolorization occurs rapidly, but as the process continues, colored intermediates are formed. These intermediates are more recalcitrant to oxidation, but are destroyed as ozonation proceeds. These authors indicate that the concentration of dissolved ozone remains substantially constant so that the kinetics of this process can be treated as involving two consecutive pseudo first-order reactions:

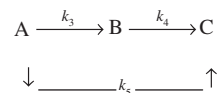


where A represents Mordant Black, B is a lumped parameter representing several persistent colored intermediates, and C represents all of the colorless solutes. At  $25^\circ\text{C}$ , pH 7.0, and an initial concentration ( $\text{A}_0$ ) of 200 mg/L, the values of  $k_1$  and  $k_2$  are  $9.12 \times 10^{-3}$  and  $1.13 \times 10^{-3} \text{ s}^{-1}$ , respectively.

- (a) Prepare plots of the concentrations of species A, B, and C as functions of time when no B or C is present initially. Determine the time corresponding to the maximum concentration of species B and the time at which the sum of the concentrations of species A and B is 20 mg/L. The latter time can be viewed as corresponding to removal of approximately 90% of the initial color values, thereby rendering the solution amenable to processing via more conventional waste treatment methods.
- (b) Now consider the demands that will be placed on the ozonation facility by a process modification that will reduce water use by 50%, thereby increasing the initial concentration of Mordant Black to 400 mg/L. For this process modification, the corresponding values of the pseudo first-order rate constants  $k_1$  and  $k_2$  at  $25^\circ\text{C}$  are  $4.16 \times 10^{-3}$  and  $6.76 \times 10^{-3} \text{ s}^{-1}$ . How long will it now take to reduce the sum of the concentrations of species A and B to 20 mg/L?
- (c) Suppose that the activation energies of the first and second reactions are 10.0 and 15.0 kcal/mol, respectively. At what temperature must the reactor be operated if the time required to reach the specified final concentration of A and B (total = 20 mg/L) is to be reduced to the same value as that required for an initial concentration of 200 mg/L?

- 5.15 Yu. G. Osokin, M. Ya. Grinberg, and V. Sh. Fel'dblyum [*Kinet. Catal.*, **17**, 1047 (1976)] studied the liquid phase isomerization of 1,5-cyclooctadiene in the presence of an iron pentacarbonyl catalyst. These researchers attempted to model the reactions of interest in two ways:

1. As a set of consecutive pseudo first-order reactions of the form  $\text{A} \xrightarrow{k_1} \text{B} \xrightarrow{k_2} \text{C}$ , where A refers to 1,5-cyclooctadiene, B to 1,4-cyclooctadiene, and C to 1,3 cyclooctadiene.
2. As a set of competitive, consecutive pseudo first-order reactions of the form



The equations describing the time-dependent behavior of the concentrations of the various species present in the system for case 1 are available in a number of textbooks. However, the corresponding solutions for case 2 are not as readily available.

- (a) For case 1 use a textbook to determine the equation that governs the time dependence of species B. Then use this relation to derive equations relating the time at which the concentration of species B passes through a maximum to the rate constants and the initial concentrations of species A and B. (Consider the general case for which the initial concentration of species B is not zero.) For what range of variables does a maximum exist?
- (b) For case 2 set up the differential equations for the time dependence of the concentrations of the various species. Solve these equations for the case in which the initial concentrations of the species of interest are  $\text{A}_0$ ,  $\text{B}_0$ , and  $\text{C}_0$ . Determine the time at which the concentration of species B is a maximum. For what range of variables does a maximum exist?
- (c) Consider the situation in which only reactant A is present initially. Prepare plots of the dimensionless concentration of species B (i.e.,  $\text{B}/\text{A}_0$ ) versus time (180 min) for each of the two cases noted above using the following values of the rate constants (in  $\text{s}^{-1}$ ) as characteristic of reaction at  $160^\circ\text{C}$ .

$$k_1 = 0.45 \times 10^{-3}$$

$$k_2 = 5.0 \times 10^{-3}$$

$$k_3 = 0.32 \times 10^{-4}$$

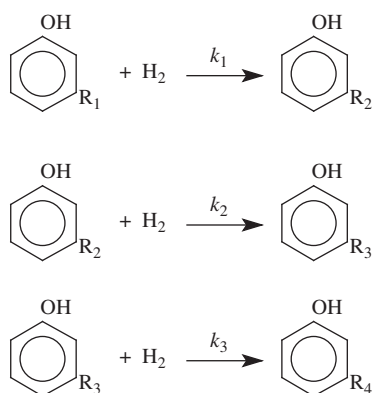
$$k_4 = 1.6 \times 10^{-4}$$

$$k_5 = 4.2 \times 10^{-4}$$

- (d) Indicate the time at which the concentration of species B is a maximum for each of the two models. The data below are available at  $160^\circ\text{C}$  for the concentrations of species B. Plot these points on the graphs prepared in part (c) and indicate which of the two models provides the best fit of the data at this temperature. The initial composition of the experimental system may be taken as 100% A.

Time (min)	B (% w/w)
0	0.0
20	2.3
30	3.5
60	5.2
90	3.2
120	2.4
180	2.2

- 5.16** V. Madhusudhan, M. A. Sivasamban, R. Vaidyeswaran, and M. Bhagawanthan Rao [*Ind. Eng. Chem. Process Des. Devel.*, **20**, 625 (1981)] studied the kinetics of the hydrogenation of cardanol over Raney nickel:



The reactions of interest involve the successive hydrogenation of tri-, di-, and monoolefinic *meta*-substituted phenols to produce 3-pentadecylphenol, where  $\text{R}_1 = \text{C}_{15}\text{H}_{25}$ ,  $\text{R}_2 = \text{C}_{15}\text{H}_{27}$ ,  $\text{R}_3 = \text{C}_{15}\text{H}_{29}$  and  $\text{R}_4 = \text{C}_{15}\text{H}_{31}$ . These four species will be referred to as A, B, C, and D, respectively.

For the experimental conditions employed (constant hydrogen pressure and constant weight of catalyst), all three reactions may be viewed as zero-order in hydrogen and first-order in the *meta*-substituted phenol. These researchers reported that at  $140^\circ\text{C}$  the pseudo first-order rate constant  $k_1 = 0.1295 \text{ min}^{-1}$ ,  $k_1/k_2 = 19.7$ , and  $k_1/k_3 = 22.9$ .

For an experiment at  $140^\circ\text{C}$  with a liquid of the initial composition

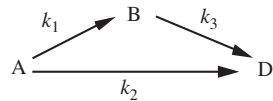
$$\begin{aligned}
 C_{A0} &= 0.8703 \text{ M} \\
 C_{B0} &= 0.7412 \text{ M} \\
 C_{C0} &= 1.4843 \text{ M} \\
 C_{D0} &= 0.0000 \text{ M}
 \end{aligned}$$

maxima were observed in the concentrations of species B and C.

- (a) At what times do these maxima occur?  
 (b) Prepare plots of the concentrations of species A, B, C, and D as functions of time for the interval from 0 to 400 min.

- 5.17** B. S. Gevert, J.-E. Otterstedt, and F. E. Massoth [*Appl. Catal.*, **31**, 119–131 (1987)] studied the kinetics of the hydrodeoxygenation of 4-methylphenol in an autoclave

over a sulfided commercial catalyst. In the presence of a large excess of hydrogen, the reactions of interest can be regarded as pseudo first-order in the various organic species, and the reaction network can be represented in symbolic fashion as



where A represents 4-methylphenol, B represents toluene, and D represents the sum of methylcyclohexane and methylcyclohexene. If the only reactive species in the initial charge to the reactor is species A, prepare plots of the dimensionless concentrations of the various species ( $\text{A}/\text{A}_0$ ,  $\text{B}/\text{A}_0$ ,  $\text{D}/\text{A}_0$ ) versus time for the following values of the pseudo first-order rate constants which are appropriate for use at the temperature and hydrogen pressure of interest:

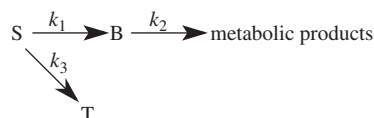
$$k_1 = 2.4 \text{ min}^{-1}$$

$$k_2 = 0.52 \text{ min}^{-1}$$

$$k_3 = 0.0026 \text{ min}^{-1}$$

Consider times up to 5.0 min. Use both graphical and analytical approaches to determine the time at which the concentration of species B reaches a maximum.

- 5.18** A. W. Jones and K. A. Jonsson [*Br. J. Clin. Pharmacol.*, **37**, 427–431 (1994)] investigated the pharmacokinetics of ethanol in men. One reaction network that can be used to describe the observed data is as follows:

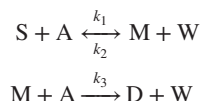


where S refers to the quantity of ethanol in the stomach and digestive tract, B refers to alcohol absorbed in the bloodstream, and T refers to alcohol absorbed directly from the stomach by other organs and tissues.

- (a) If the system of interest is modeled as a constant volume batch reactor for which  $k_1 = 0.0029 \text{ min}^{-1}$ ,  $k_2 = 750 \text{ mg/h}$ , and  $k_3 = 885 \text{ mg/min}$ , derive the equations that describe how S, B, and T (in grams) vary with time and plot the results for times from zero to 3 h. You may assume that all subjects rapidly consume 60 g of alcohol after a 10-h fast (i.e., both B and T are zero at time zero). You should note that “reactions” 2 and 3 are zero-order processes and that “reaction” 1 is a first-order process. You should also note that once S becomes zero, reactions 1 and 3 will cease and the equations that are applicable at short times will no longer be valid.  
 (b) Use the model and a nongraphical procedure to determine the maximum quantity of alcohol in the blood and the time at which this maximum is reached. The experimental data indicate that this maximum is reached approximately 1 h after ingestion of the alcohol.

- (c) If the legal limit for blood alcohol content is 0.08 g/dL, how long will it be before a person who ingests 100 g of ethanol can legally drive a vehicle? The average volume of blood in the body may be taken as 5.7 L. Plot the concentration of ethanol in the blood in g/dL for times from zero to 5 h. You may consider the circulatory system to be well mixed so that the ethanol concentration in the blood is constant throughout the body.

- 5.19** J. A. Arcos and C. Otero-Hernandez (personal communication) studied the enzyme-catalyzed reactions of various sugars (S) with fatty acids (A) to form mono- (M) and di- (D) esters. In generic form the reaction network of interest can be regarded as

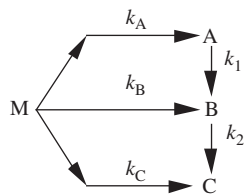


where W is water and where the rate expressions for the indicated reactions are of the mixed second-order form.

Consider these reactions as they occur in solution under conditions such that the rate expressions all degenerate to pseudo first-order forms; that is, (A) is approximately constant because of the use of a large excess of this material, and (W) is approximately constant at a low value because molecular sieves were used by these researchers to absorb the water formed in the two esterification reactions.

- (a) Derive equations for the concentrations of species S and M as functions of time for the general situation in which both species S and M are present in the initial reaction mixture. Use an overall material balance to relate the concentration of the diester D to the concentrations of S and M at any time and the initial concentrations of these species.
- (b) Prepare plots of the dimensionless concentrations of species S, M, and D as functions of dimensionless time ( $k_1 A_0 t$ ) for values of this parameter from 0 to 5. Note that the dimensionless time can be regarded as the product of the pseudo first-order rate constant ( $k_1 A_0$ ) and the actual time. The concentrations are to be normalized with respect to the initial concentration of the sugar,  $S_0$ . Prepare plots for the case where  $M_0 = 0$  for values of  $k_1 A_0 / k_2 W_0$  equal to 10 and 1, and values of  $k_3 / k_1$  equal to 0.5 and 1 (four plots). Comment, taking into account both the time necessary to achieve high conversions of the reacting sugar and the product distribution.

- 5.20** K. Yamasaki, A. Watanabe, T. Kakuda, and I. Tokue [*Int. J. Chem. Kinet.*, **30**, 47–54 (1988)] developed a new procedure for analyzing the rates of very rapid reactions. In their analysis, these investigators considered a variety of reaction networks. A particularly interesting case is that represented by the following sequence of reactions:



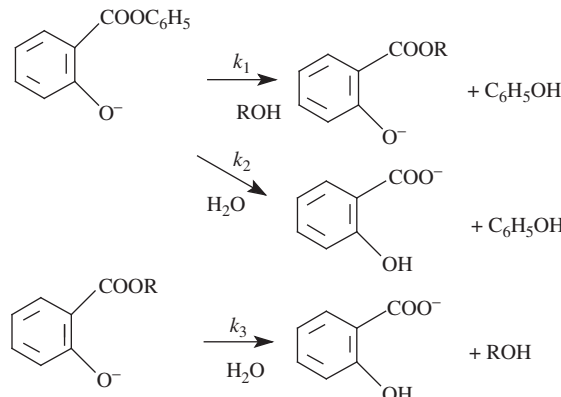
Consider these reactions as they occur isothermally in a batch reactor that initially contains only species M at a concentration  $M_0$ .

- (a) Derive equations relating the concentrations of species M, A, B, and C, the several rate constants, and time.
- (b) Prepare plots of the dimensionless concentrations  $[(M/M_0), (A/M_0), (B/M_0), \text{ and } (C/M_0)]$  for times between zero and 100  $\mu$ s and the following values of the rate constants:

$$\begin{aligned} k_A &= 2 \times 10^5 \text{ s}^{-1} \\ k_B &= 1 \times 10^5 \text{ s}^{-1} \\ k_C &= 5 \times 10^4 \text{ s}^{-1} \\ k_1 &= 1.5 \times 10^4 \text{ s}^{-1} \\ k_2 &= 5 \times 10^3 \text{ s}^{-1} \end{aligned}$$

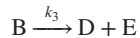
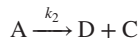
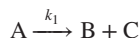
- (c) Derive a closed-form expression for the time at which species A is a maximum. What time corresponds to the values of the rate constants indicated in part (b)?
- (d) Determine the time corresponding to the maximum concentration of species B for the values of the rate constants indicated above.
- (e) How will the shapes of the various curves determined in part (b) vary if the value of  $k_1$  becomes very small compared to the values of the other rate constants? Indicate the shapes of the curves for the various species.

- 5.21** M. Niyaz Khan [*Int. J. Chem. Kinet.*, **19**, 757–776 (1987)] studied the kinetics of the alcoholysis of phenyl salicylate in aqueous mixed solvents. For reaction at 30°C in basic (0.05 M NaOH) solution containing 5% (*v/v*) methanol and 0.8% methyl cyanide, the reaction network can be described as follows:



where each of the irreversible reactions indicated is pseudo first-order in the aromatic species and where R represents

$\text{CH}_3$ . In shorthand notation these reactions may be written as



- (a) Derive equations that describe how the concentrations of the various species (A, B, C, D, and E) vary with time when the feed concentration of phenyl salicylate is  $\text{A}_0$  and no other aromatic species is present in the feed.
- (b) Prepare plots of the species concentrations for reaction at  $30^\circ\text{C}$  in this medium. At these conditions the values of the pseudo first-order rate constants are as follows:

$$k_1 = 2.01 \times 10^{-3} \text{ s}^{-1}$$

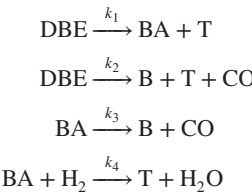
$$k_2 = 5.01 \times 10^{-4} \text{ s}^{-1}$$

$$k_3 = 1.34 \times 10^{-4} \text{ s}^{-1}$$

Use  $\text{A}_0 = 1.6 \times 10^{-4} \text{ M}$  and times ranging from 0 to 40 min.

- (c) Use both an analytical approach and a graphical approach to determine the time at which the concentration of methyl salicylate (species B) is maximized. What is the value of this concentration?

- 5.22 I. V. Kalechits, V. Yu. Korobkov, E. N. Grigor'eva, O. V. Sen'ko, and V. I. Bykov [*Kinet. Catal.*, **28**, 914 (1987)] studied the kinetics of the pyrolysis of dibenzyl ether at temperatures from 350 to  $410^\circ\text{C}$  in an environment containing both hydrogen and tetralin. These researchers have reported that the decomposition reaction can be modeled in terms of the following reaction network:



where DBE is dibenzyl ether, T is toluene, BA is benzaldehyde, and B is benzene. Because of the presence of a large excess of hydrogen, reaction 4 may be regarded as pseudo first-order in benzaldehyde.

- (a) Derive equations that describe the variation of the concentrations of DBE, BA, B, and T with time in a constant-volume batch reactor. You may assume that only DBE,  $\text{H}_2$ , and tetralin are present initially.
- (b) Use these equations to prepare plots of the concentrations of these four species for reaction at  $380^\circ\text{C}$  and times from zero to 120 min. At  $380^\circ\text{C}$ , the values of the first-order rate constants are

$$k_1 = 1.4 \times 10^{-2} \text{ min}^{-1}$$

$$k_2 = 0.45 \times 10^{-2} \text{ min}^{-1}$$

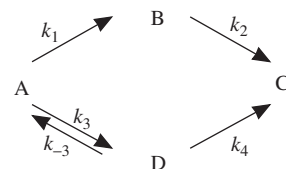
$$k_3 = 6.5 \times 10^{-4} \text{ min}^{-1}$$

$$k_4 = 1.4 \times 10^{-2} \text{ min}^{-1}$$

Express your results in dimensionless form by normalizing each concentration by the initial concentration of DBE.

- (c) Derive a closed form expression for the time at which the concentration of benzaldehyde passes through a maximum.
- (d) Compute the value of this time and compare the result with that determined from the plot in part (b).

- 5.23 M. Bikrani, L. Fidalgo, M. A. Garralda, and C. Ubide [*J. Mol. Catal.*, **118**, 47–53 (1997)] studied the catalytic activity of cationic iridium complexes for homogeneous hydrogen transfer from isopropanol to 2-cyclohexen-1-one to give cyclohexanol. The reaction network contains consecutive, competitive, and reversible elements. In isopropanol these elements can be expressed as pseudo first-order processes:



where A is 2-cyclohexen-1-one, B is cyclohexone, C is cyclohexanol, and D is 2-cyclohexenol.

- (a) Derive the equations that govern the time dependence of the concentrations of the three species of primary interest (A, B, and C) for the case in which all of the indicated reactions obey pseudo first-order kinetics and in which species D is so reactive that it never accumulates to a significant extent. The latter constraint implies that one may assume that the concentration of D is both small and substantially constant throughout the course of the reaction. You may assume that only species A is present initially.
- (b) The following rate constants are applicable at  $83^\circ\text{C}$ :

$$k_1 = 1.4 \times 10^{-3} \text{ s}^{-1}$$

$$k_2 = 1.2 \times 10^{-4} \text{ s}^{-1}$$

$$k^1 = 1.8 \times 10^{-3} \text{ s}^{-1}$$

$$k^{11} = 4 \times 10^{-4} \text{ s}^{-1}$$

where

$$k^1 = k_1 + k_3 - \frac{k_3 k_{-3}}{k_{-3} + k_4}$$

and

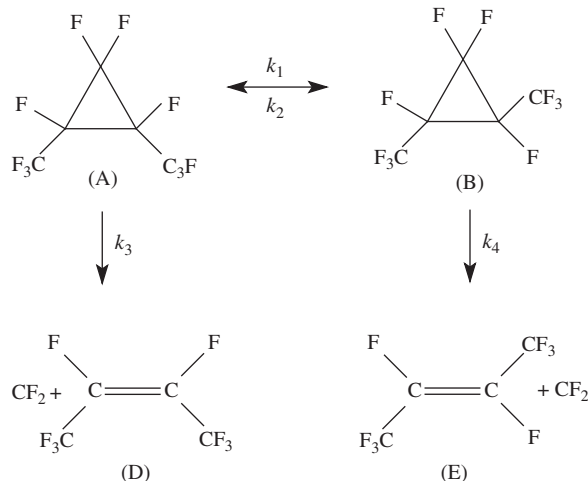
$$k^{11} = k^1 - k_1 = \frac{k_4 k_3}{k_{-3} + k_4}$$

Prepare plots of the concentrations of species A, B, and C for the time interval from zero to 3 h. Express the species concentrations relative to the initial concentration of species A.

- (c) Use the answers developed in parts (a) and (b) to determine the time at which the concentration of species B

passes through a maximum. Is the result obtained from the plot consistent with the closed form expression for this time that you derive from your expression for  $B(t)$ ?

- 5.24 J. C. Ferrero and E. H. Staricco [*Int. J. Chem. Kinet.*, **11**, 1287 (1979) studied the kinetics of the gas-phase thermal isomerization and decomposition of *cis*-bis(trifluoromethyl)-1, 2, 3, 4-tetrafluorocyclopropane (species A):



- (a) Consider the situation in which this reaction is carried out in a constant volume batch reactor starting with pure A. Derive equations that describe the variations of the concentrations of species A, B, D, and E with time.

(b) At 513.5 K the values of the rate constants are:

$$k_1 = 68.3 \times 10^{-5} \text{ s}^{-1}$$

$$k_7 = 16.14 \times 10^{-5} \text{ s}^{-1}$$

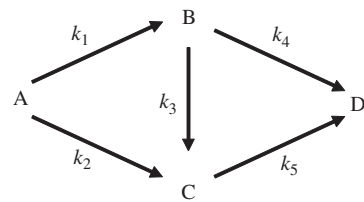
$$k_3 = 2.94 \times 10^{-5} \text{ s}^{-1}$$

$$k_4 = 1.92 \times 10^{-5} \text{ s}^{-1}$$

Use machine computation to prepare plots of the concentrations of species A, B, D, and E for isothermal reaction at this temperature for the first 10 ks of reaction (start with pure A and express all concentrations relative to  $A_0$ ).

- (c) At what time does the concentration of species B pass through a maximum when the reaction occurs isothermally at 513.5 K? Use both your plot and a closed form analytical solution to determine this time.

- 5.25 I. A. Eldib and L. F. Albright [*Ind. Eng. Chem.*, **49**, 825 (1957)] indicated that the main reactions in the catalytic hydrogenation of cottonseed oil are



where A is linoleic acid, B is *cis*-oleic acid, C is isoleic acid, and D is stearic acid.

- (a) If each of these reactions is regarded as irreversible pseudo first-order, derive equations for the time dependence of each species in terms of the initial concentrations and the appropriate rate constants. For run 3, the following parameter values were estimated.

$$k_1 = 0.0133 \text{ min}^{-1}$$

$$k_2 = 0.0108 \text{ min}^{-1}$$

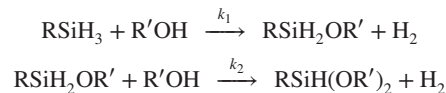
$$k_3 = 0.0024 \text{ min}^{-1}$$

$$k_4 = 0.0024 \text{ min}^{-1}$$

$$k_5 = 0.0080 \text{ min}^{-1}$$

- (b) If one were to start with pure linoleic acid, determine the time dependent behavior of all species in terms of normalized concentrations ( $C_i/C_{A0}$ ).

- 5.26** The reaction of *p*-chlorophenylsilane with benzyl alcohol may be characterized as follows:



where both reactions are second-order overall, first-order in each reactant. From the following data determine the two rate constants if the reaction of 127.3 mg of *p*-chlorophenylsilane with 198.2 mg of benzyl alcohol in the presence of metallic copper liberated hydrogen gas to the extent noted below.

Time, $t$ (s)	$\text{cm}^3 \text{ H}_2$ (at STP)
62	8.12
116	12.18
198	16.24
396	20.30
878	24.36

The initial silane concentration is equivalent to 0.5 kmol/m<sup>3</sup>.

# Chapter 6

---

## Elements of Heterogeneous Catalysis

### 6.0 INTRODUCTION

Because the chemical, petrochemical, and petroleum industries rely heavily on catalytic processing operations and because of the utility of catalysts in remediating environmental problems (e.g., emissions from motor vehicles), chemical engineers must be cognizant of the fundamental and applied aspects of catalysis. Bartholomew and Farrauto (1) have indicated the immense leverage that the use of catalysts gives the world chemical industry; from a global economic perspective, in the early twenty-first century an investment of \$10 billion in catalyst technology led to some \$10 trillion worth of gross products, a multiplicative factor of 1000. Some commercially significant catalytic processes are listed in Table 6.1. In this chapter our discussion focuses on the chemical aspects of heterogeneous catalytic phenomena. Chapter 12 is devoted to the engineering aspects of catalytic phenomena that are involved in the design of commercial scale reactors.

Centuries ago when philosophical and metaphysical ideas enjoyed precedence over experimental facts as a source of scientific theory, many of the concepts that we now interpret as catalytic in nature played a key role in the theories of that era. The “Philosopher’s Stone” was a hypothetical substance that could turn base metals into gold and could promote good health and long life. Its chemical action required that a small quantity of this substance could bring about a large change, an idea inherent in the modern view of catalysis. The aura of mysticism that is associated with catalytic phenomena reaches back to the days of the alchemist. Only in recent years has catalysis been regarded more as a science than an art. Indeed, much art remains, and our imperfect understanding of catalysts has long been reflected in the manufacturing processes employed to produce commercial catalysts.

In 1835, Berzelius coined the term *catalysis* to describe the influence of certain substances on the nature of diverse reactions, the substances themselves apparently being unchanged by the reaction. He imbued these materials with a *catalytic force* capable of awakening the potential

for chemical reaction between species that would normally be nonreactive at a given temperature. In more modern terms the following definition is appropriate: *A catalyst is a substance that affects the rate or the direction of a chemical reaction, but is not appreciably consumed in the process.* There are three important aspects of the definition. First, a catalyst may increase or decrease the reaction rate. Second, a catalyst may influence the direction or selectivity of a reaction. Third, the amount of catalyst consumed by the reaction is negligible compared to the consumption of reactants.

Catalysts that decrease reaction rates are usually referred to as *inhibitors*. They often act by interfering with the free-radical processes involved in chain reactions, and the mechanism usually differs from that involved in accelerating a reaction. The most familiar example of the use of inhibitors has historically been the addition of additives such as tetraethyllead or methyl *tert*-butyl ether to gasoline to improve its antiknock properties.

A catalyst *cannot* change the *ultimate equilibrium point* set by thermodynamics, but it can affect the rate at which this point is approached. More importantly, it can facilitate the approach to equilibrium with respect to a desired reaction while not influencing the rates of other less desirable reactions. In optimizing yields of desired products, chemical engineers are very concerned with the *selectivity* or *specificity* of a catalyst; for commercial applications, selectivity is often more important than activity per se.

The idea that a catalyst remains unaltered by the reaction it catalyzes is naive and misleading. Physical and chemical changes can and do occur either during or as a result of the catalytic process. The ratio of metal to oxygen in an oxide catalyst will frequently change with changes in temperature and in the composition of the fluids with which it is in contact. Pure metal catalysts will often change in crystal structure or surface roughness on use. Many commercial catalysts are gradually deactivated by poisoning reactions that accompany the main reaction process. The catalysts used to initiate free-radical polymerization

**Table 6.1** Large-Scale Industrial Catalytic Reactions

Type of reaction <sup>a</sup>	Reactants	Catalysts	Products
1. Ammonia synthesis	$N_2 + H_2$	Iron oxide ( $Fe_3O_4$ ) promoted with $Al_2O_3$ and $K_2O$	$NH_3$
2. Ammonia oxidation	$NH_3 + O_2$	Pt-Rh	NO used in the manufacture of $HNO_3$
3. Oxidation of sulfur dioxide	$SO_2 + O_2$	$V_2O_5$ or Pt	$SO_3$ used in the manufacture of oleum and sulfuric acid
4. Hydrogenation of fats and edible oils	Unsaturated oil + $H_2$	Ni	Saturated oil or fat
5. Cracking	Various petroleum fractions	Combinations of silica, alumina, and molecular sieves	Wide range of compounds
6. Polymerization	Ethylene	Aluminum alkyls and $TiCl_4$ , $MoO_3$ , or $CrO_3$ on alumina	Polyethylene
7. Dehydrogenation	Ethylbenzene	Iron oxide or chromia alumina	Styrene

Source: From refs. 1 to 3.

<sup>a</sup>The first five processes are among the most important commercial catalytic processes in terms of total processing capacity.

reactions end up as an integral part of the polymer formed by the reaction and are thus consumed. In neither case does a stoichiometric whole-number relationship exist between the amount of the catalyst consumed and the amounts of reactants converted to products. The number of moles of reactants converted is often orders of magnitude greater than the number of moles of catalyst consumed.

For reversible reactions the principle of microscopic reversibility (Section 4.1.5.4) indicates that a material that accelerates the forward reaction will also catalyze the reverse reaction. In several cases where the catalytic reaction has been studied from both sides of the equilibrium position, the rate expressions observed are consistent with this statement.

Catalytic reactions are often classified as homogeneous or heterogeneous. True *homogeneous catalysis* takes place when the catalyst and the reactants are both present in the same fluid phase. Acid and base catalyzed reactions in aqueous solution are reactions of this type. Reactions that occur between a gas and a liquid or between two liquid phases are also generally considered to fall in this category. Although the mass transfer characteristics in these cases differ from those in which the reaction takes place in a single phase, the reactants are mobile in both phases. The characteristics of these reactions are much more similar to those of reactions occurring in a single fluid phase than they are to those of reactions occurring at a fluid–solid interface. The term *heterogeneous catalysis* is generally restricted to catalytic phenomena involving a solid catalyst

and reactants in a gas or liquid phase. These phenomena are sometimes referred to as *contact catalysis*.

Catalysts may be employed in solid, gaseous, or liquid form. However, the overwhelming majority of industrial catalytic processes involve solid catalysts and gaseous reactants. In many cases it is possible to develop useful new catalysts on the basis of analogies drawn between the behavior of certain chemical systems in the presence of heterogeneous or homogeneous catalysts. For example, reactions that take place in the presence of strong acids in liquid solution are often catalyzed by acidic solid catalysts such as silica–alumina. In some cases, inorganic salts or metal complexes that have catalytic activity in aqueous solution will exhibit activity for the same reaction when deposited on a solid support. For example, an aqueous solution of cupric chloride and palladium chloride can be used as a catalyst for oxidizing ethylene to acetaldehyde in the Wacker process (2). These same materials can be deposited on a solid support to obtain a heterogeneous catalyst for this reaction, although this is not done in the current commercial process.

## 6.1 ADSORPTION PHENOMENA

In this section we treat chemical and physical adsorption phenomena to provide necessary background material for the discussion of catalytic reaction mechanisms in Section 6.3.1.

*Adsorption is the preferential concentration of a species at the interface between two phases.* Adsorption

on solid surfaces is a very complex process and one that is not well understood. The surfaces of most heterogeneous catalysts are not uniform. Variations in energy, crystal structure, and chemical composition will occur as one moves about on the catalyst surface. Despite this situation, one can divide virtually all adsorption phenomena involving solid surfaces into two main classes: physical adsorption (also known as *physisorption*) and chemical adsorption (or *chemisorption*). Physical adsorption arises from *intermolecular* forces involving permanent dipole, induced dipole, and quadrupole interactions. This phenomenon involves van der Waals or secondary valence forces and is akin to condensation. Chemisorption, on the other hand, involves a chemical interaction with attendant transfer of electrons between the adsorbent and the adsorbing species (*adsorbate*). The adsorbed species are held to the surface by valence forces that are the same as those that hold atoms together in a molecule.

In practice, one can usually distinguish between chemisorption and physical adsorption on the basis of experimental evidence. However, it is frequently necessary to consider several criteria in making the classification. The most important criterion for differentiating between physical and chemical adsorption is the magnitude of the enthalpy change accompanying the adsorption process. The energy evolved when physical adsorption occurs is usually similar to the heat of liquefaction of the gas (i.e., approximately 2 to 6 kcal/mol). Like condensation, the process is exothermic. For physical adsorption the heat of adsorption often lies between the heat of vaporization and the heat of sublimation. The enthalpy change accompanying chemisorption is significantly greater than that for physical adsorption and, in some cases, may exceed 100 kcal/mol. More often it will lie between 10 and 50 kcal/mol. In practice, chemisorption is regarded as an exothermic process, and in the past the view was frequently expressed that endothermic adsorption could not occur. However, if a molecule dissociates on chemisorption and the dissociation energy of the molecule is greater than the energy of formation of the bonds with the surface, the process can be endothermic. Because the Gibbs free-energy change accompanying any spontaneous process must be negative, the only cases in which endothermic adsorption can be observed are those for which there will be a large positive entropy change. The dissociative chemisorption of hydrogen on glass is endothermic and is an example of this relatively rare phenomenon. More often, dissociative chemisorption is exothermic, like other chemisorption processes.

A second criterion that is frequently used to differentiate empirically between chemical and physical adsorption is the *rate* at which the process occurs and, in particular, the temperature dependence of the rate. For physical adsorption of a gas on a solid surface, equilibrium

is usually attained very quickly and is readily reversible. The activation energy of the process is usually less than 1 kcal/mol. Physical adsorption usually takes place so fast that the rate observed is limited by the rate at which molecules can be transported to the surface instead of by the adsorption process itself. Chemisorption may occur at rates comparable to those of physical adsorption, or it may occur at much slower rates, depending on the temperatures involved. Most types of chemisorption are characterized by a significant activation energy and thus proceed at appreciable rates only above certain minimum temperatures. This type of phenomenon is referred to as *activated chemisorption*. However, in some systems, chemisorption occurs very rapidly even at very low temperatures and has an activation energy near zero. For example, chemisorption of hydrogen and oxygen occurs on many clean metal surfaces at liquid nitrogen temperatures. These cases are described as *nonactivated chemisorption*. One often observes that for a given combination of adsorbent and adsorbate, chemisorption is nonactivated initially but, subsequently, chemisorption is activated.

Another aspect of rate measurements that is useful in discriminating between the two types of adsorption involves studies of the rate of desorption. The activation energy for desorption from a physically adsorbed state is seldom more than a few kilocalories per mole, whereas that for desorption from a chemisorbed state is usually in excess of 20 kcal/mol. Consequently, the ease with which desorption occurs on warming from liquid-nitrogen temperature to room temperature is often used as a quick test for determining the nature of the adsorption process.

A third empirical criterion is based on the effect of temperature on the amount adsorbed. For physical adsorption the amount of gas adsorbed always decreases monotonically as the temperature is increased. Significant amounts of physical adsorption should *not* occur at temperatures in excess of the normal boiling point at the operating pressure. Appreciable chemisorption can occur at temperatures above the boiling point and even above the critical temperature of the material. Because chemisorption can be an activated process that takes place at a slow rate, it may be difficult to determine the amount of chemisorption corresponding to true equilibrium. Moreover, the process may not be reversible. It is also possible for two or more types of chemisorption or for chemical and physical adsorption to occur simultaneously on the same surface. These facts make it difficult to generalize with regard to the effect of temperature on the amount adsorbed. Different behavior will be observed for different adsorbent-adsorbate systems.

The experimental procedure for measuring the extent of adsorption generally involves admitting a gas to a chamber that contains the sample and waiting for a fixed period of time, during which “equilibrium” is supposedly achieved. Figure 6.1 indicates one common type of

behavior that can be observed if physical adsorption and one type of activated chemisorption are present. At low temperatures, physical adsorption processes dominate and the amount of chemisorption is insignificant. The amount of material adsorbed physically decreases as the temperature increases. Within the time frame of the normal adsorption experiment, the amount of material adsorbed via the chemisorption process will increase as the temperature increases in the low-temperature range. Consequently, its contribution to the total will become more and more significant as the temperature rises, and one eventually reaches a point at which the decrease in physical adsorption with increasing temperature is more than offset by the increase in the amount of material that can be chemisorbed in the time period involved. Consequently, the total amount adsorbed will increase with increasing temperature over a limited temperature range. At higher temperatures the rate of desorption from the chemisorbed state begins to be more important, and the curve will go through a local maximum and then decrease. At the highest temperatures equilibrium can be established with respect to the chemisorption process. Note that the discussion above and the solid curve in Figure 6.1 apply to the situation where one starts at a low temperature and increases the temperature continuously. If we start at a high temperature and move in the direction of decreasing temperature, we would not retrace the solid curve but, instead, would follow the upper dashed line in Figure 6.1 until rate considerations again become significant. Beyond this point the experimental curve will again lie below the true equilibrium curve.

Another characteristic that can be used to differentiate between chemical and physical adsorption is the degree of specificity in the gas–solid interaction. Physical adsorption is nonspecific. Physisorption will occur on all surfaces for a given gas, provided that the ratio of the adsorbate partial pressure to its saturation vapor pressure is sufficiently large. Since chemisorption is a chemical reaction confined to the surface of a solid and since the possibility of chemical reaction is highly specific to the nature of the species involved, chemisorption can take place only if the adsorbate is capable of forming a chemical bond with the adsorbent. Moreover, because it requires a chemical interaction, chemisorption is limited to a maximum of one layer of molecules on the surface (a monolayer). It frequently involves lower coverage. The valence forces holding the molecules on the surface fall off very rapidly with distance and become too small to form chemical bonds when the distance from the solid surface exceeds normal bond distances. Chemical and physical adsorption can occur together, but any adsorbed layers beyond the first must be physically adsorbed.

Physical adsorption is a readily reversible process, and alternate adsorption and desorption stages can be carried out repeatedly without changing the character of the surface or the adsorbate. Chemisorption may or may not be

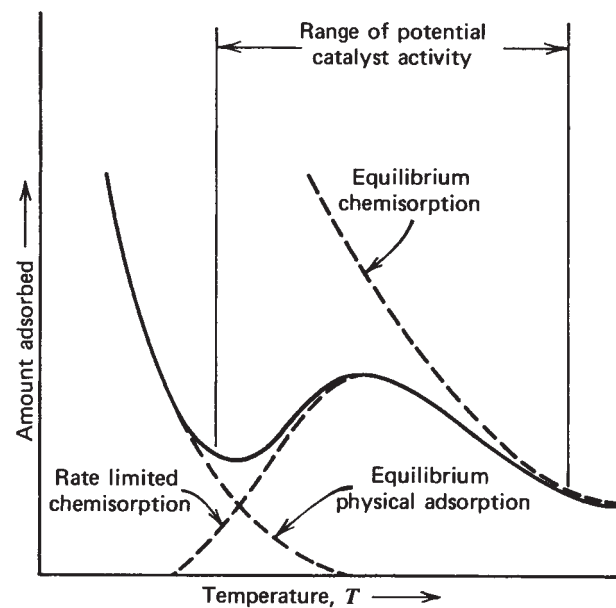


**Figure 6.1** Effects of temperature on amount adsorbed for simultaneous physical adsorption and activated chemisorption. (Adapted from J. M. Smith, *Chemical Engineering Kinetics*, 3rd ed. Copyright © 1970. Used with permission of McGraw-Hill Book Company.)

reversible. Often one species may be adsorbed and a second desorbed. Oxygen adsorbed on charcoal at room temperature is held very strongly, and high temperatures are necessary to accomplish the desorption. CO and/or  $\text{CO}_2$  are the species that are removed from the surface. Chemical changes like these are *prima facie* evidence that chemisorption has occurred.

Although no single definitive test is available to characterize the type of adsorption that takes place in an arbitrary system, the general criteria discussed above, taken collectively, provide a suitable basis for discrimination. Table 6.2 contains a summary of these criteria.

One of the basic tenets of virtually all mechanistic approaches to heterogeneous catalysis is that chemisorption of one or more reactant species is an essential step in the reaction. Because of the large changes in activation energies that are observed when shifting from a homogeneous reaction to one that is heterogeneously catalyzed, energetic considerations indicate that chemisorption must be involved. The forces involved in physical adsorption are so small relative to those involved in chemical bonding that it is difficult to imagine that they can distort the electron clouds associated with a molecule to such an extent that they have an appreciable effect on its reactivity. Many heterogeneous catalytic reactions take place at temperatures above the critical temperatures of the reactants involved and, presumably, physical adsorption cannot occur under these conditions.

**Table 6.2** Comparison of Chemisorption and Physical Adsorption

Parameter	Chemical adsorption	Physical adsorption
Bonding forces	Primary valence forces (intramolecular forces)	Secondary valence forces (intermolecular forces)
Coverage	Monolayer	Multilayer
Adsorbent	Some solids	All solids
Adsorbate	Chemically reactive vapors	All gases below critical temperature
Reversibility	May be reversible or irreversible	Readily reversible
Rate	May be fast or slow, depending on the temperature	Rapid, may be limited by diffusion
Temperature dependence	May be complex (see Figure 6.1)	Decreases with increasing temperature
Enthalpy effect	Virtually always exothermic, similar in magnitude to heats of reaction	Always exothermic, similar in magnitude to heats of condensation
Uses of adsorption studies	Determination of catalytically active surface area and elucidation of reaction kinetics	Determination of specific surface areas and pore size distributions

Chemisorption has, however, been observed in many such cases.

In this section we have treated the qualitative features of chemisorption and physical adsorption processes. Both are important to the chemical engineer who is interested in the design of heterogeneous catalytic reactors: chemisorption because it is an essential precursor of the reaction, and physical adsorption because it provides a means of characterizing heterogeneous catalysts in terms of specific surface areas and the distribution of pore sizes within a porous catalyst.

## 6.2 ADSORPTION ISOTHERMS

Plots of an amount of material adsorbed versus pressure at a fixed temperature are known as *adsorption isotherms*. They are generally classified in the five main categories described by Brunauer et al. (4). In Figure 6.2, adsorbate partial pressures ( $P$ ) are normalized by dividing by the saturation pressure at the temperature in question ( $P_0$ ). Type I, referred to as *Langmuir-type adsorption*, is characterized by a monotonic approach to a limiting amount of adsorption, which presumably corresponds to formation of a monolayer. This type of behavior is that expected for chemisorption. No other isotherms imply that one can reach a saturation limit corresponding to completion of a monolayer.

Type II is typical of the behavior normally observed for physical adsorption. At values of  $P/P_0$  approaching unity, capillary and pore condensation phenomena occur. The knee of the curve corresponds roughly to completion of a monolayer. A statistical monolayer is built up at relatively low values of  $P/P_0$  (0.1 to 0.3).

Type IV behavior is similar to type II behavior except that a limited pore volume is indicated by the horizontal approach to the right-hand ordinate axis. This type of curve is relatively common for porous structures of many kinds. Hysteresis effects associated with pore condensation are often, but not always, encountered in this type of system. They arise from the effects of surface curvature on vapor pressure.

Types III and V are relatively rare. They are typical of cases in which the forces giving rise to monolayer adsorption are relatively weak. Type V differs from type III in the same manner that type IV differs from type II.

There are three approaches that may be used in deriving mathematical expressions for an adsorption isotherm. The first utilizes kinetic expressions for the rates of adsorption and desorption. At equilibrium these two rates must be equal. A second approach involves the use of statistical thermodynamics to obtain a pseudo-equilibrium constant for the process in terms of the partition functions of vacant sites, adsorbed molecules, and gas-phase molecules. A third approach based on classical thermodynamics is also possible. Because it provides a useful physical picture of the molecular processes involved, we adopt the kinetic approach in our derivations.

The Langmuir adsorption isotherm provides a simple mechanistic picture of the adsorption process and gives rise to a relatively simple mathematical expression. This isotherm can also be used to obtain a crude estimate of specific surface areas. More important, from the viewpoint of the chemical engineer, it serves as a point of departure for formulating rate expressions for heterogeneous catalytic reactions.

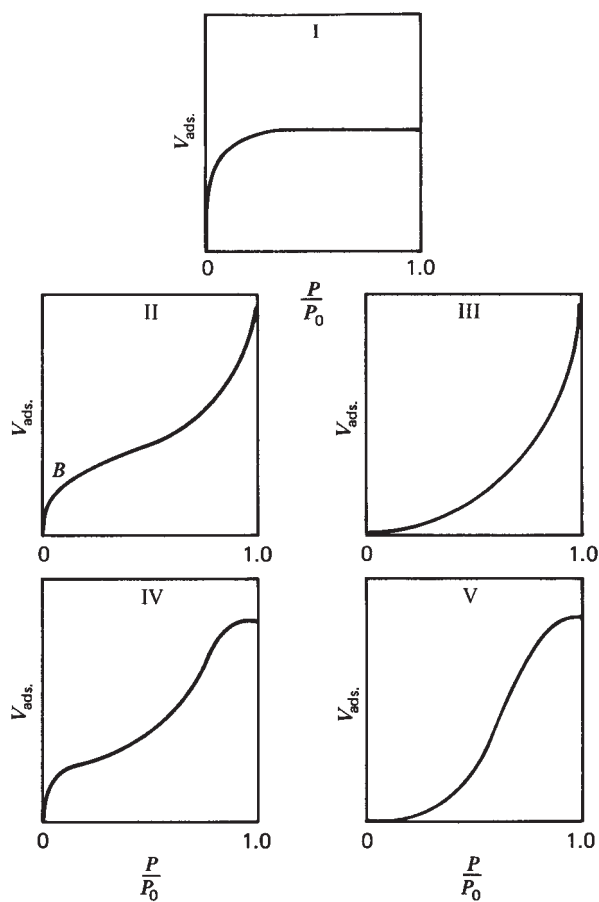


**Figure 6.2** Five types of isotherms for adsorption. (Adapted with permission from S. Brunauer, L. S. Deming, W. E. Deming, and E. Teller, On a Theory of the Van der Waals Adsorption of Gases, *J. Am. Chem. Soc.*, **62**, 1723. Copyright © 1940, American Chemical Society.)

### 6.2.1 The Langmuir Adsorption Isotherm

Virtually all theoretical treatments of adsorption phenomena are based on or can readily be related to the analysis developed by Langmuir (5, 6). The Langmuir isotherm corresponds to a highly idealized type of adsorption and the analysis is predicated on the following key assumptions.

1. Gas-phase molecules are adsorbed at discrete points of attachment on the surface that are referred to as *adsorption sites*. Each site can accommodate only a single adsorbed species.
2. The energy of an adsorbed species is the same anywhere on the surface and is independent of the presence or absence of nearby adsorbed molecules. This assumption implies that the forces between adjacent adsorbed molecules are so small as to be negligible and that the probability of adsorption on an empty site is independent of whether or not an adjacent site is

occupied. This assumption usually implies that the surface is completely uniform in an energetic sense. If one prefers to use the concept of a nonuniform surface with a limited number of active centers that are the only points at which chemisorption occurs, this approach is permissible if it is assumed that all these active centers have the same activity for adsorption and that the rest of the surface has none.

3. The maximum amount of adsorption that is possible is that which corresponds to a monolayer.
4. Adsorption is localized and occurs by collision of gas-phase molecules with vacant sites.
5. The desorption rate depends only on the amount of material on the surface.

For physical adsorption processes the third assumption is the poorest of these assumptions. For the case of chemical adsorption the worst of these assumptions is the second. There is a significant amount of experimental evidence that is contradictory to this assumption. Taylor (7) was the first person to emphasize that adsorption sites may vary in energy. He noted that atoms at peaks on the surface and along crystal edges will be in high-energy states and will be the points at which adsorption first occurs. Other evidence for the lack of surface uniformity includes experimental data indicating that:

1. Adsorption of a catalyst poison to an extent that represents only a very small fraction of a monolayer can cause an extremely disproportionate reduction in catalytic activity.
2. Heats of chemisorption usually decrease markedly as adsorption proceeds and the surface becomes covered.

In using the Langmuir adsorption isotherm as a basis for correlating heterogeneous catalytic rate data, the fact that the heat of chemisorption varies with the extent of adsorption is less significant than would appear at first glance. Molecules adsorbed on high-energy sites may be bound so strongly that they are unable to serve as intermediates in the catalytic reaction. On the low-energy sites the energy change on adsorption may be insufficient to open up the catalytic path for the reaction. It is possible that only those sites of intermediate energy are effective in catalysis.

#### 6.2.1.1 Derivation of the Langmuir Equation: Adsorption of a Single Species

The kinetic approach to deriving a mathematical expression for the Langmuir isotherm assumes that the rate of adsorption on the surface is proportional to the product of the partial pressure of the adsorbate in the gas phase and the fraction of the surface that is bare. (Adsorption may occur

only when a gas-phase molecule strikes an uncovered site.) If the fraction of the surface covered by an adsorbed gas A is denoted by  $\theta_A$ , the fraction that is bare will be  $(1 - \theta_A)$  if no other species are adsorbed. If the partial pressure of A in the gas phase is  $P_A$ , the rate of adsorption is given by

$$r_{\text{adsorption}} = kP_A(1 - \theta_A) \quad (6.2.1)$$

where  $k$  may be regarded as a “pseudo rate constant” for the adsorption process.

The rate of desorption depends only on the number of molecules that are adsorbed. Thus,

$$r_{\text{desorption}} = k'\theta_A \quad (6.2.2)$$

where  $k'$  may be regarded as a pseudo rate constant for the desorption process.

At equilibrium the rates of adsorption and desorption are equal:

$$kP_A(1 - \theta_A) = k'\theta_A \quad (6.2.3)$$

The fraction of the sites occupied by species A is then

$$\theta_A = \frac{kP_A}{k' + kP_A} \quad (6.2.4)$$

If one takes the ratio of the pseudo rate constant for adsorption to that for desorption as an equilibrium constant for adsorption ( $K$ ), equation (6.2.4) can be written as

$$\theta_A = \frac{(k/k')P_A}{1 + (k/k')P_A} = \frac{KP_A}{1 + KP_A} \quad (6.2.5)$$

The fraction of the sites that are occupied is also equal to the ratio of the volume of gas actually adsorbed to that which would be adsorbed in a monolayer ( $v_m$ ).

$$\theta_A = \frac{v}{v_m} \quad (6.2.6)$$

Both volumes are measured at standard conditions (0°C, 1 atm) or at some other fixed reference temperature and pressure.

The last two equations can be combined to give a relation between the pressure of the gas and the amount that is adsorbed:

$$v = \frac{v_m KP_A}{1 + KP_A} \quad (6.2.7)$$

A plot of  $v$  versus  $P_A$  is of the same form as the type I adsorption isotherm. At low values of  $P_A$  the term  $KP_A$  is small compared to unity, and the amount adsorbed will be linear in pressure. At high pressures the term  $KP_A$  is large compared to unity, and the surface coverage is nearly complete. In this case  $v$  will approach  $v_m$ , the volume equivalent to formation of a monolayer.

Equation (6.2.7) may be transformed into several expressions that can be used in analyzing experimental

data. However, the following form is preferred because it avoids undue emphasis on the low pressure points—those that are most susceptible to error.

$$\frac{P_A}{v} = \frac{1}{v_m K} + \frac{P_A}{v_m} \quad (6.2.8)$$

If type I adsorption behavior is obeyed, a plot of  $P_A/v$  versus  $P_A$  should be linear with slope  $1/v_m$ . Once the volume corresponding to a monolayer has been determined, it can be converted to the number of molecules adsorbed by dividing by the molar volume at the reference conditions and multiplying by Avogadro’s number ( $N_0$ ). When this number of molecules is multiplied in turn by the area covered per adsorbed molecule ( $\alpha$ ), the total surface area of the catalyst (S) is obtained. Thus,

$$S = \frac{v_m N_0}{v_{\text{reference conditions}}} \alpha \quad (6.2.9)$$

Specific surface areas are then obtained by dividing by the weight of catalyst employed in the experiments in question. It should be pointed out, however, that it is the BET adsorption isotherm that is the basis for conventional determinations of catalyst surface areas (see Section 6.2.2).

### 6.2.1.2 The Langmuir Equation for the Case Where Two or More Species May Adsorb

Adsorption isotherms for situations in which more than one species may adsorb are of considerable significance when one is dealing with heterogeneous catalytic reactions. Reactants, products, and inert species may all adsorb on the catalyst surface. Consequently, it is useful to develop generalized Langmuir adsorption isotherms for multicomponent adsorption. If  $\theta_i$  represents the fraction of the sites occupied by species  $i$  and  $\theta_v$  is the fraction of the sites that are vacant, then  $\theta_v = \left[1 - \sum_i \theta_i\right]$ , where the summation is taken over all species that can be adsorbed. The pseudo rate constants for adsorption and desorption may be expected to differ for each species, so they will be denoted by  $k_i$  and  $k'_i$ , respectively.

The rates of adsorption and desorption of each species must be equal at equilibrium. Thus:

For species A:

$$k_A P_A (1 - \theta_A - \theta_B - \theta_C \dots) = k'_A \theta_A$$

For species B:

$$k_B P_B (1 - \theta_A - \theta_B - \theta_C \dots) = k'_B \theta_B \quad (6.2.10)$$

For species C:

$$k_C P_C (1 - \theta_A - \theta_B - \theta_C \dots) = k'_C \theta_C$$

where  $P_i$  is the partial pressure of the  $i$ th species in the gas phase.

If these equations are solved for the fractions occupied by each species,

$$\begin{aligned}\theta_A &= \frac{k_A}{k'_A} P_A (1 - \theta_A - \theta_B - \theta_C \dots) \\ &= K_A P_A (1 - \theta_A - \theta_B - \theta_C \dots) \\ \theta_B &= \frac{k_B}{k'_B} P_B (1 - \theta_A - \theta_B - \theta_C \dots) \\ &= K_B P_B (1 - \theta_A - \theta_B - \theta_C \dots) \\ \theta_C &= \frac{k_C}{k'_C} P_C (1 - \theta_A - \theta_B - \theta_C \dots) \\ &= K_C P_C (1 - \theta_A - \theta_B - \theta_C \dots)\end{aligned}\quad (6.2.11)$$

where the adsorption equilibrium constants  $K_i$  have been substituted for the ratios of  $k_i$  to  $k'_i$ . If the expressions for  $\theta_i$  are added,

$$\theta_A + \theta_B + \theta_C + \dots = (1 - \theta_A - \theta_B - \theta_C \dots) \times (K_A P_A + K_B P_B + K_C P_C + \dots) \quad (6.2.12)$$

or

$$\sum \theta_i = \left(1 - \sum \theta_i\right) \left(\sum K_i P_i\right) \quad (6.2.13)$$

Solving for  $\sum \theta_i$  yields

$$\sum \theta_i = \frac{\sum K_i P_i}{1 + \sum K_i P_i} \quad (6.2.14)$$

or

$$1 - \sum \theta_i = \frac{1}{1 + \sum K_i P_i} = \theta_v \quad (6.2.15)$$

where  $\theta_v$  is the fraction of the sites that are vacant. Thus

$$\theta_A = \frac{K_A P_A}{1 + \sum K_i P_i} = \frac{K_A P_A}{1 + K_A P_A + K_B P_B + K_C P_C + \dots} \quad (6.2.16)$$

and

$$\theta_B = \frac{K_B P_B}{1 + K_A P_A + K_B P_B + K_C P_C + \dots} \quad (6.2.17)$$

Note that at low surface coverages where  $(1 + K_A P_A + K_B P_B + K_C P_C + \dots) \approx 1$ , the fraction of the sites occupied by each species will be proportional to its partial pressure.

### 6.2.1.3 The Langmuir Equation for the Case in Which Dissociation Occurs on Adsorption

There is evidence that certain chemical adsorption processes involve dissociation of the adsorbate to form two bonds with the adsorbent surface. On many metals, hydrogen is adsorbed in atomic form. For such situations the kinetic approach to the derivation of the Langmuir equation requires that the process be regarded as a reaction between the gas molecule and *two vacant surface sites*. Thus, the adsorption rate is written as

$$r_{\text{adsorption}} = k_A P_A \theta_v^2 = k_A P_A (1 - \theta_A)^2 \quad (6.2.18)$$

where we have assumed that only species A is adsorbed.

The desorption process must involve a reaction between two adsorbed atoms to regenerate the gas-phase molecules. Consequently, it may be regarded as a second-order reaction between two surface species:

$$r_{\text{desorption}} = k'_A \theta_A^2 \quad (6.2.19)$$

At equilibrium,

$$k_A P_A (1 - \theta_A)^2 = k'_A \theta_A^2 \quad (6.2.20)$$

or

$$\frac{\theta_A}{1 - \theta_A} = \sqrt{\frac{k_A P_A}{k'_A}} = \sqrt{K_A P_A} \quad (6.2.21)$$

Solving for  $\theta_A$  gives us

$$\theta_A = \frac{\sqrt{K_A P_A}}{1 + \sqrt{K_A P_A}} \quad (6.2.22)$$

At low pressures where the surface is sparsely covered, the fraction of the sites occupied by fragments of species A will be proportional to the square root of the gas-phase partial pressure.

If several species can adsorb but only species A dissociates, it is easily shown, using the type of analysis employed in Section 6.2.1.2, that

$$\theta_A = \frac{\sqrt{K_A P_A}}{1 + \sqrt{K_A P_A} + K_B P_B + K_C P_C} \quad (6.2.23)$$

and that for species that do not dissociate,

$$\theta_B = \frac{K_B P_B}{1 + \sqrt{K_A P_A} + K_B P_B + K_C P_C} \quad (6.2.24)$$

### 6.2.2 The BET Isotherm

Inasmuch as the Langmuir equation does not allow for nonuniform surfaces, interactions between neighboring adsorbed species, or multilayer adsorption, a variety of theoretical approaches that attempt to take one or more of these factors into account have been pursued by different investigators. The best known alternative is the *BET isotherm*, which derives its name from the initials of the three people responsible for its formulation: Brunauer, Emmett, and Teller (8). It takes multilayer adsorption into account and is the basis of standard methods for determining specific surface areas of heterogeneous catalysts. The extended form of the BET equation (4) can be used to derive relations for all five types of isotherms as special cases.

The BET approach is essentially an extension of the Langmuir approach. Van der Waals forces are regarded as the dominant forces, and the adsorption of all layers is regarded as physical, not chemical. One sets the rates of adsorption and desorption equal to one another, as in the Langmuir case; in addition, one requires that the rates of adsorption and desorption be identical for every molecular layer. That is, the rate of condensation on the bare surface is equal to the rate of evaporation of molecules in the first layer; the rate of evaporation from the second layer is equal to the rate of condensation on top of the first layer; and so on. One then sums over the layers to determine the total amount of adsorbed material. The derivation also assumes that the heat of adsorption of each layer other than the first is equal to the heat of condensation of the bulk adsorbate material (i.e., van der Waals forces of the adsorbent are transmitted only to the first layer). If one assumes that a very large or effectively infinite number of layers can be adsorbed, one obtains the following result after a number of relatively elementary mathematical operations:

$$v = \frac{v_m c P}{(P_0 - P) [1 + (c - 1)(P/P_0)]} \quad (6.2.25)$$

where  $c$  is a constant exponentially related to the heats of adsorption of the first layer and the heat of liquefaction, and  $P_0$  is the saturation pressure.

This equation can be rearranged to give a somewhat more familiar form,

$$\frac{x}{v(1-x)} = \frac{1}{v_m c} + \left( \frac{c-1}{v_m c} \right) x \quad (6.2.26)$$

where  $x$  is the normalized pressure ( $P/P_0$ ). If one plots the left side of equation (6.2.26) versus  $x$ , a straight line should result, with

$$v_m = \frac{1}{\text{slope} + \text{intercept}} \quad (6.2.27)$$

Equation (6.2.9) may then be used in determining the specific surface area of an adsorbent. Alternative arrangements of equation (6.2.25) are possible, but they have the inherent disadvantage of placing undue emphasis on the low-pressure data points that are most susceptible to error.

If one restricts the number of layers of adsorbate that may be stacked up, as would be the case in the very narrow capillaries of a porous catalyst, the BET analysis must be modified to allow for this. If  $n$  is the number of permissible layers, it can be shown that the adsorption isotherm becomes

$$v = \frac{v_m c x [1 - (n+1)x^n + nx^{n+1}]}{(1-x)[1 + (c-1)x - cx^{n+1}]} \quad (6.2.28)$$

When  $n = 1$ , this equation reduces to the Langmuir form. Because  $x$  is always less than unity, it does not take very large values of  $n$  to approach the limiting form indicated by equation (6.2.25). By appropriate choice of the parameters in equation (6.2.28), it is possible to generate the five types of curves shown in Figure 6.2.

Many people have developed more elegant theoretical treatments of adsorption isotherms since Brunauer, Emmett, and Teller published their classic paper. Nonetheless, the BET and Langmuir isotherms are the most significant for chemical engineering applications.

## 6.3 REACTION RATE EXPRESSIONS FOR HETEROGENEOUS CATALYTIC REACTIONS

When a heterogeneous catalytic reaction occurs, several physical and chemical processes must take place in proper sequence. Hougen and Watson (9) and others have broken down the steps that occur on a molecular scale in the following manner.

1. Mass transfer of reactants from the main body of the fluid to the gross exterior surface of the catalyst particle.
2. Molecular diffusion and/or Knudsen flow of reactants from the exterior surface of the catalyst particle into the interior pore structure.
3. Chemisorption of at least one of the reactants on the catalyst surface.
4. Reaction on the surface. (Reaction may involve several steps.)
5. Desorption of (chemically) adsorbed species from the surface of the catalyst.
6. Transfer of products from the interior of the catalyst pore structure to the gross external surface of the catalyst by ordinary molecular diffusion and/or Knudsen diffusion.

**7. Mass transfer of products from the exterior surface of the particle into the bulk of the fluid.**

Several of these steps are shown in schematic fashion in Figure 6.3. Naturally, if the catalyst is nonporous, steps 2 and 6 are absent. Steps 1, 2, 6, and 7 are obviously physical processes, while steps 3 to 5 are basically chemical in character. The rates of the various steps depend on a number of factors in addition to the concentration profiles of the reactant and product species.

Steps 1 and 7 are highly dependent on the fluid flow characteristics of the system. The mass velocity of the fluid stream, the particle size, and the diffusional characteristics of the various molecular species are the pertinent parameters on which the rates of these steps depend. These steps limit the rate observed only when the catalytic reaction is very rapid and the mass transfer is slow. Anything that tends to increase mass transfer coefficients will enhance the rates of these processes. Since the rates of these steps are influenced only slightly by temperature, the impact of these processes on the overall conversion rate will vary as the temperature changes. Their influence is often negligible

at low temperatures, but may be quite significant at higher temperatures.

There are two commonly used techniques for determining the range of process variables within which these steps influence conversion rates. The first approach involves carrying out a series of trials in which one measures the conversion achieved as a function of the ratio of the weight of catalyst ( $W$ ) to the molal feed flow rate ( $F$ ). One then repeats the experiments at a different linear velocity through the reactor (e.g., by changing the length-to-diameter ratio of the catalyst bed in a tubular reactor). The data are then plotted as shown in Figure 6.4a and b. If the two curves do not coincide as shown in Figure 6.4b, mass transfer resistances are significant, at least in the low-velocity series. If the curves coincide as shown in Figure 6.4a, mass transfer effects probably do not influence the conversion rate observed. This diagnostic test must be applied with caution; Chambers and Boudart (10) have shown that it often lacks sensitivity under conditions commonly employed in laboratory-scale studies. Heat and mass transfer coefficients are not strongly dependent on

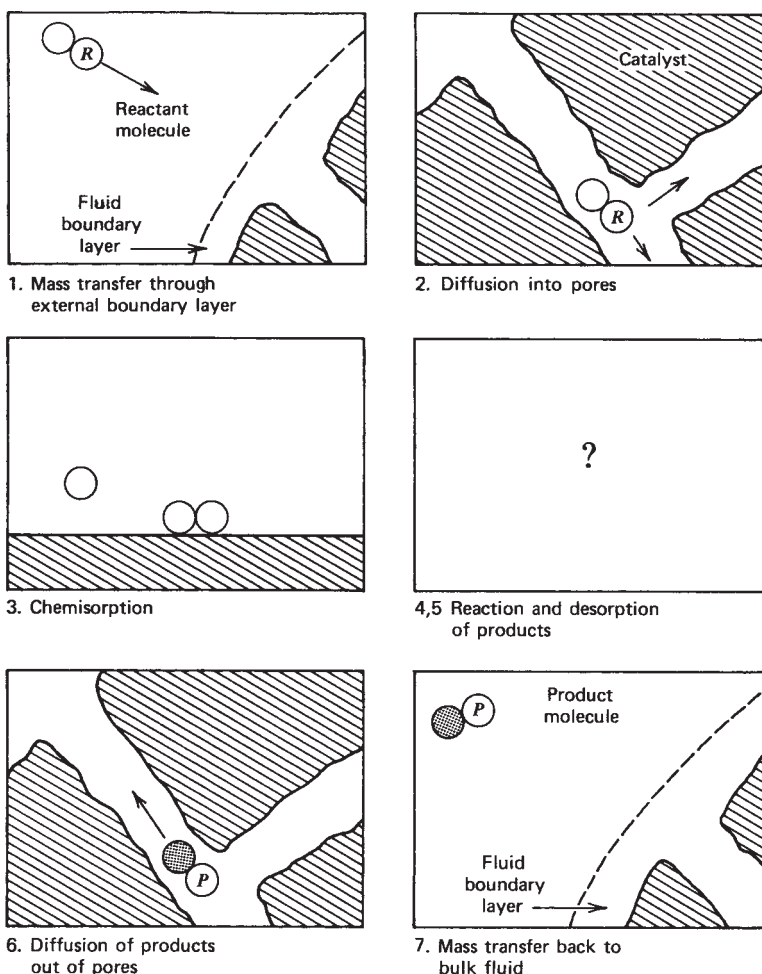


**Figure 6.3** Schematic representation of heterogeneous catalytic reaction on a porous catalyst.

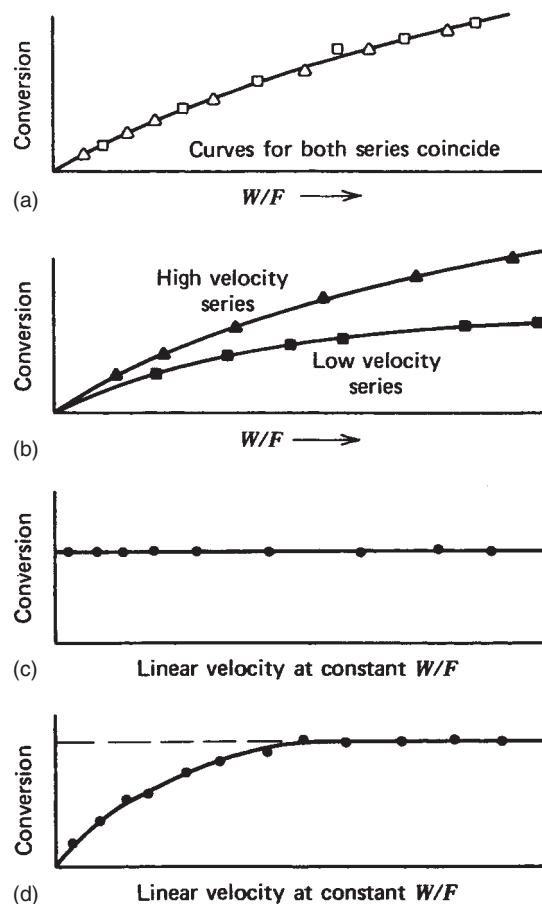


**Figure 6.4** Tests for external mass transfer limitations on conversion rates. (a, c) External mass transfer probably does not limit conversion rate. (b) Mass transfer limitations are present. (d) Mass transfer limitations are present at low velocities. [Adapted from R. H. Perry, C. H. Chilton, and S. D. Kirkpatrick (Eds.), *Chemical Engineers' Handbook*, 4th ed. Copyright © 1963. Used with permission of McGraw-Hill Book Company.]

fluid velocity for Reynolds numbers below 50. (The characteristic length dimension is taken as the pellet diameter.) Consequently, at low Reynolds numbers, the conversion will not change significantly with fluid velocity at constant  $W/F$ , even though heat or mass transfer limitations may be present. The scatter in the experimental data will often be sufficient to mask these effects for many reactions. Thus, when the experimental diagnostic test indicates that mass transfer limitations are probably not present, one's conclusions should be verified by calculations of the sensitivity of the test to variations in fluid velocity. The methods developed in Section 12.4 may be used for this purpose.

The second approach involves simultaneous variation of the weight of catalyst and the molar flow rate so as to maintain  $W/F$  constant. One then plots the conversion achieved versus linear velocity, as shown in Figure 6.4c and d. If the results are as indicated in Figure 6.4d, mass transfer limitations exist in the low-velocity regime. If the

conversion is independent of velocity, there probably are no mass transfer limitations on the conversion rate. However, this test is also subject to the sensitivity limitations noted above.

When fluid velocities are high relative to the solid, mass transfer is rapid. However, in stagnant regions or in batch reactors where no provision is made for agitation, one may encounter cases where the rate of mass transfer limits the observed reaction rate. We should also note that in industrial practice pressure drop constraints may make it impractical to employ the exceedingly high velocities necessary to overcome the mass transfer resistance associated with highly active catalysts.

For porous catalysts the external gross surface area of a particle often represents only an insignificant fraction of the total surface area that is potentially capable of catalyzing a given reaction. For these materials, diffusional processes occurring within the pores can have marked effects on the conversion rates that can be observed in the laboratory. When working with this type of catalyst, it is necessary to recognize that steps 2 and 6 enumerated above play key roles in determining how effective the total surface area is in bringing about the desired reaction. In dealing with an active catalyst, equilibrium or complete conversion may be substantially achieved in the region near the mouth of the pore, and the conversion rate observed will not differ appreciably from that which would be observed if the catalytic surface area deep within the pores were not present. The efficiency with which the internal surface area of a porous catalyst is used is an extremely important consideration in the design of catalytic reactors. This subject is treated in detail in Section 12.3. The parameters that govern the influence of pore diffusion processes on the conversion rates observed are the degree of porosity of the catalyst, the dimensions of the pores, the degree to which the pores are interconnected, the gross dimensions of the catalyst particle itself, the rate at which the reaction occurs on the catalyst surface, and the diffusional characteristics of the reaction mixture. To determine if steps 2 and 6 are influencing the overall conversion rate, examine the effect of changing the gross particle dimensions: for example, by breaking up a catalyst into smaller pieces. For a given weight of catalyst the total surface area will remain essentially unchanged as a result of this process, but the effective surface area will increase significantly when pore diffusion processes have had a strong influence on the rate observed experimentally. Reducing the gross exterior dimensions of the particles decreases the average length of the pores and makes a greater fraction of the total surface area available to the reactant species. The increase in effective surface area that accompanies particle fragmentation is shown schematically in Figure 6.5.

The three remaining steps (chemisorption of reactants, reaction on the surface, and desorption of adsorbed

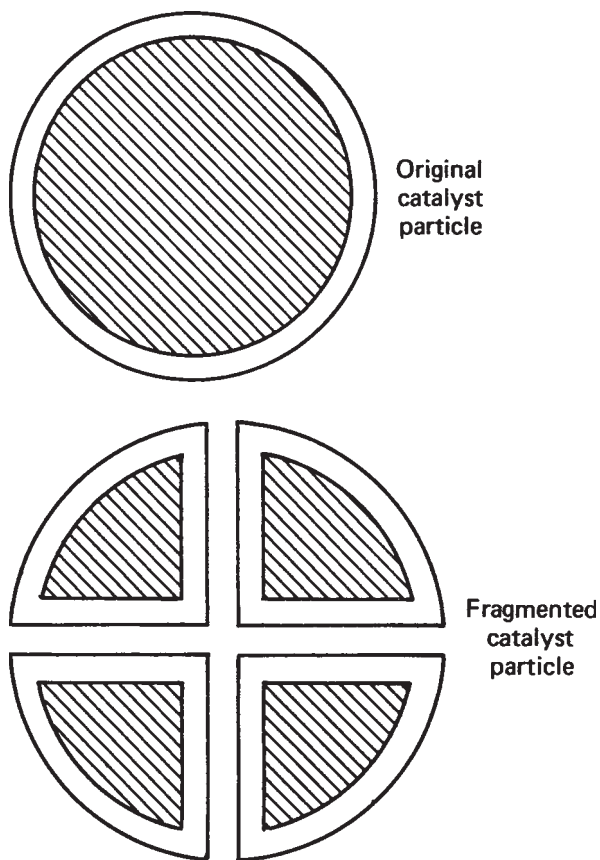


**Figure 6.5** Effect of fragmentation on catalyst utilization when intraparticle diffusion is rate controlling. (Shaded areas represent regions of the catalyst with markedly reduced concentrations of reactants.)

products) are all chemical in nature. It is convenient to employ the concept of a rate-limiting step in the treatment of these processes so that the reaction rate becomes equal to that of the slowest step. The other steps are presumed to be sufficiently rapid that quasi-equilibrium relations may be used. The overall rate of conversion will then be determined by the interaction of the rate of the process that is rate limiting from a chemical point of view with the rates of the physical mass transfer processes discussed above.

The remainder of this section is devoted to a discussion of the types of rate expressions that are obtained when purely chemical phenomena determine observed conversion rates.

### 6.3.1 Rate Expressions for Heterogeneous Catalytic Reactions Limited by the Rates of Chemical Processes

In the treatment of rate expressions for heterogeneous catalytic reactions, the definition of local reaction rates in

terms of interfacial areas [equation (3.0.10)] is appropriate:

$$r'' = \frac{1}{S} \frac{d\xi}{dt} \quad (6.3.1)$$

where  $S$  is the surface area of the solid catalyst.

If an attempt is made to fit heterogeneous catalytic reaction rate data with a power-law rate expression

$$r'' = k C_A^{\beta_A} C_B^{\beta_B} C_C^{\beta_C} \dots \quad (6.3.2)$$

one often finds that the reaction orders are not integers, that the orders depend on temperature and perhaps on concentration (or partial pressure), and that the observed activation energy may depend on temperature. Such expressions are of rather limited use for design purposes and can be used with confidence only under conditions that closely resemble those under which the experimental data were recorded. The basic reason that this sort of approach often gives rise to such difficulties is that it assumes that the driving force for reaction is the concentrations of the species present in the fluid phase. A more logical approach is to use the surface concentrations of the adsorbed species in an expression analogous to equation (6.3.2); that is,

$$r'' = k'' \theta_A^{\beta_A} \theta_B^{\beta_B} \theta_C^{\beta_C} \dots \quad (6.3.3)$$

where  $\theta_i$  is the fraction of the surface covered by species  $i$ . If the various  $\theta_i$  can be related to bulk fluid-phase concentrations, one has an appropriate mathematical form to use in testing a proposed reaction rate expression. The basis for most analyses of this type is the Langmuir isotherm. When expressions for the various  $\theta_i$  in terms of the appropriate partial pressures involved in the Langmuir isotherm are substituted into equation (6.3.3), a Langmuir–Hinshelwood or Hougen–Watson rate expression is obtained. The latter two engineers were responsible for analyzing a number of possible reaction mechanisms in these terms (11, 12) and for popularizing this approach to analyzing catalytic reaction rate data. For simplicity the term *Hougen–Watson models* will be used throughout the remainder of this book.

In addition to the assumptions implicit in the use of the Langmuir isotherm, the following assumption is applicable to all Hougen–Watson models: the reaction involves at least one species chemisorbed on the catalyst surface. If reaction takes place between two adsorbed species, they must be adsorbed on neighboring sites in order for reaction to occur. The probability of reaction between adsorbed A and adsorbed B is assumed to be proportional to the product of the fractions of the sites occupied by each species ( $\theta_A \theta_B$ ). Similar considerations apply to termolecular reactions occurring on the surface.

In addition to the aforementioned assumptions, one *normally* elects one of two mutually incompatible assumptions as a basis for his or her analysis. These two

limiting categories are indicated below and each category is discussed in turn.

*Category I. Adsorption equilibrium is maintained at all times, and the overall rate of reaction is governed by the rate of chemical reaction on the surface. The expressions developed for  $\Theta_i$  in Section 6.2 can be used for reactions in this category.*

*Category II. The rate of chemical reaction on the surface is so rapid that adsorption equilibrium is not achieved, but a steady-state condition is reached in which the amount of adsorbed material remains constant at some value less than the equilibrium value. This value is presumed to be that corresponding to equilibrium for the surface reaction at the appropriate fractional coverages of the other species involved in the surface reaction. The rate of adsorption or desorption of one species is presumed to be much slower than that of any other species. This step is then the rate-limiting step in the overall reaction.*

### 6.3.1.1 Hougen–Watson Models for the Case of Equilibrium Adsorption

In this section we treat Hougen–Watson mathematical models for cases where the rate-limiting step is the chemical reaction rate on the surface. In all cases it is assumed that equilibrium is established with respect to adsorption of all species.

**Case I: Irreversible Reaction (Unimolecular).** Consider the following mechanistic equation for a reaction occurring on a catalyst surface:



where both A and R are adsorbed in appreciable amounts. In this case the reaction rate is proportional to the fraction of the surface occupied by species A:

$$r'' = k\Theta_A \quad (6.3.5)$$

This fraction is given by equation (6.2.16), the Langmuir adsorption isotherm for the case where several species may be adsorbed. Thus,

$$r'' = \frac{kK_A P_A}{1 + K_A P_A + K_R P_R} \quad (6.3.6)$$

There are a number of limiting forms of this rate expression, depending on the magnitudes of the various terms in the denominator relative to unity and to one another. Any species that is weakly adsorbed will not appear in the denominator. If species R undergoes dissociation on adsorption, the term  $K_R P_R$  must be replaced by  $\sqrt{K_R P_R}$  according to the discussion in Section 6.2.1.3. If an inert species I is also capable of adsorption, the term  $K_I P_I$  must be added to the sum in the denominator.

If the product R is strongly adsorbed, equation (6.3.6) provides a basis for explaining inhibition of the reaction by that material. For example, if the dominant term in the denominator is  $K_R P_R$ , the appropriate approximation for the rate expression is

$$r'' = \frac{kK_A P_A}{K_R P_R} \quad (6.3.7)$$

The decomposition of ammonia on platinum has a rate expression of this form. The reaction is first-order in ammonia and inverse first-order in hydrogen.

The temperature variation of heterogeneous catalytic reaction rates can be quite complex. The apparent activation energy can in many cases be related to the activation energy of the surface reaction and the enthalpy changes accompanying adsorption of various species. If one of the terms in the denominator of the right side of equation (6.3.6) is very much larger than any of the other terms, this is possible. If not, one cannot relate the apparent activation energy to these parameters. The dependence of the adsorption equilibrium constants on temperature is given by

$$\frac{d \ln K}{d(1/T)} = \frac{-\Delta H^0}{R} \quad (6.3.8)$$

where  $\Delta H^0$  is the standard enthalpy change accompanying chemisorption. Consequently, the apparent activation energies corresponding to some limiting forms of equation (6.3.6) are as given below.

Dominant term in denominator	Limiting form of rate expression	Apparent rate constant	Apparent activation energy
1	$r'' = kK_A P_A$	$kK_A$	$E + \Delta H_A^0$
$K_A P_A$	$r'' = k$	$k$	$E$
$K_R P_R$	$r'' = \frac{kK_A P_A}{K_R P_R}$	$\frac{kK_A}{K_R}$	$E + \Delta H_A^0 - \Delta H_R^0$

where  $E$  is the activation energy of the surface reaction and  $\Delta H_i^0$  is the standard enthalpy change accompanying chemisorption of species  $i$ . In the last case, the relative magnitudes of the heats of adsorption of A and R will determine whether the apparent activation energy will be greater than or less than that of the surface reaction.

**Case II: Irreversible Bimolecular Reaction Between Adsorbed Species on the Same Type of Site.** Consider the following irreversible bimolecular reaction, which takes place between two species adsorbed on a catalyst surface:



In this case the reaction rate is assumed to be proportional to the product of the fractions of the sites occupied by species

A and B.

$$r'' = k\theta_A\theta_B \quad (6.3.10)$$

In the general case where all species may be adsorbed on the same type of surface site, equations (6.2.16) and (6.2.17) may be used for  $\theta_A$  and  $\theta_B$ . Thus,

$$r'' = \frac{kK_A K_B P_A P_B}{(1 + K_A P_A + K_B P_B + K_R P_R + K_S P_S)^2} \quad (6.3.11)$$

There are several limiting forms of this rate expression, depending on which species are strongly or weakly adsorbed.

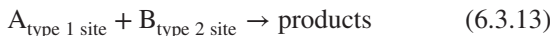
If all partial pressures except that of one reactant—say, species A—are held constant and the partial pressure of species A is varied, the rate will go through a maximum. The rate increases initially with increasing partial pressure of reactant A as the fraction of sites occupied by species A increases. However, as this fraction increases, the fraction occupied by species B declines as B molecules are displaced by A molecules. Eventually, one reaches a point where the decline in the value of  $\theta_B$  more than offsets the increase in  $\theta_A$  and the product  $\theta_A\theta_B$  goes through a maximum.

For the case of bimolecular reaction between two adsorbed A molecules, similar arguments lead to the following rate expression:

$$r'' = \frac{kK_A^2 P_A^2}{(1 + K_A P_A + K_R P_R + K_S P_S)^2} \quad (6.3.12)$$

**Case III: Irreversible Bimolecular Reactions Between Species Adsorbed on Different Types of Sites.**

With certain types of catalysts it is easy to postulate that more than one type of chemisorption site may exist on the solid surface. For example, in the case of metal oxide catalysts, one might speculate that certain species could chemisorb by interaction with metal atoms at the surface, while other species could interact with surface oxygen atoms. Consider the possibility that species A adsorbed on one type of site will react with species B adsorbed on a second type of site according to the following reaction:



For this mechanism the rate expression is given by

$$r'' = k\theta_{A1}\theta_{B2} \quad (6.3.14)$$

where  $\theta_{A1}$  is the fraction of the type 1 sites occupied by species A and  $\theta_{B2}$  is the fraction of the type 2 sites occupied by species B. If the Langmuir adsorption isotherm equation is written for each type of site, if only species A is adsorbed on type 1 sites, and if only species B is adsorbed on type 2 sites,

$$r'' = k \left( \frac{K_{A1} P_A}{1 + K_{A1} P_A} \right) \left( \frac{K_{B2} P_B}{1 + K_{B2} P_B} \right) \quad (6.3.15)$$

Rate expressions of this type have been proposed to correlate the data for the reaction between hydrogen and carbon dioxide on tungsten. Because adsorption occurs independently on each type of site and displacement of one species by another does not occur, this type of reaction will not exhibit a maximum of the type noted in case II. Instead, the rate will increase with increasing partial pressure of one reactant, eventually approaching an asymptotic limit corresponding to saturation of the type of site in question.

**Case IV: Irreversible Bimolecular Reactions Between an Adsorbed Species and a Fluid-Phase Molecule.**

The first three examples consider cases where only adsorbed species participate in the reaction. The possibility also exists that reaction may occur between a gaseous molecule and an adsorbed species. This mechanism is referred to as a Rideal mechanism. If species A refers to the adsorbed species and species B to a gas-phase molecule, one form of this bimolecular reaction may be written as



with a rate expression given by

$$r'' = k\theta_A P_B \quad (6.3.17)$$

If we consider the general case where all species may be adsorbed,  $\theta_A$  is given by equation (6.2.16), and the rate becomes

$$r'' = \frac{kK_A P_A P_B}{1 + K_A P_A + K_B P_B + K_R P_R + K_S P_S} \quad (6.3.18)$$

If species B had been adsorbed rather than species A, the corresponding rate equation would be

$$r'' = \frac{kK_B P_A P_B}{1 + K_A P_A + K_B P_B + K_R P_R + K_S P_S} \quad (6.3.19)$$

Both equations have the same mathematical form. In these cases there will not be a maximum in the rate as the pressure of one species varies. Instead, the rate will approach an asymptotic value at high pressures. Consequently, this type of mechanism can be excluded from subsequent consideration if it can be shown that the experimentally observed rate passes through a maximum as the concentration of one reactant is increased at constant values of other species concentrations.

If the surface is nearly covered ( $\theta_A \approx 1$ ), the reaction will be first-order in the gas-phase reactant and zero-order in the adsorbed reactant. On the other hand, if the surface is sparsely covered ( $\theta_A \approx K_A P_A$ ), the reaction will be first-order in each species or second-order overall. Because adsorption is virtually always exothermic, the first condition will correspond to low temperatures and the second condition to high temperatures. This mechanism thus offers

a ready explanation of a transition from quasi first- to mixed second-order kinetics with increasing temperature.

**Case V: Reversible Reactions Between Adsorbed Species (Change in Number of Moles on Reaction).** Consider the reaction



where all species are adsorbed on surface sites. It is assumed that an adsorbed A molecule reacts with a *vacant site* to form an intermediate that then dissociates to form adsorbed R and S species. This type of mechanism implies that the number of sites involved in a reaction obeys a conservation principle.

The rate of this surface reaction can be written as

$$r'' = k_1 \theta_A \theta_v - k_{-1} \theta_R \theta_S \quad (6.3.21)$$

where  $\theta_v$  is the fraction of the sites that are vacant. This quantity is given by

$$\theta_v = 1 - (\theta_A + \theta_R + \theta_S) \quad (6.3.22)$$

or

$$\begin{aligned} \theta_v &= 1 - \left( \frac{K_A P_A + K_R P_R + K_S P_S}{1 + K_A P_A + K_R P_R + K_S P_S} \right) \\ &= \frac{1}{1 + K_A P_A + K_R P_R + K_S P_S} \end{aligned} \quad (6.3.23)$$

Substitution of this result into equation (6.3.21), together with the appropriate expressions for the fractional coverages of other species gives

$$r'' = \frac{k_1 K_A P_A - k_{-1} K_R K_S P_R P_S}{(1 + K_A P_A + K_R P_R + K_S P_S)^2} \quad (6.3.24)$$

or

$$r'' = \frac{k_1 K_A \{P_A - [K_R K_S P_R P_S / (K_r K_A)]\}}{(1 + K_A P_A + K_R P_R + K_S P_S)^2} \quad (6.3.25)$$

where  $K_r$  is the equilibrium constant for the surface reaction:

$$K_r = k_1 / k_{-1}$$

If we let

$$k = k_1 K_A \quad (6.3.27)$$

and

$$K = \frac{K_r K_A}{K_R K_S} \quad (6.3.28)$$

equation (6.3.25) can be rewritten as

$$r'' = \frac{k [P_A - (P_R P_S / K)]}{(1 + K_A P_A + K_R P_R + K_S P_S)^2} \quad (6.3.29)$$

The cases discussed above represent only a small fraction of the surface reaction mechanisms that might be considered. Yang and Hougen (12) considered several additional surface reaction mechanisms and developed tables from which rate expressions for these mechanisms may be determined. They approached this problem by writing the rate expression in the form

$$\text{rate} = \frac{\text{kinetic term} \times \text{driving force}}{(\text{absorption term})^n} \quad (6.3.30)$$

Let us now examine each of the terms in this formulation of the rate expression.

*Driving force term.* In all rate expressions the *driving force* must become zero when thermodynamic equilibrium is established. The “equilibrium” constant  $K$  appearing in equation (6.3.29) can be regarded as the appropriate ratio of partial pressures for the overall reaction:

$$K \equiv \frac{K_r K_A}{K_R K_S} = \frac{P_{Re} P_{Se}}{P_{Ae}} \quad (6.3.31)$$

The value of  $K$  appearing in the driving force term is the product of the equilibrium constant for the surface reaction  $K_r$  and the product of the adsorption equilibrium constants for the reactants divided by the product of the adsorption equilibrium constants for the reaction products. Note that  $K$  is also the equilibrium constant for the overall reaction expressed in terms of gas phase partial pressures.

*Kinetic term.* The designation *kinetic term* is something of a misnomer in that it contains both rate constants and adsorption equilibrium constants. For cases where surface reaction controls the overall conversion rate, it is the product of the surface reaction rate constant for the forward reaction and the adsorption equilibrium constants for the reactant surface species participating in the reaction. When adsorption or desorption of a reactant or product species is the rate-limiting step, it will involve other factors.

*Adsorption term.* When all reactants, products, and inert are adsorbed without dissociation such that adsorption equilibrium prevails, the *adsorption term* is given by

$$1 + K_A P_A + K_B P_B + K_R P_R + K_S P_S + K_I P_I$$

where  $K_I$  and  $P_I$  are the adsorption equilibrium constant and the gas-phase partial pressure of an inert species I, respectively. When dissociation of species  $i$  occurs on adsorption, the term  $K_i P_i$  must be replaced by  $\sqrt{K_i P_i}$  as long as adsorption equilibrium holds for all species. When adsorption equilibrium is not maintained, other modifications in the adsorption term are necessary.

The exponent  $n$  on the adsorption term is equal to the number of sites participating in the surface reaction, regardless of whether they hold adsorbed species or participate as vacant sites. If more than one site is involved, we assume

that the sites must be adjacent for the surface reaction to occur.

### 6.3.1.2 Hougen–Watson Models for Cases Where Adsorption and Desorption Processes Are the Rate-Limiting Steps

When surface reaction processes are very rapid, the overall conversion rate may be limited by the rate at which adsorption of reactants or desorption of products takes place. In such situations, usually only one of the many species in a reaction mixture will not be in adsorptive equilibrium. This generalization will be taken as a basis for developing the expressions for overall conversion rates that apply when adsorption or desorption processes are rate limiting. In this treatment we assume that chemical reaction equilibrium exists between various adsorbed species *on the catalyst surface*, even though reaction equilibrium will not prevail in the fluid phase.

Consider the reversible surface reaction



in which we presume that species A is not in adsorptive equilibrium and that the rate-limiting step in the overall conversion process is the rate of adsorption of species A. When A molecules are adsorbed, the chemical reaction equilibrium existing between surface species is disturbed, and adsorbed A molecules must then react. The reaction occurs so rapidly that the adsorptive equilibrium for species A cannot be established, and  $\theta_A$  is determined by surface reaction equilibrium constraints. Because the *surface reaction* is at equilibrium,

$$k_1 \theta_A \theta_B = k_{-1} \theta_R \theta_S \quad (6.3.33)$$

Thus,

$$\theta_A = \frac{k_{-1} \theta_R \theta_S}{k_1 \theta_B} = \frac{\theta_R \theta_S}{K_r \theta_B} \quad (6.3.34)$$

where  $K_r$  is the equilibrium constant for the surface reaction.

The rates of adsorption and desorption of species B are equal. Hence,

$$k_{1B} P_B \theta_v = k_{-1B} \theta_B \quad (6.3.35)$$

where  $\theta_v$  is the fraction of the sites that are vacant, and  $k_{1B}$  and  $k_{-1B}$  are the rate constants for adsorption and desorption of species B. Solving for  $\theta_B$  yields

$$\theta_B = \frac{k_{1B} P_B \theta_v}{k_{-1B}} = K_B P_B \theta_v \quad (6.3.36)$$

A similar analysis is applicable to other species that attain adsorptive equilibrium. Thus,

$$\theta_R = K_R P_R \theta_v \quad \text{and} \quad \theta_S = K_S P_S \theta_v \quad (6.3.37)$$

The sum of the fractions of sites occupied by the various species and the fraction vacant must be unity:

$$1 = \theta_A + \theta_B + \theta_R + \theta_S + \theta_v \quad (6.3.38)$$

Combination of equations (6.3.34) and (6.3.36) to (6.3.38) gives the fraction vacant

$$\theta_v = \frac{1}{1 + (K_R K_S / K_r K_B) (P_R P_S / P_B) + K_B P_B + K_R P_R + K_S P_S} \quad (6.3.39)$$

Because the rate-limiting step in the overall process is the rate of adsorption of species A, the net rate of reaction is equal to the difference between the rates of adsorption and desorption:

$$r'' = k_{1A} P_A \theta_v - k_{-1A} \theta_A \quad (6.3.40)$$

or

$$r'' = k_{1A} \left( P_A \theta_v - \frac{\theta_A}{K_A} \right) \quad (6.3.41)$$

Combination of equations (6.3.34), (6.3.36), (6.3.37), (6.3.39), and (6.3.41) gives

$$r'' = \frac{k_{1A} \{ P_A - [(K_R K_S P_R P_S) / (K_r K_A K_B P_B)] \}}{1 + \left[ \left( \frac{K_R K_S}{K_r K_B} \right) \left( \frac{P_R P_S}{P_B} \right) \right] + K_B P_B + K_R P_R + K_S P_S} \quad (6.3.42)$$

This Hougen–Watson model for the case where the adsorption of a single species is rate limiting is of the same mathematical form as equation (6.3.30). In this case the kinetic term is merely the rate constant for the rate-controlling adsorption process. The driving-force term will depend on the stoichiometry of the surface reaction, which is presumed to be at equilibrium. The adsorption term must also be modified in these cases, the change occurring in the element in the summation corresponding to the species that is not at adsorptive equilibrium. This term will also depend on the nature of the surface reaction involved.

Extension of the analysis developed above to cases where the stoichiometry of the surface reaction differs from that considered is relatively simple and straightforward. An interesting case is that where the overall conversion rate is limited by adsorption of a species that dissociates on adsorption. Consider a reaction whose stoichiometry can be represented by



where dissociation of the  $A_2$  molecule occurs on adsorption. The mechanism of the reaction on the catalyst surface is represented by



In this case the above procedure can be used to show that

$$r'' = \frac{k_{1A} \{ P_{A_2} - [(K_R K_S P_R P_S) / (K_A K_r)] \}}{\left( 1 + \sqrt{\frac{K_R K_S P_R P_S}{K_r}} + K_R P_R + K_S P_S \right)^2} \quad (6.3.45)$$

Now consider the case where the controlling step is the rate of desorption of a product species R for a reversible surface reaction of the form



All other species are presumed to be in adsorptive equilibrium; that is,

$$\theta_A = K_A P_A \theta_v \quad \theta_B = K_B P_B \theta_v \quad \theta_S = K_S P_S \theta_v \quad (6.3.47)$$

The reaction *on the surface* is also assumed to be at equilibrium:

$$\theta_R = \frac{K_r \theta_A \theta_B}{\theta_S} \quad (6.3.48)$$

The sum of the various types of fractional coverage is unity:

$$1 = \theta_A + \theta_B + \theta_R + \theta_S + \theta_v \quad (6.3.49)$$

Combination of equations (6.3.47) to (6.3.49) and rearrangement gives

$$\theta_v = \frac{1}{1 + K_A P_A + K_B P_B + K_S P_S + \frac{K_r K_A K_B P_A P_B}{K_S P_S}} \quad (6.3.50)$$

The conversion rate is equal to the net rate of desorption of species R. Hence,

$$r'' = k_{-1R} \theta_R - k_{1R} P_R \theta_v = k_{-1R} (\theta_R - K_R P_R \theta_v) \quad (6.3.51)$$

Combination of equations (6.3.47), (6.3.48), (6.3.50), and (6.3.51) gives

$$r'' = \frac{k_{-1R} \{ [(K_r K_A K_B P_A P_B) / (K_S P_S)] - K_R P_R \}}{1 + K_A P_A + K_B P_B + K_S P_S + \frac{K_r K_A K_B P_A P_B}{K_S P_S}} \quad (6.3.52)$$

where  $k_{-1R}$  refers to the rate constant for desorption of R.

The analyses developed in this section are readily extended to reactions with different stoichiometries. Regardless of whether an adsorption or a desorption process is rate limiting, the resulting rate expressions may be written in the typical Hougen–Watson fashion represented by equation (6.3.30). A comprehensive summary of such relations has been developed by Yang and Hougen (12). Illustration 6.1 indicates the development of a Hougen–Watson model in an attempt to fit rate data for a catalytic reaction.

## ILLUSTRATION 6.1 Development of a Hougen–Watson Rate Expression for a Heterogeneous Catalytic Reaction

Oldenberg and Rase (13) studied the catalytic vapor-phase hydrogenation of propionaldehyde to propanol over a commercially supported nickel catalyst. Their data indicate that at 150°C the mathematical form of the reaction rate (at very low conversions) can be expressed quite well as

$$r = k P_P / P_{H_2}^{1/2}$$

where the subscript P refers to propionaldehyde and the subscript  $H_2$  refers to molecular hydrogen. It has been suggested that the rate-limiting step in the mechanism is the chemisorption of propionaldehyde and that hydrogen undergoes dissociative adsorption on nickel. Determine if the rate expression predicted by a Hougen–Watson model based on these assumptions is consistent with the rate expression observed experimentally.

### Solution

It is convenient to assign the following symbols before proceeding to a discussion of the mechanism proper.

P = propionaldehyde

A = propanol

$\sigma$  = surface site

$P_\sigma$  = adsorbed propionaldehyde

$\theta_P$  = surface coverage by propionaldehyde

$H_\sigma$  = atomically adsorbed hydrogen

$\theta_H$  = surface coverage by adsorbed hydrogen atoms

$A_\sigma$  = adsorbed alcohol

$\theta_A$  = surface coverage by adsorbed propional

The following mechanistic equations for chemisorption and reaction are appropriate.



$K_{H_2}$  = adsorption equilibrium constant for  $H_2$



$K_{eq}$  = equilibrium constant for surface reaction



$1/K_A$  = reciprocal of adsorption equilibrium

constant for alcohol

The rate of the overall reaction is equal to that of the rate-controlling step:

$$r'' = k_{1P}P_P\theta_v - k_{-1P}\theta_P \quad (E)$$

where  $\theta_v$  and  $\theta_P$  are the fractions of the sites that are vacant and occupied by propionaldehyde, respectively. From equation (B),

$$K_{H_2} = \frac{\theta_H^2}{P_{H_2}\theta_v^2} \quad \text{or} \quad \theta_H = \sqrt{K_{H_2}P_{H_2}}\theta_v \quad (F)$$

From equation (C),

$$K_{eq} = \frac{\theta_A\theta_v^2}{\theta_P\theta_H^2} \quad \text{or} \quad \theta_P = \frac{\theta_A\theta_v^2}{K_{eq}\theta_H^2} \quad (G)$$

From equation (D),

$$1/K_A = \frac{P_A\theta_v}{\theta_A} \quad \text{or} \quad \theta_A = K_A P_A \theta_v \quad (H)$$

The expressions for  $\theta_A$  and  $\theta_H$  may now be substituted into equation (G) to obtain

$$\theta_P = \frac{K_A P_A \theta_v}{K_{eq} K_{H_2} P_{H_2}} \quad (I)$$

The sum of the fractional coverages must be unity. Hence,

$$1 = \theta_H + \theta_P + \theta_A + \theta_v \quad (J)$$

Substitution of equations (F), (H), and (I) into equation (J) and rearrangement gives

$$\theta_v = \frac{1}{1 + K_A P_A + \sqrt{K_{H_2} P_{H_2} + [K_A P_A / (K_{eq} K_{H_2} P_{H_2})]}}$$

Substitution of this result into equation (E) gives

$$r'' = \frac{k_{1P}P_P - (k_{-1P}K_A P_A / K_{eq} K_{H_2} P_{H_2})}{1 + K_A P_A + \sqrt{K_{H_2} P_{H_2} + [K_A P_A / (K_{eq} K_{H_2} P_{H_2})]}}$$

For an initial rate study,  $P_A \approx 0$  and the preceding equation becomes

$$r''_0 = \frac{k_{1P}P_P}{1 + \sqrt{K_{H_2} P_{H_2}}}$$

If the second term in the denominator is large compared to unity,

$$r''_0 = \frac{k_{1P}P_P}{\sqrt{K_{H_2} P_{H_2}}^{1/2}}$$

Under these conditions the Hougen–Watson model is consistent with the rate expression observed experimentally.

### 6.3.2 Interpretation of Experimental Data

The problem of determining which, if any, of the Hougen–Watson models developed in Section 6.3.1 fits experimental data for a heterogeneous catalytic reaction is generally more complex than the corresponding problem for a homogeneous phase reaction. Usually, many possible controlling steps must be examined. Physical limitations on the overall reaction rate must first be eliminated by operating in a turbulent system and using sufficiently small catalyst pellets. The multitude of Hougen–Watson rate expressions for the cases where adsorption, desorption, and reaction on the surface are rate limiting are then considered. The trial-and-error procedures developed in Chapter 3 may be applied to data for catalytic reactions (i.e., one postulates a rate expression and then uses an integral or differential method to determine if the rate expression is consistent with the data). Because of the complexity of Hougen–Watson rate models, it is often convenient to use an initial rate approach to analyze the data. The remainder of this section is devoted to a discussion of the use of this approach to determine reaction rate expressions.

Studies of the influence of total pressure on the initial reaction rate for pure reactants present in stoichiometric proportions provide a means of discriminating between various classes of Hougen–Watson models. Isolation of a class of probable models by means of plots of initial reaction rate versus total pressure, feed composition, and temperature constitutes the first step in developing a Hougen–Watson rate model. Hougen (14) considered the influence of total pressure for unimolecular and bimolecular surface reactions; the analysis that follows is adopted from his monograph.

In initial rate studies no products need be present in the feed, and the terms in the rate expression involving the partial pressures of these species may be omitted under appropriate experimental conditions. The use of stoichiometric ratios of reactants may also cause a simplification of the rate expression. If one considers a reversible bimolecular surface reaction between species A and B,



an analysis of the type employed in Section 6.3.1.1 indicates that if the surface reaction is controlling, the conversion rate is given by

$$r'' = \frac{k_1 (K_A K_B P_A P_B - K_R K_S P_R P_S / K_r)}{(1 + K_A P_A + K_B P_B + K_R P_R + K_S P_S)^2} \quad (6.3.54)$$

If an equimolar feed of species A and B is used, the dependence of the *initial* rate on total pressure ( $P$ ) is given by

$$r''_0 = \frac{(k_1/4)K_A K_B P^2}{[1 + (K_A + K_B)(P/2)]^2} \quad (6.3.55)$$

In this case the initial rate increases as the square of the pressure at very low pressures and approaches a constant asymptotic limit at high pressures.

If the reaction proceeds by a mechanism requiring dissociation of one of the reactants ( $A_2$ ) on adsorption, the rate expression corresponding to the termolecular surface reaction between the two symmetric fragments of adsorbed A and an adsorbed B species is given by

$$r''_0 = \frac{k_1 K_{A_2} K_B \{P_{A_2} P_B - [(K_R K_S P_R P_S / K_r K_{A_2} K_B)]\}}{(1 + \sqrt{K_{A_2} P_{A_2}} + K_B P_B + K_R P_R + K_S P_S)^3} \quad (6.3.56)$$

This expression corresponds to the situation in which the rate-limiting step is a reaction on the surface with  $r'' = k_1 \theta_A^2 \theta_B$ .

If stoichiometric quantities of  $A_2$  and B are used, the dependence of the initial rate on the total pressure is given by

$$r''_0 = \frac{k_1 K_{A_2} K_B (P/2)^2}{[1 + \sqrt{K_{A_2} P/2} + (K_B P/2)]^3} \quad (6.3.57)$$

In the low-pressure limit the rate will increase as the square of the pressure, but at very high pressures it will fall off in a manner proportional to the reciprocal of the pressure. Consequently, as the pressure increases, the initial rate increases at first, goes through a maximum, and then declines.

In the case of a Rideal-type mechanism [equation (6.3.16)] a similar analysis indicates that for the case where the surface reaction is rate limiting, the initial rate starts out proportional to the square of the pressure and increases indefinitely with increasing total pressure. At high pressures it is linear in the total pressure. In like manner one can treat cases for which the rate-controlling step is adsorption or desorption of some species. Hougen (14) considered the effect of total pressure on initial reaction rates for several cases where these processes are rate limiting.

Studies of the effect of pressure on initial rates limit the possible Hougen–Watson rate expressions to certain classes. Subsequent studies using nonstoichiometric feeds and inerts and product species in the feed mixture further serve to determine the exact form of the reaction rate expression.

In determining the constants involved in a rate model, one often finds it convenient to invert the rate expression to obtain a form that lends itself to visualization of the overall quality of the fit of the rate expression to the data when it is linearized. For example, equation (6.3.11) can be rearranged to give

$$\left( \frac{P_A P_B}{r''} \right)^{1/2} = \frac{1}{\sqrt{k K_A K_B}} (1 + K_A P_A + K_B P_B + K_R P_R + K_S P_S) \quad (6.3.58)$$

so a multivariable regression analysis can be used to determine the five constants involved. Proper control of the nature of the experimental data can greatly simplify the problem of determining these parameters. However, this example illustrates one of the key difficulties involved in determining rate expressions for heterogeneous catalytic reactions, and we must temper any enthusiasm that we may have developed for Hougen–Watson rate models with recognition of the situations one faces in the real world. The fact that various specific models can be proposed, each leading to a corresponding mathematical formulation (which is not necessarily unique), tempts one to try to correlate experimental data by each of a variety of such mathematical forms and then to “conclude” that the one which best fits the data is the “true” kinetic mechanism. Considerably more judgment than this is required, and although a given mathematical expression may provide a good fit of the data, it does not necessarily imply that the presumed mechanism is indeed the “correct” one. For rate expressions of the form of equation (6.3.58), there are five adjustable constants; when one also considers the possibilities of reversible reactions, adsorption of inerts, or reactions in parallel or series, still more constants are introduced. With the flexibility given by these constants it is not difficult to obtain a good fit of data to a mathematical expression. In the words of one of my colleagues, “With six constants you can fit a charging rhinoceros.”

Furthermore, one often finds that “best” fits of data may give rise to negative adsorption equilibrium constants. This result is clearly impossible on the basis of physical arguments. Nonetheless, reaction rate models of this type may be entirely suitable *for design purposes* if they are not extrapolated out of the range of the experimental data on which they are based.

We should also point out that the adsorption equilibrium constants appearing in the Hougen–Watson models cannot be determined from adsorption equilibrium constants obtained from nonreacting systems if one expects the mathematical expression to yield accurate predictions of the reaction rate. One explanation of this fact is that probably only a small fraction of the catalyst sites are actually effective in promoting the reaction.

## 6.4 PHYSICAL CHARACTERIZATION OF HETEROGENEOUS CATALYSTS

The ease with which gaseous reactant molecules achieve access to the interior surfaces of a porous substance is

often of crucial significance in determining whether or not a given catalyst formulation and preparation technique will produce a material that is suitable for industrial applications. The magnitude of the surface area alone is insufficient to predict the efficacy with which a given mass of catalyst promotes a specific reaction. For fast reactions, the greater the amount of catalyst surface open to easy access by reactant molecules, the faster the rate at which reactants can be converted to products. If we are to be able to develop useful predictive models of catalyst behavior, we must know something about the interior pore structure of the catalyst and the facility with which reactant and product species can be transported within catalyst pellets.

In this section we focus on the techniques used to characterize the *physical properties* of solid catalysts. In industrial practice, the chemical engineer who anticipates the use of these catalysts in developing new or improved processes must effectively combine theoretical models, physical measurements, and empirical information on the behavior of catalysts manufactured in similar ways in order to be able to predict how these materials will behave. The complex models are beyond the scope of this book, but the principles involved are readily illustrated by the simplest model. This model requires the specific surface area, the void volume per gram, and the gross geometric properties of the catalyst pellet as input.

The specific surface area is usually determined by the BET technique discussed in Section 6.2.2. For the most reliable BET measurements the adsorbate gas molecules should be small, approximately spherical, inert (to avoid chemisorption), and easy to handle at the temperature in question. For economy, nitrogen is the most common choice, with measurements usually made at 77 K, the normal boiling point of liquid nitrogen. Krypton is another material that is frequently employed.

The remainder of this section is devoted to a discussion of the experimental techniques used to determine the other physical properties of catalysts that are of primary interest for reactor design purposes: the void volume and the pore size distribution.

### 6.4.1 Determination of Catalyst Void Volumes

The simplest method of determining the void volume or the pore volume of a given catalyst sample is to measure the increase in weight that occurs when the pores are filled with a liquid of known density. Water, carbon tetrachloride, and various hydrocarbons have been used successfully. The procedure involves boiling a known weight of dry catalyst pellets in the liquid for 20 to 30 min to displace the air in the pores. After the boiling fluid is replaced with cool liquid, the pellets are placed on an absorbent cloth and rolled to remove the excess liquid. They are then weighed. The

difference between the wet and dry weights ( $W_{\text{wet}} - W_{\text{dry}}$ ) divided by the density of the liquid imbibed ( $\rho_L$ ) gives the void volume. The void volume per gram of catalyst ( $V_g$ ) can then be determined from

$$V_g = \frac{W_{\text{wet}} - W_{\text{dry}}}{\rho_L W_{\text{dry}}} \quad (6.4.1)$$

One can employ this technique to determine the total volume of the pores with radii between approximately 10 and 1500 Å. This approach is limited in accuracy by the fact that it is difficult to dry the external surface of the particles without removing liquid from the large pores. Some liquid also tends to be retained around the points of contact between particles. These two sources of error offset one another. Any air retained within the pores after boiling will lead to erroneous results.

A much more accurate method of determining the pore volume of a catalyst sample is the helium–mercury method. One places a known weight of catalyst ( $W$ ) in a chamber of known volume. After the chamber has been evacuated, a known quantity of helium is admitted. From the gas laws and measurements of the temperature and pressure, one may then proceed to determine the volume occupied by the helium ( $V_{\text{He}}$ ). This volume is equal to the sum of the volume exterior to the pellets proper and the void volume within the pellets ( $V_{\text{void}}$ ). The helium is then pumped out and the chamber is filled with mercury at atmospheric pressure. Since the mercury will not penetrate the pores of most catalysts at atmospheric pressure, the mercury will occupy only the volume exterior to the pellets proper ( $V_{\text{Hg}}$ ). Hence,

$$V_{\text{void}} = V_{\text{He}} - V_{\text{Hg}} \quad (6.4.2)$$

and the void volume per gram ( $V_g$ ) is

$$V_g = \frac{V_{\text{He}} - V_{\text{Hg}}}{W} \quad (6.4.3)$$

This method permits one to determine the pore volume corresponding to pore radii less than 75,000 Å. By varying the pressure on the system, one can force the mercury into some of the pores and determine the void volumes corresponding to different pore radii. We shall pursue this point in the next section.

The porosity of the catalyst pellet ( $\epsilon_p$ ) is defined as the void fraction.

$$\epsilon_p = \frac{\text{void volume of catalyst particle}}{\text{total volume of catalyst particle}} \quad (6.4.4)$$

For a particle of mass  $m_p$ ,

$$\epsilon_p = \frac{m_p V_g}{m_p V_g + (m_p / \rho_{\text{skeletal}})} = \frac{V_g}{V_g + (1 / \rho_{\text{skeletal}})} \quad (6.4.5)$$

where  $\rho_{\text{skeletal}}$  is the true density of the bulk solid and where the second term in the denominator is the volume occupied by the solid proper. Many commercial catalysts have porosities in the neighborhood of 0.5, indicating that the gross particle volume is about evenly split between void space and solid material. Significantly higher porosities are not encountered in commercial catalysts because of the problems of achieving sufficient mechanical strength at these porosity levels.

The total pore volume can also be determined from adsorption measurements if one knows the *volume of vapor adsorbed under saturation conditions*. For high-surface-area catalysts, the amount of material adsorbed on particle exteriors will be negligible compared to that condensed in the pores. Hence, the liquid-phase volume equivalent to the amount of gas adsorbed is equal to the pore volume. The liquid density is assumed to be that corresponding to the saturation conditions in question. This technique is less accurate than that described previously. Illustration 6.2 indicates how void volume and surface area measurements can be combined to evaluate the parameters involved in the simplest model of catalyst pore structure.

## ILLUSTRATION 6.2 Evaluation of Parameters in a Mathematical Model of Porous Catalysts

To develop analytical models for processes employing porous catalysts, one must make assumptions about the geometry of the catalyst pores. A variety of assumptions are possible, and Thomas and Thomas (15) have discussed some of these. The simplest model assumes that the pores are cylindrical and are not interconnected. Develop expressions for the average pore radius ( $\bar{r}$ ), the average pore length ( $\bar{L}$ ), and the number of pores per particle ( $n_p$ ) in terms of parameters that can be measured in the laboratory [i.e., the apparent particle dimensions, the void volume per gram ( $V_g$ ), and the surface area per gram ( $S_g$ )].

### Solution

We start by developing an expression for the average pore radius  $\bar{r}$ . If we denote the mass of an individual catalyst particle by  $m_p$ , simple geometric considerations indicate that the void volume per particle is given by

$$m_p V_g = n_p \bar{r}^2 \bar{L} \quad (\text{A})$$

while the surface area per particle is given by

$$m_p S_g = n_p 2\pi \bar{r} \bar{L} \quad (\text{B})$$

where we have neglected the area at the end of the cylinder, since  $\bar{L} \gg \bar{r}$  for virtually all systems of interest. Division of equation (A) by equation (B) and rearrangement gives

$$\bar{r} = \frac{2V_g}{S_g} \quad (\text{C})$$

For a monodisperse distribution of pore radii, this result is in good agreement with the values obtained from pore size distribution measurements, but it can be significantly in error if one is dealing with a bimodal pore size distribution (see Section 6.4.2).

To evaluate the average pore length, it is necessary to recognize that the porosity,  $\varepsilon_p$ , will represent not only the volumetric void fraction but also at any cross section the fraction of the area occupied by the pore openings. If the average open area associated with each pore is assumed to be  $\pi\bar{r}^2$ , the definition of the porosity indicates that

$$\varepsilon_p = \frac{m_p V_g}{V_p} = \frac{n_p \pi \bar{r}^2}{S_x} \quad (\text{D})$$

where  $V_p$  and  $S_x$  are the gross geometric volume and geometric surface area, respectively. Substitution of equation (A) into equation (D) gives

$$\frac{n_p \pi \bar{r}^2 \bar{L}}{V_p} = \frac{n_p \pi \bar{r}^2}{S_x}$$

which can be rearranged to obtain

$$\bar{L} = \frac{V_p}{S_x}$$

For a spherical catalyst pellet of radius  $R$ ,

$$\bar{L} = \frac{\frac{4}{3}\pi R^3}{4\pi R^2} = \frac{R}{3}$$

The number of pores per particle may be obtained by solving equation (D) for  $n_p$  and using equation (C) to eliminate  $\bar{r}$ :

$$n_p = \frac{\varepsilon_p S_x S_g^2}{4\pi V_g^2}$$

where  $\varepsilon_p$  is determined from equation (6.4.5).

### 6.4.2 Determination of Pore Size Distributions

Scanning electron microscopy and other experimental methods indicate that the void spaces in a typical catalyst particle are not uniform in size, shape, or length. Moreover, they are often highly interconnected. Because of the complexities of most common pore structures, detailed mathematical descriptions of the void structure

are not available. Moreover, because of other uncertainties involved in the design of catalytic reactors, the use of elaborate quantitative models of catalyst pore structures is not warranted. What is required, however, is a model that allows one to take into account the rates of diffusion of reactant and product species through the void spaces. Many of the models in common use simulate the void regions as cylindrical pores; for such models a knowledge of the distribution of pore radii and the volumes associated therewith is required.

There are two well-established experimental techniques for determining the distribution of pore radii: the mercury penetration technique and the desorption isotherm method. The *mercury penetration approach* is based on the fact that liquid mercury has a very high surface tension and the observation that mercury does not wet most catalyst surfaces. This situation holds true for oxide catalysts and supported metal catalysts that make up by far the overwhelming majority of the porous commercial materials of interest. Since mercury does not wet such surfaces, the pressure required to force mercury into the pores will depend on the pore radius. This dependence provides a basis for measuring pore size distributions through measurements of the volume of mercury contained within the pores as a function of applied pressure. The smallest pores that can be observed using this approach depend on the highest pressure to which the mercury can be subjected in a particular piece of equipment. Volumes corresponding to pore radii as small as 100 to 200 Å can be measured using commercially available equipment. Beyond this point the pressures required to fill up the capillaries with smaller radii become impractical for routine use. Unfortunately, there are many catalysts of industrial significance where these very small capillaries contribute substantially to the specific surface area. Special research-grade mercury porosimeters capable of measurements down to 15 Å radii have been developed, but for routine measurements, the desorption approach described below is more appropriate for use.

The *desorption isotherm approach* is the second generally accepted method for determining the distribution of pore sizes. In principle, either a desorption or an adsorption isotherm would suffice, but in practice the desorption isotherm is much more widely used when hysteresis effects are observed. The basis of this approach is the fact that capillary condensation occurs in narrow pores at pressures less than the saturation vapor pressure of the adsorbate. The smaller the radius of the capillary, the greater is the lowering of the vapor pressure. Hence, in very small pores, vapor will condense to liquid at pressures considerably below the normal vapor pressure. Mathematical details of the analysis have been presented by Cranston and Inkley (16) and need not concern us here. The size of the largest pores that can be determined by this technique

is limited by the rapid change in meniscus radius with pressure as the relative pressure  $P/P_0$  approaches unity. This limit corresponds to pore radii in the neighborhood of 150 to 200 Å, corresponding to a relative pressure of 0.93 in the former case. The smallest pore radii that can be observed by this technique are those near 10 Å. Although measurements may be reported corresponding to smaller pore sizes, such results are suspect because the molecular diameter of the adsorbate molecules is comparable in magnitude to the pore radius in this regime. Moreover, the analysis is based on the assumption that the properties of the condensed phase in the capillaries are the same as those of bulk liquids, yet the concepts of surface tension and a hemispherical surface become hazy or unrealistic below radii of 10 Å, and perhaps even at larger radii. In the regions where the mercury penetration approach and the desorption method overlap, they agree reasonably well. However, in many cases of practical significance, it is necessary to employ both techniques to cover the entire range of pore sizes (10 to 10,000 Å) that may be present. This requirement is particularly true of catalysts such as pelleted alumina in which one has a bimodal pore size distribution of the type discussed below.

The catalysts employed in commercial fixed-bed reactors often exhibit a bimodal pore size distribution, sometimes referred to as bidisperse or macro–micro distributions. In these systems the bulk of the catalytic reaction occurs in pores with radii below 200 Å, because the bulk of the surface area resides in these very narrow pores. However, the transport of reactants to these small pores occurs primarily through macropores with radii ranging from 200 to 10,000 Å. These catalyst pellets are prepared by compacting fine porous powders. The micropore region arises from the pore structure within each of the particles of the original powder, while the macropores are formed by the passageways around the compacted particles. As the pelleting pressure is increased, the macropores become successively reduced in size, but the micropores remain unaffected unless the crushing strength is exceeded. Most commercial forms of alumina catalysts exhibit this type of bimodal pore size distribution. For example, Rothfeld (17) observed two peaks, one centered at a radius of 6250 Å and the other at 60 Å. The micropores accounted for about 99% of the surface area and 65% of the void volume. It is these pores that one would expect to be most significant from a catalytic viewpoint. Some other industrial catalysts are deliberately fabricated with a macropore–micropore structure in order to minimize or eliminate pore diffusion limitations on the reaction rate. The macropores serve as expressways that facilitate reactant transport to the internal surface area of the catalyst. The micropores are analogous to narrow one-lane roads.

## 6.5 CATALYST PREPARATION, FABRICATION, AND ACTIVATION

The task of developing a suitable catalyst for commercial applications involves many considerations, ranging from obvious factors such as catalyst activity and selectivity to variables such as the catalyst shape and the composition of the binder used in a pelletizing process. This section is devoted to a discussion of these considerations and of the techniques involved in manufacturing industrial catalysts.

Figure 6.6 illustrates some of the requirements to be kept in mind when developing a catalyst for industrial applications. The art of catalyst formulation involves reconciling conflicting demands that may be imposed by such requirements. The keystone of the arch is a material that has high intrinsic activity and selectivity for promoting the reaction of interest. This material may be used in bulk form or, more commonly, it will be supported on a carrier material that may or may not have catalytic activity of its own. The activity per unit volume is of practical significance because process economics are often strongly dependent on the cost of packed reactor volume. Consequently, the catalyst should have a high specific surface area, and it should have a pore structure such that reactants can gain easy access to the inner surfaces of the catalyst pellet. The first of these requirements follows directly from the fact that the reaction takes place at the fluid–solid interface, while the requirement for an appropriate pore structure follows from a desire to avoid diffusional and mass transfer limitations on chemical conversion rates (see Chapter 12).

The lifetime of a catalyst is another factor that plays a key role in determining process economics. This lifetime is the period during which the catalyst produces the *desired product* in yields in excess of or equal to a designated value. The life of a catalyst may terminate because of

unacceptable changes in activity and/or selectivity, because of physical attrition, or because of unacceptable changes in mechanical properties arising from thermal cycling or other factors in the process environment. Resistance to poisoning and fouling as well as to other catalyst deactivation processes is an attribute to be preferred in commercial catalysts.

Mechanical and geometric properties also play a strong role in determining if a given formulation will give rise to a commercially viable catalyst. Catalyst pellets must be suitably shaped so that the reactant fluid can pass through a packed bed without excessive pressure drop or maldistribution of the flow. The finished catalyst must also be mechanically robust to avoid attrition during handling and loading and to avoid crushing under sustained loads during fixed-bed operation. The requirements of high strength and a stable structure depend on a firm welding together of the catalyst components into a structure that is not greatly weakened or changed by sintering during use.

Very seldom does an industrial catalyst consist of a single chemical compound or metallic element. Most often a catalyst formulation consists of a multitude of components, each of which performs an essential task in the creation of a commercially viable catalyst. As indicated in Figure 6.7, the components commonly found in industrial catalysts can be classified as catalytic species, catalyst supports, and catalyst stabilizers. The support may be a ceramic matrix bound together by a hydraulic cement. The support gives body and strength to the catalyst granule and is frequently used to decrease the concentration of the usually more expensive catalyst proper. The catalytic agents consist of the catalyst proper together with any materials added to promote or modify the active surface so as to enhance either catalyst activity or selectivity. Stabilizers may be present in the form of gross crystals readily seen under the scanning electron microscope, or they may be present in highly dispersed form. They prevent sintering

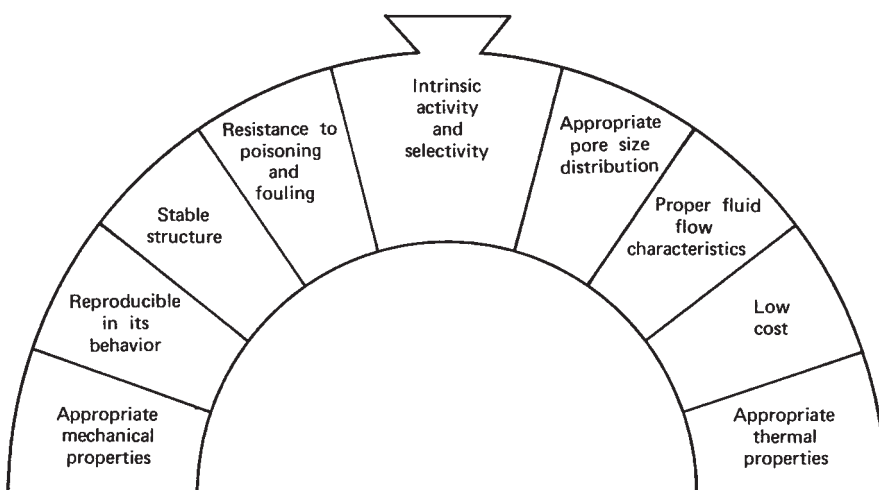


**Figure 6.6** Requirements for industrial catalysts.

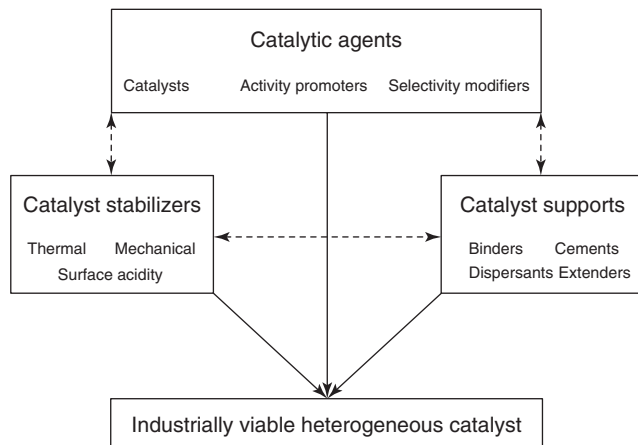


**Figure 6.7** Catalyst engineering involves an optimal combination of interdependent structural elements that yields the catalytic, mechanical, and physicochemical (specific surface area and pore size distribution, density, surface functionality, and acidity) properties desired for successful industrial applications. Solid arrows indicate primary contributions of catalyst components to the desired properties. Dashed arrows indicate secondary influences of these components via the interdependent nature of some properties.

and loss of active surface area through diffusional merging of contiguous small crystals and crystallites. Catalysts in which the active constituent is a metal with a relatively low melting point normally are stabilized through the use of refractory materials such as alumina, chromia, and magnesia, which act as spacers between the readily sinterable metal crystals. Metals are particularly susceptible to sintering when the dimensions of the crystals are very small (e.g., below 500 Å) and the temperature exceeds half their melting point. Because commercial catalysts are complex multicomponent mixtures, it is appropriate to describe in broad terms some of the procedures used in the preparation of these materials.

### 6.5.1 Catalyst Preparation

Natural products and common industrial chemicals in massive form are seldom useful as catalysts because they have low specific surface areas, may contain various amounts of impurities that have deleterious effects on catalyst performance, do not usually have the exact chemical composition desired, or are too expensive to use in bulk form. The preparation of an industrial catalyst generally involves a series of operations designed to overcome such problems. Many catalysts can be produced by several routes. The actual choice of technique for the manufacture of a given catalyst is based on ease of preparation, homogeneity of the final catalyst, stability of the catalyst, reproducibility of quality, and cost of manufacture. The two most commonly used techniques for catalyst preparation are the only ones we shall consider:

1. Precipitation or gel formation of the active component or components through the interaction of aqueous solutions of two or more chemical compounds.
  2. Impregnation of a carrier using a solution containing a compound of the catalyst component desired.

Precipitation is frequently used in the preparation of single- and multiple-component catalysts. If possible, the catalyst precursor is precipitated as a compound that will undergo some chemical change before it is converted into the substance that actually functions as the catalyst. Dehydration of a hydrated precipitate may be sufficiently drastic to accomplish this purpose. The nature of the impurities occluded or adsorbed on the precipitate must be considered in making up the starting solutions. Experience has indicated that the use of dilute solutions, nitrates or sulfates of the metal elements, and ammonia or ammonium salts as the precipitating agents generally facilitates the removal of impurities. In these cases subsequent heat treatment often suffices to drive off the impurities in volatile form. Significant variations in catalytic activity have been observed for precipitates of the same material formed under different conditions. When preparing multicomponent catalysts by coprecipitation techniques, the process variables must be manipulated to produce a uniform product. By adding a solution of two metal salts to an excess of the precipitating counter ion (carbonate, sulfide, hydroxide, etc.) simultaneous precipitation of both species is obtained. If the addition is carried out in the reverse order, there is a preferential precipitation of one metal salt relative to the other because of differences in solubility products.

One of the simplest, most commonly used techniques for preparing a catalyst involves dispersing an active component (or components) on a support material. Normally, one impregnates the carrier material with a solution of a soluble precursor of the catalyst and then converts this precursor to the product desired by oxidation, reduction, thermal decomposition, or some other suitable step. Where appropriate, it is preferable to use a granular support instead of a powder, because it eliminates the necessity for pelletizing or extrusion to obtain the final product.

In many cases, drying operations are critical to the production of successful commercial catalysts. Close control of the drying process is necessary to achieve the proper distribution of the catalyst precursor within the pore structure of the support. Drying also influences the physical characteristics of the finished catalyst and the ease with which subsequent pelleting or extrusion processes may be carried out.

In general, all materials used to catalyze reactions of a vapor-phase feed are calcined or activated at temperatures above 400 to 500°F. This heat treatment may accomplish one or more of the following tasks.

1. Reduce the moisture content to a level consistent with the temperature at which the catalyst will be employed.
2. Decompose salts containing the catalyst precursors, such as metal nitrates, formates, oxalates, or acetates. (Oxides are the usual products of the decomposition process.)
3. Form metal catalysts by reduction of metal oxides with hydrogen.
4. Increase the strength of the finished pellet or extrudate.
5. Influence the initial activity and stability of the catalyst.

The form in which the catalyst is employed is strongly dependent on the reaction involved, the scale of the process, the specific nature of the catalyst, and the type of reactor. Catalysts used for reactions carried out with a liquid feed are usually ground so as to pass through a 100- to 200-mesh screen. Catalysts employed with gaseous feeds in fixed-bed reactors are most frequently used in the form of pellets, granules, or extrusions, whereas those used in fluidized beds are usually ground to pass through a 60-mesh screen. With cylindrical pellets the ratio of length to diameter is usually kept below 3 : 1 so that the pellets will not pack parallel to one another and thus lead to excessive pressure drop or excessive bypassing, channeling, or maldistribution of the flow. The ratio of the diameter of the reaction vessel to a characteristic pellet dimension is also significant, because it is almost impossible to achieve uniform packing if this ratio is less than 5 : 1.

More detailed treatments of catalyst manufacture and activation processes are available in the literature (1, 18–23).

### 6.5.2 Catalyst Supports, Promoters, and Inhibitors

It is very seldom that a commercial catalyst consists of only a single chemical compound or element. Often, the active constituent is supported on a carrier material that may or may not possess catalytic activity of its own. Enhanced catalytic activity, selectivity, or stability may also be achieved by the addition of other materials, referred to as promoters or inhibitors.

Early workers viewed carriers or catalyst supports as inert substances that provided a means of spreading out an expensive material such as platinum or else improved the mechanical strength of an inherently weak material. The primary factors in the early selection of catalyst supports were their physical properties and their low cost; hence, pumice, ground brick, charcoal, coke, and similar substances were used. No attention was paid to the possible influence of the support on catalyst behavior; differences in behavior were attributed to variations in the distribution of the catalyst itself.

However, it is now recognized that the catalyst carrier does more than provide a physical framework on which the catalyst is supported. In many cases there is an interaction between the carrier and the active component of the catalyst, so that the character of the active surface will change. For example, the electronic character of the supported catalyst may be influenced by the transfer of electrons across the catalyst–carrier interface. In some cases the carrier itself has a catalytic activity for the primary reaction, an intermediate reaction, or a subsequent reaction, and a “dual-function” catalyst is thereby obtained. Materials of this type are employed widely in reforming processes. There are other cases in which the interaction of the catalyst and support are much more subtle and difficult to label. For example, the crystal size and structure of supported metal catalysts as well as the manner in which the metal is dispersed can be influenced by the nature of the support material.

One should distinguish between true catalyst supports and diluents. A catalyst support (or carrier) is a material on which a thin layer of catalyst is deposited; a diluent is an inert material thoroughly mixed with the catalyst to enhance the binding properties of a powdered catalyst or to assist in pelleting or extrusion fabrication procedures.

An ideal carrier is one that is:

1. Inexpensive
2. Available in large quantities of uniform composition
3. Sufficiently porous to permit dispersion of catalyst on its interior surfaces
4. Free of any components that may poison the catalyst
5. Stable under operating and regeneration conditions
6. Strong enough to resist any thermal or mechanical shocks that it is likely to suffer as well as any disruptive action arising from fouling material that may be deposited in its pores
7. Resistant to attrition
8. Inert to attack from components of the feed stream and product stream and any components present in any regeneration streams to which it may be exposed
9. Noncatalytic with regard to any undesirable side reactions

The average pore size and the pore size distribution should be such that physical limitations are not placed on the conversion of reactants to products. The particle size of the carrier must also be suitable for the purpose intended (i.e., small for fluidized-bed reactors and significantly larger for fixed-bed applications).

The types of materials used commercially as catalyst supports can be categorized as having high or low specific surface areas. The low-surface-area (up to  $1 \text{ m}^2/\text{g}$ ) materials are generally ceramic materials such as silica

or alumina. They are often formed by high-temperature fusion (2000°C) in electric furnaces. The product of this operation is crushed, sieved, and fabricated into various shapes (spheres, granules, rings, cylindrical annuli, or irregular shapes). Partial sintering is then accomplished by firing at temperatures in the neighborhood of 1400°C. The resulting products are stable mechanically and are easily impregnated with a variety of catalyst precursor solutions. The final product is quite porous, with pore sizes typically in the range 20 to 100  $\mu\text{m}$ . Low-surface-area carriers are used where the need for a high activity per unit mass of finished catalyst is less important than other factors, such as catalyst cost or selectivity.

The high-specific-surface-area supports (10 to 100  $\text{m}^2/\text{g}$  or more) are natural or manufactured materials that normally are handled as fine powders. When processed into the finished catalyst pellet, these materials often give rise to pore size distributions of the macro–micro type mentioned previously. The micropores exist within the powder itself, and the macropores are created between the fine particles when they are compressed together in a pellet press. Diatomaceous earth and pumice (or cellular lava) are naturally occurring low-cost materials that are representative of this class of catalyst support. Among the synthetic carriers that can be created by modern technology are those derived from clays, bauxite, activated carbon, and xerogels of silica gel and alumina gel.

Although a carrier is often the major constituent of a catalyst pellet, one often finds that there are materials that are added in small amounts during catalyst preparation to impart improved characteristics to the finished catalyst. These materials are referred to as *promoters*. They may lead to better activity, selectivity, or stability. In this regard, one should note that it is often economically desirable to sacrifice high initial activity for either higher selectivity or enhanced stability. The manner in which promoters act is not well understood, even though a number of plausible explanations have been set forth. They remain one of the reasons for the “black magic” aura of catalysis.

In 1920, Pease and Taylor (24) proposed a definition of promoter action that is still appropriate today. Promotion occurs in those “cases in which a mixture of two or more substances is capable of producing a greater catalytic effect than can be accounted for on the supposition that each substance in the mixture acts independently and in proportion to the amount present.” Hence “better” catalyst performance implies an improvement beyond that expected from a simple additive rule. The phenomenon is often characterized by a steep rise in activity to a sharp maximum at a low concentration of promoter followed by a decline to a lower or zero level of activity, depending on whether or not the promoter alone is capable of acting as a catalyst.

Some hypotheses that have been offered in an effort to explain promotion effects are:

1. The promoter may change the electronic structure of the solid in such a way that the activity per unit area is increased.
2. The promoter may catalyze an intermediate step in the reaction. In this sense it may act as one component of a dual-function catalyst.
3. The promoter may slow down or otherwise influence crystal formation and growth, or produce lattice defects. These effects may lead either to a higher activity per unit area or to a higher specific surface area.

Promoters may influence selectivity by poisoning undesired reactions or by increasing the rates of desired intermediate reactions so as to increase the yield of the product desired. If they act in the first sense, they are sometimes referred to as *inhibitors*. An example of this type of action involves the addition of halogen compounds to the catalyst used for oxidizing ethylene to ethylene oxide (silver supported on alumina). The halogens prevent complete oxidation of the ethylene to carbon dioxide and water, thus permitting the use of this catalyst for industrial purposes.

Another example of catalyst promotion is the use of additives to inhibit the loss of active surface area during operation. Since this effect enhances catalyst stability, such additives are often called *stabilizers*. These promoters may inhibit sintering of active sites on the surface or growth of microcrystalline regions. They may form solid solutions with higher melting points than those of the active agents alone, thus permitting a reaction to be carried out at a higher temperature than would be possible otherwise. Alumina is used for this purpose in the manufacture of iron-based ammonia synthesis catalysts.

In commercial catalysts it is often useful to employ a multiplicity of promoters, each of which serves a particular function or acts in conjunction with other constituents to produce a more desirable catalyst.

## 6.6 POISONING AND DEACTIVATION OF CATALYSTS

Since the earliest days of heterogeneous catalysis, decreases in activity during use have been observed. The rates at which catalyst deactivation processes take place may be fast or slow. In some cases the decline in activity is so rapid that the catalyst ceases to function effectively after a few minutes or hours of exposure to a reactant feed stream. On the other hand, there are cases where the deactivation processes occur so slowly that the catalyst may function effectively for months or years. In the design of commercial catalytic processes, one obviously must

take these factors into account so as to allow for periodic replacement or regeneration of the heterogeneous catalyst.

If the deactivation is rapid and caused by the decomposition or degradation of reactants or products on the catalyst surface, the process is termed *fouling*. In this case a deposit is formed on the surface or in the pores that physically blocks a portion of the catalyst and prevents it from catalyzing the reaction. Such fouling is particularly rapid with silica-alumina cracking catalysts, and in this application, the design of a unit for catalyst regeneration is as important as the design of the reactor proper. An example of a cracking reaction leading to fouling might be  $C_{10}H_{22} \rightarrow C_5H_{12} + C_4H_{10} + C$  (solid on catalyst surface). The carbon deposit may be burned off with oxygen and/or steam to regenerate the catalyst so that the active surface is no longer covered.

If the activity of the catalyst is slowly modified by chemisorption of materials that are not easily removed, the deactivation process is termed *poisoning*. It is usually caused by preferential adsorption of small quantities of impurities (poisons) present in the feed stream. Adsorption of extremely small amounts of the poison (a small fraction of a monolayer) is often sufficient to cause very large losses in catalytic activity. The bonds linking the catalyst and poison are often abnormally strong and highly specific. Consequently, the process is often irreversible. If the process is reversible, a change in the temperature or the composition of the gas to which it is exposed may be sufficient to restore catalyst activity. This process is referred to as *reactivation*. If the preferential adsorption of the poison cannot readily be reversed, a more severe chemical treatment or complete replacement of the catalyst may be necessary.

In addition to fouling and poisoning, there is a third catalyst deactivation process that is commonly encountered in industrial practice. This is the phenomenon known as *aging*. Aging involves a loss in specific activity because of a loss in catalyst surface area arising from crystal growth or sintering processes. The rate of the aging process becomes more rapid as the temperature increases. It may also be increased by the presence of certain components of the feed stream or product stream or of trace constituents of the catalyst. In some cases a flux or glaze capable of blocking catalyst pores may be produced.

Various schemes have been proposed for classifying poisons, but the one that is perhaps the most convenient for chemical engineers interested in reactor design is the classification in terms of the manner by which the poison affects chemical activity. In these terms one can distinguish between four general but not sharply differentiated classes.

**1. Intrinsic activity poisons.** These poisons decrease the activity of the catalyst for the primary chemical reaction by virtue of their direct electronic or chemical influence on

the catalyst surface or active sites. The mechanism appears to be one that involves coverage of the active sites by poison molecules, removing the possibility that these sites can subsequently adsorb reactant species. Common examples of this type of poisoning are the actions of compounds of elements of the groups Vb and VIb (N, P, As, Sb, O, S, Se, Te) on metallic catalysts.

**2. Selectivity poisons.** These poisons decrease the selectivity of the catalyst for the main reaction. In many cases impurities in the feed stream will adsorb on the catalyst surface and then act as catalysts for undesirable side reactions. The classic examples of poisons of this class are heavy metals such as Ni, Cu, V, and Fe, which are present in petroleum stocks in the form of organometallic compounds such as porphyrins. When these feedstocks are subjected to catalytic cracking, these organometallic compounds decompose and deposit on and within the catalyst. The metals then act as dehydrogenation catalysts. The product distribution is markedly affected, resulting in lower yields of gasoline and higher yields of light gas, coke, and hydrogen. Very small poison concentrations suffice to produce large changes in selectivity. In cases where a large number of parallel and series reactions are involved, the poison adsorbed is thought to change the activation energy barrier for some of the competitive intermediate steps, resulting in increased rates of undesirable side reactions relative to that of the primary reaction.

**3. Stability poisons.** These poisons decrease the structural stability of the catalytic agent or of the carrier by facilitating recrystallizations and other structural rearrangements. Steam acts as this type of a poison for silica-alumina gel catalysts. The steam acts not so much by reducing the intrinsic activity per unit surface area, but by reducing the active area, thus decreasing the activity per unit weight of catalyst. The temperature at which the reactor operates has a marked effect on stability poisoning. Sintering, localized melting, and recrystallization occur much more rapidly at high temperatures than at low temperatures.

**4. Diffusion poisons.** This phenomenon is closely akin to catalyst fouling. Blockage of pore mouths prevents full use of the interior surface area of the pellet. Entrained dust particles or materials that can react on the catalyst to yield a solid residue give rise to this type of poisoning.

Many reviews listing specific poisons for specific catalysts are available (24–27).

## LITERATURE CITATIONS

1. BARTHOLEMEW, C. H., and FARRAUTO, R. J., *Fundamentals of Industrial Catalytic Processes*, 2nd ed. Wiley-Interscience, Hoboken, NJ, 2006.

2. THOMAS, C. L., *Catalytic Processes and Proven Catalysts*, Academic Press, New York, 1970.
3. THOMSON, S. J., and WEBB, G., *Heterogeneous Catalysis*, Oliver & Boyd, Edinburgh, 1968.
4. BRUNAUER, S., DEMING, L. S., DEMING, W. E., and TELLER, E., *J. Am. Chem. Soc.*, **62**, 1723 (1940).
5. LANGMUIR, I., *J. Am. Chem. Soc.*, **38**, 221 (1916).
6. LANGMUIR, I., *J. Am. Chem. Soc.*, **40**, 1361 (1918).
7. TAYLOR, H. S., *Proc. R. Soc. London, A* **108**, 105 (1925).
8. BRUNAUER, S., EMMETT, P. H., and TELLER, E., *J. Am. Chem. Soc.*, **60**, 309 (1938).
9. HOUGEN, O. A., and WATSON, K. M., *Chemical Process Principles*, Part 3, *Kinetics and Catalysis*, pp. 906–907, Wiley, New York, 1947.
10. CHAMBERS, R. P., and BOUDART, M., *J. Catal.*, **6**, 141 (1966).
11. HOUGEN, O. A., and WATSON, K. M., *Ind. Eng. Chem.*, **35**, 529 (1943).
12. YANG, K., and HOUGEN, O. A., *Chem. Eng. Prog.*, **46** (3), 149 (1950).
13. OLDENBURG, C. C., and RASE, H. F., *AIChE J.*, **3**, 462 (1957).
14. HOUGEN, O. A., *Reaction Kinetics in Chemical Engineering*, Chem. Eng. Prog. Monograph Ser., No. 1, 47, Chap. 5, 1951.
15. THOMAS, J. M., and THOMAS, W. J., *Introduction to the Principles of Heterogeneous Catalysis*, pp. 206–211, Academic Press, New York, 1967.
16. CRANSTON, R. W., and INKLEY, F. A., *Adv. Catal.*, **9**, 143 (1957).
17. ROTHFELD, L. B., *AIChE J.*, **9**, 19 (1963).
18. CATALYST HANDBOOK, Springer-Verlag, New York, 1970.
19. CIAPETTA, F. G., and PLANK, C. J., *Catalyst Preparation*, Chap. 7 in *Catalysis*, Vol. I, P. H. EMMETT (Ed.), Reinhold, New York, 1964.
20. CIAPETTA, F. G., HELM, C. D., and BARAL, L. L., *Commercial Preparation of Industrial Catalysts*, Chap. 2 in *Catalysis in Practice*, C. H. COLLIER (Ed.), Reinhold, New York, 1957.
21. INNES, W. B., *Catalyst Carriers, Promoters, Accelerators, Poisons, and Inhibitors*, Chap. 6 in *Catalysis*, Vol. I, P. H. EMMETT (Ed.), Reinhold, New York, 1954.
22. ANDERSON, J. R., *Structure of Metallic Catalysts*, Academic Press, New York, 1975.
23. TWIGG, M. V. (Ed.), *Catalyst Handbook*, 2nd ed, Wolfe Publishers, Frome, England, 1989.
24. PEASE, R. N., and TAYLOR, H. S., *J. Phys. Chem.*, **24**, 241 (1920).
25. MAXTED, E. B., *J. Soc. Chem. Ind. London*, **67**, 93 (1948).
26. MAXTED, E. B., *Adv. Catal.*, **3**, 129 (1951).
27. BUTT, J. B., *Chemical Reaction Engineering*, *Adv. Chem. Ser.*, **109**, 259 (1972).

## PROBLEMS

**6.1** R. J. Farrauto and C. H. Bartholemew (*Fundamentals of Industrial Catalytic Processes*, p. 127, Blackie, London, 1997) reported the data in Table P6.1 for the adsorption of nitrogen at 77 K on a bayerite alumina sample.

- (a) Use these data to prepare plots of the adsorption and desorption branches of the adsorption isotherm. Comment.
- (b) Test these data to see if they can be fit by an isotherm of the Langmuir form for relative pressures up to about 0.4. Use the Langmuir equation in the form

$$\frac{P_A}{v} = \frac{1}{v_m K} + \frac{P_A}{v_m}$$

where  $P_A$  is the pressure of adsorbate and  $v$  is the corresponding equivalent volume of adsorbed material. Comment.

**Table P6.1**

Relative pressure, $P/P_0$	Data for adsorption (increasing $P$ )		Data for desorption (decreasing $P$ )	
	Volume adsorbed (cm <sup>3</sup> at STP/g)	Relative pressure, $P/P_0$	Volume adsorbed (cm <sup>3</sup> at STP/g)	
0.010	31.0	0.992	200.0	
0.020	34.4	0.990	198.7	
0.031	36.6	0.987	196.1	
0.040	38.2	0.981	192.1	
0.049	39.7	0.975	188.8	
0.079	43.6	0.968	185.7	
0.109	47.1	0.957	182.0	
0.138	50.2	0.942	178.3	
0.168	53.2	0.924	175.0	
0.198	56.3	0.905	172.2	
0.243	61.0	0.890	170.2	
0.283	65.5	0.868	167.6	
0.327	70.7	0.846	165.5	
0.369	76.4	0.822	163.1	
0.414	83.3	0.795	160.5	
0.459	90.6	0.766	157.6	
0.501	97.2	0.735	153.9	
0.546	103.1	0.701	149.1	
0.587	107.6	0.666	143.5	
0.630	111.5	0.628	136.8	
0.667	114.8	0.590	129.2	
0.698	117.4	0.545	120.1	
0.732	120.2	0.503	112.7	
0.764	123.0	0.460	99.4	
0.793	125.7	0.408	82.4	
0.818	128.3	0.371	76.5	
0.844	131.4	0.324	70.0	
0.866	134.7	0.279	64.7	
0.887	138.6	0.243	60.7	
0.906	143.4	0.202	56.4	
0.923	149.3	0.171	53.3	
0.938	155.9	0.141	50.2	
0.946	159.7			
0.965	172.7			
0.973	178.2			
0.978	182.2			
0.984	187.3			
0.987	190.8			
0.992	196.6			
0.995	201.1			

- (c) Test these data to see if they are consistent with the BET equation for values of the relative pressure below about 0.4. If they are consistent, what is the corresponding value of the BET surface area?

**Table P6.2**

H <sub>2</sub> on Cu powder at 25°C		Nitrogen on silica gel at -196°C	
Pressure (cmHg)	Volume adsorbed/ g sample (cm <sup>3</sup> at STP)	Pressure (cmHg)	Volume adsorbed/ g sample (cm <sup>3</sup> at STP)
0.097	0.163	0.6	6.1
0.110	0.171	2.5	12.7
0.190	0.221	14.9	17.0
0.265	0.256	25.0	19.7
0.405	0.321	29.8	21.5
0.555	0.371	32.8	23.0
0.750	0.411	40.2	27.7
0.815	0.421	46.0	33.5
1.195	0.471		

**6.2** The adsorption data in Table P6.2 were recorded at constant temperature for two different systems. For the data pertaining to chemisorption of hydrogen on copper powder at 25°C, prepare a Langmuir adsorption isotherm plot using coordinates that should yield a straight line. Use this plot to determine the specific surface area. For the data pertaining to the adsorption of nitrogen on silica gel at -196°C, prepare both Langmuir and BET plots using coordinates that one would expect to give rise to linear plots. What specific surface areas are predicted in each case? The areas covered per molecule of adsorbed hydrogen and nitrogen are 14.2 and 16.2 Å<sup>2</sup>, respectively. The normal boiling point of liquid nitrogen is minus 196°C. Comment on your results.

**6.3** H. S. Taylor and S. C. Liang [*J. Am. Chem. Soc.*, **69**, 1306 (1947)] studied the extent of adsorption of hydrogen on zinc oxide at a constant gas pressure and at successively increasing temperatures. A typical curve of the amount adsorbed as a function of time is shown in Figure P6.3. In this figure the curve to the left of A applies at 0°C; at A the temperature is raised to 111°C, at B to 154°C, at C to 184°C, and at D to 218°C. Interpret these data.

**6.4** R. M. Barrer and E. Strachan [*Proc. R. Soc. London, A* **231**, 52 (1955)] investigated adsorption and flow phenomena in cylindrical pellets formed from microporous carbon powder by compression to various degrees. Both monatomic and diatomic gases were studied using plots of linearized forms of the BET and Hütting equations to determine the specific surface areas of pellets characterized by different porosities. All of the pellets and the powder from which they were formed had very high specific surface areas. Pertinent data from measurements at 90 K using argon as the adsorbate at relative pressures ( $P/P_{\text{saturation}}$ ) from 0 to close to unity are given in Table P6.4.

What is your interpretation of these data, especially the fact that the specific surface area goes through a minimum as the sample is subjected to increasing degrees of compression?

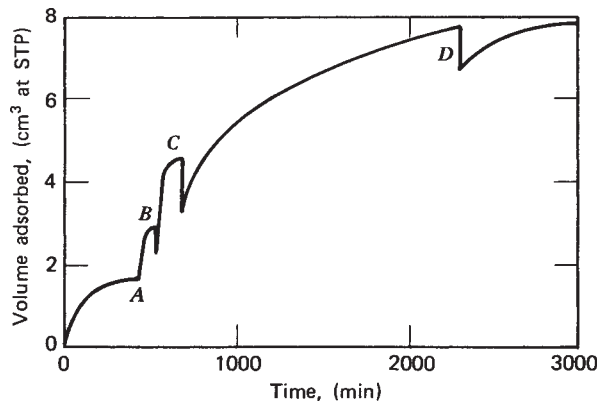


**Figure P6.3** Typical adsorption rate curve for the adsorption of hydrogen on zinc oxide at 1 atm. [Adapted with permission from H. S. Taylor and S. C. Liang, *The Heterogeneity of Catalyst Surfaces for Chemisorption*, *J. Am. Chem. Soc.*, **69**, 1306 (1947). Copyright © 1947 by the American Chemical Society.]

**6.5** E. F. Restelli and J. Coull [*AIChE J.*, **12**, 292 (1966)] studied the transmethylation reaction of dimethylamine in a differential flow reactor using montmorillonite as a catalyst. They measured initial reaction rates at steady state under isothermal conditions for this heterogeneous catalytic process. The stoichiometry of the initial reaction is



The feed stream consisted of essentially pure dimethylamine. What is your interpretation of the data presented in Figures P6.5-1 and P6.5-2? In your discussion, place particular emphasis on the various physical and chemical processes that can affect the rate of a chemical reaction.

**Table P6.4**

Porosity of pellet	Monolayer coverage via BET plot	Monolayer coverage via Hütting plot	Specific surface area via BET plot	Specific surface area via Hütting plot
	( $v_m$ in cm <sup>3</sup> )	( $v_m$ in cm <sup>3</sup> )	( $S_g$ in m <sup>2</sup> /g)	( $S_g$ in m <sup>2</sup> /g)
Loose powder	254.7	271.1	1060	1128
0.79	237.3	250.8	987	1043
0.64 (plug 6)	224.3	236.7	933	985
0.64 (plug 4)	216.5	227.3	901	946
0.53	214.0	220.9	890	919
0.45	191.1	202.0	795	841
0.45 <sup>a</sup>	204.7	215.1	803	843
0.37	201.6	211.7	839	881

<sup>a</sup>For this trial the temperature was 79 K rather than 90 K.

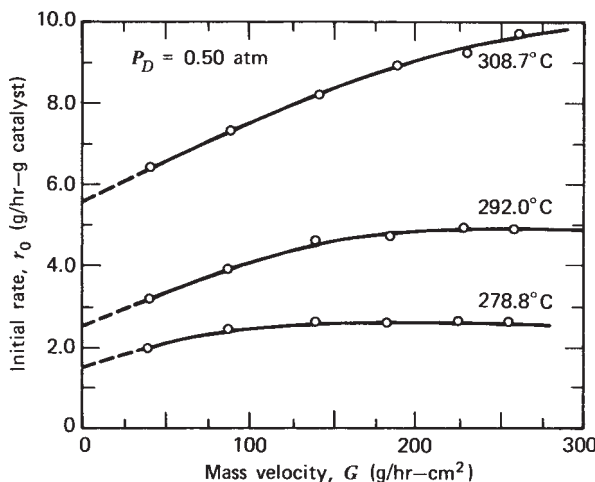


**Figure P6.5-1** Initial rate versus mass velocity. [Reprinted with permission from *AIChE J.*, **12**, 292 (1966).]

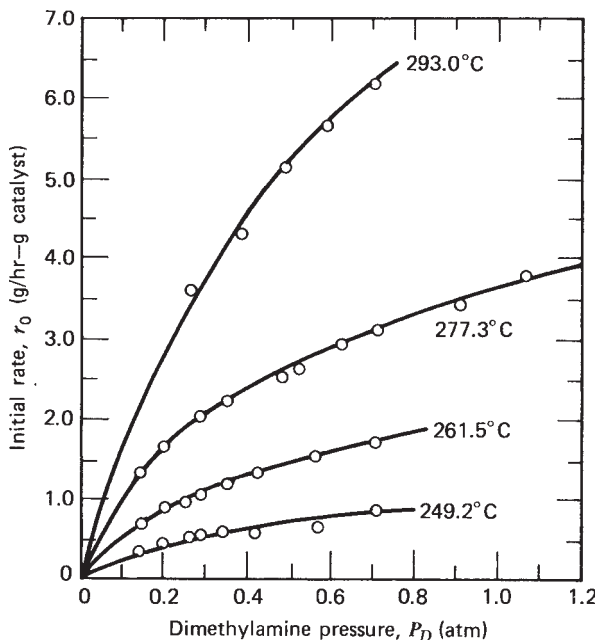


**Figure P6.5-2** Initial rate versus pressure of dimethylamine. [Reprinted with permission from *AIChE J.*, **12**, 292 (1966).]

- (a) Using a catalyst size  $-50, +60$  mesh with a feed pressure of 0.5 atm, the authors obtained the data reproduced in Figure P6.5-1.  $G$  is the mass velocity under steady-state operating conditions in grams per hour per square centimeter, and  $r_0$  is the initial reaction rate in grams per hour per gram of catalyst. The three curves correspond to three different operating temperatures.
- (b) A series of experiments involved measurement of reaction rates for different catalyst sizes, maintaining all other variables constant. The rates measured were constant for catalyst particle sizes from  $-100, +120$  to  $-30, +40$  mesh, a fourfold variation in average particle diameter. These experiments were carried out at mass

velocities corresponding to the asymptotic portions of the curves in Figure P6.5-1.

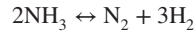
- (c) Several other experiments were also carried out at mass velocities corresponding to the asymptotic portions of the curves shown in Figure P6.5-1. Initial rates were measured as a function of the dimethylamine pressure for the four temperatures indicated in Figure P6.5-2. These data may be fit by an expression of the form  $r_0 = k_D P_D^{0.523}$ , where  $P_D$  is the partial pressure of dimethylamine. Postulate a generic Hougen-Watson model that is consistent with this rate law. What is the activation energy of this reaction?

- 6.6** R. E. Mardaleishvili, Hu Sin-Chou, and Zh. Ya. Smorodinskaya [*Kinet. Catal.*, **8**, 664 (1967)] studied the catalytic decomposition of ammonia on quartz. The following initial rate data were obtained by these investigators at  $951^\circ\text{C}$ .

Initial rate (arbitrary units)	Initial ammonia pressure (torr)
0.0033	20
0.0085	50
0.0140	90
0.0236	140

What is the order of the reaction with respect to ammonia?

- 6.7** C. N. Hinshelwood and R. E. Burk [*J. Chem. Soc.*, **127**, 1105 (1925)] studied the decomposition of ammonia over a heated platinum filament at  $1138^\circ\text{C}$ . The stoichiometry of the reaction is



Initially, pure  $\text{NH}_3$  was present in the reaction vessel. The following data are representative of the kinetics of the reaction; the reactor volume is constant.

Time, $t$ (s)	Total pressure (kPa)
0	26.7
10	30.4
60	34.1
120	36.3
240	38.5
360	40.0
720	42.7

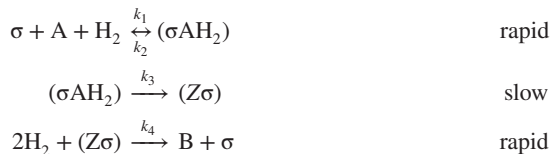
Ascertain if a rate expression of the form  $r = kP_{\text{NH}_3}/P_{\text{H}_2}$  provides a reasonable representation of the experimental data. If it does, what is the corresponding value of the rate constant? Indicate the type of Hougen-Watson model that leads to this type of rate expression.

- 6.8** V. Y. Konyukhov, N. V. Kul'kova, and M. I. Temkin [*Kinet. Catal.*, **21**, 496 (1980)] studied the kinetics of the hydrogenation of benzoic acid (A) to cyclohexylcarboxylic acid (B) over palladium on an activated charcoal catalyst.



At typical reaction conditions hydrogen gas is passed through a well-stirred solution of benzoic acid in liquid butanol in which very fine catalyst particles are suspended.

- (a) These authors suggested that the mechanism of this reaction is of the following form:



where  $\sigma$  represents a vacant surface site and where the species in parentheses represent adsorbed reaction intermediates. Because the last step occurs so rapidly, surface coverage by species Z is very, very small (i.e.,  $\theta_Z \approx 0$ ).

- (b) Figure P6.8-1 is a plot of the total rate of product formation versus mass of suspended catalyst for reaction at 130°C, an initial benzoic acid concentration of 0.4 M, and a hydrogen pressure of 50 atm. What are the implications of this figure?

Figure P6.8-2 is a plot of the reaction rate per unit mass of catalyst versus the product  $C_A P_{H_2}$ . The data correspond to reaction at 130°C at a catalyst loading of 0.5 g. The data in the figure represent two types of experiments: the diamonds correspond to data at a fixed acid concentration (0.4 M) and variable hydrogen pressure.

$P_{H_2}$ (atm)	$r$ [mmol/(g·h)]
10	3.12
20	4.72
25	5.34
30	6.00
35	6.72
40	8.16
45	7.50
50	10.36
55	8.50
60	8.16

The triangles in the figure correspond to a constant hydrogen pressure of 50 atm.

$C$ (mol/L)	$r$ [mmol/(g·h)]
0.082	2.5
0.197	4.8
0.394	8.4
0.590	12.6
0.660	11.2
0.786	12.0
1.00	13.6

Is the proposed mechanism consistent with the data? Determine numerical values for any kinetic parameters (or their products or quotients) for which this is possible.

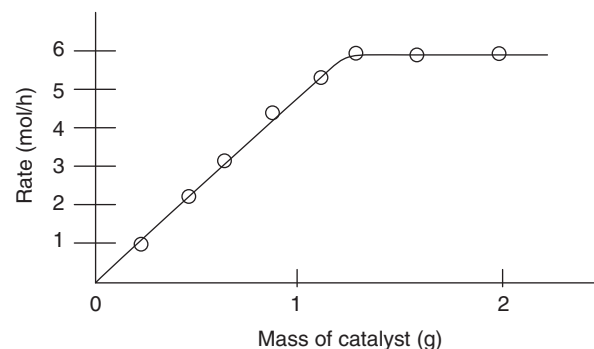


**Figure P6.8-1** Dependence of reaction rate on the mass of catalyst present.

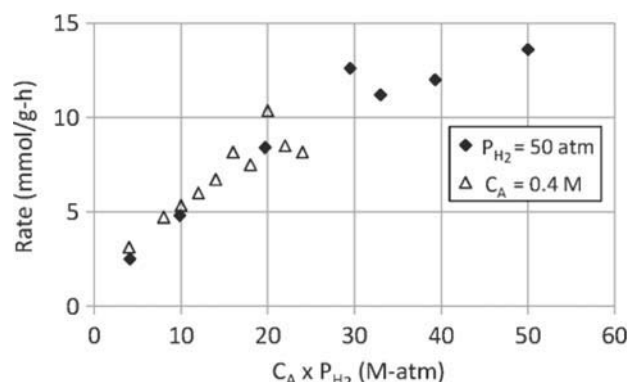
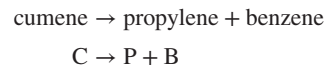


**Figure P6.8-2** Dependence of reaction rate on the presumed dependence of the rate law on the concentration of benzoic acid and hydrogen pressure.

**6.9** T. E. Corrigan, J. C. Garver, H. F. Rase and R. S. Kirk [Chem. Eng. Prog., **49**, 603 (1953)] investigated the catalytic cracking of cumene over a silica–alumina catalyst at 950°C:



They indicated that both single- and dual-site mechanisms can be postulated.

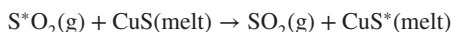
Single site	Dual site
(1) $\text{C} + \sigma \leftrightarrow \text{C}_\sigma$	(4) $\text{C} + \sigma \leftrightarrow \text{C}_\sigma$
(2) $\text{C}_\sigma \leftrightarrow \text{B}_\sigma + \text{P}$	(5) $\text{C}_\sigma + \sigma \leftrightarrow \text{B}_\sigma + \text{P}_\sigma$
(3) $\text{B}_\sigma \leftrightarrow \text{B} + \sigma$	(6) $\text{B}_\sigma \leftrightarrow \text{B} + \sigma$
	(7) $\text{P}_\sigma \leftrightarrow \text{P} + \sigma$

- (a) Assuming that the reaction is reversible and that steps 2 and 5 are rate limiting for the single- and dual-site mechanisms, respectively, derive Hougen–Watson rate expressions for these mechanisms.
- (b) These investigators also conducted some *initial* rate studies at 950 °F. Use the entries in the following table to

perform a graphical test to assess the validity of the mechanisms considered in part (a). You may assume that the range of pressures considered is sufficient to identify any maxima or minima that ought to be observed if the kinetic data are to be consistent with the rate expression associated with a particular mechanism.

Pressure (atm)	Initial rate $\times 10^2$ at 950°F [lb mol/(hr·lb catalyst)]
1.0	4.42
1.5	5.45
2.0	5.83
3.0	6.50
4.5	7.25
6.0	7.40
7.5	7.72
9.0	7.81
12.0	8.01
15.0	8.15
16.0	8.18
18.0	8.22

**6.10** P. T. Morland, S. P. Matthew, and P. C. Hayes [*Metall. Trans., 22B*, 211–217 (1991)] studied the kinetics of  $^{35}\text{S}$  isotope exchange between  $\text{SO}_2$  gas mixtures and  $\text{CuS}$  melts at 1523 K. This isotope exchange reaction can be expressed as



where  $\text{S}$  and  $\text{S}^*$  refer to normal and labeled sulfur atoms, respectively.

(a) The data in Table P6.10 have been reported as characteristic of this reaction in a gas environment comprised of  $\text{SO}_2$ ,  $\text{CO}_2$ , and  $\text{CO}$ .

For these trials there was no gaseous oxygen in the initial reaction mixture, and the concentration of this species at any time was very small. These authors have

**Table P6.10**

Run	$P_{\text{SO}_2}$ (atm)	$P_{\text{CO}}$ (atm)	$P_{\text{CO}_2}$ (atm)	Rate (mol/m <sup>2</sup> ·s)
2	0.10	0.019	0.881	0.0124
3	0.10	0.019	0.881	0.00922
4	0.10	0.019	0.881	0.0117
5	0.01	0.053	0.937	0.00197
6	0.01	0.051	0.939	0.00362
7	0.03	0.032	0.938	0.0122
8	0.03	0.032	0.938	0.0109
9	0.03	0.032	0.938	0.0067
10	0.40	0.005	0.595	0.0200
11	0.40	0.005	0.595	0.0230
13	0.20	0.009	0.790	0.0121
14	0.20	0.009	0.790	0.0145

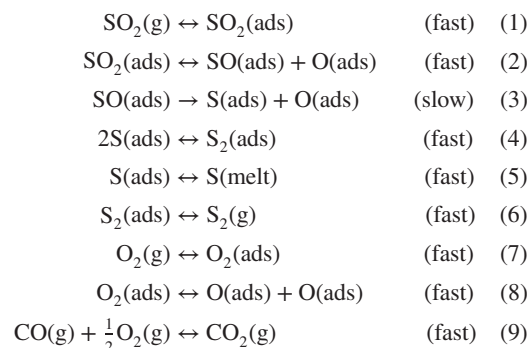
reported that this exchange reaction obeys the following rate expression:

$$r = 6.4 \left( \frac{P_{\text{CO}}}{P_{\text{CO}_2}} \right) P_{\text{SO}_2}$$

for partial pressures in atm and  $r$  in  $\text{mol}/(\text{m}^2 \cdot \text{s})$ . Analyze the data to determine if they are consistent with the rate expression proposed. In your analysis you should take into account the fact that physical considerations will require the rate to go to zero as  $P_{\text{SO}_2}$  becomes zero.

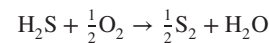
Are any other simple power law expressions (i.e., those for which all orders are either zero or positive or negative integers) consistent with the data? Consider only forms in which  $P_{\text{CO}}/P_{\text{CO}_2}$  appears as a ratio.

(b) The network of reactions indicated below has been proposed as a mechanism to explain the kinetics of this isotopic exchange reaction. Is this mechanism consistent with the experimental rate data?



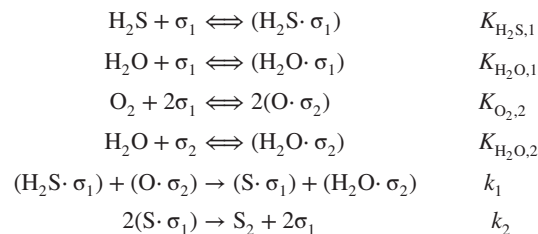
Denote the rate or equilibrium constant associated with a particular step ( $i$ ) as  $k_i$  or  $K_i$ , respectively. Let  $\theta_x$  represent the “concentration” of adsorbed species  $x$ .

**6.11** T. G. Alkhazov and N. S. Amirgulyan [*Kinet. Catal.*, **23**, 962 (1981)] studied the catalytic oxidation of  $\text{H}_2\text{S}$  in the presence of methane over a bed of iron oxide granules:



It is noteworthy that the methane does not react. Hence, one could envision a desulfurization process based on the use of this catalyst.

(a) These researchers have proposed the following two-site mechanism for this reaction.



where  $(\text{X} \cdot \sigma_i)$  refers to species  $\text{X}$  adsorbed on a site of type  $i$ . If adsorption equilibria are established with respect to

**Table P6.11-1** Rates of Oxidation of  $\text{H}_2\text{S}$  [mmol/(s·L of catalyst bed)] at Constant Space Velocity (6000 h<sup>-1</sup>) But Variable Linear Velocity

Temperature (K)	Volumetric flow rate of feed (L/s)			
	0.83	1.67	3.33	5.00
515	0.99	0.97	0.99	0.92
535	1.61	1.55	1.60	1.48
555	2.09	2.11	1.99	1.93

**Table P6.11-2** Rate of Oxidation of  $\text{H}_2\text{S}$  [mmol/(s·L of catalyst bed)] at Constant Space Velocity as a Function of Catalyst Granule Size

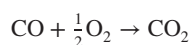
Temperature (K)	Granule size (mm)		
	0.25–0.5	0.5–1.0	1.5–2.0
515	0.73	0.71	0.69
535	1.19	1.16	1.14
555	1.53	1.54	1.52

$\text{H}_2\text{S}$  and  $\text{H}_2\text{O}$  on type 1 sites and with respect to dissociated oxygen on type 2 sites, and if the bimolecular surface reaction between adsorbed  $\text{H}_2\text{S}$  and an adsorbed oxygen atom is the rate-limiting step in this reaction, derive an expression for the expected reaction rate.

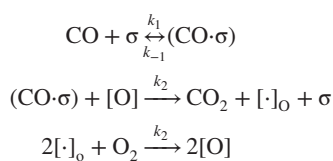
- (b) These researchers also investigated the effect of the presence of increasing amounts of water in the feed stream on the observed reaction rate. They noted that (other parameters remaining unchanged) the reaction rate decreased as the partial pressure of water in the feed stream increased. Is the mechanism above consistent with this observation?

The entries in Table P6.11-1 indicate the effects of a sixfold variation in the linear velocity of the feedstock on the observed reaction rate at a fixed space velocity in the reactor. The data in Table P6.11-2 reflect the effects of a several-fold variation in catalyst particle size on the rate observed. What are your interpretations of these data?

- 6.12 H. Collette, V. Deremince-Mathieu, Z. Gabelica, J. B. Nagy, E. G. Derouane, and J. J. Verbist [*J. Chem. Soc. Faraday Trans. 2*, **83**, 1263 (1987)] studied the catalytic oxidation of CO by  $\text{O}_2$  over a bismuth uranate ( $\text{Bi}_2\text{UO}_6$ ) catalyst:



and proposed the following mechanism:



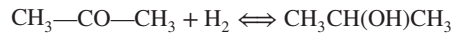
where  $[\text{O}]$  represents a lattice oxygen atom and  $[\cdot]_0$  designates an oxygen vacancy at the surface. The concentration of lattice oxygen atoms can be considered to be present in large excess. Equilibrium with respect to the adsorption step (reaction 1) is established very rapidly.

- (a) Derive the expression for the rate of formation of  $\text{CO}_2$  predicted by this mechanism. Under what circumstances is this expression consistent with the experimental data, which indicate that the reaction is zero-order in oxygen, first-order in CO at low partial pressures of CO, and zero-order at high partial pressures of CO?
- (b) The following data were obtained at 400°C over 0.5 g of catalyst. The reaction was carried out with 30 mol%  $\text{O}_2$  and the indicated partial pressure of CO. The balance of the gas mixture was  $\text{N}_2$ .

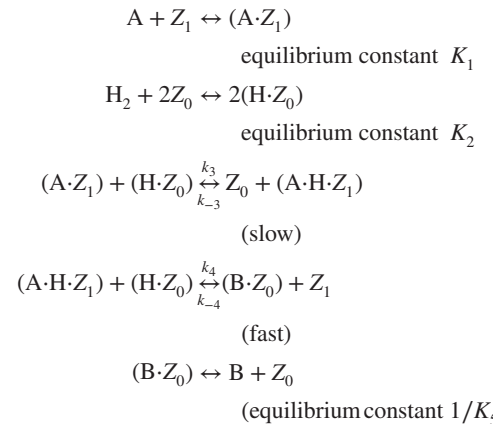
$P_{\text{CO}}$ (atm)	Rate $\times 10^4$ [(mol/(hr·g catalyst))]
0.035	8.2
0.109	19.6
0.194	27.3
0.250	31.6
0.301	35.2

Is the rate expression derived in part (a) consistent with these data? What are the values of the adsorption equilibrium constant ( $k_1/k_{-1}$ ) and the apparent rate constant for this reaction at 400°C?

- 6.13 G. I. Golodets, N. V. Pavlenko, and A. I. Tripol'skii [*Kinet. Catal.*, **27**, 296 (1986)] studied the vapor-phase hydrogenation of acetone (A) and the dehydrogenation of 2-propanol (B) over a platinum-on-alumina catalyst:



These investigators have proposed that the mechanism for this reversible reaction can be written as

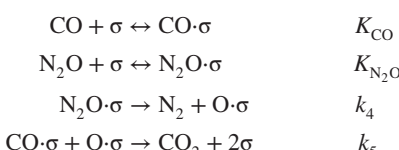


where  $\text{Z}_0$  and  $\text{Z}_1$  represent surface sites of types 0 and 1, respectively, parentheses denote surface species, B is 2-propanol [ $\text{CH}_3\text{CH(OH)CH}_3$ ], and A is acetone

$[\text{CH}_3\text{COCH}_3]$ . Reactions 1, 2, and 5 are considered to be at equilibrium. Reactions 3 and 4 are reversible, but not in equilibrium.

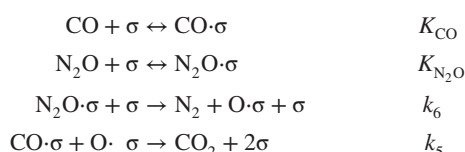
- (a) Derive the Hougen–Watson rate expression that is characteristic of this mechanism. Be sure to include the effects of both the forward and reverse reactions. Do not assume that the fraction of the surface sites of type 1 covered by the intermediate  $\text{A}\cdot\text{H}\cdot\text{Z}_1$  is negligible.
- (b) Experimentally, these researchers observed that if one examines the initial rate of formation of 2-propanol from acetone (i.e., the rate of the forward reaction) at temperatures from 387 to 423 K, the observed rate of reaction is (1) virtually independent of the partial pressure of hydrogen for values between 10 and 50 kPa (at a constant partial pressure of acetone); (2) increases with increasing acetone partial pressure for values between 10 and 40 kPa (at a constant partial pressure of hydrogen); and (3) for an acetone partial pressure of 20 kPa and a hydrogen partial pressure of 10 kPa, decreases with increasing partial pressure of alcohol. Under what conditions is the rate expression for the proposed mechanism consistent with these results? What conclusions can you draw relative to the fractional coverage of the two types of sites and the magnitudes of the various kinetic and equilibrium parameters?
- 6.14 P. Granger, P. Malfoy, P. Esteves, L. Leclercq, and G. Leclercq [J. Catal., **187**, 321–331 (1999)] studied the kinetics of the reaction between CO and  $\text{N}_2\text{O}$  over a supported platinum catalyst. These authors examined the ability of several Hougen–Watson rate expressions to fit their kinetic data.
- (a) Derive rate expressions for the five mechanisms below and indicate the corresponding mathematical forms in which the data should be plotted to test the validity of the proposed mechanism via linear regression analysis.

*Mechanism 1:*



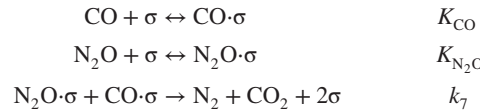
where  $\sigma$  refers to a vacant site and  $\text{X}\cdot\sigma$  refers to a site occupied by species X. The rate-controlling step for mechanism 1 is dissociation of the adsorbed  $\text{N}_2\text{O}$  species.  $K_i$  refers to an adsorption equilibrium constant and  $k_i$  to a rate constant.

*Mechanism 2:*



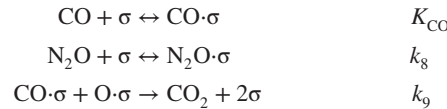
where the rate-controlling step is the reaction between an adsorbed  $\text{N}_2\text{O}$  species and a vacant site.

*Mechanism 3:*



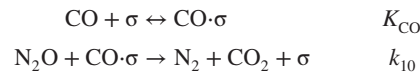
where the biomolecular surface reaction is the rate-controlling step.

*Mechanism 4:*



where the rate-controlling step is the dissociative adsorption of  $\text{N}_2\text{O}$ .

*Mechanism 5:*



where the rate-controlling step is the reaction between adsorbed carbon monoxide and gas-phase nitrous oxide.

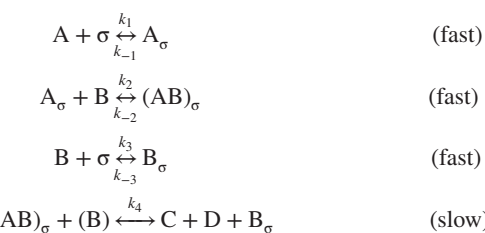
- (b) The experimental data obtained by these investigators indicate that for temperatures from 260 to 320°C the order of the reaction in CO is negative and the order of the reaction in NO is about 0.66. Can any of the mechanisms indicated above be ruled out on the basis of these data?

- 6.15 Z. Hong (Ph.D. thesis, University of Wisconsin–Madison, 1998) studied the kinetics of the isomerization of isobutane to isobutene in the presence of an H-mordenite catalyst at 200°C. In the presence of small quantities of isobutene (ca. 5 ppm) and at isobutane partial pressures of 0.1 to 0.8 atm, the observed rate expression is of the form

$$r = \frac{k P_A P_B^2}{k^* P_A + k' P_B}$$

where A refers to isobutane and B to isobutene.

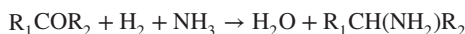
The following Hougen–Watson mechanism has been proposed to explain the kinetics observed.



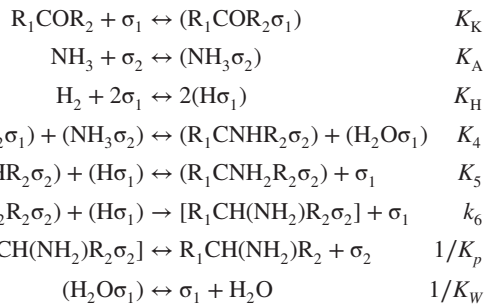
where  $\sigma$  refers to a vacant site on the surface of the catalyst and  $\text{A}_\sigma$ ,  $\text{B}_\sigma$ , and  $(\text{AB})_\sigma$  refer to adsorbed species.

Derive the rate expression associated with this mechanism. Is the general form of the rate expression associated with this mechanism consistent with the observed rate expression? Under what mathematical circumstances will the rate expression based on this mechanism be consistent with the experimental results? What conclusions can you draw concerning the surface coverages of species  $A_\sigma$ ,  $B_\sigma$ ,  $(AB)_\sigma$ , and vacant sites if the proposed mechanism is to be consistent with the observed rate expression? What additional tests can be performed to assess the validity of the proposed mechanism? Explain in detail what you would do in the laboratory and what you would expect to observe.

- 6.16** G. A. Kliger, L. S. Glebov, R. A. Fridman, E. I. Bogolepova, and A. N. Bashkirov [*Kinet. Catal.*, **19**, 489 (1978)] studied the kinetics of the hydroamination of 2-octanone and other aliphatic ketones over a sintered iron catalyst:

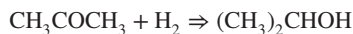


Kinetic data indicate that these reactions are zero-order with respect to both the ketone and ammonia, that the reaction is half-order with respect to hydrogen, and that water inhibits the reaction. All species are gases at the temperatures of interest. These researchers have postulated a mechanism that involves two types of sites: a  $\sigma_1$  site on which oxygen containing species and hydrogen are adsorbed and a  $\sigma_2$  site on which nitrogen containing species are adsorbed.

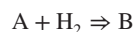


Step 6 is the slow, or rate-determining step. All other steps are presumed to be at equilibrium. If one makes appropriate assumptions, does this mechanism give rise to a rate expression that is consistent with the observed kinetics?

- 6.17** I. Tripol'skii, N. V. Pavlenko, and G. I. Golodets [*Kinet. Catal.*, **26**, 976–980 (1986)] studied the kinetics and mechanism of the vapor-phase hydrogenation of acetone over supported copper catalysts:



or



Initial rate data for experiments in which the initial concentration of hydrogen is held constant indicate that at low partial pressures of acetone, the rate increases with increasing partial pressure of acetone but then approaches an asymptotic limit. Similarly, when the partial pressure of acetone is held constant and the partial pressure of hydrogen is increased, the rate increases with increasing  $P_{H_2}$  at low partial pressure, but then approaches an asymptotic limit. The initial rate decreases with increasing concentration of 2-propanol. The selectivity of this reaction is independent of the contact time.

For this reaction one can postulate a mechanism involving only a single type of catalyst site or a mechanism involving two different types of surface sites. These mechanisms are indicated below.

#### I. Single type of site ( $\sigma$ ):



#### II. Two types of sites ( $\sigma$ and $z$ ):



- (a) Assuming that reactions (3) and (7) are reversible and that these reactions are rate limiting for mechanisms I and II, respectively, derive Hougen–Watson rate expressions for each of these mechanisms. Start by expressing the rate in terms of the fractional coverages of the active sites. Also indicate the form of these equations that corresponds to the initial rate.
- (b) Is either of these mechanisms consistent with the available experimental data? You may assume that the initial rate data cover a sufficiently wide range of partial pressures that any predicted trends will be observed. Explain.
- (c) Would it be reasonable to assume that dissociative adsorption of  $H_2$  on two sites of the same type should be constructed as a viable alternative to either or both of these mechanisms? For this alternative, the rate-limiting step would involve a termolecular surface reaction involving two adsorbed hydrogen atoms and an adsorbed acetone molecule. Explain your reasoning in a concise manner.
- 6.18** F. J. Dumez and G. F. Froment [*Ind. Eng. Chem. Process Des. Dev.*, **15**, 291 (1976)] studied the kinetics of the

dehydrogenation of 1-butene over a  $\text{Cr}_2\text{O}_3/\text{Al}_2\text{O}_3$  catalyst at 490 to 600°C:



or



They carried out a number of experimental studies in an attempt to discriminate among several Hougen–Watson models that were proposed to explain the observed kinetics. A few of these models are summarized below. Derive the corresponding Hougen–Watson rate expression for each of these models.

(a) Atomic dehydrogenation; surface recombination of hydrogen

- |  |                  |
|--|------------------|
| (1) $\text{B} + \sigma \leftrightarrow \text{B}_\sigma$  | $K_B$            |
| (2) $\text{B}_\sigma + \sigma \leftrightarrow (\text{C}_4\text{H}_7)_\sigma + \text{H}_\sigma$ | $k_f, k_r$       |
| (3) $(\text{C}_4\text{H}_7)_\sigma + \sigma \leftrightarrow \text{D}_\sigma + \text{H}_\sigma$ | $K_3$            |
| (4) $\text{D} + \sigma \leftrightarrow \text{D}_\sigma$  | $K_D$            |
| (5) $2\text{H}_\sigma \leftrightarrow (\text{H}_2)_\sigma + \sigma$                            | $K_5$            |
| (6) $\text{H}_2 + \sigma \leftrightarrow (\text{H}_2)_\sigma$                                  | $K_{\text{H}_2}$ |

Consider the case where the second reaction is rate controlling.

(b) Atomic dehydrogenation; gas-phase recombination of hydrogen

- |  |                  |
|--|------------------|
| (1) $\text{B} + \sigma \leftrightarrow \text{B}_\sigma$  | $K_B$            |
| (2) $\text{B}_\sigma + \sigma \leftrightarrow (\text{C}_4\text{H}_7)_\sigma + \text{H}_\sigma$ | $k_f, k_r$       |
| (3) $(\text{C}_4\text{H}_7)_\sigma + \sigma \leftrightarrow \text{D}_\sigma + \text{H}_\sigma$ | $K_3$            |
| (4) $\text{D} + \sigma \leftrightarrow \text{D}_\sigma$  | $K_D$            |
| (5) $\text{H}_2 + 2\sigma \leftrightarrow 2\text{H}_\sigma$                                    | $K_{\text{H}_2}$ |

(c) Molecular dehydrogenation

- |  |                  |
|--|------------------|
| (1) $\text{B} + \sigma \leftrightarrow \text{B}_\sigma$                              | $K_B$            |
| (2) $\text{B}_\sigma + \sigma \leftrightarrow \text{D}_\sigma + (\text{H}_2)_\sigma$ | $k_f, k_r$       |
| (3) $\text{D} + \sigma \leftrightarrow \text{D}_\sigma$                              | $K_D$            |
| (5) $\text{H}_2 + \sigma \leftrightarrow (\text{H}_2)_\sigma$                        | $K_{\text{H}_2}$ |

What sorts of kinetic experiments could be utilized to discriminate between the models proposed? In what manner should initial rate data be plotted to assess the validity of each of the three proposed mechanisms?

6.19 The water gas reaction takes place on a platinum catalyst in a batch reactor at 1000°C. The reaction is



No products other than  $\text{H}_2\text{O}$  or  $\text{CO}$  are formed. In a series of experiments in which the initial  $\text{CO}_2$  pressure was held constant (and in substantial excess over hydrogen), the rate of formation of  $\text{CO}$  was directly proportional to

the pressure of  $\text{H}_2$ . In another series of experiments the initial partial pressure of  $\text{H}_2$  was held constant at 100 torr, and the following partial pressures of  $\text{CO}$  were observed after 120 s.

Initial pressure of $\text{CO}_2$ (torr)	Pressure of $\text{CO}$ after 120 s (torr)
25	3.8
50	7.0
75	10.0
100	12.4
125	14.4
150	16.2
175	17.5
200	18.0
225	17.8
250	17.3
300	15.4

CO had negligible retarding influence on the rate of reaction. In all runs the water formed was removed immediately by condensation in a dry ice trap.

- (a) Derive the general Hougen–Watson rate expression that applies to this type of reaction.  
 (b) What is the simplest form to which the general equation can be reduced yet still adequately fit all the data?  
 (c) Why does the rate go through a maximum with an increase in the initial pressure of  $\text{CO}_2$ ? Explain qualitatively, in terms of the mathematical model and in mechanistic terms.

6.20 K. H. Yang and O. A. Hougen [Chem. Eng. Prog., **46**, 146, (1950)] suggested that initial rate data can be analyzed in terms of total pressure to facilitate the acceptance or rejection of a mechanism. For their analyses, experimental conditions are set such that two reactants are present in a constant ratio (often equimolar amounts).

G. P. Mathur and G. Thodos [Chem. Eng. Sci., **21**, 1191, (1966)] used the initial rate approach to analyze the kinetics of the catalytic oxidation of sulfur dioxide. They summarized the most plausible rate-controlling steps for the reaction as follows:

- (a) For sulfur dioxide chemisorbed, oxygen dissociated and chemisorbed, sulfur trioxide chemisorbed:  
 1. Adsorption of oxygen controlling  
 2. Adsorption of sulfur dioxide controlling  
 3. Desorption of sulfur trioxide controlling  
 4. Surface reaction between sulfur dioxide and atomic oxygen controlling  
 (b) For sulfur dioxide chemisorbed, oxygen in gas phase and not adsorbed, sulfur trioxide chemisorbed

**Table P6.20**

Superficial mass		Initial rate [lb mol SO <sub>2</sub> / (h-lb catalyst)]	Temperature (°F)	Grams of catalyst	
Total pressure (atm)	velocity [lbmol/h-ft <sup>2</sup> ]				
SO <sub>2</sub>	O <sub>2</sub>				
1.54	1.14	1.33	0.0322	649	3.145
2.36	1.84	2.04	0.0489	649	3.145
3.72	2.61	2.92	0.0541	649	3.145
7.12	4.93	4.99	0.0757	649	3.145
9.84	4.29	6.01	0.0585	649	3.145
1.68	1.29	1.31	0.0320	649	2.372
2.36	1.83	1.90	0.0532	649	2.372
3.72	2.59	2.90	0.0642	649	2.372
7.12	4.87	4.94	0.0642	649	2.372
9.71	4.21	5.95	0.0514	649	2.372
1.54	1.13	1.32	0.0202	701	3.145
2.36	1.84	2.04	0.0904	701	3.145
7.12	4.94	4.98	0.0496	701	3.145
1.54	1.23	1.32	0.0289	701	2.372
2.36	1.83	1.90	0.0688	701	2.372
3.04	2.10	2.48	0.0845	701	2.372
3.72	2.59	2.90	0.0894	701	2.372
7.12	4.85	4.94	0.0520	701	2.372
1.54	1.13	1.33	0.0578	752	3.145
2.36	1.85	2.04	0.0620	752	3.145
3.72	2.62	2.93	0.0659	752	3.145
5.08	3.05	2.88	0.0817	752	3.145
7.12	4.93	4.99	0.0947	752	3.145
1.68	1.29	1.31	0.0459	752	2.372
2.36	1.83	1.90	0.0592	752	2.372
3.72	2.59	2.90	0.0679	752	2.372
5.08	3.04	3.88	0.0852	752	2.372
7.12	4.89	4.93	0.1031	752	2.372

Source: Adapted from G. P. Mathur and G. Thodos, *Chem. Eng. Sci.*, **21**, 1191, copyright © 1966. Used with permission of Pergamon Press Ltd.

For a single-site mechanism:

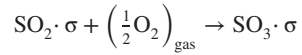
5. Adsorption of sulfur dioxide controlling
6. Desorption of sulfur trioxide controlling
7. Surface reaction between chemisorbed sulfur dioxide and gaseous oxygen controlling

For a dual-site mechanism:

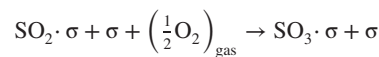
8. Adsorption of sulfur dioxide controlling
9. Desorption of sulfur trioxide controlling
10. Surface reaction between chemisorbed sulfur dioxide and gaseous oxygen controlling

I. Derive equations relating the *initial* reaction rate ( $r_0$ ) to the total pressure ( $\pi$ ) for each of the cases listed above when the sulfur dioxide and oxygen are initially present in equimolar amounts. Do this using the Hougen–Watson mechanistic models. Show your derivations.

[Hint: For the single-site mechanism assume (as Mathur and Thodos did) that the surface reaction step can be written as



For the dual-site mechanism assume (as Mathur and Thodos did) that the reaction step can be written as



II. Use the data in Table P6.20 to prepare plots of the initial rate versus  $\pi$  for each temperature. Reject any mechanisms that are grossly inadequate by *qualitative* reasoning. Do not attempt to do a complicated quantitative or statistical analysis.

(Hint 1: Although sulfur dioxide and oxygen do not appear to be present in equimolar amounts for several of the data points, you may assume, as Mathur and Thodos did, that they are close enough for the purposes of this *qualitative* analysis.)

(Hint 2: Look for the presence or absence of a maximum. Assume that the data have been taken over a wide enough range for a maximum to show up if it were going to.)

# Chapter 7

---

## Liquid Phase Reactions

### 7.0 INTRODUCTION

The dynamic behavior of reactions in liquids may differ appreciably from that of gas phase reactions in several important respects. The short-range nature of intermolecular forces leads to several major differences in the macroscopic properties of the system, often with concomitant effects on the dynamics of chemical reactions occurring in the liquid phase.

The various effects are often classified as physical or chemical, depending on the role played by solvent molecules in the course of the elementary reaction acts. The effects associated with the presence of solvent molecules are *chemical* in nature when the solvent molecules themselves (or fragments thereof) participate in the microscopic reaction events that comprise the reaction mechanism. In some cases the solvent molecules are regenerated by the sequence of reactions and, like catalysts, do not enter into the overall stoichiometry of the reaction. In other cases there may be a net increase or decrease in the amount of solvent present. However, in the majority of the situations likely to be encountered in industrial practice, the changes in solvent concentration arising from its participation in the reaction stoichiometry will not be appreciable. When solvent molecules play a chemical role, this effect is superimposed on a number of *physical* effects arising from the interplay of intermolecular forces in liquid solution. The most significant of the physical effects is ionization, which affords the possibility of alternative reaction mechanisms to those normally occurring in vapor phase reactions, with concomitant changes in the energy requirements for the molecular processes constituting the reaction mechanism. The *net* energy requirements for the conversion of reactants to products, however, remain unchanged.

In this chapter we treat those aspects of the kinetic behavior of reactions in liquid solutions that are most germane to the education of a chemical engineer. Particular emphasis is placed on catalysis by acids, bases, and enzymes and a useful technique for correlating kinetic data.

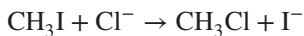
Solvent molecules may play a variety of roles in liquid phase reactions. In some cases they merely provide a physical environment in which encounters between reactant molecules take place much as they do in gas phase reactions. Thus, they may act merely as space fillers and have negligible influence on the observed reaction rate. At the other extreme, the solvent molecules may act as reactants in the sequence of elementary reactions constituting the mechanism. Although a thorough discussion of these effects would be beyond the scope of this book, the paragraphs that follow indicate some important aspects with which the budding kineticist should be familiar.

The most important physical effects associated with the presence of the solvent are electrostatic in nature. The production of ions from neutral species in the gas phase involves a large energy requirement (a few hundred kilocalories/mol). Consequently, ionic species are seldom involved in gas phase reaction mechanisms. In solution the interaction energy between the solvent molecules and the ions may often be of the same order of magnitude as the energy required for formation of ions from their neutral precursors. The interactions between reactant and solvent molecules thus may be strong enough to stabilize a charge on a fragment of a reactant molecule. Ionic species are then more likely to be present in much higher concentrations in the liquid phase than in the vapor phase and are much more likely to be involved as reaction intermediates in liquid phase reactions.

Electrostatic effects other than ionization are also important. Interactions between reacting ions depend on the local electrical environment of the ions and thus reflect the influence of the dielectric constant of the solvent and the presence of other ions and various solutes that may be present. In dilute solutions the influence of ionic strength on reaction rates is felt in the primary and secondary salt effects (see below).

Another important physical effect arising from the presence of solvent molecules is the efficiency of energy transfer. In condensed phases the rapid energy transfer in the abundant collisions between reactant and solvent

molecules maintains vibrational thermal equilibrium at all times. Other solvent effects on reaction rates and mechanisms include effects arising from the acidity of the medium; effects of selective solvation by one component in a mixed solvent or of different degrees of solvation of the reactants, reaction intermediates (including activated complexes), and reaction products; effects arising from hydrogen bonding; effects of changing from a protic solvent (one that may be regarded as a hydrogen bond donor, such as  $\text{H}_2\text{O}$ ,  $\text{NH}_3$ , and alcohols) to a dipolar aprotic solvent (not a hydrogen bond donor, such as acetone,  $\text{SO}_2$ , or nitrobenzene); and cage effects. The various solvent effects may, of course, be superimposed or overlap one another such that they are inextricably linked. The magnitude of these solvent effects may range from insignificance to several powers of 10. For example, at 25°C the reaction



occurs more than  $10^6$  times as fast in dimethyl acetamide as in acetone (1). On the other hand, the decomposition of nitrogen pentoxide in several different solvents is characterized by rate constants that lie within a factor of 2 of the gas phase rate constant (2).

Because the forces giving rise to the formation of chemical bonds are very short-range forces, reactions in liquid solutions will require some sort of encounter or “collision” between reactant molecules. These encounters will differ appreciably from gas phase collisions in that they will occur in close proximity to solvent molecules. Indeed, in liquids any individual molecule will always be interacting with several surrounding molecules at the same time, and the notion of a bimolecular collision becomes rather arbitrary. Nonetheless, a number of approaches to formulating expressions for collision frequencies in the liquid phase have appeared in the chemical literature through the years. The simplest of these approaches presumes that the gas phase collision frequency expression is directly applicable to the calculation of liquid phase collision frequencies. The rationale for this approach is that for several second-order gas phase reactions that are also second-order in various solvents, the rate constants and preexponential factors are pretty much the same in the gas phase and in various solvents. For further discussion of the collision theory approach to reactions in liquids, consult the monograph by North (3).

There is another aspect of collisions in liquid solution that is of particular interest with regard to chemical reactions. Collisions in solution are often repeated, so that multiple collisions of the same two molecules occur. Consider the molecules labeled A and B in Figure 7.1. Each molecule is surrounded by several neighboring molecules. In view of the short-range order typical of liquids, the neighboring molecules will all be located at

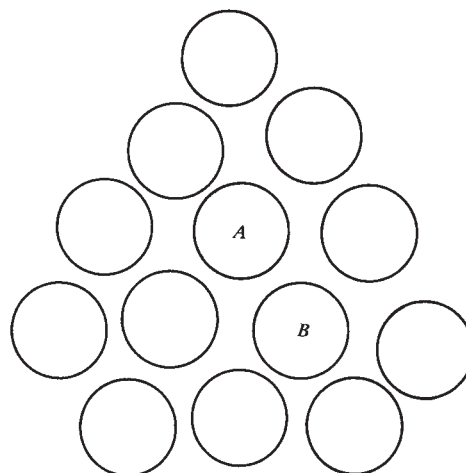


Figure 7.1 Schematic representation of the cage effect.

approximately the same distance from the molecule in question. This distance will be somewhat larger than a typical hard-sphere molecular diameter, but considerably less than twice this diameter. Consequently, geometric and molecular force considerations indicate that the passage of any specified reference molecule between any two neighbors will be restricted by the repulsive portion of the intermolecular potential. To escape from the “cage” formed by the surrounding molecules, the reference molecule must surmount the energy barrier presented by the repulsive forces.

This molecule will undergo many collisions with its nearest-neighbor molecules before it escapes from the cage. In the case of two solute molecules hemmed in by solvent molecules, multiple collisions will occur before one or both of the solute molecules can diffuse out of the cage. In liquid solution, then, the total number of collisions is comparable in magnitude to the number of gas phase collisions, but repeated collisions are favored over fresh collisions.

It has been estimated (4) that in most common solvents at room temperature two reactant molecules within a cage of solvent molecules will collide from 10 to 1000 times before they separate. The number of collisions per encounter will reflect variations in solvent viscosity, molecular separation distances, and the strength of the pertinent intermolecular forces. High viscosities, high liquid densities, and low temperatures favor many collisions per encounter.

The tendency for liquid phase collisions to occur in groups or sets does not have a very large effect for ordinary reactions that involve a significant activation energy, because no individual collision within the set is more likely to lead to reaction than any other. On the other hand, some reactions have zero or minimal energy requirements (e.g., free-radical recombination reactions). Such reactions will occur at virtually every collision. For

in these reactions the rate is limited by diffusional processes within the liquid phase in that virtually every collision between reactants leads to reaction. Since these reactions have negligible activation energies, their reaction rate constants are expected to be inversely proportional to the time elapsing between sets or groups of collisions.

The cage effect described above is also referred to as the Franck–Rabinowitch effect (5). It has one other major influence on reaction rates that is particularly noteworthy. In many photochemical reactions there is often an initiation step in which the absorption of a photon leads to homolytic cleavage of a reactant molecule with concomitant production of two free radicals. In gas phase systems these radicals are readily able to diffuse away from one another. In liquid solutions, however, the pair of radicals formed initially is trapped in a cage formed by surrounding solvent molecules and often will recombine before they can diffuse away from one another. This phenomenon is referred to as *primary recombination*, as opposed to *secondary recombination*, which occurs when free radicals combine after having previously been separated from one another. The net effect of primary recombination processes is to reduce the photochemical yield of radicals formed in the initiation step for the reaction.

## 7.1 ELECTROSTATIC EFFECTS IN LIQUID SOLUTION

In dilute solutions it is possible to relate the activity coefficients of ionic species to the composition of the solution, its dielectric properties, the temperature, and certain fundamental constants. Theoretical approaches to the development of such relations trace their origins to classic papers by Debye and Hückel (6–8). For detailed treatments of this subject, refer to standard physical chemistry texts or to treatises on electrolyte solutions [e.g., that by Harned and Owen (9)]. The Debye–Hückel theory is useless for quantitative calculations in most of the reaction systems encountered in industrial practice because such systems normally employ concentrated solutions. However, it may be used together with transition state theory to predict the qualitative influence of ionic strength on reaction rate constants.

For a bimolecular reaction between species A and B, the analysis gives an equation of the form

$$k = \frac{k_0 \gamma_A \gamma_B}{\gamma_{AB}^{\ddagger}} \quad (7.1.1)$$

where  $k_0$  is the rate constant in infinitely dilute solution and  $\gamma_A$ ,  $\gamma_B$ , and  $\gamma_{AB}^{\ddagger}$  are the activity coefficients of species A, B, and the activated complex, respectively.

If limiting forms of the Debye–Hückel expression for activity coefficients are used, this equation becomes

$$\ln k = \ln k_0 + 2Z_A Z_B \sqrt{\mu} \frac{q^3 \sqrt{8\pi N_0 / 1000}}{2(k_B T D)^{3/2}} \quad (7.1.2)$$

where  $Z_A$  and  $Z_B$  represent the number (and sign) of charges on the ions A and B,  $q$  is the charge on an electron,  $N_0$  is Avogadro's number,  $k_B$  is the Boltzmann constant,  $T$  is the absolute temperature,  $D$  is the dielectric constant of the medium, and  $\mu$  is the ionic strength of the solution:

$$\mu = \frac{1}{2} \sum (C_i \zeta_i^2) \quad (7.1.3)$$

where  $C_i$  is the molar concentration of species  $i$ .

In dilute aqueous solution at 25°C, equation (7.1.2) becomes

$$\log k = \log k_0 + 2Z_A Z_B \sqrt{\mu} (0.509) \quad (7.1.4)$$

This equation, known as the *Brønsted–Bjerrum equation*, may be derived in several ways. It predicts that a plot of  $\log k$  versus the square root of the ionic strength should be linear over the range of ionic strengths for which the Debye–Hückel limiting law is applicable. The slopes of such lines are nearly equal to the product of the ionic charges of the reactants  $Z_A Z_B$ .

There are three general classes of ionic reactions to which these equations may be applied.

1. Reactions between ions of the same sign ( $Z_A Z_B$  is positive) for which the rate constant increases with increasing ionic strength
2. Reactions between ions of opposite sign ( $Z_A Z_B$  is negative) for which the rate constant decreases with increasing ionic strength
3. Reactions between an uncharged species and an ion for which the rate constant is independent of ionic strength ( $Z_A Z_B = 0$ )

Several tests of the validity of equation (7.1.4) have been conducted. Figure 7.2 indicates the variation of  $\log(k/k_0)$  with ionic strength for a variety of reactions. All factors considered, the agreement of theory and experiment is quite remarkable for a great many reactions. Note that the bulk of the data is reported in a range of ionic strengths that would normally be expected to be outside the range of validity of the Debye–Hückel limiting law (below  $\sqrt{\mu} = 0.1$  for 1 : 1 electrolytes and below  $\sqrt{\mu} = 0.03$  for higher valence ions). Equation (7.1.2) appears to be capable of extrapolation to much higher ionic strengths for the reactions indicated. Also note that the magnitude of the effect can be quite significant, particularly for reactions that involve ions with multiple charges. Even in the case of reactions where  $Z_A Z_B = \pm 1$ , the use of “inert” salts to

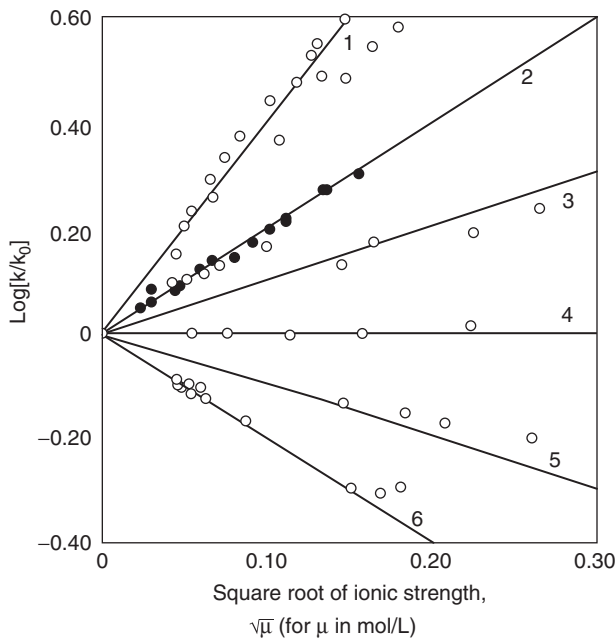


**Figure 7.2** Plots of  $\log_{10}(k/k_0)$  against the square root of the ionic strength, for reactions involving ions of various types. The lines are drawn with slopes equal to  $Z_A Z_B$ . The reactions to which the data points correspond are as follows:

1.  $2[\text{Co}(\text{NH}_3)_5\text{Br}]^{2+} + \text{Hg}^{2+} + 2\text{H}_2\text{O} \rightarrow \text{HgBr}_2 + 2[\text{Co}(\text{NH}_3)_5\text{H}_2\text{O}]^{3+}$  ( $Z_A Z_B = 4$ )  
No foreign salt added. Brönsted and Livingston: *J. Am. Chem. Soc.*, **51**, 435 (1927).
2. Open circles:  $\text{CH}_2\text{BrCOO}^- + \text{S}_2\text{O}_3^{2-} \rightarrow \text{CH}_2\text{S}_2\text{O}_3\text{COO}^- + \text{Br}^-$  ( $Z_A Z_B = 2$ )  
No foreign salt added. La Mer: *J. Am. Chem. Soc.*, **49**, 334 (1929).  
Closed circles:  $\text{S}_2\text{O}_8^{2-} + \text{I}^- \rightarrow \text{I}_2 + \text{SO}_4^{2-}$  ( $Z_A Z_B = 2$ )  
King and Jacobs: *J. Am. Chem. Soc.*, **53**, 1704 (1931).
3.  $[\text{CO}(\text{OC}_2\text{H}_5)_5\text{N} : \text{NO}_2]^- + \text{OH}^- \rightarrow \text{N}_2\text{O} + \text{CO}_3^{2-} + \text{C}_2\text{H}_5\text{OH}$  ( $Z_A Z_B = 1$ )  
Brönsted and Delbano: *Z. Anorg. Chem.*, **144**, 248 (1925).
4.  $\text{C}_{12}\text{H}_{22}\text{O}_{11}\text{OC}_2\text{H}_5 + \text{OH}^- \rightarrow$   
invert sugar ( $Z_A Z_B = 0$ )  
Arrhenius: *Z. Phys. Chem.*, **1**, 111 (1887).
5.  $2\text{H}^+ + 2\text{Br}^- + \text{H}_2\text{O}_2 \rightarrow 2\text{H}_2\text{O} + \text{Br}_2$  ( $Z_A Z_B = -1$ )  
Livingston: *J. Am. Chem. Soc.*, **48**, 53 (1926).
6.  $[\text{Co}(\text{NH}_3)_5\text{Br}]^{2+} + \text{OH}^- \rightarrow [\text{Co}(\text{NH}_3)_5\text{OH}]^{2+} + \text{Br}^-$  ( $Z_A Z_B = -2$ )  
Brönsted and Livingston: *J. Am. Chem. Soc.*, **49**, 435 (1927).

[This figure has been adapted with permission from the contribution of V. K. La Mer to *Chem. Rev.*, **10**, 179 (1932). Copyright © 1932 by the American Chemical Society.]

increase the ionic strength can cause the rate to increase or decrease by as much as 50%.

Equation (7.1.2) characterizes what is known as the *primary salt effect* (i.e., the influence of ionic strength on

the reaction rate through the activity coefficients of the reactants and the activated complex). Much early work on ionic reactions is relatively useless because this effect was not understood. Now it is common practice in studies of ionic reactions to add a considerable excess of inert salt (e.g., NaCl) to the reaction mixture. This practice ensures that the ionic strength does not vary substantially during the course of the reaction as it might if pure water were used as the solvent. To the uninitiated observer, the primary salt effect might appear to be a form of catalysis, since the rate is affected by the addition of substances that do not appear in the stoichiometric equation for the reaction. However, it is preferable not to regard this phenomenon as a form of catalysis, because the added salts affect the rate by changing the environment in which the reaction occurs through their influence on electrostatic forces rather than by opening up alternative reaction pathways.

For more detailed treatments of ion–molecule reactions in liquid solution, consult the books by Amis and Hinton (11) and Reichardt (12) and the review article by Clark and Wayne (13).

## 7.2 PRESSURE EFFECTS ON REACTIONS IN LIQUID SOLUTION

The effect of external pressure on the rates of liquid phase reactions is normally quite small, and unless one goes to pressures of several hundred atmospheres, the effect is difficult to observe. In terms of the transition state approach to reactions in solution, the equilibrium existing between reactants and activated complexes may be analyzed in terms of Le Châtelier's principle or other theorems of moderation. The concentration of activated complex species (and hence the reaction rate) will be increased by an increase in hydrostatic pressure if the volume of the activated complex is less than the sum of the volumes of the reactant molecules. The rate of reaction will be decreased by an increase in external pressure if the volume of the activated complex molecules is greater than the sum of the volumes of the reactant molecules. For a decrease in external pressure, the opposite would be true. In most cases the rates of liquid phase reactions are enhanced by increased pressure, but there are also many cases where the converse situation prevails.

To properly account for the effect of pressure on liquid phase reaction rates one should eliminate the pressure dependence of the concentration terms by expressing the latter in terms of mole ratios. It is then customary to express the general dependence of the rate constant on pressure as

$$\left( \frac{\partial \ln k}{\partial P} \right)_T = -\frac{\Delta V^\ddagger}{RT} \quad (7.2.1)$$

where  $\Delta V^\ddagger$  is the volume of activation for the reaction. If pressure dependent concentration units (e.g., moles per liter) are employed to determine the rate constant, this equation must be corrected by a term accounting for the compressibility of the solution. In many cases the correction term is negligible, but this situation does not always prevail. Nonetheless, much of the high-pressure rate constant data available in the literature do not take this factor into account, and a good design engineer must properly evaluate the validity of the reported values before using them in calculations. Because high pressures usually enhance reaction rates, activation volumes are negative for most reactions.

Equation (7.2.1) implies that the rate constant for a reaction increases with increasing pressure if  $\Delta V^\ddagger$  is negative, which is the most common situation. In this case the transition state has a smaller volume than the initial state. On the other hand, pressure increases bring about a decrease in the reaction rate if the formation of the activated complex requires a volume increase.

Substitution of typical numerical values of  $\Delta V^\ddagger$  into equation (7.2.1) indicates that at room temperature  $\Delta V^\ddagger/(RT) \sim 10^{-3} \text{ atm}^{-1}$ , so that one needs to go to pressures of several hundred or several thousand atmospheres to observe significant effects or to obtain accurate values of  $\Delta V^\ddagger$  from plots of  $\ln k$  versus pressure.

Activation volumes may be used to elucidate the mechanisms of classes of reactions involving the same functional groups, and changes in activation volumes can be used to characterize the point at which a change in the reaction mechanism takes place in a series of homologous reactions.

For a detailed treatment of the kinetics of reactions at high pressures, consult the review article by Eckert (14).

### 7.3 HOMOGENEOUS CATALYSIS IN LIQUID SOLUTION

A catalyst has been defined previously as a substance that influences the *rate* or the *direction* of a chemical reaction *without being appreciably consumed*. Another definition of a catalyst that is particularly appropriate for reactions in liquid solution is the following: “A substance is said to be a catalyst for a reaction in a homogeneous system when its concentration occurs in the velocity expression to a higher power than it does in the stoichiometric equation” (15). In the overwhelming majority of cases, catalysts influence reaction rates by opening up alternative sequences of molecular reactions linking the reactant and product states. Catalyst species participate in elementary reaction steps, forming reaction intermediates that, in turn, react to eventually yield the reaction products and regenerate the original catalyst species.

Homogeneous catalytic processes are those in which the catalyst is dissolved in a liquid reaction medium. There are a variety of chemical species that may act as homogeneous catalysts (e.g., anions, cations, neutral species, association complexes, and enzymes). All such reactions appear to involve a *chemical interaction* between the catalyst and the *substrate* (the substance undergoing reaction). The bulk of the material in this section will focus on acid–base and enzyme catalysis. Students interested in learning more about these subjects and other aspects of homogeneous catalysis should consult appropriate texts (11, 12, 16–30) or the original literature.

#### 7.3.1 Acid–Base Catalysis

In acid–base catalysis there is at least one step in the reaction mechanism that consists of a generalized acid–base reaction (a proton transfer between the catalyst and the substrate). The protonated or deprotonated reactant species or intermediate then reacts further, either with another species in the solution or by a decomposition process.

The relative ease with which proton transfer is accomplished is responsible for the importance of the generalized acid–base concept in solution chemistry. The Brønsted concept of acidity is most useful in this respect. Brønsted defined an *acid* as a species that tends to give up a proton and a *base* as a species that tends to accept a proton. In this sense any proton transfer process having the general form



may be regarded as an acid–base reaction between a Brønsted acid HX and a Brønsted base Y to form a conjugate base X and a conjugate acid HY. The various species involved in these reactions may be ions or neutral molecules.

The unique properties of the proton have been attributed by some authors to the fact that it has no electronic or geometric structure. The absence of any electron shell implies that it will have a radius that is about  $10^5$  times smaller than any other cation and that there will be no repulsive interactions between electron clouds as a proton approaches another reactant species. The lack of any geometric or electronic structure also implies that there will not be any steric limitations with regard to orientation of the proton. However, it still must attack the other reactant molecule at the appropriate site.

The small size of the proton relative to its charge makes the proton very effective in polarizing the molecules in its immediate vicinity and, consequently, leads to a very high degree of solvation in a polar solvent. In aqueous solutions, the primary solvation process involves the formation of a covalent bond with the oxygen atom of a water molecule to form a hydronium ion,  $\text{H}_3\text{O}^+$ . Secondary solvation of this

species then occurs by additional water molecules. Whenever we use the term *hydrogen ion* in the future, we are referring to the  $\text{H}_3\text{O}^+$  species.

Early studies of the catalytic hydrolysis of esters indicated that in many cases, for strong acids, the observed rate constants were independent of the anion, and it became generally accepted that the active catalyst was a hydrogen ion. In other reactions it became necessary to consider the effects of the hydroxide ion concentration and also the rate of the uncatalyzed reaction. The result was a three-term expression for the apparent rate constant:

$$k_{\text{apparent}} = k_0 + k_{\text{H}^+}[\text{H}^+] + k_{\text{OH}^-}[\text{OH}^-] \quad (7.3.2)$$

where the first term corresponds to the uncatalyzed reaction, the second to catalysis by hydrogen ions, and the third to catalysis by hydroxide ions. The three rate constants appearing in this expression vary with temperature and with the nature of the reaction involved. Depending on the reaction conditions and the reaction involved, one or two of these terms may be negligible compared to the other(s). When only the hydronium ion is effective in catalyzing the reaction, the process is referred to as *specific acid catalysis*. When only hydroxide ions are effective, the process is classified as *specific base catalysis*. When both terms are significant, the catalysis is characterized as specific acid and specific base catalysis.

Although the concepts of specific acid and specific base catalysis were useful in the analysis of some early kinetic data, it soon became apparent that any species that could effect a proton transfer with the substrate could exert a catalytic influence on the reaction rate. Consequently, it became desirable to employ the more general Brønsted–Lowry definition of acids and bases and to write the reaction rate constant as

$$k = k_0 + k_{\text{H}^+}(\text{H}_3\text{O}^+) + k_{\text{OH}^-}(\text{OH}^-) + \sum_i k_{\text{HX}_i}(\text{HX}_i) + \sum_j k_{\text{X}_j}(\text{X}_j) \quad (7.3.3)$$

where  $\text{HX}_i$  and  $\text{X}_j$  represent all other acid and base species present in the solution apart from  $\text{H}_3\text{O}^+$  and  $\text{OH}^-$ . Reactions that are dependent on the concentrations of  $\text{HX}_i$  and  $\text{X}_j$  are categorized as involving *general acid* and *general base* catalysis, respectively. Table 7.1 indicates a number of catalytic reactions of the specific and general acid–base types to provide some orientation as to the types of reactions in the various categories. A thorough discussion of these reactions is obviously beyond the scope of this book. Consult the books by Laidler (17), Moore and Pearson (18), Bender (19), and Hine (32) for a further introduction to this topic.

**Table 7.1** Examples of Acid and Base Catalysis in Aqueous Solution

Type of catalysis	Brief title of reaction	Stoichiometric equation of reaction
Specific acid	Inversion of cane sugar	$\text{C}_{12}\text{H}_{22}\text{O}_{11} + \text{H}_2\text{O} = \text{C}_6\text{H}_{12}\text{O}_6 + \text{C}_6\text{H}_{12}\text{O}_6$
	Hydrolysis of acetals	$\text{R}_1\text{CH}(\text{OR}_2)_2 + \text{H}_2\text{O} = \text{R}_1\cdot\text{CHO} + 2\text{R}_2\text{OH}$
	Hydration of unsaturated aldehydes	$\text{CH}_2:\text{CH}\cdot\text{CHO} + \text{H}_2\text{O} = \text{CH}_2\text{OH}\cdot\text{CH}_2\cdot\text{CHO}$
Specific base	Cleavage diacetone–alcohol	$\text{CH}_3\text{CO}\cdot\text{CH}_2\cdot\text{C}(\text{OH})(\text{CH}_3)_2 = 2(\text{CH}_3)_2\cdot\text{CO}$
	Claisen condensation	$\text{C}_6\text{H}_5\text{CHO} + \text{CH}_3\cdot\text{CHO} = \text{C}_6\text{H}_5\cdot\text{CH}:\text{CHO} + \text{H}_2\text{O}$
	Aldol condensation	$2\text{R}\cdot\text{CH}_2\cdot\text{CHO} = \text{R}\cdot\text{CH}_2\text{CH}(\text{OH})\cdot\text{CHR}\cdot\text{CHO}$
Specific acid and base	Hydrolysis of $\gamma$ -lactones	$\text{CH}_2\text{CH}_2\cdot\text{CH}_2\cdot\text{C}(\text{O}) + \text{H}_2\text{O} = \text{CH}_2\text{OH}\cdot\text{CH}_2\cdot\text{CH}_2\cdot\text{COOH}$
	Hydrolysis of amides	$\text{R}\cdot\text{CO}\cdot\text{NH}_2 + \text{H}_2\text{O} = \text{R}\cdot\text{COONH}_4$
	Hydrolysis of esters	$\text{R}_1\text{COOR}_2 + \text{H}_2\text{O} = \text{R}_1\cdot\text{COOH} + \text{R}_2\text{OH}$
General acid	Decomposition of acetaldehyde hydrate	$\text{CH}_3\text{CH}(\text{OH})_2 = \text{CH}_3\text{CHO} + \text{H}_2\text{O}$
	Hydrolysis of <i>o</i> -esters	$\text{HC}(\text{OC}_2\text{H}_5)_3 + \text{H}_2\text{O} = \text{H}\cdot\text{COOC}_2\text{H}_5 + 2\text{C}_2\text{H}_5\text{OH}$
	Formation of nitro compound	$\text{CH}_2:\text{NO}_2^- + \text{acid} = \text{CH}_3\cdot\text{NO}_2 + \text{base}^-$
General base	Decomposition of nitramide	$\text{NH}_2\text{NO}_2 = \text{N}_2\text{O} + \text{H}_2\text{O}$
	Bromination of nitromethane	$\text{CH}_3\text{NO}_2 + \text{Br}_2 = \text{CH}_2\text{BrNO}_2 + \text{HBr}$
	Aldol with acetaldehyde	$2\text{CH}_3\cdot\text{CHO} = \text{CH}_3\cdot\text{CH}(\text{OH})\cdot\text{CH}_2\cdot\text{CHO}$
General acid and base	Halogenation, exchange, racemization of ketones	$\text{R}\cdot\text{CO}\cdot\text{CH}_3 + \text{X}_2 = \text{R}\cdot\text{CO}\cdot\text{CH}_2\text{X} + \text{XH}$
	Addition to carbonyl	$\text{R}_1\cdot\text{CO}\cdot\text{R}_2 + \text{NH}_2\text{OH} = \text{R}_1\text{R}_2\cdot\text{COH}\cdot\text{NHOH}$

Source: Adapted from Ashmore (31).

Because the rates of acid and base catalyzed reactions are sensitive to variations in the solution pH, it is instructive to consider the types of behavior that can be observed in aqueous solution in the laboratory. The dissociation constant for water may be written as

$$K_w = [H^+][OH^-] \quad (7.3.4)$$

Combining equations (7.3.4) and (7.3.2) indicates that in aqueous media for specific acid-base catalysis,

$$k_{\text{apparent}} = k_0 + k_{H^+}[H^+] + \frac{k_{OH^-}K_w}{[H^+]} \quad (7.3.5)$$

Alternatively,

$$k_{\text{apparent}} = k_0 + \frac{k_{H^+}K_w}{[OH^-]} + k_{OH^-}[OH^-] \quad (7.3.6)$$

In many cases one or two of the three terms on the right side of these equations is negligible compared to the others. In 0.1 N strong acid, for example, the second term is  $k_{H^+} \times 10^{-1}$ , while the last term is  $k_{OH^-} \times 10^{-13}$ , because  $K_w \sim 10^{-14}$ . Consequently, unless the ratio  $k_{OH^-}/K_w$  is  $10^9$  or more, the third term will be negligible compared to the second. This large a ratio is not often encountered in practice. By the same sort of argument, it can be shown that in a 0.1 N strong base, catalysis by hydrogen ions will usually be unimportant relative to catalysis by hydroxide ions. Normally, one finds that there will be a lower limit on hydrogen ion concentration above which catalysis by hydroxide ions may be regarded as insignificant. Similarly, there is usually a range of pH values in the high-pH region where catalysis by hydrogen ions will be negligible and the hydroxide ions will be responsible for the catalytic effect. Within the pH range where the hydrogen ions are solely responsible for the catalytic effect, the apparent rate constant will be linear in the hydrogen ion concentration. Consequently, it is a straightforward task to determine  $k_{H^+}$  from a plot of the apparent rate constant versus hydrogen ion concentration. Within the pH range where hydroxide ions are solely responsible for the catalysis, one may use an analogous procedure to determine  $k_{OH^-}$ .

There are several types of pH-dependent kinetic behavior that can be interpreted in terms of one or more of the various forms of the specific acid-base catalysis relation [equation (7.3.2)]. Skrabal (33) classified the various possibilities that may arise in reactions of this type, and Figure 7.3 is based on this classification. The various forms of the plots of  $\log k$  versus pH reflect the relative importance of each of the various terms in equation (7.3.2) as the pH shifts. Curve *a* represents the most general type of behavior. This curve consists of a region where acid catalysis is superimposed on the noncatalytic reaction, a region where neither acid nor base catalysis is significant,

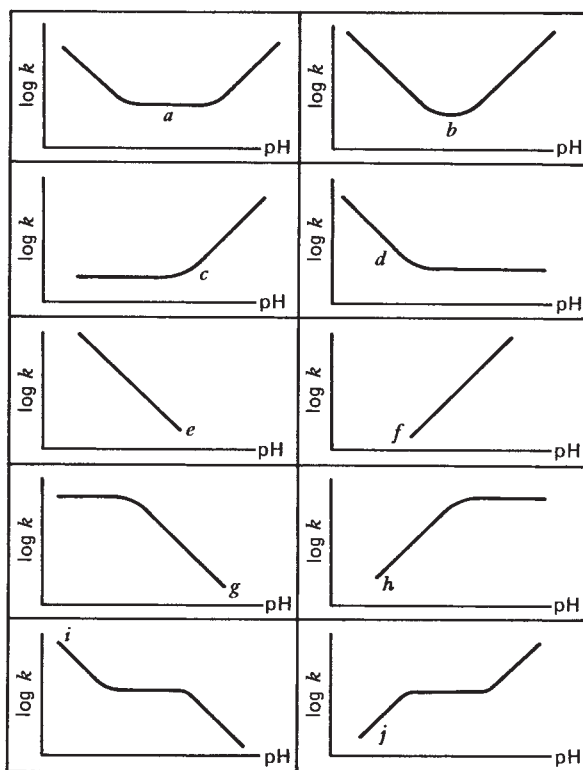


**Figure 7.3** Schematic representation of  $\log k$  versus pH profiles for various types of acid-base catalysis.

and a region where base catalysis is superimposed on the spontaneous reaction. At low pH, the bulk of the reaction may be attributed to the acid-catalyzed reaction and

$$k_{\text{apparent}} = k_{H^+}[H_3O^+] \quad (7.3.7)$$

Thus

$$\log k_{\text{apparent}} = \log k_{H^+} + \log[H_3O^+] = \log k_{H^+} - \text{pH} \quad (7.3.8)$$

The slope of the left arm of curve *a* is thus  $-1$ . At intermediate-pH values, the rate is independent of pH, so  $k_0$  may be determined directly from kinetic measurements in this pH regime. At high pH the only significant contribution to the rate constant is that attributed to specific base catalysis. In terms of equation (7.3.5),

$$k_{\text{apparent}} = k_{OH^-}K_w/[H^+] \quad (7.3.9)$$

or

$$\begin{aligned} \log k_{\text{apparent}} &= \log(k_{OH^-}K_w) - \log H_3O^+ \\ &= \log(k_{OH^-}K_w) + \text{pH} \end{aligned} \quad (7.3.10)$$

Hence, at high pH for this situation, the slope of the plot of  $\log k_{\text{apparent}}$  versus pH is  $+1$ .

The various other forms of the plots of log rate constant versus pH may be analyzed in similar terms. In curve *b*, the horizontal portion of the curve is missing, indicating that the spontaneous reaction does not contribute significantly to the reaction rate observed at any pH. If either  $k_{\text{H}^+}$  or  $k_{\text{OH}^-}$  is sufficiently small, the contribution to  $k_{\text{apparent}}$  from the catalytic effect in question will be negligible, and the corresponding arm of the curve will be missing. Hence, curve *c* reflects a combination of specific base catalysis and the intrinsic reaction, while curve *d* represents a combination of specific acid catalysis and the intrinsic reaction. If the horizontal region and one arm of the curve are missing, one has the degenerate forms of the rate constant expression indicated by equations (7.3.7) and (7.3.9). Curve *e* corresponds to specific acid catalysis and curve *f* to specific base catalysis. More complex dependencies of  $\log k$  on pH have also been observed in the laboratory, and in these more complicated systems, considerable ambiguity may arise in the interpretation of the kinetic data.

We have indicated how to determine the various kinetic constants appearing in the expression for specific acid and base catalysis. Let us now consider how to evaluate the various contributions to the rate constant in the case of general acid-base catalysis. For reactions of this type in a solution of a weak acid or base and its corresponding salt, the possible catalysts indicated by equation (7.3.3) are the hydronium ion, the hydroxide ion, the undissociated weak acid (or base), and the conjugate base (or acid). In the case of acetic acid the general acid would be the neutral  $\text{CH}_3\text{COOH}$  species and the conjugate base would be the acetate ion ( $\text{CH}_3\text{COO}^-$ ). In this case the apparent rate constant can be written as

$$k_{\text{apparent}} = k_0 + k_{\text{H}^+}(\text{H}_3\text{O}^+) + k_{\text{OH}^-}(\text{OH}^-) + k_{\text{HA}}(\text{HA}) + k_{\text{A}^-}(\text{A}^-) \quad (7.3.11)$$

The five constants appearing in this expression may be determined by a systematic variation of the experimental conditions so as to make one or more of the contributing terms negligible within a given set of experiments. By carrying out experiments in the absence of acetate ions and acetic acid, one can determine the constants  $k_0$ ,  $k_{\text{H}^+}$ , and  $k_{\text{OH}^-}$  using the procedure outlined previously for specific acid and specific base catalysis. Strong acids and strong bases whose corresponding anions and cations are known to exhibit no catalytic activity are used as the source of hydronium and hydroxide ions. One may then proceed to determine the constants characteristic of generalized acid and base catalysis by using a buffer solution of the weak acid and its conjugate base. In a series of buffer solution experiments the absolute concentrations of undissociated acetic acid species and acetate ions may be varied while maintaining a constant ratio ( $q$ ) of these concentrations. In

these experiments the ionic strength should also be maintained constant to ensure that the activity coefficients of the various species do not change.

From consideration of the dissociation equilibrium, it is evident that

$$(\text{H}^+) = \frac{K_a(\text{HA})}{(\text{A}^-)} = K_a q \quad (7.3.12)$$

where  $K_a$  is the dissociation constant for the acid. The hydrogen ion concentration will not vary if the ratio  $(\text{HA})/(\text{A}^-)$  is maintained constant. Thus, the first three terms on the right side of equation (7.3.11) may be represented by a constant  $k_1$  under these conditions. This equation may then be rewritten as

$$k_{\text{apparent}} = k_1 + (\text{HA}) \left( k_{\text{HA}} + \frac{k_{\text{A}^-}}{q} \right) \quad (7.3.13)$$

By plotting the measured rate constant versus the concentration of the undissociated acid, one obtains for this type of catalysis a straight line whose intercept is  $k_1$  and whose slope  $\alpha_1 = k_{\text{HA}} + (k_{\text{A}^-}/q)$ . If the procedure is repeated for other ratios, enough information is obtained to permit evaluation of  $k_{\text{HA}}$  and  $k_{\text{A}^-}$ . The hydrogen and hydroxide ion concentrations corresponding to a given ratio  $q$  may be determined from equation (7.3.12) and the dissociation constant for water.

It should be evident that the calculations and the necessary experimental program are simplified if one or more of the contributions is negligible under appropriate conditions. In a relatively simple system in which either  $k_{\text{HA}}$  or  $k_{\text{A}^-}$  is zero, the existence of general acid or general base catalysis may be deduced from the pH dependence of the rate constant.

A reaction catalyzed by an undissociated acid species will have the dependence of  $\log k$  on pH shown in Figure 7.3g. Specific acid and specific base catalysis are presumed to be absent. If specific and general acid and base catalysis are both operative, one is able to obtain a variety of interesting  $\log k$  versus pH curves, depending on the relative contributions of the different terms in various pH ranges. Curves *i* and *j* of Figure 7.3 are simple examples of these types.

Because specific acid and specific base catalysis and generalized acid and generalized base catalysis by cations and anions all involve ionic species, these processes are influenced by the ionic strength of the solutions in which they take place. There are two types of salt effects that are significant in acid-base catalysis. The first of these is the *primary salt effect*, discussed in Section 7.1. This effect is significant for reactions in solution involving ionic species. It operates by influencing the activity coefficients of the reactants and the activated complex. The second effect is referred to as the *secondary salt effect*. It operates by changing the actual concentrations of the catalytically active ions.

It may cause either an increase or a decrease in the rate constant, and it may be either larger or smaller than a primary salt effect. In some instances both effects occur simultaneously, and a cancellation of effects can make the reaction rate appear to be independent of ionic strength.

The secondary salt effect is important when the catalytically active ions are produced by the dissociation of a weak electrolyte. In solutions of weak acids and weak bases, added salts, even if they do not exert a common ion effect, can influence hydrogen and hydroxide ion concentrations through their influence on activity coefficients.

If one considers a reaction catalyzed by hydrogen ions formed by the dissociation of a weak acid HA, the hydrogen ion concentration is governed by the following relation:

$$K_a = \frac{\gamma_{H^+} \gamma_{A^-}}{\gamma_{HA}} \frac{(H^+)(A^-)}{(HA)} \quad (7.3.14)$$

where  $K_a$  is the equilibrium constant for the reaction and the  $\gamma$ 's are the activity coefficients of the various species. Taking logarithms and rearranging gives

$$\log(H^+) = \log K_a + \log \left[ \frac{(HA)}{(A^-)} \right] + \log \left( \frac{\gamma_{HA}}{\gamma_{H^+} \gamma_{A^-}} \right) \quad (7.3.15)$$

The concentration of hydrogen ions depends on the ionic strength through the ratio of activity coefficients appearing in the dissociation equilibrium expression. Any change in ionic strength affects the  $\gamma$  terms and thus the hydrogen ion concentration. Consequently, if a reaction is catalyzed by hydrogen (or hydroxide) ions, the rate becomes dependent on ionic strength through this secondary salt effect.

For the range of concentrations in which the Debye–Hückel theory is applicable, it is possible to place the theory of the secondary salt effect on a more quantitative basis by using Debye–Hückel relations for the various activity coefficients appearing in equation (7.3.15) or its more general analog. For an acid of charge  $z$  and its conjugate base of charge  $z - 1$ , the analogous equation is

$$\log(H^+) = \log K_a + \log \left[ \frac{(HA^z)}{(A^{z-1})} \right] + \log \left( \frac{\gamma_{HA^z}}{\gamma_{H^+} \gamma_{A^{z-1}}} \right) \quad (7.3.16)$$

If the Debye–Hückel limiting law is used to evaluate the various activity coefficients in aqueous solution at 25°C, equation (7.3.16) becomes

$$\log(H^+) = \log K_a + \log \left[ \frac{(HA^z)}{(A^{z-1})} \right] - 0.509(2)\sqrt{\mu}(z - 1) \quad (7.3.17)$$

In the most common case,  $z = 0$ , and the secondary salt effect implies that the hydrogen ion concentration will

increase with increasing ionic strength. However, the direction of the effect is determined by the sign of the quantity  $(z - 1)$ .

The existence of the primary and secondary salt effects indicates the importance of maintaining control over ionic strength in kinetics studies. One may choose to keep the ionic strength low so as to minimize its effects, or one may make a series of measurements at various ionic strengths to permit extrapolation to the limit of infinitely dilute solution. Another useful alternative is to maintain the ionic strength constant at a value that is sufficiently large that any variations caused by the progress of the reaction will be negligible. This approach is similar to the method of excess concentrations discussed in Chapter 3. It is particularly useful in attempts to determine the rate expressions for reactions that would involve significant changes in ionic strength if carried out in the absence of extraneous ionic species. Unfortunately, the rate constants determined in this fashion may be quite different from those in highly dilute solutions. Nonetheless, it is good laboratory practice to add small quantities of electrolytes to those reaction systems believed to involve ionic species to determine the possible presence of ionic strength effects. Some judgment must be used in the selection of the added ions in order to choose species that are noncatalytic in themselves and thus influence reaction rates only through the charged species resulting from electrolytic dissociation.

### 7.3.2 Catalysis by Enzymes

Enzymes are protein molecules that possess exceptional catalytic properties. They are essential to plant and animal life processes. Enzymes are remarkable catalysts in at least three respects: activity, specificity, and versatility.

The high activity of enzymes becomes apparent when the rates of enzyme catalyzed reactions are compared to those of the corresponding nonenzymatic reaction or to the same reaction catalyzed by an inorganic species. Rate enhancements by factors of  $10^8$  to  $10^{11}$  are not unusual in the presence of enzymes. Enzyme efficiencies are often measured in terms of a *turnover number*. This number is defined as the number of molecules that are caused to react in 1 min by one molecule of catalyst. For many common reactions the turnover number is in excess of  $10^3$ , and in some cases it may exceed  $10^6$ . High enzyme turnover numbers are largely the result of greatly reduced activation energies for the enzymatic reaction relative to other modes of bringing about the reactions in question.

Enzymes are often considered to function by general acid–base catalysis or by covalent catalysis, but these considerations alone cannot account for the high efficiency of enzymes. Proximity and orientation effects may be partially responsible for the discrepancy, but even the inclusion of these effects does not resolve the disparity

between the observed rates and those predicted theoretically. These and other aspects of the theories of enzyme catalysis are treated in the monographs by Bender (19) and Jencks (20).

Enzyme specificities are categorized in terms of the manner in which enzymes interact with various substrates. Some enzymes will cause only a single substrate to react. This type of specificity is known as *absolute specificity*. An example is urease, which catalyzes only the hydrolysis of urea. Other enzymes will react only with substrates having certain functional groups in certain positions relative to the bond to be attacked. This situation is called *group specificity*. An example of enzymes of this type is pepsin, which requires an aromatic group to be present in a certain position relative to a peptide linkage in order to bring about its hydrolysis. *Reaction specificity* is the least specific type of enzyme catalysis. This type of specificity requires only that a certain type of bond be present in the substrate. Enzymes such as the lipases will catalyze the hydrolysis of any organic ester. Many enzymes exhibit *stereochemical specificity* in that they catalyze the reactions of one stereochemical form but not the other. Proteolytic enzymes, for example, catalyze only the hydrolysis of peptides comprised of amino acids in the L configuration.

Enzyme specificity is often explained in terms of the geometric configuration of the active site of the enzyme. The active site includes the side chains and peptide bonds that either come into direct contact with the substrate or perform some direct function during catalysis. Each site is polyfunctional in that certain parts of it may hold the substrate in a position where the other parts cause changes in the chemical bonding of the substrate, thereby producing a reaction intermediate in the sequence of steps leading to product formation. The detailed configuration of the enzyme molecule including the conformation of the protein in folds or coils as well as the chemical structure near the active site, is quite important, and it is said that the geometric configuration is such that only molecules with certain structural properties can fit. This statement is the famous “lock and key” hypothesis for enzyme activity that dates back to the work of Fischer in 1894. More sophisticated models that purport to explain enzyme specificity have been proposed through the years, but the basic concept that specificity results from steric or geometric considerations remains unchanged.

The third remarkable aspect of enzyme catalysis is the versatility of these species. They catalyze an extremely wide variety of reactions: oxidation, reduction, polymerization, dehydration, dehydrogenation, and so on. Their versatility is a reflection of the range and complexity of the chemical reactions necessary to sustain life in plants and animals.

### 7.3.2.1 Rate Expressions for Enzyme Catalyzed Single-Substrate Reactions

The vast majority of the reactions catalyzed by enzymes are believed to involve a series of bimolecular or unimolecular steps. The simplest type of enzymatic reaction involves only a single reactant or substrate. The substrate forms an unstable complex with the enzyme, which subsequently undergoes decomposition to release the product species or to regenerate the substrate.

Reaction rate expressions for enzymatic reactions are usually derived by making the Bodenstein steady-state approximation for the intermediate enzyme–substrate complexes. This assumption is appropriate for use when the substrate concentration greatly exceeds that of the enzyme (the usual laboratory situation) or when there is both a continuous supply of reactant and a continuous removal of products (the usual cellular situation).

The “classic” mechanism of enzymatic catalysis can be written as



where E represents the enzyme, S represents the substrate, ES represents the enzyme–substrate complex, and P represents the product of the reaction. The stoichiometry of the reaction may be written as



In one sense this mechanism is akin to Lindemann’s picture of unimolecular decomposition reactions (see Section 4.3.1.3). An initial reaction produces a reactive intermediate that subsequently decomposes irreversibly to yield products or is reversibly decomposed into enzyme and substrate.

The net rate of an enzymatic reaction is usually referred to as its *velocity* and is assigned the symbol *V*. In this case

$$V = \frac{d(P)}{dt} = k_3(ES) \quad (7.3.21)$$

The concentration of the complex can be obtained by making the usual steady-state approximation:

$$\frac{d(ES)}{dt} = k_1(E)(S) - k_2(ES) - k_3(ES) \approx 0 \quad (7.3.22)$$

or

$$(ES) = \frac{k_1(E)(S)}{k_2 + k_3} \quad (7.3.23)$$

Combining equations (7.3.21) and (7.3.23) gives

$$V = \frac{k_1 k_3 (E)(S)}{k_2 + k_3} \quad (7.3.24)$$

Because most kinetic studies of this type involve initial rate experiments, it is usually necessary to rederive this expression in terms of the initial concentrations and the initial rate. From material balance considerations

$$(E_0) = (E) + (ES) \quad (S_0) = (S) + (ES) \quad (7.3.25)$$

For the conditions commonly encountered in the laboratory,  $S_0 \gg E_0$ . Because  $ES$  cannot exceed  $E_0$ , this inequality implies that  $(S_0) \approx (S)$ . Solving equation (7.3.25) for  $E$  and substituting this result into equation (7.3.22) gives

$$\frac{d(ES)}{dt} = k_1[(E_0) - (ES)](S_0) - k_2(ES) - k_3(ES) \cong 0 \quad (7.3.26)$$

or

$$(ES) = \frac{k_1(E_0)(S_0)}{k_2 + k_3 + k_1(S_0)} \quad (7.3.27)$$

Note the similarity of this expression to that for  $\theta_A$  derived for the Langmuir adsorption isotherm.  $(ES)/(E_0)$  plays a role analogous to  $\theta_A$  and  $S_0$  plays a role akin to the gas pressure. Although the expression is formally similar, we do not mean to imply that the two types of catalytic reactions proceed by similar molecular steps.

The result shown in equation (7.3.27) may be substituted into equation (7.3.21) to give

$$V_0 = \frac{k_1 k_3 (E_0) (S_0)}{k_2 + k_3 + k_1 (S_0)} \quad (7.3.28)$$

This equation predicts that the initial rate will be proportional to the initial enzyme concentration if the initial substrate concentration is held constant. If the initial enzyme concentration is held constant, the initial rate will be proportional to the substrate concentration at low substrate concentrations, and substantially independent of substrate concentration at high substrate levels. The maximum reaction rate is equal to  $k_3 E_0$ , and this product is often assigned the symbol  $V_{\max}$ . The group  $(k_2 + k_3)/k_1$  is often assigned the symbol  $K$  and is known as the *Michaelis constant*. Equation (7.3.28) can be written in terms of these parameters as

$$V_0 = \frac{V_{\max} (S_0)}{K + (S_0)} \quad (7.3.29)$$

The Michaelis constant is numerically equal to the value of the initial substrate concentration that gives an initial velocity that is half that of the maximum. Although equation (7.3.28) and, in particular, equation (7.3.29) are known as Michaelis–Menten rate expressions, these authors used a somewhat different approach to arrive at this mathematical form for an enzymatic rate expression (34).

In attempting to determine if a given set of experimental data is of the same mathematical form as equation (7.3.29), there are three routes that permit the graphical determination of the parameters  $V_{\max}$  and  $K$ . The most

frequently used plot is known as a *Lineweaver–Burk* or *reciprocal plot*. These plots are based on rearrangement of equation (7.3.29) into the form

$$\frac{1}{V_0} = \frac{1}{V_{\max}} + \frac{K}{V_{\max} (S_0)} \quad (7.3.30)$$

If the data are consistent with this mathematical model, a plot of  $1/V_0$  versus  $1/(S_0)$  should be linear with a slope  $K/V_{\max}$  and intercept  $1/V_{\max}$ . Such plots are analogous to those used in determining the constants in the Langmuir equation for adsorption on solid surfaces. Other forms that may be used to prepare linear plots are

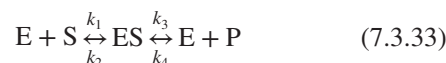
$$V_0 = V_{\max} - K \frac{V_0}{(S_0)} \quad (7.3.31)$$

and

$$\frac{(S_0)}{V_0} = \frac{K}{V_{\max}} + \frac{(S_0)}{V_{\max}} \quad (7.3.32)$$

Equation (7.3.31) gives rise to what is known as an *Eadie* or *Hofstee plot*, and equation (7.3.32) gives rise to a *Hanes plot*. The Eadie plot has the advantage of spreading the points out more evenly and of determining  $K$  and  $V_{\max}$  separately. The three types of plots are shown schematically in Figure 7.4. The Lineweaver–Burk and Eadie plots are the ones used most frequently in data analysis.

The Michaelis–Menten equation is applicable to a wide variety of enzyme-catalyzed reactions, but it is not appropriate for use in analyzing data for reversible reactions or multiple-substrate reactions. However, the generalized steady-state analysis remains applicable. Consider the case of reversible decomposition of an enzyme–substrate complex into a product molecule and an enzyme via the mechanistic equations:



In this case the net rate of reaction is given by

$$V = \frac{d(P)}{dt} = k_3(ES) - k_4(E)(P) \quad (7.3.34)$$

The steady-state approximation for the intermediate complex is

$$0 \approx \frac{d(ES)}{dt} = k_1(E)(S) - k_2(ES) - k_3(ES) + k_4(E)(P) \quad (7.3.35)$$

If the conservation equation for total enzyme concentration (7.3.25) is employed, equation (7.3.35) becomes

$$k_1[(E_0) - ES](S) - k_2(ES) - k_3(ES) + k_4[(E_0) - (ES)](P) \cong 0 \quad (7.3.36)$$

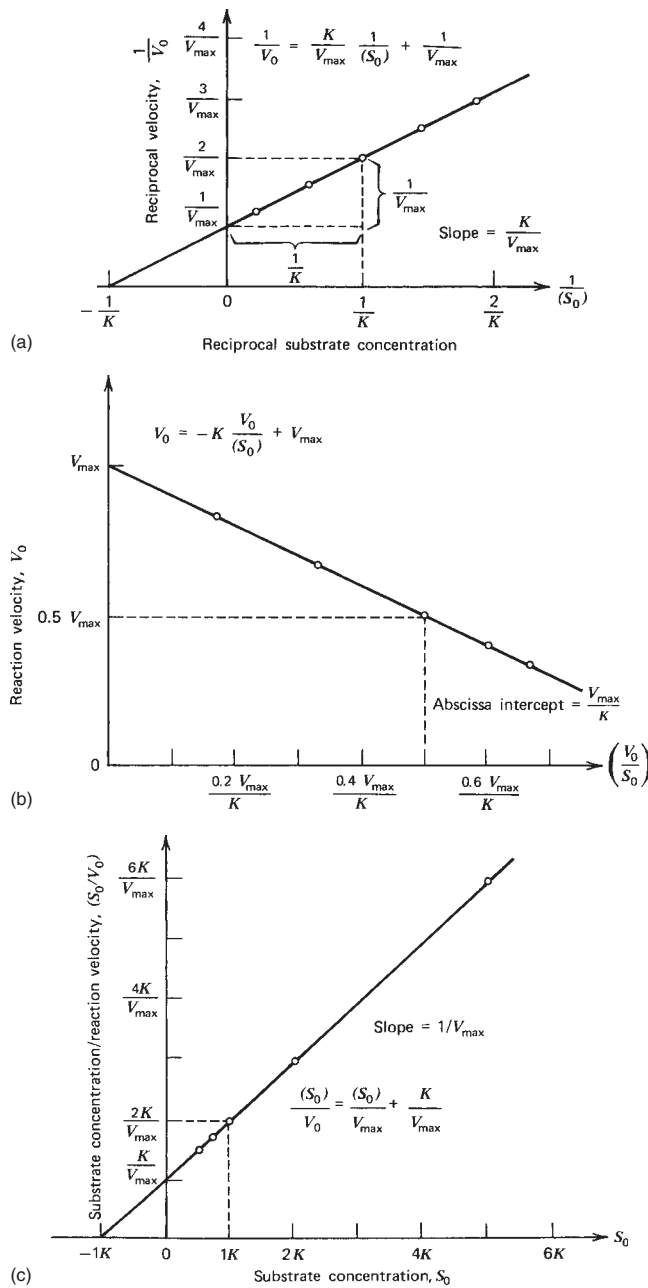


**Figure 7.4** Methods of plotting data for enzyme-catalyzed reactions: (a) Lineweaver-Burk plot; (b) Eadie or Hofstee plot; (c) Hanes plot. (Adapted from K. Plowman, *Enzyme Kinetics*. Copyright © 1972. Used with permission of McGraw-Hill Book Company.)

or

$$(ES) = \frac{k_1(E_0)(S) + k_4(E_0)(P)}{k_2 + k_3 + k_1(S) + k_4(P)} \quad (7.3.37)$$

Combining equations (7.3.25), (7.3.34), and (7.3.37) gives

$$V = \frac{k_1 k_3(E_0)(S) - k_2 k_4(E_0)(P)}{k_2 + k_3 + k_1(S) + k_4(P)} \quad (7.3.38)$$

If one defines the enzyme reaction parameters,

$$\begin{aligned} V_{1\text{ max}} &= k_3(E_0) & V_{4\text{ max}} &= k_2(E_0) \\ K_s &= \frac{k_2 + k_3}{k_1} & K_p &= \frac{k_2 + k_3}{k_4} \end{aligned} \quad (7.3.39)$$

the four kinetic constants ( $V_{1\text{ max}}$ ,  $V_{4\text{ max}}$ ,  $K_s$ , and  $K_p$ ) can be determined from initial rate studies of the forward and reverse reactions. Equation (7.3.38) can be rephrased in terms of these parameters as

$$V = \frac{K_p V_{1\text{ max}}(S) - K_s V_{4\text{ max}}(P)}{K_s K_p + K_p(S) + K_s(P)} \quad (7.3.40)$$

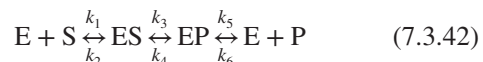
At equilibrium the net reaction velocity must be zero. In terms of the enzymatic kinetic constants, equation (7.3.40) then indicates that

$$\frac{(P)}{(S)} = K_{\text{eq}} = \frac{K_p V_{1\text{ max}}}{K_s V_{4\text{ max}}} \quad (7.3.41)$$

where  $K_{\text{eq}}$  is the thermodynamic equilibrium constant for the overall reaction. Equation (7.3.41) is known as the *Haldane relation*. This relation indicates that the enzymatic kinetic parameters are not all independent but are constrained by the thermodynamics of the overall reaction.

In the example above, the enzyme combined with either the substrate or the product to form the same complex. This assumption is not realistic, but it still leads to the correct form of the rate expression.

The following mechanism for a reaction of identical stoichiometry introduces a second complex into the sequence of elementary reactions.



where ES and EP are enzyme-substrate and enzyme-product complexes, respectively. For this mechanism, the steady-state rate equation is

$$V = \frac{(E_0)k_1k_3(S) - (E_0)k_2k_4k_6(P)}{(k_2k_5 + k_2k_4 + k_3k_5) + \sum(S) + \chi(P)} \quad (7.3.43)$$

where  $\sum \equiv k_1(k_3 + k_4 + k_5)$  and  $\chi \equiv k_6(k_2 + k_3 + k_4)$ .

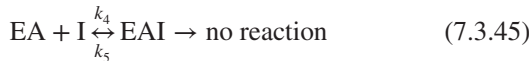
Comparison of equations (7.3.43) and (7.3.38) shows that they are of the same mathematical form. Both can be written in terms of four measurable kinetic constants in the manner of equation (7.3.40). Only the relationship between the kinetic constants and the individual rate constants differs. Thus, no distinction can be made between the two mechanisms using steady-state rate studies. In general, the introduction of unimolecular steps involving only isomerization between unstable intermediate complexes does not change the form of the rate expression.

### 7.3.2.2 Inhibition Effects in Enzyme Catalyzed Reactions

Enzyme catalyzed reactions are often retarded or inhibited by the presence of species that do not participate in the reaction in question as well as by the products of the reaction. In some cases the reactants themselves can act as inhibitors. Inhibition usually results from the formation of various enzyme–inhibitor complexes, a situation that decreases the amount of enzyme available for the normal reaction sequence. The study of inhibition is important in the investigation of enzyme action. By determining what compounds behave as inhibitors and what type of kinetic patterns are followed, one may be able to draw important conclusions about the mechanism of an enzyme's action or the nature of its active site. When this situation exists for reactions of interest to the pharmaceutical, agrichemical, and veterinary products industries, these conclusions are important to researchers seeking to identify compounds that ought to be investigated for use as potential drug products, herbicides, fungicides, and so on.

Inhibitors may act reversibly or irreversibly, but this classification is not particularly useful. This classification may even be misleading, because it suggests that reversible and irreversible inhibitors act in different ways when, in fact, both act by combining with the enzyme to give inactive complexes, but with quite different “dissociation constants.” The irreversible inhibitors give complexes that have very small dissociation constants; the reversible inhibitors have significantly higher dissociation constants.

A much more useful classification of inhibitors can be made on the basis of the mechanisms by which they act. *Competitive inhibitors* combine with the enzyme at the same site as does the substrate, thus blocking the first step in the reaction sequence. *Noncompetitive inhibitors* combine with the enzyme at some other site to give a complex that can still combine with the substrate, but the resulting ternary complex is unreactive. *Uncompetitive inhibition* results when the inhibitor and substrate combine with enzyme forms, as in the following mechanism:



These three classes of inhibition can be distinguished by virtue of the effect of variations in inhibitor concentration on the slopes and intercepts of reciprocal plots. For competitive inhibition only the slope varies when the concentration of inhibitor changes. For uncompetitive inhibition only the intercept varies, while for noncompetitive inhibition both the slope and the intercept vary when the inhibitor concentration changes.

If more than a single substrate participates in an enzymatic reaction, the kinetic effects of an inhibitor can be quite complex. In this case, the rules formulated by Cleland (36) are useful in gaining a qualitative picture of the inhibition patterns to be expected from a given mechanism. For the benefit of readers interested in interpreting data from experimental inhibition studies in assessments of the plausibility of proposed enzymatic mechanisms, we have summarized these rules below.

1. If the inhibitor combines with an enzyme form different from one with which the variable substrate combines, the vertical intercept of the corresponding reciprocal plot will be shifted.
2. If the inhibitor combines with an enzyme form that is the same as or is connected by a series of reversible steps to the same form with which the variable substrate combines, the slope of the corresponding reciprocal plot is altered.
3. These effects can occur separately (in which case the inhibition is either competitive or uncompetitive). For noncompetitive inhibition they can occur jointly.

### 7.3.2.3 The Influence of Environmental Factors on Enzyme Kinetics

Because enzymes are proteins, they are unusually sensitive to changes in their environment. This is true not only with regard to variations in inhibitor concentrations, but also with respect to variations in pH and temperature. Most enzymes are efficient catalysts only within relatively narrow ranges of pH and temperature.

When the rate of an enzyme-catalyzed reaction is studied as a function of temperature, one usually finds that the rate passes through a maximum. The existence of an optimum temperature can be explained by considering the effect of temperature on the catalytic reaction itself and on the corresponding enzyme denaturation reaction. In the low-temperature range (around room temperature) there is little denaturation, and increasing the temperature increases the rate of the catalytic reaction in the usual manner. As the temperature rises, deactivation arising from protein denaturation becomes more and more important, so the observed overall rate will eventually begin to decline. In aqueous environments at temperatures in excess of 50 to 60°C, most enzymes are completely denatured, and the rates observed are essentially zero.

Enzyme activity generally passes through a maximum as the pH of the system in question is varied. However, the optimum pH varies with substrate concentration and temperature. Provided that the pH is not changed too far from the optimum value corresponding to the maximum rate, the changes of rate with pH are reversible and reproducible. However, if the solutions are made too acid or too alkaline,

the activity of the enzyme may be irreversibly destroyed. Irreversible deactivation is usually attributed to denaturation of the proteinaceous enzyme. The range of pH in which reversible behavior is observed is generally small, and this behavior is almost certainly a consequence of changes in the amounts and activities of the various ionic forms of the enzyme, the substrate, and the enzyme complex. The maximum in the activity of the enzyme is a reflection of the maximum in the concentration of the catalytically active species.

## 7.4 CORRELATION METHODS FOR KINETIC DATA: LINEAR FREE ENERGY RELATIONS

A primary objective of the practicing kineticist is to be able to relate the rate of a reaction to the structure of the reactants. Although the collision and transition state theories provide useful frameworks for discussion of the microscopic events involved in chemical reactions, they do not in any meaningful way permit one to predict reaction rates on an *a priori* basis for even relatively simple reactions. However, chemical engineers should be aware that methods exist for correlating experimental rate data for homologous reactions. These correlations attempt to describe quantitatively the influence of variations in chemical structure on rate constants for a series of reactions involving the same functional groups. In this section we briefly describe the most useful correlation method in order to indicate to beginning kineticists an empirical approach which has given good results in the past. The useful correlation methods are based on what are referred to as linear free energy relations. These relations presume that when a selected molecule undergoes reactions with two different homologous compounds, the activation energy changes associated with the rate processes will be influenced in a similar fashion by the changes in structure. In essence one treats the molecule as if its structure can arbitrarily be broken up into a reaction center *X* and a nonreacting residue with structural elements that can influence the rate of reaction at *X*. Similar treatments are used in the correlation of free energy changes associated with reaction equilibria and hence of the equilibrium constant itself. The development and improvement in these quantitative correlations for reaction rate and equilibrium constant data have been one of the most striking developments in the evolution of physical organic chemistry. In the area of kinetics these relationships constitute a suitable framework for the extrapolation and interpolation of rate data, and they can also provide useful insights into the events that take place at a molecular level during reaction.

It is instructive to consider the rationale underlying the various linear free energy correlations and to indicate in qualitative fashion how substituents may influence reaction

rates. The relation between an equilibrium constant and the standard Gibbs free energy change accompanying a reaction is given by

$$\Delta G^0 = -RT \ln K_a \quad (7.4.1)$$

Since the transition state formulation of a reaction rate expression treats the activated complex as being in equilibrium with the reactants, the resulting expression for the reaction rate constant depends similarly on the free-energy difference between reactants and the activated complex. In this case equation (4.3.34) can be rewritten as

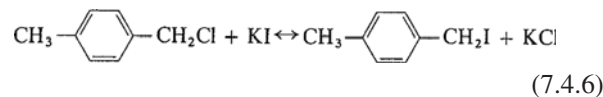
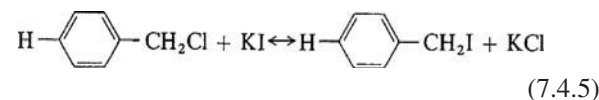
$$\Delta G^\ddagger = -RT \left[ \ln k - \ln \left( \frac{k_B T}{h} \right) \right] \quad (7.4.2)$$

where the second logarithmic term is constant at a fixed temperature. Thus, estimates of reaction rate and equilibrium constants may be regarded as equivalent to estimates of free energy differences between different species. If one examines a series of reactions, differences in  $\ln k$  or  $\ln K$  are then simply related to differences in the associated free energy changes.

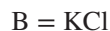
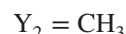
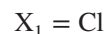
Consider two molecular processes involving the reaction of structurally similar reactants with a common reagent. For example,



where  $Y_1$  and  $Y_2$  are monovalent substituent atoms or groups;  $X_1$  and  $X_2$  are monovalent atoms or groups that may be regarded as the reactant and product group, respectively;  $N$  is the core of the molecule that links the substituent groups to the reactant and product groups; and  $A$  and  $B$  are other reactant and product molecules. A specific example of the pair of generalized reactions above is the following:



where



When one looks at the general reaction systems from the standpoint of the kineticist, species  $YX_1A^\ddagger$  would represent the transition state configuration. In this case, equation (7.4.2) indicates that

$$RT \ln\left(\frac{k_1}{k_2}\right) = \Delta G_2^\ddagger - \Delta G_1^\ddagger \quad (7.4.7)$$

Now the standard free energy content of a molecule has often been expressed as the sum of a number of contributions from the constituent parts of that molecule plus various contributions arising from the interactions of the parts with one another and with surrounding molecules (e.g., those of the solvent). Inasmuch as each chemical species represents a structurally unique combination of its constituent groups, it is possible to correlate standard free energies and many other thermodynamic properties for all known compounds by using a sufficiently large number of contributing parameters. Under a given set of standard conditions, the free energy of our representative  $Y_1NX_1$  molecule will include terms due to the individual  $Y_1$ ,  $N$ , and  $X_1$  groups and terms arising from the interactions of these groups. For a representative molecule, the standard free energy under these conditions may be written as

$$G_{Y_1NX_1}^0 = G_{Y_1} + G_N + G_{X_1} + G_{Y_1N} + G_{X_1N} + G_{Y_1X_1N} \quad (7.4.8)$$

where the singly subscripted  $G$  variables refer to individual group contributions, the  $G_{Y_1N}$  and  $G_{X_1N}$  terms to interactions between the substituent group and the core group and between the reactive group and the core group, respectively, and  $G_{Y_1X_1N}$  represents the interactions between the substituent and reactive groups through the molecular core.

The standard Gibbs free energy change for reaction (7.4.3) is given by

$$\Delta G_1^0 = G_{Y_1NX_2}^0 + G_B^0 - G_A^0 - G_{Y_1NX_1}^0 \quad (7.4.9)$$

Substitution of equation (7.4.8) and analogous equations for other compounds into equation (7.4.9), followed by simplification, gives

$$\begin{aligned} \Delta G_1^0 &= G_{X_2N} + G_{Y_1X_2N} + G_{X_2} + G_B^0 - G_A^0 \\ &\quad - (G_{X_1N} + G_{Y_1X_1N} + G_{X_1}) \end{aligned} \quad (7.4.10)$$

If we derive an analogous equation for reaction (7.4.4), we find that

$$\begin{aligned} \Delta G_2^0 &= G_{X_2N} + G_{Y_2X_2N} + G_{X_2} + G_B^0 - G_A^0 \\ &\quad - (G_{X_1N} + G_{Y_2X_1N} + G_{X_1}) \end{aligned} \quad (7.4.11)$$

Two equations of the form of equation (7.4.1) can be used with equations (7.4.10) and (7.4.11) to show that

$$RT \ln\left(\frac{K_2}{K_1}\right) = G_{Y_1X_2N} - G_{Y_2X_2N} - (G_{Y_1X_1N} - G_{Y_2X_1N}) \quad (7.4.12)$$

This relation implies that the ratio of the equilibrium constants for the two different reactions involving the same functional group but different substituents depends only on the terms for the free energies of interaction between the substituent and reactant groups. In similar fashion one may write for the ratio of reaction rate constants

$$RT \ln\left(\frac{k_2}{k_1}\right) = G_{Y_1X_2N} - G_{Y_2X_2N} - (G_{Y_1X_1N} - G_{Y_2X_1N}) \quad (7.4.13)$$

It is generally thought that the interaction energies of groups that are not bonded directly to one another result from the following effects.

- 1. Inductive or polar effects.** These effects involve electron displacements that are transmitted along a chain of atoms without any reorganization of the formal chemical bonds in the molecule. For example, the introduction of a methyl group in a pyridine ring involves a displacement of electrons to the nitrogen atom from the methyl group. This effect falls off rapidly with separation distance.
- 2. Resonance or electromeric effects.** Certain molecular structures are characterized by the possibility of having two or more compatible electronic structures and the molecules exist in a resonance state intermediate between the several extremes. These effects are particularly characteristic of aromatic structures and other molecules containing conjugate double bonds.
- 3. Steric effects.** These effects arise as a consequence of the molecular geometry of the species involved in the reaction. They include interference with internal rotations, steric compressions or strains, and so on.

These various effects combine to result in different rate and equilibrium constants for homologous reactions. The substituents influence these parameters in part by displacements of electron density of the first two types and in part by geometric effects of the last type. When some of the possible complications are considered, it is not surprising that there is no generally useful method for correlating the  $G_{YXN}$  terms with satisfactory accuracy. However, there are a number of special cases in which useful correlations can be developed. This is particularly true for those cases where  $N$  is a relatively rigid group, such as an aromatic ring. In this case the various  $X$  and  $Y$  groups will be the same distance apart in the species involved in reactions (7.4.3) and (7.4.4). Furthermore, if the  $X$  and  $Y$  groups are sufficiently far apart that there are no direct steric interactions and no direct resonance interactions between the  $X$  and  $Y$  groups, only the polar interactions contribute significantly to the  $G_{YXN}$  terms. This situation occurs in many *meta*- and *para*-substituted benzene derivatives. In this case  $G_{YXN}$  can be assumed

to be proportional to the product of parameters for the substituent group Y and the reactant group X. These parameters are referred to as *polar substituent constants*  $\sigma_{Y^N}$  and  $\sigma_{X^N}$ . The proportionality constant depends on the solvent, the temperature, and the nature of the core group N linking the substituents. It provides a measure of how effectively the influence of one group is transmitted to the other. This proportionality constant may be written as  $-\tau_N RT \ln [10]$ , so that the interaction term can be written as

$$G_{YX^N} = -(\tau_N RT \ln [10])\sigma_{Y^N}\sigma_{X^N} \quad (7.4.14)$$

Combining equations (7.4.13) and (7.4.14) then gives

$$\ln\left(\frac{k_1}{k_2}\right) = (\tau_N \ln [10])[(\sigma_{Y_1^N}\sigma_{X_2^N} - \sigma_{Y_2^N}\sigma_{X_2^N}) - (\sigma_{Y_1^N}\sigma_{X_1^N} - \sigma_{Y_2^N}\sigma_{X_1^N})] \quad (7.4.15)$$

or, on simplification,

$$\log\left(\frac{k_1}{k_2}\right) = \tau_N[(\sigma_{Y_1^N} - \sigma_{Y_2^N})(\sigma_{X_2^N} - \sigma_{X_1^N})] \quad (7.4.16)$$

Within a specific sequence of reactions involving the same groups  $X_1$  and  $X_2$  and for uniform conditions of solvent, temperature, and so on, the value of  $\tau_N(\sigma_{X_2^N} - \sigma_{X_1^N})$  will be a constant  $\rho_{X_1X_2^N}$  that characterizes the functional group interactions involved. Hence,

$$\rho_{X_1X_2^N} \equiv \tau_N(\sigma_{X_2^N} - \sigma_{X_1^N}) \quad (7.4.17)$$

and equation (7.4.16) becomes

$$\log\left(\frac{k_1}{k_2}\right) = \rho_{X_1X_2^N}(\sigma_{Y_1^N} - \sigma_{Y_2^N}) \quad (7.4.18)$$

Because only *differences* between  $\sigma$ 's for the substituents are involved, one may arbitrarily set the absolute value of one  $\sigma$  value without loss of generality. Normally one chooses a hydrogen atom as a reference substituent for which  $\sigma$  is defined as zero. All other rate constants may then be compared to the one characterizing the reaction of the reference substance ( $k_0$ ). In these terms equation (7.4.18) becomes

$$\log\left(\frac{k_1}{k_0}\right) = \rho_{X_1X_2^N}\sigma_{Y_1^N} \quad (7.4.19)$$

A corresponding equation exists for the ratio of equilibrium constants. The utility of equations of this form lies in the fact that the  $\rho$  value is characteristic of a particular reaction of functional groups, while the  $\sigma$  value is characteristic of the nonreactive functional groups. Once  $\sigma$  values have been determined for one class of reactions, they may be used for another class of reactions. Hence, knowledge of  $k_0$  and  $\rho$  for the second class permits one to obtain estimates

of the rate constants for reactions involving the various substituted compounds. As we will see in the next subsection, if equations similar to equation (7.4.19) are to be appropriate for use, they require that a certain free energy difference or free energy contribution be a linear function of some property of a substituent group. Consequently, these equations are referred to as linear free energy relations.

### 7.4.1 The Hammett Equation

The Hammett equation is the best known and most widely studied of the various linear free energy relations for correlating reaction rate and equilibrium constant data. This equation was first proposed to correlate the rate constants and equilibrium constants for the side chain reactions of *para*- and *meta*-substituted benzene derivatives. Hammett (37-39) noted that for a large number of reactions of these compounds plots of  $\log k$  (or  $\log K$ ) for one reaction versus  $\log k$  (or  $\log K$ ) for a second reaction of the corresponding member of a series of such derivatives was reasonably linear. Figure 7.5 is a plot of this type involving the ionization constants for phenylacetic acid derivatives and for benzoic acid derivatives. The point labeled *p*-Cl has for its ordinate  $\log K_a$  for *p*-chlorophenyl acetic acid and for its abscissa  $\log K_a$  for *p*-chlorobenzoic acid.

The data points approximate a straight line, which can be expressed as

$$\log K_A = \rho \log K'_A + C \quad (7.4.20)$$

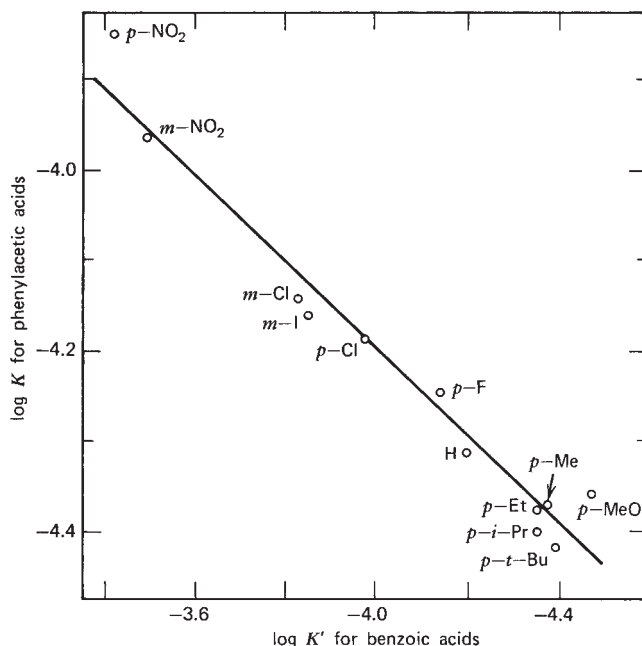


**Figure 7.5** Log-log plot of ionization constants of benzoic and phenylacetic acids in water at 25°C. (From J. S. Hine, *Physical Organic Chemistry*. Copyright © 1962. Used with permission of McGraw-Hill Book Company.)

where  $K_A$  and  $K'_A$  are the ionization constants for substituted phenylacetic and benzoic acids with a given substituent,  $\rho$  is the slope of the line, and  $C$  is the intercept. This relation may be used for any substituent, including the reference substituent, normally taken as a hydrogen atom. If the reference substance is denoted by the subscript zero, then

$$\log K_0 = \rho \log K'_0 + C \quad (7.4.21)$$

where  $K_0$  and  $K'_0$  are the ionization constants of phenylacetic and benzoic acids, respectively. Elimination of the intercept  $C$  gives

$$\log\left(\frac{K_A}{K_0}\right) = \rho \log\left(\frac{K'_A}{K'_0}\right) \quad (7.4.22)$$

Equations of this type can be written for any pair of the many reactions for which linear log-log plots could be made. Consequently, it is convenient to choose a reference reaction to which others can be compared. The large amount of accurate data on the ionization of benzoic acid derivatives at 25°C made this reaction an appropriate

choice, and a new constant  $\sigma$  was then defined as

$$\sigma_A = \log\left(\frac{K'_A}{K'_0}\right) \quad (7.4.23)$$

This constant characterizes the ionization of a particular substituted benzoic acid in water at 25°C relative to that of benzoic acid itself. This definition reduces equation (7.4.22) to

$$\log\left(\frac{K_A}{K_0}\right) = \rho\sigma_A \quad (7.4.24)$$

which is of the same form as the general linear free-energy relation introduced earlier in equation (7.4.19), although it predates the latter by many years. From this equation and from the definition of  $\sigma$ , it is evident that  $\rho$  is taken as unity for the standard reaction (i.e., the ionization of substituted benzoic acids in water at 25°C). The value of  $\sigma$  may be determined from its definition in terms of the ionization constant if the appropriate benzoic acid derivative has been measured. Such  $\sigma$  values may then be used to determine  $\rho$  values for other reactions, and these  $\rho$  values, in turn, lead to the possibility of determining new  $\sigma$  values.

Equation (7.4.24) implies that a plot of  $\log K_A$  or  $\log k_A$  versus  $\sigma_A$  should be linear for a given series of reactions

**Table 7.2** Hammett Substituent Constants<sup>a</sup>

Substituent	$\sigma$		Substituent	$\sigma$	
	Meta	Para		Meta	Para
CH <sub>3</sub>	-0.069	-0.170	O <sup>-</sup>	-0.708	-1.00
CH <sub>2</sub> CH <sub>3</sub>	-0.07	-0.151	OH	+0.121	-0.37
CH(CH <sub>3</sub> ) <sub>2</sub>	-0.068	-0.151	OCH <sub>3</sub>	+0.115	-0.268
C(CH <sub>3</sub> ) <sub>3</sub>	-0.10	-0.197	OC <sub>2</sub> H <sub>5</sub>	+0.1	-0.24
C <sub>6</sub> H <sub>5</sub>	+0.06	-0.01	OC <sub>6</sub> H <sub>5</sub>	+0.252	-0.320
C <sub>6</sub> H <sub>4</sub> NO <sub>2</sub> - <i>p</i>	—	+0.26	OCOCH <sub>3</sub>	+0.39	+0.31
C <sub>6</sub> H <sub>4</sub> OCH <sub>3</sub> - <i>p</i>	—	-0.10	F	+0.337	+0.062
CH <sub>2</sub> Si(CH <sub>3</sub> ) <sub>3</sub>	-0.16	-0.21	Si(CH <sub>3</sub> ) <sub>3</sub>	-0.04	-0.07
COCH <sub>3</sub>	+0.376	+0.502	PO <sub>3</sub> H <sup>-</sup>	+0.2	+0.26
COC <sub>6</sub> H <sub>5</sub>	—	+0.459	SH	+0.25	+0.15
CN	+0.56	+0.660	SCH <sub>3</sub>	+0.15	0.00
CO <sub>2</sub> <sup>-</sup>	-0.1	0.0	SCOCH <sub>3</sub>	+0.39	+0.44
CO <sub>2</sub> H	+0.35	+0.406	SOCH <sub>3</sub>	+0.52	+0.49
CO <sub>2</sub> CH <sub>3</sub>	+0.321	+0.385	SO <sub>2</sub> CH <sub>3</sub>	+0.60	+0.72
CO <sub>2</sub> C <sub>2</sub> H <sub>5</sub>	+0.37	+0.45	SO <sub>2</sub> NH <sub>2</sub>	+0.46	+0.57
CF <sub>3</sub>	+0.43	+0.54	SO <sub>3</sub> <sup>-</sup>	+0.05	+0.09
NH <sub>2</sub>	-0.16	-0.66	S(CH <sub>3</sub> ) <sub>2</sub> <sup>+</sup>	+1.00	+0.90
N(CH <sub>3</sub> ) <sub>2</sub>	-0.211	-0.83	Cl	+0.373	+0.227
NHCOCH <sub>3</sub>	+0.21	0.00	Br	+0.391	+0.232
N(CH <sub>3</sub> ) <sub>3</sub> <sup>+</sup>	+0.88	+0.82	I	+0.352	+0.276
N <sub>2</sub> <sup>+</sup>	+1.76	+1.91	IO <sub>2</sub>	+0.70	+0.76
NO <sub>2</sub>	+0.710	+0.778			

Source: Hine (46).

<sup>a</sup>Note that  $\sigma$  values for charged substituents may be particularly solvent dependent.

involving the same reactive groups. Extensive experimental evidence validates this relation. Table 7.2 contains some values that have been reported in the literature. Extensive tabulations of  $\sigma$  and  $\rho$  values are available (37, 40–47). Note that one requires different  $\sigma$  values for *meta* and *para* substituents but that only one  $\rho$  value is required. Typical  $\sigma$  values range from about  $-1$  to  $+2$ , while  $\rho$  values range from  $-6$  to  $+4$ . Hence, the Hammett equation may be used to correlate data covering several orders of magnitude in the rate and equilibrium constant values. Illustration 7.1 involves the use of Table 7.2 to estimate a reaction rate constant.

The substituent constants have also been associated with the ability of the substituent group to alter the charge density at the reaction site. The groups with positive  $\sigma$  values are regarded as electron withdrawers; those with negative  $\sigma$ 's refer to electron donor substituents. Reactions involving a transition state with a highly electron-deficient center would be expected to be sensitive to the stabilizing effect of substituents able to donate charge to the center. The opposite situation exists for reactions involving a reaction center with an excess electron density. In this case the stabilizing effect occurs in the presence of substituents that act to withdraw charge from the center. Reactions with positive  $\rho$  values are accelerated by electron withdrawal from the ring (positive  $\sigma$ ); those with negative  $\rho$  values are retarded by electron withdrawal.

In its original form the Hammett equation was appropriate for use with *para*- and *meta*-substituted compounds where the reaction site is separated from the aromatic group by a nonconjugating side chain. Although there have been several extensions and modifications that permit use of the Hammett equation beyond these limitations, it is not appropriate for use with *ortho*-substituted compounds, because steric effects are likely to be significant with such species. The results obtained using free radical reactions are often poor, and the correlation is more appropriate for use with ionic reactions. For a detailed discussion of the Hammett equation and its extensions, consult the texts by Hammett (37), Amis and Hinton (11), and Johnson (47).

Before terminating our discussion of the Hammett equation, we should note that the existence of linear correlations of the type indicated by equation (7.4.20) implies a linear free energy relationship. The rate or equilibrium constants can be eliminated from this equation using equation (7.4.1); that is,

$$\frac{\Delta G_A^0}{2.303RT} = \rho \frac{[\Delta G_A^0]'}{2.303RT} - C \quad (7.4.25)$$

Thus, a linear relationship between the free energies for one homologous series of reactions and those for another must exist if the Hammett equation is obeyed.

## ILLUSTRATION 7.1 Use of the Hammett Equation for the Determination of a Reaction Rate Constant

K. Kindler [*Ann. Chem.*, **450**, 1 (1926)] studied the alkaline hydrolysis of the ethyl esters of a number of substituted benzoic acids. The *m*-nitro compound has a rate constant that is 63.5 times as fast as that for the unsubstituted compound. What relative rate constant is predicted for the reaction of *p*-methoxybenzoate using the Hammett equation? The value based on experimental results is 0.214.

### Solution

From Table 7.2 the  $\sigma$  value for the *m*-nitro group is 0.710. Substitution of this value and the ratio of reaction rate constants into equation (7.4.19) gives

$$\log(63.5) = \rho(0.710)$$

or

$$\rho = 2.54$$

for the alkaline hydrolysis of ethyl benzoates. For *p*-methoxy substitution, Table 7.2 indicates that  $\sigma = -0.268$ . In this case equation (7.4.19) becomes

$$\log\left(\frac{k}{k_0}\right) = 2.54(-0.268) = -0.681$$

or

$$\frac{k}{k_0} = 0.209$$

This value compares quite favorably with the experimental result.

### 7.4.2 Other Correlations

To correlate rate constant data for aliphatic and *ortho*-substituted aromatic compounds, one must allow not only for the polar effects correlated by the Hammett equation but also for resonance and steric effects. Taft (48, 49) has shown that it is possible to extend the range of linear free-energy relations significantly by assuming that the polar, steric, and resonance effects may be treated independently. Other useful extensions of the Hammett equation include those of Swain et al. (50, 51), Edwards (52, 53), Grunwald and Winstein (54), and Hansson (55). To obtain substituent values for the parameters appearing in the various equations, consult the comprehensive review article by Hansch et al. (45), the text by Wells (40), the original references, or modern texts on physical organic chemistry such as that by Anslyn and Dougherty (56). The practicing design engineer should be aware of these

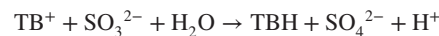
and other correlations to minimize the experimental work necessary to generate required kinetic parameters.

## LITERATURE CITATIONS

- PARKER, A. J., *Adv. Phys. Org. Chem.*, **5**, 192 (1967).
- LAIDLER, K. J., *Reaction Kinetics*, Vol. 2, *Reactions in Solution*, p. 2, Pergamon Press, Oxford, 1963.
- NORTH, A. M., *The Collision Theory of Chemical Reactions in Liquids*, Methuen, London, 1964.
- RABINOWITCH, E., and WOOD, W. C., *Trans. Faraday Soc.*, **32**, 1381 (1936).
- FRANCK, J., and RABINOWITCH, E., *Trans. Faraday Soc.*, **30**, 120 (1934).
- DEBYE, P., and HÜCKEL, E., *Phys. Z.*, **24**, 305 (1923).
- DEBYE, P., and HÜCKEL, E., *ibid.*, **25**, 145 (1924).
- DEBYE, P., and HÜCKEL, E., *Trans. Faraday Soc.*, **23**, 334 (1927).
- HARNED, H. S., and OWEN, B. B., *The Physical Chemistry of Electrolytic Solutions*, 3rd ed., Reinhold, New York, 1958.
- LA MER, V. K., *Chem. Rev.*, **10**, 179 (1932).
- AMIS, E. S., and HINTON, J. F., *Solvent Effects on Chemical Phenomena*, Academic Press, New York, 1973.
- REICHARDT, C., *Solvents and Solvent Effects in Organic Chemistry*, 3rd ed., Wiley-VCH, Weinheim, Germany, 2003.
- CLARK, D., and WAYNE, R. P., in *Comprehensive Chemical Kinetics*, Vol. 2, *The Theory of Kinetics*, pp. 302–376, Elsevier, Amsterdam, 1969.
- ECKERT, C. A., *Ann. Rev. Phys. Chem.*, **23**, 239, (1972).
- BELL, R. P., *Acid-Base Catalysis*, p. 3, Oxford University Press, Oxford, 1941.
- BREZONIK, P. L., *Chemical Kinetics and Process Dynamics in Aquatic Systems*, Lewis Publishers, Boca Raton, FL, 1994.
- LAIDLER, K. J., *Chemical Kinetics*, 3rd ed., Harper & Row, New York, 1987.
- MOORE, J. W., and PEARSON, R. G., *Kinetics and Mechanism*, 3rd ed. Wiley, New York, 1961.
- BENDER, M. L., *Mechanisms of Homogeneous Catalysis from Protons to Proteins*, Wiley-Interscience, New York, 1971.
- JENCKS, W. P., *Catalysis in Chemistry and Enzymology*, Dover, New York, 1987.
- SEGEL, I. H., *Enzyme Kinetics: Behavior and Analysis of Rapid Equilibrium and Steady State Enzyme Systems*, Wiley, New York, 1975.
- COOK, P. F., *Steady State Enzyme Kinetics*, Oxford University Press, New York, 1997.
- COOK, P. F., and CLELAND, W. W., *Enzyme Kinetics and Mechanism*, Garland Science, New York, 2007.
- PURICH, D. L., and ALLISON, R. D., *Handbook of Biochemical Kinetics*, Academic Press, San Diego, CA, 1999.
- CORNISH-BOWDEN, A., *Fundamentals of Enzyme Kinetics*, Portland Press, London, 1995.
- FERSHT, A., *Structure and Mechanism in Protein Science: A Guide to Enzyme Catalysis and Protein Folding*, W.H. Freeman, New York, 1999.
- MARANGONI, A., *Enzyme Kinetics: A Modern Approach*, Wiley-Interscience, Hoboken, NJ, 2003.
- BISSWANGER, H., *Enzyme Kinetics: Principles and Methods*, 2nd rev. ed., Wiley-VCH, Weinheim, Germany, 2008.
- PARSHALL, G. W., and ITTEL, J. D., *Homogeneous Catalysis: The Application and Chemistry of Catalysis by Soluble Transition Metal Complexes*, Wiley, New York, 1992.
- LEEUWEN, P. W. N. M., *Homogeneous Catalysis: Understanding the Art*, Springer-Verlag, New York, 2008.
- ASHMORE, P. G., *Catalysis and Inhibition of Chemical Reactions*, pp. 30–31, Butterworth, London, 1963.
- HINE, J. S., *Physical Organic Chemistry*, 2nd ed., McGraw-Hill, New York, 1962.
- SKRABAL, A., *Z. Elektrochem.*, **33**, 322 (1927).
- MICHAELIS, L., and MENTEN, M. L., *Biochem. Z.*, **49**, 333 (1913).
- PLOWMAN, K., *Enzyme Kinetics*, McGraw-Hill, New York, 1972.
- CLELAND, W. W., *Biochim. Biophys. Acta*, **67**, 188 (1963).
- HAMMETT, L. P., *Physical Organic Chemistry*, 2nd ed., McGraw-Hill, New York, 1970.
- HAMMETT, L. P., *Chem. Rev.*, **17**, 125 (1935).
- HAMMETT, L. P., *Trans. Faraday Soc.*, **34**, 156 (1938).
- WELLS, P. R., *Linear Free Energy Relationships*, Academic Press, New York, 1968.
- GORDON, A. J., and FORD, R. A., *The Chemist's Companion*, pp. 145–149, Wiley, New York, 1972.
- JAFFE, H. H., *Chem. Rev.*, **53**, 191 (1953).
- McDANIEL, D. H., and BROWN, H. C., *J. Org. Chem.*, **23**, 420 (1958).
- LEFFLER, J. E., and GRUNWALD, E., *Rates and Equilibria of Organic Reactions*, Wiley, New York, 1963.
- HANSCH, C., LEO, A., and TAFT, R. W., *Chem. Rev.*, **97**, 165 (1991).
- HINE, J. S., op. cit., p. 87.
- JOHNSON, C. D., *The Hammett Equation*, Cambridge University Press, London, 1973.
- TAFT, R. W., Jr., *J. Am. Chem. Soc.*, **74**, 2729, 3120 (1952); **75**, 4231 (1953).
- TAFT, R. W., Jr., in *Steric Effects in Organic Chemistry*, M. S. NEWMAN (Ed.), Chap. 13, Wiley, New York, 1956.
- SWAIN, C. G., and SCOTT, C. B., *J. Am. Chem. Soc.*, **75**, 141 (1953).
- SWAIN, C. G., MOSELY, R. B., and BROWN, D. E., *J. Am. Chem. Soc.*, **77**, 3731 (1955).
- EDWARDS, J. O., *J. Am. Chem. Soc.*, **76**, 1540 (1954).
- EDWARDS, J. O., *J. Am. Chem. Soc.*, **78**, 1819 (1956).
- GRUNWALD, E., and WINSTEIN, S., *J. Am. Chem. Soc.*, **70**, 846 (1948).
- HANSSON, J., *Sven. Kem. Tidsk.*, **66**, 351 (1954).
- ANSLYN, E. V., and DOUGHERTY, D. A., *Modern Physical Organic Chemistry*, University Science Books, Sausalito, CA, 2006.

## PROBLEMS

- 7.1** S. B. Jonnalagadda and N. R. Gollapalli [*J. Chem. Educ.*, **77** 506 (2000)] studied the effect of ionic strength on the kinetics of the reduction of toluidine blue ( $TB^+$ ) with sulfite ions in aqueous solution. The stoichiometry is



where  $TBH$  is toluidine white.

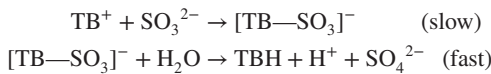
- (a)** Absorbance measurements at 596 nm were used to monitor the progress of the reaction at 25°C. The following data were obtained in a trial conducted using 0.1 M  $Na_2SO_3$  and  $2 \times 10^{-5}$  M  $TB^+$ . Analyze these data via the Guggenheim method to ascertain the pseudo first-order rate constant.

Time (s)	Absorbance
60	0.891
120	0.721
180	0.581
240	0.468
300	0.377
360	0.305
420	0.249
480	0.204
540	0.170
600	0.143
660	0.123
720	0.106
780	0.094
840	0.084
900	0.076
960	0.069
1020	0.064
1080	0.061
1140	0.058
1200	0.055

- (b) Additional experiments involving a large (but variable) excess of sulfite ions were conducted to determine the order of the reaction with respect to sulfite ions. The “adjusted” results, shown below, are expressed in terms of the dependence of the pseudo first-order rate constant ( $k^1$ ) on the concentration of sulfite ions. Throughout these trials at 25°C the ionic strength was held constant at 0.300 M. Determine the order of the reaction in  $\text{SO}_3^{2-}$  and the corresponding values of the  $n$ th-order rate constants.

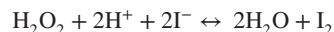
$[\text{SO}_3^{2-}]$ (M)	$k^1 \times 10^3$ ( $\text{s}^{-1}$ )
0.020	0.74
0.040	1.46
0.060	2.27
0.080	3.10
0.100	3.95

- (c) Subsequent trials were conducted at 25°C using several ionic strengths ( $\mu$ ) but with initial concentrations of  $\text{SO}_3^{2-}$  and toluidine blue held constant at 0.02 and  $2.0 \times 10^{-5}$  M, respectively. Does the Debye–Hückel model for activity coefficients accurately reflect the data below? Is the following mechanism consistent with the data for the dependence of the rate constant on the ionic strength? Comment.



$k^1$ ( $\text{s}^{-1}$ )	Ionic strength (M)
0.092	0.060
0.081	0.072
0.073	0.084
0.066	0.096
0.060	0.108
0.055	0.120

## 7.2 The oxidation of iodide ions by hydrogen peroxide,



has been studied by F. Bell, R. Gill, D. Holden, and W. F. K. Wynne-Jones [J. Phys. Chem., **55**, 874 (1951)]. At 25°C the reaction appears to proceed by two parallel paths to give an observed rate expression of the form

$$r = k_1(\text{H}_2\text{O}_2)(\text{I}^-) + k_2(\text{H}_2\text{O}_2)(\text{I}^-)(\text{H}^+)$$

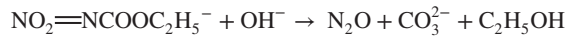
The influence of ionic strength on the two rate constants is indicated below.

$\mu$ ( $\text{kmol}/\text{m}^3$ )	$k_1$ [ $\text{m}^3/(\text{kmol}\cdot\text{s})$ ]	$k_2$ [ $\text{m}^6/(\text{kmol}^2\cdot\text{s})$ ]
0	0.658	19
0.0207	0.663	15
0.0525	0.67	12.2
0.0925	0.679	11.3
0.1575	0.694	9.7
0.2025	0.705	9.2

Are these data consistent with the results predicted using the following equation?

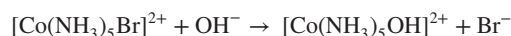
$$\log k = \log k_0 + 2Z_A z_B \sqrt{\mu}(0.509)$$

- 7.3 The reaction of the nitrourethane ions with hydroxide ions can be written as



Near room temperature the reaction is essentially irreversible and second-order. In the limit of zero ionic strength at 293 K,  $k = 2.12 \text{ m}^3/(\text{kmol}\cdot\text{ks})$ . Determine the initial reaction rate in a solution that is 0.05 kmol/m<sup>3</sup> each in potassium nitrourethanate,  $\text{KNO}_2$ ,  $\text{NH}_4\text{OH}$ , and  $\text{KCl}$ . The dissociation constant for  $\text{NH}_4\text{OH}$  at 293 K is  $1.7 \times 10^{-5} \text{ kmol/m}^3$ . The effect of the slight ionization of  $\text{NH}_4\text{OH}$  on ionic strength and the variation of activity coefficients with temperature between 293 and 298 K may be neglected.

- 7.4 The following reaction takes place in aqueous solution:



This reaction may be regarded as bimolecular and irreversible. Determine the ratio of the reaction rate in a system initially containing 10 mol/m<sup>3</sup>  $[\text{Co}(\text{NH}_3)_5\text{Br}](\text{NO}_3)_2$ , 100 mol/m<sup>3</sup>  $\text{NH}_4\text{OH}$ , and 50 mol/m<sup>3</sup>  $\text{KNO}_3$  to the rate in a system that initially contains 100 mol/m<sup>3</sup>  $\text{NH}_4\text{OH}$

and  $100 \text{ mol/m}^3$   $[\text{Co}(\text{NH}_3)_5\text{Br}](\text{NO}_3)$ . Take into account both primary and secondary salt effects, but neglect the contributions to the ionic strength of species resulting from the dissociation of  $\text{NH}_4\text{OH}$ . You may employ  $1.75 \times 10^{-5}$  as the dissociation constant for  $\text{NH}_4\text{OH}$  when concentrations are given in moles per/liter.

- 7.5 D. Chen and K. J. Laidler *Can. J. Chem.*, **37**, 599 (1959) studied the reaction of the quinoid form of bromophenol blue with hydroxide ions to give the carbinol form of the dye. The following values of the second-order rate constant at  $25^\circ\text{C}$  were reported.

Pressure (psia)	$k \times 10^4$ [L/(mol·s)]
14.7	9.298
4,000	11.13
8,000	13.05
12,000	15.28
16,000	17.94

What is the activation volume for this reaction?

- 7.6 For much of the twentieth century, the disposal of excess or obsolete chemical warfare agents and munitions in offshore ocean waters was an internationally accepted practice. Well in excess of  $10^5$  tons of such materials were disposed of in this manner prior to adoption of federal laws and international conventions in the 1970s. Loss of structural integrity by the containment vessels can release these highly toxic materials and present a major threat to both the environment and human health. The potential use of such materials by rogue nations or terrorists has led to several studies of the natural degradation of these agents in marine environments. Sarin (also known as GB or isopropyl methylphosphonofluoride) is a nerve gas that has been of particular concern. Consequently, hydrolysis reactions of GB and similar esters have been investigated by several research groups. These reactions are also of interest with respect to potential detoxification of these hazardous esters by deep well injection. Because the pressures associated with ocean depths and deep well injection are large, one must consider their effects on the rates of these aqueous-phase reactions.

As indicated by G. O. Bizzigotti, H. Castelly, A. M. Hafez, W. H. B. Smith, and M. T. Whitmire [*Chem. Rev.* **109**, 236 (2009)], GB undergoes hydrolysis by acidic, neutral, and basic mechanisms, all of which give isopropyl methylphosphonate and fluoride ions as the initial products. In seawater the rate of hydrolysis is markedly increased by the presence of magnesium and calcium hydroxocations,  $[\text{MgOH}]^+$  and  $[\text{CaOH}]^+$ . In essence the resulting rate expressions can be regarded as pseudo-first-order in GB with rate constants  $k$  of the form

$$k = k_w + k_{\text{Ca}} + k_{\text{Mg}}$$

where the constants  $k_{\text{Ca}}$  and  $k_{\text{Mg}}$  depend on temperature, pH, and the activities of the corresponding hydroxocations. In seawater the  $k_w$  term is small compared to the other terms.

The review article by Bizzigotti et al. contains kinetic data relevant to detoxification of the chemical warfare agent GB. Data for hydrolysis of this compound in seawater at a pH of 7.7 and atmospheric pressure can be correlated using the equation

$$\log \tau_{1/2} = \frac{4325}{T} - 12.84$$

for the half-life ( $\tau_{1/2}$ ) in minutes and temperature ( $T$ ) in kelvin. To effect detoxification of 99.9% of the GB originally present in a seawater sample requires nearly 10 half-lives.

- (a) If the pressure generated by a 10-m-high column of seawater is approximately 1 bar (0.987 atm), consider hydrolysis of GB in seawater at hydrostatic pressures corresponding to ocean depths of (1) 4 km (the average depth of the oceans) and (2) 10.6 km (the maximum depth of the oceans). If the volume of activation of this reaction is  $-12 \text{ cm}^3/\text{mol}$ , determine the times necessary to hydrolyze 99.9% of the GB initially present in seawater at  $5^\circ\text{C}$  and pressures corresponding to sea level and the indicated depths.
- (b) If, instead, temperature increases to  $7^\circ\text{C}$  and  $10^\circ\text{C}$  are considered, determine the times corresponding to 99.9% hydrolysis for each of the depths of interest. Comment.
- 7.7 The activation volumes associated with the formation of a transition state complex reflect two separate processes: one involving structural rearrangement of atoms in going from reactants to activated complexes (a molecular contribution), the other concerning changes in the structure of the solvent (an electrostriction contribution). For bimolecular processes the latter process causes a decrease in volume; for unimolecular processes there is a corresponding increase in volume. By contrast, reorganization of solvent molecules may be accompanied by either positive or negative changes in volume. These effects can be viewed as electrostriction effects. For reactions involving ions or highly polar molecules the effect of changes in the structure of the solvent are more important than those associated with rearrangement of atoms.

C. Cameron, P. P. S. Saliya, M. A. Floriano, and E. Whalley [*J. Phys. Chem.*, **92**, 3417 (1988)] investigated the use of activation volume measurements at very high pressures to discriminate between  $\text{S}_{\text{N}}1$  and  $\text{S}_{\text{N}}2$  mechanisms for solvolysis reactions of alkyl halides. At low pressures both of these mechanisms are characterized by negative activation volumes because the effects of electrostriction constitute the dominant contribution to  $\Delta V^\ddagger$ . These effects are caused by the large dipole moment associated with the transition state. However, at sufficiently high pressures the compressibility of the solvent becomes very small, as does the effect of the electrostriction. At such pressures the activation volume largely reflects the effect of the structural rearrangement of atoms in proceeding from reactants to products, and it is this effect that determines the sign of  $\Delta V^\ddagger$ . Consequently, at high pressures an  $\text{S}_{\text{N}}1$  reaction should have a positive activation volume and an  $\text{S}_{\text{N}}2$  reaction should have a negative activation volume.

Consider the data below for the glycerolysis of  $\text{CH}_3\text{I}$  (Table P7.7-1) and of *tert*-butyl chloride (Table P7.7-2). Use these data to characterize the mechanisms of these reactions

**Table P7.7-1** Rate Constants for the Solvolysis of Methyl Iodide in Glycerol in the Range 9.4 to 69.6 kbar

Pressure (kbar)	Temperature (°C)	Rate constant $\times 10^3$ (s <sup>-1</sup> )
9.4	75.0	0.166
12.5	75.0	0.268
15.7	75.0	0.330
18.8	75.0	0.406
21.9	75.0	0.467
20.9	74.8	0.441
34.8	75.7	0.793
46.0	75.1	0.944
58.0	75.0	1.21
70.0	74.9	1.40

**Table P7.7-2** Rate Constants for the Solvolysis of *tert*-Butyl Chloride in Glycerol at 22.0 and 32.0 °C in the Range 1.8 to 23.3 kbar

Pressure (kbar)	Rate constant $\times 10^3$ (s <sup>-1</sup> )	
	22.0 °C	32.0 °C
1.8		0.339
3.6		0.794
6.3		1.20
9.0	0.340	1.65
11.6	0.424	1.80
14.3	0.462	1.91
16.1	0.503	1.97
17.9	0.478	1.93
18.8		1.80
19.2	0.425	
19.7		1.65
20.0	0.370	
20.6	0.430	1.44
23.3		0.867

and to ascertain the activation volumes of these reactions at a mean pressure of 12 kbar.

**7.8** Maintenance of appropriate levels of disinfectants in water distribution systems is necessary to ensure the safety of potable water supplies. However, reactions of disinfectants with oxidizable species can lead to undesirable reductions in the concentration of the disinfectant. For example, Fe(II) species in aqueous solution can bring losses of monochloramine. The primary reaction leading to loss of monochloramine is a disproportionation reaction.



In a series of trials at pH 3.0, R. L. Valentine and C. T. Jafvert [*Environ. Sci. Technol.*, **22**, 691 (1988)] ascertained that in the

presence of protonated phosphate species, this disproportionation obeys a rate law that is characteristic of both specific and general acid catalysis. These researchers reported that for reaction at pH 3.0 the pseudo-second-order rate constant depended on the concentration of  $\text{H}_2\text{PO}_4^-$  ions in the following manner.

$\text{H}_2\text{PO}_4^-$ (mM)	Rate constant (M <sup>-1</sup> /s)
45	12.5
70	15
90	17
135	21
180	25.5

Determine the values of the rate constants for both specific acid and general acid catalysis under the conditions employed. When  $(\text{H}_2\text{PO}_4^-)$  is 90 mM, what fraction of the reaction takes place via the specific acid-catalyzed pathway, and what fraction via the general acid-catalyzed pathway?

**7.9** J. N. Brønsted and E. A. Guggenheim [*J. Am. Chem. Soc.*, **49**, 2554 (1927)] studied the mutarotation of glucose as catalyzed by acids and bases. The reaction takes place slowly in pure water, is weakly catalyzed by hydrogen ions, and is strongly catalyzed by hydroxide ions. When strong acids and bases are employed as catalysts, the apparent first-order rate constants can be written as

$$k = k_0 + k_{\text{H}^+}(\text{H}^+) + k_{\text{OH}^-}(\text{OH}^-)$$

where  $k_{\text{OH}^-}/k_{\text{H}^+}$  is on the order of several thousand. In the pH range 4 to 6, the contribution of the spontaneous reaction dominates, because both catalytic terms are negligible in this region. In dilute solutions the primary salt effect is not applicable to solutions of strong acids and bases. On the basis of the following data, determine the parameters  $k_{\text{OH}^-}$  and  $k_{\text{H}^+}$  at 18°C.

Solution	$k \times 10^3$ (min <sup>-1</sup> )
$1.0 \times 10^{-4}$ N $\text{HClO}_4$	5.20
$1.0 \times 10^{-4}$ N $\text{HCl}$	5.31
$1.0 \times 10^{-5}$ N $\text{HCl}$	5.23
Distilled water (contaminated by $\text{CO}_2$ from the air)	5.42
$1.0 \times 10^{-4}$ N $\text{HClO}_4 + 0.1$ N $\text{NaCl}$	5.25
$1.0 \times 10^{-4}$ N $\text{HClO}_4 + 0.2$ N $\text{NaCl}$	5.24
$1.0 \times 10^{-4}$ N $\text{HClO}_4 + 0.05$ M $\text{Ba}(\text{NO}_3)_2$	5.43
$1.0 \times 10^{-3}$ N $\text{HClO}_4$	5.42
$2.0 \times 10^{-2}$ N $\text{HClO}_4$	8.00
$4.0 \times 10^{-2}$ N $\text{HClO}_4$	11.26
$3.85 \times 10^{-2}$ N $\text{HClO}_4$	10.80
$2.50 \times 10^{-2}$ N $\text{HClO}_4 + 0.2$ N $\text{NaCl}$	8.89

Because the spontaneous reaction term dominates in the pH range 4 to 6, studies of the reaction in this range are particularly suitable for measuring the small catalytic effects of weak acids and weak bases. If one employs the more general expression for  $k$  involving contributions from the undissociated acid and the anion resulting from dissociation, determine the coefficients of these terms from the following data.

Sodium propionate normality	Propionic acid normality	Hydrogen ion concentration (kmol/m <sup>3</sup> )	$k \times 10^3$ (min <sup>-1</sup> )
0.010	0.010	—	5.65
0.040	0.020	—	6.53
0.050	0.050	—	6.81
0.075	0.075	—	7.57
0.100	0.100	—	8.21
0.125	0.125	—	9.15
0.150	0.150	—	9.85
0.040	0.020	0.00001	6.53
0.040	0.060	0.00002	6.60
0.040	0.110	0.00006	6.76
0.040	0.160	0.00010	6.77

- 7.10 R. P. Bell and E. C. Baughan [J. Chem. Soc., 1937, (1947)] investigated the generalized acid-base catalysis of the depolymerization of dimeric dihydroxyacetone. In terms of the general formulation of the first-order rate constant

$$k = k_0 + k_{\text{H}^+}(\text{H}^+) + k_{\text{OH}^-}(\text{OH}^-) + k_A(\text{A}) + k_B(\text{B})$$

where  $k_0$  is the rate constant for the water-catalyzed reaction and  $k_x$  is the catalytic constant for species  $x$ . This equation can also be written as

$$k = k^* + \alpha(\text{B})$$

where

$$k^* = k_0 + k_{\text{H}^+}(\text{H}^+) + k_{\text{OH}^-}(\text{OH}^-)$$

and

$$\alpha = k_B + \frac{k_A(\text{A})}{(\text{B})}$$

For the reactions in question, no term may be neglected and it was necessary to carefully plan the experimental program to facilitate evaluation of all five kinetic parameters. On the basis of the data below, determine these parameters when the weak acid employed is acetic acid.

CH <sub>3</sub> COOH CH <sub>3</sub> COO <sup>-</sup>	H <sub>3</sub> O <sup>+</sup> (mol/m <sup>3</sup> )	CH <sub>3</sub> COO <sup>-</sup> (mol/m <sup>3</sup> )	$k$ (ks <sup>-1</sup> )
0.980	$2.69 \times 10^{-2}$	100.4	0.707
		50.5	0.583
		31.6	0.530
		12.9	0.473
1.304	$3.56 \times 10^{-2}$	104.5	0.633
		78.5	0.558
		53.3	0.490
		20.4	0.423
3.38	$9.27 \times 10^{-2}$	102.7	0.433
		75.0	0.363
		40.9	0.278
		12.7	0.207
4.83	0.132	102.6	0.390
		87.1	0.363
		68.3	0.297
		51.2	0.262
		30.3	0.208
		10.3	0.154

- 7.11 According to P. L. Buzonick [Chemical Kinetics and Process Dynamics, p. 548, CRC Press, Boca Raton, FL, (1994)], Viscut (M.S. thesis, Asian Institute of Technology, Bangkok, 1985) studied the oxidation of ammonium ions by bacteria suspended in an aqueous solution. The data in Table P7.11 were reported for a series of trials designed to elucidate the mechanism by which sodium ions inhibit oxidation of NH<sub>4</sub><sup>+</sup>. Use Lineweaver–Burk plots to analyze these data, ascertain the kinetic parameters associated with these trials, and identify the mechanism by which inhibition proceeds.

- 7.12 The following kinetic data were reported for an enzyme catalyzed reaction of the type E + S ⇌ ES → E + P. Since these data pertain to initial reaction rates, the reverse reaction may be neglected. Use an Eadie–Hofstee plot to determine the

Table P7.11 Inhibitor Concentration

Substrate (mg/L)	Rate [mg/(L·h)]	Substrate (mg/L)	Rate [mg/(L·h)]	Substrate (mg/L)	Rate [mg/(L·h)]
0.92	0.15	1.11	0.125	1.14	0.058
2.12	0.308	1.11	0.143	2.17	0.116
5.00	0.571	2.08	0.274	4.26	0.192
10.0	1.04	2.17	0.290	4.55	0.21
25	1.67	3.85	0.435	4.76	0.244
		5.88	0.667	11.1	0.30
		11.1	0.91	11.8	0.36
		12.5	1.05	13.3	0.24
		22.2	0.83	20	0.43
		25	1.25	22.2	0.63
				25	0.47

Michaelis constant and  $V_{\max}$  for this system at the enzyme concentration employed.

Initial substrate Concentration (M)	Initial rate [ $\mu\text{mol}/(\text{L}\cdot\text{min})$ ]
$2 \times 10^{-3}$	150
$2 \times 10^{-4}$	149.8
$2 \times 10^{-5}$	120
$1.5 \times 10^{-5}$	112.5
$1.25 \times 10^{-6}$	30.0

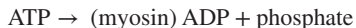
What would the initial rate be at a substrate level of  $2.0 \times 10^{-5}$  M if the enzyme concentration were doubled? At a  $2 \times 10^{-3}$  M substrate level, how long does it take to achieve 80% conversion at the new enzyme level?

- 7.13 K. J. Laidler and M. L. Barnard [*Trans. Faraday Soc.*, **52**, 497 (1956)] studied the effects of pH on the rate of the  $\alpha$ -chymotrypsin-catalyzed hydrolysis of methyl hydrocinnamate. An initial rate approach based on potentiometric measurements led to the following data for a reaction at 25°C and pH 7.8.

Substrate (M)	Initial rate $\times 10^8$ (M/s)
0.00866	16.8
0.00737	16.2
0.00650	14.85
0.00433	12.8
0.00346	11.4
0.00262	9.93

Use these data to prepare both Lineweaver–Burk and Eadie plots and determine the Michaelis–Menten parameters associated with each type of plot. Comment.

- 7.14 In aqueous solution, adenosine triphosphate (ATP) is hydrolyzed to adenosine diphosphate (ADP) and inorganic phosphate in the presence of myosin:



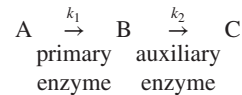
The free energy change associated with this reaction is employed by the muscle tissue of animals to produce external mechanical work. Essentially all physiological mechanisms that require energy to take place obtain this energy from stored ATP.

L. Ouellet, K. J. Laidler, and M. F. Morales [*Arch. Biochem. Biophys.*, **39**, 37 (1952)] have studied the kinetics of this enzyme-catalyzed reaction using in vitro colorimetric measurements to monitor the rate of release of phosphate. These researchers reported the data below for reaction at 25°C in the presence of 0.039 g myosin per/liter. Use Lineweaver–Burk, Eadie, and Hanes plots of these data

to ascertain whether or not the classic Michaelis–Menten rate expression for a single substrate provides an accurate description of these data. Determine the slopes and intercepts of these plots and the associated values of the Michaelis constant and  $V_{\max}$ . Comment on the consistency of the parameter values.

Substrate concentration (mmol/L)	Initial rate [ $\mu\text{mol}/(\text{L}\cdot\text{s})$ ]
0.0061	0.067
0.0117	0.099
0.0192	0.123
0.0225	0.134
0.0309	0.148
0.0505	0.165
0.0639	0.173
0.119	0.183
0.152	0.186
0.215	0.193
0.317	0.196

- 7.15 In carrying out an enzyme assay one may find it convenient to introduce an auxiliary enzyme to the system to effect the removal of a product produced by the first enzymatic reaction. R. McClure [*Biochemistry*, **8**, 2782 (1969)] described the kinetics of these coupled enzyme assays. The simplest coupled enzyme assay system may be represented as



If the first reaction is regarded as zero-order irreversible (i.e., the enzyme is saturated with substrate), and the second reaction is first-order in the product B (low coverage of species B), determine the time-dependent behavior of the concentration of species B if no B is present initially. How long does it take to reach 98% of the steady-state value if  $k_1 = 0.833 \text{ mol}/(\text{m}^3 \cdot \text{ks})$  and  $k_2 = 0.767 \text{ s}^{-1}$ ? What is this steady-state value?

- 7.16 In kinetic studies of enzymatic reactions, rate data are usually tested to determine if the reaction follows the Michaelis–Menten model of enzyme–substrate interactions. H. H. Weetall and N. B. Havewala [*Biotechnol. Bioeng. Symp.*, **3**, 241 (1972)] studied the production of dextrose from cornstarch using conventional glucoamylase and an immobilized version thereof. Their goal was to obtain the data necessary to design a commercial facility for dextrose production. Their studies were carried out in a batch reactor at 60°C. Compare the data below with those predicted from a Michaelis–Menten model with a rate expression of the form

$$r = \frac{k_3(E_0)(S)}{K_m + (S)}$$

(a) Conventional enzyme ( $E_0 = 11,600$  units)

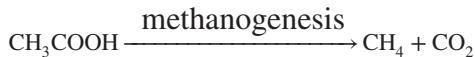
Time, $t$ (s)	Yield (mg dextrose produced/cm <sup>3</sup> )
0	12.0
900	40.0
1800	76.5
3600	120.0
5400	151.2
7200	155.7
9000	164.9

(b) Immobilized enzyme data ( $E_0 = 46,400$  units)

Time, $t$ (s)	Yield (mg dextrose produced/cm <sup>3</sup> )
0	18.4
1,800	200.0
3,600	260.0
5,400	262.0
7,200	278.0
9,000	310.0
13,500	316.0
18,900	320.0
24,900	320.0

In both cases the initial substrate concentration was  $0.14 \text{ kmol/m}^3$ . In cases (a) and (b) the Michaelis constants ( $K_m$ ) are reported to be  $1.15 \times 10^{-3}$  and  $1.5 \times 10^{-3} \text{ kmol/m}^3$ , respectively. The rate constant  $k_3$  is equal to  $1.25 \mu\text{mol}/(\text{m}^3 \cdot \text{s} \cdot \text{unit of enzyme})$  in both cases. If the data are not consistent, provide plausible explanations for the discrepancy.

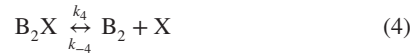
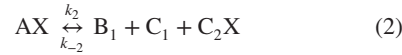
- 7.17 A. Bhadra, S. N. Mukhopadhyay, and T. K. Ghose [*Biotechnol. Bioeng.*, **26**, 257 (1984)] studied the isothermal bioconversion of acetic acid to methane and carbon dioxide by a crude culture of methanogens. The stoichiometry expected is of the form



Hence, conversion of acetic acid should produce an effluent gas with a composition of 50%  $\text{CH}_4$  and 50%  $\text{CO}_2$ . However, in all experiments they observed more than 60% methane in the effluent biogas. Consequently, some reduction of  $\text{CO}_2$  to methane must also occur.

These researchers have examined a variety of mechanisms in their efforts to explain the observed results. One of these mechanisms can be written in the following symbolic

form:



where A represents acetic acid, AX is a complex formed between acetic acid and the cell (an intermediate),  $\text{B}_1$  is methane produced directly from acetic acid,  $\text{C}_1$  is free  $\text{CO}_2$ ,  $\text{C}_2\text{X}$  is intracellularly bound  $\text{CO}_2$ ,  $\text{B}_2\text{X}$  is an intracellular methane-cell complex produced from the intracellularly bound  $\text{CO}_2$ ,  $\text{B}_2$  is methane produced by reduction of  $\text{CO}_2$ , and X is cell mass. In writing reaction (2) in the form indicated, one must recognize that when viewed from a molecular level, this reaction undoubtedly represents the net result of two or more competitive consecutive reactions. Although the authors treated the indicated reactions as mechanistic in character, the previous statement indicates that they erred in doing so. Nonetheless, you may proceed to treat reaction (2) as if it is a mechanistic equation.

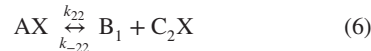
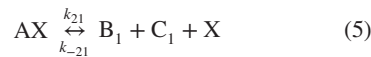
- (a) Derive the rate expressions that correspond to the cases for which:

- Reaction (1) is the rate-controlling step. In deriving the rate expressions, you may assume that all steps other than the rate-controlling step are at equilibrium. In your analysis you should recognize that a balance on the cell mass requires that

$$\text{X}_0 = \text{X} + \text{AX} + \text{C}_2\text{X} + \text{B}_2\text{X}$$

where  $\text{X}_0$  is the initial total mass of cells. Your final rate expression should contain only rate (or equilibrium) constants,  $\text{X}_0$ , and the concentrations of stable species.

- Reaction (2) is replaced by the following two parallel reactions:



Derive the rate expression for this situation for the case where reaction (1) is again the rate-controlling step. You may make the same assumptions as in case 1.

- (b) The data in Table P7.17 were also reported by these authors. Is either of the two mechanisms postulated consistent with these data if one examines the dependence of the initial rate of reaction on the initial concentration of acetic acid?
- (c) What type of kinetic data would be necessary for you to determine which of the models considered (i.e., cases 1 and 2) provides a more appropriate description of the mechanism of this reaction?

**Table P7.17**

Time (days)	<sup>a</sup> <i>r</i> for <i>C</i> = 3.0 g/L	<i>r</i> for <i>C</i> = 5.0 g/L	<i>r</i> for <i>C</i> = 7.0 g/L	<i>r</i> for <i>C</i> = 9.0 g/L
1.0	0.360	0.59	0.810	1.00
1.5	0.345	0.56	0.765	0.92
2.0	0.330	0.54	0.715	0.84
2.5	0.320	0.52	0.670	0.78
3.0	0.300	0.50	0.620	0.70

<sup>a</sup>Rates *r* are expressed in g/(L·day).

**7.18** The classic equation for the kinetics of the metabolic processes responsible for cell growth—creation of biomass from carbon-containing rate-limiting substrate—is the Monod equation. Although this relation originated as a consequence of empirical curve-fitting analysis of data of this type, the Monod equation has the same mathematical form as the simple Michaelis–Menten equation and the single-site first-order Hougen–Watson rate expression. The Monod equation for the rate of growth of biomass can be expressed as

$$\frac{d(S)}{dt} = \frac{-\mu_{\max}}{Y} \left[ \frac{(S)(X)}{K_S + (S)} \right] \quad (1)$$

with

$$\frac{d(X)}{dt} = \frac{\mu_{\max}(S)(X)}{K_S + (S)} \quad (2)$$

where *(X)* is the concentration of active cells, *Y* is the yield of cells expressed per unit degradation of substrate, and  $\mu_{\max}$  is the maximum growth rate obtained when the substrate concentration *(S)* is much greater than the  $K_S$  parameter that is akin to the Michaelis constant used as a parameter in rate expressions for enzyme-catalyzed reactions. In the Monod equation  $K_S$  is referred to as the half-maximum concentration because when  $K_S = (S)$ , the observed reaction rate will be half the maximum rate. Implicit in the Monod analysis is the assumption that the change in cell concentration is proportional to the change in the concentration of the substrate as indicated by the elimination of time as an explicit variable:

$$\frac{d(X)}{d(S)} = -Y \quad (3)$$

C. Liu and J. M. Zachara [*Environ. Sci. Technol.*, **35**, 133 (2001)] considered the problem of determining the uncertainties associated with the parameters that arise when the Monod equation is used to model the reduction of Fe(III) citrate by dissimilatory iron-reducing bacteria during microbial respiration.

Equations (1) and (2) constitute the mathematical model and the parameters reported by these researchers for reduction by *S. putrefaciens* (CN32) are:

$$Y = 1.28 \times 10^9 \text{ cells/mmol of Fe(III)}$$

$$\mu_{\max} = 0.19 \text{ h}^{-1}$$

$$K_S = 25 \text{ mM}$$

For a trial in which  $\text{Fe(III)} = 20 \text{ mM}$  at time zero, prepare two plots, the first of which can be used to assess the ability of the Monod model to accurately reflect the experimental data tabulated below, and the second of which can be used to ascertain whether or not the system of interest exhibits autocatalytic behavior. Plot  $\text{Fe(II)}$  versus time in hours for times from zero to 80 h starting with an initial cell level ( $X_0$ ) of  $1.5 \times 10^9 \text{ cells/L}$ . Plot both the data and the curve predicted using the solution to the differential equations that correspond to the indicated parameter values. In addition, plot the reaction rate evaluated using equation (1) as a function of the time elapsed during the experiment. What conclusions can you draw from these plots?

Time (h)	Fe(II) (mM)
0	0.00
5	0.59
10	1.59
15	2.95
20	4.55
25	6.70
30	9.43
35	12.27
40	14.82
45	16.82
50	17.73
55	18.41
60	18.91
65	19.15
70	19.18
75	19.20
80	19.21

**7.19** J. V. Sinisterra, J. M. Marinas, and A. Llobura [*Can. J. Chem.*, **61**, 230 (1983)] employed an extended form of the Hammett equation to correlate data for esterification of ethanol with substituted benzoic acids in the gas phase over a solid  $\text{AlPO}_4$  catalyst. The focus of their efforts was correlation of values of the adsorption equilibrium constants and apparent rate constants. Use the information tabulated below to prepare a Hammett plot of experimental absorption equilibrium constants versus the corresponding values of the  $\sigma$  parameters for the substituted benzoic acids indicated. Employ the  $\sigma$  values in Table 7.2 of the text. In principle the intercept of the best straight line through these data should correspond to the adsorption equilibrium constant for benzoic acid. By how much does this value differ from the experimental value below? What value of the parameter  $\rho$  characterizes the chemisorption of substituted benzoic acids?

Suppose that the substituent is a *p*-ethoxy group. What is your best estimate of the apparent rate constant for this compound?

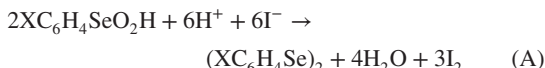
Substituent	Adsorption equilibrium constant	Apparent rate constant $\times 10^4$
H	85	10.1
<i>m</i> -CH <sub>3</sub>	84	8.7
<i>p</i> -CH <sub>3</sub>	97	10.7
<i>m</i> -OCH <sub>3</sub>	48	9.1
<i>p</i> -OCH <sub>3</sub>	130	2.7
<i>m</i> -Cl	51	8.2
<i>m</i> -Br	53	?

Prepare a second Hammett plot using the values of the apparent rate constant for the catalytic reaction. Use the Hammett relation to estimate the apparent rate constant for esterification of *m*-bromobenzoic acid over AlPO<sub>4</sub> and compare this value with the experimental value of  $(7.6 \pm 0.6) \times 10^{-4}$  [mol/(atm·g·s)]. Consider two ways to generate the equation of the line that best represents the data.

1. Use all of the rate constant data to generate the equation of the straight line that best fits these data.
2. Omit the data point that appears to be an obvious outlier when you generate the regression line as one step in your analysis.

Comment.

- 7.20** F. Ferranti and D. De Filippo [*J. Chem. Soc.*, **B1971** (1925)] studied the kinetics of the reduction of several *para*- and *meta*-substituted benzene seleninic acids by iodide ions in acidic aqueous solutions of ethanol. Absorbance measurements were used to monitor the progress of the reaction in a stopped-flow apparatus.



where X represents the various substituents on the aromatic ring. The rate laws for these reactions are all first-order in each of the three reactants, third-order overall.

- (a) The table below indicates the values of the third-order rate constants at 25°C in solutions that have a constant

ionic strength of 0.25 M. Values of the Hammett parameters corresponding to the various substituents are presented in Table 7.2. Are the kinetic data consistent with the Hammett relation? Comment.

Substituent X	$10^5 \times k$ (for $k$ in M <sup>-2</sup> /s)
H	1.342
<i>m</i> -Cl	1.522
<i>p</i> -Cl	1.435
<i>m</i> -Br	1.531
<i>p</i> -Br	1.453
<i>m</i> -NO <sub>2</sub>	1.683
<i>p</i> -NO <sub>2</sub>	1.868

- (b) Suppose that the *p*-NO<sub>2</sub> group is the member of the data set that exhibits the largest deviation from the best-fit regression line. If this data point is excluded from the data set, what would a regression analysis of the remaining data indicate is the corresponding value of the Hammett parameter  $\rho$ ? If the data for *p*-nitrobenzeneseleninic acid were to be consistent with the remainder of the data, what would we require the value of the corresponding rate constant for equation (A) to be? How does this value compare with the experimental value reported by Ferranti and De Filippo?
- (c) On the basis of the regression analysis you conducted in part (b) consider the following question. If the value of the rate constant measured for the corresponding reaction of *p*-CH<sub>3</sub>C<sub>6</sub>H<sub>4</sub>SeO<sub>2</sub>H were  $1.322 \times 10^{-5}$  M<sup>-2</sup>/s, what would you expect the value of  $\sigma$  to be for a methyl group in the *para*- position? Is this value consistent with the value of  $\sigma$  that should have been reported by Ferranti and De Filippo: namely,  $-0.170$  (the minus sign was missing in the original publication)? This error should remind you that as a practicing engineer you should always remember that everything you read on the Internet or in a book or journal should not be taken as valid and that in the practice of engineering one must always be alert to the proper use of sign conventions.

## Basic Concepts in Reactor Design and Ideal Reactor Models

### 8.0 INTRODUCTION

The chemical reactor must be regarded as the very heart of a chemical process. The reactor is the equipment in which conversion of feedstock to desired product takes place and is thus the single irreplaceable component of the process. Several different factors must be considered in selecting the physical configuration of the reactor and the mode of operation most appropriate for accomplishing a specified task. The fundamental tools employed by chemical engineers in making these decisions are the rate expressions for the reactions of interest and the laws of conservation of matter and energy as reflected in material and energy balances.

#### 8.0.1 The Nature of the Reactor Design Problem

The chemical engineer is required to choose the reactor configuration and mode of operation that yields the greatest profit consistent with market forces associated with raw material and product costs, capital and operating costs, safety considerations, environmental/pollution control requirements, and esthetic constraints that may be established by management, society, or labor unions. Usually, there are many combinations of operating conditions and reactor size and/or type that will meet the requirements imposed by nature in terms of the reaction rate expression involved and those imposed by management in terms of the production capacity required. The engineer is thus faced with the task of maintaining a careful balance between analytical reasoning expressed in quantitative terms and sound engineering judgment. In an attempt to maintain this balance, some or all of the following questions must be answered.

1. What is the composition of the feedstock, and under what conditions is it available? Are any purification procedures necessary?
2. What is the scale of the process? What capacity is required?
3. Is a catalyst necessary or desirable? If a catalyst is employed, what are the ramifications with respect to product distribution, operating conditions, most desirable type of reactor, process economics, and other pertinent questions raised below?
4. What operating conditions (temperature, pressure, degree of agitation, etc.) are required for most economical operation?
5. Is it necessary or desirable to add inerts or other materials to the feedstock to enhance yields of desired products, to moderate thermal effects, or to prolong the useful life of any catalysts that may be employed?
6. Should the process be continuous or intermittent? Would batch or semibatch operation be advantageous?
7. What type of reactor best meets the process requirements? Are there advantages associated with the use of a combination of reactor types or multiple reactors in parallel or series?
8. What size and shape reactor(s) should be used?
9. How are the energy transfer requirements for the process best accomplished? Should one operate isothermally, adiabatically, or in accord with an alternative temperature protocol?
10. Is single-pass operation best, or is recycle needed to achieve the desired degree of conversion of the raw feedstock?
11. What facilities are required for catalyst supply, activation, and regeneration?

12. What are the reactor effluent composition and conditions? Are any chemical separation steps or physical operations required to obtain an effluent that is satisfactory for the desired end use?
13. Are there any special materials requirements imposed by the process conditions? Are the process fluids corrosive? Are extremely high temperatures or pressures required?
14. If the product is a pharmaceutical, a food, or a beverage, what precautions are required to ensure that U.S. Food and Drug Administration constraints are satisfied?
15. Are there any environmental or safety aspects of the operation that need to be addressed?

In the remainder of the book we establish a rational framework within which many of these questions can be addressed. We will see that, often, considerable freedom of choice is available in terms of the type of reactor and reaction conditions that will accomplish a given task. The development of an optimum processing scheme or even of an optimum reactor configuration and mode of operation requires a number of complex calculations that often involve iterative numerical calculations. Consequently, machine computation is used extensively in industrial situations to simplify the optimization task. Nonetheless, we have deliberately chosen to present the concepts used in reactor design calculations in a framework that insofar as possible permits analytical solutions in order to divorce the basic concepts from the mass of detail associated with machine computation.

The first stage of a logical design procedure involves determination of a reaction rate expression that is appropriate for the range of conditions to be investigated in the design analysis. One requires a knowledge of the dependence of the rate on composition, temperature, fluid velocity, the characteristic dimensions of any heterogeneous phases present, and any other process variables that may be significant. There are several potential sources of the experimental data that are essential for proper reactor design.

1. *Bench-scale experiments.* The reactors used in these experiments are usually designed to operate at constant temperature under conditions that minimize heat and mass transfer limitations on reaction rates. This approach facilitates accurate evaluation of the intrinsic chemical kinetics.
2. *Pilot-plant studies.* The reactors used in these studies are significantly larger than those employed in bench-scale laboratory experiments. One uses essentially the reverse of the design procedures developed later in the chapter to determine the effective reaction rate from the pilot-plant data. In analysis of data of this type, one

may encounter difficulties in separating intrinsic chemical effects from the effects of heat and mass transfer processes that influence the rate of conversion of reactants to products.

3. *Operating data from commercial-scale reactors.* If one has access to actual operating data on another commercial installation of the same type as that contemplated, these data provide the closest approximation to the conditions likely to be encountered in industrial practice. Such access may result from licensing arrangements or from previous experience within one's company. Unfortunately, such data are often incomplete or inaccurate, and the problems of backing the intrinsic chemical kinetics out of the mass of data may be insurmountable. In such systems physical limitations on rates of heat and mass transfer may disguise the true kinetics to a significant degree.

In the design of an industrial-scale reactor for a new process, or an old one that employs a new catalyst, it is common practice to carry out both bench-scale and pilot-plant studies before finalizing the design of the commercial-scale reactor. The bench-scale studies yield the best information about the intrinsic chemical kinetics and the associated rate expression. However, when taken alone, they force the chemical engineer to rely on standard empirical correlations and prediction methods to determine the possible influence of heat and mass transfer processes on the rates that will be observed in industrial-scale equipment. The pilot-scale studies can provide a test of the applicability of the correlations and an indication of potential limitations that physical processes may place on conversion rates. These pilot-plant studies can provide extremely useful information on the temperature distribution in the reactor and on contacting patterns when more than a single-phase reactant–catalyst system is employed.

## 8.0.2 Reactor Types

In terms of the physical configurations commonly encountered in industrial practice, there are two basic types of reactors: the tank and the tube. The *ideal tank reactor* is one in which stirring is so efficient that the contents are always uniform in composition and temperature throughout. The simple tank reactor may be operated in a variety of modes: batch, semibatch, and continuous flow. These modes are illustrated schematically in Figure 8.1. In the simple *batch reactor*, the fluid elements will all have the same composition, but the composition will be time dependent. A stirred-tank reactor may also be operated in *semibatch* fashion. In this mode the tank is partially filled with reactant(s), and additional reactants are added progressively until the desired end composition is achieved. Alternatively, one may charge the reactants

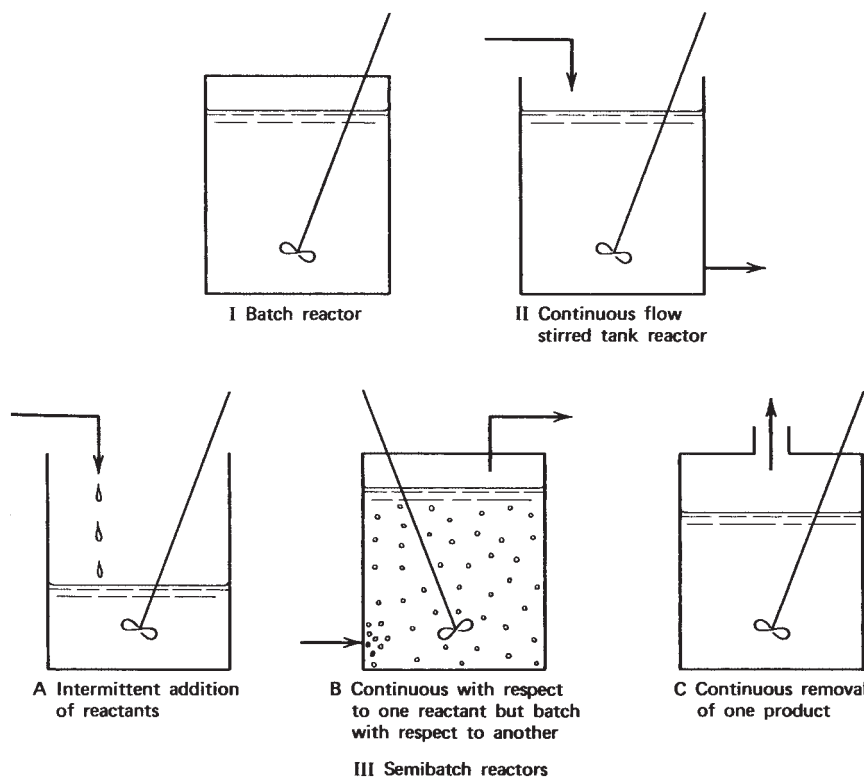


Figure 8.1 Types of tank reactors.

all at once and continuously remove products as they are formed. In the continuous flow mode of operation the stirred-tank reactor is continuously supplied with feed; at the same time an equal volume of reactor contents is discharged, to maintain a constant level in the tank. The composition of the effluent stream is identical with that of the fluid remaining in the tank.

The *ideal tubular reactor* is one in which elements of the homogeneous fluid reactant stream move through a tube as plugs moving parallel to the tube axis. This flow pattern is referred to as *plug flow* or *piston flow*. The velocity profile at a given cross section is flat and it is assumed that there is no axial diffusion or backmixing of fluid elements.

Batch reactors are often used for liquid phase reactions, particularly when the required level of production is low. They are seldom employed on a commercial scale for gas phase reactions because the quantity of product that can be produced in reasonably sized reactors is small. Batch reactors are well suited for producing small quantities of material, for producing several different products from one piece of equipment, and for situations in which sanitation considerations are paramount. Consequently, they find extensive use in the food, pharmaceutical, dye-stuff, and polymer industries and in the production of certain specialty chemicals where such flexibility is desired. When rapid fouling is encountered or contamination of fermentation cultures is to be avoided (e.g., in brewing beer), batch operation is preferable to continuous processing

because it facilitates the necessary cleaning and sanitation procedures.

When the specified production capacities are low, processes based on batch reactors will usually have lower capital investment requirements than those of processes calling for continuous operation. Hence, batch reactors are often preferred for new and untried processes during the initial stages of development. As production requirements increase in response to market demands, it may become more economical to shift to continuous processing, but even in these cases, there are many industrial situations where batch operation remains preferable. This is particularly true when the operating expenses associated with the reactor are a minor fraction of total product cost. At low production capacities, construction and instrumentation requirements for batch reactors are usually cheaper than for continuous process equipment. Moreover, it is generally easier to start up, shut down, and control a batch reactor than a continuous flow reactor of comparable capacity. The disadvantages associated with the use of a batch reactor include the high labor and materials handling costs involved in filling, emptying, and cleaning these reactors. While batch reactors are being filled, emptied, or cleaned, and while the reactor contents are being heated to the reaction temperature or cooled to a point suitable for discharge, batch reactors are not producing reaction products. The sum of the times associated with these nonproductive periods may often be comparable to the time necessary

to actually carry out the reaction. In determining long term production capacities for batch reactors, these “dead times” must be taken into account.

Continuous flow reactors are almost invariably preferred to batch reactors when the processing capacity required is large. Although the capital investment requirements will be higher, the operating costs per unit of product will usually be lower for continuous operation than for batch reaction. The advantages of continuous operation are that it:

1. Facilitates good quality control for the product through the provision of greater constancy in reaction conditions.
2. Facilitates automatic process control and stability of operation.
3. Minimizes the labor costs per unit of product.

Often, the decision to select a batch- or continuous-processing mode involves a determination of the relative contributions of capital and operating expenses to total process costs for the level of capacity proposed. As Denbigh (1) points out, what is best for a highly industrialized country with high labor costs is not necessarily best for a less well developed country. In many cases, selectivity considerations determine the processing mode, particularly when the reaction under study is accompanied by undesirable side reactions. The yield of the desired product may differ considerably between batch and continuous operation and between the two primary types of continuous processes. When the yield is lower for a continuous process, this factor may be so important in the overall process economics as to require the use of a batch reactor.

At this point we wish to turn to a brief discussion of the types of batch and flow reactors used in industrial practice for carrying out homogeneous fluid phase reactions. Treatment of heterogeneous catalytic reactors is deferred to Chapter 12, while bioreactors are discussed in Chapter 13.

### 8.0.2.1 Batch Reactors (Stirred Tanks)

Batch reactors are usually cylindrical tanks and the orientation of such tanks is usually vertical. Cylindrical vessels are employed because they are easier to fabricate and clean than other geometries and because the construction costs for high-pressure units are considerably less than for alternative configurations. For simple stirred vertical batch reactors, the depth of liquid is usually comparable to the diameter of the reactor. For greater liquid height/diameter ratios, more complex agitation equipment is necessary. Agitation can be supplied by stirrer blades of various shapes or by forced circulation with an external or built-in pump. Where more gas–liquid interfacial area is required for evaporation or gas absorption, or where it is necessary

to minimize the hydrostatic head (e.g., to minimize elevation of the boiling point), horizontal reactors may be used. The latter orientation may also be preferable when the reactor contents are quite viscous or take the form of a slurry. Batch reactors may be fabricated from ordinary or stainless steel, but there are often advantages to using glass or polymer coatings on interior surfaces to minimize corrosion or sanitation problems.

Because of the large energy effects that often accompany chemical reaction, it is usually necessary to provide for heat transfer to or from the reactor contents. Heating or cooling may be accomplished using jacketed walls, internal coils, or internal tubes filled with a heat transfer fluid that is circulated through an external heat exchanger. Energy may also be supplied by electrical heating or direct firing. If the process fluid is noncorrosive and readily and safely pumped, it may be preferable to employ an external heat exchanger and circulation pump. Good temperature control can be achieved using an external reflux condenser. For cases where appreciable vapor is given off, selection of either internal or external heat transfer equipment is governed by the area required, the susceptibility of the heat transfer surface to fouling, the temperature and pressure requirements imposed by the heat transfer medium, and the potential adverse effects that might occur if the process fluid and the heat transfer medium come in direct contact through leakage.

For high-pressure operation, safety considerations are extremely important and care must be taken to ensure proper mechanical design. Closures must be designed to withstand the same maximum pressure as that in the rest of the autoclave. Various authors have treated the problems involved in designing medium and high pressure batch reactors (2–4).

### 8.0.2.2 Continuous Flow Reactors: Stirred Tanks

The continuous flow stirred-tank reactor is used extensively in chemical process industries. Both single tanks and batteries of tanks connected in series are used. In many respects the mechanical and heat transfer aspects of these reactors closely resemble the stirred-tank batch reactors treated above in Section 8.0.2.1. However, in the present case, one must also provide for continuous addition of reactants and continuous withdrawal of the product stream.

It is possible to employ either multiple individual tanks in series or units containing multiple stages within a single shell (see Figure 8.2). Multiple tanks are more expensive but provide more flexibility in use, since they are more readily altered if process requirements change. To minimize pump requirements and maintenance, engineers often choose to allow for gravity flow between stages. When the reactants are of limited miscibility but differ in density, the

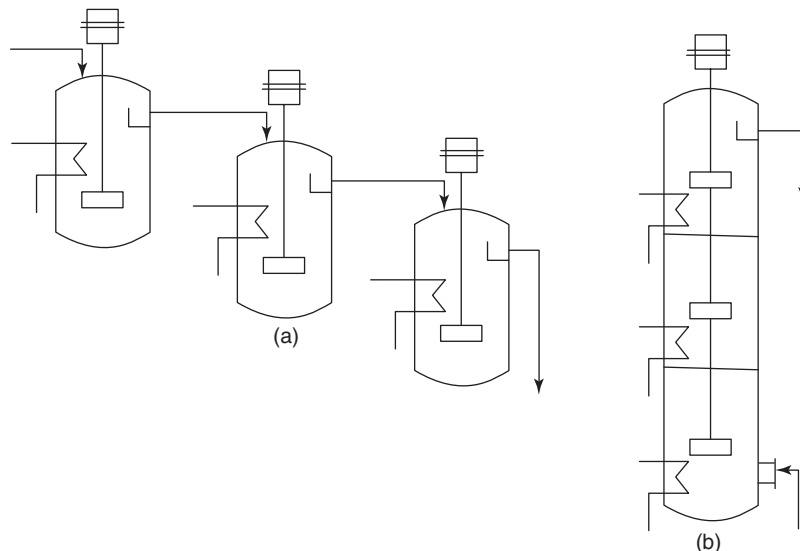


**Figure 8.2** Types of continuous-flow stirred-tank reactors: (a) three-stage cascade of stirred-tank reactors; (b) vertically staged cascade of three stirred tanks. Compartmented versions of a battery of stirred tanks in a single horizontal shell may also be employed. (Adapted from J. R. Couper, W. R. Penney, J. R. Fair, and S. M. Walas. *Chemical Process Equipment: Selection and Design*. Copyright © 2010. Used with permission of Elsevier.)

vertical staged shell lends itself to countercurrent operation. This approach is useful when dealing with reversible reactions between immiscible fluids.

For purposes of calculation, each stage in a multiple-stage unit is treated as an individual reactor. The process stream flows from one reactor to the next, so that there is essentially a step change of composition between successive reactors. The step change is a direct consequence of efficient mixing. Unless the fluid phase is highly viscous, it is not difficult to approach perfect mixing in industrial-scale equipment. All that is required is that the time necessary to distribute an entering element of fluid uniformly throughout the tank be very small compared to the average residence time in the tank.

Because of the dilution that results from the mixing of entering fluid elements with the reactor contents, the average reaction rate in a stirred tank reactor will usually be less than it would be in a tubular reactor of equal volume supplied with an identical feed stream and operating at the same temperature. Consequently, to achieve the same production capacity and conversion level, a continuous flow stirred-tank reactor or even a battery of several stirred-tank reactors must be much larger than a tubular reactor operating at the same temperature. In many cases, however, the greater volume requirement is a relatively unimportant economic factor, particularly when one operates at ambient pressure in tanks constructed of relatively inexpensive materials such as mild steel.

In addition to lower construction costs, a continuous flow stirred-tank reactor possesses other advantages relative to a tubular flow reactor, such as facilitation of temperature control. Efficient stirring of the reactor contents ensures uniform temperature and the elimination

of local hot spots. The large heat capacity of the reactor contents also acts as a heat sink to moderate temperature excursions when changes occur in process conditions. The physical configuration of cylindrical tanks provides a large heat transfer area on the external surface of the tank and permits augmentation of this area through the use of submerged coils within the tank. However, the rate of heat transfer per unit volume of reaction mixture is generally lower in a conventional stirred-tank reactor than in conventional tubular reactors because of the lower ratio of heat transfer surface area to volume in the tank reactor. Consequently, tubular reactors are preferred for fast reactions when energy transfer requirements are very large.

Ease of access to the interior surface of stirred tanks is an additional advantage of this type of reactor. This consideration is particularly significant in polymerization reactors, where one needs to worry about periodic cleaning of internal surfaces. Sanitation considerations are particularly relevant in the design of reactors for pharmaceutical and food-related applications (e.g., brewing and fermentation facilities).

Selectivity considerations may also dictate the use of stirred-tank reactors. They are preferred if undesirable side reactions predominate at high reactant concentrations, and they are also useful when one desires to “skip” certain concentration or temperature ranges where by-product formation may be excessive.

Stirred-tank reactors are also employed when it is necessary to handle gas bubbles, solids, or a second liquid suspended in a continuous liquid phase. One often finds that the rates of such reactions are strongly dependent on the degree of dispersion of the second phase, which in turn depends on the level of agitation.

Large stirred-tank reactors are generally not suited for use at high pressures because of mechanical strength limitations. *They are used mainly for liquid-phase reaction systems at low or medium pressures when appreciable residence times are required.*

### 8.0.2.3 Continuous Flow Reactors: Tubular Reactors

The tubular reactor is so named because the physical configuration of the reactor is normally such that the reaction takes place within a tube or length of pipe. The idealized model of this type of reactor is based on the assumption that an entering fluid element moves through the reactor as a differentially thin plug of material that fills the reactor cross section completely. Thus, the terms *piston flow* or *plug flow reactor* (PFR) are often employed to describe the idealized model. The contents of a specific differential plug are presumed to be uniform in temperature and composition. This model may be used to treat both the case where the tube is packed with a solid catalyst (see Section 12.1) and the case where the fluid phase alone is present.

The majority of tubular reactors may be classified in terms of three major categories:

1. Single-jacketed tubes.
2. Shell-and-tube heat exchangers.
3. Tube furnaces, in which the tubes are exposed to thermal radiation and heat transfer from combustion gases.

The single-jacketed tube reactor is the simplest type of tubular reactor to conceptualize and to fabricate. Single-jacketed tubes may be used only when the heat transfer requirements are minimal because of the low surface area/volume ratio characteristic of these reactors.

When the shell-and-tube configuration is utilized, the reaction may take place on either the tube side or the shell side. The shell-and-tube reactor has a much greater area for heat transfer per unit of effective reactor volume than the single-jacketed tube. Consequently, it may be used for reactions where the energy transfer requirements are large. On occasion the reaction zone may be packed with granular solids to promote increased turbulence or better contacting of heterogeneous fluid phases or to act as a thermal sink to facilitate control of the reactor. In many cases energy economies can be achieved using countercurrent flow of a hot product stream to preheat an incoming reactant stream to the temperature where the reaction occurs at an appreciable rate. Two commercial scale processes that employ this technique are the synthesis of ammonia from its elements and the oxidation of sulfur dioxide to sulfur trioxide.

Tubular furnaces are used only when it is necessary to carry out *endothermic* reactions at fairly high temperatures

on very large quantities of feedstock. Thermal reforming reactions and other reactions used to increase the yield of gasoline from petroleum-based feedstocks are commercial scale processes that employ this type of reactor. A tubular furnace is basically a combustion chamber with reactor tubes mounted on its walls and ceiling. Tube dimensions are typically 3 to 6 in. in diameter, with lengths ranging from 20 to 40 ft. As many as several hundred tubes may be used, with either series or parallel connections possible, depending on the required residence time.

Because there is no backmixing of fluid elements along the direction of flow for the idealized model of a tubular reactor (a PFR), there is a *continuous* gradient in reactant concentration in this direction. One does not encounter the step changes in composition or temperature that are characteristic of flow through cascades of stirred-tank reactors. Consequently, for the same feed composition and temperature, the average reaction rate will generally be significantly higher in a PFR (tubular reactor) than it would be in a single stirred tank (or a battery of stirred tanks operating isothermally) with a total volume equal to that of the tubular reactor. The more efficient utilization of reactor volume is an advantage of the tubular reactor that promotes its use in processes that require a very large capacity. Because variations in temperature and composition may occur in the axial direction in tubular reactors, these systems may be more difficult to control than continuous-flow stirred-tank reactors. However, the control problems are usually not insurmountable, and one can normally obtain steady state operating conditions that lead to uniform product quality.

Other advantages of the tubular reactor relative to stirred tanks include suitability for use at higher pressures and temperatures and the fact that severe energy transfer constraints may be surmounted readily using this configuration. The tubular reactor is usually employed for liquid phase reactions when relatively short residence times are needed to effect the desired chemical transformation. Tubular reactors are the configuration of choice for continuous flow gas phase operations.

### 8.0.2.4 Semibatch or Semiflow Reactors

Semibatch or semiflow operations usually take place in a single stirred tank using equipment extremely similar to that described for batch operations. Figure 8.1 indicates some of the many modes in which semibatch reactors may be operated.

One common mode of operation involves loading some of the reactants into a stirred tank as a single charge and then feeding in the remaining material gradually. This mode of operation is advantageous when large heat effects accompany the reaction. Exothermic reactions may be slowed down and temperature control maintained by

regulating the rate at which one of the reactants is fed. This point is demonstrated quite dramatically in Illustration 10.7. This mode of operation is also desirable when high reactant concentrations favor the formation of undesirable side products or when one of the reactants is a gas of limited solubility.

Another mode of semibatch operation involves the use of a purge stream to continuously remove one or more of the products of a reversible reaction. For example, water may be removed in esterification reactions by the use of a purge stream or by distillation of the reacting mixture. For reversible reactions continuous removal of product(s) increases the net reaction rate by slowing down the reverse reaction, thereby driving the reaction in a direction that favors a higher yield of product species.

Semibatch or semiflow processes are among the most difficult to analyze from the viewpoint of reactor design because one must deal with an open system operating under non-steady-state conditions. Hence, the differential equations governing energy and mass conservation are more complex than they would be for the same reaction carried out batchwise or in a continuous flow reactor operating at steady state.

### 8.0.3 Fundamental Concepts Used in Chemical Reactor Design

The bread-and-butter tools of the practicing chemical engineer are the material balance and the energy balance. In many respects, chemical reactor design can be regarded as a straightforward application of these fundamental principles. In this section we indicate in general terms how these principles are applied to the various types of idealized reactor models.

#### 8.0.3.1 Material and Energy Balances in the Design of Industrial Reactors

The analysis of chemical reactors in terms of material and energy balances differs from the analysis of other process equipment in that one must take into account the rate at which molecular species are converted from one chemical form to another and the rate at which energy is transformed by the process. When combined with material and energy balances on the reactor, the reaction rate expression provides a means of determining the production rate and the composition of the product stream as functions of time. Both steady-state and time-varying situations may be analyzed using the same fundamental relations. Differences in the analyses result from the retention of different terms in the basic balance equations. A material balance on a reactant species of interest for an element of volume  $\Delta V$  can be

written as

$$\begin{aligned}
 \text{rate of flow of} & \quad \text{rate of flow} \\
 \text{of reactant} & \quad \text{of reactant} \\
 \text{into volume} & \quad \text{out of volume} \\
 \text{element} & \quad \text{element} \\
 & \quad \text{rate of disappearance} \\
 & \quad \text{of reactant by chemical} \\
 & \quad \text{reactions within the} \\
 & \quad \text{volume element} \\
 & \quad \text{rate of accumulation} \\
 & \quad \text{+ of reactant within the} \\
 & \quad \text{volume element}
 \end{aligned} \tag{8.0.1}$$

or, in shorter form,

$$\begin{aligned}
 \text{input} & = \text{output} + \text{disappearance by reaction} \\
 & \quad + \text{accumulation}
 \end{aligned} \tag{8.0.2}$$

The flow terms represent the convective and diffusive transport of reactant into and out of the volume element. The third term is the product of the size of the volume element and the reaction rate per unit volume evaluated using the properties appropriate for this element. Note that the reaction rate per unit volume is equal to the intrinsic rate of the chemical reaction only if the volume element is uniform in temperature and concentration (i.e., there are no heat or mass transfer limitations on the rate of conversion of reactants to products). The final term represents the rate of change in inventory resulting from the effects of the other three terms.

In the analysis of batch reactors, the two flow terms in equation (8.0.1) are omitted. For continuous flow reactors operating at steady state, the accumulation term is omitted. However, for the analysis of continuous flow reactors under transient conditions and for semibatch reactors, it may be necessary to retain all four terms. For ideal well-stirred reactors, the composition and temperature are uniform throughout the reactor and all volume elements are identical. Hence, the material balance may be written over the entire reactor in the analysis of an individual stirred tank. For tubular flow reactors the composition is not independent of position and the balance must be written on a differential element of reactor volume and then integrated over the entire reactor using appropriate flow conditions and concentration and temperature profiles. When non-steady-state conditions are involved, it will be necessary to integrate over time as well as over volume to determine the performance characteristics of the reactor.

Because the rate of a chemical reaction is normally strongly temperature dependent, to be able to utilize equation (8.0.1) properly it is essential to know the temperature at each point in the reactor. When there are temperature gradients within the reactor, it is necessary to

utilize an energy balance in conjunction with the material balance to determine the temperature and composition prevailing at each point in the reactor at a particular time. The general energy balance for an element of volume  $\Delta V$  over a time increment  $\Delta t$  is

$$\begin{aligned} \text{accumulation of energy} &= \text{energy transferred from surroundings by heat and shaft work interactions} \\ &+ \text{energy effects associated with the entry of matter} \\ &+ \text{energy effects associated with transfer of matter to surroundings} \end{aligned} \quad (8.0.3)$$

For completeness, the terms corresponding to the entry of material to the volume element and exit therefrom must contain, in addition to the ordinary enthalpy of the material, its kinetic and potential energy. However, for virtually all cases of interest in chemical reactor design, only the enthalpy term is significant. Since only changes in internal energy or enthalpy can be evaluated, the datum conditions for the first, third, and fourth terms must be identical to achieve an internally consistent equation. Although heat interactions in chemical reactors are significant, shaft work effects are usually negligible unless one is analyzing an internal combustion engine or an electrochemical reactor (e.g., a fuel cell). The chemical reaction rate does not appear explicitly in equation (8.0.3), but its effects are implicit in all terms except the second. The first, third, and fourth terms reflect differences in temperature and/or in composition of the streams entering and leaving. The energy effects associated with composition changes are a direct reflection of the enthalpy change associated with the reaction.

There are a variety of limiting forms of equation (8.0.3) that are appropriate for use with different types of reactors and different modes of operation. For stirred tanks the reactor contents are uniform in temperature and composition throughout, and it is possible to write the energy balance over the entire reactor. In the case of a batch reactor, only the first two terms need be retained. For continuous flow systems operating at steady state, the accumulation term disappears. For adiabatic operation in the absence of shaft work effects the energy transfer term is omitted. For the case of semibatch operation it may be necessary to retain all four terms. For tubular reactors neither the composition nor the temperature need be independent of position, and the energy balance must be written on a differential element of reactor volume. The resulting differential equation

must then be solved in conjunction with the differential equation describing the material balance on the differential element.

### 8.0.3.2 Vocabulary of Terms Used in Reactor Design

Several terms used extensively throughout the remainder of the book deserve definition or comment. The concepts involved include steady state and transient operation, heterogeneous and homogeneous reaction systems, adiabatic and isothermal operation, mean residence time, contacting and holding time, and space time and space velocity. Each of these concepts is discussed in turn.

Large-scale industrial reactions are almost invariably carried out on a continuous basis, with reactants entering at one end of the reactor network and products leaving at the other. Usually, such systems are designed for *steady state* operation but, even during the design of such systems, adequate care must be made to provide for the *transient* conditions that will invariably be incurred during startup and shutdown periods. By the term *steady state operation* we imply that conditions at any point in the reactor are time-invariant. Changes in composition occur in the spatial dimension instead of in a time dimension. It should be emphasized that operation at steady state does not imply *equilibrium*. The last term is restricted to *isolated* systems that undergo no net change with time. Isolated systems are at equilibrium only when neither the conditions in the system nor those in the surroundings are changing with time. By contrast, even though a system may be operating at steady state, conditions in the surroundings may be changing with time. In such situations neither the system nor the surroundings is at equilibrium. Insofar as the analysis of continuous flow reactors is concerned, the major thrust of this and succeeding chapters involves steady state operation. The basic principles described in Section 8.0.3.1 remain valid for the analysis of transient systems. However, in most analyses of transient behavior, one must resort to numerical solutions to predict the response of a continuous flow reactor network to changes in operating conditions. Batch reactors are inherently unsteady-state systems, even when the temperature and composition of the reactor contents are uniform throughout the reactor.

Both homogeneous and heterogeneous reaction systems are frequently encountered in commercial practice. In this book the term *homogeneous reaction system* is restricted to fluid systems in which the system properties *vary continuously* from point to point within the reactor. The term embraces both catalytic and noncatalytic reactions, but it requires that any catalysts be dispersed uniformly throughout the fluid phase. The term *heterogeneous reaction system* refers to a system in which there are

two or more phases involved in the reaction process, either as reactants or as catalysts.

*Adiabatic operation* implies that there is no heat interaction between the reactor contents and their surroundings. *Isothermal operation* implies that the feed stream, the reactor contents, and the effluent stream are equal in temperature and have a uniform temperature throughout. The present chapter is devoted to the analysis of such systems. Adiabatic and other forms of nonisothermal systems are treated in Chapter 10.

The terms *holding time*, *contact time*, and *residence time* are often used in discussions of the performance of chemical reactors. As employed by reactor designers, these terms are essentially interchangeable. They refer to the length of time that an element of process fluid spends in the reactor in question. For a batch reactor it is usually assumed that no reaction occurs while the reaction vessel is being filled or emptied or while its contents are brought up to an ignition temperature. The holding time is thus the time necessary to "cook" the contents to the point where the desired degree of conversion is achieved. The terms *contact time* and *mean residence time* are used primarily in discussions of continuous flow processes. They represent the average length of time that it takes a fluid element to travel from the reactor inlet to the reactor outlet. For plug flow reactors, all fluid elements will have the same residence time. However, for stirred-tank reactors or other reactors in which mixing effects are significant, there will be a distribution of residence times for the different fluid elements. These distributions have important implications for the conversions that will be achieved in such reactors.

Although the concept of mean residence time is easily visualized in terms of the average time necessary to cover the distance between reactor inlet and outlet, it is not the most fundamental characteristic time parameter for purposes of reactor design. A more useful concept is that of the reactor *space time*. For continuous flow reactors the space time ( $\tau$ ) is defined as the ratio of the reactor volume ( $V_R$ ) to a characteristic volumetric flow rate of fluid ( $\mathcal{V}$ ).

$$\tau = \frac{V_R}{\mathcal{V}} \quad (8.0.4)$$

The reactor volume is taken as the volume of the reactor *physically occupied* by the reacting fluids. As utilized in this book, the symbol  $V_R$  does not include the volume occupied by agitation devices, heat exchange equipment, or headspace above liquids. One may arbitrarily select the temperature, pressure, and even the state of aggregation (gas or liquid) at which the volumetric flow rate to the reactor will be measured. For design calculations it is usually convenient to choose the reference conditions as those that prevail at the inlet to the reactor. However, it is easy to convert to any other basis if the pressure–volume–temperature behavior of the system is known. Since the reference

volumetric flow rate is arbitrary, care must be taken to specify the reference conditions precisely to allow for proper interpretation of the resulting space time. Unless an explicit statement is made to the contrary, *we will choose our reference state as that prevailing at the reactor inlet and emphasize this choice by the use of the subscript zero*. Henceforth,

$$\tau = \frac{V_R}{\mathcal{V}_0} \quad (8.0.5)$$

where  $\mathcal{V}_0$  is the volumetric flow rate at the inlet temperature and pressure and a fraction conversion of zero.

For this convention, a space time of 30 min means that every 30 min one reactor volume of feed (measured at inlet conditions) is processed by the reactor. One reactor volume enters and one reactor volume leaves, but this statement does *not* imply that we have simply displaced the original charge from the reactor. Some or all of the original contents may leave, and some of the fresh charge may leave as well. In the latter circumstance the reactor contents become a mixture of the original contents and new material.

The space time is not necessarily equal to the average residence time of an element of fluid in the reactor. Variations in the number of moles on reaction as well as variations in temperature and pressure can cause the volumetric flow rates at arbitrary points in the reactor to differ appreciably from those corresponding to inlet conditions. Consequently, even though the reference conditions may be taken as those prevailing at the reactor inlet, the space time need not be equal to the mean residence time of the fluid. The two quantities are equal only if *all* of the following conditions are met.

1. Pressure and temperature are constant throughout the reactor.
2. The density of the reaction mixture is independent of the extent of reaction. For gas-phase reactions this requirement implies that there is no change in the number of moles during reaction. Hence equation (3.1.45) implies that  $\delta = 0$ .
3. The reference volumetric flow rate is evaluated at reactor inlet conditions.

When the space time and the mean residence time differ, it is the space time that should be regarded as the independent process variable that is directly related to the constraints imposed on the system. We shall see in Sections 8.2 and 8.3 that it is convenient to express the fundamental design relations for continuous flow reactors in terms of this parameter. We shall also see that for these reactors the mean residence time cannot be considered as an independent variable, but that this parameter can be determined only after the nature of the changes occurring within the reactor is known.

The reciprocal of the space time is known as the *space velocity* ( $S$ ):

$$S = \frac{1}{\tau} = \frac{V}{V_R} \quad (8.0.6)$$

Like the definition of the space time, the definition of the space velocity involves the volumetric flow rate of the reactant stream measured at some reference condition. A space velocity of 10  $\text{h}^{-1}$  implies that every hour, 10 reactor volumes of feed can be processed.

When dealing with reactions in which a liquid feed must be vaporized prior to being fed to the reactor proper, one must state very clearly whether the space velocity is based on the volumetric flow rate of the feed as a liquid or as a gas. Unless an explicit statement to the contrary is made, the term *space velocity* will refer to the ratio of the volumetric flow rate *evaluated at reactor inlet conditions* to the reactor volume.

The term *space velocity* has somewhat different connotations when dealing with heterogeneous catalytic reactors. For such systems, the space velocity is the ratio of the mass flow rate of feed to the mass of catalyst used ( $W$ ):

$$\text{WHSV} = \frac{\rho V}{W} \quad (8.0.7)$$

where  $\rho$  is the mass density of the feed and WHSV is termed the *weight hourly space velocity*. Sometimes the term *volumetric hourly space velocity* (VHSV) is used to denote the ratio of the volumetric flow rate at the reactor inlet to the weight of the catalyst bed:

$$\text{VHSV} = \frac{V}{W} \quad (8.0.8)$$

On other occasions the volume of catalyst instead of the mass of catalyst may be used in the denominators of equations (8.0.7) and (8.0.8). The units associated with a particular space velocity indicate the definition employed.

## 8.1 DESIGN ANALYSIS FOR BATCH REACTORS

Batch reactors are widely used in the chemical industry for producing materials that are needed in limited quantity, particularly in those cases where the processing cost represents only a small fraction of the total value of the product. Since modern industry stresses the use of continuous processes because they lend themselves most readily to mass production, chemical engineers may, in some instances, tend to overlook the economic superiority of batch operations. One should not become so fascinated with the continuous process, or the more complex and interesting design analysis associated therewith, as to lose sight of the economic penalty exacted by this degree of technical sophistication.

The starting point for the development of the basic design equation for a well-stirred batch reactor is a material balance involving one of the species participating in the chemical reaction. For convenience we denote this species as A and let  $(-r_A)$  represent the *rate of disappearance* of this species by reaction. For a well-stirred reactor the reaction mixture will be uniform throughout the effective reactor volume, and the material balance may thus be written over the entire contents of the reactor. For a well-stirred batch reactor equation (8.0.1) becomes

$$\begin{aligned} & \text{rate of accumulation} \\ & \text{of reactant A} \\ & \text{within the reactor} \\ & \text{rate of disappearance of} \\ & = -\text{reactant A within the reactor} \quad (8.1.1) \\ & \text{by chemical reaction} \end{aligned}$$

The accumulation term is just the time derivative of the number of moles of reactant A contained within the reactor ( $dN_A/dt$ ). This term may also be written in terms of either the extent of reaction  $\xi$  or the fraction conversion of the limiting reagent ( $f_A$ ). (A is presumed to be the limiting reagent.) Thus,

$$\frac{dN_A}{dt} = \nu_A \frac{d\xi}{dt} = -N_{A0} \frac{df_A}{dt} \quad (8.1.2)$$

where  $N_{A0}$  is number of moles of species A present when the fraction conversion is zero.

The total rate of disappearance of reactant A is given by

$$\text{rate of disappearance of A} = (-r_A)V_R \quad (8.1.3)$$

We again emphasize that  $V_R$  is the volume physically occupied by the reacting fluid. Combination of equations (8.1.1) to (8.1.3) gives

$$N_{A0} \frac{df_A}{dt} = (-r_A)V_R \quad (8.1.4)$$

Rearrangement and integration give the general form of the design equation for a batch reactor:

$$t_2 - t_1 = N_{A0} \int_{f_{A1}}^{f_{A2}} \frac{df_A}{(-r_A)V_R} \quad (8.1.5)$$

where  $f_{A1}$  and  $f_{A2}$  represent the fraction conversion at times  $t_1$  and  $t_2$ , respectively. This equation is the most general form of the basic design relationship for a batch reactor. This relation is valid for both isothermal and nonisothermal operation as well as for both constant-volume and constant-pressure operation. Both the reaction rate and the reactor volume should be retained inside the integral sign, since either or both may change as the reaction proceeds.

There are a number of limiting forms of equation (8.1.5) that should be mentioned briefly. When  $t_1 = 0$  and  $f_{A1} = 0$ ,

$$t = N_{A0} \int_0^{f_A} \frac{df_A}{(-r_A)V_R} \quad (8.1.6)$$

In addition, if the reactor volume (fluid density) is constant, equation (8.1.6) becomes

$$t = C_{A0} \int_0^{f_A} \frac{df_A}{(-r_A)} = - \int_{C_{A0}}^{C_A} \frac{dC_A}{(-r_A)} \quad (8.1.7)$$

For reactions in which the fluid volume varies linearly with the fraction conversion, as indicated by equation (3.1.40), equation (8.1.6) becomes

$$\begin{aligned} t &= N_{A0} \int_0^{f_A} \frac{df_A}{(-r_A)V_{R0}(1 + \delta_A f_A)} \\ &= C_{A0} \int_0^{f_A} \frac{df_A}{(-r_A)(1 + \delta_A f_A)} \end{aligned} \quad (8.1.8)$$

where  $V_{R0}$  is the volume occupied by the reacting fluid at zero fraction conversion. This equation would be appropriate for use when low pressure gas phase reactions involving a change in the number of moles on reaction take place in a batch reactor *at constant pressure*. However, gas phase reactions are rarely carried out batchwise on a commercial scale because the quantity of product that can be produced in a reasonably sized reactor is so small. The chief use of batch reactors for gas phase reactions is to obtain the data necessary for the design of continuous flow reactors.

For reactions that obey a simple  $n$ th-order rate law and for which volumetric expansion effects may be significant, equation (8.1.8) becomes

$$\begin{aligned} t &= C_{A0} \int_0^{f_A} \frac{df_A}{k[C_{A0}(1 - f_A)/(1 + \delta_A f_A)]^n (1 + \delta_A f_A)} \\ &= \int_0^{f_A} \frac{(1 + \delta_A f_A)^{n-1} df_A}{k C_{A0}^{n-1} (1 - f_A)^n} \end{aligned} \quad (8.1.9)$$

Equations (8.1.4) to (8.1.8) may also be written in terms of the extent of reaction  $\xi$  or the extent per unit volume ( $\xi^*$ ). In terms of  $\xi$ , the most general design relation [equation (8.1.5)] becomes

$$t_2 - t_1 = \nu_A \int_{\xi_1}^{\xi_2} \frac{d\xi}{r_A V_R} = \int_{\xi_1}^{\xi_2} \frac{d\xi}{r V_R} \quad (8.1.10)$$

The use of equations like this was treated in great detail in Chapter 3. There our primary objective was determination of the mathematical form of the rate expression from data on the extent of reaction or fraction conversion versus time. At present our objective is just the reverse: to determine the time necessary to achieve a specified degree of

conversion using our knowledge of the mathematical form of the rate expression and the reaction conditions. Although it is often more convenient to work in terms of the extent of reaction when analyzing rate data, it is usually more convenient to work in terms of fraction conversion in analyzing design problems. The two concepts are simply related, and the chemical engineer should learn to work in terms of either with equal facility.

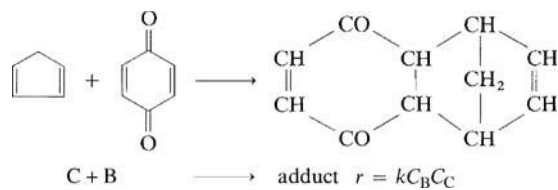
The degree of difficulty associated with evaluating the integral in any of the batch reactor design equations [equations (8.1.5) to (8.1.10)] depends on the composition and temperature dependence of the reaction rate expression. For nonisothermal systems an energy balance must be employed to relate the system temperature (and through it the reaction rate) to the fraction conversion. For isothermal systems it is not necessary to utilize an energy balance to determine the holding time necessary to achieve a specified fraction conversion. One merely substitutes rate constants evaluated at the temperature in question directly into the rate expression. However, an energy balance must be used to determine the heat transfer requirements necessary to maintain isothermal conditions. The reader should recognize that even if a simple closed form relation between time and fraction conversion cannot be obtained, it is still possible to evaluate the integral graphically or numerically using standard methods to assure convergence. The latter approach is invariably necessary when departures from isothermal conditions are large.

The following illustrations indicate how the basic design relations developed above are used to answer the two questions with which the reactor designer is most often faced.

1. What is the time required for converting a quantity of material to the level desired under specified reaction conditions?
2. What reactor volume is required to achieve a given production rate?

### ILLUSTRATION 8.1 Determination of Holding Time Requirements for the Formation of a Diels–Alder Adduct

Wassermann (6) studied the Diels–Alder reaction of benzoquinone (B) and cyclopentadiene (C) at 25°C.



Volume changes on reaction may be neglected. At 25°C the rate constant is equal to  $9.92 \times 10^{-3} \text{ m}^3/(\text{kmol}\cdot\text{s})$ . If one employs a well-stirred isothermal batch reactor to carry out this reaction, determine the holding time necessary to achieve 95% conversion of the limiting reagent using initial concentrations of 0.1 and 0.08 kmol/m<sup>3</sup> for cyclopentadiene and benzoquinone, respectively.

### Solution

The limiting reagent is benzoquinone. The rate of disappearance of this species can be written in terms of the initial concentrations and the fraction conversion as

$$-r_B = k[C_{B0}(1 - f_B)](C_{C0} - f_B C_{B0})$$

Because this liquid-phase reaction takes place at constant volume, the pertinent design relation is equation (8.1.7):

$$t = C_{B0} \int_0^{f_B} \frac{df_B}{kC_{B0}(1 - f_B)(C_{C0} - f_B C_{B0})}$$

Because the reaction occurs under isothermal conditions, the rate constant may be taken outside the integral sign. Integration and simplification then give

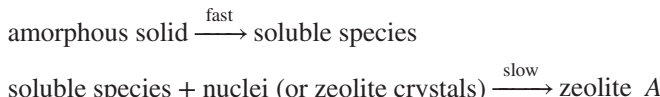
$$t = \frac{\ln\langle\{(C_{C0}/C_{B0}) - f_B\}(C_{B0}/C_{C0})\}/(1 - f_B)}{k(C_{C0} - C_{B0})}$$

Substitution of numerical values gives

$$t = \frac{\ln\langle\{(0.10/0.08) - 0.95\}(0.08/0.10)\}/(1 - 0.95)}{9.92 \times 10^{-3}(0.1 - 0.08)} \\ = 7.91 \times 10^3 \text{ s or } 2.20 \text{ h}$$

### ILLUSTRATION 8.2 Determination of Holding Time and Reactor Size Requirements for the Production of Zeolite A in a Batch Reactor

Zeolites are hydrous aluminosilicates that are widely used as catalysts in the chemical process industry. Zeolite A is usually synthesized in the sodium form from aqueous solutions of sodium silicate and sodium aluminate. Kerr (7) and Liu (8) studied an alternative method of synthesis from amorphous sodium aluminosilicate substrate and aqueous sodium hydroxide solution. The reaction (essentially a crystallization or recrystallization process) can be viewed as



Liu's description of the kinetics of the zeolite formation process can be formulated in terms of the following equation:

$$-\frac{dC_A}{dt} = \frac{k_2[\text{OH}^-]^{k_1} C_A C_Z}{k_3 C_Z + (k_3 + 1) C_A} \quad (\text{A})$$

where  $C_A$  is the concentration of amorphous substrate (kg/m<sup>3</sup>),  $[\text{OH}^-]$  the concentration of hydroxide ions (kmol/m<sup>3</sup>),  $C_Z$  the concentration of zeolite crystals (kg/m<sup>3</sup>), and  $k_1$ ,  $k_2$ , and  $k_3$  are kinetic parameters. Since the total weight of solids in a batch reactor must satisfy an overall material balance, we require that the quantity  $(C_A + C_Z)$  be a constant equal to the total weight of the charge divided by the effective reactor volume. Note that the reaction is catalyzed by the presence of product in that the zeolite concentration appears in the numerator of the rate expression. Consequently, it is desirable to include some zeolite in the feed to the reactor to enhance the reaction rate. Reactions of this type are labeled as "autocatalytic." They are treated in more detail in Section 9.4.

At 100°C the following values of the rate constants are appropriate for use.

$$k_1 = 2.36 \quad k_2 = 0.625 \text{ ks}^{-1} \quad k_3 = 0.36$$

1. If one utilizes a slurry containing 1 kg/m<sup>3</sup> of zeolite and 24 kg/m<sup>3</sup> of amorphous substrate, determine the time necessary to achieve 98% conversion of the substrate to zeolite A in a well-stirred batch reactor. The conditions to be considered are isothermal operation at 100°C and a hydroxide concentration of 1.5 kmol/m<sup>3</sup>.
2. Assuming the reaction conditions noted in part 1, determine the reactor size and total weight of charge necessary to produce zeolite A at an average rate of 2000 kg/day. Only one reactor is to be used, and it will be necessary to shut down for 1.8 ks between batches for removal of product, cleaning, and startup. The zeolite to be recycled to the reactor will come from the 2000 kg produced daily.

### Solution

Because the reaction takes place in a slurry, the reactor volume may be regarded as constant, and equation (8.1.7) is appropriate for use.

$$t = C_{A0} \int_0^{f_A} \frac{df_A}{(-r_A)} \quad (\text{B})$$

where the subscript A refers to the amorphous substrate.

The principles of stoichiometry may be used to express the rate in terms of the fraction conversion. Because the conversion desired is written in terms of the initial substrate

level,  $C_{A0} = 24 \text{ kg/m}^3$ . At any time the instantaneous concentration of substrate is given by

$$C_A = C_{A0}(1 - f_A) \quad (\text{C})$$

while the corresponding concentration of zeolite is given by

$$C_Z = C_{Z0} + f_A C_{A0} \quad (\text{D})$$

The instantaneous reaction rate can be expressed in terms of the fraction conversion by combining equations (A), (C), and (D):

$$\begin{aligned} -r_A &= \frac{-dC_A}{dt} \\ &= \frac{k_2[\text{OH}^-]^{k_1} C_{A0}(1 - f_A)(C_{Z0} + f_A C_{A0})}{k_3(C_{Z0} + f_A C_{A0}) + (1 + k_3)C_{A0}(1 - f_A)} \end{aligned}$$

Substitution of numerical values into this relation gives

$$\begin{aligned} -r_A &= \frac{(0.625)(1.5)^{2.36}(24)(1 - f_A)(1 + 24f_A)}{0.36(1 + 24f_A) + (1.36)(24)(1 - f_A)} \\ &= \frac{(39.05)(1 - f_A)(1 + 24f_A)}{33.0 - 24f_A} \end{aligned} \quad (\text{E})$$

Combining equations (E) and (B) gives

$$t = 24 \int_0^{f_A} \frac{(33.0 - 24f_A)df_A}{39.05(1 - f_A)(1 + 24f_A)}$$

This integral may be broken up into terms that can be evaluated using standard tables.

$$\begin{aligned} t &= 20.28 \int_0^{f_A} \frac{df_A}{(1 - f_A)(1 + 24f_A)} \\ &\quad - 14.75 \int_0^{f_A} \frac{f_A df_A}{(1 - f_A)(1 + 24f_A)} \end{aligned}$$

or

$$\begin{aligned} t &= \left( \frac{20.28}{25} \right) \left[ \ln \left( \frac{1 + 24f_A}{1 - f_A} \right) \right] \\ &\quad + \left( \frac{14.75}{25} \right) \left[ \ln(1 - f_A) + \frac{1}{24} \ln(1 + 24f_A) \right] \end{aligned}$$

The time required to achieve any desired degree of conversion may be calculated from this expression. The solution for  $f_A = 0.98$  is  $t = 3.54 \text{ ksec} = 0.982 \text{ hr}$ .

For part 2, for 98% conversion, each batch will require a holding time of 3.54 ks and a downtime of 1.80 ks for emptying, cleaning, and startup. The total time consumed in processing one batch is thus 5.34 ks. To produce 2000 kg of zeolite A per day, we require that to start, each batch should contain an amount of amorphous solids equal to

$$\frac{2000 \text{ kg/day}}{0.98 \text{ (% conversion)}} \times \frac{5.34 \text{ ks/batch}}{86.4 \text{ ks/day}} = 126 \frac{\text{kg}}{\text{batch}}$$

The weight of amorphous solids per batch must equal the product of the reactor volume and the solids concentration. Thus,

$$V_R = \frac{126 \text{ kg}}{24 \text{ kg/m}^3} = 5.25 \text{ m}^3 = 1387 \text{ gal}$$

Note that in this illustration the batch reactor is operating in a production mode only two-thirds of the time. This situation is not extraordinary, and to meet design requirements properly allowances must be made for downtime.

When there are significant heating and cooling periods associated with the utilization of a batch reactor, one must take these circumstances into account in design calculations. If only a single reaction is involved, the holding time computed using the methods of this section will be a conservative estimate of the length of time the reactor contents should be held at the temperature specified. However, if undesirable side reactions take place at temperatures below the operating temperature, the magnitude of the adverse effects must be considered. Should they be significant, it may be necessary to resort to rapid quenching techniques or to separate preheating of coreactants to the desired temperature.

## 8.2 DESIGN OF TUBULAR REACTORS

Tubular reactors are normally used in the chemical industry for extremely large-scale processes. When filled with solid catalyst particles, such reactors are referred to as fixed-bed or packed-bed reactors. In this section we treat general design relationships for tubular reactors in which isothermal homogeneous reactions take place. Nonisothermal tubular reactors are treated in Section 10.4 and packed-bed reactors in Section 12.7.

### 8.2.1 The Plug Flow Reactor Model: Basic Assumptions and Design Equations

The simplest model of the behavior of tubular reactors is the plug flow model. The essential features of this idealized model require that there be no longitudinal mixing of fluid elements as they move through the reactor and that all fluid elements take the same length of time to move from the reactor inlet to the outlet. The model may also be labeled the *slug flow* or *piston flow model* in that it may be convenient to picture the reaction as taking place within differentially thin slugs of fluid that fill the entire cross section of the tube and that are separated from one another by hypothetical pistons that prevent axial mixing. These plugs of material move as units through the reactor, and this assumption is conveniently expressed in terms of a requirement that

the velocity profile be flat as one traverses the tube diameter. Each plug of fluid is assumed to be uniform in temperature, composition, and pressure, which is equivalent to assuming that radial mixing is infinitely rapid. However, there may well be variations in composition, temperature, pressure, and fluid velocity as one moves in the longitudinal direction. With respect to these variations, however, the model requires that mass transport via diffusion or turbulent mixing processes be negligible. The plugs of material do, however, interact with one another with respect to both transmission of the hydrodynamic forces giving rise to the fluid motion and transfer of thermal energy from one plug to another if the plugs differ in temperature. Some of the aforementioned requirements may be removed in more complex mathematical models of tubular reactors. In the present chapter, however, we limit our discussion to the simplest possible model: the plug flow model. Nonetheless, when we attempt to compare the results predicted by the model with what we observe in the real world, we should keep in mind that the model can only reflect the idealizations built into it and that deviations from ideal behavior can fall into three categories.

1. There will be velocity gradients in the radial direction, so all fluid elements will not have the same residence time in the reactor. Under turbulent flow conditions in reactors with large length/diameter ratios, any disparities between values observed and model predictions arising from this factor should be small. For short reactors and/or laminar flow conditions, the disparities can be appreciable. Some of the techniques used in the analysis of isothermal tubular reactors that deviate from plug flow are treated in Chapter 11.
  2. There will be an interchange of material between fluid elements at different axial positions by virtue of ordinary molecular diffusion and eddy diffusion processes arising from turbulence and/or the influence of any packing in the bed. Convective mixing arising from thermal gradients in the reactor may also contribute to the exchange of matter between different fluid elements.
  3. There may be radial temperature gradients in the reactor that arise from the interaction between the energy released by reaction, heat transfer through the walls of the tube, and convective transport of energy. This factor is the greatest potential source of disparities between the predictions of the model and the behavior observed for real systems. The deviations are most significant in nonisothermal packed-bed reactors.

The tubular reactor is a convenient means of approaching the performance characteristics of a batch reactor on a continuous basis, since the distance-pressure-temperature history of the various plugs as they flow through the reactor corresponds to the time-pressure-temperature protocol

that is used in a batch reactor. Although this analogy is often useful, it may on occasion be misleading. Batch reactors are almost invariably operated under the constraint of constant volume, whereas in a tubular reactor, each plug of fluid more nearly approximates constant pressure conditions. For liquid phase reactions constraints of constant volume and constant pressure may effectively be satisfied simultaneously, and the same is true of isothermal gas phase reactions that do not involve a change in the number of gas phase moles on reaction. However, when there is a change in temperature or in the number of molecules contained within the plug, the volume of the plug can change by an appreciable fraction. To maintain a constant mass velocity at various points along a uniform-diameter tube in cases where there is an increase in the number of moles on reaction (an increase in plug volume), an increase in the volumetric flow rate must accompany the reaction. Instead of giving rise to the pressure increase that would take place in a constant volume batch reactor, the change in the number of moles on reaction causes the fluid to accelerate. Thus, the residence time of the plug in the reactor will be less than that which would have been observed if the volume of the plug remained unchanged. We turn now to the problem of developing fundamental design relationships that allow for such effects.

Consider the segment of tubular reactor shown in Figure 8.3. Because the fluid composition varies with longitudinal position, we must write our material balance for a reactant species over a different element of reactor ( $dV_R$ ). Moreover, since plug flow reactors are usually operated at steady state except during startup and shutdown procedures, the relations of major interest are those in which the accumulation term is missing from equation (8.0.1). Thus,

$$\begin{aligned} \text{rate of flow of reactant into volume element} &= \text{Rate of flow of reactant out of volume element} \\ &+ \text{rate of disappearance of reactants by chemical reactions within the volume element} \end{aligned} \quad (8.2.1)$$

If the molal flow rate of reactant A into the volume element is designated as  $F_A$ , and the molal flow rate out of the volume element is represented by  $F_A + dF_A$ , equation

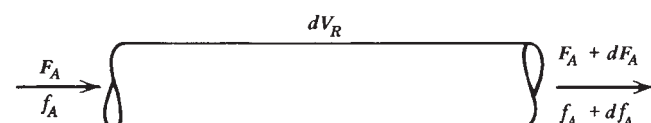


**Figure 8.3** Schematic representation of differential volume element of plug flow reactor.

(8.2.1) becomes

$$F_A = (F_A + dF_A) + (-r_A) dV_R \quad (8.2.2)$$

or

$$dF_A = r_A dV_R \quad (8.2.3)$$

At any point the molal flow rate of reactant A can be expressed in terms of the fraction conversion  $f_A$  and the molal flow rate corresponding to zero conversion  $F_{A0}$ :

$$F_A = F_{A0}(1 - f_A) \quad (8.2.4)$$

Differentiation gives

$$dF_A = -F_{A0} df_A \quad (8.2.5)$$

Combination of equations (8.2.3) and (8.2.5) gives

$$\frac{dV_R}{F_{A0}} = \frac{df_A}{(-r_A)} \quad (8.2.6)$$

which may be integrated over the entire reactor volume to obtain

$$\frac{V_R}{F_{A0}} = \int_{f_{A\text{ in}}}^{f_{A\text{ out}}} \frac{df_A}{(-r_A)} \quad (8.2.7)$$

This equation is a very useful relation that indicates the reactor size necessary to accomplish a specified change in the degree of conversion for a fixed inlet molal flow rate. However, it requires a knowledge of the relationship between the reciprocal rate of reaction and the fraction conversion. For nonisothermal systems this relationship can be quite complex, as we shall see in Chapter 10.

It should be emphasized that for *ideal* tubular reactors (PFRs), it is the *total volume* per unit of feed that determines the conversion level achieved. The ratio of the length of the tube to its diameter is irrelevant, provided that plug flow is maintained and that one uses the same flow rates and pressure-temperature profiles expressed in terms of reactor volume elements.

$F_{A0}$  may also be written as the product of a volumetric flow rate and a reactant concentration where both are measured at some reference temperature and pressure and correspond to zero fraction conversion. Thus,

$$\frac{V_R}{F_{A0}} = \frac{V_R}{C_{A0}V_0} = \frac{\tau}{C_{A0}} \quad (8.2.8)$$

where we have introduced the space time  $\tau$ . Combining equations (8.2.8) and (8.2.7) gives

$$\tau = \frac{V_R}{V_0} = C_{A0} \int_{f_{A\text{ in}}}^{f_{A\text{ out}}} \frac{df_A}{(-r_A)} \quad (8.2.9)$$

Reactor inlet conditions are particularly useful as reference conditions for the volumetric flow rate in that they not only give physical meaning to  $C_{A0}$  and  $V_0$  but also usually

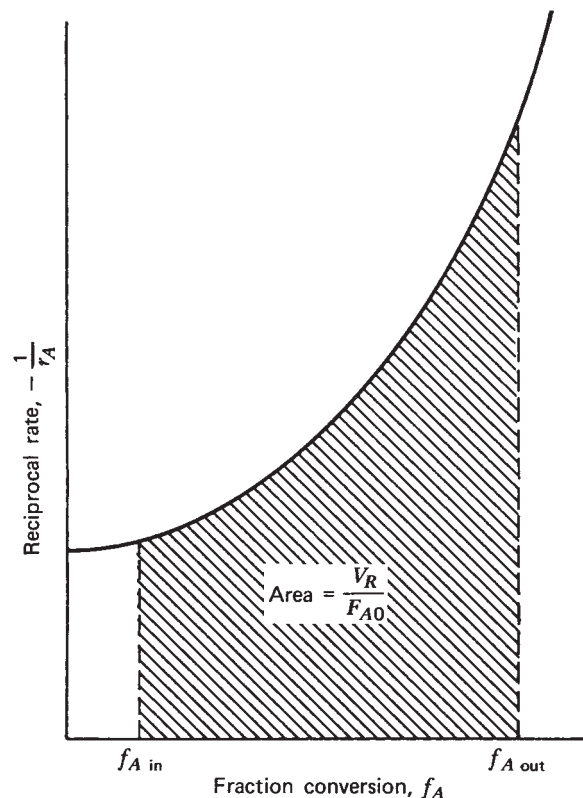


**Figure 8.4** Determination of  $V_R/F_{A0}$  from plot of reciprocal rate versus fraction conversion.

lead to cancellation of  $C_{A0}$ , with a similar term appearing in the reaction rate expression.

If the temperature is constant throughout the reactor volume, the rate constant  $k$  may be removed from the integral, and an analytic solution can often be obtained for the integral. At times it will be necessary to evaluate the integrals in equations (8.2.7) and (8.2.9) using graphical or numerical methods. Figure 8.4 indicates this schematically. For nonisothermal systems one must employ an energy balance in conjunction with the basic design equation to relate the temperature (and thus the temperature-dependent terms in the rate expression) to the fraction conversion. The relations are such that exact analytical solutions can rarely, if ever, be obtained (see Chapter 10).

For cases where  $\delta = 0$ , equation (8.2.9) can be written in terms of concentrations:

$$\tau = - \int_{C_{A\text{ in}}}^{C_{A\text{ out}}} \frac{dC_A}{(-r_A)} \quad (8.2.10)$$

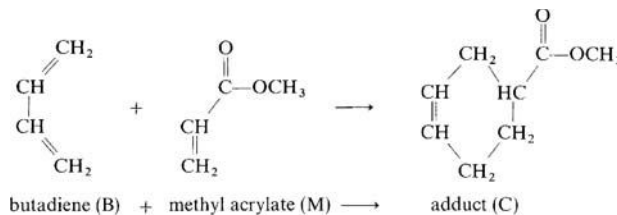
but for constant density systems only. For variable density systems it is more convenient to work in terms of the fraction conversion [equation (8.2.9)]. For constant-density systems either equation (8.2.9) or equation (8.2.10) is appropriate.

For preliminary design calculations involving tubular reactors, the usual procedure is to assume plug flow with constant pressure over the length of the reactor. However, the analysis above is appropriate regardless of whether or not a pressure drop exists. The pressure enters only through its influence on the reaction rate term. For liquid phase reactions the influence of pressure variations is usually insignificant, but for gas phase reactions or when mixtures of gases and liquids are present, the pressure drop across a given segment of the reactor must be taken into account in arriving at the reactor volume required to accomplish a specified task. No new principles are involved; one merely breaks the reactor up into a series of segments that can be assumed to operate at an appropriate average pressure. The pressure drop across a segment is calculated from the Bernoulli equation using appropriate empirical relations where necessary to estimate the friction factor, equivalent lengths for U-bends or other fittings, and losses associated with changes in tube diameter. The basic design equation is then applied to each segment using the average of the inlet and outlet pressures in the rate expression. One marches through the reactor assuming that for conversion increments that are sufficiently small, calculations allowing for the pressure drop lead to convergence of the integral.

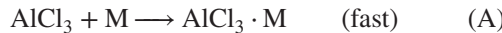
Illustrations 8.3 and 8.4 indicate the application of the analysis above to isothermal tubular reactors with negligible pressure drop.

### ILLUSTRATION 8.3 Determination of Required Plug Flow Reactor Volume for Isothermal Operating Conditions: Constant Density Case

Inukai and Kojima (9) studied the aluminum chloride-catalyzed diene condensation of butadiene and methyl acrylate in benzene solution. The stoichiometry for this Diels–Alder reaction is



The following set of mechanistic equations is consistent with their experimental results:



where reaction (B) is the rate-limiting step.  $\text{AlCl}_3 \cdot \text{M}$  and  $\text{C} \cdot \text{AlCl}_3$  represent complexes formed between the dissolved  $\text{AlCl}_3$  and the species in question. The concentration of the first reactive complex is essentially constant as long as enough methyl acrylate remains in solution to regenerate  $\text{AlCl}_3 \cdot \text{M}$  efficiently. The concentration of methyl acrylate in excess of  $\text{AlCl}_3$  will not affect the rate of reaction during the early stages of reaction, but as reaction proceeds and the methyl acrylate concentration drops below the initial  $\text{AlCl}_3$  concentration, the amount of complex present is limited by the amount of methyl acrylate remaining.

These investigators report that the second-order rate constant for reaction B is equal to  $1.15 \times 10^{-3} \text{ m}^3/(\text{mol} \cdot \text{ks})$  at  $20^\circ\text{C}$ . Determine the volume of plug flow reactor that would be necessary to achieve 40% conversion of the feed butadiene assuming isothermal operating conditions and a liquid feed rate of  $0.500 \text{ m}^3/\text{ks}$ . The feed concentrations (in  $\text{mol}/\text{m}^3$ ) are as follows: butadiene (B): 96.5; methyl acrylate (M): 184;  $\text{AlCl}_3$ : 6.63.

### Solution

Butadiene is the limiting reagent and conversions will be expressed in terms of this species. Over the composition range of interest, sufficient methyl acrylate will always be present to tie up the aluminum chloride as the complex  $\text{AlCl}_3 \cdot \text{M}$ . Consequently, the concentration of the complex  $\text{AlCl}_3 \cdot \text{M}$  will remain constant throughout the length of the reactor at a value equal to the initial  $\text{AlCl}_3$  concentration. For these conditions the reaction rate expression takes the form

$$-r_B = k C_B C_{\text{AlCl}_3 \cdot \text{M}} = k C_{B0} (1 - f_B) C_{\text{AlCl}_3,0} \quad (\text{D})$$

because the volume change accompanying liquid-phase reactions is negligible. Equation (8.2.9) may be used as the basic design relationship:

$$\begin{aligned} \tau &= C_{B0} \int_0^{f_B} \frac{df_B}{(-r_B)} \\ &= C_{B0} \int_0^{f_B} \frac{df_B}{k C_{B0} (1 - f_B) C_{\text{AlCl}_3,0}} \end{aligned} \quad (\text{E})$$

Because the quantities  $C_{\text{AlCl}_3,0}$  and  $k$  are constant for the conditions cited, equation (E) may be integrated to obtain

$$\tau = \frac{\ln[1/(1 - f_B)]}{k C_{\text{AlCl}_3,0}}$$

Substitution of numerical values gives

$$\tau = \frac{\ln[1/(1 - 0.4)]}{(1.15 \times 10^{-3})(6.63)} = 67.0 \text{ ks} = 18.6 \text{ h}$$

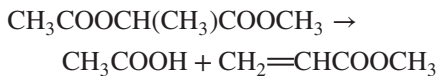
From the definition of the space time and the inlet volumetric flow rate,

$$V_R = \tau V_0 = 67.0(0.500) = 35.5 \text{ m}^3$$

The space time required to accomplish the specified conversion in a plug flow reactor (18.6 h) is sufficiently long that it makes the use of a tubular reactor impractical for the operating conditions specified. For these conditions a cascade of stirred-tank reactors would be more appropriate for use.

### ILLUSTRATION 8.4 Determination of Plug Flow Reactor Volume Required for Isothermal Operating Conditions: Variable Density Case

Ratchford and Fisher (10) studied the pyrolysis of methyl acetoxypropionate at temperatures near 500°C and a variety of pressures:



If one desires to design a pilot-scale tubular reactor to operate isothermally at 500°C, what length of 6-in. pipe will be required to convert 90% of the raw feedstock to methyl acrylate? The feedstock enters at 5 atm at a flow rate of 500 lb/h. Ideal gas behavior may be assumed. A 6-in. pipe has an area of 0.0388 ft<sup>2</sup> available for flow. Pressure drop across the reactor may be neglected. Below 565°C the pyrolysis reaction is essentially first-order with a rate constant given by  $k = 7.8 \times 10^9 e^{-19,220/T} \text{ s}^{-1}$  for  $T$  in  $K$ .

### Solution

From equation (8.2.9) and the fact that the reaction is first-order,

$$\tau = C_{A0} \int_0^{f_A} \frac{df_A}{kC_A} \quad (\text{A})$$

For the case where the feed is pure methyl acetoxypropionate,

$$\delta_A = \frac{2-1}{1} = 1$$

Because there is a change in the number of moles of gaseous species on reaction, the concentration corresponding to a given fraction conversion is

$$C_A = C_{A0} \left( \frac{1-f_A}{1+\delta_A f_A} \right) = C_{A0} \left( \frac{1-f_A}{1+f_A} \right) \quad (\text{B})$$

Combining equations (A) and (B) gives

$$\tau = \int_0^{f_A} \frac{(1+f_A)df_A}{k(1-f_A)}$$

Because the reaction takes place isothermally at 500°C, the rate constant may be moved outside the integral sign. At this temperature  $k$  is equal to 0.124 s<sup>-1</sup>. Thus,

$$0.124\tau = \int_0^{f_A} \frac{df_A}{1-f_A} + \int_0^{f_A} \frac{f_A df_A}{1-f_A}$$

Evaluation of the integrals gives

$$\begin{aligned} 0.124\tau &= -\ln(1-f_A) - f_A - \ln(1-f_A) \\ &= -2\ln(1-f_A) - f_A \end{aligned}$$

For  $f_A = 0.90$ ,

$$\tau = \frac{-2\ln(1-0.9) - 0.900}{0.124} = 29.9 \text{ s}$$

If we had erred and not included the effect of volumetric expansion on reaction, we would have calculated a space time of 18.6 s, which would have been off by 38%, and this error would propagate through the remainder of the calculations below.

If the gas behaves ideally, the volumetric flow rate at the reactor inlet is given by the product of the molal flow rate [(500/146) lb-mol/h] and the molal volume at the pressure and temperature in question. The latter may be calculated by correcting the standard molal volume (359 ft<sup>3</sup>/lb-mol) for variations in temperature and pressure between the reactor inlet and standard conditions. Hence,

$$\begin{aligned} V_0 &= \frac{500(773)(1)(359)}{146(273)(5)} \text{ ft}^3/\text{h} = 696 \text{ ft}^3/\text{h} \\ &= 0.193 \text{ ft}^3/\text{s} \end{aligned}$$

From the definition of the space time,

$$V_R = V_0\tau = 0.193(29.9) = 5.78 \text{ ft}^3$$

From geometric considerations the required length of 6-in. pipe is equal to  $(5.78 \text{ ft}^3)/(3.88 \times 10^{-2} \text{ ft}^2)$  or 149 ft.

Illustrations 8.3 and 8.4 indicate how the plug flow design equations may be applied to homogeneous fluid-phase reactions. We now wish to consider the form of the plug flow reactor design equation for heterogeneous catalytic reactions. For reactions of this type the reaction rate must be expressed per unit weight or per unit area of catalyst. Since the two are related through the specific surface area of the material, we develop relations only in terms of the former. Consider the segment of tubular reactor shown in Figure 8.3, in which we now presume

that the differential volume element  $dV_R$  contains a mass of catalyst  $dW$ . The rate of disappearance of reactant A within the differential volume element is then equal to  $(-r_{Am})dW$ . A material balance for steady-state operating conditions based on equation (8.2.1) gives

$$\begin{aligned} \text{input} &= \text{output} + \text{disappearance by reaction} \\ F_A &= F_A + dF_A + (-r_{Am})dW \end{aligned} \quad (8.2.11)$$

Introduction of the fraction conversion through equation (8.2.5) leads to the following analog of equation (8.2.7):

$$\frac{W}{F_{A0}} = \int_{f_{A \text{ in}}}^{f_{A \text{ out}}} \frac{df_A}{(-r_{Am})} \quad (8.2.12)$$

In this case the reaction rate will depend not only on the system temperature and pressure but also on the properties of the catalyst. One should note that the reaction rate term must include the effects of external and intraparticle heat and mass transfer limitations on the rate. In Chapter 12 we treat these subjects and indicate how equation (8.2.12) can be used in the analysis of packed-bed reactors.

## 8.2.2 Residence Times in Plug Flow Reactors

For plug flow reactors all fluid elements take the same length of time to travel from the reactor inlet to the reactor outlet. This time is the mean residence time  $\bar{t}$ . Consider the general case of a reaction accompanied by a volumetric expansion or contraction. The average time necessary for a plug to travel from inlet to outlet of a tubular reactor is given by

$$\bar{t} = \int_0^{V_R} \frac{dV_R}{\mathcal{V}} \quad (8.2.13)$$

where  $\mathcal{V}$  is the volumetric flow rate. At any point along the length of the tubular reactor, the volumetric flow rate can be written in terms of the inlet reference volumetric flow rate  $\mathcal{V}_0$ , the fraction conversion, and the volumetric expansion parameter:

$$\mathcal{V} = \mathcal{V}_0(1 + \delta_A f_A) \quad (8.2.14)$$

The increment in reactor volume can be written in terms of the fraction conversion using equation (8.2.6):

$$dV_R = \frac{F_{A0} df_A}{(-r_A)} \quad (8.2.15)$$

Combining equations (8.2.13) to (8.2.15) gives

$$\bar{t} = \int_{f_{A \text{ in}}}^{f_{A \text{ out}}} \frac{F_{A0} df_A}{(-r_A) \mathcal{V}_0(1 + \delta_A f_A)} \quad (8.2.16)$$

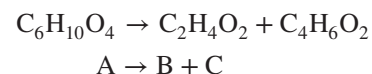
which can be rewritten in terms of the inlet reference concentration of the limiting reagent as

$$\bar{t} = C_{A0} \int_{f_{A \text{ in}}}^{f_{A \text{ out}}} \frac{df_A}{(-r_A)(1 + \delta_A f_A)} \quad (8.2.17)$$

This equation is the basic relation for the mean residence time in a plug flow reactor with arbitrary reaction kinetics. Note that this expression differs from that for the space time [equation (8.2.9)] by the inclusion of the term  $(1 + \delta_A f_A)$  and that this term appears *inside* the integral sign. The two quantities become identical only when  $\delta_A$  is zero (i.e., the fluid density is constant). The differences between the two characteristic times may be quite substantial, as we shall see in Illustration 8.5. Of the two quantities, the reactor space time is the more meaningful for reactor design purposes. Knowledge of the mean residence time  $\bar{t}$  does not permit us to determine the required reactor volume, but a knowledge of the space time  $\tau$  leads readily to this quantity. The space time is an independent variable directly related to system parameters, whereas the mean residence time is a dependent variable found by integration of equation (8.2.17) or by tracer studies (see Chapter 11).

## ILLUSTRATION 8.5 Determination of Mean Residence Time in a Plug Flow Reactor for Isothermal Operating Conditions: Variable Density Case

Consider the plug flow reactor used for the pyrolysis of methyl acetoxypropionate in Illustration 8.4:



For isothermal operation at 500°C and 5 atm, it was shown in Illustration 8.4 that the space time required to achieve 90% conversion was 29.9 s. Compare this value with the mean residence time of the material in the plug flow reactor.

### Solution

For first-order kinetics in a system where  $\delta_A$  is nonzero, the reaction rate expression is of the form

$$-r_A = k C_{A0} \left( \frac{1 - f_A}{1 + \delta_A f_A} \right)$$

In the present case  $\delta_A = 1$ . Hence, the equation for the mean residence time [equation (8.2.17)] becomes

$$\bar{t} = C_{A0} \int_0^{0.9} \frac{df_A}{\{k C_{A0}[(1 - f_A)/(1 + \delta_A f_A)]\}(1 + \delta_A f_A)}$$

Simplification gives

$$\bar{t} = \frac{1}{k} \int_0^{0.9} \frac{df_A}{1-f_A} = \frac{-\ln(1-f_A)}{k} \Big|_0^{0.9}$$

Substitution of numerical values gives

$$\bar{t} = \frac{1}{0.124} [-\ln(1-0.9)] = 18.6 \text{ s}$$

This value is considerably less than the reactor space time and differs from it by 38%.

### 8.2.3 Series-Parallel Combinations of Tubular Reactors

To achieve increases in production capacity or to obtain higher conversion levels, it may be necessary to provide additional reactor volume through the use of various series-parallel combinations of reactors. Consider  $j$  plug flow reactors connected in series and let  $f_1, f_2, f_3, \dots, f_i, \dots, f_j$  represent the fraction conversion of the limiting reagent, leaving reactors 1, 2, 3, ...  $i$ , ... ,  $j$ . For each of the reactors considered above, the appropriate design equation is (8.2.7). For reactor  $i$ ,

$$V_{Ri} = F_{A0} \int_{f_{i-1}}^{f_i} \frac{df_A}{(-r_A)} \quad (8.2.18)$$

The total reactor volume is obtained by summing the individual reactor volumes:

$$\begin{aligned} V_{R,\text{total}} &= \sum_{i=1}^j V_{Ri} \\ &= F_{A0} \left[ \int_{f_0}^{f_1} \frac{df_A}{(-r_A)} + \int_{f_1}^{f_2} \frac{df_A}{(-r_A)} + \dots + \int_{f_{j-1}}^{f_j} \frac{df_A}{(-r_A)} \right] \end{aligned} \quad (8.2.19)$$

From the principles of calculus, the quantity in brackets can be rewritten as a single integral. Hence,

$$V_{R,\text{total}} = F_{A0} \int_{f_0}^{f_j} \frac{df_A}{(-r_A)} \quad (8.2.20)$$

Thus,  $j$  plug flow reactors in series with a total volume  $V_{R,\text{total}}$  give the same conversion as a single reactor of volume  $V_{R,\text{total}}$ .

When plug flow reactors are connected in parallel, the most efficient utilization of the total reactor volume occurs when mixing of streams of differing compositions does not occur. Consequently, the feed rates to different parallel legs of a reactor network must be proportioned such that equal increments in conversion occur across each leg. For this case, too, the network acts as if it were a single plug flow reactor with a volume equal to the sum of the constituent

reactor volumes. Thus for any series-parallel combination of plug flow reactors, one can treat the entire system as a single plug flow reactor with a volume equal to the total volume of the individual reactors, provided that the fluid streams are distributed in a manner such that streams that combine have the same composition. Hence, for any units in parallel, the space times or  $V_R/F_{A0}$  must be identical. Other flow distributions would be less efficient.

## 8.3 CONTINUOUS FLOW STIRRED-TANK REACTORS

Continuous flow stirred-tank reactors are widely used in the chemical process industry. Although individual reactors may be used, it is generally preferable to employ a battery of such reactors connected in series. The effectiveness of such batteries depends on the number of reactors used, the sizes of the component reactors, and the efficiency of mixing within each stage.

Continuous flow stirred-tank reactors are normally just what the name implies: tanks into which reactants flow and from which a product stream is removed on a continuous basis. CFSTRs, CSTRs, C-star reactors, and backmix reactors are only a few of the names applied to the idealized stirred-tank flow reactor model. We will use the letters CSTR in this book. The virtues of a stirred-tank reactor lie in its simplicity of construction and the relative ease with which it may be controlled. These reactors are used primarily for carrying out liquid phase reactions in the organic chemicals industry, particularly for systems that are characterized by relatively slow reaction rates. If it is imperative that a gas phase reaction be carried out under efficient mixing conditions similar to those found in a stirred-tank reactor, one may employ a tubular reactor containing a recycle loop. At sufficiently high recycle rates, such systems approximate the behavior of stirred tanks. In this section we are concerned with the development of design equations that are appropriate for use with the idealized stirred-tank reactor model.

### 8.3.1 Individual Stirred-Tank Reactors

#### 8.3.1.1 Basic Assumptions and Design Relationships

The most important feature of a CSTR is its mixing characteristics. The idealized model of reactor performance presumes that the reactor contents are perfectly mixed so that the properties of the reacting fluid are uniform throughout. The composition and temperature of the effluent are thus identical with those of the reactor contents. This feature greatly simplifies the analysis of stirred-tank reactors vis-à-vis tubular reactors for both isothermal and nonisothermal

operation. In practice, it is not difficult to obtain a good approximation to CSTR behavior, provided that the fluid phase is not too viscous. The approximation is valid if the time necessary to disperse an entering element of fluid (e.g., a shot of dye or radioactive tracer) uniformly throughout the tank is very much shorter than the average residence time in the tank.

Unlike the situation in a plug flow reactor, the various fluid elements mix with one another in a CSTR. In the limit of perfect mixing, a tracer molecule that enters at the reactor inlet has equal probability of being anywhere in the vessel after an infinitesimally small time increment. Thus, all fluid elements in the reactor have equal probability of leaving in the next time increment. Consequently, there will be a broad distribution of residence times for various tracer molecules. The character of the distribution is discussed in Section 11.1. Because some of the molecules have short residence times, there is a rapid response at the reactor outlet to changes in the reactor feed stream. This characteristic facilitates automatic control of the reactor.

Because the mixing process makes the properties of the entire reactor contents equal to those of the effluent stream, there will be a step change in fluid composition and temperature at the point where the feed stream enters the reactor. In the present chapter, unless noted otherwise we restrict the discussion to cases where there is no temperature change

on entrance to the reactor. For these isothermal CSTRs the drop in reactant concentration as the fluid enters the reactor implies that in the vast majority of cases the volume average reaction rate will be low by comparison to that in an isothermal plug flow reactor. Consequently, when both operate at the same temperature, a CSTR will have to be significantly larger than a PFR to effect the same composition change in a given amount of fluid. (Exceptions occur in the case of autocatalytic reactions.) However, by using a battery of stirred tanks in series, differences in total volume requirements can be significantly reduced. Moreover, because of the simplicity of their construction, stirred-tank reactors normally cost much less per unit of volume than tubular reactors. Thus, in many cases it is more economical to employ a large stirred-tank reactor or a battery of such reactors than it is to use a tubular reactor. Size comparisons of these two types can be treated quantitatively, and we will return to this subject in Sections 8.3.1.3 and 8.3.2.3. First, however, we must develop the basic design equations.

Consider the schematic representation of a continuous-flow stirred-tank reactor shown in Figure 8.5. The starting point for the development of the fundamental design equation is again a generalized material balance on a reactant species. For the steady-state case the accumulation term in equation (8.0.1) is zero. Furthermore, because conditions are uniform throughout the reactor volume, the

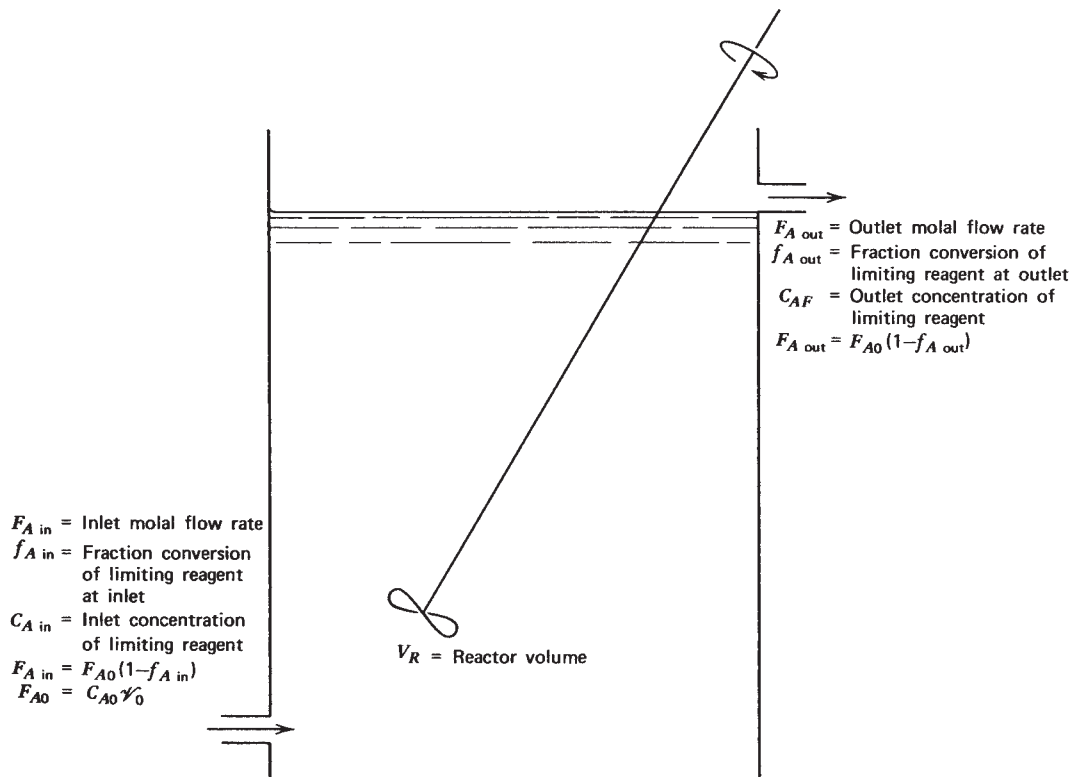


Figure 8.5 Schematic representation of a single CSTR indicating process variables.

material balance may be written over the entire reactor. Hence,

$$\begin{aligned} \text{rate of flow of reactant into reactor} &= \text{rate of flow of reactant out of reactor} \\ &\quad + \text{rate of disappearance of reactants by reaction in the reactor} \end{aligned} \quad (8.3.1)$$

In terms of the symbols indicated in Figure 8.5,

$$F_{A \text{ in}} = F_{A \text{ out}} + (-r_{AF})V_R \quad (8.3.2)$$

where we again emphasize that the appropriate volume is that physically occupied by the reacting fluid. The quantity  $(-r_{AF})$  is the rate of disappearance of reactant A evaluated at *reactor outlet conditions*.

Equation (8.3.2) may be rewritten in terms of the fraction conversion as

$$F_{A0}(1 - f_{A \text{ in}}) = F_{A0}(1 - f_{A \text{ out}}) + (-r_{AF})V_R \quad (8.3.3)$$

where  $F_{A0}$  is again the molal flow rate corresponding to zero conversion. Rearrangement gives

$$\frac{V_R}{F_{A0}} = \frac{f_{A \text{ out}} - f_{A \text{ in}}}{(-r_{AF})} \quad (8.3.4)$$

Equation (8.3.4) is an extremely useful expression relating in a simple manner the reactor volume, the molal flow rate at zero conversion, the change in fraction conversion accomplished in the reactor, and the reaction rate. Knowledge of any three of these quantities permits the fourth to be calculated directly. For reactor design purposes, the two problems of primary interest can be solved readily using this equation:

1. The size of the reactor needed to perform a specified task under specified operating conditions may be determined.
2. For a reactor of a given size, one may determine either the conversion achieved for a specified flow rate and temperature or the quantity of material that can be processed to a given degree of conversion at a specified temperature.

Equation (8.3.4) may also be used in the analysis of kinetic data taken in laboratory scale stirred-tank reactors. One may determine the reaction rate directly from a knowledge of the reactor volume, the molar flow rate of the limiting reagent, and stream compositions. The fact that one may determine the rate directly and without integration makes stirred-tank reactors particularly attractive for use in studies of reactions with complex rate expressions (e.g., enzymatic or heterogeneous catalytic reactions) or of systems in which multiple reactions take place. Equation (8.3.4) is

completely general and independent of whether the reaction occurs at constant density ( $\delta_A = 0$ ) and of whether the feed stream and the reactor contents have identical temperatures. The effective reactor volume is independent of the particular geometry giving rise to this volume. All that is required is that the contents be well mixed.

If the molal flow rate at zero fraction conversion is written in terms of the product of a reference volumetric flow rate  $V_0$  and a corresponding concentration ( $C_{A0}$ ),

$$\frac{V_R}{V_0} = \frac{C_{A0}(f_{A \text{ out}} - f_{A \text{ in}})}{(-r_{AF})} \quad (8.3.5)$$

In terms of the reactor space time,

$$\tau = \frac{C_{A0}(f_{A \text{ out}} - f_{A \text{ in}})}{(-r_{AF})} = \frac{C_{A0} \int_{f_{A \text{ in}}}^{f_{A \text{ out}}} df_A}{(-r_{AF})} \quad (8.3.6)$$

This equation differs from that for the plug flow reactor (8.2.9) in that for a CSTR the rate is evaluated at *effluent conditions* and thus appears *outside* the integral.

It is particularly convenient to choose the reference conditions at which the volumetric flow rate is measured as the temperature and pressure prevailing at the reactor inlet, because this choice leads to a convenient physical interpretation of the parameters  $V_0$  and  $C_{A0}$ , and in many cases, one finds that the latter quantity cancels a similar term appearing in the reaction rate expression. Unless otherwise specified, this choice of reference conditions is used throughout the remainder of the book. For constant-density systems and this choice of reference conditions, the space time  $\tau$  then becomes numerically equal to the average residence time of the fluid in the stirred tank.

Because one is almost always concerned with liquid-phase reactions when dealing with stirred-tank reactors, the assumption of constant fluid density is usually appropriate. In this case, for constant-density systems only, equation (8.3.6) can be written as

$$\tau = \frac{\int_{C_{A \text{ in}}}^{C_{A \text{ out}}} dC_A}{(r_{AF})} = \frac{C_{A \text{ in}} - C_{A \text{ out}}}{(-r_{AF})} \quad (8.3.7)$$

We now wish to consider some examples that indicate how to employ the foregoing equations in reactor design analyses.

## ILLUSTRATION 8.6 Determination of CSTR Volume Required for Isothermal Operating Conditions: Liquid Phase Reaction

Consider the Diels–Alder reaction between 1,4-butadiene (B) and methyl acrylate (M) to form an adduct (C):



If the operating conditions used in Illustration 8.3 are again employed, determine the volume of a single continuous flow stirred-tank reactor which will give 40% conversion of butadiene when the liquid flow rate is 0.500 m<sup>3</sup>/ks.

## Solution

For the conditions cited the reaction rate expression is of the form

$$-r_B = kC_{B0}(1 - f_B)C_{AlCl_3,0} \quad (A)$$

with

$$\begin{aligned} k &= 1.15 \times 10^{-3} \text{ m}^3/(\text{mol} \cdot \text{ks}) \\ C_{B0} &= 96.5 \text{ mol/m}^3 \\ C_{AlCl_3,0} &= 6.63 \text{ mol/m}^3 \end{aligned}$$

Equation (8.3.6) may be used as the basic design relation.

$$\tau = \frac{C_{B0} \int_0^{f_B} df_B}{(-r_{BF})} = \frac{C_{B0} f_B}{(-r_{BF})} \quad (B)$$

Combination of equations (A) and (B) gives

$$\tau = \frac{C_{B0} f_B}{kC_{B0}(1 - f_B)C_{AlCl_3,0}} = \frac{f_B}{k(1 - f_B)C_{AlCl_3,0}}$$

Substitution of numerical values gives

$$\tau = \frac{0.40}{(1.15 \times 10^{-3})(1 - 0.4)(6.63)} = 87.4 \text{ ks} = 24.3 \text{ h}$$

From the definition of the space time and the inlet volumetric flow rate,

$$V_R = \tau V_0 = 87.4(0.500) = 43.7 \text{ m}^3$$

This volume is appreciably larger than the volume of the plug flow reactor determined in Illustration 8.3 for the same reaction conditions and fraction conversion. However, the cost of such a reactor would be considerably less than the cost of a tubular reactor of the size determined in Illustration 8.3.

### 8.3.1.2 Mean Residence Time in Stirred-Tank Reactors

Stirred-tank reactors differ from plug flow reactors in that not all fluid elements remain in the CSTR for the same length of time. The characteristics of the residence-time distribution function are treated in Chapter 11. In this subsection we consider only the problem of determining the average residence time of a fluid element in an ideal CSTR. This problem is simplified considerably by the fact that the fluid properties are uniform throughout the reactor

and equal to those prevailing at the reactor exit. Thus, the mean residence time in an ideal CSTR is given by

$$\bar{\tau} = \frac{V_R}{V_F} \quad (8.3.8)$$

where the volumetric flow rate is evaluated at effluent conditions.

The effluent volumetric flow rate is also given by

$$V_F = V_0(1 + \delta_{AF}) \quad (8.3.9)$$

where  $V_0$  is the volumetric flow rate evaluated at a composition corresponding to zero fraction conversion. Combining equations (8.3.8) and (8.3.9) gives

$$\bar{\tau} = \frac{V_R}{V_0(1 + \delta_{AF})} = \frac{\tau}{1 + \delta_{AF}} \quad (8.3.10)$$

Unlike the situation in the PFR, there is always a simple relationship between the mean residence time and the reactor space time for a CSTR. Since one normally associates a liquid feed stream with these reactors, volumetric expansion effects are usually negligible ( $\delta_A = 0$ ). In this situation the mean residence time and the reactor space time become identical.

### 8.3.1.3 Relative Size Requirements for an Individual Continuous Stirred-Tank Reactor and a Plug Flow Reactor

In the development of the final reactor design for a proposed production requirement, the chemical engineer must consider a variety of reactor types and modes of operation. Several factors must be considered in the development of the final design, some of which may be related only peripherally to the kinetics of the reaction in question. Many of these factors are implicit in the questions posed in Section 8.0.1. Because a variety of operating conditions, modes of operation, and reactor types can be used to accomplish a specified task, it is not possible to generate a simple logical procedure that can be followed to arrive at a truly optimum design. A knowledge of the performance characteristics of individual ideal reactors (and combinations thereof) and sound engineering judgment based on previous design experience are both useful in arriving at a workable design. The non-analytical reasoning that must be used in design calculations is beyond the scope of this book. This capability comes only with the accumulation of experience and interactions with other people who have long been regularly engaged in the practice of reactor design. We can, however, indicate the quantitative considerations that have an important bearing on the economics of the proposed design. The choice of the reactor network employed to carry out the conversion desired will play an important role in that it will specify the size of the units needed and the distribution

of products emerging from the reactor. In this section we turn our attention to the problem of determining relative size requirements for a single ideal CSTR and a PFR where both reactors operate isothermally at the same temperature. The analysis applies to systems in which only one reaction occurs to a significant extent.

For most of the commonly encountered types of reaction rate expressions the rate decreases monotonically with increasing fraction conversion. The fact that a step change in composition occurs as a fluid enters an ideal CSTR implies that for these cases the volume average reaction rate will be much smaller in this type of reactor than it would be in a tubular reactor being used to accomplish the same composition change. Consequently, the CSTR must be significantly larger than the corresponding PFR. These considerations are evident from a brief consideration of Figure 8.6a. In a plug flow reactor one moves from right to left along the rate curve as he or she proceeds from inlet to outlet. In a CSTR, on the other hand, the reaction rate is constant throughout the reactor and equal to that prevailing at the outlet. Except in the case of autocatalytic reactions (see Section 9.4), this rate corresponds to the lowest point on the PFR rate curve and implies that a larger volume will be required to accomplish the same composition change between inlet and outlet streams.

It is possible to reduce the disparity in reactor volumes by using several tanks in a series configuration so that one obtains stepwise changes in composition as one proceeds from tank to tank. This situation is depicted in Figure 8.6b for the case of three CSTRs in series. In this case it is readily apparent that each of the CSTRs would have a larger volume than that of a PFR necessary to effect the same composition change, so that the total volume of the three CSTRs would exceed that of a single PFR used to effect the same overall change in composition. (We have shown earlier that the three PFRs in series would be equivalent to a single PFR with a volume equal to the sum of those of the individual PFRs.) As one increases the number of CSTRs in series, the disparities in total volume become less and, in the limit, as the number of identical CSTRs approaches infinity the battery will approach PFR behavior. For now, however, we will limit the discussion to comparison of the relative sizes of a single CSTR and a PFR when each operates isothermally at the same temperature.

To be able to compare relative reactor sizes, one needs a knowledge of the form of the reaction rate expression in either graphical or analytical terms. In Section 8.2.1 we showed that the area under a plot of the reciprocal reaction rate ( $-1/r_A$ ) versus fraction conversion was equal to the ratio  $V_R/F_{A0}$  for a plug flow reactor. In the case of a single CSTR, equation (8.3.4) indicates that on a similar plot, the quantity  $V_R/F_{A0}$  is equal to the rectangular area shown in Figure 8.7. Thus, the ratio of the rectangular area to the area under the curve is equal to the ratio of reactor volumes

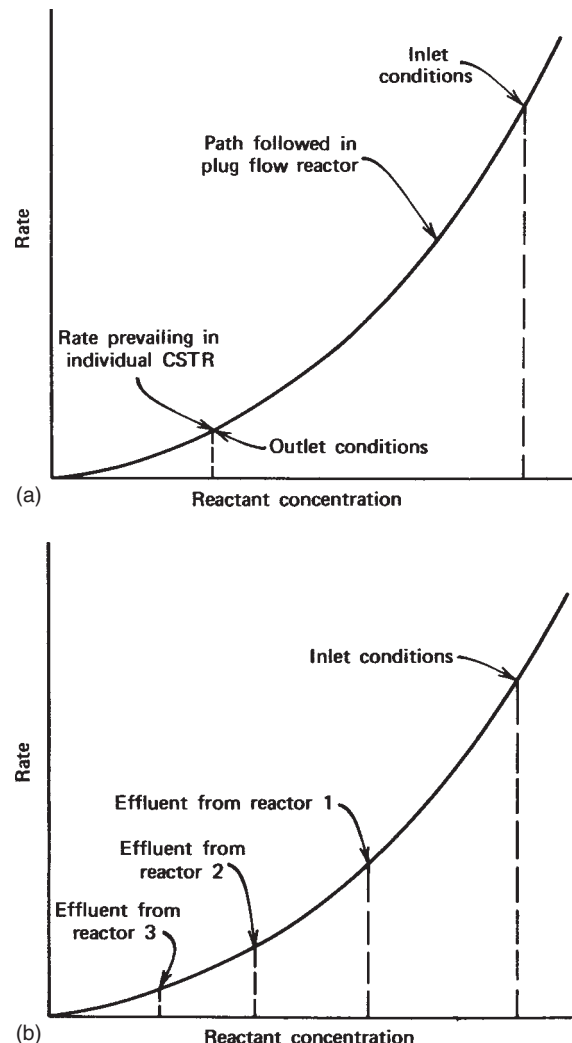


**Figure 8.6** (a) Reaction rate versus reactant concentration plot for typical reactions: single ideal CSTR reactor. (b) Reaction rate versus reactant concentration plot for typical reactions: cascade of three CSTR reactors.

if identical molar flow rates and conversion increments are employed. For any rate expression that decreases monotonically with increasing fraction conversion, the CSTR will always require a larger reactor volume than the corresponding PFR used to accomplish the same task.

If one knows the analytical form of the reaction rate expression, equations (8.2.7) and (8.3.4) may be used to determine the relative reactor volumes required. To indicate the utility of these equations, let us consider the general class of reactions that follow simple  $n$ th-order kinetics with  $n$  normally lying between zero and 3. Following Levenspiel's analysis (11), we will presume that the inlet fraction conversion is zero and that the volumetric expansion parameter ( $\delta_A$ ) has some arbitrary value. Consequently,

$$-r_A = \frac{kC_{A0}^n(1-f_A)^n}{(1+\delta_A f_A)^n} \quad (8.3.11)$$

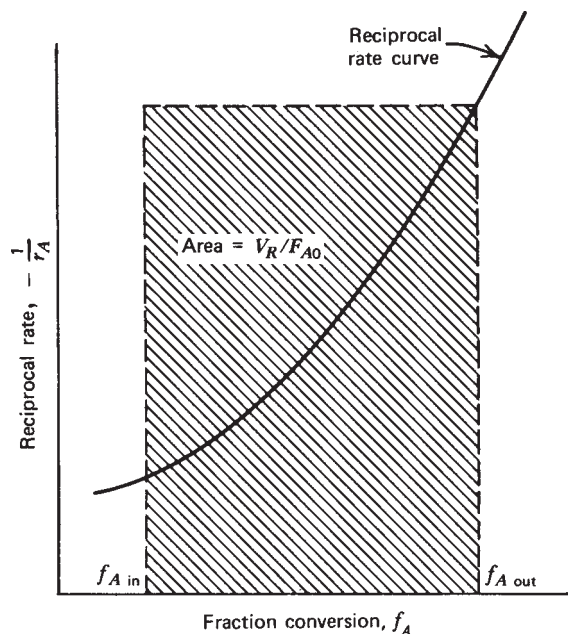


**Figure 8.7** Reciprocal rate versus fraction conversion plot for determination of  $V_R/F_{A0}$  for a single CSTR.

For these conditions the general design equation for a plug flow reactor (8.2.7) becomes

$$\left(\frac{V_R}{F_{A0}}\right)_{\text{PFR}} = \int_0^{f_A} \frac{(1 + \delta_A f_A)^n df_A}{k C_{A0}^n (1 - f_A)^n} \quad (8.3.12)$$

while that for a single CSTR [equation (8.3.4)] becomes

$$\left(\frac{V_R}{F_{A0}}\right)_{\text{CSTR}} = \frac{f_A}{k C_{A0}^n} \left( \frac{1 + \delta_A f_A}{1 - f_A} \right)^n \quad (8.3.13)$$

Division of equation (8.3.13) by equation (8.3.12) gives

$$\frac{(V_R C_{A0}^n / F_{A0})_{\text{CSTR}}}{(V_R C_{A0}^n / F_{A0})_{\text{PFR}}} = \frac{f_A [(1 + \delta_A f_A) / (1 - f_A)]^n}{\int_0^{f_A} [(1 + \delta_A f_A)^n / (1 - f_A)^n] df_A} \quad (8.3.14)$$

Levenspiel (11) has evaluated the right side of equation (8.3.14) for various values of  $n$  and  $\delta_A$ . His results are presented in graphical form in Figure 8.8. For identical feed concentrations ( $C_{A0}$ ) and molal flow rates ( $F_{A0}$ ), the ordinate of the figure indicates the volume ratio required for a specified conversion level.

There are several useful generalizations that may be gleaned from a thorough study of Figure 8.8. They include the following.

1. If the reaction order is positive, the CSTR is larger than the PFR at all conversion levels.
2. The higher the fraction conversion involved, the greater the disparity between the sizes of the CSTR and the PFR.

3. The higher the order of the reaction, the greater the ratio of sizes at a fixed conversion level. For zero-order reactions, reactor size is independent of reactor type.

4. Variations in fluid density on reaction can have significant effects on the size ratio, but the effects are secondary compared to the variations in reaction order. For positive values of the expansion parameter  $\delta_A$ , the volume ratio is increased; for negative values of  $\delta_A$ , the volume ratio decreases. However, the fact that in practice CSTRs are used only for liquid-phase reactions renders this point academic.

The larger volume requirement of the CSTR does not necessarily imply extra capital costs, especially for reactions that occur at ambient pressure. However, the fact that the required CSTR volume increases rapidly at high conversion levels leads to some interesting optimization problems in reactor design. The chemical engineer must find the point at which he obtains an economic trade-off between the high fraction conversion obtained in a large reactor versus the low conversions in a small reactor. In the first situation the equipment costs will be high and the product separation costs and raw material costs low; in the second case, equipment costs will be low and the other costs high. The optimization problem may be further complicated by allowing the number of CSTRs employed to vary, as we will see in Section 8.3.2.3.

In Illustrations 8.3 and 8.6 we considered the reactor-size requirements for the Diels–Alder reaction between 1,4-butadiene and methyl acrylate. For the conditions cited the reaction may be considered as a pseudo first-order reaction with  $\delta_A = 0$ . At a fraction conversion of 0.40, the PFR volume required was  $33.5 \text{ m}^3$ , while the CSTR volume required was  $43.7 \text{ m}^3$ . The ratio of these volumes is 1.30. From Figure 8.8 the ratio is seen to be identical with this value. Thus, this figure or equation (8.3.14) can be used in solving a number of problems involving a comparison of the performance of an individual CSTR with that of a plug flow reactor for systems that obey  $n$ th-order kinetics. Mixed second- and third-order reactions can also be handled in terms of the  $n$ th-order model if stoichiometric ratios of reactants are used. The techniques employed in solving problems using the figure are discussed in Section 8.3.2.3 after a corresponding figure has been developed for use with multiple identical CSTRs connected in series.

### 8.3.1.4 CSTR Performance Under Non-Steady-State Conditions

During startup and shutdown periods and during shifts from one steady state operating condition to a second, the design equations developed in Section 8.3.1.1 are no longer appropriate. In these cases the starting point for the analysis must be the generalized material and energy balance equations containing accumulation terms [equations

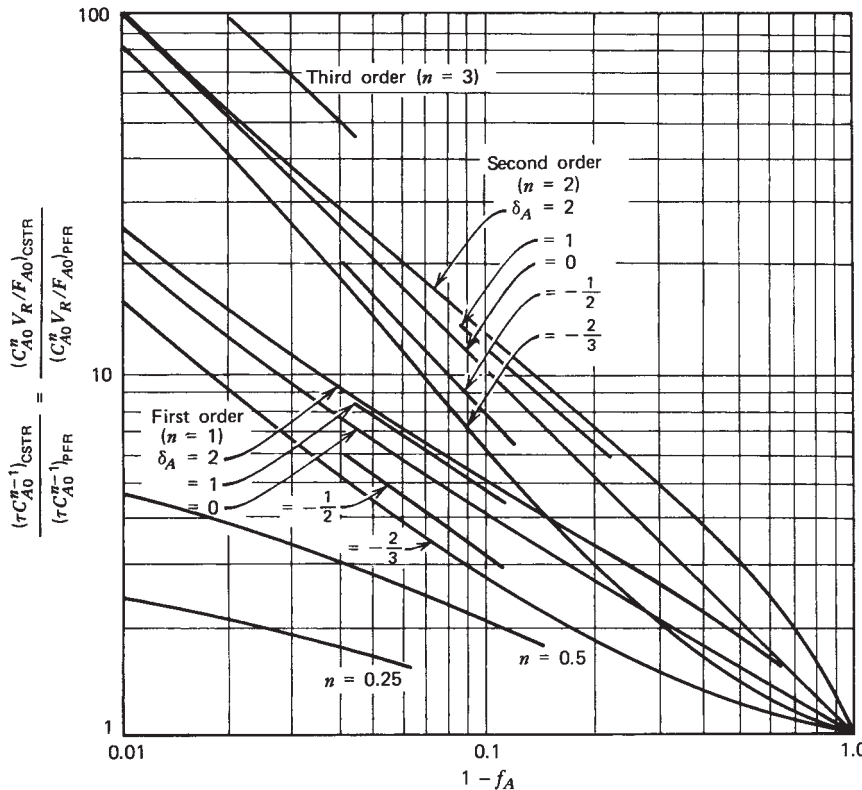


**Figure 8.8** Comparison of performance of a single CSTR and a plug flow reactor for the  $n$ -th-order reactions  $A \rightarrow$  products,  $-r_A = kC_A^n$ . The ordinate becomes the volume ratio  $V_{\text{CSTR}}/V_{\text{PFR}}$  or the space-time ratio  $\tau_{\text{CSTR}}/\tau_{\text{PFR}}$  if the same quantities of identical feed are used. (Adapted from O. Levenspiel, *Chemical Reaction Engineering*, 2nd ed., Copyright © 1972. Reprinted by permission of John Wiley & Sons, Inc.)

(8.0.1) and (8.0.3)]. To indicate the general approach to the non-steady-state analysis of reactors, we wish to consider briefly the relations that govern the transient behavior of an individual CSTR operating *under isothermal conditions*. In some cases it is possible to easily obtain analytical solutions describing the approach to the steady state because of the uniform composition of the reactor contents. This situation is in distinct contrast to that prevailing in a plug flow reactor, where one must invariably resort to numerical solutions of the transient material balance relations in order to describe the approach to steady-state conditions.

For non-steady-state operating conditions the generalized material balance on reactant A is as follows:

$$\begin{aligned} \text{input} &= \text{output} + \text{disappearance by reaction} \\ &\quad + \text{accumulation} \\ F_{A \text{ in}} &= F_{A \text{ out}} + (-r_{AF})V_R + \frac{dN_A}{dt} \end{aligned} \quad (8.3.15)$$

where the reaction rate is evaluated at the conditions prevailing at the reactor outlet and  $N_A$  is the total number of moles of species A in the reactor at time  $t$ .  $N_A$  may change as a result of changes in the volume occupied by the reacting fluid or as a result of changes in the composition of the fluid. Since

$$N_A = C_{AF}V_R \quad (8.3.16)$$

then

$$\frac{dN_A}{dt} = V_R \frac{dC_{AF}}{dt} + C_{AF} \frac{dV_R}{dt} \quad (8.3.17)$$

If the molal flow rates are written as the product of a concentration and a volumetric flow rate, and if equation (8.3.17) is combined with equation (8.3.15),

$$C_{A \text{ in}}V_{\text{in}} = C_{AF}V_{\text{out}} + (-r_{AF})V_R + V_R \frac{dC_{AF}}{dt} + C_{AF} \frac{dV_R}{dt} \quad (8.3.18)$$

For liquid-phase reactions where  $\delta_A = 0$ , the following expression is appropriate.

$$\frac{dV_R}{dt} = V_{\text{in}} - V_{\text{out}} \quad (8.3.19)$$

Combining equations (8.3.18) and (8.3.19) gives

$$\frac{dC_{AF}}{dt} - r_{AF} = (C_{A \text{ in}} - C_{AF}) \frac{V_{\text{in}}}{V_R} \quad (8.3.20)$$

There are several interesting forms of equation (8.3.20) that correspond to various limiting conditions. For example, if both  $V_R$  and  $V_{\text{in}}$  are time invariant, we have the situation corresponding to a shift from one steady-state operating condition to a second, and the quantity  $V_R/V_{\text{in}}$  is just the reactor space time  $\tau$ . Hence, for this case,

$$\frac{dC_{AF}}{dt} - r_{AF} = \frac{C_{A \text{ in}} - C_{AF}}{\tau} \quad (8.3.21)$$

It is readily apparent that equation (8.3.21) reduces to the basic design equation [equation (8.3.7)] when steady state conditions prevail. Under the presumptions that  $C_{A \text{ in}}$  undergoes a step change at time zero and that the system is isothermal, equation (8.3.21) has been solved for various reaction rate expressions. In the case of first-order reactions, solutions are available for both multiple identical CSTRs in series and individual CSTRs (12). In the case of a first-order irreversible reaction in a single CSTR, equation (8.3.21) becomes

$$\frac{dC_{AF}}{dt} = \frac{C_{A \text{ in}}}{\tau} - \frac{C_{AF}}{\tau} - kC_{AF} \quad (8.3.22)$$

This equation is an ordinary linear differential equation with constant coefficients if  $C_{A \text{ in}}$  and the rate constant are time independent. In this case the solution may be obtained by separation of variables and integration:

$$\int_{C^*}^{C_{AF}} \frac{dC_{AF}}{(C_{A \text{ in}}/\tau) - [k + (1/\tau)]C_{AF}} = \int_0^t dt \quad (8.3.23)$$

where  $C^*$  is the reactant concentration in the tank at time zero. Integration gives

$$\frac{\ln \left\{ \frac{(C_{A \text{ in}}/\tau) - [k + (1/\tau)]C^*}{(C_{A \text{ in}}/\tau) - [k + (1/\tau)]C_{AF}} \right\}}{k + (1/\tau)} = t \quad (8.3.24)$$

or

$$C_{AF} = \frac{C_{A \text{ in}}}{k\tau + 1} + \left( C^* - \frac{C_{A \text{ in}}}{k\tau + 1} \right) e^{-(k\tau + 1)t/\tau} \quad (8.3.25)$$

where the first term on the right is just the steady-state effluent concentration.

### 8.3.2 Cascades of Stirred-Tank Reactors

To reduce the disparities in volume or space-time requirements between an individual CSTR and a plug flow reactor, batteries or cascades of stirred-tank reactors are employed. These reactor networks consist of a number of stirred-tank reactors connected in series with the effluent from one reactor serving as the feed to the next. Although the concentration is uniform within any single reactor, there is a progressive decrease in reactant concentration as one moves from the initial tank to the final tank in the cascade. In effect, there are stepwise variations in composition as one moves from one CSTR to the next. Figure 8.9 illustrates the stepwise variations typical of reactor cascades. In the general nonisothermal case one will also encounter stepwise variations in temperature as one passes from one reactor to the next in the cascade.

Each of the individual CSTRs that make up the cascade can be analyzed using the techniques and concepts developed in Section 8.3.1. The present discussion concerns how one can manipulate the key relations developed earlier to obtain equations that simplify the analysis of a cascade of ideal CSTRs.

We begin by indicating a few generalizations that are relevant to the treatment of batteries of stirred-tank reactors. Consider the cascade of ideal CSTR's shown in Figure 8.10. For any individual reactor denoted by the subscript  $i$ , the basic design equation developed earlier as equation (8.3.4) is appropriate:

$$\frac{V_{Ri}}{F_{A0}} = \frac{f_{A \text{ out}} - f_{A \text{ in}}}{-r_{AF}} = \frac{f_i - f_{i-1}}{-r_{Ai}} \quad (8.3.26)$$

where the subscripts used are as indicated in the figure and  $(-r_{Ai})$  is the rate of disappearance of species A in reactor  $i$ . We wish to emphasize that  $F_{A0}$  is the molal flow rate of reactant A under conditions that would correspond to zero fraction conversion. We should also note that the conditions within any individual reactor are not influenced by what happens in reactors downstream. The conditions characteristic of its inlet stream and those prevailing within the reactor itself are the only variables that influence the performance of an individual reactor under either steady state or transient conditions.

If desired, equation (8.3.26) can also be written in terms of the reactor space time for the  $i$ th reactor as

$$\tau_i = \frac{V_{Ri}}{V_0} = \frac{C_{A0}(f_i - f_{i-1})}{-r_{Ai}} \quad (8.3.27)$$

where  $C_{A0}$  is the reactant concentration corresponding to zero conversion at the inlet temperature and pressure.

Equations (8.3.26) and (8.3.27) are generally applicable to all types of CSTR cascades. If one recognizes that the use of such cascades is almost invariably restricted to liquid systems and that in such systems density changes caused by reaction or thermal effects are usually quite small, then additional relations or simplifications can be developed from these starting equations. In particular, this situation implies that at steady state the volumetric flow rate between stages is substantially constant. It also implies that for each reactor,  $\bar{t}_i = \tau_i$ , and that the following relation between concentration and fraction conversion is appropriate:

$$C_{Ai} = C_{A0}(1 - f_i) \quad (8.3.28)$$

where  $C_{Ai}$  is the concentration of reactant A leaving the  $i$ th reactor. Throughout the remainder of Section (8.3.2) we will make the assumption of constant density. We should also recall that the development of equation (8.3.26) presumed steady state operation, and thus this assumption is also made throughout Sections 8.3.2.1 to 8.3.2.3.

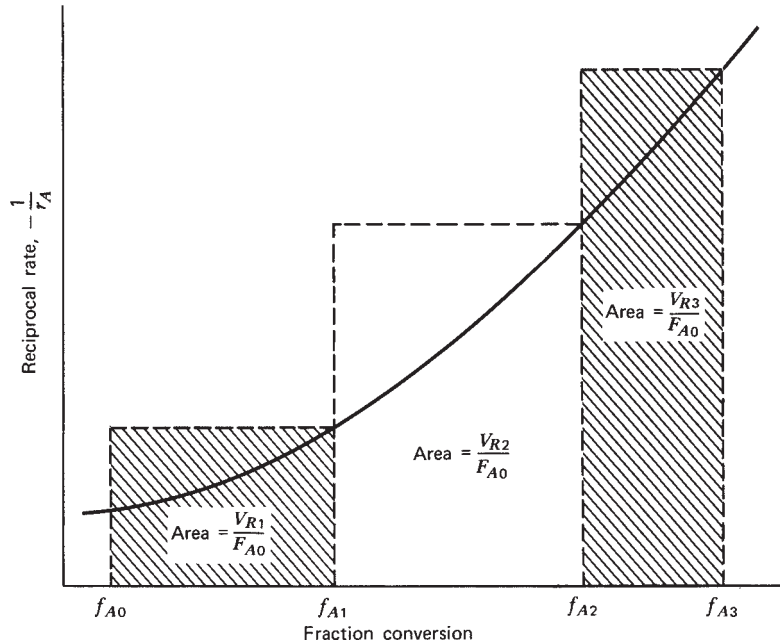
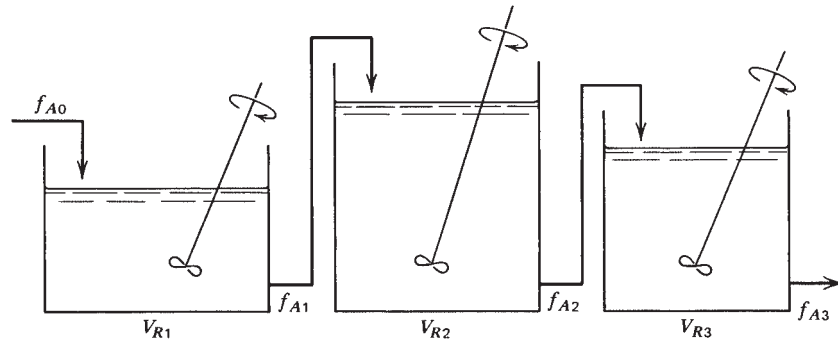


**Figure 8.9** Schematic representation of reciprocal rate curve for a cascade of three arbitrary-sized CSTRs.

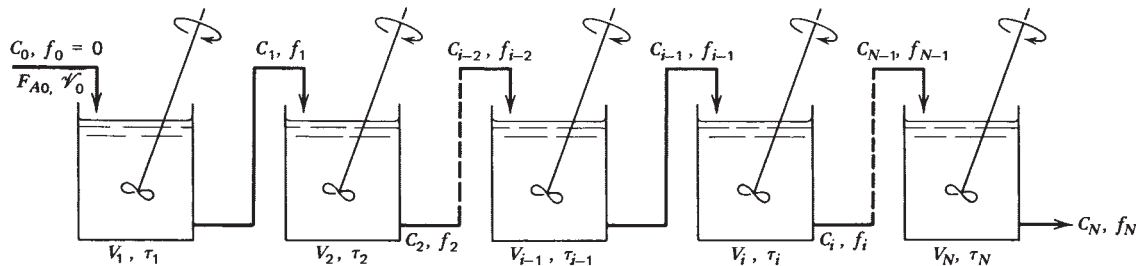


**Figure 8.10** Notation for a cascade of  $N$  CSTRs in series.

In view of equation (8.3.28) and these assumptions, equation (8.3.27) can be rewritten as

$$\tau_i = \frac{V_{Ri}}{V_0} = \frac{C_{A(i-1)} - C_{Ai}}{-r_{Ai}} \quad (8.3.29)$$

This equation is the one that is most appropriate for use in the next two subsections in that we will find it convenient to work in terms of reactant concentrations instead of conversion levels.

### 8.3.2.1 Graphical Approach to the Analysis of Batteries of Stirred-Tank Reactors Operating at Steady State

Even in reaction systems where it is not possible to determine the algebraic form of the reaction rate expression, it is often possible to obtain kinetic data that permit one to express graphically the rate as a function of the concentration of one reactant. Laboratory-scale CSTRs are

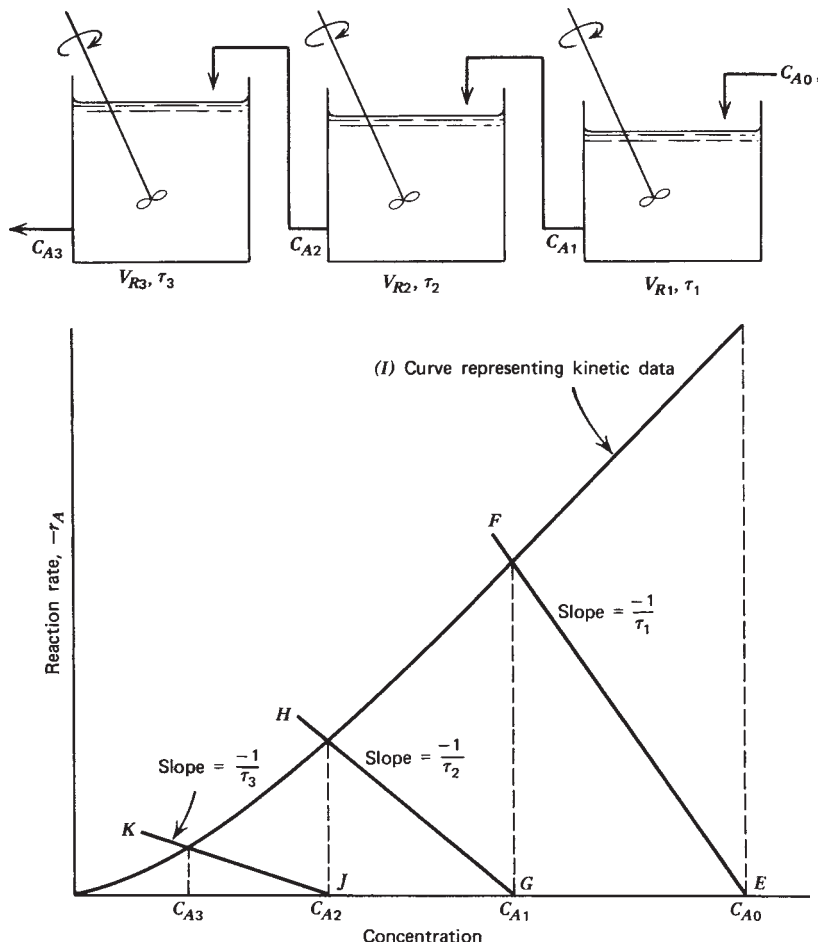


**Figure 8.11** Plot used in the graphical analysis of cascades of ideal CSTRs.

particularly appropriate for generating this type of kinetic data for complex reaction systems. In this section we presume a knowledge of the reaction rate expression as a function of the concentration of reactant A, at least in graphical terms. That is, we presume that

$$-r_A = g(C_A) \quad (8.3.30)$$

where  $g(C_A)$  characterizes this known function. For present purposes we assume that *the CSTRs all operate at the same temperature* and that  $g(C_A)$  is known at this temperature.

Equation (8.3.29) may be written in the form

$$-r_{Ai} = \frac{C_{A(i-1)} - C_{Ai}}{\tau_i} \quad (8.3.31)$$

In graphical terms this equation indicates that a plot of  $(-r_A)$  versus  $C_{Ai}$  is a straight line with a slope  $-1/\tau_i$  that cuts the abscissa at  $C_{A(i-1)}$ . An analysis of the reactor design problem involves the simultaneous solution of equation (8.3.30) and several equations of the form of equation (8.3.31) (one for each reactor). These equations are the basis for the solution of the two types of problems

with which the reactor designer is most often faced in the analysis of cascades of ideal CSTRs.

1. What is the final effluent composition from a network of such reactors? (We might also require the composition of the stream leaving each reactor.)
2. What combination of ideal CSTRs is best suited to achieving a specified conversion?

Each of these problems will be considered in turn. Consider the three ideal CSTRs shown in Figure 8.11. The characteristic space times of these reactors may differ widely. Note that the direction of flow is from right to left. The first step in the analysis requires the preparation of a plot of reaction rate versus reactant concentration based on experimental data [i.e., the generation of a graphical representation of equation (8.3.30)]. This plot is shown as curve I in Figure 8.11.

Now, for the first reactor, equation (8.3.31) becomes

$$-r_1 = \frac{C_{A0} - C_{A1}}{\tau_1} \quad (8.3.32)$$

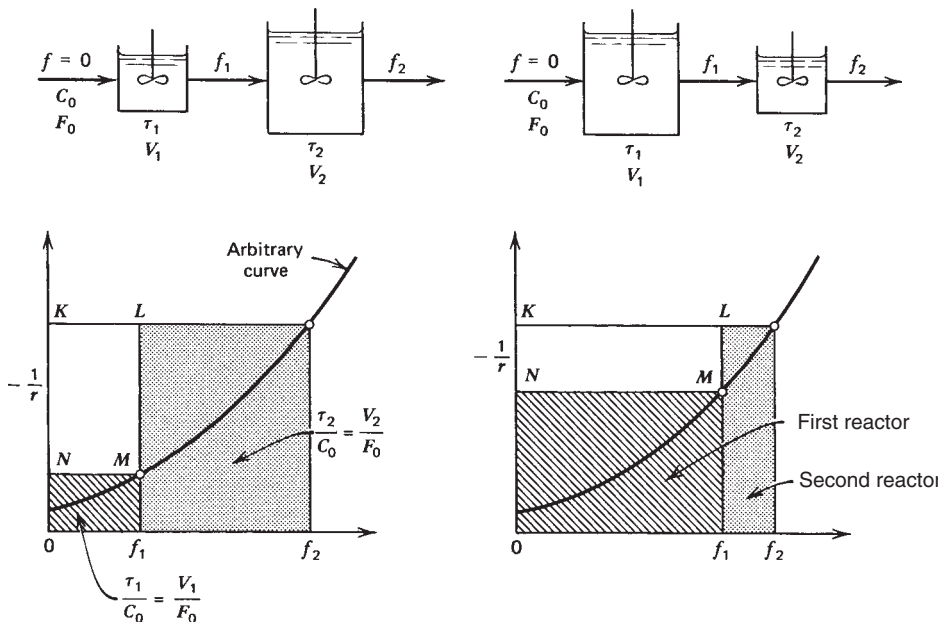


**Figure 8.12** Graphical representation of variables for the cascade of two CSTRs. Shaded rectangular areas are measures of  $V/F_0$ . (Adapted from O. Levenspiel, *Chemical Reaction Engineering*, 2nd ed., Copyright © 1972. Reprinted by permission of John Wiley & Sons, Inc.)

For a specified inlet concentration this equation indicates that a plot of  $-r_1$  versus  $C_{A1}$  is a straight line with slope  $-1/\tau_1$  that passes through the point where the ordinate is zero and the abscissa is  $C_{A0}$ . However, only the point of intersection of the straight line with the curve representing equation (8.3.30) has physical meaning. This point represents the conditions that must prevail in the first reactor. Hence, the solution to the first part of our problem consists of drawing straight line  $EF$  through point  $E$  with slope  $-1/\tau_1$ .  $C_{A1}$  is the value of the abscissa at the point of intersection of this straight line with curve  $I$  (Figure 8.11).

Now that  $C_{A1}$  is known, it is evident that a similar process can be used to find  $C_{A2}$  because, in this case, equation (8.3.31) becomes

$$-r_2 = \frac{C_{A1} - C_{A2}}{\tau_2} \quad (8.3.33)$$

Thus one may construct straight line  $GH$  in Figure 8.11 by drawing a line of slope  $-1/\tau_2$  through the point with an ordinate of zero and an abscissa of  $C_{A1}$ . The intersection of this line with curve  $I$  gives the concentration of A in the effluent from the second reactor. This procedure can be repeated for any other reactors that may be part of the cascade. The straight line  $JK$  was constructed in this fashion for the present case.

Let us turn now to the second of the problems mentioned earlier—determination of the combination of CSTRs that is best suited to achieving a specified conversion level. We begin by considering the case of a cascade of two arbitrarily sized ideal CSTRs operating under isothermal conditions and then briefly treat the problem of using multiple identical CSTRs in series. Consider the two cascade configurations shown in Figure 8.12. For the first reactor, equation

(8.3.26) becomes

$$\frac{V_{R1}}{F_{A0}} = \frac{f_1 - f_0}{(-r_{A1})} \quad (8.3.34)$$

and for the second, it becomes

$$\frac{V_{R2}}{F_{A0}} = \frac{f_2 - f_1}{(-r_{A2})} \quad (8.3.35)$$

The relations indicated by these two equations are shown graphically in Figure 8.12 for two alternative configurations. In both cases the cascade operates between the same initial and final conversion levels. The same arbitrary reaction rate expression is appropriate in both instances. As the composition of the effluent from the first reactor is changed, the relative size requirements for the two individual reactors also change, as does the total volume required. The size ratio is determined by the ratio of the two shaded areas and the total volume by the sum of these areas. The total reactor volume is minimized when rectangle  $KLMN$  is made as large as possible, so the problem of selecting the optimum sizes of the two reactor components in this sense reduces to that of selecting point  $f_1$  so that the area of rectangle  $KLMN$  is maximized. Levenspiel (13) considered this general problem. We need consider only the results of his analysis.

For reaction rate expressions of the  $n$ th-order form it can be shown that there is always one and only one point that minimizes the total volume when  $n > 0$ . This situation is obtained when the intermediate fraction conversion  $f_1$  is selected so that the slope of the curve representing the reaction rate expression at this conversion level is equal to the slope of the diagonal of rectangle  $KLMN$ , as shown in

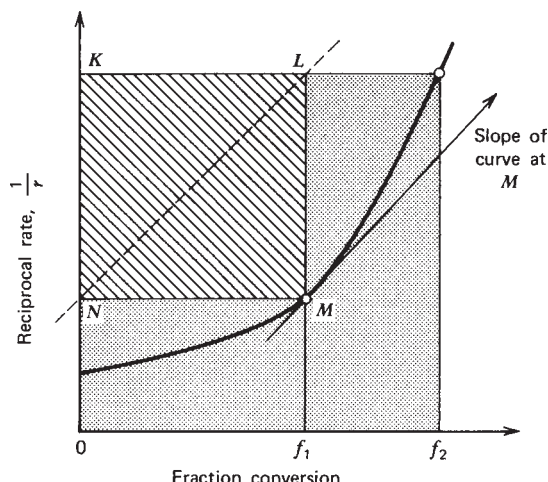


**Figure 8.13** Maximization of rectangles applied to find the optimum intermediate conversion and optimum sizes of two CSTRs in a cascade configuration. (Adapted from O. Levenspiel, *Chemical Reaction Engineering*, 2nd ed. Copyright © 1972. Reprinted by permission of John Wiley & Sons, Inc.)

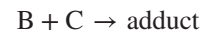
Figure 8.13. Once this conversion level is known, equations (8.3.34) and (8.3.35) may be used to determine the reactor sizes required.

As Levenspiel points out, the optimum size ratio is generally dependent on the form of the reaction rate expression and on the conversion task specified. For first-order kinetics (either irreversible or reversible with first-order kinetics in both directions), equal-sized reactors should be used. For orders above unity, the smaller reactor should precede the larger; for orders between zero and unity, the larger reactor should precede the smaller. Szepe and Levenspiel (14) presented charts showing the optimum size ratio for a cascade of two reactors as a function of the conversion level for various reaction orders. Their results indicate that the minimum in the total volume requirement is an extremely shallow one. For example, for a simple second-order reaction where 99% conversion is desired, the minimum total volume required is only about 3% less than if equal-volume tanks had been used. For 99.9% conversion the difference is only about 4%. Generally, the savings associated with this small a reduction in total volume requirements would scarcely be adequate to cover the extra costs of engineering, installing, and maintaining two tanks of different sizes. The argument for uniformity in tank sizes becomes even stronger when cascades composed of more than two reactors are considered. Consequently, except in those rare cases where there are compelling reasons to the contrary, the reactor designer tends to employ multiple identically sized CSTRs in working up design specifications. However, it may be advantageous to run the various CSTRs at different temperatures.

For cascades of multiple equal-sized CSTRs, the problem of determining the reactor sizes necessary to achieve a specified degree of conversion can be solved by a trial-and-error procedure. In this case the lines in figures analogous to Figure 8.11 will all be parallel to one another. Consequently, one draws a number of parallel lines equal to the number of CSTRs that he or she intends to use, with the first line passing through the inlet composition. When the slope used provides the necessary match with the final effluent composition specified, this slope may be used to determine the necessary reactor volume. Illustration 8.7 indicates the use of this technique.

### ILLUSTRATION 8.7 Determination of Size Requirements for Cascades Containing Different Numbers of Identical Reactors: Graphical Solution

Consider the Diels–Alder reaction between benzoquinone (B) and cyclopentadiene (C) which was discussed in Illustration 8.1.



If the reaction occurs in the liquid phase at 25°C, determine the reactor volume requirements for cascades of one and three identical CSTRs that operate at the same temperature. The rate at which liquid feed is supplied is 0.278 m<sup>3</sup>/ks. Use the graphical approach outlined previously. The following constraints are applicable:  $r = kC_B C_C$  with  $k = 9.92 \text{ m}^3/(\text{kmol} \cdot \text{ks})$ ;  $C_{C0} = 0.1 \text{ kmol/m}^3$ ;  $C_{B0} = 0.08 \text{ kmol/m}^3$ ; conversion desired = 87.5%.

### Solution

The graphical approach requires a plot of reaction rate versus the concentration of the limiting reagent (benzoquinone). To prepare this plot it is necessary to relate the two reactant concentrations to one another. From the initial concentrations and the stoichiometric coefficients.

$$C_C = C_B + 0.02$$

Thus,

$$r = kC_B(C_B + 0.02)$$

or at 25°C,

$$r = 9.92C_B^2 + 0.1984C_B \quad (\text{A})$$

where the rate is expressed in kilomol/(m<sup>3</sup> · ks) when concentrations are expressed in kilomol/m<sup>3</sup>. Equation (A) is presented in graphical form as curve M in Figure 8.7.

For 87.5% conversion the concentration of benzoquinone in the effluent from the last reactor in the cascade will be equal to  $(1 - 0.875)(0.08)$ , or 0.010 kmol/m<sup>3</sup>.

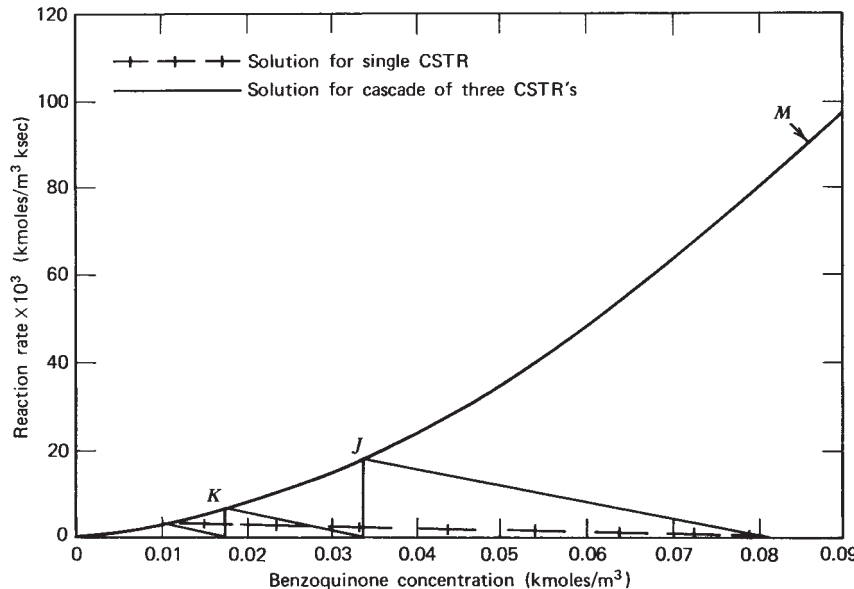


Figure I8.7 Graphical solution for cascade of CSTRs.

For the case where the cascade consists of just a single reactor, only a single straight line of the form of equation (8.3.31) is involved in the graphical solution. One merely links the point on curve  $M$  corresponding to the effluent concentration of benzoquinone with the point on the abscissa corresponding to the feed concentration. The slope of this line is equal to  $-1/\tau$  or  $-V_0/V_R$ . In the present instance the slope is equal to  $(2.976 - 0) \times 10^{-3} / (0.01 - 0.08)$  or  $-0.0425 \text{ ks}^{-1}$ . Thus,

$$V_R = \frac{V_0}{0.0425} = \frac{0.278}{0.0425} = 6.54 \text{ m}^3$$

For the case where the cascade consists of three identical reactors, a trial and-error approach is necessary to determine the reactor size required. One starts at the inlet concentration and draws a line linking this point on the abscissa with some point  $J$  on curve  $M$ . One then draws a straight line parallel to the first, but passing through the point on the abscissa corresponding to the benzoquinone concentration at point  $J$ . This straight line intersects curve  $M$  at some point  $K$ . One then repeats the procedure by drawing yet another parallel line through the point on the abscissa corresponding to the benzoquinone concentration at  $K$ . If the intersection of this straight line with curve  $M$  occurs at a reactant concentration of  $0.010 \text{ kmol/m}^3$ , the initial choice of slope was correct. If not, one must choose a new point  $J$  and repeat the procedure until such agreement is obtained. Figure I8.7 indicates the construction for this case. The slopes of the straight lines are equal to  $(18.2 - 0) \times 10^{-3} / (0.034 - 0.08)$  or  $-0.396 \text{ ks}^{-1}$ . The volume of an individual CSTR is then  $0.278/0.396$  or  $0.70 \text{ m}^3$ , and the total volume of the three CSTRs is  $2.1 \text{ m}^3$ . For the cascade the volume is reduced by more

than a factor of 3 relative to that of a single CSTR. In Section 8.3.2.3 we shall see that large volume reductions are typical for use of cascades of CSTRs.

### 8.3.2.2 Algebraic Approach to the Analysis of Cascades of Stirred-Tank Reactors Operating at Steady State

Although the graphical approach presented in Section 8.3.2.1 is quite generally applicable to the steady-state analysis of CSTR cascades, it is not highly accurate in numerical terms, particularly when the generation of the curve representing the reaction rate expression involves graphical or numerical differentiation of kinetic data. Algebraic methods are capable of greater accuracy than are graphical methods if the functional form and constants involved in the rate expression are known. In this subsection we again consider a cascade of CSTRs where the reactor volumes are not necessarily equal to one another. We again use the nomenclature shown in Figure 8.10 and start from equation (8.3.29), rearranged as follows:

$$C_{Ai} - r_{Ai}\tau = C_{A(i-1)} \quad (8.3.36)$$

Starting with the first reactor and using algebraic iteration, we proceed to analyze the cascade for particular forms of the reaction rate expression. For example, in the case of first-order kinetics,

$$C_{Ai} + k_i C_{Ai} \tau_i = C_{A(i-1)} \quad (8.3.37)$$

Thus,

$$C_{Ai} = \frac{C_{A(i-1)}}{1 + k_i \tau_i} \quad (8.3.38)$$

or

$$C_{A1} = \frac{C_{A0}}{1 + k_1 \tau_1} \quad (8.3.39)$$

and

$$C_{A2} = \frac{C_{A1}}{1 + k_2 \tau_2} = \frac{C_{A0}}{(1 + k_1 \tau_1)(1 + k_2 \tau_2)} \quad (8.3.40)$$

Finally,

$$C_{AN} = \frac{C_{A(N-1)}}{1 + k_N \tau_N} = \frac{C_{A0}}{(1 + k_1 \tau_1)(1 + k_2 \tau_2) \cdots (1 + k_N \tau_N)} \quad (8.3.41)$$

These relations are valid regardless of whether the reactors all operate at the same temperature or at different temperatures. When the cascade is isothermal and all reactors have the same size,

$$C_{AN} = \frac{C_{A0}}{(1 + k\tau)^N} \quad (8.3.42)$$

where  $\tau$  is the space time for an individual CSTR.

One may use the same general approach when the reaction kinetics are other than first-order. However, except in the case of zero-order kinetics, it is not possible to obtain simple closed-form expressions for  $C_{AN}$ , particularly if unequal reactor volumes are used. However, the numerical calculations for other reaction orders are not difficult to make for the relatively small number of stages likely to be encountered in industrial practice. The results for zero-order kinetics may be determined from equation (8.3.36) as

$$C_{AN} = C_{A0} - \sum_{i=1}^N k_i \tau_i \quad (8.3.43)$$

which is again appropriate for non-isothermal, non-equal-volume cases. If the cascade is isothermal and all reactor volumes are equal,

$$C_{AN} = C_{A0} - Nk\tau \quad (8.3.44)$$

where  $\tau$  is the space time for an individual CSTR.

Consider now the general second-order case where equation (8.3.36) becomes

$$C_{Ai} + k_1 C_{Ai}^2 \tau_i = C_{A(i-1)} \quad (8.3.45)$$

or

$$C_{Ai} = \frac{-1 + \sqrt{1 + 4k_i \tau_i C_{A(i-1)}}}{2k_i \tau_i} \quad (8.3.46)$$

where we have discarded the negative root because reactant concentrations cannot be negative. Thus,

$$C_1 = \frac{-1 + \sqrt{1 + 4k_1 \tau_1 C_0}}{2k_1 \tau_1} \quad (8.3.47)$$

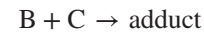
$$C_2 = \frac{-1 + \sqrt{1 + 4k_2 \tau_2 C_1}}{2k_2 \tau_2}$$

$$= \frac{-1 + \sqrt{1 + 4k_2 \tau_2 [(-1 + \sqrt{1 + 4k_1 \tau_1 C_0})/2k_1 \tau_1]}}{2k_2 \tau_2} \quad (8.3.48)$$

and so on. Although a general expression for  $C_{AN}$  would be rather complex algebraically, involving  $N$  nested square roots, the solution for the isothermal case is readily obtained numerically or graphically by the procedure outlined in Section 8.3.2.1. A number of other graphical solutions have been discussed in the reactor design literature (15–18). Illustrations 8.8 and 8.9 indicate how the techniques developed here and in Section 8.3.2.1 may be used in design analyses of cascades of stirred-tank reactors.

### ILLUSTRATION 8.8 Determination of Reactor Size Requirements for a Cascade of Identical CSTRs: Algebraic Approach

Consider the Diels–Alder reaction between benzoquinone (B) and cyclopentadiene (C), discussed in Illustrations 8.1 and 8.7.



If one employs a feed containing equimolar concentrations of reactants, the reaction rate expression can be written as

$$r = kC_C C_B = kC_B^2$$

Determine the reactor size requirements for cascades composed of one, two, and three identical CSTRs. Use an algebraic approach and assume isothermal operation at 25°C where the reaction rate constant is equal to  $9.92 \text{ m}^3/(\text{kmol} \cdot \text{ks})$ . Reactant concentrations in the feed are equal to  $0.08 \text{ kmol/m}^3$ . The liquid feed rate is equal to  $0.278 \text{ m}^3/\text{ks}$ . The desired degree of conversion is equal to 87.5%.

### Solution

For the degree of conversion specified, the effluent concentration of benzoquinone must be equal to  $(1 - 0.875) \times (0.08) = 0.01 \text{ kmol/m}^3$ .

**Case I: Single CSTR.** In this case, equation (8.3.45) can be solved for the reactor space time directly:

$$\tau = \frac{C_{A0} - C_{A1}}{kC_{A1}^2}$$

or

$$\frac{V_{R1}}{V_0} = \frac{0.08 - 0.01}{9.92(0.01)^2} = 70.56 \text{ ks}$$

Thus

$$V_{R1} = 70.56(0.278) = 19.6 \text{ m}^3$$

This value is considerably larger than that calculated in Illustration 8.7 for a nonstoichiometric feed ratio, thus indicating the potential desirability of using an excess of one reagent when it appears to be a positive power in the rate expression. In any economic analysis of a process, however, the costs of separation and recovery or disposal of the excess reagent must be taken into account.

**Case II: Two Identical CSTRs in Series.** In this case it will be necessary to determine the concentration in the effluent from the first reactor in order to determine the required reactor size. One way of proceeding is to write the design equation for each CSTR:

$$\frac{V_{R1}}{V_0} = \frac{C_{B0}(f_{B1} - 0)}{kC_{B0}^2(1 - f_{B1})^2} \quad (\text{A})$$

$$\frac{V_{R2}}{V_0} = \frac{C_{B0}(f_{B2} - f_{B1})}{kC_{B0}^2(1 - f_{B2})^2} \quad (\text{B})$$

For identical reactors, equations (A) and (B) may be combined to obtain

$$\frac{f_{B1}}{(1 - f_{B1})^2} = \frac{f_{B2} - f_{B1}}{(1 - f_{B2})^2}$$

For  $f_{B2} = 0.875$ ,

$$(1 - 0.875)^2(f_{B1}) = (0.875 - f_{B1})(1 - f_{B1})^2$$

This equation may be solved by trial and error or by graphical means to determine the composition of the effluent from the first reactor. Thus,  $f_{B1} = 0.7251$  and  $C_{B1} = 0.08(1 - 0.7251) = 0.02199 \text{ kmol/m}^3$ . Either equation (A) or (B) may now be used to determine the reactor size required. Hence,

$$V_{R1} = \frac{0.278(0.08)(0.7251)}{9.92(0.08)^2(1 - 0.7251)^2} = 3.36 \text{ m}^3$$

The total volume of the two reactors is  $6.72 \text{ m}^3$ , which is considerably less than half that required if only a single CSTR is employed.

**Case III: Three Identical CSTRs in Series.** In this case there are two intermediate unspecified reactant concentrations instead of just the single intermediate concentration

encountered in case II. At least one of these concentrations must be determined if one is to be able to size the reactors appropriately. In principle, one may follow the procedure used in case II where one writes the design equations for each CSTR and then equates the reactor space times. This procedure gives three equations and three unknowns ( $V_{R1}$ ,  $f_{B1}$ , and  $f_{B2}$ ). Thus, for the first reactor,

$$\frac{V_{R1}}{V_0} = \frac{C_{B0}(f_{B1} - 0)}{kC_{B0}^2(1 - f_{B1})^2} \quad (\text{C})$$

For the second,

$$\frac{V_{R2}}{V_0} = \frac{C_{B0}(f_{B2} - f_{B1})}{kC_{B0}^2(1 - f_{B2})^2} \quad (\text{D})$$

and for the third,

$$\frac{V_{R3}}{V_0} = \frac{C_{B0}(0.875 - f_{B2})}{kC_{B0}^2(1 - 0.875)^2} \quad (\text{E})$$

Combination of equations (C) and (E) gives

$$\frac{0.875 - f_{B2}}{(0.125)^2} = \frac{f_{B1}}{(1 - f_{B1})^2}$$

or

$$f_{B2} = 0.875 - \frac{(0.125)^2 f_{B1}}{(1 - f_{B1})^2} \quad (\text{F})$$

Combination of equations (C) and (D) yields

$$\frac{f_{B1}}{(1 - f_{B1})^2} = \frac{f_{B2} - f_{B1}}{(1 - f_{B2})^2} \quad (\text{G})$$

Now  $f_{B2}$  may be eliminated from equation (G) using equation (F):

$$\frac{f_{B1}}{(1 - f_{B1})^2} = \frac{0.875 - [(0.125)^2 f_{B1} / (1 - f_{B1})^2] - f_{B1}}{[1 - 0.875 + \{(0.125)^2 f_{B1} / (1 - f_{B1})^2\}]^2}$$

This equation may be solved numerically by trial and error, recognizing that  $f_{B1}$  must lie between 0 and 0.875. The appropriate value of  $f_{B1}$  is 0.6285. Equation (F) may now be used to determine that  $f_{B2} = 0.8038$ . With a knowledge of these conversions, equation (C), (D), or (E) may be used to determine the required reactor volume. Thus,

$$V_{R1} = \frac{0.278(0.08)(0.6285)}{9.92(0.08)^2(1 - 0.6285)^2} = 1.60 \text{ m}^3$$

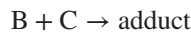
The total volume of the cascade is then  $3(1.60)$  or  $4.8 \text{ m}^3$ , which is again a significant reduction in the total volume requirement but not nearly as great as that brought about in going from one to two CSTRs in series.

Obviously, this approach is not easily extended to cascades containing more than three reactors and, in those cases, an alternative trial-and-error procedure is preferable.

One chooses a reactor volume and then determines the overall fraction conversion that would be obtained in a cascade of  $N$  reactors. When one's choice of individual reactor size meets the specified overall degree of conversion, the choice may be regarded as the solution desired. The latter approach is readily amenable to iterative programming techniques using a digital computer.

### ILLUSTRATION 8.9 Determination of Optimum Reactor Sizes for a Cascade of Two Dissimilar CSTRs

Consider the Diels–Alder reaction between benzoquinone (B) and cyclopentadiene (C) discussed in Illustrations 8.1, 8.7, and 8.8:



We wish to determine the effect of using a cascade of two CSTRs that differ in size on the volume requirements for the reactor network. In Illustration 8.8 we saw that for reactors of equal size, the total volume requirement was  $6.72 \text{ m}^3$ . If the same feed composition and flow rate as in Illustration 8.8 are employed and if the reactors are operated isothermally at  $25^\circ\text{C}$ , determine the minimum total volume required and the manner in which the volume should be distributed between the two reactors. An overall conversion of 0.875 is to be achieved.

### Solution

For the conditions cited, the reaction rate expression is of the form

$$r = kC_B^2$$

where  $k = 9.92 \text{ m}^3/\text{kmol} \cdot \text{ks}$ . From the basic design relationship for a CSTR (8.3.4),

$$\frac{V_{R1}}{F_{B0}} = \frac{f_{B1}}{kC_{B0}^2(1-f_{B1})^2} \quad (\text{A})$$

and

$$\frac{V_{R2}}{F_{B0}} = \frac{f_{B2} - f_{B1}}{kC_{B0}^2(1-f_{B2})^2} = \frac{0.875 - f_{B1}}{kC_{B0}^2(1-0.875)^2} \quad (\text{B})$$

Thus, the total reactor volume in the cascade is given by

$$V_{R1} + V_{R2} = \frac{F_{B0}}{kC_{B0}^2} \left[ \frac{f_{B1}}{(1-f_{B1})^2} + \frac{0.875 - f_{B1}}{(0.125)^2} \right] \quad (\text{C})$$

It is this sum that we desire to minimize. The easiest approach to finding this minimum is to plot the quantity in brackets versus  $f_{B1}$ . The minimum in this quantity then gives the minimum total volume, and the value of  $f_{B1}$

associated with the minimum may be used in equations (A) and (B) to determine the optimum distribution of the total volume between the two reactors. The minimum occurs when  $f_{B1} = 0.702$ .

Now

$$F_{B0} = C_{B0}V_0 = 0.08(0.278) = 0.02224 \text{ kmol/ks}$$

Thus,

$$V_{R1} = \frac{0.02224(0.702)}{9.92(0.08)^2(1-0.702)^2} = 2.77 \text{ m}^3$$

$$V_{R2} = \frac{0.02224(0.875 - 0.702)}{9.92(0.08)^2(1-0.875)^2} = 3.88 \text{ m}^3$$

and

$$V_{R1} + V_{R2} = 2.77 + 3.88 = 6.65 \text{ m}^3$$

This total differs from that for equal-sized reactors by only  $0.07 \text{ m}^3$  or approximately 1%. The benefits that would ensue from this small change would probably be far outweighed by the disadvantages associated with having reactors of different sizes, such as the costs of engineering design, construction, fabrication, and inventory of spare parts. In general, the economics associated with using reactors of different sizes are offset by the concomitant disadvantages. For further treatment of the problem of optimization of a two-tank CSTR cascade, consult the papers by Crooks (19) and Denbigh (20).

#### 8.3.2.3 Size Comparisons Between Cascades of Ideal Continuous Stirred-Tank Reactors and Plug Flow Reactors

In this section the size requirements for CSTR cascades containing different numbers of identical reactors are compared with that for a plug flow reactor used to effect the same change in composition. One may define a space time for an entire cascade ( $\tau_c$ ) in terms of the ratio of the sum of the component reactor volumes to the inlet volumetric flow rate. Hence,

$$\tau_c = \frac{\sum_{i=1}^N V_{Ri}}{V_0} = \sum_{i=1}^N \tau_i \quad (8.3.49)$$

If all component reactors have the same volume and thus the same space time ( $\tau$ ),

$$\tau_c = N\tau \quad (8.3.50)$$

For a first-order reaction, we showed that for a cascade composed of equal-sized reactors, equation (8.3.42) governed the effluent composition from the  $N$ th reactor:

$$\frac{C_{AN}}{C_{A0}} = \frac{1}{(1+k\tau)^N} \quad (8.3.51)$$

where  $\tau$  is the space time for an individual reactor. Combination of equations (8.3.50) and (8.3.51) and rearranging gives

$$\frac{C_{AN}}{C_{A0}} = \frac{1}{[1 + (k\tau_c/N)]^N} \quad (8.3.52)$$

If the right side of this equation is expanded in a binomial series,

$$\begin{aligned} \frac{C_{A0}}{C_{AN}} &= 1 + N \frac{k\tau_c}{N} + \frac{N(N-1)}{2!} \left( \frac{k\tau_c}{N} \right)^2 \\ &+ \frac{N(N-1)(N-2)}{3!} \left( \frac{k\tau_c}{N} \right)^3 + \dots \end{aligned} \quad (8.3.53)$$

and if  $e^{k\tau_c}$  is expanded in series form,

$$e^{k\tau_c} = 1 + k\tau_c + \frac{(k\tau_c)^2}{2!} + \frac{(k\tau_c)^3}{3!} + \dots \quad (8.3.54)$$

a term-by-term comparison in the limit as  $N$  approaches infinity indicates that

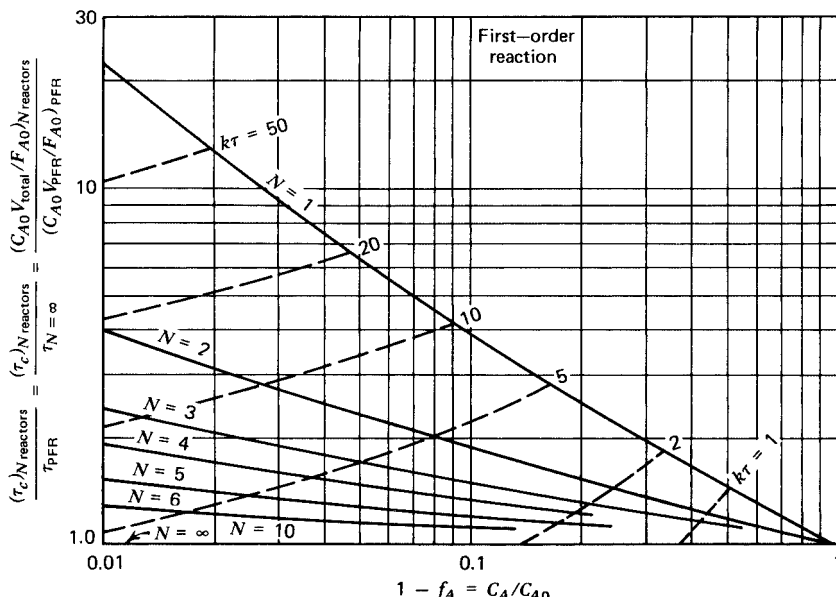
$$\frac{C_{A0}}{C_{AN}} \approx e^{k\tau_c} \quad \text{as } N \rightarrow \infty \quad (8.3.55)$$

or

$$\tau_c = \frac{1}{k} \ln \left( \frac{C_{A0}}{C_{AN}} \right) \quad \text{as } N \rightarrow \infty \quad (8.3.56)$$

This relation is identical with that which would be obtained from equation (8.2.10) for a plug flow reactor with first-order kinetics:

$$\tau_{PFR} = \frac{1}{k} \ln \left( \frac{C_{A0}}{C_{A\text{out}}} \right) \quad (8.3.57)$$



These relations support our earlier assertion that for the same overall conversion the total volume of a cascade of CSTRs should approach the plug flow volume as the number of identical CSTRs in the cascade is increased. For a finite (low) number of CSTRs in series, equation (8.3.52) can be rewritten as

$$\tau_c = \frac{N}{k} \left[ \left( \frac{C_{A0}}{C_{AN}} \right)^{1/N} - 1 \right] \quad (8.3.58)$$

The ratio of equations (8.3.58) and (8.3.57) gives the relative *total space time* requirement for a cascade of stirred-tank reactors vis-a-vis a plug flow reactor:

$$\begin{aligned} \frac{\tau_c \text{ for } N \text{ reactors}}{\tau_c \text{ for } N=\infty} &= \frac{\tau_c \text{ for } N \text{ reactors}}{\tau_{\text{plug flow}}} \\ &= \frac{N[(C_{A0}/C_{AN})_{\text{cascade}}^{1/N} - 1]}{\ln(C_{A0}/C_{A\text{out}})_{\text{plug flow}}} \end{aligned} \quad (8.3.59)$$

If the effluent streams from the two reactor configurations are to be identical and if equimolar feed rates and compositions are employed, the ratio of space times becomes equal to the ratio of the total volume requirements. For constant density systems where  $C_{A\text{out}} = C_{AN} = C_{A0}(1 - f_A)$ :

$$\frac{V_{\text{total,cascade}}}{V_{\text{PFR}}} = \frac{N\{[1/(1-f_A)]^{1/N} - 1\}}{-\ln(1-f_A)} \quad (8.3.60)$$

Figure 8.14 is in essence a plot of this ratio versus the fraction conversion for various values of  $N$ , the number of identical CSTRs employed. The larger the value of  $N$ , the smaller the discrepancy in reactor volume requirements between the CSTR cascade and a PFR reactor. Note

**Figure 8.14** Comparison of performance of a series of  $N$  equal-sized CSTR reactors with a plug flow reactor for the first-order reaction  $A \rightarrow R$ ,  $\delta_A = 0$ . For the same processing rate of identical feed, the ordinate measures the volume ratio  $V_N \text{ CSTRs}/V_{\text{PFR}}$  or the space-time ratio  $\tau_N \text{ CSTRs}/\tau_{\text{PFR}}$  directly. (Adapted from O. Levenspiel. *Chemical Reaction Engineering*, 2nd ed., Copyright © 1972. Reprinted by permission of John Wiley & Sons, Inc.)

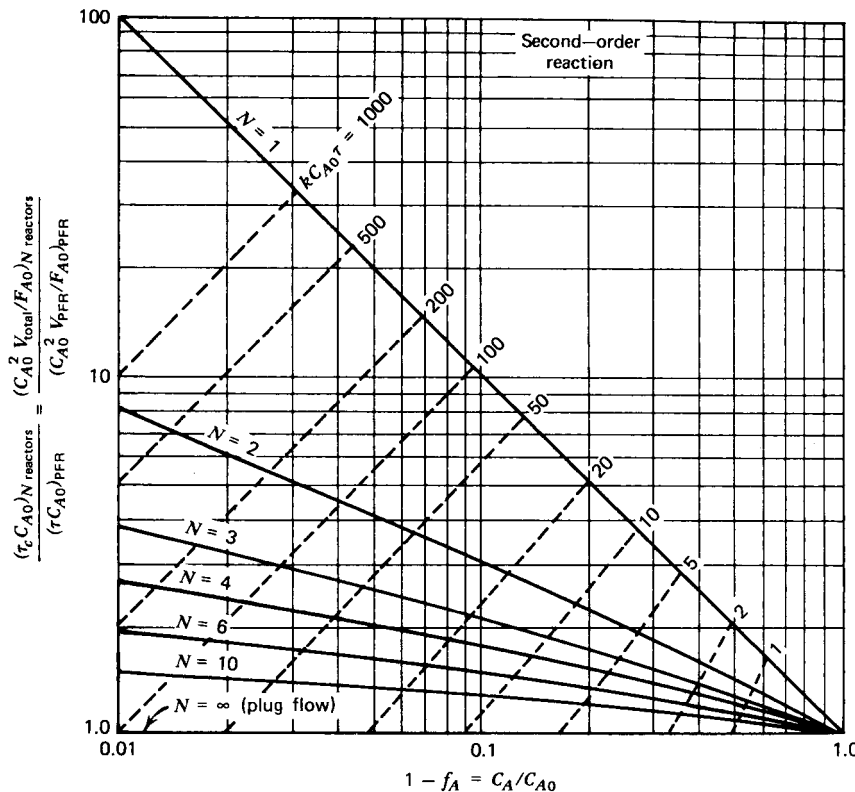


**Figure 8.15** Comparison of performance of a series of  $N$  equal-sized CSTR reactors with a plug flow reactor for elementary second-order reactions:  $2A \rightarrow \text{products}$  and  $A + B \rightarrow \text{products}$  with  $C_{A0} = C_{B0}$  with negligible expansion ( $\delta_A = 0$ ). For the same processing rate of identical feed, the ordinate measures the volume ratio  $V_N \text{ CSTRs}/V_{\text{PFR}}$  or the space-time ratio  $\tau_N \text{ CSTRs}/\tau_{\text{PFR}}$  directly. (Adapted from O. Levenspiel, *Chemical Reaction Engineering*, 2nd ed., Copyright © 1972. Reprinted by permission of John Wiley & Sons, Inc.)

how rapidly PFR behavior is approached as  $N$  increases. Levenspiel has also included lines of constant  $k\tau$  on this figure, and these lines may be useful in solving certain types of design problems, as we will see in Illustration 8.10.

Levenspiel (22) has prepared a similar plot for second-order reactions (Figure 8.15) based on a generalization of equation (8.3.46) for  $N$  identical reactors in series and the integrated form of the plug flow design equation for second-order kinetics. Inspection of Figure 8.15 again reveals that increasing the number of reactors in the cascade causes the total volume discrepancy between the cascade and a plug flow reactor to diminish rapidly, with the greatest change occurring on addition of a second tank.

Although the major thrust of the material presented in this subsection has concerned the relative size requirements for CSTR cascades and plug flow reactors, the practicing chemical engineer will be more concerned with the relative economics of the two alternative reactor network configurations. In this regard it is worth repeating that the additional capital costs associated with the larger volumes of CSTRs are relatively small, particularly when the units are designed for operation at atmospheric pressure. Consequently, a plot of the total costs associated with the use of  $N$  reactors versus the number  $N$  will usually look something like that shown in Figure 8.16. One obtains an economic trade-off between the costs associated with

the high volume requirements when very few reactors are employed and the additional engineering, fabrication, installation, and maintenance costs incurred by using a

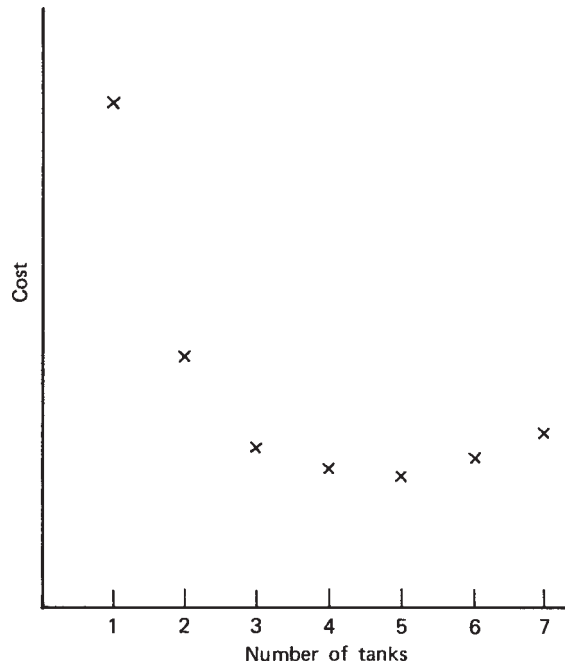


**Figure 8.16** Interaction between the cost decline associated with reduced total volume and cost increases arising from design, construction, installation, and maintenance of a number of reactors.

larger number of reactors in the cascade. Consequently, the reactor designer must consider cascades containing different numbers of reactors in the search for an economic optimum.

In Illustration 8.10 we indicate how Figures 8.14 and 8.15 are used in handling simple reactor design calculations.

### ILLUSTRATION 8.10 Use of Design Charts for Comparison of Alternative Reactor Networks

Consider the Diels–Alder reaction between benzoquinone (B) and cyclopentadiene (C) discussed in Illustrations 8.7 to 8.9:



At 25°C the reaction is first-order in each reactant with a rate constant of  $9.92 \text{ m}^3/(\text{kmol} \cdot \text{ks})$ . A feed stream containing equimolar quantities of B and C (0.1 kmol/m<sup>3</sup>) is to be processed at a rate of 0.1111 m<sup>3</sup>/ks. A tubular reactor (assume plug flow) with an effective volume of 2.20 m<sup>3</sup> is to be employed.

Use the design charts in Figures 8.8, 8.14, and 8.15 to determine the following.

1. What degree of conversion can be obtained in the tubular reactor?
2. What reactor size would be required to achieve the same conversion if a single ideal CSTR were employed?
3. What degree of conversion would be obtained in a single CSTR equal in size to the tubular reactor?
4. If two identical ideal CSTRs in series are employed (each with a volume equal to that determined in part 2), by how large a factor can the flow rate of the feed stream be increased while maintaining the conversion level constant at the value used in parts 1 and 2?
5. If one employs these same two ideal CSTRs in series and maintains a constant feed rate, what conversion is achieved?

### Solution

For an equimolar feed the reaction rate expression can be written as

$$-r_B = kC_B^2$$

#### A. Conversion for Plug Flow

The reactor space time is given by

$$\tau = \frac{V_R}{V_0} = \frac{2.2}{0.1111} = 19.80 \text{ ks}$$

Consequently, the characteristic dimensionless rate group for the second-order reaction and initial conditions is given by

$$kC_{B0}\tau = 9.92(0.1)(19.80) = 19.6$$

In Figure 8.15 the line corresponding to plug flow is that where  $V_{N \text{ CSTRs}}/V_{\text{PFR}} = 1$ . The intersection of this line and the line for a value of  $kC_{B0}\tau = 19.6$  gives the desired degree of conversion, namely 95%.

#### B. Size Requirement for CSTR for Identical Processing Task

For the same feed rate and initial concentrations, the ordinates of Figures 8.8 and 8.15 reduce to the volume ratios for the two reactors. Hence, at the same  $f_B$ , we see that  $V_{1 \text{ CSTR}}/V_{\text{PFR}} = 20$ . Thus,  $V_{1 \text{ CSTR}} = 20(2.20) = 44 \text{ m}^3$ .

#### C. Conversion in a CSTR of the Same Size as the Tubular Reactor

For a CSTR equal in volume to the tubular reactor, one moves along a line of constant  $kC_{B0}\tau$  in Figure 8.15 to determine the conversions accomplished in cascades composed of different numbers of reactors but with the same overall space time. The intersection of the line  $kC_{B0}\tau = 19.6$  and the curve for  $N = 1$  gives  $f_B = 0.80$ .

#### D. Increase in Processing Rate Arising from the Use of a Cascade of Two CSTRs at a Specified Degree of Conversion

The values of the group  $kC_{B0}\tau$  that correspond to 95% conversion and one or two CSTRs in series may be determined from Figure 8.15. They are approximately 350 and 70, respectively. Thus,

$$\frac{(kC_{B0}\tau)_{N=2}}{(kC_{B0}\tau)_{N=1}} = \frac{\tau_{N=2}}{\tau_{N=1}} = \frac{70}{350} = 0.20$$

Since

$$V_{N=2} = 2V_{N=1}$$

and

$$\frac{\tau_{N=2}}{\tau_{N=1}} = \frac{V_{N=2}}{V_{N=1}} \frac{V_{N=1}}{V_{N=2}} = 2 \frac{V_{N=1}}{V_{N=2}}$$

then

$$\frac{V_{N=2}}{V_{N=1}} = \frac{2}{0.20} = 10$$

Consequently, the processing rate for the cascade will be an order of magnitude greater than that for a single CSTR. Note that operation of the two reactors in parallel would have merely doubled the processing capacity. Hence, there is a very strong case for operating with the units in a series flow configuration.

### E. Increase in Conversion Arising from the Use of a Cascade of Two CSTRs at a Specified Feed Rate

If the feed rate is maintained constant while the number of reactors is doubled, the overall space time for the cascade will double. In the present case  $kC_{B0}\tau_{N=2} = 2(350) = 700$ . From Figure 8.15, at this value of the dimensionless group and  $N = 2$ , one finds that  $f_B = 0.99$ .

#### 8.3.2.4 Analysis of CSTR Cascades Under Non-Steady-State Conditions

In Section 8.3.1.4, equations relevant to the analysis of the transient behavior of an individual CSTR were developed and discussed. It is relatively simple to extend the most general of these relations to the case of multiple CSTRs in series. For example, equations (8.3.15) to (8.3.21) may all be applied to any individual reactor in the cascade of stirred-tank reactors, and these relations may be used to analyze the cascade in stepwise fashion. The difference in the analysis for the cascade, however, arises from the fact that more of the terms in the basic relations are likely to be time variant when applied to reactors beyond the first. For example, even though the feed to the first reactor may be time invariant during a period of non-steady-state behavior in the cascade, the feed to the second reactor will vary with time as the first reactor strives to reach its steady state condition. Similar considerations apply farther downstream. However, since there is no effect of variations downstream on the performance of upstream CSTRs, one may start at the reactor where the disturbance is introduced and work downstream from that point. In our generalized notation, equation (8.3.20) becomes

$$\frac{dC_{Ai}}{dt} - r_{Ai} = \frac{C_{A(i-1)} - C_{Ai}}{\tau_i} \quad (8.3.61)$$

where the reaction rate is evaluated at conditions prevailing in reactor  $i$  and where we have presumed both a constant density system and a constant reactor volume. In the general situation for this case the inlet and outlet concentrations [ $C_{A(i-1)}$  and  $C_{Ai}$ ] and the rate in the  $i$ th reactor in the cascade [ $-r_{Ai}$ ] may all vary with time.

For first-order irreversible reactions and identical space times it is possible to obtain closed form solutions to differential equations of the form of (8.3.61). In other cases it is usually necessary to solve the corresponding difference equations numerically.

If we were to extend the analysis developed in equations (8.3.22) to (8.3.25) to the case of just two CSTRs in series, the equation we would have to solve to determine the composition of the effluent from the second reactor

would be the following form of equation (8.3.61):

$$\frac{dC_{A2}}{dt} - kC_{A2} = \frac{1}{\tau_2} \left[ \frac{C_{A \text{ in}}}{k\tau_1 + 1} + \left( C^* - \frac{C_{A \text{ in}}}{k\tau_1 + 1} \right) e^{-(k\tau_1 + 1)t/\tau_1} - C_{A2} \right] \quad (8.3.62)$$

Mathematically inclined students are encouraged to solve this equation and to move as far downstream as they desire. All students should recognize that we have seen equations of this mathematical form in Chapter 5.

### 8.3.3 Recycle Reactors

In cases where one desires to promote backmixing in gaseous systems, it may be desirable to use a recycle reactor (Figure 8.17). The need for backmixing may arise from a desire to enhance reaction selectivity or to moderate thermal effects associated with the reaction.

Reaction takes place only within the plug flow element of the recycle reactor, and the gross product stream from this element is divided into two portions; one becomes the net product and the second is mixed with fresh feed. The mixture of the fresh feed and recycle stream is then fed to the plug flow element. By varying the relative quantities of the net product and recycle streams, one is able to obtain widely varying performance characteristics. At the limit of zero recycle the system approaches plug flow behavior, and at the limit where only an infinitesimal proportion of net product stream is produced, the system will approach CSTR behavior. To develop characteristic design equations that describe the performance of recycle reactors, we will follow Levenspiel's treatment (23). The recycle ratio  $R$  is defined as

$$R = \frac{\text{volume of fluid returned to reactor entrance}}{\text{volume of fluid leaving system in net product stream}} \quad (8.3.63)$$

The basic design equation for a plug flow reactor [equation (8.2.7)] may be used to describe the steady-state conversion achieved in the plug flow element of the recycle reactor:

$$\frac{V_R}{F'_{A1}} = \int_{f_{A1}}^{f_{A2}} \frac{df_A}{(-r_A)} \quad (8.3.64)$$

where  $F'_{A1}$  represents a hypothetical molal flow rate of A corresponding to a stream in which none of the A had reacted, where  $f_{A1}$  is the fraction of  $F'_{A1}$  that has been converted to products prior to entering the plug flow element, and where streams 2, 3, and 4 all have the same composition. No reaction takes place outside the plug flow element.

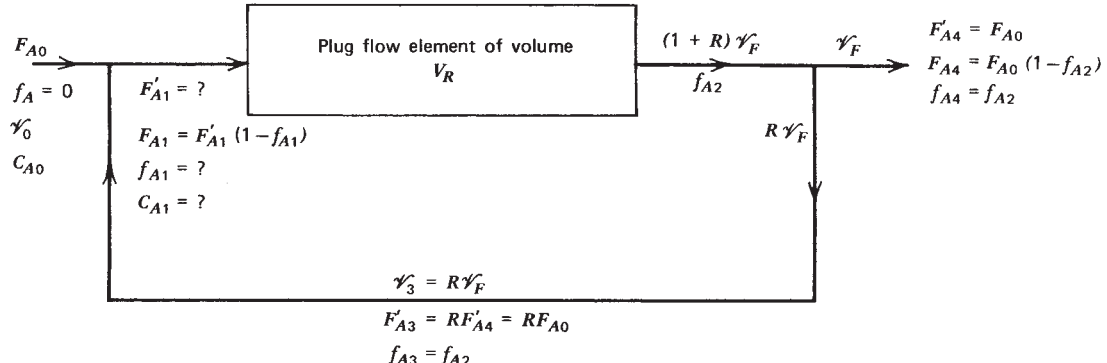


Figure 8.17 Schematic representation of recycle reactor indicating symbols used in design analysis.

Material balance considerations indicate that

$$F'_A1 = F_A0(1 + R) \quad (8.3.65)$$

In other words, the molal flow rate of A corresponding to zero fraction conversion at the inlet to the PFR element is equal to the sum of the net inlet flow rate and the amount that would have entered if none of the material in the recycle stream had undergone reaction.

The reactant concentration at the reactor inlet is given by the ratio of the molal and volumetric flow rates at the same location. Therefore,

$$C_{A1} = \frac{F_{A1}}{V_1} = \frac{F_{A0} + F_{A3}}{V_0 + V_3} \quad (8.3.66)$$

where we have recognized that for a constant-pressure system (no pressure drop through the reactor or recycle return line) there will be no volume change on mixing.

Now, from the definition of the recycle ratio,

$$V_3 = RV_4 = RV_0(1 + \delta_A f_{A2}) \quad (8.3.67)$$

and

$$F_{A3} = RF_{A4} = RF_{A0}(1 - f_{A2}) \quad (8.3.68)$$

Combining equations (8.3.66) to (8.3.68) and (3.1.47) gives

$$C_{A1} = \frac{F_{A0}[1 + R(1 - f_{A2})]}{V_0[1 + R(1 + \delta_A f_{A2})]} = C_{A0} \left( \frac{1 - f_{A1}}{1 + \delta_A f_{A1}} \right) \quad (8.3.69)$$

Thus,

$$\begin{aligned} & (1 - f_{A1})(1 + R + R\delta_A f_{A2}) \\ & = (1 + \delta_A f_{A1})(1 + R - f_{A2}R) \end{aligned} \quad (8.3.70)$$

which can be manipulated algebraically to obtain the result desired

$$f_{A1} = \frac{R}{R + 1} f_{A2} \quad (8.3.71)$$

Combining equations (8.3.64), (8.3.65), and (8.3.71) gives

$$\frac{V_R}{F_{A0}} = (R + 1) \int_{Rf_{A2}/(R+1)}^{f_{A2}} \frac{df_A}{(-r_A)} \quad (8.3.72)$$

which may be regarded as the fundamental design relationship for a recycle reactor with a zero conversion level in the feed stream mixed with the recycle stream. This relation is valid for both constant- and variable-density systems.

Examination of the limiting forms of equation 8.3.72 for  $R = 0$  and  $R = \infty$  indicates that the recycle reactor can approach either plug flow or CSTR behavior. For intermediate values of the recycle ratio this equation can be integrated if the form of the reaction rate expression is known.

## 8.4 REACTOR NETWORKS COMPOSED OF COMBINATIONS OF IDEAL CONTINUOUS FLOW STIRRED-TANK REACTORS AND PLUG FLOW REACTORS

In this section we indicate a few useful generalizations that are pertinent in considerations of series and parallel flow combinations of ideal plug flow and stirred-tank reactors operating isothermally. Parallel combinations are governed by the general principle enunciated in Section 8.2.3: *For most efficient utilization of the available reactor volume, all parallel streams that meet must have the same composition.*

Under these circumstances each parallel leg may be considered to be operating independently insofar as the space-time requirements necessary to effect a given composition change are concerned. Total feed capacity then increases in proportion to the flow rates that can be handled by the various parallel legs. The component reactors of each of the parallel legs can then be considered

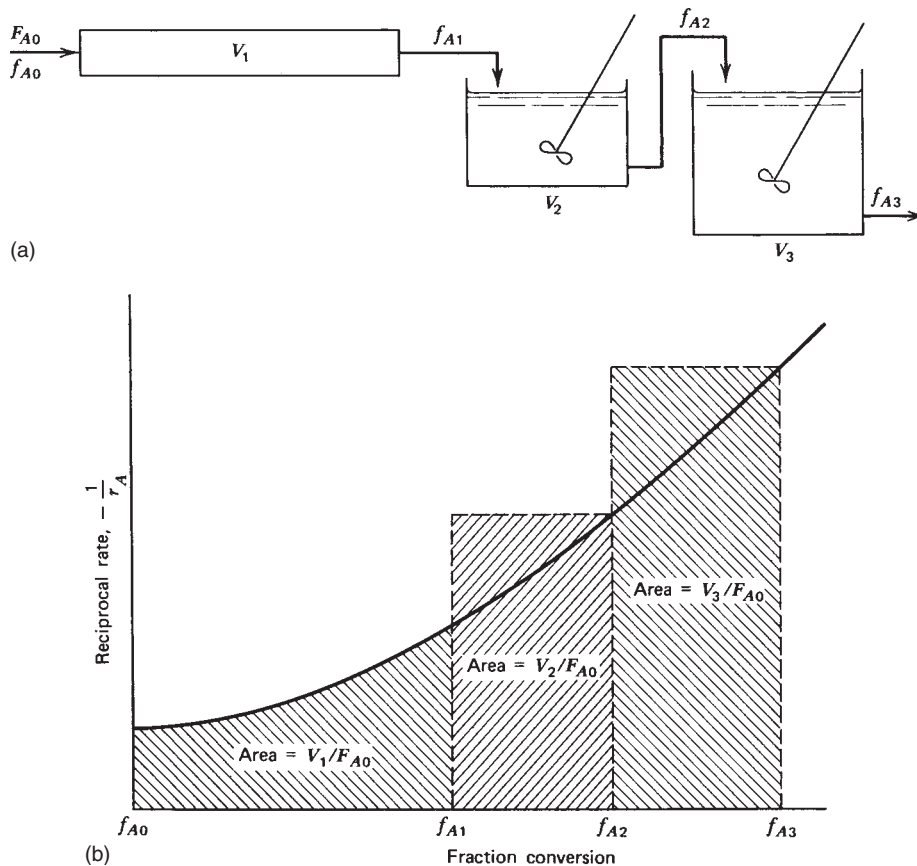


**Figure 8.18** (a) Series flow combination of a PFR and two CSTRs. (b) Graphical representation of equations (8.4.1) to (8.4.3).

as a series combination of reactors and can be optimized in terms of the general principles enunciated below.

Consider the series flow combination of a PFR and two CSTRs shown in Figure 8.18a. In terms of the fundamental design equations for these idealized reactor types [(8.2.7) and (8.3.4)], it can be said that

$$\frac{V_1}{F_{A0}} = \int_{f_{A0}}^{f_{A1}} \frac{df_A}{(-r_A)} \quad (8.4.1)$$

$$\frac{V_2}{F_{A0}} = \frac{f_{A2} - f_{A1}}{-r_{A2}} \quad (8.4.2)$$

$$\frac{V_3}{F_{A0}} = \frac{f_{A3} - f_{A2}}{-r_{A3}} \quad (8.4.3)$$

where the reaction rates in the last two equations are evaluated at the effluent conditions for each reactor and where  $F_{A0}$  is the molal flow rate of reactant A that would correspond to zero conversion. The relations above are depicted in graphical form in Figure 8.18b. If the mathematical form of the rate expression is known, these equations can be used to completely specify the necessary design parameters.

For optimum utilization of a given set of ideal reactors operating as an isothermal reactor network, an examination of the plot of  $1/(-r_A)$  versus  $C_A$  is a good way to find the best arrangement of units. The following general rules have been enunciated by Levenspiel (24).

1. For a reaction whose reciprocal rate-concentration curve rises monotonically (any  $n$ th-order reaction,  $n > 0$ ) the reactors should be connected in series. They should be ordered so as to keep the concentration of reactant as high as possible if the curve is concave ( $n > 1$ ), and as low as possible if the curve is convex ( $n < 1$ ).

For all reaction orders greater than unity, the appropriate order is plug flow, small CSTR, large CSTR. When the reaction order is less than unity, the reverse order should be employed. For a first-order reaction the conversion will be independent of the geometric arrangement of the various reactors.

2. For reactions whose plot of reciprocal rate versus concentration passes through a maximum or minimum, the arrangement of units depends on the actual shape of curve, the conversion level desired, and the units available. (See Section 9.4 for an illustration of this type.)

**Table 8.1** Summary of Design Equations Given that  $\mathcal{V} = \mathcal{V}_0(1 + \delta_A f_A)$ 

Reactor type	Measure of capacity	General design relation	Design relation for $-r_A = kC_A^n$
<b>I. Batch</b>			
A. Holding time			
1. Constant volume	$t$	$t = C_{A0} \int \frac{df_A}{(-r_A)}$	$t = \frac{1}{kC_{A0}^{n-1}} \int \frac{df_A}{(1-f_A)^n}$
2. Constant pressure	$t$	$t = C_{A0} \int \frac{df_A}{(1 + \delta_A f_A)(-r_A)}$	$t = \frac{1}{kC_{A0}^{n-1}} \int \frac{(1 + \delta_A f_A)^{n-1} df_A}{(1-f_A)^n}$
B. Equivalent space time	$\tau$	$\tau = t + t_s$	
<b>II. Plug flow</b>			
A. Mean residence time	$\bar{t}^a$	$\bar{t} = C_{A0} \int \frac{df_A}{(1 + \delta_A f_A)(-r_A)}$	$\bar{t} = \frac{1}{kC_{A0}^{n-1}} \int \frac{(1 + \delta_A f_A)^{n-1} df_A}{(1-f_A)^n}$
B. Space time	$\tau = \frac{1}{S}$	$\tau = C_{A0} \int \frac{df_A}{(-r_A)}$	$\tau = \frac{1}{kC_{A0}^{n-1}} \int \frac{(1 + \delta_A f_A)^n df_A}{(1-f_A)^n}$
<b>III. CSTR</b>			
A. Mean residence time	$\bar{t}^a$	$\bar{t} = \frac{C_{A0} \int df_A}{(-r_{AF})(1 + \delta_A f_{AF})}$	$\bar{t} = \frac{1}{kC_{A0}^{n-1}} \left[ \frac{(1 + \delta_A f_{AF})^{n-1}}{(1-f_{AF})^n} \int df_A \right]$
B. Space time	$\tau = \frac{1}{S}$	$\tau = \frac{C_{A0}}{(-r_{AF})} \int df_A$	$\tau = \frac{1}{kC_{A0}^{n-1}} \left[ \frac{(1 + \delta_A f_{AF})^n}{(1-f_{AF})^n} \int df_A \right]$

Source: Adapted from O. Levenspiel, *Chemical Reaction Engineering*, by Copyright © 1962. Reprinted by permission of John Wiley & Sons, Inc.

<sup>a</sup>Design relations indicated not recommended for use in reactor analysis.

## 8.5 SUMMARY OF FUNDAMENTAL DESIGN RELATIONS: COMPARISON OF ISOTHERMAL STIRRED-TANK AND PLUG FLOW REACTORS

Table 8.1 contains a summary of the fundamental design relations for the various types of ideal reactors in terms of equations for reactor space times and mean residence times. The equations are given in terms of both the general rate expression and *n*th-order kinetics.

If the various expressions are compared, it is evident that for constant-density situations,

$$\begin{aligned} t_{\text{batch, constant pressure}} &= t_{\text{batch, constant volume}} \\ &= \bar{t}_{\text{PFR}} = \tau_{\text{PFR}} \end{aligned} \quad (8.5.1)$$

Moreover, for negligible pressure drop through a plug flow reactor,

$$t_{\text{batch, constant pressure}} = \bar{t}_{\text{PFR}} \quad (8.5.2)$$

As we stressed earlier, the reactor space time is the independent variable at the control of the reactor designer. This

parameter is more meaningful than the mean residence time in the reactor.

If we wish to make size comparisons of batch and continuous processing equipment in terms of space time requirements, we must recognize that there are nonproductive periods associated with filling, heating, cooling, draining, cleaning, and so on, and that the long-term space-time requirement would be given by

$$\tau_{\text{batch}} = t + t_s \quad (8.5.3)$$

where  $\tau_{\text{batch}}$  is the cycle time for each batch,  $t_s$  is the average nonproductive time per batch processed, and  $t$  is given by the equations in Table 8.1.

## 8.6 SEMIBATCH OR SEMIFLOW REACTORS

For semibatch or semiflow reactors, all four of the terms in the basic material and energy balance relations [equations (8.0.1) and (8.0.3)] can be significant. The feed and effluent streams may enter and leave at different rates so as to cause

changes in both the composition and volume of the reaction mixture through the dependence of these parameters on both the operating conditions and the chemical reaction. Even in cases where the reactor operates isothermally, numerical methods may be required to solve the differential equations that govern the performance of the reactor.

It may be desirable to operate in semibatch fashion to enhance reaction selectivity or to control the rate of energy release by reaction via manipulation of the rate of addition of one reactant. Other situations in which semibatch operation is employed include a variety of biological fermentations where various nutrients may be added at predetermined rates to achieve optimum production capacity and cases where one reactant is a gas of limited solubility that can be fed only as fast as it will dissolve.

Semibatch operations usually employ a single well-stirred tank. In such cases it is possible to make the usual assumption that the composition and temperature of the fluid are uniform throughout the tank. For semibatch operation, the fraction conversion ( $f$ ) is often ambiguous for many cases of interest. If reactant is present initially in the reactor and is added or removed in feed and effluent streams, the question arises as to the proper basis for the definition of  $f$ . In such cases it is best to work either in terms of the weight fraction of a particular component present in the fluid of interest or in terms of concentrations when constant-density systems are under consideration. In terms of the symbols shown in Figure 8.19 the fundamental material balance relation becomes

$$w_0 \phi_{m0} = w_F \phi_{mF} + (-r_{AF})V_R + \frac{d}{dt}(w_F \rho_m V_R) \quad (8.6.1)$$

where  $w$  is the weight fraction reactant,  $\phi_m$  is the mass flow rate,  $\rho_m$  is the mass density of the fluid in the reactor,  $(-r_{AF})$  the reaction rate per unit volume expressed in terms of the mass of reactant A disappearing per unit time and evaluated at the conditions prevailing within the reactor, and the subscripts 0 and  $F$  indicate feed and effluent conditions, respectively. If the initial conditions of the reactor contents are known and if the feed stream conditions are specified, it is possible to solve equation (8.6.1) to determine the effluent composition as a function of time. The solution may require the use of material balance relations for other species or a total material balance. This requirement is particularly true of variable-volume situations, where the following overall material balance equation is often useful:

$$\phi_{m0} = \phi_{mF} + \frac{d}{dt}(\rho_m V_R) \quad (8.6.2)$$

By working in terms of total mass, the reaction term in equation (8.6.2) disappears because the principle of conservation of mass must be satisfied.

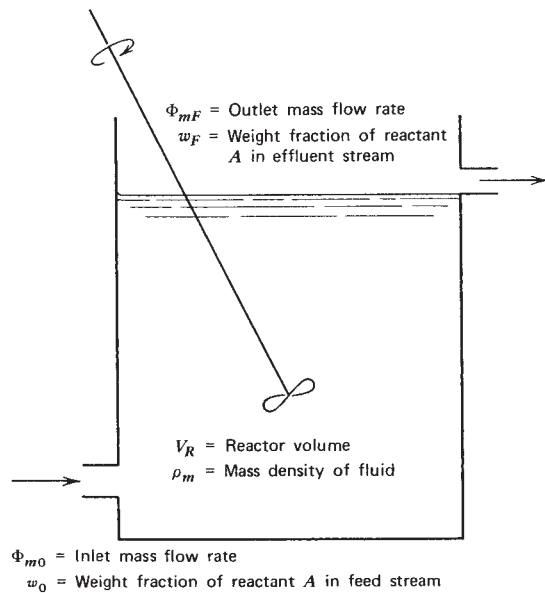


**Figure 8.19** Schematic representation of semibatch reactor indicating process variables.

There are a number of specific cases of equation (8.6.1) that are of potential interest for commercial applications. We wish to consider one mode of semibatch operation using Illustration 8.11 to indicate the general principles involved in the analysis of these systems.

Kladko (25) presented a very interesting case study of a reactor design problem involving an exothermic isomerization reaction. Although the reaction in question was well behaved in a laboratory-scale apparatus, it behaved quite differently when first conducted on a commercial scale in a batch reactor. The system ran out of control, with the temperature increasing so rapidly that the batch erupted violently through a safety valve and vented out over the building area. The fact that the strong exotherm and its concomitant effect on the reaction rate could have been predicted *a priori* on the basis of energy balance calculations indicates the necessity of considering thermal effects in reactor design calculations. These effects are the subject of Chapter 10; be particularly careful to take them into account when moving from bench- or pilot-scale reactor systems to commercial-scale equipment. Because of the proprietary nature of the product, many details of the reaction were omitted. However, by making certain assumptions or engineering estimates regarding heat capacities and molecular weights, it is possible to generate the necessary input data to permit evaluation of several alternative reactor designs. Some alternatives are considered as illustrative examples in Chapter 10, and Illustration 8.11 indicates the type of analysis appropriate to isothermal semibatch operation.

## ILLUSTRATION 8.11 Isomerization in a Semibatch Reactor

Reagent A undergoes an essentially irreversible isomerization reaction that obeys first-order kinetics:



Both A and B are liquids at room temperature and both have very high boiling points. A 1000-gallon glass-lined kettle is available for carrying out the reaction. The kettle may be maintained at essentially isothermal conditions by a heat transfer fluid that circulates through a jacket on its external surface. The heat transfer fluid may be cooled or heated as required by circulation through appropriate heat exchangers. Since the reaction is exothermic, Kladko (25) wished to consider the possibility of using cold reactant feed to provide a heat sink for some of the energy liberated by reaction. By controlling the rate of addition of feed, they could also obtain a measure of control over the rate of energy release by reaction. Hence, a semibatch mode of operation appeared to be an attractive alternative. Since cold incoming reactant would crack the hot glass liner, they considered the possibility of starting with 1500 lb of product B in the reactor so as to provide a thermal and material sump. The sump not only acts as a thermal sink for the cold incoming reactant, but also dilutes it, thereby reducing the reaction rate and the rate of energy release by reaction.

If the temperature of the reactor contents is maintained constant at 163°C, determine the total amounts of species A and B in the reactor as functions of time when it is loaded according to the following schedule:

Time, $t$ (h)	Feed rate of A (lb/h)
0–3	175
3–6	225
6–7	275
7–8	325
8–11	400
11–12	325
12–13	275
13–14	225
14–15	175
15–16	100
16–17	50
17+	0

As we shall see in Illustration 10.7, this type of filling schedule is necessary to avoid dramatic exotherms that would result from sudden termination of the feed and to ensure that the heat transfer capability of the system is not exceeded.

Data and permissible assumptions are as follows:

1. The reactor contents are perfectly mixed.
2. The rate expression is first-order in species A.
3. At 163°C the reaction rate constant is 0.8  $\text{h}^{-1}$ .

## Solution

A material balance involving the amount of species A contained within the reactor at any time can be written as

input = accumulation + disappearance by reaction

$$F_{A0} = \frac{dn_A}{dt} + kC_A V'_R \quad (\text{A})$$

where  $n_A$  is the instantaneous number of moles of species A contained within the reactor and  $V'_R$  is the instantaneous volume occupied by the liquid solution. This equation is similar to equation (8.6.1), but it lacks the term corresponding to the effluent stream and has been written in terms of moles.

Now, at any time,

$$C_A = \frac{n_A}{V'_R} \quad (\text{B})$$

Thus,

$$F_{A0} = \frac{dn_A}{dt} + kn_A \quad (\text{C})$$

Equation (A) can be rewritten in terms of the mass of species A present in the reactor as

$$\phi_{A0} = \frac{dm_A}{dt} + km_A \quad (\text{D})$$

where  $\phi_{A0}$  is the mass rate of flow of species A into the reactor.

Equation (C) may be solved in piecewise fashion to determine the mass of species A present in the reactor as a function of time. The solution can be written as

$$\int_{m_{Ai}}^{m_{A(i)}} \frac{dm_A}{\phi_{A0} - km_A} = t - t_i$$

where one uses a constant value of  $\phi_{A0}$  appropriate to the time interval in question and  $m_{Ai}$  is the mass of A in the reactor at the start of the time interval (time  $t_i$ ). Thus,

$$\frac{1}{k} \ln \left[ \frac{\phi_{A0} - km_{Ai}}{\phi_{A0} - km_A} \right] = t - t_i$$

Rearranging yields

$$m_A = m_{Ai} e^{-k(t-t_i)} + \frac{\phi_{A0}}{k} [1 - e^{-k(t-t_i)}] \quad (\text{E})$$

Using 0.8  $\text{h}^{-1}$  for  $k$  and values of  $\phi_{A0}$  given in the filling schedule, equation (E) can be solved in piecewise fashion.

**Table I8.11** Material Balance Analysis

Time, <i>t</i> (h)	<i>m</i> <sub>A</sub> (lb)	<i>m</i> <sub>B</sub> (lb)	Total mass (lb)	Fraction of input A that remains unconverted
0	0	1500	1500	0.000
1	120	1555	1675	0.686
2	175	1675	1850	0.500
3	199	1826	2025	0.379
4	244	2006	2250	0.325
5	265	2210	2475	0.272
6	274	2426	2700	0.228
7	312	2663	2975	0.212
8	364	2936	3300	0.202
9	439	3261	3700	0.200
10	473	3627	4100	0.182
11	488	4012	4500	0.163
12	443	4382	4825	0.133
13	388	4712	5100	0.108
14	329	4996	5325	0.086
15	268	5232	5500	0.067
16	189	5411	5600	0.046
17	119	5531	5650	0.029
18	54	5596	5650	0.013
19	24	5626	5650	0.006
20	11	5639	5650	0.003

The mass of B present at time *t* can be found by a material balance:

$$m_B = m_{B0} + \int_0^t \phi_{A0} dt - m_A$$

Values of the amounts of A and B present in the reactor at various times are given in Table I8.11.

## LITERATURE CITATIONS

1. DENBIGH, K. G. *Chemical Reactor Theory*. p. 3, Cambridge University Press, Cambridge, 1965.
2. GOOCH, D. B., *Ind. Eng. Chem.*, **35**, 927 (1943).
3. CLARK, E. L., GOLBER, P. L., WHITEHOUSE, A. M., and STORCH, H. H., *Ind. Eng. Chem.*, **39**, 1555 (1947).
4. MOSS, F. D., *Ind. Eng. Chem.*, **45**, 2133 (1953).
5. WALAS, S. M., *Reaction Kinetics for Chemical Engineers*, p. 79, McGraw-Hill, New York, 1959.
6. WASSERMANN, A., *J. Chem. Soc.*, 1936, 1028.
7. KERR, G. T., *J. Phys. Chem.*, **70**, 1047 (1966).
8. LIU, S., *Chem. Eng. Sci.*, **24**, 57 (1969).
9. INUKAI, T., and KOJIMA, T., *Org. Chem.*, **32**, 872 (1967).
10. RATCHFORD, W. P., and FISHER, C. H., *Ind. Eng. Chem.*, **37**, 382 (1945).
11. LEVENSPIEL, O., *Chemical Reaction Engineering*, 2nd ed., pp. 125–127, Wiley, New York, 1972.

12. MASON, D. R., and PIRET, E. L., *Ind. Eng. Chem.*, **43**, 1210 (1951).
13. LEVENSPIEL, O., *op. cit.*, pp. 139–143.
14. SZEPE, S., and LEVENSPIEL, O., *Ind. Eng. Chem. Process Des. Dev.*, **3**, 214 (1964).
15. ELDRIDGE, J. M., and PIRET, E. L., *Chem. Eng. Prog.*, **46**, 290 (1950).
16. JONES, R. W., *Chem. Eng. Prog.*, **47**, 46 (1951).
17. WEBER, A. P., *Chem. Eng. Prog.*, **49**, 26 (1953).
18. JENNEY, T. M., *Chem. Eng.*, **62**, 12 198 (1955).
19. CROOKS, W. M., *Bri. Chem. Eng.*, **2**, 710 (1966).
20. DENBIGH, K. G., *Trans. Faraday Soc.*, **40**, 352 (1944).
21. LEVENSPIEL, O., *op. cit.*, p. 136.
22. LEVENSPIEL, O., *op. cit.*, p. 137.
23. LEVENSPIEL, O., *op. cit.*, pp. 144–148.
24. LEVENSPIEL, O., *op. cit.*, p. 144.
25. KLAJKO, M., *Chemtech*, **1**, 141–146 (1971). Data from this source were used in constructing illustrative examples of worked-out problems in this and subsequent chapters. The article was published by the American Chemical Society.

## PROBLEMS

- 8.1** F. Salvador, J. L. Gonzalez, and M. A. Herraez [*Int. J. Chem. Kinet.*, **14**, 875 (1982)] studied the kinetics of the isomerization of cholest-5-en-3-one in cyclohexane in the presence of trichloroacetic acid as a catalyst. The stoichiometry of this reaction is A → B, where A refers to cholest-5-en-3-one and B to cholest-4-en-one. Species A and B both form association complexes with trichloroacetic acid. In the presence of excess acid, the kinetics of the isomerization reaction are described by a rate expression that is pseudo first-order in A:

$$r = k_{\text{observed}}(A)$$

At 25.4°C the observed rate constant is  $1.087 \times 10^{-3}$  s<sup>-1</sup> for the concentration of trichloroacetic acid employed ( $7.37 \times 10^{-3}$  M).

Consider this reaction as it takes place in a semibatch reactor operating at 25.4°C. Initially, this reactor contains 20 L of a cyclohexane solution that contains the desired amount of trichloroacetic acid, but no A. The reactor is fed with a cyclohexane solution containing species A ( $2 \times 10^{-3}$  M) and trichloroacetic acid ( $7.37 \times 10^{-3}$  M). The feed stream enters at 25.4°C at a constant rate of 5 L/min for a total time of 30 min. Subsequently, the reactor functions as a batch reactor. The reactor is well stirred during both phases of the reaction.

Prepare plots of the concentrations of species A and B as functions of time for a total elapsed time of 100 min. At what time does the concentration of species A pass through a maximum? How much total time is necessary to convert 98% of the A fed to the reactor into B?

- 8.2** J. Czarnowski and H. J. Schumacher [*Int. J. Chem. Kinet.*, **11**, 613 (1979)] studied the kinetics of the gas-phase decomposition of bispentafluorosulfur trioxide. In the presence of sufficiently high oxygen pressures, the stoichiometry is



Sue Dent has obtained the data below from experiments conducted in a tubular reactor (volume = 100 cm<sup>3</sup>) operating at room temperature (25°C) and 1 bar. Use these data to ascertain

whether this reaction is first-order in bispentafluorosulfur tri-oxide by preparing an appropriate plot of the data and testing for linearity. If this reaction is first-order, determine the value of the rate constant at this temperature. The material entering the reactor is an equimolar mixture of  $\text{SF}_5\text{O}_3\text{SF}_5$  and  $\text{O}_2$ .

Feed flow rate ( $\text{cm}^3/\text{min}$ )	Percent conversion
5.0	1.8
2.5	3.6
1.0	8.7
0.5	16.4
0.25	29.8

- 8.3** E. A. Chernishev, V. G. Bykovchenko, T. S. Kisileva, and N. N. Silkina [*Kinet. Catal.*, **27**, 1073–1076 (1986)] have studied the kinetics of the gas-phase reaction of trichlorosilane and chloroform:



The rate expression for this reaction is  $r = k(A)(B)^{0.5}$  where A is  $\text{HSiCl}_3$  and B is  $\text{HCCl}_3$ . At  $485^\circ\text{C}$ ,  $k = 0.23 \text{ M}^{-0.5} \text{ sec}^{-1}$ .

Consider the situation in which equimolar quantities of trichlorosilane and chloroform are fed to one of three reactor networks. Each network operates at a total pressure of 5 atm. Ideal gas behavior may be assumed. Determine the fraction conversion of chloroform leaving each reactor constituting the network if the total feed flow rate is  $90 \text{ ft}^3/\text{min}$  measured at reactor inlet conditions. (Express all conversions relative to the feed to the first reactor in the network.)

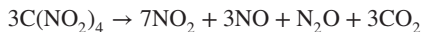
- (a) The reactor network consists of a 6-in.-ID tube that is 30 ft long followed by a 24-in.-ID tube that is 10 ft long.
- (b) The reactor network consists of a 24-in.-ID tube that is 10 ft long followed by a 6-in.-ID tube that is 30 ft long.
- (c) The reactor consists of a single tube with a total volume of  $37.31 \text{ ft}^3$  (This volume is equal to the sum of the volumes of the 6-in. and 24-in. ID reactors.)

- 8.4** P. G. Blake and S. Ijadi-Maghsoodi [*Int. J. Chem. Kinet.*, **15**, 609–618 (1983)] studied the kinetics of the gas-phase decomposition of ethyl isocyanate:



For reaction at  $500^\circ\text{C}$ , this reaction obeys a rate expression that is 1.5-order in the isocyanate. At this temperature, the value of the rate constant is  $3.03 \times 10^{-3} \text{ M}^{-1/2}/\text{s}$ . For a tubular reactor determine the space time necessary to achieve a conversion of 95%. The feedstock is at 1 atm and contains 85% v/v ethyl isocyanate and 15%  $\text{N}_2$ . You may assume that the gas phase behaves ideally. Comment on your answer.

- 8.5** Consider the task of analyzing the performance of a tubular reactor in which decomposition of tetranitromethane is taking place at steady state. The stoichiometry of the reaction is



J. M. Sullivan and A. E. Axworthy [*J. Phys. Chem.*, **70**, 3366 (1996)] reported that at  $213^\circ\text{C}$ , the first-order rate constant for this reaction is  $0.144 \text{ s}^{-1}$ .

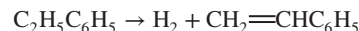
- (a) The nitromethane is present in an off-gas stream with the following composition:

Species	Percent v/v
$\text{C}(\text{NO}_2)_4$	60.0
$\text{CO}_2$	18.0
NO	15.0
$\text{N}_2\text{O}$	7.0

Determine the space time necessary to effect the decomposition of 99.9% of the entering tetranitromethane. The inlet pressure is 1.5 bar and the reactor operates isothermally at  $213^\circ\text{C}$ .

- (b) Is the mean residence time of the fluid greater than, less than, or equal to this space time? Explain your reasoning. Now validate your reasoning by determining the mean residence time. By how much does it differ from the space time?
- (c) If the activation energy for this reaction is 20 kcal/mol, what conversion would be expected at the space time determined in part (a) if the operating temperature were decreased to  $200^\circ\text{C}$  because of a malfunction of a temperature controller?
- (d) Another stream contains 60% v/v nitromethane and 40% inerts. Determine the space time necessary for a tubular reactor to effect decomposition of 99.9% of the tetranitromethane in this stream. Employ the conditions used in part (a) Comment.

- 8.6** Dehydrogenation of ethylbenzene to styrene is normally accomplished in a fixed-bed reactor. A catalyst is packed in tubes to form the fixed bed. Steam is often fed with the styrene to moderate the temperature excursions that are characteristic of adiabatic operation. The steam also serves to prolong the life of the catalyst. Consider the situation in which we model the behavior of this reactor as an isothermal plug flow reactor in which the dehydrogenation reaction occurs homogeneously across each cross section of the reactor. The stoichiometry of the primary reaction is



Consider the case for which the reaction obeys a rate law that is first-order in ethyl benzene with  $k = 3.5 \times 10^{-3} \text{ s}^{-1}$  at the temperature of interest ( $200^\circ\text{C}$ ), and the feed is 75% v/v  $\text{H}_2\text{O}$ , 15%  $\text{C}_2\text{H}_5\text{C}_6\text{H}_5$ , and 10%  $\text{H}_2$ .

If the feed stream enters at 1 atm and behaves as an ideal gas, what space time is necessary for the laboratory-scale reactor to achieve 90% conversion? What is the mean residence time of the gas under these conditions? Which of these two times is more useful for purposes of reactor design? Why?

- 8.7** G. H. Roper [*Chem. Eng. Sci.*, **2**, 27 (1953)] studied the reaction of chlorine (A) with 2-ethylhexene-1 (B) in carbon tetrachloride solution. Solutions of these materials were prepared

**Table P8.7**

Run	$C_{A0}$ (mol/m <sup>3</sup> )	$C_{B0}$ (mol/m <sup>3</sup> )	$C_{A\text{ exit}}$ (mol/m <sup>3</sup> )	Space time, ( $\tau$ ) (s)
1	91	209	23	0.600
2	91	209	32	0.376
3	91	209	45	0.284
4	110	211	34	0.525
5	110	211	46	0.324
6	110	211	59	0.232

and brought together in a mixing chamber at the inlet of a tubular reactor. The data in Table P8.7 were obtained at 20°C. The initial concentrations refer to values calculated on the basis of perfect mixing of the two solutions at the reactor inlet.

It has been suggested that the rate law is of mixed second-order form ( $r = kC_A C_B$ ). Prepare a plot of the data that permits you to determine if this expression is consistent with the data. If so, what is the reaction rate constant? If not, what do you recommend?

- 8.8** Consider the homogeneous isothermal gas-phase decomposition of acetaldehyde.



From experiments in a constant volume batch reactor at 791K, it is known that the time required for a 50% increase in total pressure is 197 s. The initial pressure is 1 bar. The reaction is known to be second-order in acetaldehyde. Determine the volume of a plug flow reactor necessary to achieve 80% conversion of 120 L/min of pure acetaldehyde gas. The feed pressure is 1 atm. The reaction is essentially irreversible. The pressure drop along the length of the reactor is negligible.

- 8.9** M. dos Santos Afonso and H. J. Schumacher [*Int. J. Chem. Kinet.*, **16**, 103–115 (1984)] reported that the rate law for the gas-phase reaction between  $\text{CF}_3\text{OF}$  and  $\text{C}_3\text{F}_6$  is

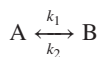
$$r = k_1(\text{CF}_3\text{OF})(\text{C}_3\text{F}_6) + k_2(\text{CF}_3\text{OF})^{3/2}(\text{C}_3\text{F}_6)^{1/2}$$

At 75°C, the values of  $k_1$  and  $k_2$  are  $8.67 \times 10^{-2}$  and  $1.16 \text{ M}^{-1}/\text{s}$ , respectively. For practical purposes, the stoichiometry of this reaction is



Consider the design of a small tubular reactor capable of processing 10 L/min of a 4 : 1 v/v mixture of  $\text{CF}_3\text{OF}$  and  $\text{F}_3\text{C}_6$  to achieve 95% conversion of the limiting reagent. The reactor is to operate isothermally at 75°C at a pressure of 1 bar. The internal diameter of the tube is 5 cm. What length of tube will be required?

- 8.10** J. C. H. Chen and W. P. Huntsman [*J. Phys. Chem.*, **75**, 430 (1979)] described a method for evaluating both rate and equilibrium constants for reversible first-order reactions of the type



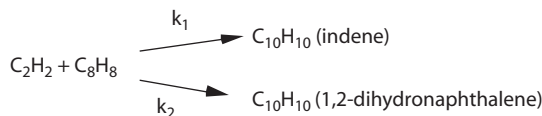
The technique involves injection of a quantity of pure reactant A into an inert carrier gas stream flowing at steady state through a tubular reactor. This injection is followed by subsequent injection of an identical amount of pure reactant B into the carrier gas. This procedure ensures identical contact times for both experiments. From a knowledge of the effluent compositions for these two trials, one can determine the equilibrium constant for the reaction. Subsequent experiments at different flow rates provide a means of determining individual rate constants.

The following data correspond to the *cis-trans* isomerization of 1,3-pentadiene at 430°C by injection of equal volumes of samples of each isomer.

Space time (s)	Conversion of <i>cis</i> isomer to <i>trans</i> isomer (%)	Conversion of <i>trans</i> isomer to <i>cis</i> isomer (%)
62.6	15.0	7.6
96.1	21.0	10.3
112.6	24.2	11.9
133.4	27.9	13.8
196.2	34.5	17.5
223.4	38.1	18.9

- (a)** Develop appropriate equations in integral form for both the case where the initial reactant is pure A and the case where it is pure B. Note that the initial concentrations and the space times are the same for both experiments. You may assume that it is appropriate to use the steady state design equation in both cases.
- (b)** Determine the equilibrium constant for each run.
- (c)** Determine the individual rate constants for the forward and reverse reactions.

- 8.11** Under appropriate conditions, mixtures of acetylene and styrene can form adducts such as methyl indene and 1,2-dihydronaphthalene, although polymers normally form under similar conditions. One of your researchers, Sue Dent, claims to have found a material which when added to the gaseous mixture inhibits both polymer formation and other side reactions. Her data indicate that at 525°C, the reactions of interest can be expressed as



At this temperature the rate expressions are

$$\begin{aligned} r_1 &= k_1(\text{C}_2\text{H}_2)(\text{C}_8\text{H}_8) \\ r_2 &= k_2(\text{C}_2\text{H}_2)(\text{C}_8\text{H}_8) \end{aligned}$$

with  $k_1 = 0.055 \text{ M}^{-1}/\text{s}$  and  $k_2 = 0.037 \text{ M}^{-1}/\text{s}$ .

For purposes of pilot-plant tests, a gaseous feedstock containing 60% v/v styrene, 30% acetylene, and 10% nitrogen is available at a volumetric flow rate of 5 m<sup>3</sup>/min

(measured at STP). If the indicated reactions are to be carried out isothermally at 525°C, what length of 2-in.-ID pipe will be required to achieve 95% conversion of the limiting reagent? Comment. The reactor will operate at a constant pressure of 5 atm. The quantity of inhibitor that must be employed is considerably less than 0.1% v/v.

- 8.12** Researchers in both industry and academia have employed immobilized enzymes as biocatalysts. Immobilization usually involves attaching enzymes to solid supports and packing the supports in a tube through which liquid flows. One application has involved conversion of the lactose in dairy fluids to glucose and galactose, which would permit conversion of the whey produced in cheese manufacture to useful by-products. By averaging over the void spaces between solid particles and the particles themselves, one can obtain an effective rate expression per unit volume of the bed of biocatalyst. The rate expression is

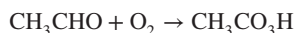
$$r = \frac{kS}{S + K_M[1 + (P_1/K_I)]}$$

for a reaction of the type



At a given temperature the parameters  $k$ ,  $K_M$ , and  $K_I$  are constants.  $K_M$  is known as a Michaelis constant and  $K_I$  as an inhibition constant.  $S$  and  $P_1$  are the concentrations of reactant  $S$  and product  $P_1$ , respectively. What effective space time for a tubular reactor will be required to obtain 80% conversion of the lactose at 40°C, where  $K_M = 0.0528$  M,  $K_I = 0.0054$  M, and  $k = 5.53$  mol/(L · min). The initial lactose concentration is 0.149 M.

- 8.13** Under appropriate conditions, the gas-phase partial oxidation of acetaldehyde to peracetic acid is autocatalytic. The reaction stoichiometry is



and the corresponding rate expression is

$$r = k_{\text{eff}}(CH_3CHO)^{1.5}[(O_2) + (CH_3CO_3H)]$$

For present purposes you may assume that

$$k_{\text{eff}} = 10^{13.78} e^{-20,000/RT}$$

for  $k_{\text{eff}}$  in  $\text{cm}^{9/2}/(\text{mol}^{3/2} \cdot \text{s})$ ,  $T$  in K, and  $R$  in  $\text{cal}/(\text{mol} \cdot \text{K})$ .

Consider a feedstock consisting of 75.0% v/v acetaldehyde, 5.0% oxygen, and 20.0% nitrogen. For a tubular reactor designed for isothermal operation at 200°C and 1.5 atm, determine the space time necessary to achieve 99% conversion of the limiting reagent. Ideal gas behavior may be assumed.

- 8.14** H. D. Martin, T. Urbandk, and R. Braun [Int. J. Chem. Kinet., **16**, 117–124 (1984)] studied the kinetics of the gas phase pyrolysis of barrelene [bicyclo(2.2.2)octa-2,5,7-triene] (B) to benzene and acetylene.



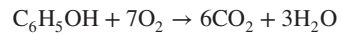
The following data are characteristic of the reaction as it occurs in a constant-volume batch reactor at 493 K.

Time (min)	Barrelene (%)
0	100
40	83.8
80	72.8
120	63.4
180	48.6
240	41.4
300	32.9

These researchers also indicated that for temperatures from 483 to 523 K, the activation energy for this reaction is 41.7 kcal/mol. Use these data to ascertain the temperature at which a plug flow reactor should be operated if one desires to decompose 98% of a pure barrelene feedstock when the barrelene enters the reactor at 2 atm. Barrelene is to be supplied at a volumetric flow rate of  $10^3$  ft<sup>3</sup>/min to a tubular reactor whose volume is 100 ft<sup>3</sup>. Comment on your answer.

What is the mean residence time of a fluid element in the reactor for operation at this temperature?

- 8.15** T. D. Thornton and P. E. Savage [AIChE J., **38**, 321–326 (1992)] studied the kinetics of the oxidation of phenol in dilute solutions under supercritical conditions. Although the overall stoichiometry is of the form



this reaction takes place in several steps. Temperatures of 300 to 420°C, pressures of 188 to 278 atm, and phenol concentrations of 50 to 330 ppm w/w were employed in these studies. Space times in a tubular reactor ranged from 1.2 to 111 s. If the rate expression for this reaction is of the form

$$r = k[C_6H_5OH]^a[O_2]^b[H_2O]^c$$

use the data in Table P8.15 to determine the orders of the reaction indicated with respect to each species and the reaction rate constant at 380°C. In each individual trial the feed concentration of phenol was  $1.3 \times 10^{-3}$  M. You may assume that the orders of the reaction with respect to phenol and oxygen are either integers or half-integers. You may also assume that within each experiment the oxygen concentration may be regarded as substantially constant over the length of the reactor because of the complex nature of the overall reaction and the fact that by monitoring the effluent phenol concentration one focuses solely on the first step in the complex sequence of reactions. Report the order with respect to water to the nearest 0.1.

- 8.16** A plant is producing nitric acid by oxidizing ammonia with air. The gases leaving the oxidation unit are cooled to condense out essentially all of the water present. The gases leaving the cooler pass to a long pipe followed by a series of absorption towers. Further oxidation of NO to NO<sub>2</sub> takes place in these towers. Of the NO present in the gases leaving the cooler, 90% is now being oxidized to NO<sub>2</sub> in the oxidizing chamber and absorption towers.

It has been suggested that the *production capacity* of the plant can be increased by introducing additional air into

**Table P8.15**

Trial	[O <sub>2</sub> ] (M)	[H <sub>2</sub> O] (M)	Space time (s)	Fraction conversion of phenol
A1	0.04	28.60	2.92	0.15
A2	0.04	28.60	4.38	0.18
A3	0.04	28.60	6.57	0.25
A4	0.04	28.60	8.76	0.33
A5	0.04	28.60	10.22	0.39
A6	0.04	28.60	13.12	0.39
A7	0.04	28.60	14.58	0.48
A8	0.04	28.60	17.54	0.48
A9	0.04	28.60	24.04	0.59
A10	0.04	28.60	32.05	0.70
A11	0.04	28.60	39.37	0.79
A12	0.04	28.60	46.73	0.86
A13	0.04	28.60	62.50	0.94
A14	0.04	28.60	68.49	0.94
A15	0.04	28.60	72.46	0.95
A16	0.04	28.60	92.59	0.98
A17	0.04	28.60	94.34	0.97
A18	0.04	28.60	98.04	0.98
B1	0.10	5.95	20.0	0.37
B2	0.10	9.59	20.0	0.56
B3	0.10	17.63	20.0	0.74
B4	0.10	27.23	20.0	0.74
C1	0.009	28.60	40.0	0.57
C2	0.009	28.60	50.0	0.64
C3	0.009	28.60	60.0	0.72
C4	0.009	28.60	70.4	0.78
D1	0.014	28.60	40.0	0.67
D2	0.014	28.60	50.0	0.74
D3	0.014	28.60	60.0	0.81
D4	0.014	28.60	70.4	0.86
E1	0.034	28.60	40.0	0.82
E2	0.034	28.60	50.0	0.88
E3	0.034	28.60	60.0	0.92
E4	0.034	28.60	70.4	0.94
F1	0.05	28.60	40.0	0.86
F2	0.05	28.60	50.0	0.92
F3	0.05	28.60	60.0	0.955
F4	0.05	28.60	70.4	0.97

the gases leaving the cooler. Buck Badger suggests that the decrease in residence time will be more than compensated for by the increased rate of reaction. He proposes that the plant throughput be increased, keeping the conversion of the NO fixed at 90%.

- (a) Is it possible to increase the production capacity as suggested?
- (b) If so, what should be the number of moles of air fed per mole of gas leaving the cooler in order to maximize

the production capacity? What is the percent increase in capacity under these conditions?

Data and suggestions include the following. The composition of the gases leaving the cooler is 83% N<sub>2</sub>, 8.8% O<sub>2</sub>, and 8.2% NO.

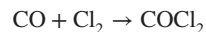
1. Assume that this composition will be unchanged by any change in the plant production capacity.
2. For simplification, assume that the gas flow approximates plug flow at a constant temperature of 30°C.
3. The oxidation reaction is homogeneous. The reverse reaction may be neglected.
4. In your analysis, obtain a first approximation to the solution by neglecting the effect of expansion that accompanies the reaction. Because of the large percentage of inerts in the feed stream, the volume change on reaction may be neglected in obtaining the approximation. To obtain a more exact result, conduct an analysis that incorporates volumetric expansion effects.
5. It may be assumed that absorption of the NO<sub>2</sub> by H<sub>2</sub>O in the absorption towers does not affect the oxidation rate.
6. The plant capacity is directly proportional to the quantity of NO<sub>2</sub> produced per unit time.
7. The rate law at 30°C is

$$\frac{-dC_{NO}}{dt} = k C_{NO}^2 C_{O_2}$$

where concentrations are expressed in kmol/m<sup>3</sup> and with  $k = 8.0 \times 10^3 \text{ m}^6/(\text{kmol}^2 \cdot \text{s})$ .

8. Composition of air: N<sub>2</sub> = 79% O<sub>2</sub> = 21%.
9. Note that the addition of air increases the O<sub>2</sub> concentration but also adds N<sub>2</sub> as an inert diluent. Thus, there will be some optimum air feed rate.
10. A useful approach is to set up an expression for the result desired in terms of the moles of air fed per 100 mol of gas leaving the cooler.

- 8.17** E. N. Shapatina, V. L. Kuchaev, B. E. Pan'kovo, and M. I. Temkin [*Kinet. Catal.*, **17**, 559 (1976)] investigated the kinetics of the industrial catalytic process for the synthesis of phosgene:



The reaction takes place at 130°C over an activated carbon catalyst. The rate expression for this irreversible reaction is

$$r = k_1 P_{CO} \left( \frac{P_{Cl_2}}{k_2 P_{CO} + P_{COCl_2}} \right)^{0.25}$$

with  $k_1 = 0.132 \text{ mol}/(\text{h} \cdot \text{atm} \cdot \text{g catalyst})$  and  $k_2 = 0.50 \text{ atm}^{-1}$  for partial pressures in atmospheres when the rate is expressed per unit weight of catalyst.

The CHE Corporation has available a pure carbon monoxide stream produced at the rate of 0.5 kmol/min. This stream will be employed to produce phosgene for use in the synthesis of several specialty chemicals. Note that pressure drop through the reactor is negligible, so that operation occurs at a constant total pressure of 1 atm.

- (a) The proposed applications are sensitive to the presence of chlorine, so the design of the phosgene reactor calls for the use of a 10% excess of carbon monoxide. If the flow through the packed-bed reactor approximates plug flow, what weight of activated carbon will be required to produce conversions of 90, 99, 99.9, 99.99, and 99.999% under isothermal conditions? Note that the pressure drop through the reactor is negligible, so that operation occurs at a constant total pressure of 1 atm. Present your results in tabular form. In your table also provide entries for the four highest conversions corresponding to the ratio of the increment in the weight of catalyst to the increment in the conversion relative to the previous entry. Comment on your results.
- (b) If the flow through the packed-bed reactor approximates plug flow and is isothermal, what weight of activated carbon will be required to effect 99.9% conversion when molar excesses of 0, 1, 2, 5, 10, and 20% are employed? Prepare a plot of the weight of activated carbon required versus the molar excess of carbon monoxide. Comment.

- 8.18** H. M. Frey and H. P. Watts [*Int. J. Chem. Kinet.*, **13**, 729 (1981)] studied the gas-phase pyrolysis of 4-methyl-3,6-dihydro-2H-pyran (P) to give 2-methylbuta-1,3-diene (D) and formaldehyde (F):

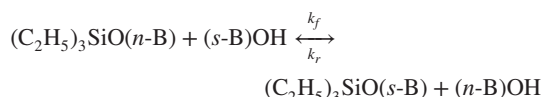


In an effort to verify the results obtained by Frey and Watts, Professor Viejo Dinosaurio has employed a laboratory scale tubular reactor that can operate isothermally at 628 K. For a reactor with an effective volume of  $2850 \text{ cm}^3$  and an operating pressure of 1 atm, he reported the data summarized below. Feed composition: P = 50% v/v; N<sub>2</sub> = 50% v/v.

Total feed flow rate at inlet (cm <sup>3</sup> /min)	Fraction conversion	
	At inlet	At exit
670	0.041	0.330
480	0.053	0.418
310	0.062	0.547
234	0.068	0.635
165	0.072	0.747
125	0.075	0.824
98	0.082	0.883

Frey and Watts reported that the relation between the rate constant and the temperature in K can be expressed as  $\log k \text{ (in sec}^{-1}\text{)} = (14.619 \pm 0.030) - [(209.48 \pm 0.35) \text{ kJ/mol} / \{RT \ln 10\}]\text{.}$  Are the pyrolysis data consistent with this correlation?

- 8.19** K. Ito and T. Ibaraki [*Int. J. Chem. Kinet.*, **19**, 841–849 (1987)] studied the kinetics of the iodine-catalyzed alcoholysis of *n*-butoxytriethylsilane in secondary butanol:

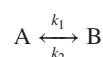


where B represents C<sub>4</sub>H<sub>9</sub> and where the rate expressions for both the forward and reverse reactions are of the mixed second-order form. (The effects of the iodine catalyst are incorporated in the second-order rate constants.) These investigators have reported that at the temperature of interest when I<sub>2</sub> = 0.015 M, the values of k<sub>f</sub> and k<sub>r</sub> are  $5.8 \times 10^{-5}$  and  $13.9 \times 10^{-5} \text{ M}^{-1}/\text{s}$ , respectively.

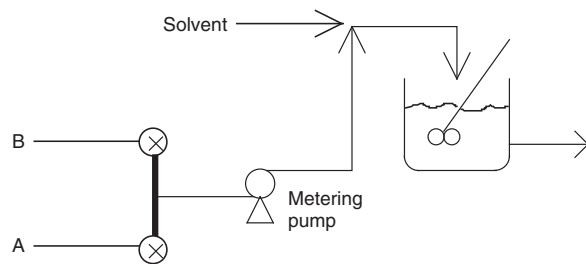
A single CSTR with a volume of 2 m<sup>3</sup> is available for carrying out this reaction. Prepare a plot of the fraction conversion versus the volumetric feed rate for the case in which the feedstock consists of a 4.1 : 1 molar ratio of *s*-butanol to *n*-butoxytriethylsilane. The concentration of I<sub>2</sub> is 0.015 M. Consider feed rates below 8.0 L/min. The feed concentration of the silane may be taken as 2.05 M.

To what does the low flow rate limit correspond? Prepare a plot of the effluent conversion versus the reactor space time.

- 8.20** J. C. H. Chen and W. P. Huntsman [*J. Phys. Chem.*, **75**, 430 (1979)] described a method for evaluating both rate and equilibrium constants for reversible reactions of the type



Although this technique was proposed originally for use with gaseous reactions occurring in a tubular reactor, one can extend their approach to encompass reactions that occur in the liquid phase in a single stirred-tank reactor. Consider the following apparatus:

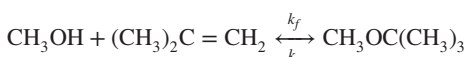


Either pure A or pure B is fed to a metering pump that serves to inject this compound into a solvent stream which then passes to a CSTR. The ratio of reactant to solvent is always maintained at a very low level. By restricting the change in operating conditions to merely opening and closing the valves connecting the reservoirs and the metering pump, one can ensure identical space times of both reactants in the stirred tank. From a knowledge of the steady-state effluent compositions corresponding to feed solutions containing either A alone or B alone, one can determine the equilibrium constant for the reaction. Experimental data for feeding either A or B alone at different flow rates of the solvent for each of the space times cited can then be used to determine the individual rate constants. The following data correspond to an arbitrary isomerization reaction of the type described above.

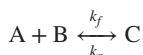
Reactor space time (ks)	Conversion of A to B (%)	Conversion of B to A (%)
0.626	15.0	7.6
0.975	21.0	10.3
1.200	24.2	11.9
1.500	27.9	13.8
2.300	34.5	17.5
2.800	38.1	18.9

- (a) Develop appropriate equations for both the case in which the initial reactant is pure A dissolved in the solvent and the case in which it is pure B dissolved in the solvent. Note that the initial concentrations and the space times are the same for both experiments. You may assume that it is appropriate to use the steady-state design equation in both cases.
- (b) Determine the equilibrium constant for each run.
- (c) Determine the individual rate constants for the forward and reverse reactions.

- 8.21 In the presence of the  $\text{H}^+$  form of a strong cation-exchange resin, methanol reacts with isobutylene to form methyl *tert*-butyl ether (MTBE), a compound that was formerly used as a high-octane blending agent for gasoline:



or



This reversible exothermic reaction was studied by M. H. Matouq and S. Goto [*Int. J. Chem. Kinet.*, **25**, 825–831 (1993)], who reported the following rate expression:

$$r = [k_f(\text{A})(\text{B}) - k_r(\text{C})](\text{catalyst})$$

where

$$k_f = \exp\left(7.16 - \frac{10,100}{T}\right) \text{ m}^6/(\text{mol} \cdot \text{s} \cdot \text{mol H}^+)$$

or

$$k_r = \exp\left(30.4 - \frac{16,100}{T}\right) \text{ m}^3/(\text{mol H}^+ \cdot \text{s})$$

Consider the problem of designing a single CSTR to carry out this reaction under conditions such that the effective concentration of the hydrogen ion catalyst is  $177 \text{ mol/m}^3$ . The feed concentrations of methanol, isobutylene, and MTBE are  $2.0$ ,  $3.0$ , and  $0.0 \text{ kmol/m}^3$ , respectively. The inlet volumetric flow rate is  $0.9 \text{ m}^3/\text{h}$ . The desired level of conversion of the limiting reagent is  $78\%$ . If the reactor is to be operated at the temperature that maximizes the reaction rate, how large must the CSTR be?

- 8.22 E. Alper, M. al-Roweih, and W. Bouhomra [*Chem. Eng. J.*, **55**, 53–59 (1994)] studied the kinetics of the reaction of carbonyl sulfide (A) with 2-amino-2-methyl-1-propanol

(B) in isopropanol solution. At  $25^\circ\text{C}$  the rate expression is  $r = k(\text{A})(\text{B})^2$  with  $k = 0.66 \text{ m}^6/(\text{kmol}^2 \cdot \text{s})$ . The stoichiometry is  $\text{A} + 2\text{B} \rightarrow \text{C} + \text{D}$ .

- (a) Consider the possibility of carrying out this reaction at  $25^\circ\text{C}$  in a single CSTR under conditions such that stoichiometric quantities of reactants are employed, the feed concentration of the carbonyl sulfide is  $1.2 \text{ M}$ , and the feed flow rate is  $8.0 \text{ m}^3/\text{h}$ . How large must this reactor be to achieve  $80\%$  conversion? If the activation energy is  $82.6 \text{ kJ/mol}$ , what would be the corresponding volume requirement for operation at  $50^\circ\text{C}$ ?

- (b) What are the corresponding reactor volume requirements for plug flow reactors operating at  $25$  and  $50^\circ\text{C}$ , all other factors remaining the same?

- 8.23 Y. Wang [*Int. J. Chem. Kinet.*, **25**, 91–96 (1993)] studied the kinetics of dimerization of arylmercuric compounds in hexamethylphosphoramide solution in the presence of a  $[\text{ClRh}(\text{CO})_2]_2$  catalyst. Consider the dimerization of  $\text{CH}_3\text{OC}_6\text{H}_4\text{HgCl}$  (species A). The stoichiometry is  $2\text{A} \rightarrow \text{B} + \text{Hg} + \text{HgCl}_2$  and the rate expression is  $r = k[\text{A}]^2$ . At  $80^\circ\text{C}$  in the presence of  $0.5\%$  catalyst,  $k = 1.50 \times 10^{-3} \text{ M}^{-1}/\text{s}$ . The feed liquid contains only species A as a solute at a concentration of  $0.19 \text{ M}$  and is supplied at a rate of  $200 \text{ L/h}$ .

Two alternative reactor configurations are to be considered for use in a pilot-plant study. The first consists of a tubular reactor with a volume of  $100 \text{ L}$  followed by a CSTR with a volume of  $200 \text{ L}$ . The second configuration consists of a CSTR with a volume of  $200 \text{ L}$  followed by a tubular reactor with a volume of  $100 \text{ L}$ . If each reactor configuration is operated isothermally at  $80^\circ\text{C}$ , determine the fraction conversion leaving the network for each configuration.

What general principle concerning the order in which different reactor types should be employed in an isothermal reactor network does this problem exemplify? (Hint: Consider rate expressions of the general  $n$ th-order form and ask yourself how the various types of reactors should be employed for optimum productivity.)

- 8.24 The rate of a chemical reaction is given by

$$r = k(\text{A})^n$$

If  $98\%$  of the reactant A is converted to products in a reactor, and if one obtains a second reactor that is half the size of the first, determine the increases in feed capacity that result from the following types of operation:

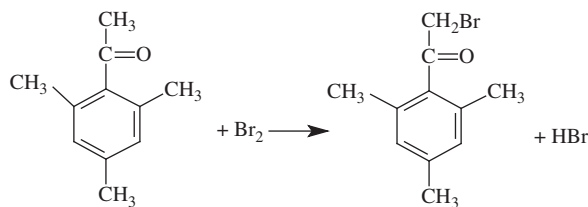
1.  $n = \frac{1}{2}$ ; two plug flow reactors in series
2.  $n = 1$ ; two plug flow reactors in series
3.  $n = 3$ ; two plug flow reactors in series
4.  $n = \frac{1}{2}$ ; two plug flow reactors in parallel
5.  $n = 1$ ; two plug flow reactors in parallel
6.  $n = 3$ ; two plug flow reactors in parallel

- (a) By what percentage can the feed flow rate be increased if two reactors are employed as indicated while maintaining a constant overall conversion? Assume that the exit composition from the last reactor remains unchanged in all

cases and that none of the A has been converted to products prior to entering the first reactor. Do not assume that  $\delta = 0$ . Obtain a general solution. In series operation the small reactor precedes the large reactor in the sequence.

- (b) Repeat part (a) for the case of continuous stirred-tank reactors. Assume that there is no change in the number of moles on reaction.
- (c) In addition, consider what happens when a second-order reaction takes place in the series configuration of CSTRs. Consider both the case where the small CSTR precedes the large CSTR and the case for which the large CSTR precedes the small CSTR. Comment on your results.

- 8.25** A. G. Pinkus and R. Gopalan [*J. Am. Chem. Soc.*, **106**, 2630 (1984)] reported that the bromination of 2,4,6-trimethylacetophenone (A) occurs rapidly in 50% v/v aqueous acetic acid in the presence of 0.1 M HBr and 0.4 M NaClO<sub>4</sub>.

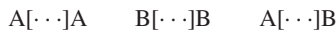


The rate expression for this reaction is  $r = k(A)(Br_2)$ . At 25°C, the second-order rate constant is  $4.34 \times 10^{-2} \text{ M}^{-1} \text{ sec}^{-1}$ . The activation energy is 61.5 kJ/mole.

Consider the following tasks associated with the design of a laboratory-scale facility for carrying out this bromination. In all cases the feed is to be 0.06 M in Br<sub>2</sub> and 0.05 M in A; overall conversion of the limiting reagent is to be 80%.

- (a) A single CSTR with a volume of 0.18 m<sup>3</sup> is to be operated at a temperature such that  $2.25 \times 10^{-4} \text{ m}^3/\text{s}$  of feed may be processed. What is this temperature?
- (b) A battery of two identical CSTRs, each with a volume of 0.09 m<sup>3</sup>, is to be operated at 48°C. By how much may the inlet feed rate of task (a) be increased while maintaining the specified degree of conversion?
- (c) Repeat task (b) for the case where a battery of three CSTRs, each with a volume of 0.06 m<sup>3</sup>, is employed.
- (d) If a tubular reactor with a volume of 0.18 m<sup>3</sup> is operated at 48°C, by how much may the feed flow rate be increased?
- (e) Note that the total reactor volume is 0.18 m<sup>3</sup> in each case. Comment on your results.
- (f) Describe the expected shape of a plot of capital costs for  $n$  CSTRs versus  $n$ . Discuss.

- 8.26** D. Beigzadeh, S. Sajjadi, and F. Afshar Taromi [*J. Polym. Sci.*, **33A**, 1505–1510 (1995)] studied the kinetics of the polyesterification reactions of ethylene glycol and fumaric acid. Fumaric acid is a diacid and ethylene glycol contains two hydroxyl groups, so that polymers of the following types can be formed in a batch reactor:



depending on the relative ratio of acidic (A) and hydroxyl (B) groups originally present in the system. The distribution of chain lengths [· · ·] at any time also reflects the ratio of acidic and hydroxyl groups, with the longest chains being formed when this ratio is unity. These investigators reported that when this reaction is carried out under self-catalyzed conditions, the rate expression is of the form

$$\frac{dp}{dt} = k_1 C_0^2 e^{\alpha p} (1-p)^2 (r-p) - k_2 [H_2O] p$$

This equation also assumes that the bulk of the water formed by the esterification reaction is removed from the reaction vessel continuously using a sweep gas. In this equation,  $p$  is the fraction of the acid groups present in their esterified forms,  $C_0$  is the original concentration of acid groups, and  $r$  is the ratio of hydroxyl groups to acid groups in the original mixture.

Consider the possibility of using a single CSTR to generate the polymeric resin formed by these polyesterification reactions. The reactor is to be operated at 180°C using a feed stream consisting of ethylene glycol and fumaric acid with a mole ratio of 1.1125. Nitrogen sweep gas is employed for continuous removal of the large majority of the water produced by reaction. The conditions are:

$$k_1 = 3.8127 \times 10^{-4} (\text{kg mixture})^2 / (\text{mol}^2 \cdot \text{min})$$

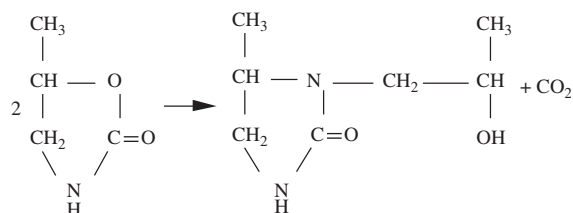
$$k_2 [H_2O] = 0.4747 \times 10^{-4} \text{ min}^{-1}$$

$$\alpha = 0.8705$$

$$C_0 = 10.7482 \text{ mol/kg mixture}$$

- (a) If one desires to process 100 kg of mixture per hour to an extent that converts 80% of the incoming acid groups to their esterified form, what is the necessary capacity of the reactor? (Note that in the present case, the space time of the reactor can be regarded as the ratio of the mass of material in the reactor to the mass flow rate of the reaction mixture.)
- (b) To what value would the capacity requirement be reduced if a cascade of two identical CSTRs is employed? You may assume that a sweep gas is used in each reactor so as to cause the concentration of water to be the same in each CSTR. Hence, one can use the same value of  $k_2 [H_2O]$  for each reactor. The overall design requirement is that the fraction of the original acid groups converted to ester bonds remains at 0.8.

- 8.27** W. E. Walles and A. E. Platt [*Ind. Eng. Chem.*, **59**(6), 41 (1967)] have reported that the thermal decomposition of 5-methyl-2-oxazolidinone is autocatalytic with a stoichiometry of the form



or



The rate expression for this liquid-phase reaction is

$$r = k_1(A)^2 + k_2(A)(B)$$

At the temperature of interest,

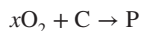
$$k_1 = 1.02 \times 10^{-6} L/(mol \cdot s)$$

$$k_2 = 75 \times 10^{-6} L/(mol \cdot s)$$

- (a) For a feedstock consisting of species A dissolved in an inert solvent at a concentration of 0.15 M, determine the fraction conversion of species A and the concentrations of species A and B that lead to the maximum rate of reaction. No B is present in the feed stream.
- (b) This reaction is to be carried out in a cascade of two identical CSTRs. The concentration of A in the feed stream is 0.15 M and the volumetric flow rate of the feed stream is 200 L/h. The first CSTR is to operate at the conversion of A corresponding to the maximum rate of reaction. Determine the reactor volume corresponding to this conversion and the concentrations of species A and B corresponding to the effluent from the second reactor.
- (c) What combination of ideal reactor types leads to the minimum requirement for total reactor volume if the feed consists solely of species A (0.15 M) in the inert solvent? If the feedstock is supplied at a volumetric flow rate of 0.2 m<sup>3</sup>/h, determine the volume of each constituent of the combination that minimizes the total volume requirement. The fraction conversion of species A leaving the last reactor is to be 0.99. Both reactors in the combination operate at the same temperature.

- 8.28** S. M. Mahajani, M. M. Sharma, and T. Sridhar [*Chem. Eng. Sci.*, **54**, 3967–3976 (1999)] studied the liquid phase partial oxidation of cyclohexene in a batch reactor. In the absence of a catalyst, a variety of products are formed, including cyclohexenol, cyclohexene hydroperoxide, cyclohexenone, and cyclohexene oxide.

This research group obtained kinetic data using a well-agitated pressure vessel in which the partial pressure of oxygen over the liquid was maintained constant by continuous addition of oxygen as the reaction proceeded. For our present purpose, we may consider the stoichiometry of the reaction to be of the general form



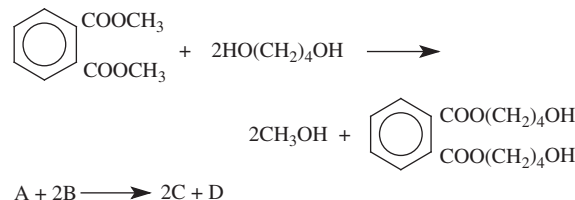
where C is cyclohexene, P is a generic product, and x is an undetermined stoichiometric coefficient. These investigators fit their data with a rate expression of the form

$$r = k(C)(P) \quad (1)$$

A rate expression of this form is characterized as being autocatalytic in that the rate depends on the concentration of the product raised to a positive power. Consider the task of designing a reactor network for carrying out this reaction. The first

reactor is to be a single CSTR in which the head space is continuously replenished with oxygen at a rate which (with the agitation provided) maintains the oxygen in solution at a level such that for reaction at 105°C, the value of the rate constant k is 0.407 M<sup>-1</sup>/h. The CSTR is to be operated under conditions that maximize the reaction rate. Species C and P are fed to the CSTR in a manner such that the blend of these streams contains concentrations of C and P of 9.31 and 0.49 M, respectively. If the working volume of the CSTR is 2000 L, what volumetric flow rate should be employed for the blend? What fraction of the C that enters the CSTR is converted to P? The second reactor is to be a plug flow reactor with an effective volume of 1600 L. Oxygen is injected at several points along the length of the reactor to maintain a constant concentration of this species over the entire length of the PFR. This concentration is such that the rate expression given by equation (1) remains valid with k = 0.407 M<sup>-1</sup>/h. What fraction of the C that enters the CSTR is converted to P in the combination of reactors indicated?

- 8.29** Butanediol (B) can be used to trans-esterify the dimethyl ester of phthalic acid (A) in the presence of an appropriate solvent:



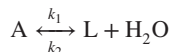
The rate expression for this reaction is  $r = k(A)(B)$ .

Consider the situation in which a single CSTR is currently being used to carry out this reaction using a feedstock in which an appropriate solvent contains the dimethyl ester of phthalic acid at a concentration of 0.2 M and butanediol at a concentration of 0.4 M. At the temperature of interest,  $k = 0.5 \text{ M}^{-1}/\text{ks}$ .

- (a) For a reactor volume of 50 m<sup>3</sup> and a total feed rate of 5 m<sup>3</sup>/ks, determine the effluent concentration of species A.
- (b) Now consider a situation in which the feed concentrations of species A and B are increased to 0.4 M and 0.8 M, respectively. Derive an expression from which one can determine the manner in which the concentration of species A varies with time being measured from the instant a step change of the type indicated is made in the feed composition. Both the reactor volume and the volumetric flow rates of the feed and effluent streams remain constant when the composition of the feed stream changes. You need not solve explicitly for  $C_{AF}$  but may leave your expression in a form in which the only variable on the left side of the equation is  $C_{AF}$  and the only variable on the right side is time.
- (c) Use the expression determined in part (b) to evaluate the effluent composition 2 ks after the step change has been made.

- (d) What is the effluent concentration of species A at the new steady-state condition?

**8.30** Consider the conversion of  $\gamma$ -hydroxybutyric acid (A) into its lactone (L) in aqueous solution:



At 25°C this reaction is first-order in A in the forward direction with  $k_1 = 0.112 \text{ ks}^{-1}$ . In the reverse direction, the reaction is pseudo-first-order in the lactone with  $k_2 = 0.042 \text{ ks}^{-1}$ . This reaction is being studied on a pilot-plant scale in a single well-stirred tank reactor (volume = 1.5 m<sup>3</sup>).

- (a) Determine the volumetric flow rate necessary to achieve 60% conversion at steady state when the feed stream is 0.182 M in A. What is the value of the corresponding equilibrium composition?
- (b) Now, suppose that the feed concentration of species A is increased at time zero to 0.200 M and maintained at this value until steady state is again achieved. Throughout this period the volumetric flow rate is held constant at the value determined in part (a). How long does it take for the effluent concentration of species A to increase to 0.075 M? Note that at time zero, the effluent concentration of species A is 0.0728 M.
- 8.31** A stream from a manufacturing operation contains  $\beta$ -nicotinamide-adenine dinucleotide (commonly referred to as NADH). A second stream contains methylene blue (MB), which can be used to catalyze the oxidation of NADH. Your co-worker Sue Dent has suggested that these streams can be blended to produce a stream containing NADH at a concentration of  $1.96 \times 10^{-4} \text{ M}$  and  $MB^+$  at a concentration of  $3.6 \times 10^{-6} \text{ M}$ . In the presence of sufficient dissolved oxygen, the NADH will be oxidized in a manner governed by the following rate law:

$$-\frac{d[NADH]}{dt} = \frac{k[NADH][MB^+]}{1 + K[NADH]}$$

P. Sevick and B. Dunford [*Int. J. Chem. Kinet.*, **27**, 925–928 (1995)] indicated that at 25°C,  $k = 4.21 \text{ M}^{-1}/\text{s}$  and  $K = 3.53 \times 10^2 \text{ M}^{-1}$  at the pH of the buffered solution (9.0) which will result from blending the two liquid streams. Furthermore, the level of dissolved oxygen in the blended stream is sufficient to ensure rapid reoxidation of the product leucomethylene blue (MBH) back to  $MB^+$  so that the concentration of MBT in this stream will be essentially invariant (i.e., the  $MB^+$  can be regarded as a catalyst for the oxidation of NADH by dissolved oxygen). This blended stream is available at a rate of 6 L/min.

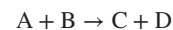
- (a) Determine the size of a single CSTR that will achieve NADH conversions from 50 to 99%. Present your data in the form of a plot of reactor volume versus the fraction conversion. Comment on the shape of your plot.
- (b) If process economics dictate that the conversion of NADH exceed 95%, determine the total volume requirements for cascades of identical CSTRs consisting of two and three CSTRs.

- (c) Repeat part (b) for the case in which the conversion level specified is 99%. Summarize your results in the form of a table which indicates the total volume requirements at the two conversion levels indicated for cascades of one, two, and three identical CSTRs.

**8.32** A second-order exothermic reaction with the stoichiometry  $A \rightarrow 2B$  takes place in organic solution. It is to be carried out in a cascade of two identical CSTRs. To equalize the heat load on these reactors, it will be necessary to operate them at different temperatures. The reaction rates in each reactor will be the same, however. To minimize solvent losses by evaporation, one must operate the second reactor at 20°C where the reaction rate constant is equal to 5 L/(mol · h). If the effluent from the second reactor corresponds to 90% conversion and if the molal feed rate to the cascade is equal to 2000 mol/h when the feed concentration of species A is 1.5 mol/L, how large must each of the reactors be? If the activation energy for the reaction is 20 kcal/g-mol, at what temperature should the first reactor be operated?

**8.33** An exothermic reaction that obeys a second-order rate expression ( $r = kC_A^2$ ) is to be accomplished in a cascade of three identical stirred tanks operating in series. To (approximately) balance the heat loads on the various reactors, each of the reactors will be operated at a different temperature. These temperatures are to be selected in a manner such that the rates of reaction are to be the same in each reactor. To minimize losses of the organic solvent during operation, it will be necessary to operate the third reactor at 140°C. At this temperature the reaction rate constant is equal to 500 L/(mol · h). If the effluent from the third reactor corresponds to 99% conversion and if the volumetric flow rate to the cascade is equal to 1.8 m<sup>3</sup>/h when the concentration of A in the feed stream is 1.5 M, how large must each of the reactors be? If the activation energy for the reaction is 20 kcal/g-mol, at what temperatures should the first and second reactors be operated?

**8.34** A condensation reaction with the generic stoichiometry



is being carried out under steady-state operating conditions in a cascade of three identical stirred-tank reactors. Each reactor operates at a different temperature. The rate expression is of mixed second-order form:

$$r = k(A)(B)$$

The liquid feed stream contains equal concentrations of species A and B (1.8 M).

To best utilize the available heat exchangers, the CSTRs are to be operated in a manner such that the reaction rate is the same in each reactor while the conversion of the limiting reagent leaving the last reactor is 96%. The first reactor operates at 40°C and the second at 60°C.

- (a) What is the activation energy of this reaction?
- (b) At what temperature must the third reactor be operated?

**8.35** Kim Enjanear has been asked to scale up an existing process to obtain increased production capacity for compound D. The stoichiometry of the liquid-phase reaction is  $A + B \rightarrow D$ . At present the process is carried out in a single large CSTR with a volume of 400 L. When operated at room temperature with a feed flow rate of 16 L/min and inlet concentrations  $C_{A0} = 3.0$  M and  $C_{B0} = 1.5$  M, this reactor is capable of producing 1.2 kmol/h of species D. It has been suggested that the inlet volumetric flow rate can be raised to 32 L/min (i.e., doubled) and that better utilization of the reactants can be achieved (i.e., one can achieve a higher degree of conversion) by using a cascade of two reactors, the first of which has an effective volume of 200 L, and the second of which is that used in the present configuration. The reaction is known to be of the mixed second-order form,  $r = kC_A C_B$ .

Does an engineering analysis support the above suggestion? What will be the conversion of the limiting reagent under the new mode of operation relative to that employed in the present case?

**8.36** A single CSTR is to be employed to effect a hydration reaction in perchloric acid solution:



Under appropriate conditions the reaction is pseudo first-order in reactant A. For these conditions the rate constant is equal to  $2.7 \times 10^{-2} \text{ min}^{-1}$ . Consider operation of a reactor with a volume of  $9.0 \text{ m}^3$  to which an aqueous solution of the reactant is being fed at a rate of 100 L/min. The feed concentration of reactant A is equal to 0.5 M.

- (a) Determine the effluent concentration of species A for the indicated operating conditions if steady state conditions prevail in the reactor.
- (b) If the volumetric flow rate is increased to 150 L/min, prepare a plot of the effluent concentration of species A as a function of time from the time at which the increase is made until 100 min later. How long does it take the effluent concentration of species A to equal 0.175 M? The reactor continues to operate at the same temperature and with the same concentration of reactant in the feed stream. Note that there is no accumulation of the liquid phase in the CSTR.

**8.37** Y. K. Kim and J. D. Hatfield [*J. Chem. Eng. Data*, **30**, 149–153 (1985)] studied the kinetics of the hydration of mesityl oxide (M) in phosphoric acid to obtain diacetone alcohol (D):



Under the conditions of interest, the rate expression can be regarded as pseudo first-order in the forward direction and first-order in the reverse direction:

$$r = k_1 a_w(M) - k_{-1}(D)$$

where  $a_w$  refers to the activity of water, which can be regarded as constant.

Consider the problem of designing a single CSTR that can be used to accomplish this reaction in an available feedstock containing 17.2% w/w  $H_3PO_4$  and 1.748 M mesityl

oxide. Volatility considerations indicate that the maximum allowable temperature will be  $70^\circ\text{C}$ . Between room temperature and  $70^\circ\text{C}$ , the activity of water in this solution is relatively constant at 0.956. The temperature dependence of the rate constants can be expressed as  $k_1 = 1.66 \times 10^5 e^{-12.668/RT}$  and  $k_{-1} = 2.69 \times 10^8 e^{-18.755/RT}$  for  $k_1$  in  $\text{s}^{-1}$ ,  $k_{-1} a_w$  in  $\text{s}^{-1}$ , and  $R$  in  $\text{cal}/(\text{mol} \cdot \text{K})$ .

- (a) Prepare a plot of the temperature at which the CSTR should be operated to achieve maximum productivity versus the fraction conversion of mesityl oxide achieved in the reactor. Consider conversions from 50 to 95% in 5% increments.
- (b) Prepare a plot of the corresponding reactor volume versus fraction conversion for each of the conversions considered in part (a). The feedstock enters at a rate of  $1.5 \text{ m}^3/\text{h}$ .
- (c) Is this reaction exothermic or endothermic? What is the standard enthalpy change for this reaction?
- (d) Suggest an appropriate mode of operation for a cascade consisting of two (nonidentical) CSTRs and calculate the total volume requirement for this cascade when the overall conversion level is to be 95%. Comment.

**8.38** Y. K. Kim and J. D. Hatfield [*J. Chem. Eng. Data*, **30**, 149–153 (1985)] studied the kinetics of the hydration of mesityl oxide (M) to diacetone alcohol (D) in aqueous phosphoric acid:



For reaction at  $39.7^\circ\text{C}$  at a constant water activity of 0.956, the rate ( $r$ ) is of the form

$$r = k_f(M) - k_r(D)$$

where the effect of the activity of water has been lumped into the pseudo first-order rate constant  $k_f$ . For the conditions cited,  $k_f = 8.51 \times 10^{-5} \text{ s}^{-1}$  and  $k_r = 7.75 \times 10^{-6} \text{ s}^{-1}$ .

- (a) This reaction is currently being carried out in a single large CSTR operating at  $39.7^\circ\text{C}$ . If this reactor has a volume of  $20 \text{ m}^3$ , the feed flow rate of the aqueous solution is  $5 \text{ m}^3/\text{h}$ , and the concentration of mesityl oxide in the feed stream is 2 M, determine the effluent concentration of mesityl oxide corresponding to steady-state operating conditions. No diacetone alcohol is present in the feed stream.
- (b) Now consider the case in which the concentration of the feed to the reactor is suddenly increased to 2.5 M. If the total quantity of solution in the CSTR remains constant, the reactor continues to operate at  $39.7^\circ\text{C}$ , and the flow rate of the feedstock remains constant, derive an equation for the effluent concentration of mesityl oxide as a function of time elapsed since the change in the feed concentration. Prepare a plot of the effluent concentration of mesityl oxide as a function of time elapsed since the step change in feed composition was made. In your derivation you will find it convenient to denote the effluent concentration of mesityl oxide corresponding to the steady-state operating conditions of part (a) as  $M^*$ . What is the value of the effluent concentration of mesityl oxide after 3 h has

elapsed? What is the new steady-state concentration of mesityl oxide?

- 8.39** A cascade consisting of two identical stirred-tank reactors is to be used to manufacture the intermediate product B, which is formed and consumed in the following sequence of liquid-phase reactions:



where the first reaction obeys first-order kinetics and the second reaction obeys second-order kinetics.

- (a) Derive the general equations that govern the steady-state concentrations of species A, B, and C that are present in the effluent from the second reactor in the cascade. It may be assumed that the feed stream consists of A dissolved in an inert solvent at a concentration  $C_{A0}$ .
- (b) Determine the concentrations of species A, B, and C in the effluent from the second reactor for the case where the feed concentration of species A is 2.7 M, each reactor has a volume of  $5.0 \text{ m}^3$ , the volumetric flow rate is  $4 \text{ m}^3/\text{h}$ , and the values of the rate constants  $k_1$  and  $k_2$  are  $1.6 \text{ h}^{-1}$  and  $0.2 \text{ M}^{-1}/\text{h}$ , respectively.
- (c) Do your calculations provide any evidence that the present mode of operation does not maximize the concentration of species B in the effluent from the second reactor? Should higher or lower flow rates be employed to increase the concentration of species B in the effluent from the second reactor? Determine the volumetric flow rate that maximizes this concentration.
- 8.40** A cascade of three identical CSTRs is currently employed to carry out an irreversible pseudo first-order reaction with water (W). The stoichiometry is



Each reactor has a volume of 500 gallons. In the presence of the acid form of an ion-exchange resin currently employed as a catalyst, the reaction is known to be first-order in species P, but the effective rate constant currently associated with this catalyst is uncertain because of losses of the solid maintained in suspension to attrition. If the cascade is operated such that the temperature of the contents of each reactor is  $50^\circ\text{C}$ , a flow rate of 25 gal/min leads to an overall conversion of species P of 93.6% (for the cascade). The concentration of species P in the feed stream is 2.2 M.

- (a) What is the value of the pseudo first-order rate constant for these operating conditions? What are the concentrations of species P and R leaving each reactor?
- (b) Consider the possibility of increasing by 40% the production capacity of the reactor network described above by employing different temperatures in the reactors in the cascade subject to the following constraints:
1. The overall conversion is to be held constant at 93.6%. The new feed rate is to be 35 gal/min.
  2. The first reactor in the cascade is to continue to operate at  $50^\circ\text{C}$ . The second and third reactors are both to operate at the same temperature, but this temperature remains to be determined.

Address the following questions: At what temperature should the second and third reactors be operated if the activation energy for the reaction is 18 kcal/mol? What are the concentrations of species P and R leaving each reactor?

- 8.41** T. D. Thornton and P. E. Savage [AIChE J., 38, 321–327 (1992)] studied the kinetics of the oxidation of phenol (P) by oxygen in supercritical water. The stoichiometry of the complete oxidation reaction is



However, this reaction does not proceed in a single step, but involves several intermediates. For pedagogical purposes we may account for the presence of these intermediates and the existence of multiple reaction pathways via the following relation

$$O_2 = [O_2]_0 - 7f_p[P]_0 \quad (2)$$

where  $f_p$  is the fraction of the phenol present in the fresh feed stream that has reacted.

Supercritical water is useful for the oxidative degradation of hazardous organic compounds because it is a good solvent for both oxygen and organic compounds. Thornton and Savage report that the rate of reaction 1 can be expressed as

$$r = k[P][O_2]^{0.5}[H_2O]^{0.7} \quad (3)$$

where

$$k = Ae^{-E/RT} \quad (4)$$

and the Arrhenius parameters are given by

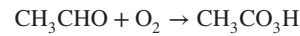
$$A = 303 \text{ M}^{-1.2}/\text{s}$$

with  $E = 12.4 \text{ kcal/mol}$ .

Consider the issue of designing a recycle reactor to accomplish the degradation of 99.99% of the phenol present at a concentration of  $1.1 \times 10^{-3} \text{ M}$  in supercritical water at  $380^\circ\text{C}$  and 278 atm. This destruction level is selected on the basis of Environmental Protection Agency standards for thermal treatment of hazardous organic wastes. The corresponding inlet concentration of oxygen is 0.08 M. Prepare a plot of the reactor volume required to process  $8 \text{ m}^3/\text{h}$  of the supercritical aqueous solution versus the recycle ratio for values of this ratio between 0 and 20. Comment.

Data concerning the PVT behavior of supercritical water are not readily available, but extrapolation of data in steam tables for pure water indicate that at 278 atm and  $380^\circ\text{C}$ , the specific volume is approximately  $0.048 \text{ ft}^3/\text{lb}$ .

- 8.42** V. A. Bryukhovetskii, S. S. Levush, F. B. Moin, and V. U. Shevchuk [Kinet. Catal., 17, 976 (1976)] studied the kinetics of the gas-phase oxidation of acetalydehyde to peracetic acid:



At temperatures in the range 170 to  $210^\circ\text{C}$  the rate expression is of the form

$$r = k_{\text{eff}} (CH_3CHO)^{1.5} [(O_2) + (CH_3CO_3H)]$$

with  $k_{\text{eff}} = 2.59 \times 10^{10} e^{-14,500/1.987T}$  for  $k_{\text{eff}}$  in  $\text{M}^{-1.5}/\text{s}$  and temperature in K. Although some by-products are formed, the selectivity to peracetic acid exceeds 90%. For present purposes you may neglect the side reactions. It has also been suggested that the use of a recycle reactor followed by a plug flow reactor would be appropriate for this autocatalytic reaction.

- (a) Determine the total reactor volume required to achieve an overall conversion of 95% of the limiting reagent when the feed composition is as follows (mole percentages):  $\text{CH}_3\text{CHO} = 80\%$ ;  $\text{O}_2 = 8.3\%$ ;  $\text{N}_2 = 11.7\%$ .

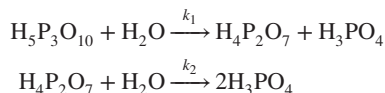
Both reactors are to operate at  $170^\circ\text{C}$  and 1 atm. The volumetric feed rate is  $3600 \text{ m}^3/\text{h}$ . Consider four recycle ratios: 0,  $1/9$ ,  $1/4$ , and  $1/2$ . The conversion leaving the recycle reactor has been selected arbitrarily as 45%. Comment on your results.

- (b) Now consider a hypothetical situation for which the autocatalytic pathway becomes more significant: namely, a rate expression of the form

$$r = k_{\text{eff}} (\text{CH}_3\text{CHO})^{1.5} [(\text{O}_2) + 5(\text{CH}_3\text{CO}_3\text{H})]$$

where  $k_{\text{eff}}$  retains the same value reported in the literature. Again determine the total reactor volume required to achieve an overall conversion of 95% of the limiting reagent for operation at the same temperature, pressure, inlet feed rate, and recycle ratios considered in part (a). You may again assume that the fraction conversion of the limiting reagent in the stream leaving the recycle reactor is 0.45.

- 8.43** E. Prodan and I. L. Shashkova [*Kinet. Catal.*, **24**, 891–894 (1984)] studied the kinetics of the decomposition of tripolyphosphoric acid in aqueous solution:



In aqueous solution, each of these reactions can be treated as if it were pseudo first-order in the participating acid. At  $40^\circ\text{C}$ , the corresponding values of  $k_1$  and  $k_2$  are 0.352 and  $0.065 \text{ h}^{-1}$ , respectively. Consider the task of analyzing the performance of a single CSTR in which these consecutive reactions are being carried out.

- (a) If the feed stream contains only  $\text{H}_5\text{P}_3\text{O}_{10}$  at a concentration of 0.10 M and is fed at a rate of 1500 L/h, determine the effluent concentrations of  $\text{H}_5\text{P}_3\text{O}_{10}$  (A),  $\text{H}_4\text{P}_2\text{O}_7$  (B), and  $\text{H}_3\text{PO}_4$  (C) from the CSTR (volume = 10,000 L) operating at steady state.
- (b) Now consider the situation in which the feed concentration of  $\text{H}_5\text{P}_3\text{O}_{10}$  is suddenly increased to 0.20 M. Derive an expression from which one can determine the manner in which the effluent concentration of  $\text{H}_5\text{P}_3\text{O}_{10}$  varies with the time measured from the instant the step change is made in the feed composition. The volumetric flow rate and the reactor volume do not change when the concentration of  $\text{H}_5\text{P}_3\text{O}_{10}$  is increased. Both the reactor volume and the volumetric flow rates of the feed and effluent streams

remain constant when the composition of the feed stream changes. Set up and solve the differential equation for the effluent concentration of  $\text{H}_4\text{P}_2\text{O}_7$  (B) as a function of time elapsed since the step change in the feed concentration of  $\text{H}_5\text{P}_3\text{O}_{10}$ .

- (c) Use the expressions determined in part (b) to prepare plots of the effluent concentrations of  $\text{H}_5\text{P}_3\text{O}_{10}$  and  $\text{H}_4\text{P}_2\text{O}_7$  for times from the moment the step change is made until 20 h later.
- (d) At the same time that the concentration of  $\text{H}_5\text{P}_3\text{O}_{10}$  is increased from 0.10 to 0.20 M, suppose that the concentration of a nonreactive species undergoes the same change. Derive the equation describing how the concentration of this species varies with time and plot it on the graph prepared for part (c).
- (e) Comment on the time constants for the various curves.

- 8.44** Consider a liquid-phase dimerization reaction



that is being carried out in a cascade of three identical CSTRs. This reaction is exothermic and it is desirable to carry out the reaction in a manner such that the heat loads on each of the component CSTRs is the same. Because the enthalpy change for the reaction is substantially independent of temperature, balancing the heat loads is equivalent to requiring that the rate of reaction in each reactor be the same. Furthermore, the last reactor in the cascade is to be operated at a temperature that maximizes the reaction rate at the desired overall conversion of 87%. The first and second reactors are to be operated at temperatures that cause the rate to be the same in each of the three reactors.

If the rate expressions for the forward and reverse reactions are given by

$$r_f = 1.10 \times 10^4 e^{-2800/T} (\text{A})^2$$

and

$$r_r = 6.3 \times 10^6 e^{-6600/T} (\text{B})$$

for temperature in K, for concentrations in M, and rates in  $\text{M}/\text{h}$ , determine:

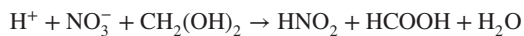
- (a) The concentration of species A leaving each reactor.
- (b) The temperatures at which the second and third reactors should be operated.
- (c) The volumes of the individual reactors that are necessary to process  $8 \text{ m}^3/\text{h}$  of feed solution if the concentration of species A in the feed is 3.0 M.

- 8.45** M. Horvath, I. Lengyel, and G. Bazsa [*Int. J. Chem. Kinet.*, **20**, 687–697 (1988)] reported that the kinetics of the oxidation of formaldehyde in aqueous nitric acid are governed by a rate expression of the form

$$-\frac{d[\text{CH}_2(\text{OH})_2]}{dt} = k(\text{NO}_3^-)(\text{H}^+)(\text{HNO}_2)[\text{CH}_2(\text{OH})_2]$$

where  $\text{CH}_2(\text{OH})_2$  represents the hydrated form of formaldehyde in aqueous solution and where  $k = 4.0 \times 10^{-5} \text{ M}^{-3} \cdot \text{s}$  at

room temperature. The stoichiometry of the reaction of interest may be regarded as



Consider the task of designing a recycle reactor network to process a volumetric flow rate of  $3.6 \text{ m}^3/\text{h}$  for a feed stream which is  $5 \text{ M}$  in  $\text{HNO}_3$ ,  $5 \times 10^{-4} \text{ M}$  in  $\text{HNO}_2$ , and  $0.21 \text{ M}$  in

$\text{CH}_2(\text{OH})_2$ . The recycle reactor is to achieve 95% conversion of the limiting reagent. Plot the reactor volume versus the recycle ratio for values of this ratio between zero and 2. What recycle ratio leads to the smallest reactor volume? What is this volume?

In working this problem you should regard the nitric acid as completely dissociated but neglect dissociation of  $\text{HNO}_2$  and  $\text{HCOOH}$ .

## Selectivity and Optimization Considerations in the Design of Isothermal Reactors

### 9.0 INTRODUCTION

In the present chapter we extend the treatment of the basic principles of reactor design to cases where multiple reactions are present. Because the choice of reactor type can have a strong influence on product distribution (and thereby on the economics of the process being investigated), the material in this chapter is inextricably linked to the problem of optimization. Rigorously speaking, the choice of the optimum reactor configuration should follow, not precede, investigations of the optimum operating conditions for each configuration. However, as far as selectivity considerations are concerned, it is usually possible to establish the most suitable reactor type by using relatively simple arguments based on the various rate expressions that are involved.

For purposes of reactor design, the distinction between a *single* reaction and *multiple* reactions is made in terms of the number of extents of reaction necessary to describe the kinetic behavior of the system, the former requiring only one reaction progress variable. Because the presence of multiple reactions makes it impossible to characterize the product distribution in terms of a unique fraction conversion, we will find it most convenient to work in terms of species concentrations. Division of one rate expression by another will permit us to eliminate time as an explicit independent variable, thereby obtaining expressions that are convenient for examining the effects of changes in process variables on the product distribution.

In discussions of systems in which only a single chemical reaction is involved, one may use the words *yield* and *conversion* as complementary terms. However, in dealing with multiple reactions, *conversion* refers to the proportion of a reagent that reacts, whereas *yield* refers to the amount of a specific product that is obtained. When a number of

alternative reaction paths are available to a given reactant, yield and conversion may not be simply related.

To avoid the possibility of obtaining yields in excess of 100%, it is necessary to employ stoichiometric coefficients to normalize one's calculations properly. It is also necessary to state whether the yield is computed relative to the amount of reactant introduced into the system or relative to the amount of reactant consumed. For example, for the reaction



where we take A to be the limiting reagent, the yield of species R ( $Y'_R$ ) may be defined as

$$Y'_R = \frac{a(N_R - N_{R0})}{r(N_{A0} - N_A)} \quad (9.0.2)$$

where  $N_R$  and  $N_A$  are the moles of species R and A present after reaction, respectively, and where the subscript zero refers to initial conditions. Use of the ratio of the stoichiometric coefficients is required to give 100% yield for complete conversion to R.

The concept of yield is useful in determining the *selectivity* of a catalyst or of a given reactor and operating conditions. Different conventions have been used in assigning numerical values to selectivity, but one that is often useful is the ratio of the amount of the limiting reagent that reacts to give the desired product to the amount that reacts to give an undesirable product.

There are many industrial situations where reactor designers have opted for selective catalysts or reaction conditions even though they lead to low reactivity. Although large reactor volumes are required, the economics of these situations are more favorable than those leading to high reactivity but low selectivity. The latter situation is

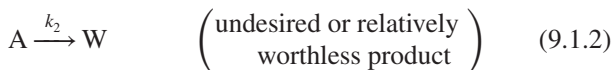
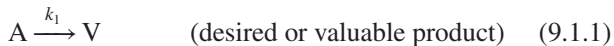
characterized by a smaller, cheaper reactor, but the raw material and separation costs necessary to produce a given amount of desired product are unacceptably high.

The bulk of this chapter is devoted to a discussion of optimization with regard to selectivity considerations. In the sections that follow we take  $\delta = 0$  in order to concentrate on the primary effects and to simplify the discussion. Consequently, in this chapter, the terms *space time*, *mean residence time*, and *holding time* may be used interchangeably.

## 9.1 COMPETITIVE (PARALLEL) REACTIONS

The possibility of a species reacting by parallel paths to yield geometric isomers or entirely different products is often responsible for low yields of a desired product. If circumstances are such that the orders of the desired and unwanted reactions are different with respect to one or more species, it is possible to promote the desired reaction by an appropriate choice of reactor type and reaction conditions.

Following the treatment of Levenspiel (1), we begin by considering a set of parallel reactions in which only a single reactant species has any influence on the corresponding rate expressions:



The corresponding rate expressions are

$$r_V = \frac{dC_V}{dt} = k_1 C_A^{\alpha_1} \quad (9.1.3)$$

$$r_W = \frac{dC_W}{dt} = k_2 C_A^{\alpha_2} \quad (9.1.4)$$

Elimination of time as a variable between equations (9.1.3) and (9.1.4) gives

$$\frac{r_V}{r_W} = \frac{dC_V}{dC_W} = \frac{k_1}{k_2} C_A^{(\alpha_1 - \alpha_2)} \quad (9.1.5)$$

It follows that for this situation one obtains maximum selectivity by choosing reaction conditions such that the ratio  $(r_V/r_W)$  always has its highest value. This ratio is often referred to as *instantaneous selectivity*.

For a specific system at a given temperature, nature dictates the values of  $k_1$ ,  $k_2$ ,  $\alpha_1$ , and  $\alpha_2$ . The only factor that the engineer is at liberty to adjust and control is  $C_A$ . This concentration may be maintained at a high level by using a batch or plug flow reactor, by operating at low conversions, by increasing the pressure in gas-phase

systems, and by avoiding the use of inert diluents in the feed. Low concentrations of a reactant are achieved using a single CSTR, operating at high conversions, decreasing the pressure in gaseous systems, and adding inert to the feed stream. Note that in this case the desire for selectivity works at cross purposes to the desire for a small reactor size so that a good design with respect to one constraint may be poor with respect to other constraints. In this situation a detailed economic analysis is necessary to optimize the design.

Let us now consider the three possible rankings of the reaction orders in order to determine when the concentration of species A should be kept at high or low values.

**Case 1:**  $\alpha_1 > \alpha_2$ . In this case the order of the desired reaction is higher than that of the unwanted reaction, so the exponent on the concentration is positive. The instantaneous selectivity is promoted by employing high concentrations of reactant. Consequently, batch or plug flow reactors are most appropriate from a selectivity viewpoint. Because the selectivity is enhanced by operating at relatively low conversions, one must strike a balance between high separation costs and selective production of the economically desirable species.

**Case 2:**  $\alpha_2 > \alpha_1$ . In this situation the order of the unwanted reaction is greater than that of the reaction desired, so the selectivity is enhanced by using low concentrations of reactant. Use of a single CSTR is appropriate from a selectivity standpoint. Unfortunately, this situation is one in which the selectivity considerations work against the desire for a small reactor size.

**Case 3:** If the orders of the two parallel reactions are identical, the selectivity is a constant given by the ratio of the rate constants:

$$\frac{r_V}{r_W} = \frac{k_1}{k_2} \quad (9.1.6)$$

The relative product yields in this case are insensitive to the type of reactor used, so reactor volume considerations will govern the choice of reactor type.

In all three cases it is possible to influence the product distribution by changing process conditions so as to bring about changes in the ratio of rate constants. The selectivity can be enhanced by changing the operating temperature if the activation energies of the two rate constants are different. Other methods by which the selectivity can be improved include use of a catalyst to accelerate the reaction desired and use of an inhibitor to repress the unwanted reaction. Use of catalysts and inhibitors may, however, lead to changes in the observed reaction orders with concomitant implications for the type of reactor that is preferred.

In the case of other parallel reactions with different reaction rate expressions, similar analyses can be used to ascertain the influence of various reactant concentrations on the selectivity of a proposed process. Such analyses

would lead to the following generalization, which is useful in considerations of parallel reactions in which the reactant concentration level influences the product distribution: *High reactant concentrations favor the reaction of higher order, while low reactant concentrations favor the reaction of lower order.*

In cases where the orders of the reactions in question are the same with respect to a particular reactant, the product distribution is independent of the concentration level of that species. It is, of course, possible to have situations in which the selectivity is enhanced by a high concentration of one reactant and by a low concentration of a second reactant. The higher the concentration dependence, the more important it is to keep a particular species at a high or a low value. Figures 9.1 and 9.2 depict some possible modes of contacting in batch and continuous flow reactors for some common situations. The most desirable contacting pattern and mode of operation can be determined only by considering several alternative processing modes and the possibility of recycle of reactants, either prior to or subsequent to separation of the products.

To determine the product distribution quantitatively, it is necessary to combine material balance and reaction rate

expressions for a given reactor type and contacting pattern. On the other hand, if the reactor size is desired, alternative design equations reflecting these rate expressions and material balances must be employed. For these purposes it may be convenient to work in terms of the fractional yield. This yield is the ratio of the amount of a product formed to the amount of reactant consumed. The *instantaneous fractional yield* of a product V (denoted by the symbol  $y$ ) is defined as

$$y = \frac{\nu_A}{\nu_V} \frac{dC_V}{dC_A} \quad (9.1.7)$$

while the *overall fractional yield*  $Y$  is defined as

$$Y = \frac{\nu_A}{\nu_V} \left( \frac{C_{VF} - C_{V0}}{C_{AF} - C_{A0}} \right) \quad (9.1.8)$$

Appropriate stoichiometric coefficients are employed to ensure that  $y$  and  $Y$  lie between zero and 1. The overall fractional yield is the average of the instantaneous fractional yield integrated over the reactor. The proper averaging technique depends on the type of reactor employed. Because the fluid composition is constant throughout the volume of a single CSTR, this type of

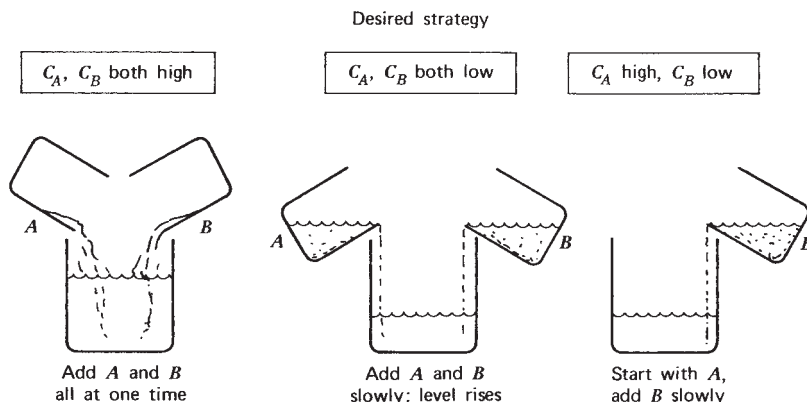


**Figure 9.1** Contacting patterns for various combinations of high and low concentrations of reactants in noncontinuous operations (batch reactors). (Adapted from O. Levenspiel, *Chemical Reaction Engineering*, 2nd ed. Copyright © 1972. Reprinted by permission of John Wiley & Sons, Inc.)

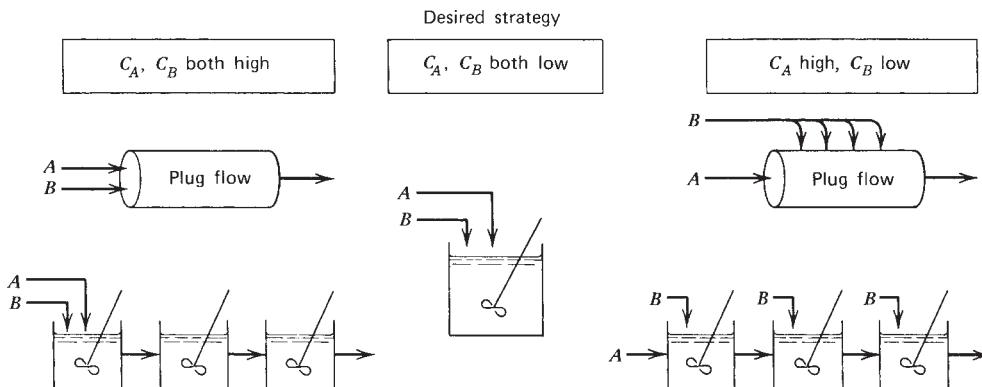


**Figure 9.2** Contacting patterns for various combinations of high and low concentrations of reactants in continuous-flow operations. (Adapted from O. Levenspiel, *Chemical Reaction Engineering*, 2nd ed. Copyright © 1972. Reprinted by permission of John Wiley & Sons, Inc.)

reactor does not present any problems with respect to the averaging process. For this case the instantaneous and overall yields are identical:

$$Y_{\text{CSTR}} = y_{\text{CSTR}} = \frac{\nu_A r_{\text{VF}}}{\nu_V r_{\text{AF}}} \quad (9.1.9)$$

where the rate expressions are evaluated at the reactor effluent composition.

For a plug flow or a batch reactor where the reactant concentration varies with position or with time, the overall yield can be determined by noting that

$$C_{\text{VF}} - C_{\text{V0}} = \int_{C_{\text{A0}}}^{C_{\text{AF}}} \frac{\nu_V y}{\nu_A} dC_A \quad (9.1.10)$$

Substitution into the definition for the overall yield gives

$$\begin{aligned} Y &= \frac{1}{C_{\text{AF}} - C_{\text{A0}}} \int_{C_{\text{A0}}}^{C_{\text{AF}}} y \, dC_A \\ &= \frac{1}{C_{\text{A0}} - C_{\text{AF}}} \int_{C_{\text{AF}}}^{C_{\text{A0}}} y \, dC_A \end{aligned} \quad (9.1.11)$$

It is possible to extend this treatment to the case of multiple CSTRs operating in series by adapting the procedure outlined by Denbigh and Turner (2). Let  $(\Delta C_A)_1$ ,  $(\Delta C_A)_2$ , and  $(\Delta C_A)_i$  represent the changes in the concentration of species A that take place in tanks 1, 2, and  $i$ , respectively.

$$(\Delta C_A)_i = (C_A)_i - (C_A)_{i-1} \quad (9.1.12)$$

where  $(C_A)_i$  is the concentration of reactant A in tank  $i$ . The associated changes in the concentrations of the valuable product V are given by

$$(\Delta C_V)_i = \frac{\nu_V}{\nu_A} (\Delta C_A)_i y_i \quad (9.1.13)$$

where  $y_i$  is the yield characteristic of the steady-state concentrations prevailing in the  $i$ th tank. This relation follows directly from equation (9.1.7) as applied to a finite process taking place at constant  $y$ . The overall change in the concentration of species V is obtained by summing over the pertinent number of tanks ( $n$ ):

$$\Delta C_V = C_{\text{Vn}} - C_{\text{V0}} = \frac{\nu_V}{\nu_A} \sum_{i=1}^n [y_i (\Delta C_A)_i] \quad (9.1.14)$$

Combination of this result with the definition of the overall yield given by equation (9.1.8) gives

$$Y = \frac{\sum_{i=1}^n [y_i (\Delta C_A)_i]}{C_{\text{An}} - C_{\text{A0}}} \quad (9.1.15)$$

This equation is the CSTR cascade analog of equation (9.1.11) for a PFR. The overall yield is a summation over

the instantaneous yields weighted by the fraction of the concentration change that takes place in each tank.

For those cases where the rate expressions for all reactions taking place in the system under study are known, the use of the instantaneous yield in the equations above does not contribute significantly to understanding the system behavior. In such cases it is easier to determine the overall yield by substituting the appropriate ratio of reaction rate expressions for the instantaneous yield in equations like equation (9.1.11) and then evaluating the integral directly. Unfortunately, there are many significant industrial reactions, particularly heterogeneous catalytic reactions involving a complex feedstock, for which formal rate expressions are not known. For these cases the concept of instantaneous yield can sometimes be quite useful. This situation occurs when the instantaneous yield depends on only a single composition variable. In such cases  $y$  can often be measured with far less effort than would be needed to determine the formal rate expressions for the various competing reactions. Plots of the instantaneous yield versus composition may be generated from the results of a series of steady-state experiments in a CSTR. All runs are carried out at the same temperature and catalyst conditions. The shape of the curve determines which type of reactor configuration gives rise to the optimum product distribution.

Figure 9.3 contains typical instantaneous yield versus reactant concentration plots. The shaded areas indicate the composition changes of the desired product that are effected by various reactor types. From the definition of the overall yield,

$$C_{\text{VF}} - C_{\text{V0}} = -\frac{\nu_V}{\nu_A} Y (C_{\text{A0}} - C_{\text{AF}}) \quad (9.1.16)$$

Combination of this equation and equation (9.1.11) gives

$$C_{\text{VF}} - C_{\text{V0}} = -\frac{\nu_V}{\nu_A} \int_{C_{\text{AF}}}^{C_{\text{A0}}} y \, dC_A \quad (9.1.17)$$

Hence, the area under the curve of  $y$  versus  $C_A$  multiplied by the ratio of stoichiometric coefficients represents the overall change in valuable product concentration between the inlet and outlet streams in a plug flow reactor or in a batch reactor. For the case of a CSTR, the instantaneous yield is evaluated at the effluent composition, and the corresponding equation is

$$C_{\text{VF}} - C_{\text{V0}} = -\frac{\nu_V}{\nu_A} y_F (C_{\text{A0}} - C_{\text{AF}}) \quad (9.1.18)$$

Thus, the pertinent area in this case is the rectangle shown in Figure 9.3b. For a staged cascade of stirred-tank reactors, a similar analysis indicates that the pertinent area is that given by the sum of the rectangles corresponding to the individual tanks.

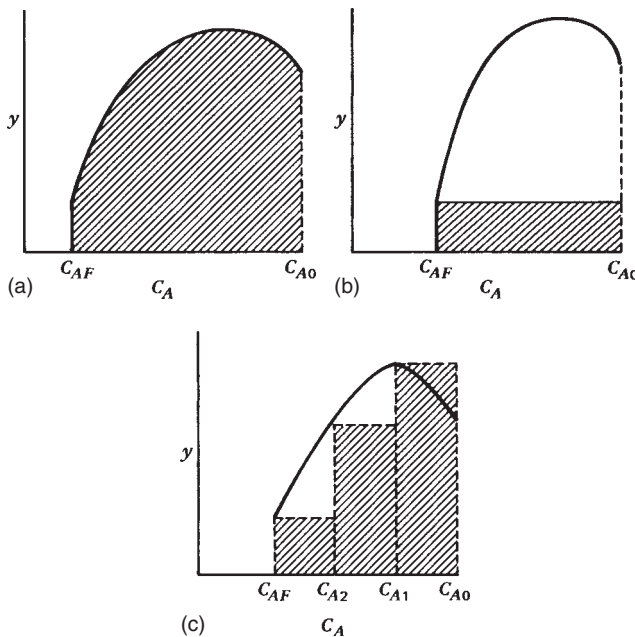


**Figure 9.3** Instantaneous yield versus reactant concentration curves and their relation to overall product concentration changes: (a) plug flow or batch reactor; (b) single CSTR; (c) cascade of three arbitrary-sized CSTRs in series. (Adapted from O. Levenspiel *Chemical Reaction Engineering*, 2nd ed. Copyright © 1972. Reprinted by permission of John Wiley & Sons, Inc.)

The shape of the instantaneous yield curve determines the optimum reactor configuration and flow pattern for a particular reaction network. For cases where the instantaneous yield increases continuously with increasing reactant concentration, the optimum reactor configuration from a product selectivity viewpoint is a plug flow or batch reactor. If the instantaneous yield decreases continuously with increasing reactant concentration, the optimum product distribution is achieved using a continuous stirred-tank reactor. When maxima or minima are observed in the instantaneous yield curve, the selectivity desired is enhanced by the use of a combination of plug flow and stirred-tank reactors. However, considerations other than selectivity may influence the final choice of reactor type, especially when the instantaneous yield curve is relatively flat over the reactant concentration range of interest.

For cases where there are three or more reactions occurring in parallel, the rate expressions may be such that the order of the reaction that leads to the product desired lies between the orders of reactions that lead to undesirable products. For this case the relative significance of the competing reactions changes as the reaction proceeds. Initially, the yield is diminished because of formation of the by-product created by the highest-order reaction. This effect decreases as the reaction progresses. At high conversions, on the other hand, the yield is decreased by formation of

by-products resulting from the low-order reaction. In this situation the yield is optimized by using a stirred-tank reactor followed by a plug flow reactor (3). This procedure permits one to “skip” the high concentration range where one of the by-products is formed.

Illustration 9.1 indicates how the principles enunciated above may be used in optimizing the yield of a desired product when dealing with parallel reactions.

### ILLUSTRATION 9.1 Quantitative Treatment of Irreversible Parallel Reactions Occurring in a Liquid Phase

Species A is present in liquid solution at an initial concentration  $C_{A0}$ . This species may undergo the reactions indicated by the following mechanistic equations:



$$\text{by isomerization} \quad r_1 = k_1 C_A$$



$$\text{disproportionation or dimerization}) \quad r_2 = k_2 C_A^2$$

Neither V nor any of the undesirable product species are present in the feed stream. For both a plug flow reactor and a single continuous flow stirred-tank reactor determine the maximum yields of V that can be obtained in the limit at which the conversion of A approaches 100%. Prepare plots of the effluent concentrations of all species versus reactor space time for each type of reactor. To quantify the concentration of the undesired products in the effluent, consider the dimerization reaction ( $2A \rightarrow D$ ) as the only significant reaction.

Parameter values:  $C_{A0} = 2 \text{ M}$ ;  $k_1 = 1.0 \text{ min}^{-1}$ ; and  $k_2 = 0.4 \text{ M}^{-1}/\text{min}$ .

### Solution

Equation (9.1.11) is appropriate for determining the overall yield in a plug flow reactor:

$$Y_{PFR} = \frac{1}{C_{A0} - C_{AF}} \int_{C_{AF}}^{C_{A0}} y \, dC_A \quad (\text{A})$$

where

$$\begin{aligned} y &= \frac{\nu_A}{\nu_V} \frac{dC_V}{dC_A} = \frac{dC_V}{dC_A} = \frac{k_1 C_A}{k_1 C_A + 2k_2 C_A^2} \\ &= \frac{1}{1 + (2k_2/k_1)C_A} \end{aligned} \quad (\text{B})$$

Thus,

$$Y_{\text{PFR}} = \frac{1}{C_{A0} - C_{AF}} \int_{C_{AF}}^{C_{A0}} \frac{dC_A}{1 + (2k_2/k_1)C_A} \quad (\text{C})$$

and integration gives

$$Y_{\text{PFR}} = \frac{k_1}{2k_2(C_{A0} - C_{AF})} \ln \left[ \frac{1 + (2k_2/k_1)C_{A0}}{1 + (2k_2/k_1)C_{AF}} \right] \quad (\text{D})$$

In the limit of complete conversion, as  $C_{AF}$  approaches zero,

$$Y_{\text{PFR}} = \frac{k_1}{2k_2C_{A0}} \ln \left[ 1 + \frac{2k_2}{k_1} C_{A0} \right] \quad (\text{E})$$

Now consider the case of a stirred-tank reactor. The overall yield is given by equation (9.1.9):

$$Y_{\text{CSTR}} = \frac{\nu_A r_{VF}}{\nu_V r_{AF}} = \frac{k_1 C_{AF}}{k_1 C_{AF} + 2k_2 C_{AF}^2} = \frac{1}{1 + (2k_2/k_1)C_{AF}} \quad (\text{F})$$

In the complete-conversion limit as  $C_{AF}$  approaches zero, the overall yield in the CSTR approaches unity. If the plug flow and stirred-tank reactors are operated at less than complete conversion, equations (D) and (F) indicate that at the same conversion the yield from the CSTR will always exceed that from the PFR.

We can quantify how the overall yield varies over the range of conversions by plotting these two curves for particular values of the rate constants and the concentration of reactant A in the feed stream. Examination of Figure 9.4 reveals that at low conversion ( $C_{AF} \approx C_{A0}$ ) each reactor gives substantially the same low yield of V from A (ca. 40%). At high conversions,  $C_{AF}$  becomes small and the undesired, second-order reaction occurs to a negligible extent. For this level of conversion there are significant benefits to operating the CSTR at the outlet concentration. The selectivity of the process for production of V from A then approaches 100%. By contrast, the selectivity for V associated with a PFR gradually increases with increasing conversion because the various fluid elements moving through the PFR experience the entire range of concentrations of species A from  $C_{A0}$  to  $C_{AF}$ . The uniform low concentrations of species A in the CSTR lead to slower reaction rates than those in the PFR. Consequently, to achieve the same conversion of A in a CSTR as in a PFR, one requires a larger space time (larger reactor).

The relations between the outlet concentrations of A, V, and D and the space times for the two types of reactors are shown in the two panels of Figure 9.5. The outlet concentrations for the PFR were obtained by numerical integration of the PFR balance equations. The CSTR results were obtained by first solving the CSTR design equation for the outlet concentration of species A, followed by use

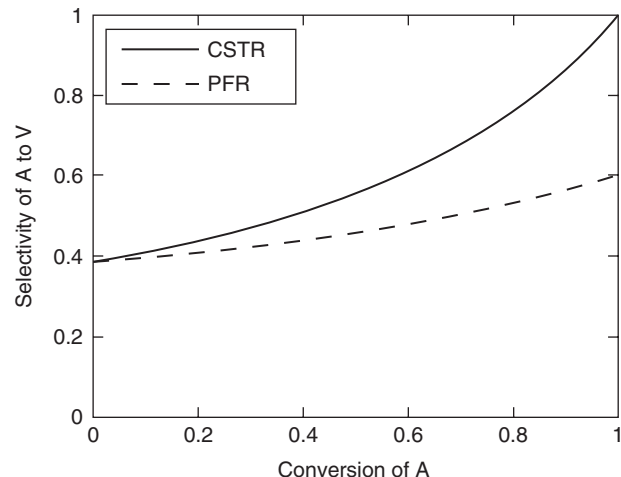


**Figure 9.4** Dependence of overall yield of V from A for both a plug flow reactor and an individual continuous flow stirred-tank reactor.

of this value to calculate the concentrations of V and D via appropriate material balances on the CSTR.

The higher selectivity obtained in a CSTR is obtained only at the expense of using a much larger reactor (larger space time). At a space time of only 5 min, the PFR achieves 99.7% conversion of A, with a maximum selectivity of A to V of 60%. In contrast, at a space time of 20 min, the CSTR reaches a conversion of only 95% but has a higher selectivity of A to V (92%); use of even larger reactor volumes can increase both conversion and selectivity to 100%.

Selection of the type of reactor to employ involves an economic compromise between the concomitant increase in the cost of the CSTR and the relative values of product V and the losses associated with the presence of unconverted A in the reactor effluent when operating at less than complete conversion.

This illustration provides a concrete example of the selectivity considerations involved in an analysis of irreversible parallel reactions. The illustration indicates in quantitative fashion the validity of the general rule of thumb that we have stated for analyzing parallel reactions. *High concentrations favor the higher-order reaction, and low concentrations favor the lower-order reaction.*

## 9.2 CONSECUTIVE (SERIES) REACTIONS: $A \xrightarrow{k_1} B \xrightarrow{k_2} C \xrightarrow{k_3} D$

There are innumerable industrially significant reactions that involve the formation of a stable intermediate product that is capable of subsequent reaction to form yet another stable product. These include condensation polymerization reactions, partial oxidation reactions, and reactions in which it is possible to effect multiple substitutions of a particular functional group on the parent species. If an intermediate is the

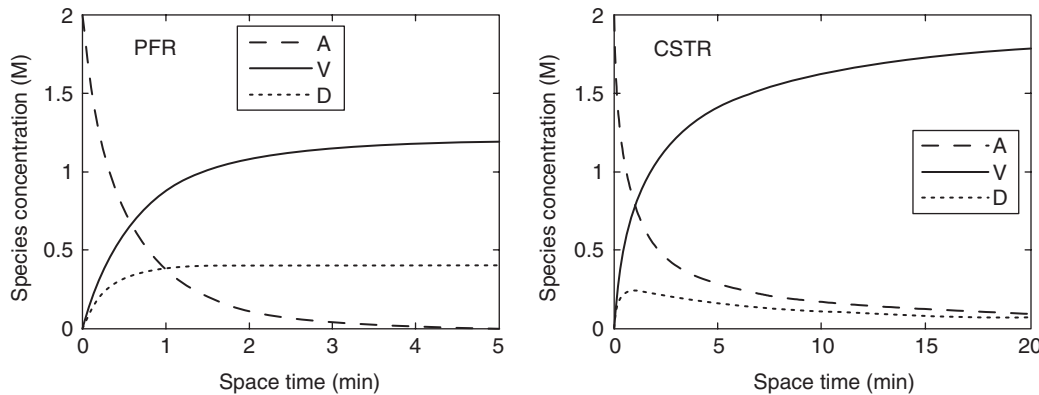


**Figure 9.5** Dependence of effluent species concentrations on reactor space time for both a plug flow reactor and an individual continuous flow stirred-tank reactor.

desired product, commercial reactors should be designed to optimize the production of this species. This section is devoted to a discussion of this and related topics for reaction systems in which the reactions may be considered as sequential or consecutive in character.

For the situation in which each of the series reactions is irreversible and obeys a first-order rate law, equations (5.3.4), (5.3.6), (5.3.9), and (5.3.10) describe the variations of the species concentrations with time in an isothermal well-mixed batch reactor. For consecutive reactions in which all of the reactions do not obey simple first-order or pseudo first-order kinetics, the rate expressions can seldom be solved in closed form, and it is necessary to resort to numerical methods to determine the time dependence of various species concentrations. Irrespective of the particular reaction rate expressions involved, there will be a specific time at which the concentration of a particular intermediate passes through a maximum. If interested in designing a continuous-flow process for producing this species, the chemical engineer must make appropriate allowance for the flow conditions that will prevail within the reactor. That disparities in reactor configurations can bring about wide variations in desired product yields for series reactions is evident from the examples considered in Illustrations 9.2 and 9.3.

### ILLUSTRATION 9.2 Quantitative Development of Consecutive Reaction Relationships for Batch and Plug Flow Reactors

For the set of first-order consecutive reactions,



determine the optimum holding time in a batch reactor and the optimum space time in a plug flow reactor in terms of

maximizing the concentration of the intermediate V. What will the maximum concentration be in each case? It may be assumed that only species A is present initially.

### Solution

For systems in which the fluid density is constant, the design equations for plug flow and batch reactors are mathematically identical in form with the space time and the holding time playing comparable roles (see Chapter 8). Consequently it is necessary to consider only the batch reactor case. The pertinent rate equations were solved in Section 5.3.1.1 to obtain the following results:

$$\frac{C_A}{C_{A0}} = e^{-k_1 t} \quad (A)$$

$$\frac{C_V}{C_{A0}} = \frac{k_1}{k_2 - k_1} (e^{-k_1 t} - e^{-k_2 t}) \quad (B)$$

$$\frac{C_W}{C_{A0}} = 1 - \frac{C_A}{C_{A0}} - \frac{C_V}{C_{A0}} \quad (C)$$

The time corresponding to maximum yield of V is obtained by differentiating equation (B) with respect to time and setting the derivative equal to zero:

$$\frac{d(C_V/C_{A0})}{dt} = \frac{k_1}{k_2 - k_1} (-k_1 e^{-k_1 t} + k_2 e^{-k_2 t}) = 0$$

or

$$\frac{k_1}{k_2} = e^{-(k_2 - k_1)t_{\text{optimum}}}$$

Hence, for a *plug flow* or *batch reactor*:

$$t_{\text{optimum}} = \frac{\ln(k_1/k_2)}{k_1 - k_2} = \frac{1}{k_{\log \text{ mean}}} \quad (D)$$

The optimum time could also have been determined by noting that this time is also that at which the rate of formation of W is most rapid.

Equation (B) may be rewritten as

$$\frac{C_V}{C_{A0}} = \frac{k_1 e^{-k_1 t}}{k_2 - k_1} [1 - e^{(k_1 - k_2)t}] \quad (\text{E})$$

Substitution of equation (D) into equation (E) gives an expression for the maximum obtainable concentration of species V.

$$\begin{aligned} \frac{C_{V,\text{max}}}{C_{A0}} &= \frac{k_1 e^{-[k_1 \ln(k_1/k_2)]/(k_1 - k_2)}}{k_2 - k_1} [1 - e^{\ln(k_1/k_2)}] \\ &= \frac{k_1}{k_2 - k_1} \left( \frac{k_1}{k_2} \right)^{-k_1/(k_1 - k_2)} \left( 1 - \frac{k_1}{k_2} \right) \end{aligned}$$

or

$$\begin{aligned} \frac{C_{V,\text{max}}}{C_{A0}} &= \frac{k_1}{k_2 - k_1} \left( \frac{k_1}{k_2} \right)^{-k_1/(k_1 - k_2)} \left( \frac{k_2 - k_1}{k_2} \right) \\ &= \left( \frac{k_1}{k_2} \right)^{1-[k_1/(k_1 - k_2)]} = \left( \frac{k_1}{k_2} \right)^{k_2/(k_2 - k_1)} \end{aligned} \quad (\text{F})$$

For the conditions cited, this is the maximum possible yield of species V.

### ILLUSTRATION 9.3 Quantitative Development of Consecutive Reaction Relationships for a Single Continuous Flow Stirred-Tank Reactor

For the set of first-order consecutive reactions considered in Illustration 9.2, determine the optimum space time in a single stirred-tank reactor from the standpoint of maximizing production of the intermediate. What will be the effluent concentration of V for this optimum operating condition? It may be assumed that species V and W are not present in the feed stream.

#### Solution

The effluent composition is readily obtained by writing a material balance on each species and solving the resulting set of equations. Hence at steady state,

input = output + disappearance by reaction

For A:

$$C_{A0}\mathcal{V} = C_{AF}\mathcal{V} + k_1 C_{AF} V_R \quad (\text{A})$$

For V:

$$0 = C_{VF}\mathcal{V} + (k_2 C_{VF} - k_1 C_{AF}) V_R \quad (\text{B})$$

For W:

$$0 = C_{WF}\mathcal{V} - k_2 C_{VF} V_R \quad (\text{C})$$

where the usual significance is attached to each symbol. From equation (A),

$$\frac{C_{AF}}{C_{A0}} = \frac{1}{1 + k_1(\mathcal{V}_R/\mathcal{V})} = \frac{1}{1 + k_1\tau} \quad (\text{D})$$

From equations (B) and (D),

$$C_{VF} = \frac{k_1 C_{AF} V_R}{\mathcal{V} + k_2 V_R} = \frac{k_1 C_{AF} \tau}{1 + k_2 \tau} = \frac{k_1 C_{A0} \tau}{(1 + k_1 \tau)(1 + k_2 \tau)} \quad (\text{E})$$

From equations (C) and (E),

$$C_{WF} = k_2 C_{VF} \frac{V_R}{\mathcal{V}} = k_2 C_{VF} \tau = \frac{k_1 k_2 C_{A0} \tau^2}{(1 + k_1 \tau)(1 + k_2 \tau)} \quad (\text{F})$$

The space time corresponding to a maximum concentration of species V is obtained by differentiating equation (E) with respect to  $\tau$ , and setting the derivative equal to zero.

$$\frac{dC_{VF}}{d\tau} = 0 = k_1 C_{A0} \times (\Psi_N/\Psi_D)$$

where

$$\Psi_N = \{(1 + k_1 \tau)(1 + k_2 \tau) - \tau[(1 + k_1 \tau)k_2 + (1 + k_2 \tau)k_1]\}$$

and where

$$\Psi_D = [(1 + k_1 \tau)^2(1 + k_2 \tau)^2]$$

Expansion of the products in the numerator leads to

$$1 - k_1 k_2 \tau_{\text{optimum}}^2 = 0$$

or

$$\tau_{\text{optimum}} = \frac{1}{\sqrt{k_1 k_2}} \quad (\text{G})$$

Substitution of this result into equation (E) gives an expression for the maximum possible effluent concentration of the desired species.

$$\begin{aligned} \frac{C_{V,\text{max}}}{C_{A0}} &= \frac{(k_1/k_2)^{1/2}}{[1 + (k_1/k_2)^{1/2}][1 + (k_1/k_2)^{1/2}]} \\ &= \frac{1}{[1 + (k_1/k_2)^{1/2}]^2} \end{aligned} \quad (\text{H})$$

The ratio of the maximum yield achievable in a CSTR to that which can be obtained in a PFR is given by the ratio of equation (H) to equation (F) of Illustration 9.2. Hence,

$$\frac{Y_{\text{max,CSTR}}}{Y_{\text{max,PFR}}} = \frac{1}{[1 + (k_1/k_2)^{1/2}]^2 (k_1/k_2)^{k_2/(k_2 - k_1)}}$$

This relative yield is plotted in Figure I9.3 as a function of the ratio of rate constants,  $k_2/k_1$ . The largest disparity in the yields is obtained when this ratio is unity (i.e., when the two rate constants are identical). The more this

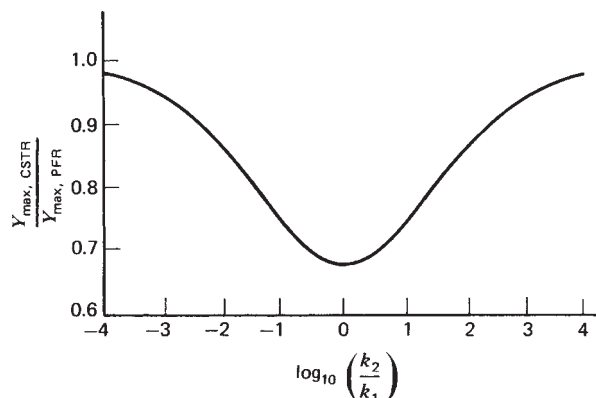


**Figure 19.3** Comparison of maximum yields for series reactions in a single stirred tank and a plug flow reactor.

ratio departs from unity, the more nearly equal the yields become. At very high and very low values of this ratio, the system behaves as if only a single reaction has any influence on the reactor design. Because the minimum value of the relative yield is 0.68, the difference in yields can have a very significant influence on the overall process economics. Figure 19.3 indicates the range of values of  $k_2/k_1$  for which the differences in yield are significant. Successive substitution reactions are often characterized by rate constants that produce results lying near the minimum in the relative yield curve.

As we noted earlier, there may be temperature control/heat transfer considerations or other factors that dictate the use of a CSTR even when the yield considerations are unfavorable. In such cases the yield of the desired product may be significantly increased by using a battery of CSTRs in series. If desired, one has the additional flexibility granted by using tanks with different volumes or tanks

operating at different temperatures in the production line. The relative capacities of the various tanks may then be chosen to optimize product yield. This problem was considered previously by Denbigh (4). He has shown that if both reactions are first-order and if isothermal conditions prevail, the capacities of all tanks should be the same. However, if the degradation reaction is of higher order than that producing the desired product, the capacities of the tanks should become smaller from the first tank onward. Conversely, if the degradation reaction is of lower order, the capacities of the tanks should increase from the first tank onward.

There are a few other points worthy of note that become evident on closer inspection of the equations developed in Illustrations 9.2 and 9.3. First, except for the case where  $k_2/k_1 = 1$ , the plug flow or batch reactor requires a lower space or holding time than a CSTR to achieve the maximum concentration of intermediate. The more this ratio departs from unity, the greater the difference in space times. This fact becomes evident on substitution of numerical values into equations (C) and (G) of Illustrations 9.2 and 9.3, respectively, or when plots of  $C_V/C_{A0}$  versus  $k_1\tau$  are prepared for various ratios of  $k_2/k_1$  [see, e.g., Levenspiel (5)]. In general, for series reactions, the maximum possible yields of intermediates are obtained when fluids of different compositions (different stages of conversion) are not allowed to mix.

Second, it is possible to plot the data in time-independent form to obtain curves that are useful in the determination of  $k_2/k_1$  in studies of reaction kinetics. The experimental points are matched with one of the families of curves on plots corresponding to the type of reactor used in the investigation. Figure 9.6 is an example of this type of plot for a continuous stirred-tank reactor.

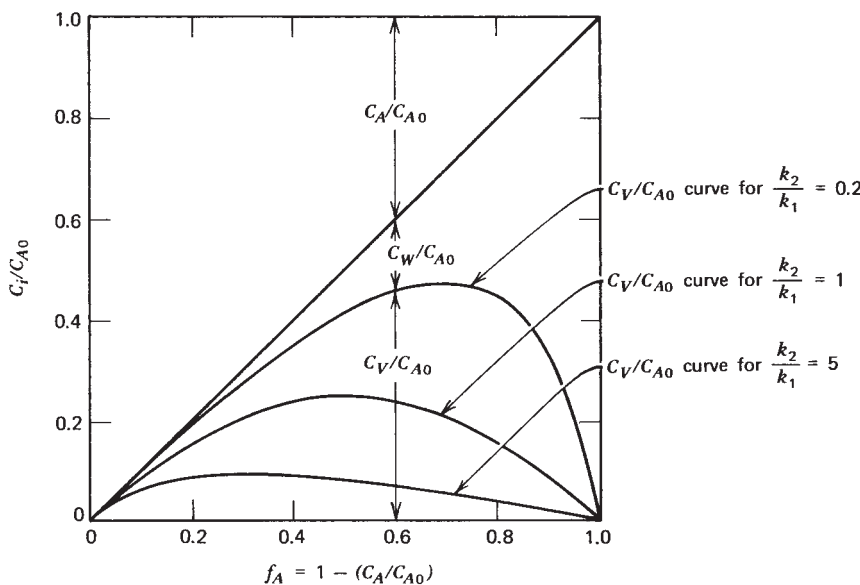


**Figure 9.6** Dimensionless representation of product distributions for consecutive first-order irreversible reactions:  $A \rightarrow V \rightarrow W$  (stirred-tank reactor).

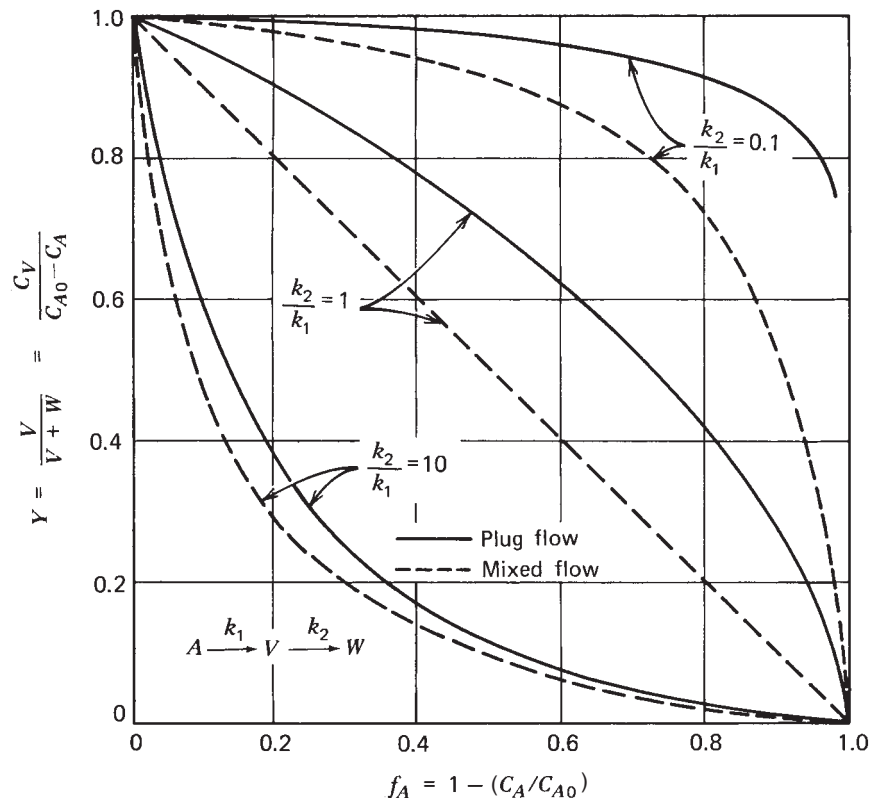


**Figure 9.7** Comparison of the fractional yields of V in mixed and plug flow reactors for the consecutive first-order reactions.  $A \rightarrow V \rightarrow W$ . (Adapted from O. Levenspiel, *Chemical Reaction Engineering*, 2nd ed. Copyright © 1972. Reprinted by permission of John Wiley & Sons, Inc.)

For cases where it is possible to readily recover unconverted reactant A from the product mixture for recycle to the reactor inlet, the use of the definition of yield employed in Illustrations 9.2 and 9.3 is not appropriate. In this situation, a more appropriate definition is

$$Y = \frac{C_V}{C_{A0} - C_A} = \frac{C_V}{C_V + C_W} \quad (9.2.1)$$

The equations derived earlier for the effluent concentrations in the PFR and CSTR cases may be substituted into equation (9.2.1) to obtain numerical values of the fractional yield of the intermediate V as a function of the fraction of the initial A converted. Levenspiel (6) has prepared such plots, and Figure 9.7 is reproduced from his textbook. This figure presents the fractional yield of intermediate V as a function of the ratio of rate constants ( $k_2/k_1$ ) and the fraction A converted. The curves indicate that the fractional yield of the intermediate species is always higher for plug flow than when extensive backmixing occurs, regardless of the conversion level. Moreover, the figure has important implications with regard to the conversion level of species A for which one should design. If the reaction under consideration has a value of  $k_2/k_1$  that is greater than unity, the fractional yield of V decreases very rapidly with increasing conversion, even at low values of the conversion of species A. Thus, to avoid excessive production of the undesirable product W, it is necessary to design for a low conversion

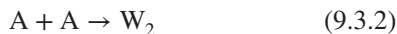
of A per pass and to recycle this species after separation from the product mixture. In such cases the load on the separation equipment will be high, and large quantities of material will have to be processed per unit of desired product. Consequently, the costs of the separation process will strongly influence the overall process economics. As the ratio  $k_2/k_1$  decreases below unity, the fractional yield of the intermediate increases at a constant level of conversion. It is evident that at low values of  $k_2/k_1$ , this yield becomes relatively insensitive to the fraction conversion until the conversion level begins to exceed 80 to 90%. In this situation one should design for relatively high conversion levels.

Although the bulk of the discussion in this section and the illustrative examples have been restricted to successive first-order reactions, concentration versus time curves can be developed for other cases, including those where the consecutive reactions differ in order from one another. For the batch and plug flow cases, the development requires the simultaneous solution of the pertinent differential equations. For stirred-tank reactors an analogous set of simultaneous algebraic equations are obtained that will generally be nonlinear. In such cases closed form solutions are generally not available, and computers must be used to obtain numerical solutions. Fortunately, the concentration versus time curves are similar in shape to those for first-order reactions, and the rules of thumb enunciated previously for that case may be regarded as general for all

irreversible consecutive reactions. Little can be said about the product distribution curves for reactions that are other than strictly first-order, because they depend on the initial reactant concentration. One may conclude, as in the case of parallel reactions, that high concentrations of reactant favor the higher-order reaction and low concentrations favor the lower-order reaction. Variations in the feed concentration will shift the location of the maximum intermediate concentration, and this variable can be used to optimize the product distribution.

### 9.3 COMPETITIVE CONSECUTIVE REACTIONS

Reaction networks that consist of a multiplicity of reactions in which steps in parallel and steps in series are both present are often referred to as *competitive-consecutive* or *series-parallel reactions*. These systems often are characterized by rate expressions that place conflicting demands on the type of contacting desired, so that it is often impossible to obtain a unique answer to a design problem. In such cases the practicing chemical engineer must exercise creativity and judgment in the choice of contacting pattern and reactor type. To illustrate the type of conflicts involved, one may consider the following combination of mechanistic equations:



where V is the desired product and  $W_1$  and  $W_2$  are undesirable products

To optimize the production of V, one would be persuaded by the presence of the consecutive reactions to use a plug flow or batch reactor. On the other hand, since the parallel reaction leading to  $W_2$  is of higher order in reactant A than that leading to V, a stirred-tank reactor is called for. These conflicting considerations imply that there will not be a unique solution as to the type of reactor and operating conditions to be employed. The answer will depend on the feed concentrations available and the values of the pertinent rate constants. To illustrate the general principles involved in tackling these design problems involving competitive-consecutive reactions, it is instructive to consider two common classes of reactions of this type: multiple substitution reactions and polymerization reactions.

#### 9.3.1 Multiple Substitution Reactions

Multiple substitution reactions are commonly encountered in industrial practice. They may be represented in general

form as



This reaction set may be regarded as parallel reactions with respect to consumption of species B and as a series reaction with respect to species A, V, and W. Common examples include the nitration and halogenation of benzene and other organic compounds to form polysubstituted compounds. To characterize the qualitative behavior of such systems, it is useful to consider reactions (9.3.3) and (9.3.4) as mechanistic equations and to analyze the effects of different contacting patterns on the yield of species V. We shall follow the treatment of Levenspiel (7).

If one has two beakers, one containing species A and the other containing species B, there are several ways in which their contents may be brought together. The mixing modes that represent limiting conditions are:

1. Add A slowly to B.
2. Add B slowly to A.
3. Mix A and B together rapidly.

By the use of the term *slowly*, we imply that the rate of addition of a particular species is slow compared to the rates of the various chemical processes involved.

In mode 1, as the first increment of A is added, it is converted rapidly to V by reaction with the B molecules. The V molecules then find themselves in the presence of excess B molecules and thus react further to yield W. The same process occurs as subsequent increments of A are supplied, the conversion rate being limited by the rate of addition of A. This mode of mixing leads to a situation in which one does not ever have significant amounts of V present in the vessel to which A is added. A is also absent from this vessel as long as any B remains, but it will be present after complete consumption of B. The vessel becomes progressively richer in W until all B is consumed. Figure 9.8 is a schematic representation of the various mole numbers present in the mixing beaker.

In mode 2, a quite different situation prevails. When the first increment of B is added slowly to A, it will react to form V. The V molecules cannot react further, since all of the B molecules have been consumed. When the second increment of B is added, the V molecules formed previously will compete with unconverted A molecules for the B molecules that have been added. Since A is present in large excess during the initial stages of the addition process, it will react with most of the B to form V. The effect, however, is to increase the amount of V to the point where in subsequent additions of B the V molecules compete more successfully for the B molecules. Eventually, one reaches a point at which enough B will have been added such that

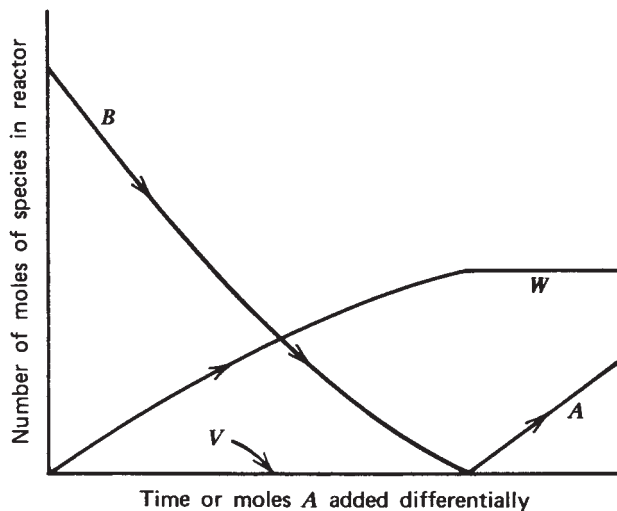


**Figure 9.8** Schematic representation of product distribution versus time for a competitive-consecutive reaction network. Case I: series component added slowly. (Adapted from O. Levenspiel, *Chemical Reaction Engineering*, 2nd ed. Copyright © 1972. Reprinted by permission of John Wiley & Sons, Inc.)

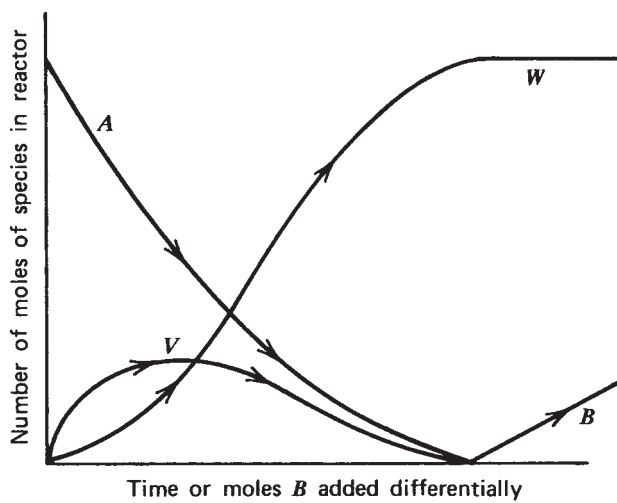


**Figure 9.9** Schematic representation of product distribution versus time for a competitive-consecutive reaction network. Case II: parallel component added slowly. (Adapted from O. Levenspiel, *Chemical Reaction Engineering*, 2nd ed. Copyright © 1972. Reprinted by permission of John Wiley & Sons, Inc.)

more V will be consumed by reaction (9.3.4) than is produced by reaction (9.3.3). Beyond this point the concentration of V continues to diminish. When 2 mol of B has been added per mole of original A, the concentration of V will reach zero and we will have a solution containing only W. Figure 9.9 is a schematic representation of the changes that occur.

In mode 3, the reaction rate is slow compared to the mixing process, and one has, in effect, a well-stirred batch

reactor. Initially, A and B combine to form V, which can then compete with other A molecules for the B molecules that remain. During the early stages of the reaction, the V molecules are at a numerical disadvantage, and more V will be produced than is consumed. As their concentration increases, the V molecules compete more successfully, so that the concentration of V eventually passes through a maximum and declines thereafter. The general behavior of this mode of mixing in terms of product distribution is roughly similar to that of mode 2, which was depicted in Figure 9.9.

The product distributions shown in Figures 9.8 and 9.9 are obviously quite different, so we again see that the manner of contacting can have significant effects on product yields. When all the A that will ever be added is present in the mixing vessel, as in modes 2 and 3, appreciable amounts of intermediate V are formed. When A is added incrementally, as in mode 1, there never are appreciable amounts of V in the reaction vessel. Such behavior is characteristic of reactions in series, as noted in Section 9.2. For such conditions species A, V, and W generally behave as if the network is analogous to that for the following mechanistic equations



Comparison of the qualitative results of modes 2 and 3 reveals that the concentration level of B does not have a major influence on the product distribution and the reaction sequences involved. (It will, however, influence the overall conversion rate.) This behavior is characteristic of parallel reactions of the same order with respect to a particular species. From the viewpoint of species B, reactions (9.3.3) and (9.3.4) may be regarded as



Levenspiel (8) discussed these examples and has proposed the following very useful rule of thumb: *Series-parallel reactions can be analyzed in terms of their constituent series reactions and parallel reactions in that optimum contacting for favorable product distribution is the same as for the constituent reactions.*

For the network described by reactions (9.3.3) and (9.3.4) where V is the product desired, the rule indicates that a mixture containing A, some of which has reacted, should not be backmixed with fresh A, while B may be added in any fashion that is convenient. One must apply the maxim with discretion, however, and where possible should work out the mathematics appropriate to the reaction set involved in order to obtain as much insight as possible into the factors that will influence the product distribution.

We are now prepared to develop quantitative relations for series-parallel reactions of the multiple substitution type considered above.

**Case I: Quantitative Treatment for Plug Flow or Batch Reactor.** The first step in the determination of the product distribution for reactions (9.3.3) and (9.3.4) is an evaluation of the instantaneous yield:

$$y = \frac{\nu_A}{\nu_V} \frac{dC_V}{dC_A} = \frac{dC_V/dt}{-dC_A/dt} = \frac{k_1 C_A C_B - k_2 C_V C_B}{k_1 C_A C_B} \quad (9.3.7)$$

Hence, for a plug flow or batch reactor,

$$\frac{dC_V}{dC_A} = \frac{k_2 C_V}{k_1 C_A} - 1 \quad (9.3.8)$$

This differential equation can be solved using an integrating factor approach. The solution consists of two parts:

$$\frac{C_V}{C_{A0}} = \frac{1}{1 - (k_2/k_1)} \left[ \left( \frac{C_A}{C_{A0}} \right)^{k_2/k_1} - \frac{C_A}{C_{A0}} \right] + \frac{C_{V0}}{C_{A0}} \left( \frac{C_A}{C_{A0}} \right)^{k_2/k_1} \quad \text{for } k_2 \neq k_1 \quad (9.3.9)$$

and

$$\frac{C_V}{C_{A0}} = \frac{C_A}{C_{A0}} \left[ \frac{C_{V0}}{C_{A0}} - \ln \left( \frac{C_A}{C_{A0}} \right) \right] \quad \text{for } k_2 = k_1 \quad (9.3.10)$$

One of the last two equations gives the relationship between  $C_V$  and  $C_A$  at any time in a plug flow or batch reactor. The stoichiometry of the system provides the additional information necessary to describe the system composition completely.

A material balance on species A indicates that

$$C_{A0} + C_{V0} + C_{W0} = C_A + C_V + C_W \quad (9.3.11)$$

which, with (9.3.9) or (9.3.10), gives  $C_W$  as a function of  $C_A$ . A material balance on species B gives

$$C_{B0} - C_B = (C_V - C_{V0}) + 2(C_W - C_{W0}) \quad (9.3.12)$$

This relation provides a means of evaluating  $C_B$  in terms of  $C_A$ .

**Case II: Quantitative Treatment of a Single Stirred-Tank Reactor.** When reactions (9.3.3) and (9.3.4) take place in a single continuous-flow stirred-tank reactor, the route to a quantitative relation describing the product distribution involves writing the material balances or design equations for species V and A:

$$\tau = \frac{C_{A0} - C_A}{-r_A} = \frac{C_{V0} - C_V}{-r_V} \quad (9.3.13)$$

or

$$\frac{C_{A0} - C_A}{k_1 C_A C_B} = \frac{C_{V0} - C_V}{-k_1 C_A C_B + k_2 C_V C_B} \quad (9.3.14)$$

Rearrangement gives

$$\frac{C_{V0} - C_V}{C_{A0} - C_A} = -1 + \frac{k_2 C_V}{k_1 C_A} \quad (9.3.15)$$

which is the difference equation analog of equation (9.3.8). Equation (9.3.15) may be solved for  $C_V$  in terms of  $C_A$  to obtain

$$\frac{C_V}{C_{A0}} = \frac{(C_{V0}/C_{A0}) + [1 - (C_A/C_{A0})]}{1 + (k_2/k_1)[(C_{A0}/C_A) - 1]} \quad (9.3.16)$$

Equations (9.3.11) and (9.3.12) are also applicable to analysis of a single CSTR, since they represent overall material balances. They provide the additional relations necessary to determine the complete effluent composition.

It is possible to represent the product distributions for both the batch and CSTR cases in the form of time-independent plots, as shown in Figures 9.10 and 9.11. These plots were prepared using equations (9.3.9) [or (9.3.10)], (9.3.11), (9.3.12), and (9.3.16). As the reaction proceeds, B is consumed, and one moves from left to right along the curve representing the appropriate value of  $k_2/k_1$ . The dashed lines with slopes equal to 2 on Figures 9.10 and 9.11 indicate the amount of B consumed to reach a particular point on the curve being followed. This value of consumption of B is independent of the manner in which B is added. It depends only on the total consumption. If one recognizes that the 45° lines in Figures 9.10 and 9.11 would represent complete conversion to the desired product, it is evident that the highest fractional yields of V are obtained at low fraction conversions of species A, regardless of whether  $k_2/k_1$  is large or small. However, the larger the value of  $k_2/k_1$ , the faster the fractional yield of V decreases with increasing conversion of A. Thus, if it is possible to remove small amounts of V cheaply from large volumes of the reaction mixture, the optimum reactor configuration and mode of operation would involve the use of a plug flow reactor with low conversions of A per pass coupled with a separator to remove the product V and to recycle unconverted reactants. The exact conversion level to be employed will depend on an economic analysis of the combined reactor-separator system.

As Levenspiel points out in his discussion of this reaction network, it is relatively easy to extend the use of figures such as Figure 9.10 to cases in which intermediates may be present in the feed to the plug flow reactor either by virtue of their presence in a recycle stream or in the fresh feed stream. The progress of the reaction will still be along the same  $k_2/k_1$  curve. However, the starting point will no longer be the point  $C_V = 0, C_A = C_{A0}$ , but the intersection of the curve corresponding to the value of  $k_2/k_1$  characteristic of the system and a straight line passing through the point  $C_V = C_A = 0$ , with a slope equal to  $-C_{V0}/C_{A0}$ . The effect of the presence of intermediate V in the feed is to reduce the net fractional yield of species V.

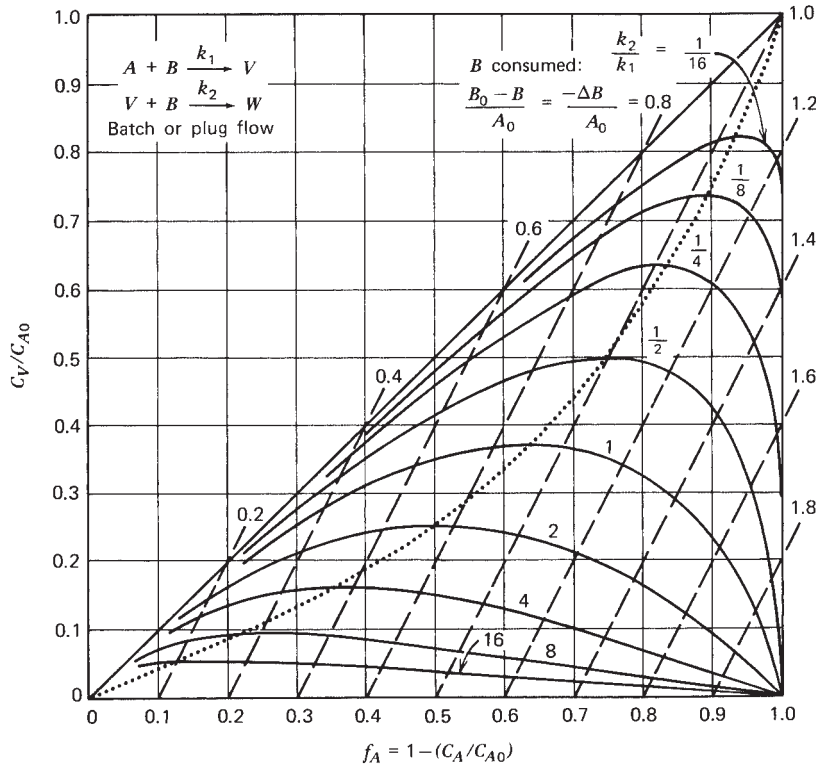


**Figure 9.10** Product distribution in batch or plug flow reactors for the reactions indicated. (Adapted from O. Levenspiel, *Chemical Reaction Engineering*, 2nd ed. Copyright © 1972. Reprinted by permission of John Wiley & Sons, Inc.)

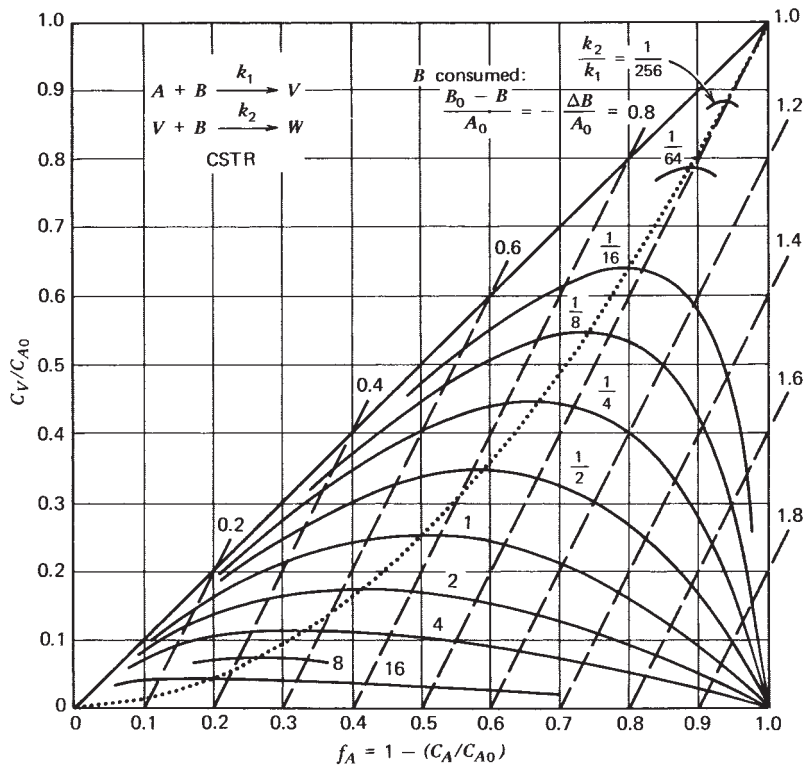
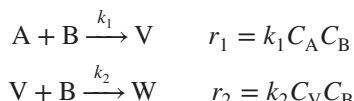


**Figure 9.11** Product distribution in a continuous flow stirred-tank reactor for the reactions indicated. (Adapted from O. Levenspiel, *Chemical Reaction Engineering*, 2nd ed. Copyright © 1972. Reprinted by permission of John Wiley & Sons, Inc.)

Illustration 9.4 indicates how the concepts presented above may be used to develop a rational reactor design for carrying out multiple substitution reactions.

### ILLUSTRATION 9.4 Design Considerations for a Specified Product Distribution

For a network of competitive-consecutive reactions represented by



it is desired to operate under conditions such that the relative yield of  $V$  is 75%, based on the amount of  $A$  that reacts. If the reaction rate constants are numerically equal, indicate briefly the constraints within which idealized reactor types must operate. Consider conversion levels, mole ratios of the feed, and the possibility of separation and recycle of reactant or product species. It may be presumed that species  $A$  is the limiting reagent.

#### Solution

Figures 9.10 and 9.11 are useful for determining the conversion level at which each type of reactor should be operated. The locus of points along which the relative overall yield  $V$  is 75% is given by the straight line linking the point  $f_A = 0$ ,  $C_V/C_{A0} = 0$  to the point  $f_A = 1$ ,  $C_V/C_{A0} = 0.75$ . Points above this straight line will correspond to yields in excess of the minimum specified value of 75%. The point where this straight line intersects the yield curve for the specified value of  $k_2/k_1$  (1.0) indicates the highest conversion level at which the product distribution specified can be achieved. When such a straight line is superimposed on Figure 9.10, one finds that for a batch or plug flow reactor, the maximum possible conversion of  $A$  that is consistent with the constraint on the product distribution is  $f_A = 0.42$ . For a CSTR the corresponding maximum conversion level may be found using Figure 9.11. For this case  $f_A = 0.25$ . At the conversion levels indicated, the product mixtures will contain substantial amounts of unreacted  $A$  and  $B$ . Thus, it is appropriate to consider the questions of separation and recycle for each species in turn.

#### Reactant A

If  $A$  has significant economic value, it should be separated from the reactor effluent stream and recycled for subsequent reuse. Since the conversion level is higher in the plug flow reactor, the recycle rate will be much smaller and

the demands on the separation equipment for reclaiming species  $A$  will also be somewhat smaller. Even when species  $A$  is of relatively little economic value, there may be circumstances when the costs associated with meeting the pollution control requirements for the process effluent will dictate separation and recycle of this reactant as the most economic alternative.

#### Reactant B

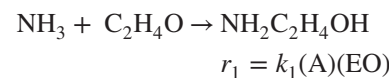
The product distribution is insensitive to the concentration of reactant  $B$ . If  $B$  is cheap and does not create a potential pollution problem downstream, its concentration may be kept at any convenient level. However, if  $B$  is costly or must be removed for other reasons, one has the options of operating with low concentrations of  $B$  at high conversions thereof in a relatively large reactor to produce a product containing very little  $B$ , or of operating at higher concentrations of  $B$  in a smaller reactor with separation and recycle of unused  $B$ . The specified product distribution requires that the mole ratio of  $V$  to  $W$  be 3 : 1. To produce 1 mol of  $W$  and 3 mol of  $V$ , one must consume 4 mol of  $A$  and 5 mol of  $B$ . The feed ratio employed in an actual situation may differ appreciably from 1.25 to enhance the reaction rate or to allow for recycling or discarding some  $A$  and  $B$ .

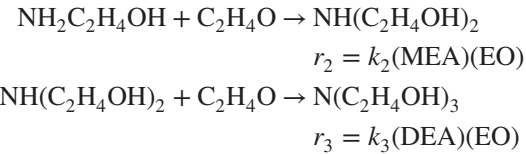
#### Products V and W

Recycle of species  $V$  or  $W$  has no merit, although there are a variety of reasons why it might be necessary to separate these materials from the product mixture: product purity specifications, pollution constraints, and so on. Neither product enhances the reaction rate. The low conversion of  $A$  that we are forced to employ is a consequence of the fact that otherwise there would be insufficient  $V$  in the product mixture.

### ILLUSTRATION 9.5 Trajectories of Product Concentrations with Increasing Reactor Space Time for Competitive-Consecutive Second-Order Reactions in Continuous-Flow Reactors

The competitive-consecutive reactions of ammonia ( $A$ ) with ethylene oxide (EO) in aqueous solution lead to production of monoethanolamine (MEA), diethanolamine (DEA), and triethanolamine (TEA). The reaction network for the stepwise formation of these products is





Viewed from the perspective of ethylene oxide, these reactions are competitive; by contrast, from the perspective of the amines, they are consecutive. An analysis to determine the concentrations of the indicated alkanolamines as functions of time in a pressurized batch reactor was considered in Illustration 5.6. However, MEA, DEA, and TEA are commodity chemicals that are produced on an industrial scale in continuous flow reactors.

Consider a flow reactor operating at 150°C and 20 bar so as to maintain all species in the liquid phase. The rate laws are of the mixed second-order form, with hypothetical rate constants  $k_1$ ,  $k_2$ , and  $k_3$  equal to 1, 0.4, and 0.1 (L/mol·min), respectively.

Determine the effluent concentrations of the three alkanolamine products as functions of the reactor space time for the range 0 to 15 min when the blended inlet feed stream is 1 M in ammonia and 2.4 M in ethylene oxide. Prepare plots of the product distributions for the synthesis of these alkanolamines in both a PFR and an individual CSTR.

## Solution

Because these coupled reactions take place at constant volume (liquid phase), the evolution of the product distribution with increasing reactor space time can be determined using either three suitable species concentrations or three extents of reaction per unit volume. In Illustration 5.6 we employed an approach based on extents of reaction. To demonstrate an alternative approach in this solution, we have elected to utilize the concentrations of the three alkanolamines [(MEA), (DEA), and (TEA)] as the reaction progress variables. Material balance considerations dictate that the concentrations of the feed species are then given by

$$(A) = (A)_0 - (\text{MEA}) - (\text{DEA}) - (\text{TEA}) \quad (\text{A})$$

$$(\text{EO}) = (\text{EO})_0 - (\text{MEA}) - 2(\text{DEA}) - 3(\text{TEA}) \quad (\text{B})$$

where  $(A)_0$  and  $(\text{EO})_0$  are the initial concentrations of the reactants.

If equations (A) and (B) are now used to express the rate laws for the three independent reactions given in the problem statement in terms of product concentrations and the initial concentrations of reactants,

$$\begin{aligned} r_1 &= k_1[(A)_0 - (\text{MEA}) - (\text{DEA}) - (\text{TEA})] \times \\ &[(\text{EO})_0 - (\text{MEA}) - 2(\text{DEA}) - 3(\text{TEA})] \quad (\text{C}) \end{aligned}$$

$$\begin{aligned} r_2 &= k_2(\text{MEA})[(\text{EO})_0 - (\text{MEA}) - 2(\text{DEA}) - 3(\text{TEA})] \\ &\quad (D) \end{aligned}$$

$$r_3 = k_3(\text{DEA})[(\text{EO})_0 - (\text{MEA}) - 2(\text{DEA}) - 3(\text{TEA})] \quad (\text{E})$$

We shall now consider utilization of equations (A) to (E) to ascertain the speciation of the effluents from a PFR and an individual CSTR.

**Case 1: Plug Flow Reactor.** The net rates at which the three alkanolamines are formed at an arbitrary location in a PFR operating at steady state are then

$$\frac{d(\text{MEA})}{d\tau} = r_1 - r_2 \quad (\text{F})$$

$$\frac{d(\text{DEA})}{d\tau} = r_2 - r_3 \quad (\text{G})$$

$$\frac{d(\text{TEA})}{d\tau} = r_3 \quad (\text{H})$$

where  $\tau$  is the space time for the reactor ( $\tau = V_R/V_0$ ). At the inlet to the reactor  $\tau = 0$  and

$$(\text{MEA})_0 = (\text{DEA})_0 = (\text{TEA})_0 = 0 \quad (\text{I})$$

Equations (F) to (H) correspond to a system of coupled, nonlinear differential equations that may be combined with the rate laws in equations (C) to (E) and integrated numerically using any suitable engineering software, such as the *ode15* or *ode23* commands in Matlab. The results for the product species concentrations are shown in the PFR panel in Figure I9.5.

**Case 2: Continuous Flow-Stirred Tank.** For operation of an individual CSTR operating at steady state, material balances on each product species yield the following relations:

For MEA:

$$V_0(\text{MEA})_0 + r_1 V_R = V_0(\text{MEA}) + r_2 V_R \quad (\text{J})$$

For DEA:

$$V_0(\text{DEA})_0 + r_2 V_R = V_0(\text{DEA}) + r_3 V_R \quad (\text{K})$$

For TEA:

$$V_0(\text{TEA})_0 + r_3 V_R = V_0(\text{TEA}) \quad (\text{L})$$

At the entrance to the CSTR where  $\tau = 0$ , equation (I) again specifies the concentrations of the various alkanolamines in the feed stream. Algebraic manipulation of equations (I) to (L) followed by introduction of the definition of the space time for the CSTR yields the following set of three algebraic equations in three unknowns:

$$\begin{aligned} 0 &= (\text{MEA}) + \tau[r_2 - r_1] \\ &= (\text{MEA}) + \tau(\text{EO})[k_2(\text{MEA}) - k_1(A)] \\ &= (\text{MEA}) + \{(\text{EO})_0 - (\text{MEA}) - 2(\text{DEA}) - 3(\text{TEA})\} \times \\ &\quad \{k_2\tau(\text{MEA}) - k_1\tau[(A)_0 - (\text{MEA}) - (\text{DEA}) - (\text{TEA})]\} \quad (\text{M}) \end{aligned}$$

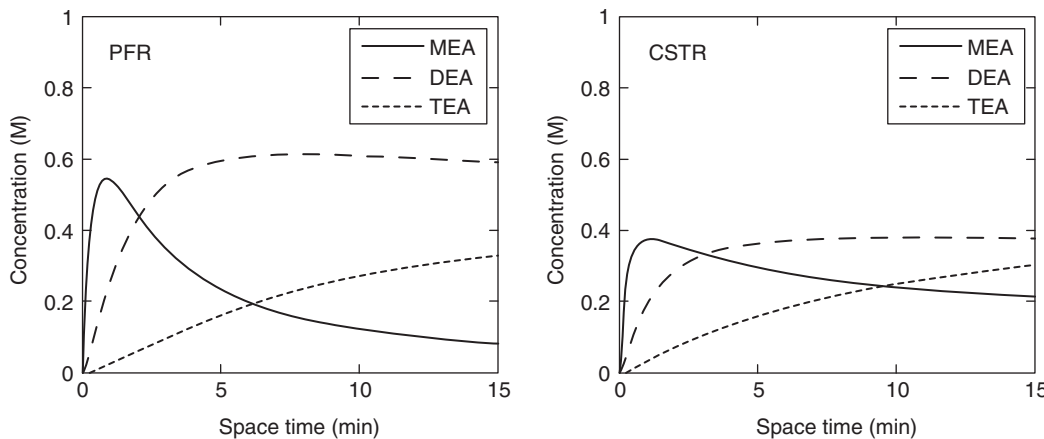


**Figure I9.5** Speciation plots for the competitive-consecutive second-order reactions of ammonia and ethylene oxide. Panel PFR: plug flow reactor; panel CSTR: individual continuous flow stirred-tank reactor.

$$\begin{aligned}
 0 &= (\text{DEA}) + \tau[r_3 - r_2] \\
 &= (\text{DEA}) + \tau(\text{EO})[k_3(\text{DEA}) - k_2(\text{MEA})] \\
 &= (\text{DEA}) + \{(\text{EO})_0 - (\text{MEA}) - 2(\text{DEA}) - 3(\text{TEA})\} \times \\
 &\quad \{k_3\tau(\text{DEA}) - k_2\tau(\text{MEA})\} \quad (\text{N}) \\
 0 &= (\text{TEA}) - r_3\tau = (\text{TEA}) - k_3\tau(\text{EO})(\text{DEA}) \\
 &= (\text{TEA}) - k_3\tau\{(\text{EO})_0 - (\text{MEA}) \\
 &\quad - 2(\text{DEA}) - 3(\text{TEA})\}(\text{DEA}) \quad (\text{O})
 \end{aligned}$$

This coupled system of equations can be solved numerically to ascertain the effluent concentrations using common engineering software tools, such as ‘fsolve’ in Matlab or a ‘given–find’ block in MathCad. The outlet concentrations of the alkanolamines over the range of reactor space times of interest are shown in the CSTR panel in Figure I9.5.

Comparison of the trajectories of the concentrations of the product species as functions of the space times for the two idealized reactor models (Figure I9.5) demonstrates that with a PFR one can elect to select a space time that produces a higher yield of either MEA or DEA. Both maxima exceed the effluent concentrations of these species from an individual CSTR at the same space time. This result is a direct consequence of the basic hypothesis of the PFR model that the contents of a differentially thin slice of fluid pass through the reactor without mixing with the contents of any other slice. By contrast, the hypothesis of perfect mixing in the CSTR produces uniform conditions (temperature and composition) throughout the entire volume of the CSTR. The net result of mixing is that the effluent contains more nearly uniform concentrations of product species as the space time increases from 0 to 15 min. Moreover, the “peaks” for MEA and DEA in the trajectories in the CSTR panel in Figure I9.5 are both shorter and broader than the corresponding peaks in the PFR panel.

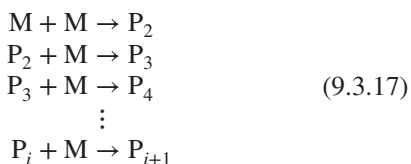
Readers should note that if one plots the results of the PFR and batch models on the same scale for the independent variable (time or space time), the trajectories of the concentrations of the three alkanolamines in the PFR panel in Figure I9.5 are identical to those in the product panel in Figure I5.6. As each little slice/plug moves through the tubular reactor, it effectively functions as a batch reactor operating at substantially constant pressure.

### 9.3.2 Polymerization Reactions

Polymerization processes represent an extremely important aspect of the chemical processing industry. Since many of the properties of polymeric materials are markedly affected by their average molecular weight and their molecular weight distribution, the design of reactors for polymerization processes offers many opportunities for the use of the principles presented earlier in this chapter. Denbigh (10) presented a systematic mathematical treatment of the manner in which these principles can be exploited to develop useful relationships for the dependence of the molecular weight distribution of polymers on the degree of polymerization for both condensation polymerization and free-radical polymerization.

Because tubular reactors are generally not suitable for use in effecting liquid-phase or emulsion polymerizations, the principal design alternatives reduce to batch reaction or the use of single or multiple stirred-tank reactors for continuous processing. In tubular reactors, the velocity profile arising from the high viscosity of the solution will imply that fluid elements near the wall have significantly longer residence times than those at the tube axis. This distribution of residence times means that the material near the wall may be polymerized to an excessive level, perhaps resulting in the precipitation of polymer and the buildup of solid material on the tube walls, eventually leading to choking or plugging of the tube.

If we represent the monomer from which a polymer is formed by M and a polymer consisting of  $i$  monomer units by  $P_i$ , a polymerization reaction can be written as



This reaction can be regarded as a series reaction from the viewpoint of the growing polymer molecule and as a parallel reaction from the viewpoint of the monomer molecules being consumed. Of course, if polymer molecules can react with one another,



A given sample of polymer is characterized by a distribution of molecular weights arising from the interaction of the network of reactions shown in equation (9.3.17) [and possibly equation (9.3.18)], and the mixing processes taking place in the reactor in which the polymer sample was prepared.

For idealized reactor types there are two opposing factors that influence the overall molecular weight distribution (10,11).

1. *Concentration history.* That is, in a batch reactor the monomer concentration decreases continuously, whereas in a CSTR it remains constant.
2. *Residence-time distribution.* All fluid elements have the same “cooking” time in a batch reactor, but there will be a wide spread in residence times in a CSTR.

In a CSTR the steady-state concentration of monomer is at a lower average value than it would be for the same feed conditions if the same reaction were carried out batch-wise. In many free radical polymerization reactions, holding the monomer concentration at a constant level has the effect of reducing the variation in degree of polymerization (or molecular weight).

As the residence time of a fluid element lengthens, it is possible for the degree of polymerization of the polymer molecules contained therein to increase. Consequently, any factor that leads to a spread in residence times of individual molecules can increase the spread in the molecular weight distribution. In a CSTR some growing polymer molecules leave after a short residence time so they do not reach a very large molecular weight. Other molecules remain in the reactor for longer than the average residence time and consequently will reach a molecular weight greater than the average value.

Whether the first or the second factor dominates depends on the type of polymerization process involved. If

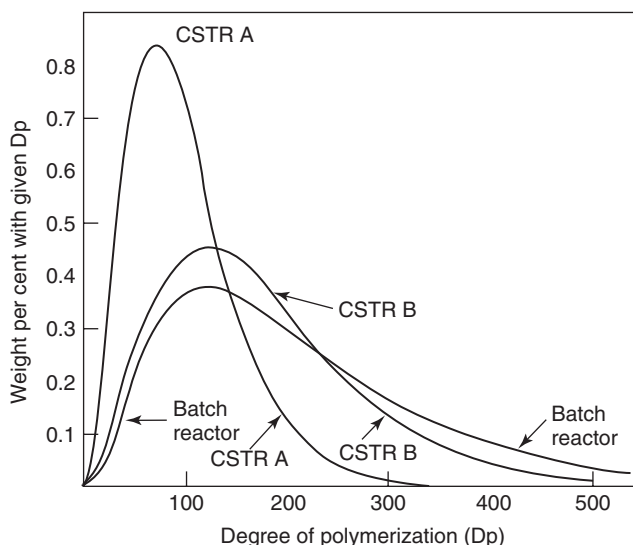


**Figure 9.12** Molecular weight distribution function for situations in which the duration of the growth stage is short compared to the residence time in the reactor (e.g., free-radical polymerization). The steady-state operating conditions in CSTR A and CSTR B correspond to relative monomer concentrations of 0.1 and 0.354, respectively. The conditions in the batch reactor involve a transition from a relative monomer concentration of 1.0 to one of 0.1. [Adapted with permission of The Royal Society of Chemistry from the contribution of K. G. Denbigh to *Trans. Faraday Soc.*, **43**, 648 (1947). Copyright © 1947, The Royal Society of Chemistry.]

the period during which the polymer molecule is growing is short compared to the residence time of the molecule in the reactor, the first factor dominates. This situation holds for many free radical and ionic polymerization processes in which the reaction intermediates are extremely short-lived. Figure 9.12 depicts the types of behavior expected for systems of this type.

For cases where the growth period is the same as the residence-time in the reactor, as in polycondensation processes, the residence-time distribution is the dominant factor influencing the molecular weight distribution. In this case one obtains a broader molecular weight distribution from a CSTR than from a batch reactor. Figure 9.13 indicates the type of behavior expected for systems of this type.

## 9.4 REACTOR DESIGN FOR AUTOCATALYTIC REACTIONS

### 9.4.1 Basic Concepts

There are many reactions in which the products formed can themselves act as catalysts for the reaction. Thus, there will be a range of compositions for which the reaction rate accelerates as the reaction proceeds. This phenomenon is known as *autocatalysis*, and reactions of this type pose

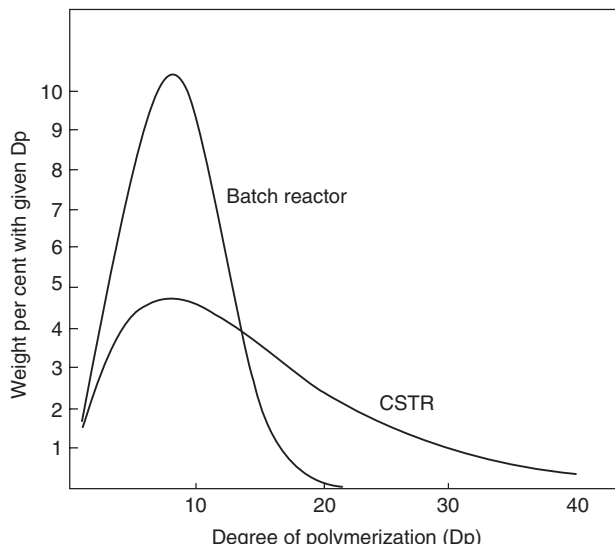


**Figure 9.13** Molecular weight distribution functions for the case where the length of the growth stage is long compared to the reactor residence time or for the case where there are no termination reactions (condensation polymerization). [Adapted with permission of The Royal Society of Chemistry from the contribution of K. G. Denbigh to *Trans. Faraday Soc.*, **43**, 648 (1947). Copyright © 1947, The Royal Society of Chemistry.]

some interesting problems in the selection of an optimum reactor configuration.

An autocatalytic reaction is one in which the reaction rate is proportional to a product concentration raised to a positive exponent. Some of the first articles in the literature of chemical kinetics deal with reactions of this type. For example, in 1857, Baeyer (12) reported that the reaction of bromine with lactose was autocatalytic. The hydrolyses of several esters also fit into the autocatalytic category, because the acids formed by reaction give rise to hydrogen ions that serve as catalysts for subsequent reaction. Among the most significant autocatalytic reactions are fermentation reactions, which involve the action of a microorganism on an organic feedstock.

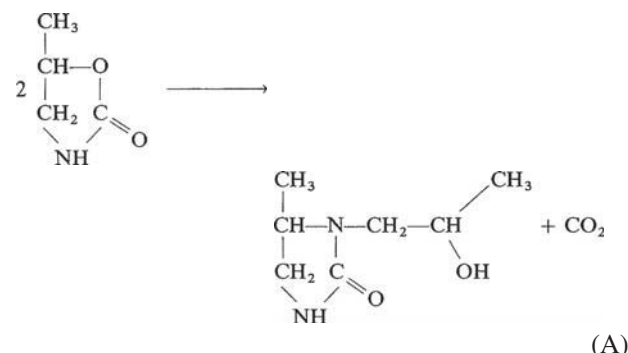
When a material reacts under normal circumstances, its initial rate of disappearance is high, but the rate decreases progressively as the reactant is consumed. For an autocatalytic reaction, on the other hand, the initial rate is relatively slow, because little or no product is present. The rate increases to a maximum as products are formed and then decreases to a low value (or zero) as reactants are consumed or equilibrium is achieved. If there are no product species present in the initial reaction mixture, autocatalytic reactions exhibit the type of behavior shown in Figure 9.14a. If the product species that is catalytic is present in the original reaction mixture, the type of behavior that the system will exhibit is shown in Figure 9.14b.

The reader should note that we have not let the initial rate become zero in Figure 9.14 even when no catalyst is present, because the possibility exists that there may be alternative paths from reactants to products, only one of which is autocatalytic. The rate observed will be the sum of the rates for the various paths. Reaction will proceed by the uncatalyzed path until sufficient products are produced to render conversion by this path negligible compared to conversion by the autocatalytic path. In practice, one always has the possibility of spiking the original mixture with adequate catalyst, but in many cases, small amounts of product species left in the reactor from previous runs may suffice to get things going again. For hydrolysis reactions that are acid catalyzed, the hydrogen ion concentration in the feed water may be sufficient to initiate reaction.

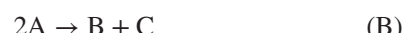
An experimental test for autocatalysis involves addition of the suspected autocatalytic species to the reaction mixture. If the material added is the responsible agent, one may generally expect behavior like that shown in Figure 9.15. Illustration 9.6 indicates one type of rate expression and reaction mechanism that may be associated with an autocatalytic reaction.

## ILLUSTRATION 9.6 Autocatalytic Decomposition of 5-Methyl-2-Oxazolidinone

When heated above 200°C, pure 5-methyl-2-oxazolidinone decomposes into two products, CO<sub>2</sub> gas and *N*-(2-hydroxy-propyl)imidazolidinone. The stoichiometry is



or



where C represents  $\text{CO}_2$ .

While we have taken some liberties with the numerical values that we will subsequently employ, the following set of mechanistic equations has been proposed in an effort to explain the observed autocatalytic kinetic behavior (13):



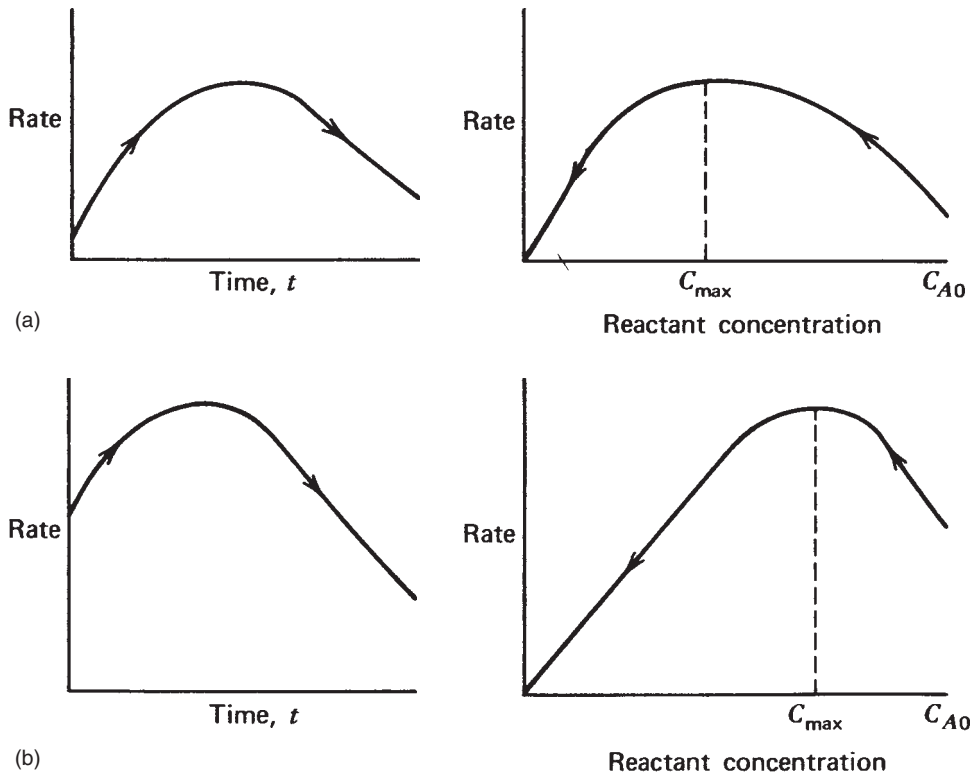


**Figure 9.14** Characteristics of autocatalytic reactions: (a) no products present in initial reaction mixture; (b) some products present in initial reaction mixture.

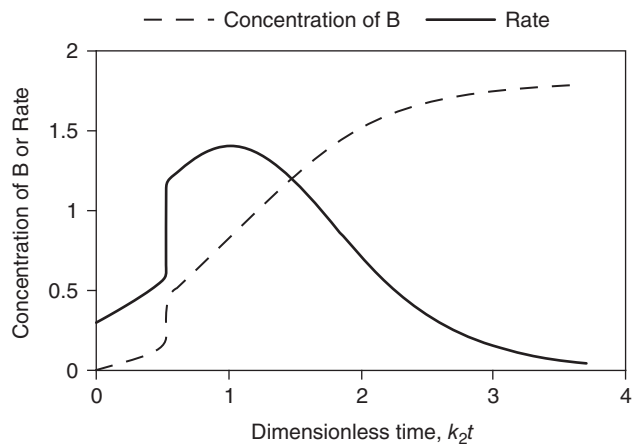


**Figure 9.15** Response of autocatalytic system to addition of autocatalytic agent. The reaction stoichiometry is  $A \rightarrow B$  and the rate law is  $r = k_1(A) + k_2(A)(B)$ . Only species A is present initially and  $k_2/k_1 = 7.5$ . Addition of B occurs at  $k_2 t = 0.526$ .



where AB is an intermediate complex. Verify that this mechanism produces autocatalytic behavior.

If the following values (in  $\text{m}^3/(\text{kmol-Msec})$ ) are assumed for the reaction rate constants:  $k_1 = 1.02$ ,  $k_2 = 150$ , and  $k_3 = 172$ , determine the fraction conversion of A that leads to the maximum rate at which B can be produced in an ideal CSTR with a fixed volume  $V_R$ . No special constraint is to be placed on the volumetric feed rate or the initial concentration of species A.

### Solution

The observed rate of consumption of species A is given by

$$-r_A = 2k_1(A)^2 + k_2(A)(B) \quad (F)$$

Thus, the mechanism is characterized by a rate expression in which product species B is responsible for the useful autocatalytic behavior.

The design equation for a CSTR is

$$\tau = \frac{V_R}{V_0} = \frac{C_{A0} \int_0^{f_A} df_A}{-r_{AF}} \quad (G)$$

which, on rearrangement for the case where the feed contains neither B nor C, becomes

$$-r_{AF}V_R = C_{A0}V_0f_A = F_{A0}f_A \quad (H)$$

The right side of this expression is identical with the rates of production of species B and C. Hence, the maximum production rate for a fixed reactor volume occurs when the reactor contents have a composition that maximizes the reaction rate [equation (F)]. Now, in terms of the fraction conversion,

$$(B) = C_{A0}f_A \quad (I)$$

Combination of equations (F) and (I) yields

$$-r_{AF} = 2k_1 C_{A0}^2 (1-f_A)^2 + k_2 C_{A0} (1-f_A) (C_{A0} f_A) \quad (J)$$

When the rate has its maximum value,

$$0 = \frac{\partial(-r_{AF})}{\partial f_A} = 2k_1 C_{A0}^2 2(1-f_A)(-1) + k_2 C_{A0}^2 (1-2f_A) \quad (K)$$

Thus,

$$4k_1(1-f_{A \max}) = k_2(1-2f_{A \max}) \quad (L)$$

or

$$f_{A \max} = \frac{k_2 - 4k_1}{2k_2 - 4k_1} \quad (M)$$

Substitution of appropriate numerical values gives

$$f_{A \max} = \frac{150 - 4(1.02)}{2(150) - 4(1.02)} = 0.493 \quad (N)$$

Illustration 9.5 indicates that one may have parallel paths leading from reactants to products and that in the case of an autocatalytic reaction, one path may be preferred over a second until the product level builds up to a point where the rate associated with the second pathway becomes appreciable. In this example, the magnitudes of the rate constants are such that the vast majority of the reaction occurs by the autocatalytic path. In cases such as these, it is desirable to use a CSTR or recycle reactor to enhance the reaction rate by virtue of the backmixing of product species.

An autocatalytic reaction does not necessarily imply a first-order dependence on the product species, or even an integer order with respect to this species. In the hydrolysis of an ester formed from a weak acid, an order approaching 1/2 may be observed.

The key characteristic of all autocatalytic rate expressions is that plots of the rate versus time are of the general form shown in Figure 9.15. When converted into plots of fraction conversion versus time, these forms give rise to a characteristic S shape. These plots first rise, showing autoacceleration as the rate increases, then pass through an inflection point as the rate reaches a maximum, and finally taper off so that the fraction conversion approaches unity or its equilibrium value as the time approaches infinity.

In the more general case for liquid-phase reactions or other cases where  $\delta = 0$ , the autocatalytic term in the rate expression ( $r_{AC}$ ) can be written as

$$r_{AC} = k(C_{A0} + \nu_A \xi^*)^{\beta_A} (C_{P0} + \nu_P \xi^*)^{\beta_P} \quad (9.4.1)$$

where A and P are reactant and product species, respectively. The extent of reaction per unit volume corresponding to the maximum autocatalytic rate may be determined by setting the derivative equal to zero:

$$\begin{aligned} \frac{dr_{AC}}{d\xi^*} &= k[\beta_A \nu_A (C_{A0} + \nu_A \xi^*)^{\beta_A-1} (C_{P0} + \nu_P \xi^*)^{\beta_P} \\ &+ \beta_P \nu_P (C_{A0} + \nu_A \xi^*)^{\beta_A} (C_{P0} + \nu_P \xi^*)^{\beta_P-1}] = 0 \end{aligned} \quad (9.4.2)$$

or

$$\beta_A \nu_A (C_{P0} + \nu_P \xi^*) + \beta_P \nu_P (C_{A0} + \nu_A \xi^*) = 0 \quad (9.4.3)$$

Solving for the extent of reaction per unit volume that gives the maximum reaction rate

$$\xi_{\max}^* = \frac{-(\beta_A \nu_A C_{P0} + \beta_P \nu_P C_{A0})}{\nu_A \nu_P (\beta_A + \beta_P)} \quad (9.4.4)$$

For the case where  $\nu_A = -1$  and  $\nu_P = 1$  and where no product is present initially,

$$\xi_{\max}^* = \frac{\beta_P}{\beta_P + \beta_A} \quad (9.4.5)$$

The maximum rate may be evaluated by combining equation (9.4.4) or (9.4.5) with equation (9.4.1).

## 9.4.2 Reactor Design Considerations

Plug flow reactors generally give greater production capacities than do CSTRs of equal volume, but in the case of autocatalytic reactions, this generalization is not valid. For this class of reactions, backmixing of reacted material with fresh feed is often beneficial in optimizing the overall reactor design. This mixing can be achieved by employing a continuous stirred-tank reactor or by recycling the unseparated product mixture. With a single CSTR it is possible to operate all the time at the highest reaction rate (i.e., at the points in Figure 9.14 labeled  $C_{\max}$ ). One could thus require a lower volume than would be required to achieve the same conversion level in a plug flow reactor, which would operate at an average rate less than the optimum. This mode of operation would require an effluent composition corresponding to  $C_{\max}$ . If lower conversions are desired, the CSTR will still require less volume than a PFR to reach this level. However, if higher conversions are desired, the optimum design solution (from the viewpoint of minimum total volume) requires

the use of a CSTR to reduce the reactant concentration from its initial value to  $C_{\max}$  and then a PFR to further reduce the reactant concentration to the level specified in the ultimate product.

In cases where unconverted reactants can readily be separated from the product stream, it may be preferable to use only the CSTR operating at the maximum rate, regardless of the conversion level desired, because the reactants separated can be recycled. In this case one must determine the relative costs of operating in the separation and recycle mode vis-a-vis the costs of utilizing the second-stage plug flow reactor and the attendant separation costs necessary to obtain the final product.

## LITERATURE CITATIONS

1. LEVENSPIEL, O., *Chemical Reaction Engineering*, 2nd ed., pp. 166–167, Wiley, New York, 1972.
2. DENBIGH, K. G., and TURNER, J. C. R., *Chemical Reactor Theory*, 2nd ed., pp. 123–124, Cambridge University Press, Cambridge, 1971.
3. TRAMBOUZE, P. J., and PIRET, E. L., *AIChE J.*, **5**, 384 (1959).
4. DENBIGH, K. G., *Chem. Eng. Sci.*, **17**, 25 (1961).
5. LEVENSPIEL, O., *op. cit.*, p. 180.
6. LEVENSPIEL, O., *op. cit.*, p. 181.
7. LEVENSPIEL, O., *op. cit.*, pp. 186–192.
8. LEVENSPIEL, O., *op. cit.*, p. 189.
9. LEVENSPIEL, O., *op. cit.*, pp. 191–192.
10. DENBIGH, K. G., *Trans. Faraday Soc.*, **43**, 648 (1947).
11. DENBIGH, K. G., and TURNER, J. C. R., *Chemical Reactor Theory*, 3rd ed., pp. 122–127, Cambridge University Press, Cambridge, 1984.
12. BAEYER, A., *Ann. Chem. Pharm.*, **103**, 178 (1857).
13. WALLE, W. E., and PLATT, A. E., *Ind. Eng. Chem.*, **59** (6), 41 (1967).

## PROBLEMS

- 9.1** Xylene isomerization reactions can be accomplished by contacting a hot gas stream with a solid catalyst. Under these conditions the isomerization reactions may be regarded as reversible and first-order. Unfortunately, the catalyst also catalyzes disproportionation reactions. These reactions may be regarded as essentially second-order and irreversible. If one desires to achieve an equilibrium mixture of isomers with minimal material losses associated with disproportionation reactions, what do you recommend concerning the mode in which one should operate a continuous-flow reactor?
- 9.2** Your company has two liquid streams available containing solutes that are not profitably marketable at the present time. One stream contains an aqueous solution of A. The second stream contains an aqueous solution of species B. Species A can react either with species B or with itself according to the following stoichiometric equations and rate expressions:



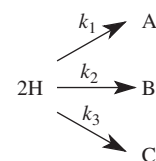
$$r_V = k_1 C_A C_B$$



$$r_W = \frac{k_2 C_A^2}{1 + k_3 C_V^{1/2}}$$

- (a) You have two beakers containing samples of the two streams and desire to carry out a small-scale laboratory experiment in which you maximize the formation of species V. In what manner should you carry out this experiment; that is, in what order and at what rate would you add each beaker of the reactants to an empty container?
- (b) If you desire to produce V in a flow reactor, what type of reactor and operating conditions do you recommend?
- (c) If the activation energies for the rate constants  $k_1$ ,  $k_2$ , and  $k_3$  are 60, 40, and 50 kJ/mol, respectively, what additional statements can you make regarding the operating conditions recommended for maximizing production of species V?

- 9.3** V. Bulatov and I. Oref [*Int. J. Chem. Kinet.*, **25**, 1019–1027 (1993)] investigated the kinetics of the dimerization of *trans*-hexatriene in toluene solution. They indicate that a simplified form of the reaction network can be written as



where H refers to *trans*-1,3,5-hexatriene and A, B, and C refer to the three dimers that can be formed. Each of the indicated reactions is second-order in species H. These researchers have reported the following expressions for the several rate constants:

$$k_1 = 3.98 \times 10^7 e^{-5048/T}$$

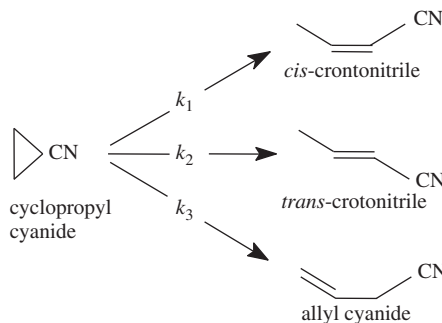
$$k_2 = 3.98 \times 10^7 e^{-4895/T}$$

$$k_3 = 2.51 \times 10^6 e^{-4502/T}$$

for  $k$  in  $M^{-1}s^{-1}$  and  $T$  in K.

- (a) If the reactions indicated occur isothermally, at what temperature should a batch reactor be operated to maximize the yield of species B? What is the maximum yield? You may assume that it will be possible to exert sufficient pressure on the reaction mixture to maintain a liquid phase. You should employ the definition of the yield based on the amount of species H that reacts.
- (b) If one desires to carry out the reactions indicated in a tubular reactor, what space time will be required to achieve 98% conversion of species H if the reactor is to operate isothermally under conditions that maximize the yield of species B? The feed concentration of species H is 0.015 M. What are the concentrations of species A, B, C, and H in the effluent from this reactor?
- (c) Now consider the possibility of carrying out the reaction in a single CSTR operating at the temperature that maximizes the yield of species B. What space time will give 98% conversion of species H? What are the corresponding effluent concentrations of species A, B, C, and H? How does the yield of species B compare to that which would be obtained in a PFR?

**9.4** D. A. Luckraft and P. J. Robinson [*Int. J. Chem. Kinet.*, **5**, 137–147 (1973)] studied the kinetics of the gas-phase unimolecular isomerization of cyclopropyl cyanide in the range 660 to 760 K and 2 to 89 torr. The major reactions involved are



with

$$\log_{10} k_1 = 14.01 - \frac{237.6}{2.303RT}$$

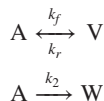
$$\log_{10} k_2 = 14.09 - \frac{243.7}{2.303RT}$$

$$\log_{10} k_3 = 14.59 - \frac{252.5}{2.303RT}$$

for  $k$  in  $\text{s}^{-1}$ ,  $R$  in  $\text{kJ}/(\text{mol}\cdot\text{K})$ , and  $T$  in K.

- (a) The desired product is *trans*-crotonitrile. If each of these reactions is irreversible, determine the temperature at which to operate an isothermal PFR to maximize the yield of *trans*-crotonitrile. What is the maximum yield?  
 (b) Do you have any reservations or cautions that should be noted before you design a reactor to operate at this temperature?

**9.5 (a)** Consider the following network of competitive first-order reactions:



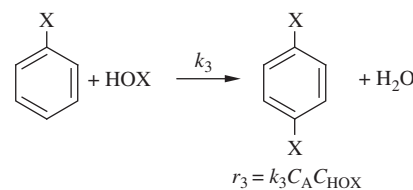
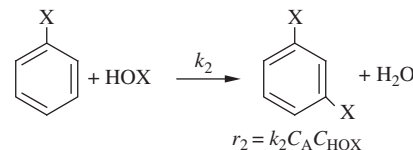
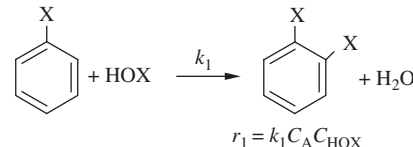
in which species V is the desired product. If these reactions take place in a CSTR operating at steady state, derive the analytical relation between the space time that maximizes the effluent concentration of species V and the kinetic parameters of the system. You may assume that the feed consists of species A dissolved in a liquid to give a concentration  $A_0$ .

- (b) If the reactor is operated at the flow rate corresponding to the optimum determined in part (a), determine the effluent concentrations of species A, V, and W when the temperature of the effluent is 60°C. At this temperature,  $k_f = 0.50$ ,  $k_r = 0.125$ , and  $k_2 = 0.08$  (all in  $\text{min}^{-1}$ ). The concentration of A in the feed stream is 2.0 M.  
 (c) For operation at the optimum space time determined in part (b), determine the rate at which thermal energy (heat) must be supplied to or removed from the reactor if the feed stream enters the reactor at 60°C. The standard enthalpy

changes for the reversible and irreversible reactions are  $-50.0$  and  $+30.0 \text{ kcal/mol}$ , respectively. Be sure to indicate the direction of heat transfer. The volume of the reactor is  $4.0 \text{ m}^3$ .

- (d) If the activation energies associated with  $k_f$ ,  $k_r$ , and  $k_2$  are 20, 30, and 40 kcal/mol, does the maximum effluent concentration of species V increase, decrease, or stay the same when the operating temperature is increased by 10 K? First present a qualitative argument and then be as quantitative as possible.

**9.6** Consider the following sequence of reactions and rate expressions:



If the rate constants for these reactions are given by the expressions below, at what temperature should a single CSTR be operated to maximize the yield of the *meta* product formed in reaction 2?

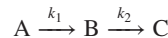
$$k_1 = 2.0 \times 10^4 e^{-6400/T}$$

$$k_2 = 3.0 \times 10^{-6} e^{-8000/T}$$

$$k_3 = 4.5 \times 10^7 e^{-9600/T}$$

for  $T$  in K.

- 9.7** R. L. Luus and O. N. Okongwu [*Chem. Eng. J.*, **75**, 1–9 (1999)] studied several issues relevant to the practical optimal control of batch reactors. In particular, they considered the sequence of consecutive first-order reactions



with

$$k_1 = 5.35 \times 10^{10} e^{-9000/T}$$

and

$$k_2 = 4.61 \times 10^{17} e^{-15000/T}$$

for  $k$  in  $\text{min}^{-1}$  and  $T$  in K.

They considered the case for which the initial concentrations of species A, B, and C were 0.95, 0.05, and 0.00, respectively. Their stated goal was to determine the temperature versus time protocol under which the reactor should be operated to maximize the concentration of species B after 30 min of reaction. Determine the temperature at which the reactor should be operated isothermally to maximize the concentration of species B at 30 min. What is the composition of the reaction mixture at this time? What is the maximum concentration of species B at this time? What is the maximum concentration of species B that could be obtained when operating at the optimum temperature if the time constraint of 30 min is not applicable? How much time would be required to achieve this maximum?

- 9.8** G. Debande and G. Huybrechts [*Int. J. Chem. Kinet.*, **6**, 545 (1974)] studied the gas-phase Diels–Alder additions of propylene (P) to cyclohexa-1,3-diene (Chd) to give the exo and endo-isomers of 5-methylbicyclo[2.2.2]oct-2-ene (MBO). The initial reaction rates were both of the mixed second-order form with

$$r_{\text{endo}} = k_{\text{endo}} C_{\text{P}} C_{\text{Chd}} \quad \text{and} \quad r_{\text{exo}} = k_{\text{exo}} C_{\text{P}} C_{\text{Chd}}$$

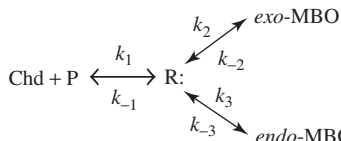
and

$$\log k_{\text{endo}} = \frac{-5698}{T} + 5.74$$

$$\log k_{\text{exo}} = \frac{-6577}{T} + 6.66$$

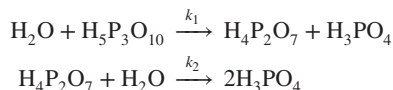
where  $T$  is expressed in K and  $k$  in  $\text{m}^3/(\text{kmol}\cdot\text{s})$ .

The following biradical mechanism has been proposed for this reaction:



- (a) Does this mechanism give rise to a rate expression that is consistent with the initial rate data?
- (b) If the reverse Diels–Alder reactions are faster than the isomerization reaction between the exo and endo forms, to what does the rate expression reduce?
- (c) If the endo form is the desired product, do you recommend operation at the high or low end of the temperature range 512 to 638 K? Determine the product distribution for 30% conversion of cyclohexadiene at the temperature specified.

- 9.9** E. Prodan and I. L. Shashkova [*Kinet. Catal.*, **24**, 891–894 (1984)] studied the kinetics of the decomposition of tripolyphosphoric acid in aqueous solution:

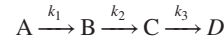


Analysis of their data indicates that at 40°C, the values of the pseudo first-order rate constants  $k_1$  and  $k_2$  are 0.353 and

$5.28 \times 10^{-3} \text{ h}^{-1}$ , respectively. Consider the situation in which a stream is available containing  $\text{H}_5\text{P}_3\text{O}_{10}$ ,  $\text{H}_4\text{P}_2\text{O}_7$ , and  $\text{H}_3\text{PO}_4$  at concentrations of 0.20, 0.004, and 0.002 M, respectively.

- (a) Determine the space time for a single CSTR at which the effluent concentration of  $\text{H}_4\text{P}_2\text{O}_7$  is a maximum. The reactor operates at 40°C. In addition, determine the effluent concentrations of the three acids.
- (b) Repeat part (a) for the case in which these reactions are carried out in a cascade of two identical CSTRs, both operating at 40°C. In this case, prepare plots of the effluent concentrations versus the space time for the cascade. Comment and indicate how your results would compare with the optimum value of the space time for a PFR.

- 9.10** I. N. Bazanova, O. V. Lefedova, V. P. Gostikin, and L. V. Kudryashova [*Kinet. Catal.*, **28**, 1177–1182 (1988)] studied the kinetics of the catalytic reduction of 2-(2'-hydroxy-5'-methylphenyl)benzotriazole over Raney nickel in 1 M NaOH. Several successive hydrogenation reactions occur such that the reaction network of interest can be regarded as a series of apparent first-order pseudo-homogeneous reactions of the form



These authors indicate that at 75°C, the value of the apparent pseudo-homogeneous rate constant  $k_1$  is  $0.53 \times 10^{-3} \text{ L}/(\text{s}\cdot\text{g catalyst})$  when the initial concentration of the benzotriazole is  $15.10 \times 10^{-3} \text{ M}$  and the catalyst loading is 0.625 g/L. Unfortunately, these authors did not report values of the other pseudo-homogeneous rate constants, but for present purposes we shall assume that  $k_2$  and  $k_3$  may be taken as  $0.40 \times 10^{-3}$  and  $0.20 \times 10^{-3} \text{ L}/(\text{s}\cdot\text{g catalyst})$ , respectively.

Consider the possibility of carrying out this reaction in a single continuous flow stirred-tank reactor operating at 75°C with a feed concentration of the benzotriazole equal to  $15.10 \times 10^{-3} \text{ M}$  and a catalyst loading of 2.5 g/L. If the volume of the reactor is 4 m<sup>3</sup>, determine the (different) volumetric flow rates of the feed stream that maximize the effluent concentrations of species B and C. Of the species of interest in the reaction network, only species A is present in the feed stream.

- 9.11** M. L. Kaliya, A. E. Nechitailo, and E. M. Guseinov [*Kinet. Katal.*, **30**, 699–702 (1990)] studied the kinetics of the hydrolysis of both cyanopyridines (C) and pyridine carboxamides (A). In basic solution these consecutive reactions can both be regarded as pseudo first-order:



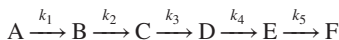
For the case where C is 2-cyanopyridine, A is picolinomide, and K is picolinic acid, consider the situation in which sufficient base is present in aqueous solution that  $k_1 = 8.41 \times 10^{-2} \text{ min}^{-1}$  and  $k_2 = 1.45 \times 10^{-2} \text{ min}^{-1}$ .

A solution of the base and 2-cyanopyridine are being fed to a batch reactor during a start up process. Consider the case in which the tank initially contains 100 L of the basic solution, the ultimate capacity of the reactor is 500 L, and the total volumetric flow rate of the entering streams is held constant at 12.5 L/min until capacity is reached. Thereafter it is zero.

Only base and species C are present in the feed stream. The concentration of species C in the feed stream is 1.2 M.

- (a) Determine the concentrations of species C, A, and K as functions of time during the time the reactor is being filled and during the period while the concentration of species A is increasing. Prepare plots of the concentrations of these three species during this period for times up to 80 min.
- (b) At what time is the fraction of species C fed to the reactor that is present as species A at its maximum value?

- 9.12** Consider the kinetics of an extended sequence of pseudo first-order reactions of the form



This reaction scheme can be employed to describe the reactions of mesonitrile (species A) in 89.8% w/w sulfuric acid.

- (a) If a single stirred-tank reactor is employed to carry out these reactions, derive expressions for the effluent compositions of all six of the species indicated as functions of the space time employed.
- (b) Use these expressions to prepare plots of the concentrations of all six species as functions of the reactor space time for space times from 0 to 12,000 s. Consider the case where the feed contains only mesonitrile in sulfuric acid. In preparing these plots, normalize the various species concentrations by dividing by the concentration of species A in the feed stream. Use the following values of the pseudo first-order rate constants (in  $s^{-1}$ ) at 98.3°C:  $k_1 = 6.61 \times 10^{-4}$ ,  $k_2 = 9.19 \times 10^{-4}$ ,  $k_3 = 1.69 \times 10^{-2}$ ,  $k_4 = 1,820$ , and  $k_5 = 4.83 \times 10^{-4}$ .
- (c) The magnitudes of the various rate constants are such that the only species present in appreciable concentrations in the effluent stream are mesonitrile (A), mesitamide (B), and the monosulfuric acid derivative (E). What reactor space times correspond to the maxima in the effluent concentrations of species B and E? What are the values of these maxima?
- (d) Comment on the relative values of the reactor space times and the effluent concentrations corresponding to the maxima for species B and E for a single CSTR and a plug flow reactor. For a batch reactor employing the same feedstock, the expression governing the time dependence of the concentration of species B is

$$B = \frac{k_1 A_0}{k_2 - k_1} [e^{-k_1 t} - e^{-k_2 t}] \quad (1)$$

- 9.13** A cascade of two identical CSTRs is being used to produce the intermediate V in the reaction sequence



In the presence of an appropriate catalyst, the first reaction is pseudo first-order:

$$r_1 = k_1 C_A$$

where the dependence of the rate on the catalyst concentration is incorporated in the rate constant. In the presence of the same

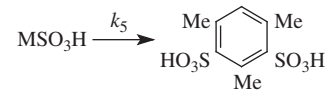
catalyst, the second reaction in the sequence is pseudo zero-order in all species:

$$r_2 = k_2$$

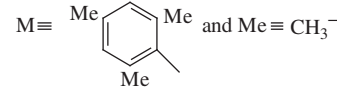
If both reactors operate at the same temperature, derive an expression for the reactor space time that leads to the maximum concentration of species V in the effluent from the second reactor. Consider the general case in which both A and V are present in the feed stream at concentrations  $C_{A0}$  and  $C_{V0}$ . Your expression need not be an explicit closed form expression for  $\tau$ . The reaction takes place in the liquid phase.

If one operates at the space time that maximizes the concentration of species V in the effluent from the second reactor, what fraction of the A fed to the cascade ends up as V when  $k_1 = 8.33 \text{ ks}^{-1}$ ,  $k_2 = 0.5 \text{ kmol}/(\text{m}^3 \cdot \text{ks})$ ,  $C_{A0} = 1.80 \text{ kmol}/\text{m}^3$ , and  $C_{V0} = 0.18 \text{ kmol}/\text{m}^3$ . Note that a trial-and-error solution will be required to arrive at a numerical answer.

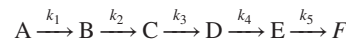
- 9.14** J. Al-ka'bi, P. H. Gore, E. F. Saad, and D. N. Waters [*Int. J. Chem. Kinet.*, **15**, 697 (1983)] analyzed the kinetics of an extended sequence of pseudo-first-order reactions. The example considered is the sequence of reactions that occur when mesitonitrile (2,4,6-trimethylbenzonitrile) is present in 89.8% w/w sulfuric acid at 98.3°C.



where



We have indicated only the core aromatic species in the scheme above because these reactions are all pseudo-first-order in these species and pseudo-zero-order in all other species when the reactions are carried out in concentrated sulfuric acid. This reaction network can also be written in symbolic form as



The following values of pseudo first-order rate constants (in  $s^{-1}$ ) are available for these reactions at the temperature indicated:

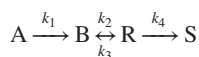
$$\begin{aligned} k_1 &= 6.61 \times 10^{-4} \\ k_2 &= 9.19 \times 10^{-4} \\ k_3 &= 1.69 \times 10^{-2} \\ k_4 &= 1820 \\ k_5 &= 4.83 \times 10^{-4} \end{aligned}$$

- (a) Consider the problem of predicting the effluent composition of a plug flow reactor as a function of the reactor space

time. Derive the equations necessary to predict the effluent concentrations of all six of the organic compounds indicated. Generate plots of these concentrations for reactor space times from 0 to 12,000 s for the case where only mesitonitrile (A) and sulfuric acid are present initially. Normalize these concentrations by dividing by the initial concentration of mesitonitrile. In the expressions for the various product species, you should place all terms preceding the same exponential function over a common denominator and factor this denominator so that each factor consists of a difference in rate constants.

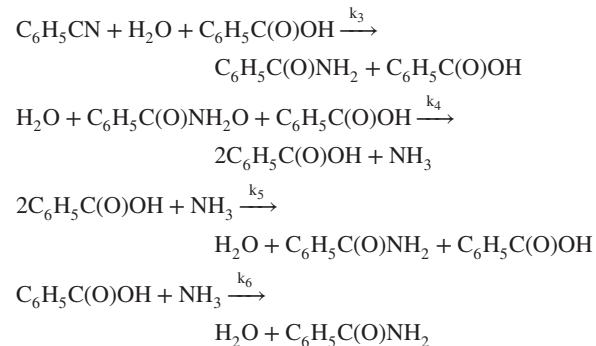
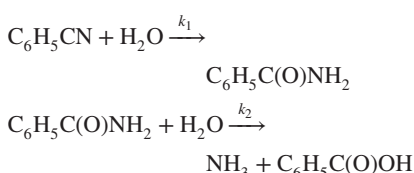
- (b) The magnitudes of the various rate constants are such that appreciable concentrations of only the intermediates mesitamide ( $\text{MCONH}_2$ ) and the monosulfonic acid derivative ( $\text{MSO}_3\text{H}$ ) are observed. At what space times are these maxima observed? What are the maximum yields of these two species relative to the initial concentration of species A? Use both a plot and an analytical solution to generate the values corresponding to the maximum concentration of mesitamide and a plot to determine the maximum concentration of the monosulfuric acid derivative.

- 9.15** It is desired to utilize a single CSTR to produce species R via the following reaction network:



The feed stream consists of species A dissolved in a liquid at a concentration of 2.0 mol/L. Each of the rate laws indicated is first-order.

- (a) Derive equations in which the effluent concentrations of species A, B, and R are each related to the several rate constants, the space time of the reactor, and the inlet concentration of reactant A. None of these three equations should contain more than a single effluent concentration.
- (b) Determine the reactor space time that maximizes the effluent concentration of species R. At the operating temperature in question, the rate constants have the following values in  $\text{h}^{-1}$ :  $k_1 = 5.4$ ,  $k_2 = 5.0$ ,  $k_3 = 0.25$ , and  $k_4 = 0.2$ . Note that a trial-and-error solution will be required. (The space time required lies between 1 and 3 h.) If the inlet concentration of species A is 2.0 mol/L, what is the maximum effluent concentration of species R?
- 9.16** B. Izzo, C. L. Harrel, and M. T. Klein [*AIChE J.*, **43**, 2048–2058 (1997)] studied the hydrolysis of nitriles in high-temperature pressurized aqueous solution. They report that the reaction is autocatalytic because of catalysis by the acid formed as a result of hydrolysis of the amide formed in the initial reaction. For benzonitrile, the reaction network can be represented as



Consider the situation in which only  $\text{C}_6\text{H}_5\text{CN}$  is present in the aqueous solution fed to the CSTR (concentration = 0.71 M) and the CSTR operates at 300°C and 87 bar, where the rate constants have the following values:  $k_1 = 7.44 \times 10^{-3} \text{ min}^{-1}$ ,  $k_2 = 1.15 \times 10^{-2} \text{ min}^{-1}$ ,  $k_3 = 1.35 \times 10^{-1} \text{ M}^{-1} / \text{min}$ ,  $k_4 = 1.72 \times 10^{-1} \text{ M}^{-1} / \text{min}$ ,  $k_5 = 1.70 \times 10^{-1} \text{ M}^{-2} / \text{min}$ ; and  $k_6 = 1.14 \times 10^{-2} \text{ M}^{-1} / \text{min}$ , where the rate constants indicated are pseudo rate constants that incorporate the effect of the concentration of water.

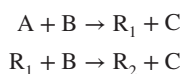
There are two scenarios for which this reaction network is of potential interest in the design of a CSTR.

1. Operation in a mode that maximizes the rate of hydrolysis of  $\text{C}_6\text{H}_5\text{CN}$ .
2. Operation under conditions that maximize the concentration of the intermediate amide in the effluent.

First consider the task of operating a single CSTR at a conversion level that maximizes the rate of destruction of the nitrile. What value of the space time corresponds to this mode of operation? Analyze this situation by developing expressions for the effluent concentrations of each species as a function of the reactor space time.

Determine the space time corresponding to the maximum rate of consumption of  $\text{C}_6\text{H}_5\text{CN}$ . Plot the rate versus the concentration of  $\text{C}_6\text{H}_5\text{CN}$ . On this plot indicate the operating line for the single CSTR. Then use the plot to determine the concentrations of benzonitrile that would be present in the effluent from each reactor in a cascade of three identical reactors, the first of which operates at the maximum rate of destruction of the nitrile. Use the plots of species concentration versus time to ascertain whether there is a space time that maximizes the concentration of the amide in the effluent from the CSTR. Comment.

- 9.17** M. R. Newberger and R. H. Kadlec [*AIChE J.*, **17**, 1381–1387 (1971)] studied the conditions for optimal operation of a tubular reactor in which consecutive second-order reactions are being carried out. Of particular interest was the saponification of diethyl adipate with sodium hydroxide in aqueous solution. The stoichiometry of these reactions can be expressed as



where A refers to the diester, B to sodium hydroxide, C to ethanol,  $\text{R}_1$  to the sodium salt of the monoester, and  $\text{R}_2$  to the sodium salt of adipic acid. The rate expressions for these

reactions are

$$r_1 = k_1(A)(B)$$

and

$$r_2 = k_2(R_1)(B)$$

with

$$k_1 = 4.87 \times 10^6 e^{-10,080/(1.987T)}$$

and

$$k_2 = 3.49 \times 10^3 e^{-5965/(1.987T)}$$

for  $k$  in  $M^{-1}/s$  and  $T$  in K.

The corresponding standard heats of reaction are

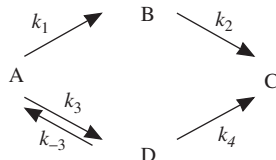
$$\Delta H_1^0 = -10.8 \text{ kcal/mol}$$

and

$$\Delta H_2^0 = -16.3 \text{ kcal/mol}$$

Determine the volumetric flow rate that maximizes the effluent concentration of monoethyl adipate if the tubular reactor is operated at a temperature of 80°C. The feed stream is 0.018 M in diethyl adipate and 0.050 M in sodium hydroxide. The tubular reactor is 6 ft long and has an internal diameter of 1.25 in. Will the relative yield of monoethyl adipate increase or decrease if the reactor is operated at a higher temperature?

- 9.18** M. Bikrani, L. Fidalgo, M. A. Garralda, and C. Ubide [*J. Mol. Catal.*, **118**, 47–53 (1997)] studied the catalytic activity of cationic iridium complexes for homogeneous hydrogen transfer from isopropanol to 2-cyclohexen-1-one to give cyclohexanol. The reaction network contains consecutive, competitive, and reversible elements. In isopropanol these elements can be expressed as pseudo first-order processes:



where A is 2-cyclohexen-1-one, B is cyclohexenone, C is cyclohexanol, and D is 2-cyclohexenol. Consider the possibility of carrying out these reactions in a tubular reactor (PFR).

- (a)** Derive the equations that govern the dependence of the effluent concentrations of the three species of primary interest (A, B, and C) for the case in which all of the reactions indicated obey pseudo-first-order kinetics and in which species D is so reactive that it is never present at a significant level. Because both the concentration of species D and its derivative with respect to longitudinal position (space time) in the reactor are small, one can make the assumption that  $dD/d\tau$  is approximately zero. ( $\tau$  is the space time for the PFR.) This assumption is the PFR analog of the steady-state approximation that could be utilized in analysis of these reactions in a batch reactor. You may assume that only species A is present in the feed stream.

- (b)** Bikrani et al. reported the following rate constants at 83°C:

$$k_1 = 1.4 \times 10^{-3} \text{ s}^{-1}$$

$$k_2 = 1.2 \times 10^{-4} \text{ s}^{-1}$$

$$k^1 = 1.8 \times 10^{-3} \text{ s}^{-1}$$

$$k^{11} = 4 \times 10^{-4} \text{ s}^{-1}$$

where

$$k^1 = k_1 + k_3 - \left( \frac{k_3 k_{-3}}{k_{-3} + k_4} \right)$$

and

$$k^{11} = k^1 - k_1 = \left( \frac{k_3 k_4}{k_{-3} + k_4} \right)$$

Prepare plots of the effluent concentrations of species A, B, and C for reactor space times from zero to 3 h. Express the species concentrations relative to the inlet concentration of species A. In addition, use the following hypothetical values of the other rate constants to plot the concentration of species D on the same figure.

$$k_3 = 4.5 \times 10^{-4} \text{ s}^{-1}$$

$$k_{-3} = 0.8 \text{ s}^{-1}$$

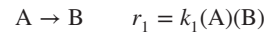
$$k_4 = 6.4 \text{ s}^{-1}$$

These values are consistent with the values of  $k^1$  and  $k^{11}$  reported by Bikrani et al. Comment on the validity of the steady-state approximation as reflected in the values calculated for  $D/A_0$ .

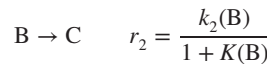
- (c)** Use the answers developed in parts (a) and (b) to determine the reactor space time at which the effluent concentration of species B is maximized. Is the result obtained from the plot consistent with the closed form expression for this space time that you derive from your expression for  $B(\tau)$ ?

- 9.19** J. Kumar and S. Nath [*Chem. Eng. Sci.*, **52**, 3455–3462 (1997)] simulated the behavior of a CSTR in which a liquid-phase autocatalytic reaction and a reaction that obeys a Michaelis–Menten rate expression are occurring simultaneously.

Consider the following specific example of their general case. The stoichiometry and rate expression for the autocatalytic reaction are



The other reaction of interest has the following stoichiometry and rate expression:



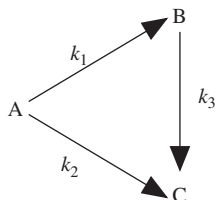
Consider the situation in which no B or C is present in the feed, the CSTR has a volume  $V_R$ , the volumetric flow rate of the feed stream is  $\mathcal{V}$ , and the feed concentration of species A is  $A_0$ .

(a) Derive closed-form expressions for the steady-state concentrations of species A, B, and C in the effluent from the CSTR as functions of the reactor volume, the volumetric flow rate, the feed concentration of species A, and the kinetic parameters,  $k_1$ ,  $k_2$ , and  $K$ . You may leave your answers in terms of three equations:

1. An expression relating A and B.
2. An expression relating C and B.
3. A quadratic equation from which the effluent concentration of B can be determined. Reduce this expression to the form  $aB_1^2 + bB_1 + c = 0$ , where  $a$ ,  $b$ , and  $c$  are functions of the reactor space time, the kinetic parameters, and the concentration of species A in the feed stream. The expression indicated may contain only the aforementioned parameters and the concentrations specified.

(b) Optimize the effluent concentration of species B by considering the specific case for which  $1$  is very large compared to  $KB$ ; that is, consider the limit of the relations derived above by letting  $K$  become zero. Derive expressions for (1) the space time corresponding to the maximum effluent concentration of species B and (2) the maximum effluent concentration itself.

**9.20** K. Kato and K. Amada [*Int. J. Chem. Kinet.*, **21**, 81–87 (1981)] studied the characteristics of a parallel consecutive reaction network as a basis for assessing the selectivity of the oxidation of ethylene to ethylene oxide. The reaction is modeled in terms of a network of first-order reactions:

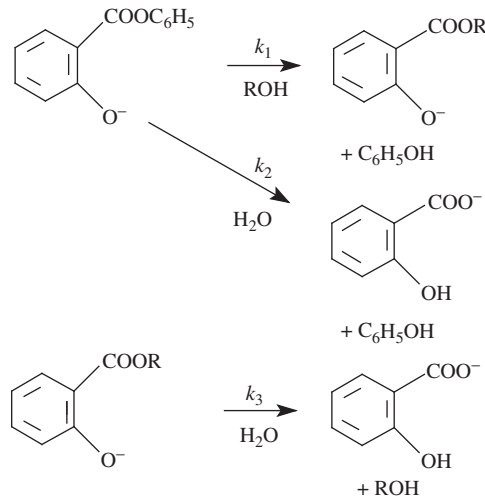


Consider the problem of predicting how the concentrations of species A, B, and C in the effluent from a tubular reactor depend on the reactor space time when the values of  $k_1$ ,  $k_2$ , and  $k_3$  are 0.20, 0.09, and  $0.04\text{ s}^{-1}$ , respectively. Prepare plots of the concentrations of each species for space times from 0 to 20 s. In addition, prepare a plot of the yield of species B per mole of A reacted [ $C_B/(C_{A0} - C_A)$ ] as a function of the space time.

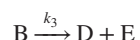
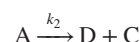
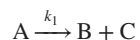
Use both a graphical/spreadsheet approach and an analytical procedure leading to a closed-form solution to determine the space time corresponding to a maximum concentration of species B in the effluent. What is the value of this concentration? What space time gives the maximum yield of species B? What is this yield? What might be a problem with operating at this space time?

**9.21** M. Niyaz Khan [*Int. J. Chem. Kinet.*, **19**, 757–776 (1987)] studied the kinetics of the methanolysis of phenyl salicylate in aqueous mixed solvents. For reaction at  $30^\circ\text{C}$  in basic ( $0.05\text{ M NaOH}$ ) solution containing 5% v/v methanol and 0.8% methyl

cyanide, the reaction network can be described as follows:



Each of the indicated irreversible reactions is pseudo first-order in the aromatic species. R represents  $\text{CH}_3$ . In shorthand notation these reactions may be written as

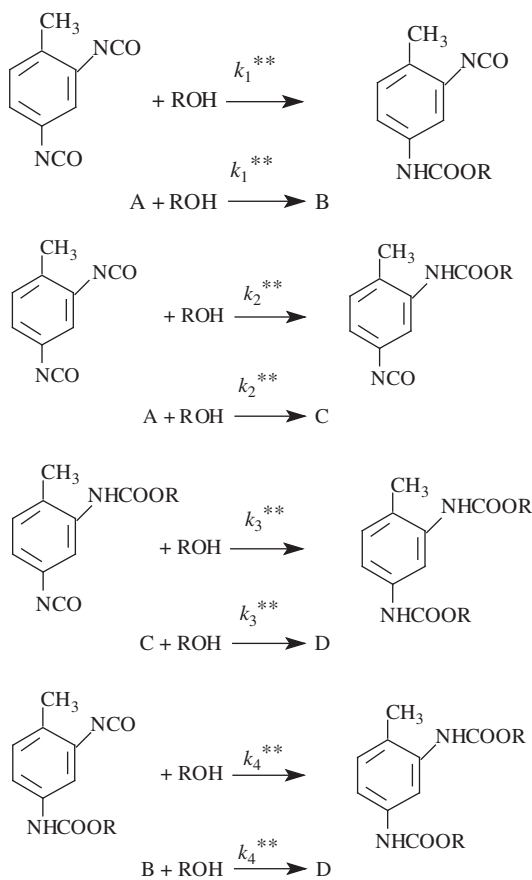


At  $30^\circ\text{C}$  the values of the pseudo-first-order rate constants (in  $\text{s}^{-1}$ ) are  $k_1 = 2.01 \times 10^{-3}$ ,  $k_2 = 5.01 \times 10^{-4}$ , and  $k_3 = 1.34 \times 10^{-4}$ . Consider the possibility of carrying out these reactions in a single CSTR under conditions that maximize the concentration of the methyl salicylate (species B) in the effluent. The reactions are to be carried out in a CSTR with a volume of  $10\text{ m}^3$ .

- (a) Determine the volumetric flow rate that maximizes the steady-state concentration of methyl salicylate in the effluent. Start by deriving expressions for the dependence of the effluent concentrations of species A, B, C, and D on the space time for the reactor. Prepare plots of dimensionless effluent concentrations versus space time. Use both graphical and analytical approaches to determine the space times corresponding to the optimum indicated. What fraction of the phenyl salicylate fed to the CSTR is converted to species B when this reactor is operated at the optimum space time?
- (b) Compare the optimum value of the space time for the CSTR with the corresponding value for a plug flow reactor. What is the corresponding value of the fraction conversion of phenyl salicylate to methyl salicylate in the effluent from a PFR operating at the optimum space time?

**9.22** I. B. Tsvetkovskii, S. B. Gordeeva, and G. N. Petrov [*Kinet. Catal.*, **28**, 262–265 (1987)] studied the kinetics of the reaction of an oligodienediol with 2,4-toluene diisocyanate. The

reactions constituting the competitive-consecutive reaction network of interest can be written as



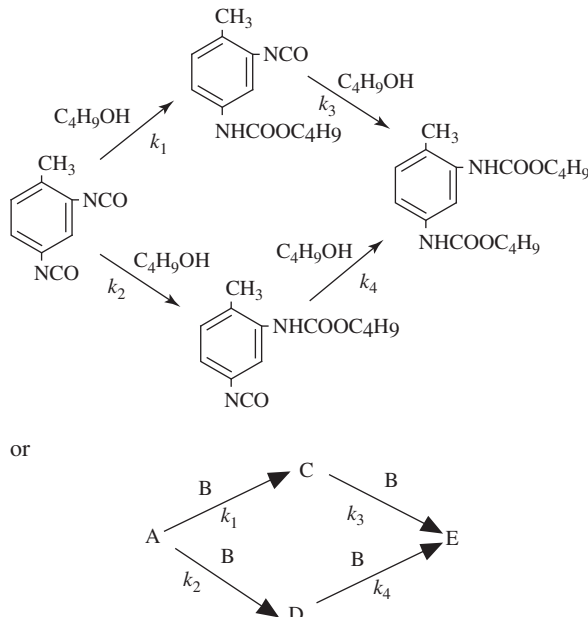
The asterisk superscripts serve to indicate that in this research the authors expressed both reaction rates and species concentrations per kg solution rather than per unit volume. At 31.5°C the values of the second-order rate constants are  $k_1^{**} = 0.085$ ,  $k_2^{**} = 0.010$ ,  $k_3^{**} = 0.030$ , and  $k_4^{**} = 0.002$ , where the units associated with rate constants are kg solution/(mol·min).

Consider the possibility of carrying out these reactions in a tubular reactor (PFR) that operates isothermally at 31.5°C. The oligodienediol is employed in large excess so that each of the four reactions can be regarded as being pseudo first-order in the indicated aromatic species. You may convert the second-order rate constants indicated to the corresponding pseudo first-order form by using a value of 10.5 mol/kg for the (essentially constant) concentration of the dienediol.

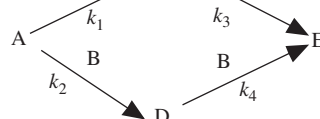
Analyze the situation in which concentration of 2,4-toluene diisocyanate in the feed is 0.5 mol/kg solution. None of the other aromatic species is present in the feed stream. Prepare plots of the composition of the effluent stream as a function of the space time for the reactor. Determine the reactor space times that maximize the concentrations of the two stable intermediates, B and C. Note that for this problem the space time can be regarded as the ratio of the mass of

liquid contained within the reactor to the entering mass flow rate.

- 9.23** V. G. Sumkina, G. M. Palyutkin, and V. V. Zharkov [*Kinet. Catal.*, **26**, 420 (1985)] studied the reactions of 2,4-toluene diisocyanate with *n*-butanol (B):



or

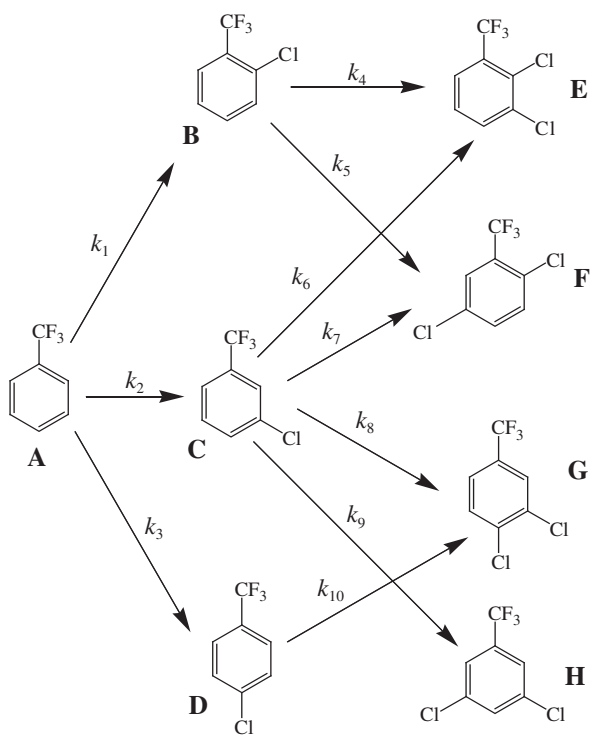


- (a)** Consider the problem of maximizing the concentration of species C in the effluent from a single stirred-tank reactor. The specified operating conditions imply that the feed concentrations of butanol (B) and the diisocyanate (A) are 4.0 M and 0.2 M, respectively. At 20°C the rate constants have the following values (in  $M^{-1}/sec^{-1}$ ):  $k_1 = 7.7 \times 10^{-4}$ ,  $k_2 = 7.0 \times 10^{-5}$ ,  $k_3 = 3.0 \times 10^{-5}$ , and  $k_4 = 2.2 \times 10^{-4}$ . Note that a vast excess of alcohol is to be employed. Under such conditions the several rate expressions may be treated as if they all obey pseudo first-order kinetics. How large must the reactor be to process 5000 L/h of feed when operating so as to maximize the effluent concentration of species C? Determine the effluent concentrations of all species for operation under these conditions.
- (b)** In the presence of 0.01 M triethylamine, which acts as a catalyst, the effective second-order rate constants (in  $M^{-1}/s$ ) for the several reactions are as follows:  $k_1 = 0.265$ ,  $k_2 = 0.101$ ,  $k_3 = 0.040$ , and  $k_4 = 0.171$ , where the effect of the catalyst concentration has been incorporated in the rate constant. In the presence of excess butanol, the several rate expressions will again degenerate to the pseudo first-order form. Determine the optimum space time for this reactor if this catalyst is employed. What would be the effluent concentrations of the various species if the optimum space time is used? The reactant concentrations in the feed would be the same as those employed in part (a).
- (c)** Indicate the advantages and disadvantages that would be associated with use of the triethylamine catalyst. Indicate

other processes that might offer advantages over the present mode of operation.

- 9.24** A. A. Ushakov, V. I. Kosorotov, G. V. Motsarev, B. Y. Stul' and R. V. Dzhagatspanyan [*Kinet. Catal.*, **20**, 1208 (1979)] reported values of rate constants at 80°C [in  $\text{m}^6/(\text{kmol}^2 \cdot \text{ks})$ ] for the competitive-consecutive reactions of chlorine with benzotrifluoride (A):

$k_1 = 0.97$	$k_6 = 0.06$
$k_2 = 9.83$	$k_7 = 0.48$
$k_3 = 1.20$	$k_8 = 1.37$
$k_4 = 0.60$	$k_9 = 0.26$
$k_5 = 2.40$	$k_{10} = 1.10$

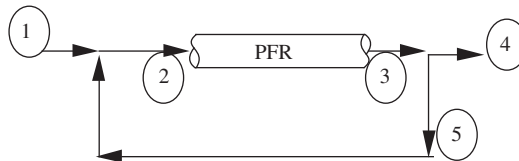


The rate expressions for each of the reactions in question are third-order overall: first-order with respect to the catalyst ( $\text{FeCl}_3$ ), chlorine, and the aromatic reactant.

- (a) For reaction in a single PFR, derive equations for and prepare plots of the relative yields of each monosubstituted product (B, C, and D) as a function of both the fraction conversion of benzotrifluoride and the reactor space time. None of the several product species is present in the feed to the reactor. You should find it useful to eliminate time (or space time) in conducting the first part of this analysis.
- (b) Perform a similar analysis for and prepare plots describing the yields of the total monosubstituted ( $B + C + D$ ) and total disubstituted products ( $E + F + G + H$ ) for reaction in a PFR. You may plot both types of product distribution on the same figure.

- (c) Prepare plots of the various product concentrations from parts (a) and (b) versus the space time for the plug flow reactor. Consider space times up to 0.8 s.

- 9.25** For autocatalytic reactions it is often appropriate to employ a reactor configuration in which a CSTR operating at the maximum rate is followed by a plug flow reactor. Another alternative would be to employ a recycle reactor in which a portion of the effluent from a PFR is recycled to the reactor inlet.



Consider an irreversible autocatalytic reaction with the stoichiometry



and a rate expression

$$r = kC_{\text{A}}C_{\text{B}}$$

This reaction takes place in the liquid phase with  $k = 0.08 \text{ L}/(\text{mol} \cdot \text{min})$  at the temperature of interest. The recycle ratio  $R$  represents the ratio of the volumetric flow rate of the material recycled to the reactor inlet (i.e., at point 5) to the volumetric flow rate of the material leaving the composite system (i.e., at point 4).

Consider a situation in which  $R = 1.5$ , the concentration of reactant A in the fresh feed (point 1) is 1.6 M, and the concentration of species B in the reactor effluent (point 3) is 1.2 M. The reactor operates isothermally. The flow rate of the feedstock at point 1 is 2 L/min.

Determine the following:

- The volumetric flow rate at point 2.
- The concentrations of species A and B at point 2.
- The total length of the PFR necessary to accomplish this reaction if the inside diameter of the reactor is 10 cm.
- What distance from the reactor inlet corresponds to the maximum rate of reaction? This point will correspond to that at which the heat transfer requirements (in or out) will be a maximum.

- 9.26** A. Komlosi, G. Porta, and G. Stedman [*Int. J. Chem. Kinet.*, **27**, 911–917 (1995)] studied the autocatalytic oxidation of formaldehyde by nitric acid in aqueous solution.



where  $\text{H}_2\text{C}(\text{OH})_2$  is a hydrated form of formaldehyde. For reaction at 20°C when  $\text{HNO}_3$  is present in large excess, the rate expression is

$$r = k[\text{H}_2\text{C}(\text{OH})_2][\text{HNO}_2]$$

with  $k = 2.47 \text{ dm}^3/(\text{mol} \cdot \text{min})$ .

For autocatalytic reactions, the minimum total volume requirement necessary to achieve a specified high degree of conversion can often be obtained by using a stirred- tank reactor operating at an extent of conversion that produces the maximum rate of reaction followed by a tubular reactor. Consider the task of producing formic acid ( $\text{HCOOH}$ ) from a feed stream containing  $\text{HNO}_3$ ,  $\text{H}_2\text{C}(\text{OH})_2$ , and  $\text{HNO}_2$  at concentrations of 7.5, 0.140, and  $0.004\text{ mol/dm}^3$ , respectively. If 98% of the feed  $\text{H}_2\text{C}(\text{OH})_2$  in a stream supplied at a rate of  $5000\text{ dm}^3/\text{h}$  is to be converted to formic acid, determine the volumes of a CSTR and a PFR that give the minimum total volume.

- 9.27** S. M. Mahajani, M. M. Sharma, and T. Sridhar [*Chem. Eng. Sci.*, **54**, 3967–3976 (1999)] studied the liquid-phase partial oxidation of cyclohexene in a batch reactor. In the absence of a catalyst, a variety of products are formed, including cyclohexenol, cyclohexene hydroperoxide, cyclohexenone, and cyclohexene oxide. This research group obtained kinetic data using a well-agitated pressure vessel in which the partial pressure of oxygen over the liquid was maintained constant by continuous addition of oxygen as the reaction proceeded. For our present purpose, we may consider the stoichiometry of the reaction to be of the general form



where C is cyclohexene and P is a generic product. Even though these authors indicated that the stoichiometric coefficient of oxygen is undetermined, you may assume it to be unity. These investigators fit their data with an autocatalytic rate expression of the form

$$r = k(\text{C})(\text{P})$$

Consider the task of designing a reactor network for carrying out this reaction. The first reactor is to be a single CSTR in which the head space is continuously replenished with oxygen at a rate which (with the agitation provided) maintains the oxygen in solution at a level such that for reaction at  $105^\circ\text{C}$ , the value of the rate constant  $k$  is  $0.407\text{ M}^{-1}/\text{h}$ . The CSTR is to be operated under conditions that maximize the reaction rate. Species C and P are fed to the CSTR in a manner such that the blend of these streams contains concentrations of C and P of 9.31 and 0.49 M, respectively. If the working volume of the CSTR is 2000 L, what volumetric flow rate should be employed for the blend? If we regard the stoichiometric coefficient of oxygen as unity, what fraction of the C that enters the CSTR is converted to P?

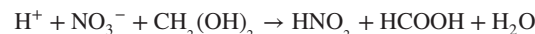
The second reactor is to be a plug flow reactor with an effective volume of 1600 L. Oxygen is injected at several points along the length of the reactor to maintain a constant concentration of this species over the entire length of the PFR. This concentration is such that the aforementioned rate expression and rate constant remain valid. What fraction of the C that enters the CSTR is converted to P in the indicated combination of reactors?

- 9.28** M. Horvath, I. Lengyel, and G. Bazsa [*Int. J. Chem. Kinet.*, **20**, 687–697 (1988)] reported that the kinetics of the oxidation of

formaldehyde in aqueous nitric acid are governed by a rate expression of the form

$$-\frac{d[\text{CH}_2(\text{OH})_2]}{dt} = k(\text{NO}_3^-)(\text{H}^+)(\text{HNO}_2)[\text{CH}_2(\text{OH})_2]$$

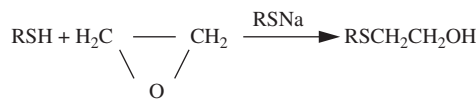
where  $\text{CH}_2(\text{OH})_2$  represents the hydrated form of formaldehyde in aqueous solution and where  $k = 4.0 \times 10^{-5}\text{ M}^{-3}/\text{s}$  at room temperature. The stoichiometry of the reaction of interest may be regarded as



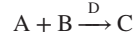
In working this problem you should regard the nitric acid as completely dissociated but neglect dissociation of  $\text{HNO}_2$  and  $\text{HCOOH}$ .

- (a) Consider the question of designing a recycle reactor network to process a volumetric flow rate of  $1.2\text{ m}^3/\text{h}$  for a feed stream that is 5 M in  $\text{HNO}_3$ ,  $5 \times 10^{-4}$  M in  $\text{HNO}_2$ , and 0.21 M in  $\text{CH}_2(\text{OH})_2$ . The recycle reactor is to achieve 95% conversion of the limiting reagent. Plot the reactor volume versus the recycle ratio for values of this ratio between zero and 2. What recycle ratio leads to the smallest reactor volume? What is this volume?
- (b) Now consider the situation in which reactor network consists of a recycle reactor followed by a tubular reactor (PFR). The overall conversion is again 95% leaving the tubular reactor. The conversion leaving the recycle reactor is the conversion corresponding to the maximum reaction rate. The recycle reactor is operated at the recycle ratio that minimizes the volume of the recycle reactor. Determine:
1. The concentration leaving the recycle reactor.
  2. A reasonable recycle ratio (consider ratios of 0, 0.1, 0.25, 0.5, 1, and 2).
  3. The volume of the corresponding recycle reactor.
  4. The volume of the PFR.
  5. The total volume of the reactor network. Comment.

- 9.29** J. Chlebicki and Z. Cichacz [*Int. J. Chem. Kinet.*, **20**, 387–395 (1988)] studied the sodium thiolate-catalyzed addition of oxirane to alkanethiols. This reaction is an important method for producing nonionic surfactants. When the alkanethiol is present in excess, the product is exclusively the alkyl-2-hydroxyethyl sulfide.



or



Consider the reaction between 1-butanethiol and oxirane. This reaction is autocatalytic with the following rate expression:

$$r = (k_1 C_A + k_2 C_C) C_B C_D$$

- (a) For autocatalytic reactions in liquid solution it may be advantageous to employ a network consisting of a CSTR operating at the maximum rate followed by a

PFR. The reactor network is to operate isothermally. Suppose that at the temperature of interest, the values of the rate constants  $k_1$  and  $k_2$  are  $2.08 \times 10^{-4}$  and  $7.57 \times 10^{-3} \text{ M}^{-2}/\text{s}$ , respectively. For a feed rate of  $3.6 \text{ m}^3/\text{h}$ , determine the volumes of the reactors that constitute the system that gives the minimum total reactor (CSTR + PFR) volume required to achieve 90% conversion of the limiting reactant. The feed concentrations are:  $C_{A0} = 5.0 \text{ M}$ ,  $C_{B0} = 1.0 \text{ M}$ ,  $C_{C0} = 0.0 \text{ M}$ , and  $C_{D0} = 0.05 \text{ M}$ .

**(b)** An alternative to the reactor combination considered in part (a) is to employ a recycle reactor for which the effluent composition corresponds to the conversion associated with the maximum rate of reaction. This reactor would then be followed by a PFR. If the temperature and the feed composition are the same as in part (a), determine the manner in which the overall reactor (recycle + PFR) volume varies with the recycle ratio when the desired conversion of the limiting reagent is 90%.

# Chapter 10

---

## Temperature and Energy Effects in Chemical Reactors

### 10.0 INTRODUCTION

The energy changes associated with chemical reactions play an extremely important role in the design of commercial-scale reactors. Even in those cases where one desires to use a mode of operation approximating isothermal behavior, energy balance considerations are important in determining the heat transfer requirements of the process. In laboratory-scale experiments it is relatively easy to maintain substantially isothermal conditions because of the large surface-to-volume ratio of small equipment and because economic aspects of the heat transfer process are unimportant. In industrial-scale equipment, both physical limitations on the rate of heat transfer and the economics of this process can become quite important, particularly when large enthalpy changes accompany the reaction.

Several factors govern the temperature range in which one may choose to operate a commercial reactor. The dependence of the reaction rate expression on temperature and the position of chemical equilibrium are two key factors influencing the choice of temperature level. The temperature dependence of the main reaction and of important side reactions will govern the selectivity of the conversion. Other properties of the reaction mixture may also influence the choice of operating temperature through secondary considerations. For example, the dew point of a gaseous mixture, the bubble point of a liquid mixture, the temperature at which a liquid separates into two immiscible phases, and the temperature dependence of corrosion reactions all can limit the temperature range within which one might choose to operate. Catalyst activity, selectivity, and deactivation must also be considered in selecting the operating temperature for catalytic processes.

To achieve adequate control during the operation of a reactor, it is necessary to maintain the temperature within at least moderate limits. Adiabatic operation is possible

only when the concomitant temperatures do not rise so high that the rate becomes excessive or drop so low that the rate becomes impractically low. This mode of operation is favored when the enthalpy change accompanying the reaction is small in magnitude, when it is possible to adjust the initial temperature of the reactant mixture to a level where subsequent changes will not take the mixture out of the workable range, or when a solvent or other inert materials can be added to the reactant mixture to moderate temperature changes via sensible or latent heat effects. In some cases it is advantageous to divide the reactor into several stages, each of which operates adiabatically but between which heat exchangers are used to heat or cool the reactant mixture. In commercial-scale equipment it is often impractical to try to maintain truly isothermal conditions, but one can often achieve adequate control at a satisfactory level of the reaction rate by exchanging heat with external heat reservoirs.

For nonisothermal reactors the key questions that the reactor designer must answer are: (1) How can one relate the temperature of the reacting system to the degree of conversion that has been accomplished? and (2) How does this temperature influence the subsequent performance of the system? In responding to these questions the chemical engineer must use two basic tools: the material balance and the energy balance. The bulk of the chapter deals with these topics. Some stability and selectivity considerations are also treated.

### 10.1 THE ENERGY BALANCE AS APPLIED TO CHEMICAL REACTORS

The principle that energy must be conserved has been expressed by innumerable textbook authors in a number of mathematical forms, depending on the particular orientation and interests of the person concerned. One form that

is especially useful for chemical engineering applications is the following:

$$\frac{dE_{\text{sys}}}{dt} = \dot{Q} - \dot{W}_s + \sum_{\text{input streams}} \left( h_{\text{in}} + \frac{v_{\text{in}}^2}{2g_c} + \frac{g}{g_c} Z_{\text{in}} \right) \dot{m}_{\text{in}} - \sum_{\text{output streams}} \left( h_{\text{out}} + \frac{v_{\text{out}}^2}{2g_c} + \frac{g}{g_c} Z_{\text{out}} \right) \dot{m}_{\text{out}} \quad (10.1.1)$$

where  $E_{\text{sys}}$  is the internal energy of a control volume or fixed region in space that has been chosen as the system to be investigated,  $t$  is time,  $\dot{Q}$  is the *rate* at which heat is being transferred *to* the system from the surroundings across boundaries that are impermeable to the flow of matter,  $\dot{W}_s$  is the rate at which *shaft work* is being done *on* the surroundings *by* the system,  $h$  is the enthalpy per unit mass,  $v^2/2g_c$  is the kinetic energy per unit mass,  $gZ/g_c$  is the gravitational potential energy per unit mass,  $\dot{m}$  is the mass flow rate into or out of the system, and the subscripts “in” and “out” refer to the conditions that prevail at the various points of entry and exit, respectively.

Recall that the term *shaft work* refers to mechanical forms of energy that are interchanged between the system and the surroundings by means of a shaft that protrudes from the equipment and either rotates or reciprocates. A shaft work interaction can take place only at those portions of the system boundary that are impermeable to the flow of matter. For further discussion of general forms of the energy balance equation as applied to chemical engineering systems, consult the textbooks by Reynolds (1), Smith and Van Ness (2), Tester and Modell (3), and Sandler (4).

Equation (10.1.1) represents a very general formulation of the first law of thermodynamics, which can readily be reduced to a variety of simple forms for specific applications under either steady-state or transient operating conditions. For steady-state applications the time derivative of the system energy is zero. This condition is that of greatest interest in the design of continuous flow reactors. Thus, at steady state,

$$\dot{Q} - \dot{W}_s = \sum_{\text{outlet streams}} \left( h_{\text{out}} + \frac{v_{\text{out}}^2}{2g_c} + \frac{g}{g_c} Z_{\text{out}} \right) \dot{m}_{\text{out}} - \sum_{\text{inlet streams}} \left( h_{\text{in}} + \frac{v_{\text{in}}^2}{2g_c} + \frac{g}{g_c} Z_{\text{in}} \right) \dot{m}_{\text{in}} \quad (10.1.2)$$

where

$$\sum_{\text{inlet streams}} \dot{m}_{\text{in}} = \sum_{\text{outlet streams}} \dot{m}_{\text{out}} \quad (10.1.3)$$

For most circumstances of interest in the design of chemical reactors, the kinetic and potential energy effects

are negligible, as is the shaft work term. Under these circumstances,

$$\dot{Q} = \sum_{\text{outlet streams}} (h_{\text{out}} \dot{m}_{\text{out}}) - \sum_{\text{outlet streams}} (h_{\text{in}} \dot{m}_{\text{in}}) \quad (10.1.4)$$

For the vast majority of situations of interest in the design of industrial-scale reactors, equation (10.1.4) provides an adequate approximation of the true situation for continuous-flow reactors operating at steady state. Because the right side of this expression represents the difference between the total enthalpy that leaves the system in time  $dt$  and the total enthalpy that enters during the same time, one often sees the statement that

$$q \approx \Delta H \quad (10.1.5)$$

where  $q$  is the amount of heat transferred *per unit mass* of entering material and  $\Delta H$  is the difference between the enthalpies per unit mass of the exit and entrance streams.

It should be emphasized that the enthalpy change indicated includes not only sensible heat effects but also a heat-of-reaction term and in some cases pressure and heat-of-solution effects. If there are multiple inlet and outlet streams, appropriate averaging techniques must be used to employ equation (10.1.5).

For batch reactors the appropriate form of the first law to use is that for closed systems:

$$\Delta E_{\text{total}} = Q - W \quad (10.1.6)$$

where  $\Delta E_{\text{total}}$  is the change in the total energy of the system,  $Q$  is the heat transferred from the surroundings to the system, and  $W$  is the work done *by the system* on the surroundings.

If one again takes note of the fact that work effects and kinetic and potential energy effects are usually negligible in chemical reactors, equation (10.1.6) simplifies to

$$\Delta E = Q_V \quad (10.1.7)$$

The subscript  $V$  is used to indicate that the volume is assumed to be substantially constant.

The vast majority of the reactions carried out in industrial-scale batch reactors involve reactants in condensed phases. Since the specific volumes of both liquids and solids are very small, the difference between internal energy and enthalpy for these materials is usually negligible. Thus, one often sees the statement that for batch reactions taking place at constant volume,

$$Q \approx \Delta H \quad (10.1.8)$$

where the  $\Delta$  now represents the difference between the final and initial values of the enthalpy of the system. For both batch and flow reactors, the enthalpy changes that

occur during the course of the reaction are then important in determining the heat transfer requirements of the system under consideration. The methods used in determining the enthalpy changes that accompany chemical reactions were discussed in detail in Section 2.2.

The rate at which heat is transferred to a system can be expressed in terms of an overall heat transfer coefficient  $U$ , the area through which the heat exchange occurs and on which  $U$  is based, and the difference between the temperature of the heat source (or sink)  $T_m$  and that of the reactor contents  $T$ :

$$\dot{Q} = UA(T_m - T) \quad (10.1.9)$$

This expression may be combined with equations (10.1.4) and (10.1.8) in order to analyze the different situations that may arise in operating the various types of ideal reactors. These analyses are the subject of Sections 10.2 to 10.4.

## 10.2 THE IDEAL WELL-STIRRED BATCH REACTOR

The key assumption on which the design analysis of a batch reactor is based is that the degree of agitation is sufficient to ensure that the composition and temperature of the contents are uniform throughout the reaction vessel. Under these conditions one may write the material and energy balances on the entire contents of the reaction vessel.

If one considers a batch reactor in which the chemistry is characterized by a single extent of reaction, the material balance analysis presented in Section 8.1 indicates that the holding time necessary to change the fraction conversion from  $f_{A1}$  to  $f_{A2}$  is given by

$$t = N_{A0} \int_{f_{A1}}^{f_{A2}} \frac{df_A}{V_R(-r_A)} \quad (10.2.1)$$

For operation in a constant pressure nonisothermal mode with a relatively low pressure *gas phase reaction*, it is convenient to approximate the reactor volume by

$$V_R = V_{R0}(1 + \delta_{AfA}) \frac{T}{T_0} \quad (10.2.2)$$

where the temperature corresponding to a given fraction conversion ( $T$ ) and that corresponding to zero conversion ( $T_0$ ) are expressed in degrees absolute. The  $\delta$  parameter in this equation represents the fractional volume change that would occur under isothermal operating conditions. Combining equations (10.2.1) and (10.2.2) leads to the following expression for the holding time for

nonisothermal gas phase reactions carried out at constant pressure.

$$t = C_{A0} \int_{f_{A1}}^{f_{A2}} \frac{df_A}{(-r_A)(1 + \delta_{AfA})(T/T_0)} \quad (10.2.3)$$

To be able to evaluate the integrals in equations (10.2.1) and (10.2.3), one must know not only the temperature dependence of the rate terms but also the relationship between the fraction conversion and the temperature of the system.

In Section 10.1 we showed that in industrial-scale batch reactors,

$$Q = \Delta H \quad (10.2.4)$$

for the vast majority of the cases of interest. Strictly speaking, equation (10.2.4) applies only to liquid phase reactions where the restrictions of constant volume and constant pressure go together and to gas phase reactions occurring at constant pressure. We should again emphasize that the enthalpy change appearing in equation (10.2.4) contains both sensible heat terms and heat of reaction terms. Consequently, one can interpret equation (10.2.4) as implying that

$$\begin{aligned} \text{heat input} &= \text{change in sensible heat} \\ &+ \text{energy transformed by reaction} \end{aligned} \quad (10.2.5)$$

or

$$Q = \int_{T_0, \xi_0}^{T_{\text{final}}, \xi_1} (m\hat{C}_p \, dT + \Delta H_R \, d\xi) \quad (10.2.6)$$

where  $\hat{C}_p$  is an appropriate average heat capacity per unit mass,  $m$  is the total mass of the system, and  $\Delta H_R$  is the enthalpy change per extent of reaction  $\xi$ .

Because enthalpy is a state variable, the integral on the right side of equation (10.2.6) is independent of the path of integration, and it is possible to rewrite this equation in a variety of forms that are more convenient for use in reactor design analyses. One may evaluate this integral by allowing the reaction to proceed isothermally at the initial temperature from extent  $\xi_0$  to extent  $\xi_1$  and then heating the final product mixture at constant pressure and composition from the initial temperature to the final temperature:

$$Q = \Delta H_R \text{ at } T_0 (\xi_1 - \xi_0) + \int_{T_0}^{T_{\text{final}}} m\hat{C}_p \, dT \quad (10.2.7)$$

where the appropriate average heat capacity to use is the mass average based on the composition of the *final* product mixture.

Further modification of these equations is possible by writing the last integral as

$$\int_{T_0}^{T_{\text{final}}} m\hat{C}_p \, dT = \sum \left( n_i \int_{T_0}^{T_{\text{final}}} \bar{C}_{pi} \, dT \right) \quad (10.2.8)$$

where the  $n_i$  are the *final mole numbers* of the various species present in the reaction mixture and the  $\bar{C}_{pi}$  are the partial molal heat capacities of these species. The summation is taken over all species (including inert) present in the system. For gaseous mixtures that follow ideal solution behavior, the partial molar quantities may be replaced by the pure component values.

Because the total heat input represents the time integral of the heat transfer rate, it is evident from equations (10.1.9), (10.2.7), and (10.2.8) that

$$\int_0^t UA(T_m - T) dt = \Delta H_{R \text{ at } T_0} (\xi_1 - \xi_0) + \sum \left( n_i \int_{T_0}^{T_{\text{final}}} \bar{C}_{pi} dT \right) \quad (10.2.9)$$

Because the various mole numbers can be expressed in terms of the extent of reaction, equation (10.2.9) expresses the relationship that must exist between the extent of reaction at time  $t$  and the temperature at that time. In terms of the fraction conversion where the fraction conversion at zero time is taken as zero,

$$\int_0^t UA(T_m - T) dt = \frac{-\Delta H_{R \text{ at } T_0}}{\nu_A} n_{A0} f_A + \sum \left( n_i \int_{T_0}^{T_{\text{final}}} \bar{C}_{pi} dT \right) \quad (10.2.10)$$

where  $n_{A0}$  is the number of moles of the limiting reagent charged to the batch reactor.

On a differential basis,

$$UA(T_m - T) = \frac{-\Delta H_R}{\nu_A} n_{A0} \frac{df_A}{dt} + \sum \left( n_i \bar{C}_{pi} \frac{dT}{dt} \right) \quad (10.2.11)$$

where the summation over the mole numbers must now be evaluated at time  $t$ . If one recognizes that the first term on the right is simply the rate at which energy is transformed by reaction ( $\Delta H_R rV_R$ ), equation (10.2.11) becomes

$$UA(T_m - T) = \Delta H_R (rV_R) + \sum \left( n_i \bar{C}_{pi} \frac{dT}{dt} \right) \quad (10.2.12)$$

For exothermic reactions  $\Delta H_R$  is negative, and the term ( $\Delta H_R rV_R$ ) will then represent the rate at which chemical energy is transformed to sensible heat and heat exchanged with the surroundings.

In general, when designing a batch reactor, it will be necessary to simultaneously solve one form of the material balance equation and one form of the energy balance equation [equations (10.2.1) and (10.2.5) or equations derived therefrom]. Because the reaction rate depends on both temperature and the extent of reaction, closed form solutions can be obtained only when the system is isothermal. One must normally employ numerical methods of solution when dealing with nonisothermal systems.

For isothermal and adiabatic modes of operation, the energy balance equations developed above will simplify so that the design calculations are not nearly as tedious as they are for the other modes of operation. In the case of adiabatic operation, the heat transfer rate is zero, so equation (10.2.10) becomes

$$\Delta H_{R \text{ at } T_0} \frac{n_{A0} f_A}{\nu_A} = \sum \left( n_i \int_{T_0}^{T_{\text{final}}} \bar{C}_{pi} dT \right) \quad (10.2.13)$$

If the partial molar heat capacities are substantially constant over the temperature range of interest, this equation may be solved to determine the relationship between the temperature and the fraction conversion:

$$T = T_0 + \frac{\Delta H_{R \text{ at } T_0} n_{A0} f_A}{\nu_A \sum (n_i \bar{C}_{pi})} \quad (10.2.14)$$

where each of the  $n_i$  in the summation is evaluated at a fraction conversion equal to  $f_A$ . When this result is substituted into batch reactor design equations, one has an integral expressed in terms of a single variable, which may then be evaluated graphically or numerically.

For the case of isothermal operation, the material and energy balance equations are not coupled, and design equations like (10.2.1) can be solved readily because the reaction rate can be expressed directly as a function of the fraction conversion. For operation in this mode, an energy balance can be used to determine how the heat transfer rate should be programmed to keep the system isothermal. For this case, equation (10.2.12) simplifies to the following expression for the heat transfer rate:

$$\dot{Q} = UA(T_m - T) = \Delta H_R rV_R \quad (10.2.15)$$

The reaction rate can be readily determined as a function of time from the design equation, and this in turn can be used to determine how  $\dot{Q}$  or  $T_m$  should be varied to approach isothermal operating conditions.

Kladko (5) presented a very interesting case study of the development of a reactor design for an exothermic reaction. When first carried out on a commercial scale in a batch reactor, the system exothermed rapidly, and the system ran out of control. The batch erupted violently through a safety valve and vented out over the building area. The fact that this result could have been predicted a priori illustrates the necessity of making the types of energy balance calculations described in this chapter when one attempts to move from bench- or pilot-scale reactor systems to commercial-scale equipment. Because of the proprietary nature of the product, many details of the reaction were omitted, but if engineering “guesstimates” of the heat capacities and molecular weights are used, it is possible to conduct an engineering analysis of the system to complement those presented by Kladko for semibatch

operation. We use his data and our guesstimates of the system properties as the basis for several illustrations in the remainder of this chapter.

### ILLUSTRATION 10.1 Determination of Required Reactor Volumes for Isothermal and Adiabatic Operation of a Batch Reactor

Reagent A undergoes an essentially irreversible isomerization reaction that obeys first-order kinetics:



Both A and B are liquids at room temperature and both have extremely high boiling points. Determine the reactor volumes necessary to produce 2 million pounds of B in 7000 h of operation:

- (a) If the reactor operates isothermally at 163°C.
- (b) If the reactor operates adiabatically.

Use the following data and assumptions.

Reaction rate expression	$r = kC_A$
Rate constant at 163°C	$0.8 \text{ h}^{-1}$
Activation energy	28,960 cal/g-mol
Heat of reaction	-83 cal/g
Molecular weight	250

The heat capacities of species A and B may be assumed to be identical and to be 0.5 cal/(g·°C). Their densities may be assumed to be 0.9 g/cm<sup>3</sup>. The times necessary to fill and drain the reactor are 10 and 12 min, respectively. It may be assumed that negligible reaction occurs during the 14 min it takes to heat the feed from the temperature at which it enters the reactor to 163°C. After 97% of the A has been isomerized, the hot product mixture is discharged to a cooling tank.

#### Solution

In a batch reactor maintained at constant volume, the holding time is given by equation (8.1.7):

$$t = C_{A0} \int_0^{0.97} \frac{df_A}{-r_A} = C_{A0} \int_0^{0.97} \frac{df_A}{kC_{A0}(1-f_A)} = \int_0^{0.97} \frac{df_A}{k(1-f_A)} \quad (\text{A})$$

For isothermal operation at 163°C the rate constant is equal to 0.8 h<sup>-1</sup>. Thus,

$$t = \frac{1}{0.8} \ln \left( \frac{1}{1-f_A} \right) \Big|_0^{0.97} = 4.38 \text{ hr}$$

The total processing time per batch is the sum of the holding time and the times necessary to fill the reactor, heat the mixture to the reaction temperature, and drain the reaction products from the reactor, or

$$\tau_{\text{batch}} = 4.38 + \frac{10 + 14 + 12}{60} = 4.98 \text{ h}$$

The total processing time per batch is thus essentially equal to 5 h. While operating 7000 h, one will be able to process 7000/5, or 1400, batches. Each batch must contain 2,000,000/[0.97(1400)], or 1473 lb. Because the liquid has a density of 0.9 g/cm<sup>3</sup>, the volume required will be 1473/[0.9 × 62.5], or 26.2 ft<sup>3</sup>. This volume is equivalent to 196 gal.

The maximum heat flux that will have to be maintained to operate isothermally will be that generated at the start of the reaction.

$$\dot{Q} = \Delta H_R (rV_R) = \Delta H_R (kC_{A0}V_R)$$

or

$$\dot{Q} = \Delta H_R (k n_{A0})$$

In consistent units,

$$\Delta H = -83 \frac{\text{cal}}{\text{g}} \times \frac{1 \text{ Btu}}{252 \text{ cal}} \times \frac{454 \text{ g}}{\text{lb}} = -149.5 \text{ Btu/lb}$$

Thus,

$$\dot{Q} = (-149.5)(0.8)(1473) = -176,000 \text{ Btu/h}$$

This cooling load is rather large for a system of this size. Kladko found it advantageous to go to a semibatch mode of operation so that incoming cold feed could be used to absorb some of the energy released by reaction and thereby drastically reduce the cooling requirements for the system. If the cold feed enters at room temperature, it acts as a heat sink that is capable of absorbing nearly 80% of the energy released by reaction. This fact enables one to consider operation in the autothermal mode discussed in Section 10.5.

We now consider operation of the batch reactor under adiabatic conditions. We will assume that we need not worry about reaching the boiling point of the liquid and that the rate of energy release by reaction does not become sufficiently great that an explosion ensues.

Equation (10.2.14) is valid for adiabatic operation

$$T = T_0 + \frac{\Delta H_R f_A n_{A0}}{\nu_A \sum (n_i \bar{C}_{pi})}$$

In the present case,

$$T = 436 + \frac{-83f_A n_{A0}}{(-1)n_{A0}(0.5)} = 436 + 166f_A \quad (\text{B})$$

where  $T$  is expressed in K. Note that the ultimate temperature rise will be more than 160 K.

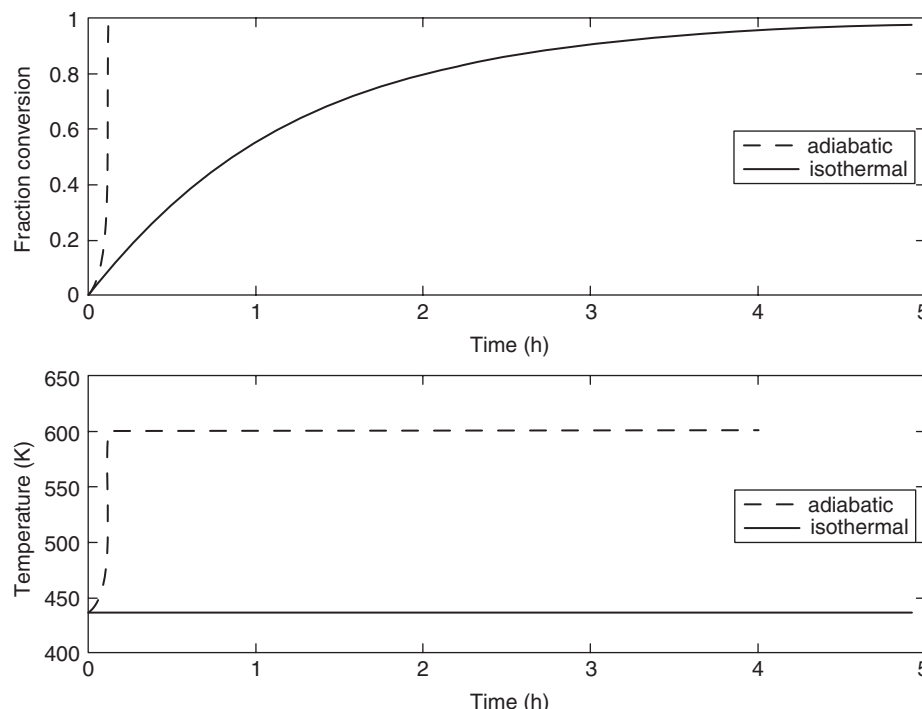
From the Arrhenius relation,  $k = Ae^{-E_a/RT}$  and at 436 K,  $0.8 = Ae^{-28,960/[1.987(436)]}$ , so

$$k = 2.61 \times 10^{14} e^{-14,570/T} \quad (\text{C})$$

Equations (B) and (C) may now be substituted into design equation (A) to solve for the holding time required using any convenient numerical integration tool. Alternatively, in anticipation of later solving the plug flow analog of this batch reactor problem for different heat transfer conditions, it is convenient to employ the differential form of the material balance to determine the trajectories of conversion and temperature versus time:

$$\frac{df}{dt} = k(1 - f_A)$$

This relation may be used with equations (B) and (C) to incorporate the change in temperature (and thus the associated reaction rate) with fractional conversion. The present problem can be solved via machine computation by choosing a reaction time sufficient to obtain  $f_A = 0.97$ . One may employ a differential equation solver such as those in Matlab, MathCad, or other engineering software. With either approach one finds that  $f_A = 0.97$  at  $t = 0.117$  h or 7.0 min. Evolution of both the fraction conversion and the temperature of the reaction mixture as functions of time is shown in the two panels of Figure I10.1. Plots of the dependent variables as functions of the time for the batch reaction



are displayed for operation of the reactor in the isothermal mode and in the adiabatic mode.

The time necessary to accomplish this exothermic reaction under adiabatic operating conditions is only an extremely small fraction of that necessary for isothermal operation. In fact, the times necessary to fill and drain the reactor and to heat it to a temperature where the rate becomes appreciable will be greater than that necessary to accomplish the reaction. Thus,

$$\tau_{\text{batch, adiabatic}} = 0.12 + \frac{10 + 12 + 14}{60} = 0.72 \text{ h}$$

This time corresponds to an upper limit because the reaction (and release of thermal energy) will begin in the hot feed stream as it approaches the reaction temperature even before entering the adiabatic region of the reactor.

While operating 7000 h, one will be able to process 7000/0.72, or 9722 batches per year. Each batch will then contain  $2 \times 10^6 / [0.97(9722)]$ , or 212 lb. The requisite reactor volume will then be 28 gal. Under these circumstances the times necessary to perform the nonreactive operations would undoubtedly be somewhat reduced. One should recognize that these steps will be the bottlenecks in this operation. The required reactor size is definitely on the small side, and it would be preferable to operate in a larger reactor and process a smaller number of batches per year with attendant reductions in labor requirements. A flow reactor would be an attractive operating mode that would avoid separate steps for the nonreactive operations, and several alternative

**Figure I10.1** Evolution of fraction conversion and temperature in a batch reactor for the isothermal and adiabatic modes of operation considered.

approaches of this type are considered in later illustrative examples in this chapter.

### 10.3 THE IDEAL CONTINUOUS FLOW STIRRED-TANK REACTOR

The ideal continuous flow stirred-tank reactor is the easiest type of continuous flow reactor to analyze in design calculations because the temperature and composition of the reactor contents are homogeneous throughout the reactor volume. Consequently, material and energy balances can be written over the entire reactor and the outlet composition and temperature can be taken as representative of the reactor contents. In general, the temperatures of the feed and effluent streams will not be equal, and it will be necessary to use both material and energy balances and the temperature-dependent form of the reaction rate expression to determine the conditions at which the reactor operates.

The material balance on a single CSTR operating at steady state may be represented by

$$F_i \text{ in} = F_i \text{ out} - r_i V_R \quad (10.3.1)$$

where the rate expression is evaluated at the effluent composition and temperature. If only one reaction is taking place, one may rewrite this equation in terms of the familiar design equation

$$\tau_{\text{CSTR}} = \frac{C_{A0}(f_{A \text{ out}} - f_{A \text{ in}})}{-r_{A \text{ F}}} \quad (10.3.2)$$

If multiple reactions are taking place and the system cannot be characterized by a single fraction conversion, an equation of the form of (10.3.1) will need to be written for each species.

The steady-state form of the energy balance for a continuous-flow stirred-tank reactor is given by equation (10.1.4):

$$\dot{Q} = \sum_{\text{outlet streams}} (h_{\text{out}} \dot{m}_{\text{out}}) - \sum_{\text{inlet streams}} (h_{\text{in}} \dot{m}_{\text{in}}) \quad (10.3.3)$$

It should be emphasized that not all of the individual enthalpy datum conditions may be chosen independently because of the presence of one or more reactions.

Because enthalpy changes are path-independent quantities, one is at liberty to choose a convenient path for making the calculation. If we carry out the reaction isothermally at the inlet temperature and then heat the products at constant composition to the effluent temperature, we find that

$$\dot{Q} = \Delta H_{R \text{ at } T_0} r V_R + \sum_i \left( F_{iF} \int_{T_0}^{T_{\text{out}}} \bar{C}_{pi} dT \right) \quad (10.3.4)$$

where the summation involves the *outlet* molal flow rates.

From a material balance on reactant A:

disappearance by reaction = input – output

$$\begin{aligned} -v_A r V_R &= F_{A0}(1 - f_{A \text{ in}}) - F_{A0}(1 - f_{A \text{ out}}) \\ &= F_{A0}(f_{A \text{ out}} - f_{A \text{ in}}) \end{aligned} \quad (10.3.5)$$

Thus,

$$\dot{Q} = \frac{F_{A0}(f_{A \text{ out}} - f_{A \text{ in}})}{-v_A} \Delta H_{R \text{ at } T_0} + \sum_i \left( F_{iF} \int_{T_0}^{T_{\text{out}}} \bar{C}_{pi} dT \right) \quad (10.3.6)$$

Equation (10.3.6), the reaction rate expression, and the design equation are sufficient to determine the temperature and composition of the fluid leaving the reactor if the heat transfer characteristics of the system are known. If it is necessary to know the reactor volume needed to obtain a specified conversion at a fixed feed flow rate and specified heat transfer conditions, the energy balance equation can be solved to determine the temperature of the reactor contents. When this temperature is substituted into the rate expression, one can readily solve the design equation for the reactor volume. On the other hand, if a reactor of known volume is to be used, a determination of the exit conversion and temperature will require a simultaneous trial-and-error solution of the energy balance, the rate expression, and the design equation.

Illustrations 10.2 and 10.3 show how the principles discussed above are applied in the design of a commercial-scale continuous flow stirred-tank reactors.

### ILLUSTRATION 10.2 Determination of Heat Transfer and Volume Requirements for Single and Multiple Continuous Flow Stirred-Tank Reactors

Consider the reaction system and production requirements discussed in Illustration 10.1. Consider the possibility of using one or more continuous flow stirred-tank reactors operating in series. If each CSTR is to operate at 163°C and if the feed stream is to consist of pure A entering at 20°C, determine the reactor volumes and heat transfer requirements for (1) a single CSTR and (2) three identical CSTRs in series.

### Solution

The rate at which A must be processed is equal to

$$\frac{2 \times 10^6}{0.97} \text{ lb} \div 7000 \text{ h} = 295 \text{ lb/h} = 133,700 \text{ g/h}$$

**Case 1: Single Stirred Tank (CSTR).** From equation (8.3.38) for a single CSTR,

$$C_{A\text{ out}} = \frac{C_{A\text{ in}}}{1 + k\tau} \quad (\text{A})$$

Now  $C_{A\text{ out}} = 0.03C_{A\text{ in}}$ . Thus,

$$0.03 = \frac{1}{1 + 0.8\tau}$$

or

$$\tau_{\text{reactor}} = \frac{1 - 0.03}{0.03(0.8)} = 40.4 \text{ h}$$

The volumetric feed rate may be determined from the production requirements and the density of the material:

$$V_0 = 133,700 \frac{\text{g}}{\text{h}} \times \frac{\text{cm}^3}{0.9 \text{ g}} \times \frac{1 \text{ gal}}{3785 \text{ cm}^3} = 39.3 \text{ gal/h}$$

The reactor volume required may now be determined from the space time and the volumetric flow rate:

$$V_R = V_0\tau = 39.3 (40.4) = 1586 \text{ gal}$$

The heat transfer rate in the reactor can be determined from the energy balance equation (10.3.6):

$$\dot{Q} = -\frac{F_{A0}(f_{A\text{ out}} - f_{A\text{ in}})}{\nu_A} \Delta H_{R\text{ at }T_0} + \sum \left( F_{iF} \int_{T_0}^{T_{\text{out}}} \bar{C}_{pi} \, dT \right) \quad (\text{B})$$

Thus,

$$\dot{Q} = 133,700(0.97)(-83) + \int_{20}^{163} 133,700(0.5) \, dT$$

or

$$\begin{aligned} \dot{Q} &= -10,764,000 + 9,560,000 = -1,204,000 \text{ cal/h} \\ &= -4780 \text{ Btu/h} \end{aligned}$$

Hence, for a single continuous-flow stirred-tank reactor, the volume required will be 1586 gal, and the amount of heat that must be *removed* is equal to 4780 Btu/h.

**Case 2: Cascade of three CSTRs.** If we denote the composition leaving the  $n$ th reactor by  $C_n$ , it is readily shown that

$$C_{A1} = \frac{C_{A0}}{1 + k\tau} \quad (\text{C})$$

$$C_{A2} = \frac{C_{A1}}{1 + k\tau} = \frac{C_{A0}}{(1 + k\tau)^2} \quad (\text{D})$$

$$C_{A3} = \frac{C_{A2}}{1 + k\tau} = \frac{C_{A0}}{(1 + k\tau)^3} \quad (\text{E})$$

where  $\tau$  is the ratio of the volume of a *single CSTR* to the input volumetric flow rate.

For 97% conversion,

$$\frac{C_{A3}}{C_{A0}} = 0.03 = \frac{1}{(1 + 0.8\tau)^3}$$

Rearrangement yields  $(1 + 0.8\tau) = 0.3107$ . Thus,

$$\tau = \frac{1 - 0.3107}{0.8(0.3107)} = 2.77 \text{ h}$$

The reactor volume required per CSTR is then equal to  $39.3 \text{ gal/h} \times 2.77 \text{ h} = 109 \text{ gal}$ .

The fraction conversion in the effluent from the first reactor can be determined from equation (C) and the definition of the fraction conversion. Because

$$C_{A1} = \frac{C_{A0}}{1 + k\tau} = C_{A0}(1 - f_{A1})$$

then

$$f_{A1} = \frac{k\tau}{1 + k\tau} = \frac{0.8(2.77)}{1 + 0.8(2.77)} = 0.689$$

From equation (D) and the definition of the fraction conversion,

$$C_{A2} = \frac{C_{A1}}{1 + k\tau} = \frac{C_{A0}(1 - f_{A1})}{1 + k\tau} = C_{A0}(1 - f_{A2})$$

Thus,

$$f_{A2} = 1 - \frac{1 - f_{A1}}{1 + k\tau} = 1 - \frac{0.311}{1 + 0.8(2.77)} = 0.903$$

The heat transfer requirements for each reactor may be determined from equations of the form of equation (B). For reactor 1,

$$\dot{Q}_1 = 133,700(0.689)(-83) + \int_{20}^{163} (133,700)(0.5) \, dT$$

or

$$\begin{aligned} \dot{Q}_1 &= -7,646,000 + 9,560,000 = 1,914,000 \text{ cal/h} \\ &= 7595 \text{ Btu/h} \end{aligned}$$

For reactors 2 and 3, there will not be any sensible heat effects because the temperatures of the entering and leaving streams are identical.

$$\begin{aligned} \dot{Q}_2 &= 133,700(0.970 - 0.689)(-83) = -2,375,000 \text{ cal/h} \\ &= -9424 \text{ Btu/h} \end{aligned}$$

and

$$\begin{aligned} \dot{Q}_3 &= 133,700(0.970 - 0.903)(-83) = -743,500 \text{ cal/h} \\ &= -2950 \text{ Btu/h} \end{aligned}$$

The equipment requirements that we have determined are well within the realm of technical feasibility and practicality. The heat transfer requirements are easily attained

in equipment of this size. The fact that some of the heat transfer requirements are positive and others negative indicates that one should probably consider the possibility of at least partial heat exchange between the incoming cold feed stream and the effluent from the second or third reactors. The heat transfer calculations show that the sensible heat necessary to raise the cold feed to a temperature where the reaction rate is appreciable represents a substantial fraction of the energy released by reaction. These calculations also indicate that it would be advisable to investigate the possibility of adiabatic operation in a cascade of CSTRs.

### ILLUSTRATION 10.3 Adiabatic Operation of a Cascade of Continuous Flow Stirred-Tank Reactors

Consider the possibility of carrying out the reaction used as the basis for Illustrations 10.1 and 10.2 under adiabatic operating conditions. How much B will it be possible to produce from 2.1 million lb/yr of species A using a pair of 1000-gal CSTRs operating in series? The feed to the first reactor has a temperature of 20°C. Assume that you will be able to operate 7000 h/yr. Use the data from Illustration 10.2.

#### Solution

The solution to this problem requires a trial-and-error iterative procedure. Because both the reactor volume and the initial volumetric flow rate are known, the space time per reactor may be calculated and we may focus our attention initially on the first reactor.

The volumetric flow rate is equal to

$$\frac{2.1 \times 10^6 \text{ lb}}{7 \times 10^3 \text{ h}} \times 454 \frac{\text{g}}{\text{lb}} \times \frac{\text{cm}^3}{0.9 \text{ g}} \times \frac{1 \text{ gal}}{3785 \text{ cm}^3} \text{ or } 40.0 \text{ gal/h.}$$

This value corresponds to a reactor space time given by

$$\tau = \frac{V_R}{V_0} = \frac{1000}{40.0} = 25 \text{ h}$$

For a first-order reaction it was shown in Illustration 10.2 that

$$f_{A1} = \frac{k\tau}{1 + k\tau} = \frac{25k}{1 + 25k} \quad (\text{A})$$

where the rate constant is a temperature dependent quantity given by equation (C) in Illustration 10.1.

$$k = 2.61 \times 10^{14} e^{-14,570/T} \quad (\text{B})$$

The energy balance equation for adiabatic operation becomes

$$0 = \frac{-F_{A0}f_{A1}}{v_A} \Delta H_{R \text{ at } T_0} + \sum \left( F_i \int_{T_0}^{T_{\text{out}}} \bar{C}_{pi} \, dT \right)$$

where the last term is equal to  $F_{A0}C_p(T_{\text{out}} - T_0)$ . Division by  $F_{A0}$  and rearrangement gives

$$f_{A1} = v_A \frac{C_p(T_{\text{out}} - T_0)}{\Delta H_{R \text{ at } T_0}} = \frac{0.5(T_{\text{out}} - 293)}{83} \quad (\text{C})$$

Equations (A) to (C) must now be solved simultaneously. Combining these equations gives

$$f_{A1} = v_A \frac{C_p(T_{\text{out}} - T_0)}{\Delta H_{R \text{ at } T_0}} = \frac{0.5(T_{\text{out}} - 293)}{83} = \frac{25k}{1 + 25k} \quad (\text{D})$$

where  $k$  is given by equation (B) with  $T = T_{\text{out}}$ . This equation can be solved for  $T$  using a trial-and-error procedure. This exercise gives  $T = 410 \text{ K}$ . Thus,

$$f_{A1} = \frac{0.5(410 - 293)}{83} = 0.705$$

From Illustration 10.2,

$$f_{A2} = 1 - \frac{1 - f_{A1}}{1 + k\tau} = \frac{f_{A1} + k\tau}{1 + k\tau}$$

or

$$f_{A2} = \frac{0.705 + 25k}{1 + 25k} \quad (\text{E})$$

where  $k$  is given by equation (B).

The energy balance equation for adiabatic operation becomes

$$0 = \frac{F_{A0}(f_{A2} - f_{A1})}{v_A} \Delta H_{R \text{ at } T_0} + F_{A0} \int_{T_0}^{T_2} C_p \, dT - F_{A0} \int_{T_0}^{T_1} C_p \, dT$$

Division by  $F_{A0}$  and combination of the integrals gives

$$(f_{A2} - f_{A1}) \frac{\Delta H_{R \text{ at } T_0}}{v_A} = \int_{T_1}^{T_2} C_p \, dT$$

or

$$f_{A2} = f_{A1} + \frac{v_A \int_{T_1}^{T_2} C_p \, dT}{\Delta H_{R \text{ at } T_0}} = 0.705 + \frac{0.5(T_2 - 410)}{83} \quad (\text{F})$$

Combination of equations (B), (E), and (F) gives

$$0.705 + \frac{0.5(T_2 - 410)}{83} = \frac{0.705 + 25(2.61 \times 10^{14} e^{-14,570/T_2})}{1 + 25(2.61 \times 10^{14} e^{-14,570/T_2})} \quad (\text{G})$$

A trial-and-error solution gives  $T_2 = 458.5 \text{ K}$  (approximately 186°C) and  $f_{A2} = 0.997$ .

With this reactor configuration one would be able to produce in excess of 2 million pound of B annually if side

reactions do not occur at this higher temperature and if the vapor pressure of the solution still lies within a range that does not create problems.

## 10.4 TEMPERATURE AND ENERGY CONSIDERATIONS IN TUBULAR REACTORS

In this section we treat the material and energy balance equations for a plug flow reactor. For steady-state operation the energy balance analysis leading to equation (10.1.4) is appropriate:

$$\dot{Q} = \sum_{\text{outlet streams}} (h_{\text{out}} \dot{m}_{\text{out}}) - \sum_{\text{inlet streams}} (h_{\text{in}} \dot{m}_{\text{in}}) \quad (10.4.1)$$

while the design equation appropriate for these conditions is

$$\tau = C_{A0} \int_{f_A \text{ in}}^{f_A \text{ out}} \frac{df_A}{-r_A} \quad (10.4.2)$$

These equations must be solved simultaneously using a knowledge of the temperature dependence of reaction rate expression.

Note that in the case of the plug flow reactor, there may be a variation in the temperature of the reactor contents from point to point along the length of the reactor. This condition is in contrast to the two ideal reactor cases discussed earlier, where the temperature of the contents of a single reactor was assumed to be constant throughout. The presence of temperature gradients in the *same* direction as the flow is by no means contrary to the assumption of plug flow. In this chapter we confine our analysis to situations in which both the temperature and the composition are uniform across the cross section of the reactor. The complications arising from the existence of radial temperature gradients and variations in the composition with radial position are treated implicitly in conjunction with the discussion of the two-dimensional model of fixed bed reactors in Section 12.7. For homogeneous systems the effects are usually small.

If one considers the rate at which heat is being supplied to a differential length of a tubular reactor, geometric considerations imply that

$$d\dot{Q} = U(T_m - T) dA = U(T_m - T) \frac{4}{D} dV_R \quad (10.4.3)$$

where  $D$  is the inside diameter of the tubular reactor.

A material balance on this differential reactor volume yields the following result:

$$F_{A0} df_A = -r_A dV_R \quad (10.4.4)$$

Combining equations (10.4.3) and (10.4.4) gives

$$d\dot{Q} = U(T_m - T) \frac{4}{D} F_{A0} \frac{df_A}{(-r_A)} \quad (10.4.5)$$

and the energy balance on this differential volume element then becomes

$$U(T_m - T) \frac{4}{D} F_{A0} \frac{df_A}{(-r_A)} = \sum \left( F_i \int_{T_0}^{T \text{ out of element}} \bar{C}_{pi} dT \right) - \sum \left( F_i \int_{T_0}^{T \text{ into element}} \bar{C}_{pi} dT \right) - \frac{F_{A0} \Delta H_R \text{ at } T_0}{\nu_A} df_A \quad (10.4.6)$$

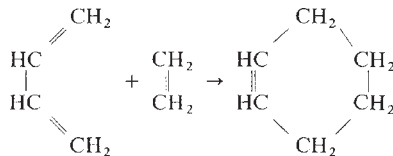
where the first summation involves the molal flow rates of the various species leaving the volume element, and the second summation involves the molal flow rates entering the volume element. The datum for the enthalpy calculations has been taken as the temperature prevailing at the inlet to the reactor. This equation may also be integrated between the reactor inlet and a point downstream where the fraction conversion is  $f_A$  to obtain

$$\int_{f_A \text{ in}}^{f_A \text{ out}} U(T_m - T) \frac{4}{D} F_{A0} \frac{df_A}{(-r_A)} = \sum \left( F_i \int_{T_0}^T \bar{C}_{pi} dT \right) - \frac{F_{A0} \Delta H_R \text{ at } T_0}{\nu_A} (f_A \text{ out} - f_A \text{ in}) \quad (10.4.7)$$

The summation involves the effluent molal flow rates. This equation and equation (10.4.2) must be solved simultaneously to determine the tubular reactor size and to determine the manner in which the heat transfer requirements are to be met. For either isothermal or adiabatic operation, one of the three terms in equation (10.4.7) will drop out, and the analysis will be much simpler than in the general case. In the illustrations that follow, two examples are treated in detail to indicate the types of situations that one may encounter in practice and to indicate in more detail the nature of the design calculations.

### ILLUSTRATION 10.4 Determination of the Volume Requirements for Adiabatic Operation of a Tubular Reactor with Exothermic Reaction

Butadiene will react with ethylene in the gas phase at temperatures above 500°C. This reaction is a simple example of a Diels–Alder reaction.



If an equimolar mixture of butadiene and ethylene at 450°C and 1 atm is fed to a tubular reactor, determine the space times required to convert 10% of the butadiene to cyclohexene for isothermal and for adiabatic modes of operation.

Wasserman (6) reported the following data for this reaction:

$$k = 10^{7.5} e^{-27,500/RT} \text{ L/(mol}\cdot\text{s)}$$

$$\Delta H_R = -30,000 \text{ cal/g-mol}$$

The reverse reaction may be neglected. The following values of gas-phase heat capacities may be assumed to be constant over the temperature range of interest.

$$C_{p,C_4H_6} = 36.8 \text{ cal/(g-mol}\cdot\text{K)}$$

$$C_{p,C_2H_4} = 20.2 \text{ cal/(g-mol}\cdot\text{K)}$$

$$C_{p,C_6H_{10}} = 59.5 \text{ cal/(g-mol}\cdot\text{K)}$$

## Solution

From the units on the reaction rate constant, the reaction is second-order. There is a volume change on reaction and  $\delta_a = (-1/2)$ . Thermal expansion will also occur, so equations (3.1.44) and (3.1.47) must be combined to obtain the reactant concentrations. Because equimolar concentrations of reactants are used, the design equation becomes

$$\begin{aligned} \tau &= C_{A0} \int_0^{0.1} \frac{df_A}{kC_{A0}^2 \{(1-f_A)^2/[1-(f_A/2)]^2(T_0/T)^2\}} \\ &= \int_0^{0.1} \left( \frac{T}{T_0} \right)^2 \frac{[1-(f_A/2)]^2 df_A}{kC_{A0}(1-f_A)^2} \end{aligned} \quad (\text{A})$$

The initial reactant concentration can be determined from the ideal gas law:

$$C_{A0} = \frac{Y_A P_{\text{tot}}}{RT_0} = \frac{0.5(1)}{0.08206(723)} = 8.43 \times 10^{-3} \text{ g-mol/L}$$

For isothermal operation at 450 °C the rate constant is equal to 0.156 liters/mol-sec and

$$kC_{A0}\tau = \int_0^{0.1} \frac{\left[1 - \left(\frac{f_A}{2}\right)\right]^2 df_A}{(1-f_A)^2}$$

With  $\Psi = 1 - f_A$  as a dummy variable, integration of the above equation gives

$$kC_{A0}\tau = \left\{ \frac{1}{\Psi} - \left[ \frac{1}{\Psi} + \ln(\Psi) \right] - \frac{1}{4} \left[ \Psi - 2\ln(\Psi) - \frac{1}{\Psi} \right] \right\} \Big|_{\Psi=1}^{\Psi=0.9}$$

or

$$\tau = \left\{ \frac{-\frac{1}{2} \ln(\Psi) + \left[ \frac{(1-\Psi)(1+\Psi)}{4\Psi} \right]}{0.156(8.43 \times 10^{-3})} \right\} \Big|_{\Psi=1}^{\Psi=0.9} = 80.19 \text{ sec}$$

For adiabatic operation the temperature must be related to the fraction conversion so that equation (A) can be integrated.

Equation (10.4.7) is appropriate for use if we set the heat transfer term equal to zero.

$$\sum \left( F_i \int_{T_0}^T \bar{C}_{pi} dT \right) = \frac{F_{A0} \Delta H_R \text{ at } T_0 (f_{A \text{ out}} - f_{A \text{ in}})}{v_A} \quad (\text{B})$$

From the reaction stoichiometry and the tabulated values of the heat capacities the contributions to the summation may be written as:

Butadiene:

$$F_i C_{pi}(T - T_0) = F_{A0}(1 - f_A) 36.8(T - T_0)$$

Ethylene:

$$F_i C_{pi}(T - T_0) = F_{A0}(1 - f_A) 20.2(T - T_0)$$

Cyclohexene:

$$F_i C_{pi}(T - T_0) = F_{A0} f_A (59.5)(T - T_0)$$

Hence,

$$\sum \left( F_i \int_0^T C_{pi} dT \right) = (57.0F_{A0} + 2.5f_A F_{A0})(T - T_0)$$

Substitution of numerical values into equation (B) and rearrangement then gives

$$T = 723 + \frac{30,000f_A}{57.0 + 2.5f_A} \quad (\text{C})$$

where  $T$  is expressed in K. At a fraction conversion of 0.1, the gas temperature will have risen to 775 K. The design equation then becomes

$$\tau = \int_0^{0.1} \left( \frac{T}{723} \right)^2 \frac{[1 - (f_A/2)]^2 df_A}{10^{7.5} e^{-27,500/1.987T} (8.43 \times 10^{-3})(1-f_A)^2}$$

where  $T$  is given by equation (C).

Numerical evaluation of this integral gives  $T = 47.11$  s. This space time is about 59% of that required for isothermal operation. This number may be somewhat low because the reaction is exothermic and the rate of

the reverse reaction may be appreciable at the highest temperatures involved in our calculation.

We now wish to examine the case where we allow for heat exchange with a substantially constant temperature heat sink (e.g., an evaporating or condensing fluid or a material flowing at a velocity such that its temperature change over the reactor length is quite small compared to the driving force for heat transfer).

### ILLUSTRATION 10.5 Determination of the Volume Requirements for Operation of a Tubular Reactor Under Nonisothermal Conditions with Heat Exchange

Consider the reaction used as the basis for Illustrations 10.1 to 10.3 ( $A \rightarrow B$ ). Determine the volume required to produce 2 million pounds of B annually in a plug flow reactor operating under the conditions described below. The reactor is to be operated 7000 h annually with 97% conversion of the A fed to the reactor. The feed enters at 163°C. The internal pipe diameter is 4 in. and the piping is arranged so that the effective reactor volume can be immersed in a heat sink maintained at a constant temperature of 160°C. The overall heat transfer coefficient based on the inside area of the pipe may be taken as 200 kcal/(h·m<sup>2</sup>·K). Volumetric expansion effects are negligible.

#### Solution

For this case it will be necessary to calculate the steady-state temperature and fractional conversion profiles along the length of the tubular reactor. For a plug flow reactor the appropriate differential material balance for the reaction at hand is

$$\frac{df}{d\tau} = k(T)(1 - f_A) \quad (A)$$

From equation (C) of Illustration 10.1,

$$k = 2.61 \times 10^{14} e^{-14,570/T} \text{ h}^{-1} \quad (B)$$

The temperature may be related to the fraction conversion by the differential form of the energy balance [e.g., (10.4.7)].

$$\left[ \sum F_i C_{pi} \right] \frac{dT}{dV_R} = U(T_m - T) \frac{4}{D} + \frac{F_{A0} \Delta H_R}{\nu_A} \frac{df_A}{dV_R}$$

or, using  $\tau = V_R / \mathcal{V}_0$  and  $F_{A0} \mathcal{V}_0 C_{A0}$ ,

$$\frac{dT}{d\tau} = \left[ \frac{U(T_m - T)(4/D)}{C_{A0}} + \frac{\Delta H_R}{\nu_A} \left( \frac{df_A}{d\tau} \right) \right] \frac{1}{\bar{C}_p} \quad (C)$$

where we have introduced a molar average heat capacity at constant pressure,  $\bar{C}_p$ .

For this illustration

$U$	200,000 cal/(m <sup>2</sup> ·hr·K)
$T_m$	433K
$D$	$4(2.54 \times 10^{-2}) = 0.1016 \text{ m}$
$F_{A0}$	133,700 g/h (from Illustration 10.2)
$C_p$	0.5 cal/(g·K)
$T_0$	436 K
$\Delta H_R / \nu_A$	83 cal/g

The initial reactant concentration is equal to 0.9 g/cm<sup>3</sup> or  $9 \times 10^5$  g/m<sup>3</sup> in units that are consistent with the other parameters we are using. Insertion of the reaction rate expression and numerical values into the combined material and energy balance equation (C) gives

$$\begin{aligned} \frac{dT}{d\tau} &= \left[ 200,000 (T_m - T) \left( \frac{4}{0.1016} \right) \right. \\ &\quad \times \left. \left( \frac{1}{900,000} \right) + 83 \frac{df_A}{d\tau} \right] \frac{1}{0.5} \\ &= 17.5(433 - T) + 166 \frac{df_A}{d\tau} \end{aligned} \quad (D)$$

Equations (A) and (D) are subject to the initial conditions at the entrance to the reactor where  $\tau$  is zero: namely, that  $f_A = 0$ , and  $T = 436$  K. Equations (A), (B), and (D) can be solved with standard numerical tools for integrating systems of coupled differential equations, such as *ode15s* in Matlab. The profiles of fractional conversion and temperature with reactor space time are shown by the solid lines in Figure I10.5.

The space time corresponding to the operating conditions outlined above is equal to 4.66 h. The required reactor volume is then equal to

$$V_R = \tau \mathcal{V}_0 = 4.66(39.3) = 183.1 \text{ gal}$$

or

$$V_R = 24.5 \text{ ft}^3$$

This volume corresponds to a reactor length of 70.2 ft of 4-in.-ID pipe. Such a reactor is most conveniently constructed using 14 parallel pipes 5 ft in length, or any other collection of shorter pipes in parallel to achieve the same aggregate length and residence time in a footprint convenient for construction and utilization.

The temperature of the reactor contents rises from 436 K at the inlet to 443.2 K at a point corresponding to  $f_A = 0.22$  and then drops to a temperature of 433.2 K at the reactor outlet. The maximum temperature is significantly less than that which would be obtained by adiabatic operation (597 K). This fact may be important in design considerations when side reactions have significant reaction rates at high temperatures. The required reactor volume will be greater than that for isothermal operation because, under the specified operating conditions, once a

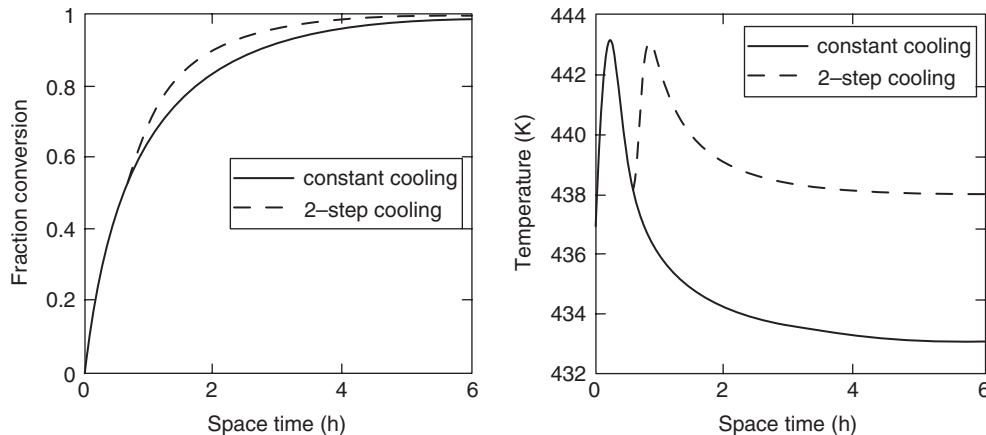


**Figure I10.5** Space time profiles of fractional conversion and reactor temperature in a PFR. These profiles correspond to the constant cooling and two step cooling cases.

fraction conversion of 0.63 is obtained, the temperature of the reactant mixture drops below the feed temperature and the reaction rate constant is correspondingly reduced. This effect more than offsets the increase in reaction rate accompanying the temperature increase in the early portion of the reactor. In practice one might wish to dispense with all or part of the cooling capacity in the later portions of the reactor. This technique would have the effect of reducing the required reactor volume. For example, the average operating temperature can be increased while keeping the maximum temperature below 445 K by dividing the reactor into two segments and changing the temperature of the heat transfer fluid to 466 K after  $f_A = 0.6$  ( $\tau = 1.2$  h). In this case, the specified conversion of 97% is accomplished at a reactor space time  $\tau$  of 3.266 h or  $V_R = 128.4$  gal. The concomitant significant reduction in reactor volume is achieved by allowing the reactor to operate at the slightly higher temperature for the latter portion of the reaction. The trajectories of fractional conversion and temperature experienced by a fluid element as it moves through the tubular reactor are shown by the dashed lines in Figure I10.5. Other temperature profiles that result from a variety of heat transfer conditions may be employed, limited only by one's imagination or by practicalities of implementation.

## 10.5 AUTOTHERMAL OPERATION OF REACTORS

In the design of processes involving exothermic reactions it is generally desirable to use the energy liberated by reaction at some other point in the process or to make it available for use elsewhere in the industrial plant. For example, it can be used to preheat the feed components, particularly when the reaction takes place at high temperatures and the feed components are supplied at much lower temperatures. The

term *autothermal operation* is applied to modes of processing in which exothermic reactions are carried out such that the energy released by reaction is fed back to the incoming reactant stream. Use of this term implies that the reactor system is to a large extent self-supporting in terms of its thermal energy requirements. Consequently, it is possible to run at the desired operating temperature without using external heat sources to preheat the feed. An autothermal reaction is akin to the autocatalytic reactions discussed in Section 9.4 in the sense that a product of the reaction (in this case, thermal energy) serves to enhance the reaction rate.

Because operation in an autothermal mode implies a feedback of energy to preheat the feed, provision must be made for "ignition" of the reaction to attain steady-state operation. The ordinary gas burner and many other rapid combustion reactions are examples of autothermal reactions in which the reactants are preheated to the reaction temperature by thermal conduction and radiation. (Back diffusion of free radicals also plays an important role in many combustion processes.)

There are several techniques by which the feedback of energy may be accomplished.

1. In a semibatch reactor, a cold feed may be heated by mixing with the reactor contents. This technique is discussed in Illustration 10.7.
2. In reactors operating under continuous flow conditions, there may be heat exchange between the effluent stream or the reactor contents and the feed stream. This exchange may occur in the reactor proper, in heat exchangers between various portions of a reactor network, or by various fluid mixing processes. In a stirred-tank reactor the fresh feed is mixed rapidly with the reactor contents to promote energy transfer. Energy feedback in tubular reactors can be accomplished by recycling a fraction of the reactor effluent for mixing with the fresh feed.

In Illustration 10.2 we saw that when one uses a battery of stirred tanks for carrying out an exothermic reaction under isothermal conditions, there may be occasions when the heat requirements for the various tanks may be of opposite sign. Some tanks will require a net input of thermal energy, while others will need to be cooled. It is often useful in such situations to consider the possibility of adiabatic operation of one or more of the tanks in series, remembering the constraints that one desires to place on the temperatures of the process streams. Another means of achieving autothermal operation is to use a network consisting of a stirred-tank reactor followed by a tubular reactor. This case is considered in Illustration 10.6.

### ILLUSTRATION 10.6 Autothermal Operation of a Reactor Network Consisting of a Stirred-Tank Reactor Followed by a Plug Flow Reactor

Consider the reaction studied in Illustration 10.1. Autothermal operation is to be achieved using a CSTR with an effective volume of 1000 gal followed by a PFR of undetermined volume. Pure species A enters at a rate of 40.0 gal/h and at a temperature of 20°C. The overall fraction conversion is to be 0.97. This flow rate and conversion level will suffice to meet the annual production requirement of 2 million pounds of B. Both the CSTR and the PFR are to be operated adiabatically. What PFR volume will be required, and what will be the temperature of the effluent stream?

### Solution

The analysis of the performance of the CSTR is identical with that of the first CSTR considered in Illustration 10.3. The space time for the CSTR is

$$\tau = \frac{V_R}{V_0} = \frac{1000}{40.0} = 25 \text{ h}$$

The fraction conversion at the CSTR exit for this first-order reaction is given by

$$f_{A1} = \frac{k\tau}{1 + k\tau} = \frac{25k}{1 + 25k} \quad (\text{A})$$

The rate constant is given by

$$k = 2.61 \times 10^{14} e^{-14.570/T} \quad (\text{B})$$

The energy balance equation for adiabatic operation is

$$0 = -\frac{F_{A0}f_{A1}}{\nu_A} \Delta H_{R \text{ at } T_0} + F_{A0} \int_{T_0}^{T_{\text{out}}} C_p \, dT$$

or, assuming a constant heat capacity for the liquid,

$$f_{A1} = \frac{\nu_A C_p (T_{\text{out}} - T_0)}{\Delta H_{R \text{ at } T_0}} = \frac{0.5(T_{\text{out}} - 293)}{83} \quad (\text{C})$$

Equations (A) to (C) can now be solved simultaneously using a trial-and-error iterative procedure. One finds that  $f_{A1} = 0.705$  and  $T = 410\text{K}$ . These properties are those of the stream entering the plug flow reactor. The design equation for this reactor is

$$\tau = C_{A0} \int_{0.705}^{0.97} \frac{df_A}{kC_{A0}(1-f_A)} = \int_{0.705}^{0.97} \frac{df_A}{k(1-f_A)} \quad (\text{D})$$

where  $k$  is again given by equation (B).

An energy balance on the PFR operating at steady state is given by equation (10.4.6). For adiabatic operation this equation becomes

$$0 = \frac{F_{A0}(f_{A2} - f_{A1})}{\nu_A} \Delta H_{R \text{ at } T_0} + F_{A0} \int_{T_0}^{T_{\text{leaving PFR}}} C_p \, dT - F_{A0} \int_{T_0}^{T_{\text{entering PFR}}} C_p \, dT \quad (\text{E})$$

Because the heat capacity of the reaction mixture is described as being independent of temperature and composition, equation (E) simplifies to

$$0 = \frac{(f_{A2} - f_{A1}) \Delta H_{R \text{ at } T_0}}{\nu_A} + C_p (T_{\text{leaving PFR}} - T_{\text{entering PFR}}) \quad (\text{F})$$

The relationship between the temperature and the fraction conversion at a particular point in the plug flow reactor can be obtained by setting  $f_{A2} = f_A$  and  $T_{\text{leaving PFR}}$  equal to  $T$ . Hence

$$T = T_{\text{entering PFR}} + \frac{\Delta H_{R \text{ at } T_0}}{\nu_A C_p} + (f_A - f_{A1}) \quad (\text{G})$$

In numerical terms,

$$T = 410 + \frac{-83}{-1 (0.5)} (f_A - 0.705) = 410 + 166(f_A - 0.705) \quad (\text{H})$$

At the exit from the PFR, the temperature will be 454 K or 181°C.

Equations (B), (D), and (H) may now be solved simultaneously to determine the space time required for the plug flow reactor. For the present situation  $\tau = 3.72$  h so the required PFR volume is  $3.72(40) = 148.8$  gal or 19.8 ft<sup>3</sup>. By operating in this mode, one eliminates or minimizes the necessity for using heat exchangers. If one regards the exit temperature of 181°C as excessive, a heat exchanger could be used between the CSTR and the PFR, or arrangements could be made for internal cooling within the PFR.

In Illustration 10.7 we consider how to meet the vast majority of the heat transfer requirements for operation of a semibatch reactor by a semi-autothermal mode of processing. By intermittent addition of a cold reactant stream to the hot contents of a well-stirred semibatch reactor, it is possible to maintain the system temperature within prescribed limits.

### ILLUSTRATION 10.7 Quasi-Autothermal Operation of a Semibatch Reactor Using Addition of Cold Feed

At the time Kladko's article (5) was prepared, market conditions dictated that it would not be financially remunerative to develop a continuous process for producing B by the reaction discussed in Illustration 10.1 and other illustrations in this chapter. Consequently, they considered the possibility of using a semibatch reactor with continuous addition of cold feed to maintain the temperature of the reactor contents within prescribed limits. The basic problem was considered in Illustration 8.11. However, in addition to the material balance aspects of the design, we now wish to consider the heat transfer requirements for operation in accordance with the filling schedule outlined earlier. For the conditions indicated in Illustration 8.11 (isothermal, 163°C); determine the direction and magnitude of the heat transfer requirements.

#### Solution

The material balance equations have been solved earlier with the result that

$$m_A = m_{Ai} e^{-k(t-t_i)} + \frac{\phi_{A0}}{k} [1 - e^{-k(t-t_i)}]$$

where  $m_A$  is the mass of A remaining in the reactor at time  $t$ ,  $m_{Ai}$  is the mass of A in the reactor at time  $t_i$ , and  $\phi_{A0}$  is the mass feed rate of A appropriate to the time interval between  $t$  and  $t_i$ .

An energy balance on the reactor can be derived from equation (10.1.1) by omission of appropriate terms:

$$\frac{dE_{\text{sys}}}{dt} = \dot{Q} + h_{\text{in}} \dot{m}_{\text{in}}$$

Multiplying by  $dt$  and integrating between time zero and time  $t$  gives

$$E_{\text{sys}} - E_{\text{sys},0} = Q + h_{\text{in}} m_{\text{in}}$$

If the temperature of the inlet stream is taken as the datum temperature for enthalpy and internal energy calculations,

$$h_{\text{in}} = 0$$

and

$$E_{\text{sys}} - E_{\text{sys},0} = Q$$

However, for condensed phases, the difference between internal energy and enthalpy is usually negligible:

$$Q \approx H_{\text{sys}} - H_{\text{sys},0} \quad (\text{A})$$

The enthalpy difference is given by

$$H_{\text{sys}} - H_{\text{sys},0} = \int_{20^\circ\text{C}}^{163^\circ\text{C}} (m_A + m_B - m_{B0}) \hat{C} \, dT + \Delta H_R \text{ at } 20^\circ\text{C} (m_B - m_{B0}) \quad (\text{B})$$

where  $\hat{C}$  is the average heat capacity per unit mass and where we have assumed that the initial material sump ( $m_{B0}$ ) is at 163°C.

Equations (A) and (B) can be combined with appropriate numerical values to obtain

$$\begin{aligned} Q &= (m_A + m_B - m_{B0})(0.5)(163 - 20) - 83(m_B - m_{B0}) \\ &= (m_A + m_B - m_{B0})71.5 - 83(m_B - m_{B,0}) \\ &= 71.5m_A - 11.5(m_B - m_{B0}) \end{aligned}$$

where  $Q$  is expressed in calories and  $m$  is expressed in grams. If  $m$  is expressed in pounds and  $Q$  in Btu, then

$$Q = 128.7m_A - 20.7(m_B - m_{B0})$$

The numerical values characterizing  $m_A$  and  $m_B$  at various times are obtained as indicated in Illustration 8.11. They may be used to determine the net heat required between time zero and time  $t$ . The pertinent results are presented in Table I10.7-1. It is evident that heat must be supplied to the reactor during the first several hours, but the reactor then reaches a point beyond which cooling must be supplied.

Instantaneous heat transfer requirements may be determined by recognizing that the thermal energy supplied must be used to effect either a sensible heat change or the reaction. If  $\dot{Q}$  is the heat transfer rate,

$$\dot{Q} = \phi_{A0} \int_{T_0}^T \hat{C} \, dT + rV_R \Delta H_R$$

where  $V'_R$  is the liquid-phase volume at time  $t$ . Because  $C_A = m_A/V'_R$  and the reaction obeys first-order kinetics,

$$\dot{Q} = \phi_{A0} \int_{T_0}^T \hat{C} \, dT + km_A \Delta H_R$$

Substitution of numerical values gives

$$\begin{aligned} \dot{Q} &= \phi_{A0}(0.5)(163 - 20) + 0.8m_A(-83) \\ &= 71.5\phi_{A0} - 66.4m_A \end{aligned}$$

**Table I10.7-1 Material and Energy Balance Analysis**

Time (h)	$m_A$ (lb)	Total mass (lb)	$Q_{\text{total}} \times 10^{-3}$ (Btu)	$\dot{Q} \times 10^{-3}$ (Btu/h) <sup>a</sup>
0	0	1500	0	22.52
1	120	1675	14.31	8.18
2	175	1850	18.90	1.61
3	199	2025	18.86	5.18
4	244	2250	20.93	-0.20
5	265	2475	19.41	-2.71
6	274	2700	16.10	2.65
7	312	2975	16.08	4.54
8	364	3300	17.12	7.98
9	439	3700	20.05	-0.98
10	473	4100	16.85	-5.04
11	488	4500	10.81	-16.49
12	443	4825	-2.64	-17.55
13	388	5100	-16.55	-17.41
14	329	5325	-30.02	-16.79
15	268	5500	-42.76	-19.16
16	189	5600	-56.63	-16.15
17	119	5650	-68.13	-14.22
18	54	5650	-77.84	-6.45
19	24	5650	-82.32	-2.87
20	11	5650	-84.26	-1.31

<sup>a</sup>Instantaneous heat transfer rates are calculated after changes are made in the mass flow rates at the times indicated.

where  $\dot{Q}$  is expressed in cal/h,  $\phi_{A0}$  is expressed in g/h, and  $m_A$  is expressed in grams.

In more conventional engineering units,

$$\dot{Q} = 128.7\phi_{A0} - 119.5m_A$$

where  $\dot{Q}$  is now expressed in Btu/h,  $\phi_{A0}$  is expressed in lb/h, and  $m_A$  is expressed in pounds. Calculated values of  $\dot{Q}$  are also presented in Table I10.7-1.

If one were to operate this semibatch reactor under a filling schedule, which for the first 11 h is identical to that considered previously, and then proceed to feed A at the maximum rate of 400 lb/h for an additional 2.875 h, the same total amount of A would have been introduced to the reactor. However, in this case, the heat transfer requirements would change drastically. There would be a strong exotherm beginning at the moment the cold feed is stopped. The results for this case are presented in Table I10.7-2.

Consequently, if one desires to minimize the possibility that this reaction will run away (be out of control) as a result of exceeding the capacity of the cooling network, it would be advisable to operate in a mode such that the feed rate is gradually diminished instead of being abruptly terminated at a high feed flow rate.

**Table I10.7-2 Results of Analysis for Abrupt Termination of Feed at 13.875 h**

Time (h)	$m_A$ (lb)	Total mass (lb)	$Q_{\text{total}} \times 10^{-3}$ (Btu)	$\dot{Q} \times 10^{-3}$ (Btu/h) <sup>a</sup>
11	488	4500	10.81	-6.84
12	494	4900	3.42	-7.55
13	498	5300	-4.26	-8.03
13.875	499	5650	-11.35	-59.63
14.00	452	5650	-18.38	-54.01
14.50	303	5650	-40.64	-36.21
15.0	203	5650	-55.58	-24.26
15.50	136	5650	-65.59	-16.25
16.00	91	5650	-72.31	-10.87
17	41	5650	-79.78	-4.90
18	18	5650	-83.22	-2.15
19	8	5650	-84.71	-0.96

<sup>a</sup>Instantaneous heat transfer rates are calculated after changes are made in the mass flow rates at the times indicated.

## 10.6 STABLE OPERATING CONDITIONS IN STIRRED TANK REACTORS

In Illustrations 10.2 and 10.3 the temperatures and degrees of conversion leaving stirred-tank reactors were determined by simultaneous solution of rate, material balance, and energy balance equations. In this section we see that there may be circumstances when there will be more than one set of operating conditions that will satisfy these equations. In such cases questions arise as to the stability of the operating points corresponding to these solutions. For the elementary cases that are treated in this book, the stability can be determined readily on the basis of simple physical arguments. There are more complex cases in the general area of reactor stability, however, that require sophisticated mathematical analysis. Many of these cases have been treated in the extensive body of literature that exists on this subject. Perlmutter (7) has summarized much of this material in textbook form.

When a reactor is operating at steady state, the rate of energy release by chemical reaction must be equal to the sum of the rates of energy loss by convective flow and heat transfer to the surroundings. This statement was expressed in algebraic form in equations (10.3.4) and (10.4.6) for the CSTR and PFR, respectively. This statement can serve as the physical basis for examination of the stability of various operating points.

Let  $Q_g$  represent the rate at which thermal energy is released by an exothermic chemical reaction in a CSTR. If  $Q_g$  is plotted versus the temperature of the reactor contents for a fixed feed rate and feed composition, there are several curves that may result, depending on the nature of the

reaction or reactions involved. Figure 10.1 shows the nature of the curve for the case of a simple first-order irreversible reaction. At low temperatures the reaction rate is negligible, so very little energy is released. At high temperatures the reaction rate constant is so large that very little unreacted material remains in the effluent stream. Consequently, still higher values of  $T$  cannot increase  $Q_g$  significantly, and the curve must approach an asymptote. At intermediate temperatures one has a competition between the increase in reaction rate arising from the effect of increased temperature and the negative effect on the rate arising from depletion of the reactants. The equation of the curve is easily obtained from first principles:

$$Q_g = rV_r|\Delta H| \quad (10.6.1)$$

where  $|\Delta H|$  is the magnitude of the heat of reaction for the exothermic reaction. For a first-order irreversible reaction with  $\nu_A = -1$

$$r = -r_A = kC_A \quad (10.6.2)$$

If there is no volume change because of reaction, the design equation for a CSTR indicates that

$$\tau = \frac{V_R}{V_0} = \frac{C_{A0} - C_{AF}}{-r_{AF}} = \frac{C_{A0} - C_{AF}}{kC_{AF}} \quad (10.6.3)$$

or

$$C_{AF} = \frac{C_{A0}}{1 + k\tau} \quad (10.6.4)$$

Combination of equations (10.6.1), (10.6.2), and (10.6.4) gives

$$Q_g = \frac{kC_{A0}V_R|\Delta H_R|}{1 + k\tau} \quad (10.6.5)$$

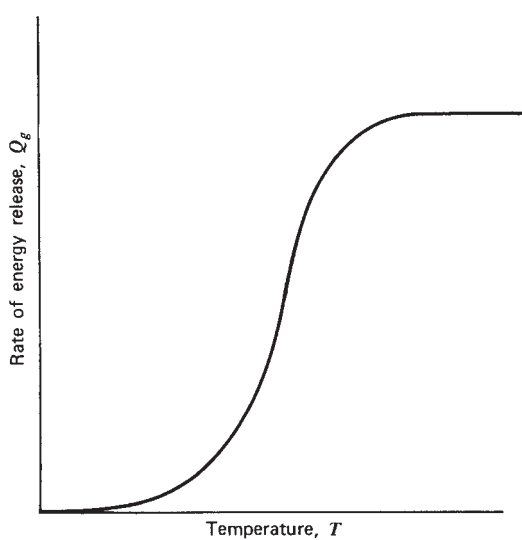


**Figure 10.1** Rate of energy release by reaction versus temperature for an irreversible exothermic reaction carried out in a CSTR.

If  $k$  is now written in the Arrhenius form,

$$Q_g = \frac{Ae^{-E/RT} C_{A0} V_R |\Delta H_R|}{1 + (V_R/V_0)Ae^{-E/RT}} \quad (10.6.6)$$

This expression for  $Q_g$  depends on temperature in the manner shown in Figure 10.1.

Other reactions will have somewhat different forms for the curve of  $Q_g$  versus  $T$ . For example, in the case of a reversible exothermic reaction, the equilibrium yield decreases with increasing temperature. Because one cannot exceed the equilibrium yield within a reactor, the fraction conversion obtained at high temperatures may be less than a subequilibrium value obtained at lower temperatures. Since the rate of energy release by reaction depends only on the fraction conversion attained and not on the position of equilibrium, the value of  $Q_g$  may thus be lower at the higher temperature than it was at a lower temperature. Figure 10.2 indicates the general shape of a  $Q_g$  versus  $T$  plot for a reversible exothermic reaction. For other reaction networks, differently shaped plots of  $Q_g$  versus  $T$  will exist.

The rate at which energy is removed from the system,  $Q_r$ , is equal to the rate at which it is being lost by heat transfer processes plus the mass flow rate times the gain in sensible heat per unit mass. Thus,

$$Q_r = UA(T - T_m) + \phi_m \hat{C}(T - T_0) \quad (10.6.7)$$

where  $T_m$  is the temperature of the heat transfer medium (assumed constant),  $\phi_m$  the mass flow rate,  $\hat{C}$  the average heat capacity per unit mass appropriate to the temperature range in question, and  $T_0$  the feed temperature. Equation (10.6.7) can be rewritten as

$$Q_r = T(UA + \phi_m \hat{C}) - UAT_m - \phi_m \hat{C}T_0 \quad (10.6.8)$$

to emphasize the fact that  $Q_r$  will be essentially linear in  $T$  if  $U$  and  $C$  are not strong functions of temperature.

At steady state the rate of transformation of energy by reaction must be equal to the sum of the energy losses by convective transport and heat transfer through the walls of the reactor. This statement implies that the intersection(s) of

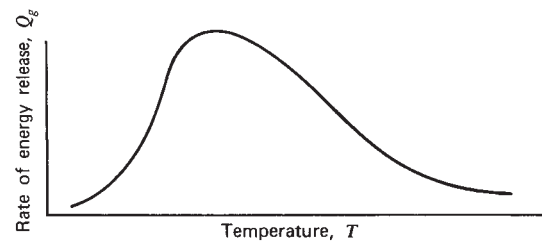


**Figure 10.2** Rate of energy release by reaction versus temperature for a reversible exothermic reaction carried out in a CSTR.

the curves given by equations (10.6.6) and (10.6.8) will represent the solution(s) of the combined material and energy balance equations. The positions at which the intersections occur depend on the variables appearing on the right side of equations (10.6.6) and (10.6.8). Figure 10.3 depicts some of the situations that may be encountered.

If the rate of energy removal is represented by line 1 in Figure 10.3, the reaction mixture is cooled to such an extent that steady-state operation is possible only at a very low degree of conversion and a very low temperature. If the variables influencing the  $Q_g$  and  $Q_r$  curves are examined, one sees that this type of steady state is favored by:

1. Low magnitudes of the heat of reaction.
2. Large values of the  $UA$  product.
3. Low values of  $T_m$  or  $T_0$ .
4. Low feed rates ( $V_0$ ).
5. Long residence times ( $V_R/V_0$ ).
6. Small rate constants.

If  $Q_r$  is represented by line 3, substantially complete conversion is achieved. This type of steady state is favored by conditions that are opposite to those enumerated above.

Because of the sigmoid shape of the thermal energy generation curve, intersections at high or very low degrees of conversion are more probable than intersections at intermediate levels. This conclusion is in agreement with observations of the performance of stirred-tank reactors. Nonetheless, it is the situation where the intersection occurs at an intermediate value of the conversion (or of  $Q_g$ ) that is of greatest interest from a stability analysis viewpoint.

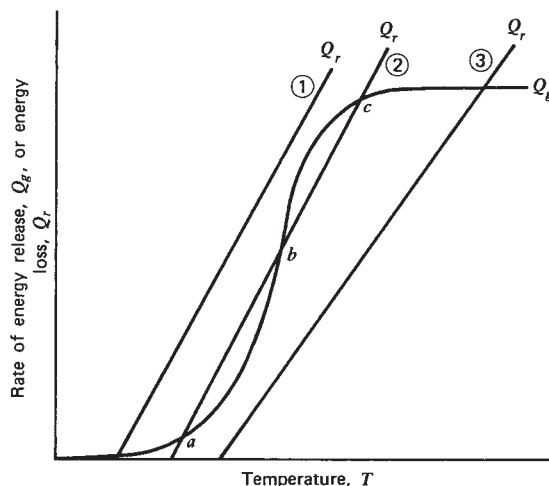


Figure 10.3 Energy release and energy loss curves for an irreversible reaction in a CSTR.

If the  $Q_r$  curve is given by the straight line numbered 2, it is evident that there are three points of intersection with the thermal energy generation curve. This case could be achieved by reducing the cooling capacity employed in the first case, or by dropping the feed temperature and/or increasing the cooling capacity employed in case 3.

Of the three operating conditions indicated in Figure 10.3, only two (*a* and *c*) are stable; the third (*b*) is unstable. The stability of the various points can be examined in terms of the slopes of the  $Q_g$  and  $Q_r$  curves at the point in question. When operating at point *c*, if a small positive temperature fluctuation occurred, one would move into a region where the rate of energy loss is greater than the rate of release of energy by chemical reaction. Consequently, the system will suffer a net loss of thermal energy and cool down until it returns to point *c*. On the other hand, if there were a negative temperature fluctuation, one would move to a region where more energy is transformed by reaction than is lost by heat transfer and convective flow. There would then be a net gain of energy, and the system temperature would rise until point *c* was reached again. Because departures from this point lead to conditions tending to restore the system to the original point, *c* represents a *stable* operating condition. By the same reasoning it can be shown that point *a* and the intersections of curves 1 and 3 with the  $Q_g$  curve are stable operating points.

However, with regard to temperature fluctuations the characteristics of point *b* are quite different. At this point the slope of the energy transformation curve is greater than the slope of the energy-loss curve. If a small positive temperature fluctuation were to occur, one would be in a region where energy stored in the form of chemical bonds would be transformed by reaction faster than it could be dissipated by convective transport and heat transfer. This condition would cause the system to increase further in temperature. The temperature deviation would continue to be amplified until the reactor arrived at point *c*, the upper stable operating point. A negative temperature fluctuation would also be amplified, the system losing energy faster than the energy stored in the form of chemical bonds is transformed by the exothermic reaction. In this case the temperature decreases until the lower stable operating point is attained. This situation corresponds to extinguishing the reaction. Because of the nature of its response to deviations in temperature, point *b* is referred to as an *unstable* operating point.

To operate at a point like *c* on curve 2 in Figure 10.3, one must provide a means of bypassing or circumventing the lower stable state *a* and the unstable state *b*. This result may be accomplished by preheating the feed, temporarily operating at a reduced flow rate, or reducing the capacity of the cooling system. These procedures will permit one to move to the right of point *b* and "ignite" the reaction.

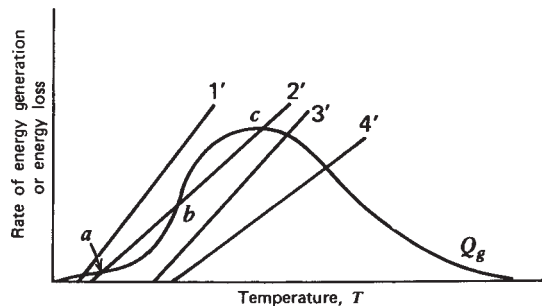


**Figure 10.4** Energy release and energy loss curves for a reversible exothermic reaction in a CSTR.

These stability considerations are not limited to first-order irreversible reactions. Figure 10.4 depicts the  $Q_g$  and  $Q_r$  curves for a reversible exothermic reaction. The intersections of the  $Q_g$  curve and lines 3' and 4' represent stable operating conditions, as do points *a* and *c*. Point *b*, however, is unstable. Also note that a relatively small slope for the heat-loss curve will give rise to a high reaction temperature and low yield. If the cooling capacity is increased, one moves from line 4' to line 3' and achieves a higher degree of conversion for this equilibrium-controlled reaction. The highest yield evidently corresponds to using an energy-loss curve that intersects the energy-release curve near or at its peak. However, because of the shape of the curve, it may be very difficult from a process control viewpoint to operate at this condition. Increases in the cooling rate can increase the slope of the energy-loss curve, possibly leading to extinction of the reaction. This situation can be visualized by rotating line 2' to the left about its intersection on the  $T$  axis.

The problem of ignition and extinction of reactions is basic to that of controlling the process. It is interesting to consider this problem in terms of the variables used in the earlier discussion of stability. When multiple steady-state solutions exist, the transitions between the various stable operating points are essentially discontinuous, and hysteresis effects can be observed in these situations.

Consider the energy-release and energy-loss curves shown in Figure 10.5. These curves correspond to three different operating conditions where one would be varying either the temperature of the feed stream,  $T_0$ , or the temperature of the medium to which heat is being transferred,  $T_m$ . The intercepts on the temperature axis corresponding to the three cases are  $T'$ ,  $T''$ , and  $T'''$ . We will assume that all other operating variables are held constant. When the temperature intercept is  $T'$ , the reactor may operate in a stable mode at point *A*.

However, if the cooling rate is increased (by decreasing  $T_m$ ) or if the temperature of the feed stream drops, curve  $Q'_r$  will move to the left and the reaction will be

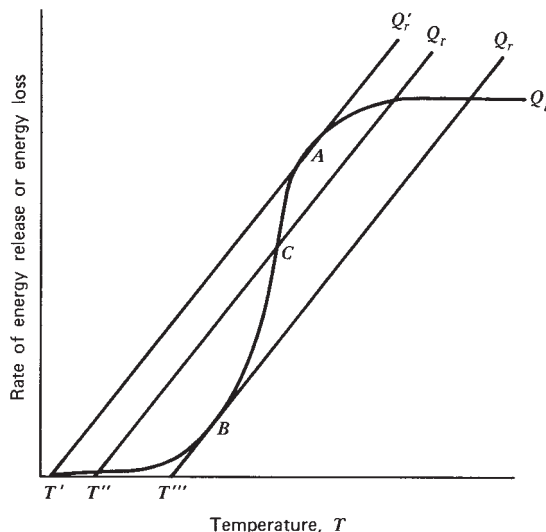


**Figure 10.5** Influence of operating conditions on ignition and extinction of reactions.

extinguished. Consequently, point *A* represents a critical extinction point. For combustion reactions the temperature at this point may be referred to as a *minimum combustion temperature*. This temperature cannot be regarded as having an absolute value characteristic of the reaction. It depends on the various factors that influence the relative positions of the  $Q_g$  and  $Q_r$  curves and their point of tangency. The heat transfer coefficient, reactant feed composition, volumetric flow rate, physical properties of the reactants, and characteristic properties of the reaction all influence the absolute value of this point.

The tangent indicated at point *B* also represents a critical reaction condition, but of a somewhat different type. In this case the reactor temperature corresponding to point *B* represents the minimum temperature at which autoignition will occur. In this sense it can be regarded as a *minimum ignition temperature*. Like the critical extinction point, this temperature should not be regarded as an absolute value but as a function of various operating parameters. If the temperature intercept of the energy-loss curve lies between those corresponding to the minimum ignition temperature and to the critical extinction point (e.g., at  $T'$ ), ignition can occur only if the unstable operating point *C* can be bypassed.

We should note that hysteresis effects could be observed in situations such as those depicted in Figure 10.5. Suppose that the temperature of the feed stream is such that the temperature intercept moves from slightly below  $T'$  to slightly above  $T''$ . Assuming that all other independent variables are held constant, the temperature of the reactor contents will rise slowly, because the conversion

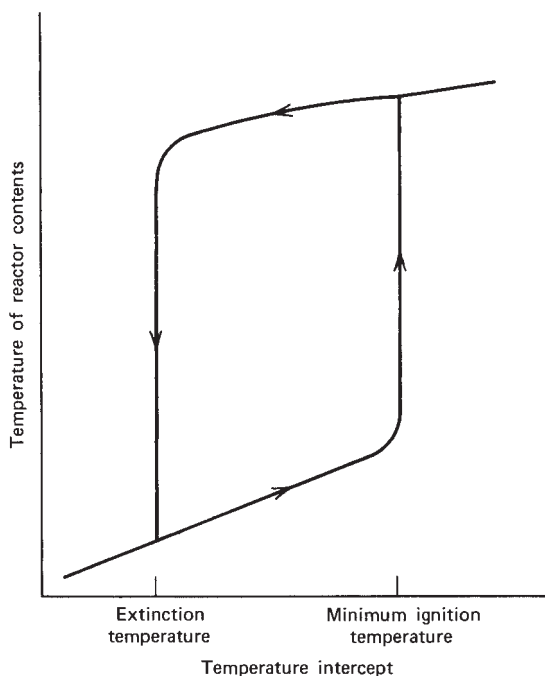


**Figure 10.6** Ignition and extinction hysteresis effects in a CSTR.

levels achieved will be those corresponding to the lowest stationary-state condition. Once intercept  $T''$  is exceeded, however, autoignition will occur and the temperature of the reactor contents will increase very markedly. The conversion level now will be significantly higher than it was previously. If the temperature of the feed stream is now reduced so that the temperature intercept moves to the left of  $T''$ , the temperature of the reactor contents will diminish slowly moving along the  $Q_g$  curve. The reactor will continue to operate at a high conversion level, corresponding to the upper steady state. Eventually, the temperature intercept will drop below  $T'$  and the reaction will be extinguished. The temperature of the reactor contents and the fraction conversion will then drop to low levels. Figure 10.6 illustrates the hysteresis phenomenon involved.

Ignition and extinction phenomena can be examined with respect to each of the various parameters of the system using the general approach outlined above. It should be noted that in these analyses and in the discussion above, one is restricted to changes that occur so slowly that the corresponding changes in reactor conditions can be regarded as a series of pseudo stationary states. It is instructive to consider the effects of opening and closing the valve on a propane torch or of varying the gas flow rate to a bunsen burner in terms of the material we have presented in this section. The basic problem of obtaining a stable flame can be analyzed in terms of the concepts developed above, even though other phenomena are undoubtedly of importance.

## 10.7 SELECTION OF OPTIMUM REACTOR TEMPERATURE PROFILES: THERMODYNAMIC AND SELECTIVITY CONSIDERATIONS

In this section we treat the selection of optimum temperature progressions for systems in which multiple reactions can occur. In a batch reactor this progression is the time schedule that the temperature should follow as a function of reactant conversion. In a tubular reactor it is the profile along the length of the reactor. In a series of stirred-tank reactors it is the change in temperature from stage to stage. For a single reversible reaction, the optimum temperature progression is chosen as that which minimizes the required reactor volume for a given fraction conversion and feed rate. For multiple reactions, optimization involves manipulation of the temperature to obtain a favorable product distribution.

### 10.7.1 Optimum Temperature Schedules

To minimize the reactor volume required for a given type of reactor and level of conversion, one must always operate with the reactor at a temperature where the rate is a maximum. For irreversible reactions the reaction rate always increases with increasing temperature, so the highest rate occurs at the highest permissible temperature. This temperature may be selected on the basis of constraints established by the materials of construction, phase changes, or side reactions that become important at high temperatures. For reversible reactions that are endothermic, the same considerations apply, since both the reaction rate and the equilibrium yield increase with increasing temperature.

For reversible exothermic reactions the situation is more complicated, because kinetic and thermodynamic considerations work against one another when the temperature is raised. The rates of the forward and reverse reactions both increase with increasing temperature, but the latter increases faster than the former. Therefore, the equilibrium yield or maximum attainable conversion decreases with increasing temperature. Because of this, it is advisable to use a high temperature when the system is far from equilibrium to take advantage of the influence of temperature on the forward reaction rate. When equilibrium is approached, the temperature should be decreased to shift the equilibrium yield to a higher value. The optimum temperature sequence is then one that starts out high and decreases with increasing conversion.

For a single plug flow reactor, optimum conditions for adiabatic operation are obtained by varying the feed temperature so that the average reaction rate has the highest possible value. For endothermic reactions this implies the maximum practical feed temperature. For exothermic

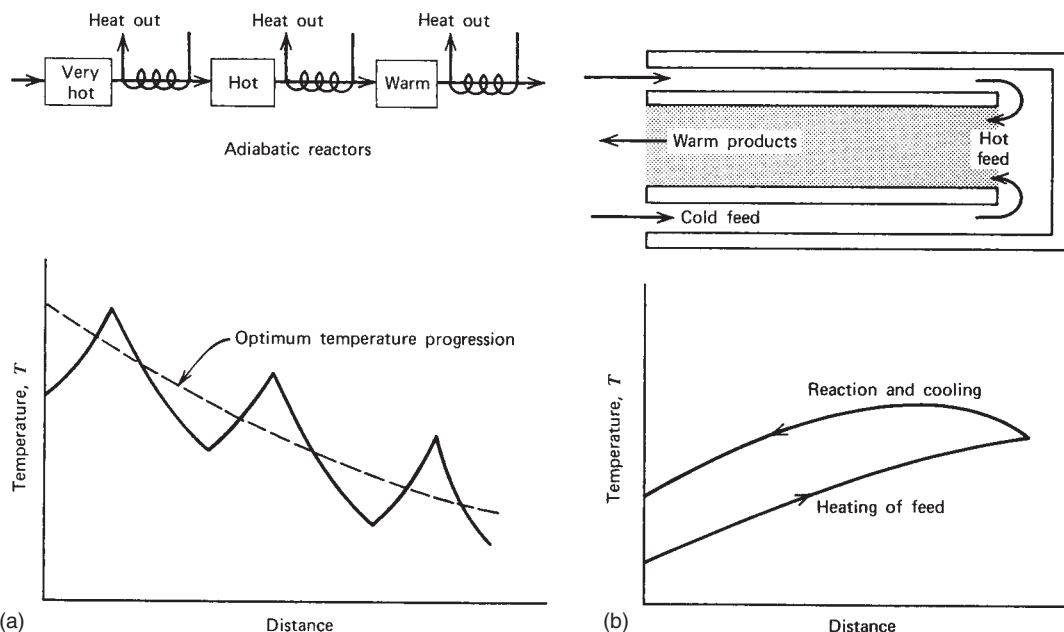


**Figure 10.7** Techniques for approaching optimum temperature profiles for exothermic reaction: (a) adiabatic operation of reactors with interstage cooling; (b) countercurrent heat exchange. (Adapted from O. Levenspiel, *Chemical Reaction Engineering*, 2nd ed., Copyright © 1972. Reprinted by permission of John Wiley & Sons, Inc.)

reactions, optimization of the temperature profile implies that the exit temperature should lie below that corresponding to equilibrium at the fraction conversion desired and above that corresponding to the maximum rate at this conversion. A trial-and-error procedure can locate an exit temperature within this range that corresponds to the minimum reactor volume. For a CSTR the reactor effluent temperature should be that which gives a maximum rate at the conversion level desired. The inlet temperature may be adjusted to give this effluent condition when the reactor is operated adiabatically.

For an exothermic reaction, adiabatic operation gives an increase in temperature with increasing conversion. However, the optimum temperature profile is one in which the temperature declines with increasing conversion. Severe heat transfer requirements may be needed to make the actual temperature profile approach the ideal desired. Two ways in which this may be achieved are indicated in Figure 10.7. Illustration 10.8 indicates how one determines the optimum temperature at which a single CSTR should be operated.

The case of internal heat exchange between the reaction mixture and the feed stream has been discussed by Van Heerden (8) and Kramers and Westerterp (9). The other alternative is to use staged operations with interstage cooling between adiabatic sections. This case has also been treated by Kramers and Westerterp (9). For endothermic reactions, multiple stages with reheating between stages are commonly used to keep the temperature from dropping too far.

### ILLUSTRATION 10.8 Determination of Optimum Temperature for Operation of a Single CSTR in Which a Reversible Exothermic Reaction is Being Carried Out

The following reversible reaction takes place in a CSTR:



where both the forward and the reverse reaction obey first-order kinetics. The rate constants may be written in the Arrhenius form as

$$k_1 = A_1 e^{-E_1/RT}$$

$$k_2 = A_2 e^{-E_2/RT}$$

Determine the minimum reactor volume that will be required to obtain a fraction conversion  $f_C$  if the feed is pure C and the volumetric feed rate is  $V_0$ . What will be the temperature of the effluent stream?

#### Solution

For this CSTR the appropriate design equation is

$$\tau = \frac{V_R}{V_0} = \frac{C_{C0} \int_0^{f_e} df_c}{-r_{CF}} = \frac{C_{C0} f_e}{-r_{CF}} \quad (A)$$

with

$$-r_{CF} = k_1 C_{CF} - k_2 C_{BF} \quad (B)$$

From stoichiometric considerations

$$C_{CF} = C_{C0}(1 - f_c) \quad (C)$$

$$C_{BF} = C_{C0}f_c \quad (D)$$

Combining equations (A) to (D) gives

$$\frac{V_R}{V_0} = \frac{f_c}{k_1(1 - f_c) - k_2f_c} = \frac{f_c}{k_1 - f_c(k_1 + k_2)}$$

To minimize the required reactor volume, one may set the temperature derivative of  $V_R$  equal to zero:

$$\left( \frac{\partial V_R}{\partial T} \right)_{f_c} = \frac{-V_0 f_c \frac{\partial}{\partial T} [k_1 - f_c(k_1 + k_2)]}{[k_1 - f_c(k_1 + k_2)]^2} = 0$$

or

$$\frac{\partial k_1}{\partial T} - f_c \left( \frac{\partial k_1}{\partial T} + \frac{\partial k_2}{\partial T} \right) = 0$$

However, from the Arrhenius relation,

$$\frac{d \ln k}{dT} = \frac{E_A}{RT^2} \quad \text{or} \quad \frac{dk}{dT} = \frac{kE_A}{RT^2}$$

Thus, the optimum temperature will be that at which

$$\frac{k_1 E_1}{RT^2} (1 - f_c) - f_c \frac{k_2 E_2}{RT^2} = 0$$

or

$$\frac{k_1}{k_2} = \frac{E_2}{E_1} \left( \frac{f_c}{1 - f_c} \right)$$

Substitution of the Arrhenius form of the rate constants yields

$$\frac{A_1 e^{-E_1/RT}}{A_2 e^{-E_2/RT}} = \frac{E_2}{E_1} \left( \frac{f_c}{1 - f_c} \right)$$

One can then solve for the optimum temperature:

$$\frac{1}{T} \left( -\frac{E_1}{R} + \frac{E_2}{R} \right) = \ln \left[ \left( \frac{E_2 A_2}{E_1 A_1} \right) \left( \frac{f_c}{1 - f_c} \right) \right] \equiv \ln \beta$$

or

$$T = \frac{E_2 - E_1}{R \ln \{ [(E_2 A_2)/(E_1 A_1)] [f_c/(1 - f_c)] \}} = \frac{E_2 - E_1}{R \ln \beta}$$

At this temperature

$$k_1 = A_1 e^{-(E_1 \ln \beta)/(E_2 - E_1)} = A_1 \beta^{-E_1/(E_2 - E_1)}$$

and

$$k_2 = A_2 \beta^{-E_2/(E_2 - E_1)}$$

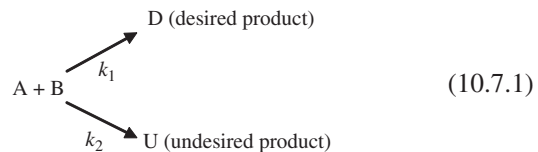
Thus, the minimum reactor volume is given by

$$V_R = \frac{V_0 f_c}{A_1 \beta^{-E_1/(E_2 - E_1)} (1 - f_c) - A_2 \beta^{-E_2/(E_2 - E_1)} f_c}$$

### 10.7.1.1 The Influence of Selectivity Considerations on the Choice of Reactor Operating Temperatures

When multiple reactions are possible, certain of the products have greater economic value than others, and one must select the type of reactor and the operating conditions so as to optimize the product distribution and yield. In this subsection we examine how the temperature can be manipulated with these goals in mind. In our treatment we ignore the effect of concentration levels on the product distribution by assuming that the concentration dependence of the rate expressions for the competing reactions is the same in all cases. The concentration effects were treated in detail in Chapter 9.

Consider the following simple parallel reactions:



It is evident that

$$\frac{dD}{dU} = \frac{k_1}{k_2} \quad (10.7.2)$$

If reaction 1 is to be enhanced and reaction 2 suppressed, the ratio of the rate constants must be made as large as possible. This ratio may be written in the Arrhenius form as

$$\frac{k_1}{k_2} = \frac{A_1 e^{-E_1/RT}}{A_2 e^{-E_2/RT}} = \frac{A_1}{A_2} e^{-(E_1 - E_2)/RT} \quad (10.7.3)$$

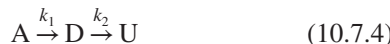
This ratio changes with temperature in a manner that depends on whether  $E_1$  is greater than or less than  $E_2$ . When the temperature increases, the ratio increases if  $E_1 > E_2$  and decreases if  $E_2 > E_1$ . Consequently, the reaction having the larger activation energy is the one that is most sensitive to variations in temperature. The following general rule is appropriate to competing reactions: *High temperatures favor the reaction with the higher activation energy, and lower temperatures favor the reaction with the lower activation energy.*

For the parallel reactions in equation (10.7.1), one may use this general rule to select the following operating conditions as optimum from a selectivity viewpoint when the reactor operates isothermally. If  $E_1 > E_2$ , use a high temperature. If  $E_2 > E_1$ , use a low temperature.

On the other hand, if it is possible to use a temperature progression scheme and if one desires to obtain the maximum amount of the desired product per unit time per unit reactor volume, somewhat different considerations are applicable. If  $E_1 > E_2$ , one should use a high temperature throughout, but if  $E_2 > E_1$ , the temperature should increase

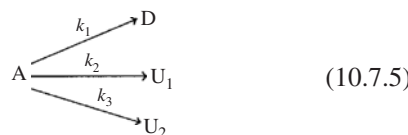
with time in a batch reactor or with distance from the reactor inlet in a plug flow reactor. It is best to use a low temperature initially to favor conversion to the desired product. In the final stages of the reaction a higher temperature is more desirable in order to raise the reaction rate, which has fallen off because of depletion of reactants. Even though this temperature increases production of the undesirable product, considerably more of the desired product is formed than would otherwise be the case. Thus one obtains a maximum production capacity for the desired product.

Now consider the basic series reaction scheme



where species  $D$  is the desired product. In this case the desired product distribution is favored when the ratio of the rate constants ( $k_1/k_2$ ) is made very large. Therefore, for operation at a single temperature, one should use a high temperature if  $E_1 > E_2$  and a low temperature if  $E_2 > E_1$ . On the other hand, if a temperature progression is to be employed, the relative magnitudes of the activation energies determine whether the initial temperature should be greater than or less than the final temperature. For example, if  $E_2 > E_1$ , the temperature should start out high to accelerate the first reaction and thus obtain a large output from a given reactor volume. However, the temperature should be progressively reduced as species  $D$  accumulates, to take advantage of the fact that the undesirable side reaction  $D \rightarrow U$  slows down faster with decreasing temperature than does the useful reaction. The problem of selecting an optimum temperature schedule has been treated by Bilous and Amundson (10).

For competitive-consecutive combinations of reactions a number of possible situations can arise. Two general guidelines are useful to keep in mind (11). First, if one has two undesirable products being formed in parallel with a desired species or with an intermediate product that can subsequently react to form the desired species,



there are three significant orderings of the activation energies. The type of temperature to use for each of these cases is as follows:

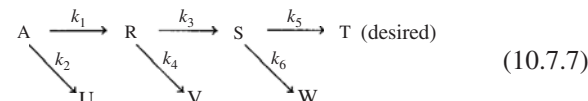
1.  $E_1 > E_2$  and  $E_1 > E_3$ ; use a high temperature.
2.  $E_1 < E_2$  and  $E_1 < E_3$ ; use a low temperature.
3.  $E_1 > E_2$  and  $E_1 < E_3$ , or  $E_1 < E_2$  and  $E_1 > E_3$ ; use an intermediate temperature.

In case 3 an intermediate temperature will give the most favorable product distribution. If  $E_1 > E_2$  and

$E_1 < E_3$ , one can show that the optimum temperature is given by

$$T = \frac{E_3 - E_2}{R \ln\{[(E_3 - E_1)/(E_1 - E_2)](A_3/A_2)\}} \quad (10.7.6)$$

A second generalization is applicable to steps occurring in series. If an early step requires a high temperature and a subsequent step is favored by a low temperature, a temperature sequence that decreases with increasing space time or reactor holding time should be used. Levenspiel (12) gives the following example of a situation of this type:



where  $E_1 > E_2$ ,  $E_4 > E_3$ , and  $E_5 > E_6$ .

The optimum temperature progression to use in this sequence is a high temperature to start, followed by lower temperatures where the concentration of species  $R$  is high and then increasing temperatures when the concentration of species  $S$  becomes appreciable. Levenspiel (13) summarized the results of several analyses of the optimum temperature level and progression to be used for several general reaction schemes.

Although a determination of the operating temperature that produces the most favorable product distribution is important in working up a reactor design for a reaction scheme involving multiple reactions, other considerations may be equally important from a design viewpoint. Optimization of the reactor economics requires a favorable product distribution, high conversions, and low capital costs. If the most favorable product distribution is obtained at low temperatures, very little of any product will be formed. In this case it will be more economical to use an intermediate temperature, because the adverse effects of a change in the product distribution will be more than offset by the increase in reaction rate and conversion. This approach will have the effect of increasing the production capacity of a given reactor. In the case where the most favorable product distribution is favored by operation at high temperatures, the highest permissible temperature should be used, because the reaction rates will be high and the requisite reactor size small.

## LITERATURE CITATIONS

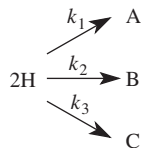
1. REYNOLDS, W. C., *Thermodynamics*, McGraw-Hill, New York, 1965.
2. SMITH, J. M., VAN NESS, H. C., and ABBOTT, M., *Introduction to Chemical Engineering Thermodynamics*, Seventh Edition, McGraw-Hill, New York, 2004.
3. TESTER, J. W., and MODELL, M., *Thermodynamics and Its Applications*, 3rd ed., Prentice Hall, Upper Saddle River, NJ, 1996.
4. SANDLER, S. I., *Chemical, Biochemical, and Engineering Thermodynamics*, Fourth Edition, Wiley, Hoboken, (2006).

5. KLAJKO, M., *Chem. Technol.*, **1** 141, (1971).
6. WASSERMAN, A., *Diels-Alder Reactions*, pp. 42, 50, and 52, Elsevier, London, 1965.
7. PERLMUTTER, D. D., *Stability of Chemical Reactors*, Prentice-Hall, Englewood Cliffs, NJ, 1971.
8. VAN HEERDEN, C., *Ind. Eng. Chem.*, **45** 1242 (1953).
9. KRAMERS, H., and WESTERERP, K. R., *Elements of Chemical Reactor Design and Operation*, pp. 124–128, Academic Press, New York, 1963.
10. BILOUS, O., and AMUNDSON, N. R., *Chem. Eng. Sci.*, **5**, 81,115 (1956).
11. LEVENSPIEL, O., *Chemical Reaction Engineering*, 2nd ed., p. 239, Wiley, New York, 1972.
12. *Ibid.*, p. 240.
13. *Ibid.*, p. 241.

## PROBLEMS

**10.1** A second-order exothermic reaction with the stoichiometry  $A \rightarrow 2B$  takes place in organic solution in a cascade of two identical CSTRs. To equalize the heat load on the two reactors it will be necessary to operate them at different temperatures. The reaction rates in each reactor will be the same, however. To minimize solvent losses by evaporation it will be necessary to operate the second reactor at 120°C, where the reaction rate constant is equal to 5 L/(mol·h). If the effluent from the second reactor corresponds to 90% conversion and if the molal feed rate to the cascade is 2000 mol/h when the feed concentration is 1.5 mol/L, how large must each of the reactors be? If the activation energy for the reaction is 20 kcal/mol, at what temperature should the first reactor be operated?

**10.2** V. Bulatov and I. Oref [*Int. J. Chem. Kinet.*, **25**, 1019–1027 (1993)] investigated the kinetics of the dimerization of *trans*-hexatriene in toluene solution. They indicate that a simplified form of the reaction network can be written as



where H refers to *trans*-1,3,5-hexatriene and A, B, and C refer to the three dimers that can be formed. Each of the reactions indicated is second order in species H. These researchers have reported the following expressions for the several rate constants:

$$\begin{aligned} k_1 &= 3.98 \times 10^7 e^{-5048/T} \\ k_2 &= 3.98 \times 10^7 e^{-4895/T} \\ k_3 &= 2.51 \times 10^6 e^{-4502/T} \end{aligned}$$

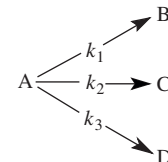
for  $k$  in  $M^{-1}/s$  and  $T$  in K.

(a) If the reactions indicated occur isothermally, at what temperature should a batch reactor be operated to maximize the yield of species B? What is the maximum yield? You may assume that it will be possible to exert sufficient pressure on the reaction mixture to maintain a liquid phase. You should employ the definition of the yield based on the amount of species H that reacts.

(b) If one desired to carry out the reactions indicated in a tubular reactor, what space time will be required to achieve 98% conversion of species H if the reactor is to operate isothermally under conditions that maximize the yield of species B? The feed concentration of species H is 1.5 M. What are the concentrations of species A, B, C, and H in the effluent from this reactor? What is the yield of species B?

(c) Now consider the possibility of carrying out the reaction in a single CSTR operating at the temperature that maximizes the yield of species B. What space time will give 98% conversion of species H? What are the corresponding effluent concentrations of species A, B, C, and H? How does the yield of species B compare to that obtained in the PFR?

**10.3** F. Thurner and U. Mann [*Ind. Eng. Chem. Process Des. Dev.*, **20**, 482 (1981)] investigated the kinetics of the pyrolysis of wood in the range 300 to 400°C at atmospheric pressure. A simplified view of the reactions involved may be expressed as



where A, B, C, and D represent wood, gas, tar, and char, respectively, and where

$$\begin{aligned} k_1 &= 8.607 \times 10^5 e^{-88.6/RT} \\ k_2 &= 2.475 \times 10^8 e^{-112.6/RT} \\ k_3 &= 4.426 \times 10^7 e^{-106.5/RT} \end{aligned}$$

for  $k$  in  $min^{-1}$ ,  $T$  in K, and  $R$  in  $kJ/(mol \cdot K)$ .

- (a) If the reactions above are regarded as irreversible, and if these reactions are to be accomplished in a batch reactor operating isothermally, determine the temperature at which the reactor should be operated to maximize the amount of char formed per unit of wood consumed.
- (b) Determine the time necessary to achieve 95% conversion of the wood in a batch reactor operating at the optimum temperature determined in part (a). What yields of the three product species will be obtained when operating at such conditions?
- (c) Consider operation of a batch reactor in which the batch starts at 300 K and is heated at a rate of 40 K/min until a temperature of 630 K is reached. What time is required to achieve a 95% conversion in this case? Will there be a major change in the product distribution observed if this mode of processing is employed?

**10.4** D. S. Sabo and J. S. Dranoff [*AICHE J.*, **16**, 211 (1970)] considered the question of the stability of a single CSTR in which the following consecutive first-order reactions occur:  $A \xrightarrow{k_1} V \xrightarrow{k_2} W$ . The article cited indicates that for appropriate property values, it is possible to obtain three steady-state

**Table P10.4**

Fluid density	60 lb/ft <sup>3</sup>
Reactor volume	100 ft <sup>3</sup>
Heat capacity of reaction mixture	1.0 Btu/[lb·°R]
Standard enthalpy changes	$\Delta H_{R1}^0 = -9885 \text{ Btu/lb}$ $\Delta H_{R2}^0 = -7000 \text{ Btu/lb}$
Rate constants for $k$ in $\text{s}^{-1}$ , $T$ in $^{\circ}\text{R}$ , and $R = 1.987 \text{ Btu}/(\text{lb mol} \cdot ^{\circ}\text{R})$	$k_1 = 6.08 \times 10^{15} e^{-47,000/RT}$ $k_2 = 5.40 \times 10^{12} e^{-35,000/RT}$
Overall heat transfer coefficient	60.57 Btu/(ft <sup>2</sup> ·s·°R)
Area for heat transfer	500 ft <sup>2</sup>
Volumetric feed rate	1800 ft <sup>3</sup> /s
Temperature of heat transfer medium	546°R
Feed temperature	690°R
Feed concentration of species A	0.50 lb/ft <sup>3</sup>
Feed concentrations of species C and W	0.0 lb/ft <sup>3</sup>

operating conditions. Determine the operating temperatures and effluent compositions corresponding to the process variables in Table P10.4. Indicate which of the steady-state conditions correspond to stable and which to unstable operating conditions. (Note that the conditions employed by Sabo and Dranoff have been modified so that  $k_1 \neq k_2$  and  $\Delta H_{R1}^0 \neq \Delta H_{R2}^0$ .)

- (a) Prepare a plot of the rate at which energy is being transformed by reaction versus the temperature of the reactor contents.
- (b) Prepare a plot of the rate at which the contents of the reactor are losing energy by the sum of thermal losses to the coolant and the difference between the sensible heats of the leaving and entering streams.
- (c) Indicate the conditions that prevail at steady state and discuss the stability of each steady state.
- 10.5** M. Shacham, N. Bauner, and M. B. Cutlip [*Chem. Eng. Edu.*, **28**, 30–35 (1994)] discussed the existence of multiple steady states for exothermic reactions being carried out in a single CSTR. In particular, these authors considered an irreversible first-order reaction of the form



as it takes place in an ideal CSTR equipped with a cooling jacket. The rate at which thermal energy is transferred from the contents of the reactor to the coolant flowing through the cooling jacket ( $Q$ ) is given by

$$Q = UA(\Delta T)_{lm}$$

where  $U$  is the overall heat transfer coefficient,  $A$  the area across which heat transfer takes place, and  $(\Delta T)_{lm}$  the log mean temperature difference between the contents of the CSTR and the coolant.

Use the parameter values summarized below to determine the steady-state temperature of both the reactor contents and the coolant stream exiting the jacket, as well

as the conversion level(s) corresponding to the specified operating conditions.

The liquid coolant is supplied to the jacket at a flow rate of 49.9 ft<sup>3</sup>/h and a temperature of 530°R. The coolant has a density of 62.3 lb/ft<sup>3</sup> and a heat capacity of 1.0 Btu/(lb mol·°R). The feedstock enters the reactor at a flow rate of 40 ft<sup>3</sup>/h and a temperature of 530°R. The reactor volume is 48 ft<sup>3</sup>. The feedstock has a density of 50 lb/ft<sup>3</sup> and a heat capacity of 0.75 Btu/(lb mol·°R). This heat capacity does not depend on the composition of this stream. The concentration of reactant M in the feed stream is 0.50 lb mol/ft<sup>3</sup>. The volumetric flow rate, density, and heat capacity of the effluent are the same as the corresponding properties of the feedstock.

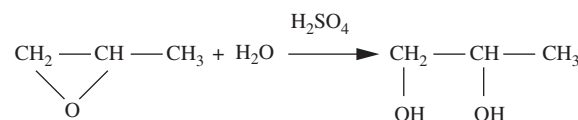
The area for heat transfer is 48 ft<sup>2</sup> and the value of the overall heat transfer coefficient is 150 Btu/(h·ft<sup>2</sup>·°R). The Arrhenius form of the rate constant is

$$k = 7.08 \times 10^{10} e^{-30,000/1.987T}$$

for  $k$  in  $\text{h}^{-1}$  and  $T$  in  $^{\circ}\text{R}$ . The standard enthalpy change for the reaction is  $-30,000 \text{ Btu/lb mol}$ .

- (a) Prepare a plot of the rate at which energy is being transformed by reaction versus the temperature of the reactor contents.
- (b) Prepare a plot of the rate at which the contents of the reactor are losing energy by the sum of thermal losses to the coolant and the difference between the sensible heats of the leaving and entering streams.
- (c) What conditions prevail at steady state? Discuss the stability of each steady-state condition.

- 10.6** T. Furusawa, H. Nashimura, and T. Miyauchi [*J. Chem. Eng. Jpn.*, **2**, 95–100 (1969)] studied stability phenomena in a single stirred-tank reactor using hydrolysis of propylene oxide as a model reaction:



Their results indicated that for this liquid-phase reaction enthalpy changes associated with both mixing streams of different composition and reaction were significant. Consider the problem of determining the steady-state operating conditions for a single CSTR. The reactor is well insulated and two feed streams enter the reactor, each at 18°C. The first feed stream consists of approximately equal volumes of propylene oxide and an inert solvent (methanol). The second feed stream is an aqueous solution of  $\text{H}_2\text{SO}_4$  (0.1% w/w). Additional operating parameters and physical property data are presented in the Table P10.6. The tabulated heat of formation data correspond to formation of the compounds as liquids. The total volumetric flow rate to the reactor is 14.41 m<sup>3</sup>/h. Volumetric expansion effects accompanying the reaction or mixing of the two feed streams may be regarded as negligible.

The rate expression may be regarded as pseudo first-order with  $k = 4.71 \times 10^9 e^{-18,000/RT} \text{ s}^{-1}$  for  $R$  in calories/(g·mol·K) and  $T$  in K.

**Table P10.6**

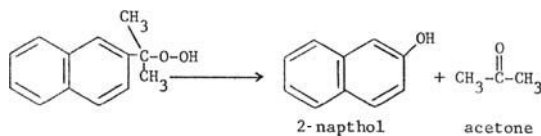
Species	Inlet flow rate (kg-mol/h)	$\Delta H_{f298}^0$ (kJ/g-mol)	Mean heat capacity [J/(mol·K)]
Propylene oxide	40	-122.6	125.6
Water	500	-285.8	75.35
Propylene glycol	0	-485.7	182.5
Methanol (inert)	67	-239.1	80.4

The enthalpy change associated with mixing the entering solution of propylene oxide in methanol with the incoming dilute solution of  $H_2SO_4$  is very significant in this system. For the ratio of feedstocks employed in the system being subjected to analysis, the enthalpy change can be regarded as equivalent to  $-9\text{ kJ/g-mol}$  of propylene oxide fed to the CSTR (i.e., the mixing process is exothermic and the energy liberated produces an effect that is equivalent to increasing the temperature of the inlet streams and neglecting the heat of mixing effect).

Conduct analyses that permit you to determine steady-state (and adiabatic) operating conditions (temperature and fraction conversion) for a single CSTR with a volumes of (1) 500 L, (2) 750 L, and (3) 1000 L.

Comment on the stability characteristics of the operating conditions you identify for each reactor. Can you relate your comments to something you may have observed in a chemistry laboratory or when watching a welder operate an acetylene torch?

**10.7** F. G. Boyaci, S. Takaç, and T. H. Özdamar [*Ind. Eng. Chem. Res.*, **38**, 3838 (1999)] studied the kinetics of the decomposition of 2-isopropynaphthalene hydroperoxide in the presence of acetic acid and hydrogen peroxide:



Professor Viejo Dinosaurio wishes to utilize this reaction as the basis for a laboratory demonstration that would illustrate both autothermal operation of a CSTR and reactor stability concepts. He plans to use a well-insulated reactor with an effective liquid volume of 1.0 L. The feed is to consist of a mixture of the hydroperoxide (HP), acetone (A), and acid catalyst at 25°C. Initial concentrations of hydroperoxide and acetone are 0.5 and 1.0 mol/L, respectively. The following property values are available: the standard heat of reaction at 25°C (estimated) =  $-60.5\text{ kcal/g-mol}$  and the heat capacity per liter of fluid (estimated) =  $406\text{ cal/(L}\cdot^\circ\text{C)}$ . This value may be taken as independent of the fraction conversion.

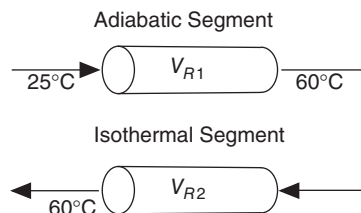
The rate expression,  $r = k_{\text{effective}} C_{\text{HP}}$  and at 60°C,  $k_{\text{effective}} = 0.543\text{ min}^{-1}$ . The activation energy is 25 kcal/g-mol.

If the feed rate is 1.0 L/min, determine the effluent conditions (temperature and degree of conversion). You may

assume that the boiling point of the liquid is not exceeded. Rumor has it that the effluent temperature is between 30 and 120°C and that Professor Dinosaurio may be asking a trick question that has two solutions within the temperature range indicated, only one of which corresponds to a stable operating point. Determine both solutions and perform calculations that indicate their stabilities.

**10.8** The irreversible enzyme-catalyzed reaction  $2\text{A} \rightarrow \text{B} + \text{C}$  is to be carried out in the liquid phase in a tubular reactor. The feedstock contains A at a concentration of 300 g/L and enters at a temperature of 25°C. The density of the feed stream is 0.95 kg/L and its volumetric flow rate is 0.8 m<sup>3</sup>/h. Thermochemical data indicate that at 25°C, the standard heat of reaction is  $-200\text{ cal/g}$  of A reacting. Experimental measurements indicate that the heat capacity of the liquid is essentially  $0.92\text{ cal/(g}\cdot^\circ\text{C)}$ , regardless of the extent of reaction. Bench-scale measurements indicate that over the temperature range of interest, the dependence of the first-order rate constant on temperature is given by  $k = 3.0 + 0.6(T - 25)$  for  $k$  in  $\text{h}^{-1}$  and  $T$  in °C.

Although it would be desirable from the standpoint of minimizing the reactor volume to operate the reactor adiabatically, the enzyme catalyst rapidly loses its activity when the temperature rises above 60°C. Hence, it is suggested that the following combination of adiabatic and isothermal tubular reactors be employed to achieve 90% conversion of A to B:



- Determine the volume requirements for both the adiabatic and isothermal segments of the reactor network.
- What are the heat transfer requirements for the isothermal segment of the reactor? Is thermal energy added to or removed from the isothermal segment?

**10.9** J. M. Castro, S. D. Lipshitz, and C. W. Macosko [*AIChE J.*, **28**, 973 (1982)] modeled a thermosetting polymerization reaction in a laminar flow reactor under several different operating conditions. Demonstrate your ability to simulate the performance of a plug flow reactor for this reaction under both isothermal and adiabatic reaction conditions. In particular, determine the reactor space times necessary to achieve 73% conversion for both modes of operation and the following parameter values for a (3/2)-order reaction ( $r = kc^{1.5}$ ).

$$k = Ae^{-E/RT} \text{ with } A = 3.14 \times 10^8 (\text{m}^3/\text{g-equiv})^{0.5}/\text{min}$$

$$E = 64.64 \text{ kJ/mol}$$

$$\Delta H_R^0 = -60.33 \text{ kJ/g-equiv}$$

$$C_p = 1.875 \text{ kJ/(kg}\cdot\text{K)}$$

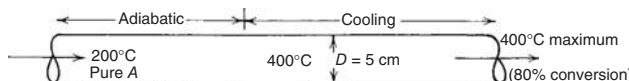
$$\rho = 1075 \text{ kg/m}^3$$

The liquid feedstock consists of an extended diisocyanate prepolymer and a caprolactone-based triol. The feed enters the reactor at 318 K with an initial reactive group concentration of  $2.64 \times 10^3$  g-equiv/m<sup>3</sup>. The feed flow rate is 1.05 m<sup>3</sup>/min. What reactor volumes are required in each case? At what rate must thermal energy be removed to keep the system isothermal? What is the effluent temperature when the reactor operates adiabatically?

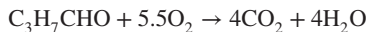
- 10.10** The liquid-phase reaction  $A \rightarrow B$  is to be carried out in a tubular reactor operating at a constant pressure of 202.6 kPa. The feed rate is 600 kmol/ks of pure A with an inlet temperature of 200°C. Pure A has a specific volume of 0.056 m<sup>3</sup>/kmol. The heat of reaction at 200°C is -15 kJ/mol. The molar specific heats of A and B are both 42 J/(mol·K). The reaction rate constant near this temperature can be approximated by

$$k = 110 + 0.8(T - 200)$$

for  $k$  in ks<sup>-1</sup> and  $T$  in °C. Although it would be desirable to run the reactor adiabatically, the maximum reaction temperature allowable is 400°C. Above this temperature undesirable byproducts are formed. Calculate the *minimum* reactor volume required to obtain 80% conversion of A. What must the heat transfer rate be in the cooled section of the reactor?



- 10.11** A. S. Dryakhlov, N. N. Golubeva, L. I. Kalinkina, V. A. Prokhorov, V. M. Kisarov, and S. L. Kiperman [*Kinet. Catal.*, **22**, 757 (1979)] studied the kinetics of the oxidation of small quantities of butyraldehyde in air as a vehicle for modeling the problem of combustion of the volatile organic compounds that are by-products of synthetic fatty acid production. The reaction stoichiometry is



Over the Pt/Al<sub>2</sub>O<sub>3</sub> catalyst employed by these researchers, the effective rate expression, expressed per unit volume of catalyst bed, is of the form

$$r = \frac{kC_4}{1 + k_1 C_4}$$

for  $r$  in mmol/(m<sup>3</sup>·s) and  $C_4$  in mmol/m<sup>3</sup>, and where the kinetic parameters ( $k$  and  $k_1$ ) are  $5.28 \times 10^6 e^{-11,072/T} \text{ s}^{-1}$  and  $0.72 \times 10^{-4} e^{2466/T} \text{ m}^3/\text{mmol}$ , respectively, for  $T$  in K. This expression is valid for small particles where heat and mass transfer effects are negligible. For our present purposes, it will be assumed to be applicable to the temperature range 300 to 750 K.

If 1000 m<sup>3</sup>/h of effluent gases containing 10 mmol/m<sup>3</sup> of C<sub>3</sub>H<sub>7</sub>CHO (remainder is air) is to be treated to reduce the effluent concentration of C<sub>3</sub>H<sub>7</sub>CHO to 0.5 mmol/m<sup>3</sup> or less, determine the volume of tubular reactor (packed with catalyst) necessary to effect the desired conversion if adiabatic

operation is utilized. Prepare a plot of reactor volume versus the fraction of the C<sub>3</sub>H<sub>7</sub>CHO that reacts for effluent concentration values between 0.5 and 0.01 mmol/m<sup>3</sup>.

The properties of the feed and effluent streams are essentially those of pure air at 1 atm and the temperature in question [ $C_p \approx 7.0 \text{ cal}/(\text{mol} \cdot \text{C})$ ]. Ideal gas behavior may be assumed. For the reaction above, the standard heat of reaction may be taken as independent of temperature and equal to -558.4 kcal/mol C<sub>3</sub>H<sub>7</sub>CHO. The feed gases enter the reactor at 650 K. Remember that at a fixed pressure and composition, the volume of an ideal gas is proportional to its absolute temperature.

- 10.12** Consider the reaction used as the basis for Illustrations 10.1 to 10.3. Determine the volume that would be required to produce 2 million pounds of B annually in a plug flow reactor operating isothermally at 163°C. Assume that 97% of the A fed to the reactor is to be converted to B and that the reactor can be operated for 7000 h annually. Determine the manner in which the heat transfer requirement is distributed along the length of the reactor, that is, what fraction of the heat evolved must be removed in the first 10% of the reactor length, the second 10%, the third 10%, etc.?

- 10.13** Consider the cascade of two nonidentical CSTRs and associated heat exchangers shown in Figure P10.13. In particular, consider the problem of steady-state operation of this cascade in an autothermal mode in which the feed stream flows in countercurrent fashion through heat exchangers in each reactor so as to be heated to a temperature at which the reaction becomes self-sustaining. The areas of the heat exchangers in the two reactors differ appreciably.

The overall rate of heat transfer to the contents of a particular reactor is described by a relation of the form  $Q = UA\Delta T$  where the appropriate temperature difference is a logarithmic mean temperature difference between the temperature of the fluid flowing through a particular heat exchanger and the temperature of the contents of the corresponding reactor.

The reaction A + B → C is characterized by a mixed second-order rate expression  $r = kC_A C_B$  and a standard heat of reaction of -80.0 kJ/mol. The feed stream is a liquid with a density of 0.8 kg/L and a heat capacity of 3.6 J/(g·°C). The flow rate of the feed stream is 4000 L/h. The concentrations of species A and B in the feed stream are 2.0 and 2.5 M, respectively. The feed stream enters heat exchanger 2 (HE2) at 20°C and leaves this exchanger at 40°C. The effluent from HE2 flows through a well-insulated line to the heat exchanger in reactor 1 (HE1) and leaves this exchanger at 60°C. The temperature of the reaction mixture leaving the first reactor is 70°C. The rate constant  $k$  is given by the expression

$$k = 1.397 \times 10^{22} e^{-(150,000/RT)}$$

for  $k$  in M<sup>-1</sup>/h<sup>-1</sup>,  $R$  in J/(mol·K), and  $T$  in K.

- (a) Determine the requisite size of each individual CSTR and the conversion leaving the first reactor.  
 (b) Determine the temperature at which the reaction mixture leaves the second reactor if the specified value for the overall conversion in the cascade is 95%.

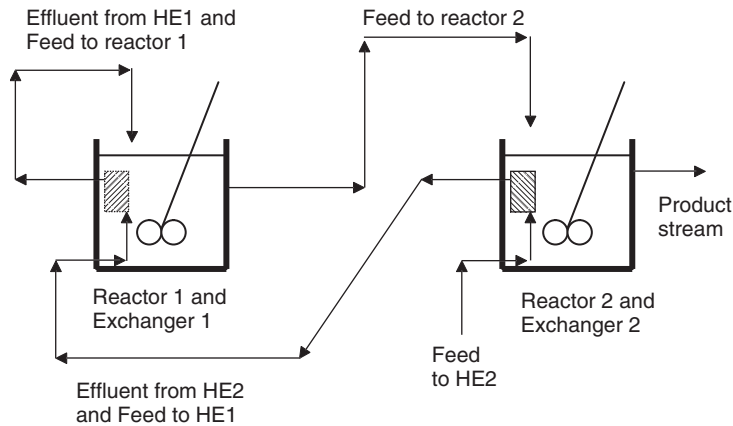
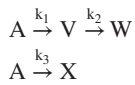


**Figure P10.13** Schematic diagram of cascade of stirred-tank reactors and associated heat exchangers.

- (c) If the overall heat transfer coefficients in each reactor are the same, and if  $10 \text{ m}^2$  of heat transfer area are provided in the first reactor, what is the area required for the heat exchanger in the second reactor?

- 10.14** Consider a reactor network consisting of two identical CSTRs operating in a cascade configuration. The feed stream consists of reactant A dissolved in an inert liquid. Species A may react according to the reaction scheme:



where each of the reactions indicated is first-order. Consider first the general case in which each reactor will operate at a different temperature.

- (a) Derive general equations for the concentrations of species A, V, W, and X leaving each reactor in terms of the space time for a single reactor  $\tau$ . Express your answers in terms of  $C_{A0}$ ,  $k_1^I$ ,  $k_1^I$ ,  $k_1^I$ ,  $k_3^I$ ,  $k_1^{II}$ ,  $k_2^{II}$ ,  $k_3^{II}$ , and  $\tau$ . The superscripts on the rate constants indicate the temperature at which they are evaluated (I for that of reactor 1 and II for reactor 2).

- (b) The temperature at which the effluent leaves the first reactor is  $150^\circ\text{C}$ . At this temperature,  $k_1^I = 0.023 \text{ min}^{-1}$ ,  $k_2^I = 0.014 \text{ min}^{-1}$ , and  $k_3^I = 0.006 \text{ min}^{-1}$ . If the first reactor is operated adiabatically, determine the standard heat of reaction for the second reaction. In addition, determine the amount of heat removed (or added) in the second reactor if the temperatures of the feed to and the effluent from this reactor are both  $150^\circ\text{C}$ . If species V is the desired product, what do you recommend?

- (c) If the cooling capacity of the second reactor is increased so that the effluent from the second CSTR is now at  $140^\circ\text{C}$ , the rate constants at this temperature become  $k_1^{II} = 0.020 \text{ min}^{-1}$ ,  $k_2^{II} = 0.007 \text{ min}^{-1}$ , and  $k_3^{II} = 0.003 \text{ min}^{-1}$ . If the feed to the second CSTR remains at  $150^\circ\text{C}$ , determine the new effluent composition and the new heat transfer requirements. Comment.

Potentially useful data for parts (b) and (c):

$$\Delta H_1^0 = -20,000 \text{ cal/mol, independent of temperature}$$

$$\Delta H_3^0 = -15,000 \text{ cal/mol, independent of temperature}$$

The standard enthalpy change for reaction 2 is also independent of temperature. The heat capacity of the reacting liquid is  $0.8 \text{ cal}/(\text{cm}^3 \cdot ^\circ\text{C})$ .

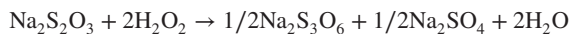
$$\text{reactor volume} = 1000 \text{ L}$$

$$\text{volumetric flow rate} = 10 \text{ L}/\text{min}$$

$$C_{A0} = 2.5 \text{ mol/L}$$

$$\text{temperature of feed to first reactor} = 50^\circ\text{C}$$

- 10.15** The reaction between sodium thiosulfate and hydrogen peroxide in aqueous solution



is characterized by a rate expression of the form

$$r = k C_A C_B$$

where A refers to thiosulfate and B to peroxide.

As reported by K. F. Lin and L. L. Wu [*Chem. Eng. Sci.*, **36**, 435 (1981)],

$$k = 2.00 \times 10^{10} e^{-68,200/RT}$$

for  $k$  in  $\text{m}^3/(\text{kmol}\cdot\text{s})$ ,  $R$  in  $\text{J}/(\text{mol}\cdot\text{K})$ , and  $T$  in  $\text{K}$ .

The aforementioned researchers have utilized experimental and computer simulation studies of this reaction to assess the performance of adiabatic reactors subjected to various modes of operation. An analysis of the performance of a plug flow reactor operated adiabatically with a feed entering at  $20^\circ\text{C}$  that is  $0.4 \text{ M}$  in thiosulfate and  $0.6 \text{ M}$  in hydrogen peroxide indicates that the space time necessary to achieve 70% conversion of the limiting reagent is 38.9 s.

- (a) What is the temperature of the effluent from the plug flow reactor if the enthalpy change accompanying the reaction at  $25^\circ\text{C}$  is  $-586.2 \text{ kJ}/(\text{mol Na}_2\text{S}_2\text{O}_3 \text{ reacted})$ , and the heat capacity of the process fluid is  $4.186 \text{ kJ}/(\text{L}\cdot\text{K})$ ?

- (b) Consider the corresponding analysis of a single CSTR that is operated adiabatically. For this type of reactor, what is the space time necessary to achieve 70% conversion? What is the corresponding effluent temperature?
- (c) Comment on the relative volumes required to achieve 70% conversion for adiabatic operation of the PFR and the CSTR.
- 10.16** Consider a reactor network consisting of a CSTR followed by a PFR. The CSTR has a volume of 4.0 m<sup>3</sup> and is operated adiabatically for the reversible exothermic reaction of interest: namely,



This reaction is first-order in both the forward and reverse directions: that is,

$$r = k_f(B) - k_r(D)$$

The feed to the CSTR consists solely of B dissolved in an inert organic solvent at a concentration of 4.2 M. The effluent from the CSTR is characterized by a temperature of 250°C. The volumetric feed rate is to be determined from the constraint that the temperature leaving the CSTR is that which maximizes the reaction rate at the effluent conversion.

The rate constants for this reversible reaction can be written as

$$k_f = A_f e^{-E_f/RT} \text{ and } k_r = A_r e^{-E_r/RT}$$

where

$$A_f = 1306 \text{ s}^{-1}$$

$$A_r = 2.82 \times 10^5 \text{ s}^{-1}$$

$$E_f = 14,500 \text{ cal/mol}$$

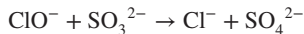
$$E_r = 20,000 \text{ cal/mol}$$

**(a)** Determine:

1. The fraction conversion leaving the CSTR.
2. The appropriate volumetric flow rate.
3. The temperature at which the process fluid enters the CSTR.

**(b)** On exiting the CSTR, the process fluid enters the tube side of a single pass shell-and-tube heat exchanger. The fraction conversion leaving the heat exchanger (based on the feed to the CSTR) is 0.80. The volumetric heat capacity of the process fluid is  $9.24 \times 10^5 \text{ cal/(m}^3 \cdot ^\circ\text{C)}$ . If the temperature of the effluent from the heat exchanger is 100°C, determine the rate at which thermal energy is transferred in the heat exchanger. Is heat added to, or removed from, the process fluid?

- 10.17** NaOCl is often added to power plant cooling water streams to keep condenser tubes free from slime. When such streams are discharged to the environment, they threaten aquatic life unless the residual hypochlorite is removed by reaction. One route by which such removal can be accomplished is by addition of sodium sulfite to effect the reaction



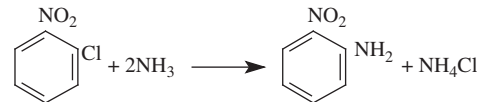
R.D. Srivastava, P. C. Nigam, and S. K. Goyal [*Ind. Eng. Chem. Fundam.*, **19**, 207 (1980)] reported that this reaction obeys second-order kinetics:

$$r = k(\text{ClO}^-)(\text{SO}_3^{2-})$$

with a rate constant of 1730 L/(mol·sec) at 15°C and an activation energy of 15.6 kcal/mol. If a cooling water stream containing ClO<sup>-</sup> is blended with a stream containing Na<sub>2</sub>SO<sub>3</sub> to produce a stream for discharge at 15°C in which the residual ClO<sup>-</sup> and SO<sub>3</sub><sup>2-</sup> concentrations are 0.050 M and 0.055 M, respectively, determine the residual ClO<sup>-</sup> level in the effluent from a discharge tube that is 2 m long and 7.5 cm in diameter. The discharge rate is 60 L/s and conditions are such that heat transfer to or from the discharge tube is negligible. How does this answer compare with that predicted by the assumption of isothermal operation at 15°C?

The thermodynamic properties of the discharge stream are equal to those of pure water. The standard enthalpy change for the reaction of interest is -81.3 kcal/mol.

- 10.18** M. D. Gordon, G. J. O'Brien, C. J. Hensler, and K. Marcali [*Plant/Oper. Prog.*, **1**, 27 (1982)] utilized a mathematical model to assess the thermal hazard (explosion potential) associated with the amination of ortho-nitrochlorobenzene (ONCB) with aqueous ammonia:



The following rate expression is applicable:

$$r = \frac{-d(\text{ONCB})}{dt} = 1.52 \times 10^8 [\text{NH}_3][\text{ONCB}]_{aq} e^{-E/RT}$$

where  $E = 94.2 \text{ kJ/mol}$ ,  $T$  is expressed in K, concentrations in mol/L, and the rate in mol/(L·min). Amination is assumed to occur in the aqueous phase in which the solubility of [ONCB] may be limited, depending on the temperature and ammonia concentration. Although the organic product of this reaction is itself susceptible to explosive decomposition, we wish to consider only the aforementioned reaction as a basis for a preliminary determination of reactor productivity subject to the requirement that the temperature of the reactor effluent not exceed 240°C.

- (a)** If the autoclave is modeled as a single CSTR with a volume of 400 L, and if no solubility limits are incurred, determine the rate at which thermal energy must be added (or removed) if the autoclave is to operate at 220°C when the total volumetric feed rate is 16 L/min. The feed stream enters the reactor at 210°C. The feed stream is 0.635 M in ONCB and 4.2 M in ammonia. The heat capacity of the process fluid is 3.97 kJ/(L·°C). Sufficient pressure is maintained in the autoclave to ensure that the process fluid remains liquid. The standard enthalpy change for the reaction may be taken as -126 kJ/mol within the temperature range from 150 to 300°C. What conversion will be achieved under these

conditions? Do not make any more assumptions than are absolutely necessary to solve this problem. In particular, you should not assume that the reaction obeys pseudo first-order kinetics.

- (b) To approximate the maximum temperature rise that will occur if the flow of coolant is lost, analyze the autoclave as if it were operating adiabatically. The flow rate and composition of the feed stream are the same as in part (a). Determine the effluent temperature and the fraction of the ONCB that is converted to the product amine. Note that a trial-and-error approach or use of an equation solver will be required. As a first guess, consider an effluent conversion of 60% and refine this value in subsequent iterations to obtain an answer containing three significant figures.

- 10.19** A battery of two identical CSTRs is currently employed to effect a reversible hydration reaction with a stoichiometry of the form



Because the reaction takes place in aqueous solution, the concentration of water (W) remains substantially constant throughout the course of the reaction. Hence, the rate expression for the forward reaction can be regarded as pseudo first-order in the reactant E. The rate of the reverse reaction is first-order in the product P. Each reactor has a volume of 500 gal.

- (a) If the battery is operated so that the temperature of the contents of each reactor is 50°C, determine the steady-state concentrations of species E and P in the effluent stream when the feed flow rate is 20 gal/min. At 50°C the apparent rate constants for the forward and reverse reactions are

$$k_f = 0.12 \text{ min}^{-1}$$

$$k_r = 3 \times 10^{-3} \text{ min}^{-1}$$

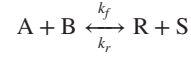
The concentration of species E in the feed stream is 2.5 M. Species P is not present in the feed stream to the first reactor.

- (b) Consider the possibility of increasing by 25% the production capacity of the reactor network described above by employing different temperatures in the reactors in the cascade (subject to the constraints described below).
1. The overall conversion at steady state must be at least as large as that obtained in part (a). The new feed rate is to be 25 gal/min.
  2. The first reactor in the cascade is to continue to operate at 50°C. The second reactor is to operate at a higher temperature, but this temperature remains to be determined.

At what temperature should the second reactor be operated if the activation energies for the forward and reverse reactions are 18 and 20 kcal/mol, respectively? Determine the conversion in the effluent from the second reactor when it operates at 60°C and then indicate whether the requisite temperature will be greater or less

than this value. Comment on the values you calculate for the effluent concentrations of species E for each reactor in part (b).

- 10.20** Consider the problem of minimizing the volume of a tubular reactor that is to be operated under nonisothermal conditions. The gas-phase reaction of interest has a stoichiometry of the form



with a rate expression

$$r = k_f C_A C_B - k_r C_R C_S$$

where

$$k_f = 30 e^{-9500/RT} \text{ m}^3 / (\text{kmol} \cdot \text{s})$$

$$k_r = 4.3 \times 10^4 e^{-16,000/RT} \text{ m}^3 / (\text{kmol} \cdot \text{s})$$

for  $T$  in K and  $R$  in cal/(mol·K).

- (a) Derive the equation relating the temperature and the fraction conversion that leads to the minimum space time necessary to accomplish a specified conversion task. Consider the case in which the inlet concentrations are  $C_{A0} = C_{B0} = 50 \text{ mol/m}^3$  and  $C_{R0} = C_{S0} = 3 \text{ mol/m}^3$ . Prepare a plot of the optimum operating temperature versus fraction conversion for conversions of the A fed to the reactor ranging from 0.00 to 0.80. Be sure to incorporate volumetric expansion effects associated with thermal expansion of the gas in your analysis. The inlet temperature corresponding to the cited value of  $C_{A\text{in}}$  is 1466 K.
- (b) Determine the minimum tubular reactor volumes required to obtain 70% and 80% conversion of the A fed to the reactor when the optimum temperature profile is employed. The inlet volumetric flow rate is 500  $\text{m}^3/\text{h}$ .
- (c) Now consider an alternative mode of operation. Suppose that the first portion of the tubular reactor is operated isothermally at 600 K until the fraction conversion reaches 22.0% and thereafter at the optimum temperatures determined in part (b) until the overall conversion reaches the desired level. The feed concentrations are as stated in part (a). Remember to correct for the difference in the inlet temperature of part (a) and the new feed temperature of 600 K. What volumes now correspond to conversions of 70% and 80%? Comment on the difference in volume requirements.

- 10.21** Consider the task of designing a reactor network for a reversible exothermic reaction with the stoichiometry  $A \leftrightarrow B$ . The rate expression is

$$r_B = k_1 C_A C_B - k_2 C_B^2$$

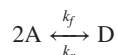
with  $k_1 = 31.4 e^{-7,200/RT}$  and  $k_2 = 3.48 \times 10^8 e^{-18,200/RT}$  for  $k$  in  $\text{L}/(\text{mol} \cdot \text{s})$ ,  $T$  in K,  $R$  in  $\text{cal}/(\text{mol} \cdot \text{K})$ , and  $r_B$  in  $\text{mol}/(\text{L} \cdot \text{s})$ .

To take advantage of the autocatalytic nature of this reaction, it has been suggested that the first reactor in the network be a CSTR operating under conditions that maximize

the rate. Determine the temperature and extent of conversion that correspond to the optimum. The feed consists of a solution that is 2.0 M in species A and 0.04 M in species B. What space time should be employed for the CSTR if one is to operate under conditions that maximize the reaction rate?

Because this autocatalytic reaction is reversible and exothermic, the maximum extent of reaction is limited by thermodynamic considerations. If the CSTR operating at a temperature corresponding to the maximum rate is followed by a second CSTR operating at the same temperature so that an overall conversion based on the amount of species A fed to the reactor is 30%, what would be the space time for this CSTR? This conversion is slightly below the equilibrium conversion of 32%. The search for conditions that would give a much higher yield (say 83%) of product would require use of an additional reactor operating at a lower temperature because of the exothermic nature of the reaction. Consider adding a PFR operating at room temperature (298 K) following the second CSTR. What should the corresponding space time for the CSTR be?

- 10.22** In the presence of an appropriate catalyst, monomer A reacts to form dimer D in a reversible reaction,



with a rate expression  $r = k_f(A)^2 - k_r(D)$  in which the influence of the catalyst is incorporated in the rate constants  $k_f$  and  $k_r$ .

The rate constants can be written as

$$k_f = 4.10 \times 10^6 e^{-15,000/RT}$$

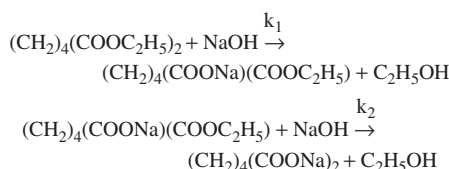
$$k_r = 1.22 \times 10^9 e^{-20,000/RT}$$

for  $R$  in cal/(mol·K),  $T$  in K,  $k_f$  in  $M^{-1}s^{-1}$  and  $k_r$  in  $s^{-1}$ .

A solution of A (3.0 M) at 300 K is fed to a cascade of two stirred tanks at a rate of 250 L/h. Process specifications require that 80% of the monomer be converted to dimer. The second reactor in the cascade is to be operated at the temperature that maximizes the reaction rate at this conversion. The first reactor operates at 325 K.

- (a) If both reactors are to be the same size, how large must they be?  
 (b) What is the value of the standard enthalpy change for this reaction?  
 (c) Determine the rate at which thermal energy must be delivered to or removed from the second reactor if the heat capacity of the process fluid is 850 cal/(L·C).

- 10.23** M. R. Newberger and R. H. Kadlec [AIChE J., **19**, 1272 (1973)] studied the saponification of diethyl adipate (A) in alkaline solution. The chemical reactions of interest are



The rate constants for these reactions are given by

$$k_1 = 4.87 \times 10^6 e^{-42.2/RT}$$

$$k_2 = 3.49 \times 10^3 e^{-25.0/RT}$$

for rate constants in  $m^3/(kmol \cdot s)$ , temperature in K, and  $R$  in  $MJ/(kmol \cdot K)$ . (The preexponential factor for the second rate constant was actually reported as 1000 times larger. However, according to other data in the article cited, the correct value is as stated.)

The corresponding standard heats of reaction are

$$\Delta H_1 = -45.2 \text{ MJ/kmol}$$

$$\Delta H_2 = -68.0 \text{ MJ/kmol}$$

Consider a cascade of two identical stirred tanks that is being used to carry out these reactions. The feed stream enters at a rate of 100  $m^3/h$  and a temperature of 300 K. Both reactors operate at the same temperature. When operating at steady state, each reactor is characterized by a space time of 72.5 s. The initial concentrations of NaOH and diethyl adipate are 0.5 and 0.2 kmol/ $m^3$ , respectively.

- (a) Determine the composition of the effluent from each reactor.  
 (b) What is the rate at which thermal energy must be removed from each reactor to sustain isothermal operation?  
 (c) Now consider the case of adiabatic operation. If the entire cascade is adiabatic and if the heat capacity of the solution is equal to that of water (4.186 MJ/ $m^3$ ), determine the temperature of the effluent from each reactor and the concentrations of reactants and products in the effluent from each reactor.

- 10.24** For a hypothetical reversible exothermic reaction of the type  $A \xrightleftharpoons[k_r]{k_f} B$ , a plot of fraction conversion in a single CSTR versus the operating temperature exhibits a maximum because of the interplay between kinetic and thermodynamic effects. Consider the case for which both the forward and reverse reaction rate expressions are first-order. Use the rate constants below to prepare a plot of the equilibrium fraction conversion as a function of temperature. In addition, prepare a plot of the fraction conversion that will be achieved at a flow rate of 0.1  $m^3/min$  in an ideal CSTR with a volume of 1.0  $m^3$  versus the temperature of the reactor contents. Use these curves and the data given below to ascertain optimum operating conditions.

- (a) What are the activation energies of the forward and reverse reactions? What is the standard enthalpy change for the reaction? Is the reaction exothermic or endothermic?  
 (b) What fraction conversion corresponds to a flow rate of 0.08  $m^3/min$  and an effluent temperature of 340 K?  
 (c) Derive the equation for the curve describing the energy balance on the CSTR for adiabatic operation. To maximize production of B when the flow rate is 0.1  $m^3/min$ , what inlet temperature should be specified?

The rate constants for the forward and reverse reactions can be written in Arrhenius form as

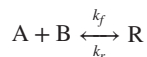
$$k_f = 5.3 \times 10^6 e^{-12,500/RT} \text{ min}^{-1}$$

$$k_r = 2.5 \times 10^{17} e^{-29,700/RT} \text{ min}^{-1}$$

where  $R$  is 1.987 cal/(g-mol·K) and  $T$  is expressed in K.

The feed stream contains species A at a concentration of 1.5 M dissolved in a solvent S. The heat capacity of the solution is 800 kcal/(m<sup>3</sup>·K), regardless of the extent of reaction.

- 10.25** Consider the task of designing a single stirred-tank reactor for accomplishing the reversible addition reaction



The feed flow rate is to be 0.20 m<sup>3</sup>/h and the feed concentrations of species A and B are to be 1.5 M and 0.75 M, respectively. The CSTR is to be operated at the temperature that maximizes the reaction rate at an effluent conversion of

70% of the limiting reagent. If the feedstock enters at 25°C, determine:

- the temperature at which the CSTR should operate,
- the volume of the CSTR,
- the heat transfer rate required for the CSTR.

The data are as follows:

$$k_f = A_f e^{-E_f/RT}$$

$$k_r = A_r e^{-E_r/RT}$$

$$A_f = 31.4 \text{ L/(mol·s)}$$

$$A_r = 3.06 \times 10^7 \text{ s}^{-1}$$

$$E_f = 7.20 \text{ kcal/mol}$$

$$E_r = 18.00 \text{ kcal/mol}$$

$$\Delta H_R^0 = -10.80 \text{ kcal/mol}$$

for the temperatures of interest

For the temperature range of interest, the density of the feed stream is 0.90 kg/L and its heat capacity is 0.95 cal/(g·C).

# Chapter 11

---

## Deviations from Ideal Flow Conditions

### 11.0 INTRODUCTION

The flow patterns in real reactors do not conform exactly to those postulated for the ideal plug flow and continuous flow stirred-tank reactor models. Nonetheless, the conversions achieved in many real reactors so closely approximate those predicted on the basis of the idealized models that the design equations for these reactors can be used in preliminary design calculations with negligible error. In other cases, significant differences are noted between observed and predicted results. These differences may arise from a number of sources: from channeling of fluid as it moves through the reaction vessel, from longitudinal mixing caused by vortices and turbulence, from the presence of stagnant regions within the reactor, from bypassing or short-circuiting of portions of a packed reactor bed, from the failure of impellers or other mixing devices to provide perfect mixing, and so on. In this chapter we aim to establish a rational basis for examining quantitatively and qualitatively the effect of departures from idealized flow behavior on the performance of a reactor. Read this chapter with a view toward developing a “seat of the pants” feeling for the magnitude of deviations from ideal flow conditions in various types of reactors so that you will know when these effects can be neglected and when they must be treated by the techniques developed in this chapter. In principle, if the temperatures, velocities, flow patterns, and local rates of mixing of every element of fluid in a reactor were known, and if the differential material and energy balances could be integrated over the reactor volume, one could obtain an exact solution for the composition of the effluent stream and thus the degree of conversion that takes place in the reactor. However, most of this information is lacking for the reactors used in laboratory or commercial practice. Consequently, it has been necessary to develop approximate methods for treating nonideal flow systems in terms of data that are easily obtained experimentally. From measurements on the feed and effluent streams, one may develop parameters that can be used to characterize

the magnitude of system nonidealities and to serve as input to more complex models of reactor behavior than ideal CSTRs and PFRs. We begin by indicating how such measurements can be used to determine the residence time distribution function for a reactor, and then treat three different mathematical models that permit estimation of the conversion that will be attained. Throughout this chapter we restrict our discussion to systems in which a single reaction takes place in a homogeneous isothermal reactor. Volume changes on reaction are also assumed to be negligible ( $\delta \approx 0$ ). These restrictions will permit us to focus our attention on the nonideal flow conditions.

### 11.1 RESIDENCE TIME DISTRIBUTION FUNCTIONS, $F(t)$ AND $dF(t)$

Except for the case of an ideal plug flow reactor, different fluid elements will take different lengths of time to flow through a chemical reactor. To be able to predict the behavior of a given piece of equipment as a chemical reactor, one must be able to determine how long different fluid elements remain in the reactor. One does this by measuring the response of the effluent stream to changes in the concentration of inert species in the feed stream: called the *stimulus-response technique*. In this section we discuss the analytical form in which the distribution of residence times is cast, derive relationships of this type for various reactor models, and illustrate how experimental data are treated to determine the distribution function.

The mathematical relations expressing the different amounts of time that fluid elements spend in a given reactor may be expressed in a variety of forms [see, e.g., Levenspiel (1–3) and Himmelblau and Bischoff (4)]. In this book we utilize the cumulative residence-time distribution curve [ $F(t)$ ], as defined by Danckwerts (5) for this purpose. For a continuous flow system,  $F(t)$  is the volume fraction of

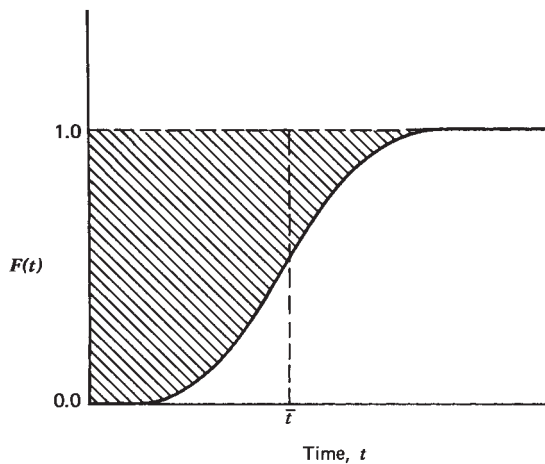


**Figure 11.1** Determination of average residence time from the cumulative residence time distribution function.

the fluid at the outlet that has remained in the system for a time less than  $t$ . In other words, if we were to assign “ages” to the various fluid elements leaving the system,  $F(t)$  would be the volume fraction of the outlet stream having an age less than  $t$ , age being measured relative to the time at which the fluid element entered the reactor. For constant density systems, volume fractions are identical with weight fractions, and  $F(t)$  is also the weight fraction of the effluent with an age less than  $t$ . In accordance with this definition of the  $F(t)$  curve, the probability that an element of volume entering the system at time  $t = 0$  has left it within a period of time  $t$  is just equal to  $F(t)$ . The probability that it is still in the reactor and will leave at a time later than  $t$  is  $1 - F(t)$ . It will always take a finite time for a fluid element to traverse the system, so  $F(t) = 0$  at  $t = 0$ . Similarly, none of the material can remain in the flow reactor indefinitely, so  $F(t) = 1.0$  at  $t = \infty$ . Figure 11.1 indicates these limiting values for an arbitrary  $F(t)$  curve.

Because  $F(t + dt)$  represents the volume fraction of the fluid having a residence time of less than  $t + dt$ , and  $F(t)$  represents that having a residence time of less than  $t$ , the differential of  $F(t)$ , namely,  $dF(t)$ , will be the volume fraction of the effluent stream having a residence time between  $t$  and  $t + dt$ . Hence,  $dF(t)$  is known as the *differential residence-time distribution function*. From the principles of probability the average residence time ( $\bar{t}$ ) of a fluid element is given by

$$\bar{t} = \int_{F(t)=0}^{F(t)=1} t \, dF(t) \quad (11.1.1)$$

or

$$\bar{t} = t = \int_{t=0}^{t=\infty} t \left( \frac{dF(t)}{dt} \right) dt \quad (11.1.2)$$

Consequently, the shaded area in Figure 11.1 is equal to  $\bar{t}$  and the shaded area to the right of  $t = \bar{t}$  must be equal to the unshaded area to the left of  $1$ .

### 11.1.1 Experimental Determination of Residence Time Distribution Functions

To be able to make use of the cumulative residence-time distribution function in the analysis of a specific reactor network, one must be able to determine this function experimentally. This task is accomplished by changing some property of the fluid entering the network as a function of time and then noting the resulting response of the effluent stream. The method most commonly employed is to change the concentration of one of the nonreactive components of the feed stream. This tracer component is generally chosen on the basis of the convenience and accuracy with which it may be measured. The properties that are most often used for monitoring the concentration of these tracers are electrical conductivity, absorbance, and emission of beta and gamma rays. In choosing the tracer, one must take care to ensure that significant amounts of tracer do not disappear during the course of the experimental measurement (e.g., by selective adsorption on the walls of the reaction vessel or on heterogeneous catalysts present in the reactor, by settling out or being filtered out as it moves through the reactor, or by chemical reaction in the case of nonradioactive tracers).

There are three general stimulus techniques that may be used in theoretical and experimental analyses of reactor networks to characterize their dynamic behavior:

1. A step function stimulus in which the entrance concentration is changed from one steady-state level to another.
2. A pulse stimulus in which a relatively small amount of tracer is injected at the reactor entrance in the shortest possible time.
3. A sinusoidal stimulus. The frequency of the sinusoidal variation is changed and the steady-state response of the effluent at different input frequencies is determined, thereby generating a frequency-response diagram for the system.

The time variations of the effluent concentration of tracer in response to step and pulse stimuli and the frequency-response diagram all contain essentially the same information. In principle, any one of these three types of response can be mathematically transformed into the other two. However, since it is easier experimentally to effect a change in the feed concentration of tracer that approximates a step change or an impulse function, and since the measurements associated with sinusoidal variations are much more time consuming and require special

equipment, the latter are used much less often in simple reactor studies. Even in the first two cases, one can obtain good experimental results only if the average residence time in the system is relatively long.

Kramers and Alberda (6) discussed the manner in which sinusoidal variations are analyzed, but we discuss only the first two types of stimuli. They are sufficient for the analysis of the majority of situations that will be encountered by chemical engineers engaged in the practice of designing chemical reactors.

The interpretation of the  $F(t)$  curve as the probability that a fluid element entering the reactor at time zero has left by time  $t$  may be used to indicate how the curve may be generated from experimental data. Let us consider the case where at time zero one makes a step change in the weight fraction tracer in the feed stream from  $w_0^-$  to  $w_0^+$ . A generalized stimulus-response curve for this system is shown in Figure 11.2.

At time  $t$  the fraction of the effluent fluid characterized by an age less than  $t$  (and thus with a composition  $w_0^+$ ) is just equal to  $F(t)$ . At the same time, the fraction of the effluent characterized by an age greater than  $t$  (with the original inlet composition  $w_0^-$ ) is equal to  $1 - F(t)$ . The time dependence of the weight fraction tracer in the effluent  $w_E(t)$  is then given by

$$w_E(t) = w_0^+ F(t) + w_0^- [1 - F(t)] \quad (11.1.3)$$

Thus,

$$F(t) = \frac{w_E(t) - w_0^-}{w_0^+ - w_0^-} \quad (11.1.4)$$

and we see that in general  $F(t)$  would give the relative response of the system to a step function stimulus.

Now consider the case for which the stimulus is a pulse of tracer. The amount of tracer leaving in a time increment  $dt$  is  $w_E \phi_m dt$ , where  $\phi_m$  is the mass flow rate. For constant-density systems, mass and volume fractions are identical

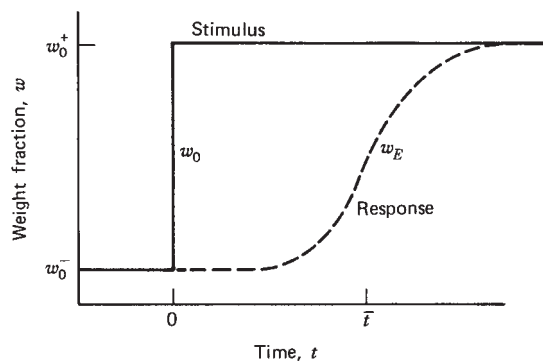


**Figure 11.2** Generalized response of an arbitrary reactor to a step change in the feed concentration of tracer.

and the basic definition of  $F(t)$  indicates that

$$F(t) = \frac{\int_0^t w_E \phi_m dt}{\int_0^\infty w_E \phi_m dt} = \frac{\int_0^t w_E \phi_m dt}{m_T} \quad (11.1.5)$$

where we have identified the term in the denominator as the total mass of tracer recovered from a pulse stimulus. Differentiation of equation (11.1.5) gives

$$\frac{dF(t)}{dt} = \frac{w_E \phi_m}{\int w_E \phi_m dt} = \frac{w_E \phi_m}{m_T} \quad (11.1.6)$$

For linear systems the relative response to a pulse stimulus is equal to the derivative of the relative response to a step stimulus. Illustration 11.1 indicates how the response of a reactor network to a pulse stimulus can be used to generate an  $F(t)$  curve.

### ILLUSTRATION 11.1 Determination of an $F(t)$ Curve from the Response of a Reactor to a Pulse Stimulus

A slug of dye is placed in the feed stream to a stirred reaction vessel operating at a steady state. The dye concentration in the effluent stream was monitored as a function of time to generate the data in the table below. Times are measured relative to the instant at which the dye was injected.

Time, $t$ (s)	Tracer concentration (g/m <sup>3</sup> )
0	0.0
120	6.5
240	12.5
360	12.5
480	10.0
600	5.0
720	2.5
840	1.0
960	0.0
1080	0.0

Determine the average residence time of the fluid and the  $F(t)$  curve for this system.

### Solution

For a constant-density system, concentrations are directly proportional to weight fractions. Thus, equation (11.1.5) becomes

$$F(t) = \frac{\int_0^t C_E \phi_m dt}{\int_0^\infty C_E \phi_m dt}$$

where  $C_E$  is the tracer concentration in the effluent.

**Table I11.1** Data Workup

Time, $t$ (s)	$C_E$ (g/m <sup>3</sup> )	$\sum_0^t (C_E)$ (g/m <sup>3</sup> )	$F(t)$	$tC_E$ (s·g/m <sup>3</sup> )	$t^2C_E$ (s <sup>2</sup> ·g/m <sup>3</sup> )
0	0.0	0.0	0	0	0
120	6.5	6.5	0.13	780	93,600
240	12.5	19.0	0.38	3,000	720,000
360	12.5	31.5	0.63	4,500	1,620,000
480	10.0	41.5	0.83	4,800	2,304,000
600	5.0	46.5	0.93	3,000	1,800,000
720	2.5	49.0	0.98	1,800	1,296,000
840	1.0	50.0	1.00	840	705,600
960	0.0	50.0	1.00	0	0
1080	0.0	50.0	1.00	0	0
		$\sum_0^\infty (C_E) = 50.0$			$\sum_0^\infty (tC_E) = 18,720$

One must replace the integrals by finite sums to be able to make use of the data given. Thus

$$F(t) = \frac{\sum_{t=0}^{t=t} (C_E \Phi_m \Delta t)}{\sum_{t=0}^{t=\infty} (C_E \Phi_m \Delta t)}$$

The data are reported at evenly spaced time increments, and the mass flow rate is invariant for steady state operation. Thus

$$F(t) = \frac{\sum_{t=0}^{t=t} (C_E)}{\sum_{t=0}^{t=\infty} (C_E)}$$

The average residence time is given by equation (11.1.2). Combination of this equation with equations (11.1.5) and (11.1.6) gives

$$\bar{t} = \frac{\int_{t=0}^{t=\infty} t w_E \Phi_m dt}{\int_{t=0}^{t=\infty} w_E \Phi_m dt}$$

In terms of the data and the aforementioned assumptions this equation becomes

$$\bar{t} = \frac{\sum_{t=0}^{t=\infty} (t C_E)}{\sum_{t=0}^{t=\infty} (C_E)}$$

Table I11.1 contains a workup of the data in terms of the analysis above. In the more general case one should be sure to use appropriate averaging techniques or graphical integration to determine both  $F(t)$  and  $\bar{t}$ . When there is an abundance of data, plot it, draw a smooth curve, and integrate graphically instead of using the strictly numerical procedure employed above. On the basis of the tabular entries,

$$\bar{t} = \frac{18,720}{50.0} = 374.4 \text{ s}$$

### 11.1.2 $F(t)$ Curves for Ideal Flow Patterns

For a few highly idealized systems, the residence-time distribution function can be determined a priori without the need for experimental work. These systems include our two idealized flow reactors—the plug flow reactor and the continuous-flow stirred-tank reactor—and the tubular laminar flow reactor. The  $F(t)$  and response curves for each of these three types of well-characterized flow patterns will be developed in turn.

The plug flow reactor has a flat velocity profile and no longitudinal mixing. These idealizations imply that all fluid elements leaving the reactor have the same age ( $\bar{t}$ ). The  $F(t)$  function for this system must then be

$$F(t) = \begin{cases} 0 & \text{for } 0 < t < \bar{t} \\ 1.0 & \text{for } t > \bar{t} \end{cases} \quad (11.1.7)$$

The responses of this system to ideal step and pulse stimuli are shown in Figure 11.3. Because the flow patterns in real tubular reactors will always involve some axial mixing and boundary layer flow near the walls of the vessels, they will distort the response curves for the ideal plug

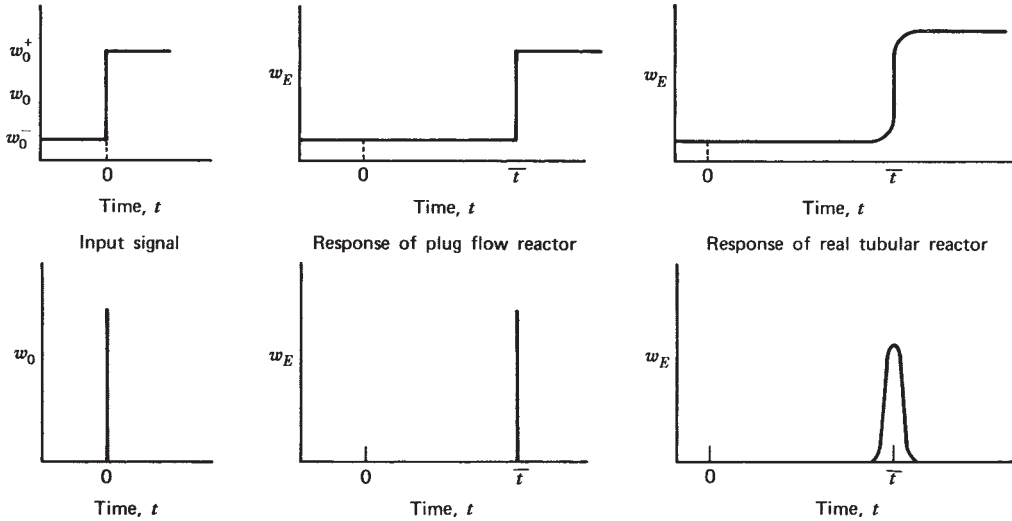


Figure 11.3 Responses of ideal plug flow reactor and a real tubular reactor to step change and pulse stimuli.

flow reactor. Consequently, the responses of a real tubular reactor to these stimuli may look like those shown in Figure 11.3.

The next case to be considered is the ideal continuous flow stirred-tank reactor. The key to the derivation of the  $F(t)$  curve for this type of reactor is the realization that the assumption of perfect mixing implies that upon entry in the reactor an element of volume can instantaneously appear in any position in the reactor. Therefore, its past or future history cannot be derived from its current position. Furthermore, the probability that it will leave the system by some future time will be independent of its past history. These statements require that the probability that a fluid element will remain in the system longer than a time  $t_1 + t_2$  will be the product of the two independent probabilities that it will remain in longer than times  $t_1$  and  $t_2$ , respectively.

$$1 - F(t_1 + t_2) = [1 - F(t_1)][1 - F(t_2)] \quad (11.1.8)$$

If we now replace  $t_1$  by  $t$  and consider the case where we let  $t_2$  become very small ( $\Delta t$ ),

$$1 - F(t + \Delta t) = [1 - F(t)][1 - F(\Delta t)] \quad (11.1.9)$$

For a perfectly mixed reactor, all fluid elements have an equal chance of leaving the reactor, so that for a small time increment  $\Delta t$ , the probability that a given fluid element will leave is just the ratio of the mass of fluid leaving to the total mass contained within the reactor.

$$F(\Delta t) = \frac{\phi_m \Delta t}{\rho V_R} = \frac{V_0 \Delta t}{V_R} = \frac{\Delta t}{\bar{t}} \quad (11.1.10)$$

where  $\rho$  is the fluid density and  $\bar{t}$  is the mean residence time.

Combination of equations (11.1.9) and (11.1.10) gives

$$F(t + \Delta t) - F(t) + F(t) \frac{\Delta t}{\bar{t}} = \frac{\Delta t}{t} \quad (11.1.11)$$

Dividing by  $\Delta t$  and taking the limit as  $\Delta t$  approaches zero yields

$$\frac{dF(t)}{dt} + \frac{F(t)}{\bar{t}} = \frac{1}{t} \quad (11.1.12)$$

The solution to this differential equation subject to the boundary condition that  $F(t) = 0$  is

$$F(t) = 1 - e^{-t/\bar{t}} \quad (11.1.13)$$

The same result can be obtained by considering the response of the composition of the effluent from a CSTR to a step function change in the feed concentration and using equation (11.1.4) to determine  $F(t)$ .

The relative response of a single CSTR to an ideal pulse input may be obtained by taking the time derivative of equation (11.1.13):

$$\frac{dF(t)}{dt} = \frac{e^{-t/\bar{t}}}{\bar{t}} \quad (11.1.14)$$

From this equation it is evident that there is a wide distribution of residence times in a stirred-tank reactor.

The responses of a single ideal stirred-tank reactor to ideal step and pulse stimuli are shown in Figure 11.4. Note that any change in the reactor inlet stream shows up immediately at the reactor outlet in these systems. This fact is used to advantage in the design of automatic control systems for stirred-tank reactors.

The performance of the stirred-tank flow reactors that are encountered in industrial practice may differ significantly from the ideal case discussed above. The feed stream entering the stirred region will not be dispersed and mixed instantaneously with the entire contents of the vessel. The mixing process will require a finite amount of time to produce a microscopically homogeneous solution, so there will be a time lag between the change in the input stream and the

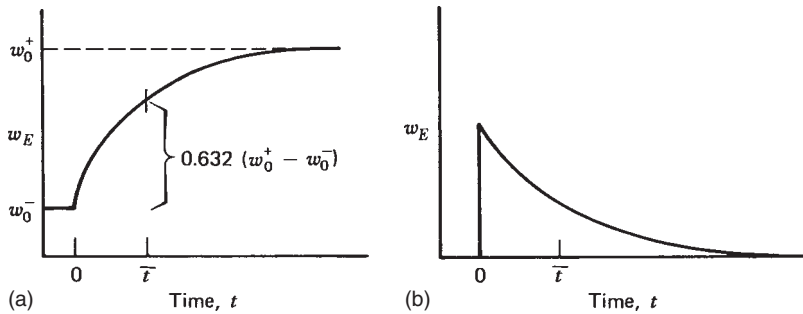


**Figure 11.4** Responses of an ideal continuous-flow stirred-tank reactor to (a) step change and (b) pulse stimuli.

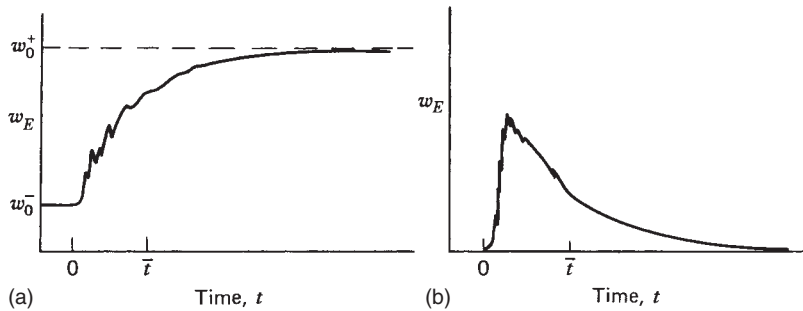


**Figure 11.5** Responses of a real stirred-tank reactor to (a) step change and (b) pulse stimuli.

change in the characteristics of the effluent stream. However, this time lag is generally very small compared to the average residence time in the tank. Nonetheless, portions of the feed stream may pass through the reactor outlet without undergoing complete mixing.

These portions may lead to an irregular response curve. This effect cannot be described quantitatively for a general system because it will depend on the relative orientations of the inlet and outlet with respect to the impellers and any baffles present in the system. Examples of possible response curves are shown in Figure 11.5. The effluent response will also be strongly dependent on the mixing time. The approximation of an actual stirred-tank reactor by an ideal CSTR improves as the ratio of the mean residence time to the mixing time increases. For most design purposes a ratio greater than 10 gives a very good approximation (7).

The final idealized flow situation that we consider is laminar flow in a tubular reactor in the absence of either radial or longitudinal diffusion. The velocity profile in such a reactor is given by

$$u = u_0 \left[ 1 - \left( \frac{r}{R} \right)^2 \right] \quad \text{for } 0 \leq r \leq R \quad (11.1.15)$$

where  $u_0$  is the centerline velocity,  $r$  the distance from the centerline of the pipe, and  $R$  the inside radius of the pipe.

The average velocity with which a fluid element moves is given by

$$\bar{u} = \frac{u_0}{2} \quad (11.1.16)$$

Because  $u$  varies with  $r$ , the residence times of the various fluid elements will also vary with  $r$ . The time that it will

take a fluid element to traverse the length of the reactor is

$$t = \frac{L}{u} = \frac{L}{u_0[1 - (r/R)^2]} \quad (11.1.17)$$

where  $L$  is the length of the reactor.

The average residence time  $\bar{t}$  is

$$\bar{t} = \frac{2L}{u_0} \quad (11.1.18)$$

Combination of equations (11.1.17) and (11.1.18) yields

$$\frac{\bar{t}}{2t} = \left[ 1 - \left( \frac{r}{R} \right)^2 \right] \quad (11.1.19)$$

The fluid at the centerline is moving the fastest, so this material will be the first to leave. This fluid leaves at a time  $t_{\min}$  given by

$$t_{\min} = \frac{L}{u_0} = \frac{\bar{t}}{2} \quad (11.1.20)$$

Thus,

$$F(t) = 0 \quad \text{for } t < \frac{\bar{t}}{2} \quad (11.1.21)$$

The fraction of the volumetric flow rate that takes place in the region bounded by  $r = 0$  and  $r = r$  will be equal to  $F(t)$  where  $t$  is equal to the time necessary for a fluid element to traverse the reactor length at a given radius  $r$  [equation (11.1.17)]. Thus,

$$F(t) = \frac{\left[ \begin{array}{l} \text{volumetric flow rate} \\ \text{between } r = 0 \text{ and } r = r \end{array} \right]}{\text{total volumetric flow rate}} \quad (11.1.22)$$

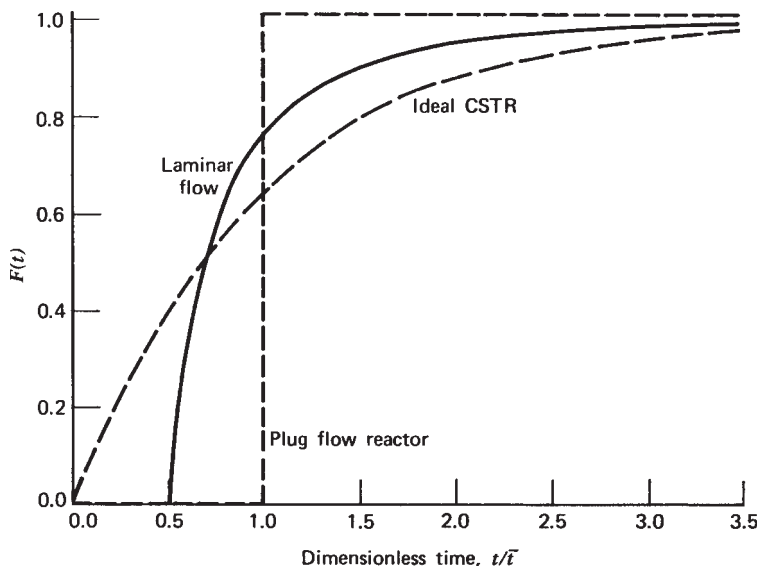


**Figure 11.6**  $F(t)$  curves for reactors with idealized flow patterns.

or

$$F(t) = \frac{\int_0^r u(r) 2\pi r dr}{\int_0^R u(r) 2\pi r dr} \quad (11.1.23)$$

Combining equations (11.1.15) and (11.1.23) and simplifying gives

$$F(t) = \frac{\int_0^r [1 - (r/R)^2] r dr}{\int_0^R [1 - (r/R)^2] r dr} \quad (11.1.24)$$

Integration gives

$$F(t) = \frac{(r^2/2) - (r^4/4R^2)}{(R^2/2) - (R^4/4R^2)} = \left(\frac{r}{R}\right)^2 \left[2 - \left(\frac{r}{R}\right)^2\right] \quad (11.1.25)$$

From equation (11.1.19),

$$\left(\frac{r}{R}\right)^2 = 1 - \frac{\bar{t}}{2t} \quad (11.1.26)$$

Substitution of this result into equation (11.1.25) yields, for  $t \geq \bar{t}/2$ ,

$$F(t) = \left(1 - \frac{\bar{t}}{2t}\right) \left[2 - \left(1 - \frac{\bar{t}}{2t}\right)\right] = 1 - \left(\frac{\bar{t}}{2t}\right)^2 \quad (11.1.27)$$

The  $F(t)$  curve for a laminar flow tubular reactor with no diffusion is shown in Figure 11.6. Curves for the two other types of idealized flow patterns are shown for comparison.

### 11.1.3 Models for Nonideal Flow Situations

Different reactor networks can give rise to the same residence time distribution function. For example, a CSTR

characterized by a space time  $\tau_1$  followed by a PFR characterized by a space time  $\tau_2$  has an  $F(t)$  curve that is identical to that of these two reactors operated in reverse order. Consequently, the  $F(t)$  curve alone is not sufficient, in general, to permit one to determine the conversion in a nonideal reactor. As a result, several mathematical models of reactor performance have been developed to provide estimates of the conversion levels that will be obtained in nonideal reactors. These models vary in their degree of complexity and range of applicability. In this book we confine the discussion to models in which a single parameter is used to characterize the nonideal flow pattern. Multi-parameter models have been developed for handling more complex situations (e.g., that which prevails in a fluidized-bed reactor), but these are beyond the scope of this book [see Levenspiel (2) and Himmelblau and Bischoff (4)].

It is convenient to classify deviations from ideal flow conditions into two categories:

1. Different fluid elements may move through the reactor at different velocities. The elements remain *segregated* as they move through the reactor.
2. Fluid elements with different ages may mix on a microscopic scale. However, the *mixing* does not occur to the extent that it does in an ideal CSTR.

These two types of deviations occur simultaneously in actual reactors, but the mathematical models we discuss assume that the residence-time distribution function may be attributed to one or the other of these flow situations. The first class of nonideal flow conditions leads to the segregated flow model of reactor performance. This model may be used with the residence-time distribution function to predict conversion levels accurately for first-order reactions that occur isothermally (see Section 11.2.1). The second

class may be modeled in several ways, depending on the additional assumptions one is willing to make concerning the nature of the mixing processes. Once these assumptions are made, the parameters of the mathematical model can be determined from the  $F(t)$  curve. The remainder of this section is devoted to a discussion of the interpretation of response data in terms of two of these mixing models.

### 11.1.3.1 The Axial Dispersion Model

The *axial dispersion model* is often used to describe the behavior of tubular reactors. This model characterizes mass transport in the axial direction in terms of an effective or apparent longitudinal diffusivity  $D_L$  that is superimposed on the plug flow velocity. The model also involves the assumption that the fluid velocity and reactant concentration are constant across the tube diameter. The magnitude of the dispersion is assumed to be independent of position within the vessel, so there will be no stagnant regions and no bypassing or short-circuiting of fluid in the model reactor. By changing the magnitude of the dispersion parameter, one may vary the performance of the reactor from that of plug flow ( $D_L = 0$ ) to that of a single continuous flow stirred-tank reactor ( $D_L = \infty$ ).

The axial dispersion parameter  $D_L$  accounts for mixing by both molecular diffusion processes and turbulent eddies and vortices. Because these two types of phenomena are to be characterized by a single parameter, and because we force the model to fit the form of Fick's law of diffusion,  $D_L$  should be regarded as an *effective* dispersion coefficient having the units of an ordinary molecular diffusivity (length<sup>2</sup>/time). However, it is significantly greater in magnitude because of turbulence effects.

The response of the axial dispersion model to step or pulse tracer stimuli can be determined by writing a material balance over a short segment of the tubular reactor and then solving the resulting differential equations. A transient material balance on a nonreactive tracer for a cylindrical element of length  $\Delta Z$  gives

$$\begin{aligned} & \left[ \left( -D_L \frac{\partial C}{\partial Z} + uC \right) \pi R^2 \right]_Z \Delta t \\ &= \left[ \left( -D_L \frac{\partial C}{\partial Z} + uC \right) \pi R^2 \right]_{Z+\Delta Z} \Delta t + \pi R^2 \Delta Z \Delta C \end{aligned} \quad (11.1.28)$$

input = output + accumulation

where the input and output terms allow for both dispersive and convective transport. Division of both sides by the cross-sectional area,  $\Delta t$ , and  $\Delta Z$ , and taking the limit as the last two parameters approach zero gives

$$D_L \frac{\partial^2 C}{\partial Z^2} - u \frac{\partial C}{\partial Z} = \frac{\partial C}{\partial t} \quad (11.1.29)$$

The initial and boundary conditions that apply to this equation depend on whether one is dealing with a pulse or a step stimulus and the characteristics of the system at the tracer injection and monitoring stations. At each of these points the tubular reactor is characterized as "closed" or "open," depending on whether or not plug flow into or out of the test section is assumed. A *closed boundary* is one at which there is plug flow outside the test section; an *open boundary* is one at which the same dispersion parameter characterizes the flow conditions within and adjacent to the test section. There are then four different possible sets of boundary conditions on equation (11.1.29), depending on whether a completely open or completely closed vessel, a closed-open vessel, or an open-closed vessel is assumed. Different solutions will be obtained for different boundary conditions. Fortunately, for small values of the dispersion parameter, the numerical differences between the various solutions will be small.

If we now consider a step change in tracer concentration in the feed to an open tube that can be regarded as extending to infinity in both directions from the injection point, the appropriate initial and boundary conditions on equation (11.1.29) are

$$C = \begin{cases} C_0^- & \text{for } Z > 0 \text{ at } t = 0 \\ C_0^+ & \text{for } Z < 0 \text{ at } t = 0 \end{cases} \quad (11.1.30)$$

and

$$C = \begin{cases} C_0^+ & \text{at } Z = -\infty \text{ for } t \geq 0 \\ C_0^- & \text{at } Z = +\infty \text{ for } t \geq 0 \end{cases} \quad (11.1.31)$$

where  $C_0^+$  and  $C_0^-$  are the tracer concentrations before and after the step change, respectively. In this case a closed-form solution is possible with

$$\frac{C - C_0^-}{C_0^+ - C_0^-} = \frac{1}{2} \left[ 1 - \text{erf} \left( \frac{Z - ut}{\sqrt{4D_L t}} \right) \right] \quad (11.1.32)$$

where the term in parentheses is the argument of the error function.<sup>†</sup>

The relative response at the end of a tubular reactor of length  $L$  is identical to the  $F(t)$  curve at  $Z = L$ . If we define  $\bar{t}^* = L/u$ ,

$$F(t) = \frac{1}{2} \left[ 1 - \text{erf} \left\{ \frac{1}{2} \sqrt{\frac{uL}{D_L}} \left( \frac{1 - t/\bar{t}^*}{\sqrt{t/\bar{t}^*}} \right) \right\} \right] \quad (11.1.33)$$

This equation is plotted in Figure 11.7 for different values of the parameter  $D_L/uL$ . When this parameter is zero,

<sup>†</sup>The error function is tabulated in most handbooks of mathematical tables. Readers should note that  $\text{erf}(-x) = -\text{erf}(x)$  and that

$$\text{erf}(x) = \frac{2}{\sqrt{\pi}} \int_0^x e^{-y^2} dy$$

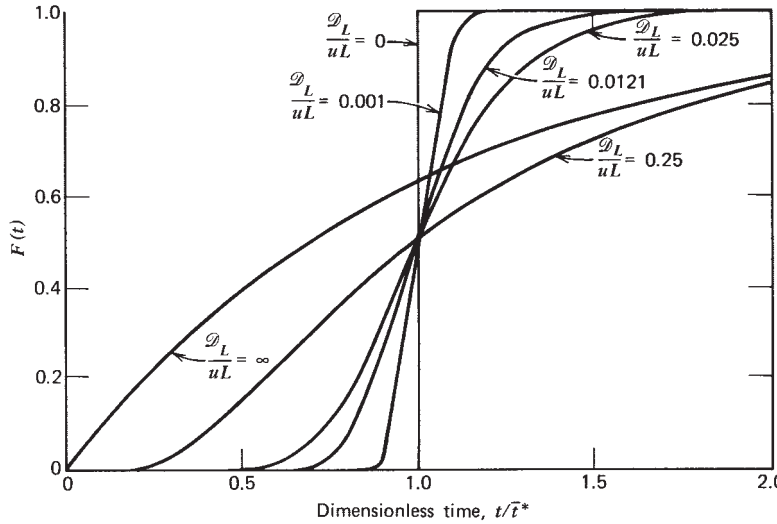


**Figure 11.7** Cumulative residence time distribution curves for the axial dispersion model.

there is no axial dispersion, and the reactor acts as a plug flow reactor. The response in this case is shown in Figure 11.7 to be the step-function response expected. At the other extreme, a value of  $D_L/uL$  equal to infinity corresponds to an ideal stirred-tank reactor.

When one injects a perfect pulse of tracer, Levenspiel and Smith (8) have shown that the solution to equation (11.1.29) is

$$C = \frac{m_T L}{2V_R \sqrt{\pi D_L t}} e^{-(Z-ut)^2 / 4D_L t} \quad (11.1.34)$$

where  $m_T$  is the amount of tracer injected in consistent units, and  $L$  and  $V_R$  are the length and volume of the test section, respectively. At  $Z = L$ ,

$$C_L(t) = \frac{m_T L}{2V_R \sqrt{\pi D_L t}} e^{-(L-ut)^2 / (4D_L t)} \quad (11.1.35)$$

For constant-density systems the variable  $\bar{t}^*$  becomes

$$\bar{t}^* = \frac{L}{u} = \frac{V_R}{V_0} \quad (11.1.36)$$

and equation (11.1.36) becomes

$$\begin{aligned} C_L(t) &= \frac{m_T L}{2V_R \sqrt{\pi D_L t}} e^{\left\{ -L^2 \left( 1 - \frac{ut}{L} \right)^2 / 4D_L t \right\}} \\ &= \frac{m_T L}{2V_R \sqrt{\pi D_L t} \frac{L}{ut^*}} e^{\left\{ \left[ 1 - \left( t / \bar{t}^* \right) \right]^2 / \left[ \left( \frac{4D_L}{uL} \right) \left( t / \bar{t}^* \right) \right] \right\}} \\ &= \frac{m_T}{2V_R \sqrt{\pi \left( \frac{D_L}{uL} \right) \left( t / \bar{t}^* \right)}} e^{\left\{ \left[ 1 - \left( t / \bar{t}^* \right) \right]^2 / \left[ \left( \frac{4D_L}{uL} \right) \left( t / \bar{t}^* \right) \right] \right\}} \end{aligned} \quad (11.1.37)$$

Because an overall material balance requires that all the tracer pass the monitoring station,

$$\int_0^\infty C_L(t) V_0 dt = m_T \quad (11.1.38)$$

Combination of equations (11.1.36) to (11.1.38) gives

$$\begin{aligned} &\frac{C_L(t)}{\int_0^\infty C_L(t) d(t/\bar{t}^*)} \\ &= \frac{1}{2\sqrt{\pi \left( \frac{D_L}{uL} \right) \left( t / \bar{t}^* \right)}} e^{-\left\{ \left[ 1 - \left( t / \bar{t}^* \right) \right]^2 / \left[ \left( \frac{4D_L}{uL} \right) \left( t / \bar{t}^* \right) \right] \right\}} \end{aligned} \quad (11.1.39)$$

If the right side of this equation is plotted versus dimensionless time for various values of the group  $D_L/uL$  (the reciprocal Péclet number), the types of curves shown in Figure 11.8 are obtained. The skewness of the curve increases with increasing  $D_L/uL$ , and for small values of this parameter, the shape approaches that of a normal error curve. In physical terms this behavior implies that when  $D_L/uL$  is small, the shape of the axial concentration profile does not change appreciably in the time interval required for the fluid to pass the monitoring station. However, when  $D_L/uL$  is of order 0.01 or greater, the shape changes significantly in this time interval.

Differentiation of equation (11.1.39) with respect to  $t/\bar{t}^*$  can be used to determine the time at which the maximum tracer concentration is observed at the monitoring station. The result is

$$\left( \frac{t}{\bar{t}^*} \right)_{\max} = \sqrt{\left( \frac{D_L}{uL} \right)^2 + 1} - \frac{D_L}{uL} \quad (11.1.40)$$

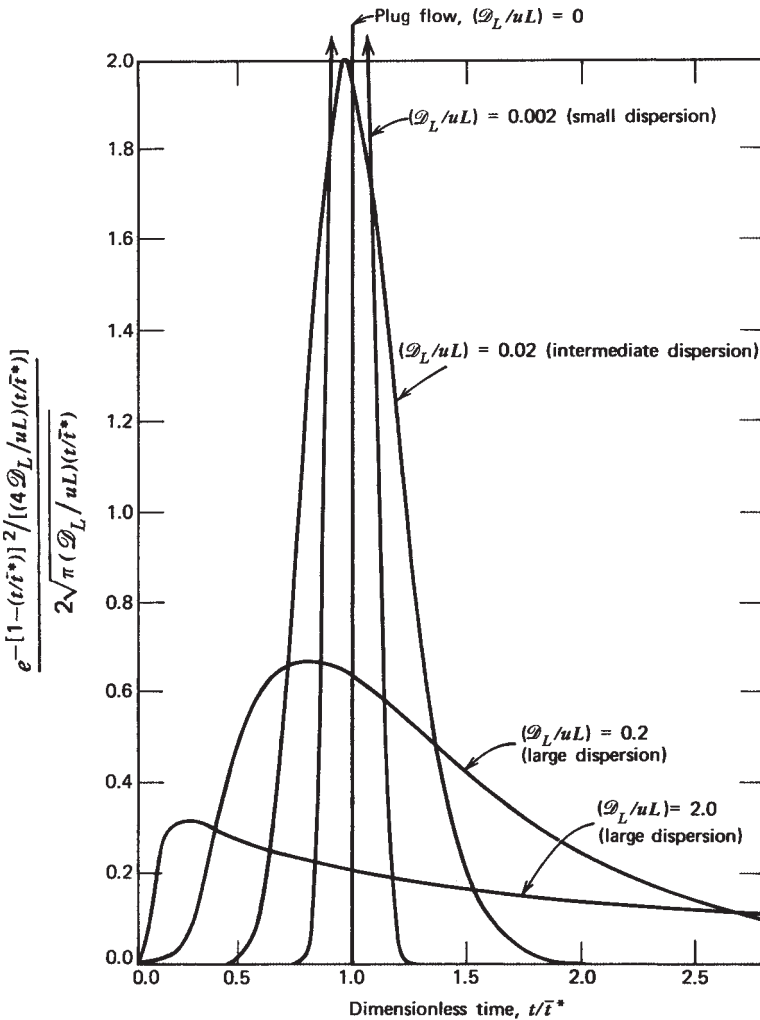


**Figure 11.8** Effluent response curves for perfect impulse injection of tracer (axial dispersion model). (Adapted from O. Levenspiel, *Chemical Reaction Engineering*, 2nd ed. Copyright © 1972. Reprinted with permission of John Wiley & Sons, Inc.)

or

$$\left(\frac{t}{\bar{t}^*}\right)_{\max} = \frac{\mathcal{D}_L}{uL} \left[ \sqrt{1 + \left(\frac{uL}{\mathcal{D}_L}\right)^2} - 1 \right] \quad (11.1.41)$$

Inspection of equation (11.1.40) indicates that the time at which the maximum concentration is reached must lie between zero and  $\bar{t}^*$  and that for very small values of  $\mathcal{D}_L/uL$ , the maximum is very close to  $\bar{t}^*$ .

Equations (11.1.33) and (11.1.39) provide the basis for several methods of estimating dispersion parameters. Tracer experiments are used in the absence of chemical reactions to determine the dispersion parameter  $\mathcal{D}_L$ ; this value is then employed in a material balance for a reactive component to predict the reactor effluent composition. We now indicate some methods that can be used to estimate the dispersion parameter from tracer measurements.

One method of estimating  $\mathcal{D}_L$  from experimental tracer data is based on evaluation of the slope of the  $F(t)$  curve at

$t = \bar{t}^*$ . At this point the derivative of equation (11.1.33) is

$$\left[ \frac{dF(t)}{d(t/\bar{t}^*)} \right]_{(t/\bar{t}^*)=1} = \frac{1}{2} \sqrt{\frac{uL}{\pi \mathcal{D}_L}} \quad (11.1.42)$$

This approach to determining  $\mathcal{D}_L$  suffers from several disadvantages:

1. Only a small portion of the available data (i.e., those near  $t = \bar{t}^*$ ) is used.
2. The process of taking the derivative of experimental data often leads to considerable uncertainty in the dispersion parameter.
3. Equation (11.1.33) is strictly applicable only for an ideal step change stimulus and the boundary conditions cited. The plant or laboratory situation may not correspond to these assumptions.

For small values of the dispersion parameter, one may take advantage of the fact that equation (11.1.37) takes the shape of a normal error curve. This situation implies that for

a step function stimulus a plot of  $(C - C_0^-)/(C_0^+ - C_0^-)$  or  $F(t)$  versus time on probability paper will be linear. Because the dispersion parameter is related to the variance of the curve (see below), it is a simple matter to use this plot to determine  $\mathcal{D}_L$ . For a normal error curve, one standard deviation on either side of the mean comprises 68% of the total area under the curve. Thus, the 16th and 84th percentile points on the  $F(t)$  curve are two standard deviations apart, and  $t_{84\%} - t_{16\%} = 2\sigma_t$ . Using relations developed below for small  $\mathcal{D}_L/uL$  (say,  $<0.01$ );

$$\frac{\mathcal{D}_L}{uL} \cong \frac{1}{2} \left[ \frac{\sigma_t^2}{(\bar{t}^*)^2} \right] \quad (11.1.43)$$

Alternative methods of estimating  $\mathcal{D}_L$  are based on the response of the reactor to an ideal pulse stimulus. For example, equation (11.1.39) may be used to calculate the mean residence time and its variance. Levenspiel and Bischoff (9) indicate that for the boundary conditions cited,

$$\bar{t} = \bar{t}^* \left( 1 + \frac{2\mathcal{D}_L}{uL} \right) = \frac{V_R}{V_0} \left( 1 + \frac{2\mathcal{D}_L}{uL} \right) \quad (11.1.44)$$

and

$$\sigma_t^2 = (\bar{t}^*)^2 \left[ \frac{2\mathcal{D}_L}{uL} + 8 \left( \frac{\mathcal{D}_L}{uL} \right)^2 \right] \quad (11.1.45)$$

For other boundary conditions or for imperfect pulse injections, modifications must be made in these expressions. For example, for a closed-closed vessel, Levenspiel and Bischoff (9) indicate that

$$\bar{t} = \bar{t}^* \quad (11.1.46)$$

and

$$\sigma_t^2 = (\bar{t}^*)^2 \frac{2\mathcal{D}_L}{uL} \left[ 1 - \frac{\mathcal{D}_L}{uL} (1 - e^{-uL/\mathcal{D}_L}) \right] \quad (11.1.47)$$

For situations where  $\mathcal{D}_L/uL$  is small (say, less than 0.01), the various expressions for  $\sigma_t^2$  become

$$\sigma_t^2 \cong (\bar{t}^*)^2 \frac{2\mathcal{D}_L}{uL} \quad (11.1.48)$$

This approximation is valid to within 5% at this limit. Because the axial dispersion term itself may be viewed as a perturbation or correction term for real tubular reactors, errors of this magnitude in  $\mathcal{D}_L$  lead to relatively minor errors in the conversions predicted using the model.

In principle, any of equations (11.1.40), (11.1.44), (11.1.45), (11.1.47), or (11.1.48) could be used to determine the dispersion parameter. However, both equations (11.1.40) and (11.1.44) require that one accurately determine a small difference in large numbers to evaluate  $\mathcal{D}_L/uL$ . Hence, equations (11.1.45) and (11.1.47) are

preferred for evaluation of  $\mathcal{D}_L/uL$  for open and closed vessels, respectively. For small  $\mathcal{D}_L/uL$ , equation (11.1.48) is appropriate.

The discussion thus far presumes that a perfect pulse or step stimulus is employed when, in fact, such stimuli can only be approximated. In the case of pulse stimuli, one is also faced with two conflicting constraints in attempting to generate a perfect pulse or delta function. Because a finite amount of tracer cannot be injected in zero time, as much material should be injected in as short a time as possible to approximate a delta function. However, the injection process should not disturb the system significantly. The latter requirement implies that the tracer should be injected very slowly. Fortunately, these difficulties may be circumvented by using the imperfect pulse method described by Aris (10), Bischoff (11), and Bischoff and Levenspiel (12). The technique involves monitoring the concentration at two points in the test section instead of at a single point. It does not matter where the injection point is located, provided that it is upstream of the two monitoring stations. Any type of imperfect pulse stimulus may be employed. The variances of the concentration-time curves at the two monitoring stations are determined and their difference is taken:

$$\Delta\sigma^2 = \sigma_2^2 - \sigma_1^2 \quad (11.1.49)$$

where the subscripts 1 and 2 refer to the upstream and downstream locations, respectively. This equation reflects the fact that variances are additive for flow through *independent* vessels or regions. This property implies that the variance of the residence-time distribution can be determined for any region if the variances of the inlet and effluent streams are known. In a similar fashion, mean residence times are additive; thus, for the test section,

$$\bar{t}_{\text{test}} = \bar{t}_{\text{out}} - \bar{t}_{\text{in}} \quad (11.1.50)$$

Aris (10), Bischoff (11) and Bischoff and Levenspiel (12) have derived equations relating the measured mean residence times and variances to the Péclet number or dispersion parameter for the test section. For the case where the conditions at both monitoring probes correspond to a doubly infinite pipe, it can be shown that

$$\Delta\sigma^2 = \frac{2\mathcal{D}_L}{uL} \quad (11.1.51)$$

If the measuring points are chosen far enough away from the ends of the test vessel so that end effects are negligible, this expression may be used with confidence. Bischoff and Levenspiel (12) have presented design charts that permit one to locate monitoring stations so as to avoid end effects. For example, in a packed-bed reactor with a tube to pellet diameter ratio of 15, where the packed bed is followed by an open tube, at least 8 pellet diameters are

required between the measurement point and the open tube if errors below 1% are to be obtained.

In addition to the aforementioned slope and variance methods for estimating the dispersion parameter, it is possible to use transfer functions in the analysis of residence-time distribution curves. This approach reduces the error in the variance approach that arises from the “tails” of the concentration versus time curves. These tails contribute significantly to the variance and can be responsible for significant errors in the determination of  $\mathcal{D}_L$ .

A linear system may be described by a transfer function  $\hat{F}(p)$ :

$$\hat{F}(p) = \frac{C_2(p)}{C_1(p)} = \frac{\int_0^\infty C_2(t)e^{-pt} dt / (\int_0^\infty C_2(t) dt)}{\int_0^\infty C_1(t)e^{-pt} dt / (\int_0^\infty C_1(t) dt)} \quad (11.1.52)$$

where  $C_1(t)$  and  $C_2(t)$  are the tracer concentrations (as functions of time) at the upstream and downstream monitoring stations, respectively. Material balance considerations indicate that

$$\int_0^\infty C_2(t) dt = \int_0^\infty C_1(t) dt \quad (11.1.53)$$

Hence,

$$\hat{F}(p) = \frac{\int_0^\infty C_2(t)e^{-pt} dt}{\int_0^\infty C_1(t)e^{-pt} dt} \quad (11.1.54)$$

The material balance characterizing the axial dispersion model is equation (11.1.29), which can be rewritten as

$$\frac{\mathcal{D}_L}{uL} \frac{\partial^2 C}{\partial(Z/L)^2} - \frac{\partial C}{\partial(Z/L)} - \frac{L}{u} \frac{\partial C}{\partial t} = 0 \quad (11.1.55)$$

where  $L$  is the distance between monitoring stations and  $L/u$  is again defined as  $\bar{t}^*$ . For a section of a continuous system in which end effects are negligible, Mixon et al. (13) and Østergaard and Michelsen (14) have shown that the transform of this equation with respect to time leads to the following expression:

$$\begin{aligned} \hat{F}(p) &= \exp \left[ \frac{uL}{2\mathcal{D}_L} \left\{ 1 - \left( 1 + \frac{4\mathcal{D}_L}{uL} \left[ \frac{L}{u} \right] p \right)^{1/2} \right\} \right] \\ &= \exp \left[ \frac{uL}{2\mathcal{D}_L} \left\{ 1 - \left( 1 + \frac{4\mathcal{D}_L}{uL} \bar{t}^* p \right)^{1/2} \right\} \right] \end{aligned} \quad (11.1.56)$$

Rearrangement and algebraic manipulation of the logarithmic form of this equation gives

$$\frac{1}{\ln[1/\hat{F}(p)]} = \frac{p\bar{t}^*}{\{\ln[1/\hat{F}(p)]\}^2} - \frac{\mathcal{D}_L}{uL} \quad (11.1.57)$$

Numerical values of  $\hat{F}(p)$  may be calculated from the experimental data for arbitrary values of  $p$  using equation (11.1.54). One takes these values and prepares a plot of the left side of equation (11.1.57) versus  $p / \{\ln[1/\hat{F}(p)]\}^2$  for test data. This procedure should give a straight line of slope  $\bar{t}^*$  and intercept  $-\mathcal{D}_L/uL$ . Hopkins et al. (15) have shown that some discretion must be used in selecting the “arbitrary”  $p$  values to minimize the error involved in determining  $\mathcal{D}_L/uL$ . Low values of the group  $p\bar{t}^*$  lead to large errors in  $\mathcal{D}_L/uL$  because the transfer function is relatively insensitive to variations in  $\mathcal{D}_L/uL$  at low  $p\bar{t}^*$ . Large values of the group  $p\bar{t}^*$  are also disadvantageous because of the effect of the exponential  $e^{-pt}$  on the individual values of the integrands in equation 11.1.54. The weighting factor  $e^{-pt}$  minimizes the influence of the tail but emphasizes the values of  $C(t)$  at short times when concentration fluctuations may be important. Hopkins et al. (15) recommend that values of  $p\bar{t}^*$  between 2 and 5 be used when dealing with flow through packed beds.

In addition to the three methods described above, non-linear regression methods or other transform approaches may be used to determine the dispersion parameter. For a more complete treatment of the use of transform methods, consult the articles by Hopkins et al. (15) and Østergaard and Michelsen (14).

Illustration 11.2 indicates the use of the slope and variance methods for evaluating  $\mathcal{D}_L/uL$ .

## ILLUSTRATION 11.2 Determination of Dispersion Parameter from Experimental Residence-Time Measurements

In Illustration 11.1 we considered the response of an arbitrary reactor to a pulse stimulus and used these data to determine the average residence time and the  $F(t)$  curve. If the pulse is assumed to be perfect, what value of  $\mathcal{D}_L/uL$  gives a reasonable fit of the experimental data? Use the slope and variance methods to evaluate this parameter.

### Solution

First consider the slope method for determining  $\mathcal{D}_L/uL$ . From the plot of the  $F(t)$  curve in Illustration 11.1, the value of  $dF(t)/dt$  at  $t = \bar{t} = 374.4$  s or 0.3744 ks is equal to  $2.17 \text{ ks}^{-1}$ . From equation (11.1.42),

$$\frac{dF(t)}{d(t/\bar{t})}_{t/\bar{t}=1} = \frac{1}{2} \sqrt{\frac{uL}{\pi \mathcal{D}_L}} = 0.3744(2.17)$$

Thus,

$$\frac{\mathcal{D}_L}{uL} = 0.121$$

The  $F(t)$  curve for this value of the dispersion parameter can be generated using equation 11.1.33 (see Figure 11.7).

Now consider determination of this parameter using the variance of the response to a pulse stimulus. The variance measures the spread of the distribution about the mean. For a continuous distribution it is defined as

$$\sigma^2 = \frac{\int_0^\infty (x - \mu)^2 f(x) dx}{\int_0^\infty f(x) dx}$$

where  $\mu$  is the mean,  $x$  the property being investigated, and  $f(x) dx$  the distribution function.

In terms of the present problem for the response to a pulse, the variance in  $t$  is given by

$$\begin{aligned} \sigma_t^2 &= \frac{\int_0^\infty (t - \bar{t})^2 [dF(t)/dt] dt}{\int_0^\infty [dF(t)/dt] dt} \\ &= \int_0^\infty t^2 \frac{dF(t)}{dt} dt - \bar{t}^2 \end{aligned}$$

If steady-state operation, invariant mass flow rate, and evenly spaced time increments are assumed, as in Illustration 11.1, this equation may be written as

$$\sigma_t^2 = \frac{\sum_{t=0}^{t=\infty} [t^2 C_E]}{\sum_{t=0}^{t=\infty} [C_E]} - \bar{t}^2$$

From the data in Table I11.1 it is evident that

$$\sigma_t^2 = \frac{1}{50.0} \left( \begin{array}{l} 0 + 93,600 + 720,000 \\ + 1,620,000 + 2,304,000 \\ + 1,800,000 + 1,296,000 \\ + 705,600 + 0 \end{array} \right) - (374.4)^2$$

or

$$\sigma_t^2 = 30,609 \text{ s}^2$$

To proceed from this point to a determination of the dispersion parameter, one must know something about the experimental apparatus. For an open vessel, equation (11.1.45) indicates that

$$\sigma_t^2 = (\bar{t}^*)^2 \left[ \frac{2D_L}{uL} + 8 \left( \frac{D_L}{uL} \right)^2 \right]$$

Because no information is available concerning  $L/u$  or  $V_R/V_0$ , we assume as a first approximation that  $\bar{t}^* = \bar{t} = 374.4 \text{ s}$ . Thus,

$$30,609 = (374.4)^2 (2) \left[ \frac{D_L}{uL} + 4 \left( \frac{D_L}{uL} \right)^2 \right]$$

or

$$4 \left( \frac{D_L}{uL} \right)^2 + \frac{D_L}{uL} = \frac{30,609}{(374.4)^2 (2)} = 0.1092$$

Solving for  $D_L/uL$  gives 0.0822.

A more refined value may be obtained using equation (11.1.44) to determine  $\bar{t}^*$ :

$$\bar{t}^* = \frac{\bar{t}}{1 + 2(D_L/uL)} = \frac{374.4}{1 + 2(0.0822)} = 321.5$$

As a second approximation based on equation (11.1.45),

$$4 \left( \frac{D_L}{uL} \right)^2 + \frac{D_L}{uL} = \frac{30,609}{(321.5)^2 (2)} = 0.1481$$

or  $D_L/uL = 0.104$ .

Subsequent iterations lead to the conclusion that  $D_L/uL = 0.113$ . This result differs from that obtained using the slope approach by 7%. The variance approach to determination of  $D_L/uL$  is preferred to the slope method because the variance is based on the totality of the data set used to determine  $F(t)$ . By contrast, the slope approach generates a value of  $D_L/uL$  that is based primarily on the subset of data in the vicinity of  $t = \bar{t}$ .

Note that if one has a value for  $V_R/V_0$  as in the normal situation, the iterative procedure is unnecessary. However, in this case, equation (11.1.44) should not be used to determine  $D_L/uL$ , because significant errors may be involved in accurately determining a small difference in large numbers.

### 11.1.3.2 The Stirred Tanks in Series Model

Another model that is frequently used to simulate the behavior of actual reactor networks is a cascade of ideal stirred-tank reactors. The actual reactor is replaced by  $n$  identical stirred-tank reactors whose *total* volume is the same as that of the actual reactor.

$$V_R = nV_{\text{CSTR}} \quad (11.1.58)$$

One determines the value of  $n$  that gives the best fit of the response curve of the actual reactor by the response curve of the model. Consequently, it is necessary to develop an analytical expression for the latter. For the  $n$ th stirred-tank reactor in the series, the time-dependent form of the material balance equation becomes (in the absence of reaction)

$$C_{n-1}V_0 = C_nV_0 + V_{\text{CSTR}} \frac{dC_n}{dt} \quad (11.1.59)$$

Rate of input = rate of output + rate of accumulation

Because the *total average residence time in the actual reactor* ( $\bar{t}$ ) is given by

$$\bar{t}_{\text{cascade}} = \frac{V_{\text{Rcascade}}}{V_0} = \frac{nV_{\text{CSTR}}}{V_0} \quad (11.1.60)$$

equation (11.1.59) may be rewritten as

$$\frac{dC_n}{dt} + \frac{nC_n}{\bar{t}} = \frac{nC_{n-1}}{\bar{t}} \quad (11.1.61)$$

where  $\bar{t}$  is the mean residence time for the cascade.

If we are determining the response of the series of stirred-tank reactors to a step change in inlet tracer concentration from 0 to  $C_0^+$  at time zero, the initial condition for this differential equation is

$$C_n = 0 \quad \text{for } t = 0 \text{ and } n > 0$$

The solution to this equation may be obtained using an integrating factor approach to obtain

$$C_n = e^{-nt/\bar{t}} \int_0^t \frac{nC_{n-1}}{\bar{t}} e^{nt/\bar{t}} dt \quad (11.1.62)$$

The integral may be evaluated for each stage of the reactor network in turn. For the first stage,  $C_{n-1} = C_0^+$ , so that

$$C_1 = e^{-t/\bar{t}} \int_0^t \frac{C_0^+}{\bar{t}} e^{t/\bar{t}} dt \quad (11.1.63)$$

or

$$\frac{C_1}{C_0^+} = e^{-t/\bar{t}} (e^{t/\bar{t}} - 1) = 1 - e^{-t/\bar{t}} \quad (11.1.64)$$

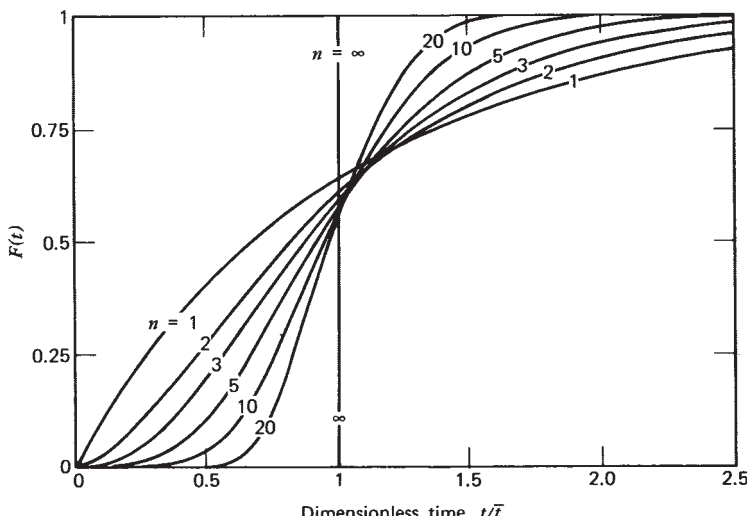
when there is just a single CSTR (a single stage).

If there are  $n$  identical reactors in series,  $\bar{t}_{\text{1 reactor}} = \bar{t}/n$  and

$$\frac{C_1}{C_0^+} = 1 - e^{-nt/\bar{t}} \quad (11.1.65)$$

where  $\bar{t}$  here is the mean residence time for the entire network.

Equations (11.1.62) and (11.1.65) may be combined to obtain the equation for the tracer concentration in the effluent from the second reactor when two reactors comprise the



network.

$$C_2 = e^{-2t/\bar{t}} \int_0^t \frac{2C_0^+}{\bar{t}} (1 - e^{-2t/\bar{t}}) e^{2t/\bar{t}} dt \quad (11.1.66)$$

or

$$\begin{aligned} \frac{C_2}{C_0^+} &= e^{-2t/\bar{t}} \frac{2}{\bar{t}} \int_0^t (e^{2t/\bar{t}} - 1) dt = e^{-2t/\bar{t}} \left\{ \left[ \left( e^{2t/\bar{t}} - \frac{2t}{\bar{t}} \right) \right]_0^t \right\} \\ &= e^{-2t/\bar{t}} \left( e^{2t/\bar{t}} - 1 - \frac{2t}{\bar{t}} \right) = 1 - e^{-2t/\bar{t}} \left( 1 + 2 \frac{t}{\bar{t}} \right) \end{aligned} \quad (11.1.67)$$

where  $\bar{t}$  is the mean residence time for the two-reactor cascade.

One may proceed stepwise in this fashion to develop a general recursion expression for the concentration leaving reactor  $j$  in an  $n$ -reactor cascade.

$$\begin{aligned} \frac{C_j}{C_0^+} &= 1 - e^{-nt/\bar{t}} \left[ 1 + \frac{nt}{\bar{t}} + \frac{1}{2!} \left( \frac{nt}{\bar{t}} \right)^2 + \frac{1}{3!} \left( \frac{nt}{\bar{t}} \right)^3 + \dots \right. \\ &\quad \left. + \frac{1}{(j-1)!} \left( \frac{nt}{\bar{t}} \right)^{j-1} \right] \end{aligned} \quad (11.1.68)$$

The response curve for the network as a whole is obtained by setting  $j$  equal to  $n$  in equation (11.1.68). Note that  $\bar{t}$  is given by equation (11.1.60).

$$\begin{aligned} F(t) &= \frac{C_n}{C_0^+} = 1 - e^{-nt/\bar{t}} \left[ 1 + \frac{nt}{\bar{t}} + \frac{1}{2!} \left( \frac{nt}{\bar{t}} \right)^2 + \dots \right. \\ &\quad \left. + \frac{1}{(n-1)!} \left( \frac{nt}{\bar{t}} \right)^{n-1} \right] \end{aligned} \quad (11.1.69)$$

Note that in this case the right side of equation (11.1.68) is zero for  $t = 0$  and unity for  $t = \infty$ . Figure 11.9 contains several  $F(t)$  curves for various values of  $n$ . As  $n$  increases, the spread in residence time decreases. At the limit, as  $n$  approaches infinity, the  $F(t)$  curve approaches

Figure 11.9 Cumulative residence time distribution curves for the  $n$ -CSTR model.

that for an ideal plug flow reactor. If the residence time distribution function given by (11.1.69) is differentiated, one obtains an equation for the slope of the curve from which  $n$  may be determined by comparison with the experimental  $F(t)$  curve.

$$\frac{dF(t)}{d(t/\bar{t})} = ne^{-nt/\bar{t}} \left[ 1 + \frac{nt}{\bar{t}} + \frac{1}{2!} \left( \frac{nt}{\bar{t}} \right)^2 + \cdots + \frac{1}{(n-1)!} \left( \frac{nt}{\bar{t}} \right)^{n-1} \right] - e^{-nt/\bar{t}} \left[ n + \frac{n^2 t}{\bar{t}} + \frac{n^3}{2!} \left( \frac{t}{\bar{t}} \right)^2 + \cdots + \frac{n^{n-1}}{(n-2)!} \left( \frac{t}{\bar{t}} \right)^{n-2} \right] \quad (11.1.70)$$

or

$$\frac{dF(t)}{d(t/\bar{t})} = ne^{-nt/\bar{t}} \frac{1}{(n-1)!} \left( \frac{nt}{\bar{t}} \right)^{n-1} \quad (11.1.71)$$

At  $t/\bar{t} = 1$ , the slope is given by

$$\left[ \frac{dF(t)}{d(t/\bar{t})} \right]_{t/\bar{t}=1} = \frac{n^n e^{-n}}{(n-1)!} = \frac{n^{n+1} e^{-n}}{n!} \quad (11.1.72)$$

For  $n > 5$  we may use Stirling's approximation and retain an accuracy of 2%.

$$n! \approx n^n e^{-n} \sqrt{2\pi n} \quad (11.1.73)$$

Combination of equations (11.1.72) and (11.1.73) gives

$$\left[ \frac{dF(t)}{d(t/\bar{t})} \right]_{t/\bar{t}=1} \approx \sqrt{\frac{n}{2\pi}} \quad \text{for } n > 5 \quad (11.1.74)$$

Approximate values of the slope at  $t/\bar{t} = 1$  for  $n \leq 5$  are:

$n$	Slope
1	0.368
2	0.541
3	0.672
4	0.781
5	0.877

The  $n$ -CSTR model suffers from the fact that it allows only integer values of  $n$  and that it may not be possible to obtain a match of the residence-time distribution function at both high and low values of  $F(t)$  with the same value of  $n$ . Buffham and Gibilaro (16) generalized the model to include noninteger values of  $n$ . The technique outlined by these authors is particularly useful in obtaining better fits of the data for cases in which  $n$  is less than 5.

A preferable alternative to the slope approach to determining the appropriate value of  $n$  for use in model calculations is based on a determination of the variance of the response of the actual reactor to a *pulse* stimulus. For linear systems this is equivalent to determining the variance of the derivative of the  $F(t)$  curve. The response of the

series of reactors to a pulse stimulus is given by equation (11.1.71). The variance of this expression is given by its second moment:

$$\sigma_{t/\bar{t}}^2 = \int_0^\infty \left( \frac{t}{\bar{t}} - 1 \right)^2 \frac{n^{n+1}}{n!} e^{-nt/\bar{t}} \left( \frac{t}{\bar{t}} \right)^{n-1} d \left( \frac{t}{\bar{t}} \right) \quad (11.1.75)$$

Evaluation of this integral leads to the surprisingly simple result that

$$\sigma_{t/\bar{t}}^2 = \frac{1}{n} \quad (11.1.76)$$

Thus,

$$\sigma_t^2 = \frac{(\bar{t})^2}{n} \quad (11.1.77)$$

Hence by determining the variance of the response of a system to a *pulse* stimulus, one may obtain an estimate of  $n$  for use in subsequent reactor design calculations.

For experimental trials in which two monitoring stations are used, equation (11.1.49) is applicable, and

$$\frac{\Delta\sigma^2}{(\bar{t})^2} = \frac{\sigma_2^2 - \sigma_1^2}{(\bar{t})^2} = \frac{1}{j} \quad (11.1.78)$$

where  $j$  is now the equivalent number of stirred tanks between the two stations. Illustration 11.3 indicates how  $n$  may be determined using each of the two methods discussed above.

### ILLUSTRATION 11.3 Use of Experimental Response Data to Determine the Number of Stirred-Tank Reactors in Series

Use the data of Illustration 11.1 for the response of a reactor network to a pulse stimulus to determine the number of identical stirred tank reactors in series that gives a reasonable fit of the experimental data. Use both the slope and variance methods described above.

#### Solution

From a plot of the data for Illustration 11.1,

$$\left[ \frac{dF(t)}{d(t/\bar{t})} \right]_{(t/\bar{t})=1} = \left[ \bar{t} \frac{dF(t)}{dt} \right]_{\bar{t}} = 0.3744(2.17) = 0.81$$

For small values of  $n$ , the corresponding values of the slope at the point where  $t/\bar{t} = 1$  are tabulated below equation (11.1.74). Inspection of these values in the light of the slope value of 0.81 above indicates that  $n$  must lie between 4 and 5.

The variance approach is preferred for use in determining  $n$ . From Illustration 11.2 the variance of the response data based on dimensionless time is  $30,609/(374.4)^2$ , or

0.218. From equation (11.1.76) it is evident that  $n$  is 4.59. Thus, the results of the two approaches are consistent. However, a comparison of the  $F(t)$  curves for  $n = 4$  and  $n = 5$  with the experimental data indicates that these approaches do not provide very good representations of the data. For the reactor network in question it is difficult to model the residence-time distribution function in terms of a single parameter. This is one of the potential difficulties inherent in using such simple models of reactor behavior. For more advanced methods of modeling residence-time effects, consult the review article by Levenspiel and Bischoff (3) and textbooks written by these authors (2, 4).

## 11.2 CONVERSION LEVELS IN NONIDEAL FLOW REACTORS

In the present section we indicate how tracer residence time data may be used to predict the conversion levels that will be obtained in reactors with nonideal flow patterns. As indicated earlier, there are two types of limiting processes that can lead to a distribution of residence times within a reactor network.

1. A flow pattern in which the various fluid elements follow different paths without mutual mixing on a microscopic scale. An example of this case is laminar flow.
2. Mixing of fluid elements having different ages. Microscopic mixing produced by eddy diffusion effects is an example of this case.

Because these two types of processes have drastically different effects on the conversion levels achieved in chemical reactions, they provide the basis for the development of mathematical models that can be used to provide approximate limits within which one can expect actual isothermal reactors to perform. In the development of these models we define a *segregated system* as one in which the first effect is *entirely responsible* for the spread in residence times. When the distribution of residence times is established by the second effect, we refer to the system as *mixed*. In practice, one encounters various combinations of these two limiting effects.

We can characterize the mixed systems most easily in terms of the longitudinal dispersion model or in terms of the cascade of stirred-tank reactors model. The maximum amount of mixing occurs for the cases where  $D_L = \infty$  or  $n = 1$ . In general, for reaction orders greater than unity, these models place a lower limit on the conversion that will be obtained in an actual reactor. The applications of these models are treated in Sections 11.2.2 and 11.2.3.

In the *segregated flow model* the contents of the volume elements of the fluid do not mix with one another as they move through the reactor. Each element may be considered as a small closed system that moves through the reactor.

The different elements spend various amounts of time in the reactor, giving rise to the measured residence-time distribution function. The closest approximation to this condition that one commonly encounters in engineering practice is a laminar flow reactor, in which molecular diffusion in both longitudinal and radial directions is negligible. Another real life situation in which a segregated flow pattern is largely responsible for the spread in residence times is one in which there is some short-circuiting or bypassing of portions of the reactor volume as the fluid moves through the reactor. The bypassed regions may be considered as "dead" spaces that contribute to the total reactor volume but that do not contribute to the overall conversion rate in proportion to their volume. Because they are not effectively purged by the prevailing flow pattern, they often contain fluid in which the reaction has gone substantially to completion. It should be evident that this situation should be avoided in the proper design of chemical reactors. In general, for reaction orders greater than unity, the segregated flow model places an upper limit on the conversion that will be obtained in an actual reactor. For a first-order reaction occurring isothermally, the model can be used to accurately predict the conversion that will be attained in a real reactor whose  $F(t)$  curve is known. The details of the analysis are discussed in Section 11.2.1.

In general, the larger the breadth of the distribution of residence times, the greater the discrepancy between the conversion levels predicted on the basis of the segregated flow model and those predicted by the various mixing models. For narrow distribution functions, the conversions predicted by both models will be in good agreement with one another.

To illustrate the nature of the limits that the segregated flow and mixing models place on the conversion level expected, it is useful to examine what happens to two elements of fluid that have the same volume  $V$  but that contain different reactant concentrations  $C_1$  and  $C_2$ . We may imagine two extreme limits on the amount of mixing that may occur.

S: No mixing of the contents of the elements as they move through the reactor (complete segregation).

M: Complete mixing of the contents immediately on entrance followed by flow through the reactor in the completely mixed state.

If the rate expression is of the form

$$r = kC^n \quad (11.2.1)$$

the total conversion rates under the two limiting circumstances outlined above are given by

$$R_S = V(k(C_1^n + C_2^n)) \quad (11.2.2)$$

and

$$R_M = 2Vk \left( \frac{C_1 + C_2}{2} \right)^n \quad (11.2.3)$$

For a differential reactor and the same residence time, the ratio of these rates will be equal to the ratio of the conversion levels attained.

$$\frac{f_S}{f_M} = \frac{R_S}{R_M} = \frac{C_1^n + C_2^n}{2[(C_1 + C_2)/2]^n} \quad (11.2.4)$$

Because

$$\frac{C_1^n + C_2^n}{2} \neq \left( \frac{C_1 + C_2}{2} \right)^n \quad (11.2.5)$$

unless  $n = 1$  or  $n = 0$ , these are the only cases for which the two extreme situations will converge to the same limit. In these cases the fraction conversion will be the same whether or not fluid elements having different reactant concentrations remain segregated or are mixed prior to or during the reaction.

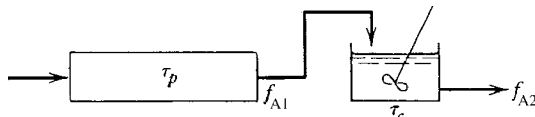
For reaction orders greater than unity, the segregated flow model will predict a higher conversion level than the various mixing models. For reaction orders less than unity, the mixing models will predict higher conversion levels than the segregated flow model. The magnitudes of the differences for representative cases are shown in Illustrations 11.5 to 11.7. The following illustration shows that for the first-order case, reactor combinations involving different mixing patterns but the same residence-time distribution function will lead to the same predicted conversion.

#### ILLUSTRATION 11.4 Comparison of Conversion Levels Attained in Two Different Reactor Combinations Having the Same Residence-Time Distribution Curve: First-Order Reaction

The  $F(t)$  curve for a system consisting of a plug flow reactor followed by a continuous-flow stirred-tank reactor is identical to that of a system in which the CSTR precedes the PFR. Show that the overall fraction conversions obtained in these two combinations are identical for the case of an irreversible first-order reaction. Assume isothermal operation.

#### Solution

Let  $\tau_p$  and  $\tau_c$  represent the space times of the plug flow reactor and the continuous-flow stirred-tank reactor, respectively. Consider the following reactor combination:



where  $f_{A1}$  and  $f_{A2}$  are the conversions at the outlet of the first and second reactors, respectively.

From the design equation for a PFR,

$$\tau_p = C_{A0} \int_0^{f_{A1}} \frac{df_A}{kC_{A0}(1-f_A)}$$

Integration gives

$$k\tau_p = -\ln(1-f_{A1})$$

or

$$f_{A1} = 1 - e^{-k\tau_p}$$

From the design equation for a CSTR,

$$\tau_c = \frac{C_{A0} \int_{f_{A1}}^{f_{A2}} df_A}{kC_{A0}(1-f_{A2})} = \frac{f_{A2} - f_{A1}}{k(1-f_{A2})}$$

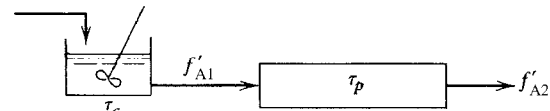
Solving for  $f_{A2}$  yields

$$f_{A2} = \frac{f_{A1} + k\tau_c}{1 + k\tau_c}$$

or

$$f_{A2} = \frac{1 + k\tau_c - e^{-k\tau_p}}{1 + k\tau_c}$$

Now consider the alternative arrangement,



where  $f'_A1$  and  $f'_A2$  are the conversions at the outlet of the CSTR and the PFR, respectively. From the design equation for the CSTR,

$$\tau_c = \frac{C_{A0} \int_0^{f'_A1} df_A}{kC_{A0}(1-f'_A1)} = \frac{f'_A1}{k(1-f'_A1)}$$

or

$$f'_A1 = \frac{k\tau_c}{1 + k\tau_c} \quad (A)$$

From the design equation for the PFR,

$$\tau_p = C_{A0} \int_{f'_A1}^{f'_A2} \frac{df_A}{kC_{A0}(1-f_A)}$$

Integration gives

$$k\tau_p = \ln \left[ \frac{1-f'_A1}{1-f'_A2} \right]$$

or

$$1 - f'_{A2} = (1 - f'_{A1})e^{-k\tau_p} \quad (B)$$

Combination of equations (A) and (B) and rearranging gives

$$f'_{A2} = 1 - \frac{e^{-k\tau_p}}{1 + k\tau_c} = \frac{1 + k\tau_c - e^{-k\tau_p}}{1 + k\tau_c}$$

This relation is identical to that obtained for the first reactor configuration. This illustration provides an example of the general principle that for irreversible first-order reactions carried out isothermally, all reactor combinations having the same residence-time distribution function lead to the same overall conversion.

Students should repeat the analysis for a second-order reaction to verify that for other reaction orders the overall conversion will depend on whether the PFR precedes the CSTR or vice versa.

### 11.2.1 The Segregated Flow Model

The basic premise of the segregated flow model is that the various fluid elements move through the reactor at different speeds without mixing with one another. Consequently, each little fluid element will behave as if it were a batch reactor operating at constant pressure. The conversions attained within the various fluid elements will be equal to those in batch reactors with holding times equal to the residence times of the different fluid elements. The average conversion level in the effluent is then given by

$$\langle f_A \rangle = \sum \left( \begin{array}{l} \text{fraction conversion expressed as} \\ \text{a function of residence time} \\ \times \text{fraction of the fluid elements having} \\ \text{residence times between } t \text{ and } t + dt \end{array} \right) \quad (11.2.6)$$

where the summation extends over all possible residence times. In terms of an integral,

$$\langle f_A \rangle = \int_{F(t)=0}^{F(t)=1.0} f_A(t) \, dF(t) \quad (11.2.7)$$

An alternative interpretation of the segregated flow model that leads to precisely the same result involves replacing the actual reactor by a number of plug flow reactors in parallel so that the combination will give rise to the  $F(t)$  curve observed experimentally. Under these conditions the degree of conversion in a fraction of the effluent stream  $dF(t)$  is equal to that which would occur in an ideal PFR with a residence time  $t$ . When the different streams are recombined at the outlet, the average conversion level is again given by equations (11.2.6) and

(11.2.7). To indicate how one makes use of these relations, consider Illustration 11.5.

### ILLUSTRATION 11.5 Use of the Segregated Flow Model to Determine the Conversion Level Attained in a Nonideal Flow Reactor

Use the  $F(t)$  curve generated in Illustration 11.1 to determine the fraction conversion that will be achieved in the reactor if it is used to carry out a first-order reaction with a rate constant equal to  $3.33 \times 10^{-3} \text{ s}^{-1}$ . Base the calculations on the segregated flow model.

#### Solution

Equation (11.2.7) is the key to the solution of this problem.

$$\langle f_A \rangle = \int_{F(t)=0}^{F(t)=1.0} f_A(t) \, dF(t) \quad (A)$$

For a first-order reaction,

$$f_A(t) = 1 - e^{-kt}$$

so that equation (A) becomes

$$\langle f_A \rangle = 1 - \int_{t=0}^{t=\infty} e^{-kt} \frac{dF(t)}{dt} dt$$

Substitution of equation (11.1.6) into this relation gives

$$\langle f_A \rangle = 1 - \frac{\int_{t=0}^{t=\infty} e^{-kt} w_E \phi_m \, dt}{\int_0^{\infty} w_E \phi_m \, dt} \quad (B)$$

If we assume a constant density system and a constant mass flow rate and replace the integrals by finite sums, we have

$$\langle f_A \rangle = 1 - \frac{\sum_0^{\infty} (e^{-kt} w_E \Delta t)}{\sum_0^{\infty} (w_E \Delta t)}$$

If we now replace the mass fractions by concentrations and note that the data are recorded at evenly spaced time increments,

$$\langle f_A \rangle = 1 - \frac{\sum_0^{\infty} (e^{-kt} C_E)}{\sum_0^{\infty} (C_E)}$$

The data were worked up as shown in the next table (page 355).

Time, $t$ (s)	$C_E$	$e^{-kt}$	$C_E e^{-kt}$
0	0.0	1.00	0.0
120	6.5	0.670	4.36
240	12.5	0.449	5.61
360	12.5	0.301	3.76
480	10.0	0.202	2.02
600	5.0	0.135	0.68
720	2.5	0.091	0.23
840	1.0	0.061	0.06
960	0.0	—	0.0
1080	0.0	—	0.0
$\sum_{t=0}^{t=\infty} (C_E) = 50.0$		$\sum_{t=0}^{t=\infty} (C_E e^{-kt}) = 16.72$	

Thus,

$$\langle f_A \rangle = 1 - \frac{16.72}{50.00} = 0.666$$

As an alternative to this numerical procedure, graphical integration of the terms in equation (B) could be employed.

Because the reaction under consideration is a first-order reaction, this result should be in good agreement with the conversions predicted on the basis of various mixing models. That this is true can be seen from a comparison of the result obtained above with those that will be obtained in Illustrations 11.6 and 11.7.

For systems characterized by a wide distribution of residence times, the degree of conversion can be calculated accurately only in the case of a first-order reaction. However, if it is possible to estimate in some rough fashion the extents to which mixing and segregation effects contribute to the observed residence-time distribution, one can bracket the actual performance of the reactor with the solutions obtained from the completely segregated flow model and those obtained from models consisting of various combinations of ideal reactors. It is an extremely rare situation in which one knows the flow pattern in the reactor sufficiently well that an exact calculation of the conversion can be performed. Instead, one must be satisfied with bracketing the solution in terms of models based on segregated flow and various mixing effects. Two commonly used mixing models are described in the next two sections.

## 11.2.2 The Longitudinal Dispersion Model in the Presence of a Chemical Reaction

In Section 11.1.3.1 we considered the longitudinal dispersion model for flow in tubular reactors and indicated how one may employ tracer measurements to determine the magnitude of the dispersion parameter used in the model. In this section we consider the problem of determining the

conversion that will be attained when the model reactor operates *at steady state*. We proceed by writing a material balance on a reactant species A for a tubular reactor. A mass balance over a reactor element of length  $\Delta Z$  yields

$$\begin{aligned} \left[ \left( -D_L \frac{dC}{dZ} + uC \right) \pi R^2 \right]_Z &= \left[ \left( -D_L \frac{dC}{dZ} + uC \right) \pi R^2 \right]_{Z+\Delta Z} \\ \text{Input} & \quad \text{Output} \\ + (-r_A) \pi R^2 \Delta Z & \quad (11.2.8) \\ \text{Disappearance by reaction} \end{aligned}$$

where we have taken into account the fact that material enters and leaves the volume element by bulk flow and by longitudinal dispersion. If we divide by  $\Delta Z$ , take the limit as  $\Delta Z$  approaches zero, and rearrange equation (11.2.8), we find that

$$D_L \frac{d^2 C_A}{dZ^2} - u \frac{dC_A}{dZ} + r_A = 0 \quad (11.2.9)$$

Note the similarities and differences between this equation and the time-dependent equation used to evaluate the dispersion parameter [equation (11.1.29)].

For a first-order irreversible reaction, equation (11.2.9) becomes

$$D_L \frac{d^2 C_A}{dZ^2} - u \frac{dC_A}{dZ} - kC_A = 0 \quad (11.2.10)$$

Wehner and Wilhelm (17) obtained an analytical solution to this equation for the case where  $\delta_A = 0$ . The solution is valid both when one has plug flow and when one has dispersion in the regions adjacent to the test section.

$$\frac{C_A}{C_{A0}} = 1 - f_A = \frac{4\beta e^{uL/2D_L}}{(1+\beta)^2 e^{\beta uL/2D_L} - (1-\beta)^2 e^{-\beta uL/2D_L}} \quad (11.2.11)$$

where

$$\beta = \left[ 1 + 4k \left( \frac{D_L}{uL} \right) \left( \frac{L}{u} \right) \right]^{1/2} \quad (11.2.12)$$

Levenspiel and Bischoff (18) compared this solution with that for the plug flow case:

$$\frac{C_{A \text{ plug}}}{C_{A0}} = 1 - f_A = e^{-k\tau} = e^{-kL/u} \quad (11.2.13)$$

They determined the ratio of the volume of a tubular reactor with dispersion to that for a plug flow reactor capable of accomplishing the same degree of conversion for several values of the dimensionless dispersion parameter  $D_L/uL$ . Figure 11.10 provides a graphical summary of their results. Inspection of this figure indicates that for high conversions and large  $D_L/uL$  significantly larger reactors are required than would be predicted by a plug

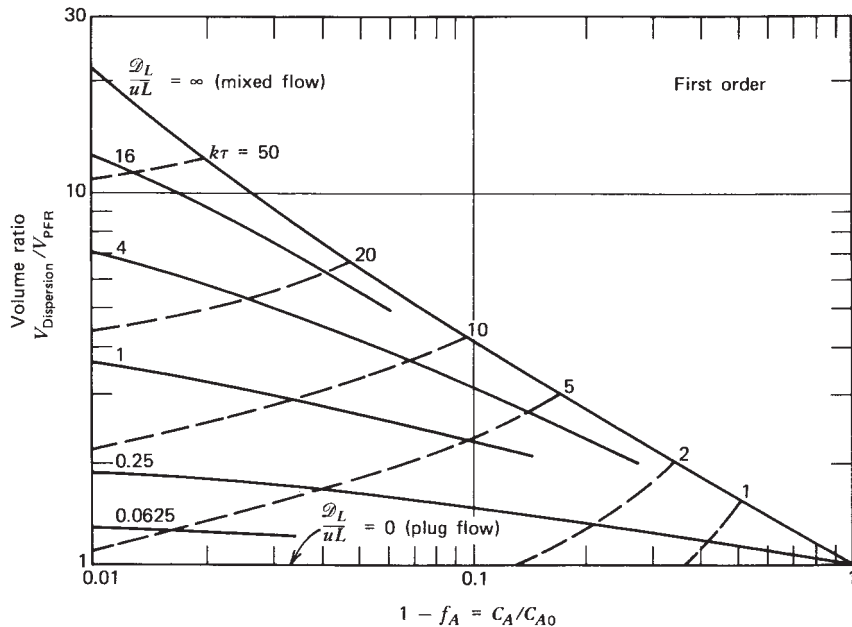


**Figure 11.10** Comparison of real and plug flow reactors for the first-order reaction  $A \rightarrow$  products, assuming negligible expansion ( $\delta_A = 0$ ). (Adapted from O. Levenspiel, *Chemical Reaction Engineering*, 2nd ed. Copyright © 1972. Reprinted by permission of John Wiley & Sons, Inc.)

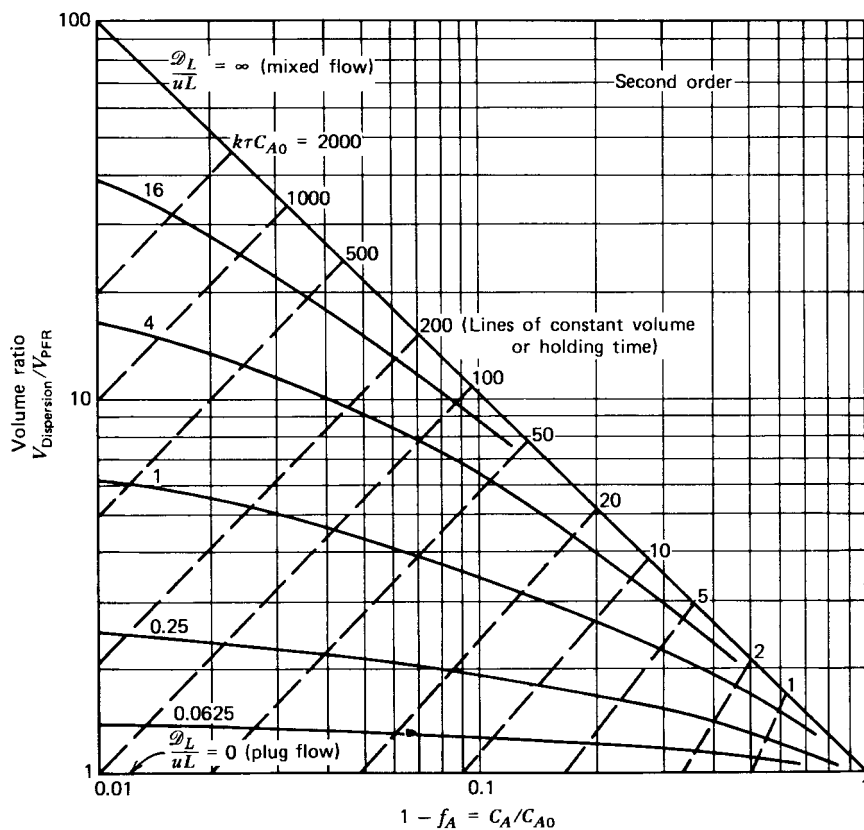


**Figure 11.11** Comparison of real and plug flow reactors for the second-order reactions  $A + B \rightarrow$  products ( $C_{A0} = C_{B0}$ ) and  $2A \rightarrow$  products, assuming negligible expansion ( $\delta_A = 0$ ). (Adapted from O. Levenspiel, *Chemical Reaction Engineering*, 2nd ed. Copyright © 1972. Reprinted by permission of John Wiley & Sons, Inc.)

flow analysis. However, at large  $D_L/uL$ , the dispersion model may well be inappropriate for use. Consequently, only the lower segment of Figure 11.10 is of general utility for design calculations.

Numerical solutions to equation (11.2.9) have been obtained for reaction orders other than unity. Figure 11.11 summarizes the results obtained by Levenspiel and Bischoff (18) for second-order kinetics. Like the chart for

first-order kinetics, it is most appropriate for use when the dimensionless dispersion group is small. Fan and Bailie (19) have solved the equations for quarter-order, half-order, second-order, and third-order kinetics. Others have used perturbation methods to arrive at analogous results for the dispersion model (e.g., 20, 21).

There are several closed form approximate solutions to both the general and first-order forms of the dispersion equations (11.2.9) and (11.2.10). For example, Levenspiel and Bischoff (2-4) indicate that for small dispersion numbers  $D_L/uL$ , equation (11.2.11) can be rewritten in the following form if one expands the exponentials and drops higher-order terms:

$$\ln\left(\frac{C_A}{C_{A0}}\right) = -k\frac{L}{u} + \left(\frac{kL}{u}\right)^2 \frac{D_L}{uL} = -k\tau + (k\tau)^2 \frac{D_L}{uL} \quad (11.2.14)$$

or, using equation (11.2.13) for the same reactor space time and the same reactor volume,

$$\ln\left(\frac{C_A \text{ dispersion}}{C_A \text{ plug}}\right) = (k\tau)^2 \frac{D_L}{uL} \quad (11.2.15)$$

This equation indicates that the conversion in the tubular reactor with dispersion will always be less than that in the plug flow reactor ( $C_A \text{ dispersion} > C_A \text{ plug}$ ). For the case where one fixes the effluent composition instead of the reactor size, equations (11.2.13) and (11.2.14) can be manipulated to show that for small  $D_L/uL$  at the same conversion,

$$\frac{L_{\text{dispersion}}}{L_{\text{plug flow}}} = \frac{V_{\text{dispersion}}}{V_{\text{plug flow}}} = 1 + k\tau \left(\frac{D_L}{uL}\right) \quad (11.2.16)$$

Levenspiel and Bischoff (3) used a derivation by Pasquon and Dente (20) to obtain an expression that gives an approximate solution to equation (11.2.9) for small  $D_L/uL$  and an arbitrary rate law:

$$C_A \text{ dispersion} = C_A \text{ plug} + \frac{D_L}{uL} (r_{A \text{ exit}} \tau) \ln\left(\frac{r_{A \text{ exit}}}{r_{A0}}\right) \quad (11.2.17)$$

where  $r_{A \text{ exit}}$  and  $r_{A0}$  are the rates at the exit and entrance of a plug flow reactor with the same space time as the tubular reactor with dispersion.

The influence of dispersion on the yield of an intermediate produced in a series of consecutive reactions has also been studied. When  $D_L/uL$  is less than 0.05, Tichacek's results (22) indicate that the fractional decrease in the maximum amount of intermediate formed relative to plug flow conditions is approximated by  $D_L/uL$  itself. Results obtained at higher dispersion numbers are given in the original article. Douglas and Bischoff (23) considered the influence of volumetric expansion effects on the yields obtained with dispersion. Illustration 11.6 indicates how the longitudinal dispersion model may be used to predict reactor performance.

## ILLUSTRATION 11.6 Use of the Dispersion Model to Determine the Conversion Level obtained in a Nonideal Reactor

Use the dispersion parameter determined in Illustration 11.2 to predict the conversion that will be attained in the reactor of Illustration 11.1. Assume that the value of the first-order rate constant is  $3.33 \times 10^{-3} \text{ s}^{-1}$ .

### Solution

Equation (11.2.11) is applicable in this case. Using the results obtained in Illustrations 11.1 and 11.2 yields

$$\beta = [1 + 4(3.33 \times 10^{-3})(0.113)(374.4)]^{1/2} = 1.25$$

where we have used the value of  $D_L/uL$  determined by the variance approach. From equation (11.2.11),

$$\frac{C_A}{C_{A0}} = \frac{4(1.25)e^{1/[2(0.113)]}}{(1 + 1.25)^2 e^{1.25/[2(0.113)]} - (1 - 1.25)^2 e^{-1.25/[2(0.113)]}} = 0.327$$

Thus,

$$f_A = 1 - 0.327 = 0.673$$

This result compares favorably to the value of 0.666 predicted on the basis of the segregated flow model. Excellent agreement should be obtained for the first-order case if the dispersion parameter gives a good fit of the experimental  $F(t)$  curve. For reaction orders other than unity, the agreement of the values predicted using the two models will not be nearly as good.

### 11.2.3 Determination of Conversion Levels Based on the Cascade Model of Stirred-Tank Reactors

In Section 11.1.3.2 we considered a model of reactor performance in which the actual reactor is simulated by a cascade of equal-sized continuous-flow stirred-tank reactors. We indicated how the cumulative residence-time distribution function can be used to determine the number of tanks that best model the tracer measurement data. Once this parameter has been determined, the techniques discussed in Section 8.3.2 can be used to determine the effluent conversion level.

For an irreversible first-order reaction, a material balance on the  $n$ th CSTR in a cascade of equal-sized reactors gives

$$C_{n-1} V_{n-1} = C_n V_n + k C_n \frac{V_R}{n} \quad (11.2.18)$$

input = output + disappearance by reaction

where  $V_R$  is the volume of the actual reactor and  $V_R/n$  is the volume of an individual CSTR used in the cascade model. Equations of this form were treated in Section 8.3.2.2. For a constant-density system,

$$C_n = \frac{C_{n-1}}{1 + (k\tau/n)} \quad (11.2.19)$$

where

$$\tau = \frac{V_R}{V} \quad (11.2.20)$$

The final effluent concentration is related to the inlet concentration in the following manner:

$$C_n = \frac{C_0}{[1 + (k\tau/n)]^n} = C_0(1 - f_n) \quad (11.2.21)$$

where  $f_n$  is the fraction conversion leaving tank  $n$  in the model. The use of the reactor cascade model to estimate the conversion level attained in a first-order reaction is discussed in Illustration 11.7.

### ILLUSTRATION 11.7 Use of the Cascade of Stirred-Tank Reactors Model to Predict Reactor Performance

Use the model based on a cascade of stirred-tank reactors to predict the conversion that will be attained in the reactor of Illustration 11.1. Assume that the value of the first-order rate constant is  $3.33 \times 10^{-3} \text{ s}^{-1}$ .

In Illustration 11.1 we found  $\bar{t}$  or  $\tau$  to be 374.4 s, while in Illustration 11.3 we determined that the value of  $n$  must lie between 4 and 5. From equation (11.2.21), with  $n = 4$ ,

$$f = 1 - \frac{1}{[1 + 3.33 \times 10^{-3}(374.4)/4]^4} = 1 - 0.337 \\ = 0.663$$

For  $n = 5$ ,  $f = 0.671$ , and for  $n = 4.59$ ,  $f = 0.668$ . All these values are close to those predicted using the segregated flow and dispersion models.

### 11.3 GENERAL COMMENTS AND RULES OF THUMB

In Section 11.2 we indicated how various mathematical models may be used to simulate the performance of a reactor in which the flow patterns do not fit either ideal CSTR or PFR conditions. The models treated represent only a small fraction of the large number that have been proposed by various authors. However, they are among the simplest and most widely used models, and they permit

one to bracket the expected performance of an isothermal reactor. However, *small variations in temperature can lead to much more significant changes in reactor performance than do reasonably large deviations in flow patterns from idealized conditions*. Because the rate constant depends exponentially on temperature, uncertainties in this parameter can lead to design uncertainties that will make any quantitative analysis of performance in terms of the residence-time distribution function little more than an academic exercise. Nonetheless, there are many situations where such analyses are useful.

Denbigh (24) provided a set of generalizations that are useful in deciding when the conversions attained in tubular reactors will deviate significantly from those predicted on the basis of the plug flow model. For laminar flow, molecular diffusion in the longitudinal direction will not affect reactor performance appreciably if the reactor length is much greater than its diameter. Molecular diffusion in the radial direction tends to destroy any concentration gradients that have been established and thus serves to offset deviations resulting from the velocity profile. In other words, it works in favor of the idealized assumptions instead of against them. For turbulent flow, eddy diffusion is the dominant mode of dispersion, and it can significantly affect reactor performance. A crude generalization that is valid for simple reactions is that if the Reynolds number is greater than  $10^4$  and if the ratio of the reactor length to its diameter is at least 50, deviations from plug flow because of longitudinal dispersion may be neglected. However, if these criteria are not met, the reactor size may have to be increased to a value appreciably greater than that required by plug flow conditions. The additional volume requirements may be determined using the models described previously.

Note that even though various flow models will often predict conversion levels that are within a few percent of one another, one must be extremely careful in the overall design calculations, particularly if the conversion level is high. If an ideal plug flow reactor gives a conversion of 98% and proper accounting for nonideal flow conditions by various models gives a range of conversion levels from 95 to 97%, the magnitude of subsequent separation problems will vary widely depending on the model chosen. For example, if product specifications call for a purity of 99% or better, the separations required would be quite different. In the ideal case, one would have to reduce the impurity level from 2% to 1%; in the nonideal flow model it would have to be reduced from 5% to 1%. The costs of the equipment necessary to accomplish this task would vary greatly, depending on the input impurity level. Of course, it is only fair to point out that any other sources of error in the conversion estimate (e.g., temperature variations) would have the same effect.

The dispersion and stirred-tank models of reactor behavior are in essence single parameter models. The literature contains an abundance of more complex multiparameter models. For an introduction to such models, consult the review article by Levenspiel and Bischoff (3) and the texts by these authors (2, 4). The texts also contain discussions of the means by which residence-time distribution curves may be used to diagnose the presence of flow maldistribution and stagnant region effects in operating equipment.

## LITERATURE CITATIONS

1. LEVENSPIEL, O., *Chemical Reaction Engineering*, pp. 244–253, Wiley, New York, 1962.
2. LEVENSPIEL, O., *Chemical Reaction Engineering*, 2nd ed., pp. 253–314, Wiley, New York, 1972.
3. LEVENSPIEL, O., and BISCHOFF, K. B., *Adv. Chem. Eng.*, **4**, 95 (1963).
4. HIMMELBLAU, D. M., and BISCHOFF, K. B., *Process Analysis and Simulation*, pp. 59–86, Wiley, New York, 1968.
5. DANCKWERTS, P. V., *Chem. Eng. Sci.*, **2**, 1 (1953).
6. KRAMERS, H., and ALBERDA, G., *Chem. Eng. Sci.*, **2**, 173 (1953).
7. KRAMERS, H., and WESTERTERP, K. R., *Elements of Chemical Reactor Design and Operation*, Academic Press, New York, 1963.
8. LEVENSPIEL, O., and SMITH, W. K., *Chem. Eng. Sci.*, **6**, 227 (1957).
9. LEVENSPIEL, O., and BISCHOFF, K. B., loc. cit., p. 112.
10. ARIS, R., *Chem. Eng. Sci.*, **9**, 266 (1959).
11. BISCHOFF, K. B., *Chem. Eng. Sci.*, **12**, 69 (1960).
12. BISCHOFF, K. B., and LEVENSPIEL, O., *Chem. Eng. Sci.*, **17**, 245 (1962).
13. MIXON, F. O., WHITAKER, D. R., and ORCUTT, J. C., *AIChE J.*, **13**, 21 (1967).
14. ØSTERGAARD, K., and MICHELSSEN, M. L., *Can. J. Chem. Eng.*, **47**, 107 (1969).
15. HOPKINS, M. J., SHEPPARD, A. J., and EISENKLAM, P., *Chem. Eng. Sci.*, **24**, 1131 (1969).
16. BUFFHAM, B. A., and GIBILARO, L. G., *AIChE J.*, **14**, 805 (1968).
17. WEHNER, J. F., and WILHELM, R. H., *Chem. Eng. Sci.*, **6**, 89 (1959).
18. LEVENSPIEL, O., and BISCHOFF, K. B., *Ind. Eng. Chem.*, **51**, 1431 (1959).
19. FAN, L. T., and BAILIE, R. C., *Chem. Eng. Sci.*, **13**, 63 (1960).
20. PASQUON, L., and DENTE, M., *J. Catal.*, **1**, 508 (1962).
21. BURGHARDT, A., and ZALESKI, T., *Chem. Eng. Sci.*, **23**, 575 (1968).
22. TICHACEK, L. J., *AIChE J.*, **9**, 394 (1963).
23. DOUGLAS, J. M., and BISCHOFF, K. B., *Ind. Eng. Chem. Process Des. Devel.*, **3**, 130 (1964).
24. DENBIGH, K. G., *Chemical Reactor Theory*, pp. 50–51, Cambridge University Press, London, 1965.

## PROBLEMS

- 11.1** D. G. Tajbl, J. B. Simons, and J. J. Carberry [*Ind. Eng. Chem. Fundam.*, **5**, 171 (1966)] developed a stirred-tank reactor for studies of catalytic reactions. Baskets containing catalyst pellets are mounted on a drive shaft that can be rotated at different speeds. The unit is designed for continuous flow operation. To determine if the performance

of the unit approximated that of an ideal continuous flow stirred-tank reactor, these investigators carried out a series of tracer experiments at different agitator speeds and different volumetric flow rates. The response of a nonreacting system to a pulse stimulus of helium injected into a steadily flowing airstream was used to characterize the reactor. The data are normalized by assuming that the concentration of the effluent at time zero is equal to the total mass of tracer injected divided by the effective volume of the reactor.  $C_0$  is the normalizing concentration. On the basis of the two sets of data presented below, does the reactor appear to provide a good approximation to an ideal CSTR? Be sure to use *all* the data in your analysis.

### Run 1

Volumetric flow rate	6.25 cm <sup>3</sup> /s
Agitator speed	1290 rpm
Dimensionless time, $t/\tau$	
$C_{\text{effluent}}/C_0$	
0.85	0.13
0.72	0.30
0.51	0.65
0.37	0.95
0.275	1.25
0.215	1.55
0.16	1.85

### Run II

Volumetric flow rate	10.6 cm <sup>3</sup> /s
Agitator speed	630 rpm
Dimensionless time, $t/\tau$	
$C_{\text{effluent}}/C_0$	
0.80	0.20
0.65	0.40
0.49	0.70
0.34	1.10
0.26	1.25
0.19	1.63
0.14	2.05

- 11.2** The concepts of residence time distribution and mean residence time can be employed in a wide range of disciplines other than chemical reactor design (e.g., in the analysis of equipment used in separation processes and sewage treatment plants). Another example is the analysis of the behavior of pharmaceuticals in humans and animals. Such information is important in determining the conditions necessary to maintain efficacy of these materials *in vivo*. The data from the pharmacokinetic study presented below pertain to a drug that was being studied as a potential inhibitor of the HIV virus.

J. H. Beijnen, P. L. Meenhorst, H. Rosing, R. Van Gijn, G. Los, and J. H. Underberg [J. Drug Devel., **3**, 127–133 (1990)] developed a procedure for analysis of 2',3'-dideoxyinsine (ddI) in blood plasma samples. To demonstrate the applicability of the assay to in vivo studies, these researchers injected a bolus of a saline solution of this drug into the tail of a rat. At the time intervals indicated below, 300- $\mu$ L samples of blood were withdrawn from the carotid artery and analyzed by HPLC.

- (a) Determine if the circulatory system can be modeled as a simple CSTR (use a graphical approach).  
 (b) Plot the  $F(t)$  curve for this system.

Time (min)	$C_{ddI}$ (ng/mL)
0.5	160,000
8	50,000
15	14,000
30	2,700
60	700
90	375
120	240
180	80

- (c) Determine the mean residence time of the drug in the circulatory system of the rat.

In your analysis in parts (b) and (c) you should employ appropriate methods of extrapolation (via curve fitting) to arrive at meaningful answers.

- 11.3** G. Barnett, R. Hawks, and R. Resnick [J. Ethnopharmacol., **3**, 353 (1981)] of the National Institute on Drug Abuse have studied cocaine pharmacokinetics in the human body. Cocaine was given to human subjects by intravenous administration. Gas chromatography–mass spectroscopy was used to determine the concentration of this drug in blood plasma samples. From the measurements reported below, determine whether the data are consistent with the response of a single CSTR to a pulse injection of tracer. Also determine the mean residence time of the material in the body.

Time (min)	Concentration (mg/mL)
5	921
15	815
30	667
60	430
120	190
180	75
240	28
300	16
360	8

- 11.4** In an effort to determine the cause of low yields from a reactor network, your technicians have carried out some

tracer studies in which 4.000 kg of an inert material is quickly injected at the feed port. The tracer levels leaving the reactor at various times after injection are listed below.

Time, $t$ (s)	Tracer concentration (kg/m <sup>3</sup> )
12	1.960
24	1.930
120	1.642
240	1.344
600	0.736
1200	0.268
2400	0.034
3600	0.004

You may assume that for times greater than or equal to 3600 s, no tracer is present in the effluent.

At any time the reactor contains 2 m<sup>3</sup> of fluid. The feed and effluent flow rates remain constant at 3.4 m<sup>3</sup>/ks.

Does the response of the system approximate that of any simple ideal reactor? What conversion level is expected if the reaction has a first-order rate constant of 15 ks<sup>-1</sup>?

- 11.5** Z. Kemblowski and J. Torzecki [Polym. Eng. Sci., **22** (3), 141 (1982)] have applied the concept of a residence time distribution function to analyze the potential for thermal degradation of poly(ethylene terephthalate) (PET) as it is transported in molten form to spinning machines. The time during which the molten polymer is stable ( $t_s$ ) is temperature dependent, varying from ca. 120 min at 275°C to ca. 25 min. at 295°C. For a PET sample with a weight average molecular weight of 44,000, the time during which the PET is stable at a specified temperature is given by

$$t_s = 4.32 \times 10^{-18} e^{26,843/T}$$

for  $t_s$  in seconds and  $T$  in K.

Because laminar flow occurs in the piping leading to the spinning machines, it is impossible to avoid degradation of polymer in the entire volume of the melt flowing through a pipe. Consider the problem of determining the relationship between the volume fraction of polymer which has degraded (i.e., has a residence time greater than  $t_s$ ) and the mean residence time in the pipe. Specifically, for operation at 285°C in a pipe with an ID of 4.48 cm and a length of 18 m, determine the volume fraction degraded at a mass flow rate of 0.167 kg/s. The density of molten PET at this temperature is 1170 kg/m<sup>3</sup>.

Start with the expression for a parabolic velocity profile:

$$v(r) = v_0 \left[ 1 - \left( \frac{r}{R} \right)^2 \right]$$

where  $v_0$  represents the centerline velocity,  $r$  the radial position, and  $R$  the tube radius. Then derive expressions for the corresponding  $F(t)$  curve (in dimensionless terms involving the ratio of the actual residence time to the mean residence time) and the fraction of the fluid volume with a residence time greater than  $t_s$ . Will the indicated operating conditions

produce an extent of degradation in excess of the quality control standard of 0.1%?

- 11.6** R. L. Bell [AIChE J., **18**, 495 (1972)] investigated residence time distributions on commercial-scale distillation trays using a fiber optic technique. A pulse of a 10-g/L solution of Rhodamine-B dye was injected into the downcomer of the top tray. The response data are summarized below.

Time (min)	Output (V) voltage
0.0	0.00
0.1	0.00
0.2	2.80
0.3	4.48
0.4	3.32
0.5	1.70
0.6	0.84
0.7	0.39
0.8	0.18
0.9	0.11
1.0	0.07
1.1	0.03
1.2	0.04
1.3	0.01
1.4	0.01
1.5	0.01
1.6	0.00
1.7	0.01
1.8	0
1.9	0

The output voltage is proportional to the concentration of the dye.

- (a) Determine the mean residence time and  $F(t)$  curve characteristic of this system.  
 (b) Use the longitudinal dispersion model and the variance method for determining  $D_L/uL$ .  
 (c) Estimate the number of equal-sized CSTRs in series that will give a dispersion comparable to that observed experimentally.  
 (d) Comment on your results.
- 11.7** A problem commonly encountered in the development of both gas and liquid phase chromatographic methods of analysis is that of “tailing.” In such cases it is difficult to characterize the retention time of a particular species because of the long “tail” associated with the peak. Consider the detector output indicated in Figure P11.7. The time dependence of the effluent concentration of this species can be represented by

$$C_A = \begin{cases} 0 & \text{for } 0 < t < 8.5 \text{ min} \\ 105 e^{-2t} & \text{for } t > 8.5 \text{ min} \end{cases}$$

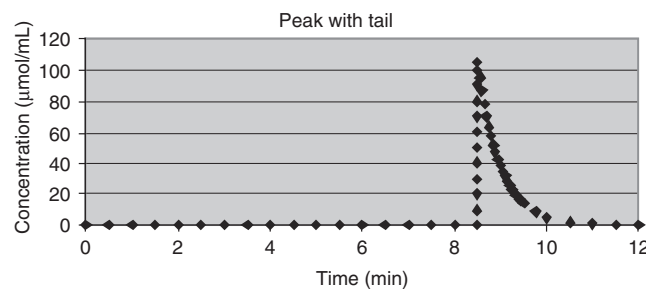
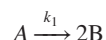


**Figure P11.7** Chromatographic peak with long tail.

for  $C_A$  in  $\mu\text{mol}/\text{mL}$ . This curve was generated by injecting a pulse of a sample containing species A into a solvent flowing through the chromatographic column at a constant flow rate.

- (a) Determine the mathematical form of the  $F(t)$  curve corresponding to the response to the pulse test.  
 (b) Use this  $F(t)$  curve to determine the average residence time of species A in the column.  
 (c) Suppose that a catalyst is present in dilute solution of species A ( $100 \mu\text{mol}/\text{mL}$ ) in the liquid carrier. In addition, suppose that this solution does not produce a measurable difference in the flow conditions or the residence times of fluid elements in the column [relative to parts (a) and (b)]. If the reaction in question is of the form



with  $k_1 = 0.12 \text{ min}^{-1}$ , use the segregated flow model to determine the average effluent concentration of species B.

- 11.8** S. M. Mahajani, M. M. Sharma, and T. Sridahar [Chem. Eng. Sci., **54**, 3967–3976 (1999)] studied the liquid phase partial oxidation of cyclohexene in a batch reactor. In the absence of a catalyst, a variety of products are formed, including cyclohexenol, cyclohexene hydroperoxide, cyclohexenone, and cyclohexene oxide. This research group obtained kinetic data for this autocatalytic reaction using a well-agitated pressure vessel in which the partial pressure of oxygen over the liquid was maintained constant by continuous addition of oxygen as the reaction proceeded. The stoichiometry of the reaction is of the general form



where C is cyclohexene, P is a generic product, and  $x$  is an undetermined stoichiometric coefficient. These investigators fit their data for this batch reactor with a rate expression of the form

$$r = k(C)(P) \quad (1)$$

This reaction is currently being carried out in a reactor network of unusual design in which injection of oxygen at several points is sufficient to maintain the partial pressure of oxygen at a value equal to that employed in the batch reactor

study. For operation at 105°C, the corresponding value of the second-order rate constant is 0.407 M<sup>-1</sup>/h.

One component of the reactor network is characterized by a cumulative residence time distribution that can be represented as

$$F(t) = \begin{cases} 0 & \text{for } 0 \leq t \leq 1 \text{ h} \\ 0.625(t-1) & \text{for } 1 \leq t \leq 2.6 \text{ h} \\ 1 & \text{for } t \geq 2.6 \text{ h} \end{cases}$$

- (a) Determine the mean residence time of the process fluid in this component of the reactor network.
- (b) Use the segregated flow model to predict the concentration of cyclohexene in the effluent from this component of the reactor network. The concentrations of C and P at the inlet to this component are 9.31 and 0.49 M, respectively. The fluid flow rate is identical with that used to generate the  $F(t)$  curve.

- 11.9 M. Y. Lyu and J. L. White [*Polym. Eng. Sci.*, **38**, 1366–1377 (1998)] studied residence time distributions for melting and flow of chemoplastic resins in a Buss kneader. For an experiment involving injection of a spike of 5 g of aluminum flakes into polystyrene, they reported the following data for a feed rate of 22.7 kg/h.

Time (s)	Aluminum (% w/w)
0	0.000
30	0.000
50	0.000
70	0.000
87	0.341
100	1.091
113	1.045
133	0.625
150	0.375
181	0.216
227	0.125
267	0.068
300	0.034
400	0.008
500	0.002
600	0.000

- (a) Prepare plots of the response curve and the cumulative residence time distribution function.
- (b) Determine the mean residence time.
- (c) Use the segregated flow model to predict the fraction of the polymer that will be thermally degraded if the degradation reaction obeys pseudo first-order kinetics with a rate constant equal to  $3 \times 10^{-5} \text{ s}^{-1}$ . Will the process meet specifications that require less than 0.5% of the polymer to be degraded in the kneader?

- 11.10 W. Zhu and Y. Jaluria [*Polym. Eng. Sci.*, **41**, 1280–1291 (2001)] determined residence time distribution curves for a twin-screw extruder in which gelatinization of cornmeal

takes place. The cornmeal enters as a solid, is heated to the reaction temperature, and is extruded as a gel.

The following data correspond to the effluent concentration of a dye in the response to a pulse injection of dye when the extruder is operating at 250 rpm, a mass flow rate of 25 kg/h, and 150°C.

Time (s)	Concentration (% w/w)
0–40	0
42	0
44	0.023
46	0.038
48	0.050
50	0.054
52	0.055
54	0.052
56	0.046
58	0.042
60	0.034
62	0.028
64	0.022
66	0.018
68	0.012
70	0.006
72	0.003
74	0.002
76	0.001
78	0.001
80	0.0005
82 = $\infty$	0

- (a) Use these data to generate a plot of the cumulative residence time distribution function,  $F(t)$ , and to determine the mean residence time.
- (b) Gelatinization of cornmeal may be regarded as a first-order reaction with  $k = 1.28 \times 10^{11} e^{-86.19/RT} \text{ min}^{-1}$  for  $R$  in kJ/mol, and  $T$  in K. Hence, at 150°C,  $k = 2.90 \text{ min}^{-1}$  or  $k = 4.834 \times 10^{-2} \text{ s}^{-1}$ .
1. Determine the conversion predicted using the segregated flow model if the extruder operates isothermally at 150°C.
  2. Determine the conversion predicted using the longitudinal dispersion model. Use open–open boundary conditions.
  3. Determine the conversion predicted using the  $n$ -CSTR model.
  4. Determine the conversion that would be obtained at 150°C in a PFR with a mean residence time equal to that in the extruder.
- (c) Comment on your results. The conversion observed experimentally is ca. 70%. Why might the observed conversion be significantly less than the conversion predicted by the various models? Suppose that the uncertainty in the operating temperature is  $\pm 5^\circ\text{C}$ . What is the corresponding uncertainty in the conversion predicted using the PFR model?

- 11.11** Consider a reactor network that consists of a cascade of two well-stirred reactors that differ in size but behave as ideal CSTRs. Prior to initiation of a trial designed to determine the average residence time for the cascade, the reactors are operating at steady state at a volumetric flow rate  $V$ . The volumes of the first and second CSTRs are  $V_{R1}$  and  $V_{R2}$ , respectively.

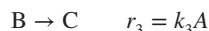
At time zero the tracer concentration in the feed stream is changed from zero to  $w_0^+$  as a step stimulus. The equation governing the time history of the concentration of tracer in the effluent from the first CSTR ( $w_1$ ) is  $w_1 = w_0^+ (1 - e^{-t/\tau_1})$ , where  $t$  is time and  $\tau_1$  is the space time for the first stirred tank.

- Derive the equation describing the time history of the concentration of tracer in the effluent from the second tank ( $w_2$ ).
- Determine the cumulative residence time distribution function,  $F(t)$ , for the cascade of two tanks that differ in size from one another.
- Use the  $F(t)$  curve to *derive* the mean residence time for the cascade in terms of the space times of the constituent reactors.

- 11.12** The cumulative residence time distribution function [ $F(t)$ ] for a cascade consisting of two nonidentical stirred-tank reactors can be represented by a mathematical expression of the form

$$F(t) = 1 + 4e^{-0.125t} - 5e^{-0.100t} \quad \text{for } t \text{ in min}$$

- Determine the mean residence time for this cascade.
- The following set of isomerization reactions takes place in the liquid phase:



Use the segregated flow model to determine the effluent concentration of species B if the values of the rate constants are 0.80, 0.10, and  $0.15 \text{ min}^{-1}$  for  $k_1$ ,  $k_2$ , and  $k_3$ , respectively.

For the conditions of interest, only species A is present in the feed to the first reactor. The feed concentration of species A is 2.0 M.

- If the reactor network is modeled as consisting of two CSTRs with space times of 8 and 10 min, determine the different concentrations of species B for each of the three possible configurations of the reactor network: the cascades in which the large reactor precedes the small CSTR, the cascade in which the small CSTR precedes the large CSTR, and the arrangement in which the two reactors are operated in parallel with one another with the feed divided evenly between the two reactors. Comment on the results obtained for the various cases.

- 11.13** The response of a “black box” reactor network to an ideal pulse of tracer can be described in terms of the following

equations for the effluent concentration of tracer:

$$C = \begin{cases} 0 & \text{for } 0 < t < \tau_1 \\ C_1 e^{-(t-\tau_1)/\tau_2} & \text{for } t > \tau_1 \end{cases}$$

The volumetric flow rate throughout the network is constant during the measurements.

- Use this information to generate a cumulative residence-time distribution function,  $F(t)$ , for this network.
- Now consider the sequence of consecutive first-order reactions



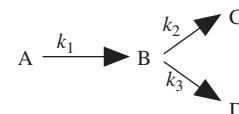
Use the segregated flow model to predict the effluent concentration of species A and V for the reactor network whose  $F(t)$  curve was determined in part (a). The feed contains only species A at an initial concentration  $A_0$ .

- 11.14** Tracer studies indicate that at an inlet volumetric flow rate of  $25 \text{ m}^3/\text{min}$ , the cumulative residence time distribution function for a reactor network is

$$F(t) = 1 - e^{-2t}$$

for  $t$  in min.

- Determine the mean residence time in this network.
- The following set of reactions takes place in the gas phase within the indicated reactor network:



The feed consists of pure A at 2 atm and  $400^\circ\text{C}$ . Each of the reactions of interest is first-order in the reactant. Use the segregated flow model to derive an expression for the effluent concentration of species B. What is this concentration if the values of  $k_1$ ,  $k_2$ , and  $k_3$  are 16.0, 1.0, and  $0.5 \text{ min}^{-1}$ , respectively?

- 11.15** A second-order reaction with a stoichiometry



takes place isothermally in a high boiling liquid that flows through a tubular reactor. The concentration of reactant A in the feed stream is 2.5 M. At the temperature of interest, the second-order rate constant is  $0.04 \text{ L}/(\text{mol} \cdot \text{min})$ . The liquid feedstock is sufficiently viscous that the flow is laminar.

The  $F(t)$  curve for the reactor is given by

$$F(t) = 0 \quad \text{for } 0 < t < 5 \text{ min}$$

and

$$F(t) = 1 - \frac{25}{t^2} \quad \text{for } t > 5 \text{ min}$$

- Determine the mean residence time of the fluid and the volume of the reactor if the volumetric flow rate is  $0.5 \text{ L}/\text{min}$ . Sketch the shape of the  $F(t)$  curve for times from 0 to 20 min.

- (b) Determine the effluent concentration of species A using the segregated flow model.
- (c) Is the concentration determined in part (b) greater than, less than, or equal to that which would be obtained in a plug flow reactor with the same mean residence time? Back up your answer with appropriate calculations.

- 11.16** The response of a reactor network to a step change in the concentration of a nonreactive tracer in the feed stream at time zero can be characterized by a parameter ( $C$ ) that represents the concentration of tracer (M) in the liquid effluent stream. For one experimental trial, the response curve can be represented in algebraic form as

$$C(t) = \begin{cases} 0.04 & \text{for } 0 \leq t \leq 3 \\ 0.04 + 0.02(t-3) & \text{for } 3 \leq t \leq 5 \\ 0.08 & \text{for } 5 \leq t \leq 8 \\ 0.08 + 0.03(t-8) & \text{for } 8 \leq t \leq 10 \\ 0.14 & \text{for } t \geq 10 \end{cases}$$

where  $t$  is expressed in minutes.

- (a) Determine the expressions that describe the  $F(t)$  curve for this network.
- (b) Determine the mean residence time for this system.
- (c) It has been suggested that this reactor network be utilized to carry out an irreversible liquid phase reaction whose stoichiometry is  $2A \rightarrow B$ . The corresponding rate expression is  $r = k[A]^{3/2}$ , where  $k = 0.2 \text{ min}^{-1} \cdot \text{L}^{1/2}/\text{mol}^{1/2}$  at the temperature of interest. If one employs the same flow rate used in the determination of the  $F(t)$  curve, what effluent concentration of species B is predicted using the segregated flow model? The feedstock is 0.81 M in species A. No B is present in the feed.
- (d) Does the value of the effluent concentration of species B predicted in part (c) represent a lower or an upper bound on this concentration?

- 11.17** In the development of the  $n$ -CSTR model, the concentration of a nonreactive tracer leaving the second reactor in the cascade of identical ideal stirred tanks varies with time in the following manner when the concentration of tracer in the feed to the first CSTR undergoes a step change from zero to  $C_0^+$ :

$$\frac{C_2}{C_0^+} = 1 - e^{-2t/\tau_2^*} \left( 1 + \frac{2t}{\tau_2^*} \right)$$

In this equation  $\tau_2^*$  refers to the total space time for the cascade of two identical CSTRs.

- (a) Determine how the effluent concentration from the third identical reactor in the cascade varies with time. Begin by writing a material balance on the third reactor and then solve this equation for  $C_3$  as a function of time. What is the corresponding equation for  $F(t)$  for a cascade consisting of three identical CSTRs?
- (b) Consider a first-order reaction of the form  $A \xrightarrow{k_1} B$  with  $k = 0.05 \text{ min}^{-1}$  at the temperature of interest. Use the

segregated flow model to predict the concentration of reactant A in the effluent from the third CSTR if the total volumetric flow rate is 40 L/min and the volume of each individual CSTR is 800 L. The inlet concentration of A is 3.0 M. How does this result compare with that obtained from the general recursion relation

$$\frac{C_{An}}{C_{A0}} = \frac{1}{(1 + k\tau_1)^n}$$

where  $\tau_1$  is the space time for an individual reactor and  $n$  is the number of identical CSTRs constituting the cascade?

- 11.18** Consider a reactor network whose cumulative residence-time distribution function,  $F(t)$ , is given by

$$F(t) = 1 - e^{-\alpha t} - \alpha t e^{-\alpha t}$$

where  $\alpha$  is related to the volume occupied by the reacting fluid and the volumetric flow rate of the process fluid. This network produces a valuable product V and an undesirable by-product W by the following sequence of catalytic reactions:



In the presence of an appropriate catalyst, the first reaction obeys a first-order rate expression [ $r_1 = k_1(A)$ ] in which the effect of the catalyst is incorporated in the rate constant. When this catalyst is employed, the rate of the second reaction is pseudo zero-order in all species. Hence, during the time that any V is still present,  $r_2 = k_2$ . The reactor network operates isothermally at a temperature such that  $k_1 = 0.06 \text{ min}^{-1}$  and  $k_2 = 1.8 \times 10^{-3} \text{ kmol}/(\text{m}^3 \cdot \text{min})$ . The feed concentration of species A is 0.81 kmol/m<sup>3</sup>.

Use the segregated flow model to predict the effluent concentration of species V as a function of  $\alpha$ . If the value of  $\alpha$  that maximizes the effluent concentration of species V is  $0.03 \text{ min}^{-1}$ , what is the corresponding effluent concentration of species V?

If you have difficulty in evaluating the integrals, it may be helpful to recall l'Hôpital's rule.

- 11.19** Sue Dent has measured the response of a tubular reactor to a step change in the inlet concentration of an inert solute. Her data are depicted in Figure P11.19. The ordinate,  $w/w_0^+$ , represents the normalized response at the outlet to a step change in the solute concentration at the inlet from 0 to  $w_0^+$ . Sue's statistical analysis of her data indicates that to a very good approximation the  $F(t)$  curve can be represented by

$$F(t) = \begin{cases} 0 & \text{for } 0 \leq t \leq 25 \text{ s} \\ 1 - \left( \frac{25}{t} \right)^2 & \text{for } t \geq 25 \text{ s} \end{cases}$$

- (a) Use the expression for  $F(t)$  to determine the mean residence time of the fluid for these flow conditions.
- (b) Now consider the possibility that a liquid-phase dimerization reaction of the form



is occurring in this reactor as it operates at a steady state with the same volumetric flow rate as employed in the

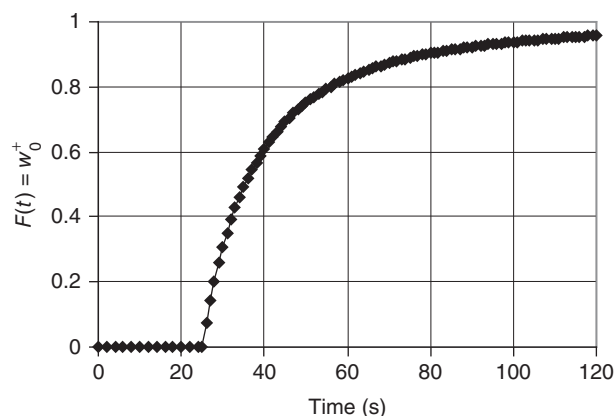


Figure P11.19 Cumulative residence time distribution.

residence time distribution study. At the temperature of interest this reaction obeys a second-order rate expression  $r = kC_A^2$ . Use the segregated flow model to predict the effluent concentration of species A when  $C_{A0} = 1.5 \text{ M}$  and  $k = 0.004 \text{ M}^{-1}/\text{s}$ .

- (c) Do you expect the result determined in part (b) to be less than, equal to, or greater than the effluent concentration of species A that will be observed in the laboratory? Explain your expectation.
- (d) One interpretation of the indicated residence time distribution function is that it corresponds to a laminar flow reactor. A second plausible interpretation is that it corresponds to an ideal plug flow reactor with a space time of 25 s followed by a somewhat less than ideal CSTR with a space time of approximately 25 s. Use this combination of reactors to predict the effluent concentration of species A.

**11.20** T. R. Hanley and R. A. Mischke [*Ind. Eng. Chem. Fundam.*, **17**, 51–58 (1978)] studied the influence of the degree of mixing on both the residence time distribution function for a tank and the extent of conversion achieved for a second reaction carried out in the tank under continuous-flow conditions. The data in Table P11.20 are characteristic of the two types of mixing behavior that were investigated. Case I corresponds to a high level of agitation and case V to minimal agitation. The tabulated data correspond to the response of the effluent composition to a pulse stimulus of tracer. Where necessary, the data have been extrapolated to provide an adequate basis for responding to the questions raised below. The tabular entries correspond to effluent concentrations measured in arbitrary units. The feed flow rate is 400 mL/min.

- (a) Prepare  $F(t)$  plots for the two cases of interest. Test the data for the well-mixed tank to ascertain whether or not they are consistent with ideal CSTR behavior. Determine the mean residence time of the fluid in the reactor for each of the two mixing situations.
- (b) Employ both the  $n$ -CSTR model and the segregated flow model to predict upper and lower bounds on the conversion expected when the second-order reaction between NaOH and ethyl acetate is carried out in the reactor. The feed to the reactor consists of two streams, one of which

Table P11.20

Time (min)	Effluent concentration (arbitrary units)	
	Case I	Case V
10	0.813	0.210
20	0.633	0.288
30	0.483	0.338
40	0.383	0.350
50	0.300	0.338
60	0.225	0.300
70	0.175	0.263
80	0.150	0.250
90	0.125	0.226
100	0.098	0.213
110	0.075	0.194
120	0.050	0.175
130	0.041	0.156
140	0.033	0.144
150	0.026	0.134
160	0.023	0.120
170	0.018	0.110
180	0.014	0.101
190	0.011	0.092
200	0.008	0.083
210	0.007	0.076
220	0.005	0.070
230	0.004	0.064
240	0.003	0.058
250	0.002	0.053
260	0.002	0.049
270	0.001	0.043
280	0.001	0.038
290	0.001	0.033
300	0.001	0.028
310	0.001	0.024
320	0.000	0.020
330	0.000	0.016
340	0.000	0.013
350	0.000	0.009
360	0.000	0.006
370	0.000	0.004
380	0.000	0.002
390	0.000	0.002
400	0.000	0.001
410	0.000	0.001
420	0.000	0.001
430	0.000	0.000
440	0.000	0.000
450	0.000	0.000
460	0.000	0.000
470	0.000	0.000
480	0.000	0.000
490	0.000	0.000
500	0.000	0.000

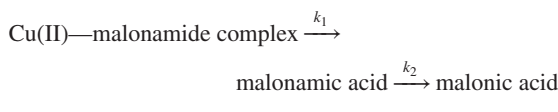
is 0.08 M in NaOH, the other being 0.08 M in ethyl acetate. Each stream enters at a flow rate of 200 mL/min so that the effective entering concentration of each reactant is 0.04 M. The rate expression for this reaction is

$$r = k (\text{NaOH})(\text{ethyl acetate})$$

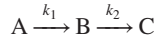
where  $\ln(k) = 16.47 - (11,200/RT)$  for  $T$  in K,  $R$  in cal/(mol·K), and  $k$  in L/(mol·s).

How do the predicted conversions compare with the conversion that would be achieved in a single ideal CSTR whose space time is the same as that for the real tank? Consider both good and poor mixing.

- 11.21** M. Arif Niaz and A. Aziz Khan [*Int. J. Chem. Kinet.*, **23**, 799–805 (1991)] studied the kinetics of the base-catalyzed hydrolysis of a Cu(II) malonamide complex in aqueous sodium hydroxide (0.25 M). The reaction network of interest can be regarded as a series of pseudo-first-order reactions.



or



where the dependence of the first-order rate constants on the NaOH concentration is given by

$$\frac{1}{k_1} = \alpha_1 + \frac{\alpha_2}{[\text{OH}^-]}$$

$$\frac{1}{k_2} = \beta_1 + \frac{\beta_2}{[\text{OH}^-]}$$

where

$$\alpha_1 = 1.14 \times 10^2 \text{ min}$$

$$\alpha_2 = 39.25 \text{ M} \cdot \text{min}$$

$$\beta_1 = 2.41 \times 10^3 \text{ min}$$

$$\beta_2 = 8.92 \times 10^2 \text{ M} \cdot \text{min}$$

- (a) If the plug flow model of reactor performance is applicable, determine the reactor space time that maximizes the effluent concentration of species B. What are the corresponding effluent concentrations of species A and B if the feed concentration of species A is 0.8 M?
- (b) Now assume that the performance of the reactor is best modeled in terms of the longitudinal dispersion model.

1. Prepare a plot of the effluent fraction conversion of species A as a function of the ratio  $L/u$  for a value of the dispersion number,  $D_L/uL$ , equal to 0.06.
2. Use the technique of eliminating time as a variable to determine the relationship between the concentrations of species A and B prevailing at any point in the reactor. Use this relation and the information from part (b1) to prepare a plot of the malonamic acid concentration in the effluent that would reflect the influence of a dispersion number  $D_L/uL$  of 0.06.

How does the value of  $L/u$  corresponding to the maximum concentration of species B correspond to the space time determined in part (a)? What is the ratio of the maximum effluent concentration of species B predicted using the longitudinal dispersion model to that predicted using the PFR model? Which conversions of species A correspond to the maxima for the two reactor models? Comment.

- 11.22** J. Fernandez-Sempere, R. Font-Montesinos, and O. Espejo-Alcaraz [*Chem. Eng. Sci.*, **50**, 223–230 (1995)] studied the residence times of possible polluting agents discarded into a municipal sewage system. A single pulse of concentrated NaCl solution (1.162 kg of Na<sup>+</sup> ions) was injected and the effluent from the sewage system was analyzed by flame spectrophotometry for Na<sup>+</sup> ions. In the table that follows, corrections have been made for any Na<sup>+</sup> ions present in the effluent before the injection. The mass flow rate may be assumed to be constant.

Time (s)	Concentration (kg/m <sup>3</sup> )
0	0.0000
300	0.0000
600	0.0000
900	0.0000
1200	0.0000
1500	0.0000
1800	1.4856
2100	1.4476
2400	0.6206
2700	0.3376
3000	0.1786
3300	0.1186
3600	0.0646
3900	0.0446
4200	0.0356
4500	0.0266
4800	0.0186
5100	0.0156
5400	0.0786
5700	0.1256
6000	0.0486
6300	0.0225
6600	0.0194
6900	0.0094
7200	0.0044

- (a) Prepare a plot of the cumulative residence-time distribution function,  $F(t)$ , for the sewage system (assume constant density).
- (b) Calculate the mean residence time in the sewage system.
- (c) Prepare an appropriate plot of the data to determine whether or not this system can be modeled as a simple, single CSTR.

- (d) If a single CSTR is not appropriate for characterizing this system, determine the number of identical stirred-tank reactors that could be used to characterize the system.
- (e) If the biological oxygen demand (BOD) of the sewage is destroyed at a rate that is pseudo first-order in the BOD concentration and if the effective rate constant is  $1.3 \times 10^{-3} \text{ s}^{-1}$  at  $60^\circ\text{F}$ , what fraction of the original BOD will remain in the effluent from the sewage system? Use both the  $n$ -CSTR model and the segregated flow model to estimate the residual BOD in the effluent. How do these conversions compare with the conversion that would be obtained in a PFR with a mean residence time equal to that of the sewage system?
- (f) Suppose that the temperature decreases by  $3^\circ\text{F}$ . By how much would the conversion achieved in the PFR decrease if the activation energy is 20 kcal/mol? Comment.
- (g) Suggest another model and use it to estimate the expected conversion.

- 11.23** Consider the following set of consecutive first-order reactions:



which take place in the liquid phase. A flow reactor with the following cumulative residence time distribution function is to be used in carrying out these reactions:

$$F(t) = 1 - e^{-t/\tau}$$

where  $\tau$  is the reactor space time.

Demonstrate your familiarity with the segregated flow model by using this model to predict the effluent concentration of species V from this reactor by proceeding in the manner indicated below. Although you may recognize the  $F(t)$  curve as that for a CSTR, you may not assume CSTR behavior for purposes of solving this problem: that is, you may not employ the design equation for a CSTR or a material balance on a CSTR in arriving at your solution.

- (a) Derive expressions for the concentrations of species A and V as functions of time in a batch reactor. The concentrations of these species at time zero are  $C_{A0}$  and  $C_{V0}$ , respectively.
- (b) Use the  $F(t)$  curve to determine the effluent concentration of species V as a function of the first-order rate constants  $k_1$  and  $k_2$ , the space time for the flow reactor, and the initial concentrations of species A and V.
- (c) If the volume of the flow reactor is  $4.0 \text{ m}^3$  and the rate constants  $k_1$  and  $k_2$  are  $3.2 \times 10^{-3}$  and  $2.0 \times 10^{-4} \text{ min}^{-1}$ , respectively, what flow rate gives the maximum concentration of species V in the effluent stream? Consider two cases: (1)  $C_{V0} = 0$  and (2)  $C_{V0} = 0.2C_{A0}$ . What are the values of  $C_V$  corresponding to the maximum for each case?

- 11.24** M. J. Hopkins, A. J. Sheppard, and P. Eisenklam [*Chem. Eng. Sci.*, **24**, 1131 (1969)] have indicated that the data in Figure P11.24 can be used to determine the dimensionless dispersion parameter,  $\mathcal{D}_L/uL$ . Use the transfer function method to

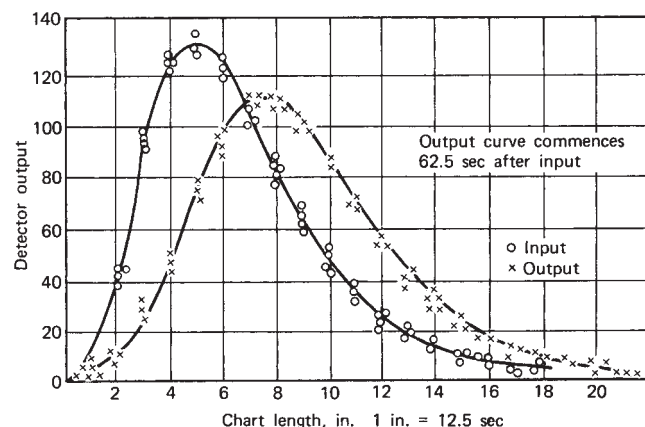


**Figure P11.24** Tracer response curve. [Reprinted from M. J. Hopkins, A. J. Sheppard, and P. Eisenklam, *Chem. Eng. Sci.*, **24**, 1131 (1969). Used with permission of Pergamon Press, Ltd.]

**Table P11.24**

Time (s)	Feed		Effluent	
	Response (arbitrary units)	Time (s)	Response (arbitrary units)	Time (s)
0	0	0	0	0
12.5	10.7	50	0	0
25.0	40.0	62.5	0	0
37.5	88.0	75	4.0	0
50.0	126.0	87.5	10.2	0
61.0	133.3	100.0	22.5	0
75.0	126.0	112.5	50.0	0
85.6	104.3	123.5	75.5	0
100.0	80.0	137.5	99.8	0
111.0	63.6	148.1	110.0	0
125.0	46.3	162.5	110.0	0
134.7	36.0	171.1	103.8	0
150.0	25.0	187.5	85.0	0
160.3	18.7	197.2	70.9	0
175.0	13.3	212.5	58.0	0
186.1	10.7	222.8	45.0	0
200	6.7	237.5	32.5	0
212.5	4.7	248.6	24.0	0
225	2.7	262.5	16.0	0
236.4	0.8	275	12.0	0
250	0.0	287.5	8.7	0
		298.9	6.7	0
		312.5	5.2	0
		325.0	3.8	0

evaluate the mean residence time and  $\mathcal{D}_L/uL$  for a system subjected to the arbitrary stimulus shown in the figure. Note that the output response has been shifted to the left by 62.5 s. Detector response values for the feed and effluent streams were as given in Table P11.24

- 11.25** D. Wolf and D. White [*AIChE J.*, **22**, 128 (1976)] investigated residence times in an extruder with a view toward examination of the possibilities of combining reaction and extrusion in a single piece of equipment. The following data correspond to the response at the exit of the extruder to injection of a single pulse of radioactive tracer.

Time interval (s)	Count rate (counts/s)
0–5	0
5–10	0
10–15	0
15–20	0
20–25	0
25–30	0
30–35	0
35–40	17,460
40–45	34,120
45–50	29,000
50–55	1,270
55–60	80
60–65	20
65–70	30
70–75	20
75–80	55
80–85	10
85–90	15
90–95	5
95–100	15
100–105	5
105–110	0
110–115	5
115–120	0
120–125	0

A polymer P is to be formed by a reaction in this extruder. Assume that the reaction can be approximated by first-order kinetics with  $k = 0.047 \text{ s}^{-1}$  and assume that the residence times can be approximated by these data.

- (a) Prepare a plot of the cumulative residence-time distribution function  $F(t)$  for the extruder.
- (b) Determine the mean residence-time characteristic of this system.
- (c) Determine the fraction conversion  $f_A$  that would be obtained in an ideal plug flow reactor operating at a space time equal to the mean residence time found in part (b).
- (d) Determine the value of  $f_A$  predicted using the segregated flow model with the  $F(t)$  plot generated in part (a).
- (e) Determine the value of the conversion predicted using the longitudinal dispersion model. Use the variance method to determine  $D_L/uL$ . Compare this value of  $f_A$  with the corresponding value obtained using the approximate solution of Levenspiel and Bischoff for small dispersion numbers. Comment on your results.

- (f) Determine the value of the conversion predicted using the  $n$ -CSTR model.

- (g) Calculate the fraction conversion assuming that the reaction is carried out in a cascade of two CSTRs. The space time for each reactor in this cascade is 22 s. Comment on your results.

- 11.26** R. S. Peterson [*Ph.D. thesis, University of Wisconsin - Madison* (1987)] carried out a series of residence time measurements on a Damrace immobilized enzyme reactor used to effect the hydrolysis of lactose to glucose and galactose. The effluent composition data given below correspond to an experiment in which a pulse of sodium acetate was injected at the reactor entrance. The liquid flow rate was maintained constant at  $6 \text{ cm}^3/\text{min}$ .

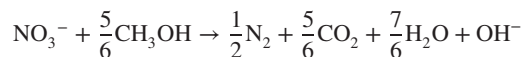
- (a) Use these data to determine the mean residence time of the fluid in the reactor.
- (b) Use the variance method to determine the dimensionless dispersion number,  $D_L/uL$ .
- (c) Use the variance method to determine the number of stirred tanks in series that would give a residence-time distribution comparable to that observed in the present experiment.
- (d) Comment on the appropriateness of using a plug flow model to predict approximate profiles of conversion versus reactor space time. The rate expression is of the form

$$r = \frac{V_m S}{K_m [1 + (P_2/K_i)] + S}$$

where S refers to lactose,  $P_2$  to the product galactose, and  $K_m$ ,  $K_i$ , and  $V_m$  are kinetic constants characteristic of the enzyme in question.

Time (min)	NaCl concentration (M) $\times 10^4$	Time (min)	NaCl concentration (M) $\times 10^4$
0.0	0	6.5	5.500
0.5	0	7.0	3.905
1.0	0	7.5	2.426
1.5	0	8.0	1.399
2.0	0	8.5	1.026
2.5	0	9.0	0.761
3.0	0	9.5	0.633
3.5	0	10.0	0.219
4.0	0.214	10.5	0.088
4.5	1.175	11.0	0.100
5.0	3.361	11.5	0.113
5.5	5.702	12.0	0

- 11.27** A. L. Parker, L. J. Sikora, and R. R. Hughes [*AIChE J.*, **22**, 851 (1976)] studied biological denitrification of wastewater streams in packed beds. For steady-state microbe populations and feed nitrate concentrations of less than 100 mg/L, the reaction



obeys a rate expression of the form

$$r = \mu Y C_N$$

where  $\mu$  is the specific nitrate removal rate,  $Y$  the biological yield coefficient,  $C_N$  is nitrate concentration, and the product  $\mu Y$  can be regarded as a pseudo-first-order rate constant for the conditions cited.

These investigators reported the following effluent response data for a 25-cm<sup>3</sup> pulse of aqueous solution containing chloride ion at the 1000-ppm level:

Time (min)	Concentration (arbitrary units)
0	0.00
10	0.00
20	0.00
30	0.00
40	0.10
50	0.38
60	0.99
70	1.40
80	1.46
90	1.31
100	1.10
110	0.86
120	0.62
130	0.40
140	0.22
150	0.08
160	0.02
170	0.00
180	0.00
190	0.00
200	0.00

- (a) Prepare a plot of the  $F(t)$  curve for this reactor.
- (b) Determine the mean residence time of the fluid in the reactor.
- (c) Calculate  $D_L/uL$  for this system using a variance approach. Use this value to determine the conversion predicted using the dispersion model in the case for which  $\mu Y = 0.451 \text{ h}^{-1}$ . Compare this result with that which would be obtained in an ideal PFR with the mean residence time obtained in part (b).
- (d) Calculate the conversion that would be obtained in a cascade of CSTRs whose  $F(t)$  curve would closely resemble that obtained in part (a).
- (e) Calculate the conversion predicted using the segregated flow model.
- 11.28** The techniques developed in this chapter for the analysis of residence-time distribution functions can be used in analyzing flow conditions in a stream or river where one wishes to determine the dispersion of pollutants from a source. The data that follow were taken from a U.S. Geological Survey study of the South Platte River (R. E. Glover, Dispersion of

Dissolved or Suspended Materials in Flowing Streams, *Geological Survey Professional Paper 433-B*, 1964). The average flow rate is 554 ft<sup>3</sup>/s, the length of reach is 19,900 ft, and the naturally occurring concentration of K<sup>+</sup> ions in the stream is 8.2 mg/L.

At time zero, 1000 lb of K<sub>2</sub>CO<sub>3</sub> is dumped into the upstream end of the reach. Periodically, samples were taken at the downstream end of the reach and analyzed for K<sup>+</sup> ions. The results are tabulated below.

Time, $t$ (min)	K <sup>+</sup> at downstream end (g/m <sup>3</sup> )
0	8.2
60	8.2
75	8.2
90	8.2
105	8.4
120	9.6
130	13.6
132.5	14.8
134	14.8
138	14.6
142.5	13.2
150	12.8
165	10.0
180	9.2
195	8.2
210	8.2
$\infty$	8.2

- (a) Calculate the fraction of the tracer that was recovered.
- (b) Basing your calculations on the amount of tracer recovered, compute the  $F(t)$  curve. Also compute the average residence time  $\bar{t}$  and prepare plots of the effluent concentration of K<sup>+</sup> that exceeds the background level and  $F(t)$  versus  $t/\bar{t}$ .
- (c) An organic species A is a potential pollutant that is present in the waste stream from a factory that empties into the upper end of the reach. The mixing cup average concentration of A at the upper end of the reach is 100 mg/L. Species A is converted to a product that is harmless by a first-order reaction in solution. What fraction of the initial concentration of species A is present at the downstream end of the reach? The effective rate constant at the stream temperature is equal to 0.01 min<sup>-1</sup>. Use the segregated flow model for this calculation.
- (d) Based on the  $F(t)$  curve, what is the apparent axial dispersion coefficient of the tracer if one assumes that the stream approximates a nonideal plug flow reactor with axial dispersion?
- (e) Based on the model of part (d), and using the axial dispersion coefficient calculated therein, determine if the average concentration of A present at the downstream end of the reach is greater than, less than, or equal to that predicted in part (c)?

**11.29** When catalytic reactions are carried out in a fluidized-bed reactor, one may observe conversions lower than those predicted using either PFR or CSTR models. Such observations are often attributed to gas bypassing by bubbles that do not contact the catalyst efficiently. M. Iwasaki, I. Furuoya, H. Sueyoshi, T. Shirasaki, and E. Echigoya [*Kagaku Kogaku*, **29** (11), 892 (1965)] have described a method for measuring the distribution of times that reactive gases are in contact with the solid. The technique is based on pulse injections of two gases, one of which is adsorbed by the solid and the second of which is not adsorbed. Typical data are given in Table P11.29.

- (a) Assuming injection of an ideal pulse, determine:
1. The  $F(t)$  curves for both the inert gas and the reactive gas.
  2. The  $F(t)$  curve for the contact-time distribution.
  3. The effective dispersion parameter for the inert gas case,  $D_L/uL$ .
- (b) For a first-order irreversible isomerization reaction ( $A \rightarrow R$ ) with  $k = 0.45 \text{ s}^{-1}$ , determine the conversions predicted using the following reactor models: plug flow with  $\tau = \bar{t}$  for the reactive gas experiment and with  $\tau =$  average contact time.

**Table P11.29** Pulse Stimulus–Response Data for Inert and Adsorbed Gases

Time, $t$ (s)	Concentration (arbitrary units)	
	Inert gas	Adsorbed gas
0.0	0.0	0.0
0.8	0.0	0.0
1.6	0.0	0.0
2.4	0.01	0.01
3.2	5.0	5.0
4.0	10.0	7.5
4.8	8.0	8.5
5.6	4.0	8.0
6.4	0.0	6.5
7.2	0.0	4.0
8.0	0.0	2.0
8.8	0.0	1.0
9.6	0.0	0.0

# Chapter 12

---

## Reactor Design for Heterogeneous Catalytic Reactions

### 12.0 INTRODUCTION

Heterogeneous catalytic reactors are the most important single class of reactors utilized by the chemical industry. Whether their importance is measured by the wholesale value of the goods produced, the processing capacity, or the overall investment in the reactors and associated peripheral equipment, there is no doubt as to the prime economic role that reactors of this type play in modern industry. The focus of this chapter is the design of heterogeneous catalytic reactors. Particular emphasis is placed on the concept of catalyst effectiveness factors and the implications of heat and mass transfer processes for fixed bed reactor design.

### 12.1 COMMERCIALLY SIGNIFICANT TYPES OF HETEROGENEOUS CATALYTIC REACTORS

The types of reactors used in industry for carrying out heterogeneous catalytic reactions may be classified in terms of a relatively small number of categories. One simple means of classification is in terms of the relative motion of the catalyst particles, or lack thereof. In the sections that follow we consider:

1. Reactors in which the solid catalyst particles remain in fixed positions relative to one another (fixed bed, trickle bed, and moving bed reactors).
2. Reactors in which the particles are suspended in a fluid and are moving about constantly (fluidized bed and slurry reactors).

#### 12.1.1 Heterogeneous Catalytic Reactors in Which the Motion of the Catalyst Particles Relative to One Another Is Insignificant

##### 12.1.1.1 Fixed Bed Reactors

In its most basic form, a fixed bed reactor consists of a cylindrical tube filled with catalyst pellets. Such reactors are also known as packed bed reactors. Reactants flow through the catalyst bed and are converted into products. They may be regarded as the workhorse of the chemical industry with respect to the number of reactors employed and the economic value of the materials produced. Ammonia synthesis, sulfuric acid production (by oxidation of  $\text{SO}_2$  to  $\text{SO}_3$ ), and nitric acid production (by oxidation of  $\text{NH}_3$ ) are only a few of the extremely high tonnage processes that make extensive use of various forms of packed bed reactors.

The catalyst constituting the fixed bed will generally be employed in one of the following configurations:

1. A single large bed.
2. Multiple horizontal beds supported on trays arranged in a vertical stack.
3. Multiple parallel packed tubes in a single shell.
4. Multiple beds each in its own shell.

The use of configurations employing multiple beds of catalyst usually arises because of the need to maintain adequate temperature control within the system. Other constraints leading to the use of multiple beds include those of pressure drop or adequate fluid distribution. In addition to the shell-and-tube configuration, some of the possibilities

for heat transfer to or from fixed bed reactors include the use of internal heat exchangers, annular cooling spaces or cooling thimbles, and circulation of a portion of the reacting gases through an external heat exchanger.

The packing itself may consist of spherical, cylindrical, or randomly shaped pellets, wire screens or gauzes, crushed particles, or a variety of other physical configurations. The particles usually are 0.25 to 1.0 cm in diameter. The structure of the catalyst pellets is such that the internal surface area far exceeds the superficial (external) surface area, so that the contact area is, in principle, independent of pellet size. To make effective use of the internal surface area, one must use a pellet size that presents negligible diffusional resistance within the catalyst pellet but that also gives rise to an acceptable pressure drop across the catalyst bed. Some considerations that are important in the handling and use of catalysts for fixed bed operation in industrial situations are discussed elsewhere (1,2).

The most commonly used direction of reactant flow is downward through the bed. This approach gives a stable bed that will not fluidize, dance, or lift out of the reactor. This approach minimizes catalyst attrition and potential entrainment of catalyst fines. When processing conditions are such that the reactor is subjected to wide variations in feed flow rates or when the feed is a dense fluid, it is imperative that the flow direction be downward. The attendant disadvantages of downward flow are the tendency of the bed to compress itself and the gravitation of catalyst fines (resulting from attrition) down through the bed. Both phenomena may lead to increased pressure drop and channeling or maldistribution of the flow.

Upflow has the advantage of lifting catalyst fines or fragmented particles from the bed, thereby avoiding channeling and blockage of the bed. However, this mode of operation is disadvantageous because it may lead to unstable beds at high flow rates. It leads to dancing particles in a pulsating flow that causes catalyst abrasion and, in unusual circumstances, may lead to fluidization.

A fixed bed reactor has many unique and valuable advantages relative to other reactor types. One of its prime attributes is its simplicity, with the attendant consequences of low costs for construction, operation, and maintenance relative to moving bed or fluidized bed operation. Fixed bed reactors require a minimum of auxiliary equipment and are particularly appropriate for use in small commercial units when investments of large sums for control, catalyst handling, and supporting facilities would be economically prohibitive. Another major advantage of this mode of operation is implicit in the use of the term *fixed bed reactor* (i.e., there are no problems in separating the catalyst from the reactor effluent stream). (In many fluidized bed systems, catalyst recovery can be quite troublesome and require substantial equipment costs.) Another important attribute of fixed bed reactors is the wide variation in

space times at which they can be operated. This flexibility is extremely important in situations where one is likely to encounter wide variations in the quantity or quality of the feedstock to be processed. For extremely high temperature or high pressure reactions employing solid catalysts, economic considerations usually dictate that the process becomes commercially viable only when a fixed bed reactor is employed.

There are some cases where the disadvantages of fixed bed operation prevent the use of such reactors. Heat transfer to or from a large fixed bed of catalyst often represents a significant problem. In some cases it is possible to circumvent this potential difficulty by appropriate variations in the physical configuration of the catalyst bed (e.g., using a shell-and-tube arrangement). There are also a variety of operating techniques that can be used to facilitate control over the bed temperature. These include the use of inert diluents in the feed stream to moderate the temperature changes, and the use of the *cold shot* or *gas bypass technique*, in which a fresh cold reactant stream is mixed with a hot stream that has undergone partial reaction. Recycle of a product stream and partial temporary poisoning of the catalyst are two other expedients that can be used to help regulate the temperature in fixed-bed reactors.

The problem of heat transfer is a difficult one because the rate of energy release or consumption along the length of the reactor is not uniform. The major share of the reaction often takes place near the reactor inlet. In an exothermic reaction, the rate will be relatively large near the inlet because of high reactant concentrations. If the rate of energy release is greater than the rate at which heat can be transferred to a coolant fluid, the temperature of the reacting fluid will continue to increase, leading to an even faster reaction rate. This phenomenon continues as the mixture moves down the tube, until the decline in reactant concentration has a larger effect on the rate than does the temperature increase. The net result is that for exothermic reactions one often observes a maximum in a plot of temperature versus distance from the reactor inlet.

The maintenance of uniform flow distribution in fixed bed reactors is frequently a problem. Undesirable flow patterns lead to excessive spreads in the distribution of residence times with adverse effects on the reactor performance, particularly when consecutive reactions are involved. Poor flow distributions may aggravate problems of hot-spot formation and lead to regions of the reactor where undesired reactions predominate. Disintegration or attrition of the catalyst may lead to or may aggravate flow distribution problems.

Another disadvantage of fixed bed reactors is associated with the fact that the minimum pellet size that can be used is restricted by the permissible pressure drop through the bed. Thus, if the conversion rate is potentially subject to

diffusional limitations within the catalyst pore structure, it may not be possible to fully utilize all the catalyst area (see Section 12.3). The smaller the pellets, the more efficiently the internal area is used, but the greater the pressure drop across the bed of catalyst.

One of the major disadvantages of fixed bed operation is that catalyst regeneration or replacement is relatively difficult to accomplish. If the catalyst deactivation rate is sufficiently rapid, costs associated with the catalyst regeneration or replacement step may render the entire process unattractive from a commercial standpoint. The effective catalyst life necessary to render the process economic for fixed bed operation depends on the details of the process under study, but if the lifetime is not at least several months, the costs of the shutdowns will normally be exorbitant. In situ regeneration offers a possible way around this difficulty, but if continuous operation is to be maintained, the use of in situ regeneration requires two or more reactors in parallel with concomitant higher capital costs. The most successful fixed bed operations are those in which the catalyst activity does not decline markedly over long time periods. A technique that can occasionally be used to prolong the time between regenerations and shutdowns is the use of catalyst beds that are longer than are required to accomplish the desired degree of conversion. If the bed depth required is relatively short, doubling or tripling the depth of the catalyst packing will greatly prolong the time that the unit can remain onstream. When the unit is first brought onstream, the desired conversion will be accomplished in the first portion of the bed. As the catalyst activity declines, the portion of the bed in which the bulk of the reaction is accomplished will move down the bed until, finally, insufficient catalyst activity remains to accomplish the required degree of conversion. Unfortunately, this approach can be used only with certain reactions, the most well known example being the ammonia synthesis reaction.

### 12.1.1.2 Trickle Bed Reactors

A trickle bed reactor utilizes a fixed bed over which liquid flows without entirely filling the void spaces between particles. The liquid usually flows downward under the influence of gravity, while the gas flows upward or downward through the void spaces between the catalyst pellets and the liquid holdup. Generally, co-current downward flow of liquid and gas is preferred because this mode of operation facilitates a uniform distribution of the liquid across the catalyst bed and permits the employment of higher liquid flow rates before encountering flooding constraints.

The primary uses of trickle bed reactors are for hydrodesulfurization, hydrocracking, and hydrotreating of various high-boiling petroleum fractions. The direct and capital costs are significantly less for trickle bed operation than for an equivalent hydrodesulfurization unit operating

entirely in the vapor phase. The use of this reactor type makes it possible to process feedstocks with such high boiling points that straight vapor-phase operation would lead to excessive undesirable side reactions.

Despite the fact that trickle bed reactors often approach plug flow behavior, the use of a liquid phase in the feed introduces several complications in the design analysis. The nature and extent of the liquid distribution within the catalyst bed vary drastically with changes in the liquid and vapor flow rates, the properties of the reaction mixture (especially its viscosity and wetting characteristics), and the design of the reactor (especially the liquid distribution system). As the liquid distribution changes, there are concomitant changes in the contacting efficiencies between the liquid, vapor, and catalyst. Usually, gaseous reactants must first be absorbed and transported across a thin liquid film to the exterior of the catalyst pellet. They must subsequently be transported through liquid-filled pores to sites in the catalyst interior. By using a low ratio of liquid to catalyst in the reactor, one is able to minimize the extent of the homogeneous reaction. However, a balance must be struck for highly exothermic reactions, because the energy released by reaction may be sufficient to volatilize the liquid in substantial portions of the bed. In such cases, portions of the bed will not be wetted, and there will be poor contacting between liquid and catalyst.

One often finds that either external or intraparticle mass transfer effects are significant in trickle bed reactors. Although the treatments of these topics outlined in Sections 12.3 and 12.4 are in general applicable to trickle bed reactors, analyses specific to such reactors have been reviewed by Gianetto and Specchia (3).

### 12.1.1.3 Moving Bed Reactors

In moving bed reactors, a fluid phase passes upward through a packed bed of catalyst pellets. Pellets are fed to the top of the bed, move downward under the influence of gravity in a manner approximating plug flow, and are removed from the bottom. The catalyst pellets are then transferred in continuous fashion to the top of the reactor using external equipment to effect pneumatic or mechanical transport. During the period when the catalyst pellets are not in the reactor proper, they may be regenerated or reconditioned in an auxiliary facility.

It is necessary to design special control valves to provide proper solids flow and to maintain close control over the solids level within the reactor. Moreover, care must be taken in the design of these reactors to prevent bypassing of the bed by the fluid reactant stream and to ensure good distribution of the solids at all levels. These potential difficulties indicate why these types of reactors are less frequently used than fixed or fluidized bed reactors. When catalyst decay is slow, so that fixed

bed operation is satisfactory with infrequent shutdown for catalyst regeneration, moving bed operation does not offer a viable alternative. In catalytic cracking where catalyst deactivation is so rapid that fixed beds must be regenerated after only a few minutes of time on stream, the disadvantages of these reactors are obvious. Either moving bed or fluidized bed operation is imperative in such cases. The primary disadvantage of moving bed operation vis-à-vis fluidized bed operation is in its reduced capability to facilitate heat transfer in either the reactor proper or the regeneration unit. This reduced capability makes it difficult to achieve the control of the catalyst temperature necessary to prevent high-temperature deactivation processes. In instances where catalyst deactivation is not rapid but is still appreciable and can be circumvented by intermittent regeneration, moving bed operation may offer advantages over using several fixed bed reactors in parallel. Because the process economics are dependent on the deactivation rate and other process details, no general rule of thumb is applicable.

The catalyst in moving bed operations usually has an important role as a heat-carrying medium. The energy released by carbon burnoff in exothermic regeneration reactions can be used to supply some of the energy requirements of endothermic cracking reactions with attendant savings in overall energy costs.

## 12.1.2 Heterogeneous Catalytic Reactors in Which There Is Significant Motion of the Catalyst Particles Relative to One Another

### 12.1.2.1 Fluidized Bed Reactors

A fluidized bed reactor is one in which relatively small particles of catalyst are suspended by the upward motion of the reacting fluid. In virtually all industrial applications the fluid is a gas that flows upward through the solid particles at a rate that is sufficient to lift them from a supporting grid, but which is not so large as to carry them out of the reactor or to prevent them from falling back into the fluidized phase above its free surface. The particles are in constant motion within a relatively confined region of space, and extensive mixing occurs in both the radial and longitudinal directions of the bed.

Fluidized bed reactors were first employed on a large scale for the catalytic cracking of petroleum fractions, but more recently they have been employed for an increasingly large variety of reactions, both catalytic and noncatalytic. The catalytic reactions include the partial oxidation of naphthalene to phthalic anhydride and the formation of acrylonitrile from propylene, ammonia, and air. Noncatalytic applications include the roasting of ores and fluorination of uranium oxide.

Typically, the catalyst particles used in fluidized bed operations have dimensions in the range of 10 to 300  $\mu\text{m}$ . For optimum fluidization, it is important to employ the proper particle size distribution. Beds of large, uniformly sized solids often fluidize poorly with bumping, slugging, and spouting, which can cause serious structural damage in large beds. In such cases the quality of the fluidization can frequently be drastically improved by adding small amounts of fines. Fine particles with a relatively wide distribution of particle diameters will remain fluidized over a wide range of gas flow rates, permitting flexible operation with relatively large beds. Commercial scale fluidized bed reactors may be extremely large pieces of equipment. Diameters of 10 to 30 ft are not unusual for catalytic cracking units. Typically, height/diameter ratios of 2 : 1 or greater are employed. Large systems are required in part to accommodate heat transfer equipment, cyclone separators, and other internal equipment.

Several advantages are associated with the use of fluidized bed reactors. A remarkably uniform temperature can be maintained throughout the catalyst bed. This property is a consequence of the high degree of turbulence within the bed, the high heat capacity of the solid catalyst comprising the bed relative to the gas contained therein, and the extremely high interfacial area for heat transfer between the solid and the gas phase. These factors facilitate control over the temperature of the reactor and its contents. Better control in turn enhances the selectivity that can be achieved and permits very large scale operations.

The primary advantage of fluidized bed reactors, however, is that they permit continuous, automatically controlled operations using reactant–catalyst systems that require catalyst regeneration at very short intervals. Fluidized bed operation permits one to easily add or remove the catalyst from the reactor or the regenerator. Regeneration can be accomplished by any convenient procedure, but the use of fluidized bed regeneration permits continuous operation and is usually most economical. Furthermore, the circulation of solids between two fluidized beds makes it possible to transport large quantities of energy between the reactor and the regenerator. This feature is particularly useful in catalytic cracking reactions where exothermic regeneration reactions can be harnessed to supply some of the energy requirements for endothermic cracking reactions.

Still another advantage of fluidized bed operation is that it leads to more efficient contacting of gas and solid than many competitive reactor designs. Because the catalyst particles employed in fluidized beds have very small dimensions, one is much less likely to encounter mass transfer limitations on reaction rates in these systems than in fixed bed systems.

Disadvantages are also associated with fluidized bed reactors. These reactors cannot be used with catalyst

solids that will not flow freely or that have a tendency to agglomerate. Attrition of the solids also causes some loss of material as fines, which are blown out of the reactor. Extensive solids collection systems, including cyclone separators and electrostatic precipitation, must often be provided to minimize catalyst losses and contamination of the environment. Another disadvantage of fluidized bed operation is that it leads to a larger pressure drop than fixed bed operation with concomitant higher operating costs. Erosion of pipes and reactor internals via abrasion caused by the particles can occur. In general, operating and maintenance costs will be relatively high for this mode of operation compared with operations at a similar scale with other reactor types. Fluidized bed operations also have the disadvantage that the fluid flow deviates markedly from plug flow, and the bypassing of solids by bubbles can lead to inefficient contacting. This problem is particularly significant when dealing with systems in which high conversions are desired. The problem can be circumvented to some extent by using multiple beds in series or internal staging.

Despite the drawbacks enumerated above, fluidized bed reactors have a number of compelling advantages, as we noted previously. By proper design one can overcome their deficiencies so that their advantages predominate. In this book we do not discuss in detail the manner in which this problem can be solved, although the design considerations outlined in subsequent sections of this chapter are quite pertinent. For detailed treatments of fluidized bed reactor design, consult the works by Kunii and Levenspiel (4) and Yang (5).

### 12.1.2.2 Slurry Reactors

Slurry reactors are commonly used in situations where it is necessary to contact a liquid reactant or a solution containing the reactant with a solid catalyst. To facilitate mass transfer and effective utilization of the catalyst, one usually suspends a powdered or granular form of the catalyst in the liquid phase. This type of reactor is useful when one of the reactants is normally a gas at the reaction conditions and the second reactant is a liquid (e.g., in the hydrogenation of various oils). The reactant gas is bubbled through the liquid, dissolves, and then diffuses to the catalyst surface. Mass transfer limitations on reaction rates can be quite significant in those instances where three phases (the solid catalyst and the liquid and gaseous reactants) are present and necessary to proceed rapidly from reactants to products.

Satterfield (6) discussed several advantages of slurry reactors relative to other modes of operation. They include the following.

1. A well-agitated slurry may be kept at a uniform temperature throughout, eliminating "hot" spots, which have adverse effects on catalyst selectivity.

2. The high heat capacity associated with the large mass of liquid facilitates control of the reactor and provides a safety factor for exothermic reactions that might lead to thermal explosions or other "runaway" events.
3. Because liquid phase heat transfer coefficients are large, heat recovery is practical with these systems.
4. The small particles used in slurry reactors may make it possible to obtain much higher rates of reaction per unit weight of catalyst than would be achieved with the larger pellets that would be required in trickle bed reactors. This situation occurs when the trickle bed pellets are characterized by low effectiveness factors (see Section 12.3).
5. Essentially continuous regeneration of the catalyst can be obtained by continuously removing a fraction of the slurry from which the catalyst is then separated, regenerated, and returned to the reactor.
6. Because fine catalyst particles are desired, the costs associated with the pelleting process are avoided, and it becomes possible to use catalysts that are difficult or impossible to pelletize.

A major deterrent to the adoption of continuous slurry reactors is the fact that published data are often inadequate for design purposes. Solubilization and mass transfer processes may influence observed conversion rates, and these factors may introduce design uncertainties. One also has the problems of developing mechanical designs that will not plug up and of selecting carrier liquids in which the reactants are soluble, yet which remain stable at elevated temperatures in contact with reactants, products, and the catalyst. An additional disadvantage of the slurry reactor is that the ratio of liquid to catalyst is much greater than in a trickle bed reactor. Hence, the relative rates of undesirable homogeneous liquid phase reactions will be greater in the slurry reactor, with a potentially adverse effect on the process selectivity.

Slurry reactors may take on several physical forms: They may be simple stirred autoclaves, they may be simple vessels fitted with an external pump to recirculate the liquid and suspended solids through an external heat exchanger, or they may resemble a bubble-tray rectifying column with several stages placed above one another in a single shell. Because a single slurry reactor has a residence time distribution approximating that of a CSTR, the last mode of construction gives an easy means of obtaining stagewise behavior and more efficient utilization of the reactor volume.

For more detailed treatments of slurry reactors, see the text of Satterfield (6) and the review by Wang et al. (7).

## 12.2 MASS TRANSPORT PROCESSES WITHIN POROUS CATALYSTS

Heterogeneous catalysis involves an interaction between a solid substrate and reactant molecules in a fluid phase. This interaction occurs at the interface between the two phases, and efficient utilization of the catalyst may require that the surface area per unit weight of catalyst be as large as possible. For commercial applications, this requirement implies that the catalyst should be porous with a large internal surface area. Typical industrial catalysts have specific surface areas, ranging from 1 to 1000 m<sup>2</sup>/g. With the exception of the use of wire gauzes for high-temperature oxidation processes (e.g., oxidation of NH<sub>3</sub> or SO<sub>2</sub>), nonporous catalysts have not been used extensively in commercial applications. For porous catalysts the superficial external surface of the catalyst will normally represent only an insignificant fraction of the total surface area. A spherical catalyst pellet with a diameter of 0.5 cm weighing 0.1 g would have an apparent external geometric surface area of only  $7.8 \times 10^{-5}$  m<sup>2</sup>. If it had a modest specific surface area of 10 m<sup>2</sup>/g, the internal surface area would be 1 m<sup>2</sup>. Hence, even a thin outer shell of the catalyst, which is only 0.05 cm deep, would have an associated surface area that would be orders of magnitude greater than the external surface area. Consequently, to obtain high specific activities, it is necessary to use highly porous catalysts in industrial situations.

One requires only an extremely limited knowledge of fluid flow processes to recognize that the pressure drop through a typical fixed bed of catalyst is not sufficient to force any perceptible amount of fluid through the very small pores of catalyst particles that are required to obtain surface areas of from 1 to 1000 m<sup>2</sup>/g. If reactants are to come in contact with the interior surface of catalyst particles, they must do so by diffusion. If one has a fast reaction and relatively long catalyst pores, reactant molecules will be converted to products before they have time to diffuse very far into the pore structure. In this case, the interior of the particle will be filled primarily with product molecules, and only the outer peripheral layer of the catalyst pellet will be fully effective in promoting reaction. The problem of determining what fraction of the total catalyst surface area is used effectively in promoting chemical reaction and the implications of this situation for chemical reactor design are treated in Section 12.3. In the most general case, the problem involves a complex interaction between chemical reaction, diffusive mass transfer, and heat transfer processes.

One must understand the physical mechanisms by which mass transfer takes place in catalyst pores to comprehend the development of mathematical models that can be used in engineering design calculations to estimate what fraction of the catalyst surface is effective in promoting

reaction. There are several factors that complicate efforts to analyze mass transfer within such systems. These complications include the facts that (1) the pore geometry is extremely complex, and not subject to realistic modeling in terms of a small number of parameters, and that (2) different molecular phenomena are responsible for the mass transfer. Consequently, it is often useful to characterize the mass transfer process in terms of an *effective diffusivity*, that is, a transport coefficient that pertains to a porous material in which the calculations are based on *total area* (void plus solid) *normal to the direction of transport*. For example, in a spherical catalyst pellet, the appropriate area to use in characterizing diffusion in the radial direction is  $4\pi r^2$ .

Unfortunately, it is not possible to obtain effective diffusivities merely by correcting bulk phase diffusivities for the reduction in cross-sectional area associated with the solid phase. Two primary factors render this simple approach invalid:

1. The geometry of the pore structure makes it impossible to accurately determine the effective length of the diffusion path. Interconnections within the pore structure, the tortuous character of individual pores, and variations in cross-sectional area along the pore length all contribute to the difficulty of the task.
2. One or more of several different mechanisms may be responsible for the mass transfer process. These include ordinary bulk diffusion, Knudsen diffusion, surface diffusion, and bulk flow. For the majority of the catalysts and conditions used in industrial practice, the only significant mechanisms are bulk diffusion and Knudsen diffusion. The relative importance of these two processes depends on the relative values of the mean free path and the pore dimensions.

*Ordinary or bulk diffusion* is primarily responsible for molecular transport when the mean free path of a molecule is small compared with the diameter of the pore. At 1 atm the mean free path of typical gaseous species is on the order of 10<sup>-5</sup> cm or 10<sup>3</sup> Å. In pores with diameters larger than 10<sup>-4</sup> cm, the mean free path is much smaller than the diameter, and collisions with other gas-phase molecules will occur much more often than collisions with the pore walls. Under these circumstances the effective diffusivity will be independent of the pore diameter, and within a given catalyst pore, ordinary bulk diffusion coefficients may be used with Fick's first law to evaluate the rate of mass transfer and the concentration profile in the pore. In industrial practice there are three general classes of reaction conditions for which use of the bulk value of the diffusion coefficient is appropriate. For all catalysts, these include liquid-phase reactions and very high pressure reactions in which the fluid density approaches the critical density of the material. The third class is made up of low-pressure

gas phase reactions that take place over catalysts with very large pores, say greater than 5000 Å in diameter. When bulk diffusion is operative, a number of correlations may be used to estimate the ordinary molecular diffusivity in the absence of experimental data. Poling et al. (8) summarized these correlations in convenient form.

*Knudsen diffusion* will be the dominant mechanism of mass transfer whenever the mean free path between collisions is large compared with the pore diameter. This situation prevails when the gas density is low or when the pore dimensions are very small. This mechanism is not observed with liquids. The molecules hitting the walls are adsorbed momentarily and then are given off in random directions (diffusely reflected). After a collision with the pore wall, the molecule will usually move to another spot on the wall before having a collision with a second gas-phase molecule. Many collisions with the walls will take place for each collision between gas-phase molecules. The molecule moves down the catalyst pore by a series of random flights, interrupted by collisions with the pore walls. The gas flux is reduced by the wall "resistance." The resulting transport of these molecules is delayed because of the finite time the molecules are adsorbed on the pore walls and because after a collision with the wall, the molecule is just as apt to reverse its direction as it is to continue along its original path. If the equation for the gas flow in a *straight cylindrical pore* for the case of Knudsen flow is analyzed according to the principles of the kinetic theory of gases, it can be shown that the molar flow rate ( $F$ ) can be expressed as

$$F = -\pi\bar{r}^2 \frac{2}{3}\bar{r} \sqrt{\frac{8RT}{\pi M}} \frac{\Delta C}{\Delta X} \quad (12.2.1)$$

where  $\bar{r}$  is the mean pore radius,  $R$  the gas constant,  $T$  the absolute temperature,  $M$  the molecular weight, and  $\Delta C/\Delta X$  the concentration gradient along the pore.

Because  $\pi\bar{r}^2$  is the cross-sectional area for flow and the term under the radical is the average molecular velocity ( $\bar{v}$ ), equation (12.2.1) can be written in the form of Fick's first law as

$$\frac{F}{\pi\bar{r}^2} = -D_K \frac{\Delta C}{\Delta X} \quad (12.2.2)$$

where the Knudsen diffusivity  $D_K$  is

$$D_K = \frac{2}{3}\bar{r} \sqrt{\frac{8RT}{\pi M}} = \frac{2}{3}\bar{r} \bar{v} \quad (12.2.3)$$

The Knudsen diffusivity is thus directly proportional to the pore radius,  $\bar{r}$ . Equation (12.2.3) is often written in cgs units as

$$D_K = 9.7 \times 10^3 \bar{r} \sqrt{\frac{T}{M}} \quad (12.2.4)$$

where  $D_K$  is expressed in  $\text{cm}^2/\text{s}$ ,  $\bar{r}$  is expressed in centimeters, and  $T$  is expressed in  $\text{K}$ .

The symbols refer to a single component. Because molecular collisions are rare events in Knudsen flow, flow and diffusion are synonymous and each component of a mixture behaves as if it alone were present. Numerical values of the Knudsen diffusivity for molecules of ordinary weight at the temperatures of primary interest range from  $0.01 \text{ cm}^2/\text{s}$  for pores with a radius of 10 Å to roughly  $10 \text{ cm}^2/\text{s}$  for pores with 10,000-Å radii.

By comparing the relative magnitudes of the mean free path ( $\lambda$ ) and the pore diameter ( $2\bar{r}$ ), it is possible to determine whether bulk diffusion or Knudsen diffusion may be regarded as negligible. Using the principles of the kinetic theory of gases, one can show that this ratio is equal to the ratio of the bulk diffusivity ( $D_{AB}$ ) to the Knudsen diffusivity:

$$\frac{\lambda}{2\bar{r}} = \frac{D_{AB}}{D_K} \quad (12.2.5)$$

Obviously, there will be a range of pressures or molecular concentrations over which the transition from ordinary molecular diffusion to Knudsen diffusion takes place. Within this region both processes contribute to the mass transport, and it is appropriate to utilize a combined diffusivity ( $D_c$ ). For species A the correct form for the combined diffusivity is the following:

$$D_c = \frac{1}{[1/D_K] + [(1 - \alpha Y_A)/D_{AB}]} \quad (12.2.6)$$

where  $Y_A$  is the mole fraction of species A in the gas phase,  $D_{AB}$  the bulk diffusivity in a binary gaseous mixture of A and B, and  $\alpha$  is given by

$$\alpha = 1 + \frac{N_B}{N_A} \quad (12.2.7)$$

where  $N_A$  and  $N_B$  are the molar fluxes of A and B relative to a fixed coordinate system.

The combined diffusivity is defined as the ratio of the molar flux to the concentration gradient, irrespective of the mechanism of transport. Equation (12.2.7) was derived by separate groups working independently (9–11). It is important to recognize that the molar fluxes ( $N_i$ ) are defined with respect to a fixed catalyst pellet rather than to a plane of no net transport. Only when there is equimolar counterdiffusion do the two types of flux definitions become equivalent. For a more detailed discussion of this point, interested readers should consult Bird et al. (12). When there is *equimolar* counterdiffusion,  $N_B = -N_A$  and equation (12.2.6) reduces to

$$D_c = \frac{1}{(1/D_K) + (1/D_{AB})} \quad (12.2.8)$$

Equimolar counterdiffusion takes place in catalyst pores when a reaction with a stoichiometry of the form  $A \rightarrow B$  occurs under steady state conditions.

In the case of nonequimolar counterdiffusion, equation (12.2.6) suffers from the serious disadvantage that the combined diffusivity is a function of the gas composition in the pore. This functional dependence carries over to the effective diffusivity in porous catalysts (see below) and makes it difficult to integrate the combined diffusion and transport equations. As Smith (13) points out, the variation of  $D_c$  with composition ( $Y_A$ ) is not usually strong, and it has been almost universal practice to use a composition independent form of  $D_c$  (12.2.8) in assessing the importance of intrapellet diffusion. In fact, the concept of a single effective diffusivity loses its engineering utility if the dependence on composition must be retained.

Whether Knudsen or bulk diffusion dominates the mass transport process depends on the relative magnitudes of the two terms in brackets in the denominator of equation (12.2.6). The ratio of the two diffusivity parameters is obviously important in establishing these magnitudes. In this regard it is worth noting that  $D_K$  is proportional to the pore diameter and independent of pressure, whereas  $D_{AB}$  is independent of pore size and inversely proportional to the pressure. Consequently, the higher the pressure and the larger the pore, the more likely it is that ordinary bulk diffusion will dominate.

*Surface diffusion* is yet another mechanism that is invoked to explain mass transport in porous catalysts. An adsorbed species may be transported either by desorption into the gas phase or by migration to an adjacent site on the surface. It is this latter phenomenon that is referred to as surface diffusion. This phenomenon is poorly understood and the rate of mass transfer by this process cannot be predicted with a reasonable degree of accuracy. Classic discussions of this subject are presented by Satterfield (14) and Barrer (15), while modern animations are contained in *Wikipedia* (16).

Bulk or forced flow of the Hagan–Poiseuille type does not, in general, contribute significantly to the mass transport of gases in porous catalysts. For fast reactions in which there is a change in the number of moles on reaction, significant pressure differentials can arise between the interior and the exterior of the catalyst pellets. This phenomenon occurs because there is insufficient driving force for effective mass transfer of gas-phase species by forced flow. Molecular diffusion occurs much more rapidly than forced flow in most porous catalysts.

Our discussion of the various types of diffusion has presumed that the diffusion takes place in a well-characterized pore structure, that is, straight cylindrical pores. However, the catalysts used in industry have extremely complex structures with interconnecting pores, tortuous pores, and wide variations in pore diameter as one moves along the length of the pore. Consequently, we need to convert the combined diffusivities that are appropriate for Knudsen and/or bulk diffusion into effective

diffusivities, which are required for use in systems of unspecified pore geometry. These effective diffusivities can be calculated if we presume some sort of realistic model for the geometry of the pore structure. The test of the model is, of course, whether or not it predicts results that are in accord with what is observed in the laboratory or the plant. The preferred method of obtaining an effective diffusivity for design calculations involves measurement of this property. It should be noted, however, that the values obtained should be interpreted with care. We discuss briefly both calculational and experimental routes to effective diffusivity values in the paragraphs below.

If the pores of a catalyst pellet are randomly oriented, geometric considerations require that if one takes an arbitrary cross section of the porous mass, the fraction of the area occupied by the solid material will be a constant that will be identical with the volume fraction solids  $[(1 - \varepsilon_p)$ , where  $\varepsilon_p$  is the porosity of the pellet]. Similarly, the fraction of the cross-sectional area through which mass transfer can take place is identical with the void fraction  $\varepsilon_p$ . Consequently, our first step in obtaining an effective diffusivity will be to multiply our combined diffusivity by  $\varepsilon_p$ , because the area available for mass transport has been reduced by this factor from the gross area of a cross section normal to the direction of flow. The second step requires recognition that the length of the diffusion path that the molecules must traverse in real pores will be greater than that of a straight line linking the origin and termination of the diffusion path. In addition, the avenues through which diffusion proceeds are irregular in shape and vary in cross section. Since the constrictions offer resistances to diffusion that are not offset by enlargements, both of these factors cause the flux to be less than it would be in a straight cylindrical pore of the same length and mean radius. Consequently, if we introduce a length factor  $L'$  and a shape factor  $S'$  (both of which are greater than unity) to allow for these effects, the relation between the effective diffusivity and the combined diffusivity may be written as

$$D_{\text{eff}} = \frac{D_c \varepsilon_p}{L' S'} = \frac{D_c \varepsilon_p}{\tau'} \quad (12.2.9)$$

where the tortuosity factor  $\tau'$  is used to replace the factor  $L' S'$ , because it is virtually impossible to separate these factors for most real porous systems. For accurate work this parameter, or  $D_{\text{eff}}$  itself, must be determined experimentally. There have been several attempts to relate  $L'$  and/or  $S'$  to other readily measured properties of catalyst pellets, but they are of limited applicability. The combined factor  $\tau'$  has been measured for a variety of commercial catalysts. Tortuosity factors from slightly more than 1 to greater than 10 have been reported (17). Values of 3 to 7 are easily reconciled with physical reality by multiplying together physically reasonable values of  $L'$  and  $S'$ .

In the discussion above we have presumed that the tortuosity factor  $\tau'$  is characteristic of the pore structure but not of the diffusing molecules. However, when the size of the diffusing molecule begins to approach the dimensions of the pore, one expects the solid to exert a retarding influence on the flux, and this effect may also be incorporated in the tortuosity factor. This situation is likely to be significant in dealing with catalysis by zeolites (molecular sieves).

Because a priori estimates of effective diffusivities are not adequate for accurate design calculations and recourse must be made to experimental methods to evaluate these parameters, a few comments on the techniques used in these studies are in order. Since catalytic reactors are normally operated at steady state and nearly constant pressure, effective diffusivities are often measured under these constraints. The most commonly used apparatus for measuring counter diffusion rates was first described by Wicke and Kallenbach (18). It involves sealing off the sides of a cylindrical pellet and flowing two different pure gases over the two flat faces. The rate of steady-state diffusion through the pellet is determined by analyzing each of the two pure streams for contamination by the other component. One difficulty with this approach is that because it measures diffusion through the pellet, it ignores dead-end pores, which may contribute to reaction and which are included in a measured pore-size distribution. This method can be used over a wide range of pressures but cannot be readily adapted to temperatures much above ambient. The principles of kinetic theory can be used to calculate effective diffusivities for both species from measurements on only one of the two gas fluxes. In practice, however, measurements of both fluxes are desirable to facilitate the detection of leaks in the apparatus and of the presence of surface diffusion.

A second approach to measuring effective diffusivities involves filling the pore structure with one component and then measuring the rate of efflux of this component into a second component. Although somewhat simpler experimentally, this efflux method has the disadvantage that adsorption-desorption effects on the surface can conceivably complicate the results for high-surface-area materials. Because it is not a steady-state experiment, the equations for non-steady-state diffusion must be used in interpreting data. For gases and typical catalyst pellets, the time frame of the experiment is so short that it is difficult to obtain accurate diffusivity values. Consequently, the technique is largely restricted to liquids or to very finely porous solids, which give rise to very low effective diffusivities (e.g., zeolites).

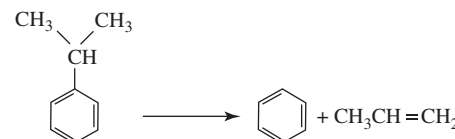
Barrer (19) developed another widely used non-steady-state technique for measuring effective diffusivities in porous catalysts. In this approach, an apparatus configuration similar to the steady-state apparatus is used. One side of the pellet is first evacuated and then the increase in the downstream pressure is recorded as a function of time,

the upstream pressure being held constant. The pressure drop across the pellet during the experiment is also held relatively constant. There is a time lag before a steady-state flux develops, and effective diffusion coefficients can be determined from either the transient or steady-state data. For the transient analysis, one must allow for accumulation or depletion of material by adsorption if this occurs.

The following illustration indicates how the concepts we have developed thus far in this chapter can be used in determining effective diffusivities for use in the analyses we develop in subsequent sections.

### ILLUSTRATION 12.1 Estimation of Combined Diffusivity for Cumene in a Cracking Catalyst

The cumene (isopropyl benzene) cracking reaction is often used as a model reaction for determining the relative activities of cracking catalysts.



This reaction takes place on silica-alumina catalysts in the temperature range 300 to 600°C. There is negligible production of by-products in this reaction.

For the purposes of this illustrative example, we wish to calculate the combined and effective diffusivities of cumene in a mixture of benzene and cumene at 1 atm total pressure and 510°C within the pores of a typical TCC (Thermofor catalytic cracking) catalyst bead. For present purposes, the approximation to the combined diffusivity given by equation (12.2.8) will be sufficient because we will see that the Knudsen diffusion term is the dominant factor in determining the combined diffusivity.

The following property values are associated with the TCC beads:

$S_g$	342 m <sup>2</sup> /g
$\epsilon_p$	0.51
equivalent particle diameter	0.43 cm
density of an individual particle $\rho_p$	1.14 g/cm <sup>3</sup>

A narrow pore size distribution and a tortuosity factor of 3 may be assumed. Use of the methods suggested by Poling et al. (8) indicates that the ordinary molecular diffusivity ( $D_{AB}$ ) is 0.150 cm<sup>2</sup>/s.

### Solution

The Knudsen diffusion coefficient may be evaluated from equation (12.2.4) if the catalyst property values are used

to estimate the average pore radius. From equation (C) of Illustration 6.2,

$$\bar{r} = \frac{2V_g}{S_g}$$

In terms of the property values indicated,

$$V_g = \frac{\epsilon_p}{\rho_p} = \frac{0.51}{1.14} = 0.447 \text{ cm}^3/\text{g}$$

Hence,

$$\bar{r} = \frac{2(0.447)}{342 \times 10^4} = 2.61 \times 10^{-7} \text{ cm} = 2.61 \text{ nm} = 26.1 \text{ \AA}$$

and

$$D_k = 9.7 \times 10^3 (2.61 \times 10^{-7}) \sqrt{\frac{783}{120.19}} \\ = 6.46 \times 10^{-3} \text{ cm}^2/\text{s}$$

Substitution of the numerical values for the bulk and Knudsen diffusion coefficients into equation (12.2.8) gives

$$\frac{1}{D_c} = \frac{1}{6.46 \times 10^{-3}} + \frac{1}{0.150} = 154.8 + 6.67$$

or

$$D_c = 6.19 \times 10^{-3} \text{ cm}^2/\text{s}$$

From the magnitudes of the diffusion coefficients, it is evident that under the conditions cited, the majority of the mass transport will occur by Knudsen diffusion. Equation (12.2.9) and the tabulated values of the porosity and tortuosity may be used to determine the effective diffusivity:

$$D_{\text{eff}} = \frac{D_c \epsilon_p}{\tau'} = \frac{(6.19 \times 10^{-3})(0.51)}{3} = 1.05 \times 10^{-3} \text{ cm}^2/\text{s}$$

## 12.3 DIFFUSION AND REACTION IN POROUS CATALYSTS

When diffusion and reaction occur simultaneously within a porous solid structure, concentration gradients of reactant and product species are established. If the various diffusional processes discussed in Section 12.2 are rapid compared with the chemical reaction rate, the entire accessible internal surface of the catalyst will be effective in promoting reaction because the reactant molecules will spread essentially uniformly throughout the pore structure, before they have time to react. Here only a small concentration gradient will exist between the exterior and interior of the particle, and there will be diffusive fluxes of reactant molecules in and product molecules out that suffice to balance the reaction rate within the particle. In

this case we measure true intrinsic kinetics. On the other hand, if the catalyst is very active, many reactant molecules will have been converted to products before they have had time to diffuse very far into the pore structure. There will be steep concentration gradients of both reactant and product species near the periphery of the particle. Within the central core of the particle, the reactant concentrations will be very low and their gradients will be small. In the core the product concentrations will be high. Virtually the entire reaction will take place within a thin shell on the periphery of the particle. In this case the internal surface area is not used effectively. Still, under steady state operating conditions, diffusion of reactants in and products out must balance the rate of reaction within the pore. Here, however, it is large peripheral concentration gradients rather than high diffusivities that are primarily responsible for achieving the necessary mass transfer rate. Assuming that the catalyst particle is isothermal, the average reaction rate under these conditions will, in general, be less than that which would prevail if there were no mass transfer limitations. In this case, one does *not* measure true intrinsic kinetics. In this section we examine the general problem of determining what fraction of the catalyst surface area is effective when reaction and intraparticle mass transfer processes interact. Our objective is to develop expressions for the rate of reaction averaged over the entire catalyst particle, but expressed in terms of the temperature and concentrations prevailing at its exterior surface.

Quantitative analytical treatments of the effects of mass transfer and reaction within a porous structure were apparently first carried out by Thiele (20) in the United States, Damköhler (21) in Germany, and Zeldovitch (22) in Russia, all working independently and reporting their results between 1937 and 1939. Since these early publications, a number of different research groups have extended and further developed the analysis. Of particular note are the efforts of Wheeler (23, 24), Weisz (25–28), Wicke et al. (29–32), and Aris (33–36). More recently, several groups have extended the analysis to include enzymes immobilized in porous media or within permselective membranes, while others have treated photocatalytic phenomena (37). The important consequence of these analyses is the development of a technique that can be used to quantitatively analyze the factors that determine the effectiveness with which the surface area of a porous catalyst is used. For this purpose we define an effectiveness factor  $\eta$  for a catalyst particle as

$$\eta = \frac{\text{measured rate for entire catalyst particle}}{\left[ \frac{\text{rate expression evaluated at exterior}}{\text{surface conditions for entire particle}} \right]} \quad (12.3.1)$$

Hence, the effectiveness factor is the ratio of the actual reaction rate to that which would be observed if the total

surface area throughout the catalyst interior were exposed to a fluid at the same conditions (composition, temperature, etc.) as those prevailing at the outside surface of the particle. By proper choice of experimental conditions, one can ascertain the intrinsic rate expression. Such conditions require the elimination of both external and intraparticle mass transfer resistances. Once the intrinsic chemical kinetics have been determined, the problem that we are addressing reduces to one of evaluating the effectiveness factor  $\eta$ . The general approach to analyzing this problem involves the development and solution of differential equations for simultaneous reaction and diffusion within a catalyst particle. In the case of nonisothermal catalyst pellets, we also require an additional differential equation for energy transport within the particle.

### 12.3.1 Effectiveness Factors for Isothermal Catalyst Pellets

This section is concerned with analyses of simultaneous reaction and mass transfer within porous catalysts under isothermal conditions. Several factors that influence the final equation for the catalyst effectiveness factor are discussed in the various subsections. The factors considered include different mathematical models of the catalyst pore structure, the gross catalyst geometry (i.e., its apparent shape), and the rate expression for the surface reaction.

#### 12.3.1.1 The Effectiveness Factor for a Straight Cylindrical Catalyst Pore: First-Order Reaction

To illustrate the basic features of an analysis for catalyst effectiveness factors, we consider the problem of a first-order reaction taking place on the surface of a straight cylindrical catalyst pore. It is assumed that there is no change in the number of moles of gas-phase species during reaction ( $\delta = 0$ ). Figure 12.1 indicates the geometric parameters characterizing the cylindrical pore and the differential element of length over which we write a mass balance.

If the catalyst pellet is assumed to contain  $n_p$  identical pores of this type, the analysis in Illustration 6.2 indicates that the model parameters  $\bar{r}$ ,  $\bar{L}$ , and  $n_p$  (the number of pores

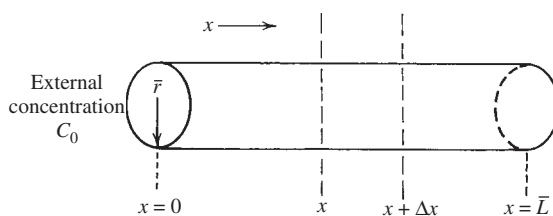


**Figure 12.1** Schematic representation of straight cylindrical catalyst pore.

per catalyst particle) can be related to experimentally measurable properties as follows:

$$\bar{r} = \frac{2V_g}{S_g} \quad (12.3.2)$$

$$\bar{L} = \frac{V_p}{S_x} \quad (12.3.3)$$

$$n_p = \frac{\varepsilon_p S_x S_g^2}{4\pi V_g^2} \quad (12.3.4)$$

where  $V_g$  is the void volume per gram of catalyst,  $S_g$  the surface area per gram of catalyst,  $V_p$  the gross volume of the catalyst particle,  $S_x$  the gross exterior surface area of the particle (geometric area), and  $\varepsilon_p$  the catalyst porosity. For a surface reaction that is first-order in gas phase reactant concentration, the rate *per unit surface area* may be written as

$$r = k_1'' C \quad (12.3.5)$$

where  $C$  refers to the reactant concentration, the subscript 1 indicates that the reaction is first-order, and the superscript (") emphasizes that the reaction rate is expressed per unit surface area.

If a material balance is written over the differential element of pore length shown in Figure 12.1, one finds that at steady state:

$$\text{input} = \text{output} + \text{disappearance by reaction}$$

$$\pi\bar{r}^2 \left( -D_c \frac{dC}{dx} \right)_x = \pi\bar{r}^2 \left( -D_c \frac{dC}{dx} \right)_{x+\Delta x} + (2\pi\bar{r} \Delta x) k_1'' C \quad (12.3.6)$$

where we have used the symbol  $D_c$  to emphasize the fact that the diffusive flux may represent a combination of Knudsen and ordinary molecular diffusion. We have also assumed that the stoichiometric coefficient of the reactant for which we are writing the material balance is  $-1$  and that the length of the pore is sufficiently large relative to the diameter that the circular area at the end of the pore is negligible compared to that of the walls.

Dividing through by  $\Delta x$ , taking the limit as  $\Delta x$  goes to zero, and rearranging gives

$$D_c \frac{d^2C}{dx^2} = \frac{2k_1'' C}{\bar{r}} \quad (12.3.7)$$

This second-order differential equation is subject to the boundary conditions

$$C = C_0 \quad \text{at } x = 0 \quad (12.3.8)$$

$$\frac{dC}{dx} = 0 \quad \text{at } x = \bar{L} \quad (12.3.9)$$

The second boundary condition meets the requirement that there be no flow of matter out of the closed end of the pore.

Equation (12.3.7) may be rewritten as

$$\frac{d^2C}{d(x/\bar{L})^2} = \left( \frac{2k_1'' \bar{L}^2}{\bar{r} D_c} \right) C \quad (12.3.10)$$

The term in parentheses on the right is a dimensionless group that plays a key role in determining the limitations that intraparticle diffusion places on observed reaction rates and the effectiveness with which the catalyst surface area is utilized. We define the Thiele modulus,  $h_T$ , as

$$h_T^2 = \frac{2k_1'' \bar{L}^2}{\bar{r} D_c} \quad (12.3.11)$$

so that equation (12.3.10) may be rewritten as

$$\frac{d^2C}{d(x/\bar{L})^2} = h_T^2 C \quad (12.3.12)$$

The solution to this equation may be written in the form

$$C = \frac{C_0 \cosh\{h_T[1 - (x/\bar{L})]\}}{\cosh h_T} \quad (12.3.13)$$

which describes the concentration profile along the length of the pore. Although this equation is not our ultimate goal, a brief digression to examine a possible physical interpretation of the square of the Thiele modulus may shed some light on the discussion that follows.

Equation (12.3.11) may be rewritten as

$$h_T^2 = \frac{(2\pi\bar{r}\bar{L})k_1'' C_0}{\pi\bar{r}^2 \{D_c[(C_0 - 0)/\bar{L}]\}} \quad (12.3.14)$$

The numerator on the right side of this equation is equal to the chemical reaction rate that would prevail if there were no diffusional limitations on the reaction rate. In this situation, the reactant concentration is uniform throughout the pore and equal to its value at the pore mouth. The denominator may be regarded as the product of a hypothetical diffusive flux and a cross-sectional area for flow. The hypothetical flux corresponds to the case where there is a linear concentration gradient over the pore length equal to  $C_0/\bar{L}$ . The Thiele modulus is thus characteristic of the ratio of an intrinsic reaction rate in the absence of mass transfer limitations to the rate of diffusion into the pore under a specified concentration gradient.

Now, at steady state, the observed rate of reaction within the pore balances the rate of diffusion of reactant into the pore:

$$r_{\text{pore}} = -D_c \left( \frac{dC}{dx} \right)_{x=0} \pi\bar{r}^2 \quad (12.3.15)$$

From equation (12.3.13), the concentration gradient at the pore mouth is

$$\begin{aligned} \left( \frac{dC}{dx} \right)_{x=0} &= \frac{C_0}{\cosh h_T} \left\{ \sinh \left[ h_T \left( 1 - \frac{x}{\bar{L}} \right) \right] \right\} \left( -\frac{h_T}{\bar{L}} \right) \Big|_{x=0} \\ &= -\frac{h_T C_0}{\bar{L}} \frac{\sinh h_T}{\cosh h_T} = \frac{-h_T C_0}{\bar{L}} \tanh h_T \end{aligned} \quad (12.3.16)$$

According to this model, the reaction rate that would be observed within the catalyst pore is given by a combination of equations (12.3.15) and (12.3.16):

$$r_{\text{pore}} = \pi\bar{r}^2 \frac{D_c h_T C_0}{\bar{L}} \tanh h_T \quad (12.3.17)$$

If no limitations were placed on the reaction rate by intraparticle diffusion (i.e., if the reactant concentration were  $C_0$  throughout the pore), the reaction rate would be given by

$$r_{\text{ideal}} = 2\pi\bar{r}\bar{L}k_1'' C_0 \quad (12.3.18)$$

From the definition of the effectiveness factor and equations (12.3.17) and (12.3.18),

$$\begin{aligned} \eta &= \frac{r_{\text{pore}}}{r_{\text{ideal}}} = \frac{\pi\bar{r}^2 (D_c h_T C_0 / \bar{L}) \tanh h_T}{2\pi\bar{r}\bar{L}k_1'' C_0} \\ &= \left( \frac{\bar{r} D_c}{2\bar{L} k_1''} \right) h_T \tanh h_T \end{aligned} \quad (12.3.19)$$

Equation (12.3.11) indicates that the term in parentheses on the right is  $1/h_T^2$ . Hence,

$$\eta = \frac{\tanh h_T}{h_T} \quad (12.3.20)$$

Figure 12.2 is a plot of the effectiveness factor  $\eta$  versus the Thiele modulus  $h_T$ . For low values of  $h_T$  (slow reaction, rapid diffusion), the effectiveness factor approaches unity. For values of the Thiele modulus of 2.0 or larger,  $\tanh h_T \approx 1$  and the effectiveness factor may be approximated by

$$\eta \approx \frac{1}{h_T} \quad (12.3.21)$$

The approximation is quite good for many engineering purposes, particularly when one recognizes the disparity between the physical reality represented by a real porous catalyst and the assumptions implied by the model.

The effectiveness factor for a single pore is identical with that for the particle as a whole. Thus, the reaction rate per unit mass of catalyst can be written as

$$r_{\text{mass}} = \eta k_1'' C_0 S_g \quad (12.3.22)$$

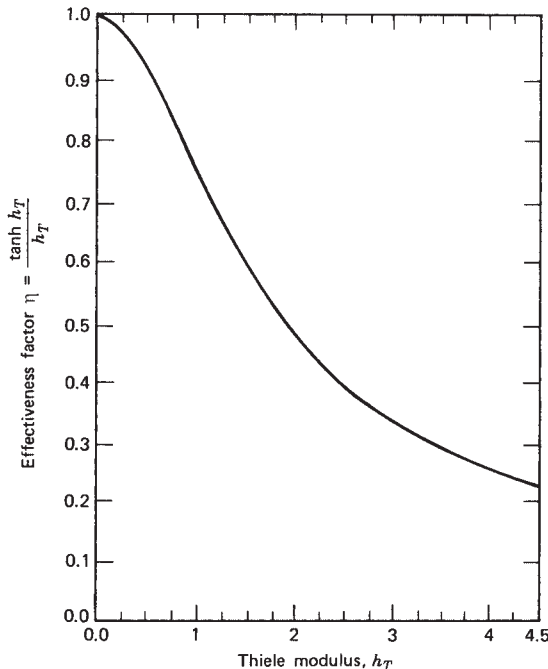


**Figure 12.2** Plot of effectiveness factor versus Thiele modulus for the first-order reaction  $h_T = L \sqrt{2k_1''/(\bar{r}D_c)}$ .

By definition the first-order rate constant measured per unit area of catalyst must be equal to the product  $(\eta k_1'')$ . Hence, an alternative interpretation of the effectiveness factor is

$$\eta = \frac{k_1'' \text{ measured}}{k_1'' \text{ intrinsic}} \quad (12.3.23)$$

The effectiveness factor may thus be regarded as the ratio of the measured rate constant to the intrinsic (true) rate constant.

The Thiele modulus may be written in terms of measurable quantities using equations (12.3.2) and (12.3.3):

$$h_T = \bar{L} \sqrt{\frac{2k_1''}{\bar{r}D_c}} = \frac{V_p}{S_x} \sqrt{\frac{k_1'' S_g}{D_c V_g}} \quad (12.3.24)$$

For  $h_T > 2$  the reaction rate observed can be approximated by combining equations (12.3.21), (12.3.22), and (12.3.24):

$$r_{\text{mass}} = \frac{S_x}{V_p} \sqrt{\frac{V_g D_c}{k_1'' S_g}} (k_1'' S_g) C_0 = \frac{S_x}{V_p} \sqrt{V_g D_c k_1'' S_g} C_0 \quad (12.3.25)$$

There are two points worth noting relative to equation (12.3.25). First, the ratio of the external surface area  $S_x$  to the gross geometric volume of a catalyst particle is inversely proportional to a characteristic dimension of the particle. For geometrically similar particles, this fact implies that the rate observed per unit mass of catalyst will

be inversely proportional to the particle size. Second, the rate observed will be proportional to the square root of the true rate constant. Consequently, over the temperature range where intraparticle mass transfer strongly influences the reaction rate, the apparent activation energy for the reaction will be approximately one-half the true activation energy for the surface reaction.

If reactor designers desire to make use of the analysis developed thus far in this subsection, they must have a means of evaluating the effectiveness factor for the catalyst particles they plan to use in their reactor. There are two basic routes to the evaluation of  $\eta$ . Each is discussed in turn.

The first method of determining  $\eta$  is based on equation (12.3.23). This method requires experimental data on the rate constant (or the reaction rate at similar external concentrations) as a function of the gross particle size of the catalyst. Experiments are carried out using smaller and smaller particles (obtained by grinding or crushing the large particles that are intended for use in the commercial-scale reactor). When one reaches a size regime in which the rate constant is independent of particle size, one is measuring the true or intrinsic rate constant. This parameter gives us the denominator of equation (12.3.23). The corresponding numerator is the apparent rate constant measured for the particle size one intends to use in the reactor. This method requires rate measurements on at least two different size catalysts, and preferably more.

A second approach to determining  $\eta$  requires rate measurements on only a single size of catalyst, but it requires that one knows  $V_p$ ,  $S_x$ ,  $V_g$ , and  $S_g$  and that one knows, or can estimate,  $D_c$ . From a single rate measurement, one can obtain  $k_1''$  or its equivalent,  $k_1'' S_g$ . Then there are alternative means of solving equations (12.3.11), (12.3.20), and (12.3.23) for  $\eta$  in terms of the input parameters. A simple trial-and-error technique consists of the following steps.

1. Assume a value for  $\eta$ .
2. Calculate  $h_T$  from equation (12.3.20) or read the value of this parameter from the curve in Figure 12.2.
3. Calculate the intrinsic rate constant from the known input parameters, using equation (12.3.24).
4. Compare the measured rate constant  $k_1''$  with the product of the assumed  $\eta$  and the intrinsic rate constant determined in step 3. If the two are equal, the assumption in step 1 was correct; if they are not equal, one assumes a new value of  $\eta$  and iterates until consistent results are obtained.

A variation on the second approach involves a somewhat different manner of combining the equations used in the trial-and-error procedure. From equation (12.3.11),

$$k_1'' = \frac{\bar{r}D_c}{2\bar{L}^2} h_T^2 \quad (12.3.26)$$

and from equations (12.3.23) and (12.3.20),

$$k''_1 = \frac{k''_{1 \text{ measured}}}{\eta} = \frac{h_T k''_{1 \text{ measured}}}{\tanh h_T} \quad (12.3.27)$$

Combining equations (12.3.26) and (12.3.27) gives

$$k''_{1 \text{ measured}} = h_T (\tanh h_T) \frac{\bar{r} D_c}{2L} \quad (12.3.28)$$

which can be written in terms of experimentally measurable variables using equations (12.3.2) and (12.3.3):

$$k''_{1 \text{ measured}} = h_T (\tanh h_T) \frac{V_g S_x^2 D_c}{S_g V_p^2} \quad (12.3.29)$$

This equation can be solved for  $h_T$ , and equation (12.3.20) may then be used to determine the effectiveness factor.

The equations for effectiveness factors that we have developed in this subsection are strictly applicable only to reactions that are first-order in the fluid phase concentration of a reactant whose stoichiometric coefficient is unity. They further require that no change in the number of moles take place on reaction and that the pellet be isothermal.

Illustration 12.2 indicates how this idealized cylindrical pore model is used to obtain catalyst effectiveness factors.

### ILLUSTRATION 12.2 Determination of Catalyst Effectiveness Factor for Cumene Cracking from Measurement of an Apparent Rate Constant

The cumene cracking reaction has been studied by a number of investigators because it is a relatively clean reaction that can be used as a measure of the relative activities of different cracking catalysts. Some of the data on this reaction have been obtained using integral flow reactors. For this type of reactor, the variation of conversion with reactor space time is relatively insensitive to variations in the form of the reaction rate expression at degrees of conversion that are far from equilibrium. Consequently, data on these systems are often reported in terms of a simple first-order reaction rate constant, assuming that the volume change accompanying the reaction is negligible. An expression that is often used to determine this constant is

$$\frac{W}{F_{A0}} = \int_0^{f_A} \frac{df_A}{(-r_{A_m})} = \int_0^{f_A} \frac{df_A}{kC_{A0}(1-f_A)} = \frac{-\ln(1-f_A)}{kC_{A0}}$$

where  $W$  is the weight of catalyst employed and the reaction rate constant is expressed per unit weight of catalyst. [The basic equation was derived earlier as equation (8.2.12).] If the data of Corrigan et al. (38) are expressed in these terms,

the *apparent rate constant* at 510°C is approximately 0.716  $\text{cm}^3/(\text{s} \cdot \text{g catalyst})$ , as determined from Figure 6 of the reference cited. If the catalyst employed in this study has the properties enumerated below, determine the effectiveness factor for the catalyst. The value of the combined diffusivity from Illustration 12.1 may be used in your analysis.

Data on catalyst properties (silica–alumina) follow.

Equivalent diameter	0.43 cm
Particle density	1.14 g/cm <sup>3</sup>
Specific surface area	342 m <sup>2</sup> /g
Porosity	0.51
Void volume per gram	0.447 cm <sup>3</sup> /g

### Solution

Because we are given the apparent rate constant rather than the true rate constant, a trial-and-error solution will be required. Either of the approaches described earlier may be used, but we shall employ equation (12.3.29). Since our apparent rate constant is expressed per unit weight of catalyst rather than per unit surface area, the first step involves multiplying both sides of this equation by  $S_g$ :

$$k''_{1 \text{ measured}} S_g = h_T (\tanh h_T) \frac{V_g S_x^2 D_c}{V_p^2}$$

where the left side is equal to  $0.716 \text{ cm}^3/(\text{s} \cdot \text{g catalyst})$ . The equivalent radius of the catalyst particles is 0.215 cm. Hence,

$$V_p = \frac{4}{3}\pi R^3 = \frac{4}{3}\pi(0.215)^3 = 0.0416 \text{ cm}^3$$

and

$$S_x = 4\pi R^2 = 4\pi(0.215)^2 = 0.581 \text{ cm}^2$$

Thus,

$$0.716 = h_T (\tanh h_T) \frac{0.447(0.581)^2(6.19 \times 10^{-3})}{(0.0416)^2}$$

or

$$h_T \tanh h_T = 1.327$$

This transcendental equation for  $h_T$  may be solved to obtain  $h_T = 1.47$ . Equation (12.3.20) then gives  $\eta = (\tanh 1.47)/1.47 = 0.61$ . This value is considerably higher than the experimental value (0.17) obtained from rate measurements on different size particles, but several factors may be invoked to explain the inconsistency. There will be a distribution of both pore radii and pore lengths present in the actual catalyst rather than uniquely specified values. Alumina catalysts often have a bimodal pore-size distribution. Our estimate of an apparent first-order rate constant using the method outlined above will be somewhat in error. The catalyst surface may not be equally active

throughout if selective deactivation has taken place and the peripheral region is less active than the catalyst core. Other sources of error are the failure to allow for the change in the number of moles on reaction, and the possibility that the pellets cannot be maintained in an isothermal condition for this endothermic reaction (see Section 12.3.2). The discrepancy indicates the necessity for good experimental data as input to reactor design calculations for heterogeneous catalytic reactions. Model predictions will not reflect the real world if the assumptions on which they are based are in error. For best results, one should use experimental data taken under conditions approximating the proposed industrial application.

### 12.3.1.2 Effectiveness Factors for a Straight Cylindrical Pore: Second- and Zero-Order Reactions

In this section we indicate the predictions of the straight cylindrical pore model for isothermal reactions that are zero- or second-order in the gas phase concentration of reactant. Equimolal counterdiffusion is assumed ( $\delta_A = 0$ ). For a second-order reaction, a material balance on a differential element of pore length leads to the differential equation

$$\mathcal{D}_c \frac{d^2 C}{dx^2} = \frac{2k_2''}{\bar{r}} C^2 \quad (12.3.30)$$

where we have used the subscript 2 to indicate that we are dealing with a second-order rate constant. This equation is subject to the boundary conditions given by equations (12.3.8) and (12.3.9). In dimensionless form, this equation can be written as

$$\frac{d^2(C/C_0)}{d(x/\bar{L})^2} = \frac{2k_2'' C_0 \bar{L}^2}{\bar{r} \mathcal{D}_c} \left( \frac{C}{C_0} \right)^2 = h_2^2 \left( \frac{C}{C_0} \right)^2 \quad (12.3.31)$$

where the Thiele modulus for the second-order reaction ( $h_2$ ) is defined as

$$h_2 = \bar{L} \sqrt{\frac{2k_2'' C_0}{\bar{r} \mathcal{D}_c}} \quad (12.3.32)$$

This equation can be solved exactly in terms of elliptic integrals, but said solution is somewhat complex. However, by a slight modification of the boundary condition at the end of the pore, it is possible to obtain a good engineering approximation that is useful for fast reactions. In this approximation, we replace the boundary condition at the end of the pore by

$$C = C_L \quad \text{at } x = \bar{L} \quad (12.3.33)$$

To evaluate the effectiveness factor we require only the derivative of the concentration at the pore mouth. This

parameter may be obtained by multiplying both sides of equation (12.3.31) by  $d(C/C_0)/d(x/\bar{L})$ :

$$\begin{aligned} \frac{d(C/C_0)}{d(x/\bar{L})} \frac{d^2(C/C_0)}{d(x/\bar{L})^2} &= \frac{1}{2} \frac{d}{d(x/\bar{L})} \left[ \frac{d(C/C_0)}{d(x/\bar{L})} \right]^2 \\ &= h_2^2 \left( \frac{C}{C_0} \right)^2 \frac{d(C/C_0)}{d(x/\bar{L})} \end{aligned} \quad (12.3.34)$$

Integration gives

$$\frac{1}{2} \left[ \frac{d(C/C_0)}{d(x/\bar{L})} \right]^2 = \frac{h_2^2 (C/C_0)^3}{3} + C_1 \quad (12.3.35)$$

where  $C_1$  is a constant of integration.

At  $x/\bar{L} = 1$ , the first derivative must be zero and  $C/C_0$  must be  $C_L/C_0$ . Hence,

$$-\frac{d(C/C_0)}{d(x/\bar{L})} = h_2 \sqrt{\frac{2}{3} \left[ \left( \frac{C}{C_0} \right)^3 - \left( \frac{C_L}{C_0} \right)^3 \right]} \quad (12.3.36)$$

or

$$-\frac{dC}{dx} = \frac{C_0}{\bar{L}} h_2 \sqrt{\frac{2}{3} \left[ \left( \frac{C}{C_0} \right)^3 - \left( \frac{C_L}{C_0} \right)^3 \right]} \quad (12.3.37)$$

The reaction rate within the pore is equal to the rate of diffusion into the pore at  $x = 0$  as indicated by equation (12.3.15). Thus,

$$r_{\text{pore}} = \pi \bar{r}^2 \mathcal{D}_c \left\{ \frac{C_0}{\bar{L}} h_2 \sqrt{\frac{2}{3} \left[ 1 - \left( \frac{C_L}{C_0} \right)^3 \right]} \right\} \quad (12.3.38)$$

where the term in curly brackets arises from the derivative of the concentration evaluated at the pore mouth.

In the absence of diffusional limitations,

$$r_{\text{ideal}} = 2\pi \bar{r} \bar{L} k_2'' C_0^2 \quad (12.3.39)$$

The effectiveness factor is given by the ratio of equation (12.3.38) to (12.3.39):

$$\eta = \frac{\bar{r} \mathcal{D}_c h_2}{2 \bar{L}^2 k_2'' C_0} \sqrt{\frac{2}{3} \left[ 1 - \left( \frac{C_L}{C_0} \right)^3 \right]} \quad (12.3.40)$$

If we make use of equation (12.3.32), equation (12.3.40) becomes

$$\eta = \frac{1}{h_2} \sqrt{\frac{2}{3} \left[ 1 - \left( \frac{C_L}{C_0} \right)^3 \right]} \quad (12.3.41)$$

This relation is an exact consequence of the differential equation (12.3.30), but it suffers from the disadvantage that it contains an unknown parameter,  $C_L$ , the reactant concentration at the end of the pore. However, for even moderately fast reactions we can say that  $C_L$  is significantly less than  $C_0$ , and because of the nature of the function under the radical sign, it is a very good approximation to say that

$$\eta \approx \frac{1}{h_2} \sqrt{\frac{2}{3}} = \frac{0.8165}{h_2} \quad \text{for } h_2 > 2.5 \quad (12.3.42)$$

Curve *B* of Figure 12.3 represents the dependence of the effectiveness factor on Thiele modulus for second-order kinetics (39). Values of  $\eta$  for first- and zero-order kinetics in straight cylindrical pores are shown as curves *A* and *C*, respectively. Each curve is plotted versus its corresponding modulus.

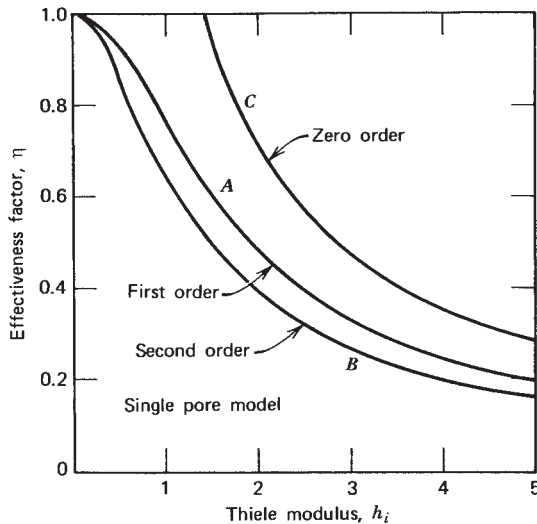


**Figure 12.3** Plots of effectiveness factors versus corresponding Thiele moduli for zero-, first-, and second-order kinetics based on the straight cylindrical pore model. For large  $h_T$ , values of  $\eta$  are as follows:

Zero-order:

$$\eta = \frac{\sqrt{2}}{h_0} \quad \text{with } h_0 = \bar{L} \sqrt{\frac{2k''_0}{\bar{r}D_c C_0}}$$

First-order:

$$\eta = \frac{1}{h_1} \quad \text{with } h_1 = \bar{L} \sqrt{\frac{2k''_1}{\bar{r}D_c}}$$

Second-order:

$$\eta = \frac{\sqrt{2/3}}{h_2} \quad \text{with } h_2 = \bar{L} \sqrt{\frac{2k''_2 C_0}{\bar{r}D_c}}$$

[From A. Wheeler, *Adv. Catal.*, **3**, 249 (1951). Copyright © 1951.

Used with permission of Academic Press.]

Notice that in the region of fast chemical reaction, the effectiveness factor becomes inversely proportional to the modulus  $h_2$ . Because  $h_2$  is proportional to the square root of the external surface concentration, these two fundamental relations require that for second-order kinetics, the fraction of the catalyst surface that is effective will increase as one moves downstream in an isothermal packed-bed reactor.

For the case of a zero-order reaction, one can readily obtain an analytical solution for  $\eta$  based on the straight cylindrical pore model. For this case the dimensionless form of the differential equation for the concentration profile is

$$\frac{d^2(C/C_0)}{d(x/\bar{L})^2} = \frac{2\bar{L}^2 k''_0}{\bar{r}D_c C_0} = h_0^2 \quad (12.3.43)$$

subject to the boundary conditions of equations (12.3.8) and (12.3.9). The parameter  $k''_0$  is the zero-order rate constant based on unit surface area of the catalyst and  $h_0$  is the Thiele modulus for the zero-order reaction.

The solution to equation (12.3.43) can be written as

$$\frac{C}{C_0} = 1 - h_0^2 \left[ \frac{x}{\bar{L}} - \frac{1}{2} \left( \frac{x}{\bar{L}} \right)^2 \right] \quad (12.3.44)$$

The reactant concentration  $C$  will be greater than zero throughout the entire length of the pore provided that  $h_0 < \sqrt{2}$ . For such conditions the effectiveness factor will be unity because the reaction rate is independent of concentration. For values of  $h_0 > \sqrt{2}$ , equation (12.3.44) would call for negative values of the reactant concentration at large values of  $x/\bar{L}$ , a situation that is clearly physically impossible. Hence, the boundary conditions on equation (12.3.43) must be changed so that both the reactant concentration and its gradient become zero at a point in the pore that we label with a coordinate  $x_c$ . In this situation, the concentration profile becomes

$$C = 0 \quad \text{for } x \geq x_c \quad (12.3.45)$$

$$\frac{C}{C_0} = 1 - 2 \left[ \frac{h_0 x}{\bar{L} \sqrt{2}} - \frac{1}{2} \left( \frac{h_0 x}{\bar{L} \sqrt{2}} \right)^2 \right] \quad \text{for } x \leq x_c \quad (12.3.46)$$

where  $x_c$  can be determined from the point at which  $dC/dx = 0$ ; that is,

$$x_c = \frac{\bar{L} \sqrt{2}}{h_0} \quad \text{for } h_0 > \sqrt{2} \quad (12.3.47)$$

Thus, for  $h_0 > \sqrt{2}$ , the effectiveness factor is given by

$$\eta = \frac{2\pi\bar{r}x_c k_0''}{2\pi\bar{r}\bar{L}k_0''} = \frac{x_c}{\bar{L}} = \frac{\sqrt{2}}{h_0} \quad (12.3.48)$$

This function is plotted as curve C in Figure 12.3.

### 12.3.1.3 The Effectiveness Factor Analysis in Terms of Effective Diffusivities: First-Order Reactions on Spherical Pellets

Useful expressions for catalyst effectiveness factors may also be developed in terms of the concept of effective diffusivities. This approach permits one to write an expression for the mass transfer within the pellet in terms of a form of Fick's first law based on the superficial cross-sectional area of a porous medium. We thereby circumvent the necessity of developing a detailed mathematical model of the pore geometry and size distribution. This subsection is devoted to an analysis of simultaneous mass transfer and chemical reaction in porous catalyst pellets in terms of the effective diffusivity. To use the analysis with confidence, the effective diffusivity should be determined experimentally because it is difficult to obtain accurate estimates of this parameter on an a priori basis.

Consider the spherical catalyst pellet of radius  $R$  shown in Figure 12.4. The effective diffusivity approach presumes that for each chemical species diffusion of all types can be represented in terms of Fick's first law and an overall effective diffusion coefficient that can be taken as a constant. That is, the appropriate flux representation is

$$N_r = -D_{\text{eff}} \frac{dC}{dr} \quad (12.3.49)$$

where  $N_r$  is the diffusive *flux outward* in the radial direction. As before, we assume steady state reaction conditions, a simple irreversible first-order reaction with  $\delta = 0$ , and an isothermal pellet. We focus our attention on

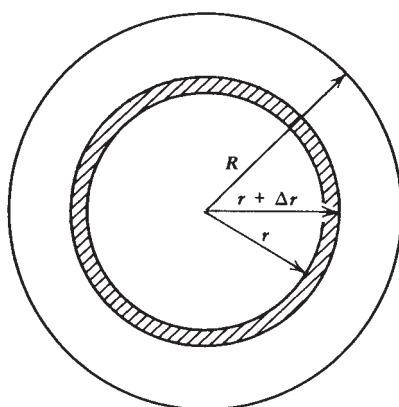


Figure 12.4 Schematic diagram of a porous spherical catalyst pellet.

the spherical shell of porous material contained within the region between  $r$  and  $(r + \Delta r)$  and write a material balance on this differential element. Reactants are transported into and out of the annular shell by diffusion and are consumed within it by reaction. For a surface reaction that is first-order in the gas phase reactant, the reaction rate within the differential volume element can be written as

$$r = k_1'' \rho_p S_g (4\pi r^2 \Delta r) C \quad (12.3.50)$$

where  $\rho_p$  is the apparent density of the catalyst particle (mass per total particle volume) and  $4\pi r^2 \Delta r$  is the differential volume element. Notice that the group  $k_1'' \rho_p S_g$  may be regarded as an apparent first-order rate constant per unit volume of catalyst pellet.

Assuming that the stoichiometric coefficient of the reactant is  $-1$  and that there is no change in the number of moles on reaction, one can write the material balance on the volume element at steady state as

$$\begin{aligned} & \text{rate of input by diffusion at } r + \Delta r \\ &= \text{rate of efflux by diffusion at } r \\ &+ \text{rate of disappearance by chemical reaction} \end{aligned}$$

$$\left\{ 4\pi r^2 \left[ \left( D_{\text{eff}} \frac{dC}{dr} \right) \right] \right\}_{r+\Delta r} = \left[ 4\pi r^2 \left( D_{\text{eff}} \frac{dC}{dr} \right) \right]_r + k_1'' \rho_p S_g C (4\pi r^2 \Delta r) \quad (12.3.51)$$

The differential equation governing simultaneous chemical reaction and diffusion then becomes

$$\frac{d}{dr} \left( r^2 D_{\text{eff}} \frac{dC}{dr} \right) - k_1'' \rho_p S_g C r^2 = 0 \quad (12.3.52)$$

If the effective diffusivity can be treated as a constant, one can write equation (12.3.52) as

$$\frac{d^2C}{dr^2} + \frac{2}{r} \frac{dC}{dr} - \frac{k_1'' \rho_p S_g C}{D_{\text{eff}}} = 0 \quad (12.3.53)$$

The boundary conditions for this differential equation require that (1) at  $r = R$ ,

$$C = C_0 \quad (12.3.54)$$

and (2) at  $r = 0$ ,

$$\frac{dC}{dr} = 0 \quad (12.3.55)$$

The first condition requires that locally the reactant concentration at the external surface of the catalyst can be viewed as fixed. The second condition implies that there can be no diffusive flux through the center of the pellet because this is a point of symmetry.

It is convenient to define a new Thiele-type modulus  $\phi_s$  for this spherically symmetric problem as<sup>†</sup>

$$\phi_s = R \sqrt{\frac{k_1'' \rho_p S_g}{D_{\text{eff}}}} \quad (12.3.56)$$

Combining equations (12.3.53) and (12.3.56) gives

$$\frac{d^2C}{dr^2} + \frac{2}{r} \frac{dC}{dr} = \left(\frac{\phi_s}{R}\right)^2 C \quad (12.3.57)$$

The conventional approach to solving this linear differential equation is to introduce a new variable  $z$  defined such that  $C = z/r$ . This substitution converts equation (12.3.57) to

$$\frac{d^2z}{dr^2} = \left(\frac{\phi_s}{R}\right)^2 z \quad (12.3.58)$$

This equation is of the same form as equation (12.3.10), and the solution can be expressed in terms of exponential functions as

$$z = Cr = C_1 e^{\phi_s r/R} + C_2 e^{-\phi_s r/R} \quad (12.3.59)$$

where the constants of integration  $C_1$  and  $C_2$  can be evaluated from the boundary conditions. At  $r = 0$ , the fact that  $dC/dr = 0$  implies that

$$C_1 = -C_2 \quad (12.3.60)$$

Equation (12.3.59) can thus be rewritten in terms of hyperbolic functions as

$$C = \frac{2C_1}{r} \sinh\left(\frac{\phi_s r}{R}\right) \quad (12.3.61)$$

Use of the boundary condition at the external surface of the spherical pellet ( $r = R$ ) leads to the following expression for the concentration profile in the spherical pellet:

$$\frac{C}{C_0} = \frac{R \sinh[\phi_s(r/R)]}{r \sinh \phi_s} \quad (\text{first-order rate law}) \quad (12.3.62)$$

Figure 12.5 contains a series of curves representing the concentration profile in the spherical pellet for different values of the Thiele modulus  $\phi_s$ . For small values of  $\phi_s$  (say less than 0.5) the concentration profile is relatively flat and the reactant concentration is reasonably uniform throughout the particle. For large values of  $\phi_s$  (say greater

<sup>†</sup>We would be remiss if we did not indicate that some authors have defined yet another Thiele-type modulus ( $\phi'_s$ ) for this problem as  $\phi'_s = \phi_s/3$ , and they have developed their analysis according to this parameter. In using plots of  $\eta$  versus  $\phi_s$  one must be careful to determine which of the two alternative definitions has been adopted for  $\phi_s$ . Otherwise, the value for  $\eta$  may be considerably in error. A variety of other symbols for dimensionless groups akin to the Thiele modulus have been employed by different authors.

than 5), the reaction is rapid relative to diffusion and the reactant concentration at the center of the catalyst pellet is less than 7% of that at the external surface. Notice that in all cases the concentration gradient approaches zero at the center of the pellet.

We now wish to evaluate the total reaction rate for the entire catalyst pellet. This quantity may be obtained by writing an expression for the reaction rate in the spherical annulus of Figure 12.4 in terms of the local reactant concentration as given by equation (12.3.62) and then integrating this expression over the entire sphere. However, a simpler procedure involves recognizing that the overall rate of reaction within the spherical pellet must be equal to the rate of mass transfer into the pellet at steady state:

$$\text{rate} = 4\pi R^2 D_{\text{eff}} \left(\frac{dC}{dr}\right)_{r=R} \quad (12.3.63)$$

where we have eliminated the negative sign on the derivative because we are interested in the net flux *into* the pellet.

The concentration gradient at the exterior surface can be obtained by differentiating equation (12.3.62) with respect to  $r$ :

$$\frac{dC}{dr} = C_0 \left[ \left(\frac{\phi_s}{r}\right) \frac{\cosh(\phi_s r/R)}{\sinh(\phi_s)} - \left(\frac{R}{r^2}\right) \frac{\sinh(\phi_s r/R)}{\sinh(\phi_s)} \right] \quad (12.3.64)$$

and evaluating the derivative at the surface:

$$\begin{aligned} \left(\frac{dC}{dr}\right)_{r=R} &= C_0 \left(\frac{\phi_s}{R}\right) \left[ \frac{\cosh(\phi_s)}{\sinh(\phi_s)} - \frac{1}{R} \right] \\ &= \left(\frac{C_0 \phi_s}{R}\right) \left[ \frac{1}{\tanh(\phi_s)} - \frac{1}{\phi_s} \right] \end{aligned} \quad (12.3.65)$$

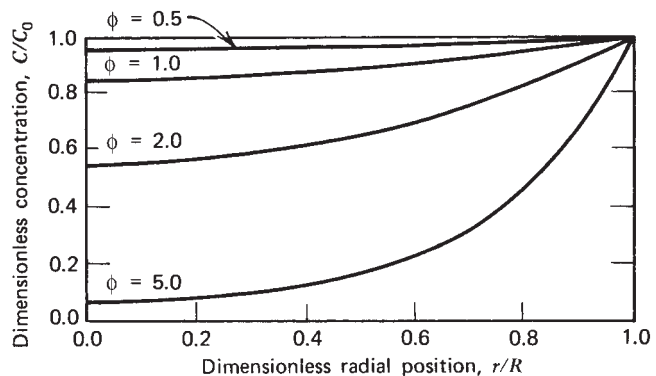


Figure 12.5 Dimensionless plot of reactant concentration versus distance from the center of the spherical pellet.

Combining equations (12.3.63) and (12.3.65) gives

$$\text{rate} = 4\pi R D_{\text{eff}} C_0 \phi_s \left( \frac{1}{\tanh \phi_s} - \frac{1}{\phi_s} \right) \quad (12.3.66)$$

If the entire active surface of the spherical pellet were exposed to reactant at a concentration  $C_0$ , the rate corresponding to this condition would be given by

$$\begin{aligned} \text{rate for } C = C_0 \text{ throughout pellet} \\ = \rho_p (4/3)\pi R^3 S_g k''_1 C_0 \end{aligned} \quad (12.3.67)$$

The effectiveness factor is then given by the ratio of equation (12.3.66) to (12.3.67):

$$\begin{aligned} \eta &= \frac{3D_{\text{eff}}\phi_s}{\rho_p R^2 k''_1 S_g} \left[ \frac{1}{\tanh(\phi_s)} - \frac{1}{\phi_s} \right] \\ &= \frac{3}{\phi_s} \left[ \frac{1}{\tanh(\phi_s)} - \frac{1}{\phi_s} \right] \end{aligned} \quad (12.3.68)$$

where we have used the defining equation for  $\phi_s$  (12.3.56). For large values of  $\phi_s$  the hyperbolic tangent approaches unity and the effectiveness factor approaches  $3/\phi_s$ . Figure 12.6 is a plot of the function described by equation (12.3.68). It is appropriate for an isothermal first-order irreversible reaction in a spherical catalyst pellet. At

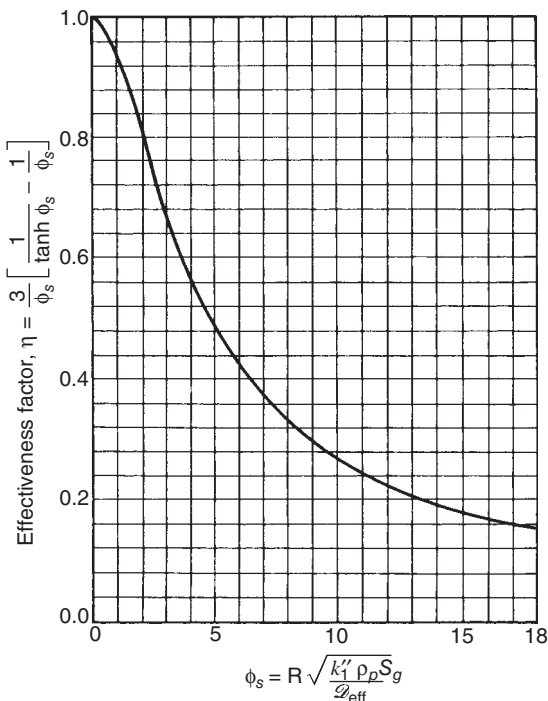


**Figure 12.6** Effectiveness factor plot for spherical catalyst pellets based on the effective diffusivity model for a first-order reaction.

low values of  $\phi_s$ , the effectiveness factor approaches unity.

Illustration 12.3 indicates the use of the effective diffusivity approach for estimating catalyst effectiveness factors when this diffusivity is determined experimentally or can be estimated.

### ILLUSTRATION 12.3 Determination of Catalyst Effectiveness Factor for the Cumene Cracking Reaction Using the Effective Diffusivity Approach

Use the effective diffusivity approach to evaluate the effectiveness factor for the silica–alumina catalyst pellets considered in Illustration 12.2. Assume that the effective diffusivity for cumene in these particles is equal to  $1.2 \times 10^{-3} \text{ cm}^2/\text{s}$ , which is a typical value for silica–alumina TCC beads (40).

#### Solution

The trial-and-error procedure outlined in Section 12.3.1.1 is quite general if appropriate modification is made for the use of  $\phi_s$  values and effective diffusivities. Thus, we will start by assuming that  $\eta = 0.20$ . From Figure 12.6 we find that  $\phi_s = 13.4$ . Substitution of numerical values into the defining equation for  $\phi_s$ , (12.3.56) gives

$$13.4 = \frac{0.43}{2} \sqrt{\frac{k''_{1 \text{ true}} S_g (1.14)}{1.2 \times 10^{-3}}}$$

or

$$k''_{1 \text{ true}} S_g = 4.081$$

The measured value of  $k''_1 S_g$  is  $0.716 \text{ cm}^3/(\text{s} \cdot \text{g catalyst})$ . If our assumption was correct, the ratio of this value to  $k''_{1 \text{ true}} S_g$  should be equal to the value assumed for the effectiveness factor. The actual ratio is 0.175, which is at variance with the assumed value. Hence, we pick a new value of  $\eta$  and repeat the procedure until agreement is obtained. This iterative approach produces an effectiveness factor of 0.238, which corresponds to a  $\phi_s$  value of 11.5. This result differs from the experimental value (0.17) and that calculated by the cylindrical pore model (0.61). In the calculations above, an experimental value of  $D_{\text{eff}}$  was not available and this circumstance is largely responsible for the discrepancy. If the combined diffusivity determined in Illustration 12.1 is converted to an effective diffusivity using equation (12.2.9), the value used above corresponds to a tortuosity factor of 2.6. If we had employed  $D_c$  from Illustration 12.1 and a tortuosity factor of unity to calculate  $D_{\text{eff}}$ , we would have determined that  $\eta = 0.65$ , which is consistent with the

value obtained from the straight cylindrical pore model in Illustration 12.2.

### 12.3.1.4 The Effectiveness Factor Analysis in Terms of Effective Diffusivities: Extension to Reactions Other than First-Order and Various Catalyst Geometries

The analysis developed in Section 12.3.1.3 may be extended in a straightforward manner to other integer-order rate expressions and to other catalyst geometries, such as flat plates and cylinders. Some of the key results from such extensions are treated briefly below.

For a zero-order chemical reaction, an analysis similar to that employed in Section 12.3.1.2 indicates that

$$\eta = \begin{cases} 1 & \text{for } \phi_{s0} < \sqrt{6} \\ 1 - \frac{4}{3} \frac{\pi r_c^3}{\frac{4}{3} \pi R^3} = 1 - \left(\frac{r_c}{R}\right)^3 & \text{for } \phi_{s0} > \sqrt{6} \end{cases} \quad (12.3.69)$$

where

$$\phi_{s0} = R \sqrt{\frac{k_0'' S_g \rho_p}{D_{\text{eff}} C_0}} \quad (12.3.70)$$

and where  $r_c$  is the radius at which the reactant concentration goes to zero. This radius may be determined from the constraints that both the reactant concentration and its gradient go to zero at the critical radius; hence,  $r_c$  is a root of the equation

$$\frac{1}{2} - \frac{3}{\phi_{s0}^2} = \frac{3}{2} \left(\frac{r_c}{R}\right)^2 - \left(\frac{r_c}{R}\right)^3 \quad (12.3.72)$$

where  $\phi_{s0}^2 \geq 6$  and  $r_c \leq R$ .

The analysis of simultaneous diffusion and chemical reaction in porous catalysts in terms of effective diffusivities is readily extended to geometries other than a sphere. Consider a flat plate of porous catalyst in contact with a reactant on one side but sealed with an impermeable material along the edges and on the side opposite the reactant. If we assume simple power law kinetics, a reaction in which there is no change in the number of moles on reaction, and an isothermal flat plate, a material balance on a differential thickness of the plate leads to the differential equation

$$D_{\text{eff}} \frac{d^2 C}{dx^2} = \rho_p S_g k_n'' C^n \quad (12.3.73)$$

where  $n$  is the reaction order and  $x$  is the distance in from the open side. One also assumes that the effective diffusivity is constant throughout the porous material. The boundary conditions for the physical situation described above require that at  $x = 0$ ,  $C = C_0$ , and at  $x = L$  (the plate thickness),  $dC/dx = 0$ .

The analyses of simultaneous reaction and mass transfer in this geometry are similar mathematically to those of the straight cylindrical pore model considered previously, because both are essentially one-dimensional models. In the general case, the Thiele modulus for semi-infinite flat-plate problems becomes

$$\phi_{Ln} = L \sqrt{\frac{\rho_p S_g k_n'' C_0^{n-1}}{D_{\text{eff}}}} \quad (12.3.74)$$

and the equations developed earlier for  $\eta$  in terms of the moduli  $h_0$ ,  $h_1$ , and  $h_2$  can be used to estimate  $\eta$  for flat-plate geometries, merely by replacing  $h_n$  and  $D_c$  by  $\phi_{Ln}$  and  $D_{\text{eff}}$ , respectively.

Figure 12.7 contains a plot showing how the effectiveness factors for different geometries and reaction orders vary with the appropriately defined Thiele modulus. In each case, at sufficiently low values of the Thiele modulus, the effectiveness factor approaches unity asymptotically. Conversely, at large values of the Thiele modulus, where the reaction is fast and diffusion throughout the porous catalyst is slow, reaction proceeds only in a small domain near the external surface and the effectiveness factor becomes proportional to  $1/\phi$ . The first- and zero-order curves provide limiting behavior for simple, single-site Langmuir–Hinshelwood–Hougen–Watson kinetics for reactions on catalytic surfaces. Catalysts where concentrations span the regime where the reaction kinetics undergo the transition from zero-order at high concentrations to first-order at low concentrations require calculations including the effects of both LHHW rate parameters and are slightly more complex. Other plots by Satterfield (40, 41) show similarly displaced curves for power law kinetics with higher reaction orders.

Analyses have been carried out for a variety of other catalyst geometries, including among others, porous rods

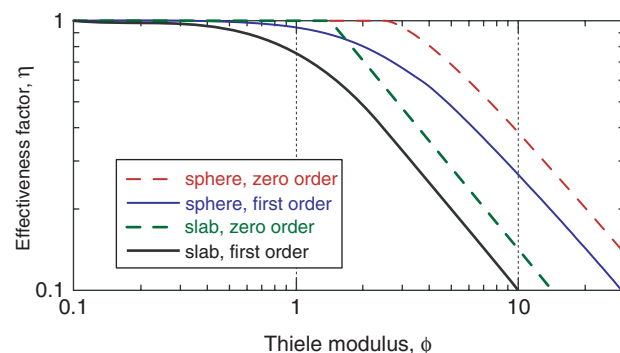


**Figure 12.7** Effectiveness factor plots for sphere and slab geometries for first- and zero-order kinetics. The Thiele modulus is given by  $\phi_{\text{sphere},n} = R \sqrt{\rho_p S_g k_n'' C_0^{n-1} / D_{\text{eff}}}$  for spherical catalysts or by  $\phi_{\text{slab},n} = L \sqrt{\rho_p S_g k_n'' C_0^{n-1} / D_{\text{eff}}}$  for slabs.

of infinite length (or with sealed ends), a porous rod with open ends, and the case of gases contacting the inside of a porous annulus. Refer to Satterfield (42) and Aris (35) for additional discussion along these lines and the pertinent references. However, we should point out that Luss and Amundson (43) have demonstrated that for simple first-order isothermal reactions, the spherical particle has the lowest effectiveness factor for all possible shapes having the same volume. This demonstration is largely a consequence of the fact that the sphere has the lowest possible external surface/volume ratio. One is tempted to conclude that catalyst particles should be fabricated in shapes other than spheres to minimize intraparticle diffusional limitations on the reaction rate. However, in practice, other considerations, such as the associated pressure drop across a packed bed, the flow distribution through the bed, and the ease of manufacture weigh heavily in determining the particular geometric shape in which the catalyst will be employed.

For spherical pellets, for semi-infinite slabs, and for infinite cylinders at sufficiently large values of the Thiele modulus,  $\phi_s$ , the effectiveness factor, becomes inversely proportional to the modulus, with the constant of proportionality depending on the gross catalyst geometry and the order of the reaction. Under these conditions, the reactant concentrations approach zero rapidly as one penetrates the catalyst, and it is only the outer periphery of the catalyst that is effective in promoting reaction. This region is very thin when  $\phi$  is large and in many respects may be regarded as a semi-infinite flat plate with a thickness  $V_p/S_x$ , irrespective of the actual catalyst geometry. This limiting condition gives rise to “asymptotic forms” of the relation between the effectiveness factor and the Thiele modulus, in which the inverse proportionality noted above is observed. This approach is extremely appealing from the viewpoint of the mathematician, because it emphasizes the mathematical similarity of the differential equations and their corresponding boundary conditions when one analyzes simultaneous diffusion and chemical reaction in porous catalysts of different geometries. For a discussion of the asymptotic solution approach to catalyst effectiveness factors, see the work of Aris (36, 44).

### 12.3.1.5 Isothermal Effectiveness Factors: Miscellaneous Considerations

**12.3.1.5.1 Implications of Nonequimolal Counterdiffusion for Effectiveness Factors** When there is a change in the number of gas phase species on reaction, there has to be at steady state a net molar flux either into or out of a porous catalyst. When bulk diffusion is responsible for all or even a reasonably significant fraction of the total mass transfer, the pressure gradient through the pellet will usually be negligible, but an increase in the

number of moles on reaction makes it more difficult for reactants to diffuse into the catalyst, thereby decreasing the effectiveness factor. A decrease in the number of moles facilitates diffusion of reactants into the pellet relative to the equimolal counterdiffusion case, thereby increasing the catalyst effectiveness factor. Although we have previously neglected consideration of these phenomena, we now wish briefly to consider the influence on catalyst effectiveness factors of changes in the number of gas phase species during reaction. Treatments of this subject date back to the classic paper of Thiele (20), but the most comprehensive general treatment is that of Weekman and Goring (45), who analyzed isothermal zero-, first-, and second-order reactions in porous spherical catalysts at constant total pressure. They described the response of the effectiveness factor to changes in the number of moles on reaction in terms of a volume change modulus  $\tilde{\theta}$  and the conventional Thiele modulus  $\phi_s$ . The volume change modulus is defined as

$$\tilde{\theta} = \left( \sum \nu_i \right) Y \quad (12.3.75)$$

where the sum of the stoichiometric coefficients is the increase in the number of moles on reaction and  $Y$  is the mole fraction reactant at the external surface of the catalyst. Their results were summarized in the form of plots of the ratio of the effectiveness factor for the volume change case ( $\eta'$ ) to that for no volume change ( $\eta$ ) versus the volume change modulus  $\tilde{\theta}$  at various values of the Thiele modulus  $\phi_s$ . Figure 12.8 is a reproduction of their curves for first-order reactions. The more significant the departures of  $\tilde{\theta}$  and  $\phi_s$  from zero, the greater the departure of the ratio  $\eta'/\eta$  from unity. The departure of  $\eta'/\eta$  from unity also becomes more significant as the order of the reaction increases, but at low values of  $\phi_s$  that effect is relatively small compared to the effects of variations in  $\tilde{\theta}$  or variations in  $\phi_s$ . Because the volume change modulus is directly proportional to the reactant mole fraction at the external surface of the catalyst, one expects the influence of  $\tilde{\theta}$  to be most significant near the inlet to a plug flow reactor *vis-à-vis* its effects at other points along the reactor length. Moreover, the effect should be small in cases where the reactants are highly diluted by the presence of inerts. This approach has also been extended to nonisothermal systems (46).

**12.3.1.5.2 Implications of the Effectiveness Factor Concept for Kinetic Parameters Measured in the Laboratory** It is useful at this point to discuss the effects of intraparticle diffusion on the kinetic parameters that are observed experimentally. Unless one is aware that intraparticle diffusion may obscure or disguise the true intrinsic chemical kinetics, he or she may draw incorrect conclusions regarding the reaction order and the

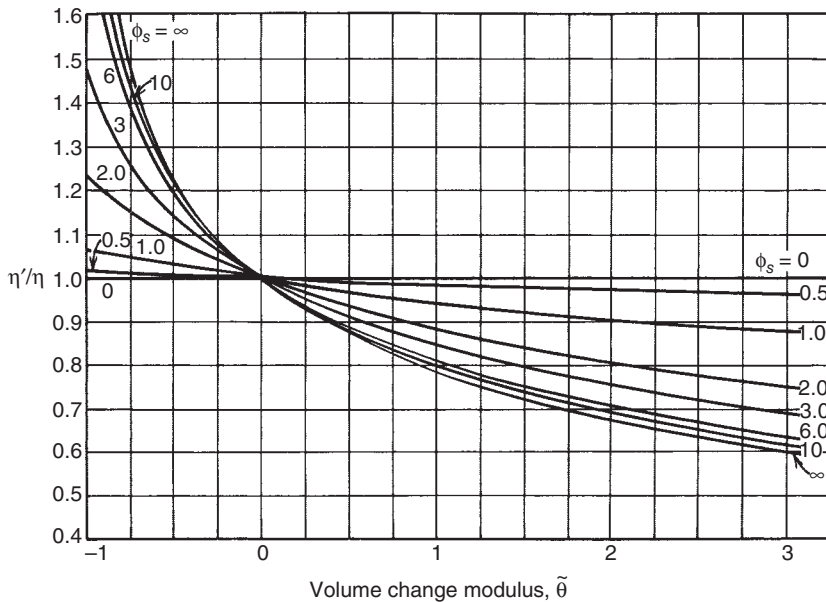


**Figure 12.8** Effectiveness factor ratios for first-order kinetics on spherical catalyst pellets.  $\eta'/\eta$  = (factor in the presence of volume change)/(factor in the absence of volume change). [From V. W. Weekman and R. L. Goring, *J. Catal.*, **4**, 260 (1965). Copyright © 1965. Used with permission of Academic Press.]

temperature dependence of the intrinsic chemical reaction. If one is interested in the fundamental nature of the chemical reaction, it is important to employ experimental conditions that eliminate the influence of both external and intraparticle mass transfer processes on the rate observed. From the viewpoint of the chemical engineer engaged in the practice of reactor design, it is even more important to recognize that in dealing with pelletized heterogeneous catalysts, the apparent kinetics may differ appreciably from the true intrinsic kinetics.

If we consider a reaction with intrinsic kinetics of simple  $n$ th-order form that takes place within the pores of a catalyst pellet, the rate of reaction observed per unit mass of catalyst may be written as

$$r_{\text{obs}} = \eta k'' C_0^n S_g \quad (12.3.76)$$

where  $C_0$  is the reactant concentration in the gas phase.

If we adopt the straight cylindrical pore model and write a material balance over a differential element of pore length, we find that for  $n$ th-order kinetics, the analog of equations (12.3.10), (12.3.31), and (12.3.43) becomes

$$\begin{aligned} \frac{d^2(C/C_0)}{d(x/\bar{L})^2} &= \left( \frac{2k'' \bar{L}^2}{\bar{r} D_c} \right) \left( \frac{C}{C_0} \right) = \left[ \frac{2k'' \bar{L}^2 C_0^{n-1}}{\bar{r} D_c} \right] \left( \frac{C}{C_0} \right)^n \\ &= h_n^2 \left( \frac{C}{C_0} \right)^n \quad (12.3.77) \end{aligned}$$

where the square of the generalized Thiele modulus (the quantity in brackets) is proportional to the external concentration of reactant raised to the power  $(n - 1)$ .

In the limit of low effectiveness factors where  $\eta$  becomes inversely proportional to the Thiele modulus,

the apparent order of the reaction may differ from the true order. In this case, because the rate is proportional to the product of the effectiveness factor and the external concentration raised to the  $n$ th power, it can be said that

$$r_{\text{obs}} \propto \frac{1}{h_n} C_0^n \propto \frac{C_0^n}{C_0^{(n-1)/2}} = C_0^{(n+1)/2} \quad (12.3.78)$$

Thus, a zero-order reaction appears to be  $\frac{1}{2}$ -order and a second-order reaction appears to be  $\frac{3}{2}$ -order when dealing with a fast reaction taking place in porous catalyst pellets. First-order reactions do not appear to undergo a shift in reaction order in going from high to low effectiveness factors. These statements presume that the combined diffusivity lies in the Knudsen range, so that this parameter is pressure independent.

If the dominant mode of transport within the catalyst pores is ordinary molecular diffusion, the analysis becomes somewhat more complex. The ordinary molecular diffusivity is inversely proportional to the pressure ( $P$ ), so that in this case

$$h_n \propto (C_0^{n-1})^{1/2} P^{1/2} \quad (12.3.79)$$

If the reactant is by far the dominant species, equation (12.3.79) can be written as

$$h_n \propto (C_0^{n-1})^{1/2} (C_0/RT)^{1/2} \text{ or } h_n \propto C_0^{n/2} \quad (12.3.80)$$

and in the limit of low effectiveness factors, the rate law will be of the form

$$r_{\text{obs}} \propto \frac{C_0^n}{C_0^{n/2}} = C_0^{n/2} \quad (12.3.81)$$

so that here one would again observe discrepancies between the orders of the reaction that are observed and those that are true.

In a similar fashion, it is easily shown that the apparent activation energy of the reaction may differ appreciably from the intrinsic activation energy of the chemical reaction. The apparent rate constant is equal to the product of the effectiveness factor and the true rate constant, and *in the limit of low effectiveness factors* it can be said that

$$k_{\text{apparent}} \propto \frac{k_{\text{true}}}{h_n} \quad (12.3.82)$$

In terms of the generalized Thiele modulus of equation (12.3.77), the last equation becomes

$$k_{\text{apparent}} \propto \frac{k_{\text{true}}}{\sqrt{k_{\text{true}}/D_c}} = \sqrt{D_c k_{\text{true}}} \quad (12.3.83)$$

where we have retained only the temperature dependent terms from the Thiele modulus.

If the combined diffusivity is written as

$$D_c = A e^{-E_{\text{diffusion}}/RT} \quad (12.3.84)$$

(where  $A$  is a temperature-independent quantity), the Arrhenius relation can be used with equations (12.3.83) and (12.3.84) to show that

$$E_{\text{apparent}} = \frac{E_{\text{diffusion}} + E_{\text{true}}}{2} \quad (12.3.85)$$

If ordinary molecular diffusion is the dominant mass transfer process, the kinetic theory of gases indicates that the diffusivity is proportional to  $T^{3/2}$  and it is easily shown that

$$E_{\text{diffusion}} = \frac{3RT}{2} \quad (12.3.86)$$

If Knudsen diffusion dominates,

$$E_{\text{diffusion}} = \frac{RT}{2} \quad (12.3.87)$$

Under normal circumstances the true activation energy term in equation (12.3.85) will far exceed the diffusional activation term calculated from either equation (12.3.86) or (12.3.87), and to a good approximation it may be said that in the limit of low effectiveness factors,

$$E_{\text{apparent}} \approx \frac{E_{\text{true}}}{2} \quad (12.3.88)$$

At low temperatures, diffusion will be rapid compared to chemical reaction and diffusional limitations on the reaction rate will not be observed. In this temperature regime, one will observe the intrinsic activation energy of the reaction. However, because chemical reaction rates increase much more rapidly with increasing temperature

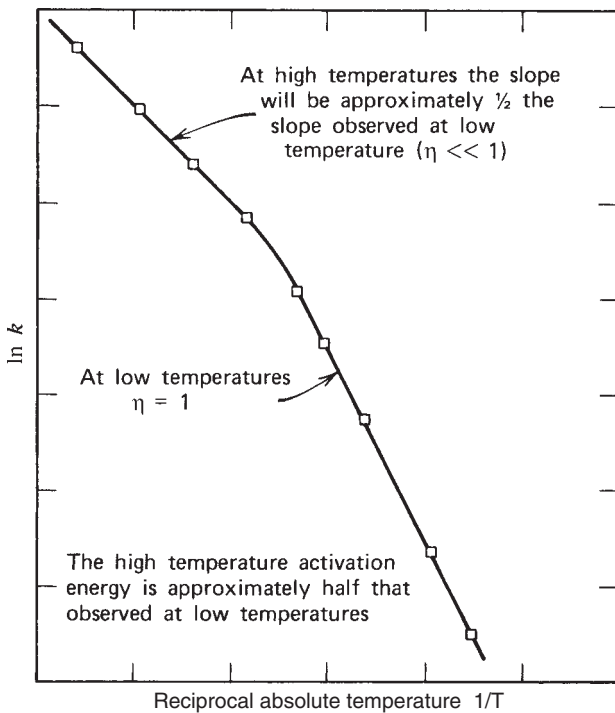


**Figure 12.9** Schematic representation of shift in activation energy when intraparticle mass transfer effects become significant.

than do diffusional processes, at higher temperatures one is much more likely to observe such limitations. In the regime where catalyst effectiveness factors become small, one will observe an activation energy that is given by equation (12.3.85). A typical Arrhenius plot for the range of temperatures where this change takes place will resemble that shown in Figure 12.9.

### 12.3.1.5.3 Effectiveness Factors for Hougen-Watson Rate Expressions

The discussion thus far and the vast majority of the literature dealing with effectiveness factors for porous catalysts are based on the assumption of an integer-power reaction rate expression (i.e., zero-, first-, or second-order kinetics). In Chapter 6, however, we stressed the fact that heterogeneous catalytic reactions are more often characterized by more complex rate expressions of the Hougen-Watson type. Over a narrow range of reactant concentrations, it is often possible to approximate a Hougen-Watson rate expression by an integer power law relation. However, if the diffusional limitations within a porous catalyst pellet are important (i.e., the effectiveness factor is low), there may be a significant gradient in reactant concentration across the pellet. The reactant partial pressure will vary from its value at the exterior surface to a value approaching zero at the center of the pellet. In this case, the range of partial pressures can be quite significant and it is not really appropriate to use the

approximate integer degenerate forms of Hougen–Watson rate expressions. Several analyses of this problem have appeared in the literature, dating back to a study by Chu and Hougen (47).

The procedure for determining catalyst effectiveness factors for generalized Hougen–Watson rate expressions is basically the same as that for integer-power rate expressions. One sets up and solves the differential equation for simultaneous diffusion and reaction inside the catalyst pellet. However, unlike the isothermal integer rate law cases, it is not possible to obtain closed-form solutions for these rate expressions, and recourse must be made to numerical solutions or various approximations that simplify the mathematical treatment. Roberts and Satterfield (48–51) developed a generalized method for predicting catalyst effectiveness factors for reactions that are first- or second-order in the fraction of the surface covered by reactant species. Their approach allows for inhibition by both reactant and product species. They found that under certain isothermal conditions, it is possible for the effectiveness factor to exceed unity. Consult the references cited above for the generalized charts and procedural details necessary to employ their numerical solutions. Some reversible first-order reactions of the Hougen–Watson form have been treated in the literature (52), and other extensions of this technique are covered in the text by Wijngaarden et al. (53).

**12.3.1.5.4 Effectiveness Factors for Reversible Reactions** The vast majority of the literature dealing with catalyst effectiveness factors presumes the reactions to be irreversible. However, in some cases it is possible to extend the analysis to certain reversible reactions. First-order reversible reactions have been treated for various catalyst geometries. For flat-plate geometry where only one side of the plate is exposed to reactant gases, one may proceed as in previous subsections to show that for mechanistic equations of the form



the effectiveness factor is given by

$$\eta = \frac{\tanh(\phi_{L,rev})}{\phi_{L,rev}} \quad (12.3.90)$$

where

$$\phi_{L,rev} = L \sqrt{\frac{(k'_1 + k''_{-1})S_g \rho_p}{D_{eff,A}}} \quad (12.3.91)$$

In terms of the equilibrium constant for the reaction, the Thiele modulus becomes

$$\phi_{L,rev} = L \sqrt{\frac{k'_1 (K + 1) S_g \rho_p}{K D_{eff,A}}} \quad (12.3.92)$$

Because the factor  $(K + 1)/K$  is always greater than unity,  $\phi_{L,rev}$  will always be greater (and  $\eta$  less) than the corresponding Thiele modulus for the forward reaction alone, other conditions remaining constant.

Analysis of the same reaction carried out using spherical catalyst pellets leads to similar results and conclusions, because the first-order rate constant is again replaced by the group  $k'_1 (K + 1)/K$ .

### 12.3.2 The Consequences of Intraparticle Temperature Gradients for Catalyst Effectiveness Factors

When catalytic reaction rates become very large, it is possible that the energy transformed (released or consumed) by reaction cannot be dissipated (or supplied) at a rate that is sufficient to keep the entire catalyst pellet at the same temperature as that of the surrounding fluid. Temperature gradients may exist within the particle itself or within the boundary layer separating the particle from the bulk fluid. The presence of such gradients can have significant consequences for reactor design calculations. In this section we treat the influence of intraparticle temperature gradients in terms of their influence on catalyst effectiveness factors. This influence is most significant in cases where highly exothermic reactions are carried out using catalyst pellets that have low effective thermal conductivities. If catalyst effectiveness factors are defined in terms of the ratio of the observed rate to a rate law evaluated assuming that the reactant concentration and the temperature at the pore mouths prevail throughout the pellet, it is possible to observe values of the effectiveness factor in excess of unity. When the catalyst interior is hotter than the peripheral regions, the increase in temperature as one moves inward may more than offset the decline in reactant concentrations, so that one obtains faster local rates of reaction in the interior than in the peripheral regions.

#### 12.3.2.1 Effective Thermal Conductivities of Porous Catalysts

The effective thermal conductivity of a porous catalyst plays a key role in determining whether or not appreciable temperature gradients will exist within a given catalyst pellet. By the term *effective thermal conductivity*, we imply that it is a parameter characteristic of the porous solid structure that is based on the gross geometric area of the pellet perpendicular to the direction of heat transfer. For example, if one considers the radial heat flux in a spherical pellet, one can say that

$$q_r = -4\pi r^2 k_{eff} \frac{dT}{dr} \quad (12.3.93)$$

where  $q_r$  is the rate of heat transfer in the outward radial direction and  $k_{\text{eff}}$  is the effective thermal conductivity.

The effective thermal conductivities of common commercial porous catalysts are quite low and fall within a surprisingly narrow range. The heat transfer path through the solid phase offers considerable thermal resistance for many porous materials, particularly if the pellet is formed by tableting of microporous particles. Such pellets may be regarded as an assembly of particles that contact one another at only a relatively small number of points that act as regions of high thermal resistance.

An approximate relationship that is sometimes useful in predicting effective thermal conductivities is the geometric average value discussed by Woodside and Messmer (54).

$$k_{\text{eff}} = k_s^{1-\varepsilon_p} k_f^{\varepsilon_p} = k_s \left( \frac{k_f}{k_s} \right)^{\varepsilon_p} \quad (12.3.94)$$

where  $k_f$  and  $k_s$  are the thermal conductivities of the bulk fluid and solid, respectively, and  $\varepsilon_p$  is the porosity of the pellet.

Despite the difficulties of predicting  $k_{\text{eff}}$  on an a priori basis, it is still possible to choose a value that is reasonably correct because the possible range of values is roughly only 0.1 to 0.4 Btu / (h·ft·°F) or 1.6 to  $6.4 \times 10^{-3}$  J/(s·cm·°C). Typically, the thermal conductivity of reactant gases at room temperature will range from 8 to  $24 \times 10^{-5}$  J/(s·cm·°C), and these values are an order of magnitude less than those of most porous catalysts under vacuum. Consequently, in such situations the bulk of the energy transport will occur through the solid phase. On the other hand, for liquids, the thermal conductivity will be an order of magnitude greater, and when the catalyst pores are filled with liquid, both phases will make significant contributions to the heat transfer process. Butt (55) has developed a useful model for the thermal conductivity of porous catalysts, while Madzhidov (56) has probed the influence of the filling fluid on thermal conductivity.

### 12.3.2.2 Effectiveness Factors for Nonisothermal Catalyst Pellets

Here we indicate how previous effectiveness factor analyses may be extended to situations where the pellet is not isothermal. Consider the case of a spherical pellet within which a catalytic reaction is taking place. If we examine an infinitesimally thin spherical shell with internal radius  $r$  similar to that shown in Figure 12.4 and write a steady-state energy balance over the interior core of the pellet, it is obvious that the heat flow outward by conduction across the sphere of radius  $r$  must be equal to the energy transformed by reaction within the central core. The latter quantity is just

the product of the reaction rate and (minus) the enthalpy change accompanying the reaction ( $\Delta H$ ). Hence,

$$-4\pi r^2 k_{\text{eff}} \frac{dT}{dr} \Big|_r = -\Delta H \mathcal{R} \quad (12.3.95)$$

where  $\mathcal{R}$  is the reaction rate in the interior core. Because the reaction rate within the core must also be equal to the rate of transfer of reactant *into* the core by diffusion, equation (12.3.95) may also be written as

$$-4\pi r^2 k_{\text{eff}} \frac{dT}{dr} \Big|_r = -\Delta H \left( 4\pi r^2 D_{\text{eff}} \frac{dC}{dr} \Big|_r \right) \quad (12.3.96)$$

Negative signs are required on the right sides of equations (12.3.95) and (12.3.96) so that for exothermic reactions, the temperature will be hotter in the core than at the periphery. Integration of the last equation between radius  $r$  and the gross pellet radius  $R$  gives

$$k_{\text{eff}}(T - T_0) = \Delta H D_{\text{eff}}(C - C_0) \quad (12.3.97)$$

where  $T_0$  and  $C_0$  are the temperature and reactant concentration at the external surface of the pellet, respectively. Rearrangement gives

$$T - T_0 = \frac{\Delta H D_{\text{eff}}}{k_{\text{eff}}}(C - C_0) \quad (12.3.98)$$

This equation is a general result first derived by Damköhler (57). It is applicable for any form of the reaction rate expression because this quantity was eliminated through the requirement that the rate of mass transport equal the reaction rate.

The maximum temperature difference between the center of the pellet and the external surface ( $T_c - T_0$ ) occurs when the reactant concentration vanishes at  $r = 0$ :

$$(T_c - T_0)_{\text{max}} = -\frac{\Delta H D_{\text{eff}} C_0}{k_{\text{eff}}} \quad (12.3.99)$$

Evaluation of the maximum temperature difference provides a useful criterion for determining if departures from isothermal behavior are significant. Substitution of the following property values into the relation (12.3.99) leads to a temperature difference of 200°C between the center of the pellet and the exterior surface:

$$\Delta H = -80,000 \text{ J/mol}$$

$$D_{\text{eff}} = 10^{-1} \text{ cm}^2/\text{s}$$

$$C_0 = 4 \times 10^{-5} \text{ mol/cm}^3 \text{ (at 1 atm)}$$

$$k_{\text{eff}} = 16 \times 10^{-4} \text{ J/(cm·s·°C)} \text{ (alumina)}$$

Obviously, if the reactant concentration does not go to zero at the center, the temperature difference will be less,

but in many cases it will still be quite large. Large values of this temperature difference can lead to effectiveness factors for exothermic reactions that are considerably in excess of unity.

In Section 12.3.1.3 it was shown that for a first-order reaction of the type  $A \rightarrow B$ , a material balance on the infinitesimally thin spherical shell of Figure 12.4 leads to the differential equation

$$\frac{d^2C}{dr^2} + \frac{2}{r} \frac{dC}{dr} = \frac{k_1'' \rho_p S_g C}{D_{\text{eff}}} \quad (12.3.100)$$

with boundary conditions

$$C = C_0 \text{ at } r = R \quad \text{and} \quad \frac{dC}{dr} = 0 \text{ at } r = 0 \quad (12.3.101)$$

At steady state, an energy balance on this same volume element gives

output – input (*by conduction*)

= energy transformed by reaction

$$\begin{aligned} \left( -4\pi r^2 k_{\text{eff}} \frac{dT}{dr} \right)_{r+\Delta r} - \left( -4\pi r^2 k_{\text{eff}} \frac{dT}{dr} \right)_r \\ = -4\pi r^2 \Delta r (k_1'' C S_g \rho_p) \Delta H \end{aligned} \quad (12.3.102)$$

Rearranging and taking the limit as  $\Delta r \rightarrow 0$  gives

$$\frac{d}{dr} \left( r^2 \frac{dT}{dr} \right) = r^2 \frac{k_1'' C S_g \rho_p \Delta H}{k_{\text{eff}}} \quad (12.3.103)$$

or

$$\frac{d^2T}{dr^2} + \frac{2}{r} \frac{dT}{dr} = \frac{k_1'' C S_g \rho_p \Delta H}{k_{\text{eff}}} \quad (12.3.104)$$

The boundary conditions on equation (12.3.104) require that

$$T = T_0 \text{ at } r = R \quad \text{and} \quad \frac{dT}{dr} = 0 \text{ at } r = 0 \quad (12.3.105)$$

Because the rate constant appearing in equations (12.3.100) and (12.3.104) depends exponentially on temperature, these equations are coupled in a nonlinear fashion and cannot be considered independently.

Exact analytical solutions of the coupled equations for simultaneous mass transfer, heat transfer, and chemical reaction can rarely be obtained. However, various authors have employed linear approximations (58, 59), perturbation techniques (60), or asymptotic approaches (61) to obtain approximate analytical solutions to these equations. Numerical solutions have also been obtained (62, 63). Once the solution for the concentration profile has been determined, equation (12.3.98) may be used to determine the temperature profile. The effectiveness factor

may also be determined from the concentration profile, using the approach we have used throughout the chapter. It is important to remember that here the effectiveness factor is defined as the ratio of the actual rate to the one that would occur if all portions of the interior of the pellet were exposed to reactant at the same concentration and the same temperature as exist at the outside surface of the pellet.

Regardless of the approach used to generate values of the effectiveness factor, this parameter can be expressed in terms of three dimensionless groups:

- I.** A Thiele-type modulus, which is defined for first-order kinetics as

$$\phi_s = R \sqrt{\frac{k_1'' S_g \rho_p}{D_{\text{eff}}}} \quad (12.3.106)$$

where the rate constant is evaluated at the external surface temperature  $T_0$ .

- II.** An Arrhenius number,

$$\gamma = \frac{E}{R_g T_0} \quad (12.3.107)$$

where  $R_g$  is the gas constant and  $E$  is the intrinsic activation energy of the reaction.

- III.** An energy conversion parameter,

$$\beta = \frac{(-\Delta H) D_{\text{eff}} C_0}{k_{\text{eff}} T_0} \quad (12.3.108)$$

where  $\beta$  is positive for an exothermic reaction.

The parameter  $\gamma$  reflects the sensitivity of the reaction rate to temperature variations. The parameter  $\beta$  represents the ratio of the maximum temperature difference that can exist within the particle [equation (12.3.99)] to the external surface temperature. This parameter reflects the transformation of energy stored in the form of chemical bonds to thermal energy. For isothermal pellets,  $\beta$  may be regarded as zero ( $k_{\text{eff}} = \infty$ ). Weisz and Hicks (63) summarized their numerical solutions for first-order irreversible reactions on spherical catalyst pellets in terms of four figures in which  $\eta$  is plotted versus  $\phi_s$ . Each figure represents a fixed Arrhenius number and contains a series of curves for values of the energy transformation parameter  $\beta$  ranging from  $-0.8$  to  $+0.8$ . Figure 12.10 is adapted from their work and represents an Arrhenius number that corresponds to a set of variables that might typically be encountered in industrial practice (i.e.,  $E = 28,000$  cal/g-mol,  $T = 700$  K). Their original article also contains curves for Arrhenius numbers of 10, 30, and 40.

Inspection of Figure 12.10 indicates that for exothermic reactions ( $\beta > 0$ ), the effectiveness factor can exceed unity by a considerable amount. This situation occurs

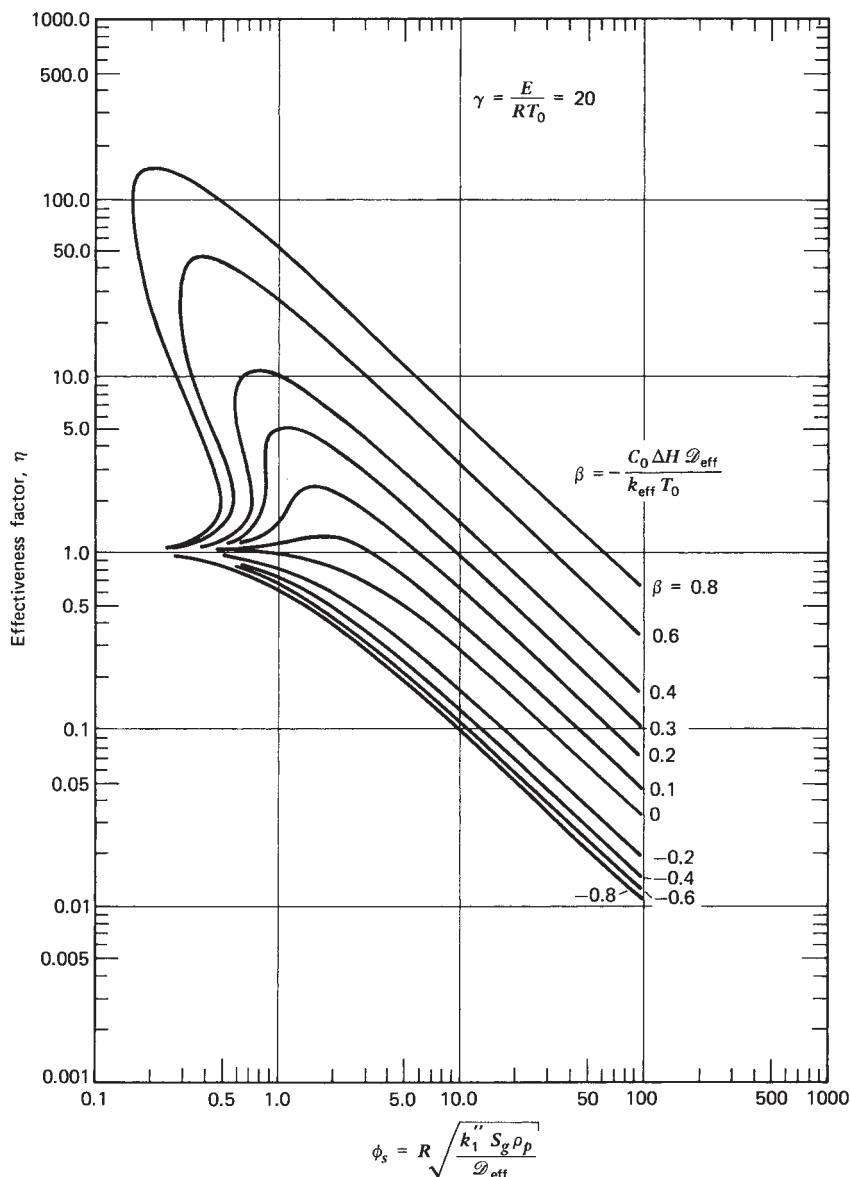


**Figure 12.10** Effectiveness factor chart for first-order reaction in spherical pellets for  $\gamma = 20$ . [From P. B. Weisz and J. S. Hicks, *Chem. Eng. Sci.*, **17**, 265 (1962). Copyright © 1962. Reprinted with permission of Pergamon Press.]

when circumstances are such that the increase in rate caused by the increase in temperature as one moves toward the center of the pellet more than offsets the decrease in reactant concentration accompanying this movement. The overall rate of reaction is therefore greater than it would be if the same temperature and reactant concentration prevailed throughout the catalyst pellet. While values of  $\eta$  that exceed unity might be thought to imply efficient catalyst utilization, there may be concomitant disadvantages. The large temperature increase at the center of the pellet may hasten catalyst deactivation processes in the interior core, or it may lead to adverse effects on catalyst selectivity if the activation energies of reactions leading to

undesired products are greater than that of the reaction of interest.

Close examination of the numerical solutions indicates that under conditions where  $\eta \gg 1$ , there is a large temperature gradient at the periphery of the pellet, but the gradient flattens out considerably as one approaches the center of the pellet. For fast exothermic reactions (large  $\phi_s$ ,  $\beta > 0$ ), the interior of the pellet will be at a relatively uniform high temperature, but there will be a fairly sharp decrease in temperature as one nears the exterior surface. In this regime  $\eta$  becomes inversely proportional to  $\phi_s$  as in the isothermal case, and the large majority of the reaction takes place in the nonisothermal shell of catalyst at its periphery.

The shapes of the curves in Figure 12.10 that correspond to highly exothermic reactions are such that a single value of  $\phi_s$  may give rise to as many as three values of  $\eta$  at fixed values of  $\gamma$  and  $\beta$ . These three values correspond to three different sets of circumstances in which the rate of energy release by reaction equals the rate of heat removal. In many respects the situation is akin to the problem of stability for a CSTR treated in Section 10.6. The intermediate value of  $\eta$  for given values of  $\phi_s$ ,  $\gamma$ , and  $\beta$  corresponds to unstable conditions. The high and low values of  $\eta$  represent stable conditions, and both can be realized in practice. Which condition will prevail in the real world depends on the direction from which the steady state condition is approached. The highest value of  $\eta$  corresponds to a steep temperature profile in the pellet. For this value physical transfer processes limit the overall reaction rate. The lowest value of  $\eta$  will be close to unity, and in this case the temperature gradients within the pellet will be quite small. In the latter instance the overall rate is controlled by the rate of the chemical reaction on the catalyst surface.

We would be remiss in our obligations to the reader if we did not point out that the regions of multiple solutions are seldom encountered in industrial practice, because of the large values of  $\beta$  and  $\gamma$  required to enter this regime. The conditions under which a unique steady state will occur have been described in a number of publications, and the interested student should consult the literature for additional details. It should also be stressed that it is possible to obtain effectiveness factors greatly exceeding unity at relatively low values of the Thiele modulus. An analysis that presumed isothermal operation would indicate that the effectiveness factor would be close to unity at the low moduli involved. Consequently, failure to allow for temperature gradients within the catalyst pellet can lead to major errors.

Under isothermal conditions, we have seen that the apparent activation energy of the reaction is approximately one half the intrinsic value when  $\eta$  is sufficiently low. When  $\eta$  exceeds unity, an opposite effect occurs (i.e., the apparent activation energy will exceed the true activation energy).

Consideration of Figure 12.10 indicates that for endothermic reactions ( $\beta < 0$ ), nonisothermal conditions do not have as significant an effect on  $\eta$  as they do for exothermic cases. For endothermic reactions,  $\eta$  is always less than unity and the temperature within the catalyst interior is less than that at the exterior surface. Both concentration and temperature decrease as one moves radially inward. A good approximation for the effectiveness factor can be obtained by considering only the temperature gradient through the pellet and neglecting concentration gradients, even when they are appreciable. This approach has been described by Maymo et al. (64).

Illustration 12.4 indicates how experimental and calculated values of catalyst effectiveness factors may be determined for a specific case.

### ILLUSTRATION 12.4 Effectiveness Factor Determination for a Nonisothermal Catalyst Pellet Employed to Effect an Exothermic Reaction

Cunningham et al. (65) studied the rate of hydrogenation of ethylene at 1 atm over a copper–magnesium oxide catalyst. They used flow reactors to study the reaction kinetics over both finely divided catalyst particles and spherical pellets, made by compressing these particles in a steel mold. They also measured the temperature difference between the center of the pellet and the external surface.

The reactor feed mixture was prepared so as to contain less than 17% ethylene (remainder hydrogen) so that the change in total moles within the catalyst pore structure would be small. This approach reduced the variation in total pressure and its effect on the reaction rate, so as to permit comparison of experiment results with theoretical predictions [e.g., those based on the work of Weisz and Hicks (63)]. Because the numerical solutions to the nonisothermal catalyst problem also presumed first-order kinetics, they determined the Thiele modulus by forcing the observed rate to fit this form even though they recognized that a Hougen–Watson type of rate expression would have been more appropriate. Hence, their Thiele modulus was defined as

$$\phi = R \sqrt{\frac{\rho_p \mathcal{R}_m}{C_0 D_{\text{eff}}}} \quad (\text{A})$$

where  $\mathcal{R}_m$  was the reaction rate per unit weight of catalyst for very small catalyst particles, and  $C_0$  was the reactant concentration at the external surface of the pellet.

Using this definition of the Thiele modulus, the reaction rate measurements for finely divided catalyst particles noted below, and the additional property values cited below, determine the effectiveness factor for 0.5-in. spherical catalyst pellets fabricated from these particles. Comment on the reasons for the discrepancy between the calculated value of  $\eta$  and the ratio of the rate observed for 0.5 in. pellets to that for fine particles.

Data are as follows:

Particle size	–100 to +150 Tyler mesh
Pellet size	0.5-in. diameter = 1.27 cm
Effective diffusivity for ethylene in pellet (estimated)	$3.0 \times 10^{-2} \text{ cm}^2/\text{s}$
Effective thermal conductivity of pellets (measured)	$3.5 \times 10^{-4} \text{ cal}/(\text{cm} \cdot \text{s} \cdot ^\circ\text{C})$

Pellet density	1.16 g/cm <sup>3</sup>
Void volume/gram	0.236 cm <sup>3</sup> /g
Specific surface area	90 m <sup>2</sup> /g
Enthalpy change for reaction	-32,700 cal/mol
Temperature	80°C
Total pressure	1 atm
Activation energy for reaction based on small particle rate measurements	17,800 cal/mol
Measured rate for small particles (extrapolated)	$8 \times 10^{-7}$ mol/(s·g catalyst)
Measured rate for 0.5-in. pellets	$1.8 \times 10^{-6}$ mol/(s·g catalyst)

## Solution

The Arrhenius number is given by equation (12.3.107):

$$\gamma = \frac{E}{R_g T_0} = \frac{17,800}{1.987(353)} = 25.4$$

The energy transformation parameter can be determined from equation (2.3.108):

$$\beta = \frac{(-\Delta H)D_{\text{eff}}C_0}{k_{\text{eff}}T_0}$$

The external ethylene surface concentration at 80°C, 1 atm, and an ethylene mole fraction of 0.17 may be estimated using the ideal gas law as  $5.87 \times 10^{-6}$  mol/cm<sup>3</sup>. Hence,

$$\beta = \frac{32,700(3.0 \times 10^{-2})}{(3.5 \times 10^{-4})(353)} (5.87 \times 10^{-6}) = 0.047$$

This value of  $\beta$  corresponds to a maximum temperature difference between the center and the surface of the pellet of 16.2°C. Values of the difference measured for this catalyst were 14 to 15°C, as reported by the authors.

The pseudo Thiele modulus may be calculated from equation (A):

$$\phi = \frac{1.27}{2} \sqrt{\frac{1.16(8 \times 10^{-7})}{(5.87 \times 10^{-6})(3.0 \times 10^{-2})}} = 1.46$$

Using Figure 12.10, one can determine that the catalyst effectiveness factor will be approximately 1.0. This figure corresponds to  $\gamma = 20$ , but consideration of the curve for  $\gamma = 30$  in the original article leads to the same conclusion.

On the basis of the experimental measurements,

$$\eta = \frac{1.8 \times 10^{-6}}{8 \times 10^{-7}} = 2.25$$

The value calculated here is at variance with the value listed in Table 3 of reference 65 because the indicated authors used  $\beta = 0.27$ , based on a calculation in which the total gas-phase concentration was used. Consequently, they predicted an effectiveness factor of 20.

There are several factors that may be invoked to explain the discrepancy between predicted and measured results, but the discrepancy highlights the necessity for good pilot-scale data to design these types of reactors properly. Obviously, the reaction does not involve simple first-order kinetics or equimolar counterdiffusion. The fact that the catalyst activity varies significantly with time onstream and some carbon deposition is observed indicates that perhaps the coke residues within the catalyst may have effects like those to be discussed in Section 12.3.3. Consult the original article for further discussion of the nonisothermal catalyst pellet problem.

### 12.3.3 The Influence of Catalyst Poisoning Processes on Catalyst Effectiveness Factors

In the design of commercial-scale heterogeneous catalytic reactors, the activity of the catalyst will almost invariably change with time. We now wish to focus our attention on the implications of poisoning reactions for efficient use of catalyst surface areas. Because reactant molecules must interact with unpoisoned catalyst sites before reaction can occur, the poisoning process may have two effects on the reaction rate that one observes.

1. It always decreases the total number of catalytic sites or the fraction of the total surface area that has the capability of promoting reaction.
2. It may increase the average distance a reactant molecule must diffuse through the pore structure before undergoing reaction.

The poisoning reaction must be viewed like any other chemical interaction between a gas-phase reactant and the solid surface. The manner in which the poisoned sites are distributed throughout the pore structure is a direct consequence of the relative values of the rate at which the poison diffuses into the pore and the rate at which the poisoning reaction takes place. The problem of determining this distribution is the same as the more general problem we have been analyzing in the last several subsections: What do the concentration profiles of reactant and product species look like for a given catalyst particle? If the poisoning reaction is slow relative to diffusion of the poison, the poisoned sites will be distributed uniformly throughout the porous catalyst and we will have *homogeneous poisoning* of the catalyst. This situation obviously corresponds to that in which the effectiveness factor for the poisoning reaction is essentially unity. On the other hand, if the poisoning reaction is rapid relative to diffusion of the poison, the outer periphery of the catalyst particle will be completely poisoned before the interior core suffers significant activity loss. This situation is termed *pore-mouth poisoning*. As poisoning proceeds, the inactive shell thickens and, under

extreme conditions, the rate of the catalytic reaction may become limited by the rate of diffusion of reactants past the poisoned pore mouths. The apparent activation energy of the reaction under these extreme conditions will be typical of the temperature dependence of diffusion coefficients. If the catalyst and reaction conditions in question are characterized by a low effectiveness factor, one may find that poisoning only a small fraction of the surface gives rise to a disproportionate drop in activity. In a sense one observes a form of *selective poisoning*.

The two limiting cases for the distribution of deactivated catalyst sites are representative of some of the situations that can be encountered in industrial practice. The formation of coke deposits on some relatively inactive cracking catalysts would be expected to occur uniformly throughout the catalyst pore structure. In other situations the coke may deposit as a peripheral shell that thickens with time on-stream. Poisoning by trace constituents of the feed stream often falls in the pore-mouth category.

By analyzing both of the limiting situations described above, Wheeler (66, 67) was able to show that the interaction of the poisoning process with the influence of intra-particle diffusion on the rates of the primary and poisoning reactions can lead to a variety of interesting relations between observed catalytic activity and the fraction of surface poisoned. Each of the limiting cases is analyzed below in terms of the mathematical model set forth by Wheeler. In both cases the reaction is presumed to proceed isothermally in a manner that is first-order in the gas-phase concentration of reactant. For convenience, the straight cylindrical pore model of the catalyst is used, but the qualitative results may be regarded as essentially independent of the model employed.

### 12.3.3.1 Uniform Distribution of Activity Loss

If the species giving rise to the poisoning reaction must make several collisions with the catalyst surface before adsorption can occur, these molecules will have a chance to diffuse deep into the catalyst pore structure before chemisorbing on the surface. Here deactivation of the catalyst will occur uniformly throughout the pore structure (homogeneous poisoning). If we denote the fraction of the surface that is poisoned by  $\alpha$ , the fraction that is intrinsically capable of promoting reaction is equal to  $1 - \alpha$ . For a first-order reaction, the rate per unit surface area will then be  $k_1''(1 - \alpha)C$ .

A material balance over a differential element of pore length leads to the following analog of equation (12.3.10):

$$\frac{d^2C}{d(x/\bar{L})^2} = \frac{2k_1''(1 - \alpha)\bar{L}^2}{\bar{r}D_c}C \quad (12.3.109)$$

The appropriate Thiele modulus for use with this differential equation is

$$h_p^2 = \frac{2k_1''\bar{L}^2(1 - \alpha)}{\bar{r}D_c} = h_T^2(1 - \alpha) \quad (12.3.110)$$

where  $h_T$  is the Thiele modulus for the unpoisoned case and  $h_p$  is the Thiele modulus for the poisoned case.

Following the procedure used in Section 12.3.1.1 for the first-order case, it is readily shown that the effectiveness factor for the poisoned surface is given by

$$\eta_{\text{poisoned}} = \frac{\tanh h_p}{h_p} \quad (12.3.111)$$

The ratio  $\mathcal{F}$  of the reaction rate for the poisoned pore to that for the unpoisoned pore is given by

$$\mathcal{F} = \frac{\eta_{\text{poisoned}} k_1''(1 - \alpha)C_0}{\eta_{\text{unpoisoned}} k_1'' C_0} \quad (12.3.112)$$

or, using equations (12.3.111) and (12.3.20),

$$\mathcal{F} = \left[ \frac{\tanh h_p}{\tanh h_T} \right] \left[ \frac{h_T(1 - \alpha)}{h_p} \right] \quad (12.3.113)$$

With equation (12.3.110), equation (12.3.113) becomes

$$\begin{aligned} \mathcal{F} &= \left[ \frac{\tanh(h_T \sqrt{1 - \alpha})}{\tanh h_T} \right] \left[ \frac{h_T(1 - \alpha)}{h_T \sqrt{1 - \alpha}} \right] \\ &= \left[ \frac{\tanh(h_T \sqrt{1 - \alpha})}{\tanh h_T} \right] \left[ \sqrt{1 - \alpha} \right] \end{aligned} \quad (12.3.114)$$

When the Thiele modulus for the unpoisoned pore is small (i.e., when the surface is completely available), the hyperbolic tangent terms become equal to their arguments and  $\mathcal{F}$  is given by

$$\mathcal{F} = 1 - \alpha \quad \text{for small } h_T \quad (12.3.115)$$

This relation is plotted as curve A in Figure 12.11 and represents the “classical case” of nonselective poisoning in which the apparent fraction of the activity remaining is equal to the fraction of the surface remaining unpoisoned. This same result is evident from equation (12.3.112) by recognizing that both effectiveness factors are unity for this situation.

On the other hand, when the Thiele modulus for the unpoisoned reaction is very large, both hyperbolic tangent terms in equation (12.3.114) become equal to unity and  $\mathcal{F}$  is given by

$$\mathcal{F} = \sqrt{1 - \alpha} \quad \text{for large } h_T \quad (12.3.116)$$

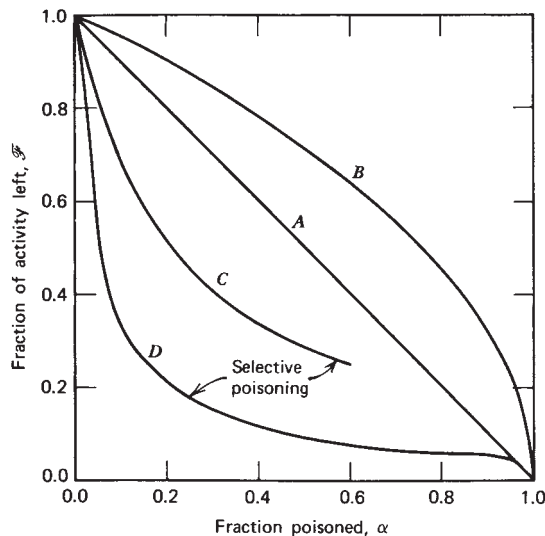


**Figure 12.11** Poisoning curves for porous catalysts. Curve A is for a porous catalyst with  $h_T$  very small and the poison distributed homogeneously. Curve B is for large  $h_T$  and the poison distributed homogeneously. Curves C and D correspond to preferential adsorption of the poison near the pore mouths. For curve C,  $h_T = 5$ , and for curve D,  $h_T = 20$ .

This relation is plotted as curve B in Figure 12.11. Smith (68) has shown that the same limiting forms for  $\mathcal{F}$  are observed using the concept of effective diffusivities and spherical catalyst pellets. Examination of curve B indicates that for fast reactions on catalyst surfaces where the poisoned sites are uniformly distributed over the pore surface, the apparent activity of the catalyst declines much less rapidly than for the case where catalyst effectiveness factors approach unity. Under these circumstances, the catalyst effectiveness factors are considerably less than unity, and the effects of the portion of the poison adsorbed near the closed end of the pore are not as apparent as in the earlier case for small values of  $h_T$ . With poisoning, the Thiele modulus  $h_p$  decreases, and the reaction merely penetrates deeper into the pore.

### 12.3.3.2 Pore-Mouth or Selective Poisoning

Because many metallic catalysts have high adsorption affinities, we often find that certain poison molecules are adsorbed in an immobile form after only a very few collisions with the catalyst surface. In this situation, the outer periphery of the catalyst particle will be completely poisoned whereas the inner shell will be nearly completely free of poison. The thickness of the poisoned shell grows with prolonged exposure to poison molecules until the pellet is deactivated completely. During the poisoning process, the boundary between active and deactivated regions is relatively sharp.

If a fraction  $\alpha$  of the total catalyst surface has been deactivated by poison, the essential assumption underlying

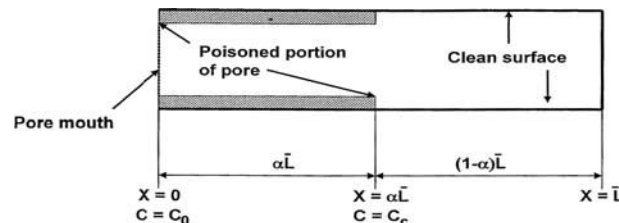


**Figure 12.12** Schematic representation of the preferential adsorption of poison near the mouth of a pore. [Adapted from A. Wheeler, *Adv. Catal.*, **3**, 249 (1951). Copyright © 1951. Used with permission of Academic Press.]

the pore-mouth poisoning model is that a cylindrical region of length  $(\alpha L)$  nearest the pore mouth will have no catalytic activity, whereas a region of length  $(1 - \alpha)L$  will be catalytically active (see Figure 12.12). The reactant concentration at the pore mouth is  $C_0$ , and that at  $x = \alpha\bar{L}$  is  $C_c$  (an unknown).

Under steady-state conditions, the reaction rate is equal to the rate of diffusion of reactant through the poisoned region. The latter may be written as

$$\text{rate of diffusion} = \pi \bar{r}^2 D_c \frac{dC}{dx} = \pi \bar{r}^2 D_c \left( \frac{C_0 - C_c}{\alpha \bar{L}} \right) \quad (12.3.117)$$

where the derivative of the concentration has been replaced by a linear gradient for a straight cylindrical pore. The rate of reaction in the unpoisoned segment of the pore can be written as the product of an effectiveness factor for a pore of length  $(1 - \alpha)\bar{L}$  exposed to a reactant concentration  $C_c$  at its mouth, and the rate of reaction within such a pore, assuming that the reactant concentration is  $C_c$  throughout the length  $(1 - \alpha)\bar{L}$ . Thus, for a first-order reaction,

$$\text{rate of reaction within the pore} = \eta(2\pi\bar{r})(1 - \alpha)\bar{L}k_1'' C_c \quad (12.3.118)$$

where  $\eta$  can be determined from equations (12.3.11) and (12.3.20) to be

$$\eta = \frac{\tanh \left[ (1 - \alpha)\bar{L} \sqrt{2k_1'' / (\bar{r}D_c)} \right]}{(1 - \alpha)\bar{L} \sqrt{2k_1'' / (\bar{r}D_c)}} \quad (12.3.119)$$

Thus, the rate of reaction within the poisoned pore can be written as

$$r_{\text{poisoned}} = \frac{\left\{ \tanh \left[ (1 - \alpha)\bar{L} \sqrt{2k_1'' / (\bar{r}D_c)} \right] \right\} 2\pi\bar{r}(1 - \alpha)\bar{L}k_1'' C_c}{(1 - \alpha)\bar{L} \sqrt{2k_1'' / (\bar{r}D_c)}} \\ = \tanh[(1 - \alpha)h_T] \sqrt{2k_1'' \bar{r}D_c \pi\bar{r} C_c} \quad (12.3.120)$$

where  $h_T$  is the Thiele modulus for the *unpoisoned* reaction.

The unknown concentration  $C_c$  can be eliminated between equations (12.3.117) and (12.3.120) to obtain

$$\begin{aligned} C_c &= \frac{C_0}{1 + \{\tanh[(1 - \alpha)h_T]\}\alpha L \sqrt{2k_1''/(\bar{r}D_c)}} \\ &= \frac{C_0}{1 + \alpha h_T \tanh[(1 - \alpha)h_T]} \end{aligned} \quad (12.3.121)$$

The reaction rate within the pore may now be obtained by combining equations (12.3.120) and (12.3.121):

$$r_{\text{poisoned}} = \frac{\tanh[(1 - \alpha)h_T] \sqrt{2k_1'' \bar{r}D_c \pi \bar{r}C_0}}{1 + \alpha h_T \tanh[(1 - \alpha)h_T]} \quad (12.3.122)$$

For an unpoisoned pore,  $\alpha = 0$  and the rate is given by

$$r_{\text{unpoisoned}} = \tanh h_T \sqrt{2k_1'' \bar{r}D_c \pi \bar{r}C_0} \quad (12.3.123)$$

The fraction of the surface that is then apparently available for reaction is given by the ratio of the poisoned rate to the unpoisoned rate:

$$\mathcal{F} = \frac{r_{\text{poisoned}}}{r_{\text{unpoisoned}}} \quad (12.3.124)$$

Combination of equations (12.3.122), (12.3.123), and (12.3.124) leads to the desired result:

$$\mathcal{F} = \frac{\tanh[(1 - \alpha)h_T]}{\tanh h_T} \left\{ \frac{1}{1 + \alpha h_T \tanh[(1 - \alpha)h_T]} \right\} \quad (12.3.125)$$

To demonstrate the selective effect of pore-mouth poisoning, it is instructive to consider the two limiting cases of reaction conditions corresponding to large and small values of the Thiele modulus for the poisoned reaction. For the case of active catalysts with small pores, the arguments of all the hyperbolic tangent terms in equation (12.3.125) will become unity and

$$\mathcal{F} \approx \frac{1}{1 + \alpha h_T} \quad \text{for } h_T(1 - \alpha) > 2 \quad (12.3.126)$$

This equation indicates that a small amount of poisoned surface can lead to a sharp decline in apparent activity. For example, if only 10% of the catalyst surface has been deactivated in the case where the Thiele modulus for the unpoisoned reaction is 40,  $\mathcal{F} = 0.200$ , so that the apparent activity has dropped by some 80%. In this situation, both the primary reaction and the poisoning reaction try to take place on the same surface near the pore mouth. As this region is poisoned, the reactants are forced to diffuse farther into the pore before encountering a

catalytically active surface. This restriction has a concomitant strong adverse effect on the observed reaction rate. Curve *D* in Figure 12.11 is representative of this type of behavior.

Now consider the other extreme condition in which diffusion is rapid relative to chemical reaction [i.e.,  $h_T(1 - \alpha)$  is small]. In this situation the effectiveness factor will approach unity for both the poisoned and unpoisoned reactions, and we must retain the hyperbolic tangent terms in equation (12.3.125) to properly evaluate  $\mathcal{F}$ . Curve *C* in Figure 12.11 is calculated for a value of  $h_T = 5$ . It is apparent that in this instance the activity decline is not nearly as sharp at low values of  $\alpha$  as it was at the other extreme, but it is obviously more than a linear effect. The reason for this result is that the regions of the catalyst pore exposed to the highest reactant concentrations do not contribute proportionately to the overall reaction rate because these regions have suffered a disproportionate loss of activity when pore-mouth poisoning takes place.

For situations in which the reaction is very slow relative to diffusion, the effectiveness factor for the poisoned catalyst will be unity, and the apparent activation energy of the reaction will be the true activation energy for the intrinsic chemical reaction. As the temperature increases, however, the reaction rate increases much faster than the diffusion rate and one may enter a regime in which  $h_T(1 - \alpha)$  is larger than 2, so that the apparent activation energy will drop to that given by equation (12.3.85) (approximately half the value for the intrinsic reaction). As the temperature increases further, the Thiele modulus,  $h_T(1 - \alpha)$ , continues to increase with concomitant decreases in both the effectiveness with which the catalyst surface area is used and the depth to which the reactants are capable of penetrating. In instances for which  $h_T(1 - \alpha)$  is large (say, greater than 6) and  $\alpha$  is appreciable (say, between 0.2 and 0.8), we find that the deactivated portion of the pore represents by far the major portion of the depth to which reactants are capable of penetrating in appreciable concentrations. In this case the overall reaction rate becomes limited by the rate of diffusion through the poisoned region, and the activation energy will reflect the temperature dependence of the combined diffusivity (i.e., it will be a kilocalorie or so). Thus, as the temperature increases, there is a transition from the activation energy of the intrinsic chemical reaction to an activation energy characteristic of molecular diffusion processes.

### 12.3.4 The Influence of Intraparticle Mass Transfer Limitations on Catalyst Selectivity

In the present section we deal with the influence of intraparticle mass transfer processes on catalyst selectivity

following the basic pattern established by Wheeler (66, 67) in his classic papers.

### 12.3.4.1 Independent Parallel Reactions of Different Species on the Same Catalyst

One often requires a catalyst that promotes the reactions of one component of a feedstock but does not promote the reactions of other constituents of the mixture. For example, one might desire to dehydrogenate six-membered rings but not five-membered rings. This type of selectivity behavior may be represented by mechanistic equations of the form



The corresponding rate equations for constant volume systems can be written as

$$\frac{d(A)}{dt} = -k_1 \eta_1(A) \quad (12.3.129)$$

$$\frac{d(X)}{dt} = -k_2 \eta_2(X) \quad (12.3.130)$$

where the effective rate constants are  $k_1 \eta_1$  and  $k_2 \eta_2$ , respectively.

The resulting selectivity of the catalyst can be described by the ratio of equations (12.3.129) and (12.3.130):

$$\frac{d(A)}{d(X)} = \frac{k_1 \eta_1(A)}{k_2 \eta_2(X)} \quad (12.3.131)$$

For an isothermal system, separation of variables followed by integration gives

$$\ln \left[ \frac{(A)}{(A_0)} \right] = \frac{k_1 \eta_1}{k_2 \eta_2} \ln \left[ \frac{(X)}{(X_0)} \right] \quad (12.3.132)$$

or

$$\ln(1 - f_A) = \frac{k_1 \eta_1}{k_2 \eta_2} \ln(1 - f_X) \quad (12.3.133)$$

where  $f_A$  and  $f_X$  are the fraction conversions of A and X, respectively. The relative conversions are dependent only on the ratio of the apparent rate constants, and this group may be defined as the selectivity  $S$ :

$$S \equiv \frac{(X)}{(A)} \frac{d(A)}{d(X)} = \frac{(X)}{(A)} \frac{d(V)}{d(W)} = \frac{k_1 \eta_1}{k_2 \eta_2} \quad (12.3.134)$$

When the effectiveness factors for both reactions approach unity, the selectivity for two independent simultaneous reactions is the ratio of the two intrinsic reaction rate constants. However, at low values of both effectiveness factors, the selectivity of a porous catalyst may be greater than or less than that for a planar catalyst surface. For

a porous spherical catalyst at large values of the Thiele modulus  $\phi_S$ , the effectiveness factor becomes inversely proportional to  $\phi_S$ , as indicated by equation (12.3.68). In this situation, equation (12.3.134) becomes

$$S = \frac{k_1}{k_2} \frac{\phi_{s,2}}{\phi_{s,1}} = \sqrt{\frac{k_1 D_{A,\text{eff}}}{k_2 D_{X,\text{eff}}}} \quad (12.3.135)$$

where we have used the definition of  $\phi_S$  given by equation (12.3.56). If the ratio of the effective diffusivities is less than the ratio of the intrinsic rate constants (e.g., when the larger molecule is the more reactive), the selectivity ratio will decline as the effectiveness factors decrease. However, if the more reactive species also has a higher effective diffusivity, it is possible to obtain an *enhanced* selectivity for the porous catalyst. This situation may readily occur in dealing with molecular sieve catalysts in which certain reactants can essentially be excluded from the catalytically active regions by virtue of their molecular size or shape.

### 12.3.4.2 Independent Parallel Reactions of the Same Species

Independent parallel reactions of the same species may be represented in *stoichiometric* form as



These are the types of reactions discussed in Section 9.1, and that discussion is relevant to our present considerations. A selective catalyst is one that will promote one of these reactions relative to the other.

If the two competing reactions have the same concentration dependence, the catalyst pore structure does not influence the selectivity because at each point within the pore structure the two reactions will proceed at the same *relative* rate, independent of the reactant concentration. However, if the two competing reactions differ in the concentration dependence of their rate expressions, the pore structure may have a significant effect on the product distribution. For example, if V is formed by a first-order reaction and W by a second-order reaction, the yield of V observed will increase as the catalyst effectiveness factor decreases. At low effectiveness factors there will be a significant gradient in the reactant concentration as one moves radially inward. The lower reactant concentration within the pore structure would then favor the lower-order reaction. For the case cited above, the yield of V relative to W will increase. When the desired reaction is of lower order than the reaction that is not desired, catalyst properties that lead to low effectiveness factors give a higher

selectivity than those that lead to an effectiveness factor of unity. If the product desired is formed by the higher-order reaction, we should minimize the concentration gradient in the pellet and thus should use catalysts with effectiveness factors approaching unity.

### 12.3.4.3 Consecutive Reactions for Which an Intermediate Is the Desired Product

Consecutive reactions in which an intermediate species (V) is the desired product are often represented as a series of pseudo-first-order reactions:



Good yields of the desired product can be obtained only when  $k_1 > k_2$ . Among the industrially significant reactions of this type are those involving partial oxidation or multiple substitutions, hydrogenations, halogenations, etc. Reactions represented by equation (12.3.137) were discussed in detail in Section 9.2, and that material is also pertinent here.

For a catalyst-reactant system in which the effectiveness factors for the first and second reactions both approach unity, the analysis presented in Sections 9.2 and 9.3 is appropriate. If yields are based on the initial concentration of reactant A and if no V or W is present in the original feed, equations (9.3.9) and (9.3.10) can be rearranged to express the yield of V as a function of the fraction A reacted:

For  $k_2 \neq k_1$ :

$$Y_V = \frac{1}{1 - (k_2/k_1)} (1 - f_A) [(1 - f_A)^{(k_2/k_1)-1} - 1] \quad (12.3.138)$$

For  $k_2 = k_1$ :

$$Y_V = (1 - f_A) \ln \left[ \frac{1}{1 - f_A} \right] \quad (12.3.139)$$

Figure 12.13 contains a plot of the yield of the intermediate V as a function of the fraction A reacted for a value of  $k_1/k_2$  equal to 5. In this case we see that the maximum yield of V based on the initial concentration of A is equal to 66.9%.

When consecutive reactions take place within a porous catalyst, the concentrations of A and V within the pellet will be significantly different from those prevailing at the external surface. The intermediate V molecules formed within the pore structure have a high probability of reacting further before they can diffuse out of the pore. Consequently, catalysts with small-diameter pores should give lower yields of V than those with large pores.

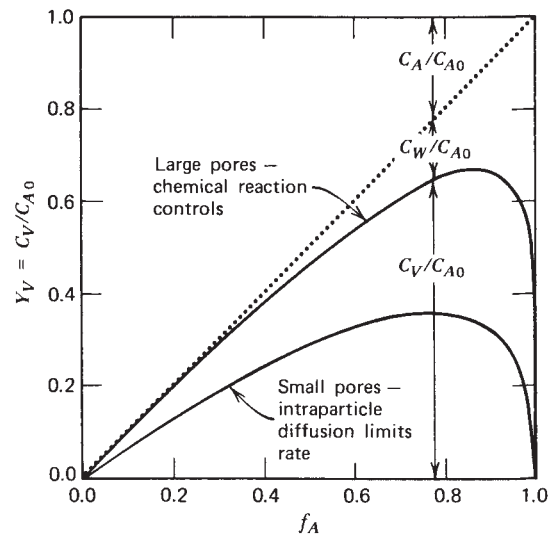


Figure 12.13 Yield of intermediate versus fraction conversion for  $k_1''/k_2'' = 5$ . Upper curve:  $\eta = 1$ ; lower curve  $\eta < 0.3$ .

The concentration profile of reactant A within the cylindrical pore is the same as that which prevails in the absence of the second reaction and is given by equation (12.3.13). The fact that V is a potentially reactive intermediate in no way influences the rate of reaction of A. The concentration of V within the pore under steady-state operating conditions is governed by an equation obtained in a manner similar to that used to arrive at equation (12.3.7), but in this case, the right side must allow for both the production and disappearance of V by surface reactions. Hence,

$$D_V \frac{d^2 C_V}{dx^2} = \frac{2}{r} (k_2'' C_V - k_1'' C_A) \quad (12.3.140)$$

where  $C_V$  and  $C_A$  are the concentrations of V and A, respectively, at a distance  $x$  from the pore mouth, and  $D_V$  represents the *combined diffusivity* for species V. This equation indicates that at steady state the rate of diffusive flow into the pore must equal the net rate of reaction within the pore. Combination of equations (12.3.13) and (12.3.140) gives

$$D_V \frac{d^2 C_V}{dx^2} = \frac{2}{r} \left[ k_2'' C_V - \frac{k_1'' C_{A_g} \cosh [h_T \{ 1 - (x/\bar{L}) \}]}{\cosh h_T} \right] \quad (12.3.141)$$

where  $C_{A_g}$  is the gas-phase concentration of reactant A at the pore mouth, and

$$h_T = \bar{L} \sqrt{\frac{2k_1''}{r D_A}} \quad (12.3.142)$$

( $D_A$  is the *combined diffusivity* of species A.) Equation (12.3.141) can be rewritten in dimensionless form as

$$\frac{d^2(C_V/C_{Ag})}{d(x/\bar{L})^2} = \left[ \frac{2k_2''\bar{L}^2}{\bar{r}D_V} \right] \left[ \frac{C_V}{C_{Ag}} \right] - \left[ \frac{2k_1''\bar{L}^2}{\bar{r}D_V} \right] \frac{\cosh[h_T\{1-(x/\bar{L})\}]}{\cosh h_T} \quad (12.3.143)$$

If we define new dimensionless variables for the ratios of rate constants and diffusivities in equation (12.3.143),

$$\kappa = k_1''/k_2'' \quad \text{and} \quad \Psi = D_A/D_V \quad (12.3.143a)$$

we can convert (12.3.143) to the following second-order differential equation

$$\frac{d^2(C_V/C_{Ag})}{d(x/\bar{L})^2} = \frac{h_T^2\Psi}{\kappa} \left\{ \left( \frac{C_V}{C_{Ag}} \right) - \frac{\cosh[h_T\{1-(x/\bar{L})\}]}{\cosh h_T} \right\} \quad (12.3.144)$$

or

$$\left[ \frac{\kappa}{h_T^2\Psi} \right] \frac{d^2(C_V/C_{Ag})}{d(x/\bar{L})^2} = \frac{C_V}{C_{Ag}} - \left\{ \frac{\cosh[h_T\{1-(x/\bar{L})\}]}{\cosh h_T} \right\} \quad (12.3.145)$$

The boundary conditions on this second-order differential equation are:

at the open end of the pore where  $x = 0$

$$C_V = C_{Vg} \quad (12.3.146)$$

at the closed end of the pore where  $x = \bar{L}$

$$\frac{dC_V}{dx} = 0 \quad (12.3.147)$$

The solution to equation (12.3.144) may be written in the following form

$$\frac{C_V}{C_{Vg}} = \left[ 1 + \frac{C_{Ag}\kappa}{C_{Vg}[(\kappa/\Psi) - 1]} \right] \times \left[ \frac{\cosh \left[ \sqrt{h_T^2(\Psi/\kappa)} \left[ 1 - (x/\bar{L}) \right] \right]}{\cosh \left( \sqrt{h_T^2(\Psi/\kappa)} \right)} \right] - \left\langle \frac{C_{Ag}}{C_{Vg}} \frac{\kappa \cosh \left\{ h_T \left[ 1 - (x/\bar{L}) \right] \right\}}{\{[(\kappa/\Psi) - 1] \cosh h_T\}} \right\rangle \quad (12.3.148)$$

The rate of production of  $V$  within a single pore must be equal to the net rate of diffusion *out* of the pore.

$$r_{V, \text{pore}} = \pi \bar{r}^2 D_V \left( \frac{dC_V}{dx} \right)_{x=0} \quad (12.3.149)$$

Evaluation of the derivative and substitution of this result into equation (12.3.149) gives

$$r_{V, \text{pore}} = \left[ \frac{\pi \bar{r}^2 D_V C_{Ag}}{\bar{L}} \right] \left\{ -\frac{C_{Vg}}{C_{Ag}} - \left[ \frac{\kappa\Psi}{(\kappa - \Psi)} \right] \times \beta \right\}$$

where  $\beta = \left\langle h_T \sqrt{\frac{\Psi}{\kappa}} \tanh \left( h_T \sqrt{\frac{\Psi}{\kappa}} \right) + h_T \tanh h_T \right\rangle$

$$(12.3.150)$$

The relative rate at which the external gas-phase concentrations change is given by the ratio of the rate at which  $V$  is produced within a pore (12.3.150) to the rate at which  $A$  is consumed within a pore (12.3.17):

$$-\Psi \frac{dC_{Vg}}{dC_{Ag}} = \left[ \frac{\left( \frac{C_{Vg}}{C_{Ag}} + \frac{\kappa\Psi}{(\kappa - \Psi)} \right) \sqrt{\frac{\Psi}{\kappa}} \tanh \left( h_T \sqrt{\frac{\Psi}{\kappa}} \right)}{\tanh h_T} \right] \quad (12.3.151)$$

This equation gives the differential yield of  $V$  for a porous catalyst at a point in a reactor. For equal combined diffusivities and the case where  $h_T$  approaches zero (no diffusional limitations on the reaction rate), this equation reduces to equation (9.3.8), because the ratio of the hyperbolic tangent terms becomes  $\sqrt{\Psi/\kappa}$ . As  $h_T$  increases from about 0.3 to about 2.0, the selectivity of the catalyst falls off continuously. The selectivity remains essentially constant when both hyperbolic tangent terms approach unity. This situation corresponds to low effectiveness factors and, in this case, equation (12.3.151) becomes

$$-\frac{dC_{Vg}}{dC_{Ag}} + \sqrt{\frac{1}{\kappa\Psi}} \left[ \frac{C_{Vg}}{C_{Ag}} \right] = \frac{\kappa/\Psi - \sqrt{\kappa/\Psi}}{(\sqrt{\kappa/\Psi} - 1)(\sqrt{\kappa/\Psi} + 1)} \quad (12.3.152)$$

Simplification gives

$$-\frac{dC_{Vg}}{dC_{Ag}} = \frac{\sqrt{\kappa/\Psi}}{\sqrt{\kappa/\Psi} + 1} - \frac{C_{Vg}}{C_{Ag}} \sqrt{\frac{1}{(\kappa\Psi)}} \quad (12.3.153)$$

This equation may be solved using an integrating factor approach to determine the absolute yield of  $V$  as a function

of the fraction A reacted in an isothermal reactor. For the situation in which neither V nor W is present in the original gas stream, integration gives

$$\frac{C_{Vg}}{C_{A0}} = \frac{\left(\frac{\kappa}{\Psi} - \sqrt{\frac{1}{\Psi}}\right)}{\left(\frac{\kappa}{\Psi} - 1\right)\left(1 - \sqrt{\frac{1}{\kappa\Psi}}\right)} \times \sigma \quad (12.3.154)$$

$$\text{where } \sigma = \left[ \left( \frac{C_{Ag}}{C_{A0}} \right)^{\sqrt{1/(\kappa\Psi)}} - \left( \frac{C_{Ag}}{C_{A0}} \right) \right],$$

where  $C_{A0}$  is the concentration of reactant at the entrance to the catalytic reactor, and  $C_{Ag}$  is the local gas-phase concentration. This equation gives the yield of V based on the initial reactant concentration as a function of the fraction conversion of A

$$Y_V = \frac{\left(\frac{\kappa}{\Psi} - \sqrt{\frac{1}{\Psi}}\right) \left[ (1 - f_A)^{\sqrt{1/(\kappa\Psi)}} - (1 - f_A) \right]}{\left(\frac{\kappa}{\Psi} - 1\right) \left(1 - \sqrt{\frac{1}{\kappa\Psi}}\right)} \quad (12.3.155)$$

The lower curve in Figure 12.13 is a plot of the yield of V versus the fraction conversion of species A for  $\mathcal{D}_V = \mathcal{D}_A$ ,  $k_1''/k_2'' = 5$ , and low effectiveness factors for the first reaction. In general, for the low effectiveness factor regime and comparable combined diffusivities, the maximum yield of an intermediate in a series of consecutive reactions will be only about half that achieved when the effectiveness factor approaches unity (66). At effectiveness factors below 0.3, the observed selectivity is nearly independent of the Thiele modulus and the effectiveness factor. The major decline in selectivity takes place as the effectiveness factor drops from unity to 0.3. If one is interested in the intermediate produced by consecutive reactions, and the reactions in question are being carried out on catalyst pellets characterized by an effectiveness factor for the initial reaction that lies between 0.3 and 1, it is possible to increase the yield of this intermediate by going to smaller catalyst pellets or by altering the pore structure so as to increase the effective diffusivity. However, if the effectiveness factor lies well below 0.3, it is necessary to go to very large reductions in pellet size or to a much more open pore structure to bring about a significant improvement in selectivity.

Wheeler's classic analysis (66, 67) has also been extended to nonisothermal situations (69–72). Generally, under either isothermal or nonisothermal conditions, intra-particle diffusional limitations are undesirable because they reduce the selectivity below that which can be achieved in their absence. The exception to this generalization is a set of endothermic reactions that take place in nonisothermal

pellets where the second reaction has an activation energy that is less than that of the first.

## 12.4 MASS TRANSFER BETWEEN THE BULK FLUID AND EXTERNAL SURFACES OF SOLID CATALYSTS

When a solid acts as a catalyst for a reaction, reactant molecules are converted into product molecules at the fluid–solid interface. To use the catalyst efficiently, we must ensure that fresh reactant molecules are supplied and product molecules removed continuously. Otherwise, chemical equilibrium would be established in the fluid adjacent to the surface, and the desired reaction would proceed no further. Ordinarily, supply and removal of the species in question depend on two physical rate processes in series. These processes involve mass transfer between the bulk fluid and the external surface of the catalyst and transport from the external surface to the internal surfaces of the solid. The concept of effectiveness factors developed in Section 12.3 permits one to average the reaction rate over the pore structure to obtain an expression for the rate in terms of the reactant concentrations and temperatures prevailing at the exterior surface of the catalyst. In some instances, the external surface concentrations do not differ appreciably from those prevailing in the bulk fluid. In other cases, a significant concentration difference arises as a consequence of physical limitations on the rate at which reactant molecules can be transported from the bulk fluid to the exterior surface of the catalyst particle. Here, we discuss this transport process and its implications for chemical reactor design.

In trying to analyze the flow fields within a heterogeneous catalytic reactor, we encounter an extremely complex problem, regardless of whether we consider a fixed bed, a trickle bed, a fluidized bed, or any other commonly used industrial configuration. We can, in principle, set up differential equations for the conservation of mass, momentum, and energy that take into account the chemical reaction at the fluid–solid interface. Appropriate equations are needed both for processes taking place external to the catalyst particle and for those occurring within the particle. The sets of equations are coupled through the conditions at the exterior surface of the particle, and here one must match the local fluxes of energy and chemical species as well as the local temperatures and compositions. Although these equations are readily written, no completely general method of solution exists. Sometimes it is possible to obtain analytical solutions by making appropriate assumptions so as to simplify the problem. Although the assumptions are in many cases inconsistent with physical reality as expressed by the situations normally encountered in industrial practice, the predictions of conversion may well be within the

accuracy of the kinetic information. Some of these analytical approaches are described in the text by Petersen (73), and interested students should consult this source. There are several intrinsic problems and/or limitations with such analyses, particularly when one attempts to employ conventional film theory. We shall find it to be more convenient to utilize average mass transfer coefficients in our analyses and to make use of the semiempirical correlations of these parameters that have been developed over the years.

### 12.4.1 External Mass Transfer in Packed Bed Reactors

The velocity patterns within a fixed-bed reactor reflect the interactions between fluid elements flowing over different particles, variations in the available cross section for flow, the intrinsic physical properties of the fluid, and the average rate at which the fluid is supplied. The problems of analyzing the various physical transport processes in a fixed bed reactor are thus extremely complex. The conventional engineering approach to analyzing such systems involves the definition of *average* heat and mass transfer coefficients for the bed. Such coefficients are presumed to apply to the entire external surface of a given catalyst particle, even though experimental studies have shown that this situation does not correspond to physical reality. This assumption is sometimes stated by saying that the surface is *uniformly accessible*. It implies that the equations describing the transport processes can be treated as unidimensional.

The errors that result from the use of average transport coefficients are not particularly serious. The correlations that are normally employed to predict these parameters are themselves determined from experimental data for packed beds. Therefore, the applications of the correlations and the data on which they are based correspond to similar physical configurations.

Depending on the driving force one chooses to employ in the analysis, there are several definitions of mass transfer coefficients that may be considered appropriate for use. If we consider an arbitrary interface between a fluid and the external surface of a catalyst particle, we might choose to define a mass transfer coefficient based on a concentration driving force ( $k_c$ ) as

$$k_c = \frac{J_i}{C_{i,B} - C_{i,ES}} \quad (12.4.1)$$

where  $J_i$  is the molar flux of species  $i$  toward the surface relative to the molar average velocity and  $C_{i,B}$  and  $C_{i,ES}$  are the concentrations of species  $i$  in the bulk and at the solid surface, respectively.

In gas phase systems, it is convenient to define a mass transfer coefficient based on a partial pressure driving force

( $k_G$ ) as

$$k_G = \frac{J_i}{P_{i,B} - P_{i,ES}} \quad (12.4.2)$$

where  $P_{i,B}$  and  $P_{i,ES}$  are the partial pressures of species  $i$  in the bulk and at the surface, respectively. If the gas behaves ideally, then

$$k_c = k_G R_g T \quad (12.4.3)$$

where  $R_g$  is the gas constant and  $T$  is the absolute temperature. To explore further the uses of these and other mass transfer coefficients, consult standard references on transport phenomena or unit operations (74–76).

Dimensional analysis of the variables characteristic of mass transfer under flow conditions suggests that the following dimensionless groups are appropriate for correlating mass transfer data:

$$\text{Reynolds number} = N_{\text{Re}} = \frac{D_p G}{\mu} \quad (12.4.4)$$

$$\text{Schmidt number} = N_{\text{Sc}} = \frac{\mu}{\rho D} \quad (12.4.5)$$

$$\text{Sherwood number} = N_{\text{Sh}} = \frac{k_c D_p}{D} \quad (12.4.6)$$

where  $D_p$  is the equivalent diameter of the catalyst particle,  $G$  the mass velocity based on the total (superficial) cross-sectional area of the reactor,  $\mu$  the fluid viscosity,  $\rho$  the fluid density, and  $D$  the molecular diffusivity of the species being transferred in the system of interest.

The Sherwood number is also known as the Nusselt number for mass transfer. Notice that the diameter of the catalyst pellet is used in the Reynolds and Sherwood numbers as the characteristic length dimension of the system. For flow through packed beds, the transition between laminar and turbulent flow occurs at a Reynolds number of approximately 40.

The equivalent particle diameter appearing in these dimensionless groups is the diameter of a sphere having the same external surface area as the particle in question. Thus for a cylinder of length  $L_c$  and radius  $r_c$ , the equivalent particle diameter is given by

$$4\pi \left( \frac{D_p}{2} \right)^2 = 2\pi r_c L_c + 2\pi r_c^2 \quad (12.4.7)$$

or

$$D_p = \sqrt{2r_c L_c + 2r_c^2} \quad (12.4.8)$$

The most convenient mathematical form for correlating mass transfer data is in terms of the well-known Chilton–Colburn (77, 78)  $j_D$  factor:

$$j_D = \frac{k_c \rho}{G} N_{\text{Sc}}^{2/3} \quad (12.4.9)$$

**Table 12.1** Correlations for Mass Transfer Factors ( $j_D$ ) in Packed Beds

Fluid	Reference	Range of $N_{Re}$ and/or $\varepsilon_B$ where applicable	Correlation	Equation number
Gas	Petrovic and Thodos (80)	$3 < N_{Re} < 2000$	$\varepsilon_B j_D = \frac{0.357}{N_{Re}^{0.359}}$	(12.4.10)
Liquid	Wilson and Geankoplis (81)	$55 < N_{Re} < 1500$	$\varepsilon_B j_D = \frac{0.250}{N_{Re}^{0.31}}$	(12.4.11)
		$0.35 < \varepsilon_B < 0.75$		
		$0.0016 < N_{Re} < 55$	$\varepsilon_B j_D = \frac{1.09}{N_{Re}^{2/3}}$	(12.4.12)

The functional dependence of  $j_D$  on the Reynolds number has been the subject of study by many investigators [e.g., Thodos and his co-workers (79, 80), and Wilson and Geankoplis (81)]. Various equations have been proposed as convenient representations of the experimental data. Many of these correlations also employ the bed porosity  $\varepsilon_B$  as an additional correlating parameter. This porosity is the ratio of the void volume *between* pellets to the total bed volume. Some of the more useful relations are summarized in Table 12.1.

At high Reynolds numbers the correlations for liquids and gases are quite similar, but axial mixing effects become increasingly significant in gases at low Reynolds numbers. The values of  $j_D$  predicted using equations (12.4.10) and (12.4.11) differ at most by 15% for  $55 < Re < 1500$ , but for low Reynolds numbers  $j_D$  for liquids will be less than  $j_D$  for gases. These equations apply to packed beds in which a single fluid fills the voids between particles. The problem of predicting appropriate mass transfer coefficients in trickle-bed reactors is much more complex, and it is beyond our scope here. For an introduction to the problems involved, consult Satterfield's monograph (82). For other catalyst geometries (e.g., woven screens) or flow conditions (e.g., pulsatile flow),  $j_D$  factors are available and may be obtained from the current literature or standard handbooks. In addition, it is possible to estimate mass transfer coefficients using data on heat transfer coefficients, because the  $j_D$  factor is equal to an analogous factor ( $j_H$ ) defined for the correlation of heat transfer data (see Section 12.5).

## 12.4.2 External Mass Transfer in Fluidized-Bed Reactors

Because the catalysts employed in fluidized bed reactors for gas feedstocks have characteristic dimensions in the range 10 to 300  $\mu\text{m}$ , the external surface area per unit weight of catalyst is significantly greater than that characteristic of fixed-bed reactors. This fact ensures that even in relatively low density fluidized beds, overall mass transfer rates

will be high compared to those in fixed beds. The large extent of turbulent mixing within such systems also serves to enhance the mass transfer coefficient, but it is the high ratio of the external surface area to the volume of the fluidized particles that is most significant in ensuring rapid mass transfer rates.

Table 12.2 is a summary of useful correlations for  $j_D$  and  $j_H$  that have been proposed by various investigators. The indicated correlations are quite consistent with one another in the regions where they overlap. Although the mass transfer coefficients determined from these correlations are not particularly large, they lead to high mass transfer rates when they are multiplied by the external surface area of the bed. For more detailed treatments of mass transfer in fluidized beds, see the text of Kunii and Levenspiel (83) and the review by Beek (84).

## 12.4.3 Implications of External Mass Transfer Processes for Reactor Design Calculations

The only instances in which external mass transfer processes can influence observed conversion rates are those in which the intrinsic rate of the chemical reaction is so rapid that an appreciable concentration gradient is established between the external surface of the catalyst and the bulk fluid. The rate at which mass transfer to the external catalyst surface takes place is greater than the rate of molecular diffusion for a given concentration or partial pressure driving force because turbulent mixing or eddy diffusion processes will supplement ordinary molecular diffusion. Consequently, for porous catalysts one does not encounter external mass transfer limitations except in those circumstances in which intraparticle diffusional limitations are also present.

In the presence of intraparticle mass transfer limitations, the rate per particle is expressed in terms of the species concentrations prevailing at the exterior of the catalyst. However, when external mass transfer limitations are also present, these concentrations will differ from

**Table 12.2** Correlations for Mass and Heat Transfer Factors in Fluidized Beds

Reference	Range of variables where applicable	Correlation	Equation number
Chu et al. (85)	$1 < N'_{\text{Re}} < 30$	$j_D = 5.7(N'_{\text{Re}})^{-0.78}$	(12.4.13)
	$30 < N'_{\text{Re}} < 10^4$	$j_D = 1.77(N'_{\text{Re}})^{-0.44}$	(12.4.14)
Riccetti and Thodos (86)	$100 < N'_{\text{Re}} < 7000$	$j_D = \frac{1}{(N'_{\text{Re}})^{0.40} - 1.5}$	(12.4.15)
Sen Gupta and Thodos (87)	$\frac{\sqrt{A_p}G}{\mu} > 50$	$\frac{\varepsilon_B j_D}{\psi} = \frac{0.300}{\left(\sqrt{A_p}G/\mu\right)^{0.35} - 1.90}$	(12.4.16)

$$N'_{\text{Re}} = \frac{D_p G}{\mu(1 - \varepsilon_B)} \quad (12.4.17)$$

$G$  is the superficial mass velocity based on total cross-sectional area,  $\varepsilon_B$  the void fraction of bed arising from spaces between particles,  $A_p$  the surface area of a single particle, and  $\psi$  the area availability factor (1.0 for spheres, 1.16 for cylinders in fluidized beds).

those prevailing in the bulk. Because bulk concentrations are what one measures in the laboratory, exterior surface concentrations must be eliminated to express the observed conversion rate in terms of measurable concentrations. In the paragraphs that follow, the manner in which one eliminates surface concentrations is indicated in some detail for a specific case.

Consider an irreversible reaction of the form



that takes place on a solid catalyst surface. For the moment we shall presume that the intrinsic chemical reaction rate follows an arbitrary kinetic expression with a functional form

$$r_m = \phi(\text{species concentrations, temperature}) \quad (12.4.19)$$

where the rate is expressed per unit mass of catalyst. If we take intraparticle mass transfer limitations into account, the relation (12.4.19) may be written as

$$r_m = \eta\phi'(\text{species concentrations, temperature}) \quad (12.4.20)$$

where the new function  $\phi'$  must be expressed in terms of the temperature and species concentrations prevailing at the exterior surface of the catalyst pellet. For reactions that obey rate expressions that differ from simple first-order kinetics,  $\eta$  itself depends on the species concentrations, and the apparent order of the reaction observed in the laboratory may differ from the intrinsic order, as we noted in Section 12.3.1.5.2.

Under steady-state operating conditions, the observed reaction rate must be exactly counterbalanced by the rate at which reactants are supplied to the exterior surface of the particle. On a unit mass basis, the latter rate can be written as

$$r_m = k_G(P_{\text{A,B}} - P_{\text{A,ES}})a_m \quad (12.4.21)$$

where  $P_{\text{A,B}}$  and  $P_{\text{A,ES}}$  are the partial pressures of reactant A in the bulk fluid and at the external surface of the catalyst, respectively,  $k_G$  is the mass transfer coefficient in appropriate units, and  $a_m$  is the *external* surface area per unit mass of catalyst.

In equation (12.4.21) the entire exterior surface of the catalyst is assumed to be uniformly accessible. Because equimolar counterdiffusion takes place for stoichiometry of the form of equation (12.4.18), there is no net molar transport normal to the surface. Hence there is no convective transport contribution to equation (12.4.21).

Let us now consider two limiting conditions for steady-state operation. First, suppose that the intrinsic reaction as modified by intraparticle diffusion effects is extremely rapid. In this case  $P_{\text{A,ES}}$  will approach zero, and equation (12.4.21) indicates that the observed rate per unit mass of catalyst then becomes

$$r_m = k_G a_m P_{\text{A,B}} \quad (12.4.22)$$

The reaction will then appear to follow first-order kinetics, *regardless of the functional forms of the intrinsic rate expression and of the effectiveness factor*. This first-order dependence is characteristic of reactions that are mass-transfer-limited. The term *diffusion controlled* is often applied to reactions that occur under these conditions, although *mass transfer controlled* would be more proper terminology.

Now consider the other extreme, in which the external mass transfer rate is sufficiently rapid to ensure that  $P_{\text{A,ES}}$  approaches  $P_{\text{A,B}}$ . In this case, the concentration dependence of the reaction rate is given by equation (12.4.20). The apparent orders of the reaction will be given by the functional form of  $\eta\phi'$ . One *may or may not* observe first-order kinetics. The apparent order will depend on the

interaction of the intrinsic surface reaction and intraparticle diffusion effects.

To illustrate the masking effects that arise from intraparticle and external mass transfer effects, consider a surface reaction whose intrinsic kinetics are second-order in species A. For this rate expression, equation (12.4.20) can be written as

$$r_m = \eta k_{\text{intrinsic}} P_A^2 \quad (12.4.23)$$

In the limit of low effectiveness factors where  $\eta$  is proportional to  $1/h_T$ , equation (12.3.78) indicates that when the dominant mode of transport is Knudsen diffusion the observed rate becomes

$$r_m = k_{\text{observed}} P_A^{3/2} \quad (12.4.24)$$

Equations (12.4.22) and (12.4.24) indicate that the observed reaction order will differ from the intrinsic reaction order in the presence of intraparticle and/or external mass transfer limitations. To avoid drawing erroneous conclusions about intrinsic reaction kinetics, we must be careful either to eliminate these limitations by proper choice of experimental conditions or to take them properly into account in our data analysis.

Let us now consider how the external surface concentrations can be eliminated when a reaction follows simple irreversible first-order kinetics. In this instance, equation (12.4.20) becomes

$$r_m = \eta k''_{\text{true}} S_g P_{A,ES} \quad (12.4.25)$$

At steady state, this rate is balanced by the mass transfer rate [equation 12.4.21],

$$r_m = \eta k''_{\text{true}} S_g P_{A,ES} = k_G (P_{A,B} - P_{A,ES}) a_m \quad (12.4.26)$$

The exterior surface concentration is then given by

$$P_{A,ES} = \frac{k_G a_m P_{A,B}}{k_G a_m + \eta k''_{\text{true}} S_g} = \frac{P_{A,B}}{1 + \eta k''_{\text{true}} S_g / (k_G a_m)} \quad (12.4.27)$$

With respect to the bulk concentration, the rate observed per unit weight of catalyst then becomes

$$r_m = \frac{\eta k''_{\text{true}} S_g P_{A,B}}{1 + \eta k''_{\text{true}} S_g / (k_G a_m)} = \frac{P_{A,B}}{1 / (\eta k''_{\text{true}} S_g) + 1 / (k_G a_m)} \quad (12.4.28)$$

The apparent rate constant per unit mass that one would observe in the laboratory would then obey the relation

$$\frac{1}{k_{\text{apparent}}} = \frac{1}{\eta k''_{\text{true}} S_g} + \frac{1}{k_G a_m} \quad (12.4.29)$$

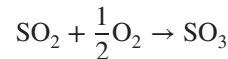
When  $k_G a_m$  is very large compared to  $\eta k''_{\text{true}} S_g$ , the exterior surface concentration is not appreciably different from the bulk fluid concentration, and the apparent rate constant

is equal to  $\eta k''_{\text{true}} S_g$ , an expression that reflects the interaction of the intrinsic chemical reaction and intraparticle diffusion processes. When  $k_G a_m$  is very small in comparison with  $\eta k''_{\text{true}} S_g$ , the exterior surface concentration will be significantly less than the bulk fluid value, and the apparent rate constant becomes equal to  $k_G a_m$ .

The above discussion indicates an approach that may be used in deriving an expression for the reaction rate in terms of the physical and chemical parameters of the system. However, for most practical catalyst systems, it will not be possible to arrive at closed-form expressions for the reaction rate per unit mass of catalyst. Consequently, this approach is of extremely limited utility for reactor design purposes. The most common approach to the analysis of external mass transfer limitations in heterogeneous catalytic reactors is usually couched in terms of calculations of the difference in reactant concentrations between the bulk fluid and the exterior surface. Illustration 12.5 indicates the manner in which one can calculate such differences.

### ILLUSTRATION 12.5 Mass Transfer in a Fixed Bed Reactor: Concentration Gradients Between the Bulk Fluid and the External Catalyst Surface

Olson et al. (88) have studied the catalytic oxidation of sulfur dioxide in a differential fixed bed reactor:



The catalyst employed consisted of platinum deposited on the external surface of  $\frac{1}{8} \times \frac{1}{8}$  in. cylindrical alumina pellets. The data below were obtained in run C-127S. Determine the composition at the exterior surface of the catalyst.

Temperature	458°C
Pressure	790 torr
Superficial mass velocity	245 lb/(h·ft <sup>2</sup> )
SO <sub>2</sub> feed rate	0.0475 g-mol/min
Air feed rate	0.681 g-mol/min
Reaction rate	0.0940 g-mol SO <sub>3</sub> produced/(h·g catalyst)
External surface area/mass catalyst	5.12 ft <sup>2</sup> /lb
Viscosity of reaction mixture	0.032 cp
Pellet density	112.8 lb/ft <sup>3</sup> = 1.81 g/cm <sup>3</sup>
Bed porosity (estimated)	0.40

The methods outlined by Poling et al. (8) have been used to estimate the diffusivities characteristic of binary mixtures of the various components of the fluid in the

reactor.

$$\begin{aligned}\mathcal{D}_{N_2-O_2} &= 0.900 \text{ cm}^2/\text{s} & \mathcal{D}_{O_2-SO_2} &= 0.598 \text{ cm}^2/\text{s} \\ \mathcal{D}_{N_2-SO_2} &= 0.602 \text{ cm}^2/\text{s} & \mathcal{D}_{O_2-SO_3} &= 0.471 \text{ cm}^2/\text{s} \\ \mathcal{D}_{N_2-SO_3} &= 0.515 \text{ cm}^2/\text{s} & \mathcal{D}_{SO_2-SO_3} &= 0.303 \text{ cm}^2/\text{s}\end{aligned}$$

## Solution

For a differential reactor, the change in composition across the reactor will be very small, and the bulk fluid composition may be estimated from the inlet molal flow rates. Assuming that the inlet air is 79% nitrogen and 21% oxygen, the calculations below indicate the bulk fluid mole fractions and partial pressures of the various components of the reaction mixture.

$$y_{SO_2} = \frac{0.0475}{0.0475 + 0.681} = 0.0652$$

$$P_{SO_2} = y_{SO_2} P_{\text{total}} = \frac{0.0652(790)}{760} = 0.0678 \text{ atm}$$

$$y_{O_2} = \frac{0.21(0.681)}{0.0475 + 0.681} = 0.1963$$

$$P_{O_2} = \frac{0.1963(790)}{760} = 0.2040 \text{ atm}$$

$$y_{N_2} = \frac{0.79(0.681)}{0.0475 + 0.681} = 0.7385$$

$$P_{N_2} = \frac{0.7385(790)}{760} = 0.7677 \text{ atm}$$

The average molecular weight of the mixture is then

$$\overline{M} = 0.0652(64) + 0.1963(32) + 0.7385(28) = 31.1 \text{ g/mol}$$

The diffusivity of species A in a gas mixture is given by

$$\mathcal{D}_{Am} = \frac{1 - (y_A/N_A) \left( \sum_{i=1}^n (N_i) \right)}{\sum_{j=1}^n \left\{ \frac{1}{\mathcal{D}_{Aj}} \left[ y_j - y_A \left( \frac{N_j}{N_A} \right) \right] \right\}} \quad (\text{A})$$

where the  $N_j$  are the molar fluxes, ratios of which can be determined from the reaction stoichiometry.  $\mathcal{D}_{Am}$  is the pseudo binary diffusivity of component A in the mixture, and  $\mathcal{D}_{Aj}$  is the diffusivity characteristic of a binary mixture of species A and  $j$ .

Equation (A) may now be used to determine the diffusivity of sulfur dioxide in the gas mixture. The flux ratios

may be determined from the reaction stoichiometry.

$$\begin{aligned}N_{O_2} &= \frac{N_{SO_2}}{2} & N_{SO_2} &= N_{SO_2} \\ N_{N_2} &= 0 & N_{SO_3} &= -N_{SO_2}\end{aligned}$$

Thus,

$$\sum_{i=1}^n (N_i) = \frac{N_{SO_2}}{2}$$

The summation of the individual terms in the denominator of equation (A) can be expressed as

$$\mathcal{D}_{SO_2-m} = \frac{1 - y_{SO_2} \left( \frac{N_{SO_2}/2}{N_{SO_2}} \right)}{Z_1 + Z_2 + Z_3 + Z_4}$$

where

$$\begin{aligned}Z_1 &= \frac{y_{SO_2} - (y_{SO_2})1}{\mathcal{D}_{SO_2-SO_2}} & Z_2 &= \frac{y_{O_2} - (y_{SO_2})(1/2)}{\mathcal{D}_{SO_2-O_2}} \\ Z_3 &= \frac{y_{N_2} - y_{SO_2}(0)}{\mathcal{D}_{N_2-SO_2}} & Z_4 &= \frac{y_{SO_3} - y_{SO_2}(-1)}{\mathcal{D}_{SO_2-SO_3}}\end{aligned}$$

or

$$\mathcal{D}_{SO_2-m} = \frac{1 - \frac{1}{2}y_{SO_2}}{\left( \frac{y_{O_2} - \frac{1}{2}y_{SO_2}}{\mathcal{D}_{O_2-SO_2}} + \frac{y_{N_2}}{\mathcal{D}_{N_2-SO_2}} + \frac{y_{SO_3} + y_{SO_2}}{\mathcal{D}_{SO_2-SO_3}} \right)}$$

Substitution of numerical values ( $y_{SO_3} \approx 0$ ) gives

$$\begin{aligned}\mathcal{D}_{SO_2-m} &= \frac{1 - (0.0652/2)}{\frac{0.1963 - (0.0652/2)}{0.598} + \frac{0.7385}{0.602} + \frac{0.0652}{0.303}} \\ &= 0.564 \text{ cm}^2/\text{s}\end{aligned}$$

Similarly, we find the following values (all in  $\text{cm}^2/\text{s}$ ) for the diffusivities of the other species in the reaction mixture.

$$\mathcal{D}_{O_2-m} = 0.502 \quad \mathcal{D}_{N_2-m} = 1.808 \quad \mathcal{D}_{SO_3-m} = 0.484$$

The ideal gas law may be used to determine the molar density of the reaction mixture:

$$\rho = \frac{P}{RT} = \frac{790/760}{82.06(731)} = 1.73 \times 10^{-5} \text{ g-mol/cm}^3$$

Because the molecular weight of the mixture is 31.1, the corresponding mass density is  $(1.73 \times 10^{-5}) \times 31.1$ , or  $5.39 \times 10^{-4} \text{ g/cm}^3$ .

Schmidt numbers may now be calculated for each component.

$$(N_{Sc})_i = \frac{\mu}{\rho D_{im}} = \frac{3.2 \times 10^{-4}}{5.39 \times 10^{-4} D_{im}} = \frac{0.594}{D_{im}}$$

Thus,

$$\begin{aligned} (N_{Sc})_{O_2} &= \frac{0.594}{0.502} = 1.18 & (N_{Sc})_{SO_2} &= \frac{0.594}{0.564} = 1.05 \\ (N_{Sc})_{SO_3} &= \frac{0.594}{0.484} = 1.23 & (N_{Sc})_{N_2} &= \frac{0.594}{1.818} = 0.327 \end{aligned}$$

The particle diameter to be employed in the mass transfer calculations is that of a sphere with the same area as that of the pellets. From equation (12.4.8) with  $r_c = 1/16$  and  $L_c = 1/8$ ,

$$D_p = \sqrt{2 \left( \frac{1}{16} \right) \left( \frac{1}{8} \right) + 2 \left( \frac{1}{16} \right)^2} = 0.153 \text{ in.} = 0.389 \text{ cm}$$

The superficial mass velocity can be expressed in cgs units as

$$\begin{aligned} G &= \frac{245 \text{ lb}}{\text{h} \cdot \text{ft}^2} \times \frac{1 \text{ h}}{3600 \text{ s}} \times \frac{454 \text{ g}}{\text{lb}} \times \frac{\text{ft}^2}{144 \text{ in}^2} \times \left( \frac{\text{in.}}{2.54 \text{ cm}} \right)^2 \\ &= 3.33 \times 10^{-2} \text{ g}/(\text{cm}^2 \cdot \text{sec}) \end{aligned}$$

The Reynolds number in consistent units is then

$$N_{Re} = \frac{D_p G}{\mu} = \frac{0.389(3.33 \times 10^{-2})}{3.2 \times 10^{-4}} = 41$$

The  $j$ -factor correlations in Table 12.1 may now be used to determine  $j_D$ . At the Reynolds number in question, equation (12.4.10) is appropriate for use.

$$j_D = \frac{0.357}{\varepsilon_B N_{Re}^{0.359}} = \frac{0.357}{0.40(41)^{0.359}} = 0.235$$

From the definition of the mass transfer  $j$  factor,

$$k_{c,i} = \frac{G}{\rho} (N_{Sc})_i^{-2/3} j_D \quad (\text{B})$$

At steady state, the rate of mass transfer must equal the reaction rate. Hence,

$$N_i a_m = \frac{\text{reaction rate}}{\text{mass catalyst}} = -\nu_i r_m \quad (\text{C})$$

where  $a_m$  is the external area per unit mass of catalyst and  $N_i$  is the molar flux of species  $i$  to the external surface of the catalyst. Because there is a change in the number of moles on reaction, we do not have equimolar counterdiffusion, and the flux of species  $i$  relative to a fixed coordinate system becomes

$$N_i = y_i \sum_{j=1}^c [N_j] + k_{c,i} (C_{i,B} - C_{i,ES})$$

where the subscripts  $B$  and  $ES$  refer to bulk and external surface values, respectively, and where the summation involves all  $c$  components of the mixture. The various fluxes are related by the reaction stoichiometry, and it is then convenient to write the preceding equation as

$$N_i = \frac{k_{c,i} (C_{i,B} - C_{i,ES})}{1 - (y_i/N_i) \sum_{j=1}^c N_j}$$

where the term in the denominator represents the drift factor commonly encountered in mass transfer calculations. Now

$$N_j = \frac{\nu_j}{\nu_i} N_i$$

Hence,

$$N_i = \frac{k_{c,i} (C_{i,B} - C_{i,ES})}{1 - \left[ (y_i/\nu_i) \sum_{j=1}^c \nu_j \right]} \quad (\text{D})$$

Combination of equations (C) and (D) gives

$$C_{i,B} - C_{i,ES} = -\frac{\nu_i r_m}{a_m k_{c,i}} \left( 1 - \frac{y_i}{\nu_i} \sum_{j=1}^c [\nu_j] \right) \quad (\text{E})$$

which, with equation (B), gives

$$C_{i,B} - C_{i,ES} = -\frac{\nu_i r_m \rho N_{Sc}^{2/3}}{a_m j_D G} \left( 1 - \frac{y_i}{\nu_i} \sum_{j=1}^c [\nu_j] \right)$$

In consistent units,

$$\begin{aligned} r_m &= \frac{0.0940 \text{ g-mol SO}_3 \text{ produced}}{\text{g catalyst} \cdot \text{h}} \times \frac{\text{h}}{3600 \text{ s}} \\ &= 2.61 \times 10^{-5} \frac{\text{g-mol}}{\text{s} \cdot \text{g catalyst}} \end{aligned}$$

and

$$\begin{aligned} a_m &= 5.12 \frac{\text{ft}^2}{\text{lb}} \times \frac{1 \text{ lb}}{454 \text{ g}} \times 9.29 \times 10^2 \frac{\text{cm}^2}{\text{ft}^2} \\ &= 10.48 \text{ cm}^2/\text{g catalyst} \end{aligned}$$

Hence,

$$\begin{aligned} C_{i,B} - C_{i,ES} &= \nu_i \frac{2.61 \times 10^{-5} (5.39 \times 10^{-4}) (N_{Sc})_i^{2/3}}{(10.48)(0.235)(3.33 \times 10^{-2})} \left[ 1 - \frac{y_i}{\nu_i} \left( -\frac{1}{2} \right) \right] \\ &= -1.72 \times 10^{-7} (N_{Sc})_i^{2/3} \nu_i \left( 1 + \frac{y_i}{2\nu_i} \right) \text{ g-mol/cm}^3 \end{aligned}$$

From the ideal gas law,

$$C_i = \frac{y_i P_{\text{total}}}{RT}$$

Thus,

$$y_{i,B} - y_{i,ES} = \frac{-(82.06)(731)}{790/760} (1.72 \times 10^{-7}) (N_{Sc})_i^{2/3} \left( \nu_i + \frac{y_i}{2} \right)$$

$$= -9.93 \times 10^{-3} (N_{Sc})_i^{2/3} \left( \nu_i + \frac{y_i}{2} \right)$$

Substitution of the Schmidt numbers and composition values calculated previously, and an appropriate average value for  $y_i$  permits one to determine the difference in mole fractions. In the present instance, we may use  $y_{i,B}$  values without significant error. Hence,

Species	$y_{i,B} - y_{i,ES}$	$y_{i,B}$	$y_{i,ES}$
$\text{SO}_2$	0.0099	0.0652	0.0553
$\text{N}_2$	-0.0017	0.7385	0.7402
$\text{O}_2$	0.0045	0.1963	0.1918
$\text{SO}_3$	-0.0114	$\cong 0.00$	0.0114

The difference in mole fractions is most significant in the case of  $\text{SO}_2$ , where this difference is 15% of the bulk phase level. This result indicates that external mass transfer limitations are indeed significant and that this difference should be taken into account in the analysis of kinetic data from this system. Note that there is a difference in nitrogen concentration between the bulk fluid and the external surface because there is a change in the number of moles on reaction, and there is a net molar flux toward the catalyst surface. Hence, one must establish a concentration difference for nitrogen so that the backward diffusion of nitrogen exactly counterbalances the convective transport to the catalyst surface. We should also indicate that the mole fractions at the external surface sum to only 0.9987. In large measure this discrepancy arises because we have used feed composition values in our calculations rather than local average bulk fluid compositions.

We would be remiss if we did not indicate that a significant temperature difference also exists between the bulk fluid and the external surface. This  $\Delta T$  has a far greater effect on the observed rate than does the difference in  $\text{SO}_2$  concentrations. Illustration 12.6 indicates how the temperature difference may be calculated.

In view of the fact that our results are reasonably sensitive to the estimate of the bed porosity used in the analysis, these results are not bad. If one had employed a value of 0.3 or 0.5 rather than 0.4 for  $\epsilon_B$ ,  $j_D$  would change significantly and this change would have a major influence on the calculated values of the concentration (or mole fraction) differences. Unfortunately, bed porosity data were not noted in the article cited. In an experimental program being conducted as an aspect of a reactor design, this parameter could easily be determined.

Yoshida et al. (89) have developed a nomograph that in essence is based on the procedure employed in Illustration 12.5. Although it employs a  $j_D$  correlation that predates those given in Table 12.1 and thus is less accurate, it eliminates many of the detailed calculations involved in determining when significant external concentration differences exist. For all practical purposes, the results obtained by using the nomograph are indistinguishable from those obtained using the procedure employed in Illustration 12.5.

Before terminating the discussion of external mass transfer limitations on catalytic reaction rates, we should note that in the regime where external mass transfer processes limit the reaction rate, the *apparent* activation energy of the reaction will be quite different from the intrinsic activation energy of the catalytic reaction. In the limit of complete external mass transfer control, the apparent activation energy of the reaction becomes equal to that of the mass transfer coefficient, typically a kilocalorie or so per gram-mole. This decrease in activation energy is obviously much greater than the decrease encountered when intraparticle diffusion processes limit the catalytic reaction rate.

## 12.5 HEAT TRANSFER BETWEEN THE BULK FLUID AND EXTERNAL SURFACES OF SOLID CATALYSTS

The energy effects that accompany chemical reactions can lead to significant temperature differences between a bulk fluid and the external surface of a catalyst on which reaction is taking place. At steady state, the rate of energy release (or consumption) by reaction must equal the rate at which heat is transferred to the fluid. The temperature gradient necessary to sustain the heat transfer may be appreciable, even in situations where concentration differences between the bulk fluid and the external catalyst surface are negligibly small. Consequently, these temperature differences can act to obscure the reaction kinetics in many more situations than can the mass transfer effects discussed previously. In laboratory studies aimed at a determination of the rate expression for the intrinsic chemical reaction, external gradients in temperature and concentration can be rendered negligible by operating under the following constraints.

1. Using a reactant stream that is diluted with inert to reduce the reaction rate so that the energy evolved per unit volume is greatly reduced below that encountered in the absence of inert.
2. Employing high mass velocities to minimize resistances to heat and mass transfer.

In such studies one may also eliminate intraparticle gradients of temperature and composition by using very fine catalyst particles or by confining the catalytic species

to the exterior surface of a nonporous or impervious pellet. Unfortunately, the conditions that are optimum for elucidation of the intrinsic chemical kinetics are often inappropriate for use in commercial scale reactors, and the design engineer must be able to take into account both exterior and intraparticle gradients in concentration and temperature. We discuss here the methods used to evaluate exterior temperature gradients in both fixed and fluidized bed reactors.

Heat transfer between a fluid and a catalyst particle occurs primarily through the same combination of molecular and convective processes that are responsible for mass transfer in such systems. At sufficiently high temperatures, one must also allow for radiation contributions to the energy transfer processes within the reactor. Radiation effects are not considered in the correlations discussed below. They are not significant at temperatures below 400°C for packed-bed reactors comprised of pellets with characteristic dimensions of less than  $\frac{1}{4}$  in. (90). At higher temperatures, they may be included in an energy balance on a segment of the reactor if appropriate view factors and other geometric considerations are specified. For present purposes, however, their inclusion would greatly complicate the analysis that follows, without shedding additional light on the fundamental principles involved.

The approach we use in analyzing the heat exchange between a solid catalyst particle and the surrounding fluid to determine if a significant temperature difference exists is in many respects quite similar to that employed in the analysis of mass transfer in Section 12.4. Both analyses are based largely on the Chilton–Colburn analogies for the corresponding transport processes. However, our earlier comment that external mass transfer limitations are less significant than intraparticle limitations cannot be generalized to the heat transfer process. At high Reynolds numbers, the heat transfer coefficients, like the mass transfer coefficients, will be large and the corresponding temperature and concentration differences between the bulk fluid and the exterior surface of the catalyst will be small. However, at low Reynolds numbers where both transfer coefficients are small, it is quite possible for substantial temperature differences to exist between the bulk fluid and the external surface, even when the corresponding concentration differences are small and when intraparticle concentration and temperature gradients are negligible ( $\eta \approx 1$ ). The major resistance to heat transfer is the laminar film adjacent to the solid surface rather than the pellet itself.

Experimental data for heat transfer in fixed- and fluidized-bed reactors are correlated in terms of a  $j$  factor for heat transfer:

$$j_H \equiv \frac{h}{C_p G} \left( \frac{C_p \mu}{\kappa} \right)^{2/3} = \frac{h}{C_p G} N_{Pr}^{2/3} \quad (12.5.1)$$

where  $\mu$  is the fluid viscosity,  $C_p$  the constant pressure heat capacity per unit mass of fluid,  $\kappa$  the thermal conductivity of the fluid,  $h$  the heat transfer coefficient between the catalyst particle and the bulk fluid, and  $N_{Pr}$  is the Prandtl number.

The functional dependence of  $j_H$  on Reynolds number has been the subject of study by many investigators, and a variety of equations have been proposed for correlation of the available data for fixed-bed (79, 89) and fluidized-bed reactors (85–87). Boundary layer theory indicates that the Chilton–Colburn analogy,  $j_H = j_D$ , represents an asymptotic solution for forced convection in three-dimensional flows in any geometry, provided that the Péclét number is large (91). [The Péclét number for mass transfer is the product of the Reynolds and Schmidt numbers ( $D_p G / D\mu$ ), while the Péclét number for heat transfer is the product of the Reynolds and Prandtl numbers ( $D_p G C_p / \kappa$ ).] The relation  $j_D = j_H$  agrees well with experimental data for many flow geometries. Although the literature correlations frequently indicate that the ratio  $j_H/j_D$  is slightly greater than unity for flow through packed beds (e.g., 81), the deviations are usually small. They may be explained by the fact that measured rates of vaporization or sublimation cancel out of the expression for the ratio  $j_H/j_D$  when one attempts to calculate these parameters from conventional experimental data. The deviation from unity then merely reflects an average of values determined from a large number of readings with a particular humidity chart (92).

For most purposes, the correlations for  $j_D$  presented in Tables 12.1 and 12.2 also suffice for estimating  $j_H$ . There is, however, one additional correlation for fluidized beds that is worth noting. On the basis of data for the fluidization of 20 to 40 mesh silica and alumina gel particles in air at Reynolds number values ( $D_p G / \mu$ ) ranging from 9 to 55, Kettenring et al. (93) suggest that

$$\frac{h D_p}{\kappa} = 0.0135 (N_{Re})^{1.3} \quad (12.5.2)$$

Notice, however, that none of these correlations is appropriate for use when radiation makes a significant contribution to the heat transfer process.

At steady state, the rate at which reactants are supplied to the external surface of the catalyst by mass transfer must be equal to the rate at which they are consumed by the catalytic reaction. Per unit mass of catalyst, the rate of disappearance of species A is then given by

$$-r_{A,m} = \frac{k_{c,A} (C_{A,B} - C_{A,ES}) a_m}{1 - (y_A / \nu_A) \left( \sum_{j=1}^c (\nu_j) \right)} \quad (12.5.3)$$

where the denominator is the drift factor. The rate of reaction multiplied by the energy release per unit extent of reaction must also equal the rate at which thermal energy is

exchanged between the fluid and the solid catalyst:

$$r_m(-\Delta H) = ha_m(T_{ES} - T_B) \quad (12.5.4)$$

Noting that  $r_{Am} = \nu_A r_m$ , one can combine equations (12.5.3) and (12.5.4) to obtain

$$\frac{k_{c,A}(C_{A,B} - C_{A,ES})a_m(-\Delta H)}{-\nu_A \left[ 1 - \left( y_A / \nu_A \right) \sum_{j=1}^c (\nu_j) \right]} = ha_m(T_{ES} - T_B) \quad (12.5.5)$$

or

$$T_{ES} - T_B = \frac{k_{c,A} \Delta H (C_{A,B} - C_{A,ES})}{h \left[ \nu_A - y_A \sum_{j=1}^c (\nu_j) \right]} \quad (12.5.6)$$

If the expressions for  $h$  and  $k_{c,A}$ , derived from equations (12.5.1) and (12.4.9), are substituted into equation (12.5.6), we find that

$$T_{ES} - T_B = \frac{j_D}{j_H} \left( \frac{N_{Pr}}{N_{Sc}} \right)^{2/3} \left( \frac{\Delta H / \nu_A}{\rho C_p} \right) \times \left[ \frac{C_{A,B} - C_{A,ES}}{1 - y_A \sum_{j=1}^c (\nu_j / \nu_A)} \right] \quad (12.5.7)$$

The temperature difference is thus directly proportional to the heat of reaction per mole of diffusing species and to the difference in concentration between the bulk fluid and the exterior surface of the solid. If we recognize that  $j_D \approx j_H$  from the Chilton–Colburn relation and the fact that the ratio of Prandtl and Schmidt numbers is close to unity for many simple gas mixtures, the relation (12.5.7) may be approximated as

$$T_{ES} - T_B \approx \frac{\Delta H}{\nu_A \rho C_p} \frac{(C_{A,B} - C_{A,ES})}{\left[ 1 - y_A \sum_{j=1}^c (\nu_j / \nu_A) \right]} \quad (\text{for gases}) \quad (12.5.8)$$

Thus, if the method developed in Section 12.4 is used to evaluate the concentration difference, this equation may be used to determine an approximate value for the temperature difference. [In many cases the drift factor term (in brackets) is essentially unity.]

In the limit at which the external surface concentration becomes very small compared to the bulk fluid concentration, we obtain the maximum temperature difference.

$$\Delta T_{\max} = \frac{\Delta H C_{A,B} / (\nu_A \rho C_p)}{1 - y_A \sum_{j=1}^c (\nu_j / \nu_A)} \quad (\text{for gases}) \quad (12.5.9)$$

In many cases of interest, the maximum temperature difference will be over 100°C, and values of this magnitude have been observed experimentally for several catalytic reactions.

Combination of equations (12.5.8) and (12.5.9) gives

$$T_{ES} - T_B = \left( 1 - \frac{C_{A,ES}}{C_{A,B}} \right) (\Delta T)_{\max} \quad (12.5.10)$$

Because of the large magnitude of  $(\Delta T)_{\max}$ , it is quite possible that significant temperature differences will exist, even when the ratio  $C_{A,ES}/C_{A,B}$  is close to unity. For example, if the exterior surface concentration is 95% of the bulk fluid level and the adiabatic temperature rise for the reaction is 300°C, equation (12.5.10) indicates that the catalyst surface is 15°C hotter than the bulk fluid. This difference would be sufficient to lead to a significant enhancement in the rate relative to bulk fluid conditions.

Another approach to estimating the temperature difference involves the solution of equation (12.5.4) for the temperature difference using measured reaction rates and empirical correlations for heat transfer coefficients. Hence,

$$T_{ES} - T_B = \frac{r_m(-\Delta H)}{ha_m} \quad (12.5.11)$$

which may also be written in terms of the  $j_H$  factor as

$$T_{ES} - T_B = \frac{r_m(-\Delta H)}{C_p G j_H N_{Pr}^{-2/3} a_m} \quad (12.5.12)$$

Yoshida et al. (89) have also developed nomographs for the solution of equation (12.5.12). Illustration 12.6 indicates an analytical approach by which the temperature difference can be evaluated using the correlations given in Tables 12.1 and 12.2.

## ILLUSTRATION 12.6 Heat Transfer in a Fixed Bed Reactor: Temperature Gradients Between the Bulk Fluid and the External Catalyst Surface

In Illustration 12.5 we considered the problem of estimating the concentration differences that exist between the bulk fluid and a catalyst used for the oxidation of sulfur dioxide. If the reported temperature is that of the bulk fluid, determine the external surface temperature corresponding to the conditions cited. Additional useful data are:

Heat of reaction evaluated for the temperature range of interest	-96.95 kJ/mol
Heat capacity ( $C_p$ ) of the reaction mixture	1.07 J/(g·K)
Thermal conductivity of the reaction mixture	$3.70 \times 10^{-4}$ J/(cm·s·K)

## Solution

The data for the thermal conductivity and the heat capacity permit us to calculate the Prandtl number for the conditions of interest.

$$N_{Pr} = \frac{C_p \mu}{\kappa} = \frac{[1.07 \text{ J/(g}\cdot\text{K)}][3.2 \times 10^{-4} \text{ g/(cm}\cdot\text{s)}]}{3.70 \times 10^{-4} \text{ J/(cm}\cdot\text{s}\cdot\text{K)}} = 0.93$$

For the conditions cited,  $j_D$  was 0.235, and by the Chilton–Colburn analogy,  $j_H$  has the same value. From the definition of the heat transfer factor  $j_H$ , it follows that

$$h = j_H C_p G (N_{Pr})^{-2/3}$$

Hence,

$$\begin{aligned} h &= 0.235(1.07)(3.33 \times 10^{-2})(0.93)^{-2/3} \\ &= 8.79 \times 10^{-3} \text{ J/(cm}^2\cdot\text{s}\cdot\text{K)} \end{aligned}$$

At steady state, equation (12.5.11) must be satisfied. Thus,

$$T_{ES} - T_B = \frac{(2.61 \times 10^{-5})(96,950)}{(8.79 \times 10^{-3})(10.48)} = 27.5^\circ\text{C}$$

or

$$T_{ES} = 27.5^\circ\text{C} + 458 = 486^\circ\text{C}$$

Thus, for this reaction, a substantial temperature difference exists between the solid surface and the bulk fluid. This difference has a far greater influence on the observed rate than does the corresponding concentration difference. Differences of this magnitude can clearly lead to complications in the analysis of data obtained in laboratory-scale reactors. If such differences will exist at the operating conditions to be employed in a commercial-scale reactor, the design engineer must be sure to take them into account in analysis of this reactor.

## 12.6 GLOBAL REACTION RATES

The rates at which chemical transformations take place are in some circumstances strongly influenced by mass and heat transfer processes (see Sections 12.3 to 12.5). In the design of heterogeneous catalytic reactors, it is essential to utilize a rate expression that takes into account the influence of physical transport processes on the rate at which reactants are converted to products. Smith (94) has popularized the use of the term *global reaction rate* to characterize the overall rate of transformation of reactants to products in the presence of heat and mass transfer limitations. We shall find this term convenient for use throughout the remainder of the chapter. Global rate expressions then include both external heat and mass transfer effects on the reaction rate and the efficiency with which the internal

surface area of a porous catalyst is used. Here we indicate how to employ the concepts developed in Sections 12.3 to 12.5 to arrive at global rate expressions.

In Section 6.3 we indicated that a catalytic reaction taking place on the surface of a porous solid involves the following sequence of physical and chemical processes.

1. Mass transfer of reactants from the bulk fluid to the gross exterior surface of the catalyst particle
2. Transport of reactants by diffusion from the exterior surface into the pores of the catalyst
3. Chemisorption of one or more reactant species
4. Reaction on the surface
5. Desorption of products
6. Transport of products by diffusion from the interior pores to the gross external surface of the catalyst
7. Mass transfer of products from the external surface to the bulk fluid

At steady state, the rates of each of the individual steps will be the same, and this equality is used to develop an expression for the global reaction rate in terms of bulk fluid properties. Actually, we have already employed a relation of this sort in the development of equation (12.4.28), where we examined the influence of external mass transfer limitations on observed reaction rates. Generally, we must worry not only about concentration differences between the bulk fluid and the external surface of the catalyst, but also about temperature differences between these points and intraparticle gradients in temperature and composition.

In laboratory experiments carried out to obtain rate data for subsequent design calculations, we normally try to operate under conditions that minimize the effects of heat and mass transfer limitations on conversion rates so as to facilitate the extraction of the rate expression for the intrinsic chemical reaction from the observed reaction rate (the global rate). We use very fine particles and high fluid velocities to minimize these limitations so that differences in composition and temperature between the bulk fluid and the fluid within the pore structure of the catalyst are insignificant. In the absence of such differences, the global reaction rate corresponds to the intrinsic reaction rate, evaluated at the bulk fluid composition and temperature. When such differences are significant, the global rate may be appreciably higher or appreciably lower than the intrinsic rate corresponding to bulk fluid properties.

Laboratory reactors and industrial-scale equipment are seldom operated under similar flow and heat transfer conditions. To obtain a global rate that is useful for design purposes, one must combine the intrinsic chemical reaction rate expression with expressions for heat and mass transfer rates corresponding to industrial operating conditions. As a general rule, the global rate reduces to the intrinsic

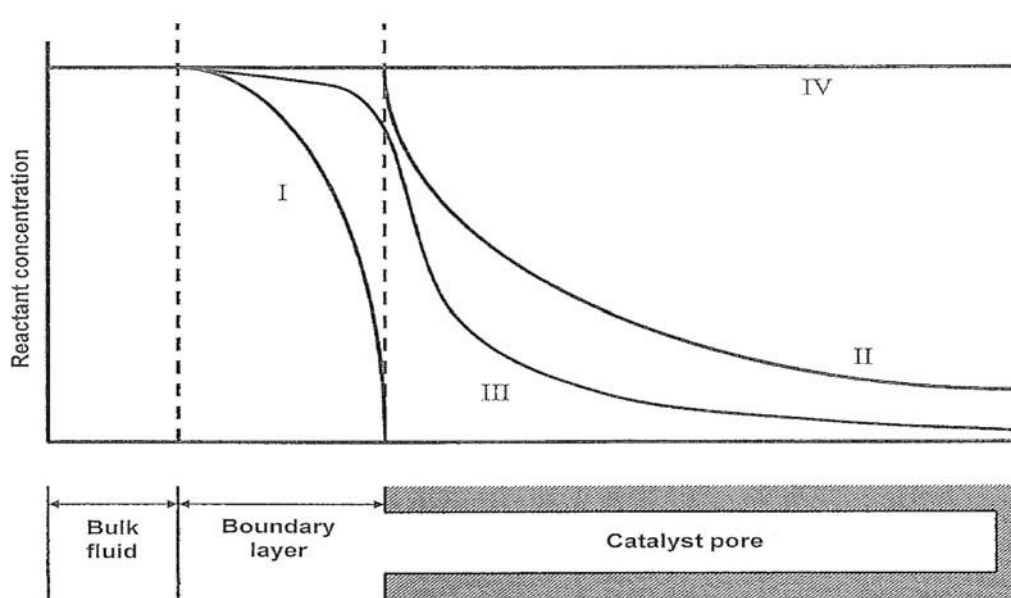


**Figure 12.14** Schematic representation of reactant concentration profiles in various global rate regimes: (I) external mass transfer limits rate; (II) pore diffusion limits rate; (III) both mass transfer effects are present; (IV) mass transfer has no influence on rate.

expression evaluated at bulk fluid properties when one of the chemical steps at the catalyst surface is slow. However, if economic considerations require the use of fluid velocities or catalyst pellet sizes that differ from those employed in the laboratory, the global rate may be quite different from the intrinsic rate at bulk fluid conditions. In such cases the reaction may be mass or heat transfer limited, or controlled by pore diffusion processes. Figure 12.14 indicates some of the reactant concentration profiles that may result from control by various steps in the sequence enumerated earlier. In commercial-scale fixed-bed reactors, external resistances to mass transfer are usually small compared to the intraparticle resistance for normal operating conditions. However, we have seen earlier that significant external temperature differences can exist even when the external concentration difference is small. In fact, for gaseous reactants the external temperature difference will probably be much greater than any intraparticle differences.

Let us now turn our attention to the problem of determining the global reaction rate at some arbitrary point in a heterogeneous catalytic reactor from knowledge of the following parameters:

1. The intrinsic rate expression
2. The properties of the bulk fluid for the region in question (temperature and composition)
3. The flow conditions (mass velocity, reactor diameter, etc.)
4. The heat of reaction at the bulk fluid temperature
5. The physical properties of the fluid (Schmidt and Prandtl numbers, heat capacity, etc.)

6. The shape and size of the catalyst
7. The physical properties of the catalyst (specific surface area, porosity, effective thermal conductivity, effective diffusivity, pellet density, etc.)
8. The porosity of the bed ( $\varepsilon_B$ )

Values of all of these parameters must be available or estimated if one is to determine the global reaction rate. Some of these quantities can be evaluated from standard handbooks of physical property data, or generalized correlations such as those compiled by Poling et al. (8). Others can be determined only by experimental measurements on the specific reactant/catalyst system under consideration.

Determination of the global reaction rate that applies to a given segment of reactor volume involves the use of equations developed earlier. The rate of mass transfer to the external surface of the catalyst is given by equation (E) of Illustration 12.5.

$$r_m = \frac{k_c a_m (C_{A,B} - C_{A,ES})}{\left[ \nu_A - y_A \sum_{j=1}^c (\nu_j) \right]} \quad (12.6.1)$$

where the mass transfer coefficient ( $k_c$ ) is that for species A.

The reaction rate averaged over the catalyst pellet can be expressed in terms of the effectiveness factor  $\eta$  as

$$r_m = \eta \psi_m (C_{ES}, T_{ES}) \quad (12.6.2)$$

where the functional form of  $\psi_m$  is presumed to be known. The subscript  $m$  is employed to emphasize the fact that  $\psi_m(C_{ES}, T_{ES})$  is the reaction rate per unit mass of catalyst in

the absence of intraparticle diffusional limitations. To determine a global rate expression from equations (12.6.1) and (12.6.2) we also need to know the dependence of  $\eta$  on the Thiele modulus  $\phi_s$ , the definition of the Thiele modulus for the intrinsic reaction kinetics involved, the Arrhenius number  $\gamma$  (12.3.107), and the energy transformation function  $\beta$  (12.3.108). To relate bulk fluid and external surface temperatures, equations (12.5.4) and (12.5.5) are employed:

$$r_m(-\Delta H) = ha_m(T_{ES} - T_B) \quad (12.6.3)$$

or, using equation (12.6.1),

$$\frac{k_c a_m (C_{A,B} - C_{A,ES})(-\Delta H)}{\left[ \nu_A - y_A \sum_{j=1}^c (\nu_j) \right]} = ha_m(T_{ES} - T_B) \quad (12.6.4)$$

Equations (12.6.2) to (12.6.4) and the relations between  $\eta$ ,  $\phi_s$ ,  $\gamma$ , and  $\beta$  are sufficient to calculate the global rate at specified values of  $T_B$  and  $C_B$ . Unfortunately, information on relation (12.6.4) is usually rather limited. The curves presented in Figure 12.10 and reference 63 give the desired relation for first-order kinetics, but numerical solutions for other reaction orders are not available to this extent; we will presume that numerical solutions may be generated if needed for design purposes.

For isothermal systems, it is occasionally possible to eliminate the external surface concentrations between equations (12.6.1) and (12.6.2) and arrive at a global rate expression involving only bulk fluid compositions [e.g., equation (12.4.28) was derived in this manner]. In general, however, closed-form solutions cannot be achieved and an iterative trial-and-error procedure must be employed to determine the global rate. One possible approach is summarized below.

1. Use the  $j$ -factor correlations of Section 12.4 to determine appropriate heat and mass transfer coefficients.
2. Assume a value for  $T_{ES}$ .
3. Determine  $C_{ES}$  from (12.6.4).
4. From the effectiveness factor relation, determine  $\eta(T_{ES}, C_{ES})$ .
5. Calculate the reaction rate per unit mass using equation (12.6.2). (This step implies knowledge of the intrinsic rate expression.)
6. Determine  $T_{ES}$  from equation (12.6.3) using the reaction rate determined in step 5.
7. Compare the initial guess of  $T_{ES}$  with the calculated value and iterate until agreement is reached.
8. Substitution of the final values of  $T_{ES}$  and/or  $C_{ES}$  into any of the various equations for  $r_m$  gives the global rate.

This procedure obviously requires machine computation capability if it is to be employed in reactor design

calculations. Fortunately, there are many reactions for which the global rate reduces to the intrinsic rate. Such situations avoid the necessity for calculations of this type. On the other hand, several high-tonnage processes (e.g.,  $\text{SO}_2$  oxidation) are influenced by heat and mass transfer effects and one must be fully cognizant of their implications for design purposes.

## 12.7 DESIGN OF FIXED BED REACTORS

Fixed or packed bed reactors have many advantages relative to other types of heterogeneous catalytic reactors and, consequently, are employed much more widely in the chemical industry than any other basic reactor type. In this section we indicate in some detail the procedures involved in the design of a tubular fixed-bed reactor. This task involves the use of global rate information obtained through the techniques developed earlier to predict the composition of the effluent from a reactor for a given set of design parameters.

The design problem can be approached at various levels of sophistication using different mathematical models of the packed bed. In cases of industrial interest, it is not possible to obtain closed-form analytical solutions for any but the simplest of models under isothermal operating conditions. However, numerical procedures can be employed to predict effluent compositions on the basis of the various models. In the subsections that follow, we consider first the fundamental equations that must be obeyed by all packed-bed reactors under various energy transfer constraints, and then discuss some of the simplest models of reactor behavior. These discussions are limited to pseudo steady-state operating conditions (i.e., the catalyst activity is presumed to be essentially constant for times that are long compared to the fluid residence time in the reactor).

Models of fixed bed reactors can be categorized in a couple of ways. One basis lies in the number of spatial coordinates employed in the equations used to describe the model. One dimensional models take into account variations in composition and temperature along the length of the reactor, while two dimensional models also allow for variations of these properties in the radial direction. A second basis for categorizing reactor models lies in the manner in which one envisions the reaction as being distributed throughout the catalyst bed. In this sense, the models are viewed as either pseudo homogeneous or heterogeneous. For pseudo homogeneous models, one envisions the reactions as taking place throughout the reactor volume, not as localized at the catalyst surface. The rate expressions for use with these models are obtained by taking the product of the global reaction rate per unit mass of catalyst and the *bulk density* ( $\rho_B$ ) of the catalyst (i.e., the total mass of

catalyst divided by the *total volume* of the reactor):

$$r_V = r_m \rho_B \quad (12.7.1)$$

The units of  $r_V$  are moles converted/(volume·time), and  $r_V$  plays a role similar to the rates employed in homogeneous reactor design. Consequently, the design equations developed earlier for homogeneous reactors can be extended for use in obtaining estimates of fixed bed reactor performance. Two dimensional pseudo homogeneous models can also be developed to allow for radial dispersion of mass and energy.

Heterogeneous models of fixed bed reactors account explicitly for the presence of the solid catalyst by writing material and energy balance equations for both the solid and fluid phases. Several types of heterogeneous models can be employed, depending on the complications that one is willing to introduce. The basic heterogeneous model considers only transport by plug flow, but differentiates between bulk fluid properties and those prevailing at the external surface of the catalyst pellet. Models may also be developed that allow for intraparticle gradients and for radial variations in system properties. The necessity of using a heterogeneous model can be circumvented through the use of *global rate* expressions in terms of  $r_V$  in the corresponding pseudo homogeneous models described in Section 12.7.2. We have chosen to utilize this approach for the level of this book. [See Froment (95, 96) for critical reviews of several heterogeneous models.]

## 12.7.1 General Considerations

Prediction of the performance of a fixed-bed reactor under specified operating conditions is a problem whose solution is readily expressed in words. Unfortunately, this solution is not so easily expressed in the quantitative terms that the engineer needs to prepare equipment specifications and cost estimates. In principle, the solution involves the use of a heterogeneous reaction rate expression in a set of material balance equations for various chemical species and a corresponding conservation equation for energy. The resulting differential equations and the attendant boundary conditions are then evaluated over the catalyst bed to determine the conditions at the reactor outlet. Before discussing these equations in detail, however, we consider briefly a few subjects that are relevant to the general problem of fixed-bed reactor design. These include pressure drop, dispersion, and heat transfer in fixed beds.

### 12.7.1.1 Pressure Drop in Fixed Bed Reactors

To simplify a preliminary reactor design analysis, engineers often assume that the pressure drop across a reactor is negligible and has little influence on reactor size requirements.

However, there are some situations in reactor design where it is important to consider the implications of pressure drop, particularly when dealing with the flow of compressible fluids through a fixed or fluidized bed reactor. Because of its significance in a wide variety of chemical engineering operations, flow through packed beds has been studied by many investigators. The most useful approaches to predicting pressure drop through packed beds are those based on empirical correlations for the friction factor ( $f_M$ ), defined in the following manner:

$$\frac{\mathcal{P}_0 - \mathcal{P}_L}{L} = \frac{4f_M}{D_p^*} \left( \frac{1}{2} \rho v_0^2 \right) \quad (12.7.2)$$

where  $L$  is the length of the packed column,  $\rho$  is the fluid density,  $v_0$  the superficial velocity (the average linear velocity the fluid would have in the absence of packing), and  $D_p^*$  is the equivalent particle diameter, defined as

$$D_p^* = \frac{6}{a_V} \quad (12.7.3)$$

where  $a_V$  is the area per unit volume of an individual particle and  $\mathcal{P}$  represents the combined effects of static pressure ( $P$ ) and gravitational force and is defined as

$$\mathcal{P} = P + \rho g z \quad (12.7.3)$$

where  $z$  is the distance upward (as opposed to gravity) from a chosen reference plane. Subscripts 0 and  $L$  refer to inlet and outlet  $\mathcal{P}$  values, respectively.

Several correlating equations for the friction factor have been proposed for both the laminar and turbulent flow regimes, and plots of  $f_M$  (or functions thereof) versus Reynolds number are frequently presented in standard fluid flow or chemical engineering handbooks (e.g., 74, 97). Perhaps the most useful of the correlations is that represented by the Ergun equation (98):

$$\left( \frac{(\mathcal{P}_0 - \mathcal{P}_L) \rho}{G^2} \right) \left( \frac{D_p^*}{L} \right) \left( \frac{\epsilon_B^3}{1 - \epsilon_B} \right) = \frac{150(1 - \epsilon_B)}{D_p^* G / \mu} + 1.75 \quad (12.7.4)$$

where each term in parentheses on the left is a dimensionless group. At high Reynolds numbers, the first term on the right drops out, and we obtain the Burke–Plummer equation for the turbulent flow regime. Similarly, at low Reynolds numbers, the second term drops out, and the Ergun equation reduces to the Blake–Kozeny relation for the laminar flow regime.

Notice that the superficial mass velocity  $G$  is constant throughout the bed but that  $\rho$  will vary for compressible fluids. When the pressure drop is small relative to the absolute pressure, equation (12.7.4) may be used for gases by employing the arithmetic average of the inlet and outlet densities. This approximation is useful in solving design problems via machine computation.

### 12.7.1.2 Dispersion in Packed Bed Reactors

In Chapter 11 we indicated that deviations from plug flow behavior could be quantified in terms of a dispersion parameter that lumped together the effects of molecular diffusion and eddy diffusivity. A similar dispersion parameter is used to characterize transport in the radial direction, and these two parameters can be used to describe radial and axial transport of matter in packed bed reactors. In packed beds, the dispersion results not only from ordinary molecular diffusion and the turbulence that exists in the absence of packing, but also from lateral deflections and mixing arising from the presence of the catalyst pellets. These effects are the dominant contributors to radial transport at the Reynolds numbers normally employed in commercial reactors.

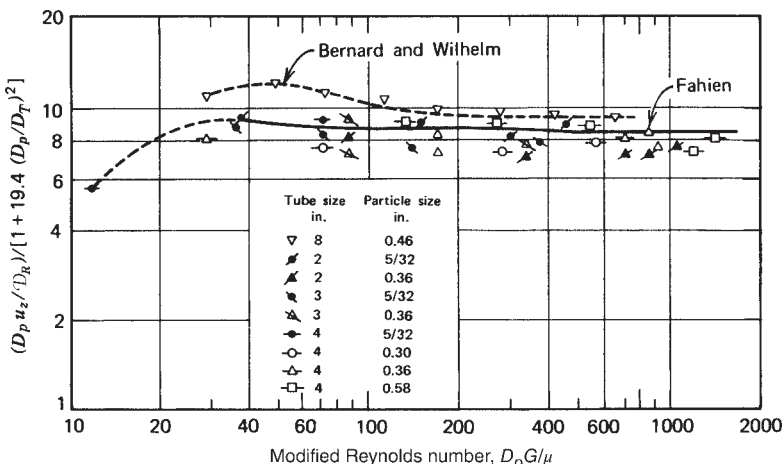
If there is no correlation between the directions in which a given fluid molecule is deflected at successive layers of pellets, the *radial distance* through which the molecule is transported as it moves longitudinally through the bed can be described using Einstein's random walk approach. Each deflection will be comparable in magnitude to the characteristic dimensions of the pellet. If a large number of molecules are considered, the effect is that of radial diffusion characterized by an apparent diffusion coefficient in the radial direction that is given by (99)

$$\mathcal{D}_R = \frac{u_z D_p}{11.2} \quad (12.7.5)$$

where  $u_z$  is the superficial velocity in the axial direction. For gases, the magnitude of  $\mathcal{D}_R$  is usually much greater than the molecular diffusion coefficient. This disparity is even greater for liquids. The dimensionless group  $u_z D_p / \mathcal{D}_R$  is known as the Péclet number for radial transport:

$$N_{Pe,r} \equiv \frac{u_z D_p}{\mathcal{D}_R} \quad (12.7.6)$$

At high Reynolds numbers where molecular diffusion effects are negligible, experimental evidence confirms the



general validity of equation (12.7.5). Figure 12.15 indicates how the Péclet number for radial mixing varies with the fluid Reynolds number. Above a Reynolds number of 40, the radial Péclet number is approximately 10.

The Péclet number for axial dispersion is defined in a manner similar to the radial parameter:

$$N_{Pe,z} \equiv \frac{u_z D_p}{\mathcal{D}_L} \quad (12.7.7)$$

where  $\mathcal{D}_L$  is the longitudinal dispersion parameter. Using a mathematical model that regards the interstices in the packing as a series of mixing chambers, Aris and Amundson (100) have estimated that the longitudinal Péclet number should have a value of approximately 2. Experimental results indicate that for gases  $N_{Pe,z}$  is equal to 2 for modified Reynolds numbers ( $D_p G / \mu$ ) above 10. For liquids, the longitudinal Péclet number is less, particularly at low Reynolds numbers. It should be emphasized that  $u_z$  is the apparent superficial velocity in the longitudinal direction (i.e., it is based on total area, voids plus solid). Similarly, in packed beds both  $\mathcal{D}_L$  and  $\mathcal{D}_R$  are normally based on the corresponding total cross section.

The extent to which longitudinal dispersion must be taken into account depends on the ratio of the reactor length to the size of the particles. If the ratio is 100 or more, as is the usual case in commercial reactors, the effect of longitudinal dispersion is negligible relative to the mass transport associated with bulk flow. Only in very short reactors at high conversions and low velocities is the effect significant. In such cases, however, dispersion models of the reactor would not be realistic because channeling and nonuniform flow distribution effects would normally be significant.

### 12.7.1.3 Heat Transfer in Fixed Bed Reactors

In reactor design, it is important to be able to describe in quantitative terms the heat transfer processes taking place within the reactor. In the design of homogeneous

**Figure 12.15** Correlation of average Péclet number with Reynolds number and the ratio of particle to tube diameter ( $D_p / D_r$ ). (Adapted from J. M. Smith, *Chemical Engineering Kinetics*, 3rd ed. Copyright © 1981. Used with permission of McGraw-Hill Book Company.)

reactors, one normally assumes that radial mixing is sufficiently rapid that all the resistance to energy transfer is concentrated at the wall and that the heat transfer can be described by a single heat transfer coefficient. However, in fixed bed reactors, the catalyst pellets inhibit radial mixing of the fluid, and significant gradients in temperature can exist in both the radial and axial directions. Here, we treat heat transfer between the containing wall of the reactor and its contents and heat transfer within the packed bed. The latter process is described in terms of an effective thermal conductivity that lumps together contributions from a number of heat transfer mechanisms. Both this parameter and the wall heat transfer coefficient can be estimated on the basis of correlations that summarize extensive experimentation in this area.

#### 12.7.1.3.1 Heat Transfer to the Containing Wall

Heat transfer between the container wall and the reactor contents enters into the design analysis as a boundary condition on the differential or difference equation describing energy conservation. If the heat flux through the reactor wall is designated as  $\dot{q}_w$ , the heat transfer coefficient at the wall ( $h_w$ ) is defined as

$$h_w \equiv \frac{\dot{q}_w}{T_w - T_B} \quad (12.7.8)$$

where  $T_w$  is the wall surface temperature and  $T_B$  is the mean temperature of the bulk fluid in the volume element at the axial position in question

Normally, such heat transfer coefficients for packed beds are significantly greater than those for empty tubes at the same gas flow rate. Early reports of such data were usually reported as ratios of the coefficient in the packed bed to that in the empty tube. Typical ratios range from 5 to 7.8, depending on the ratio of the pellet diameter to the tube diameter. Jakob (101) has proposed the following correlation for wall heat transfer coefficients as a generalization of an earlier correlation by Colburn (102):

$$\frac{h_w D_T}{\kappa_g} = f^* D_T^{0.17} \left( \frac{D_p G}{\mu} \right)^{0.83} N_{Pr} \quad (12.7.9a)$$

where  $D_T$  is the tube diameter in feet,  $D_p$  is the particle diameter in feet,  $\kappa_g$  is the thermal conductivity of the fluid in  $\text{Btu}/(\text{h}\cdot\text{ft}^2\cdot^\circ\text{F})$ ,  $h_w$  is the wall heat transfer coefficient in  $\text{Btu}/(\text{h}\cdot\text{ft}^2\cdot^\circ\text{F})$ ,  $\mu$  is the fluid viscosity in  $\text{lb}_m/(\text{h}\cdot\text{ft})$ ,  $G$  is the superficial mass velocity in  $\text{lb}_m/(\text{h}\cdot\text{ft}^2)$ , and  $f^*$  is a coefficient given by the correlation in equation (12.7.9b) with  $x = D_p/D_T$  for  $D_p$  in inches and  $D_T$  in feet:

$$f^* = 12.912x^3 - 10.443x^2 + 2.4172x + 0.0646 \quad (12.7.9b)$$

Equation (12.7.9b) provides an excellent fit of the data reported by Jakob (101) for values of  $x$  between 0.03

and 0.35. This correlation indicates that the ratio of the fixed-bed coefficient to the empty tube coefficient goes through a maximum, as  $D_p/D_T$  is varied.

Other useful correlations of heat transfer coefficients in packed beds have been proposed. Among these is a simple relation of Calderbank and Pogorski (103):

$$\frac{h_w D_p}{\kappa_g} = 3.6 \left( \frac{D_p G}{\mu \varepsilon_B} \right)^{0.365} \quad (12.7.10)$$

where the symbols have their usual significance. Leva (104) has also proposed two correlations for heating:

$$\text{For } \frac{D_p}{D_T} < 0.35 \quad h_w = 0.813 \frac{\kappa_g}{D_T} e^{-6D_p/D_T} \left( \frac{D_p G}{\mu} \right)^{0.90} \quad (12.7.11)$$

$$\text{For } 0.35 < \frac{D_p}{D_T} < 0.6 \quad h_w = 0.125 \frac{\kappa_g}{D_T} \left( \frac{D_p G}{\mu} \right)^{0.75} \quad (12.7.12)$$

and one for cooling:

$$\frac{h_w D_T}{\kappa_g} = 3.50 \left( \frac{D_p G}{\mu} \right)^{0.70} e^{-4.6D_p/D_T} \quad (12.7.13)$$

#### 12.7.1.3.2 Energy Transfer Within a Packed Bed

Energy transfer within packed beds is an extremely complicated process because it involves multiple mechanisms within a complex geometric structure. It may involve conduction through the pellets, conduction between pellets at points in contact, conduction through the fluid, radiation, turbulent transport by eddy diffusion processes, and conventional convective transport. These mechanisms combine and interact in a complex fashion to produce the observed transfer of thermal energy. Consequently, reactor designers find it convenient to use effective thermal conductivities ( $\kappa^*$ ), which encompass all contributions to the transport of thermal energy except convection by plug flow. These transport coefficients are employed in pseudo homogeneous models of packed bed reactors that picture the reactor contents as a homogeneous body through which heat is transferred by conduction. Consider the volume element shown in Figure 12.16 (see page 422). It consists of a cylindrical shell of radius  $R$ , thickness  $\Delta R$ , and length  $\Delta z$ , which is concentric with the tube axis. If an energy balance is written for the volume element, the following energy input terms are necessary:

Input of energy by convective transport in the axial direction:

$$2\pi R \Delta R \rho u_z \hat{C}_p (T - T_0)|_z \Delta t$$

Input of thermal energy by effective radial conduction:

$$-\kappa^* 2\pi R \Delta z \left( \frac{\partial T}{\partial R} \right)|_R \Delta t$$

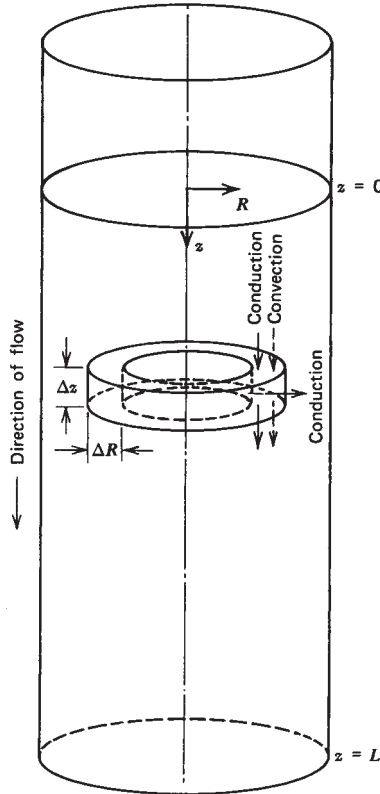


**Figure 12.16** Annular ring over which energy balance is made. (From R. B. Bird, W. E. Stewart, and E. N. Lightfoot, *Transport Phenomena*. Copyright © 1960. Reprinted with permission of John Wiley & Sons, Inc.)

Input of thermal energy by effective longitudinal conduction:

$$-\kappa_z^* 2\pi R \Delta R \left( \frac{\partial T}{\partial z} \right) \Big|_z \Delta t$$

input	$(2\pi R) \Delta R \rho u_z C_p (T - T_0) \Big _z \Delta t - \kappa_R^* (2\pi R) \Delta z \frac{\partial T}{\partial R} \Big _R \Delta t - \kappa_z^* (2\pi R) \Delta R \frac{\partial T}{\partial z} \Big _z \Delta t$
+ generation	$+ r_v (-\Delta H) 2\pi R (\Delta R) (\Delta z) (\Delta t)$
= output	$= (2\pi R) \Delta R \rho u_z C_p (T - T_0) \Big _{z+\Delta z} \Delta t - \kappa_R^* (2\pi R) \Delta z \frac{\partial T}{\partial R} \Big _{R+\Delta R} \Delta t - \kappa_z^* (2\pi R) \Delta R \frac{\partial T}{\partial z} \Big _{z+\Delta z} \Delta t$
+ accumulation	$+ [\varepsilon_{\text{total}} (\rho C_p)_{\text{gas}} + (1 - \varepsilon_{\text{total}}) (\rho C_p)_{\text{solid}}] \Delta t (2\pi R) \Delta R \Delta z$

(12.7.14)

Division by  $2\pi \Delta R \Delta z \Delta t$  and rearrangement gives

$$\begin{aligned}
 & [\varepsilon_{\text{total}} (\rho C_p)_{\text{gas}} + (1 - \varepsilon_{\text{total}}) (\rho C_p)_{\text{solid}}] R \frac{\Delta T}{\Delta t} = R r_v (-\Delta H) + \frac{\rho u_z C_p R (T - T_0) \Big|_z - \rho u_z C_p R (T - T_0) \Big|_{z+\Delta z}}{\Delta z} \\
 & + \frac{\kappa_R^* R (\partial T / \partial R) \Big|_{R+\Delta R} - \kappa_R^* R (\partial T / \partial R) \Big|_R}{\Delta R} + \frac{\kappa_z^* R (\partial T / \partial z) \Big|_{z+\Delta z} - \kappa_z^* R (\partial T / \partial z) \Big|_z}{\Delta z}
 \end{aligned} \quad (12.7.15)$$

where  $T_0$  is the datum temperature for enthalpy calculations,  $\hat{C}_p$  is an appropriate average heat capacity between the datum temperature and the temperature in question for the gaseous mixture,  $u_z$  is the superficial velocity in the  $z$ -direction corresponding to the point  $(R, z)$ ,  $\rho$  is the fluid density,  $\kappa_R^*$  and  $\kappa_z^*$  are the effective thermal conductivities in the radial and axial directions, respectively, and  $\Delta t$  is a short time increment. For convenience, we shall choose  $T_0$  to be close to  $T$  so that we may employ a constant-pressure heat capacity value corresponding to temperature  $T$ . Thus, we may delete the average symbol and let  $C_p$  refer to the heat capacity of the gas at temperature  $T$ .

Similar terms exist for output of thermal energy by these mechanisms. In addition to the input and output terms, we also need terms for the transformation of energy by chemical reaction,

$$r_v (-\Delta H) 2\pi R (\Delta R) (\Delta z) (\Delta t)$$

and the accumulation of energy within the volume element,

$$[\varepsilon_{\text{total}} (\rho C_p)_{\text{gas}} + (1 - \varepsilon_{\text{total}}) (\rho C_p)_{\text{solid}}] (\Delta T) 2\pi R (\Delta R) (\Delta z)$$

where  $r_v$  is the pseudo-homogeneous reaction rate per unit volume (solid plus fluid),  $\Delta H$  is the enthalpy change for reaction at the indicated conditions, and the term in brackets is an effective mean heat capacity per unit volume. The porosity in the last term represents the ratio of the sum of external and intraparticle void volumes to the total volume. The quantity  $\Delta T$  represents the temperature change occurring within the volume element in time  $\Delta t$ .

A typical balance equation can then be written as:

and in the limit, as the various deltas approach zero,

$$\begin{aligned} R[\varepsilon_{\text{total}}(\rho C_p)_{\text{gas}} + (1 - \varepsilon_{\text{total}})(\rho C_p)_{\text{solid}}] \frac{\partial T}{\partial t} \\ = Rr_v(-\Delta H) - R \frac{\partial}{\partial z}(\rho u_z C_p T) \\ + \frac{\partial}{\partial r} \left( \kappa_R^* R \frac{\partial T}{\partial R} \right) + R \frac{\partial}{\partial z} \left( \kappa_z^* \frac{\partial T}{\partial z} \right) \quad (12.7.16) \end{aligned}$$

The effective thermal conductivities in the axial and radial directions depend on such variables as temperature, gas flow rate, the thermal conductivities of the gas and solid phases, particle diameter and porosity, packing geometry, and the emissivity of the solid. In general,  $\kappa_R^*$  should depend on radial position, but this effect is almost always neglected. Moreover, transport of energy in the direction of flow by convective flow is normally so much greater than the effective thermal conduction that the last term in (12.7.16) is virtually always neglected. It is significant only in very short beds at low velocities. These assumptions lead to the following energy balance equation for pseudo homogeneous models of fixed bed reactors:

$$\begin{aligned} [\varepsilon_{\text{total}}(\rho C_p)_{\text{gas}} + (1 - \varepsilon_{\text{total}})(\rho C_p)_{\text{solid}}] \frac{\partial T}{\partial t} \\ = r_v(-\Delta H) - \frac{\partial}{\partial z}(\rho u_z C_p T) + \kappa_R^* \left( \frac{\partial^2 T}{\partial R^2} + \frac{1}{R} \frac{\partial T}{\partial R} \right) \quad (12.7.17) \end{aligned}$$

For steady-state operation, the time derivative vanishes and we have the form that is of greatest interest for our purposes here:

$$\frac{\partial}{\partial z}(\rho u_z C_p T) = r_v(-\Delta H) + \kappa_R^* \left( \frac{\partial^2 T}{\partial R^2} + \frac{1}{R} \frac{\partial T}{\partial R} \right) \quad (12.7.18)$$

This equation may be used as an appropriate form of the law of energy conservation in various pseudo homogeneous models of fixed bed reactors. Radial transport by effective thermal conduction is an essential element of two dimensional reactor models, but for one dimensional models, the last term must be replaced by one involving heat losses to the walls.

Equation (12.7.18) has been used by numerous investigators to evaluate effective thermal conductivities from experimental data. Figure 12.17 indicates the range of effective thermal conductivities typical of various Reynolds numbers. The data presented are most appropriate for use at temperatures below 300°C, where radiation heat transfer is negligible.

Argo and Smith (105, 106) have presented a detailed discussion of heat transfer in packed beds and have

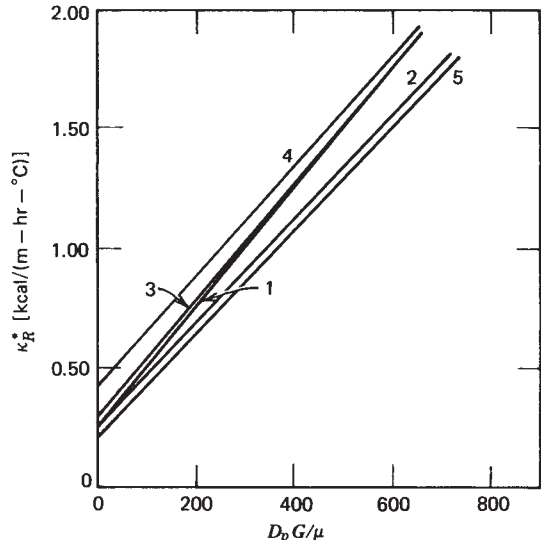


**Figure 12.17** Heat transfer in packed beds. Effective thermal conductivity as a function of Reynolds number. Curve 1, Coberly and Marshall; curve 2, Campbell and Huntington; curve 3, Calderbank and Pogorski; curve 4, Kwong and Smith; curve 5, Kunii and Smith. (Adapted from G. F. Froment and K. B. Bischoff, *Chemical Reactor Analysis and Design*, p. 533. Copyright © 1979. Used with permission of John Wiley & Sons, Inc.)

proposed the following relation for the effective thermal conductivity in packed beds:

$$\begin{aligned} \kappa^* = \varepsilon_B \left[ \kappa_g + \frac{D_p C_p G}{N_{Pe,r} \varepsilon_B} + \frac{4\sigma}{2 - \sigma} D_p (0.173) \frac{T^3}{100^4} \right] \\ + (1 - \varepsilon_B) \frac{h' \kappa_s D_p}{2\kappa_s + h' D_p} \quad (12.7.19) \end{aligned}$$

where  $\sigma$  is the emissivity of the solid,  $\kappa_g$  and  $\kappa_s$  are the thermal conductivities of fluid and pellet, respectively, and  $h'$  is a heat transfer coefficient that characterizes the thermal interaction between adjacent particles. The terms on the right of equation (12.7.19) represent, in order, the effects of molecular conduction through the fluid, the effects of transport by turbulent motion of fluid eddies, the effects of radiation transport through the void spaces, and the effects of conduction through the solid. The last term lumps together a number of effects associated with energy transfer from one pellet to adjacent pellets by radiation, point contacts, and convective transport to and from the fluid. The numerical constant in the radiation term implies that British engineering units (with time in hours) must be used for the various parameters and, in particular, the bed temperature  $T$  must be expressed in degrees Rankine.

Most of the data available have been recorded under conditions such that only the terms for eddy transport and conduction through the solid are significant. Equation (12.7.19) requires that  $\kappa^*$  increase with particle diameter,

mass velocity, and the conductivity of the solid. These requirements are consistent with data for low-conductivity solids, but some discrepancies arise for very high-conductivity solids (107). At Reynolds numbers greater than 40, the contribution of the molecular conduction term is negligible.

The parameter  $h'$ , which combines several effects, must be at least as large as the convective heat transfer coefficient ( $h_c$ ), calculated from the  $j_H$  factor correlations discussed in Section 12.5. It is given by an expression of the form

$$h' = h_c + h_R + h_p \quad (12.7.20)$$

where  $h_R$  and  $h_p$  represent the contributions of radiation between particles and conduction for pellets in contact. These quantities can be estimated as

$$h_R = \left( \frac{2\kappa_s + h'D_p}{D_p\kappa_s} \right) \left( \frac{4\sigma}{2 - \sigma} \right) D_p (0.173) \frac{T^3}{100^4} \quad (12.7.21)$$

and

$$h_p = \left( \frac{2\kappa_s + h'D_p}{D_p\kappa_s} \right) \kappa_p \quad (12.7.22)$$

where

$$\log \kappa_p = -1.76 + 0.0129 \left( \frac{\kappa_s}{\epsilon_B} \right) \quad (12.7.23)$$

in which  $\kappa_s$  is the thermal conductivity of the bulk solid. Equations (12.7.20) to (12.7.23) constitute a transcendental relation for  $h'$  that can be solved by trial-and-error procedures. Again because of the numerical constant in the radiation equation, we must employ British engineering units (with time in hours) in these relations. Illustration 12.7 indicates how to estimate an effective thermal conductivity for use with two dimensional pseudo homogeneous packed bed models.

### ILLUSTRATION 12.7 Determination of the Effective Thermal Conductivity of a Packed Bed of Catalyst Pellets

In Illustrations 12.5 and 12.6, some data for the catalytic oxidation of  $\text{SO}_2$  were used to determine composition and temperature differences between the bulk fluid and the fluid at the pellet–gas interface. Use the data and results of these illustrations and the new data given below to predict the effective thermal conductivity of the bed.

Data and results from Illustrations 12.5 and 12.6:

$$\begin{aligned} T & 458^\circ\text{C} = 731 \text{ K} = 1316^\circ\text{R} \\ P & 790 \text{ torr} \end{aligned}$$

$G$	$245 \text{ lb}/(\text{h}\cdot\text{ft}^2) = 3.33 \times 10^{-2} \text{ g}/(\text{s}\cdot\text{cm}^2)$
$\kappa_g$	$3.70 \times 10^{-4} \text{ J}/(\text{cm}\cdot\text{s}\cdot\text{K}) = 0.0214 \text{ Btu}/(\text{h}\cdot\text{ft}\cdot{}^\circ\text{F})$
$\mu$	0.032 cp
$\rho_p$	$1.81 \text{ g}/\text{cm}^3$
$\epsilon_B$	0.40
$D_p$	$0.389 \text{ cm} = 1.276 \times 10^{-2} \text{ ft}$
$N_{\text{Re}}$	41
$j_D$	0.235
$C_p$	$1.07 \text{ J}/(\text{g}\cdot\text{K}) = 0.255 \text{ Btu}/(\text{lb}\cdot{}^\circ\text{R})$
$N_{\text{Pr}}$	0.92
$h_c$	$8.79 \times 10^{-3} \text{ J}/(\text{cm}^2\cdot\text{s}\cdot\text{K})$

Additional data:

$D_T$	$1.770 \text{ in.} = 0.1475 \text{ ft}$
$\sigma$	0.65
$\kappa_s$	$1.8 \text{ Btu}/(\text{h}\cdot\text{ft}\cdot{}^\circ\text{F})$

### Solution

Equations (12.7.20) to (12.7.23) may be used to evaluate the parameter  $h'$ . We begin by converting the convective heat transfer coefficient  $h_c$  determined in Illustration 12.6, to British engineering units.

$$\begin{aligned} h_c &= 8.79 \times 10^{-3} \text{ J}/(\text{cm}^2\cdot\text{s}\cdot\text{K}) \\ &= 15.56 \text{ Btu}/(\text{ft}^2\cdot\text{h}\cdot{}^\circ\text{R}) \end{aligned}$$

From equation (12.7.20) it is evident that  $h'$  must be at least as large as  $h_c$ , and this fact provides a useful starting point for solving these transcendental equations. We begin by assuming that  $h' = 35 \text{ Btu}/(\text{h}\cdot\text{ft}^2\cdot{}^\circ\text{R})$ . From equation (12.7.23),

$$\log \kappa_p = -1.76 + 0.0129(1.8/0.40)$$

or

$$\kappa_p = 0.0199$$

From equation (12.7.22),

$$\begin{aligned} h_p &= \frac{2(1.8) + 35(0.01276)}{0.01276(1.8)}(0.0199) \\ &= 3.51 \text{ Btu}/(\text{h}\cdot\text{ft}^2\cdot{}^\circ\text{R}) \end{aligned}$$

From equation (12.7.21),

$$\begin{aligned} h_R &= \frac{2(1.8) + 35(0.01276)}{0.01276(1.8)} \left[ \frac{4(0.65)}{2 - 0.65} \right] \\ &\quad \times \left[ (0.01276)(0.173) \frac{(1316)^3}{(100)^4} \right] \\ &= 17.07 \text{ Btu}/(\text{h}\cdot\text{ft}^2\cdot{}^\circ\text{R}) \end{aligned}$$

From equation (12.7.20),

$$h' = 15.56 + 3.51 + 17.07 = 36.14 \text{ Btu}/(\text{h}\cdot\text{ft}^2\cdot{}^\circ\text{F})$$

Because the relations for  $h_g$  and  $h_p$  are not very sensitive to the value of  $h'$ , we need not iterate again. We can use the value above for subsequent purposes.

The radial Péclét number may now be estimated using Figure 12.15 at  $N_{Re} = 41$ ,

$$\begin{aligned}\frac{D_p u_z}{D_R} &= 9 \left[ 1 + 19.4 \left( \frac{D_p}{D_T} \right)^2 \right] \\ &= 9 \left[ 1 + 19.4 \left( \frac{0.01276}{0.1475} \right)^2 \right] = 10.3\end{aligned}$$

We now have numerical values for all of the quantities appearing in equation (12.7.19). However, consistent units must be employed and, because of the 0.173 factor appearing in the radiation term, British engineering units are appropriate. The various terms in this equation may be evaluated as follows:

$$\begin{aligned}\kappa_g &= 0.0214 \text{ BTU}/(\text{h}\cdot\text{ft}\cdot{}^{\circ}\text{F}) \\ \frac{D_p C_p G}{N_{Pe,r} \varepsilon_B} &= \frac{(1.276 \times 10^{-2})(0.255)(245)}{10.3(0.40)} \\ &= 0.1935 \text{ BTU}/(\text{h}\cdot\text{ft}\cdot{}^{\circ}\text{F}) \\ \frac{4\sigma}{2-\sigma} D_p (0.173) \frac{T^3}{100^4} &= \frac{4(0.65)}{2-0.65} (1.276 \times 10^{-2})(0.173) \frac{(1316)^3}{(100)^4} \\ &= 0.0969 \text{ BTU}/(\text{h}\cdot\text{ft}\cdot{}^{\circ}\text{F}) \\ \frac{(1-\varepsilon_B)h' \kappa_s D_p}{2\kappa_s + h'D_p} &= \frac{(1-0.40)(36.1)(1.8)(1.276 \times 10^{-2})}{2(1.8) + (36.1)(1.276 \times 10^{-2})} \\ &= 0.1225 \text{ BTU}/(\text{h}\cdot\text{ft}\cdot{}^{\circ}\text{F})\end{aligned}$$

Thus,

$$\begin{aligned}\kappa^* &= 0.40(0.0214 + 0.1935 + 0.0969) + 0.1225 \\ &= 0.247 \text{ BTU}/(\text{h}\cdot\text{ft}\cdot{}^{\circ}\text{F})\end{aligned}$$

The result is the average effective thermal conductivity of the bed. The reader should be aware, however, that the correlation employed is probably only good to 10 to 20% at best. In using such values in design calculations, one should examine the sensitivity of the results to variations in parameters that are characterized by such large uncertainties.

## 12.7.2 Pseudo Homogeneous<sup>‡</sup> Models of Packed Bed Reactors

Pseudo homogeneous models of fixed bed reactors are widely employed in reactor design calculations. Such

models assume that the fluid within the volume element associated with a single catalyst pellet or group of pellets can be characterized by a given bulk temperature, pressure, and composition and that these quantities vary continuously with position in the reactor. In most industrial scale equipment, the reactor volume is so large compared to the volume of an individual pellet and the fraction of the void volume associated therewith that the assumption of continuity is reasonable.

Pseudo homogeneous models require global rate expressions of the type discussed in Section 12.6, and the analysis that follows presumes that such expressions are available. To solve the differential equations representing material and energy balances, we use appropriate global rate expressions and boundary conditions to generate relations between the effluent conditions (composition and temperature) and the reactor volume. Usually, it is necessary to transform the coupled differential equations into difference equations and to use numerical methods to solve the transformed equations. The conventional approach to this problem involves the use of a stepwise procedure in which one starts at the reactor inlet and marches longitudinally through the reactor in appropriate volume increments. One or two dimensional models may be employed depending on the degree of sophistication desired, the level of approximation required, and time and cost constraints. Either model can be handled by modern computing machines, but the one dimensional model is used most often in preliminary design calculations because it provides a good approximation to the result desired and because it can easily be used to determine the effects of changes in design parameters and operating conditions on effluent conditions (see Section 12.7.2.1). The two dimensional model is more complex but provides essential information about radial temperature profiles within the bed. Such information is particularly useful in evaluating the potential for runaway reactor conditions and catalyst deactivation problems, as well as in dealing with systems in which selectivity considerations are significant (see Section 12.7.2.2).

The computational effort required to carry out the design analysis is determined mainly by the magnitude and spatial distribution of the temperature variations that are taken into account. The maximum temperature difference between the inlet and outlet of the reactor occurs when the reactor operates adiabatically. In this case, heat transfer to the reactor wall is neglected, so there is no temperature variation in the radial direction. However, the temperature does vary in the axial direction, so the material and energy balance equations are coupled through the dependence of the reaction rate on temperature. If the reactor is well insulated and/or of large diameter, the adiabatic model may provide a good representation of actual operating experience.

<sup>‡</sup>The term *pseudo homogeneous model* has been popularized by Froment (95, 96).

However, the most complex analysis is that in which heat transfer through the reactor walls is taken into account. This type of operation must be employed when it is necessary to supply or remove energy from the system so as to moderate the temperature excursions that would otherwise ensue. This mode of operation is frequently employed in industrial reactors, and to model such systems, one must often resort to two-dimensional models of the reactor that allow the concentration and temperature to vary in both the radial and axial directions. In the analysis of such systems, we make incremental calculations across the diameter of a given longitudinal segment of the packed-bed reactor, and then proceed to repeat the process for successive longitudinal increments.

The various energy transfer constraints enter into the analysis primarily as boundary conditions on the difference equations, and we now turn to the generation of the differential equations on which the difference equations are based. Because the equations for the one-dimensional model are readily obtained by omitting or modifying terms in the expressions for the two-dimensional model, we begin by deriving the material balance equations for the latter. For purposes of simplification, it is assumed that only one independent reaction occurs within the system of interest. In cases where multiple reactions are present, one merely adds an appropriate term for each additional independent reaction.

Consider the element of reactor volume shown in Figure 12.16. The cylindrical shell is concentric with the cylinder axis, about which there is general symmetry. A material balance on the volume element requires consideration of several terms. The amount of a particular species

A that enters the volume element during a time increment  $\Delta t$  consists of material entering by longitudinal bulk flow,

$$C_A u_z (2\pi R) \Delta R_z \Delta t$$

material entering as a consequence of axial dispersion,

$$-D_L (2\pi R) \Delta R \left( \frac{\partial C_A}{\partial z} \right)_z \Delta t$$

and material entering by radial dispersion,

$$-D_R (2\pi R) \Delta z \left( \frac{\partial C_A}{\partial R} \right)_R \Delta t$$

where  $D_L$  and  $D_R$  are effective dispersion parameters that lump together molecular diffusion and eddy diffusion arising from turbulence and packing effects. As used in the pseudo-homogeneous models, both diffusivities are based on the total area (void plus solid) normal to the direction of transport. These parameters are those involved in the definition and discussion of the Péclet numbers presented in Section 12.7.1.2.

The amount of species A that leaves the volume element during the time increment  $\Delta t$  consists of three similar terms. The amount of A that accumulates within the volume element during time  $\Delta t$  is  $\Delta C_A (2\pi R) \Delta R \Delta z$ , and the amount of A that is generated by chemical reaction within the volume element is  $\nu_A r_v (2\pi R) \Delta R \Delta z \Delta t$ , where  $r_v$  is the reaction rate expressed in pseudo-homogeneous form [i.e., the number of moles transformed per unit time per unit of total reactor volume (voids plus solid)].

The various terms may be combined in a generalized material balance to give:

input	$[C_A u_z (2\pi R) \Delta R]_z \Delta t - \left[ D_L (2\pi R) \Delta R \frac{\partial C_A}{\partial z} \right]_z \Delta t - \left[ D_R (2\pi R) \Delta z \frac{\partial C_A}{\partial z} \right]_R \Delta t$
+ generation	$+ \nu_A r_v (2\pi R) \Delta R \Delta z \Delta t$
= output	$= [C_A u_z (2\pi R) \Delta R]_{z+\Delta z} \Delta t - \left[ D_L (2\pi R) \Delta R \frac{\partial C_A}{\partial z} \right]_{z+\Delta z} \Delta t - \left[ D_R (2\pi R) \Delta z \frac{\partial C_A}{\partial z} \right]_{R+\Delta R} \Delta t$
+ accumulation	$+ (\Delta C_A) (2\pi R) \Delta R \Delta z$

(12.7.24)

Division by  $2\pi \Delta R \Delta z \Delta t$  and rearrangement gives

$$\begin{aligned} & \frac{[D_L R (\partial C_A / \partial z)]_{z+\Delta z} - [D_L R (\partial C_A / \partial z)]_z}{\Delta z} \\ & + \frac{[D_R R (\partial C_A / \partial R)]_{R+\Delta R} - [D_R R (\partial C_A / \partial R)]_R}{\Delta R} \\ & - \frac{(C_A u_z R)_{z+\Delta z} - (C_A u_z R)_z}{\Delta z} + \nu_A r_v R = R \frac{\Delta C_A}{\Delta t} \end{aligned} \quad (12.7.25)$$

and in the limit as  $\Delta R$ ,  $\Delta z$ , and  $\Delta t$  all approach zero,

$$\begin{aligned} & D_L R \frac{\partial^2 C_A}{\partial z^2} + D_R \frac{\partial}{\partial R} \left( R \frac{\partial C_A}{\partial R} \right) \\ & - R \frac{\partial (C_A u_z)}{\partial z} + \nu_A R r_v = R \frac{\partial C_A}{\partial t} \end{aligned} \quad (12.7.26)$$

where we have presumed that  $D_L$  and the tube diameter are constant over the length of the reactor and that  $D_R$  is constant over the reactor diameter. It is necessary to retain  $u_z$

within the partial derivative to cover those cases in which there is a change in fluid density on reaction. When there is an increase or decrease in the number of moles on reaction, or a change in fluid temperature or pressure, the velocity component in the longitudinal direction will vary along the length of the reactor. For gas-phase reactions, this effect can be very significant.

Equation (12.7.26) can be rewritten as

$$\mathcal{D}_L \frac{\partial^2 C_A}{\partial z^2} + \mathcal{D}_R \left( \frac{\partial^2 C_A}{\partial R^2} + \frac{1}{R} \frac{\partial C_A}{\partial R} \right) - \frac{\partial(C_A u_z)}{\partial z} + \nu_A r_v = \frac{\partial C_A}{\partial t} \quad (12.7.27)$$

At steady state, the right side vanishes and one obtains an equation that describes in pseudo-homogeneous fashion the concentration profile in the reactor:

$$\mathcal{D}_L \frac{\partial^2 C_A}{\partial z^2} + \mathcal{D}_R \left( \frac{\partial^2 C_A}{\partial R^2} + \frac{1}{R} \frac{\partial C_A}{\partial R} \right) - \frac{\partial(C_A u_z)}{\partial z} + \nu_A r_v = 0 \quad (12.7.28)$$

For isothermal systems this equation, together with an appropriate expression for  $r_v$ , is sufficient to predict the concentration profiles through the reactor. For nonisothermal systems, this equation is coupled to an energy balance equation [e.g., the steady-state form of equation (12.7.16)] by the dependence of the reaction rate on temperature.

$$\kappa_L^* \frac{\partial^2 T}{\partial z^2} + \kappa_R^* \left( \frac{\partial^2 T}{\partial R^2} + \frac{1}{R} \frac{\partial T}{\partial R} \right) - \frac{\partial}{\partial z} (\rho u_z C_p T) - (\Delta H) r_v = 0 \quad (12.7.29)$$

Equations (12.7.28) and (12.7.29) provide a two dimensional pseudo homogeneous model of a fixed bed reactor. The one-dimensional model is obtained by omitting the radial dispersion terms in the mass balance equation and replacing the radial heat transfer term by one that accounts for thermal losses through the tube wall. Thus, the material balance becomes

$$\mathcal{D}_L \frac{\partial^2 C_A}{\partial z^2} - \frac{\partial(C_A u_z)}{\partial z} + \nu_A r_v = 0 \quad (12.7.30)$$

The corresponding energy conservation equation is

$$\kappa_L^* \frac{\partial^2 T}{\partial z^2} - G \frac{\partial}{\partial z} (C_p T) - \frac{4}{D_T} h_w (T - T_w) - r_v \Delta H = 0 \quad (12.7.31)$$

where  $T_w$  is the tube wall temperature.

The boundary conditions that govern both the one- and two-dimensional models are usually stated in the following

manner:

$$C_A = C_{A0} \quad \text{at } z = 0 \text{ for all } R \quad (12.7.32)$$

$$T = T_0 \quad \text{at } z = 0 \text{ for all } R \quad (12.7.33)$$

$$\frac{\partial C_A}{\partial R} = 0 \quad \text{at } R = 0 \text{ for all } z \quad (12.7.34)$$

$$\frac{\partial T}{\partial R} = 0 \quad \text{at } R = 0 \text{ for all } z \quad (12.7.35)$$

$$\frac{\partial C_A}{\partial R} = 0 \quad \text{at } R = R_0 \text{ for all } z \quad (12.7.36)$$

$$u_z C_{A0}|_{z=0^-} = - \left( \mathcal{D}_L \frac{\partial C_A}{\partial z} \right)_{z=0^+} + u_z C_A|_{z=0^+} \quad \text{at } z = 0 \text{ for all } R \quad (12.7.37)$$

In the formulation of the boundary conditions, it is presumed that there is no dispersion in the feed line and that the entering fluid is uniform in temperature and composition. In addition to the boundary conditions above, it is also necessary to formulate appropriate equations to express the energy transfer constraints imposed on the system (e.g., adiabatic, isothermal, or nonisothermal–nonadiabatic operation). For the one-dimensional models, boundary conditions (12.7.34) and (12.7.35) hold for all  $R$ , not just at  $R = 0$ .

When the velocity  $u_z$  varies with *radial* position, equation (12.7.28) must be solved by a stepwise numerical procedure. Experimental evidence indicates that the axial velocity does indeed vary with radial position in fixed-bed reactors. The velocity profile is relatively flat in the center of the tube. As one moves radially outward, the velocity increases gradually until a maximum is reached at a point about one pellet diameter from the tube wall. The local velocity then falls rapidly, until it reaches zero at the wall. If the ratio of the tube diameter to the pellet diameter exceeds 30, a plug flow model of the velocity profile provides a good representation of the actual profile across the central core of the tubular reactor. Departures from the average velocity are significant only in the thin annular region near the tube walls. In single-tube commercial scale reactors this criterion is usually met [e.g., if the pellets have a characteristic dimension of 0.6 cm ( $\sim \frac{1}{4}$  in.), the required tube diameter is only 18 cm ( $\sim 7$  in.)]. However, in the multtube reactors required to meet the large heat transfer requirements of very rapid highly exothermic reactions, the assumption of a relatively flat velocity profile is not a good one. Such systems are difficult to model in mathematical terms. To generate the data necessary for the design of such reactors, the practicing engineer frequently has to resort to pilot scale reactors that consist of one or more tubes of the same diameter and length as those to be employed in the commercial scale multtube reactor.

We turn now from a discussion of general principles to specific models of reactor behavior.

### 12.7.2.1 The One Dimensional Pseudo Homogeneous Model of Fixed Bed Reactors

The design of tubular fixed bed catalytic reactors has generally been based on a one dimensional model that assumes that species concentrations and fluid temperature vary *only* in the axial direction. Heat transfer between the reacting fluid and the reactor walls is considered by presuming that all of the resistance is contained within a very thin boundary layer next to the wall and by using a heat transfer coefficient ( $h_w$ ) based on the temperature difference between the bulk fluid and the wall. Per unit area of the tube wall, the heat flow rate from the reactor contents to the wall is then  $h_w(T - T_w)$ . The correlations for  $h_w$  presented in Section 12.7.1.3 may be used to estimate this parameter.

The one dimensional model is advantageous because it provides a rapid means of (1) obtaining an estimate of the reactor size necessary to achieve a given conversion, and (2) examining the influence of several design variables on the behavior of the reactor. Unfortunately, the model provides no information concerning the possibility of achieving an excessive temperature at the center of the tube that may be markedly different from the mean temperature at the same longitudinal position. Such temperatures may be unacceptable for reasons of reactor stability, process selectivity, or catalyst deactivation. To ensure that such excessive temperatures are not achieved along the reactor axis, one should determine if they are present using a two-dimensional model to analyze those sets of operating conditions that the one-dimensional model indicates might lead to excessively high temperatures along the centerline of the tube. The two dimensional model is discussed in Section 12.7.2.2.

The equation describing the steady state material balance for tubular packed bed reactors can be obtained from the more general relation (12.7.28) by omitting the terms corresponding to radial transport of matter. Hence, the material balance relation becomes

$$D_L \frac{\partial^2 C_A}{\partial z^2} - \frac{\partial(C_A u_z)}{\partial z} + \nu_A r_v = 0 \quad (12.7.38)$$

Further simplification of the material balance equation occurs if the axial dispersion term is neglected. In this case,

$$\frac{\partial(C_A u_z)}{\partial z} - \nu_A r_v = 0 \quad (12.7.39)$$

If one recognizes that

$$F_A = C_A u_z \frac{\pi D_T^2}{4} \quad (12.7.40)$$

and that

$$V_R = \frac{\pi D_T^2}{4} z \quad (12.7.41)$$

equation (12.7.39) can be written as

$$\frac{dF_A}{dV_R} - \nu_A r_v = \frac{dF_A}{dV_R} - r_{Av} = 0 \quad (12.7.42)$$

Now,  $dF_A = -F_{A0} df_A$ , so equation (12.7.42) can be written as

$$\frac{V_R}{F_{A0}} = \int \frac{df_A}{-r_{Av}} \quad (12.7.43)$$

which is identical with the equation for an ideal plug flow reactor, derived as equation (8.2.7). If both sides of this relation are multiplied by the bulk density of the catalyst, we again generate equation (8.2.12):

$$\frac{\rho_B V_R}{F_{A0}} = \frac{W}{F_{A0}} = \int \frac{\rho_B df_A}{(-r_{Av})} = \int \frac{df_A}{(-r_{Av})} \quad (12.7.44)$$

The *general* energy balance for the one dimensional packed bed reactor *cannot* be obtained by omitting the radial derivatives of the temperature in equation (12.7.29), because these terms ultimately lead to heat transfer through the walls of the reactor. These terms can be omitted *only for situations involving adiabatic operation*. In the general case of a one dimensional model, the rate of heat loss through the wall must be considered. For a differential length of reactor ( $\Delta z$ ), this loss is given by

$$h_w \pi D_T (T - T_w) \Delta z$$

where  $D_T$  is the tube diameter,  $T_w$  the local wall temperature, and  $h_w$  a wall heat transfer coefficient that can be evaluated from the empirical correlations presented in Section 12.7.1.3.1.

An energy balance over the differential length of reactor for steady-state operating conditions is then given by

$$\begin{aligned} & \text{Input by convection} & \text{Transformation by reaction} \\ & \rho u_z \frac{\pi D_T^2}{4} C_p (T - T_0)_z + r_v (-\Delta H) \frac{\pi D_T^2}{4} \Delta z \\ & + \left( -\kappa_L^* \frac{\pi D_T^2}{4} \frac{\partial T}{\partial z} \right)_z & \\ & = \rho u_z \frac{\pi D_T^2}{4} C_p (T - T_0) \Big|_{z+\Delta z} + h_w \pi D_T (T - T_w) \Delta z \\ & + \left( -\kappa_L^* \frac{\pi D_T^2}{4} \frac{\partial T}{\partial z} \right)_{z+\Delta z} & \text{Losses through wall} \end{aligned} \quad (12.7.45)$$

which leads to the following differential equation:

$$\begin{aligned} & -\frac{\partial}{\partial z} \left( \kappa_L^* \frac{\partial T}{\partial z} \right) + \frac{\partial}{\partial z} (\rho u_z C_p T) \\ & + \frac{4}{D_T} h_w (T - T_w) = r_v (-\Delta H) \end{aligned} \quad (12.7.46)$$

This equation can also be rewritten in terms of the superficial mass velocity  $G$ , which does not vary along the length of the reactor.

$$-\frac{\partial}{\partial z} \left( \kappa_L^* \frac{\partial T}{\partial z} \right) + G \frac{\partial}{\partial z} (C_p T) + \frac{4}{D_T} h_w (T - T_w) = r_v (-\Delta H) \quad (12.7.47)$$

As indicated earlier, the axial conduction term is almost always negligible compared to the convective enthalpy transport term. Therefore, equation (12.7.47) is usually simplified to obtain

$$G \frac{\partial}{\partial z} (C_p T) + \frac{4}{D_T} h_w (T - T_w) = r_v (-\Delta H) \quad (12.7.48)$$

Equations (12.7.48) and (12.7.39) provide the simplest one-dimensional mathematical model of tubular fixed-bed reactor behavior. These equations neglect longitudinal dispersion of both matter and energy and, in essence, are completely equivalent to the plug flow model for homogeneous reactors that was examined in some detail in Chapters 8 to 10. Various simplifications in these equations will occur for different constraints on the energy transfer to or from the reactor. Normally, equations (12.7.48) and (12.7.39) are coupled through the dependence of the reaction rate on temperature. However, for isothermal operation, the equations are not coupled, and  $\partial T/\partial z$  becomes zero. For adiabatic operation, the heat losses through the wall are negligible, and the energy balance becomes

$$G \frac{\partial}{\partial z} (C_p T) = r_v (-\Delta H) \quad (\text{adiabatic case}) \quad (12.7.49)$$

Depending on the operational constraints, one of the two equations (12.7.48) or (12.7.49) or the choice of isothermal behavior must be used, together with the general material balance relation (12.7.39), to determine the composition and temperature profiles along the length of the reactor.

In many instances, the pressure drop through the reactor will be relatively small so that we may employ a mean value for the total pressure in our calculations. However, the Ergun equation presented in Section 12.7.1.1 may be used, if necessary, to evaluate the pressure at various points in the bed. Solutions of the appropriate material and energy balance equations for this simplified one-dimensional model can be obtained by straightforward numerical procedures employing machine computation to solve the corresponding difference equations. Although the correspondence of these solutions to the behavior of actual reactors must be viewed as only an approximation, this model provides a means of simulating the steady-state response of the system under investigation to changes in various process parameters at minimum cost in computer time and programming effort. The simulations enable one to answer questions such as:

1. What tube length will be required to achieve a given conversion?
2. What will be the corresponding effluent temperature?
3. What does the longitudinal temperature profile look like for specified inlet temperatures and/or wall temperature profiles? Are the hot spots excessive for reasons of selectivity, catalyst deactivation, and so on?
4. How do changes in the tube diameter influence the design calculations?
5. How do changes in catalyst pellet size affect system behavior?
6. How can one avoid excessive sensitivity of the performance of the reactor to changes in process parameters?

Question 6 pertains to the problem of parametric sensitivity. There is extensive literature dealing with this topic, but it is beyond the scope of this book.

A more general one-dimensional model of tubular packed-bed reactors is contained within equations (12.7.38) and (12.7.47). These equations include all of the elements of the simple model discussed above and, in addition, account for the longitudinal dispersion of both thermal energy and matter. The dispersion that represents the combined effects of molecular diffusion, normal fluid turbulence, and the influence of the packing is accounted for by superimposing "effective" heat and mass transfer terms on the plug flow equations. Because of the assumptions involved in the definitions of the effective thermal conductivity and dispersion terms, they implicitly contain the effect of radial velocity profiles within the tubes. Normally, one uses values averaged over the tube diameter, as expressed by Péclet numbers for heat and mass transfer. However, the velocity profile is not considered explicitly. For design purposes, we take the longitudinal Péclet number based on a pellet diameter to be approximately 2. Effective thermal conductivities may be estimated using the method described in Section 12.7.1.3.2.

In many respects, the solutions to equations (12.7.38) and (12.7.47) do not provide sufficient additional information to warrant their use in preliminary design calculations. It has been clearly demonstrated that for the fluid velocities used in industrial practice, the influence of axial dispersion of both heat and matter on the conversion achieved is negligible provided that the packing depth is in excess of 100 pellet diameters (108). Such shallow beds are only employed as the first stage of multibed adiabatic reactors. There is some question as to whether or not such short beds can be described adequately by an effective transport model. Thus, for most preliminary design calculations, the simplified one-dimensional model discussed earlier is preferred. The discrepancies between model simulations and actual reactor behavior are not resolved by the inclusion of longitudinal dispersion terms. Their effects

are small compared to the influence of radial gradients in temperature and composition. Consequently, for more accurate simulations, chemical engineers typically employ two dimensional models (see Section 12.7.2.2).

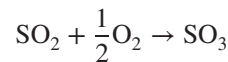
Nevertheless, one feature of the one dimensional model containing dispersion terms is of considerable interest. These terms increase the order of the partial differential equations and, under certain conditions, lead to nonuniqueness of the steady state profile through the reactor (109). For certain ranges of operating conditions and parameter values, three or more steady state profiles can be obtained for the same feed conditions. The two outlying steady-state profiles will be stable (at least to small perturbations), whereas the intermediate profile will be unstable. The profile generated as a solution to equations (12.7.38) and (12.7.47) will depend on the initial guesses for  $T$  and  $C$  involved in the trial-and-error solution.

In physical terms, the corresponding analysis implies that the steady state that would be achieved in a real reactor will depend on the initial profile in the reactor. For all situations where the initial values differ from the feed conditions, we must solve the time dependent differential equations describing the reactor to determine which profile will prevail. To determine if such computations are necessary, one must know whether or not multiple steady states are possible. Several criteria that permit us to make this decision on an a priori basis have been discussed by various authors (110–112). For details of these analyses, consult the references indicated. For present purposes we are interested only in the general conclusions derived from such studies. The range within which such multiple steady states are possible is very narrow, and such conditions are rarely encountered in either laboratory or industrial scale reactors. They are most likely to be realized for highly exothermic reactions carried out in extremely short beds under adiabatic operating conditions. The length of virtually all industrial scale reactors precludes the necessity of including longitudinal dispersion terms in a one dimensional model of reactor behavior and of worrying about their implications for multiple steady states. The effects of radial temperature gradients are much more likely to be significant. Illustrations 12.8 and 12.9 indicate the manner in which the one dimensional model is employed in reactor design analyses.

### ILLUSTRATION 12.8 Production of Sulfur Trioxide in an Adiabatic Fixed Bed Reactor

Industrial-scale production of sulfuric acid is dependent on the oxidation of sulfur dioxide to sulfur trioxide in

fixed bed catalytic reactors:



Through the years, several catalyst formulations have been employed, but one of the traditional catalytic agents has been vanadium pentoxide. Calderbank (113) has indicated that for a catalyst consisting of  $\text{V}_2\text{O}_5$  supported on silica gel, the kinetic data are represented by a rate expression of the form

$$r_m = \frac{k_1 P_{\text{SO}_2} P_{\text{O}_2} - k_2 P_{\text{SO}_3} P_{\text{O}_2}^{1/2}}{P_{\text{SO}_2}^{1/2}} \quad (\text{A})$$

that may be regarded as a degenerate form of typical Hougen–Watson rate laws. The rate constants are given by

$$\ln k_1 = 12.07 - \frac{31,000}{RT} \quad (\text{B})$$

and

$$\ln k_2 = 22.75 - \frac{53,600}{RT} \quad (\text{C})$$

where  $T$  is expressed in K,  $R$  is the gas constant expressed in cal/(mol·K),  $k_1$  is expressed in mol/(s·g catalyst·atm<sup>3/2</sup>), and  $k_2$  is expressed in mol/(s·g catalyst·atm). For present purposes, the global rate expression may be presumed to be represented by equation (A).

The reaction is highly exothermic and must be regarded as reversible. Consequently, although high temperatures enhance the initial rate, they limit the conversion that can be achieved. This limitation can be circumvented by cooling a hot effluent to a temperature at which the equilibrium is more favorable, and then contacting this stream with additional catalyst. Determine the catalyst requirements for a two-stage adiabatic fixed bed reactor with interstage cooling. Production requirements specified are 50 tons of  $\text{H}_2\text{SO}_4$  per day.

The feed composition (in mol%):  $\text{SO}_2$ , 8.0;  $\text{O}_2$ , 13.0;  $\text{N}_2$ , 79.0.

Total pressure	1 atm
First-stage inlet temperature	370°C
First-stage effluent temperature	560°C
Second-stage inlet temperature	370°C
Overall conversion of $\text{SO}_2$	99%

The heat capacities [in cal/(g-mol·K)]:  $\text{N}_2$ , 6.42 +  $1.34 \times 10^{-3}T$ ;  $\text{SO}_2$ ,  $9.52 + 3.64 \times 10^{-3}T$ ;  $\text{O}_2$ ,  $6.74 + 1.64 \times 10^{-3}T$ ;  $\text{SO}_3$ ,  $12.13 + 8.12 \times 10^{-3}T$ , where  $T$  is expressed in K. The heat of reaction at temperature  $T$  (k/g-mol) is  $-24.60 + 1.99 \times 10^{-3}T$  for  $T$  in K, the bulk density of catalyst is 0.6 g/cm<sup>3</sup>, and the reactor diameter is 6 ft.

**Table I12.8-1** Mole Table

Species	Initial moles	Moles at fraction conversion $f$	Mole fraction at conversion $f$
SO <sub>2</sub>	8.0	8.0(1 - $f$ )	8.0(1 - $f$ )/(100 - 4.0 $f$ )
N <sub>2</sub>	79.0	79.0	(79.0)/(100 - 4.0 $f$ )
O <sub>2</sub>	13.0	13.0 - (8.0 $f$ /2)	(13.0 - 4.0 $f$ )/(100 - 4.0 $f$ )
SO <sub>3</sub>	0.0	8.0 $f$	8.0 $f$ /(100 - 4.0 $f$ )
Total	100.0	100 - 4.0 $f$	1.000

The first-stage effluent temperature has been limited to 560°C to prevent excessive catalyst activity losses. The heat of reaction data are slightly inconsistent with the activation energies reported, but use of this expression demonstrates the ease with which temperature-dependent properties may be incorporated in the one dimensional model.

### Solution

Because the reaction rate per unit mass of catalyst and the reaction rate per unit volume of bed are simply related by the bulk density of the catalyst, one can readily adopt the procedures employed in Illustration 10.4 to solve this problem. However, we wish to indicate a slightly different approach that is appropriate for use in preliminary calculations that might be carried out using spreadsheet or equation solver software. By virtue of the arguments presented earlier, longitudinal dispersion of energy and matter are presumed to be negligible compared to convective transport. The appropriate equations for the one-dimensional plug flow model, assuming adiabatic operation, are then equation (12.7.49) for the energy balance:

$$G \frac{\partial}{\partial z} (C_p T) = r_v (-\Delta H) = r_m \rho_B (-\Delta H) \quad (\text{D})$$

and equation (12.7.39) for the material balance:

$$\frac{\partial}{\partial z} (C_A u_z) = \nu_A r_v = \nu_A r_m \rho_B \quad (\text{E})$$

Because there is a change in the number of moles on reaction, the volumetric expansion parameter  $\delta$  will be nonzero. Consequently,

$$u_z = u_0 (1 + \delta f) \frac{T}{T_0} \quad \text{and} \quad C_A = C_{A0} \left( \frac{1 - f}{1 + \delta f} \right) \left( \frac{T_0}{T} \right)$$

Equation (E) then becomes

$$\frac{\partial}{\partial z} (C_A u_z) = \frac{\partial}{\partial z} [C_{A0} u_0 (1 - f)] = -C_{A0} u_0 \frac{\partial f}{\partial z} \quad (\text{F})$$

Combining equations (E) and (F) and recognizing that  $\nu_A = -1$  gives

$$\frac{C_{A0} u_0}{\rho_B} \left( \frac{\partial f}{\partial z} \right) = r_m \quad (\text{G})$$

The partial pressures of the various species are numerically equal to their mole fractions because the total pressure is one atmosphere. These mole fractions can be expressed in terms of a single reaction progress variable—the degree of conversion—as indicated in a mole table (see Table I12.8-1).

It is convenient to break up the rate law for this catalytic reaction in the following manner to satisfy column width constraints.

$$\begin{aligned} \Theta_1 &= k_1 \left[ \frac{(8.0)(1 - f)}{(100 - 4.0f)} \right] \left[ \frac{13.0 - 4.0f}{100 - 4.0f} \right] \\ \Theta_2 &= k_2 \left[ \frac{8.0f}{100 - 4.0f} \right] \left[ \frac{13.0 - 4.0f}{100 - 4.0f} \right]^{1/2} \\ r_m &= \frac{\Theta_1 - \Theta_2}{\{[(8.0)(1 - f)]/[100 - 4.0f]\}^{1/2}} \end{aligned} \quad (\text{H})$$

The mass velocity  $G$  will be constant over the reactor length, and this quantity may be determined from the specified production rate and the reactor dimensions. To produce 50 tons/day of 100% H<sub>2</sub>SO<sub>4</sub>, the number of lb-mol of SO<sub>2</sub> that must be oxidized per second is

$$\begin{aligned} 50 \frac{\text{tons}}{\text{day}} \times \frac{\text{day}}{24 \text{h}} \times \frac{\text{h}}{3600 \text{ s}} \times \frac{2000 \text{ lb}}{\text{ton}} \\ \times \frac{\text{lb-mol H}_2\text{SO}_4}{98 \text{ lb H}_2\text{SO}_4} = 1.18 \times 10^{-2} \text{ lb-mol/s} \end{aligned}$$

For 99% conversion of the inlet SO<sub>2</sub>, the inlet molar flow rate must be

$$\frac{1.18 \times 10^{-2}}{0.99(0.08)} = 0.149 \text{ lb-mol/s}$$

The average molecular weight of the inlet gas is  $[(0.08)(64) + 0.13(32) + 0.79(28)] = 31.4$ . The mass velocity  $G$  is then  $\{(0.149)(31.4)/[\pi(6^2/4)]\} = 0.165 \text{ lb}/(\text{ft}^2 \cdot \text{s})$ .

We now wish to examine the heat capacity per unit mass to determine if it varies significantly with conversion. At the inlet conditions, the molal heat capacity of the gaseous feed will be equal to  $\sum(y_i C_{pi})$ . Hence, at  $f = 0$ , with  $C_p$  in units of cal/(g·K) and  $T$  in K, the heat capacity of the mixture per unit mass ( $C_{pm}$ ) may be calculated using

the following relation

$$C_{pm} = \frac{\sum (y_i C_{pi})}{\bar{M}}$$

where  $\bar{M}$  is the average molecular weight of the mixture (31.4).

$$\sum (y_i C_{pi}) = \begin{cases} 0.79 (6.42 + 1.34 \times 10^{-3}T) \\ + 0.08(9.52 + 3.64 \times 10^{-3}T) \\ 0.13(6.75 + 1.64 \times 10^{-3}T) \end{cases}$$

and

$$C_{pm} = \frac{\sum (y_i C_{pi})}{\bar{M}} = 0.214 + 4.98 \times 10^{-5}T \quad (I)$$

If complete conversion were to take place ( $f = 1$ ), the heat capacity of the effluent mixture could be evaluated in a similar manner using some of the entries in Table I12.8-1. The result is

$$C_{pm(f=1)} = 0.212 + 5.91 \times 10^{-5}T \quad (J)$$

Equations (I) and (J) indicate that for the temperature range of interest (640 to 830 K), the heat capacity per unit mass is substantially independent of the conversion level. Furthermore, the temperature-dependent contribution to the heat capacity will not vary much over the temperature range involved. Hence, without introducing errors comparable to those inherent in the use of a one-dimensional model, we may take the heat capacity as constant at 0.250 cal/(g·K) or 0.250 Btu/(lb·°F).

Combination of equations (G) and (D) indicates that

$$GC_p \frac{\partial T}{\partial z} = (-\Delta H) C_{A0} u_0 \frac{\partial f}{\partial z}$$

where we have used our assumption that  $C_p$  is a constant. Integration of this equation between the reactor inlet and axial location  $z$  gives us

$$GC_p (T - T_0) = (-\Delta H) C_{A0} u_0 (f - f_0) \quad (K)$$

The product  $C_{A0} u_0$  is the molar mass velocity of reactant A, which is equal to

$$\frac{0.08(0.149)}{\pi(6)^2/4} = 4.22 \times 10^{-4} \text{ lb-mol}/(\text{ft}^2 \cdot \text{s})$$

Substitution of numerical values into equation (K) gives

$$\begin{aligned} 0.165(0.250)1.8(T - T_0) \\ = 10^3(24.60 - 1.99 \times 10^{-3}T) \left[ \frac{454}{252} \right] \times \\ (4.22 \times 10^{-4})(f - f_0) \quad (L) \end{aligned}$$

where the 1.8 factor is necessary to convert  $T$  in K to consistent units. Hence, the relation between the temperature and the fraction conversion at any point in the adiabatic reactor is given by

$$T - T_0 = (251.9 - 0.0204T)(f - f_0)$$

or

$$T = \frac{T_0 + 251.9(f - f_0)}{1 + 0.0204(f - f_0)} \quad (M)$$

Equations (G) and (H) may be combined to obtain

$$\begin{aligned} \frac{C_{A0} u_0}{\rho_B} \frac{\partial f}{\partial z} &= \frac{k_1 [8.0(1-f)]^{1/2} (13.0 - 4.0f)}{(100 - 4.0f)^{3/2}} \\ &\quad - \frac{k_2 (8.0f) (13.0 - 4.0f)^{1/2}}{[(8.0)(1-f)]^{1/2} (100 - 4.0f)} \quad (N) \end{aligned}$$

Appropriate numerical values for use in this equation are

$$\begin{aligned} C_{A0} u_0 &= 4.22 \times 10^{-4} \text{ lb-mol}/(\text{ft}^2 \cdot \text{s}) \\ \rho_B &= 0.60 \text{ g/cm}^3 = 37.4 \text{ lb}/\text{ft}^3 \end{aligned}$$

$$\begin{aligned} k_1 &= e^{12.07} e^{-31,000/RT} \frac{\text{g-mol}}{\text{g catalyst} \cdot \text{atm}^{3/2} \cdot \text{s}} \\ &= 1.746 \times 10^5 e^{-31,000/RT} \frac{\text{lb-mol}}{\text{lb catalyst} \cdot \text{atm}^{3/2} \cdot \text{s}} \\ k_2 &= e^{22.75} e^{-53,600/RT} \frac{\text{g-mol}}{\text{g catalyst} \cdot \text{atm} \cdot \text{s}} \\ &= 7.589 \times 10^9 e^{-53,600/RT} \frac{\text{lb-mol}}{\text{lb catalyst} \cdot \text{atm} \cdot \text{s}} \end{aligned}$$

Substituting numerical values and writing equation (N) in terms of finite increments gives

$$\begin{aligned} \frac{\Delta f}{\Delta z} &= \frac{4.38 \times 10^{10} (1-f)^{1/2} (13 - 4f)}{e^{31,000/1.987T} (100 - 4f)^{3/2}} \\ &\quad - \frac{1.9 \times 10^{15} f (13 - 4f)^{1/2}}{e^{53,600/1.987T} (1-f)^{1/2} (100 - 4f)} \quad (O) \end{aligned}$$

Equations (M) and (O) may now be solved numerically to determine the bed depth corresponding to a specific conversion. If we rewrite equation (O) as

$$\Delta z = \bar{\beta}(\Delta f) \quad (P)$$

where  $\beta = \frac{(100-4f)}{\Gamma_1 - \Gamma_2}$  with

$$\Gamma_1 = \frac{4.38 \times 10^{10} (1-f)^{1/2} (13 - 4f) e^{-31,000/1.987T}}{(100 - 4f)^{1/2}}$$

and

$$\Gamma_2 = \frac{1.90 \times 10^{15} f (13 - 4f)^{1/2}}{(1-f)^{1/2}} e^{-53,600/1.987T}$$

The coefficient  $\beta$  may be evaluated at the beginning and the end of the conversion increment, and an average value employed to determine  $\Delta z$ .

At the inlet to the first reactor  $f = 0$  and  $T_0 = 370^\circ\text{C} = 643.16\text{ K}$ . Hence,

$$\beta_0 = \frac{(100)^{3/2}}{(4.38 \times 10^{10})(13)e^{-31,000/(1.987)(643.16)}} = 60.2$$

If we chose our first conversion increment as  $\Delta f = f_1 - f_0 = 0.05$ , equation (M) indicates that

$$T_1 = \frac{643.16 + 251.9(0.05)}{1 + (0.0204)(0.05)} = 655.09\text{ K}$$

Thus

$$\beta_1 = \frac{[100 - 4(0.05)]}{\Lambda_2 - \Lambda_1} = 40.2$$

with

$$\Lambda_2 = \frac{4.38 \times 10^{10}(1 - 0.05)^{1/2}[13 - 4(0.05)]}{[100 - 4(0.05)]^{1/2}e^{31,000/(1.987)(655.09)}}$$

and

$$\Lambda_1 = \frac{1.90 \times 10^{15}(0.05)[13 - 4(0.05)]^{1/2}}{(1 - 0.05)^{1/2}e^{53,600/(1.987)(655.09)}}$$

Thus

$$\Delta z = z_2 - z_1 = \frac{60.2 + 40.2}{2}(0.05) \text{ or } z_1 = 2.51\text{ ft}$$

**Table I12.8-2** Temperature and Conversion Profiles for Packed-Bed Reactor Combination

$f_A$	Stage 1		Stage 2		
	Temperature (K)	Catalyst depth (ft)	$f_A$	Temperature (K)	Catalyst depth (ft)
0	643	0.00	0.81	643	0.00
0.05	655	2.51	0.83	648	3.36
0.10	667	4.20	0.85	653	6.37
0.15	679	5.36	0.87	657	9.12
0.20	691	6.17	0.89	662	11.65
0.25	703	6.74	0.91	667	14.05
0.30	714	7.15	0.93	672	16.39
0.35	726	7.45	0.95	676	18.81
0.40	738	7.68	0.97	681	21.68
0.45	750	7.85	0.98	684	23.65
0.50	761	7.98	0.985	685	25.11
0.55	773	8.09	0.9875	685	26.21
0.60	785	8.18	0.99	686	28.76
0.65	796	8.25			
0.70	808	8.32			
0.75	820	8.38			
0.80	831	8.46			
0.81	833	8.48			

Proceeding to the next increment for  $\Delta f$  again equal to 0.05, we find that  $f_2 = 0.10$  and

$$T_2 = \frac{643.16 + 251.9(0.10)}{1 + 0.0204(0.10)} = 666.99\text{ K}$$

Thus,

$$\beta_2 = \frac{[100 - 4(0.1)]}{\Gamma_3 - \Gamma_2} = 27.4$$

with

$$\Gamma_3 = \frac{4.38 \times 10^{10}(1 - 0.1)^{1/2}[13 - 4(0.1)]}{[100 - 4(0.1)]^{1/2}e^{31,000/(1.987)(666.99)}}$$

and

$$\Gamma_2 = \frac{1.90 \times 10^{15}(0.1)[13 - 4(0.1)]^{1/2}}{(1 - 0.1)^{1/2}e^{53,600/(1.987)(666.99)}}$$

Consequently

$$\Delta z = z_2 - z_1 = \frac{40.2 + 27.4}{2}(0.05) = 1.69\text{ ft}$$

or

$$z_2 = 2.51 + 1.69 = 4.20\text{ ft}$$

The procedure above may be repeated to determine the depth of catalyst necessary to achieve a specific conversion level. Table I12.8-2 summarizes the results of such calculations. Notice that if the first-stage effluent is to be kept below  $560^\circ\text{C}$ , equation (M) indicates that the conversion

leaving this stage will be 0.81. More accurate results could be obtained using smaller values of  $\Delta f$ .

A similar procedure can be used to analyze the second stage of the reactor network. In this case, equation (M) becomes

$$T = \frac{643.16 + 251.9(f - 0.81)}{1 + 0.0204(f - 0.81)}$$

This equation and equation (O) suffice to determine the temperature and conversion profiles in the second stage of the reactor. The results of these calculations are also summarized in Table I12.8. Analysis of the tabular entries reveals that the bulk of the catalyst (77%) must be present in the second stage. Furthermore, a substantial fraction (27%) of the total is required merely to go from 95% to 99% conversion. Notice that the catalyst requirements for the second stage cannot be reduced significantly by changing the second-stage inlet temperature. The effluent conditions are approaching the equilibrium conditions for 99% conversion ( $T = 691\text{ K}$ ), and this restraint is largely responsible for the larger catalyst depth requirement in the second stage. Thermodynamic equilibrium does not limit the conversion in the first reactor, but catalyst deactivation processes do. We could, of course, consider the possibility of using a third stage to reduce catalyst requirements, but we would have to be willing to incur the associated capital charges.

The total weight of catalyst required is given by the product of the bulk density and the total reactor volume

$$\begin{aligned} \text{weight of catalyst} &= 37.4 \left[ \frac{\pi(6)^2}{4} \right] (8.48 + 28.76) \\ &= 39,400 \text{ lb or } 19.7 \text{ tons} \end{aligned}$$

In practice, one could oversize both stages and operate with reduced inlet temperatures that could subsequently be raised as catalyst deactivation occurs.

Before proceeding to Illustration 12.9, it is instructive to see if our assumption of constant total pressure was indeed appropriate. If one assumes  $\frac{1}{4}\text{-in.}$  spherical pellets, a nominal gas viscosity of  $0.09 \text{ lb/h-ft}$  and a bed porosity of 0.4, the Reynolds number of the gas is given by

$$N'_{\text{Re}} = \frac{D_p G}{\mu} = \frac{(\frac{1}{4})(\frac{1}{12})(0.165)(3600)}{0.09} = 137.5$$

From equation (12.7.4),

$$\left[ \frac{(\mathcal{P}_0 - \mathcal{P}_L) \rho}{G^2} \right] \frac{D_p}{L} \left[ \frac{\epsilon_B^3}{1 - \epsilon_B} \right] = \frac{150(1 - 0.4)}{137.5} + 1.75 = 2.40$$

where

$$\rho \approx \frac{PM}{RT} = \frac{1(31.4)}{0.73(670)(1.8)} = 3.6 \times 10^{-2} \text{ lb/ft}^3$$

Hence,

$$\begin{aligned} \mathcal{P}_0 - \mathcal{P}_L &= 240 \left( \frac{1 - 0.4}{0.4^3} \right) \left[ \frac{37.24}{\frac{1}{4} \left( \frac{1}{12} \right)} \right] \frac{(0.165)^2}{3.6 \times 10^{-2} \text{ ft-s}^2} \text{ lb} \\ &= 3.05 \times 10^4 \frac{\text{lb}_m}{\text{ft-s}^2} \times \frac{\text{lb}_f \text{s}^2}{32.2 \text{ lb}_m - \text{ft}} \times \frac{\text{ft}^2}{144 \text{ in}^2} \\ &= 6.57 \text{ psi} \end{aligned}$$

This pressure drop is a significant fraction of the total pressure (14.7 psi). Consequently, the analysis should be repeated, breaking up the reactor into segments that could be treated as having a constant average pressure. As an alternative, we could go to larger-diameter shorter beds of catalyst to reduce the pressure drop while maintaining the same conversion according to the one-dimensional homogeneous model. For example, by going to a 9-ft-diameter bed, the total bed length could be reduced from 37.24 to 16.6 ft and the pressure drop to 0.7 psi. Total catalyst requirements would be unchanged. Such trade-offs indicate why large-diameter beds with small length/diameter ratios are often employed in catalytic reactors.

### ILLUSTRATION 12.9 Production of Sulfur Trioxide in a Fixed Bed Reactor with Thermal Losses

While adiabatic operation may be approached by the use of efficient insulation techniques, heat losses from insulated reactors can be appreciable. Indeed, it may be prohibitively expensive to accomplish large reductions in thermal energy losses beyond a certain point, because of the material and labor costs involved.

Repeat the analysis of Illustration 12.8, assuming that the heat transfer to the surroundings can be characterized by an overall heat transfer coefficient based on the temperature difference between the reactor contents and ambient conditions ( $70^\circ\text{F}$ ). When based on the inside area of the reactor tube, the heat transfer coefficient has a numerical value of  $1.2 \text{ Btu}/(\text{hr-ft}^2 \cdot ^\circ\text{F})$  or  $6.0 \times 10^{-4} \text{ [Btu/(s-ft}^2 \cdot \text{K}]\text{.}}$  The second-stage inlet temperature may be taken as  $410^\circ\text{C}$  instead of  $370^\circ\text{C}$ , as in Illustration 12.8.

### Solution

The finite-difference form of the material balance equation developed in Illustration 12.8 [equation (P)] is again applicable:

$$\Delta z = \bar{\beta} \Delta f \quad (\text{A})$$

where

$$\frac{1}{\beta} = \frac{4.38 \times 10^{10} (1-f)^{1/2} (13-4f) e^{-31,000/1.987T}}{(100-4f)^{3/2}} - \frac{1.90 \times 10^{15} f (13-4f)^{1/2} e^{-53,600/1.987T}}{(1-f)^{1/2} (100-4f)}$$

However, the energy balance equation appropriate for use in this illustration differs from that employed in Illustration 12.8 because thermal losses through the reactor walls must be accounted for. This equation will be of the same general form as equation (12.7.48), but with the wall heat transfer coefficient replaced by an overall heat transfer coefficient ( $U$ ) and with a corresponding change in the temperature driving force.

$$G \frac{\partial}{\partial z} (C_p T) + \frac{4}{D_T} U (T - T_{\text{ambient}}) = (-\Delta H) r_v$$

The right side of this equation can be rewritten in terms of the fraction conversion using equations (E) and (G) of Illustration 12.8:

$$G \frac{\partial}{\partial z} (C_p T) + \frac{4}{D_T} U (T - T_{\text{ambient}}) = r_m \rho_B (-\Delta H) = (-\Delta H) C_{A0} u_0 \frac{\partial f}{\partial z}$$

Substitution of appropriate numerical values gives

$$0.165(0.250)(1.8) \frac{\partial T}{\partial z} + \frac{4}{6} (6.0 \times 10^{-4}) (T - 294.27) = 10^3 (24.60 - 1.99 \times 10^{-3} T) \left( \frac{454}{252} \right) (4.22 \times 10^{-4}) \frac{\partial f}{\partial z}$$

where  $T$  is in  $K$  and  $z$  is measured in feet. Evaluation of the numerical constants gives

$$dT = (251.9 - 0.0204T) df - 5.387 \times 10^{-3} (T - 294.27) dz$$

or, in finite difference form,

$$\Delta T = (251.9 - 0.0204T) \Delta f - 5.387 \times 10^{-3} (T - 294.27) \Delta z \quad (\text{B})$$

Equations (A) and (B) may now be solved to determine the temperature and conversion profiles for the reactor. As before, one may begin by choosing a small increment in the conversion. However, solution of the difference equations requires knowledge of the temperature at the end of the conversion increment. Consequently, a trial-and-error procedure is indicated. One assumes a value for the temperature at the end of the increment, computes  $\Delta z$  from equation (A), and checks the temperature assumption using equation (B). Under normal circumstances, the thermal loss term will be small compared to the heat of reaction term and we may obtain a reasonable first estimate of  $\Delta T$  by neglecting the thermal loss term. On the basis of Illustration 12.8, we shall

use  $T_1 = 655.09$  K as our first estimate of the temperature at the end of the first conversion increment ( $\Delta f = 0.05$ ). We will indicate the calculations for the first two conversion increments in some detail. From Illustration 12.8,  $\beta_0 = 60.2$ ,  $\beta_1 = 40.2$ , and  $\Delta z = 2.51$  ft, for an assumed temperature of 655.09 K ( $\Delta T = 11.93$  K). Substitution of these values in equation (B) gives

$$\Delta T = \left[ 251.9 - 0.0204 \left( \frac{655.09 + 643.16}{2} \right) \right] (0.05) - 5.387 \times 10^{-3} \left( \frac{655.09 + 643.16}{2} - 294.27 \right) \quad (2.51)$$

Thus,  $T_1 = 643.16 + 7.13 = 650.29$  K.

Because the preliminary estimate of  $\Delta T$  is significantly larger than the value calculated from equation (B), we should iterate using the last value of  $T_1$  as our initial estimate. For a temperature of 650.29,  $\beta_1 = 47.9$ . Thus, from equation (A),

$$\Delta z = \frac{60.2 + 47.9}{2} (0.05) = 2.70 \text{ ft}$$

and from equation (B),

$$\Delta T = \left[ 251.9 - 0.0204 \left( \frac{650.29 + 643.16}{2} \right) \right] (0.05) - 5.387 \times 10^{-3} \left( \frac{650.29 + 643.16}{2} - 294.27 \right) \quad (2.70) \\ = 6.81 \text{ K}$$

or  $T_1 = 649.97$  K. This new value is in much better agreement with the initial estimate of 650.29. To achieve the desired degree of agreement, one may iterate as often as necessary.

For the second conversion increment ( $\Delta f = 0.05$ ;  $f = 0.10$ ), we will assume that at the end of the increment,  $T = 657$  K ( $\Delta T = 7.03$  K). Here,

$$\beta_2 = 39.0$$

and from equation (A),

$$\Delta z = \frac{48.5 + 39.0}{2} (0.05) = 2.19 \text{ ft}$$

where a revised value of  $\beta_1$  corresponding to 649.97 K has been employed.

From equation (B),

$$\Delta T_2 = \left[ 251.9 - 0.0204 \left( \frac{657 + 649.97}{2} \right) \right] (0.05) - 5.387 \times 10^{-3} \left( \frac{657 + 649.97}{2} - 294.27 \right) \quad (2.19) \\ = 7.69 \text{ K}$$

Thus,  $T_2 = 649.97 + 7.69 = 657.66$  K. A second iteration using this temperature as an initial estimate gives  $T_2 = 657.69$  K and  $\Delta z = 2.17$  ft.

**Table I12.9** Conversion and Temperature Profiles for Packed Bed Reactor

First stage			Second stage		
Conversion, $f$	Temperature, $T$ (K)	Catalyst depth, $z$ (ft)	Conversion, $f$	Temperature, $T$ (K)	Catalyst depth, $z$ (ft)
0.00	643.16	0	0.87	683.16	0
0.05	650.0	2.70	0.89	685.6	1.12
0.10	657.7	4.87	0.91	687.9	2.29
0.15	666.3	6.55	0.93	689.9	3.56
0.20	675.6	7.84	0.95	691.5	5.04
0.25	685.5	8.81	0.97	691.8	7.12
0.30	695.8	9.54	0.98	690.6	8.81
0.35	706.5	10.09	0.985	688.8	10.22
0.40	717.4	10.50	0.9875	686.9	11.36
0.45	728.6	10.81	0.99	683.1	13.45
0.50	739.8	11.05			
0.55	751.2	11.24			
0.60	762.7	11.39			
0.65	774.2	11.51			
0.70	785.7	11.62			
0.75	797.2	11.72			
0.80	808.7	11.82			
0.85	820.0	11.97			
0.86	822.3	12.02			
0.87	824.4	12.14			

In the manner described above we may proceed downstream in the reactor until we either reach the desired conversion level, run into thermodynamic limitations on the reaction rate, or exceed the effluent temperature constraint (see Table I12.9). Such calculations are readily carried out in a spreadsheet format to accomplish the necessary iterations. In the present case, thermodynamic constraints on the rate indicate that the first-stage effluent should correspond to a conversion in the vicinity of 0.87 and an effluent temperature near 824.4 K. Beyond this point, the system is so close to thermodynamic equilibrium that substantial increments in the reactor length do not produce noticeable increments in the conversion.

Here, one may employ a higher temperature for the second-stage feed and still achieve the desired conversion level. The conversion and temperature profiles as calculated from equations (A) and (B) are given in Table I12.9. Analysis of the tabular entries indicates that the total weight of catalyst required is equal to

$$37.4 \left[ \frac{\pi(6)^2}{4} \right] (12.14 + 13.45) = 27,060 \text{ lb} = 13.53 \text{ tons}$$

This value is considerably less than that obtained for purely adiabatic operation (19.7 tons). The heat losses tend to partially remove thermodynamic constraints on the reaction rate and permit a closer approach to the optimum

temperature profile corresponding to minimum catalyst requirements.

A few words concerning the results of our analyses in Illustrations 12.8 and 12.9 are in order. Obviously, better estimates of the catalyst requirements could be obtained by using smaller conversion increments. We have not attempted to fully optimize the reactor stages in terms of catalyst minimization. Furthermore, we have again neglected pressure drop in each stage. Further calculations would remedy each of the aforementioned shortcomings of the analysis. They are readily accomplished with the aid of machine computation.

### 12.7.2.2 The Two Dimensional, Pseudo Homogeneous Model of Fixed Bed Reactors

Two dimensional models permit more realistic simulation of fixed bed reactor behavior than the one-dimensional models discussed previously. Experimental measurements indicate that the fluid temperature and composition are not uniform across a section of the tube normal to the flow. The one dimensional models discussed earlier neglect the radial resistance to heat and mass transfer and thereby assume a uniform temperature and composition for each longitudinal position. This assumption is a vast oversimplification when

reactions with large heat effects are considered. Whenever there is extensive heat exchange between the packed bed reactor and its surroundings, one requires at least a two dimensional model to simulate the reactor performance. In such cases, the design engineer requires a model that predicts the detailed temperature and composition patterns in the reactor to be able to avoid hot spots along the reactor axis when they would be detrimental for reasons of selectivity, catalyst deactivation, and so on.

A complete two dimensional model would account for the radial distribution of velocity, for the radial concentration and temperature gradients in terms of Péclet numbers that themselves varied with radial location, and for axial dispersion of heat and mass. With machine computation, such considerations may be handled if the cost in computer time and programming effort can be withstood. However, the most significant aspects of two-dimensional models can be demonstrated by considering simple two-dimensional models. Such models assume that the mass velocity  $G$  and the radial Péclet numbers for heat and mass transfer are constant across the tube diameter and that the effective thermal conductivity and effective dispersion contributions to longitudinal transport of energy and mass are insignificant (compared to the convective transport terms). The appropriate material and energy balance equations that provide a two dimensional description of the reactor performance at steady state have been derived earlier in discussing general aspects of heat transfer and of mass conservation in packed beds. They consist of an alternative form of equation (12.7.18) for energy conservation:

$$G \frac{\partial(C_p T)}{\partial z} - \kappa_R^* \left( \frac{\partial^2 T}{\partial R^2} + \frac{1}{R} \frac{\partial T}{\partial R} \right) + r_v \Delta H = 0 \quad (12.7.50)$$

and a simplified form of equation (12.7.28) for mass conservation:

$$D_R \left( \frac{\partial^2 C_A}{\partial R^2} + \frac{1}{R} \frac{\partial C_A}{\partial R} \right) - \frac{\partial(C_A u_z)}{\partial z} + v_A r_v = 0 \quad (12.7.51)$$

These coupled partial differential equations can be solved for the temperature and composition at any point in the catalyst bed by using numerical procedures to solve the corresponding difference equations. As boundary conditions, one needs to know the temperature and composition profile across the tube diameter at the reactor inlet. In addition, the solution must satisfy the requirements of cylindrical symmetry that

$$\frac{\partial C_A}{\partial R} = 0 \quad \text{at } R = 0 \text{ for all } z \quad (12.7.52)$$

$$\frac{\partial T}{\partial R} = 0 \quad \text{at } R = 0 \text{ for all } z \quad (12.7.53)$$

and that

$$\frac{\partial C_A}{\partial R} = 0 \quad \text{at } R = \frac{D_T}{2} = R_0 \text{ (tube wall)} \quad (12.7.54)$$

because the tube is not permeable to the fluid. The boundary condition at the wall on the energy conservation equation can be framed as a requirement that the heat flux at the wall be of the following form:

$$q = -\kappa_R^* \left( \frac{\partial T}{\partial R} \right)_{R_0} = h_w (T_{R_0} - T_w) \quad (12.7.55)$$

where  $T_w$  is the inside wall surface temperature,  $T_{R_0}$  the local temperature of the adjacent fluid, and  $h_w$  is a heat transfer coefficient. This approach in essence assumes a temperature discontinuity at the wall. Alternative methods of formulating this constraint have also been proposed (95, 96, 114), together with empirical methods of evaluating the heat transfer coefficients introduced by each method.

Various numerical procedures may be employed to solve the difference equations corresponding to equations (12.7.50) and (12.7.51). Many sophisticated numerical procedures may be employed, but they are more properly treated in textbooks dealing with numerical methods or more advanced texts in chemical reactor design.

For a general introduction to some of the techniques employed to solve difference equations of the types encountered in chemical engineering, consult the text by Lapidus (115). Detailed numerical examples of one method of numerical solution to the two dimensional reactor problem are contained in the texts of Smith (116) and Jenson and Jeffreys (117).

## 12.8 DESIGN OF FLUIDIZED BED CATALYTIC REACTORS

The design of a commercial scale fluidized bed reactor for a new process is in many respects one of the most challenging technical projects to which a practicing chemical engineer can be assigned. Even a superficial study of an operating unit reveals its intrinsic complexity. Such systems pose tremendous analytical problems for someone trying to develop realistic mathematical models of the interactions between the chemical reaction phenomena and the various physical transport processes that occur in these reactors. Not only do we have to worry about the possibilities of intraparticle and external mass and heat transfer limitations of the types discussed previously, but we must also be concerned with the complexity of the fluid–solid contacting process and the manner in which the gas and solid catalyst are distributed throughout the reactor.

Within a fluidized bed, low-density regions or “gas bubbles” are formed at apparently unpredictable rates.

These bubbles may subsequently coalesce, split, or grow, perhaps even to the extent that their size approaches the physical dimensions of the reactor. Indeed, in some cases it is necessary to provide for reactor internals to limit bubble size and the problems of slugging, poor contacting, and mechanical vibration, which become serious when the bubbles become too large. Experimental studies clearly demonstrate that there is significant movement of gas from the high solids density regions through the bubbles and back to the high density regions. The extent of this interchange between the gas bubbles and the remainder of the bed has obvious implications with respect to the degree of conversion that can be expected in a fluidized bed reactor. The bubbles are essentially empty, although from time to time a quantity of particles may rain through the bubble from the roof. In some cases, this movement may cause the bubble to split. The lowest third of a sphere enclosing the bubble contains a wake of particles that travel upward with the bubble. Solid particles also move in streamlines around each rising bubble, so that a spout of material is also drawn up behind the bubble. The solids moving upward in the wake behind the bubble and in the spout below provide rapid mixing of solids from bottom to top.

These factors combine to make it extremely difficult not only to develop predictive analytical models of the performance of such systems, but also to scale up experimental data from laboratory operations, particularly when the commercial scale equipment may contain baffles, heat exchangers, and other internal fixtures within the bed. Some useful models have been developed for fluidized beds, but the design of industrial scale reactors is generally dominated by empirical correlations and component designs that have proven useful in past generations of equipment. This feature is particularly true of the equipment used for distribution of the incoming gas. This component has a marked effect on the solids recirculation pattern and on potential channeling through the bed.

The velocity at which gas flows through the dense phase corresponds approximately to the velocity that produces incipient fluidization. The bubbles rise, however, at a rate that is nearly an order of magnitude greater than the minimum fluidization velocity. In effect, then, as a consequence of the movement of solids within the bed and the interchange of fluid between the bubbles and the particle rich regions of the bed, there are wide disparities in the residence times of various fluid elements within the reactor and in the times that the fluid elements are effectively in contact with the catalyst particles.

From the standpoint of attempting to develop mathematical models for the simulation of fluidized-bed reactors, one must determine if the phenomena mentioned above and other aspects of the behavior of fluidized beds can

be described in terms of a relatively small number of parameters. In particular, those aspects of the behavior of fluidized beds that have a significant influence on the conversion achieved must be characterized adequately by the model if it is to be useful for purposes of reactor design. Many models, especially if they are sufficiently complex and contain many "constants," can describe a given set of data equally well. However, if the models are to be useful for design purposes, it should be possible to determine the parameters appearing therein from simple laboratory experiments or from correlations of experimental data. Indeed, the utility of the model is judged by the success obtained when extrapolating data from one set of experimental reaction conditions (usually, bench or pilot scale experiments) to accurately predict the behavior of a large scale unit.

The physical situation in a fluidized-bed reactor is far too complicated to be modeled by an ideal plug flow reactor or an ideal stirred-tank reactor, although under certain conditions, either of these ideal models may provide a fair representation of the behavior of a fluidized-bed reactor. In other cases, the behavior of the system can be characterized as plug flow modified by longitudinal dispersion, and the unidimensional pseudo homogeneous model (Section 12.7.2.1) can be employed to describe the fluidized-bed reactor. As an alternative, a cascade of CSTRs (Section 11.1.3.2) may be used to model the fluidized-bed reactor. Unfortunately, none of these models provides an adequate representation of reaction behavior in fluidized beds, particularly when there is appreciable bubble formation within the bed. This situation arises mainly because knowledge of the residence time distribution of the gas in the bed is insufficient to permit accurate prediction of degrees of conversion, because there is not an equal distribution of catalyst between the bubble and dense phases. It is the presence of bubbles and their effect on gas-solid contacting and mixing that lies at the root of the problem and that causes the discrepancy between the residence time distribution (easily measured) and the contact time distribution (not easily measured).

Because of the inadequacies of the aforementioned models, a number of papers in the 1950s and 1960s developed alternative mathematical descriptions of fluidized beds that explicitly divided the reactor contents into two phases, a bubble phase and an emulsion or dense phase. The bubble or lean phase is presumed to be essentially free of solids, so that little, if any, reaction occurs in this portion of the bed. Reaction takes place within the dense phase, where virtually all of the solid catalyst particles are found. This phase may also be referred to as a particulate phase, an interstitial phase, or an emulsion phase by various authors. Figure 12.18 is a schematic representation of two-phase models of fluidized beds. Some models also

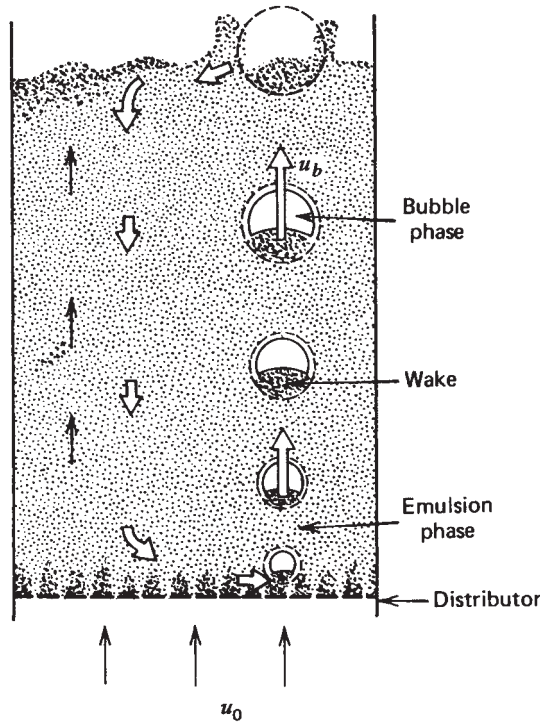


**Figure 12.18** Basic two-phase model of fluidized bed. Open arrows indicate movements of solids. Solid arrows indicate movement of gas. The symbols  $u_0$  and  $u_b$  represent the superficial velocity of the gas and the velocity at which the bubble rises, respectively. [Adapted from D. Kunii and O. Levenspiel, Bubbling Bed Model in *I & EC Fundam.*, 7(3), 447 (1968). Copyright ©1968. Used with permission of the American Chemical Society.]

define a cloud phase as the region of space surrounding the bubble that acts as a source and a sink for gas exchange with the bubble.

On the basis of different assumptions about the nature of the fluid and solid flow within each phase and between phases as well as about the extent of mixing within each phase, it is possible to develop many different mathematical models of the two-phase type. Pyle (118), Rowe (119), and Grace (120) have critically reviewed models of these types. Treatment of these models is clearly beyond the scope of this book. In many cases, insufficient data exist to provide critical tests of model validity. This situation is especially true of large-scale reactors that are the systems of greatest interest from industry's point of view. The student should understand, however, that there is an ongoing effort to develop mathematical models of fluidized-bed reactors that will be useful for design purposes. Our current capabilities in this area have not been developed to the extent that they have in fixed bed reactor design, but fluidized beds are inherently much more complex systems. Indeed, the design of fluidized bed reactors is largely dominated by empirical procedures, particularly with

regard to the design and operation of the gas distributor and the construction of reactor internals. Treatments of mathematical models of fluidized bed reactor performance are appropriate subject material for advanced texts in reactor design [see Kunii and Levenspiel (4) and Davidson and Harrison (121)].

## LITERATURE CITATIONS

- GOODMAN, D. R., Handling and Using Catalysts on the Plant, in the *Catalyst Handbook*, 2nd ed., M. V. TWIGG (Ed.), Wolfe Publishing, London, 1989.
- BARTHOLOMEW, C. H., and FARRAUTO, R. J., *Fundamentals of Industrial Catalytic Processes*, 2nd ed., Wiley, New York, 2005.
- GIANETTO, A., and SPECCHIA, V., *Chem. Eng. Sci.*, **47**, 3197 (1992).
- KUNII, D., and LEVENSPIEL, O., *Fluidization Engineering*, 2nd ed., Butterworth Heinemann, Newton, MA, 1991.
- YANG, W.-C. (Ed.), *Handbook of Fluidization and Fluid-Particle Systems*, Marcel Dekker, New York, 2003.
- SATTERFIELD, C. N., *Mass Transfer in Heterogeneous Catalysis*, pp. 107–128, MIT Press, Cambridge, MA, 1970.
- WANG, T., WANG, J., and JIN, Y., *Ind. Eng. Chem. Res.*, **46**, 5824 (2007).
- POLING, B. E., PRAUSNITZ, J. M., and O'CONNELL, J. P., *The Properties of Gases and Liquids*, 5th ed., McGraw-Hill, New York, 2001.
- EVANS, R. B., III, WATSON, G. M., and MASON, E. A., *J. Chem. Phys.*, **35**, 2076 (1961).
- SCOTT, D. S., and DULLIEN, F. A. L., *AIChE J.*, **8**, 113 (1962).
- ROTHFELD, L. B., *AIChE J.*, **9**, 19 (1963).
- BIRD, R. B., STEWART, W. E., and LIGHTFOOT, E. N., *Transport Phenomena*, 2nd ed., Chaps. 17 and 19, Wiley, New York, 2002.
- SMITH, J. M., *Chemical Engineering Kinetics*, 2nd ed., p. 403, McGraw-Hill, New York, 1970.
- SATTERFIELD, C. N., op. cit., pp. 47–54, 1970.
- BARRER, R. M., *Appl. Mater. Res.*, **2**(3), 129 (1963).
- Wikipedia*, Surface Diffusion, Nov. 18, 2009.
- SATTERFIELD, C. N., op. cit., pp. 37–40, 1970.
- WICKE, E., and KALLENBACH, R., *Kolloid Z.*, **97**, 135 (1941).
- BARRER, R. M., *J. Phys. Chem.*, **57**, 35 (1953).
- THIELE, E. W., *Ind. Eng. Chem.*, **31**, 916 (1939).
- DAMKÖHLER, G., *Der Chemie-Ing.*, **3**, 430 (1937).
- ZELDOVITCH, Y. B., *Acta Physicochim. URSS*, **10**, 583 (1939), in English. Also *Z. Fiz. Chim.*, **13**, 163 (1939).
- WHEELER, A., *Adv. Catal.*, **3**, 249 (1951).
- WHEELER, A., *Catalysis*, **2** (104), P. H. EMMETT (Ed.), Reinhold, New York, 1955.
- WEISZ, P. B., *Adv. Catal.*, **13**, 137 (1962).
- WEISZ, P. B., and HICKS, J. S., *Chem. Eng. Sci.*, **17**, 265 (1962).
- WEISZ, P. B., *Chem. Eng. Prog. Symp. Ser.*, **55**(25), 29 (1959).
- WEISZ, P. B., and PRATER, C. D., *Adv. Catal.*, **6**, 143 (1954).
- WICKE, E., and KALLENBACH, R., *Kolloid Z.*, **97**, 135 (1941).
- WICKE, E., and BROTZ, W., *Chem.-Ing.-Tech.*, **21**, 219 (1949).
- WICKE, E., and HEDDEN, K., *Z. Elektrochem.*, **57**, 636 (1953).
- WICKE, E., *Chem.-Ing.-Tech.*, **29**, 305 (1957).
- ARIS, R., *Chem. Eng. Sci.*, **6**, 262 (1957).
- ARIS, R., *Ind. Eng. Chem. Fundam.*, **4**, 227 (1965).
- ARIS, R., *Ind. Eng. Chem. Fundam.*, **4**, 487 (1965).
- ARIS, R., *The Mathematical Theory of Diffusion and Reaction in Permeable Catalysts*, Vols. I and II, Clarendon Press, Oxford, 1975.
- EDWARDS, M. E., VILLA, C. M., CHAPMAN, T. W., and HILL, C. G., Jr., *Ind. Eng. Chem. Res.*, **35**, 712 (1996).

38. CORRIGAN, T. E., GARVER, J. C., RASE, H. F., and KIRK, R. S., *Chem. Eng. Prog.*, **49**, 603 (1953).
39. WHEELER, A., op. cit., p. 136, 1955.
40. SATTERFIELD, C. N., op. cit., pp. 152, 1970.
41. SATTERFIELD, C. N., op. cit., pp. 134, 1970.
42. SATTERFIELD, C. N., op. cit., pp. 135–138, 1970.
43. LUSS, D., and AMUNDSON, N. R., *AIChE J.*, **13**, 759 (1967).
44. ARIS, R., *Introduction to the Analysis of Chemical Reactors*, Prentice-Hall, Englewood Cliffs, NJ, 1965.
45. WEEKMAN, V. W., JR., and GORING, R. L., *J. Catal.*, **4**, 260 (1965).
46. WEEKMAN, V. W., JR., *J. Catal.*, **5**, 44 (1966).
47. CHU, C., and HOUGEN, O. A., *Chem. Eng. Sci.*, **17**, 167 (1962).
48. ROBERTS, G. W., and SATTERFIELD, C. N., *Ind. Eng. Chem. Fundam.*, **4**, 288 (1965).
49. ROBERTS, G. W., and SATTERFIELD, C. N., *Ind. Eng. Chem. Fundam.*, **5**, 317 (1966).
50. KNUDSEN, C. W., ROBERTS, G. W., and SATTERFIELD, C. N., *Ind. Eng. Chem. Fundam.*, **5**, 325 (1966).
51. SATTERFIELD, C. N., op. cit., pp. 176–200, 1970.
52. KAO, H. S-P., and SATTERFIELD, C. N., *Ind. Eng. Chem. Fundam.*, **7**, 664 (1968).
53. WIJNGAARDEN, R. J., WESTERTURP, K. R., and KRONBERG, A., *Industrial Catalysis: Optimizing Catalysts and Processes*, Wiley-VCH, Weinheim, Germany, 1998.
54. WOODSIDE, W., and MESSMER, J. H., *J. Appl. Phys.*, **32**, 1688 (1961).
55. BUTT, J. B., *AIChE J.*, **11**, 106 (1965).
56. MADZHIDOV, K., *J. Eng. Phys. Thermophys.*, **69**, 120 (1996).
57. DAMKÖHLER, G., *Z. Phys. Chem.*, **A193**, 16 (1943).
58. SCHILSON, R. E., and AMUNDSON, N. R., *Chem. Eng. Sci.*, **13**, 226, 237 (1961).
59. BEEK, J., *AIChE J.*, **7**, 337 (1961).
60. TINKLER, J. D., and PIGFORD, R. L., *Chem. Eng. Sci.*, **15**, 326 (1961).
61. PETERSEN, E. E., *Chem. Eng. Sci.*, **17**, 987 (1962).
62. TINKLER, J. D., and METZNER, A. B., *Ind. Eng. Chem.*, **53**, 663 (1961).
63. WEISZ, P. B., and HICKS, J. S., *Chem. Eng. Sci.*, **17**, 265 (1962).
64. MAYMO, J. A., CUNNINGHAM, R. E., and SMITH, J. M., *Ind. Eng. Chem. Fundam.*, **5**, 280 (1966).
65. CUNNINGHAM, R. A., CARBERRY, J. J., and SMITH, J. M., *AIChE J.*, **11**, 636 (1965).
66. WHEELER, A., *Adv. Catal.*, **3**, 249, Academic Press, New York, 1951.
67. WHEELER, A., *Catalysis*, **2**, 105, P. H. EMMETT (Ed.), Reinhold, New York (copyright © 1955 by Litton Educational Publishing, Inc.).
68. SMITH, J. M., op. cit., pp. 457–462.
69. CARBERRY, J. J., *Chem. Eng. Sci.*, **17**, 675 (1962).
70. OSTERGAARD, K., *Acta Chem. Scand.*, **15**, 2037 (1961).
71. BUTT, J. B., *Chem. Eng. Sci.*, **21**, 275 (1966).
72. HUTCHINGS, J., and CARBERRY, J. J., *AIChE J.*, **12**, 20 (1966).
73. PETERSEN, E. E., *Chemical Reaction Analysis*, pp. 129–164, Prentice-Hall, Englewood Cliffs, NJ, 1965.
74. BIRD, R. B., STEWART, W. E., and LIGHTFOOT, E. N., *Transport Phenomena*, 2nd ed., Wiley, New York, 2002.
75. GEANKOPLIS, C. J., *Transport Processes and Separation Process Principles (Includes Unit Operations)*, 4th ed., Prentice Hall, Englewood Cliffs, NJ, 2003.
76. McCABE, W. L., SMITH, J. C., and HARRIOTT, P., *Unit Operations of Chemical Engineering*, 7th ed., McGraw-Hill, New York, 2004.
77. CHILTON, T. H., and COLBURN, A. P., *Ind. Eng. Chem.*, **26**, 1183 (1934).
78. COLBURN, A. P., *Trans. AIChE*, **29**, 174 (1933).
79. ACETIS, J., and THODOS, G., *Ind. Eng. Chem.*, **52**, 1003 (1960).
80. PETROVIC, L. J., and THODOS, G., *Ind. Eng. Chem. Fundam.*, **7**, 274 (1968).
81. WILSON, E. J., and GEANKOPLIS, C. J., *Ind. Eng. Chem. Fundam.*, **5**, 9 (1966).
82. SATTERFIELD, C. N., *Mass Transfer in Heterogeneous Catalysis*, pp. 79–97, MIT Press, Cambridge, 1970.
83. KUNII, D., and LEVENSPIEL, O., op. cit., Chap. 7.
84. BEEK, W. J., *Mass Transfer in Fluidized Beds*, in *Fluidization*, J. F. DAVIDSON and D. HARRISON (Ed.), Academic Press, New York, 1971.
85. CHU, J. C., KALIL, J., and WETTEROTH, W. A., *Chem. Eng. Prog.*, **49**, 141 (1953).
86. RICCETTI, R. E., and THODOS, G., *AIChE J.*, **7**, 442 (1961).
87. SEN GUPTA, A., and THODOS, G., *Chem. Eng. Prog.*, **58** (7), 58 (1962).
88. OLSON, R. W., SCHULER, R. W., and SMITH, J. M., *Chem. Eng. Prog.*, **46**, 614 (1950).
89. YOSHIDA, F., RAMASWAMI, D., and HOUGEN, O. A., *AIChE J.*, **8**, 5 (1962).
90. ARGO, W. B., and SMITH, J. M., *Chem. Eng. Prog.*, **49**, 1443 (1953).
91. STEWART, W. E., *AIChE J.*, **9**, 528 (1963).
92. SHERWOOD, T. K., *Trans. AIChE*, **39**, 583 (1943).
93. KETTENRING, K. N., MANDERFIELD, E. L., and SMITH, J. M., *Chem. Eng. Prog.*, **46**, 139 (1950).
94. SMITH, J. M., op. cit., Chaps 10–12.
95. FROMENT, G. F., “Analysis and Design of Fixed Bed Catalytic Reactors,” in *Chemical Reaction Engineering, Adv. Chem. Ser.* **109**, 1, American Chemical Society, Washington, DC, 1972.
96. FROMENT, G. F., *Fifth European Symposium on Chemical Reaction Engineering*, Elsevier, Amsterdam, 1972.
97. GREEN, D. W., and PERRY, R. H., *Perry’s Chemical Engineer’s Handbook*, 8th ed., McGraw-Hill, New York, 2007.
98. ERGUN, S., *Chem. Eng. Prog.*, **48**, 93 (1952).
99. WEHNER, J. F., and WILHELM, R. H., *Chem. Eng. Sci.*, **6**, 89 (1956).
100. ARIS, R., and AMUNDSON, N. R., *AIChE J.*, **3**, 280 (1957).
101. JAKOB, M., *Heat Transfer*, p. 553, Wiley, New York, 1957.
102. COLBURN, A. P., *Ind. Eng. Chem.*, **23**, 910, (1931).
103. CALDERBANK, P. H., and POGORSKI, L. A., *Trans. Inst. Chem. Engrs. London*, **35**, 195 (1957).
104. LEVA, M., *Ind. Eng. Chem.*, **42**, 2498 (1950).
105. ARGO, W. B., and SMITH, J. M., *Chem. Eng. Prog.*, **49**, 443 (1953).
106. SMITH, J. M., op. cit., pp. 513–522.
107. BEEK, J., *Adv. Chem. Eng.*, **3**, 229 (1962).
108. CARBERRY, J. J., and WENDEL, M., *AIChE J.*, **9**, 132 (1963).
109. RAYMOND, L. R., and AMUNDSON, N. R., *Can. J. Chem. Eng.*, **42**, 173 (1964).
110. LUSS, D., and AMUNDSON, N. R., *Chem. Eng. Sci.*, **22**, 253 (1967).
111. LUSS, D., *Chem. Eng. Sci.*, **23**, 1249 (1968).
112. HLAVACEK, V., and HOFMANN, H., *Chem. Eng. Sci.*, **25**, 173, 187 (1970).
113. CALDERBANK, P. H., *Chem. Eng. Prog.*, **49**, 585 (1953).
114. FROMENT, G. F., *Ind. Eng. Chem.*, **59**, 18 (1967).
115. LAPIDUS, L., *Digital Computation for Chemical Engineers*, McGraw-Hill, New York, 1960.
116. SMITH, J. M., op. cit., pp. 536–547.
117. JENSON, V. G., and JEFFREYS, G. V., *Mathematical Methods in Chemical Engineering*, pp. 412–428, Academic Press, New York, 1963.
118. PYLE, D. L., in “Chemical Reaction Engineering,” *ACS Adv. Chem. Ser.* **109**, 106 (1972).
119. ROWE, P. N., *Fifth European Symposium on Chemical Reaction Engineering*, Elsevier, Amsterdam, 1972.
120. GRACE, J. R., *AIChE Symp. Ser.*, **67**(116), 159 (1971).
121. DAVIDSON, J. F., and HARRISON, D., *Fluidized Particles*, Cambridge University Press, London, 1963.

## PROBLEMS

- 12.1** Thiophene ( $C_4H_4S$ ) is representative of the organic sulfur compounds that are hydrogenated in the commercial hydrodesulfurization of petroleum naphtha. Estimate both the combined and effective diffusivities for thiophene in hydrogen at 660 K and 3.04 MPa in a catalyst with a BET surface area of  $168 \text{ m}^2/\text{g}$ , a porosity of 0.40, and an apparent pellet density of  $1.40 \text{ g}/\text{cm}^3$ . A narrow pore size distribution and a tortuosity factor of 2.5 may be assumed. The following Lennard-Jones parameters for thiophene and hydrogen may be useful in estimating the ordinary molecular diffusivity.

	$\sigma$ (nm)	$\varepsilon/k_B$ (K)
Thiophene	0.562	454
Hydrogen	0.2827	59.7

Use your best judgment in estimating the binary molecular diffusivity. However, it may be assumed that the value of interest lies in the region where the binary molecular diffusivity is inversely proportional to the pressure.

- 12.2** R. H. Villet and R. H. Wilhelm [*Ind. Eng. Chem.*, **53**, 837 (1961)] studied the Knudsen diffusion of hydrogen in porous silica-alumina cracking catalyst pellets. They used an apparatus of the type depicted in Figure P12.2. The entire apparatus was immersed in a constant temperature bath at  $25^\circ\text{C}$ . The upstream hydrogen pressure was maintained constant at 770 torr. The pressure in the constant volume container ( $500 \text{ cm}^3$ ) varied with time in the following manner:

Time, $t$ (min)	Pressure (torr)
0	610.0
20	611.0
40	612.1
60	613.2
80	614.3
100	615.5

For present purposes, the pellet may be considered as cylindrical with a diameter of 0.32 cm. and a length of

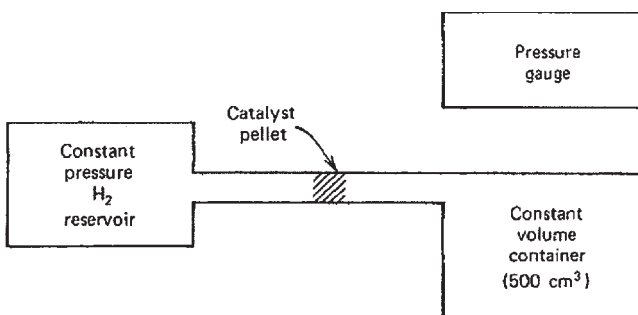


**Figure P12.2** Schematic diagram of diffusivity measurement apparatus.

0.12 cm. The porosity is 0.464 and the specific surface area is  $243 \text{ m}^2/\text{g}$ . What is the effective diffusivity of the hydrogen under these conditions?

It may be assumed that the accumulation of hydrogen within the pellet is negligible and that the pellet may be treated as being in a quasi steady state condition. The finite difference form of Fick's first law may be used to determine the flow rate of hydrogen through the pellet. The diffusion constant appearing in this equation may be considered an effective Knudsen diffusion coefficient.

- 12.3** This problem was contributed by the late Professor C. N. Satterfield of MIT and is used with his permission.

In a discussion of catalyst testing procedures, D. A. Dowden and G. A. Bridger [*Adv. Catal.*, **9**, 669 (1957)] reported the effect of particle size and mass velocity on the rate of oxidation of  $\text{SO}_2$  to  $\text{SO}_3$ . They studied this reaction at  $400$  and at  $470^\circ\text{C}$  using commercial catalyst pellets (5.88 mm in diameter) and two sizes of crushed pellets (2.36 and 1.14 mm in diameter). In all runs the feed stream composition was kept constant.

The effect of mass velocity on the conversion rate was studied using a tube of fixed diameter that was filled with a sample of a given catalyst diameter to give beds with volumes of either 10 or 20  $\text{cm}^3$ . At a constant ratio of catalyst weight to reactant feed rate, this method of varying the bed volume has the effect of varying the mass velocity through the bed. The data in Figure P12.3 indicate

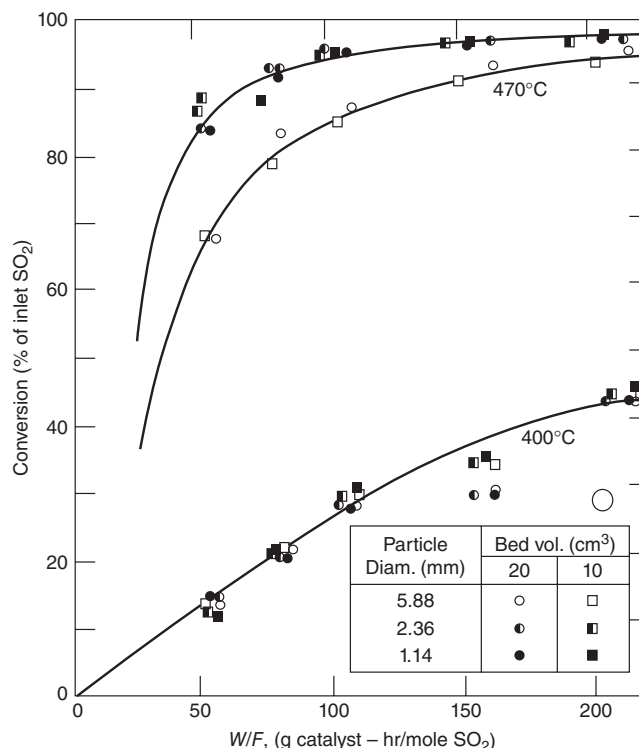


**Figure P12.3** Effects of particle size and linear velocity on conversion. (Reprinted with permission from the contribution of D. A. Dowden and G. A. Bridger to *Adv. Catal.*, **9**, 669. Copyright © 1957 by Academic Press.)

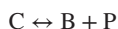
the conversion achieved for different operating conditions. What is your interpretation of these data?

- 12.4** The *ortho-para* conversion of molecular hydrogen is catalyzed by NiO. A supported catalyst of this type is available with a specific surface area of 305 m<sup>2</sup>/g and a void volume of 0.484 cm<sup>3</sup>/g. This spherical catalyst pellet has an apparent density of 1.33 g/cm<sup>3</sup> and a diameter of 0.5 cm. If the system is not far from equilibrium, an apparent first-order rate constant ( $k_r$ ) can be defined in the following manner:

$$\text{rate of approach to equilibrium} = k_r(C - C_{\text{eq}})$$

When the hydrogen pressure is 1 atm and the temperature is 77 K, the experimentally observed (apparent) rate constant is 0.159 cm<sup>3</sup>/(s·g catalyst). Determine the mean pore radius, the combined diffusivity for hydrogen in the pores of this catalyst, and the catalyst effectiveness factor based on the straight cylindrical pore model.

- 12.5** A catalyst for a generic reaction of the form indicated below is available commercially in the form of 0.35-cm-diameter spherical pellets.



The feed stock is pure C, and the reactor operates at a pressure of 2 atm. The molecular weight of species C is 120.19. The pellets have a specific surface area of 480 m<sup>2</sup>/g and a void volume of 0.42 cm<sup>3</sup>/g. If the apparent first-order rate constant for this reaction is 1.49 cm<sup>3</sup>/(s·g catalyst) at 412°C, determine the effectiveness factor of the catalyst. You may assume that Knudsen diffusion is the dominant mode of transport within the pellets.

- 12.6** L. G. Barnett, R. E. C. Weaver, and M. M. Gilkeson [AIChE J., 7, 211, (1961)] studied the catalytic dehydrogenation of cyclohexane to benzene over a platinum-on-alumina catalyst. A 4:1 mole ratio of hydrogen to cyclohexane was used to minimize carbon formation on the catalyst. Studies were conducted in an isothermal, continuous flow reactor. The results of a trial involving 0.32-cm-diameter spherical catalyst pellets are given below.

Temperature	705 K
H <sub>2</sub> feed rate	8 mol/ks
Quantity of catalyst	10.4 g
Pressure	1.480 MPa
Cyclohexane feed rate	2 mol/ks
Conversion of cyclohexane	15.5%

#### Catalyst Properties:

Pore volume	0.48 cm <sup>3</sup> /g
Pellet density	1.332 g/cm <sup>3</sup>
Surface area	240 m <sup>2</sup> /g
Pellet porosity	0.59 cm <sup>3</sup> voids/cm <sup>3</sup>

If the effectiveness factor of the catalyst is 0.42, the reaction obeys first-order kinetics, and Knudsen diffusion is the dominant mode of molecular transport, estimate the

tortuosity factor of the catalyst. Comment on the uniqueness of the value you calculate. (*Hint:* Consider both an “effective property” approach and a straight cylindrical pore model.)

- 12.7** V. P. Gupta and W. J. M. Douglas [AIChE J., 13, 883 (1967)] studied the catalytic hydration of isobutylene to *t*-butanol in a continuous flow stirred-tank reactor when the reaction is mediated by a cation exchange resin catalyst:



Water is present in such large excess relative to the concentrations of isobutylene and *t*-butanol that the reaction may be regarded as pseudo first-order in both directions.

Determine the effectiveness factor for the ion exchange resin at 85°C, assuming that the reaction is reversible (even though the authors presumed the reaction to be irreversible in reporting their data). They noted that at 100°C the equilibrium for the reaction corresponds to a conversion greater than 94%. If the equilibrium constant for the reaction is expressed as the ratio of the *t*-butanol concentration to the isobutylene concentration and corrected for the temperature change in going from 100°C to 85°C, a value of 16.6 may be considered appropriate for use.

The reaction over the ion-exchange particles may be regarded as isothermal, and the effective diffusivity of isobutylene within the particles may be taken as  $2.0 \times 10^{-5}$  cm<sup>2</sup>/s. The resin particles may be considered as spheres with radii equal to 0.0213 cm. The density of the swollen resin is 1.0 g/cm<sup>3</sup>.

Rate measurements for reaction over these particles indicate that at 85°C the rate is equal to  $1.11 \times 10^{-2}$  mol/(ks·g catalyst) when the conversion achieved is only 3.9%. Calculations based on the thermodynamic equilibrium data contained within the article indicate that a good estimate of the isobutylene concentration in the reactor at the exterior surface of the resin is  $1.65 \times 10^{-5}$  mol/cm<sup>3</sup>.

- 12.8** D. N. Miller and R. S. Kirk [AIChE J., 8, 183 (1962)] studied the kinetics of the catalytic dehydration of primary alcohols to produce the respective olefins. These investigators employed a TCC silica-alumina catalyst in a fixed bed reactor operating at 1 atm and temperatures from 400 to 700°F. The catalyst is characterized by a specific surface area of 350 m<sup>2</sup>/g and a porosity of ca. 0.5. Within the bed the apparent density of the catalyst is 1.15 g/cm<sup>3</sup>. The density of the nonporous bulk solid silica-alumina is 2.30 g/cm<sup>3</sup>. The catalyst received from the vendor was sieved to obtain five sets of particles with apparent particle diameters equal to 0.40, 2.30, 3.05, 4.06, and 5.11 mm.

Figure P12.8-1 contains plots of the data obtained in *n*-butanol dehydration trials conducted with each of these batches of catalyst at 600°F and 1 atm. Figure P12.8-2 contains cross plots of the smoothed data in Figure P12.8-1 that indicate the dependence of the observed rate on the diameter of the catalyst beads at conversions of 7, 14, and 21%. The experimental conditions are such that the catalyst beads are at the same temperature throughout and that there are no significant temperature gradients within the fixed bed.

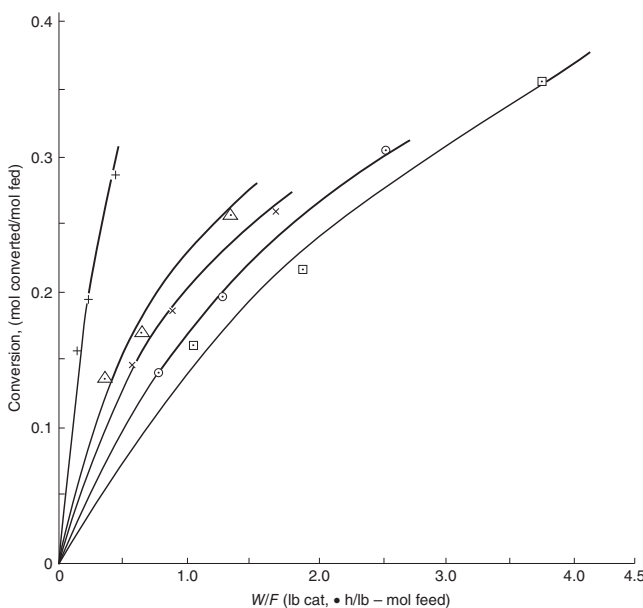


**Figure P12.8-1** Conversion of *n*-butanol versus  $W/F$  for operation of the reactor at 1 atm and 600°F using beads of different diameters. +, 0.40 mm;  $\Delta$ , 2.30 mm;  $x$ , 3.05 mm; O, 4.06 mm;  $\square$ , 5.11 mm.  
[Reprinted with permission from the contribution of D. N. Miller and R. S. Kirk to the *AIChE J.*, **8**, 183 (1962).]

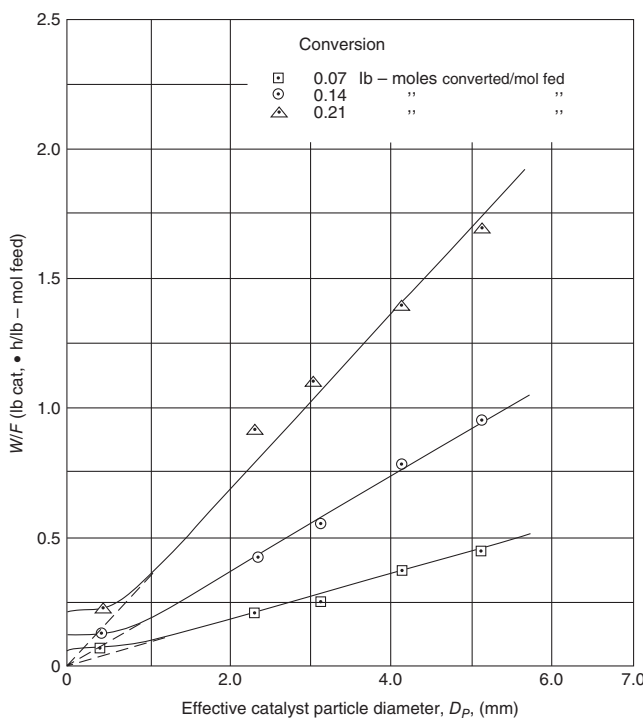


**Figure P12.8-2** Dependence of  $W/F$  on the diameter of the catalyst particles for dehydration of *n*-butanol at 1 atm and 600°F. [Reprinted with permission from the contribution of D. N. Miller and R. S. Kirk to the *AIChE J.*, **8**, 183 (1962).]

(a) If the bulk of the catalyst surface area is contained within its micropores and if the pore size distribution is relatively narrow, determine the value of the mean pore radius.

(b) Use the data in Figure P12.8-2 to prepare a table that indicates the dependence of the effectiveness factors on the diameters of the catalyst particles at conversion levels of 7, 14, and 21%. The quasilinear nature of the initial portions of the five plots in Figure P12.8-1 indicates that to a first approximation the order of the reaction is sufficiently close to unity that the effectiveness factors may be considered to be substantially independent of the reactant concentration at the mouths of the catalyst pores. A Hougen-Watson mechanism of the type indicated in part (e) of this problem will have an order in *n*-butanol that lies between zero and unity. For a first-order reaction, the effectiveness factor is independent of the concentration of reactant at the pore mouth, while for a zero-order reaction the effectiveness factor is either unity for low values of the Thiele modulus or at high values inversely proportional to the square root of the concentration at the pore mouth. For present purposes as a first approximation, we regard the effectiveness factor for a catalyst with a specified composition as relatively independent of conversion for reactions conducted under isothermal conditions.

(c) Both the straight cylindrical pore model and the effective diffusivity model of catalyst effectiveness factors indicate that for simple  $n$ th-order rate laws the effectiveness factor should be inversely proportional to a characteristic dimension of the catalyst particle. Are the data in Figure P12.8-2 consistent with this expectation? Do you expect the effectiveness factor of this catalyst to increase, decrease, or stay the same when the temperature of the fixed-bed reactor is increased by 100°F? Discuss each of these issues briefly, rather than merely providing a yes or no answer.

(d) If one assumes that the rate law can be approximated as a first-order irreversible reaction, estimate the tortuosity factor of the pores in the catalyst beads that have a diameter of 3.05 mm and are being used at a temperature that gives an effectiveness factor of 0.2. Is your answer physically realistic, and does it lie within the range of tortuosity factors expected for high-surface-area materials? Comment.

(e) Plots of the data of Miller and Kirk in the form of the ratio of the initial total pressure ( $\pi_0$ ) to the initial rate ( $r_0$ ) versus  $\pi_0$  for catalyst particles with a diameter of 4.06 mm are linear (but do not pass through the origin) at temperatures from 500 to 700°F. Are such plots consistent with a mechanism in which the rate-controlling step is a first-order surface reaction of an adsorbed *n*-butanol species? There is only one type of site on the catalyst surface. Only *n*-butanol and water can adsorb on such sites. The olefinic product (butene-1) does not adsorb on the surface of the catalyst. The mechanism proposed for

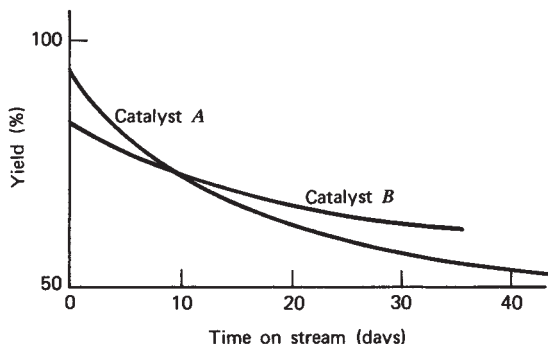
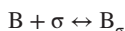


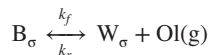
Figure P12.9 Catalyst deactivation curves

the first-order surface reaction consists of the following three steps:

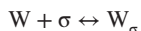
Fast, adsorption equilibrium constant  $K_B$ :



Slow, rate constants for the forward ( $k_f$ ) and reverse ( $k_r$ ) reactions on the catalyst surface:



Fast, adsorption equilibrium constant  $K_w$ :



- 12.9 A well-insulated pilot-scale packed-bed reactor (5 m long  $\times$  5 cm diameter) is being used to carry out an irreversible reaction of the type



All species are gases at the conditions of interest. The reaction is quite exothermic ( $\Delta H_R^0 = -120 \text{ kJ/mol}$ ). Side reactions are unimportant.

There are two different catalyst manufacturers whose products are being considered for use in a commercial-scale reactor facility. Both products are 3.2-mm-diameter spherical pellets that are believed to be essentially the same in chemical composition. Results of pilot-plant trials indicate that the deactivation characteristics of the two catalysts are somewhat different. The same gas pressure, feed composition, and molar feed rate were employed in all trials. For an inlet temperature of 550°C, the behavior indicated in Figure P12.9 was observed.

If the feed temperature was reduced to 475°C, both catalysts exhibited little loss of activity with time on stream, and both catalysts give essentially the same yield. (However, this yield was significantly lower than the yield obtained when the feed temperature was 550°C.) The deactivation behavior of both catalysts is very reproducible.

- How do you interpret these data?
- What modifications in the manufacturing or operating conditions do you suggest to obtain improved performance from catalyst A?

12.10 L. G. Barnett, R. E. C. Weaver, and M. M. Gilkeson [AIChE J., 7, 211 (1961)] studied the dehydrogenation of cyclohexane to benzene over a platinum-on-alumina pelleted catalyst. Using a 4:1 feed ratio of hydrogen to cyclohexane and an operating pressure of 200 psig, these authors studied the effects of particle size and poisoning on the observed reaction rate. The reaction follows first-order kinetics over the temperature range from 640 to 910°F. Arrhenius plots of their data are shown in Figure P12.10.

For the poisoned catalyst, the fraction that is poisoned ( $\alpha$ ) is estimated to be 0.78. This catalyst was used in runs 41 to 45 for which the following additional data are available.

Run	Thiele modulus for reaction over unpoisoned catalyst	Ratio of rate over poisoned catalyst to rate over unpoisoned catalyst
45	0.77	0.22
44	1.78	0.26
41	4.24	0.214
42	4.40	0.210
43	6.95	0.153

What is your interpretation of these data? Do the data indicate whether homogeneous or pore-mouth poisoning took place?

Catalyst properties:

$V_g$	0.48 cm <sup>3</sup> /g
$S_g$	204 m <sup>2</sup> /g
Average pore radius	47 Å
Pellet density, $\rho_p$	1.332 g/cm <sup>3</sup>
Skeletal density	3.25 g/cm <sup>3</sup>
Pellet porosity, $\epsilon_p$	0.59
Tortuosity factor	≈ 8

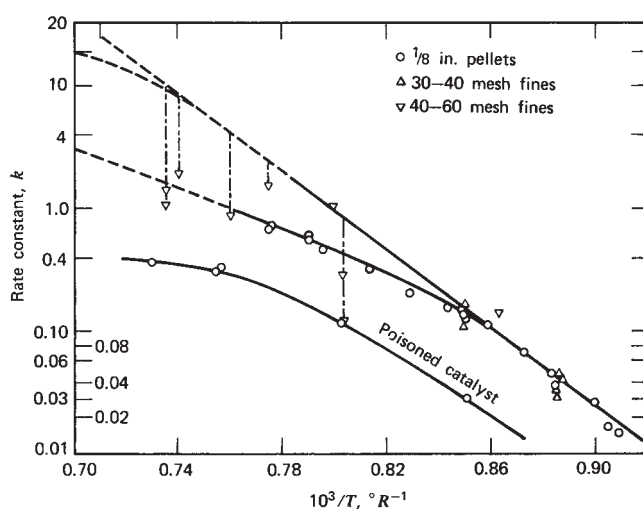
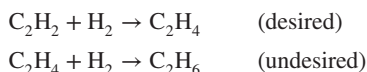


Figure P12.10 Arrhenius plots for poisoned and unpoisoned catalysts. [From L. G. Barnett, R. E. C. Weaver, and M. M. Gilkeson, AIChE J., 7 211 (1961). Used with permission.]

**12.11** Before ethylene feedstocks produced by thermal cracking can be used chemically for most applications, it is necessary to remove the traces of acetylene present in such streams. This purification can be accomplished by selective hydrogenation of acetylene to ethylene. The process involves adding sufficient hydrogen to the feedstock so that the mole ratio of hydrogen to acetylene marginally exceeds unity. Using a palladium-on-alumina catalyst under typical reaction conditions (25 atm, 50 to 200°C), one can achieve extremely high selectivity for the hydrogenation of acetylene. As long as acetylene is present, it is selectively adsorbed and hydrogenated. However, once it disappears, hydrogenation of ethylene takes place. The competitive reactions may be written as



The intrinsic rate expressions for these reactions are each first-order in hydrogen and zero-order in acetylene or ethylene. If there are diffusional limitations on the acetylene hydrogenation reaction, the acetylene concentration will go to zero at some point within the core of the catalyst pellet. Beyond this point within the central core of the catalyst, the undesired hydrogenation of ethylene takes place to the exclusion of the acetylene hydrogenation reaction.

- (a) In light of the facts above, what do the principles enunciated in the text of Chapter 12 have to say about the manner in which the reactor should be operated and the manner in which the catalyst should be fabricated?
- (b) It is often observed that the catalysts used for this purpose in commercial installations do not achieve maximum *selectivity* until they have been on stream for several days. How do you explain this observation?

**12.12** R. A. Cunningham, J. J. Carberry, and J. M. Smith [*AIChE J.*, **11**, 636 (1965)] have studied the catalytic hydrogenation of ethylene over a copper–magnesium oxide catalyst.



To minimize the complications arising from a change in the total number of moles within the catalyst particles, they restricted their studies to feeds containing less than 17% ethylene. They used continuous-flow reactors operating at steady state to obtain the data reported in Table P12.12. The pressure was 1 atm. Two forms of catalyst were used in their studies: (1) granular particles (100 to 150 Tyler mesh; equivalent diameter = 0.13 mm) and (2) spherical pellets (1.27 cm diameter) fabricated by compressing unreduced granular particles in a steel mold.

Pellets of three different densities were studied. They were obtained by varying the quantity of particles and the pressure used in the molding process. Pertinent physical property data for the various forms of catalyst used in these studies are summarized in Table P12.12.

Analysis of the entries in Table P12.12 indicates that the specific surface area is essentially determined by the area

**Table P12.12**

Catalyst	Apparent density of particle or pellet (g/cm <sup>3</sup> )	Equivalent diameter	$S_g$ (m <sup>2</sup> /g)	$V_g$ (cm <sup>3</sup> /g)	Total porosity, $\epsilon_{\text{total}}^a$
Granular particles	2.14	0.13 mm	90	0.18	0.38
Pellet A	1.16	1.28 cm	90	0.46	0.53
Pellet B	0.92	1.27 cm	90	0.73	0.77
Pellet C	0.72	1.27 cm	90	1.17	0.84

<sup>a</sup> $\epsilon_{\text{total}}$  refers to the ratio of the void volume within and between pellets to the total volume.

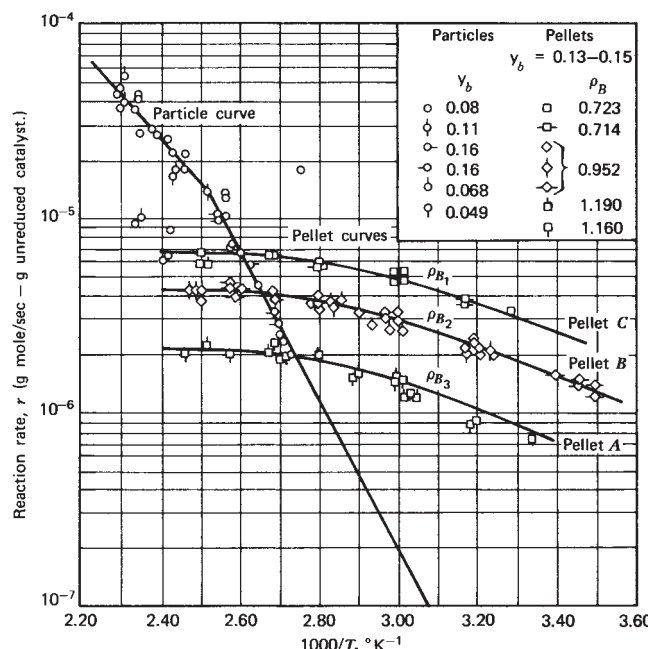


**Figure P12.12** Arrhenius plots for catalyst particles and pellets.

$y_b$  = ethylene mole fraction. [Adapted with permission from the contribution of R. A. Cunningham, J. J. Carberry, and J. M. Smith to the *AIChE J.*, **11**, 636 (1965).]

within the pores of the granular particles and that the dominant contributor to the void volume per gram of catalyst is the space between the particles constituting the pellets.

Rate data were reported as a function of temperature (see Figure P12.12). The form of the intrinsic rate equation for hydrogenation of ethylene over this specific catalyst is not known. However, other studies of the catalytic hydrogenation of ethylene indicate that one might anticipate a rate law of the form

$$r = \frac{k K_{\text{C}_2\text{H}_4} P_{\text{H}_2} P_{\text{C}_2\text{H}_4}}{1 + K_{\text{C}_2\text{H}_4} P_{\text{C}_2\text{H}_4}}$$

What is your interpretation of the data shown in Figure P12.12? If it is possible to back up your arguments using

semiquantitative arguments, do so using *rough* numbers. *If multiple interpretations are possible, state them.* In the low-temperature region, the intrinsic activation energy based on the particle data is 17.8 kcal/g-mol. However, the apparent activation energy at high temperatures drops to 11.8 kcal/g-mol. Employ a value of  $2 \times 10^{-3}$  J/(s·cm·°C) for the effective thermal conductivity of the porous pellet.

(Note: Engineering estimates of property values have been used, where necessary, to fill in the gaps in the data reported in the original article.)

- 12.13** It is instructive to consider the relative rates of mass transfer in fixed and fluidized bed reactors. The rapid rate in the fluidized bed is attributed not so much to the high mass transfer coefficients involved, but to the very large exterior surface area per unit volume of reactor. If one assigns the weight of catalyst per unit volume of reactor the symbol  $\rho_B$ , the rate of mass transfer to the external surface per unit reactor volume is given by

$$r_{MT} = k_m a_m (C_B - C_{ES}) \rho_B = k_m a_v (C_B - C_{ES}) \quad (1)$$

where we have assumed equimolar counterdiffusion ( $\delta = 0$ ) to simplify the analysis. The product  $a_m \rho_B$  represents the external surface area of catalyst per unit volume of bed  $a_v$ . For spherical pellets of radius  $R$ , this area is given by

$$a_v = \frac{4\pi R^2 \rho_B}{\rho_p [(4/3)\pi R^3]} = \frac{3}{R} \frac{\rho_B}{\rho_p}$$

where  $\rho_p$  is the apparent (gross) density of a catalyst pellet. The ratio of the catalyst density within the entire bed to that of a single pellet is equal to the ratio of the volume occupied by the pellets themselves to the entire bed volume. In terms of the external void fraction of the bed ( $\varepsilon_B$ ), the volume fraction occupied by the pellets is equal to  $1 - 0.68$ , or 0.32. Hence,

$$\frac{\rho_B}{\rho_p} = 1 - \varepsilon_B \quad (2)$$

Thus,

$$a_m \rho_B = \frac{3}{R} (1 - \varepsilon_B) = \frac{6(1 - \varepsilon_B)}{D_p} \quad (3)$$

Combining equations (1) and (3) gives

$$r_{MT} = 6k_m \left( \frac{1 - \varepsilon_B}{D_p} \right) (C_B - C_{ES}) \quad (4)$$

If the same concentration driving force exists in both fixed and fluidized beds, use typical property values to determine the relative rates of mass transfer in these systems. Mass velocities employed for operation of fixed and fluidized beds may be taken as 0.15 and 0.03 g/(cm<sup>2</sup>·s), respectively. Bed void fractions may be taken as 0.30 and 0.80 for the fixed and fluidized beds, respectively. The corresponding catalyst sizes may be taken as 0.5 cm and 0.0063 cm (250 mesh). These numbers are chosen so as to favor fixed bed mass transfer. The reacting fluid may be regarded as a gas with a viscosity of  $3.30 \times 10^{-4}$  g/(cm·s).

- 12.14** Sue Dent has been assigned the task of identifying a heterogeneous catalyst that would be appropriate for use in hydrogenation: a liquid natural product whose gross composition resembles that of an oil in that it is composed primarily of acylglycerols but in its natural state also contains a variety of other compounds. The laboratory of her research supervisor contains a large number of inorganic materials that have been prepared in previous catalyst screening studies. These materials exist as powders or other finely ground solids and include both supported and unsupported materials.

Sue has been asked to employ a simple batch reactor system for her screening studies. To date her experimental protocol has consisted of adding 0.5 g of a potential catalyst to 150 mL of the natural product and observing the rate at which hydrogen is consumed by measuring the decrease in the pressure of a hydrogen reservoir. Sufficient agitation is provided to maintain an apparently uniform suspension of the catalyst. The reactor operates isothermally. Sue has identified a pair of catalysts that appear to have comparable activities as reflected in the rates at which hydrogen is taken up by the oil. However, Sue is concerned that more detailed studies of these catalysts yield results that she does not understand. Can you provide a rational explanation of the observations she has summarized below?

1. Catalyst Abracadabra is a supported metal catalyst and trials involving 0.5 g of the support alone indicate that the support itself does not function as a hydrogenation catalyst. However, if she adds 2.0 g of this support to a suspension containing 0.5 g of the supported catalyst and conducts a trial using the resulting composite well-agitated suspension, she observes that the rate of consumption of hydrogen increases significantly. Complete reaction was observed in 0.5 h rather than the 1.5 h required to achieve complete reaction with a suspension containing only 0.5 g of Catalyst Abracadabra.
2. Catalyst Balakazam is an unsupported catalyst with a relatively high specific surface area. In a trial in which 1.0 g of this catalyst and 150 mL of the natural product, the rate of consumption of hydrogen was four to five times faster than that observed in a trial at the same temperature which employed only 0.5 g of solid from the same catalyst preparation. However, in a third trial in which 1.0 g of this catalyst was suspended in 300 mL of the natural product, Sue observed that the agitation was again sufficient to yield an apparently uniform suspension. In this trial the overall rate of consumption of hydrogen increased, but the rate per gram of catalyst was statistically the same as that observed in a trial involving 0.5 g of this catalyst in 150 mL of the oil.

How can Sue's observations be reconciled with what is known about the susceptibility of catalysts to lose activity during use?

- 12.15** This problem has been adapted with permission from the late Professor C. N. Satterfield of MIT. The data in Table P12.15 were obtained by I. M. Karpenko in an unpublished study described by P. N. Rylander in *Catalytic Hydrogenation Over Platinum Metals* (p. 39, Academic Press, New York, 1967). Nitrobenzene in ethanol was hydrogenated at

**Table P12.15**

Supported catalyst (mg)	Palladium (mg)	Rate of hydrogen uptake (cm <sup>3</sup> /s)			
		Total		Per mg Pd	
		Shaker	Stirrer	Shaker	Stirrer
52	2.6	0.042	0.042	0.016	0.016
105	5.2	0.72	0.52	0.138	0.100
210	10.5	1.97	0.92	0.187	0.088
420	21.0	2.57	0.92	0.122	0.044

room temperature and 1 atm over various amounts of 5% Pd on carbon. Four loading levels of catalyst were used. Each reduction proceeded at a nearly constant rate until the nitrobenzene was nearly exhausted. At each level of catalyst, the reduction was carried out in two types of batch reactor:

1. An equipoise shaker that gives very vigorous agitation
2. A flask stirred by a rotating magnetic bar that gives relatively poor agitation

What is your interpretation of the data?

- 12.16** M. Zajcew [J. Am. Oil Chem. Soc. **37**, 11 (1960)] studied the hydrogenation of fatty oils for shortening stock using a palladium catalyst. The experiments were carried out in a 1-gallon hydrogenator provided with mechanical agitation, a gas-dispersing system, and heating and cooling capabilities. Hydrogen gas is fed at the reactor bottom and is rapidly consumed. Figure P12.16 indicates the time necessary to achieve a specified conversion as a function of catalyst loading level. Note that log-log coordinates are employed. The table that follows reformulates the data in terms of the number of iodine units of reduction per minute per 1% of catalyst.

% Pd	Rate per % of catalyst
0.02	18
0.01	40
0.005	72
0.0025	130
0.00125	215
0.00050	354

What is your interpretation of the data?

- 12.17** This problem has been adapted with permission from the late Professor C. N. Satterfield of MIT. R. H. Price and R. B. Schiewetz [Ind Eng. Chem., **49**, 807 (1957)] studied the catalytic liquid-phase hydrogenation of cyclohexene in a laboratory-scale semibatch reactor. A supported platinum catalyst was suspended in a cyclohexene solution of the reactant by mechanical agitation of the solution. Hydrogen was bubbled through the solution continuously. The reactor is described in their words as follows:

*The reactor consisted of a 1-liter three-necked Morton flask. This flask has four equally spaced perpendicular indentations about its periphery and a concave bottom, which aid the action of the agitator. A*

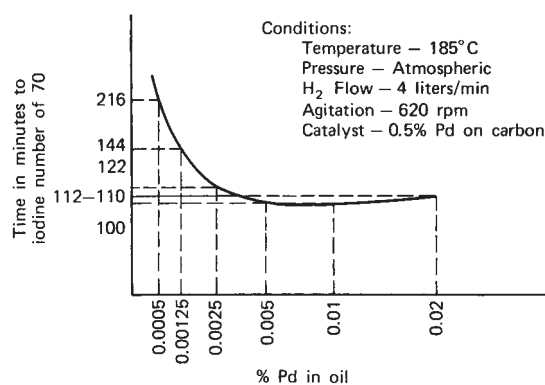


**Figure P12.16** Hydrogenation rate as a function of catalyst concentration. [Adapted from M. Zajcew, The Hydrogenation of Fatty Oils with Palladium Catalyst: III. Hydrogenation of Fatty Oils for Shortening Stock with permission of Springer Science + Business Media: *Journal of the American Oil Chemists' Society*, **37**, 11 (1960).]

*four-bladed stirrer driven by a variable-speed motor extended into the flask through a packing gland in the center neck. Tubes were sealed into one side neck for hydrogen delivery, sample withdrawal, and a thermocouple well. An ice water condenser on the exit neck minimized solvent escape by entrainment or vaporization. Hydrogen was dispersed into the reacting solution by a 20 mm sintered-glass tube extending to the bottom of the flask. The entire assembly was immersed in a constant temperature bath maintained to within  $\pm 0.1^\circ\text{C}$ . However, because of the exothermic nature of the reaction, a temperature rise of 1 to 2°C occurred in the reactor.*

At 25°C the equilibrium constant for the reaction of cyclohexene with hydrogen to form cyclohexane is  $2 \times 10^8$ . Consequently, the reaction may be regarded as irreversible. These investigators reported the data indicated on Figures P12.17-1 to P12.17-6. Provide an interpretation of each

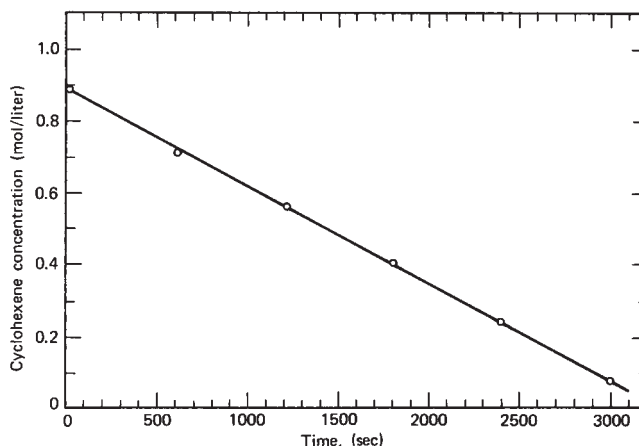


**Figure P12.17-1** Typical concentration versus time plot for experimental trials. Temperature, 26°C; pressure, 746 torr; hydrogen flow rate,  $30.7 \times 10^{-5}$  mol/s; catalyst weight, 0.975 g; stirrer speed, 1100 rpm; slope,  $13.7 \times 10^{-5}$  mol/(L·s).

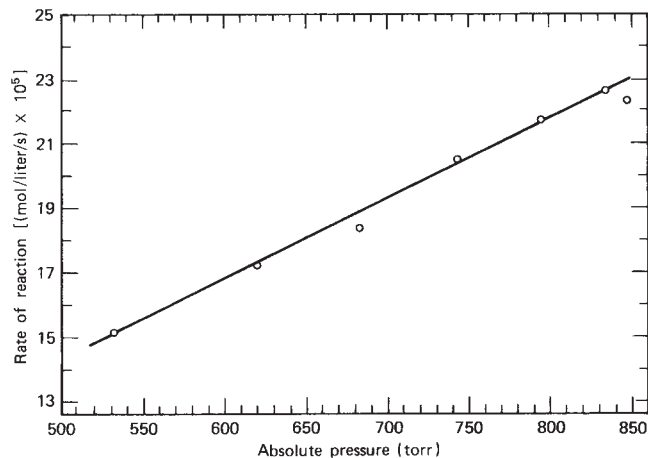


**Figure P12.17-2** Effect of pressure on the reaction rate.  
Temperature, 25 to 26°C; hydrogen flow rate,  $27.6 \times 10^{-5}$  mol/s;  
catalyst weight, 0.976 g; stirrer speed, 1500 rpm.

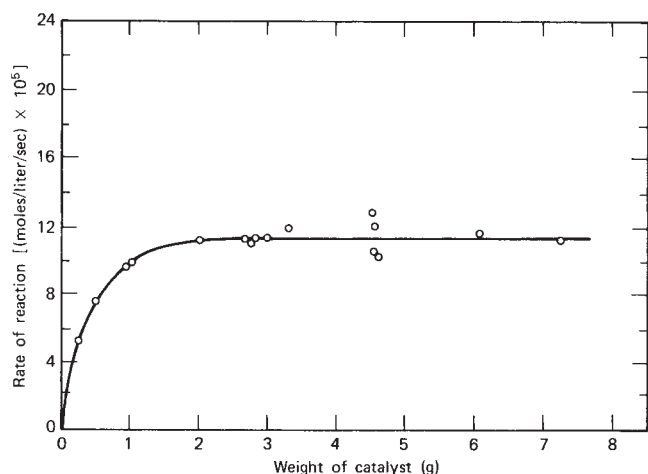


**Figure P12.17-3** Effect of catalyst weight on the rate of reaction.  
Temperature, 25°C; pressure, 748 torr; hydrogen flow rate,  $31.3 \times 10^{-5}$  mol/s; stirrer speed, 1000 rpm.

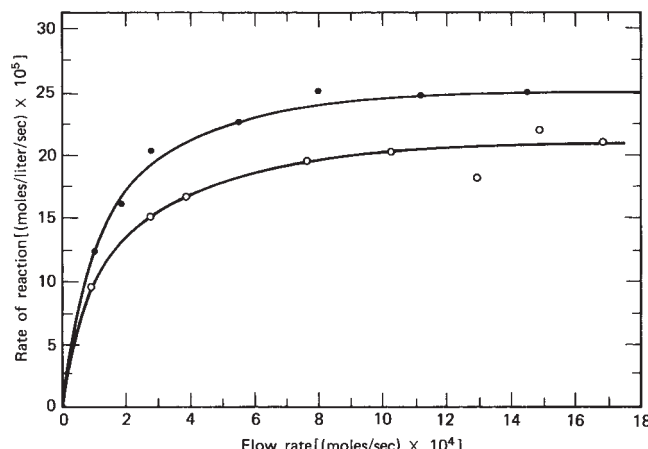


**Figure P12.17-4** Effect of hydrogen flow rate on the reaction rate.  
Temperature, 25 to 27°C; pressure, 534 (○) or 741 (●) torr; catalyst  
weight, 0.974 g; stirrer speed, 1500 rpm.

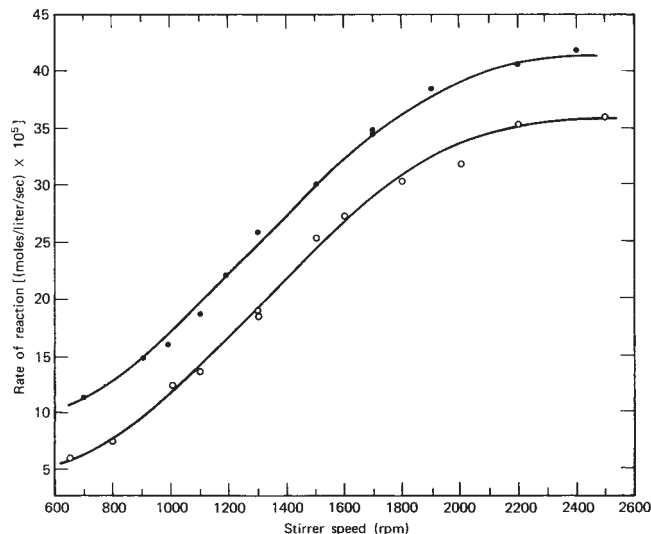


**Figure P12.17-5** Effect of stirring speed on reaction rate.  
Temperature, 25 to 27°C; pressure, 746 torr; hydrogen flow rate,  $29.6 \times 10^{-5}$  (○) or  $81.5 \times 10^{-5}$  (●) mol/s; catalyst weight, 0.976 g.

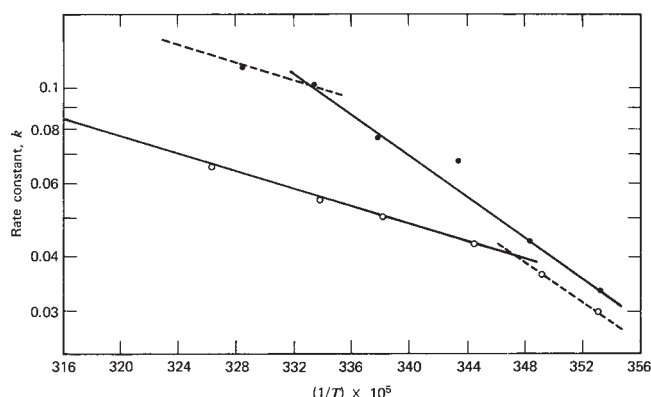
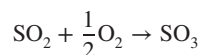


**Figure P12.17-6** Evaluation of apparent energies of activation.  
Stirring speed, 1300 rpm (○) or 2500 rpm (●).

figure individually and then an overall analysis of the factors that govern the rate of this reaction. Where multiple interpretations of an individual figure are possible, indicate them. Notice that in Figure P12.17-6, the apparent activation energies determined from the slopes of the solid lines are 4.8 and 12.8 kcal/g-mol at 1300 and 2500 rpm, respectively.

This material and the figures are reprinted, with permission, from R. H. Price and R. B. Schiewtz, *Ind. Eng. Chem.*, **49**, 807 (1957). Copyright © by the American Chemical Society.

**12.18** Vanadium pentoxide may be used as a catalyst for the oxidation of sulfur dioxide to sulfur trioxide:



In a series of laboratory-scale experiments, streams of oxygen and sulfur dioxide were fed at different rates to a differential reactor containing 2.372 g of catalyst. The

**Table P12.18**

Inlet pressure (atm)	Mass velocities [lb mol/(h·ft <sup>2</sup> )]		Percent conversion of SO <sub>2</sub>	Initial rate (lb mol SO <sub>2</sub> converted per h·lb catalyst)
	SO <sub>2</sub>	O <sub>2</sub>		
2.36	1.83	1.90	4.22	0.053
3.72	2.59	2.90	3.6	0.064
5.08	3.03	3.88	3.43	0.0717
5.76	3.24	4.26	3.10	0.0692
7.12	4.87	4.96	1.91	0.0642

data below were recorded under essentially isothermal conditions at 649°F. The rate expression pertinent to these experimental conditions is believed to be of the form

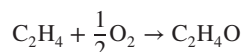
$$r = \frac{kP_{SO_2}P_{O_2}^{1/2}}{(1 + K_{SO_2}P_{SO_2})^2} \quad (1)$$

The data in Table P12.18, reported by G. P. Mathur and G. Thodos [*Chem. Eng. Sci.*, **21**, 1191 (1966)], are sufficient for an initial rate analysis of this heterogeneous catalytic process.

(a) Determine the constants  $k$  and  $K_{SO_2}$ .

(b) If pure SO<sub>2</sub> and O<sub>2</sub> are both fed to a reactor at flow rates of 100 lb mol/h, how many pounds of catalyst will be required for 20% conversion? The initial feed pressure is 1 atm. Assume that the aforementioned rate expression is valid over the range of variables concerned. The reactor may be assumed to operate isothermally at 649°F.

**12.19** S. W. Wan [*Ind. Eng. Chem.*, **45**, 234 (1953)] studied the partial oxidation of ethylene to ethylene oxide:



The catalyst consists of silver supported on alumina and, while it is reasonably selective, appreciable amounts of CO<sub>2</sub> and H<sub>2</sub>O are also formed. Over the range of interest, the yield of ethylene oxide is relatively constant so that for present purposes, we may regard the reaction stoichiometry as



The rate law is

$$r = 1.17 \times 10^6 e^{-9713/T} P_{C_2H_4}^{0.341} P_{O_2}^{0.672}$$

where the partial pressures are expressed in atmospheres,  $T$  is expressed in K, and  $r$  is expressed in lb-mol/(lb catalyst · h).

If (1/8)-in. catalyst pellets are packed in 1-in.-ID tubes, which in turn are immersed in a liquid bath that maintains the tube walls at 240°F, consider the effects of varying the feed temperature and of diluting the feed with N<sub>2</sub> to moderate the thermal effects accompanying the reaction. Consider

inlet temperatures from 350 to 480°F and N<sub>2</sub>/C<sub>2</sub>H<sub>4</sub> ratios from 0 to 5.0. Your analysis should be governed by the following constraints.

- (a) If the temperature at any point in the reactor exceeds 550°F, the conditions will be inappropriate because explosions may occur in this regime.
- (b) If the temperature decreases as one moves down the reactor, the reaction must be regarded as self-extinguishing.
- (c) If the pressure drop exceeds 14 atm, the calculations must be terminated. Determine the range of satisfactory performance and the resulting yields for various reactor lengths for the following operating specifications:

1. Inlet gas pressure = 15 atm.
2. Inlet C<sub>2</sub>H<sub>4</sub>/O<sub>2</sub> ratio (moles) = 4 : 1.
3. Superficial mass velocity = 8000 lb/(h·ft<sup>2</sup>).
4. Bulk density of catalyst = 83.5 lb/ft<sup>3</sup>.

External heat and mass transfer effects are to be neglected in your analysis, but you should estimate the potential magnitudes of these effects.

Not many problems dealing with the various fixed bed reactor models are set forth above, because we feel that the best means of demonstrating the features thereof is through case studies. We find that the principles involved are clarified by realistic examples involving the design of commercial scale reactors using machine computation where appropriate. One could employ studies of the effects of multiple process variables on the reactor performance as additional problems or else state the assignment in more general terms, as in the problem below. Space limitations preclude setting forth many such problems, but the book *Catalytic Processes and Proven Catalysts*, by C. L. Thomas, and the descriptions of new and current catalyst technology that appear frequently in the literature provide appropriate starting points for the acquisition of the necessary data for problem formulation. Old issues of *Hydrocarbon Processing* and *Industrial and Engineering Chemistry* and the quarterlies evolving from the latter journal are also good sources of essential data on catalyst activity. A more limited source of relevant information of this type and useful references are contained in the book *Fundamentals of Industrial Catalytic Processes* by C. H. Bartholemew and R. J. Farrauto (Wiley-Interscience, Hoboken, NJ, 2006). The literature of various catalyst manufacturers also provides information on the physical properties of general catalyst types when such information is not included with the activity data. As stated, the problems normally require literature searches, and students usually find that information necessary to complete the design is often missing and must be estimated using good engineering judgment.

**12.20** Oxidative Dehydrogenation of Butene to Butadiene

To: Student Team "Blue"

From: Big Red, Group Leader, re: butadiene production

A proposed expansion of the company's styrene–butadiene rubber production will require an additional 10,000 tons/yr of butadiene as a raw material. For many years, butadiene has been manufactured by dehydrogenating butene or butane over a catalyst at appropriate combinations of temperature and pressure. It is customary to dilute the butene feed with steam (10 to 20 mol  $H_2O$ /mol butene) to stabilize the temperature during the endothermic reaction and to help shift the equilibrium conversion in the desired direction by reducing the partial pressures of hydrogen and butadiene. The current processes suffer from two major disadvantages:

1. Catalyst onstream periods are short, because coke builds up rapidly on the catalyst. Hence, catalyst regeneration must take place at frequent intervals.
2. Equilibrium yields of butadiene are relatively low. For example, the yield is 35% at 930°F and 71% at 1110°F when using a hydrocarbon feed partial pressure of 0.1 atm.

Considerable research effort has been invested in trying to develop an oxidative process to accomplish the transformation desired. Several catalyst formulations with good selectivities for the desired reaction have been developed, and you are asked to determine the desirability of using one of these formulations in a fixed-bed reactor configuration. Several advantages are claimed for the oxidative processes:

1. The constraint of thermodynamic equilibrium for dehydrogenation of butene is effectively removed because hydrogen is converted to water by oxidation. Maximum yields then approach 100% over the complete temperature and partial pressure range of interest.

2. Selectivities are high, typically in excess of 90%.
3. Longer times onstream are facilitated by the presence of oxygen in the feed. Oxygen inhibits carbon buildup on the catalyst, thereby permitting one to operate for months without regeneration.
4. Input energy requirements for the process are reduced significantly because the energy released by exothermic oxidation reactions serves as a driving force for the endothermic dehydrogenation reaction.

For preliminary discussions of the expansion program proposed, it is desirable to determine the basic equipment requirements, although a detailed economic evaluation is not essential. An article by J. S. Sterrett and H. G. McIlvried [*Ind. Eng. Chem. Process Des. Develop.*, **13**, 54 (1974)] describes the use of a ferrite catalyst for the application desired. The article contains kinetic data for this catalyst and several references to other oxidative dehydrogenation catalysts. Select a promising catalyst material and prepare a reactor design proposal using a fixed-bed configuration. You are asked to consider factors such as:

1. The desirability of adding steam to the feed stream to moderate temperature excursions
2. The optimum steam/butene ratio in the feed for operation as a single adiabatic reactor
3. The desirability of using several adiabatic reactors in series with steam injection between stages
4. Temperature profiles and the possibility of hot spots within a given reactor network configuration
5. Volume requirements for different reactor network configurations
6. Effect of catalyst pellet size on reactor volume and pumping cost requirements
7. Inter-stage heat transfer requirements for different reactor network configurations
8. Concentration profiles for a given reactor network
9. Other factors that you deem pertinent

# Chapter 13

---

## Basic and Applied Aspects of Biochemical Transformations and Bioreactors

### 13.0 INTRODUCTION

In recent decades, biotechnology and biochemical reactions have played increasingly important roles in modern society. More and more frequently, government officials, industrial leaders, and public citizens concerned with issues related to the environment, individual and public health, energy, agriculture, sustainability of resources, and national defense are calling on engineers and scientists to develop technically and economically viable solutions to a multitude of problems requiring expertise in biological phenomena. In light of these circumstances, many departments of chemical engineering have modified both their names and their curricula to address those aspects of biology that their students are most likely to utilize during their professional careers. Addition of this chapter to those contained in the first edition of this book reflects the increasing importance of biology in the area of chemical reactor design.

Chemical engineers have long played important roles in achieving solutions to numerous problems related to biological phenomena and processes. In collaboration with scientists and engineers from a variety of disciplines, chemical engineers have applied their expertise to develop a large array of processes and materials that involve applications of biology and its principles to solve pressing problems in the areas noted above. Examples include industrial processes for production of penicillin and other antibiotics, permselective membrane technology associated with dialysis for amelioration of kidney problems, synthesis of biocompatible materials for use in fabricating replacement body parts, waste treatment facilities employing activated sludge treatment as a unit operation, enzymatic modification of naturally occurring fats and oils to carry out replacement of fatty acid residues with negative health implications by residues

that confer therapeutic or prophylactic health benefits, and a wide variety of commercial products whose creation and manufacture benefit from genetic manipulation techniques.

From a macroscopic standpoint, one can view every living plant or animal cell as a bioreactor that takes in nutrients from its environment, processes these nutrients to obtain metabolic products and biomass components while exchanging energy with its environment, and discharges some of these products to the surroundings. Microorganisms of various sorts perform a variety of similar tasks on a microscopic scale. In this sense, bioreactors have existed on Earth since the moment that life in any form first appeared. From a more pragmatic viewpoint, the earliest forms of bioreactors can be said to have been thoughtfully utilized by humankind 5000 or more years ago. Historical evidence concerning the earliest use of primitive bioreactors is unclear, but the first forms of bioreactors might have been either (1) the vessels in which primitive peoples produced various alcoholic beverages (i.e., beer, wine, etc.) by fermentation of fruits, vegetables, or grains; or (2) the inflated stomachs of sheep and other mammals used by prehistoric peoples as storage containers for milk. The process of cheese-making was probably discovered accidentally when the milk was subsequently found to have been converted to cheese and whey via the influence of rennet present in the stomach tissue. However, it was not until the middle of the twentieth century that the foundations of biotechnology as we now define this field were established. Early practitioners of fermentation for production of alcoholic beverages and those engaged in making cheese, cultured milk products, and a variety of other foods would have difficulty recognizing the equipment employed in modern biotechnology.

The term *bioreactor* can be applied to various types of industrial-scale equipment, but there is no commonly

accepted definition of this term. When they refer to a bioreactor, practitioners of biotechnology working on routine production of a common antibiotic for a pharmaceutical company, on a cutting-edge application involving genetic manipulation of cells for medical purposes, or on biological detoxification of industrial waste waters can be referring to equipment with vastly different capacities, physical configurations, and necessary auxiliary equipment. However, for our purposes here we define a bioreactor as apparatus designed for use in one or more of the following processes: (1) conversion of a biological feedstock to a value-added product using large-scale equipment of the type characteristic of the chemical process industry, including any associated waste treatment facilities; and (2) use of a biocatalyst (enzymes or whole cells) to bring about a desired biosynthesis reaction or chemical transformation.

The kinetics of reactions mediated by soluble enzymes are discussed in Section 7.3.2, and the principles underlying the design of reactors for carrying out homogeneous phase reactions are covered in Chapters 8 to 11. These principles remain applicable to reactions catalyzed by soluble enzymes. Mass transfer phenomena may limit the rates of reactions catalyzed by immobilized enzymes or whole cells. The discussions of intraparticle diffusion in porous materials and external mass transfer effects in fixed-bed reactors (see Chapter 12) are also relevant to the design of reactors that employ immobilized biocatalysts. Research groups investigating problems involving diffusion and mass transfer effects in heterogeneous catalysis over inorganic materials and groups concerned primarily with catalysis by immobilized enzymes have independently employed similar approaches to the development of mathematical models of the interplay of diffusion, mass transfer, and chemical reactions. The basic concepts developed in Chapter 12 provide sufficient basis for design of biochemical reactors in which immobilized enzymes or cells are used to mediate reactions. The focus of this chapter is on the fundamental aspects of the design of reactors in which entire microorganisms (whole cells) are either the desired product, function as biocatalysts for chemical transformations, or are employed in waste treatment processes. The entries in Table 13.1 indicate the wide scope of applications of whole-cell bioreactors and industrial fermentation technology.

The fundamental principles employed in the design of bioreactors are the same as those employed in designing reactors for carrying out homogeneous reactions and heterogeneous catalytic reactions (see Chapters 8 to 12): namely, the laws of conservation of matter and energy. Our focus in this chapter is to teach readers how to combine appropriate conservation equations for bioreactors with an empirical expression describing the reaction kinetics so as to transform abstract conservation laws into results that are useful in the practice of (bio)reaction engineering. In those

cases for which the apparent rate of reaction is limited by some form of mass transfer process, the rate law takes the form of an expression for a mass transfer rate.

The primary difference between conventional chemical reactors and bioreactors in which microorganisms are either a product of interest or are employed as biocatalysts is that microbiological reactions can be characterized as being “autocatalytic” in the sense that the formation of one of the products of interest (new microorganisms) serves to increase the overall rate of reaction. In the absence of these microorganisms the reaction cannot take place. Consequently, one must plan to retain a portion of this product within the manufacturing facility for subsequent use, regardless of whether one is concerned with a batch reactor process or a continuous flow process. Because of the important role that the cell growth cycle plays in considerations of both the design of bioreactors and analysis of their performance, our discussion of bioreactor design begins in Section 13.1 with a treatment of this cycle. In Section 13.2 we focus on considerations that are important in the design of a bioreactor and the complexities that they add to the treatments of reactor design presented in Chapters 8 to 12. Applications of the principles of bioreactor design to situations of particular interest to chemical engineers are presented in Section 13.3. References suggested for further reading are presented in Appendix C.

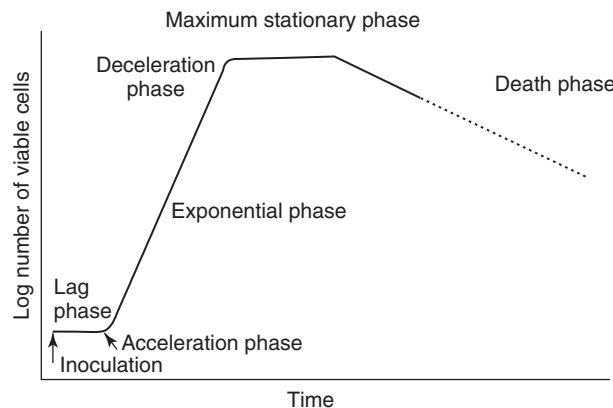
## 13.1 GROWTH CYCLES OF MICROORGANISMS: BATCH OPERATION OF BIOREACTORS

### 13.1.1 Introduction to Growth Cycles

The classic approach to the development of a commercial biochemical process is that of batch cultivation of microorganisms that are suspended in a liquid medium. One begins with an aqueous solution containing appropriate nutrients and inoculates that solution with living cells of the requisite type. In a strictly batch mode of operation, nothing further is added to or removed from the liquid suspension in the reactor. This type of bioreactor is often referred to as a *fermenter*. For culture of cells under aerobic conditions, air (or oxygen) may be bubbled through the solution to provide a nutrient essential to the growth of the microorganisms of interest and to provide some agitation that facilitates maintaining the suspension of cells at a uniform temperature and composition. The gas is typically introduced below the mixing impeller and liquid is admitted at the top of the reactor. Supplementary mechanical agitation may also be utilized. In other situations, bubbles of gaseous products (e.g.,  $\text{CH}_4$  and  $\text{CO}_2$ ) may contribute to the agitation needed to form a uniform suspension.

**Table 13.1** Products Obtained Via Industrial Fermentations

Generic category	Examples		
Antibiotics	Bacitracin Cephalosporin	Neomycin Penicillins	Streptomycin Tetracyclines
Antibodies			
Biopharmaceuticals	Taxol	Other taxanes	
Biopolymers	Xanthan gums	Polysaccharides	Polyesters
Chemicals/solvents/fuels	Ethanol; 1,3-propanediol	Glycerol	Butanol
Enzymes	Amylase; catalase	Glucose oxidase; invertase	Penicillinase; protease
Hormones	Insulin	Growth hormone	
Organic acids	Acetic; amino acids (e.g., lysine)	Citric; gluconic	Glutamic; lactic
Steroids	Cortisone	Prednisone	
Vitamins			
Waste treatment	Activated sludge; anaerobic digestion	Anaerobic oxidation of NH <sub>3</sub> ; biogas	Bioremediation processes

**Figure 13.1** Schematic representation of the growth cycle of microorganisms. At time zero, the growth medium is inoculated.

In batch fermentation, the number of cells of the microorganism present in the reactor typically varies with time in the manner shown in Figure 13.1. Readers should note that the scale of the ordinate is logarithmic while that of the abscissa is linear. Some authors describe the cell growth cycle shown in Figure 13.1 in terms of the four primary phases, while others include two smooth transitions between primary phases as additional growth phases.

Our discussion of the growth cycle is developed following the approach of Bailey and Ollis (1, 2). Growth depends on the ability of organisms to form new protoplasm from nutrients in the surrounding environment. *Growth* is defined as an organized increase in the quantity of cellular constituents, either as a consequence of an increase in the mass of individual cells or as a consequence of division of cells to bring about an increase in the number of cells present. Our treatment of the growth cycle begins at the point at which a growth medium contained in a

stirred-tank reactor is inoculated with cells of a generic microorganism.

For each phase of the growth cycle, we first provide a qualitative description of the biological phenomena involved in that phase in a stirred-tank reactor and then indicate how one can quantitatively characterize both the number of viable microorganisms present in this batch reactor and the rates at which products are created during the normal course of events.

Because a strictly batch reactor is a closed system and because no cells are added to the liquid suspension even if gas bubbles might be present, the suspension of microorganisms can be regarded as a closed system whose boundaries exclude the gas bubbles and the confining walls of the reactor proper. In such situations the number of microorganisms cannot increase indefinitely.

For some time after inoculation of the growth medium the *number of cells in the medium remains substantially constant* and equal to the number in the inoculum. However, during this initial period the amount of biomass present in the reactor will increase as the cells of the microorganism increase in size and weight as they muster resources (nutrients) from their environment and either activate or construct and install the biological machinery necessary to survive and reproduce. This period is known as the *lag phase* of the growth cycle. The lag phase is followed by an *acceleration phase* that provides a smooth transition to an *exponential growth phase*. The latter phase is typically characterized by rapid growth in both the number of cells and the quantity of biomass present.

During the acceleration phase, biosynthesis of some constituents of the cytoplasm takes place to allow the cells of the organism to adjust in response to the transition from the original environment of the inoculum to that of the growth medium. In effect, the organisms are either

activating or synthesizing and installing the biological constituents necessary to implement the process of cell propagation. When the cells in the culture are capable of propagation, the exponential growth phase begins. The exponential phase is characterized by *balanced growth* in which all components of the cells grow at the same rate (i.e., the average composition of an individual cell remains the same). During this phase, all of the requisite nutrients are readily available and the cells grow at their maximum rate; this rate is normally independent of the concentrations of those nutrients that are present in excess of stoichiometric requirements. In essence, the growth rate obeys a zero-order rate law with respect to these nutrients because under these conditions the growth rate is governed by a rate law that depends on the concentration of the limiting nutrient (in stoichiometric terms) and the number of microorganisms present in the bioreactor. The rate of growth is first-order in the number of cells present. This exponential phase is also commonly referred to as the *logarithmic phase of growth*. During balanced growth, the cells are able to adjust their metabolism to account for the effects of changes in the external (growth medium) conditions so as to keep the composition of the biomass constant despite changes in nutrient levels in the environment. Eventually, nature will exert its influence so as effectively to limit the number of cells in the bioreactor by decreasing the growth rate in response to the decreased availability of resources: substrates, light, space, available sites on enzymes involved in the metabolic reaction network of the organism at which the enzyme(s) are free to bind substrates, and so on. The accumulation of waste products often leads to inhibition of biochemical reactions so that unlimited growth cannot occur.

Nature places a finite limit on the number of microorganisms that can be suspended in the process fluid contained in a batch reactor. The period of decreasing growth rate between the exponential growth phase and the stationary phase is known as the *deceleration* (or *decline*) *phase*. The decline in growth rate is attributed to creation of an environment in which either (1) key nutrients are no longer present in sufficient quantities to sustain a high growth rate; (2) particular metabolic products accumulate to the point that they inhibit cell growth; (3) metabolic waste products act as toxins to the microorganisms; (4) the available space is exhausted, or (5) the intensity of incident light is diminished as a consequence of attenuation produced by the growing cells themselves. During the deceleration phase, the stresses imposed on the cells by the phenomena just enumerated lead to restructuring of the cells to enhance their chances for survival in the now hostile environment. During the deceleration phase some cells may die or undergo changes that negate their ability to contribute to cell growth. These changes decrease the

rate at which cells grow so as to create a quasi-steady-state condition known as the *stationary phase*.

During the stationary phase there is no net growth of the cells. The steady-state limit defines the stationary phase that, in essence, establishes a cap on the population of living cells—the maximum stationary phase. For analyses involving the number of viable cells present during the stationary phase, it is normally immaterial whether some cells are dying and an equal number of cells are dividing, or whether the entire cell population has simply ceased to grow and divide. If incubation of the cell culture continues after its arrival at the stationary phase, some cells will die, causing a decline in the population of living organisms. The decline is typically exponential. This final phase of the growth cycle is known as the *death* (or *decline*) *phase*.

The number of microorganisms present at any time during the growth cycle can be determined quantitatively by writing the population balances appropriate to each phase and then solving the differential equations pertinent to each phase using suitable boundary conditions (see Section 13.1.2). The chemical engineer engaged in the design of bioreactors must recognize that the governing equations for the design, operation, and optimization of a biochemical process will depend on the particular phase of the growth cycle in which the microorganisms find themselves. At times it may be desirable to operate a bioreactor in a batch mode; at others, a semibatch or continuous-flow mode of operation will be more appropriate. A common solution to the problem of optimizing production of a particular microorganism is first to inoculate a growth medium in a stirred-tank reactor and to operate the reactor in a batch mode under conditions that minimize the length of the lag phase of the growth cycle. After substantial growth takes place during the exponential phase, a transition to the stationary phase of the growth cycle occurs via the deceleration phase. At that time the mode of operation may be changed to a continuous flow mode to address the issue of providing an adequate supply of nutrients. (In a batch reactor, one can obtain only a small number of generations of organisms because of the limited supply of nutrients.) By shifting the reactor to a continuous flow mode of operation, the chemical engineer is able to replenish the nutrients that were depleted during batch operation for the early stages of the exponential growth phase. Issues relative to inhibition of cell growth or toxicity effects are resolved by removal of offending metabolites in the effluent from what is now the functional equivalent of a CSTR.

Given the autocatalytic nature of the growth cycle for microorganisms, an alternative solution to circumventing problems associated with the absence of reactor productivity during the lag phase is to employ a cascade of CSTRs. The stirred tanks may differ in size, with the first reactor operating at a point in the growth cycle where the

microorganisms are experiencing the high growth rate characteristic of the exponential phase. Process conditions in subsequent reactors in the cascade may be altered using supplementary feed streams containing nutrients that serve to emphasize or inhibit other biochemical reactions that shift the distribution of product species in preferred directions.

To quantitatively analyze the potential performance of a bioreactor operating under a specified protocol, the design engineer will find it necessary to employ appropriate material and energy balances on the reactor, together with a rate law that describes the kinetics of the chemical transformations of interest. In general, the equations generated during the analysis will differ for the various phases of the growth cycle. The design engineer must be prepared to employ either time-dependent analyses or steady-state analyses to describe the behavior of the reactor contents throughout the growth cycle.

We turn our attention next to the rate laws and principles of applied reaction kinetics typically associated with various phases of cell growth.

### 13.1.2 Rate Laws and Mathematical Descriptions of Phases of the Growth Cycle

Industrial scale microbiological processes employ organic compounds as key constituents of the reaction medium in which microorganisms are suspended. These compounds serve as a source not only of the chemical energy necessary to drive the chemical transformations of interest but also of the carbon atoms necessary for both continued growth of the microorganisms and biosynthesis of the metabolic products whose production may be the primary goal of the bioprocess. Usually, the conditions for operation of the bioreactor are such that those components of the nutrient mixture that are consumed in relatively low amounts are provided in excess of stoichiometric requirements. For such situations, the rate at which the carbon source in the growth medium is supplied often governs the rate of the biochemical process.

There is abundant literature describing many growth media that have been employed for the culture of cells and microorganisms of various types. Media can be purchased from multiple vendors with presterilized media available for use with cultures being conducted in single-use bioreactors (see Section 13.3.5) or in other situations where such a medium is desirable and cost-effective. We shall not discuss the formulation of these highly complex solutions of organic and inorganic solutes because the composition of the optimum growth medium is strongly dependent on the particular cell line being cultured and on the biosynthetic pathway of primary interest. Instead, we presume that those chemical engineers engaged in the design of

bioreactors will consult carefully with microbiologists and other scientists to develop growth media that enable the cell line of interest to achieve a high rate of production of the desired product per unit time per unit volume of reactor, as well as to ensure that the cell line is genetically stable. Both of these factors are extremely important in obtaining a commercially viable process that will meet all constraints imposed by regulatory agencies. Considerable research can be invested in ascertaining that the medium addresses multiple aspects of the metabolic pathways associated with the biosynthesis of those metabolites with high commercial value, as well as genetic stability issues and the entire composition of the spent medium from which the products of interest are to be recovered. Identification of a cell line that is highly productive in biosynthesis of the desired product under the conditions employed in its culture and is not susceptible to mutation or other forms of genetic instability is a crucial element in the development of an economically viable bioprocess.

#### 13.1.2.1 Characterization and Modeling of the Lag Phase

The lag phase of cell growth can play a very important role in an analysis of the economic potential of a proposed fermentation process, especially when it is likely that either a batch or fed-batch reactor will be employed in an industrial situation. In particular, optimization of the process economics usually requires that the length of the lag phase be minimized. As noted in our earlier discussion of conventional batch reactors in Section 8.0.2, one must account for both the time that a batch reactor is actually producing the desired product and the nonproductive periods associated with turning the reactor around so that the next cycle of production can be initiated. For a bioreactor that is employed in a batch mode during all or part of a production cycle, one must consider not only the time during which the actual chemical transformations are taking place, but also the times when chemical reactions are not occurring to any significant extent. For bioreactors the design engineer must add to the nonproductive periods associated with cleaning, sanitizing, filling, heating, cooling, and emptying the bioreactor both the lag time and the time necessary for inoculation of the growth medium. Hence, in a batch reaction process for which a microorganism is either the primary product or a biocatalyst, the design engineer must recognize that it is not just the exponential growth phase of the microorganism that governs the process economics. The most productive use of a batch bioreactor will generally occur when the length of the lag phase is minimized.

The ability of a particular microorganism to survive and reproduce is determined by the temperature, pH, and ambient conditions in the environment where it is located.

Survival depends on the ability of the microorganism to successfully metabolize the nutrients available in that environment. The various reactions that make up the metabolic network of the microorganism are catalyzed by enzymes of the variety of types necessary to sustain the life processes of that organism. Analysis and experimental manipulation of the pathways that make up these networks constitute the field of metabolic engineering, an area of study described in depth in the classic text by Stephanopoulos et al. (3). However, we should note that just as knowledge of a reaction mechanism is not essential in the design of a reactor to carry out that reaction, knowledge of the metabolic network for an organism is not essential to the design of a bioreactor. In both cases *what is required is a valid rate expression* for the chemical transformation and process conditions of interest.

There are several levels at which one might approach the problem of building a mathematical model of the kinetics of cell growth. Some approaches are both highly idealized and vast oversimplifications of what is found in nature, but benefit from the fact that they involve only a few parameters that are subject to determination by relatively simple measurements in the laboratory. Other models are highly complex in mathematical terms and often involve a multitude of parameters, some of which can be linked to known aspects of the biochemical reactions associated with the metabolic network of a particular microorganism. However, the task of quantifying the values of the large array of parameters of models which recognize that cultures are really a heterogeneous collection of discrete microorganisms is a forbidding task, especially if one recognizes that the various parameters may depend on temperature, pH, and/or the intensity of the electromagnetic radiation necessary for biophotosynthetic reactions. Because the growth of microorganisms is a highly complex process, drastic simplifications must be made to obtain a useful mathematical model of the growth process. An approach to the design of bioreactors that employs relatively simple mathematical models may not be accurate in predicting the detailed behavior of suspensions of the microorganisms present in a bioreactor, but it may nonetheless reveal the most important features of that behavior and, more importantly, serve the very functional purpose of facilitating certain aspects of the design of a bioreactor. For well over a century, chemical engineers have been able to make significant contributions to society by generating solutions to poorly defined problems that are not readily amenable to closed-form mathematical solutions. In making these contributions, chemical engineers have employed empirical relations, mathematical analyses, simplifying assumptions, computer simulations, heuristic analyses based on “rules of thumb,” sound judgment, concern for the safety of both employees and the general public, and respect for governmental regulations to arrive at workable solutions to problems of societal

interest. The solutions must not only be economically and technically feasible but may also need to satisfy a variety of political and regulatory constraints. Working together, chemical engineers and applied microbiologists have long achieved success in extending this approach to the design of bioreactors for use in manufacture of an extensive array of useful products.

### 13.1.2.1.1 Factors Influencing the Length of the Lag Phase

The length of the lag phase of the growth cycle depends on properties of both the growth medium and the particular type of microorganism to be employed, as well as its age and previous history of exposure to different environments. The modes of regulation and control of individual enzyme activities within a potential metabolic pathway are subject to the ability of a microorganism to adapt to an environment. Such acclimatization occurs when an organism is exposed to a different environment than that in which it has previously been present. Changes in the length of the lag phase of cell growth often reflect the necessity for individual cells to carry out the biosynthesis of the cell components, amino acids, enzymes, cofactors, vitamins, etc., necessary to activate or build an alternative pathway to replace a portion of a metabolic network that was not functioning as desired or otherwise needed to be modified. The need for modification arises because one (or more) of the pathways in the original network is no longer a functional contributor to the suite of metabolic reactions necessary for the microorganism to survive. For example, when a particular nutrient that plays a key role in the metabolism of the microorganism is exhausted, it *may* be possible for the organism to utilize a second nutrient already present in the fermentation medium via an alternative pathway that does not yet exist or has been “switched off” by the organism, but that could be created via biosynthesis of the necessary cell components. In essence, when the biosynthesis tools available to a microorganism no longer suffice to accomplish the metabolic task desired, the organism may be able to create new tools to accomplish the chemical transformations necessary to remain alive. Situations in which construction of the new pathway occurs at a rate that depends on the complexity of the particular stages associated with the new pathway may in some cases lead to a lag phase that is substantially longer than that observed originally. In other situations, the length of the lag phase may reflect not a necessity for creation of an *alternative* pathway, but for the need to obtain nonmultiplicative growth of the microorganism so as to increase the level(s) of the enzyme(s) associated with the original pathway. Decreases in the concentration of a critical nutrient are not believed to be reflected in changes in the length of the lag stage; instead, the system enters the exponential growth phase.

However, one typically does observe a decrease in the rate of growth of the microorganism.

As noted above, microorganisms can usually grow on different substrates. However, even if several substrates are present at a particular time in the growth medium, only one of these substrates is typically utilized by the microorganism being cultured. Only when the substrate preferred by the organism as the primary source of energy and carbon is exhausted do the cells construct the enzymatic pathways necessary to metabolize another substrate that meets the cell's requirements for energy and carbon atoms. The price the cells pay for renovation of the metabolic machinery of the organism is additional lag time. The ability of microorganisms to employ multiple substrates in this manner leads to what is referred to as *diauxic growth*.

The ages of the particular microorganisms constituting the inoculum can also have a major influence on the length of the lag phase. The particular behavior observed will reflect not only the age of the microorganism, but also the nature of the environments between which the microorganism is transitioning. Bailey and Ollis (2) cite an example of transfer of young cells of a specific organism for which in one medium the lag time increases with increasing age until an asymptotic limit is reached, while in a second medium the lag time goes through a minimum as the age of the microorganism increases. By contrast, transfer of an older population in a slow-growth-rate state (because of depletion of nutrients) into a fresh medium results in an increase in the length of the lag phase because the organisms must acclimate by increasing their metabolic rates in response to higher concentrations of nutrients and/or to transfer of inhibitors out of the old cells into the fresh medium.

In summary, the time between inoculation of the growth medium and initiation of the acceleration phase (i.e., the length of the lag phase) is dependent primarily on four variables: (1) the age of the cells in the inoculum, (2) the composition of the liquid suspension from which the inoculum is taken, (3) the composition of the growth medium that receives the inoculum; and (4) the ratio of the volume of the growth medium to that of the inoculum. In general, the lag time is minimized when the inoculum contains young cells in the exponential phase of their growth cycle and when the composition of the liquid phase of the inoculant and the growth medium are similar in nutrient content. The presence of both nutrients and metabolic intermediates (such as amino acids) in the growth medium will facilitate growth and reproduction of the microorganism, thereby contributing to minimization of the lag time.

Bailey and Ollis (1) have summarized the crucial features of a mathematical model developed by Dean and Hinshelwood (4) to characterize qualitatively the response of the lag time to changes in process parameters. The Dean–Hinshelwood model is based on the assumption

that when the concentration of some (unspecified) critical substance ( $C$ ) in a cell reaches a threshold value  $C'$ , the lag phase ends and the acceleration phase begins. The model is described by the following equation for the concentration of the critical substance within the cells as a function of the time elapsed since inoculation ( $t$ ):

$$C = aV + a'n_0t + a''t \quad (13.1.1)$$

where  $V$  is the volume of the liquid phase of the inoculant,  $n_0$  is the number of cells contained in the inoculum ( $n_0$  is also equal to the number of cells in the suspension of cells in the batch reactor throughout the lag phase because of the constraint that no growth occur during the lag phase),  $a$  is a parameter of the model that represents the product of the concentration of the critical substance per unit volume of the inoculum and the ratio of the volume of the inoculant to the sum of the volumes of the growth medium and the inoculant,  $a'$  is a parameter of the model that represents the contributions of other cells to the average increase per unit time per unit volume in the concentration of the critical substance in an individual cell, and  $a''$  is a parameter of the model that represents the average increase in the concentration of the critical substance in an individual cell per unit time that is attributable to metabolic production by the cell itself.

For pedagogical purposes it is useful to write equation (13.1.1) at the time ( $t_{\text{lag}}$ ) when the concentration of the critical nutrient reaches a value  $C'$ , and then rearrange that equation to obtain a relation that provides useful information concerning the effects of the size and age of the inoculum on the lag time:

$$t_{\text{lag}} = \frac{(C'/a') - (aV/a')}{n_0 + a''/a'} \quad (13.1.2)$$

Careful consideration of equation (13.1.2) indicates that if the size of the inoculum is quite small ( $n_0 \ll a''/a'$ ), the lag time will be inversely proportional to the productivity of a single young cell (assumed to be a constant). This lag time will then be long with a concomitant negative impact on process economics. By contrast, if  $n_0 \gg a'/a''$ , the lag time will be inversely proportional to the size of the inoculum, and short lag times are observed for large amounts of an inoculum comprised of young cells. Typically in industrial situations, one employs a volume of inoculant that is roughly 5 to 10% of the volume of the growth medium.

Even though there is no apparent net growth in the *number* of cells during the lag phase, the organisms are metabolizing nutrient substrates to create the changes in cellular structure that are necessary for the organisms to survive and grow in the environment in which they are located. The cells seek to accomplish two primary tasks: (1) conduct those metabolic activities necessary to maintain viability, and (2) establish a foundation in

terms of cellular structures that will provide for subsequent growth and reproduction.

### 13.1.2.2 Kinetics of the Exponential Phase

Microorganisms enter the exponential phase having utilized the acceleration phase to make the adjustments in their biological machinery and metabolic pathways that are necessary for them to multiply rapidly in the growth medium. The number of cells present in the reactor increases at a rate that is first-order in the number of cells present:

$$\frac{dn}{dt} = \mu_R n \quad (13.1.3)$$

where  $\mu_R$  is the specific rate of replication (with units of  $\text{time}^{-1}$ ). Subject to the boundary condition that at the start of the exponential growth phase, the number of cells is  $n_0^*$  and the time corresponding to the end of the acceleration phase is  $t^*$ , integration of equation (13.1.3) yields

$$n = n_0^* e^{\mu_R(t-t^*)} \quad (13.1.4)$$

The length of time necessary for the number of cells in the culture to double can be obtained using equation (13.1.4):

$$\ln\left(\frac{n}{n_0^*}\right) = \ln 2 = \mu_R(t - t^*) \quad (13.1.5)$$

or

$$t = t^* + \frac{\ln 2}{\mu_R} = t^* + \frac{0.693}{\mu_R} \quad (13.1.6)$$

The elapsed time necessary to double the number of cells in the culture is thus  $0.693/\mu_R$ .

The onset of the *deceleration phase* is identified as the time when the net rate of cell growth decreases. Decreases observed in the rate of increase of the number of cells are a direct consequence of the effects enumerated in Section 13.1.1. The point at which the *net* rate of cell growth becomes zero marks the onset of the *stationary phase*.

### 13.1.2.3 Kinetic Aspects of the Stationary Phase

The term *stationary phase* is in many respects a misnomer because it implies a lack of activity within the culture. In truth, there is no phase of the growth cycle of microorganisms in which intracellular activity is absent. Even the phrase “steady state” does not provide an accurate depiction of the states through which various individual microorganisms are passing during the stationary phase. During the stationary phase, metabolic activities are involved not only in maintenance of viability, growth, and reproduction of the microorganism, but also in the production of secondary metabolites.

*Metabolism* refers to those biochemical processes involving the consumption of nutrients by an organism to synthesize an array of biochemicals (and reaction intermediates) that are utilized in its growth, development, and reproduction. *Primary metabolites* are produced primarily during the exponential phase of cell growth and become constituents of the organism being cultured. They are essential to maintaining cell viability. The metabolic network of living cells is also responsible for the generation of substances that are not essential for cell viability. These substances are known as *secondary metabolites* (e.g., antibiotics, hormones, vitamins, and growth factors). The term *metabolite* is usually restricted to relatively small molecules.

The rates at which primary metabolites are produced follow the same general time course as the rate of normal cell growth (Figure 13.1) and are proportional to the growth rate of the organism. Secondary metabolites are not involved in those metabolic pathways that lead to growth. Often, they are produced subsequent to the exponential phase of cell growth. The presence of secondary metabolites in the growth medium can lead to enhancement of the growth rate of the microorganism only under certain specific circumstances. When these metabolites are not present, the cells do not die immediately, but their long-term survivability comes into question. During the stationary phase of the growth cycle, biosynthesis of some secondary metabolites (e.g., antibiotics and some hormones) is enhanced because their production is closely regulated by the microorganism.

Shuler and Kargi (6) have indicated that during the course of the stationary phase, one or more of the following phenomena may be observed:

1. The total amount of biomass in the reactor may remain constant, but the number of viable cells may decrease.
2. Lysis of cells may occur with concomitant release of the contents of these cells. (*Lysis* refers to a process involving breakage of cell walls via one of several possible mechanisms, either naturally via viral infections or osmotic phenomena, or via human intervention in the form of treatment with enzymes, chemicals, or sonication.) When lysis occurs, a microorganism may subsequently engage in a second growth phase (*cryptic growth*) if it is able to metabolize the cellular components released by lysis of other cells.
3. Microorganisms may engage in a destructive form of metabolism in which complex molecules within a cell (e.g., starches, proteins, fats) are broken down into simpler molecules that can be utilized as nutrients for further growth. In essence, an organism can deplete reserves stored within the cell during periods when these resources are abundant. These substances are employed in the biosynthesis of other components of

the cell (or in obtaining the energy needed for creating these components) or in other activities associated with maintenance of cell activity. In the past, such activities have often been referred to as *endogenous metabolism*, but in recent years it is more common to refer to them as cell maintenance requirements. This form of metabolism can be viewed as a reduction of metabolic activity toward the minimum level necessary to maintain viability.

- Even though there is no net growth of the microorganism the cells remain active in metabolic terms by producing secondary metabolites. In the stationary phase the mechanisms for regulation of cellular processes may be altered to yield secondary metabolites from nutrients containing carbon, nitrogen, and phosphate.

During the stationary phase the equation that describes how the mass of the microorganism present in the bioreactor declines as a consequence of the cell's requirements for maintenance energy and/or losses associated with lysis of cells can be written in differential form as

$$\left(\frac{dX}{dt}\right)_{\text{stationary}} = -k_{cm}X \quad (13.1.7)$$

where  $X$  refers to the total mass of live cells in the bioreactor and  $k_{cm}$  refers to the first-order rate constant characteristic of cell maintenance effects. Separation of variables and integration yield

$$X = X_{S0}e^{-k_{cm}t_{SP}} \quad (13.1.8)$$

where  $X_{S0}$  is the mass of live cells at the beginning of the stationary phase and  $t_{SP}$  is the time elapsed since the beginning of the stationary phase.

#### 13.1.2.4 Kinetics of Cell Death

The rate at which individual cells within a culture die is important not only in terms of its implications for the productivity of a fermentation process, but also because a knowledge of this rate is essential in the proper design of isolated sterilization/pasteurization equipment for use in the manufacture of food and pharmaceuticals. Determination of the death rate is also very important in establishing the procedural protocols used in sterilization. Thus far in this chapter we have utilized an approach based on the assumption that the various cells present in a culture play similar roles in the growth and proliferation of a particular organism. Such a description is not always accurate in that there may be some cells that are not able to grow and reproduce either because they are no longer living or because of some malfunction of their biological machinery. From a pragmatic point of view, the design engineer regards the offending organisms as if they were dead for purposes of

preparing specifications for bioreactors that will employ the culture in an industrial situation. The offenders do not contribute to the bottom line of a balance sheet and may be an early warning sign that something is awry with the source or mode of utilization of the microorganism.

The rate at which cells die is normally assumed to be proportional to the number of viable organisms present:

$$\frac{dn}{dt} = -k_d n \quad (13.1.9)$$

where  $n$  is the number of microorganisms present at time  $t$  and  $k_d$  is a pseudo-first-order rate constant for the various events that can cause a cell to die or lose its effectiveness as a potentially productive organism. Separation of variables and integration subject to the constraint that at the time the death phase begins ( $t_{d0}^*$ ), the number of viable organisms is  $n^*$  gives the following expression for the time dependence of the number of viable cells during the death phase of the growth cycle:

$$\ln\left(\frac{n}{n^*}\right) = -k_d(t - t_{d0}^*) \quad (13.1.10)$$

#### 13.1.3 Reaction Rates in Bioreactors and the Monod Equation

A key component of the analysis of any type of biochemical reactor is a mathematical expression that describes the rate at which a biochemical reaction takes place. Modeling the kinetics of a chemical transformation involves a compromise between recognizing that the model must be sufficiently complex to provide an accurate representation of the events that occur, but simple enough that the parameters of the model can be determined from a statistical analysis of readily obtainable experimental data. The most common starting point for modeling the kinetics of biochemical reactions involving either fermentation or biocatalysis by whole cells is the Monod equation. There is no single equation that provides an accurate description of all fermentation processes, but for microbial fermentations involving bacteria or yeast, the Monod equation is the relation that often serves as a useful point of departure for preliminary assessment in the design of a proposed bioreactor. First, however, we need to address the manner in which reaction rates are defined for the heterogeneous mixture that is contained within a bioreactor. Frequently, three phases are present: an aqueous solution containing the substrate nutrients, a solid phase consisting of the cells of the microorganism, and a gas phase that may contain air or oxygen as a substrate in the culture of various kinds of cells. At times metabolic products such as  $\text{CO}_2$  and  $\text{CH}_4$  may be also be present as components of the gas phase. The cells are suspended in the aqueous phase, either as individual cells or as agglomerates of individual cells.

The rates of the biochemical transformations that take place in a bioreactor are proportional to the quantity of biomass present. If we presume that species S is the substrate whose concentration in the growth medium limits the extent of reaction, the rate of consumption of this species per unit quantity of biomass can usually be expressed as

$$-r_{S,m} = -\frac{1}{X} \frac{dS}{dt} \quad (13.1.11)$$

where  $-r_{S,m}$  is the rate of consumption of substrate per unit of biomass present, X is the total quantity of biomass present, and S is the total quantity of substrate present. Comparison of equation (13.1.11) with an equivalent fundamental definition of the rate for a homogeneous reaction in equation (3.0.4) reveals that the rates of biochemical transformations are normalized with respect to the quantity of biomass present rather than with respect to the volume of a homogeneous phase.

An alternative approach that makes use of the concentration of biomass suspended in the growth medium is

$$-r_{S,m} = -\frac{1}{xV} \frac{dS}{dt} \quad (13.1.12)$$

where x is the concentration of biomass present in a volume V:  $x = X/V$ . Equations (13.1.11) and (13.1.12) explicitly indicate that the key to the design and analysis of bioreactors is recognition that the rate law is proportional to the quantity of biomass present.

Sometimes, volumetric expansion and contraction effects for biochemical transformations can be neglected. However, there are many situations in which it is imperative that the design engineer take into account the changes that occur in the volume of the aqueous growth medium that are brought about by bioconversion of soluble substrates into cellular matter, thereby decreasing the volume of aqueous phase present. At other times, decreases in the volume of the aqueous phase may result from vaporization of water that is swept out of the bioreactor in effluent gas streams as a consequence of humidification of the sterile dry air or oxygen streams that supply oxygen for use as a substrate in cultures requiring aerobic conditions. Increases in the volume of the aqueous phase can also occur. To maintain a constant pH of the growth medium, one may need to add a solution of a base or acid to offset the effects of reaction products that have the potential to alter the pH (e.g., CO<sub>2</sub>). Fed-batch operation of a bioreactor is yet another situation that leads to an increase in the amount of cell-free liquid in a bioreactor (see Illustration 13.4).

In writing the derivative terms in equations (13.1.11) and (13.1.12) we are transitioning from the symbolism of the chemical engineer that was employed in Chapters 8 to 11 for the design of chemical reactors to the symbolic language of the biochemist. In these chapters, species A identifies the limiting reagent, but in the present chapter we

use the symbol S to represent the quantity (mass or moles) of the stoichiometrically limiting *substrate* in the growth medium to stress a shift toward the conventional nomenclature of biochemists and applied microbiologists.

The *Monod equation* describes the rate of consumption of the substrate that limits the extent of the biochemical reaction as

$$-r_{S,m} = \frac{-1}{X} \frac{ds}{dt} = \mu = \frac{\mu_{\max} s}{K_S + s} \quad (13.1.13)$$

where X is the total mass of the microorganism in the bioreactor, where we have employed the Monod relation to explicitly describe the dependence of the specific growth rate ( $\mu$ ) on the concentration of the limiting substrate ( $s$ ), and where  $\mu_{\max}$  and  $K_S$  are the kinetic parameters of the Monod rate law.

In writing equations (13.1.11) to (13.1.13), we are recognizing the requirement that the reaction rate observed in the laboratory be proportional to the mass concentration of microorganism present. The dependence of the specific growth rate ( $\mu$ ) on substrate concentration ( $s$ ) is depicted in Figure 13.2. The expression for the specific growth rate contains two parameters that can be determined from kinetic data via analyses similar to those used to determine the parameters of rate laws of general Michaeli–Menten form (see Section 7.3.2.1). For example, one can rearrange equation (13.1.13) to obtain a form similar to that employed in Lineweaver–Burk plots for determination of the parameters of enzymatic reactions that are expected to obey Michaelis–Menten kinetics. Thus, from equation (13.1.13),

$$\frac{1}{\mu} = \frac{1}{\mu_{\max}} + \frac{K_S}{\mu_{\max}(s)} \quad (13.1.14)$$

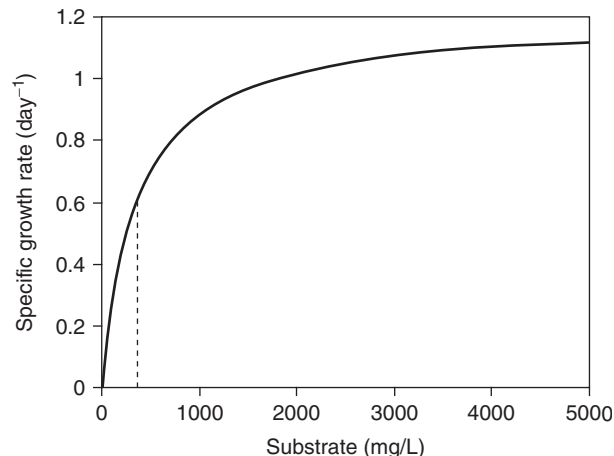


**Figure 13.2** Plot of the specific growth rate versus substrate concentration for an aerobic mixed culture on a glucose growth medium with the half-saturation constant  $K_S = 355$  mg/L and  $\mu_{\max} = 1.2$  day<sup>-1</sup>. The vertical line at a substrate concentration of 355 mg/L, a value equal to that of  $K_S$ , corresponds to a specific growth rate that is half the maximum value.

A double reciprocal plot of kinetic data for a biochemical reaction that obeys a Monod rate law will yield a value of  $\mu_{\max}$  from the reciprocal of the intercept of the  $y$ -axis. The corresponding slope is equal to  $K_S/\mu_{\max}$ . At high values of the substrate concentration ( $s \gg K_S$ ), the growth rate observed is pseudo zero-order in the substrate concentration and first-order in the mass concentration of cells. At very low values of the substrate concentration ( $(s) \ll K_S$ ), the rate observed per unit volume appears to be first-order in the concentrations of both the substrate and the microorganism. Although one can determine parameters of the Monod equation from data obtained using a bioreactor operating in a batch mode, more accurate values can usually be obtained from data generated in trials employing a laboratory-scale continuous flow stirred-tank reactor known as a *chemostat* [see equation (13.2.21) in Section 13.2.1].

The final form of the Monod relation in equation (13.1.13) is also of the same mathematical form as the Langmuir adsorption isotherm (see Section 6.2.1) and rate laws of the general Langmuir–Hinshelwood–Hougen–Watson (LHHW) type for heterogeneous catalytic reactions (see Section 6.3.1). At low values of the independent variable in these relations, the dependent variable is nearly linear in the independent variable. However, at large values of the independent variable, the dependent variable approaches an asymptotic limit (see Figure 13.2).

In equation (13.1.13),  $\mu_{\max}$  is the maximum achievable growth rate when  $(s) \gg K_S$ . The parameter  $K_S$  is referred to by various authors as the *saturation constant*, as the *half-velocity constant*, or as the *half-saturation constant*. In this book we employ the term *half-saturation constant*. The value of  $K_S$  in the Monod model represents the half-saturation constant for the overall growth process, not just the half-saturation constant for consumption of substrate (because of circumstances under which some substrate must be metabolized for purposes of cell maintenance). The values of  $K_S$  obtained in studies of the growth of microorganisms are typically quite small, often in the mg/L range for carbohydrates and in the  $\mu\text{g}/\text{L}$  range for amino acids. Because the concentrations of the growth-limiting substrate encountered in engineering practice usually exceed  $K_S$  by a factor of 10 or more, the growth rate can often be well approximated by a rate law that is zero-order in the substrate so that  $\mu$  in equation (13.1.13) approaches  $\mu_{\max}$ . Consequently, the assumption that  $\mu = \mu_{\max}$  is often made in preliminary considerations of the design of a biochemical reactor. When consumption of the limiting substrate reduces the substrate concentration to the point that it becomes comparable to  $K_S$ , the growth rate may decline to an extent that it is reflected in what appears to be an abrupt transition from a logarithmic phase to a stationary phase. Such a transition reflects rapid consumption of the remaining substrate in the presence of a large number of microorganisms.

The Monod model often provides a good representation of specific growth rate data for circumstances in which growth of the microorganism is not only slow and substrate limited, but also such that the number density of the microorganism is low. Under these conditions the value of  $(s)$  appearing in the Monod equation is simply related to conditions in the growth medium.

It has been argued that the rationale underlying use of the Monod equation as a mathematical model of the kinetics of biochemical reactions is that (1) within the metabolic network of a microorganism there lies a single metabolic pathway that controls the rate of growth of that microorganism; (2) that within this pathway there is a crucial enzymatic reaction for which a Michaelis–Menten rate law governs the rate of uptake of the limiting substrate; and (3) that either the concentration of the critical enzyme or its intrinsic activity is so low that this reaction controls the rate at which the microorganism can grow. However, we would be remiss in our obligations to the reader if we did not indicate that the Monod equation is an *empirical* relation that finds validation primarily in the fact that it has traditionally provided satisfactory representations of data for a wide variety of organisms and experimental conditions. Readers should not misconstrue the quality of these representations of the data by assigning mechanistic implications to the constituent terms in the Monod equation as one does with Michaelis–Menten and LHHW equations for enzymatic and heterogeneous catalytic rate expressions, respectively. There are no simple molecular-scale interpretations of the parameters of the Monod equation as there are for the parameters of the Michaelis–Menten and LHHW rate laws.

The ability of Monod's empirical relation to fit kinetic data for biochemical reactions has its foundations in generalizations of two phenomena frequently observed for fermentation processes: (1) nature places a cap on the quantity of microorganism that can be achieved during the exponential phase of growth in a bioreactor operating in a batch mode; and (2) as the concentration of the limiting substrate approaches zero, the rate laws for biochemical reactions approach pseudo-first-order behavior with respect to that substrate. The cap indicated on the cell growth rate has been associated with the natural limit on the maximum rate at which replication of DNA can be achieved.

Because of the failure of the Monod equation to find universal applicability, many researchers have suggested variations on the form of this equation in attempts to better characterize the kinetic behavior of substrate-limited growth of microorganisms. There are several more complex mathematical models that take into account not only inhibition by substrates and/or products of biochemical reactions, but also other factors, such as cell death and cell maintenance effects and multiple limiting substrates (5, 6).

Interested readers are encouraged to consult the literature for up-to-date perspectives.

### 13.1.4 Specific Growth Rates, Yield Coefficients, and Stoichiometric Considerations

In an environment that is conducive to the growth of a particular microorganism, cells regulate their metabolism and control their growth rate by adjusting the rates of various intracellular reactions to produce *balanced growth*. In batch cultures, balanced growth is most likely to be observed during the exponential phase of growth. During balanced growth the regulatory machinery of the cell adjusts the rates of the intracellular reactions to maintain a constant composition of the biomass despite variations in the composition of the growth medium in which the organism finds itself. For this condition to be sustainable temporarily, the specific rates of production of the various constituents of the microorganism must be proportional to one another and to the specific growth rate of the cell itself:

$$r_\chi = \mu \chi \quad (13.1.15)$$

where  $\chi$  refers to the total mass of an arbitrary constituent of the microorganism,  $r_\chi$  is the rate of production of the mass of constituent  $\chi$  per unit quantity of biomass in the suspension of microorganisms, and  $(\chi)$  is the concentration of constituent  $\chi$  within the bioreactor. Consequently, for balanced growth, the doubling time for each component of the microorganism is identical to that for the entire organism. Balanced growth cannot be maintained, however, if changes in the growth medium affect the specific growth rate of the cells.

If we combine equations (13.1.13) and (13.1.15) and introduce a yield coefficient  $Y_{X/S}$  (see below), we find that

$$r_\chi = Y_{X/S} \frac{\mu_{\max}(s)}{K_S + (s)} (\chi) \quad (13.1.16)$$

Equations of this form can be written for each of the various products of the reaction, as well as for consumption of the limiting substrate. Additional stoichiometric relations can also be developed for other species that are utilized as non-limiting substrates by the microorganism undergoing fermentation. However, because the stoichiometry associated with the production of biomass is well established for only a very few simple fermentations, biochemists and others engaged in the design of bioreactors find it useful to employ the concept of *yield coefficients* in their efforts to analyze the performance of proposed bioreactors. In essence, these researchers determine the yield coefficients experimentally in a manner akin to the technique of eliminating time as a variable in considerations of competitive and consecutive reactions (see Chapter 9).

An *overall yield coefficient*,  $Y_{X/S}$ , is defined as the ratio of the total amount of *new product X obtained* (in mass or moles) *per unit consumption of substrate S* (again in mass or moles) over the entire course of a biochemical reaction.

$$Y_{X/S} = -\frac{\Delta X}{\Delta S} = -\frac{X_F - X_0}{S_F - S_0} = \frac{X_F - X_0}{S_0 - S_F} \quad (13.1.17)$$

where the minus sign in front of the first two terms on the right side of the equation stresses the fact that one species is a reactant and the other is a product. One normally thinks of yields as positive quantities. Hence, we need the minus signs to account for the fact that the change in the quantity of the limiting substrate present ( $\Delta S$ ) is a negative quantity.

[Cautionary Note: Readers should note that numerous inconsistencies in the definitions, signs, and symbols (including subscripts) employed for the yield coefficients are present in various textbooks and scientific publications. These inconsistencies create considerable ambiguity in the minds of readers concerning the proper use of this parameter. In his book, Hochfeld (7) defines an overall yield coefficient,  $Y_{X/S}$ , as the absolute value of  $\Delta X/\Delta S$ . He subsequently relies on physical intuition in assigning positive or negative signs to the various terms involved in analyses of the rates at which products and substrates of metabolic reactions are formed or consumed, respectively. As we have defined  $Y_{X/S}$  here, this parameter is a positive quantity.]

While presentation of the concept of the number of moles of a microorganism is not an integral part of the training of a chemical engineer, one can view the concept as equivalent to the number of gram-atoms of carbon present in that microorganism at the time of interest and make appropriate adjustments in the yield coefficient to keep track of the stoichiometry. In essence what one does is to use elemental analyses to generate a hypothetical chemical formula for a microorganism that is of the form  $\text{CH}_u\text{O}_v\text{N}_w$ , where the subscripts  $u$ ,  $v$ , and  $w$  refer to the ratios of the atom percentages of H, O, and N to the atom percentage of C, respectively. Hypothetical chemical formulas can also be generated for other potential fermentation products, such as carbohydrates, enzymes and other proteins, biopolymers, and others.

The instantaneous yield coefficient,  $y_{X/S}$ , is a useful concept when yields can vary appreciably during the course of a culture (as might be the case for a batch reaction). In the limit as  $\Delta S$  approaches zero,

$$y_{X/S} = -\frac{dX}{dS} \quad (13.1.18)$$

The instantaneous yield can also be viewed as the ratio of the rate of formation of product X to the rate of consumption of substrate S:

$$y_{X/S} = -\frac{dX/dt}{dS/dt} = \frac{r_X}{-r_S} \quad (13.1.19)$$

Because S is a substrate, this species is consumed rather than produced, so its net rate of production,  $r_S$ , is a negative quantity.

Readers should note that two subscripts are needed to define yield coefficients properly. The first subscript denotes the species whose rate of *formation* ( $r_X$ ) appears in the numerator of equation (13.1.19) for the ratio of reaction rates, while the second subscript is associated with the rate of production of the species appearing in the corresponding denominator. This cautionary note should indicate to the reader that there are circumstances under which both the numerator and the denominator of equations similar to equations (13.1.17) to (13.1.19) can refer to two different product species. For example, the symbol  $Y_{P/X}$  refers to the mass (or moles) of product P formed per unit mass (or moles) of biomass formed. The extension of the yield concept in this direction is significant when selectivity considerations are important in a particular fermentation. In such cases it is helpful to examine the relative rates at which two different products are formed as an analytical tool that facilitates identification of optimum operating conditions to enhance production of a desired product V relative to that of a less desirable product W. In this

situation, as seen below, we arrive at a useful parameter that is similar in notation to an instantaneous “yield” coefficient but in truth has a significantly different physical basis:

$$\frac{r_V/(-r_S)}{r_W/(-r_S)} = \frac{y_{V/S}}{y_{W/S}} = \frac{dV/dt}{dW/dt} = y_{V/W} \quad (13.1.20)$$

For competitive (parallel) reactions, one can extend the yield concept further to arrive at relations for the relative rates of consumption of different substrates.

The substrates consumed by microorganisms during the course of a fermentation are frequently utilized for a variety of purposes (e.g., growth, cell maintenance, and production of primary and secondary metabolites). The regulatory machinery of individual cells determines how the substrates taken up by a cell are distributed among those constituent pathways of a metabolic network that are seeking allocations of particular substrates. Figure 13.3 is a schematic diagram of representative allocations of substrates at different stages of the cell growth cycle (8).

The selectivity of a microbiological process can be quantified in terms of the principles of stoichiometry by analyzing these allocations. Per unit of consumption of the

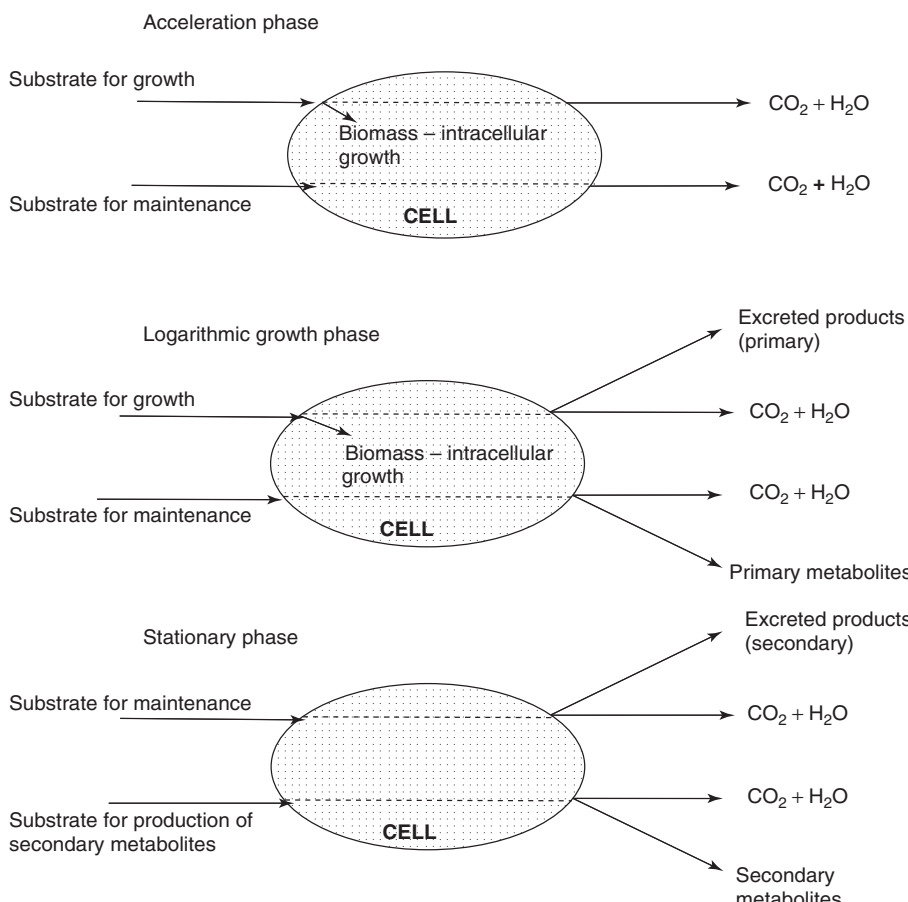


**Figure 13.3** Substrate uptake by microorganisms. From top to bottom: metabolism during the acceleration phase is directly coupled to energy metabolism to construct the cellular machinery for growth and survival; production of primary metabolites during the exponential phase is a combination of processes directly coupled to energy metabolism and processes not directly coupled to energy metabolism; production of secondary metabolites occurs during the stationary phase. Cells that grow to a critical mass are subsequently capable of dividing to form additional cells during the acceleration and logarithmic growth phases. (Adapted from P. M. Doran, *Bioprocess Engineering Principles*, p. 284, with permission from Academic Press, San Diego CA, an imprint of Elsevier.)

stoichiometrically limiting substrate or nutrient, the distribution of metabolic products resulting from the chemical transformation can be characterized via a material balance:

$$Y_{X/S} + Y_{\text{maintenance}/S} + Y_{P1/S} + Y_{P2/S} + Y_{P3/S} + Y_{P4/S} + \dots = 1 \quad (13.1.21)$$

where  $Y_{X/S}$  refers to the fractional conversion of the substrate to additional microorganism(s),  $Y_{\text{maintenance}/S}$  indicates the fraction of the substrate consumed that is utilized in maintenance activities of the cell, and where  $Y_{Pi/S}$  refers to the fractional conversion of the substrate to metabolic product  $i$ . For purposes of bioreactor design, we regard these yield coefficients as being parameters that are determined experimentally (apparent or observed values) rather than as quantities that can accurately be predicted from theoretical considerations of the stoichiometry of the reaction (sometimes misleadingly referred to as “true” yield coefficients). Because multiple reactions are occurring simultaneously during metabolic processes, it is important to distinguish between actual (or observed yields) and theoretically predicted “yields.” The former are much more important in considerations of engineering design.

The total yield of a particular product (e.g., additional biomass in the form of cell growth or an increased number of cells with associated biomass) may be calculated using the proper overall yield coefficient and the amount of substrate consumed using the following linear relation:

$$\text{additional biomass} = \Delta X = X - X_0 = Y_{X/S}(S_0 - S) \quad (13.1.22)$$

where  $S_0$  and  $S$  refer to the amounts of substrate present initially and at the time the measurement of the overall yield of biomass is desired. The yield of a particular product can be enhanced by manipulating the yield of that component relative to the yields of the other products and the microorganism(s). To accomplish this enhancement, one might chose to employ another strain of the microorganism, to inhibit undesirable reactions by changing the composition of the fermentation medium, or to modify the microorganism genetically in a manner that alters the original product distribution given in equation (13.1.21). In addition to the microbiological properties of the biocatalyst, the relative yields of the various products may be affected by physical parameters of the reaction medium: pH, ionic strength, temperature, intensity and wavelength of incident electromagnetic radiation, and chemical composition. The utility of the discussion above lies in its straightforward extension to the conclusion that the rate of production of a particular product is given by the product of the yield coefficient for that product relative to the limiting substrate and the rate of consumption of that substrate. For example, the rate of production of

microorganisms is linked to the rate of consumption of the limiting substrate by

$$\begin{aligned} & \text{microorganism production} \\ &= Y_{X/S} \times \text{substrate consumption} \quad (13.1.23) \end{aligned}$$

or

$$\frac{dX}{dt} = Y_{X/S} \times \left( -\frac{dS}{dt} \right) \quad (13.1.24)$$

Hence, to design a bioreactor when one knows the various yield coefficients, the other primary need for assessment of the selectivity of the biochemical transformation is a valid mathematical relation for the rate of consumption of the limiting substrate.

An alternative approach to consideration of the multiple routes by which the limiting substrate is consumed in a bioreactor is to reexamine the pathways shown in Figure 13.3 and to write an expression for the rate of consumption of the limiting substrate when it proceeds via a particular pathway. The total rate at which substrate is consumed can then be written as the sum of the rates of consumption via the individual pathways. Thus, in terms of our formulation of the convention for yield coefficients for metabolism of cells that takes place in a constant-volume closed system, the rate of consumption of substrate can be expressed as a sum of terms associated with the rates at which biomass and other products of metabolic processes are formed plus a maintenance coefficient,  $m_S$ , that characterizes the rate at which a cell in a resting state must consume substrate for maintenance activities if it is to remain alive:

$$-r_S = \frac{r_X}{Y_{X/S}} + \frac{r_P}{Y_{P/S}} + m_S X \quad (13.1.25)$$

In a resting state, a cell is neither reproducing nor generating products.

The basic interpretation of equation (13.1.25) is that it describes the distribution of substrate consumption into three portions: assimilation of substrate into biomass constituents, synthesis of products, and provision of the energy necessary to survive. Aspects of viability incorporated in the term for maintenance activities include facilitating transport of ions or other solutes across cell membranes and synthesizing cell constituents as replacements for damaged or malfunctioning constituents of the metabolic network of the cell, thereby repairing those pathways essential to the life of the microorganism.

A more useful approach to quantifying the relative amounts of substrate that are allocated to different metabolic pathways by individual cells is to employ the concept of *biomass specific rates*, sometimes referred to as *q-rates*. In a sense, these rates are analogous to the expression of rates per unit surface area that is often employed in heterogeneous catalysis (see Chapters 6 and 12). The various *q*-rates are defined by normalizing the

rate at which a particular rate process is occurring with respect to the quantity of cells present that are both viable and functional with respect to growth, reproduction, and metabolic activity. For example, the biomass specific rate at which substrate is consumed is often described by the Monod equation. The *biomass specific rate* for production of biomass is expressed as the ratio of the total quantity of biomass produced per unit time to the total quantity of (viable) biomass present at a particular time. Use of biomass specific rates is a more fundamental approach in considerations of biochemical transformations than are the volumetric rate terms  $r_S$  and  $r_X$  contained in equations such as (13.1.19) and (13.1.20). The various biomass specific rates characterize the average activities of the individual microorganisms rather than the behavior of the entire contents of the reactor. A biomass specific rate can be expressed as either (g product/g biomass)/time or simply time<sup>-1</sup>. Other mass units or molar units may be employed in either the numerator or the denominator of the term in parentheses.

Values of biomass specific rates are influenced by both genetic and environmental factors. The genes of a particular microorganism and the composition of the growth medium (including the presence of coenzymes, vitamins, hormones, mineral salts, and a variety of other soluble substrates) can affect the numerical values of the various  $q$ -rates. Other environmental variables that may influence  $q$ -rates are temperature, pH, intensity and wavelength of incident radiation, and ionic strength.

If we divide equation (13.1.25) by the quantity of biomass present in a bioreactor at any time and utilize the general definition of  $q$ -rates:

$$\begin{aligned} \frac{-r_S}{X} &= -q_S = \frac{r_X}{XY_{X/S}} + \frac{r_P}{XY_{P/S}} + m_S \\ &= \frac{q_{X/S}}{Y_{X/S}} + \frac{q_{P/S}}{Y_{P/S}} + m_S \end{aligned} \quad (13.1.26)$$

The biomass specific growth rate  $\mu$  is the most important  $q$ -rate. To determine other significant  $q$ -rates, one need only recognize that in a time increment  $dt$  the change in the amount of substrate  $dS$  that can be attributed to the pathway leading to production of biomass is given by

$$dS = q_S X dt \quad (13.1.27)$$

while the corresponding change in the amount of biomass present is

$$dX = Y_{X/S} \mu X dt \quad (13.1.28)$$

where we have employed the definition of the yield coefficient [equation (13.1.23)].

The yield coefficient provides a key link between actual production of biomass and consumption of the limiting substrate. Considerations of the accuracies of the analytical

chemistry methods used to quantify the amounts of biomass and substrate(s) present in a bioreactor operating in a batch mode lead to the methodology described in Illustration 13.1 for calculating  $q$ -rate values.

### ILLUSTRATION 13.1 Determination of Biomass Specific Rates ( $\mu_{\max}$ , $q_X$ , and $q_S$ ) and Yield Coefficients from Data Obtained Using a Batch Reactor

The data (hypothetical for pedagogical reasons) in Table I13.1-1 represent the growth of a generic microorganism on a glucose substrate in a batch reactor. The data have been chosen to illustrate that under circumstances that lead to a change in the volume of the growth medium in a batch reactor, one must be sure to base the calculations of  $\mu$  and the  $q$ -rates on the total quantity of biomass present rather than on the volume occupied by the growth medium. The tabular entries below are readily measured variables. Because the microorganism has been acclimated to the growth medium prior to initiation of the “experiment,” there are no substantive lag-time effects.

- Determine both the total rate of consumption of substrate and the total rate of production of biomass.
- Determine the values of  $\mu$ ,  $q_X$ , and  $q_S$  that correspond to the tabular entries.
- Comment on your answers to parts (a) and (b).

### Solution

It is important to recognize that in this analysis one must take into account the very marked decrease (32%) in the volume of the growth medium during the course of the fermentation. We can utilize the data provided in the problem

**Table I13.1-1** Results of a Kinetic Trial Involving Fermentation of a Generic Microorganism

Time (min)	Glucose (substrate) concentration (g/L)	Biomass concentration <sup>a</sup> (g/L)	Volume of growth medium (mL)
0	20.17	6.00	1000
40	20.07	6.20	991
80	20.03	6.44	978
160	19.72	6.88	962
320	19.13	7.95	920
640	17.03	10.67	837
1280	6.44	19.55	682

<sup>a</sup>Dry weight of biomass per liter.

statement, together with an Excel spreadsheet, to calculate the total amounts of substrate and biomass present at any of the indicated times, recognizing that at any time these totals are equal to the product of the volume of the cell-free growth medium and the corresponding concentration of biomass or glucose. The results of these calculations are summarized in Table I13.1-2, which also contains estimates of the total rates of consumption of substrate ( $-R_S$ ) and production of biomass ( $R_X$ ) that were obtained by simple numerical differentiation of the appropriate entries in Table I13.1-2: for example,

$$\frac{dX}{dt} = \frac{X_i - X_{i-1}}{t_i - t_{i-1}} \quad (\text{A})$$

This simple approach was adopted in order to circumvent the complications that are introduced by the fact that the volume of the liquid phase in the reactor varies with time. When the volume of the aqueous growth medium varies during the course of the reaction, an approach based on integration of a proposed rate law is problematic, although numerical integration would be possible. An additional reason for employing the differential approach below is that for rate laws that are other than those of the simple nth-order form (such as a Monod rate expression) a differential method of data analysis is often adequate for preliminary considerations involved in the design of a bioreactor that is intended to operate in a batch mode.

If one examines the entries in Table I13.1-2 for the total quantities of substrate and biomass present as functions of time, it is evident that the total amount of substrate declines continuously while the total biomass increases as the reaction proceeds. Note that on a mass basis the total rate of consumption of substrate always significantly exceeds the total rate of formation of biomass. Moreover, the magnitudes of both of these rates increase as time elapses, an indication that this reaction is indeed autocatalytic.

Although there are entries in Table I13.1-2 for the rate at which the total amount of biomass is increasing, it is preferable to use the entries in Table I13.1-1 to calculate the biomass specific growth rate ( $\mu$  or  $q_{X/S}$ ) using the following relation derived from equation (13.1.28):

$$\begin{aligned} \mu = \frac{1}{X} \frac{dX}{dt} &= \frac{d\ln X}{dt} \approx \frac{\ln X_i - \ln X_{i-1}}{t_i - t_{i-1}} \\ &= \frac{\ln(X_i/X_{i-1})}{t_i - t_{i-1}} \end{aligned} \quad (\text{B})$$

From the entries for the rate of consumption of substrate in Table I13.1-2, one can estimate the biomass specific rate of consumption of substrate ( $q_S$ ) by dividing the entries for the former rate by the amount of biomass present at the corresponding time. Estimates for both  $q_X$  and  $q_S$  are presented in Table I13.1-3 together with the corresponding values of the yield of biomass in grams of dry weight per gram of substrate consumed ( $Y_{X/S}$ ).

Inspection of the values of  $q_X$  and  $q_S$  in Table I13.1-3 indicates that even in terms of our unsophisticated approach to the determination of these parameters, the percentage variations are surprisingly small. The fact that the variations are small can be attributed to a situation in which the Monod parameter  $K_S$  in equation (13.1.13) is much less than the substrate concentration ( $s$ ). Consequently, the Monod rate law reduces to a pseudo-zero-order form

$$\mu \approx \mu_{\max} \quad (\text{C})$$

Such results are observed sufficiently often that  $q$ -rate parameters may be employed in preliminary considerations of the design of a bioreactor.

The biomass specific growth  $\mu$  can be written as

$$\mu = q_{X/S} = Y_{X/S}(-q_S) \quad (\text{D})$$

where  $Y_{X/S}$  can be regarded as the actual yield of biomass per unit of substrate consumed. Note from the entries in

**Table I13.1-2** Determination of Concentrations and Total Masses for Substrate and Cells for a Trial Involving Growth of a Generic Microorganism on Glucose

Time (min)	Total substrate (glucose) (g)	Total biomass (dry weight) (g)	Rate of substrate production, <sup>a</sup> $R_S \times 10^3$ (g/min)	Rate of biomass production, $R_X \times 10^3$ (g/min)
0	20.170	6.000		
40	19.889	6.144	-7.016	3.605
80	19.589	6.298	-7.501	3.853
160	18.971	6.619	-7.734	4.003
320	17.600	7.314	-8.569	4.347
640	14.254	8.931	-10.45	5.052
1280	4.392	13.333	-15.41	6.879

<sup>a</sup>The rate of production of substrate is (minus) the rate of consumption of substrate.

**Table I13.1-3** Determination of Biomass Specific *q*-Rates ( $\mu$  and  $q_S$ ) and Yield Coefficients for a Trial Involving Growth of a Generic Microorganism on Glucose

Time (min)	<i>q</i> -rate glucose, $q_S \times 10^3$ [(g/g) min $^{-1}$ ]	<i>q</i> -rate biomass, $q_X$ (a.k.a. $\mu$ ) $\times 10^4$ [(g/g) min $^{-1}$ ]	Yield coefficient, $Y_{X/S}$ (g/g)
0			
40	-1.142	5.937	0.52
80	-1.191	6.194	0.52
160	-1.168	6.199	0.53
320	-1.172	6.245	0.53
640	-1.171	6.241	0.53
1280	-1.156	6.262	0.54
Average	-1.17	6.18	0.53

Table I13.1-2 that the yield coefficients are positive (the biomass increases as substrate is *consumed*). Values of the biomass yield coefficients,  $Y_{X/S}$ , for many fermentations are typically about 0.5.

Readers are encouraged to consult modern texts focusing on cell kinetics and yield and selectivity considerations for additional details concerning how best to exploit experimental data to determine values of the parameters appearing in equations (13.1.17) and (13.1.25). However, readers are cautioned that for biochemical reactions it is normally preferable to employ a chemostat operating at steady state to generate kinetic data rather than a batch reactor. Such use of a chemostat not only circumvents issues associated with the lag time but also avoids the necessity of having to differentiate the data graphically or numerically. Chemical analyses of the compositions of the feed and product streams, coupled with measurement of the volumetric flow rate provide sufficient information to calculate the reaction rate directly using an equation such as (13.2.21).

In developing the solution to Illustration 13.1, we utilized a variation of the traditional material balance on a batch reactor that is often useful in the analysis of biochemical transformations carried out in batch and semibatch modes of operation. In particular, we took into account variations in the volume of the broth in the bioreactor by first converting concentrations of biomass and substrate into the total quantities of these materials present in the bioreactor. In so doing we were implicitly recognizing that the proper form of a material balance on species  $i$  for variable-volume situations is

$$\text{rate of accumulation} = \frac{d(C_i V)}{dt} = \frac{dN_i}{dt} = r_{ix} X \quad (13.1.29)$$

where  $C_i$  is the concentration of species  $i$  in the growth medium at time  $t$ ,  $V$  is the volume of cell-free growth

medium in the bioreactor,  $N_i$  is a measure of the mass or moles of species  $i$  present in the reactor,  $r_{ix}$  is a rate law expressed per unit of biomass in the reactor (e.g., a biomass-specific growth rate), and  $X$  is the quantity of biomass present in the bioreactor.

A few additional comments are worthy of note concerning the volume term that appears in many of the equations that we have introduced in our discussion of bioreactors operating in a batch mode. First, we need to emphasize that one's first action in analyzing a sample of broth removed from a bioreactor should be to remove the cells in order to obtain a supernatant liquid that is stable. Removal of the cells will quench biochemical consumption of the limiting substrate. Otherwise, the biomass would continue to act on the substrates so as to alter their concentrations as well as to produce additional biomass and other products. Next, one proceeds to assay the supernatant liquid to determine both the concentration of the analyte or substrate of interest and the total volume of the supernatant liquid relative to the total volume of the broth sample. The volume referred to in the equations pertinent to the design of a batch bioreactor [such as (13.1.29)] is the volume of cell-free liquid in the bioreactor, and the concentration of species  $i$  in the product on the left side of this equation also refers to the cell-free liquid. This approach presumes that the analyte of interest is present only in the supernatant and not in the biomass proper. Otherwise, one must also account for this situation.

Just as knowledge of the reaction rate per unit volume is very helpful in determinations of the size of a particular type of reactor for carrying out a homogeneous phase reaction (see Table 8.1), so too is it beneficial to be able to relate the various *q*-rates to reaction rates per unit volume. The several *q*-rates are expressed per unit of biomass. Hence, the corresponding rates per unit volume of reactor can be expressed as

$$r_i = q_i x \quad (13.1.30)$$

where  $x$  is the concentration of biomass in the suspension.

The solution to Illustration 13.1 indicates how one can derive values of *q*-rate kinetic parameters from experimental data characteristic of the fermentation of a generic microorganism. Analysis of the data was complicated by the fact that the volume of the fermentation broth varied substantially during the course of the reaction. The focus of Illustration 13.2 is on providing an indication of how one can utilize *q*-rate values to estimate the manner in which the masses of substrate and biomass vary with time of reaction. The ability of the *q*-rate model to fit a data set is assessed in this example by visual comparison of plots generated using the model to the initial synthetic "data points" analyzed in determining the parameters of the model.

## ILLUSTRATION 13.2 Use of Biomass Specific Growth Parameters to Determine the Time Course of a Biochemical Transformation

Consider the task of ascertaining the time variation of the total masses of both substrate and microorganisms for a fermentation that takes place in a laboratory-scale batch reactor with a working volume of 1 L. Initially, the bioreactor contains 20.17 g of glucose and 6.00 g (dry weight) of an unspecified microorganism. The values of the biomass specific growth rate ( $\mu_{\max}$ ) and the substrate  $q$ -rate ( $q_{\max}$ ) are  $6.18 \times 10^{-4} \text{ min}^{-1}$  and  $1.17 \times 10^{-3} \text{ (g substrate/g dry weight biomass \cdot min)}$ , respectively. The yield coefficient  $Y_{X/S}$  is 0.53 g dry weight biomass/g substrate. Solve the corresponding differential equations and use the solution to generate plots of the total biomass and the total amount of substrate present in the reactor at times from zero to 1600 min. Superimpose the data points on which the parameters of the model are based (see Illustration 13.1) on this plot. Comment.

### Solution

The results obtained in Illustration 13.1 indicate that for the biochemical reaction of interest the biomass specific growth rate is essentially constant. This fact, in turn, implies that the parameter  $K_S$  in the Monod equation is sufficiently small that it can be neglected over the large majority of the time that the biochemical transformation is taking place. Under these circumstances a mass balance for the microorganism leads to the following developments for circumstances when the volume of the growth medium remains constant:

$$\frac{1}{X} \frac{dX}{dt} = \mu = \mu_{\max} \quad (\text{A})$$

Separation of variables and integration yield

$$\int_{X_0}^X \frac{dX}{X} = \int_0^t \mu_{\max} dt \quad (\text{B})$$

or

$$\ln \left( \frac{X}{X_0} \right) = \mu_{\max} t \quad (\text{C})$$

where  $X_0$  is the mass of cells present at time zero, when the cells are presumed to be in the exponential stage of the growth cycle. Because the microorganism has been acclimated to the growth medium prior to initiation of the “experiment,” there are no substantive lag-time effects. Exponentiation of both sides of this equation followed by rearrangement produces the relation

$$X = X_0 e^{\mu_{\max} t} \quad (\text{D})$$

We can now proceed to write a material balance for the substrate in the form of equation (13.1.27) as

$$dS = q_s X dt \quad (\text{E})$$

where we may again take the appropriate value of  $q_s$  as that corresponding to the maximum biomass-specific growth rate. Substitution of equation (D) into equation (E) yields

$$\frac{dS}{dt} = q_{S\max} X = q_{S\max} X_0 e^{\mu_{\max} t} \quad (\text{F})$$

Integration then gives

$$\int_{S_0}^S dS = \int_0^t q_{S\max} X_0 e^{\mu_{\max} t} dt \quad (\text{G})$$

or

$$S = S_0 + \frac{q_{S\max} X_0}{\mu_{\max}} (e^{\mu_{\max} t} - 1) \quad (\text{H})$$

Readers should note from the entries in Table I13.1-3 that  $q_{S\max}$  is negative (the total amount of substrate in the batch reactor declines as fermentation proceeds). Combination of equations (C) and (H) yields

$$S = S_0 + \frac{q_{S\max} (X - X_0)}{\mu_{\max}} \quad (\text{I})$$

Substitution of the average values of the biomass specific  $q$ -rates into equations (D) and (I) yields relations that may be employed in a spreadsheet format to generate plots of the total masses of substrate and cells present in the bioreactor as functions of time. These plots are shown in Figure I13.2 together with “points” representing the data employed in Illustration 13.1 to determine the  $q$ -rate values used here in Illustration 13.2.

Examination of Figure I13.2 indicates that the model fits the biomass data very well; by contrast, the quality of the fit of the model to the substrate data is not nearly as good, especially at long fermentation times. For fermentation times less than 10 h, the quality of the substrate fit is good, but for longer times the model significantly overpredicts the amount of substrate remaining. Readers are cautioned, however, that the  $q$ -rate model requires analysis of experimental data to generate the parameters of the model and that these parameters are specific to a particular microorganism and the environment in which the organism finds itself. The model is a well-tested semiempirical approach rather than a correlation based on theoretical considerations.

The shapes of the plots for substrate consumption and biomass production, as well as both the entries in the underlying spreadsheet and equations (D) and (H) of this illustration, indicate that not only is the rate of growth of the microorganism exponential but so too is the rate at which the mass of substrate present declines.

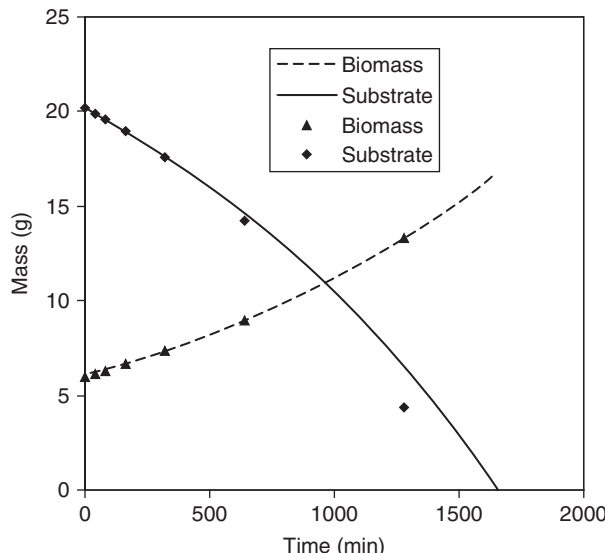


**Figure I13.2** Plots of values of the total masses of cells and substrate predicted using the  $q$ -rate parameters determined in Illustration 13.1, together with the corresponding “data” points. The smooth curves are the values predicted using the model; the triangles and diamonds correspond to the synthetic data points for biomass and substrate, respectively.

The approach utilized in this illustration can be employed to ascertain the time at which one may regard a batch culture as being completed (i.e., the time at which further production of biomass is no longer possible). For example, equation (I) indicates that when substrate is no longer present in the growth medium,

$$X_F = X_0 + \frac{\mu_{\max}}{q_{s\max}}(-S_0) \quad (J)$$

Substitution of the numerical values from the problem statement into equation (D) gives a numerical value for the final quantity of biomass in the reactor ( $X_F$ ):

$$X_F = 6.00 + \frac{6.18 \times 10^{-4}}{-1.17 \times 10^{-3}}(-20.17) = 16.65 \text{ g} \quad (K)$$

From equation (C),

$$t_{\text{final}} = \frac{\ln(X_{\text{final}}/X_0)}{\mu_{\max}} = \frac{\ln(16.65/6.00)}{6.18 \times 10^{-4}} = 1652 \text{ min}$$

Both this time and the final concentration of biomass are consistent with the plots in Figure I13.2.

### 13.1.5 The Luedeking–Piret Model

Our presentation of methodologies for interpretation of kinetic data from a bioreactor operated in a batch mode would not be complete without a brief discussion of the Luedeking–Piret model. In a sense this model is related to

our discussion of the allocation of substrates to the various metabolic pathways accessible to the microorganism of interest. Luedeking–Piret plots are employed in efforts to gain insight into the fundamental aspects of metabolic processes that occur during a particular biochemical reaction. The Luedeking–Piret model is an empirical model that is based on the observation that the metabolic pathways leading to production of primary and secondary metabolites can usually be classified as being *growth-associated*, *non-growth-associated*, or *anomalous* (i.e., involving both growth-associated and non-growth-associated pathways). This classification of metabolites via the Luedeking–Piret model is reflected in the mathematical form of the model.

$$\frac{dP}{dt} = \alpha \frac{dX}{dt} + \beta X \quad (13.1.31)$$

where  $dP/dt$  is the rate at which product  $P$  is formed during fermentation,  $X$  is the total mass of the microorganism in the bioreactor, and  $\alpha$  and  $\beta$  are empirical constants. Division by the mass of cells present leads to the form that is used in preparing plots that are useful in the interpretation of kinetic data for the rate of product formation:

$$\frac{1}{X} \frac{dP}{dt} = \alpha \frac{d\ln X}{dt} + \beta \quad (13.1.32)$$

where the first term on the right side is growth-associated and reflects the energy used for growth of the microorganism. The second term on the right is non-growth-associated. It reflects the energy requirements for cell maintenance. One can determine the parameters  $\alpha$  and  $\beta$  from a plot of the left side of equation (13.1.32) versus  $d\ln X/dt$ . These parameters correspond to the slope and intercept, respectively.

### 13.1.6 Mass Transfer Effects on Rates of Reaction in Suspensions of Microorganisms: The Role of Oxygen as a Limiting Substrate in Aerobic Bioreactions

Because of the heterogeneous nature of the contents of a bioreactor, the pathways along which substrates and components of microorganisms travel during the course of a biochemical transformation are necessarily complex and involve not only chemical reactions but also physical transport phenomena. The rate of transport of nutrients from the aqueous growth medium to the locations within a cell at which reactions occur and the rate of transport of metabolites from the protoplasm of the cell back to the bulk of the growth medium must be comparable if one is to obtain quasi-optimal operating conditions. In Chapter 12 we found that in the design of heterogeneous catalytic reactors one must provide for the possibility that mass transfer phenomena can limit the rates observed in the

laboratory. In Figure 6.3 we indicated in schematic fashion the sequence of individual stages by which reactants in a bulk fluid are transformed on the surface of a porous solid catalyst into products that in turn are subsequently transported back to the bulk of the fluid. Figure 13.4 is a corresponding schematic representation of the sequence of physical and chemical events that would occur during an bioprocess in which air or oxygen is bubbled continuously through a suspension of a microorganism in a growth medium. This figure and parts of the discussion below have been adapted from Doran (9). While the presentation by Doran terminates with intracellular transport of oxygen, readers should recognize that after an oxygen molecule arrives at the site of the biological machinery within the cell where oxygen combines with an enzyme to form an enzyme–substrate complex, reaction takes place, and the products are then returned to the aqueous phase. If we begin our verbal description of the sequence depicted in Figure 13.4 with an oxygen molecule in the interior of a gas bubble, the ensuing molecular events are as follows:

1. Diffusion of oxygen from the bulk gas to the gas–liquid interface. Even when the gas forming the bubble is air, diffusion of oxygen across the boundary layer of gas adjacent to the interface occurs rapidly.
2. Transport across the gas–liquid interface. Equilibrium of these two phases is established very rapidly. The relationship between the interfacial concentrations of

oxygen in the gas and liquid phases is governed by Henry's law for sparingly soluble gases:

$$P_{O_2} = H_{O_2} C_{O_2} \quad (13.1.33)$$

where  $C_{O_2}$  is the concentration of oxygen in the liquid phase at the interface,  $H_{O_2}$  is the Henry's law constant for oxygen, and  $P_{O_2}$  is the partial pressure of oxygen in the gas phase at the interface.

3. Diffusion of oxygen through the liquid boundary layer adjacent to the interface. This step occurs slowly and is usually regarded as rate-limiting. The aqueous medium offers much more resistance to mass transfer than does the gas phase.
4. Transport of oxygen through the well-mixed growth medium to the exterior surface of a relatively stagnant boundary layer that surrounds an individual cell or an agglomeration of cells. This step occurs rapidly in well-mixed laboratory-scale bioreactors, but may occur much more slowly in large-scale industrial equipment. Such equipment may not be able to generate sufficient interfacial area per unit volume between the gas and liquid phases to ensure that the liquid phase is not quickly depleted in oxygen as the reaction takes place.
5. Diffusion of oxygen through the relatively stagnant liquid film surrounding the agglomerated microorganisms.

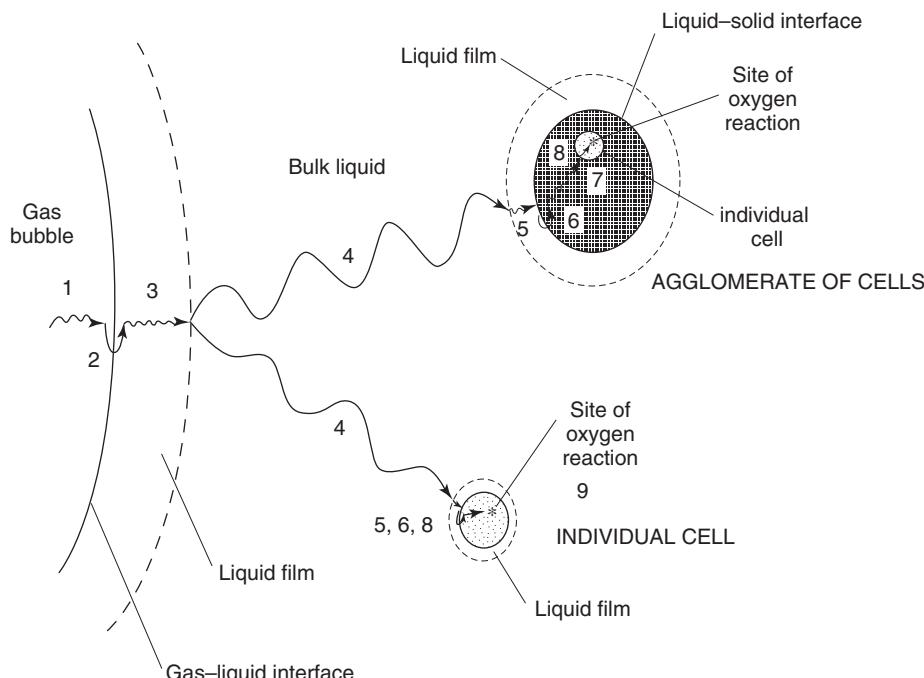


**Figure 13.4** Sequence of steps for transport of oxygen from a gas bubble to an individual cell in an aerobic bioprocess. (Adapted from P. M. Doran, *Bioprocess Engineering Principles*, p. 200, with permission from Academic Press, San Diego, CA, an imprint of Elsevier.)

6. Transfer of oxygen across the liquid–solid interface at the exterior surface of the agglomerated cells.
7. Transport of oxygen to the external surface wall of an individual cell within the agglomerate.
8. Transport of oxygen across the cell wall.
9. Diffusion of oxygen from the interior surface of the cell wall to the intracellular sites where metabolic processes occur.

Because of the very small dimensions and large specific surface areas of the cells, steps 7 to 9 occur very rapidly.

10. Transport of metabolites (reaction products) to the well-mixed growth medium via processes that are akin to steps 5 to 9 but which involve product species moving in directions opposite to those of the incoming oxygen.

When the suspensions are sufficiently dilute that agglomeration of cells does not occur, steps 6 and 7 are absent.

Mass transfer and transport phenomena are core subject areas in chemical engineering curricula and are discussed extensively in textbooks such as Treybal (10), Bird et al. (11), and McCabe et al. (12).

At ambient conditions (1 atm of air, 25°C) the solubility of oxygen in aqueous solutions is roughly 1 mmol/L or ca. 10 ppm. This solubility decreases with increasing temperature and with increasing concentration of electrolytes. Because of the low solubility of oxygen in aqueous growth media, under normal operating conditions the oxygen requirements of an actively respiring population of microorganisms are significantly in excess of the carrying capacity of the growth medium. In the absence of a continuous supply of fresh oxygen to the growth medium in a bioreactor, the concentrations of microorganisms typically found in industrially useful suspensions of cells require only seconds to deplete the dissolved oxygen completely. To maintain a viable population of microorganisms within a bioreactor, one must continuously provide these organisms with very substantial quantities of dissolved oxygen. Indeed, one often finds that the rate at which a particular aerobic bioprocess proceeds is limited by the rate of dissolution of oxygen.

The rationale underlying the analysis of mass transfer between bubbles containing oxygen and the aqueous growth medium has its roots in the two-film theory of Lewis and Whitman (13). At steady state the flux of oxygen across the gas–medium interface must be equal to both the flux of oxygen from the gas phase to the interface and the flux of oxygen through the liquid phase away from the interface. On the gas side of the interface the flux of oxygen ( $N_O$ ) is

$$N_O = k_g(P_g - P_{gi}) = k_g H(C_l^* - C_{li}) \quad (13.1.34)$$

where  $P_g$  and  $P_{gi}$  refer to the partial pressures of oxygen in the bulk of the gas bubble and at the gas–liquid interface, respectively,  $k_g$  is the mass transfer coefficient for oxygen in the gas phase. We have employed Henry's law via equation (13.1.34) to relate the (equilibrium) concentration of oxygen on the liquid side of the interface to the partial pressure of oxygen on the gas side. The (hypothetical) concentration of oxygen in the liquid phase that would be in equilibrium with an oxygen partial pressure  $P_i$  is designated as  $C_l^*$ . This parameter is sometimes referred to as the *solubility* of oxygen in the growth medium at the partial pressure of interest.

On the liquid side of the interface the flux of oxygen is

$$N_O = k_l(C_{li} - C_l) \quad (13.1.35)$$

where  $C_{li}$  and  $C_l$  are the concentrations of oxygen on the liquid side of the interface and in the bulk liquid, respectively, and  $k_l$  is a liquid-phase mass transfer coefficient for oxygen. Although the interfacial concentrations cannot be measured easily, one can eliminate the interfacial concentrations by taking advantage of assumptions that (1) equilibrium of the two phases is rapidly established at their interface, and (2) there is no accumulation of oxygen at the interface. Hence, one can equate the flux terms in equations (13.1.34) and (13.1.35) to obtain

$$k_g H(C_l^* - C_{li}) = k_l(C_{li} - C_l) \quad (13.1.36)$$

Algebraic manipulation to solve for  $C_{li}$  yields

$$C_{li} = \frac{k_g H C_l^* + k_l C_l}{k_g H + k_l} \quad (13.1.37)$$

Substitution of this result into equation (13.1.36) gives

$$\begin{aligned} N_O &= k_l \left( \frac{k_g H C_l^* + k_l C_l}{k_g H + k_l} - C_l \right) \\ &= \frac{k_l}{k_g H + k_l} (k_g H C_l^* + k_l C_l - k_l C_l - k_g H C_l) \\ &= \frac{k_l k_g H}{k_g H + k_l} (C_l^* - C_l) \end{aligned} \quad (13.1.38)$$

At this point it is convenient to define an overall mass transfer coefficient,  $K_l$ , based on a difference in liquid-phase concentrations to characterize the flux of oxygen across the interface such that

$$N_O = K_l(C_l^* - C_l) \quad (13.1.39)$$

Comparison of equations (13.1.38) and (13.1.39) yields the definition of  $K_l$ :

$$K_l \equiv \frac{k_l k_g H}{k_l + k_g H} \quad (13.1.40)$$

If we take the reciprocal of both sides of this equation, we obtain

$$\frac{1}{K_l} = \frac{1}{k_l} + \frac{1}{k_g H} \quad (13.1.41)$$

Equation (13.1.41) is the well-known relation between the overall liquid-phase mass transfer coefficient and the physical parameters of the two-film theory,  $k_g$  and  $k_l$ . This equation in essence states that the overall resistance to mass transfer of a substance between a gas and a liquid can be viewed as the sum of the resistances to the transport of this substance within each phase. For sparingly soluble gases such as oxygen in water, the large majority of the resistance to mass transfer is offered by the liquid phase, that is,

$$k_g H \gg k_l \quad (13.1.42)$$

Consequently, to a very good approximation

$$K_l \approx k_l \quad (13.1.43)$$

The oxygen transfer rate per unit volume of the bioreactor,  $Q_{O_2}$ , can then be expressed as

$$\begin{aligned} Q_{O_2} &= \text{rate of absorption of oxygen} \\ &= (\text{flux}) \times (\text{interfacial area}) / \text{liquid volume} \\ &= k_l (C_l^* - C_l) \frac{A}{V} = k_l a_V (C_l^* - C_l) \end{aligned} \quad (13.1.44)$$

where  $a_V$  is the gas–liquid interfacial area per unit volume of the liquid phase, and where we have employed equation (13.1.43).

Proper design of impellers, baffles, and other internal structures for use in aerobic bioreactors is also important to ensure that adequate levels of dissolved oxygen are present. The goal of these designs is to provide mechanisms for generating large gas–liquid interfacial areas. In practice, it is far easier to manipulate the interfacial area than it is to significantly alter either the driving force for mass transfer ( $C_l^* - C_l$ ) or the mass transfer coefficient itself. Nonetheless, equations for estimating parameter values based on correlations of experimental data are expressed in terms of the product  $k_l a_V$  rather than  $a_V$  alone. Because of the numerous parameters on which  $k_l a_V$  depends, large uncertainties are associated with the use of existing empirical correlations for estimation of  $k_l a_V$ . There are several experimental methods for measuring this product, but these are somewhat problematic in terms of their relevance because of differences between the properties of a suspension of cells (and the industrial-scale mixing equipment associated with the bioreactor) and the model liquid systems used in a piece of small-scale apparatus. Moreover, one must recognize that the agitation conditions employed to ensure that the growth medium is nearly saturated with oxygen do not necessarily create situations that are favorable to maintaining the viability of the cells in the bioreactor, especially when these cells originate in humans or other mammals.

## 13.2 PRINCIPLES AND SPECIAL CONSIDERATIONS FOR BIOREACTOR DESIGN

Fermenters and bioreactors typically contain three phases: solid, liquid, and gas. The solid phase consists primarily of the cells or microorganisms of interest, although some solids produced by biochemical reactions (e.g., sparingly soluble extracellular polysaccharides) may also be present. The biomass constituting the solid phase is sometimes referred to as a *biotic phase*. In their normal states viable cells and microorganisms contain considerable water and thus have a density that differs only slightly from that of the aqueous solution constituting the growth medium. Consequently, mild agitation suffices to produce the very low hydrodynamic drag forces necessary to maintain the microorganisms in suspension. This agitation may be produced by mechanical devices to promote stirring or by injection of oxygen or air through spargers located near the bottom or along the sides of the bioreactor. The aqueous growth medium in which the microorganisms are suspended may contain nutrients and other low-molecular-mass solutes that function as substrates for the various enzymatic reactions associated with the metabolic processes of the microorganism. True homogeneity cannot be obtained throughout a multiphase system such as that characteristic of bioreactors, but sufficiently vigorous agitation yields pseudo-homogeneous liquid phases in which only very small concentration gradients can exist. Under such conditions the cells present in the bioreactor will all be subjected to essentially the same environmental conditions, regardless of their position. This state approaches that of an ideal stirred-tank reactor in which each minuscule volume element is equally likely to be found anywhere within the bioreactor. If this stirred-tank reactor is operated in a continuous flow mode, its performance will resemble that of a CSTR. By contrast, a PFR represents the other extreme of mixing effectiveness—as the fluid elements pass through the reactor, there is complete segregation of fluid elements. There is absolutely no exchange of matter between these elements as they move through an ideal PFR. The influence of the extent of mixing that occurs within a bioreactor on the performance of that reactor can be analyzed using the techniques and models presented in Chapter 11.

There are three primary modes of operation to be considered in the design of a bioreactor. These modes include operation as

1. A well-mixed batch reactor whose contents are regarded as pseudo-homogeneous in temperature and composition throughout the entire volume occupied by the suspended cells. Aerobic bioreactions are often carried out in a semibatch mode of operation in which oxygen or air is bubbled continuously through the

aqueous suspension to provide an essential substrate for the microorganisms. Oxygen has a very low solubility in aqueous solutions. Consequently, one must continuously replenish the dissolved oxygen that is consumed by the microorganisms. This approach circumvents the limitations imposed on a batch reactor by exhaustion of the oxygen dissolved in the growth medium. Otherwise, the dissolved oxygen will be quickly depleted by metabolic processes of the suspended microorganisms, and the reactions that utilize oxygen as a substrate will come to a halt. The approach involving continuous bubbling of a gas containing oxygen through the growth medium is a typical example of a fed-batch (also known as semibatch) mode of operation. Batch and semibatch modes of operation of bioreactors are discussed in Section 13.2.1. Operation of a stirred-tank reactor in a batch mode for the initial phase of a production run followed by shifting to operation in a fed-batch mode can often have the advantage of enhancing the overall productivity of the reactor (see Illustration 13.4).

2. A continuous flow stirred-tank bioreactor (CSTBR). At times it may be desirable to employ either a cascade of such reactors or a combination of a single CSTBR and a separation device for recovery of the solids present in the effluent from the CSTBR so as to permit recycle of a portion of the product microorganisms. This approach is discussed in Section 13.2.4. It has the advantage that it enables one to exploit the autocatalytic nature of the chemical transformations involved in cell cultivation. We have elected to utilize the acronym CSTBR in this chapter rather than continuing to use CSTR to emphasize to the reader that analyses of stirred-tank reactors in which live cells participate in chemical reactions obey rate laws that differ in a very important respect from the laws associated with conventional reactions. The rates of biochemical reactions are expressed per unit of biomass present. At times one may choose to apply this constraint via inclusion of the product of the concentration of biomass ( $x$ ) and the reactor volume ( $V_R$ ) in writing material balances containing terms for biochemical reactions. However, even this approach at its core focuses on the quantity of biomass present rather than merely the volume of growth medium in which the biochemical reaction occurs.
3. The functional equivalent of a PFBR (plug flow bioreactor) when selectivity, inhibition by product species, or other considerations dictate the desirability of striving to avoid mixing of volume elements that are characterized by different degrees of conversion.

The primary modes of operation mentioned above for bioreactors are similar to those for the conventional

chemical reactors considered in Chapters 8 to 12. Portions of Sections 13.2.2 and 13.2.3 deal with aspects of the design and operation of bioreactors in CSTR and quasi-PFR modes, respectively. In this chapter we refer to these types of bioreactors as CSTBRs and PFBRs, respectively.

### 13.2.1 Batch and Semibatch Operation of Bioreactors

#### 13.2.1.1 Design of a Batch Bioreactor

Batch fermentation is not only an extremely common method for carrying out controlled large-scale bioreactions, but also one of the very oldest. Modern applications include the manufacture of a variety of pharmaceutical products as well as production of alcoholic beverages. The batch approach is suitable for use in these situations because once the containment vessel has been sterilized and sealed securely there is little chance of adulteration by foreign organisms or other contaminants. As noted in Section 8.0.2, the advantages of batch operation include lower capital costs and greater flexibility with respect to multiple-use applications. The attendant disadvantages for bioreactor applications include (1) the nonproductive aspects of a batch cycle (sterilizing, filling, heating, inoculating, the lag phase of the growth cycle, cooling, emptying, and cleaning the reactor); (2) higher labor costs because of the necessity for carrying out the nonproductive steps of the batch cycle; (3) increased danger of inadvertent release of potentially hazardous microorganisms or chemicals; and (4) the stress placed on reactor instrumentation because of the need for frequent sterilization. Efforts to circumvent the last-named disadvantage and other sterilization-related problems have led to increased employment of single-use disposable containment vessels and related equipment (see Section 13.3.5).

For bioprocesses conducted under aerobic conditions, one can utilize a semibatch mode of operation in which a sterile growth medium in the bioreactor is inoculated with the microorganism. Sterile oxygen (or air) is bubbled continuously through the resulting suspension of the microorganism. This approach is a direct consequence of the rapidity with which the oxygen dissolved in the growth medium is depleted to meet the metabolic requirements of the organism. Fed-batch operation can also be based on the use of a liquid solution or suspension as a vehicle for augmenting substrate concentrations in the bioreactor.

The material and energy balance equations used in the design and analysis of a well-agitated batch reactor were presented earlier as equations (8.1.5) and (10.2.6), respectively:

$$t_2 - t_1 = N_{A0} \int_{f_{A1}}^{f_{A2}} \frac{df_A}{(-r_A)V_R} \quad (8.1.5)$$

$$Q = \int_{T_0, \xi_0}^{T_{\text{final}}, \xi_1} (m \hat{C}_p \, dT + \Delta H_R \, d\xi) \quad (10.2.6)$$

These equations remain valid for bioreactors provided that one employs a suitable mathematical representation of the rate of disappearance of the substrate that is the limiting reagent. In Illustration 13.3 we employ an alternative form of the design equation to determine the holding time necessary to achieve a specified degree of conversion in a strictly batch bioreactor. This illustrative example also indicates how overall yield coefficients are employed as a vehicle for taking the stoichiometry of the reaction into account. Illustration 13.4 describes how one type of semi-batch operation (the fed-batch mode) can be exploited to combine the potential advantages of batch and continuous flow operation of a stirred-tank reactor.

Fed-batch operation is an approach that offers enhanced opportunities for process optimization with respect to several objective functions. Two common strategies for optimization of production are to:

1. Choose a feed rate that gives a constant volumetric rate of production of biomass. Situations when this strategy might be chosen include both those in which the requirement for dissipation of the thermal energy produced by the reaction might place a constraint on the rate at which products are formed and those in which the resulting level of substrate may be insufficient to meet requirements for cell maintenance.
2. Choose a feed rate corresponding to a constant specific growth rate to optimize use of the substrate for growth rather than for cell maintenance. In this approach the substrate level is maintained constant at a concentration below that at which a significant portion of the substrate is converted to undesirable products or directed primarily toward cell maintenance activities.

### ILLUSTRATION 13.3 Determination of the Holding Time Necessary to Achieve 98% Conversion of the Limiting Substrate in a Batch Fermentation

Consider the fermentation of a representative microorganism in a well-agitated laboratory-scale bioreactor with an initial working volume of 1 L and sufficient headspace to accommodate any volume changes that accompany the biochemical reactions taking place. (See also Illustration 13.4 concerning fed-batch operation of this reactor.) Solute S is the substrate species that limits the growth of the microorganism. Immediately after inoculation of the growth medium, the concentrations of solute S and the microorganism are 35 and 2.5 g/L, respectively. Data

from previous experimental trials indicate that the yield coefficient for the microorganism is substantially constant over the course of the experiment:  $Y_{X/S} = 0.709$ .

The rate at which the microorganism grows obeys a Monod rate expression with a maximum specific growth rate of  $3.16 \text{ day}^{-1}$ . We are asked to ascertain the manner in which the rate at which soluble substrates are transformed to biomass depends on the half-saturation constant by considering the effect of variations in the value of this parameter on the time necessary to achieve a specified level of consumption of the limiting substrate. In particular, consider the times necessary to achieve 98% consumption of the limiting substrate for  $K_S$  values of 0.278, 2.78, and 27.8 g/L. These values of the half-saturation constant cover the range of conditions from situations in which  $K_S$  is small compared to the concentration of the limiting substrate to those in which  $K_S$  is comparable in magnitude to the initial concentration of substrate. The largest parameter value is quite large compared to those typically encountered in industrial-scale biotransformations.

Determine the holding time in the bioreactor necessary to accomplish the conversion specified and the total cycle time for each batch. To facilitate the analysis for this illustrative example, you may presume that the working volume of the growth medium remains constant because the volume of the incoming solution used to control the pH is controlled to exactly offset the volume change what would otherwise accompany the transformation of soluble substrates into biomass. The sum of the nonproductive times during the cycle for a single experimental trial is 6.6 h, of which 3.5 h is associated with the lag period for growth of the microorganism.

### Solution

The design equation for a batch bioreactor is a variation of equation (8.1.5). This equation can be expressed in terms of the total mass of the microorganism, X, in the bioreactor as

$$\frac{dX}{dt} = \mu X \quad (A)$$

where the specific growth rate is of the Monod form,

$$\mu = \frac{\mu_{\text{max}} s}{K_S + s} \quad (B)$$

and where s is the concentration of the substrate in the aqueous growth medium. Combination of equations (A) and (B) followed by integration yields

$$\begin{aligned} t_{\text{batch}} &= \int_{X_0}^X \frac{(K_S + s) \, dX}{\mu_{\text{max}} s X} \\ &= \frac{1}{\mu_{\text{max}}} \left( \int_{X_0}^X \frac{K_S \, dX}{s X} + \int_{X_0}^X \frac{dX}{X} \right) \end{aligned} \quad (C)$$

The variables  $s$  and  $X$  can be related using the overall yield coefficient

$$V_R(s_0 - s) = \frac{X - X_0}{Y_{X/S}} \quad (\text{D})$$

or

$$s = s_0 - \frac{X - X_0}{V_R Y_{X/S}} \quad (\text{E})$$

Combination of equations (C) and (E) gives

$$\begin{aligned} \mu_{\max} t_{\text{batch}} &= K_S \int_{X_0}^X \frac{dX}{X \{s_0 - [(X - X_0)/(V_R Y_{X/S})]\}} \\ &+ \int_{X_0}^X \frac{dX}{X} \end{aligned} \quad (\text{F})$$

Integration gives

$$\begin{aligned} \mu_{\max} t_{\text{batch}} &= \frac{K_S}{s_0 + [X_0/(V_R Y_{X/S})]} \times \\ &\ln \left[ \frac{X}{s_0 - [(X - X_0)/(V_R Y_{X/S})]} \right]_{X_0}^X + \ln \left[ \frac{X}{X_0} \right] \\ &= \left[ \frac{K_S}{s_0 + [X_0/(V_R Y_{X/S})]} + 1 \right] \ln \left[ \frac{X}{X_0} \right] \\ &- \left[ \frac{K_S}{s_0 + [X_0/(V_R Y_{X/S})]} \right] \times \\ &\ln \left[ \frac{s_0 - [X - X_0]/(V_R Y_{X/S})}{s_0} \right] \end{aligned} \quad (\text{G})$$

Equation (G) may be simplified using equation (E) to obtain

$$\begin{aligned} \mu_{\max} t_{\text{batch}} &= \left[ \frac{K_S}{s_0 + [X_0/(V_R Y_{X/S})]} + 1 \right] \times \\ &\ln \left( \frac{X}{X_0} \right) - \left[ \frac{K_S}{s_0 + [X_0/(V_R Y_{X/S})]} \right] \ln \left( \frac{s}{s_0} \right) \end{aligned} \quad (\text{H})$$

or

$$t_{\text{batch}} = \frac{1}{\mu_{\max}} \left\{ \left[ \frac{K_S}{s_0 + [X_0/(V_R Y_{X/S})]} \right] \times \right. \\ \left. \ln \left( \frac{X s_0}{X_0 s} \right) + \ln \left( \frac{X}{X_0} \right) \right\} \quad (\text{I})$$

Moreover, the cycle time per batch is the sum of the productive and nonproductive periods:

$$t_{\text{cycle}} = t_{\text{batch}} + t_{\text{nonproductive}} \quad (\text{J})$$

At 98% conversion of the limiting substrate,

$$(S) = (1 - f_S)(S_0) = (1 - 0.98)(35) = 0.70 \text{ g} \quad (\text{K})$$

From equation (D) one can determine the amount of biomass formed at the time 98% of the limiting substrate has been consumed:

$$\begin{aligned} X &= X_0 + Y_{X/S} [s_0 - s] = 2.5 + 0.709[35 - 0.70] \\ &= 26.82 \text{ g} \end{aligned} \quad (\text{L})$$

If we had waited until the time at which no more biomass was being formed (when  $s = 0$ ) we would find that regardless of the value of  $K_S$ ,  $X_\infty = 27.32 \text{ g}$ .

At this point we have all the pieces necessary to ascertain the fermentation times and cycle times corresponding to the three values of the half-saturation constant indicated in the problem statement. These calculations are readily accomplished using a spreadsheet based on equations (H)–(K). The results are summarized in the following table.

$K_S$ (g/L)	$\frac{K_S}{s_0 + [X_0/(V_R Y_{X/S})]}$	$t_{\text{batch}}$ (h)	$t_{\text{cycle}}$ (h)
0.278	0.00722	18.37	24.97
2.78	0.0722	21.47	28.07
27.8	0.722	52.48	59.08

Inspection of the spreadsheet from which the values were derived indicates that the total quantity of microorganism produced at 98% conversion of the substrate in this strictly batch process is equal to 26.82 g. Equations (I) to (L) can be utilized in a spreadsheet format to prepare plots of the masses of cells and substrate in the bioreactor versus the holding time. Examination of the entries in the table indicates that as  $K_S$  decreases, the time necessary to achieve 98% conversion of the limiting substrate decreases. The most significant decrease in absolute terms is observed when transitioning from the condition in which  $K_S$  is comparable to the initial value of the substrate concentration to the condition in which  $K_S$  is comparable to the value the substrate concentration at ca. 92% consumption. Figure I13.3 depicts the time courses of the masses of substrate and cells in the bioreactor for the latter case in which  $K_S$  is 2.78 g/L.

### 13.2.1.2 Logistic Approach to Analysis of Microorganism Growth in a Batch Bioreactor

Logistic equations for design of bioreactors are a set of equations that characterize cell growth in terms of the *carrying capacity* of the bioreactor. One form of the logistic equation approach to analysis of the performance of a bioreactor operating in a batch mode expresses the specific growth rate as

$$\mu_{\text{net}} = k \left( 1 - \frac{X}{X_\infty} \right) \quad (13.2.1)$$

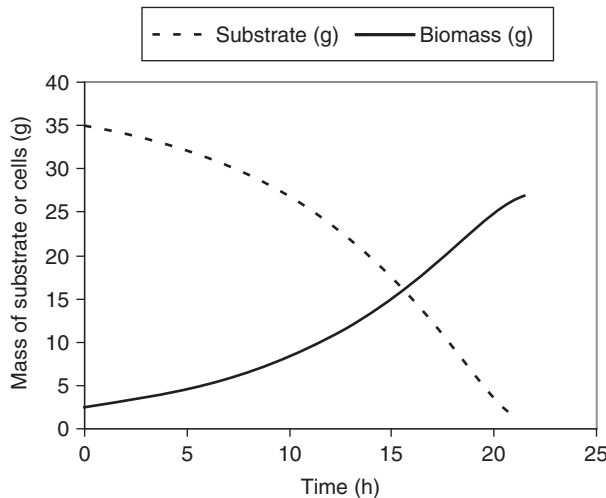


**Figure I13.3** Mass versus time profiles of substrate and biomass for a batch reaction in a fermenter. Monod rate law with  $K_S = 2.78 \text{ g/L}$  and  $\mu_{\max} = 3.16 \text{ day}^{-1}$ .

where  $X$  and  $X_\infty$  refer to the instantaneous and infinite time masses of the microorganism in the reactor, respectively. Thus, as  $X$  approaches  $X_\infty$ , growth ceases and both the residual carrying capacity and the net growth rate become zero. This approach to the design of a well-agitated batch reactor employs a formulation akin to the use of unaccomplished temperature differences in analyses of heat transfer phenomena.

When the progress of cell growth in a closed system (batch reactor) is plotted on conventional graph paper with arithmetic coordinates the resulting curve has a sigmoid shape (see the biomass curve in Figure I13.3). A mathematical description of the shape of the curve can be developed via an analysis involving the following differential equation for cell growth:

$$\frac{dX}{dt} = k \left(1 - \frac{X}{X_\infty}\right) X \quad (13.2.2)$$

subject to the initial condition that at time zero  $X = X_0$ . Separation of variables and integration give

$$\begin{aligned} \int_0^t k \, dt = kt &= \int_{X_0}^X \frac{dX}{[1 - (X/X_\infty)]X} \\ &= \ln \left[ \frac{X}{1 - (X/X_\infty)} \right]_{X_0}^X \end{aligned} \quad (13.2.3)$$

or

$$kt = \ln \left[ \frac{X}{X_0} \right] - \ln \left[ \frac{1 - (X/X_\infty)}{1 - (X_0/X_\infty)} \right] \quad (13.2.4)$$

Exponentiation of both sides of this equation gives

$$\begin{aligned} e^{kt} &= \frac{X[1 - (X_0/X_\infty)]}{X_0[1 - (X/X_\infty)]} \\ &= \frac{X(X_\infty - X_0)}{X_0(X_\infty - X)} \end{aligned} \quad (13.2.5)$$

Algebraic rearrangement gives

$$\begin{aligned} \frac{X}{X_0} &= \frac{e^{kt}}{1 - (X_0/X_\infty)(1 - e^{kt})} \\ &= \frac{X_\infty e^{kt}}{X_\infty + X_0(e^{kt} - 1)} \end{aligned} \quad (13.2.6)$$

A plot of equation (13.2.6) in dimensionless form is shown in Figure 13.5.

The differential equation form of the logistic model of cell growth is basically a two-parameter ( $k$  and  $X_\infty$ ) representation of cell growth that is largely empirical in character. There have been numerous attempts to extend and interpret the model so as to identify parameters in other variations or extensions of the model. One approach commonly described in the literature begins by expressing the Monod equation (13.1.13) for the rate of substrate consumption as

$$\mu_{\text{growth}} = \frac{\mu_{\max} s}{K_s + s} \quad (13.2.7)$$

and then recognizing that the net specific growth rate takes into account not only the gross rate of growth, but also several phenomena that reduce the potential for growth via consumption of substrate such as cell lysis and death, cell maintenance, and so on. Each phenomenon that has a negative effect on the cell growth rate is expected to occur at a rate that is proportional to the amount of microorganism present. Hence, we can characterize the sum of these effects

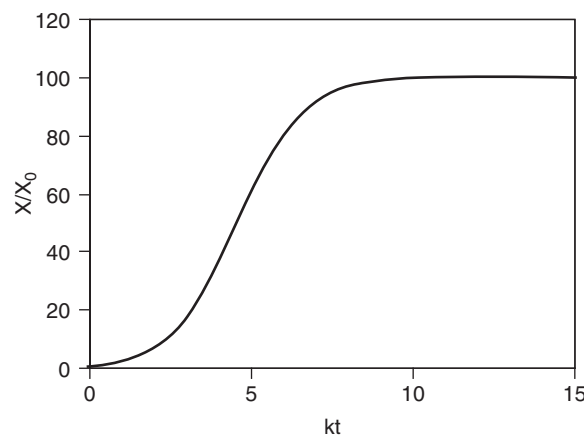


**Figure 13.5** Dimensionless representation of logistic curve for cell growth in a batch bioreactor when  $X_\infty/X_0 = 100$ .

in terms of a single lumped parameter written as a rate constant  $k_d$  and employ an expression for  $\mu_{\text{net}}$  of the form

$$\mu_{\text{net}} = \mu_{\text{growth}} - k_d \quad (13.2.8)$$

Combination of equations (13.2.7) and (13.2.8) gives

$$\mu_{\text{net}} = \frac{\mu_{\text{max}}s}{K_s + s} - k_d \quad (13.2.9)$$

If we now assume that  $s \gg K_s$ , as is commonly observed because the concentration of the limiting substrate often exceeds  $K_s$  by an order of magnitude or more, equation (13.2.9) reduces to

$$\mu_{\text{net}} = \mu_{\text{max}} - k_d \quad (13.2.10)$$

where all terms are constants. Substitution of this relation into the equation for cell growth gives

$$\frac{dX}{dt} = (\mu_{\text{max}} - k_d)X \quad (13.2.11)$$

Separation of variables and integration give

$$\int_{X_0}^X \frac{dX}{X} = \int_0^t (\mu_{\text{max}} - k_d) dt \quad (13.2.12)$$

or

$$\ln \left( \frac{X}{X_0} \right) = (\mu_{\text{max}} - k_d)t \quad (13.2.13)$$

or

$$\frac{X}{X_0} = e^{(\mu_{\text{max}} - k_d)t} \quad (13.2.14)$$

If we assume further that the growth term is significantly larger than any of the death-related processes that reduce the net growth rate and are subsumed in  $k_d$ , then

$$\mu_{\text{net}} \approx \mu_{\text{max}} \quad (13.2.15)$$

and the differential equation governing the rate of cell growth becomes

$$\frac{dX}{dt} = \mu_{\text{max}}X \quad (13.2.16)$$

while the corresponding integral form becomes

$$\frac{X}{X_0} = e^{\mu_{\text{max}}t} \quad (13.2.17)$$

Equations (13.2.14) and (13.2.17) suffer from a common deficiency: namely, both equations indicate that the mass concentration of cells increases without limit as time elapses. Neither provides a limit to the maximum number of cells that can exist within the bioreactor, whereas nature does impose such a limit.

The concept of the *carrying capacity* of the environment of the cell is a feature of the logistic approach to growth phenomena that can be utilized to impose a limit

on the maximum extent of growth. The carrying capacity of a population represents the absolute maximum number of cells that can exist in a specific environment based on the availability of a particular limiting resource. We can incorporate a factor into our growth equation that indicates at any time the fraction of the carrying capacity that is available for use by the organism. If we denote the maximum possible quantity of microorganisms that can exist in a particular environment by  $X_\infty$ , the fraction of the capacity that has been utilized at a biomass level  $X$  is  $(X/X_\infty)$ . The fraction unutilized is then  $(1 - (X/X_\infty))$ . If we introduce this factor into our equations for cell growth, the effect is to cap the population of microorganisms at a concentration  $X_\infty$ . Thus, in terms of the a logistic approach that would apply to the exponential phase of cell growth, equation (13.2.16) becomes

$$\frac{dX}{dt} = (\mu_{\text{max}} - k_d)X \left( 1 - \frac{X}{X_\infty} \right) \quad (13.2.18)$$

This differential equation is of the same mathematical form as equation (13.2.2) where in the present instance  $k = \mu_{\text{max}} - k_d$ . Hence, the solution is the analog of equation (13.2.6):

$$\frac{X}{X_0} = \frac{e^{(\mu_{\text{max}} - k_d)t}}{1 - (X_0/X_\infty)[1 - e^{(\mu_{\text{max}} - k_d)t}]} \quad (13.2.19)$$

Equations (13.2.6) and (13.2.19) are both examples of logistic growth models. Both will yield growth curves with sigmoid shapes, although the curves will reflect the fact that the characteristic time constants for the two curves differ (at least in principle) because one curve provides for cell death and related effects, whereas the other does not. They provide frameworks that are at heart two-parameter empirical models of cell growth in a batch bioreactor that are useful in generating sigmoid-shaped plots of the evolution of the population of cells in the bioreactor. Equation (H) of Illustration 13.3 also provides a vehicle for generating a characteristic S-shaped growth curve, albeit from a somewhat different perspective.

### 13.2.1.3 Fed Batch Operation of Stirred-Tank Bioreactors

A semibatch mode of operation known as *fed batch* or *extended culture fermentation* can be employed to circumvent or minimize substrate inhibition effects. Fed batch operation may also be referred to as semicontinuous culture. In this mode of operation the substrate is fed continuously or intermittently in a manner that maintains the concentration of substrate at a low level that provides sufficient substrate to sustain cell growth, but that also is low enough to mitigate the negative effects of substrate

inhibition to a tolerable level. Depending on the circumstances of a particular cell culture, it may or may not be desirable to remove a portion of the suspension of cells periodically, perhaps with separation and recycle of some cells to the bioreactor. In this context it is informative to consider expansion of Illustration 3.3, which dealt with cell cultivation in a strictly batch mode to variable volume extended batch operation of a bioreactor.

### ILLUSTRATION 13.4 Extended Culture (Fed Batch) Operation of a Well Agitated Bioreactor

In Illustration 13.3 we considered the relations between the holding time in a batch reactor, the fraction of the initial substrate that remained unreacted ( $S/S_0$ ), and the ratio of the final to the initial mass concentration of the microorganism ( $X_\infty/X_0$ ). Now consider an alternative mode of operation of the bioreactor: namely, *extended batch operation*, in which a bioreactor with a working volume of 1 L is operated initially as in Illustration 13.3. However, beginning at the time 98% conversion of the limiting substrate is obtained, more substrate is continuously added to the bioreactor at a rate that is equal to the rate at which the substrate is being consumed by fermentation. The other substrates can be regarded as present in sufficient excess that they have no influence on the conversion rate before or after the shift to an extended batch mode of operation is made. When necessary, the feed stream may also contain solutes other than the limiting substrate to ensure that these species are always present in large excess. Analyze the situation for which  $K_S = 2.78 \text{ g/L}$ .

- How much time is required to achieve 98% conversion of the limiting substrate? What is the total mass of cells present at this time?
- Now suppose that at the moment 98% conversion is reached, the operation shifts to a fed batch mode. The rate law will continue to be a Monod relation [equation (13.1.13)] with the concentration of substrate in the feed stream remaining constant at 50 g/L for a period of extended batch operation. The volumetric flow rate of the substrate makeup stream is varied in a manner that keeps the concentration of the substrate in the bioreactor constant at the concentration prevailing at the time the strictly batch operation is terminated and fed batch operation is initiated. The microorganism continues to grow but at a rate that now reflects the rate of consumption of the substrate. Use a spreadsheet to prepare a plot that indicates how the total amount of microorganism produced during the combination of batch and semibatch operation varies with time when the reactor is operated according to this protocol. By

how much would the production of cells increase if the fed-batch segment of the cycle is employed for 48 h after 98% conversion of the initial charge of substrate is achieved? Comment.

### Solution

Equations (I), (J), and (K) of Illustration 13.3 may be used to determine both the amount of microorganism present at the time when the conversion of the limiting substrate reaches 98% and the time necessary to achieve this conversion. At 98% conversion of the limiting substrate,

$$S_{98} = (1 - 0.98)S_0 = 0.02(35) = 0.70 \text{ g}$$

and the total mass of the microorganism is

$$\begin{aligned} X_{98} &= X_0 + (Y_{X/S} V_R)(s_0 - s_{98}) \\ &= 2.5 + (0.709)1.0(35 - 0.70) = 26.82 \text{ g} \end{aligned}$$

From Table I13.1 for  $K_S = 2.78 \text{ g/L}$ , the corresponding value of  $K_S/\{S_0 + [X_0/(V_R Y_{X/S})]\}$  is 0.0722. Recall that equation (I) of Illustration 13.3 is

$$t_{\text{batch}} = \frac{1}{\mu_{\text{max}}} \left\{ \frac{K_S}{(S_0) + [X_0/(V_R Y_{X/S})]} \right\} \times \left\{ \ln \left[ \frac{(X)(S_0)}{(X_0)(S)} \right] + \ln \left[ \frac{(X)}{(X_0)} \right] \right\}$$

Substitution of the values of S and X at 98% conversion of the limiting substrate into the preceding equation gives

$$\begin{aligned} t_{\text{batch}} &= \frac{1}{3.16} \left[ 0.0722 \ln \left( \frac{26.82(35)}{2.5(0.70)} \right) + \ln \left( \frac{26.82}{2.5} \right) \right] \\ &= 0.895 \text{ day} = 21.47 \text{ h} \end{aligned}$$

Thus, the operator begins feeding the bioreactor with a stream containing 50.0 g/L of the limiting substrate 21.47 h after the growth medium is inoculated with the microorganism.

Now we need to consider the equations that describe the operation of the bioreactor once the feed of fresh substrate to the reactor is initiated. For subsequent times, the volume of the suspension of the microorganism will be given by a relation of the form

$$V_R = V_{R0} + \int_{t_{98}}^t \mathcal{V} dt \quad (\text{A})$$

where  $V_R$  and  $V_{R0}$  are the volumes of the suspension at any time ( $t$ ) and initially, respectively. The parameter  $t_{98}$  is the time that it takes the contents of the bioreactor to achieve 98% conversion of the limiting substrate while operating in a strictly batch mode. The parameter  $\mathcal{V}$  is the volumetric flow rate of the stream fed to the bioreactor to make up for

the substrate that has been consumed by the bioconversion process. This flow rate will be controlled to match the rate of consumption of fresh substrate in the bioreactor.

For pedagogical purposes in Illustrations 13.3 and 13.4, we arbitrarily selected 98% conversion of the limiting substrate as the level of conversion at which the change from pure batch to extended culture operation is made. However, in industrial practice determination of the level of conversion at which the transition should be made is a fairly complex optimization problem that is beyond the scope of this book. Additional analyses of fed batch operation may be found in books by Nielsen and Villadsen (14) and Lim and Shin (15).

We next wish to perform a material balance over the bioreactor for the microorganism assuming that the feed contains substrate but not biomass (i.e., it is sterile). If biomass neither enters nor leaves the bioreactor and if we assume that the rate of cell death is negligible compared to the rate of cell growth, we find that

$$\frac{d[xV_R]}{dt} = Y_{X/S}\mu xV_R \quad (B)$$

or

$$x\frac{dV_R}{dt} + V_R\frac{dx}{dt} = Y_{X/S}\mu xV_R \quad (C)$$

where  $x$  is the mass concentration of the microorganism in the bioreactor. Combination of equations (A) and (C) gives

$$xV + V_R\frac{dx}{dt} = Y_{X/S}\mu xV_R \quad (D)$$

Rearrangement yields

$$\frac{dx}{dt} = x\left(Y_{X/S}\mu - \frac{V}{V_R}\right) \quad (E)$$

The ratio of the volumetric flow rate to the volume occupied by the suspension is defined by microbiologists as the *dilution rate* ( $D$ ).

$$D = \frac{V}{V_R} = \frac{V}{V_{R0} + \int_{t_0}^t V dt} \quad (F)$$

In fed batch systems when the volumetric flow rate of the feed stream varies in a manner that maintains the concentration of the limiting substrate constant, the dilution rate must increase as time elapses because the volume occupied by the aqueous solution increases as more feed enters. Combination of equations (E) and (F) gives

$$\frac{dx}{dt} = x(Y_{X/S}\mu - D) \quad (G)$$

The rate at which the substrate is consumed by the bioconversion process will be assumed to be described by a

Monod relation:

$$-r_s = \left(\frac{\mu_{\max} s}{K_S + s}\right)x = \left(\frac{\mu_{\max} s_{98}}{K_S + s_{98}}\right)x \quad (H)$$

where we have recognized that the substrate concentration is a constant for the fed-batch portion of the trial and that the reaction remains autocatalytic. Moreover,

$$r_x = Y_{X/S}(-r_s) = Y_{X/S} \left(\frac{\mu_{\max} s_{98}}{K_S + s_{98}}\right)x \quad (I)$$

Because we know the concentrations of substrate and biomass present in the bioreactor at the moment the fed-batch operation begins (0.70 and 26.82 g/L, respectively), we can employ equation (H) to calculate the rate at which substrate is being consumed at this time.

$$\begin{aligned} -r_s &= \left(\frac{\mu_{\max} s_{98}}{K_S + s_{98}}\right)X = \left[\frac{3.16(0.70)}{2.78 + 0.70}\right] \\ &= 17.05 \text{ g/(L-day)} \end{aligned} \quad (J)$$

This consumption rate determines the initial rate at which substrate must be fed to the bioreactor if the concentration of substrate in the reactor is to remain constant at 0.70 g/L.

A material balance on the substrate for times greater than 21.47 h leads to the equation

$$\frac{d[s_{98}V_R]}{dt} = \mathcal{V}_{\text{feed}} - \left(\frac{\mu_{\max} s_{98}}{K_S + s_{98}}\right)xV_R \quad (K)$$

or

$$\begin{aligned} s_{98}\frac{d[V_R]}{dt} + V_R\frac{ds_{98}}{dt} &= s_{98}\mathcal{V} + V_R\frac{ds_{98}}{dt} \\ &= \mathcal{V}_{\text{feed}} - \left(\frac{\mu_{\max} s_{98}}{K_S + s_{98}}\right)xV_R \end{aligned} \quad (L)$$

where  $s_{98}$  refers to the constant concentration of substrate in the well-agitated growth medium. However, the mode of operation has been chosen to maintain the concentration of substrate in the aqueous phase constant ( $ds_{98}/dt = 0$ ) and the time derivative of the reactor volume is equal to the volumetric flow rate of the entering stream. The concentration of substrate in the aqueous phase within the reactor is equal to  $s_{98}$  for a well-stirred system. Thus, equation (L) becomes

$$\mathcal{V}(s_{\text{feed}} - s_{98}) = \mu X = \left(\frac{\mu_{\max} s_{98}}{K_S + s_{98}}\right)xV_R \quad (M)$$

From a physical interpretation of this relation, it becomes obvious that if the amount of biomass in the reactor is to grow the concentration of substrate in the feed stream must exceed the concentration of substrate in the growth medium. Otherwise, the constraints on the fed batch operation would not be satisfied with respect to the desire for a constant substrate concentration during the

fed batch period. As the concentration of substrate in the feed stream increases, the smaller the volumetric flow rate of the feed stream can be and the longer will be the time necessary to exceed the volumetric capacity of the bioreactor. There are multiple possibilities for the combinations of dilution rate and the feed concentration of substrate that will satisfy equation (M). The upper limit on the substrate concentration is established by its solubility in the growth medium. In terms of equation (M) the volumetric flow rate of the entering stream would be selected so that the product  $\mathcal{V}(S_{\text{feed}} - S_{98})$  is equal to the rate of consumption of substrate given by the Monod equation. Thus, at the time use of the feed stream is initiated, equation (M) indicates that

$$\mathcal{V}[(50) - (0.70)] = \left[ \frac{3.16(0.70)}{2.78 + 0.70} \right] \quad (26.82) \quad (\text{N})$$

or  $\mathcal{V} = 0.346 \text{ L/day} = 0.0144 \text{ L/h}$ . This flow rate will need to be increased as the amount of time the additional substrate is fed increases. An increased feed rate is necessary to offset the increase in the rates of consumption of substrate and production of additional biomass, as well as dilution effects caused by the increase in the fluid volume within the bioreactor. The numbers above indicate that the daily change in volume is a very significant fraction of the working volume of the bioreactor (1 L). Nonetheless, the volume change will not prevent us from solving this problem provided that there is sufficient head space within the bioreactor to accommodate the increase in volume of the aqueous phase.

Equation (I) describes the rate at which biomass is being produced during the fed-batch period. It can also be written as

$$\frac{dX}{dt} = Y_{X/S} \left( \frac{\mu_{\max} s_{98}}{K_S + s_{98}} \right) x V_R \quad (\text{O})$$

Separation of variables and integration subject to the initial condition that at the time the fed-batch phase of the operation begins,  $X = X_{98}$  gives

$$\int_{X_{98}}^X \frac{dX}{X} = \int_{21.47}^t Y_{X/S} \left( \frac{\mu_{\max} s_{98}}{K_S + s_{98}} \right) dt \quad (\text{P})$$

or

$$\ln \left( \frac{X}{X_{98}} \right) = Y_{X/S} \left[ \frac{\mu_{\max} s_{98}}{K_S + s_{98}} \right] (t - 21.47) \quad (\text{Q})$$

Substitution of numerical values gives

$$\begin{aligned} \ln \left( \frac{X}{26.82} \right) &= 0.709 \left[ \frac{(3.16/24)(0.70)}{2.78 + (0.70)} \right] (t - 21.47) \\ &= 0.01878(t - 21.47) \end{aligned} \quad (\text{R})$$

If fed-batch operation is employed for a total of 48 h ( $t = 69.47 \text{ h}$ ), equation (R) indicates that

$$X = 66.06 \text{ g} \quad (\text{S})$$

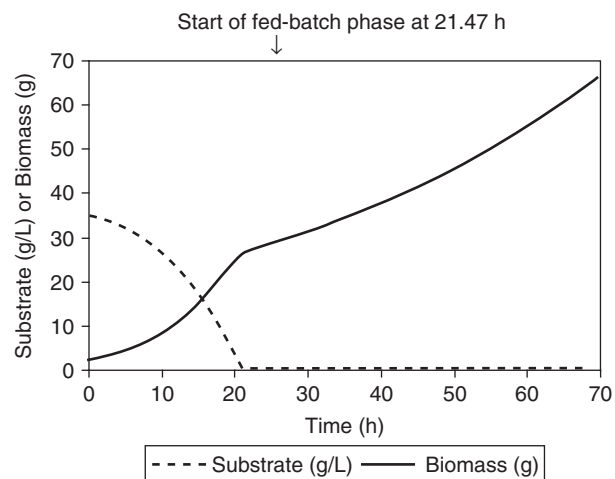


**Figure I13.4** Speciation plots for batch operation of a bioreactor to achieve 98% conversion (21.47 h) followed by fed-batch operation for an additional 48 h while maintaining a constant substrate concentration of 0.70 g/L in the growth medium.

The amount of biomass produced via the combination of batch and fed-batch operation is 2.46 times as great as that produced in the strictly batch portion of the fermentation. However, the total time involved in the fed-batch operation is greater than that for strict batch operation by a factor of  $69.47/28.07 = 2.47$ . Hence, there does not appear to be a major advantage in terms of biomass production per unit time in going to a fed-batch mode of operation for the second stage of production. Nonetheless, examination of Figure I13.4 indicates that application of the fed-batch mode of operation produces substantial amounts of biomass over and above that produced during the strictly batch portion of the reaction. Analysis of the slopes of the biomass plot in the figure during the two stages of the reaction indicates that the reaction rate is fastest during the last portion of the strictly batch stage of the process cycle.

Readers should note that for purposes of process control the flow rate of the feed stream can be determined at any time using equation (M) and the value of the total weight of biomass in the bioreactor at that time. When the fed batch phase of operation is initiated, the requisite feed rate is 14.4 mL/h, and at the end of this phase the necessary feed rate is 35.5 mL/h.

### 13.2.2 Continuous Flow Stirred Tank Bioreactors and Chemostats

In principle the use of a well-stirred bioreactor in a continuous flow mode offers significant advantages over operation in a batch or semibatch mode, but the majority of bioreactors in industrial use are operated in the latter modes. However, the actual performance of single CSTR or a cascade of such reactors often fails to meet the expectations

of the designer; a spontaneous mutation of the microorganism may occur with significant loss of production capacity; failure of the sterile feed system may lead to contamination by alien microorganisms, and so on. Nonetheless, there are many situations in which operation of a bioconversion system in a continuous manner is most economic. These applications often involve production of materials that are not intended for consumption by (or medical treatment of) humans or animals. Consequently, engineers engaged in the design of bioreactors must be capable of designing bioreactors for continuous operation as a single CSTR or a cascade of such reactors.

When used in laboratory-scale operations CSTRs are frequently referred to as *chemostats*. Chemostats are often employed in scientific studies intended to elucidate the metabolic processes associated with particular microorganisms because they are better equipped to monitor transient situations involving a transition from one set of operating conditions to another, for example, when there is a shift in the composition of the stream being fed to a unit operating at steady state. By comparison with large-scale CSTBRs, small-scale chemostats are characterized by shorter response times and are more readily instrumented to facilitate acquisition of data that are useful in optimization of the performance of these reactors.

For industrial applications the advantages of CSTBRs include improved utilization of capital investment because of continuous operation with attendant low labor costs, productivity benefits from the autocatalytic nature of fermentations because of the internal feedback inherent in the perfect mixing characteristics of an ideal CSTR, constant quality of the product, and suitability for automated operation. However, use of continuous-flow bioreactors is not appropriate in situations where flexibility for producing a variety of products is required. Moreover, when dealing with situations involving prolonged (weeks or months) campaigns for the manufacture of a particular bio product, design engineers must recognize the necessity of working with microbiologists and others to develop a strain of the organism that is characterized by both high productivity and very high genetic stability. Organisms that are susceptible to genetic variations that lead to degradation of those metabolic pathways essential to the growth of the organism and to production of desired metabolites do not provide a solid foundation for substantive investments in industrial-scale bioreactors. Such degradation might occur via mutation or via a variety of other spontaneous events that occur as a consequence of interactions between the organism and its environment. Both fed batch and single CSTBR modes of operation require strains of the organism that possess the desired productivity and genetic stability characteristics if the ultimate process design is to be economically viable. By contrast, for batch

operation it is always possible to employ a freshly prepared inoculum, thereby obviating stability problems. Usually, batch reactors are also less susceptible to infection and contamination by undesirable microorganisms.

Relative to strictly batch bioreactors, continuous and fed batch bioreactors require more connections to process streams through which sterility must be maintained throughout the entire period the reactor is onstream. When contamination does occur in equipment used to carry out a continuous process, it can rapidly spread to downstream units. By contrast, confinement or isolation of contaminants can be accomplished more readily in a batch reactor and its associated auxiliary facilities.

Many aspects of the design of single and multiple CSTRs were covered in Chapters 8 to 11. That material remains relevant to the design of bioreactors for use in a CSTR mode. The major differences between the applications involving bioreactors and conventional chemical reactors lie in (1) the necessity for maintaining reaction environments that are free from contamination by undesirable alien microorganisms; (2) differences in the mathematical forms of the rate laws for the chemical transformations of interest, especially the autocatalytic nature of transformations involving microorganisms; and (3) the greater difficulty in accounting for the stoichiometry of the bioconversion because the reactions involved do not obey a simple form of the law of definite proportions. Instead biotransformations involve more complex stoichiometric relations to describe the conversion of multiple substrates to living biomass,  $\text{CO}_2$ ,  $\text{H}_2\text{O}$ , and variety of primary and secondary metabolites.

Section 8.3.1 contains several equations that are useful in the design of individual CSTRs. For situations in bioreactors where volumetric expansion or contraction effects are negligible for suspensions of microorganisms in a growth medium, the following extension of equations (8.3.5) and (8.3.7) is a useful starting point for our discussion of how to design and analyze an individual CSTBR operating at steady state:

$$[sV]_0 - [sV]_F = (-r_{S\text{ out}})V_R \quad (13.2.20)$$

where  $V$  is the volumetric flow rate of the cell-free aqueous process stream,  $s$  the concentration of the stoichiometrically limiting substrate in the aqueous growth medium,  $-r_{S\text{ out}}$  the rate expression for consumption of the limiting substrate per unit volume evaluated at the effluent conditions,  $V_R$  the volume of the reactor occupied by the cell-free growth medium, and the subscripts 0 and  $F$  refer to the inlet and effluent streams, respectively.

Equation (13.2.20) can be manipulated and the discussion phrased in terms of the vocabulary of the microbiologist by proceeding as follows. We begin by solving equation (13.2.20) for the rate of consumption of the limiting substrate under steady state operating conditions. At

steady-state for situations in which volumetric expansion and contraction effects are negligible, the volumetric flow rates of the inlet and outlet streams may be assumed to be identical. Thus,

$$(-r_{SF}) = \frac{\mathcal{V}}{V_R}(s_0 - s_F) \quad (13.2.21)$$

This expression is the basis for employing chemostats for investigations of kinetic processes involving growth of microorganisms and the dependence of the growth rates on process parameters. By contrast with the situation for kinetic investigations in batch reactors, use of a CSTBR or chemostat permits one to determine reaction rates directly from easily measured variables [see the right side of equation (13.2.21)] rather than having to resort to graphical or numerical differentiation of concentration versus time data from a batch reactor. Hence, from data for trials in a chemostat, one can readily assess the validity of a proposed rate law using equation (13.2.21) to generate values of the rate as a function of other process variables. In the parlance of the microbiologist, the ratio  $\mathcal{V}/V_R$  in equation (13.2.21) is referred to as the *dilution rate* ( $D$ ) rather than the space velocity or the reciprocal of the space time ( $\tau$ ). Readers should recall that for reactions that occur in liquid solutions or suspensions, the space time is numerically equal to the mean residence time. Thus, from equation (13.2.21),

$$(-r_{S_{\text{out}}}) = D(s_{\text{in}} - s_{\text{out}}) \quad (13.2.22)$$

Another way of looking at the kinetic behavior of biotransformations in a CSTBR is to consider a reactor operating at steady state under conditions for which there is no biomass in the feed stream (i.e., the feed is sterile). We can then write a material balance on the biomass, equating the change in the amount of biomass contained in the reactor to the difference between the increase in the amount of biomass present in the working volume resulting from cell growth and the net amount of biomass leaving in the effluent stream. Thus, for a bioreactor containing biomass at an average concentration  $x$  within a working volume  $V_R$ , the change in the total amount of biomass present that occurs during a time increment  $\Delta t$  can be expressed in terms of a material balance on the cells as

$$\Delta(V_R x) = V_R \mu x \Delta t - \mathcal{V} x \Delta t \quad (13.2.23)$$

where we have made the usual assumption for a well-stirred reactor that the composition of the effluent is identical to that of the reactor contents.

We now divide this equation by  $\Delta t$  and take the limit as  $\Delta t$  approaches zero to obtain

$$V_R \frac{dx}{dt} + x \frac{dV_R}{dt} = V_R(\mu x) - \mathcal{V} x \quad (13.2.24)$$

Division by  $V_R$ , coupled with recognition that for a reactor operating at steady state both time derivatives are zero, leads to

$$0 = \left( \mu - \frac{\mathcal{V}}{V_R} \right) x = (\mu - D)x \quad (13.2.25)$$

where the ratio  $\mathcal{V}/V_R$  is the dilution rate ( $D$ ). Equation (13.2.25) indicates that for a CSTBR operating at steady state the specific growth rate must be equal to the dilution rate:

$$\mu = D \quad (13.2.26)$$

Substitution of the formulation of the Monod relation in terms of  $\mu_{\text{max}}$ ,  $s_F$ , and  $K_S$  into this equation followed by rearrangement yields

$$(K_S + s_F)D = \mu_{\text{max}}s_F \quad (13.2.27)$$

Solving for the effluent concentration of the substrate at steady state gives

$$s_F = \frac{K_S D}{\mu_{\text{max}} - D} \quad (13.2.28)$$

where the subscript  $F$  explicitly indicates the assumption that the average concentration of the substrate in a perfectly mixed reactor is identical with its effluent concentration.

We can also write an equation akin to equation (13.2.22) for the growth-limiting substrate that takes into account the manner in which the substrate is used by the microorganism for growth, maintenance, product formation, and so on. A balance on this substrate for a time increment  $\Delta t$  can be expressed as

$$\begin{aligned} \text{net change} &= \text{input} - \text{output} \\ &\quad - \text{consumption of substrate by reaction} \end{aligned} \quad (13.2.29)$$

where the substrate consumption term encompasses allocations to cell growth, maintenance, product formation, and so on.

$$\begin{aligned} \Delta(s_F V_R) &= s_0 \mathcal{V} \Delta t - s_F \mathcal{V} \Delta t - V_R \left( \frac{\mu x_F}{Y_{X/S}} + \mu x_F Y_{P/X} \right. \\ &\quad \left. + k_m x_F + \mu x_F Y_{CO_2/X} + \mu x_F Y_{H_2O/X} \Delta t \right) \end{aligned} \quad (13.2.30)$$

where  $V_R$  is the working volume of the aqueous phase in the bioreactor;  $s_F$  is the concentration of the limiting substrate in the well-stirred growth medium and in the effluent stream;  $\mathcal{V}$  is the volumetric flow rate (assumed to be essentially the same at the inlet and outlet of the bioreactor because of controlled balancing of losses associated with evaporation of water from the growth medium by addition of aqueous solutions designed to

maintain a constant pH and a constant quantity of water in the reactor): the subscripts 0 and  $F$  refer to the inlet and outlet streams, respectively;  $\mu$  is the specific growth rate;  $x$  is the concentration of biomass;  $k_m$  is the maintenance coefficient (g substrate consumed for metabolic functions in the absence of cell growth/g of cells);  $Y_{X/S}$  is the yield coefficient for biomass formation (g biomass formed/g substrate utilized);  $Y_{P/X}$  is the yield coefficient for product formation (g product formed/g cells formed); and  $Y_{CO_2/X}$  and  $Y_{H_2O/X}$  are the yield coefficients for formation of  $CO_2$  and  $H_2O$  (g  $CO_2$  or  $H_2O$  formed/g biomass formed).

If conditions in the bioreactor are such that cell growth is the sole metabolic event occurring, then after reduction to a differential equation, equation (13.2.30) becomes

$$\frac{d(s_F)}{dt} = D(s_0 - s_F) - \frac{\mu x_F}{Y_{X/S}} \quad (13.2.31)$$

where we have also recognized that the concentration of substrate in the tank at time  $t$  is equal to  $s_F$ .

At steady state not only are both the mass concentration of cells and the concentration of substrate in the bioreactor constant, but in addition,  $\mu = D$ . Hence, equation (13.2.31) leads to a relation for the steady-state concentration of biomass in the effluent stream

$$x_F = Y_{X/S}(s_0 - s_F) \quad (13.2.32)$$

Substitution of the steady state concentration of substrate in the effluent given by equation (13.2.28) into equation (13.2.32) yields

$$x_F = Y_{X/S} \left( s_0 - \frac{K_S D}{\mu_{\max} - D} \right) \quad (13.2.33)$$

Equation (13.2.33) provides the basis for determining a critical limit on the dilution rate ( $D_w$ ). Dilution rates in excess of this limit lead to steady-state conditions under which no biomass remains in the bioreactor ( $x_F = 0$ ). This reduction of the effluent concentration of biomass to zero is a phenomenon known as *washout* (see Figure 13.6). The corresponding equation for the concentration of substrate in the effluent from the CSTBR is equation (13.2.28). The dependence of the effluent substrate concentration on the dilution rate is also shown in Figure 13.6. During washout, microorganisms are being removed from the reactor by convective transport faster than they are being created by cell growth.

The criterion for ascertaining the dilution rate at which washout occurs is that the term in parentheses in equation (13.2.33) becomes zero, or that the dilution rate is at least

$$D_w = \frac{\mu_{\max} s_0}{K_S + s_0} \quad (13.2.34)$$

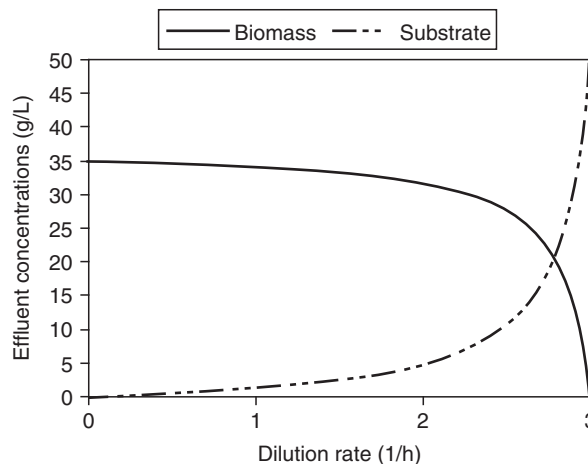


**Figure 13.6** Effect of dilution rate on the effluent concentrations of biomass and substrate for  $K_S = 2.78$ ,  $\mu_{\max} = 3.16 \text{ h}^{-1}$ ,  $s_0 = 50$ , and  $Y_{X/S} = 0.7$ .

For the conditions shown in Figure 3.6, the critical dilution rate is  $2.993 \text{ h}^{-1}$ . Readers should note the precipitous nature of the decline in the steady-state effluent concentration of biomass as the washout condition is approached. The substrate concentration must exhibit a contrary behavior. While  $D$  increases continuously, the substrate concentration first increases slowly from zero in quasilinear fashion, but then increases rapidly as  $D$  approaches its washout value.

If  $K_S$  is very small compared to  $s_0$ , equation (13.2.34) reduces to

$$D_w = \mu_{\max} \quad (13.2.35)$$

One can employ the definition of the dilution rate to ascertain the volumetric flow rate  $V_w$  at which washout is observed:

$$V_w = \mu_{\max} V_R \quad (13.2.36)$$

When  $V_w$  exceeds  $\mu_{\max} V_R$ , the rate at which the cells are carried out of the reactor in the effluent stream is faster than the rate at which they are formed in the reactor:

$$x_F V_w > \mu_{\max} x_F V_R \quad (13.2.37)$$

Readers should be cognizant of the sensitivity of conditions in the process effluent to changes in the dilution rate as washout conditions are approached. Small changes in  $D$  can be reflected in large changes in effluent substrate and biomass concentrations, especially when nature supplies kinetic parameters that exacerbate the situation and make the reactor difficult to control as the dilution rate approaches washout conditions.

One could start again with equation (13.2.29) and explore other situations of engineering interest that would lead to other constraints on operation of the bioreactor provided that the various kinetic and yield parameters are

known. Here we restrict further discussion of the design relations for a single continuous-flow stirred-tank bioreactor to optimizing the productivity that can be achieved under steady-state conditions.

The productivity ( $\mathcal{P}$ ) of a CSTBR is defined as the amount of product formed per unit time per unit volume of reactor. Another way to characterize the productivity is to employ the product of the dilution rate ( $D$ ) and the effluent concentration of the fermentation product of primary interest. Thus, if the biomass itself is the desired product,

$$\mathcal{P} = \frac{Vx_F}{V_R} = Dx_F = DY_{X/S}(s_0 - s_F) \quad (13.2.38)$$

where  $x_F$  is the effluent concentration of biomass, and where we have recognized that the yield coefficients are positive for situations where products are formed and substrates are consumed.

Combination of equations (13.2.32), (13.2.33) and (13.2.38) yields

$$\mathcal{P} = DY_{X/S} \left( s_0 - \frac{K_S D}{\mu_{\max} - D} \right) \quad (13.2.39)$$

This equation indicates that initially the steady-state productivity of the bioreactor at constant product concentration increases quasi-linearly with the dilution rate (see Figure 13.7). The maximum productivity (subject to the constraints implicit in equations (13.2.38) and (13.2.39)) may be determined by differentiating equation (13.2.39) with respect to the dilution rate and identifying the dilution rate that makes the derivative ( $d\mathcal{P}/dD$ ) equal to zero:

$$d\mathcal{P}/dD = \frac{d}{dD} \left[ DY_{X/S} \left( s_0 - \frac{K_S D}{\mu_{\max} - D} \right) \right] = 0 \quad (13.2.40)$$

$$\begin{aligned} d\mathcal{P}/dD &= Y_{X/S} \left[ \left( s_0 - \frac{K_S D}{\mu_{\max} - D} \right) \right] \\ &+ Y_{X/S} D \left[ -\frac{(\mu_{\max} - D) K_S - K_S D(-1)}{(\mu_{\max} - D)^2} \right] = 0 \end{aligned} \quad (13.2.41)$$

Simplification yields

$$(\mu_{\max} - D)^2 s_0 - (\mu_{\max} - D) K_S D - D(\mu_{\max} K_S) = 0 \quad (13.2.42)$$

or

$$(s_0 + K_S)D^2 - [2\mu_{\max}(s_0 + K_S)]D + \mu_{\max}^2 s_0 = 0 \quad (13.2.43)$$

Because equation (13.2.43) is quadratic in  $D$ , it is convenient to define the following groups of parameters as:

$$a = [s_0 + K_S] \quad (13.2.43a)$$

$$b = -2\mu_{\max}(s_0 + K_S) \quad (13.2.43b)$$

$$c = \mu_{\max}^2 s_0 \quad (13.2.43c)$$

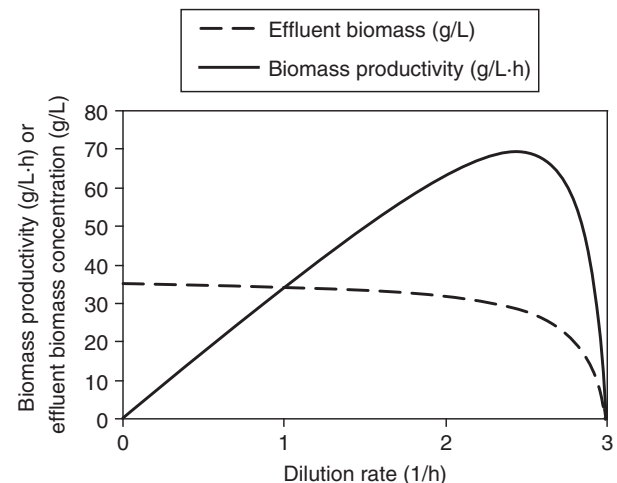


**Figure 13.7** Effects of dilution rate on the productivity of a CSTBR and on the effluent concentration of biomass at steady state. The maximum productivity is observed at a dilution rate of  $2.43 \text{ h}^{-1}$ . Parameter values:  $K_S = 2.78$ ,  $\mu_{\max} = 3.16 \text{ h}^{-1}$ ,  $s_0 = 50$ , and  $Y_{X/S} = 0.7$ .

The quadratic formula indicates that the solution to equation (13.2.43) is

$$D = \frac{-b \pm \sqrt{b^2 - 4ac}}{2a} \quad (13.2.44)$$

Extensive algebraic manipulation of equations (13.2.43) and (13.2.44) then gives

$$\begin{aligned} D &= \mu_{\max} \left[ 1 \pm \sqrt{1 - \frac{s_0}{s_0 + K_S}} \right] \\ &= \mu_{\max} \left[ 1 \pm \sqrt{\frac{K_S}{s_0 + K_S}} \right] \end{aligned} \quad (13.2.45)$$

The term containing the positive square root can be discarded as physically unrealistic because if the dilution rate exceeds  $\mu_{\max}$ , washout will occur and at steady state there will be no cells in the reactor effluent. Hence, the root that is consistent with physical constraints is

$$D_{\max p} = \mu_{\max} \left[ 1 - \sqrt{\frac{K_S}{s_0 + K_S}} \right] \quad (13.2.46)$$

where we have labeled the dilution rate that corresponds to maximum productivity as  $D_{\max p}$ . In this case the growth rate,  $\mu_{\max}$ , will exceed the dilution rate. Hence, at steady state the effluent concentration of biomass will be a positive quantity.

The effluent concentration of biomass may be determined by first rewriting equation (13.2.33) in the form

$$x_F = Y_{X/S} \left[ s_0 - \frac{K_S D_{\max p}}{\mu_{\max} - D_{\max p}} \right] \quad (13.2.47)$$

and then using equation (13.2.46) to find that

$$\mu_{\max} - D_{\max p} = \mu_{\max} \sqrt{\frac{K_S}{s_0 + K_S}} \text{ and that}$$

$$\frac{D_{\max p}}{\mu_{\max}} = \left[ 1 - \sqrt{\frac{K_S}{s_0 + K_S}} \right] \quad (13.2.48)$$

Combination of equations (13.2.47) and (13.2.48) yields

$$x_F = Y_{X/S} \left[ s_0 - \left[ 1 - \sqrt{\frac{K_S}{s_0 + K_S}} \right] \sqrt{K_S(s_0 + K_S)} \right]$$

$$x_F = Y_{X/S} [s_0 - [\sqrt{K_S(s_0 + K_S)} - K_S] \quad (13.2.49)$$

For situations in which  $s_0 \gg K_S$ , equation 13.2.49 indicates that

$$x_F = Y_{X/S} s_0 \quad (13.2.49b)$$

To indicate the need for caution in selecting the dilution rate at which to operate, we have prepared plots of the productivity  $P$  and the effluent concentration of biomass versus the dilution rate  $D$  (see Figure 13.10) using equations (13.2.39) and (13.2.33) as the basis for spreadsheet calculations. Readers should note that the dilution rate that maximizes the productivity of the CSTBR approaches  $\mu_{\max}$  for small values of  $K_S$ . Consequently, the bioengineer may be required to forego operating at the dilution rate that maximizes production of biomass in order to stay within the regime where the operating conditions are sufficiently robust that there is adequate room for the reactor operator and the process control system to maneuver in response to natural fluctuations in process parameters or process upsets. Considerations of sustainable operability, reliability, and safety are all as important in optimizing the design as are the mathematical considerations leading to the expression for ascertaining the dilution rate [equation (13.2.46)] that maximizes the productivity of the reactor.

### 13.2.3 Relative Productivities of a Chemostat and a Batch Reactor

Decisions as to whether a chemostat or a batch reactor is preferable for use in a particular application depend on a number of factors. However, an important consideration is whether or not the enhancement in productivity associated with the use of a continuous fermentation process is sufficient to offset the difficulties associated with this mode of operation: the need for continuously feeding sterile supplies of the growth medium and (if appropriate) either air or oxygen, the potential for other modes of contamination of the fermentation broth, the potential for mutation of the microorganism, and so on. As an introduction to these considerations, let us consider the relative productivities of

batch and continuous modes of operation as measured by the ratio of the maximum quantity of biomass produced to the time associated with that production.

For a chemostat or a single CSTBR, the maximum rate of production ( $P$ ) of biomass is equal to the product of the dilution rate and the effluent concentration of biomass corresponding to complete conversion of substrate to biomass:

$$P_{\text{CSTBR}} = D_{\max p} x_F = D_{\max p} (Y_{X/S} s_0) = \mu_{\max} Y_{X/S} s_0 \quad (13.2.50)$$

where we have recognized that for steady-state operation,  $D_{\max p} = \mu_{\max}$  and that  $Y_{X/S}$  is a positive quantity.

To determine an equivalent rate of production of biomass in a batch reactor we must utilize the ratio of the maximum quantity of biomass that can be obtained in a batch reactor to the sum of the cooking time for a batch and the various times during a production cycle when biochemical transformations are not taking place (i.e., the lag time, the time between inoculation and the beginning of the exponential growth phase, the times for cleaning, sterilizing, loading, heating, etc). We shall express this sum in terms of the parameter  $t_S$  with the rationale that either a negligibly small amount of growth is occurring or that no relevant reactions take place during these periods. By far the most productive portion of the growth cycle is the exponential growth phase. Hence, if we inoculate a batch reactor with a quantity of biomass  $X_0$  at time zero, the time necessary for the organism to grow from a mass  $X_0$  to a mass  $X_{\max}$  can be determined by solving the following differential equation subject to the constraint that at time zero,  $X = X_0$ :

$$\frac{dX}{dt} = \mu_{\max} X \quad (13.2.51)$$

Separation of variables followed by integration and exponentiation leads to

$$\frac{X_{\max}}{X_0} = e^{\mu_{\max} t_{\text{batch}}} \quad (13.2.52)$$

For any individual cycle of batch operation the total amount of time associated with the growth of a quantity of biomass from  $X_0$  to  $X_{\max}$  in the batch reactor is then  $(t_S + t_{\text{batch}})$ . The maximum quantity of biomass that can be produced from a fixed mass of substrate is given by  $(Y_{X/S} S_0)$ . The corresponding gross productivity of a batch reactor is then

$$P_{\text{batch}} = \frac{Y_{X/S} S_0}{t_{\text{batch}} + t_S} \quad (13.2.53)$$

Combination of equations (13.2.52) and (13.2.53) gives

$$P_{\text{batch}} = \frac{Y_{X/S} S_0}{[\ln(X_{\max}/X_0)/\mu_{\max}] + t_S} \quad (13.2.54)$$

The ratio of the productivity of a chemostat to that of a batch reactor is then

$$\frac{P_{CSTBR}}{P_{batch}} = \frac{\mu_{max} Y_{X/S} s_0}{Y_{X/S}(s_0)/(t_{batch} + t_s)} = \mu_{max}(t_{batch} + t_s) \\ = \ln(X_{max}/X_0) + \mu_{max} t_s \quad (13.2.55)$$

where we have employed equation (13.2.52).

Even in the best-case situation, for the batch reactor in which  $t_s$  approaches zero (a highly unlikely scenario!) the productivity of the CSTBR will exceed that of a batch reactor whenever the ratio ( $X_{max}/X_0$ ) exceeds  $e$ , the base of natural logarithms (2.718). Despite this fact, the disadvantages of employing a CSTBR noted in the introduction to this section can outweigh its productivity advantage.

### 13.2.4 Operation of a Single CSTBR in Conjunction with Cell Separation and Recycle

Biochemical transformations that are mediated by microorganisms are characterized by autocatalytic behavior. The fact that the rates of these reactions increase as the concentration of the organism increases provides opportunities for engineers to consider a variety of modes of operation to enhance the performance (and productivity) of a CSTBR facility. One fruitful approach is to do a partial separation and concentration of the cells contained in the effluent from the CSTBR (see Figure 13.8) and recycle the resulting process stream back to a point where it is mixed with the contents of the CSTBR.

Use of a recycle stream can lead to significant increases in the steady-state concentration of cells in the CSTBR above that which is obtained in the absence of recycle. Recovery of cells can be accomplished using one of several alternative unit operations, such as centrifugation, membrane filtration, or settling. In Figure 13.8 we have depicted a generic separation device because our primary focus here is to demonstrate that use of an appropriate recycle stream can markedly enhance productivity during operation at steady state. Subscripts are employed in this figure to identify the usual process variables at particular points in the flow sheet.

In addition to the variables we have used previously in our analysis of the behavior of a CSTBR, we employ the *recycle ratio* ( $R$ ) to represent the ratio of the volumetric flow rate of the suspension of cells leaving the separation device to the volumetric flow rate of the net product stream. The symbol  $\psi$  represents the ratio of the concentration of biomass in the recycle stream to that in the gross product stream so  $\psi = x_2/x_1$ . This concentration factor characterizes the degree to which the separation operation increases the amount of biomass present in the recycle stream beyond

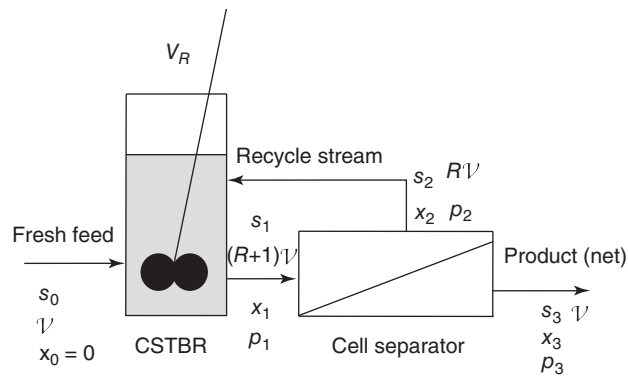


**Figure 13.8** Schematic flow sheet for a process coupling use of a CSTBR and a generic unit operation for separation and concentration of a suspension of cells for recycle to enhance reactor productivity. The concentration factor  $\psi = x_2/x_1$ .

that present in the effluent from the CSTBR. In our analysis we presume that the system is operating at steady state, a condition that will subsequently permit us to draw useful conclusions regarding the process variables.

The volumetric flow rates at various points in the process flow sheet are indicated in Figure 13.8. The relative flow rates of the recycle and net product streams are linked by the definition of the recycle ratio  $R$ . If one presumes that any differences in the densities of the fresh feed and net product streams are inconsequential, an overall material balance indicates that the volumetric flow rates of these streams are then essentially identical. In similar fashion one can conclude that total mass balances around the CSTBR and around the separator dictate that the volumetric flow rates of the recycle stream and the effluent from the CSTBR proper are  $R'V$  and  $(1 + R)V$ , respectively.

A material balance for the microorganism around the CSTBR in Figure 13.8 indicates that for a sterile feed ( $x_0 = 0$ ) the rates of various terms obey the relation

$$\text{accumulation} = \text{input} - \text{output} + \text{production by reaction} \quad (13.2.56)$$

$$\frac{d(x_{CSTBR} V_R)}{dt} = 0 + x_2 R'V - x_{CSTBR} (1 + R)V \\ + \mu_{net} x_{CSTBR} V_R \quad (13.2.57)$$

where  $\mu_{net}$  represents the difference between the biomass specific growth rate and those terms that effectively reduce the specific growth rate (and are proportional to the quantity of biomass present, such as the death rate and the effects of those maintenance activities essential to the life of the cell). At steady state the time derivative in equation (13.2.57) is zero (as are  $dV_R/dt$  and  $dx_{CSTBR}/dt$ ). Thus if we employ the definition of  $\psi$ , equation (13.2.57) becomes

$$\psi R'V - (1 + R)V + \mu_{net} V_R = 0 \quad (13.2.58)$$

Here we have also recognized that if the contents of the bioreactor are perfectly mixed,  $x_1 = x_{\text{CSTBR}}$ . Algebraic manipulation of equation (13.2.58) combined with use of the definition of the dilution rate yields

$$\mu_{\text{net}} = D[(1 + R) - \psi R] = D[1 + R(1 - \psi)] \quad (13.2.59)$$

Because the concentration factor  $\psi$  must exceed unity to render operation in a recycle mode viable, the quantity  $R(1 - \psi)$  must be negative and the dilution rate  $D$  must exceed  $\mu_{\text{net}}$ . Consequently, the use of separation and recycle of a portion of the cells permits one to operate with a steady-state dilution rate that exceeds the net biomass specific growth rate in the CSTBR.

Material balances on the substrate and the product species can be used with a rate expression and yield coefficients to specify completely the compositions of the remaining streams in Figure 13.8. For a generic biomass specific rate law and steady-state operation, a balance on the growth-limiting substrate around the combination of the mixing point and the bioreactor indicates that

$$\text{accumulation} = \text{input} - \text{output} + \text{production by reaction} \quad (13.2.60)$$

$$\begin{aligned} \frac{d(s_{\text{CSTBR}} V_R)}{dt} &= \mathcal{V} s_{\text{feed}} + R V s_{\text{CSTBR}} \\ &\quad - (1 + R) V s_{\text{CSTBR}} - \mu \frac{X_{\text{CSTBR}}}{Y_{X/S}} \\ &= \mathcal{V} s_{\text{feed}} - \mathcal{V} s_{\text{CSTBR}} - \mu \frac{X_{\text{CSTBR}}}{Y_{X/S}} \end{aligned} \quad (13.2.61)$$

where  $\mu$  is a generic specific growth rate. At steady state the accumulation term is zero. If we assume that cell death, maintenance metabolism, and similar effects can be neglected, and that we can replace the generic factor  $\mu$  by a Monod expression, we can manipulate equation (13.2.61) to obtain

$$\begin{aligned} X_{\text{CSTBR}} &= x_{\text{CSTBR}} V_R \\ &= \left( \frac{K_S + s_{\text{CSTBR}}}{\mu_{\text{max}} s_{\text{CSTBR}}} \right) Y_{X/S} \mathcal{V} (s_{\text{feed}} - s_{\text{CSTBR}}) \end{aligned} \quad (13.2.62)$$

Introduction of the definition of the dilution rate gives

$$x_{\text{CSTBR}} = \left( \frac{K_S + s_{\text{CSTBR}}}{\mu_{\text{max}} s_{\text{CSTBR}}} \right) Y_{X/S} D (s_{\text{feed}} - s_{\text{CSTBR}}) \quad (13.2.63)$$

When  $s_{\text{CSTBR}} \gg K_S$ , equation (13.2.63) reduces to

$$x_{\text{CSTBR}} = \frac{Y_{X/S} D}{\mu_{\text{max}}} (s_{\text{feed}} - s_{\text{CSTBR}}) \quad (13.2.64)$$

Combination of equations (13.2.59) and (13.2.64) gives

$$x_{\text{CSTBR}} = \frac{Y_{X/S} (s_{\text{feed}} - s_{\text{CSTBR}})}{1 + R(1 - \psi)} \quad (13.2.65)$$

Inspection of equation (13.2.65) indicates that the effect of the recycle is to reduce the amount of biomass in the effluent from the CSTBR by the factor  $1 + R(1 - \psi)$  relative to the total amount of biomass that would be obtained from a single CSTBR operating at steady state. Consequently, the biomass in the recycle stream can serve to increase the amount of biomass in the CSTBR well above that obtained in the absence of recycle.

The corresponding concentration of the substrate in the effluent from the CSTBR can be determined by recognizing that (1) at steady state, equation (13.2.59) is again applicable, and (2) in the absence of cell death and cell maintenance effects, the biochemical reaction obeys a biomass-specific rate law of the Monod form:

$$\mu = D[1 + R(1 - \psi)] = \frac{\mu_{\text{max}} s_{\text{CSTBR}}}{K_S + s_{\text{CSTBR}}} \quad (13.2.66)$$

Algebraic manipulation of equation (13.2.66) gives

$$s_{\text{CSTBR}} = \frac{K_S D [1 + R(1 - \psi)]}{\mu_{\text{max}} - \{D[1 + R(1 - \psi)]\}} \quad (13.2.67)$$

Combination of equations (13.2.65) and (13.2.67) followed by further algebraic manipulation gives the following relation for the steady-state concentration of cells in the effluent from the CSTBR:

$$x_{\text{CSTBR}} = \frac{Y_{X/S}}{1 + R(1 - \psi)} \left\{ s_{\text{feed}} - \frac{K_S D [1 + R(1 - \psi)]}{\mu_{\text{max}} - D[1 + R(1 - \psi)]} \right\} \quad (13.2.68)$$

Equation (13.2.68) was used as a basis for spreadsheet calculations leading to the plots in Figure 13.9 indicating

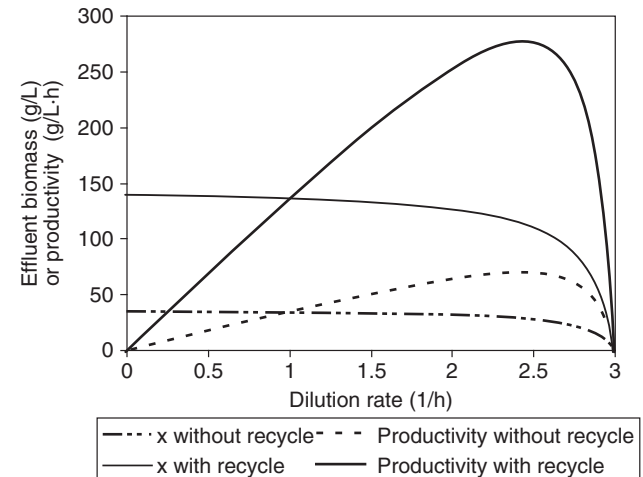


**Figure 13.9** Effects of dilution rate on the total quantity of biomass produced and on the rate of production of biomass during steady-state operation in the presence and absence of partial separation and recycle of biomass to the entrance of a single CSTBR. Parameter values used in generating plots:  $K_S = 2.78 \text{ g/L}$ ;  $\mu_{\text{max}} = 3.16 \text{ h}^{-1}$ ;  $Y_{X/S} = 0.7$ ;  $s_0 = 50 \text{ g/L}$ ;  $\psi = 2.5$ ;  $R = 0.5$ .

the effects of dilution rate on the total quantity of biomass produced and the productivity of a single CSTBR when some of the biomass is recycled. Analysis of these plots indicates that there is a very marked increase in the concentration of biomass in the CSTBR when separation and partial recycle of biomass is employed. The effect of recycle of some biomass on the productivity of a single CSTBR is even more striking (see the solid curves in Figure 13.9). The productivity ( $P$ ) of a bioreactor is defined as the product of the dilution rate and  $x_{\text{CSTBR}}$ :

$$P = Dx_{\text{CSTBR}} \quad (13.2.69)$$

Physically, the productivity can be regarded as the total rate at which the desired product (cells in this case) is produced per unit time per unit working volume of reactor. Combination of equations (13.2.68) and (13.2.69) yields

$$P = \frac{DY_{X/S}}{1 + R(1 - \psi)} \left\{ s_{\text{feed}} - \frac{K_S D [1 + R(1 - \psi)]}{\mu_{\text{max}} - D[1 + R(1 - \psi)]} \right\} \quad (13.2.70)$$

Figure 13.9 also contains plots of the productivity of the CSTBR as a function of the dilution rate for operation with and without recycle of cells. The recycled cells enable one to operate at dilution rates considerably above those characteristic of the close-to-washout conditions that would prevail in the absence of recycle. The higher density of cells leads to very substantial increases in reactor productivity. The recycle mode of operation is particularly important in the use of microorganisms for the treatment of wastewaters (see Section 13.3.1).

### 13.2.5 Batteries of CSTBRs: Cascades of Chemostats

The discussion in Section 8.3.2 indicated that dramatic reductions in reactor volume requirements can be obtained by using a number of individual CSTRs connected in a series flow configuration rather than an individual CSTR. The effluent from one reactor in the cascade serves as the feed stream for the next reactor. Although the composition and temperature are uniform throughout any individual reactor, there can be marked changes in temperature, pH, and composition as one follows an element of fluid from the first tank in a cascade to the last. Similar situations arise when chemostats are connected in series.

For CSTBRs, the use of multistage series flow configurations offers several advantages in addition to the drastic reduction in reactor size requirements that takes place when additional stirred tank reactors are connected in series to an individual CSTBR. For example, if the

environmental conditions that are conducive to the growth of microorganisms differ from those that are optimum for the synthesis of particular metabolic products, the design engineer has the option of growing up the biomass in the first reactor in a cascade to take advantage of the autocatalytic character of the growth process and to employ a subsequent CSTBR characterized by different environmental conditions to bring about enhanced selectivity for production of a desired metabolite. Such shifts in the intended purpose of an individual chemostat in a cascade can be brought about by adding to that reactor a second feed stream that shifts the pH or chemical composition of the growth medium in a manner that achieves the desired selectivity for the biochemical reactions of interest. Operating individual reactors at different temperatures can also be a useful tool in manipulating the selectivity of the primary biochemical reactions. Examples of situations in which one might employ a supplementary feed stream subsequent to the first reactor in the cascade are the synthesis of recombinant proteins and the production of metabolites that are not linked directly to energy metabolism.

For steady-state operation, each stirred tank in a cascade of CSTBRs is characterized by conditions that are similar to those of the environment at a point on the growth curve of a microorganism in a batch reactor. As a suspension of cells in a growth medium moves from one stirred tank to the following tank in a cascade, it effectively experiences a step change in the average physiological state of the biomass. These changes in state reflect the metabolic pathways available to the individual cells in the culture present in a particular stirred tank and the evolution of cell growth processes as the various cells attempt to transition to the next point on the cell growth curve for a batch reactor whose physical and chemical properties are identical with those of the contents of a CSTBR that is present in the downstream portion of the cascade.

An additional benefit of employing multiple CSTBRs in series is the possibility of using a quasi-“cross-flow” mode of operation in which the feed to the second (and/or subsequent) reactor in the cascade consists of a second fresh feed stream in addition to the effluent from the previous reactor. Use of a second fresh feed stream is optional, but this mode of operation is advantageous when this stream contains an inducer to elicit production of a targeted protein in order to circumvent problems of genetic instability.

The design equations for batteries of chemostats can be derived by appropriate extensions of the material balance relations developed in Section 8.3.2 for cascades of CSTRs. Steady-state operation is assumed for each stirred tank, but students must be careful in writing the reaction rate terms that appear in these relations. Details

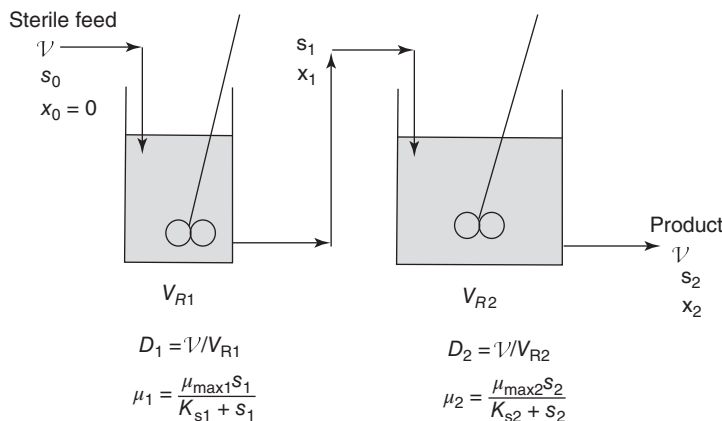
of such analyses for bioreactors are available elsewhere [e.g., van't Riet and Tremper (16), Clark and Blanch (17), Shuler and Kargi (18), and Panda (19)]. However, there is one important caveat that the reader should bear in mind: In a cascade of well-stirred fermentation vessels the cells may go through periods of unbalanced growth as they transition from one environment to another (one tank to another). The associated pseudo-lag-time effects necessary to bring about adjustments or repurposing of the metabolic machinery of individual cells may be responsible for discrepancies between actual results and results predicted using simple kinetic models. The agreement between predicted and actual results may not always be as good as one might desire.

As is the case for conventional homogeneous reactions taking place in batteries of CSTRs, one quickly reaches a point of diminishing returns with respect to the benefits of addition of another identical CSTR to a cascade. Because issues of genetic stability and prevention of contamination by alien microorganisms exacerbate the problem of diminishing returns, very rarely does a cascade of CSTBRs exceed three or four in number.

Consider a cascade of CSTBRs consisting of two reactors with different working volumes,  $V_{R1}$  and  $V_{R2}$  (see Figure 13.10). The stream fed to the first reactor in the cascade is sterile ( $x_0 = 0$ ), but it enters at a volumetric flow rate  $\mathcal{V}$  and contains a concentration  $s_0$  of the limiting substrate. The effluent from the first reactor contains biomass and the limiting substrate at concentrations  $x_1$  and  $s_1$ , respectively. The effluent from the second chemostat (volume  $V_{R2}$ ) contains these species at concentrations  $x_2$  and  $s_2$  and leaves at a volumetric flow rate  $\mathcal{V}$ .

For the first chemostat, stoichiometric yield considerations indicate that

$$x_1 = Y_{X/S}(s_0 - s_1) \quad (13.2.71)$$



If cell death and maintenance metabolic effects are negligible, and if the Monod rate law is applicable to this system, the steady-state material balance on the biomass can be expressed as

$$\text{input} = \text{output} + \text{disappearance by reaction} \quad (13.2.72)$$

$$0 = x_1 \mathcal{V} - \mu_1 x_1 V_{R1} \quad (13.2.73)$$

where we have recognized that the pertinent concentration for the reaction rate term is  $x_1$  because this is the concentration of biomass within the first chemostat. Simplification and introduction of the dilution rate ( $D_1 = \mathcal{V}/V_{R1}$ ) gives

$$0 = x_1 (D_1 - \mu_1) \quad (13.2.74)$$

Consequently, at steady state in the first chemostat, the dilution rate must be equal to the biomass specific growth rate:

$$D_1 = \mu_1 = \frac{\mu_{\max 1} s_1}{K_{s1} + s_1} \quad (13.2.75)$$

or

$$s_1 = \frac{K_{s1} D_1}{\mu_{\max 1} - D_1} \quad (13.2.76)$$

To analyze the second chemostat in the cascade, one can again write the steady-state material balances for both the biomass and the substrate. For the biomass,

$$\mu_2 x_2 V_{R2} = \mathcal{V} x_2 - \mathcal{V} x_1 \quad (13.2.77)$$

Introduction of the dilution rate for the second chemostat and rearrangement yields

$$\mu_2 = D_2 \left( 1 - \frac{x_1}{x_2} \right) \frac{\mu_{\max 2} s_2}{K_{s2} + s_2} \quad (13.2.78)$$

The corresponding steady state material balance on the limiting substrate for the second chemostat is

$$\frac{\mu_2 x_2 V_{R2}}{Y_{X/S}} = \mathcal{V} s_1 - \mathcal{V} s_2 \quad (13.2.79)$$

**Figure 13.10** Cascade of two CSTBRs (two chemostats) with different working volumes.

In terms of the dilution rate,

$$s_2 = s_1 - \frac{\mu_2}{D_2 Y_{X/S}} = s_1 - \frac{\mu_{\max,2} s_2}{(D_2 Y_{X/S})(K_{S2} + s_2)} \quad (13.2.80)$$

Given the volumes of the CSTBRs constituting the cascade and the pertinent parameters for the Monod relations, one can solve equations (13.2.71), (13.2.76), (13.2.78), and (13.2.80) simultaneously to ascertain the concentrations of substrate and biomass in the effluents from each of the two chemostats. This task is readily accomplished using engineering software (such as Mathcad) that contains an equation solver.

As we saw in Section 8.3.2, one can develop equations describing the performance of an arbitrary CSTR in a cascade of CSTRs. We can also develop the corresponding equations for the  $n$ th bioreactor in an extended cascade of stirred tanks by conducting an analysis on the  $n$ th bioreactor. The feed stream exiting bioreactor  $n - 1$  and entering reactor  $n$  has a volumetric flow rate  $\mathcal{V}$ , a concentration of the limiting substrate equal to  $s_{n-1}$ , and a biomass concentration  $x_{n-1}$ . This stream enters well-stirred reactor  $n$ , which has a working volume  $V_{Rn}$ . Associated with this reactor are an exit volumetric flow rate  $\mathcal{V}$ , a substrate concentration  $s_n$  and a biomass concentration  $x_n$ . By analogy with equations (13.2.78) and (13.2.80), the equations that constitute the steady-state material balances across the  $n$ th bioreactor for the concentrations of substrate, biomass, and product are as follows:

Biomass:

$$\mu_n = D_n \left( 1 - \frac{x_{n-1}}{x_n} \right) = \frac{\mu_{\max,n} s_n}{K_{S_n} + s_n} \quad (13.2.81)$$

Limiting substrate:

$$\begin{aligned} s_n &= s_{n-1} - \frac{\mu_n}{D_n Y_{X/S}} \\ &= s_{n-1} - \frac{\mu_{\max,n} s_n}{D_n Y_{X/S} (K_{S_n} + s_n)} \end{aligned} \quad (13.2.82)$$

Product:

$$\begin{aligned} p_n &= p_{n-1} + \frac{\mu_n}{D_n Y_{P/S}} \\ &= p_{n-1} + \frac{\mu_{\max,n} s_n}{D_n Y_{P/S} (K_{S_n} + s_n)} \end{aligned} \quad (13.2.83)$$

where  $D_n$  is the dilution rate for the  $n$ th reactor

$$D_n = \mathcal{V}/V_{Rn} \quad (13.2.83a)$$

Here we have also assumed that the rate law is of the simple Monod form. Equations of the form of equations (13.2.81) to (13.2.83) can be written for each reactor in a cascade and the resulting set of equations can be readily solved using engineering software. Students should note

that implicit in such an analysis is the assumption that the volumetric flow rate throughout the cascade is constant.

Even in the absence of the indicated software, one can employ material balances on the first CSTBR in the cascade and the composition of the feed stream ( $x_0$ ,  $s_0$ , and  $p_0$ ), together with a knowledge of the Monod constants ( $\mu_{\max,1}$  and  $K_{S1}$ ) at the conditions of the first reactor, to ascertain the steady state composition of the effluent from this reactor. In turn, one can utilize this composition as that of the stream fed to the second CSTBR, together with the values of the Monod constants ( $\mu_{\max,2}$  and  $K_{S2}$ ), in the steady state material balances on the second reactor to determine the composition of the effluent from the second reactor. One can then employ this approach to analyze the third and subsequent CSTBRs, marching forward with knowledge of the composition of the effluent from the previous CSTBR as an essential element of the analysis of the steady-state behavior of the next CSTBR in the cascade.

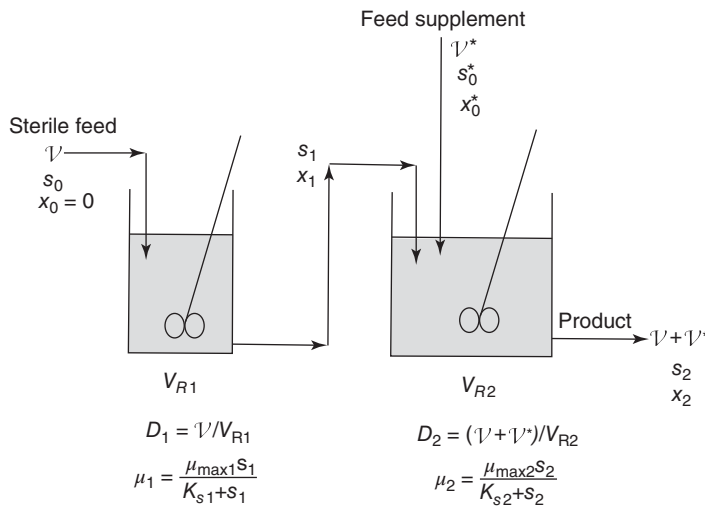
At this point in our discussion of well-stirred continuous-flow bioreactors it is helpful to consider a straightforward extension of our analysis to encompass the possibility of using more than a single feed stream. Illustration 13.5 considers a situation in which a supplementary feed stream is supplied to the second CSTBR. This illustration lets us address situations in which it is desirable to include additional components (e.g., inducers) in the growth medium to enhance the selectivity of the cascade for the production of desired product species. *Induction* enhances the production of secondary metabolites because of the presence of particular chemical species in the growth medium.

### ILLUSTRATION 13.5 Analysis of a Cascade of Two CSTBRs in the Presence of a Second Feed Stream

Consider the cascade of two chemostats shown in Figure I13.5. This physical configuration differs from that analyzed in equations (13.2.71) to (13.2.80) in that the feed to the second chemostat consists of two streams: the effluent from the first chemostat and a supplementary sterile feed stream that is characterized by a volumetric flow rate  $\mathcal{V}^*$  and a concentration of the limiting substrate equal to  $s_0^*$ . Derive the equations for the concentrations of biomass and the limiting substrate in the effluent from the second reactor for the situation in which the limiting substrate is the same in both chemostats.

### Solution

Consider the steady state material balance equations for the first chemostat. These relations are the same as those given by equations (13.2.71) and (13.2.76) for the biomass and



limiting substrate, respectively. However, for the second chemostat we must reformulate the steady state material balances even though they are of the usual form:

$$\text{input} = \text{output} + \text{disappearance by reaction}$$

$$x_1 V + 0 = (V + V^*)x_2 - \mu_2 x_2 V_{R2} \quad (\text{A})$$

where we have assumed that the volumetric flow rate of the effluent from the second reactor is equal to the sum of the flow rates of the two incoming streams. Algebraic manipulation of this equation yields

$$\mu_2 = \frac{V + V^*}{V_{R2}} - \frac{x_1 V}{x_2 V_{R2}} \quad (\text{B})$$

where the first term on the right of equation (B) can be interpreted as a dilution rate based on the volumetric flow rate of the effluent from the second chemostat. The biomass specific growth rate in the second chemostat can be expressed in terms of the Monod equation as

$$\mu_2 = \frac{\mu_{\max 2} s_2}{K_{s2} + s_2} \quad (\text{C})$$

where the kinetic parameters are evaluated at the environmental conditions prevailing in the second chemostat. The corresponding material balance on the limiting substrate for steady-state operation of the second chemostat is

$$s_1 V + s_0^* V^* = (V + V^*)s_2 + \frac{\mu_2 x_2 V_{R2}}{Y_{X/S}} \quad (\text{D})$$

In this situation the equation for the concentration of biomass in the effluent from the second chemostat becomes

$$x_2 = \frac{Y_{X/S}[(s_1 - s_2)V + (s_0^* - s_2)V^*]}{\mu_2 V_{R2}} \quad (\text{E})$$

At this point one can employ machine computation to determine the compositions of the effluent streams from each

**Figure I13.5** Cascade of two CSTBRs (two chemostats) with different working volumes with supplementation of the feed to the second CSTBR.

of the two chemostats using equations (13.2.71), (13.2.76), (B), (C), and (E), together with specified values of appropriate process parameters.

Illustration 13.6 presents a method for analyzing the operation of a cascade of three CSTBRs. This method employs graphical forms of both the material balance relations and the rate law for a biochemical reaction.

### ILLUSTRATION 13.6 Graphical Method for Analysis of a Cascade of Three CSTBRs

Figure I13.6 contains a plot of rate versus cell concentration for an autocatalytic biochemical reaction whose rate law is of the logistic form

$$r_x = \mu_{\max} \left( 1 - \frac{x}{x_{\infty}} \right) x \quad (\text{A})$$

with  $\mu_{\max} = 1.2 \text{ g}/(\text{L}\cdot\text{day})$  and  $x_{\infty} = 140 \text{ g}/\text{L}$ . Consider carrying out this reaction in a cascade of three CSTBRs that differ from each other in size. Use a graphical approach to ascertain the dilution rates and working volumes for each of these reactors if the volumetric flow rate to the first CSTBR is 4000 L/day. You may assume that (1) the cascade operates at steady state; (2) the feed to the first CSTBR is sterile; (3) the working volume of the second reactor is 50% larger than that of the first; (4) the working volume of the third reactor is 50% larger than that of the second; and (5) the first CSTBR is operated at conditions corresponding to the maximum in the rate curve. What combinations of biomass concentration and reaction rate characterize each of these reactors?

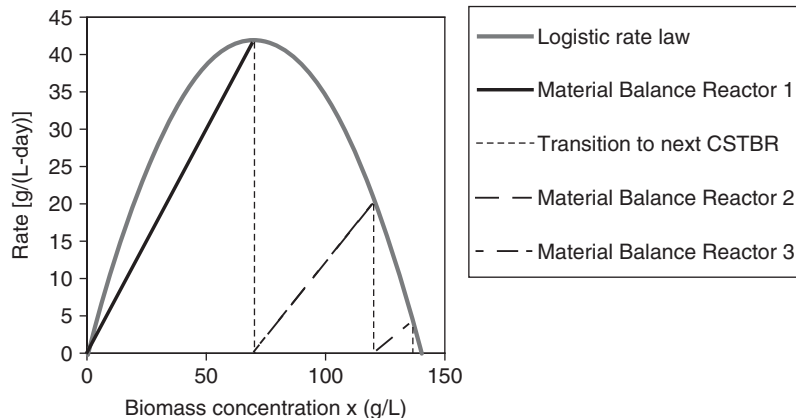


**Figure I13.6** Plots of reaction rate versus biomass concentration for the logistic rate model and material balances on each member of a cascade of three (nonidentical) CSTBRs.

## Solution

The maximum reaction rate corresponds to a condition for which the derivative of the rate law with respect to the concentration of biomass is zero.

$$0 = \frac{dr_x}{dx} = \mu_{\max} \frac{d\{[1 - (x/x_{\infty})]x\}}{dx} \\ = \left(1 - \frac{x}{x_{\infty}}\right) + x \left(\frac{-1}{x_{\infty}}\right) \quad (\text{B})$$

Thus, at the maximum rate,

$$x = \frac{x_{\infty}}{2} = \frac{140}{2} = 70 \text{ g/L} \quad (\text{C})$$

The corresponding rate is

$$r_{x1} = 1.2 \left(1 - \frac{70}{140}\right) 70 = 42 \text{ g/(L·day)} \quad (\text{D})$$

A steady state material balance on the biomass around the first reactor in the cascade yields

$$\text{input} = \text{output} + \text{disappearance by reaction} \quad (\text{E})$$

$$0 = x_1 V - r_{x1} V_{R1} \quad (\text{F})$$

where we have designated the concentration of biomass leaving the first CSTBR as  $x_1$ . The corresponding rate of production of biomass per unit volume of this reactor is  $r_{x1}$ . Rearrangement of equation (F) and introduction of the dilution rate ( $D_1 = V/V_{R1}$ ) gives

$$r_{x1} = x_1 \frac{V}{V_{R1}} = D_1 x_1 \quad (\text{G})$$

Equation (G) indicates that a plot of  $r_1$  versus  $x_1$  representing the material balance on the first CSTBR will be a straight line linking the origin and the point  $x_1$ ,  $r_{x1}$ . The slope of this line is the dilution rate for the first CSTBR ( $D_1$ ). The intersection of this straight line and the graphical representation of the logistic rate law (expressed per unit volume of growth medium) will correspond to steady-state

conditions in the first CSTBR. To minimize the volume of the first reactor, we specified operation of this reactor at the maximum in the plot of the rate versus biomass concentration curve (see Figure I13.6): namely, at  $x = 70 \text{ g/L}$  and  $r_{x1} = 42 \text{ g/(L·day)}$ . The value of the dilution rate is equal to the slope of the line linking the origin and the point of intersection of the straight line with the logistic rate curve: namely,  $0.6 \text{ day}^{-1}$ . Thus, from equation (G),

$$V_{R1} = \frac{V}{D_1} = \frac{4000}{0.6} = 6667 \text{ L} \quad (\text{H})$$

The volume of the first CSTBR is 6667 L.

The volumes of the second and third reactors are each 50% larger than the volume of the previous reactor. Hence,

$$V_{R2} = 1.5V_{R1} = 1.5(6667) = 10,000 \text{ L} \quad (\text{I})$$

and

$$V_{R3} = 1.5V_{R2} = 1.5(10,000) = 15,000 \text{ L} \quad (\text{J})$$

The dilution rates corresponding to these reactor volumes are

$$D_2 = \frac{V}{V_{R2}} = \frac{4000}{10,000} = 0.4 \text{ day}^{-1} \quad (\text{K})$$

$$D_3 = \frac{V}{V_{R3}} = \frac{4000}{15,000} = 0.26667 \text{ day}^{-1} \quad (\text{L})$$

Material balances around the second and third CSTBRs lead to the following analogs of equation (F):

$$r_{x2} = D_2(x_2 - x_1) \quad \text{for the second CSTBR} \quad (\text{M})$$

and

$$r_{x3} = D_3(x_3 - x_2) \quad \text{for the third CSTBR} \quad (\text{N})$$

The straight lines describing the material balances on the second and third CSTBRs [equations (M) and (N), respectively] can be drawn through the point  $x = 70$ ,  $r = 0$  with

slope = 0.4 for the second reactor, and through the point  $x = 120.45$ ,  $r = 0$  with slope 0.26667 for the third reactor (see Figure I13.6). The intersections of these straight lines with the curve representing the rate law indicate the following values for biomass concentrations and rates of reaction.

$$\begin{aligned} x_2 &= 120.45 \text{ g/L} & x_3 &= 136.37 \text{ g/L} \\ r_2 &= 20.18 \text{ g/(L·day)} & r_3 &= 4.245 \text{ g/(L·day)} \end{aligned}$$

We have listed above more significant figures than one would expect for a graphical solution. The excess was determined using the spreadsheet on which Figure I13.6 is based. One could obtain similar results using engineering software containing an equation solver and equations (I) to (N).

Readers may wish to compare and contrast the methods of analysis and results of this illustrative example with the corresponding aspects of Illustration 8.7. This example employed a graphical approach to analyze the behavior of a cascade of three reactors employed to conduct a reaction whose rate increased continuously with reactant concentration.

### 13.2.6 The Ideal Plug Flow Bioreactor

In Chapters 8 to 11 we provided extensive discussions of the assumptions underlying the ideal PFR model that is widely employed in preliminary design considerations of the behavior of tubular reactors and their potential for accomplishing a specific chemical transformation to the extent desired. The assumptions from which the PFBR (plug flow bioreactor) model is constructed are the same as those used in the development of the PFR model: flat velocity profile, no longitudinal dispersion of any chemical species or energy, no radial gradients in temperature or composition. The additional assumption of steady-state operation leads to the PFR design relation given in equation (8.2.7). The primary difference between the PFR and PFBR models lies in the form of the rate law that one utilizes in the model. For homogeneous reactions in a PFR, the reaction rate is usually expressed per unit volume of process fluid, but for heterogeneous catalytic reactions, it is preferable to express the rate per unit mass or per unit area of catalyst. For the PFBR model the conventional approach is to utilize a rate law based on a unit of biomass. In effect, regardless of whether or not the engineer's primary focus is on production of additional biomass, or on specific metabolic products, it is often desirable to employ a specific growth rate term, often of the Monod form, so that the rate of consumption of substrate per unit volume can be written as

$$-r_S = \frac{\mu_{\max}(s)}{K_S + (s)} x \quad (13.2.84)$$

where  $x$  is the concentration of biomass. The microorganisms may be present as a relatively homogeneous suspension in the growth medium or immobilized via one of a variety of immobilization techniques, many of which are also employed to immobilize enzymes. Consequently, one can employ the techniques for either homogeneous reaction conditions in Chapters 8 to 11 or heterogeneous reactions in Chapter 12 to attack problems concerning bioreactors that are not well mixed. Illustration 13.7 indicates how one might utilize the design equations for a plug flow reactor to size a packed bed bioreactor employed for denitrification of streams containing less than 100 mg/L of nitrates at temperatures from 5 to 20°C.

### ILLUSTRATION 13.7 Modeling Denitrification of a Waste Stream in a Packed-Bed Bioreactor

Wastewaters containing nitrates (e.g., those from septic tank sewage systems, agricultural runoff, and some food-related industries) can present serious pollution hazards for aquatic environments containing marine life. These wastewaters often represent a primary source of nutrients for the growth of those microorganisms that are the root cause of eutrophication of surface waters. A classic approach to the problem of removal of nitrogenous compounds from waste streams involves aerobic nitrification of the waste stream, followed by anaerobic denitrification. In this process facultative heterotrophic bacteria reduce nitrate ions to nitrogen



A. L. Parker, L. J. Sikora, and R. R. Hughes (20) studied biological denitrification of wastewater streams in packed beds at temperatures from 5 to 20°C. For steady state microbe populations and feed nitrate concentrations of less than 100 mg/L, the reaction above obeys a rate expression of the form

$$r = \mu^* Y C_{\text{NO}_3}$$

where  $\mu^*$  is the rate constant for pseudo first-order removal of nitrates,  $Y$  the biochemical yield coefficient, and  $C_{\text{NO}_3}$  the nitrate concentration.

Residence time distribution studies by these researchers indicated that for a tube packed with 3-mm glass beads, an appropriate  $n$ -CSTR model to use involves a number of stirred tanks that is in the high teens. Consequently, the authors concluded that the extent of longitudinal dispersion was relatively small. Indeed, it is not unreasonable to assume that a PFBR model might provide good estimates of the conversion to be expected in packed beds of this type. If a similar packed bed is

operating at steady state at a temperature for which the  $\mu Y$  product is  $0.309 \text{ h}^{-1}$  and for which the inlet concentration of nitrate ions is  $80 \text{ mg/L}$ , what space time is necessary to reduce this concentration to  $20 \text{ mg/L}$ ?

### Solution

The fact that the residence time data exhibit relatively little axial dispersion suggests that it would be appropriate to consider the performance of the reactor as governed by an equation of the form of equation (8.2.9):

$$\tau = C_{S0} \int \frac{df_S}{-r_S} \quad (\text{A})$$

Because the solution is very dilute, volumetric expansion effects can be neglected. Hence, one can regard the concentration of the substrate as given by

$$C_S = C_{S0}(1 - f_S) \quad (\text{B})$$

and the rate expression as

$$-r_S = \mu Y C_{S0}(1 - f_S) \quad (\text{C})$$

Combination of equations (A) and (C) coupled with formal recognition of the limits on the integral gives

$$\begin{aligned} \tau &= \int_0^{0.75} \frac{df_S}{\mu Y(1 - f_S)} = \frac{-\ln(1 - f_S)}{\mu Y} = \left| \frac{-\ln(1 - f_S)}{\mu Y} \right|_0^{0.75} \\ &= \frac{-\ln(1 - 0.75)}{0.309} = 4.49 \text{ h} \end{aligned}$$

Hence, for high flow rates one would require an extremely long reactor or a very large volume of packed bed.

### 13.2.7 Operation of Bioreactors in a Perfusion Mode

Operation of various types of bioreactors in a perfusion mode (21, 22) enables the design engineer to combine several advantages of traditional modes of operation of well-stirred bioreactors (e.g., semibatch operation in a fed batch mode or use of recycle with a chemostat). *Perfusion* consists of operation in a mode in which a fresh growth medium (possibly together with a recycled growth medium) is fed to a bioreactor containing viable cells that are retained within the bioreactor by permselective membranes, microfilters, immobilization, or by partial separation and recovery from the reactor effluent followed by recycle to the entrance of the reactor.

Operation in a perfusion mode can be viewed as a form of recycle of biomass that permits one to substantially increase the amount of biomass in the bioreactor. In a batch reactor used for cultivation of mammalian cells, the maximum cell concentration is roughly 1 million cells/mL. By

contrast, continuous operation of a bioreactor in a perfusion mode permits one to increase the cell density by an order of magnitude, to 10 million cells/mL. Associated with this increase in cell density is a very substantial increase in the productivity of the reactor. Moreover, such cell levels lead to a concomitant increase in the critical dilution rate necessary to achieve washout. The expansion in the range of viable dilution rates increases flexibility of operation and enhances the ability of the operator to control the reactor.

While one can utilize a CSTBR in conjunction with a centrifuge or permselective membrane separation device to achieve perfusion (see Figure 13.11), biochemical reactions and separations can be combined in the same piece of equipment by utilizing an apparatus whose geometric configuration resembles that of a shell-and-tube heat exchanger or hollow-fiber membrane separation device of the type employed for reverse osmosis or ultrafiltration. By tailoring the *permselective* properties of the fibers to the application of interest (proper selection of the *molecular weight cutoff* of the fiber), one can effectively discriminate between those molecules capable of permeating the membrane and those that are not. Physical entrapment of microorganisms in the intra-annular region on the shell side of the apparatus confines the organisms within a fixed region of space while the permselective nature of the membrane determines which species are able to permeate across the membrane to bring about cell growth and removal of metabolic products. Manifolds for connecting the solutions contained in the lumens of the fibers effectively provide the configuration necessary for both continuous supply of nutrients at the entrance to the lumens and continuous removal of unreacted substrates and metabolic products at the exit from the lumens. Ports giving access to the manifolds enable access to a supply of the growth medium and a route by which the complex broth containing reaction products and unused substrates may exit for subsequent downstream processing. Ports connecting to the intra-annular region permit inoculation of the solution of growth medium contained in this region when startup takes place and removal of the biomass product when desired. In this manner one can confine the cells in an untethered form (as opposed to immobilization of cells via chemical binding) while meeting the metabolic demands of the cells. Physical confinement rather than chemical attachment leaves the cells in a state that more closely resembles the “natural” environment in which the cells can grow and produce the desired metabolic products. Membrane separation units in perfusion systems may utilize several of the geometric configurations commonly employed for commercial ultrafiltration membranes: hollow fibers, flat sheets, spiral-wound modules, and large-diameter tubes. The effluent from the bioreactor may be subjected to one or more bioseparation processes that lead to recovery and purification of desired product(s) from

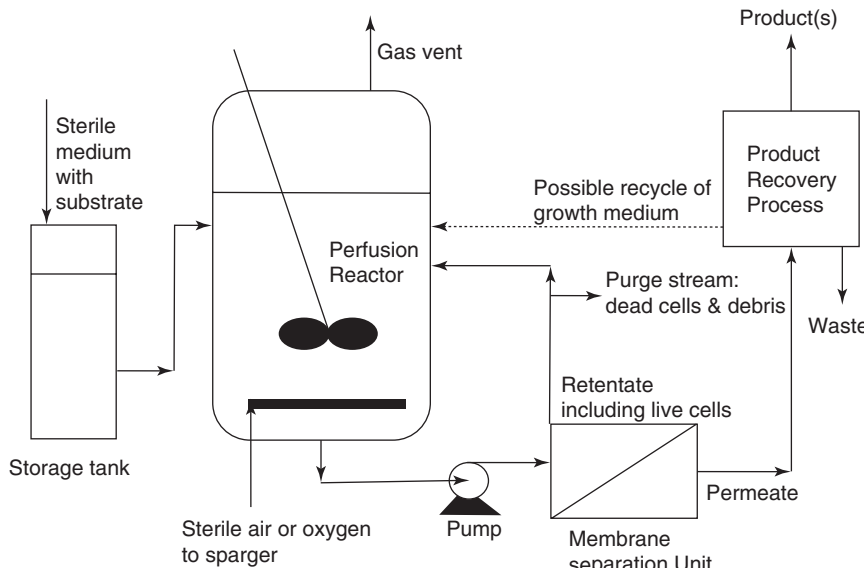


**Figure 13.11** Schematic representation of generic perfusion bioreactor.

an effluent stream containing spent medium, unreacted substrate, metabolic waste products from maintenance metabolism and other biochemical reactions, dead cells, and cellular debris.

Operation in a perfusion mode differs from fed batch operation in that the former not only involves a continuous supply of fresh substrate in the feed stream, but also continuous removal of soluble metabolic products and waste components present in the process fluid. Such removal minimizes the potential for inhibition of the biochemical reaction by soluble products. Perfusion systems are most frequently employed in the cultivation of mammalian cells (see Section 13.3.2.2). However, readers should note that diffusional or mass transfer limitations on biochemical reactions may be imposed by the use of permselective membranes.

Among the advantages of perfusion reactors (21) are: (1) high volumetric productivity; (2) partial purification of the product by removal of cell debris and inhibitory byproducts, as well as enzymes (released by dead cells) that may destroy desirable products; (3) imposition of limits on the amount of time that metabolic products are exposed to potentially harmful processing conditions; and (4) facilitation of process control via ease of regulation and maintenance of the environments of the cells.

The associated disadvantages include (1) requirements for large quantities of nutrients (growth medium) relative to batch and fed batch modes of operation; (2) high material costs associated with purchase and preparation/sterilization of the growth medium; (3) elevated waste treatment costs; and (4) fouling of the surfaces of permselective membranes or conventional or membrane microfiltration devices, which can lead to marked decreases in the flux of

substrates and reaction products with concomitant losses in productivity.

### 13.3 COMMERCIAL SCALE APPLICATIONS OF BIOREACTORS IN CHEMICAL AND ENVIRONMENTAL ENGINEERING

Currently, several different physical configurations of bioreactors are employed in a variety of modes of operation to culture cells for use in addressing problems ranging from mundane (but nonetheless important) treatment of industrial wastewaters to charismatic biosynthesis of cutting-edge biopharmaceutical products with enormous potential for improving health care. Several other significant applications of the bioreactor component of biotechnology were indicated in the introduction to this chapter. In this section we discuss a limited number of these applications as a vehicle for educating students regarding additional important considerations relevant to designing and operating bioreactor facilities.

Because activated sludge facilities have been utilized successfully for decades in the treatment of industrial wastewaters, and because of the similarity of the analysis of the performance of the constituent bioreactor to that for an individual CSTR operating with partial recycle of cells (see Section 13.2.4), we first consider how to develop steady state models of these bioreactors. We then proceed to matters related to the use of bioreactors for cultivation of animal and plant cells, including information pertinent to their susceptibility to damage in shear fields. We conclude with discussions of aspects of two interesting evolving

subject areas in the area of bioreactor design and operation: photo-bioreactors and single-use (disposable) bioreactors.

### 13.3.1 Bioremediation of Wastewaters: Secondary Treatment with Activated Sludge

Remediation of environmental problems often involves employing microorganisms that consume a wide variety of environmental contaminants as substrates in biochemical reactions that lead to benign products such as  $H_2O$  and  $CO_2$ . These remediation efforts may involve various unit operations in modern sewage treatment plants, applications involving mixed cultures of microorganisms whose composition is tailored to a situation needing remediation, or even *in situ* use of microorganisms in treating contaminated soils. Both anaerobic and aerobic processes are present in the arsenal of tools employed by engineers and scientists in their efforts to resolve problems amenable to attack via biochemical routes.

The bioreactors used in industrial-scale waste treatment activities encompass a wide variety of geometric configurations and sizes. The most common processes incorporate one or more of the following facilities: activated sludge processing, trickling filters, rotating biological contactors, and oxidation ponds. Of these, the activated sludge process involves equipment that is most akin to what a typical engineer would consider to be a bioreactor. In practice, biological processes are often employed as a secondary treatment step in a wastewater processing operation. This treatment follows the primary treatment stages that accomplish removal of coarse solids and suspended materials via screening, filtration, and other physical operations. Adjustments of pH and addition of the nutrients required in the biological treatment step (such as phosphate and ammonium ions) may also occur immediately following the primary stage. Our focus here is on the activated sludge process (23–25).

The various contaminants present in wastewaters and their concentrations depend on the origin and history of the wastewater. There are two major categories of wastewaters: *industrial* and *domestic*, the latter being more commonly referred to as *sewage*. Often, these two types of wastes are merged, as when the industrial wastes are discharged into domestic sewers.

An activated sludge facility typically consists of a containment vessel through which there is a continuous flow of biologically active microorganisms (that ultimately form the sludge) suspended in wastewater followed by a settling tank for recovery and recycle of a portion of the sludge (see Figure 13.12). The recycle stream serves as a vehicle for both continuous inoculation of the liquid in the containment vessel and extension of the mean residence time of the biomass, thereby facilitating adaptation of the

cells to the array of nutrients available in this vessel. The process stream is both well agitated and aerated extensively. Whether the flow through the containment vessel more closely approximates CSTBR or PFBR behavior depends on the flow rate, the extent of turbulence and mixing phenomena, the geometric configuration, and the physical character of the containment vessel, including the effects of any auxiliary equipment contained therein. Removal of contaminants from the aqueous phase occurs via both biochemical oxidation reactions and adsorption on the suspended microorganisms.

The sludge itself may contain a multitude of constituent microorganisms, some of which may be incorporated because of their ability to contribute to the multiple capabilities that are critical for successful treatment of particular wastewaters. The essential goals of the treatment include not only reduction of contaminants to levels that satisfy environmental regulations but also achieve safe sustainable operation that is cost-effective and robust in the face of the variable nature of both the quantity and the composition of the wastewaters. Readers should note that some of the constituent microorganisms in the mixed culture are incorporated because they facilitate flocculation and agglomeration of flocs of microorganisms. In particular, *Zoogloea ramigera* is a bacterium that plays a key role in the formation of the flocs that we refer to as *activated sludge*. This bacterium is important because of its ability to synthesize and secrete a polysaccharide gel. The resulting flocs have very high affinities for attachment of suspended solids. Indeed, a very significant aspect of biodegradation of organic species present in the bioreactor is that attachment of these species to the floc is a precursor to their subsequent biooxidation by the organisms present therein.

At times, floc formation and agglomeration may lead to mass transfer limitations on the rates of the biological oxidation reactions of soluble organic substrates that bring about reductions of the biological and chemical oxygen demand (BOD and COD) of the process stream. Nonetheless, proper floc formation is essential in obtaining efficient operation of the process in the sense that relatively large dense flocs are necessary to obtain the sedimentation rates required in the settling tank. Just as the use of cell separation and recycle as an auxiliary aspect of the operation of a CSTBR leads to improved productivity for this reactor (see Figure 13.9), so does the productivity of an activated sludge bioreactor improve when there is efficient recovery of the biomass entering the settling tank. The rates at which the activated sludge is either recycled to the containment vessel (bioreactor) or deemed present in excess are used in the control strategy for the activated sludge process.

Another factor that is critical in the design, operation, and control of an activated sludge bioreactor is obtaining

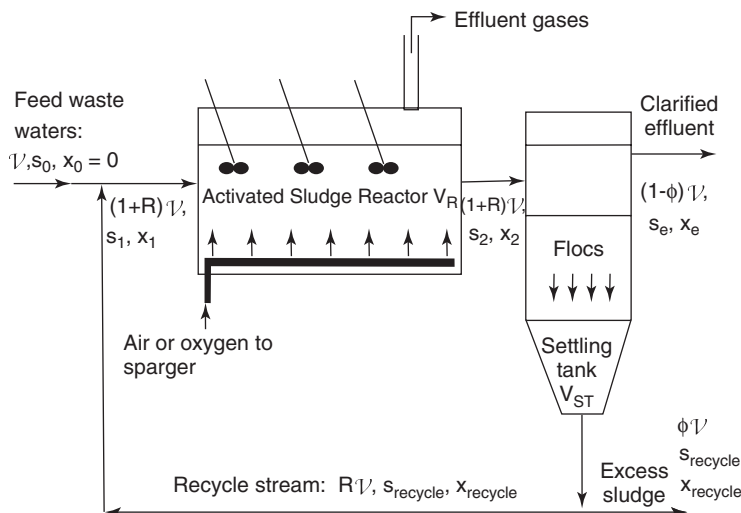


**Figure 13.12** Schematic diagram of activated sludge facility (not to scale) indicating nomenclature employed in our analysis.  $R$  represents the recycle ratio and  $\phi$  is the ratio of the volumetric flow rate of the excess sludge to that of the feed stream.

adequate oxygen content in the aqueous phase. One can employ a variety of aeration devices such as spargers discharging air or oxygen well below the surface of the containment vessel. For shallow activated sludge tanks, surface aerators may also be employed to generate fine sprays of the wastewaters to create high interfacial area between the process liquid and the ambient air. Alternatively, an aerator may consist of a partially submerged impeller that not only creates turbulence to increase the interfacial area between the surface of the wastewater and the ambient air, but also provides mechanical agitation below the surface. This agitation serves both to maintain a well-mixed suspension of the microorganisms and to promote mass transfer of gas between submerged bubbles and what is effectively a suspension of microorganisms in a growth medium.

People who are responsible for the safe and effective operation of waste treatment facilities may be faced with situations in which neither the flow rate nor the composition of the incoming process stream is well controlled. Nature and process upsets may cause uncontrolled disturbances in either the quantity of wastewaters to be processed or their composition. During such periods the effluent from the activated sludge facility may no longer meet process specifications or environmental regulations. Consequently, the flexibility to handle disturbances must be taken into account in the design and operation of an activated sludge facility. An upstream disturbance that produces abnormally high concentrations of solutes that are toxic or deleterious to the microorganisms present in the sludge (thereby markedly reducing its carrying capacity) is referred to as *shock loading*. The slug or spike of toxic solutes that passes through the facility has the greatest potential for causing excursions from normal operation when the flow through the unit resembles plug flow rather than CSTR behavior. Effective mixing of the

toxic constituents with other constituents of the aqueous suspension of microorganisms dilutes the incoming toxins most rapidly when the flow resembles that of a CSTBR. Another approach that can be employed in designing to minimize the potential for process upsets via shock loading is to provide for a number of points along the containment vessel for admittance of fresh feed. This strategy is akin to that employed in cross-flow reactors to enhance reaction selectivity (see the last flow configuration illustrated in Figure 9.2).

Even though the cells present in an activated sludge bioreactor represent a mixture of microorganisms, the analysis of such facilities is normally based on a lumped-parameter approach that simplifies the kinetics of BOD removal. In many respects the resulting analysis resembles that developed in Section 13.2.4, the major difference being the inclusion of a term to account for the kinetics of cell death. For example, in the present analysis, we can express the net rate of cell growth per unit mass of microorganism as

$$\mu_{\text{net}} = \frac{\mu_{\text{max}}s}{K_S + s} - k_d \quad (13.3.1)$$

If we assume that the flow of the suspension through the containment vessel approaches CSTBR behavior and proceed to write the steady-state forms of the material balance equations around this unit (see Figure 13.12), we find that

$$\text{input} + \text{generation by reaction} = \text{output}$$

Biomass

$$x_{\text{recycle}}R'V + \mu_{\text{net}}x_2V_R = x_2(1+R)V \quad (13.3.2)$$

## Substrate

$$s_0\mathcal{V} + s_{\text{recycle}}R\mathcal{V} - \left( \frac{\mu_{\text{max}}s_2}{K_S + s_2} \right) \left( \frac{x_2V_R}{Y_{X/S}} \right) = s_2(1 + R)\mathcal{V} \quad (13.3.3)$$

In equation (13.3.2) we have also assumed that the rate at which biomass enters in the original wastewater is negligible ( $x_0 = 0$ ) compared to the rate at which biomass enters the containment vessel via the recycle stream. Readers should note the presence of different subscripts on the specific growth rate ( $\mu$ ) in equations (13.3.2) and (13.3.3). The subscript “net” implies the presence of a cell death term, whereas the subscript “max” does not. For the substrate, the Monod form of the rate law is appropriate for use.

If we recognize that the mean residence time of the process fluid in the containment vessel is typically much greater than that associated with the settling tank, we can omit the biochemical reaction term in the corresponding material balance equations around the settling tank. We then obtain:

## Biomass

$$x_2(1 + R)\mathcal{V} = x_{\text{recycle}}(R + \phi)\mathcal{V} + x_e(1 - \phi)\mathcal{V} \quad (13.3.4)$$

When there is no fractionation or segregation of the substrate in the settling operation, one can say that  $s_{\text{recycle}} = s_2 = s_e$ , thereby making redundant the corresponding material balance equation around the settling tank for the substrate.

Rearrangement of equation (13.3.4) yields

$$x_2(1 + R)\mathcal{V} - x_{\text{recycle}}R\mathcal{V} = x_e(1 - \phi)\mathcal{V} + x_{\text{recycle}}\phi\mathcal{V} \quad (13.3.5)$$

Combination of equations (13.3.1), (13.3.2), and (13.3.5) and rearrangement yields

$$\frac{\mu_{\text{max}}s_2x_2V_R}{K_S + s_2} = k_dx_2V_R + x_e(1 - \phi)\mathcal{V} + x_{\text{recycle}}\phi\mathcal{V} \quad (13.3.6)$$

or in terms of the specific growth rate ( $\mu_g$ ),

$$\mu_gx_2V_R = k_dx_2V_R + x_e(1 - \phi)\mathcal{V} + x_{\text{recycle}}\phi\mathcal{V} \quad (13.3.7)$$

This relation indicates that the rate at which cells are produced during growth is balanced by the sum of the rates at which cells die (or must address maintenance metabolism effects) and the rates at which cells exit the bioreactor-settler combination in the clarified effluent and the excess sludge.

Introduction of the dilution rate  $D$  gives

$$\mu_gx_2 = k_dx_2 + D[x_e(1 - \phi) + x_{\text{recycle}}\phi] \quad (13.3.8)$$

This equation can also be written in terms of the reactor space time  $\tau$ :

$$\tau = \frac{V_R}{\mathcal{V}} = \frac{x_e(1 - \phi) + x_{\text{recycle}}\phi}{(\mu_g - k_d)x_2} \quad (13.3.9)$$

This expression for the reactor space time is equivalent to the mean residence time of the aqueous phase (growth medium) in the bioreactor if no significant volumetric expansion or contraction effects accompany the biochemical reaction. Moreover, solution of (13.3.8) for  $x_2$  gives

$$x_2 = \frac{Dx_e}{\mu_g - k_d} \left[ 1 + \left( \frac{x_{\text{recycle}}}{x_e} - 1 \right) \phi \right] \quad (13.3.10)$$

By appropriate manipulation of equations (13.3.1) to (13.3.10), one can obtain relations that provide additional perspectives on the design and operation of an activated sludge/settler facility. Consider an alternative form of equation (13.3.7):

$$\frac{1}{\mu_{\text{net}}} = \frac{1}{\mu_g - k_d} = \hat{t}_{\text{cells}} = \frac{x_2V_R}{\mathcal{V}[x_e(1 - \phi) + x_{\text{recycle}}\phi]} \quad (13.3.11)$$

We may identify the reciprocal of  $\mu_{\text{net}}$  with the mean residence time of the cells in the bioreactor because the numerator of the extreme right side is equal to the total amount of biomass in the bioreactor at steady state and the denominator reflects the total mass flow rate at which the cells exit the bioreactor-settler combination. Sometimes this mean residence time is referred to as the *age of the sludge*, typically somewhere between a few days and two weeks.

If there is no fractionation of substrate in the settling tank,  $s_2 = s_{\text{recycle}} = s_e$ , and equation (13.3.3) becomes

$$(s_0 - s_2)\mathcal{V} = \left( \frac{\mu_{\text{max}}s_2}{K_S + s_2} \right) \left( \frac{x_2V_R}{Y_{X/S}} \right) = \frac{\mu_gx_2V_R}{Y_{X/S}} \quad (13.3.12)$$

The first term on the right can be recognized as the Monod form of the specific growth rate ( $\mu$ ). One can rearrange equation (13.3.12) to obtain an estimate of the volume of bioreactor necessary to bring about a reduction in the concentration of the limiting substrate (e.g., BOD) from  $s_0$  to  $s_2$ .

$$V_R = \frac{Y_{X/S}(s_0 - s_2)\mathcal{V}}{\mu_gx_2} \quad (13.3.13)$$

Combination of equations (13.3.11) and (13.3.13) gives

$$V_R = \frac{Y_{X/S}(s_0 - s_2)\mathcal{V}\hat{t}_{\text{cells}}}{(1 + k_d\hat{t}_{\text{cells}})x_2} \quad (13.3.14)$$

It is also possible to express the requisite reactor volume in terms of the recycle ratio by combining equations (13.3.5)

and (13.3.11):

$$\begin{aligned} V_R &= \mathcal{V} \hat{t}_{\text{cells}} \left[ (1 + R) - \frac{x_{\text{recycle}}}{x_2} R \right] \\ &= \mathcal{V} \hat{t}_{\text{cells}} \left[ 1 + R \left( 1 - \frac{x_{\text{recycle}}}{x_2} \right) \right] \end{aligned} \quad (13.3.15)$$

Except for the presence of the cell death/maintenance metabolism term in the present analysis and the need to identify the factor  $\Psi$  in Figure 13.8 with the ratio of the concentrations in equation (13.3.15), the analysis above gives results similar to those for a chemostat operating in a biomass recycle mode.

When one considers the relative simplicity of the design analysis above with the complicated nature of the physical and biological processes involved in the operation of an activated sludge facility, it is remarkable that equations (13.3.1) to (13.3.14) provide a reasonable description of the steady-state behavior of the concentrations of the limiting substrate and the lumped microorganisms when one has access to the corresponding kinetic parameters ( $\mu_{\max}$ ,  $K_S$ ,  $k_d$ , and  $Y_{X/S}$ ) obtained using a chemostat to study the mixed culture. However, the situation is quite different when one attempts to model the transient behavior of the facility in response to variations in species concentrations or flow rates. Every day, functioning activated sludge facilities are subjected to process disturbances that require operators to exercise a control strategy to return to conditions that give satisfactory performance. Much more complex models are required to obtain descriptions of the dynamics of an activated sludge facility that are adequate for purposes of process control.

The extended discussion and analysis of activated sludge bioreactors that we have presented here is *not* intended to convey the impression that these bioreactors are the sole form of bioreactor employed in processing industrial wastewaters. Readers should note that Lin et al. (26) published a comprehensive critical review of the literature concerning applications of several types of membrane bioreactors in treatment of a wide variety of industrial and agricultural wastewaters. Activated sludge bioreactors are a long established form of biotechnology that is widely used, but multiple types of bioreactors find applications in treating wastewaters from the following industries: food processing, pulp and paper, textile, pharmaceutical, and petroleum and petrochemical, to name just a few.

### 13.3.2 Culture of Animal Cells

Three major categories of commercially valuable products highlight the technical evolution of animal cell culture: viral vaccines, recombinant glycosylated proteins, and monoclonal antibodies. Historical and general background information concerning these technologies are presented

below. Subsequent sections deal with important aspects of the culture of mammalian cells and human stem cells.

Deliberate culture of animal cells originated in the late nineteenth century when embryonic chick cells were maintained in saline solution. However, it was not until the 1940s and 1950s that demand for efficacious viral vaccines to combat major epidemics of poliomyelitis provided a compelling incentive for large-scale culture of animal cells. Enders et al. (27) demonstrated in 1949 that the polio virus could be grown in cultures of human embryonic cells. Their research paved the way for development of a vaccine based on the deactivation of polio virus. This vaccine was one of the first commercial products based on animal cell culture technology. Since the 1950s, large numbers of human and veterinary vaccines based on commercial-scale culture of animal cells have been approved by regulatory authorities.

In the 1970s major advances were made in animal cell biotechnology with developments in *recombinant deoxyribonucleic acid* (rDNA) techniques. The term *recombinant DNA* refers to the molecular-scale process of taking a piece from one of the DNA molecules that form a “double-stranded helix” and combining it with one or more such snippets from other DNA molecules to form a new strand of DNA. The most common recombinant process involves combining segments of DNA from two different organisms. Originally, this technology was employed for expression of mammalian genes in bacteria, especially *Escherichia coli*. To this day, this technology remains an important component of the bioengineer’s tool kit.

Naturally occurring bacteria do not contain the metabolic machinery necessary to bring about genuine humanization of the proteins synthesized by these bacteria. Complete humanization would require manufacture of additional and/or alternative *glycosylated structures* to reproduce the bioactivity, antigenicity, pharmacokinetics, and other aspects of the therapeutic activity profile of the corresponding genuine human protein as it exists *in vivo*. Consequently, genetically engineered mammalian cells have been developed with the glycosylation machinery necessary to approximate the characteristics and behavior of the corresponding human proteins for medically (and commercially) important therapeutic proteins such as tissue plasminogen activator, erythropoietin, and clotting factor VIII. Genetic engineering technology has also been utilized to develop similar protein glycosylation capabilities in insect and plant cells.

The development of cell fusion technology in the 1960s and 1970s is a third significant enabling technique in the commercial evolution of animal cell biotechnology. Kohler and Milstein (28) produced *hybridoma cells* that are capable of continuous production of a single type of antigen. These monoclonal antibodies are medically important as

both diagnostic and therapeutic agents because of their ability to bind specific antigens selectively.

The growth cycle for mammalian cells very closely resembles that of microbes. However, bioreactors for the culture of animal cells differ in several important respects from those employed in the culture of microorganisms, as well as from traditional fermentation equipment. These differences have their genesis in the nature of the “walls” that encapsulate the mammalian cells, especially the responses of these walls to shear stresses during culture. Indeed, some have suggested that because these walls are so thin relative to those of the bacteria and yeasts traditionally used in fermentation, it would be more appropriate to label the structure that differentiates the animal cell from its environment as a membrane rather than a cell wall.

It was not until well into the twentieth century that the culture of animal cells had evolved sufficiently to be employed in industrial practice. Nonetheless, between 1990 and 2010, significant innovations in this biotechnology led to its adoption in a large variety of medical applications, both human and veterinary. Existing and potential uses for animal cells as biocatalysts for the production of a long list of medicinal proteins reflect the important charismatic role that this biotechnology is playing in the evolution of cutting-edge medicine. Products generated or processed using animal cell cultures include important high molecular weight therapeutic proteins, monoclonal and polyclonal antibodies, and viral vaccines for prevention of disease. For example, the Salk polio vaccine (*inactivated poliovirus vaccine*) is based on three reference strains of virus grown in a type of monkey kidney tissue culture. The viruses are then inactivated using formalin (an aqueous solution of formaldehyde). Other evolving applications include regenerative medicine in which bone marrow cells and stem cells are of interest, as well as the generation of functional tissues for transplantation. The responses of animal cell cultures to pharmaceutical products, cosmetics, household products such as detergents and other cleaning agents, and so on, permit manufacturers to address some aspects of product toxicity and carcinogenicity using *in vitro* tests rather than using whole-animal trials prior to tests on humans.

Warnock and Al-Rubeai (29) have reviewed bioreactor systems for the production of biopharmaceuticals via culture of animal cells. They describe the advantages and disadvantages of several types of bioreactors and the huge expansion of commercial-scale culture facilities in the early 2000s. Early bioreactor designs for culture of animal cells focused on anchorage-dependent cell lines (see below), but in many cases these bioreactors may also be adapted for the culture of suspended cells.

To initiate the culture of animal cells, very small pieces of tissue (ca. 1 or 2 mm<sup>3</sup>) are excised and transferred to a growth medium using aseptic techniques. These cells form

*a primary culture*. Primary mammalian cells often grow in the form of monolayers on solid surfaces such as the glass or polymeric surface of the containment vessel or bioreactor. These bioreactors may be small flasks, roller bottles, or flat plates. Cells growing on solid surfaces are referred to as *anchorage-dependent cells*. Surface attachment is necessary to establish a foundation that serves to align internal structures of the cell in a configuration that permits subsequent three-dimensional growth. The attached or anchored cells grow to form a monolayer on the surface of the original bioreactor. A sequence of several wet chemistry manipulations under aseptic conditions then serves to remove the adherent cells from the surface of the containment vessel to produce a suspension of cells in a growth medium for additional culture and further growth.

Cells taken from the primary culture and used to inoculate a growth medium form what is referred to as a *secondary culture*. Many secondary cell lines are capable of being adapted to growth in suspension and in this adaptation can be viewed as *non-anchorage-dependent*. Readers should recognize that some animal cells can be grown directly in suspension culture following excision from animal tissue. These cells are also known as non-anchorage-dependent cells. One way of generating large surface areas to which the animal cells may attach is to employ microcarriers, which may, in turn, be suspended in a growth medium. (We have elected not to include a discussion of immobilization of cells in our treatment of bioreactors in order to provide a balanced presentation of the chemical, biological, and engineering aspects of chemical engineering kinetics and reactor design. There is an abundant literature concerning immobilized cell technology and its practical applications.)

When only small quantities of product are required, scale-up of production via roller bottles in a laboratory robot assisted facility may be feasible, but this approach is susceptible to contamination. Moreover, ensuring uniform environmental conditions throughout a multitude of bottles is not a trivial task. Control of a small stirred tank bioreactor is more readily accomplished. The kinetics of product formation in animal cells can often be represented in terms of the Luedeking–Piret model (see Section 13.1.5).

To circumvent mass transfer limitations, shear sensitivity, and equipment footprint problems associated with the scale-up of processes involving anchorage-dependent cells, one may resort to use of cell lines that have been adapted for growth in suspension culture. In such cases, stirred-tank reactors akin to those used in the culture of microorganisms can be employed first in batch and subsequently in fed batch culture of animal cells. Warnock and Al-Rubeai (29) provide useful discussions of the relative merits of stirred tanks and several other reactor configurations and modes of operation that have been used in the manufacture of biopharmaceuticals. During the past half-century, especially in

the past decade, use of stirred-tank reactors in a fed batch mode has become quite common in the biopharmaceutical industry. Stirred-tank reactors are widely utilized because they have a long history of successful applications in culture of both microorganisms and animal cells and because of their ease of operation. Single-use disposable reactors are also generating wide interest for manufacture of biopharmaceuticals.

In the remainder of this section we treat several important aspects of animal cell culture, beginning with a discussion of the significance of mixing and shear stress phenomena in the culture of animal cells. Subsequent sections treat fundamental aspects of the culture of mammalian cells and human stem cells.

### 13.3.2.1 Mixing and Shear Stress Considerations

The solids suspended in the growth medium in a bioreactor vary substantially in size. Microorganisms such as single-cell bacteria and yeast typically have characteristic dimensions in the range 1 to 10  $\mu\text{m}$  and are not very sensitive to damage by shear forces, but for animal cells the characteristic dimension is 20  $\mu\text{m}$ . Plant cells have a characteristic dimension of 100  $\mu\text{m}$ , and aggregates of these cells may have dimensions as large as 1 to 2 cm. Relative to microorganisms, both animal and plant cells are highly susceptible to damage when exposed to shear forces. Cells typically contain a high percentage of water, and in aqueous suspensions the difference in density between the cells and the aqueous growth medium is sufficiently small that it is relatively easy to maintain dilute suspensions of cells for long periods using mechanical stirrers or spargers that inject bubbles of gas into a bioreactor or fermenter. For concentrated suspensions, especially those that have apparent viscosities greater than that of pure water, one of the primary functions of the mixing equipment in a bioreactor is to maintain the cells in a uniform suspension. Accumulation of cells at the bottom of the vessel or in stagnant regions that are not subjected to regular sweeping by the circulation of the fluid in the tank is highly undesirable. Such conditions facilitate agglomeration of cells and deny access of nutrients and oxygen to cells positioned underneath other cells, thereby imposing mass transfer limitations on the growth of these cells, starving them of the nutrients and substrate(s) necessary to manufacture biomass.

Both macroscopic and microscopic phenomena are involved in the use of mechanical devices to achieve homogeneity within bioreactors. The agitation device must provide good circulation of the bulk fluid throughout the vessel to minimize the effects of stagnant zones. In addition, micromixing at or near the molecular level is essential to ensure appropriate access of the cells to nutrients. Often, the limiting factor in achieving a homogeneous suspension

is macromixing of the fluid contents. Tracer studies of the type discussed in Chapter 11 can be utilized to determine how effectively the mixing system is operating with respect to what would be expected for an ideal CSTBR. Empirical correlations and the techniques of fluid mechanics may be employed for estimating the effects of process scale-up on mixing phenomena (30, 31).

The domain of fluid mechanics encompasses issues concerning the development of shear stresses in fluids in the presence of velocity gradients. In turbulent flow these stresses are significantly greater than those encountered in laminar flow. The unsteady velocity components associated with turbulent eddies lead to fluctuating shear stresses that are superimposed on the main flow pattern. For turbulent flow there are considerable variations in shear stress as time evolves and as one moves from one location to another in an agitated bioreactor. In an aqueous growth medium, these stresses act to break up and disperse gas bubbles and/or flocs of cells. The turbulent velocity fluctuations of the moving fluid cause deformation of gas bubbles such that surface tension forces are no longer able to maintain a quasi-spherical shape. The bubbles stretch and deform to the extent that individual bubbles may divide into smaller bubbles. Collisions of bubbles induced by the fluid flow may also lead to coalescence of bubbles to form fewer larger bubbles. Eventually, one achieves a balance of the various forces involved to obtain a distribution of bubble sizes that reflects the various interactions. For suspended solids, if the stresses induced by the flow exceed the mechanical strength of the cells or aggregates, they break up, causing dispersion of aggregates and possibly cell death.

While decreases in bubble size are desirable to facilitate mass transfer of oxygen to cells, disruption of individual cells and cell death are counterproductive. During normal operation of a bioreactor, different types of cells are characterized by differences in their susceptibility to a variety of degradation processes, including cell death. Collectively, these processes define the phenomenon known as *shear sensitivity*, regardless of whether or not the damage originates as a consequence of exposure to fluid velocity gradients. For yeast and bacteria, the characteristic dimensions of individual cells are sufficiently small that these microorganisms are relatively insensitive to the hydrodynamic forces to which they are subjected when agitated. Their size is typically smaller than the characteristic dimensions of eddies resulting from mechanical mixing phenomena. Yeast and bacteria cells are readily entrained within turbulent eddies and follow the laminar stream lines within an individual eddy. This situation, coupled with the minimal difference in density between the organism and the suspending fluid, means that there is very little relative motion between the organism and the local suspending fluid. The

attendant shear stresses are then insufficient to cause damage to these cells.

By contrast to the situation for yeast and bacteria, much of the relevant literature indicates that mammalian, insect, and plant cells are particularly sensitive to damage by hydrodynamic shear forces (32–34). Animal and plant cells are considerably larger than yeast and bacterial cells. They can easily be larger than the size of an eddy and may thus be subjected to the influence of velocity gradients that are sufficiently large to cause damage to these cells.

Characteristic sizes of eddies can be measured in terms of the Kolmogorov scale (35). The Kolmogorov number,  $\lambda$ , is given by

$$\lambda = \left( \frac{\nu^3}{\epsilon} \right)^{1/4} \quad (13.3.16)$$

where  $\nu$  is the kinematic viscosity and where  $\epsilon$  is the rate of dissipation of turbulence kinetic energy per unit mass of fluid. As the viscosity of the suspension increases, so does the size of the smallest eddy. Hence, one expects reductions in cell damage when the viscosity of the growth medium is increased, as is observed experimentally. Similar considerations of the effect expected when adding thickening agents (viscosity enhancers) to the growth medium are confirmed by corresponding experimental data. Croughan et al. (36) reported that moderate increases in the viscosity of a suspension of cells were reflected in significant reductions in cell mortality.

The relevant literature stresses the necessity of taking the shear sensitivity of plant and animal cells into account in the design and operation of bioreactors for the culture of these cells (37, 38). Nonetheless, one must still provide sufficient mixing to avoid mass transfer limitations on substrate utilization and also to ensure that adequate supplies of dissolved oxygen are present. In this context, one must recognize not only that shear phenomena can lead to cell damage and death but also to such less obvious effects as declines in the rates of cell growth and product synthesis, dehydration of extracellular proteins, and thickening of cell walls in response to the stimulus of shear forces.

Doran (39) has presented a summary of phenomena to which investigators have attributed cell damage in bioreactors:

1. Interactions between cells and turbulent eddies
2. Collisions of cells with one another, with mixing impellers, or with stationary surfaces in the reaction vessel
3. Interactions between cells and shear forces in the boundary layers and wakes near solid objects in the bioreactor, especially impellers
4. Interactions between cells and the mechanical forces associated with gas bubble formation at the sparger and with bubble rise phenomena

## 5. Interactions between cells and gas bubbles bursting at the upper surface of the liquid phase.

Substantial forces and very high levels of energy dissipation are associated with the rupture of bubbles as the liquid film surrounding a rising bubble breaks and drains into the liquid below. This problem is often exacerbated in many animal cell cultures because of attachment of cells to rising bubbles. If these cells are retained in the thin film of liquid at the top of the rising bubble, they are subjected to the most severe stresses at the moment the bubble bursts. As the film drains back into the bulk fluid, the cells are again subjected to severe stresses associated with the high velocities at which the liquid drains, leading to concomitant damage to the cells. In some situations it is possible to mitigate the damaging effects of shear on animal cells by adding a protective surfactant such as Pluronic F68 (a copolymer of propylene and ethylene oxides) to the aqueous phase to alter the interfacial tension and the rate at which liquid drains back into the bulk liquid. In addition, the presence of the surfactant has been observed to reduce the probability for physical attachment of cells to a rising bubble. In media containing Pluronic F68, the surfactant causes a stable foam to form. Concentration dependent reductions in cell damage are then observed. Because participation of the cells in disengagement of gas bubbles from the liquid medium is reduced in the presence of Pluronic F68, the decrease observed in cell damage is attributed to the associated reduced exposure of the cells to the turbulence and high shear forces associated with disengagement of the bubbles at the liquid surface (34).

In a review of reactor engineering for the large-scale culture of animal cells, Nienow (40) indicated that for free suspension culture in the large agitated bioreactors ( $> 10,000$  L) used widely by industry, problems of shear sensitivity associated with agitation and bursting bubbles are no longer regarded as major problems. However, he also indicated that in large-scale bioreactors, problems of heterogeneity of pH and nutrients remain significant issues. Submerged culture remains the option of choice for culture of animal cells despite clean-in-place concerns.

Definitive data regarding mixing and shear sensitivity in industrial-scale systems are sparse for both cells in free suspension and cells immobilized on microcarriers. Practicing engineers and scientists lack a complete understanding of these aspects of bioreactor design and operation. Consequently, in bioreactor design these persons are forced to rely as much on their previous experience and heuristic principles of problem solving or “rules of thumb” as they are on a basic knowledge of the interactions of hydrodynamic phenomena and the mechanical properties of living materials. Those readers interested in learning more about mixing in bioreactors and cell damage in bioreactors are referred to discussions of this topic in publications by Nienow (40),

Harnby et al. (41), Chalmers (42), Wu (43), and Papoutsakis (44).

### 13.3.2.2 Culture of Mammalian Cells

Successful cultivation of mammalian cells requires a comprehensive understanding of biological, biochemical, and engineering fundamentals and their applications to develop the equipment and operating protocols that will form the foundation for a successful process that will satisfy industry and government requirements for human health and safety. Mammalian cell culture employs cells that have their genesis in mammalian tissues but are subjected to further cultivation and controlled reproduction in an artificial medium under *in vitro* conditions to propagate a cell line. Because animal cells are large (10 to 20  $\mu\text{m}$  in diameter) and exhibit a high degree of shear sensitivity, culture of these cells should involve gentle aeration and mild agitation. Shear sensitivity is strain-dependent, as is whether or not the cells are anchorage-dependent. Hence, design of bioreactors for culture of animal cells requires careful consideration of the properties of the particular cell line to be cultured.

In general, the primary advantage of cultivation of cells lies in the improved consistency and reproducibility of results obtained using a batch of cells of a single type, preferably from a homogeneous population (*clones*) (45). The consistency of the results obtained using animal cell cultures contrasts with those obtained using homogenates of animal tissue that contain a heterogeneous mixture of cells at different stages of growth or viability or from different locations in an organ or tissue (45). Disadvantages include problems with the differences in cell population distributions over time because the cells that grow the fastest will come to dominate the population that evolves in a culture containing a mixed population of cell types.

One of the most important advantages of mammalian cells for production of recombinant biologicals is their ability to perform post-translational modifications of the preliminary protein structures to obtain glycosylated forms that closely resemble those produced *in vivo*. For human and veterinary therapeutic applications, glycosylation using mammalian cells is more likely than use of other cell types to yield better matches to the bioactivity, antigenicity, pharmacokinetic, and other properties of the corresponding genuine animal proteins *in vivo*.

The mammalian cell lines most commonly employed for production of recombinant proteins are the Chinese hamster ovary and baby hamster kidney cells. These cell lines are used in both anchorage-dependent and suspension forms for the production of proteins whose glycoforms are very similar to the native human forms of the corresponding proteins (46). Protein post-translational modifications increase the functional diversity of the

proteins that constitute the proteome. These modifications in the chemical structure of proteins occur by covalent addition of functional groups or proteins, proteolytic cleavage of regulatory subunits, or degradation of entire proteins. These modifications include reactions leading to glycosylation, phosphorylation, nitrosylation, methylation, acetylation, lipidation, and proteolysis. The resulting modified proteins influence almost all aspects of normal cell biology and pathogenesis. Consequently, modified recombinant proteins are subjected to post-translational modifications to achieve desired biological activities that are important in human (and veterinary) therapeutic and preventive vaccine applications. The modified proteins regulate activity, localization, and interactions with other cellular molecules, such as proteins, nucleic acids, lipids, and cofactors. In addition, these proteins help in using identical proteins for different cellular functions in different types of cells.

The major source of failure associated with the culture of mammalian cells (indeed, any type of cell) is the problem of contamination by microorganisms, especially the bacteria that are always present to some degree in virtually every laboratory and manufacturing environment. Animal cell cultures are susceptible to being overwhelmed by bacteria because of the substantial difference in the doubling times typically associated with animal cells (ca. 24 h) and bacteria (ca. 30 min) (47). Over the course of a day the number of animal cells present in a culture will merely double, whereas the number of bacteria will increase by a factor in excess of  $10^{14}$ . When one fails to maintain aseptic conditions, the explosion in the growth of the cell population is clearly centered in the bacteria.

Although originally developed to improve the productivity of cultivation of microbes in batch reactors, the fed batch mode of operation has been widely employed in cultivation of mammalian cells. Several types of bioreactors and modes of operation can be employed for the production of biologic materials, but fed batch operation of stirred tanks has become the primary approach used in large scale facilities for the production of biopharmaceuticals and other biologics. The rationale for early adoption of fed batch culture of animal cells was that adding nutrients to a batch culture increases the amount of product that one can harvest. Operation of a batch reactor in a *perfusion mode*, in which the harvest of products occurs concurrently with an extended supply of nutrients, brings some of the same advantages of fed batch operation, but Whitford (48) indicates that advances in available cell lines and growth media have dramatically increased per cell yields in fed batch operation to offset some early perceptions of the benefits of a perfusion approach. In particular, the resulting concentrations of viable cells and the corresponding high volumetric productivity support use of fed batch operation

for large scale culture of animal cells. Fed batch operation involves lower direct costs than batch or perfusion operation because it leads to less consumption of growth medium, reduced generation of waste, and requirements for fewer personnel for overall conduct of the process. Moreover, preliminary results are obtained quickly and cheaply during fed batch operation. Whitford has also indicated that the following practical considerations favor fed batch operation over perfusion operation: reliability; ease of process characterization, validation, and control; consistency of lot quality; range of application; simplicity of design and operation that lend themselves to flexibility with respect to changing products and cell lines within a given facility; shorter turnaround times for shifts in products between manufacturing campaigns; ease of scalability; greater compatibility with respect to emerging technologies such as single use and disposable reactors and downstream separation facilities; support of alterations in both absolute and relative values of nutrient levels, including provisions for metered feeding of concentration sensitive nutrients; and better suited for production of secondary metabolites, including non-growth-associated products such as recombinant products.

Whitford (48) provides much more information that is of interest to chemical engineers involved in the design and operation of fed batch processes for culture of animal cells. Shukla and Thömmes (49) discussed additional aspects of fed batch culture of mammalian cells for large scale production of monoclonal antibodies and related proteins. Further information concerning the use of bioreactors for culture of mammalian cells is contained in the article Mammalian Cell Bioreactors by Zhou and co-workers in the *Encyclopedia of Industrial Biotechnology* (50).

In vitro fabrication of three-dimensional mammalian tissues for therapeutic and artificial internal organs remains an extraordinary challenge for research teams working on tissue growth. A variety of unusual bioreactor configurations have been explored in order to accommodate requirements for nutrient supply and removal of the waste products of cell growth. In many designs, oxygen supply is one of the most important factors limiting tissue growth. To develop the tissue thicknesses required for human applications, diffusive transport of oxygen and other nutrients must be accomplished at rates that balance the rate of the ongoing metabolic processes that produce the mammalian cells that grow on the scaffolds with which they are provided. In addition to mass transfer constraints, researchers in this area face a major challenge in the necessity of growing cells to high densities. Martin and Vermette (51) described multiple aspects of bioreactor design and operation for culture of tissue masses. Their review indicates the very formidable obstacles that need to be overcome if commercially viable products are ever to emerge from research efforts in this area. Additional

information concerning use of bioreactors for tissue culture is contained in the volume edited by Eibl et al. (52).

### 13.3.2.3 Culture of Human Stem Cells

*Stem cells* differ from other types of cells in two crucial aspects:

1. Stem cells are undifferentiated cells found in all multicellular organisms; stem cells are capable of renewing themselves indefinitely via *mitosis* (cell division), sometimes after extended periods of inactivity. As long as the animal in which the stem cells are present is living, stem cells can divide essentially without limit to repair or replenish other types of cells and rehabilitate the necessary functionality of the organ or tissue in which the stem cells are present.
2. Under appropriate (micro-) environmental conditions, stem cells can be manipulated using wet chemistry to become cells with the functional attributes associated with particular organs, tissues, or types (e.g., brain cells, muscle cells, or red blood cells). Stem cells in some locations (e.g., those in the bone marrow) regularly divide to replace or repair damaged or diseased cells; however, stem cells in other locations (such as the heart or pancreas) can divide only under very specific conditions.

Given their unique regenerative capabilities, stem cells offer possibilities for new therapeutic approaches to several severely debilitating diseases, such as cardiovascular diseases, Parkinson's, and diabetes. However, much remains to be learned and developed on laboratory and clinical scales before these approaches can evolve to the point where they can be regarded as efficacious therapeutic protocols. This promising new field of medicine is sometimes referred to as *regenerative or reparative medicine*. Research involving studies of stem cells also contributes more generally to our knowledge about how a living organism develops from a single cell to an adult mammal, how healthy cells replace damaged or diseased cells in adults, how new pharmaceuticals or biopharmaceuticals interact with mammalian cells during drug-screening tests and clinical trials, and the potential implications of these interactions with respect to identification of the cause(s) of birth defects.

In 1981, scientists discovered how to derive embryonic stem cells from early-stage mouse embryos. Subsequent studies of these stem cells and the biology of mice led to the 1998 discovery of a method for obtaining stem cells from human embryos and the technology for growing these cells in the laboratory. The embryos used in these studies were created during the course of in vitro fertilization studies and were donated with informed consent by the patients involved when the embryos were no longer

needed for reproductive purposes. These types of stem cells are referred to as *human embryonic stem cells*. These cells are derived from the inner cell mass of 5-day-old embryos during what is known as the *blastocyst* stage of development. In a developing embryo, the stem cells can self-differentiate into all of the specialized forms found in adult animals. These stem cells are *pluripotent*. The adjective *pluripotent* is used to describe stem cells that have the potential to differentiate into more than a single type of cell. Indeed, they can differentiate into any type of cell except for extra-embryonic (placenta) tissue. Other types of stem cells may be referred to as *totipotent*. Pluripotent stem cells are derived from totipotent stem cells. Nonembryonic stem cells are referred to as *somatic* or *adult stem cells*. Adult stem cells are found in diverse tissues and organs of the body of an animal. In 2006, researchers made another important breakthrough in stem cell technology with the discovery of conditions that permit some specialized adult human cells to be “reprogrammed/repurposed” genetically so that they can assume a state akin to that of stem cells. These types of cells are referred to as *induced pluripotent stem cells* (iPSCs). These cells are not identical with *adult stem cells* but, rather, with adult cells (e.g., epithelial cells) that have been genetically reprogrammed using protein transcription factors that give rise to pluripotent capabilities. With these capabilities, the iPSCs exhibit functionalities that are essentially equivalent to those of embryonic stem cells.

In mid-2012, Hambor (53) reviewed future prospects in the areas of bioreactor design and control for industrial stem cell production processes. Much of the discussion that follows has its roots in his review. Hambor pointed out that for many of the then-developing cell therapies, clinical trials indicated that the efficacy of the therapy was related to the cell dose utilized, thereby highlighting the need to employ sufficiently large numbers of cells to achieve the desired therapeutic effect. However, for many of the evolving medical protocols, the number of cells necessary to produce such results greatly exceeds the number of cells available from donors for either autologous (harvested from the patient, multiplied/expanded, and subsequently returned to the same patient) or allogeneic (obtained originally from genetically matched donors) transplants of stem cells. The magnitude of typical insufficiencies and the critical nature of the disease conditions for which remedies are sought emphasizes the necessity of developing cell-based protocols for treatment of various forms of cancer and other devastating diseases.

Consequently, bioreactors must be employed as vehicles for creating and maintaining controlled physicochemical environments in which stem cells can be multiplied to obtain the number of cells necessary for cell therapies. This multiplication should occur in an automated, standardized,

cost-effective manner that satisfies current good manufacturing practice (cGMP), U.S. Food and Drug Administration (FDA), and other regulatory requirements for clinical applications and that can be readily validated. Operation of the reactor should be sustainable despite the variability of cells from different donors and must have safety procedures in place for rectification and revalidation of the process in the event of microbial contamination or discovery of potential tumorigenic effects of fast-growing cells.

Most large-scale facilities for stem cell culture and FDA-approved biopharmaceutical processes employ agitated tank bioreactors in large measure because the vast amount of experience accumulated with these types of reactors in culturing microorganisms and other types of cells facilitates the transition to culture of stem cells. In addition, agitation by mechanical or magnetic stirrers or by sparging with air or oxygen serves to eliminate gradients in composition within the suspension. Such bioreactors typically permit noninvasive sampling and control of temperature, dissolved oxygen, and pH. They offer flexibility of operation, so they can be operated in batch, fed batch, or perfusion modes. Commercial scale stirred or agitated tanks are available from multiple vendors in presterilized, preassembled, single-use formats (see Section 13.3.5), with several options for sources of agitation.

Combination of agitated culture vessels with three-dimensional strategies for cell growth has led to significant advances in stem cell bioprocessing by enhancing yields obtained in efforts to expand cell numbers, improving efficiencies for cell differentiation, and enhancing cell functionality (53). The three-dimensional culture mode more nearly resembles the *in vivo* situation than do methods of culture intended to create suspensions of cells that are uniform in distribution and composition throughout. This three-dimensional mode of culture may involve an approach based on creating aggregates of stem cells or cultivation of these cells in or on microcarriers. (Microcarriers can function as support matrices for attachment and growth of anchorage-dependent cells so as to enable quasi suspension culture.)

Numerous designs have been proposed for bioreactors intended for use in the culture and differentiation of stem cells in their various manifestations, but few bioreactors that are appropriate in all respects for industrial or clinical use are yet available commercially. This situation reflects the fact that each disease or condition presents its own problems with respect to formulation and development of treatment protocols for cell therapy. Efficacious cell products must be developed for each therapeutic intervention while developing protocols in situations where it is not clear initially which form of cell structure will be most effective (e.g., undifferentiated stem cells, partially differentiated intermediate cells, lineage-committed progeny, tissue-specific mature cells, or even three-dimensional

tissue structures). When generating specific types of stem cells for particular therapeutic applications, one must ensure that their future is precisely controlled in the sense that the yield of the target-specialized cell is both high and reproducible, as well as that the purity of the progeny is high. Immense challenges exist as scientists, medical practitioners, and engineers work together in interdisciplinary efforts to address these matters, but the evolution of knowledge in this area holds great promise for future success. The literature describing interdisciplinary research on the use of bioreactors for expansion and controlled differentiation of stem cells and their progeny to meet clinical demands is copious, but here we cite only three representative examples (54–56).

### 13.3.3 Culture of Plant Cells and Tissues

#### 13.3.3.0 Preliminary Considerations

Plants are a vital source of an amazing array of raw materials that are used in producing life-enriching substances: foods and beverages, construction materials, clothing, energy, pharmaceuticals, pesticides, natural rubber, and other invaluable products. However, only a relatively small number of plant species have been exploited commercially. Much remains to be learned before humankind can markedly increase the extent to which members of the plant kingdom are utilized. Culture of plant cells offers tantalizing prospects of long-term success, but commercialization has long been inhibited by questions of economic viability that reflect biological and engineering factors and their complex interactions.

In a natural environment some constituents of cells are synthesized only during a very short period during the life of the plant and may subsequently be consumed in other life processes. Other highly-sought-after products of biochemical reactions may be present in such scarce proportions that nature cannot match the supply of such materials to the demands of society. One such naturally occurring compound is the anticancer agent paclitaxel, popularly known as Taxol, a registered trademark of Bristol-Myers Squibb. Obtaining 1 kg of paclitaxel originally required the bark of more than 1000 Pacific yew (*Taxus brevifolia*) trees, each more than 100 years old. This approach was clearly not a viable long-term solution to the task of supplying adequate paclitaxel to satisfy the demand for this biopharmaceutical. In the absence of equally efficacious and cost-competitive pharmaceutical products for the treatment of various cancers, a development strategy based on sustainable production was a medical imperative. Total synthesis of this compound was later reported, but this method of producing paclitaxel was not economically sustainable on a large scale either. Not until Bristol-Myers

Squibb developed a semisynthetic process for production of this pharmaceutical did a viable route to this drug become available (57). The FDA granted approval for use of this drug in treating ovarian cancer in 1992, and subsequent approvals have been granted for several other forms of cancer.

Selection of plant biotechnology over conventional agriculture (or the vegetation produced by natural processes on uncultivated lands) as the source of the starting material for production of a specific biochemical is based primarily on analyses of the costs at which this material can be sold. Potential manufacturers must be able to produce substantive volumes of this biochemical consistently in sufficiently pure form to satisfy the constraints imposed by government regulatory agencies, their competitors in the marketplace, and the desires of stockholders to earn a suitable return on their investment. Other very important factors in this selection are the consistency and the stability of the source of starting materials.

Plant cells are considerably larger than cells of microorganisms and typical animal cells. Plant cell diameters may range from 10 to 100  $\mu\text{m}$ . This size is large compared to the characteristic dimensions of turbulent eddies resulting from mechanical mixing phenomena (see Section 13.3.2.1). Consequently, plant cells are susceptible to damage in vigorously agitated bioreactors; often, design engineers employ sparging with oxygen or air as a superior method for mixing suspension cultures of plant cells (or perhaps they may utilize a form of airlift bioreactor).

Industrial-scale airlift bioreactors typically have height/diameter ratios of 8 or greater. The presence of a draft tube serves to create internal circulation/mixing of the suspension of cells. Only a portion of the reactor is sparged with gas. This portion has a lower effective density than the bubble-free zones. Differences in density between the sparged region and the bubble-free zones cause a difference in hydrostatic pressure that causes the fluids in the sparged region to move upward. This draft markedly improves circulation and mass transfer of oxygen between the gas bubbles and the aqueous phase. Because there is no mechanical stirring, the plant cells are not susceptible to the shear forces that damage or kill the cells. Different placements of the draft tube and sparger enable one to create multiple physical configurations of airlift and bubble column bioreactors.

For plant cells, suspension cultures can reach high cell densities (at times comprising more than two-thirds of the working volume of a reactor). These dense suspensions have correspondingly high viscosities. However, plant cells have long doubling times, often measured in days. Consequently, for low to intermediate cell densities, the associated rate of consumption of oxygen may be sufficiently low that one can achieve adequate mass transfer of  $\text{O}_2$  to the suspended cells without having to resort to

the high rates of mechanical stirring that would damage plant cells. Associated with the long doubling times for culture of plant cells is the fact that it may take as long as several weeks to a month to complete the bioreaction phase of a process. Care must be taken to ensure that aseptic conditions are maintained throughout this period—not a trivial task.

In suspension culture, plant cells are seldom present as isolated individual cells, more commonly being present as agglomerates of cells. By proper manipulation of the environmental conditions (i.e., hormones, nutrients, growth factors, etc.), one can entice suspended plant cells to undergo differentiation and structural organization. Ultimately, the original undifferentiated cells can be converted to shoots, roots, plant embryos, and other forms suitable for propagation.

An additional complication associated with the culture of plant cells is that the products of cell growth include carbon dioxide and ethylene ( $C_2H_4$ ). Both of these gases can influence the rates of the biochemical reactions associated with cell growth to the extent that their partial pressures (as well as that of oxygen) must be controlled. Ethylene is of special interest because it is a naturally occurring plant hormone that has a strong influence on several plant growth processes beginning with cell function and development and encompassing cell separation, seed development, germination, fruit ripening, senescent processes, and plant-pathogen interactions.

Readers seeking more information concerning plant cell and tissue culture than space limitations permit here are referred to book-length references 52 and 58.

### 13.3.3.1 Culture of Plant Cells

Production of biochemicals via the culture of plant cells or tissues offers a number of *potentially* significant benefits (59, 60) over conventional cultivation of whole plants:

1. Control over the supply of the biochemical independent of the availability of the plant because of natural disasters, inappropriate local climate, political concerns, acts of war, lack of geographic proximity, high crop prices, soil conditions, and so on.
2. Better control over the physical environment and growth conditions for the cells: composition, temperature, and pH of the growth medium to permit optimization of productivity and selectivity of metabolite production.
3. Reproducible processing conditions, leading to improved quality control and optimization of the yield(s) of the desired product(s). Cultured cells would be free from the presence of microbes and insects.
4. Strain improvement via evolutionary optimization in programs analogous to those used for microorganisms.

5. Improved control over scale-up of the process and faster response to the demands of the marketplace.
6. Higher densities of those cells most involved in the biosynthesis of target metabolites.
7. Easier separation and recovery of targeted metabolites because of reduced complexity of the plant cell extracts. Isolation of the phytochemical can be rapid and efficient relative to extraction from whole plants.
8. Inclusion of molecular analogs of natural substrates in the growth medium may enable synthesis of novel secondary metabolites with potential biopharmaceutical implications.

However, realization of these potential benefits has seldom been achieved in an economically viable manner. Commercial applications of the biotechnology of plant cell culture historically have been concerned primarily with the production of high-value secondary metabolites. This aspect of plant biotechnology is not only complex from a science and engineering standpoint, but also a very costly business: expensive in terms of the necessary investment in research and development personnel, facilities, and clinical trials, in addition to the capital costs required to construct and validate the complex manufacturing equipment and supporting infrastructure necessary to meet the cGMP standards and FDA requirements.

In the mid-1990s, a second thrust of plant cell suspension culture began to evolve into a commercial reality—use of this type of culture for production of recombinant proteins. This route to recombinant proteins for human therapeutic use (i.e., as biopharmaceutical proteins) has a number of advantages over both microbial and mammalian cell culture for production of these proteins. In particular, the products of plant cell culture are intrinsically safer because they do not propagate mammalian viruses or pathogens. Moreover, they are superior in terms of both cost-effective downstream processing and their capacity for post-translational modifications. Unlike prokaryotic hosts, plant cells are capable of bringing about complex post-translational processing such as protein folding, glycosylation, signal peptide cleavage, and numerous modification reactions that are functionally important in the therapeutic applications of recombinant proteins if the expressed heterologous proteins are to be biologically active with respect to their intended use. [The term *heterologous* implies that the proteins of interest were created (or cloned) from a different type of cell whose genetic material is not native to the recipient cell but, instead, was produced by the genetic machinery of that cell using complementary DNA that had previously been added to the recipient cell. The nonnative genetic material has its origin in a different species.]

Huang and McDonald (61) reviewed several bioreactor engineering aspects of these emerging biotherapeutic

proteins, including types of possible reactor configurations and modes of operation, as well as optimization strategies that have been employed successfully to date. Su (62) also reviewed important aspects of bioreactor engineering associated with use of plant cell suspension culture for production of recombinant proteins.

Huang and McDonald (61) indicate that in 2006 the FDA granted approval to the first transgenic tobacco cell culture produced recombinant glycoprotein protein, a veterinary vaccine based on a particular antigen. They also cited development of a plant cell based approach to the production of glucocerebrosidase as a biotherapeutic enzyme for use in treating Gaucher's disease, an inherited metabolic disease that leads to liver and bone problems. Annual treatment costs are estimated at \$200,000 per patient even though the manufacturer uses a type of disposable reactor (see Section 13.3.5) rather than a conventional stainless steel reactor of the type used in the culture of animal cells and microorganisms. This enzyme is an extremely expensive pharmaceutical, one of the most expensive in recent use.

Utilization of a particular mode of plant cell or tissue culture depends on the intended use of the products of that culture and the associated economics. Clark and Blanch (63) indicated that five general categories of plant culture can be distinguished.

1. *Cell culture*: aseptic suspension culture of cells in liquid media in aerated, agitated bioreactors (60, 64). The products of primary interest are high-value secondary metabolites.
2. *Organ culture*: aseptic culture of plant embryos, root shoots, ovaries, or other organs of plants on media containing appropriate nutrients. Rather than targeting secondary metabolites, this form of culture is usually employed for the purpose of improving particular properties of specific plants (60, 65).
3. *Callus culture*: culture of cell mass on solid media (e.g., agar). The culture is initiated using an explant of a seedling or other plant source. An explant is living tissue excised aseptically from the natural site of growth and placed in a medium for culture.
4. *Meristem culture*: aseptic culture of shoot meristems or other explant tissues on nutrient media for the purpose of growing whole plants. Plant meristems are centers of mitotic cell division. They are composed of a group of undifferentiated self-renewing stem cells from which most plant structures originate to form the mature bodies of vascular plants. Meristem culture has been used widely in horticulture (63).
5. *Protoplast culture*: aseptic isolation and culture of plant protoplasts from cultured cells or plant tissues (66). This type of culture is usually employed to

obtain somatic hybridization by fusion of protoplasts. *Somatic fusion* (also referred to as *protoplast fusion*) is a type of genetic modification in which protoplasts from two distinct species of plants are fused together to form a somatic hybrid with the characteristics of both precursors. Such hybrids have been produced between either different varieties of the same species (e.g., between nonflowering potato plants and flowering potato plants) or between two different species (e.g., between wheat triticum and rye secale to produce triticale).

The three primary approaches to plant biotechnology involve suspensions of plant cells in aqueous media, culture of plant organs, and use of immobilized plant cells. Additional information concerning the first two modes of culture is provided below.

The most important products of plant cell culture are secondary metabolites. Among the well-known examples of these products are several plant biopharmaceuticals. These drugs (and their therapeutic use) include codein (analgesic), scopolamine (anti-hypertensive), quinine (anti-malarial), atropine (an anti-cholinergic and anti-spasmodic alkaloid), morphine (analgesic, anti-tussive, and an adjunct to anesthesia), cocaine (local anesthetic for certain eye and ear problems and some types of surgery), L-dopa (treatment of Parkinson's disease), and digoxin (treatment of congestive heart failure; decreasing the heart rate in patients with atrial fibrillation). Agrochemical products of plant cell culture include pyrethrin (insecticide) and rotenone (broad spectrum insecticide and pesticide). The rates at which these plant cell culture conversions take place are typically slower than conversions involving either animal cells or microorganisms. Readers may recall that for plant cells, doubling times are often in excess of a day. Consequently, it is not unusual to need to maintain aseptic conditions in a bioreactor for several weeks.

Only a very few plants have been cultured successfully in applications oriented toward production of biochemicals. The economics of plant culture are such that only very high-value products have the opportunity to succeed. Implementation of plant cell culture has been constrained by the economic implications of:

1. The slow rate at which plant cells grow.
2. High initial capital costs and high labor costs.
3. Low yields of the secondary metabolites desired. (Typically, but not always, the yields obtained by culture of plant organs are inferior to those obtained via culture of plant cells.)
4. Low product concentrations and productivities.

### 13.3.3.2 Culture of Plant Tissue

In the 1990s, an important development in plant biotechnology was the use of plant organ cultures in which the materials being cultured retain a substantial portion of the high-level organization of mature plants that enables cell-to-cell communications to be sustained and that leads to enhanced genetic stability of the resulting plants. Unlike microorganisms, cells of higher plants do not live in isolation but are part of an organized structure containing several plant organs. Division of a plant cell is not always followed by separation of the daughter cells. Instead, the daughter cells remain in intimate contact with their neighbors via microscopic pores called *plasmodesmata*. This contact permits cell-to-cell communication with their neighbors, both directly via protoplasmic connections and indirectly via establishment of macrogradients of the chemical potentials of hormones, elicitors, growth-promoting and growth-retarding regulators, vitamins, oxygen, and other substrates. In whole plants, cells make multiple connections to other cells via the  $10^3$  to  $10^5$  plasmodesmata that they typically contain. These micropores have a width of roughly 3 nm and permit the transport of water and low molecular weight solutes (up to roughly 800 or 1000 Da) from the cytoplasm of one cell to that of another cell via the plasmodesmata.

Plant cell cultures (including suspension cultures) contain aggregates of cells that were either present at the origin of the culture (as in organ, meristem, and callus cultures) or form during preparation of the suspension culture). Regardless of the type of culture employed, it is essential for commercial applications that one use a highly productive cell line. This factor has its origin in the genetics of the plant cell and, more than any other consideration, is extremely influential in determining the productivity of the bioreactor and thus the ultimate prospects for commercial success. In aggregates with sufficiently large dimensions, the constituent cells will be exposed to the concentration gradients of nutrients, hormones, and so on, that exist within the aggregate and thus be exposed to different microenvironments. Cells located at different positions in the aggregate reflect their individual and collective histories of experiences in these microenvironments by evolving with different structural morphologies and (bio)chemical compositions, even though only cells from a single species of plant may be present. Cell-to-cell communications of the growing cells facilitate organogenesis such that growth leads eventually to creation of a plantlet with genetics and properties similar to those of the plant that was the original precursor from which the culture was generated.

By contrast, in suspension culture, communications between cells are largely eliminated. As a consequence, the range of morphologies of the cell types (and their associated functionalities) that are formed are more diverse,

lack a coherent structure, and have different properties with respect to growth rate and accumulation of secondary metabolites. (It is this characteristic of cell differentiation that is the scientific basis underlying the commonly used strategy of employing different growth media for the phases of exponential growth and product accumulation.) Nonetheless, by suitable controlled manipulation of the conditions in the growth medium (temperature, pH, chemical composition, illumination conditions, etc.) and the gas phase [ $O_2$ ,  $CO_2$ , and ethylene (a reaction product that functions as a hormone)], even plant cells in suspension can be made to undergo differentiation and organization on a higher level. Plant embryos, shoots, and roots can be derived from aggregates in suspended culture. Such differentiation can be brought about even for cells in suspension that have experienced extended culture in an undifferentiated state. The phenomenon of regeneration of entire plants from undifferentiated cells is known as *totipotency*. This property is essential to the micropropagation of plants and is frequently associated with the formation of secondary metabolites (67).

#### 13.3.3.2.1 Culture of Plant Organs

Two types of plant organ culture (68) are *transformed shoot culture* and *transformed root culture (hairy root culture)*. Use of the word *transformed* implies that a suitable experimental protocol has previously been employed to introduce foreign genes into the genome of the transformed culture, thereby offering additional possibilities for manipulation of the culture to obtain increased productivity and/or improved properties of the sought after products. Transformation of plants is both a practical tool for improvement of cultivars and a central research tool in plant biology. Two types of transformed plant culture are discussed below: transformed shoot cultures and transformed root cultures.

##### 13.3.3.2.1.1 Transformed Shoot Cultures

There are relatively few articles in the archival literature concerning production of secondary metabolites via shoot cultures, but Yesil-Celiktas et al. (69) discussed this topic extensively. This biotechnology is more useful for the micropropagation of plants, but even this application is limited because alternative superior methods exist. Shoot cultures such as spherical meristematic or bud cultures in liquid media are prolific, rapidly growing systems that are susceptible to automated inoculation, controlled delivery of medium components, mechanical separation, and delivery to the final stage of plant growth. In the past decade, major advances have been made in the design and automation of bioreactors for the propagation of plants, reflecting advances in machine vision and recognition as well as in robotics. These reactors differ significantly in physical configuration and modes of operation from traditional bioreactors, but they have demonstrated advantages in

efficiency and ease of automated operation. Nonetheless, the technical requirements of combining automated mass propagation of plants with economic viability creates a challenging obstacle to widespread adoption of bioreactor technology for plant propagation. It should also be noted that the cultivation of shoots at times requires illumination of the shoots, further complicating the physical design of the bioreactor.

Yesil-Celiktas et al. (69) reviewed the literature concerning large-scale cultivation of plant cell and tissue culture in bioreactors, and Ziv (70) reviewed bioreactor technology for the micropropagation of plants.

**13.3.3.2.1.2 Transformed Root Cultures** Transformed root cultures are popularly known as hairy root cultures. The transformation of conventional roots to hairy roots takes place by infection with the gram-negative soil bacterium *Agrobacterium rhizogenes*. Infection of a plant or explant brings about the transfer and integration into the genome of host plant cells of DNA originating in the root-inducing plasmid. The transformed cells that result acquire the ability to develop into a root system at the infection site. This system proliferates and forms a network of root branches whose extent greatly exceeds those of the corresponding systems typical of uninfected plants. Moreover, the roots of infected plants are covered by tiny root hairs—hence the name “hairy root culture.”

Culture of hairy roots in bioreactors focuses on the production of secondary metabolites via growth of the biomass in root tissues. These products are useful as pharmaceuticals and cosmetics. Perhaps the greatest advantage of hairy root culture is that cultures of this type display about the same (or even greater) biosynthetic capabilities as those of the mother plants. These cultures are also characterized by long-term genetic stability. Hairy root cultures produce secondary metabolites similar to those of conventional root cultures, and their yields of these metabolites are much higher than the corresponding yields obtained in cell culture. The growth of biomass and the production of particular secondary metabolites are controlled by the genetic characteristics of the plant and are strongly influenced by the physical conditions and chemical compositions of the micro-environments in which they are grown. Not only are the properties of the growth medium (i.e., temperature, pH, composition and concentrations of both micro- and macrosolutes) and the configuration and mode of operation of the bioreactor of interest, but so is the composition of the gas phase, especially its CO<sub>2</sub>, O<sub>2</sub>, and C<sub>2</sub>H<sub>4</sub> content.

Optimum doubling times for hairy root cultures are comparable to typical values for suspension cultures. However, because required processing times can exceed a month [42 days for ginseng root culture (71)], it is

challenging to maintain an aseptic environment for such an extended period. Another major disadvantage of large-scale hairy root cultures is the formation of *root mats*, which inhibit fluid flow, can entrap gas bubbles and float, inhibit mass transfer of oxygen in the liquid phase, and present difficulties in maintaining a uniform environment throughout the culture vessel. Indeed, one of the major engineering challenges in the bioreactor culture of transformed roots is the problem of nonuniform distribution of biomass, especially the formation of aggregates or clumps of root tissue. These aggregates can produce local root densities that are so high that local consumption of oxygen during submerged culture becomes so rapid as to substantially deplete the dissolved oxygen.

Even though the root hairs have high surface/volume ratios, they may play a negative role in mass transfer of oxygen. Their presence inhibits fluid flow on a microscale, thereby creating quasi-stagnant boundary layers and contributing to the possibility that the rate of mass transfer of oxygen may limit the rates of biomass growth and production of metabolites.

Another problem associated with the formation of aggregates of hairy roots is that entrapped bubbles of gas can coalesce to form large bubbles that lead to channeling and bypassing effects that adversely affect mass transfer of O<sub>2</sub> to the roots. (Rise velocities of large bubbles are greater than those of small dispersed bubbles.)

Culture vessels (bioreactors) of a wide variety of types and configurations have been employed in the culture of transformed roots. The book edited by Eibl et al., (72) includes schematic drawings of 11 different configurations of bioreactors for hairy root culture, and several additional types of bioreactors are described in the text. These reactors include vessels that employ steel mesh, polyurethane foam, or hangers on the walls of a cylindrical vessel to immobilize roots submerged in the growth medium, segmented bubble columns, recirculating convective transport (loop) reactors, airlift reactors of various configurations, spray and trickle-bed reactors, mist reactors, and wave reactors (see Figure 13.13 in Section 13.3.5). These systems have evolved to optimize the productivity and the transformed root bioprocess. Kim et al. (73) have also discussed the implications of the type of bioreactor employed on secondary metabolism in hairy root cultures.

### 13.3.3.3 Productivity Considerations in Culture of Plant Cells and Tissue

Production of secondary metabolites in vitro can occur at nearly any stage of cell culture. For large-scale production of these metabolites to be effective, it is important to understand during which phase of cell growth a specific secondary product is formed. This information can then

be used as the basis for developing and carrying out a strategy for production of the metabolite of particular interest. For example, if this metabolite is formed during the exponential growth phase, one might consider using a culture strategy based on fed-batch operation to ensure that the culture would be growing actively throughout the production cycle, thereby maximizing production of the secondary metabolite. Because secondary metabolites in plants are present in such low concentrations in nature, and because the commercial exploitation of these metabolites often requires complex and expensive separation processes to produce biopharmaceuticals and other biologics, one must identify and employ a highly productive cell line as a point of departure for serious research on optimization of the growth medium and the bioreactor. This cell line must have appropriate genetic, physiological, and biochemical characteristics.

Generally during the initial stages of a project, only limited levels of production of the desired secondary product are achieved. Typically, for one to be able to satisfy the demands of the market and economic viability constraints, the productivity of this cell line under appropriate conditions (expressed in terms of yield of metabolite per unit volume of bioreactor per unit time) must be increased by orders of magnitude. Under normal circumstances the research team must utilize multiple growth-enhancing techniques and modes of operation of the bioreactor to achieve such a large increase. Such a multipronged approach sometimes results in synergistic interactions or multiplicative effects that produce the large increases in secondary metabolite yields necessary to render a project viable. The classic example of manipulation of a variety of product inducing factors—optimization of the growth medium in terms of its nutrient composition, use of elicitors, optimization of the gas composition, use of media with high osmotic pressures, feeding of precursors or sugars, operating strategies for the bioreactor (fed batch cultivation, two-stage cultivation under continuous operation, perfusion culture, etc.)—is the use of plant cell culture for production of paclitaxel and other taxanes. [As an indication of the range of possible partial pressure effects, we note that for production of paclitaxel, the most effective gas composition is 10% v/v O<sub>2</sub>, 0.5% CO<sub>2</sub>, and 5 ppm C<sub>2</sub>H<sub>4</sub> (74).] Zhong (74) discusses the aforementioned approaches and describes several additional tools used to achieve the advances in the culture of taxanes necessary to enable commercial production of these biopharmaceuticals for use in the treatment of several forms of cancer. Several of these approaches are discussed elsewhere in this chapter, but here we make special mention of induction.

*Induction* is employed to enhance the production of a desired secondary metabolite by adding particular chemical solutes to the growth medium or by use of particular strategic modes of operation. Induction is the approach that

is most likely to bring about dramatic increases in the yields of secondary metabolites. Production of many secondary metabolites is associated with the responses of plants to the stresses imposed by their environments. *Inducers* (also referred to as *elicitors* in the earlier literature) are able to mobilize the defenses of plant cells against pathogens and drought, wounds of various sorts, osmotic stress, and other sources of physiologic stress. Inducers/elicitors can be biotic: low-molecular-mass organic acids, glycoproteins, glucan polymers, polysaccharides/pectin, bacterial and fungal cell walls; or abiotic: ultraviolet irradiation, inorganic salts of heavy metals and various chemicals, and ultrasonic pulsed electrical fields (64, 74). Methyl jasmonate is particularly efficacious in the production of paclitaxel and other taxoids (74).

### **13.3.3.4 Plant Propagation Considerations**

In monetary terms the most significant role that bioreactors play in plant biotechnology is that of employing plant cells to produce biopharmaceutical products for therapeutic (secondary metabolites) and prophylactic (preventive vaccines) purposes. However, unusual forms of bioreactors can also be utilized as vessels for the micropropagation of transgenic plants or other high-value elite plants. The high efficiency with which plants can be propagated using bioreactors has been demonstrated by various research groups (75) using several species of plants. However, many problems still exist in terms of how best to proceed in extending this technology to new species and in scaling up existing technology to larger commercial bioreactors. The primary difficulties lie in the high labor costs associated with preparing, cleaning, and sanitizing these bioreactors, validating their use with respect to cGMP, preparing “seed cultures” for inoculation of the bioreactor contents, and determining those conditions that optimize the performance of the bioreactor in terms of micropropagation of particular species of plants.

The primary advantage of using bioreactors to carry out the propagation lies not just in their efficiency, but also in their ease of operation. Nonetheless, the aseptic and materials handling aspects of the use of bioreactors for this application present very formidable challenges to process engineers and others involved in process automation via the use of machine vision and robotics for cutting, sorting, and dispensing plant micropropagules. (*A propagule* is any of several structures of a plant, such as transformed shoots and roots, somatic embryos, tubers, seeds, and spores, that can give rise to a new individual plant.)

A primary goal of commercial scale plant cell based bioprocessing is to conduct an economically viable biosynthesis of substances with biopharmaceutical implications. Synthesis goals are to produce compounds that are bioactive with respect to one or more of the following types of

physiological activity: anti-carcinogenic, anti-viral, anti-microbial, anti-inflammatory, anti-parasitic, hypoglycemic, tranquilizing, and/or immunomodulatory. To date, only a relatively small number of secondary metabolites have been manufactured using plant cell biotechnology. Nonetheless, the large number of experimental, biochemical, biological, and optimization techniques for manipulating the behavior of plant cells (and the bioreactors in which they may be produced) suggests that this biotechnology will become increasingly important in the future. The secondary metabolites of interest are constituents of extremely complex biosynthetic networks. In many cases the mechanism of the biosynthetic process, or even the enzyme(s) involved, remains to be elucidated. In their review of approaches to the production of secondary plant metabolites, Hussein et al. (76) indicated the rapid rate at which this biotechnology is evolving and its great potential for technological success. However, matters of economic viability remain open questions in a myriad of applications with important health implications for humans and animals alike.

### 13.3.4 Photo-bioreactors

Diverse forms of biomass are of interest to researchers in a wide variety of industrial, academic, and governmental laboratories, both for use as a source of energy and as a potential feedstock from which biorefineries can produce multiple organic compounds and valuable microorganisms for a multitude of applications. Use of photo-bioreactors to facilitate the fermentation of both micro- and macro-algae represents intriguing possibilities for production of value added materials for use in formulating food, pharmaceutical, and cosmetic products. For example, polyunsaturated omega-3 fatty acids such as DHA and EPA (docosahexaenoic and eicosapentaenoic acids) are of interest to manufacturers of nutraceuticals targeted for sale to persons at high risk for cardiovascular problems or certain forms of cancer. Additional commercial applications exist in the fields of agriculture and aquaculture.

Presently, major barriers preclude significant commercial development of photo-bioreactor technology, even allowing for the rapid evolution of biotechnology for genetic manipulation of microorganisms. The economic potential for successful development of viable industrial-scale bioreactors will necessarily be long in achieving fruition because of the difficulties associated with achieving the necessary intensity of radiation (photons) at the surfaces of microorganisms, in large measure because of the “shadowing” effects of other microorganisms and/or structural components of the reactor itself. These factors severely constrain the efficacy with which incident radiation can be captured and utilized. Light, either natural or artificial, is the principal energy source

for photoautotrophic life. Consequently, the low efficiency with which photons emitted by a light source can be absorbed by biological materials and put to effective use in human-made reactors makes developing commercially viable photo-bioreactor technology a very formidable task. Another major barrier to commercialization of photo-bioreactor technology is proper maintenance of appropriate  $\text{CO}_2$  and  $\text{O}_2$  levels in the suspensions being processed. To obtain a high rate of photosynthesis, the  $\text{CO}_2/\text{O}_2$  ratio must be controlled such that in high-density cell cultures the  $\text{CO}_2$  is readily available. However, the concentrations of oxygen produced by photosynthesis must simultaneously be sufficiently low that oxygen is not used by the cells for photorespiration. The  $\text{O}_2$  has to be removed before it participates in other undesirable reactions or reaches an inhibitory level.

Two methods of classifying photo-bioreactors are based on whether or not the growth of microorganisms occurs in natural waters (lakes, lagoons, ponds) or in manufactured facilities and on whether or not the light source is natural sunlight or artificial illumination. Systems for cultivation of microalgae that are open to the air and natural sunlight are found in a wide variety of geographical locations and most closely resemble the environment in which microalgae are present in nature. A common design is that of the raceway cultivator in which paddlewheels or other primitive sources of power are used to circulate suspended biomass through relatively shallow channels. (Photosynthesis can occur only in shallow waters, but excessive light can lead to photo inhibition effects.) Such installations suffer from the disadvantage of evaporative losses, as well as evolution of  $\text{CO}_2$  from the aqueous phase to the surrounding air. The vagaries of the weather and the time of day or night produce concomitant variability in the intensity of the incident light. Moreover, these facilities have large equipment footprints and are subject to a high probability of contamination by undesired microorganisms. Monoseptic cultures of the type that seek to produce higher-value microorganisms (such as those of interest to the pharmaceutical and cosmetic industries) require fully closed systems to be consistent with cGMP.

Closed photobioreactors are designed in a manner that addresses the disadvantages of the open systems noted above, especially those of contamination and losses of  $\text{CO}_2$  and  $\text{H}_2\text{O}$  to the surroundings. Enclosed photo-bioreactors are amenable to regulation and control of the biotechnologically important process parameters, including light intensity and the frequency of the incident radiation. These reactors consist of arrays of tubes of glass or transparent plastic through which the suspensions of interest are pumped. References to several physical configurations are noted in a review article on photo-bioreactors by Pulz (77). Particularly for processes involving high-value products, closed photo-bioreactor systems appear to be

more appropriate than open systems for future applications of commercial interest.

### 13.3.5 Single-Use (Disposable) Bioreactors

During the period since World War II, collaborations between biochemists, applied microbiologists, and chemical engineers have evolved in several complementary directions, as their joint efforts have led to the successful development of innovative processes based on biochemical transformations that take place in creatively designed fermenters and bioreactors. This equipment has been tailor-made to satisfy not only the safety, sanitation, and microbiological constraints imposed by the FDA and its counterparts in other nations, but also the labile and shear-sensitive nature of animal and plant cells. The equipment used in traditional facilities for manufacturing biopharmaceutical products consists of stainless steel bioreactors/fermenters, tanks, piping, valves, and so on, that are quasi permanent installations.

However, since the late 1990s many vendors, pharmaceutical manufacturers, and consultants have encouraged efforts to develop the bioreactor technology necessary to fabricate and employ single-use (disposable) bioreactors fabricated largely from polymeric materials. These bioreactors offer several advantages over traditional fixed equipment, including reduced capital costs, reduced consumption of water and energy, smaller footprints, and shorter time requirements for turnarounds [because of elimination of clean-in-place (CIP) and sterilize-in-place (SIP) requirements by using presanitized disposable equipment].

Single-use bioreactors are utilized extensively in the culture of mammalian cells and are being increasingly used in preclinical, clinical, and developmental scale facilities. This biotechnology has been the beneficiary of rapid innovations in both the basic disposable equipment and optimization of culture conditions and laboratory protocols. However, much of the impetus for these innovations arises from demands by manufacturers of vaccines, antibiotics, and other biologicals for upgrades in the capabilities of single-use bioreactors. A variety of single-use bioreactor designs are currently marketed covering working volumes from laboratory scale (1 L or less) to units with volumes of 2000 L. These bioreactors may differ with respect to mode of agitation, instrumentation and control systems, the multilayer sandwiches of polymers used to construct the disposable polymeric “bag” that constitutes the core of the single-use bioreactor, and the extent to which the auxiliary capabilities (stirrers, sensors, spargers, etc.) are also treated as single-use. The polymeric bags and any pre-installed accompanying auxiliary equipment are delivered

presterilized by the supplier prior to being installed in a reusable holder.

In important economic and microbiological respects these disposable reactors are viable alternatives to traditional stainless steel or glass bioreactors for laboratory and pilot scale culture of microorganisms and cells. As this biotechnology continues to benefit from ongoing incremental improvements and extension of the disposable approach to bioprocess design, utilization of single use bioreactors and related equipment is expected to continue to both penetrate existing markets and create new markets. It is not only in the bioreactor proper, but also in upstream and downstream processing operations that the single use approach is disrupting traditional thinking about bioprocesses and implementation thereof. In both commercial and research and development applications of biochemical principles, a paradigm shift is under way with respect to the optimum size of process units and to the compromises being made in process economics between the high initial capital costs of large stainless steel reaction vessels, high energy costs, and lost production time for CIP and SIP operations, as well as elevated labor costs for operation of complex facilities vis-à-vis significantly lower cost single-use bioreactors whose use does not entail lost production time for cleaning and sterilization activities and which may be coupled with downstream purification devices that are also disposable and are simpler to fabricate and operate.

Single use bioreactors differ from the vessels traditionally used to culture microorganisms in that the suspension of the organism being cultured is often contained in a disposable bag fabricated from several thin layers of various polymers rather than being held in a stainless steel or glass vessel. Typically, such a bag might consist of a composite layered sandwich of at least three polymers: one layer (e.g., PET [poly(ethylene terephthalate)] or LDPE (low-density polyethylene)) provides mechanical strength, toughness, and to some degree, stability; a second layer (e.g., PVA [poly(vinyl alcohol)] or PVC [poly(vinyl chloride)]) acts as an impermeable barrier to ambient gases (especially O<sub>2</sub> and CO<sub>2</sub>); and because the third layer is in direct contact with the suspension of the organism in the growth culture, it must be suitable for sterilization (gamma irradiation) and have no adverse effects on, or negative interactions with, either the suspended cells or products present in the growth medium. The polymer composite films can either be laminated using a thermosetting polymer adhesive or coextruded to form a multilayer film that is bonded together by a tacky thermoplastic polymer.

The typical disposable stirred bag cultivation container has a cylindrical geometry with a low aspect ratio of roughly 1 to 2. For mechanical support, large bags may be mounted in a stand fastened to a skid.

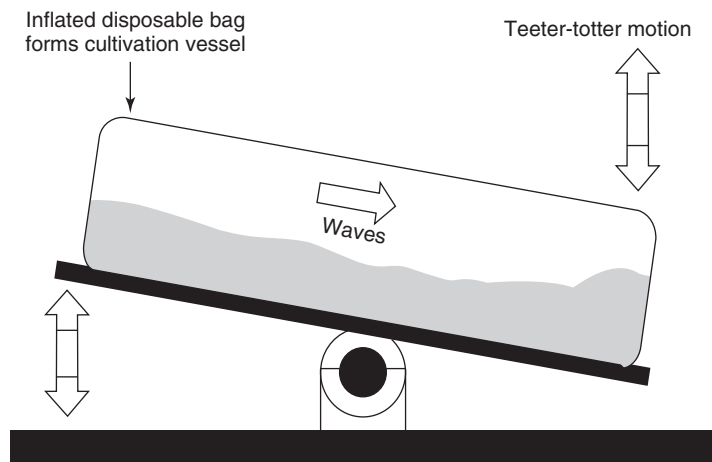


**Figure 13.13** Schematic representation of a wave-mixed disposable bag bioreactor.

The bags employed in single use bioreactors are presterilized prior to use in cultivation of cells. Several forms of disposable bag bioreactors are available from multiple vendors. Examples include physically stirred bag bioreactors and wave-mixed bag bioreactors. A schematic diagram of a wave-mixed bag bioreactor is shown in Figure 13.13. Bag bioreactors are used in the production of therapeutic recombinant proteins and monoclonal antibodies. Other types of single use bioreactors include permselective membrane reactors in both hollow-fiber and flat-sheet membrane configurations (see Section 13.2.7).

Advantages of bag bioreactors include low initial investment costs; low risk of cross-contamination; flexibility and simplicity of operation; suitability for use with commercially available presterilized growth media; reduced lifetime energy and operating costs because of the elimination of requirements for CIP and SIP equipment and the downtime associated these operations; ease of scale-up and replication of process equipment at multiple geographically dispersed sites; and facilitation of validation of process equipment before restarting process operations. Because bag reactors are presterilized and prepackaged, startup and changeover to a new biochemical reaction are facilitated, as is process development activity. Improvements in cell strains and media composition, together with evolving process optimization based on operating experience in the years since the turn of the century, have led to marked increases in the productivity per unit of bioreactor volume, thereby enabling manufacturers to meet market needs with smaller bioreactors. These advances increase the feasibility and economic viability of utilizing geographically dispersed production facilities.

Because of the necessity for CIP and SIP steps before use of a traditional stainless steel bioreactor for the manufacture of biopharmaceutical products, validation of the reactor can be expensive in terms of lost production,

labor, and energy costs. Use of a presterilized disposable reactor eliminates these steps. In the manufacture of biopharmaceutical products, validation of the equipment prior to restarting operations represents a very significant component of the operating costs. The flexibility of single-use technology makes it readily adaptable to varying production schedules, facilitating not only normal operations but also establishing surge capacity and making it easier and faster to “mothball” equipment or alter its purpose.

Disadvantages of bag bioreactors include potential problems with respect to obtaining adequate mass transfer of oxygen as a substrate for cell growth; and maintenance of sterile operating conditions by use of aseptic connections where analytical probes, ports for entry and exit of process streams, including the possibility of use of some form of disposable impeller and/or sparger. Some commercially available bag bioreactors contain stirrers and sensors built into the bag to facilitate (pre)sterilization of these components.

To ensure that the cells have adequate access to the substrates necessary to accomplish the biochemical reactions of interest, one must make provisions in the design of the bioreactor for adequate mixing of the suspension of cells. For bioreactors with volumes of 1000 L or less, one can agitate the contents of a disposable bag using some form of rocking device (Figure 13.13) or orbital shaker. Stirrers can also be employed on a similar or larger scale. In some situations the stirrers are integrated into the bag to the extent that the stirrers, too, become disposable. In these cases the closed bag containing the stirrer and sparger is presterilized by the vendor, and magnetic coupling is used to drive the stirrer.

Wave-mixed bioreactors are an interesting variation on the bag bioreactor theme that was introduced in the late 1990s. In this type of bioreactor a presterilized composite polymer bag of the type described above is fastened to a

platform that shakes or rocks (see Figure 13.13). The teeter-totter motion of the platform produces waves in the suspension of cells so that there is a turnover of the fluid at the interface with the gas. This turnover periodically renews the surface layers of liquid, thereby enhancing the rate of mass transfer of oxygen from the gas phase into the bulk liquid. For these reactors mechanical power supplied by the moving platform serves to maintain the cells in suspension, facilitates oxygenation of the growth medium from the gas phase, and creates a moving interface between the suspension and the gases above the liquid. The shear stresses associated with the movements of the liquid are relatively low, so cell damage is acceptably low.

Wave-mixed disposable bioreactors have gained considerable popularity in several commercial applications, especially for moderate-scale processes, seed culture preparation for inoculation of larger-scale bioreactors, and preclinical or clinical applications. However, the archival literature contains very little quantitative data concerning the performance of wave-mixed bioreactors. The scarcity of data is in part a consequence of the proprietary nature of the uses to which these reactors have been put and in part a paucity of appropriate sensors for use in accurately monitoring the progress of the cultivations of interest while scrupulously maintaining the microbiological integrity of the contents of this type of bag bioreactor.

Thoroughly documented life-cycle analyses of the merits of single-use bag bioreactors relative to traditional stainless steel or glass bioreactors are not available in the public domain. However, Mauter (78) has discussed important components of an environmental impact study of such an analysis. Her discussion is helpful from an initial screening perspective. She has also indicated that there are circumstances when certain manufacturing considerations will weigh more heavily than the results of necessarily incomplete economic analyses. Single-use bioreactors may provide viable alternatives to stainless steel or glass construction under circumstances when rapid process development is imperative to avoid lost opportunity costs; there are major space (footprint) constraints; avoidance of high initial capital costs is more essential than avoidance of short-term operating costs; validation costs are significantly lower for the disposable reactor; and flexibility with respect to the requisite capacity at various geographic locations is necessary (dispersed manufacturing facilities).

Sinclair et al. (79) have compared the environmental (primarily carbon) footprint of a monoclonal antibody (mAb) production facility using traditional stainless steel bioreactors with that of a facility utilizing disposable equipment for cell culture, mixing solutions, holding tanks, and liquid transfer. The mAbs are intended for use in therapeutic applications and are produced in a facility containing three 2000-L disposable bioreactors. The authors' cradle-to-grave analysis took into account facility

size, water consumption, energy use, and carbon emissions (including mining iron ore), equipment fabrication and installation, transportation of materials and employees to and from the facility, and incineration of disposable polymers. These investigators noted that water consumption was 87% less for the disposables oriented facility than for the plant using equipment constructed of stainless steel (no need for CIP or SIP capabilities). Steam costs and labor costs were also reduced substantially, largely for the same reason. CO<sub>2</sub> emissions were reduced by roughly 25%. The footprint of the facility was reduced by 38% and operating energy by 30%. However, the authors noted a substantial increase in the volume of plastic waste in the form of upstream consumables. The authors indicated that by far the largest contribution to the carbon footprint of the single-use bioreactor facility was linked to transportation of employees to and from work (80%). Even if there are substantial errors in the numerical values cited, these values nonetheless indicate that individuals responsible for the design and operation of bioreactors need to be aware of the potential benefits of single-use bioprocessing facilities. Sinclair et al. concluded that the use of disposable bioreactor technology for the production of mAbs can lead to a smaller overall environmental impact than technology based on stainless steel equipment.

The evolution of disposable bioreactor technology in response to demands for decentralized production facilities that can be readily replicated has been accompanied by concomitant demands for improved cost-effective sensors for data acquisition. Such data are essential in developing and implementing appropriate process control strategies. Increased recognition of the significance of such data has accompanied an initiative of the FDA in the area of process analysis technology. For disposable bioreactors, the initial sensing element must be installed within the sterility boundary prior to sterilization of the bag. Consequently, the sensing element must be able to retain the desired functionality during the sterilization step. Research on new sensor development focuses on *in situ* technology that employs noninvasive spectroscopic techniques via fiber optic technology linked to various types of spectrometers through disposable sensing connectors, optical windows, and so on. Review articles by Beutel and Henkel (80) and Glindkamp et al. (81) describe the large menu of analytical approaches that can be employed to monitor the progress of biochemical reactions. The latter reference is particularly germane to the issue of sensors for use in disposable reactors.

Spectrometers and other forms of analytical instrumentation can be utilized to monitor the progress of a biochemical reaction via *in situ*, *online*, and *ex situ* measurements. *In situ* measurements frequently use a noninvasive physical method to monitor the reaction medium directly to discern the progress of a reaction (see Section 3.2.2.2). The response times of such instruments

are typically inconsequential relative to the slow pace of most biochemical reactions. Changes in the property of interest provide an essentially continuous stream of data concerning variables such as temperature, electrical conductivity, partial pressures of  $O_2$  and  $CO_2$ , chemical composition, and so on. However, problems in obtaining appropriate data may arise from interference(s) from fluid motion as well as from the bubbles and cells that may be present within the bioreactor. *Ex situ* measurements are akin to the chemical approach to obtaining kinetic data described in Section 3.2.2.2. *Ex situ* measurements require removing a sample from the reaction medium and quenching the reaction. Critical issues of sampling are obtaining a representative sample and maintaining the sterility of the reactor contents. Obtaining meaningful data for purposes of process control can also be highly challenging because of the delays involved in quenching the reaction and analyzing the sample. Glindkamp et al. (81) describe some approaches to the use of *ex situ* methods for obtaining samples that can be analyzed using traditional methods of chemical analysis. Online measurements also provide essentially continuous measurements, but of the contents of a special portion of the bioreactor such as a bypass line rather than the well-mixed core of the suspension.

The aqueous phase that constitutes the growth medium in a bioreactor contains multiple species whose concentrations may be of interest for purposes of maximizing reactor productivity and it may well be impossible to utilize a single analytical technique to determine the levels of these species present in the reactor at particular times. Often, researchers may have to utilize principal components analysis and other mathematical/chemometric techniques to sift through the data to obtain the desired information. The array of analytical techniques that one could consider for use with single-use bioreactors is not as extensive as that which might be employed in work involving traditional stainless steel bioreactors, but it is nonetheless imposing. Some possibilities include:

- Fluorometry of various types
- Ultraviolet/visible spectroscopy
- Infrared spectroscopy in various manifestations (especially NIR)
- Raman spectroscopy in its various forms
- Optical chemosensors
- Optical oxygen sensors
- Optical pH sensors
- Optical  $pCO_2$  sensors
- In situ* microscopy
- Chemical field-effect transistors in various forms
- Conductivity sensors
- Sensors based on ultrasonic signals

Only a few of these techniques are both sufficiently inexpensive and sufficiently advanced in their development that they are economically viable for use in single-use bioreactors (even if only a portion of the instrumentation is actually considered disposable). Individuals with responsibilities in this area have to utilize not only their knowledge of biochemistry and engineering, but also creativity and imagination in facilitating further evolution of disposable bioreactor technology.

Additional descriptive material concerning single-use bioreactors is provided in the publications of Eibl and Eibl (82), Eibl et al. (83), Zhou et al. (50), and Warnock and Al-Rubeai (29).

## LITERATURE CITATIONS

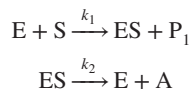
1. BAILEY, J. E., and OLLIS, D. F., *Biochemical Engineering Fundamentals*, pp. 337–369, McGraw-Hill, New York, 1977.
2. BAILEY, J. E., and OLLIS, D. F., *Biochemical Engineering Fundamentals*, 2nd ed., pp. 394–408, McGraw-Hill, New York, 1986.
3. STEPANOPoulos, G. N., ARISTIDOU, A. A., and NIELSEN, J., *Metabolic Engineering: Principles and Methodologies*, Academic Press, San Diego, CA, 1998.
4. DEAN, A. C. R., and HINSELWOOD, C. N., *Growth, Function and Regulation in Bacterial Cells*, Oxford University Press, London, 1966.
5. HOCHFELD, W. L., *Producing Biomolecular Substances with Fermenters, Bioreactors, and Biomolecular Synthesizers*, Chap. 9, CRC Press/Taylor & Francis Group, Boca Raton, FL, 2006.
6. SHULER, M. L., and KARGI, F., *Bioprocess Engineering: Basic Concepts*, 2nd ed., pp. 176–189, Prentice Hall, Upper Saddle River, NJ, 2002.
7. HOCHFELD, W. L., *op. cit.*, pp. 242–243.
8. DORAN, P. M., *Bioprocess Engineering Principles*, p. 284, Academic Press, San Diego, CA, 1995.
9. DORAN, P. M., *op. cit.*, p. 200.
10. TREYBAL, R. E., *Mass Transfer Operation*, 3rd ed., McGraw-Hill, New York, 1980.
11. BIRD, R. B., STEWART, W. E., and LIGHTFOOT, E. N., *Transport Phenomena*, 2nd ed., Wiley, New York, 2002.
12. McCABE, W. L., SMITH, J. C., and HARRIOT, P., *Unit Operations of Chemical Engineering*, 7th ed., McGraw-Hill, Boston, 2005.
13. LEWIS, W. K., and WHITMAN, W. G., *Industrial and Engineering Chemistry*, **16**(12), 1215 (1924).
14. NIELSEN, J., and VILLADSEN, J., *Bioreaction Engineering Principles*, pp. 391–398, Plenum Press, New York, 1994.
15. LIM, H. C., and SHIN, H. S., *Fed-Batch Cultures: Principles and Applications of Semi-batch Bioreactors*, Cambridge University Press, Cambridge, 2013.
16. VAN'T RIET, K., and TREMPER, J., *Basic Bioreactor Design*, Marcel Dekker, New York, 1991.
17. CLARK, D. S., and BLANCH, H., *Biochemical Engineering (Chemical Industries)*, pp. 294–297, Marcel Dekker, New York, 1997.
18. SHULER, M. L., and KARGI, F., *op. cit.*, pp. 250–256.
19. PANDA, T., *Bioreactors: Analysis and Design*, pp. 223–232, Tata McGraw-Hill, New Delhi, India, 2011.
20. PARKER, A. L., SIKORA, L. J., and HUGHES, R. R., *AIChE J.*, **22**, 851 (1976).
21. SHULER, M. L., and KARGI, F., *op. cit.*, p. 262.
22. PANDA, T., *op. cit.*, pp. 70–72.
23. SHULER, M. L., and KARGI, F., *op. cit.*, pp. 491–508.

24. BAILEY, J. E., and OLLIS, D. F., *op. cit.*, 926–938 (1986).
25. CLARK, D. S., and BLANCH, H., *op. cit.*, 322–328.
26. LIN, H., GAO, W., MENG, F., LIAO, B.-Q., LEUNG, K.-T., ZHAO, L., CHEN, J., and HONG, H., Membrane Reactors for Industrial Wastewater Treatment: A Critical Review, *Critical Reviews in Environmental Science and Technology*, **42**(7), 677–740 (2012).
27. ENDERS, J. F., WELLER, T. H., and ROBBINS, F. C., *Science*, **109**, 85 (1949).
28. KOHLER, G., and MILSTEIN, C., *Nature (London)*, **256**, 495 (1975).
29. WARNOCK, J. N., and AL-RUBEAI, M., *Biotechnol. Appl. Biochem.*, **45**, 1–12 (2006).
30. DORAN, P. M., *Bioprocess Engineering Principles*, 2nd ed. Chap. 8, Academic Press, San Diego, CA, (2013).
31. OLDSHUE, J. Y., *Fluid Mixing Technology*, McGraw-Hill, New York, 1983.
32. DORAN, P. M., *op. cit.*, 315–322 (2013).
33. SHULER, M. L., and KARGI, F., *op. cit.*, pp. 396–399.
34. THOMAS, C. R., in WINKLER, M. A. (Ed.), *Chemical Engineering Problems in Biotechnology*, Critical Reports on Applied Chemistry, Vol. 29, 23–88, Elsevier, London, 1990.
35. THOMAS, C. R., *loc. cit.*, p. 29.
36. CROUGHAN, M. S., SAYRE, E. S., and WANG, D. I. C., *Biotech. Bieng.*, **33**, 862 (1989).
37. DORAN, P. M., *op. cit.*, 318 (2013).
38. THOMAS, C. R., *loc. cit.*, 84.
39. DORAN, P. M., *op. cit.*, 317 (2013).
40. NIENOW, A. W., *Cytotechnology*, **50**, 9–33 (2006).
41. HARNBY, N., EDWARDS, M. F., and NIENOW, A. W. (Eds.), *Mixing in the Process Industries*, 2nd ed., Butterworth Heinemann, London, 1992.
42. CHALMERS, J., in *Encyclopedia of Cell Technology*, R. E. SPIER (Ed.), Vol. 1, pp. 41–51, Wiley, Hoboken, NJ, 2000.
43. WU, J., *J. Biotechnol.*, **43**, 81 (1995).
44. PAPOUTSAKIS, E. T., *Trends Biotechnol.*, **9**, 427 (1991).
45. BUTLER, M., *Animal Cell Culture and Technology*, 2nd ed., p. 2, Garland/BIOS, London, 2004.
46. BUTLER, M., *op. cit.*, p. 113–123.
47. BUTLER, M., *op. cit.*, p. 52.
48. WHITFORD, W. G., *Bioproc. Int.*, April, 30–40 (2006).
49. SHUKLA, A. A., and THÖMMES, J., *Trends Biotechnol.*, **28**(5), 253 (2010).
50. ZHOU, W., SETH, G., GUARDIA, M. J., and HU, W.-S., Mammalian Cell Bioreactors, in *Encyclopedia of Industrial Biotechnology: Bioprocess, Bioseparation, and Cell Technology*, FLICKINGER, M. C. (Ed.), pp. 3219–3230, Wiley, Hoboken, NJ, 2010.
51. MARTIN, Y., and VERMETTE, P., *Biomaterials*, **26**, 7481 (2005).
52. EIBL, R., EIBL, D., PORTNER, R., CATAPANO, G., and CZERMAK, P. (Eds.), *Cell and Tissue Reaction Engineering*, Springer-Verlag, Berlin, 2009.
53. HAMBOR, J. E., *Bioproc. Int.*, **10**, June, 22–33, (2012).
54. KRAWETZ, R., TAIANI, J. T., LIU, S., MENG, G., LI, X., KALLOS, M. S., and RANCOURT, D. E., *Tissue Eng., Part C*, **16**(4), 209 (2010).
55. KEHOE, D. E., JING, D., LOCK, L. T., and TZAANAKAKIS, E., *Tissue Eng., Part A*, **16**(2), 405 (2010).
56. BAGHBADERANI, B. A., MUKHIDA, K., SEN, A., KALLOS, M. S., HONG, M., MENDEZ, I., BEHIE, L. A., *Biotechnol. Bioeng.*, **105**, 823 (2010).
57. KIERAN, P. M., MACLOUGHLIN, P. F., and MALONE, D. M., *J. Biotechnol.*, **59**, 39 (1997).
58. DUTTA GUPTA, S., and IBARAKI, Y. Eds., *Plant Tissue Culture Engineering*, Springer-Verlag, Berlin, 2006.
59. SHULER, M. L. and KARGI, F., *op. cit.*, p. 406.
60. YESIL-CELIKTAŞ, O., GUREL, A., and VARDAR-SUKAN, F., *Large Scale Cultivation of Plant Cell and Tissue Culture in Bioreactors*, p. 3, Transworld Research Network, Kerala, India, 2010.
61. HUANG, T.-K., and McDONALD, K. A., *Biochem. Eng. J.*, **45**, 168 (2009).
62. SU, W. W., Bioreactor Engineering for Recombinant Protein Production Using Plant Cell Suspension Culture, in DUTTA GUPTA, S., and IBARAKI, Y. (Eds.), *Plant Tissue Culture Engineering*, pp. 135–159, Springer-Verlag, Berlin, 2006.
63. CLARK, D. S., and BLANCH, H., *op. cit.*, pp. 219–225.
64. EIBL, R., and EIBL, D., in EIBL, R., Eibl, D., PORTNER, R., CATAPANO, G., and CZERMAK, P. (Eds.), *Cell and Tissue Reaction Engineering*, pp. 315–356, Springer-Verlag, Berlin, 2009.
65. ADELBERG, J., Agitated Thin Films of Liquid Media for Efficient Micropropagation, pp. 101–107, in *Plant Tissue Culture Engineering*, Dutta Gupta, S., and Ibaraki, Y., (Editors). Springer-Verlag, Berlin, 2006.
66. DAVEY, M. R., ANTHONY, P., POWER, J. B., and LOWE, K. C., *Biotechnol. Adv.*, **23**, 131 (2005).
67. SHULER, M. L., and KARGI, F., *op. cit.*, p. 408.
68. WILSON, P. D. G., and HILTON, M. G., in *Bioreactor System Design*, ASENJO, J. A., and MERCHUK, J. C. (Eds.), pp. 413–439, Marcel Dekker, New York, 1995.
69. YESIL-CELIKTAŞ, O., et al. *op. cit.*
70. ZIV, M., Bioreactor Technology for Plant Micropropagation, JANICK, J. (Ed.), *Hortic. Rev.*, **24**, 1–30 (2000).
71. CHOI, Y.-E., KIM, Y.-S., and PAEK, K.-Y. in DUTTA GUPTA, S., and IBARAKI, Y. (Eds.), *Plant Tissue Culture Engineering*, p. 166, Springer-Verlag, Berlin, 2006.
72. EIBL, R., EIBL, D., PORTNER, R., CATAPANO, G., and CZERMAK, P., *Cell and Tissue Reaction Engineering*, p. 336, Springer-Verlag, Berlin, 2009.
73. KIM, Y., WYSLOUZIL, B. E., and WEATHERS, P. J., *In Vitro Cell Devel. Biol.—Plant*, **38**, 1 (2002).
74. ZHONG, J.-J., *J. Biosci. Bioeng.*, **94**(6), 591 (2002).
75. YESIL-CELIKTAŞ, O., et al., *op. cit.*, p. 42.
76. HUSSAIN, M., FAREED, S., RAHMAN, M., AHMAD, I. Z., and MOHD, S., *J. Pharm. Bioll. Sci.*, **4**, 10 (2012).
77. PULZ, O., *Appl. Microbiol. Biotechnol.*, **57**, 287 (2001).
78. MAUTER, M., *Bioproc. Int.*, April, Supplement, pp. 18–29 (2009).
79. SINCLAIR, A., LEVEEN, L., MONGE, M., LIN, J., and COX, S., Environmental Impact of Disposable Technologies, Biopharm International.com, November 2, 2008.
80. BEUTEL, S., and HENKEL, S., *Appl. Microbiol. Biotechnol.*, **91**, 1493–1505 (2011).
81. GLINDKAMP, A., REICHERS, D., REHBOCK, C., HITZMANN, B., SCHEPER, T., and REARDON, K. F., *Adv. Biochem. Eng. Biotechnol.*, **115**, 145–169 (2010).
82. EIBL, R., and EIBL, D., *Single-Use Technology in Biopharmaceuticals Manufacture*, e-book, Wiley, New York.
83. EIBL, R., EIBL, D., PORTNER, R., CATAPANO, G., and CZERMAK, P., *Cell and Tissue Reaction Engineering*, pp. 242–245, Springer-Verlag, Berlin, 2009.
84. LIM, H. C., and SHIN, H. S., *op. cit.*, p. 5.

## PROBLEMS

Although the present chapter does not contain material relative to the design of enzyme-mediated reactions, we have chosen to include in this collection of problems several reactor design problems involving extension of the material concerning enzymatic reactions in Chapter 7. Students should be able to solve these problems using the fundamental concepts of reactor design analyses presented in Chapters 8 to 12.

- 13.1** M. L. Bender and T. H. Marshall [*J. Am. Chem. Soc.*, **90**, 201(1968)] studied the elastase-mediated hydrolysis of *p*-nitrophenyl trimethylacetate to produce *p*-nitrophenol. These authors have proposed the following mechanism for this reaction:



where S, the substrate, is *p*-nitrophenyl trimethylacetate; P<sub>1</sub> the product, is *p*-nitrophenol; and A is trimethylacetic acid.

$$k_1 = 150 \text{ m}^3/\text{mole-ksec} \text{ and } k_2 = 2.60 \text{ ksec}^{-1}.$$

- (a) Derive an equation for the rate of production of species P<sub>1</sub> in terms of k<sub>1</sub>, k<sub>2</sub>, E<sub>0</sub> (the total elastase concentration in its two forms, E and ES), and S the instantaneous concentration of substrate.
- (b) Lucky Bucky Chemical Company is investigating the production of *p*-nitrophenol by this process in a continuous-flow stirred-tank reactor with a volume of 0.3 m<sup>3</sup>. If 90% of the substrate is to be converted to the product, how large a volumetric flow rate can be processed in this reactor when the initial enzyme and substrate concentrations are 1 and 100 mol/m<sup>3</sup>, respectively?
- 13.2** There is continuing interest in the dairy industry in processes that employ immobilized enzymes as biocatalysts for adding value to various process streams. These processes involve attaching enzymes to solid supports and packing the supports in a tube through which a liquid dairy product flows. One application involves the conversion of an aqueous solution of lactose (de-proteinized cheese whey) into glucose and galactose. In considerations of immobilized enzyme processes, one can average over the void spaces between particles of the solid support and the particles themselves to obtain an effective rate expression per unit volume of packed bed:

$$r = \frac{ks}{s + K_M[1 + (p_1/K_I)]}$$

At a fixed temperature the parameters k, K<sub>M</sub> and K<sub>I</sub> are constants. K<sub>M</sub> is known as a Michaelis constant and K<sub>I</sub> as an inhibition constant. The concentrations of reactant S and product P<sub>1</sub> are represented by s and p<sub>1</sub>, respectively. What effective space time for a tubular reactor will be required to obtain 80% conversion of the lactose at 40°C where K<sub>M</sub> = 0.0528 M, K<sub>I</sub> = 0.0054 M, and k = 5.53 mol/(L·h). The initial lactose concentration may be taken as 0.149 M.

- 13.3** As indicated in Illustration 13.7, A. L. Parker, L. J. Sikora, and R. R. Hughes [*AIChE J.*, **22**, 851 (1976)] studied biological denitrification of wastewater streams in packed beds. For steady state microbe populations and feed nitrate concentrations of less than 100 mg/L, the rate law is of the form

$$r = \mu Y C_N$$

where  $\mu$  is the specific nitrate removal rate, Y the biological yield coefficient, C<sub>N</sub> the nitrate concentration, and the

product  $\mu Y$  can be regarded as a pseudo first-order rate constant for the conditions cited.

These investigators reported the following effluent response data for a 25-cm<sup>3</sup> pulse of aqueous solution containing chloride ion at the 1000-ppm level:

Time (min)	C/C <sub>standard</sub>
0	0.00
10	0.00
20	0.00
30	0.00
40	0.10
50	0.38
60	0.99
70	1.40
80	1.46
90	1.31
100	1.10
110	0.86
120	0.62
130	0.40
140	0.22
150	0.08
160	0.02
170	0.00
180	0.00
190	0.00
200	0.00

- (a) Prepare a plot of the F(t) curve for this reactor.
- (b) Determine the mean residence time of the fluid in the reactor.
- (c) Calculate  $D_L/uL$  for this system using a variance approach. Use this value to determine the conversion predicted by the dispersion model in the case for which  $\mu Y = 0.451 \text{ h}^{-1}$ . Compare this result with that which would be obtained in an ideal PFBR with the mean residence time obtained in part (b).
- (d) Calculate the conversion that would be obtained in a cascade of CSTRs whose F(t) curve would closely resemble that obtained in part (a).
- (e) Calculate the conversion predicted using the segregated flow model.

- 13.4** A new process has been proposed for ultra high temperature sterilization of whey. The purpose of the process is to destroy 99.99% of the microorganisms in the whey. If very high temperatures are used for short times, this result can be obtained without degrading the protein of the whey, which, besides ruining the food value, gives it a bad taste.

A PFBR has been designed in which steam is injected into the whey as it enters the reactor. At 127°C, a holding time of 7 sec is needed to kill 99.99% of the cells. After the whey passes through the PFBR, the temperature is dropped rapidly to 10°C, where the rate of degradation is negligible. For the whey to meet health and flavor tests, a maximum

of 5% degradation of protein is to be allowed. As a first approximation in your analysis, the reaction is to be treated as isothermal at 127°C.

Another research group previously conducted tests on protein denaturation kinetics and reported the data below. Determine if the data are consistent with the principles of the kinetics of cell death phenomena. Estimate the first-order rate constant for cell death at the conditions employed in the sterilization reactor. Will the proposed process meet the standards for protein degradation?

Typically lactalbumin and lactoglobulin are present in whey at concentrations of 1.5 and 3.0 kg/m<sup>3</sup>, respectively. At 85°C the following data are available on the kinetics of protein degradation, using initial concentrations that are the same as those in whey.

Lactalbumin		Lactoglobulin	
Time, <i>t</i> (s)	Residual protein (%)	Time, <i>t</i> (s)	Residual protein (%)
0	100	0	100
120	82.5	20	83
250	72.5	35	77
360	65	80	67.5
725	47.5	100	58
850	42	125	54.5
960	39	140	52.5
1075	35	160	48
1200	30	180	44.5

Because the whey fed to the sterilization reactor is subject to an indeterminate amount of degradation as it is heated to the sterilization temperature, there are problems associated with the determination of time zero for these reactions. You may assume that the orders of both reactions are integers, although not necessarily the same integer.

Over the temperature range of interest, the activation energy for the lactalbumin degradation reaction is 25.1 kJ/mol while that for the lactoglobulin degradation reaction is 121 kJ/mol.

- 13.5** A classic paper in the evolution of knowledge of the kinetics of biochemical reactions is that of J. Monod [*Ann. Rev. Microbiol.*, **3**, 371 (1942)]. His paper indicates that the kinetics of the growth of *E. coli* are of the form

$$\frac{dx}{dt} = \frac{\mu_{\max} s}{K_s + s} x$$

with  $\mu_{\max} = 1.35 \text{ h}^{-1}$ ,  $K_s = 0.00396 \text{ g/L}$ , and for  $s$  and  $x$  measured in g/L. Consider an experiment in a batch reactor for which the initial concentration of this organism is 2 g (dry weight)/L and the initial concentration of the limiting substrate is 20 g/L.

- (a)** If the yield factor for this reaction is 0.54 g cells/g substrate consumed, prepare plots of the concentrations of cells and the limiting substrate as functions of time.

- (b)** You should also prepare a plot of the growth rate as a function of time to demonstrate the autocatalytic nature of biochemical reactions that produce microorganisms. What is the key feature of such a plot?

- 13.6** S. L. Gilani, G. D. Najafpour, H. D. Heydarzadeh, and H. Zare [*Chem. Ind. Chem. Eng. Q.*, **17**(2), 179 (2011)] modeled the kinetics of the production of xanthan gum by fermentation with *Xanthomonas campestris*. Xanthan gum has multiple applications in the food, cosmetic, and petroleum industries. Fermentations were carried out in 1000-mL Erlenmeyer flasks containing 300 mL of growth medium at temperatures from 25 to 36°C. Agitation was provided by a shaker/incubator. These researchers employed multiple mathematical models in the analysis of their data. For a rate law of the form

$$\frac{dx}{dt} = \mu x$$

with  $\mu = \mu_{\max}[1 - (x/x_{\infty})]$ , where  $x_{\infty}$  is the maximum obtainable concentration of biomass, these investigators reported that the following values of the parameters of the logistic equation provided a good fit of the data for a trial conducted at 30°C with an initial concentration of the limiting substrate glucose equal to 30 g/L:  $x_0 = 0.12 \text{ g/L}$ ,  $\mu_{\max} = 0.09 \text{ h}^{-1}$ ,  $x_{\infty} = 2.1 \text{ g/L}$ , and  $Y_{X/S} = 0.0698 \text{ g dry cells/g substrate}$ . Use these parameter values to estimate the levels of biomass and substrate present in the flask after 48 h of fermentation. If the initial concentration of the xanthan gum is zero and that at 48 h is 15 g/L, what is the average value of the yield coefficient  $Y_{P/X}$  during this period?

- 13.7** This problem has been contributed by Professor Jennifer Reed of the Department of Chemical and Biological Engineering of the University of Wisconsin–Madison. It is used with her permission.

The Mega-Buggy Chemical Corporation is ascertaining the viability of producing dodecanoic acid ( $C_{12}H_{24}O_2$ ) from glucose using a recently discovered bacterium to accomplish this biochemical transformation. The product is intended for use as a biofuel. As a recent hire, you have been assigned the task of estimating the concentration of this fatty acid in the effluent from a chemostat operating at steady state. Your predecessor on this project has determined the following information:

1. The kinetics of cell growth are governed by a Monod rate law for which the kinetic parameters at the operating conditions proposed are  $\mu_{\max} = 0.7 \text{ h}^{-1}$  and  $K_s = 0.2 \text{ g glucose/L}$ .
2. The concentration of glucose in the feed to the chemostat is 10 g/L.
3. The maximum yield of biomass ( $Y_{X/S}$ ) is 0.5 g (dry weight)/g glucose.
4. The maximum yield of dodecanoic acid is 0.35 g acid/g glucose.
5. Cell death and cell maintenance effects are negligible ( $k_d = 0$ ).
6. For present purposes it is desired to operate the chemostat at a dilution rate of  $0.5 \text{ h}^{-1}$ .

7. The specific rate of formation of dodecanoic acid ( $q_p$ ) is given by

$$q_p = \frac{\alpha\mu}{\beta + \mu + \gamma\mu^2} \quad (1)$$

with  $\alpha = 0.044$  g dodecanoic acid/(h·[g dry biomass]),  $\beta = 0.17$  h<sup>-1</sup>, and  $\gamma = 3.4$  h.

[Parameter values are from J. T. Youngquist, R. M. Lennen, D. R. Ranatunga, W. H. Bothfeld, W. D. Marner, II, and B. F. Pfleger, *Biotech. Bioeng.*, **109**(6), 1518–27 (2012).]

- (a) Estimate the concentration of this fatty acid in the effluent when the chemostat is operating at steady state.  
 (b) If the dilution rate is increased to 0.68 h<sup>-1</sup>, what are the effects of this change on the effluent concentration of dodecanoic acid and on the productivity of the chemostat as measured in terms of the total amount of fatty acid produced per unit volume of reactor per unit time? What *physical* circumstances produce these effects?

- 13.8 This problem has been contributed by Dr. Ernesto Favela of the Universidad Autónoma Metropolitana-Iztapalapa, Mexico and is used with his permission.

Consider the growth of *Saccharomyces cerevisiae* in continuous culture under conditions at which the Monod parameters are  $\mu_{\max} = 0.835$  h<sup>-1</sup> and  $K_S = 0.025$  g/L. The yield coefficient  $Y_{X/S}$  is 0.48 g dry biomass/g substrate. Prepare plots of the mass of biomass and substrate present in the bioreactor as functions of the dilution rate of the growth medium for feed concentrations of the limiting substrate equal to 20, 40, and 60 g/L. The feed is sterile (i.e., no microorganisms are present in the feed).

- 13.9 Consider the operation of a chemostat with a working volume of 2 L. The results of preliminary batch cultivation studies of the biochemical reaction and growth medium of interest indicate that the rate law is of the Monod form with  $\mu_{\max} = 0.1$  h<sup>-1</sup>. However, the reported value of the half-saturation constant is suspect, although it is thought to be quite small compared to the concentration of substrate in the feed ( $s_0 \gg K_S$ ). Use this information to obtain a preliminary estimate of the maximum feed flow rate that can be accommodated by this apparatus when it operates at steady state. Employ two approaches: for part A, obtain a crude estimate of the feed rate by assuming that  $K_S$  is zero; then refine this estimate to obtain an improved value of  $K_S$  based on the information in part B. For Part B the effluent concentration of substrate may differ from that of Part A.

- (a) The concentration of the limiting substrate in the feed stream is 0.8 g/L and that in the effluent is 0.10 g/L. If the flow rate of the growth medium is set at 75% of the washout rate, determine the productivity of the chemostat in grams of cells produced per hour. The yield coefficient  $Y_{X/S}$  is 0.38 g dry biomass/g substrate.  
 (b) Verify whether or not the half-saturation constant is truly negligible compared to the concentration of

substrate in the chemostat when it operates at the steady-state condition corresponding to 75% of the fluid flow rate at washout. By what percentage do the answers you obtain in Parts A and B differ?

- 13.10 M. Vázquez and A. M. Martin [*J. Sci. Food Agric.* **76**, 481 (1998)] employed a chemostat to investigate the kinetics of the growth of *Phaffia rhodozyma* on a medium containing peat hydrolysate. On this substrate this yeast produces cells containing an orange–pink carotenoid that is often found in marine animals (e.g., lobsters, shrimp, crab, salmon): namely, astaxanthin (3-3'-dihydroxy-β-β-carotene-4,4-dione). This substance also protects the DNA of these animals from damage by singlet oxygen, so provision of this yeast as a constituent of the diet of salmon is of major interest.

Continuous culture of *P. rhodozyma* was studied in a chemostat in which steady states were achieved within 48 h of introduction of fresh medium. The chemostat has a working volume of 2 L. The growth medium contained the peat hydrolysate at a concentration of 15 g/L. When this substance was the limiting substrate, the rate law was of the general Monod form with  $\mu_{\max} = 0.08$  h<sup>-1</sup> and a half-saturation constant  $K_S = 26.2$  g/L. For present purposes you may neglect cell death and maintenance effects even though the authors indicate that the latter are significant. Use both spreadsheet/graphical and analytical methods of determining the maximum productivity of this reactor.

If the yield coefficient  $Y_{X/S} = 0.54$  g biomass/g substrate, determine the space times of the chemostat that correspond to washout and to maximum productivity of the yeast. What are the effluent concentrations of the hydrolysate and the yeast when the dilution rate is 0.022 h<sup>-1</sup>? What is the corresponding value of the productivity?

- 13.11 This problem has been contributed by Professor Jennifer Reed of the Department of Chemical and Biological Engineering of the University of Wisconsin–Madison. It is used with her permission.

Bacteria can be utilized to degrade phenolic compounds to benign products. Such compounds are frequently present in the effluents from petroleum refineries, petrochemical plants, and pharmaceutical manufacturing plants. However, many phenolic compounds are strong inhibitors of the growth of bacterial cells. One way of circumventing this inhibition problem is to employ a cascade of two CSTBRs of the type considered in Illustration 13.5 and depicted in Figure I13.5. The illustration considers a situation in which two feed streams are fed to the second reactor in the cascade, one being the effluent from the first CSTBR and the second being a supplementary feed stream that can serve to make significant changes in the composition of the aqueous medium. The composition of the growth medium in the first reactor is chosen so as to promote the growth of bacterial cells; there are no phenolic compounds present in this medium. By contrast, the composition of the aqueous phase in the second CSTBR is formulated so that its essential functions are to maintain the cells in a viable but nongrowing state and to provide a route for the waste waters containing phenolic compounds to proceed

directly to the second CSTBR. It is also important that the medium in the second reactor optimizes conditions for degradation of the phenolic compounds. As part of your engineering responsibilities you are charged with analysis of the viability of using the two-stage cascade under the conditions indicated below for remediation of the process effluent. Comment on your results.

Specifications and potentially helpful information for use in analysis of the cascade:

1. The CSTBRs are not necessarily identical in size.
2. Of the glucose that is fed to the first CSTBR in the cascade, 95% (mass basis) is converted to biomass in this bioreactor.
3. Of the phenolic compounds that are fed to the second CSTBR in the cascade, 99% (mass basis) is converted to benign products in this bioreactor.
4. There are no phenolic compounds in the effluent from the first CSTBR. The concentration of phenolics in the supplementary feed stream to the second CSTBR is 1.2 g/L.
5. Growth of the bacterial cells occurs only in the first CSTBR. The kinetics of cell growth are described by the Monod equation with  $\mu_{\max} = 0.6 \text{ h}^{-1}$  and  $K_S = 4 \text{ g/L}$ . In the second CSTBR the phenolic compounds are such strong inhibitors of cell growth that no growth occurs in this bioreactor even though all of the incoming bacterial cells remain alive. The yield coefficient for conversion of substrate glucose to biomass ( $Y_{X/S}$ ) is 0.5 g (dry weight) cells/g glucose.
6. The feed to the first CSTBR is sterile and is characterized by a volumetric flow rate of 10 L/h. The limiting substrate is present at a concentration of 40 g/L.
7. The effluent from the first CSTBR flows directly to the second reactor, where it is mixed with the incoming supplementary feed stream. The latter stream contains 1.2 g/L of phenolics and enters at a rate of 2 L/h.
8. In the second CSTBR the specific rate at which the degradation proceeds is 0.085 g phenolics/(g cells·h). This parameter is functionally similar to a  $q$ -value but refers to the rate of degradation of a solute rather than a rate of formation of a desired product. The degradation reaction has no impact on cellular growth processes.

What is the required size of each reactor? What is the concentration of biomass leaving each reactor? What is the concentration of the limiting substrate leaving the first CSTBR?

- 13.12** Sue Dent is assessing her ability to analyze data for the kinetics of cell growth in a well-mixed batch reactor. She recognizes that it would be preferable to employ a chemostat to investigate the kinetics of cell growth, but all that is currently available to her is a batch reactor. Her data correspond to the fermentation of an unknown microorganism identified as RUcrazy. Data were obtained using a batch reactor with a working volume of 2 L. She has conducted a series of laboratory scale trials at 25°C using an inoculum that has been acclimated in a growth medium that is identical to that employed in her most recent trial. Consequently, she suggests that any data analysis can neglect the induction time of the microorganism relative to the times at which she took

samples of the reactor contents and quenched them to prevent further cell growth.

Time (h)	Limiting substrate (g/L)	Biomass (g dry biomass/L)
0	40	2
12	36	5
24	28	10
36	18	18
48	10	23
60	5	27

Sue proposes to analyze these data to determine whether or not her analysis yields kinetic parameters for a Monod rate law that are consistent with the parameters reported in Example 11.1 of J. M. Santamaría, J. Herguido, M. A. Menéndez, and A. Monzón, *Ingeniería de Reactores*, Editorial Sintesis, Madrid, 1999. Does the Monod model provide a good fit of the data? Comment on your faith in the validity of the kinetic parameters that you would determine from the fit of an appropriate form of the following equation to the data:

$$\mu_{\max} t_{\text{batch}} = \left\{ \frac{K_S}{s_0 + [X_0 / (V_R Y_{X/S})]} + 1 \right\} \ln \left( \frac{X}{X_0} \right) - \frac{K_S}{s_0 + [X_0 / (V_R Y_{X/S})]} \ln \left( \frac{s}{s_0} \right) \quad (1)$$

where  $X$  and  $X_0$  refer to the total mass of cells present at times  $t$  and zero, respectively, in a reactor with a working volume  $V_R$ .

- 13.13** Consider a cascade of three CSTBRs that may differ in volume from one another. Within any individual tank, the volume of the aqueous phase remains constant as the biochemical reactions proceed. The corresponding volumes of the aqueous phase are  $V_{R1}$ ,  $V_{R2}$ , and  $V_{R3}$ . Each reactor is supplied with a feed stream containing the limiting substrate at a concentration  $s_0$ . The volumetric flow rates of these feed streams are  $V_1$ ,  $V_2$ , and  $V_3$ , for the first, second, and third reactors, respectively. In addition, the first reactor is fed at a volumetric flow rate  $V_0$  with a sterile growth medium ( $x_0 = 0$ ) that does not contain the limiting substrate ( $s^* = 0$ ). The second and third bioreactors are fed with the effluent from the preceding CSTBR. The concentrations of the limiting substrate in reactors 1, 2, and 3 are  $s_1$ ,  $s_2$ , and  $s_3$ . The corresponding concentrations of the microorganism in these CSTBRs are  $x_1$ ,  $x_2$ , and  $x_3$ . The yield coefficient  $Y_{X/S}$  is the same in all three CSTBRs (0.48).

- (a) For each reactor in the cascade, write the general time-dependent forms of the material balance equations for the microorganism and the limiting substrate. Denote the rates of production of the microorganism per unit volume of working fluid in reactor  $i$  by  $R_{xi}$  and the corresponding rate of consumption of the limiting substrate by  $-R_{si}$ .
- (b) Convert the equations presented in part (a) to their steady-state forms and then manipulate them to obtain relations for the six rate expressions of interest ( $R_{xi}$  and  $-R_{si}$  for values of  $i$  from 1 to 3).

(c) Now consider the mode of operation in which the concentration of the limiting substrate in each reactor is  $s$  ( $s_1 = s_2 = s_3 = s$ ). Operation of the cascade under these conditions is of special interest when the biochemical reactions are subject to substantive substrate inhibition effects. Develop the corresponding relations for the rates of consumption of the limiting substrate in each CSTBR. Express your results in terms of the individual parameters  $V_{R1}$ ,  $V_{R2}$ ,  $V_{R3}$ , the various volumetric flow rates, the substrate concentrations  $s_0$  and  $s$ , and the yield coefficient  $Y_{X/S}$ .

(d) If the rate law for the reaction of interest is of the Monod form, determine the steady-state concentrations of biomass in each of these reactors for the following combination of process parameters:

Reactor volumes (in liters):

$$V_{R1} = 5,000; V_{R2} = 8,000; V_{R3} = 12,000$$

Volumetric flow rates (in liters/hr):

$$\mathcal{V}_0 = 1,000; \mathcal{V}_1 = 600; \mathcal{V}_2 = 1,000; \text{ and } \mathcal{V}_3 = 1,500$$

Kinetic parameters:

$$\mu_{\max} = 1.8 \text{ h}^{-1}; \quad K_S = 0.5 \text{ g/liter}$$

Concentrations of limiting substrate:

$$s_0 = 80 \text{ g/liter}; \quad s = 0.8 \text{ g/liter}$$

Note that for this component of the problem, you are asked to install the reactors in a configuration that has the smallest reactor first and the largest reactor last, as is the normal arrangement for conventional homogeneous reactions in which there is no autocatalytic effect.

(e) Now consider the reverse order of arrangement of the CSTBRs in the cascade and corresponding modifications of the volumetric flow rates so that for this component of the problem the new process parameters are:

Reactor volumes (in liters):

$$V_{R1} = 12,000; V_{R2} = 8,000; V_{R3} = 5,000$$

Volumetric flow rates (in liters/hr):

$$\mathcal{V}_0 = 1,000; \mathcal{V}_1 = 1,500; \mathcal{V}_2 = 1,000; \text{ and } \mathcal{V}_3 = 600$$

Other parameters remain the same.

**13.14** This problem has been contributed by Dr. Ernesto Favela of the Universidad Autónoma Metropolitana-Iztapalapa, Mexico and is used with his permission.

Studies of the production of an organic acid using *Aspergillus niger* in continuous cultivation with recirculation of the biomass indicate that under the conditions employed  $\mu_{\max} = 0.835 \text{ h}^{-1}$  and  $K_S = 0.10 \text{ g/L}$ . The yield coefficient  $Y_{X/S}$  is  $0.01 \text{ g dry biomass/g substrate}$  and  $Y_{P/S}$  is  $0.48 \text{ g/g}$ . Use a spreadsheet to prepare plots of the concentrations of biomass, substrate, and product leaving the CSTBR, as well as the productivity of the process,

as functions of the dilution rate of the growth medium. The concentration of substrate in the fresh feed stream is  $80 \text{ g/L}$ . Determine the concentrations of biomass, substrate, and product in the effluent from the CSTBR and a quasi optimum value for the fraction of the effluent subjected to recirculation when operating at a dilution rate equal to  $2\mu_{\max}$ . Comment on the expected effects of changes in the recycle ratio and the concentration enrichment factor associated with the process. Use your spreadsheet to start with a base case for which the enrichment factor is 2.0 and then modify this factor to ascertain what happens when you employ values of 1.25 and 3.0. Your base-case analysis should yield a recycle ratio that maximizes the productivity at a dilution rate equal to  $2\mu_{\max}$ . Comment.

**13.15** Stuart Dent is studying the effects of cell recycle on steady state productivity for culture of a yeast strain in a CSTBR with a working volume of  $20 \text{ L}$ . The growth medium contains  $30 \text{ g/L}$  of the limiting substrate and the sterile fresh feed stream is supplied at a rate of  $25 \text{ L/h}$ . Determine the concentrations of yeast ( $x$ ) and substrate ( $s$ ) in the effluent from the process depicted in Figure P13.15.

The subscripts on the usual process parameters indicate the positions in the process to which these parameters refer. The kinetics of yeast growth can be described by a Monod rate expression with  $\mu_{\max} = 0.625 \text{ h}^{-1}$  and  $K_S = 2 \text{ g/L}$ . Cell death and cell maintenance effects are negligible, as is formation of products other than yeast cells. The yield coefficient  $Y_{X/S}$  is  $0.44$ . The effluent from the bioreactor flows directly to a membrane filtration apparatus. The membrane is completely permeable to the substrate, so the concentrations of the substrate in the CSTBR, the effluent from the bioreactor, and the permeate from the membrane and in the recycle stream are all identical. The membrane rejects a substantial proportion of the yeast cells so that the ratio of the concentration of yeast in the recycle stream is a factor of 4 larger than that in the effluent from the CSTBR. Volumetric expansion and contraction effects may be considered negligible.

(a) Determine the concentrations of yeast and substrate in the effluent for the overall process, the reactor effluent, and in the recycle stream as functions of the recycle ratio  $R$  when operating at the specified values of the process parameters.

(b) Suppose that the pump feeding the membrane separation apparatus malfunctions so that this apparatus fails to

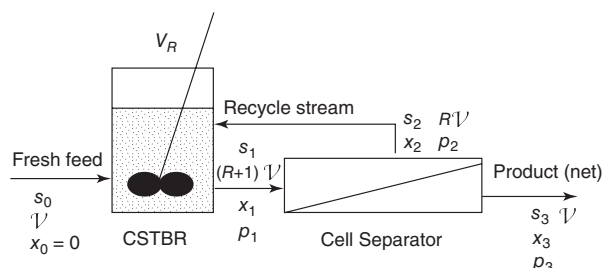


**Figure P13.15** Continuous culture of yeast in a CSTBR with recycle of cells using a membrane separation device from which the retentate is returned to the CSTBR.

operate and the flow rate of the recycle stream drops to zero. If a valve position is switched by the process control system so that the reactor effluent now becomes the process effluent stream, determine the new steady-state concentrations  $x_1$  and  $s_1$  as well as the observed shift in the productivity of the process.

- 13.16** Consider the growth of a generic microorganism in a small industrial-scale CSTBR (volume =  $0.5 \text{ m}^3$ ) that is operating at steady state. The growth of this microorganism obeys Monod kinetics with  $K_s = 1.23 \text{ kg/m}^3$  and  $\mu_{\max} = 0.202 \text{ h}^{-1}$ . The feed to the reactor is sterile, and the concentration of the limiting substrate in this stream is  $80 \text{ kg/m}^3$ . The reactor is being employed to produce a secondary metabolite P whose yield coefficient  $Y_{P/S}$  is  $0.072 \text{ g product/g substrate}$ .

- Determine the functional dependence of the effluent concentration of the microorganism on the volumetric flow rate of the growth medium. Present your results in both analytical and graphical forms.
- At what flow rate does the effluent concentration of the microorganism become zero so that the microorganism can no longer produce the desired product?
- Prepare a plot of the effluent concentration of product P as a function of the volumetric flow rate. In addition, generate a plot of the total productivity of the system versus the flow rate. Use both an analytical and a graphical approach to determine the volumetric flow rate that optimizes the productivity.

- 13.17** This problem has been adapted from a contribution of Professor Jennifer Reed of the Department of Chemical and Biological Engineering of the University of Wisconsin–Madison, with her permission.

Consider the task of designing a cascade of two CSTBRs for fermentation of a generic microorganism in a growth medium for which the limiting substrate is solute S. In each CSTBR the rate law is of the Monod form with  $\mu_{\max} = 0.35 \text{ h}^{-1}$  and  $K_s = 0.4 \text{ g/L}$ . The concentration of the limiting substrate in the feed stream ( $s_0$ ) is  $80 \text{ g/L}$ . The feed is sterile ( $x_0 = 0$ ) and the only point at which the substrate enters the cascade is the entrance to the first CSTBR. The yield coefficient  $Y_{X/S}$  is 0.45. The flow rate of the entering growth medium is  $500 \text{ L/h}$ . The specification for the concentration of the limiting substrate in the effluent from the second CSTBR is  $1.6 \text{ g/L}$ .

Simon LeProf desires to consider several options for the design of this cascade. He has assigned Sue Dent the task of determining the minimum total volume requirement for three different cases of potential interest:

- The first CSTBR operates in a manner such that the rate of production of biomass in this reactor is maximized. The second CSTBR is sufficiently large to meet the specification of the desired effluent concentration of substrate.
- The total volume of the cascade is minimized.
- Each reactor has the same volume.

For each case determine the volume of each reactor and the compositions (concentrations of the limiting substrate and the microorganism) of each process stream. Prepare a table summarizing the results of your three analyses to facilitate comparisons of the significant results.

- 13.18** This problem has been adapted from a contribution of Professor Jennifer Reed of the Department of Chemical and Biological Engineering of the University of Wisconsin–Madison, with her permission.

The fact that the rates of biochemical transformations increase as the concentration of the organism increases is indicative of autocatalytic behavior that provides opportunities for engineers to consider a variety of modes of operation to enhance the performance (and productivity) of a CSTBR facility. One fruitful approach is to do a partial separation and concentration of the cells contained in the effluent from the CSTBR (see Figure P13.18) and recycle the resulting process stream back to the CSTBR, where it is mixed with contents of the reactor.

Recovery of cells can be accomplished using one of several alternative unit operations, such as centrifugation, membrane filtration, or settling. Subscripts are employed in the figure to identify the usual process variables at particular points in the diagram. We employ the *recycle ratio* ( $R$ ) to represent the ratio of the volumetric flow rate of the suspension of cells leaving the separation device to the volumetric flow rate of the net product stream. The symbol  $\psi$  represents the ratio of the concentration of biomass in the recycle stream to that in the effluent from the CSTBR. You may assume that the system is operating at steady state and that the feed is sterile.

For purposes of the analysis, you may assume that cell death and cell maintenance metabolism effects are negligible, as is formation of any products other than biomass. The concentration of substrate in the feed is  $25 \text{ g/L}$  and the yield coefficient  $Y_{X/S}$  is  $0.52 \text{ g cells (dry weight)/g substrate}$ . The kinetics of cell growth are characterized by a rate law of the Monod form with  $\mu_{\max} = 0.6 \text{ h}^{-1}$  and  $K_s = 0.5 \text{ g/L}$ . The dilution rate for the CSTBR is  $0.95 \text{ h}^{-1}$  and the concentration factor  $\psi$  is 2.5.

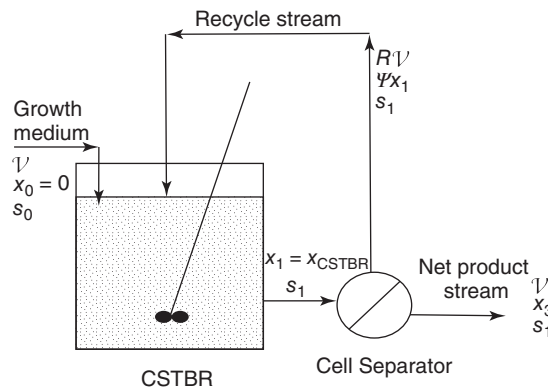


**Figure P13.18** Schematic flow sheet for a process coupling use of a CSTBR and a generic unit operation for separation and concentration of a suspension of cells for recycle to enhance reactor productivity.

The densities of the feed and net product streams are substantially the same. If the recycle ratio is 0.45, what are the steady-state concentrations  $x_1, x_2, x_3$ , and  $s_1$ ?

- 13.19** The use of submerged aerobic fermentation of a strain of the fungus *Aspergillus niger* is a much studied technology for the production of citric acid. In this and other commercial fermentation processes, fed batch modes of operation of stirred-tank reactors find extensive use in the production of a variety of amino acids, antibiotics, enzymes, and solvents (84). Citric acid is a primary metabolite that finds a multiplicity of applications in the food industry. In this application the growth medium is often formulated so that cane or beet molasses can be used as the substrate. For pedagogical reasons we have elected to employ kinetic parameters for a hypothetical strain of a related fungus, *A. bracadabra*, to simplify analysis of fed batch (also known as extended batch) operation. This approach permits us to utilize the concepts presented in Section 13.2.1.3 and in the book by Lim and Shin (15). Our interest in this problem is in the analysis of the behavior of a stirred-tank reactor that is employed first in a batch mode of operation but which subsequently transitions to semibatch operation in which it is fed continuously with a growth medium. However, for fed batch operation, no growth medium is removed from the reactor at any time while biochemical reactions are occurring.

Our task is to generate trajectories of the concentrations of *A. bracadabra*, citric acid, and sucrose (and their masses in the reactor) as time evolves during fed batch operation. The volume of the aqueous phase (growth medium) is constant during the batch stage of the process but increases continuously during the feeding stage. Several strategies exist for the manner in which the substrate for the culture is supplied, depending on the particular fermentation of interest. Some of these are discussed by Lim and Shin (15). The strategy employed in a particular situation is chosen by the design engineer on the basis of the characteristics of the particular fermentation of interest and associated economic factors.

Carry out a reactor design analysis of the fed batch process described below in which the volumetric flow rate of the entering feed stream is held constant. Use the following data and assumptions as guides in your analysis

- Immediately after inoculation the volume of the growth medium present in the stirred-tank reactor is 20 L. The level of the *A. bracadabra* fungus (dry basis) suspended in the growth medium is 40 g/L and the concentration of sucrose in the molasses-based growth medium is 140 g/L. The lag time associated with the growth of the *A. bracadabra* fungus in the strictly batch phase of the process is 8.0 h. No citric acid is present in the stirred tank reactor at the time of inoculation.
- The rate of growth of *A. bracadabra* obeys a Monod rate law with  $K_S = 0.15$  g/L and  $\mu_{\max} = 0.024$  h<sup>-1</sup>. The yield of citric acid (C) based on the amount of sucrose consumed ( $Y_{C/S}$ ) is 0.65 g/g. The corresponding yield coefficient for the biomass ( $Y_{X/S}$ ) is 0.272 g/g. Production of citric acid may be assumed to be growth-associated.

The transition from strictly batch operation to fed batch operation occurs when the concentration of sucrose drops

to 1.5 g/L. Determine the time elapsed since inoculation at which this transition is made. The extended batch phase of the process is terminated when the volume of the suspension in the reactor reaches 150 L. Following this step the fungus continues to grow until all of the substrate present at that time is consumed. At that time the production process is terminated. There are several approaches that one can employ in determining the point at which the transition should be made from strictly batch to fed batch operation. These approaches present problems in optimization and process control that are beyond the scope of this book but are treated in extensive detail in the archival literature as well as in the book by Lim and Shin (15). Our specification of a point of transition to fed batch operation at a substrate concentration of 1.5 g/L is somewhat arbitrary but not unrealistic in terms of the type of conversion level that might be employed in practical situations. This specification is advantageous in terms of drastically simplifying the mathematical analysis necessary to develop the equations required to generate speciation plots over the range of times that are of interest from a pedagogical standpoint.

- Prepare plots of the concentrations of the substrate sucrose, the product citric acid, and the biocatalyst *A. bracadabra* versus time for times between the instant of inoculation and the time the volume of the broth reaches 150 L. Indicate the total quantities (masses) of citric acid and fungus produced during both the batch and extended-batch stages of operation. What is the total mass of substrate consumed in each phase of the process? You may neglect consumption of substrate for cell maintenance activities.
- To prolong the fed-batch phase, use a concentrated solution of the limiting substrate (212 g/L) beginning at the moment strictly batch operation is terminated. The volumetric flow rate of the feed stream is to be held constant until the capacity of the reactor is reached. After the batch phase of the process and again after termination of the feed stream, the microorganism continues to grow at a rate that reflects the rate of consumption of the substrate. Use a spreadsheet to prepare a plot that indicates how the total mass of fungus produced during the sequence of batch/semibatch/batch operation varies with time when the reactor is operated according to this protocol. Time zero refers to the instant that the contents of the reactor are inoculated with the fungus. Relative to strictly batch operation during the first stage, by how much does the production of cells increase if the fed-batch segment of the cycle is employed until the working capacity of the stirred tank is reached? How much of each species is formed during the second batch stage? Note that no growth medium ever leaves the stirred tank reactor until the biochemical reaction is terminated when the second batch stage leads to complete consumption of the limiting substrate.

#### Additional hints concerning the solution to problem 13.19 and other semibatch reactor analyses

The material in this book provides the necessary background for solving the problems contained therein. However, there

are a number of nontraditional methods employed in the mathematical analysis of bioreactors, especially those employed in a semibatch mode of operation. For this reason readers may find it helpful to consider the material below in conducting an analysis of the fed batch process of interest in problem 13.19.

For a well-agitated reactor being used to carry out the culture of a microorganism in a working volume ( $V$ ) during the feeding stage of fed batch operation, the material balance equation for total mass can be expressed as

$$\rho_1 \frac{dV}{dt} = \mathcal{V}_0 \rho_0 \quad (\text{A})$$

Subscripts 1 and 0 refer to the properties of the growth medium in the reactor and in the feed stream, respectively.

If one recognizes that the densities of the growth medium in the reactor and that of the incoming feed stream are essentially the same, equation (A) becomes

$$\frac{dV}{dt} = \mathcal{V}_0 \quad (\text{B})$$

In the general case, the volumetric feed rate can be a function of time, even though in the context of problem 13.19 we shall consider it to be constant. For this case integration yields

$$V = V_0 + \int_{t_{\text{FB}}}^t \mathcal{V}_0 \, dt = V_0 + \mathcal{V}_0(t - t_{\text{FB}}) \quad (\text{C})$$

where  $t_{\text{FB}}$  is the time at which fed batch operation is initiated. Moreover at times greater than  $t_{\text{FB}}$ ,

$$V = V_0 \left[ 1 + \left( \frac{\mathcal{V}_0}{V_0} \right) (t - t_{\text{FB}}) \right] = V_0[1 + D_0^*(t - t_{\text{FB}})] \quad (\text{D})$$

Even though there is no effluent from the stirred tank reactor during processing, one can consider the ratio ( $\mathcal{V}_0/V_0$ ) as a type of dilution rate. This parameter has the dimensions of inverse time and decreases with increasing time to reflect that fact that the volume of the growth medium increases with increasing time:

$$\begin{aligned} D^* = D^*(t) &= \frac{\mathcal{V}_0}{V(t)} = \frac{\mathcal{V}_0}{V_0[1 + D_0^*(t - t_{\text{FB}})]} \\ &= \frac{D_0^*}{[1 + D_0^*(t - t_{\text{FB}})]} \end{aligned} \quad (\text{E})$$

Equations (D) and (E) are valid for the period

$$t_{\text{FB}} < t < t_{\text{FB}} + (V_C - V_0)/\mathcal{V}_0 \quad (\text{F})$$

where  $V_C$  is the capacity (maximum working volume) of the stirred tank for the growth medium.

If the feed for the fed batch phase of the process is sterile ( $x_0 = 0$ ) and if the Monod rate law is applicable, the material balance for the fungus becomes:

$$\begin{aligned} \frac{d(Vx_1)}{dt} &= \mathcal{V}_0 x_0 + Y_{X/S} \left( \frac{\mu_{\text{max}} s_1}{K_S + s_1} \right) (Vx_1) \\ &= Y_{X/S} \left( \frac{\mu_{\text{max}} s_1}{K_S + s_1} \right) (Vx_1) \end{aligned} \quad (\text{G})$$

This equation can also be expressed in terms of the specific growth rate  $\mu$  as

$$\frac{d(Vx_1)}{dt} = Y_{X/S} \mu(Vx_1) \approx Y_{X/S} \mu_{\text{max}} (Vx_1) \quad (\text{H})$$

where we have noted that for the situation in which over the vast majority of the range of accessible concentrations  $s_1 \gg K_S$ . Thus the Monod expression for the specific reaction rate degenerates to the constant  $\mu_{\text{max}}$ . For the specified value of  $K_S = 0.15 \text{ g/L}$ , this approach provides a good approximation for  $\mu$  even when the conversion exceeds 98% of the original substrate content of the CSTBR. For times greater than  $t_{\text{FB}}$  we can say that for the balance on the fungus it is appropriate to write equation (H) in the form

$$\frac{d(Vx_1)}{(Vx_1)} = \frac{dX}{X} = Y_{X/S} \mu_{\text{max}} \, dt \quad (\text{I})$$

where  $X$  is the total mass of *A. bracadabra* in the reactor.

The dependence of the total mass of fungus suspended in the growth medium on time can be determined by integration of equation (I) subject to the constraint that at  $t = t_{\text{FB}}$ ,  $X = X_{\text{FB0}}$ . Consequently,

$$\ln \left( \frac{X_{\text{FB}}}{X_{\text{FB0}}} \right) = Y_{X/S} \mu_{\text{max}} (t - t_{\text{FB}}) \quad (\text{J})$$

or

$$X = X_{\text{FB0}} e^{Y_{X/S} \mu_{\text{max}} (t - t_{\text{FB}})} \quad (\text{K})$$

The corresponding concentration of *A. bracadabra* in suspension in the growth medium can then be determined using equations (C) and (K):

$$x_1 = \frac{X(t)}{V(t)} = \frac{X_{\text{FB0}} e^{Y_{X/S} \mu_{\text{max}} (t - t_{\text{FB}})}}{V_0[1 + D_0^*(t - t_{\text{FB}})]} = \frac{x_{\text{FB0}} e^{Y_{X/S} \mu_{\text{max}} (t - t_{\text{FB}})}}{1 + D_0^*(t - t_{\text{FB}})} \quad (\text{L})$$

One way of expressing the material balance on the total mass of substrate present in the reactor during the fed batch mode of operation is

$$\frac{d(Vs_1)}{dt} = V \frac{ds_1}{dt} + s_1 \frac{dV}{dt} = \mathcal{V}_0 s_F - \left( \frac{\mu_{\text{max}} s_1}{K_S + s_1} \right) (x_1 V) \quad (\text{M})$$

where  $s_F$  is the concentration of substrate in the feed stream. Combination of equations (B) and (M) then yields

$$\frac{ds_1}{dt} = \frac{\mathcal{V}_0}{V} (s_F - s_1) - \left( \frac{\mu_{\text{max}} s_1}{K_S + s_1} \right) x_1 \quad (\text{N})$$

If we restrict our consideration to systems in which  $s_1$  significantly exceeds  $K_S$ , we can again approximate expression (N) as

$$\frac{ds_1}{dt} = \frac{\mathcal{V}_0}{V} (s_F - s_1) - \mu_{\text{max}} x_1 \quad (\text{O})$$

If one uses the principles of stoichiometry to relate  $x_1$  to  $s_1$ , one could employ that relation in equation (O), separate variables, and integrate to obtain the relation between  $s_1$  and the elapsed time ( $t - t_{\text{FB}}$ ) for operation in the fed-batch mode. Because that approach is cumbersome, we shall employ a somewhat different route based on an analysis described by Lim and Shin (15).

One way of expressing the material balance on the total mass of substrate in the reactor is

$$\frac{d(Vs_1)}{dt} = \mathcal{V}_0 s_F - \left( \frac{\mu_{\max} s_1}{K_S + s_1} \right) \left( \frac{Vx_1}{Y_{X/S}} \right) \quad (P)$$

As we have noted above, we can approximate the Monod term as  $\mu_{\max}$  because the substrate concentrations greatly exceed the value of  $K_S$ . Under these circumstances we can say that the total masses of substrate and biomass obey the relation

$$\frac{d(Vs_1)}{dt} = \mathcal{V}_0 s_F - \mu_{\max} \frac{X}{Y_{X/S}} \quad (Q)$$

Each term in this equation can be integrated under the assumptions that  $\mathcal{V}_0$ ,  $s_F$ ,  $\mu_{\max}$ , and  $Y_{X/S}$  are all invariant.

$$(Vs_1)|_t - (Vs_1)|_{t_{FB}} = \mathcal{V}_0 s_F (t - t_{FB}) - \frac{\mu_{\max}}{Y_{X/S}} \int_{X_{FB0}}^X X \, dt \quad (R)$$

in which the integral over time can be evaluated using equation (K).

Now

$$\begin{aligned} \int_{t_{FB}}^t X \, dt &= \int_{t_{FB}}^t X_{FB0} e^{Y_{X/S} \mu_{\max} (t - t_{FB})} \, dt \\ &= \frac{X_{FB0} e^{Y_{X/S} \mu_{\max} (t - t_{FB})} - X_{FB0}}{Y_{X/S} \mu_{\max}} \end{aligned} \quad (S)$$

where  $t_{FB}$  is the time at which the transition from strictly batch to fed-batch operation takes place. Combination of equations (R) and (S) yields

$$\begin{aligned} (Vs_1)|_t &= S_1(t) = (S_1)|_{t_{FB}} + \mathcal{V}_0 s_F (t - t_{FB}) \\ &\quad - \frac{X_{FB0} \{ e^{[Y_{X/S} \mu_{\max} (t - t_{FB})]} - 1 \}}{Y_{X/S}} \end{aligned} \quad (T)$$

We can calculate  $s_1$  at various times using equations (C) and (T) to determine the ratio of  $S_1(t)$  to  $V(t)$ .

If the yield coefficient for the product citric acid is constant, a similar strategy can be employed to derive the equations that describe the trajectories of the concentration and total mass of this species as functions of time. If we represent the concentration and total mass of citric acid by  $c$  and  $C$ , respectively, the material balance for this species during the fed-batch stage can be expressed as

$$\begin{aligned} \frac{d(Vc_1)}{dt} &= Y_{C/S} \left( \frac{\mu_{\max} s_1}{K_S + s_1} \right) Vx_1 \approx Y_{C/S} \mu_{\max} X \\ &= Y_{C/S} \mu_{\max} X_{FB0} e^{Y_{X/S} \mu_{\max} (t - t_{FB})} \end{aligned} \quad (U)$$

where we have recognized that no citric acid is present in the feed, that no product is removed, that we can reduce the Monod term to  $\mu_{\max}$  (because  $s_1 \gg K_S$ ), and that equation (K) is applicable. The rate of accumulation of this metabolite is thus equal to its rate of production. Equation (U) is subject to the constraint that at time  $t_{FB}$ , the concentration of citric acid is equal to that prevailing at the end of the strictly batch stage of the process. Integration in the light of this constraint then gives

$$C_t - C_{t_{FB}} = Y_{C/S} \mu_{\max} \int_{t_{FB}}^t X_{FB0} e^{Y_{X/S} \mu_{\max} (t - t_{FB})} \, dt \quad (V)$$

Combination of equations (K) and (U) yields

$$C_t = C_{t_{FB}} + X_{FB0} [e^{Y_{X/S} \mu_{\max} (t - t_{FB})} - 1] \quad (W)$$

The corresponding concentration of citric acid is

$$\frac{C_t}{V} = \frac{C_{t_{FB}} + X_{FB0} [e^{Y_{X/S} \mu_{\max} (t - t_{FB})} - 1]}{V_0 + \mathcal{V}_0 (t - t_{FB})} \quad (X)$$

Readers can employ machine computation to prepare appropriate plots (masses and concentrations) of the trajectories of all three species that apply to each of the three stages of fed batch operation employed here, as well as a composite plot of the concentrations of the three species as functions of time.

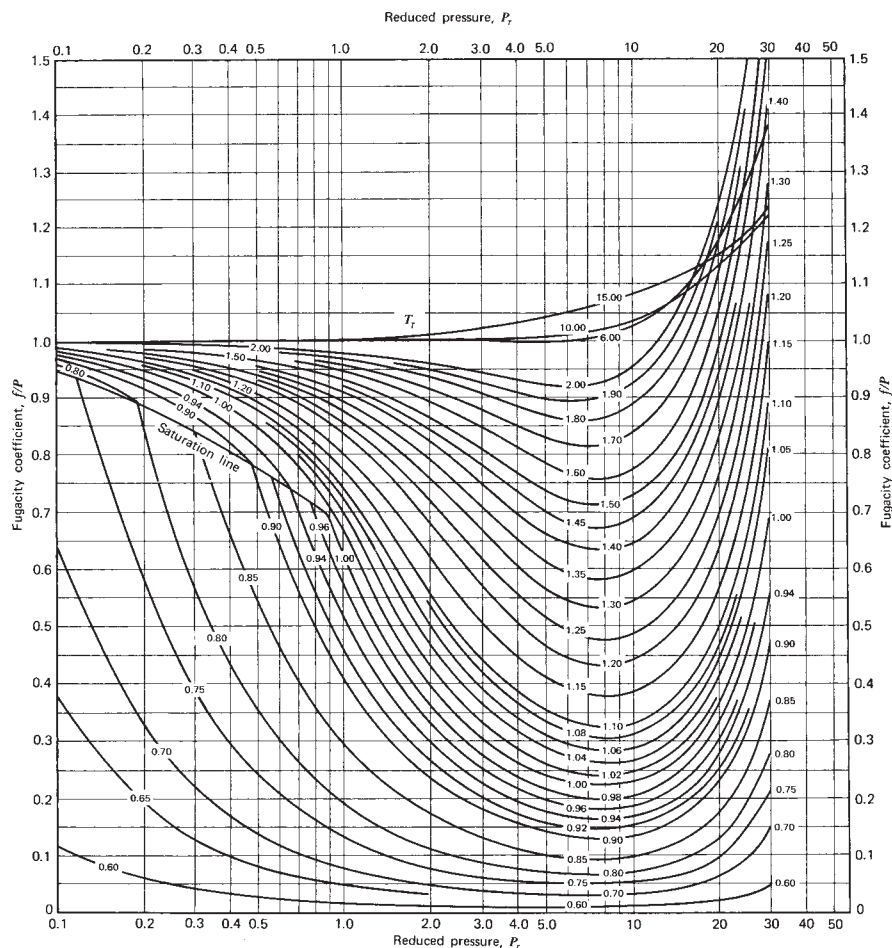
At this point, our material balance analysis has led to expressions for several parameters of interest, each of which is expressed as a function of time.

Variable	Equation(s)
$V(t)$ volume of growth medium	C
$X(t)$ total biomass	K
$x(t)$ concentration of fungus	C and K
$S(t)$ total substrate	R
$s(t)$ concentration of substrate	T
$C(t)$ total citric acid	U
$c(t)$ concentration of citric acid	U and C

For times in excess of that at which the capacity of the stirred tank is reached, one can conduct a strictly batch analysis to determine the instantaneous mass and concentration of a particular species. Use of machine computation to determine these parameters leads to the desired result.

# Appendix A

## Fugacity Coefficient Chart



Generalized fugacity coefficients of pure gases and liquids ( $Z_c = 0.27$ ). (Reprinted from O. A. Hougen, K. M. Watson, and R. A. Ragatz, *Chemical Process Principles Charts*, 3rd ed. Copyright © 1964. Reprinted by permission of John Wiley & Sons, Inc.)

Generalized fugacity coefficients of pure gases and liquids for a critical compressibility ( $Z_c$ ) of 0.27. The critical properties of most species of interest to students are normally readily available via a search of the Web or standard handbooks. The reduced pressures ( $P_r$ ) and

temperatures ( $T_r$ ) indicated on the fugacity coefficient chart are equal to the ratio of the actual absolute temperature or pressure to the corresponding critical property ( $T_c$  or  $P_c$ ):

$$T_r = T/T_c \quad P_r = P/P_c$$

# Appendix B

---

## Nomenclature

<i>Symbol</i>	<i>Meaning</i>
$a$	activity
$a$	external (superficial) surface area
$a, a', a''$	cell growth coefficients
$a_V$	gas-liquid interfacial area per unit volume of liquid
$A$	preexponential factor in rate constant
$A_i$	representative chemical species
$C$	concentration
$C_{Ai}$	concentration of reactant A at time $t_i$ or in effluent from reactor $i$
$C_p$	constant-pressure heat capacity
$C_l^*$	hypothetical concentration of gas in the liquid phase
$C^*$	reactant concentration at time zero in a CSTR operating under transient conditions
$D$	diameter
$D$	dielectric constant
$D$	dilution rate
$D_{AB}$	bulk diffusivity
$D_K$	Knudsen diffusivity
$\mathcal{D}$	dispersion or diffusivity parameter
$\mathcal{D}_{Am}$	pseudo-binary diffusivity of species A in a multicomponent gas mixture
$\mathcal{D}_c$	combined diffusivity
$E$	energy or activation energy
$E_c$	relative kinetic energy directed along the line of centers in a collision (on a per mole basis)
$E_{\text{diffusion}}$	activation energy for diffusion
$E_0$	energy increase accompanying reaction at absolute zero
$E_0$	initial enzyme concentration
$f$	fraction conversion
$f_i^0$	fugacity of pure species $i$ at pressure $P$
$\hat{f}_i$	fugacity of species $i$ as it exists in the reaction mixture
$f_M$	friction factor
$(f/P)_i$	fugacity coefficient for species $i$
$F$	molal flow rate
$F'_A$	hypothetical molal flow rate of species A corresponding to a stream in which none of the A has reacted
$F(t)$	cumulative residence time distribution function
$\mathcal{F}$	ratio of reaction rate for poisoned catalyst to that for unpoisoned catalyst
$g$	gas phase
$G$	Gibbs free energy
$G$	mass velocity
$h$	specific enthalpy
$h_c$	convective heat transfer coefficient
$h_i$	Thiele modulus for $i$ th-order reaction
$h_p$	Thiele modulus for poisoned catalyst
$h_T$	Thiele modulus

Symbol	Meaning
$H$	Henry's law constant
$j_D$	Chilton–Colburn factor for mass transfer
$j_H$	Chilton–Colburn factor for heat transfer
$J_i$	Molar flux of species $i$ relative to the molar average velocity
$k$	reaction rate constant
$k$	thermal conductivity
$k_B$	Boltzmann constant
$k_c$	mass transfer coefficient
$k_d$	pseudo first-order rate constant for cell death
$k_{em}$	pseudo first-order rate constant for endogenous metabolism
$k_f$	thermal conductivity of bulk fluid
$k_g$	mass transfer coefficient for the gas phase
$k_G$	mass transfer coefficient defined
$k_{H^+}$	rate constant for acid-catalyzed reaction
$k_l$	mass transfer coefficient for the liquid phase
$k_m$	maintenance coefficient
$k_m$	mass transfer coefficient
$k_0$	rate constant in infinitely dilute solution or for uncatalyzed reaction
$k_{OH^-}$	rate constant for base-catalyzed reaction
$k'$	pseudo rate constant for desorption
$K$	equilibrium constant
$K$	Michaelis constant
$K_a$	equilibrium constant for reaction expressed in terms of activities
$K_i$	adsorption equilibrium constant
$K_l$	overall liquid phase mass transfer coefficient
$K_p$	equilibrium constant expressed in terms of partial pressures
$K_r$	equilibrium constant for surface reaction expressed in terms of fractional surface coverages $\theta_i$
$K_S$	half-saturation constant
$K_w$	dissociation constant for water
1	liquid phase
$l$	parameter involved in definition of termolecular collisions
$L$	reactor length
$L$	average chain length
$\bar{L}$	average pore length
$m$	mass
$m$	overall order of reaction
$m_S$	maintenance coefficient for cell
$m_T$	mass of tracer injected as a pulse stimulus
$\dot{m}$	mass flow rate
$M$	molecular weight
$n$	number of cells
$n$	number of possible adsorption layers
$n$	number of stirred-tank reactors in a cascade
$n$	reaction order
$n_i$	moles of species $i$
$n_i^*$	number of viable cells at the time the death phase of the cell growth cycle begins
$n'_i$	number density of molecules of species $i$
$n_p$	number of pores per catalyst particle
$n_0$	number of cells in the inoculum
$n_0^*$	number of cells at the start of the exponential growth phase of the cell growth cycle
$N$	molar flux
$N$	number of CSTR reactors in cascade
$N_{A0}$	number of moles of species A at the start of a batch reaction
$N_i$	number of moles of species $i$ contained within a reactor
$N_0$	Avogadro's number
$N_{Pe}$	Péclet number

Symbol	Meaning
$N_r$	diffusive flux in radial direction
$N_{Re}$	Reynolds number
$N_{Sc}$	Schmidt number
$N_{Sh}$	Sherwood number
$p$	transfer function variable
$P$	pressure
$P_c$	critical pressure
$P_0$	saturation pressure, or pressure at reactor inlet
$P_s$	steric probability factor
$\mathcal{P}$	productivity
$\mathcal{P}$	parameter representing the combined effects of static pressure and gravitational force
$q$	charge on an electron
$q$	heat evolved in Semenov's correlation of activation energies and the exothermicity of reactions of small atoms and radicals
$q$	heat flux
$q$	heat transfer rate
$q_s$	biomass specific $q$ -rate
$Q$	heat transferred from surroundings to system
$Q$	partition function
$Q_r$	rate at which energy is removed from a system
$Q_g$	rate at which thermal energy is transformed by an exothermic chemical reaction
$\dot{Q}$	rate or heat transfer from surroundings to system
$r$	radius
$r$	reaction rate
$-r_A$	rate of disappearance of species A
$-r_{Ai}$	rate of disappearance of species A in CSTR $i$
$r_i$	rate of appearance of species $i$
$r_{ix}$	biomass specific growth rate for species $i$
$-r_{S,m}$	rate of disappearance of substrate per unit of biomass
$-r_{S,out}$	rate of disappearance of substrate per unit of biomass evaluated at the effluent conditions
$r_v$	reaction rate employed in pseudo homogeneous models of packed-bed reactors
$r_v$	reaction rate in a constant volume system
$r_{xy}$	interatomic separation distance between atoms X and Y
$r_X$	rate of production of X per unit of biomass
$\bar{r}$	average pore radius
$R$	gas constant
$R$	radius
$R$	recycle ratio
$-\mathcal{R}_S$	total rate of consumption of limiting substrate
$\mathcal{R}_X$	total rate of production of biomass
$s$	concentration of limiting substrate
$S$	number of squared terms contributing to the activation energy of a reaction
$S$	selectivity
$S$	space velocity
$S$	surface area
$S$	total quantity of limiting substrate
$S_g$	specific surface area of catalyst
$S_0$	initial substrate concentration
$S_x$	gross geometric surface area of catalyst pellet
$t$	time
$t_f$	time to achieve a specified fraction conversion $f$
$t_i$	time at which reactant concentration $C_{Ai}$ is measured
$t_{lag}$	lag time associated with the growth cycle for microorganisms
$t_s$	shutdown time in batch reactor
$t_{SP}$	time elapsed since the start of the stationary phase
$\bar{t}$	average residence time

Symbol	Meaning
$t^*$	relaxation time
$t^*$	time corresponding to the end of the acceleration phase of the cell growth cycle
$t_{d0}^*$	time at which the death phase of the cell growth cycle begins
$\bar{t}^*$	ratio of reactor length to average linear velocity
$T$	temperature (absolute)
$T_C$	temperature at center of catalyst pellet or critical temperature
$T_m$	temperature of heat source or sink
$u$	linear velocity
$U$	overall heat transfer coefficient
$v$	volume of gas adsorbed
$v_m$	volume of gas adsorbed in a monolayer
$\bar{v}$	average molecular velocity
$\vec{v}^\ddagger$	velocity with which activated complexes move from left to right across the transition state
$V$	velocity of an enzymatic reaction
$V$	volume
$V_g$	void volume per gram of catalyst
$V_p$	gross geometric volume of catalyst pellet
$V_R$	reactor volume
$V'$	volume of solid catalyst
$V$	volumetric flow rate
$V_0$	volumetric flow rate at inlet of reactor network
$w$	weight fraction
$W$	weight of solid catalyst
$W$	work done by system on surroundings
$\dot{W}_s$	rate at which shaft work is done by system
$x$	concentration of biomass
$x$	distance from pore mouth
$x$	normalized pressure ( $P/P_0$ )
$x_c$	distance from pore mouth at which reactant concentration vanishes
$X$	total mass of live cells
$X_F$	total mass of live cells when the biochemical reaction ceases
$X_{S0}$	mass of live cells at the start of the stationary phase
$X_\infty$	mass of cells at infinite time in the logistic model
$y$	instantaneous fractional yield
$y_{X/S}$	instantaneous yield coefficient in a biochemical reaction
$Y_{X/S}$	overall yield coefficient
$Y'_R$	overall fractional yield of species R
$Z$	distance from inlet of tubular reactor
$Z_{AB}$	bimolecular collision frequency for molecules A and B
$Z_{ABC}$	termolecular collision frequency
$Z_i$	number (and sign) of charges on ion $I$

### Greek Symbols

$\alpha$	area covered per molecule adsorbed
$\alpha$	branching coefficient in chain reaction mechanism
$\alpha$	coefficient in Luedeking–Piret equation
$\alpha$	dimensionless concentration variable
$\alpha$	fraction of catalyst surface that is poisoned
$\beta$	dimensionless concentration variable for competitive consecutive reactions [defined by equation (5.4.18)]
$\beta$	energy conversion function used in determination of the effectiveness factor for a nonisothermal catalyst pellet
$\beta$	coefficient in Luedeking–Piret equation
$\beta_i$	order of the reaction with respect to species $i$
$\gamma$	activity coefficient
$\gamma$	Arrhenius number
$\delta_A$	volumetric expansion parameter

$\delta^*$	reaction progress variable for consecutive reactions
$\delta^\neq$	characteristic length dimension of the transition state
$\Delta$	time separating rate measurements
$\Delta E_{\text{total}}$	change in total energy
$\Delta G$	Gibbs free energy change
$\Delta H$	enthalpy change
$\Delta S$	entropy change
$\Delta \xi^*$	deviation from equilibrium conditions
$\epsilon$	rate of dissipation of turbulent energy
$\epsilon_B$	bed porosity
$\epsilon_c$	relative kinetic energy directed along the line of centers in a collision
$\epsilon_p$	porosity of pellet or particle
$\epsilon_{\text{total}}$	total porosity of packed bed
$\eta$	catalyst effectiveness factor
$\theta_i$	fraction of catalyst surface covered by species $i$
$\theta_v$	fraction of surface sites that are vacant
$\kappa$	conductivity
$\kappa$	ratio of rate constants for consecutive reactions
$\lambda$	generalized physical property
$\lambda$	mean free path
$\lambda$	Kolmogorov number
$\mu$	specific growth rate
$\mu$	viscosity
$\mu$	ionic strength
$\mu_i$	chemical potential of species $i$
$\mu_{AB}$	reduced mass
$\mu_{\text{max}}$	maximum specific growth rate
$\mu_{\text{net}}$	net specific growth rate
$\mu_R$	specific rate of replication
$\nu$	kinematic viscosity
$\nu_i$	stoichiometric coefficient for species $i$
$\xi$	extent of reaction
$\xi^*$	extent of reaction per unit volume in constant-volume systems
$\prod_i$	product of the $i$ terms that follow
$\rho$	density
$\rho_B$	bulk density of catalyst
$\rho_i$	Hammett reaction constant
$\sigma$	surface site
$\sigma$	emissivity of solid
$\sigma_i$	hard-sphere diameter for molecule $i$
$\sigma_i$	Hammett substituent constant
$\sigma_{AB}$	effective hard-sphere diameter for bimolecular collision
$\sigma^2$	variance of residence-time distribution curve
$\sum_i$	sum of the $i$ terms that follow
$\tau$	reactor space time
$\tau_c$	space time for a cascade of CSTR reactors
$\tau_i$	space time for reactor $i$
$\tau_N$	proportionality constant associated with deviation of the Hammett equation
$\tau_p$	space time for a plug flow reactor
$\tau_{1/2}$	reaction half-life
$\tau'$	tortuosity factor
$\tau^*$	dimensionless time variable for competitive consecutive reactions
$\phi$	parameter used in analysis of the activated sludge process
$\phi(C_i)$	concentration-dependent portion of reaction rate expression
$\phi_{Ln}$	Thiele modulus for an infinite flat plate catalyst

$\phi_s$	Thiele modulus for a spherically symmetric catalyst pellet
$\phi_m$	mass flow rate
$\chi$	total quantity of an arbitrary constituent of a microorganism
$\psi(C_i)$	linearized integrated rate expression
$\Psi$	concentration factor for a stirred-tank fermenter employed in separation/recycle mode

### Subscripts

A	generalized chemical species A
batch	associated with a batch reactor
B	bulk fluid property
cycle	associated with the growth cycle of a microorganism
d	associated with cell death
e	equilibrium
em	endogenous metabolism
eff	effective
E	effluent stream property or equilibrium property
ES	external surface of catalyst pellet
f	refers to reactions involving formation of a compound from its elements
f	refers to forward reaction
F	property evaluated at final or effluent conditions
FB	fed batch
g	gas phase
i	refers to species $i$ , reaction $i$ , or reactor $i$ in a CSTR network
in	refers to inlet stream property
l	liquid phase
lag	lag time for growth of microorganism
lim	refers to limiting reagent
L	property value at end of catalyst pore or in longitudinal direction
m	property value per unit mass of catalyst
max	maximum or extremum value
MT	mass transfer
n	property value leaving reactor $n$
net	net specific biomass growth rate associated with the logistic model
nonproductive	associated with the times during the production cycle when a biochemical reaction is not occurring
out	refers to outlet stream property
p	pellet or particle value
PE	pseudo equilibrium
r	reverse reaction
R	reaction or property value in radial direction
RLS	rate-limiting step
S	half-saturation constant in Monod rate law
S	solid
S	substrate
SS	steady state
SP	stationary phase
sys	system
T	tube
v	property value per unit volume of catalyst bed
w	wall
X/S	defines the substances associated with the yield coefficient
z	property value in longitudinal direction
0	property value at time zero, reactor inlet, or at mouth of catalyst pore
$\infty$	value at infinite time
$\infty$	in the logistic model, this symbol refers to the infinite time mass of the microorganism

***Superscripts***

$0$	refers to variables associated with standard states of materials
$"$	variable is expressed per unit surface area
$''$	variable is expressed per unit volume of solid catalyst
$\ddagger$	refers to variable associated with transition state
$\wedge$	average value of property

# Appendix C

---

## Supplementary References

This book is intended to provide an introduction to the subjects of chemical kinetics and chemical reactor design. Consequently, all topics of potential interest cannot be treated to the depth that individual readers may require. To facilitate further reading in these areas, we have listed references that readers may find helpful.

### References Pertinent to the Chemical Aspects of Kinetics

1. C. H. BAMFORD and C. F. H. TIPPER (Eds.), *The Practice of Kinetics*, Vol. I, Elsevier, Amsterdam, 1969.
2. P. L. BREZONIK, *Chemical Kinetics and Process Dynamics in Aquatic Systems*, CRC Press, Boca Raton, FL, 1994.
3. K. A. CONNERS, *Chemical Kinetics: The Study of Reaction Rates in Solution*, Wiley-VCH, New York, 1990.
4. P. L. HOUSTON, *Chemical Kinetics and Reaction Dynamics*, McGraw-Hill, New York, 2001.
5. K. J. LAIDLER, *Chemical Kinetics*, 3rd ed., Harper & Row, New York, 1987.
6. J. W. MOORE and R. G. PEARSON, *Kinetics and Mechanism*, 3rd ed., Wiley, New York, 1981.
7. P. ZUMAN and R. C. PATEL, *Techniques in Organic Reaction Kinetics*, Krieger Publishing, Malabar, FL, 1992.

### References Pertinent to the Engineering or Reactor Design Aspects of Kinetics

1. J. B. BUTT, *Reaction Kinetics and Reactor Design*, 2nd ed., Prentice Hall, New York, 2000.
2. M. E. DAVIS and R. J. DAVIS, *Fundamentals of Chemical Reaction Engineering*, McGraw-Hill, New York, 2003.
3. K. G. DENBIGH and J. C. R. TURNER, *Chemical Reactor Theory*, 3rd ed., Cambridge University Press, London, 1984.
4. H. S. FOGLER, *Elements of Chemical Reaction Engineering*, 4th ed., Prentice Hall, Englewood Cliffs, NJ, 2005.
5. G. F. FROMENT and K. B. BISCHOFF, *Chemical Reactor Analysis and Design*, 2nd ed., Wiley, New York, 1990.
6. R. E. HAYES, *Introduction to Chemical Reactor Analysis*, Gordon & Breach, New York, 2001.
7. O. LEVENSPIEL, *Chemical Reaction Engineering*, 3rd ed., Wiley, New York, 1999.
8. O. LEVENSPIEL, *The Chemical Reactor Omnibook*, Oregon State University, Corvallis, OR, 1979.

9. U. MANN, *Principles of Chemical Reactor Analysis and Design*, Plains Publishing, Lubbock, TX, 1999.
10. J. B. RAWLINGS and J. G. EKERDT, *Chemical Reactor Analysis and Design Fundamentals*, Nob Hill Publishing, Madison WI, 2002.
11. G. W. ROBERTS, *Chemical Reactions and Chemical Reactors*, Wiley, New York, 2008.
12. L. D. SCHMIDT, *The Engineering of Chemical Reactions*, Oxford University Press, Oxford, 1998.
13. F. TISCAREÑO LECHUGA, *ABC para Comprender Reactores Químicos con Multireacción*, Editorial Reverte, Mexico City, 2008.
14. S. M. WALAS, *Chemical Reaction Engineering Handbook of Solved Problems*, Gordon & Breach, New York, 1995.

### References Pertinent to Heterogeneous Catalysis

1. C. H. BARTHOLOMEW and R. J. FARRAUTO, *Fundamentals of Industrial Catalytic Processes*, 2nd ed., Wiley-Interscience, Hoboken, NJ, 2006.
2. J. A. DUMESIC, D. F. RUDD, L. M. APARICIO, J. E. REKOSKE, and A. TREVIÑO, *The Microkinetics of Heterogeneous Catalysis*, American Chemical Society, Washington, DC, 1993.
3. B. C. GATES, *Catalytic Chemistry*, Wiley, New York, 1992.
4. J. T. RICHARDSON, *Principles of Catalyst Development*, Plenum Press, New York, 1989.
5. C. N. SATTERFIELD, *Heterogeneous Catalysis in Practice*, 2nd ed., McGraw-Hill, New York, 1991.
6. G. A. SOMORJAI, *Introduction to Surface Chemistry and Catalysis*, Wiley, New York, 1994.
7. A. B. STILES, *Catalyst Manufacture*, Marcel Dekker, New York, 1983.
8. Z. G. SZABO and D. KALLO, *Contact Catalysis* (2 vols.), Elsevier, Amsterdam, 1976.
9. C. L. THOMAS, *Catalytic Processes and Proven Catalysts*, Academic Press, New York, 1970.
10. M. V. TWIGG (Ed.), *Catalyst Handbook*, 2nd ed., Wolfe Publishing, London, 1989.

### References Pertinent to Biochemical Reactions, Fermentation and BioReactors

1. J. E. BAILEY and D. F. OLLIS, *Biochemical Engineering Fundamentals*, 2nd ed., McGraw-Hill, New York, 1986.
2. M. BUTLER, *Animal Cell Culture and Technology*, 2nd ed., Garland Science/BIOS Scientific Publishers, London (2004).

3. D. S. CLARK and H. BLANCH, *Biochemical Engineering (Chemical Industries)*, Marcel Dekker, New York, 1997.
4. P. M. DORAN, *Bioprocess Engineering Principles*, 2nd ed., Academic Press, San Diego, 2013.
5. S. DUTTA GUPTA and Y. IBARAKI (Eds.), *Plant Tissue Culture Engineering*, Springer-Verlag, Berlin, 2006.
6. R. EIBL and D. EIBL, *Single-Use Technology in Biopharmaceuticals Manufacture*, e-book, Wiley, Hoboken, NJ.
7. R. EIBL, D. EIBL, R. PORTNER, G. CATAPANO, and P. CZERMAK (Eds.), *Cell and Tissue Reaction Engineering*, Springer-Verlag, Berlin, 2009.
8. W. L. HOCHFELD, *Producing Biomolecular Substances with Fermenters, Bioreactors, and Biomolecular Synthesizers*, CRC Press/Taylor & Francis, Boca Raton, FL, 2006.
9. H. C. LIM and H. S. SHIN, *Fed-Batch Cultures: Principles and Applications of Semi-batch Bioreactors*, Cambridge University Press, Cambridge, 2013.
10. B. McNEIL and L. M. HARVEY, *Practical Fermentation Technology*, Wiley, Hoboken, NJ, 2008.
11. J. NIELSEN and J. VILLADSEN, *Bioreaction Engineering Principles*, Plenum Press, New York, 1994.
12. T. PANDA, *Bioreactors: Analysis and Design*, Tata McGraw-Hill, New Delhi, India, 2011.
13. K. SCHÜGERL, *Bioreaction Engineering: Reactions Involving Microorganisms and Cells*, Vol. 1 (V. Cottrell, transl.), Wiley, New York, 1987.
14. A. H. SCRAGG (Ed.), *Bioreactors in Biotechnology*, E. Horwood, New York, 1991.
15. M. L. SHULER and F. KARGI, *Bioprocess Engineering: Basic Concepts*, 2nd ed., Prentice Hall, Upper Saddle River, NJ, 2002.
16. G. N. STEPANOPoulos, A. A. ARISTIDOU, and J. NIELSEN, *Metabolic Engineering: Principles and Methodologies*, Academic Press, San Diego, CA, 1998.
17. J. M. VLAK, C. D. DE GOOIJER, J. TRAMPER, and H. G. MILLENBURGER, *Insect Cell Culture: Fundamental and Applied Aspects*, Kluwer Academic, Dordrecht, The Netherlands, 1996.
18. W. ZHOU, G. SETH, M. J. GUARDIA, and W.-S. HU, Mammalian Cell Bioreactors, in *Encyclopedia of Industrial Biotechnology: Bioprocess, Bioseparation, and Cell Technology*, M. C. FLICKINGER (Ed.), pp. 3219–3230, Wiley, Hoboken, NJ, 2010.

# Author Index

---

- Abdalla, B. K., 55  
Abella, L. C., 57  
Acetis, J., 440  
Adlington, D. G. 327  
Afshar Taromi, F., 266  
Ahmad, I. Z., 517  
Ahmad, I., 106, 111  
Alberda, G., 339, 359  
Albright, L. F., 151  
Aldridge, H. K., 65  
Al-Hamdany, R., 110  
Al-ka'bi, J., 297  
Alkhazov, T. G., 183  
Alley, F. C., 145  
Alper, E., 265  
Al-Roweih, M., 265  
Al-Rubeai, M., 500, 516–517  
Amada, K., 300  
Amirgulyan, N. S., 183  
Amis, E. S., 192, 206–207  
Amundson, N. R., 327–328, 391, 420,  
    439–440  
Anderson, J. R., 179  
Anderson, R. B., 80, 103  
Antelo, J.M., 143  
Anthony, P., 517  
Aparicio, L. M., 535  
Arce, F., 143  
Arcos, J. A., 149  
Argo, W. B., 423, 440  
Arif Niaz, M., 365  
Aris, R., 15, 347, 359, 380, 391, 420,  
    439–440  
Aristidou, A. A. 456, 516  
Asenjo, J. A., 517  
Ashmore, P. G., 195, 207  
Ashraf, C. M., 111  
Askey, P. J., 42, 53  
Axworthy, A. E., 260  
Aziz Khan, A. 365  
Bacaloglu, R., 60, 69  
Baeyer, A., 291, 294  
Baghbaderani, B. A., 517  
Bailey, J. E., 453, 457, 516–517  
Bailie, R. C., 357, 359  
Balaceanu, J. C., 53  
Bamford, C. H., 53, 93, 103, 535  
Banerji, K., 56  
Baral, L. L., 179  
Bard, J. R., 57, 70  
Barnett, G., 360  
Barnett, L. G., 442, 444  
Barrer, R. M., 180, 378–379, 439  
Bartholemew, C. H., 152, 179, 449, 535  
Bashkirov, A. N., 186  
Baughan, E. C., 211  
Bauner, N., 329  
Bazanova, I. N., 296  
Bazsa, G., 271, 303  
Bedzhanyan, Yu., 114  
Beek, J., 439–440  
Beek, W. J., 408, 440  
Behie, L. A., 517  
Beigzadeh, D., 266  
Beijnen, J. H., 360  
Bell, F., 208  
Bell, R. L., 361  
Bell, R. P., 207, 211  
Bender, M. L., 194, 198, 207, 518  
Benson, S. W., 7, 17, 53, 103–104, 106,  
    137, 142  
Berman, A. D., 144  
Berzelius, J. J., 152  
Beutel, S., 517  
Bhadra, A., 213  
Bhagawanthan Rao, M., 148  
Bikrani, M., 150, 299  
Bilous, O., 327–328  
Biordi, J. C., 50, 53  
Bird, R. B., 377, 423, 439, 440, 471, 516  
Bischoff, K. B., 337, 343, 347, 352,  
    355–357, 359, 421, 535  
Bizzigotti, G. O., 209  
Bjerrum, N., 191  
Blake, F. E., 105  
Blake, N. J., 419  
Blake, P. G., 105–106, 260  
Blanch, H. 489, 508, 516–517  
Bodenstein, M., 75, 77, 84, 87, 88, 92, 103,  
    114, 198  
Bogolepova, E. I., 186  
Bond, A. C., 108  
Boudart, M., 24, 53, 103, 161, 179  
Bouhomra, W., 265  
Boyaci, F. G., 330  
Braun, R., 262  
Brezonik, P. L., 535  
Bridger, G. A., 441  
Brønsted, J. N., 191–194, 210  
Brotz, W., 439  
Brown, D. E., 207  
Brown, H. C., 207  
Brunauer, S., 156–157, 160, 179  
Bryukhovetskii, V. A. 270  
Buffham, B. A., 351, 359  
Bulatov, V., 294, 328  
Bunker, D. L., 104  
Bunnet, J. F., 30, 41, 53  
Burghardt, A., 359  
Burk, D., 460  
Burk, R. E., 59, 65, 181  
Burke, S. P., 419  
Burkus, J., 141–142

- Burton, M., 103  
 Butler, M., 517  
 Butt, J. B., 179, 395, 439, 535  
 Buzonick, P. L., 211  
 Bykov, V. I., 150  
 Bykovchenko, V. G., 260
- Cain, J. C., 62  
 Calderbank, P. H., 421, 430, 440  
 Cameron, C., 209  
 Campbell, T. M., 421  
 Carberry, J. J., 359, 440, 445  
 Castellano, E., 115  
 Castelly, H., 209  
 Castro, J. M., 330  
 Catapano, G., 517  
 Chadhuri, B., 144  
 Chakma, A., 56  
 Chalmers, J., 517  
 Chambers, R. P., 161, 179  
 Chang, C. D., 15  
 Chen, D., 209  
 Chen, J. 499, 517  
 Chen, J. C. H., 261, 264  
 Chen, J.-H., 147  
 Chen, J.-T., 147  
 Chernishev, E. A., 260  
 Chilton, C. H., 162, 440  
 Chilton, T. H., 162, 407, 414–415, 440, 529  
 Chinoy, P. B., 17, 20  
 Chlebicki, J., 303  
 Choi, Y.-E., 517  
 Christiansen, J. A., 84, 103  
 Chu, C., 394, 439  
 Chu, J. C., 409, 440  
 Chuchani, G., 63  
 Ciapetta, F. G., 47, 53, 103, 179  
 Ciardelli, G., 69  
 Cichacz, Z., 303  
 Clark, D., 192, 207  
 Clark, D. S., 489, 508, 516–517  
 Clark, E. L., 259  
 Cleland, W. W., 201, 207  
 Coberly, C. A., 421  
 Colburn, A. P., 407, 414–415, 421, 440, 529  
 Collette, H., 184  
 Collier, C. H., 179  
 Connors, K. A., 535  
 Cooke, H.G., Jr., 67  
 Corcoran, W. H., 54, 110  
 Corrigan, T. E., 182, 384, 439  
 Coull, J., 180  
 Couper, J. R., 220  
 Coussemant, F., 53  
 Cox, S., 517  
 Cranston, R. W., 173, 179  
 Cremer, H. W., 15, 327  
 Cristallini, C., 69  
 Croce, A.E., 115
- Crooks, W. M., 249, 259  
 Croughan, M. S. 517  
 Csunderlik, C., 60, 69  
 Cunningham, R. A., 398, 440, 445  
 Cunningham, R. E., 398, 440  
 Cutlip, M. B., 329  
 Czarnowski, J., 63–64, 105, 259  
 Czermak, P., 517
- Daasch, L. W., 57, 70  
 Dabbagh, A. M. 110  
 Dainton, F. S., 103  
 Damköhler, G., 380, 395, 439  
 Danckwerts, P. V., 337, 359  
 Daniels, F., 103  
 Davey, M. R., 517  
 Davidson, J. F., 439–440  
 Davis, A. M., 54, 110  
 Davis, M. E., 535  
 Davis, R. J., 535  
 De Donder, Th., 2, 3  
 De Filippo, D., 215  
 Dean, A. C. R., 457, 516  
 Debande, G., 296  
 Debye, P., 191, 197, 207–208  
 Dec, J., 67  
 Deming, L. S., 157, 179  
 Deming, W. E., 157, 179  
 Denbigh, K. G., 81, 103, 124–125, 142, 219, 249, 259, 275, 281, 289–291, 294, 358–359, 535  
 Dente, M., 357, 359  
 Deremince - Mathieu, V., 184  
 Derouane, E. G., 184  
 Diaz Peña, M., 63, 142  
 Dickson, P. F., 58, 106  
 Dillon, R. T., 41–42, 53  
 Dominguez, R. M., 63  
 Doona, C. J., 69  
 Doran, P. M., 463, 470, 502, 516–517  
 dos Santos Afonso, M. 55, 61, 115, 261  
 Douglas, J. M., 357, 359, 442  
 Douglas, W. J. M., 442  
 Dowden, D. A. 441  
 Dranoff, J. S., 328  
 Dryakhlov, A. S., 331  
 Dullien, F. A. L., 439  
 Dumba, M., 66, 107  
 Dumesic, J. A., 535  
 Dumez, F. J., 186  
 Dunford, B., 269  
 Dutta Gupta, S., 517  
 Dzhagatspanyan, R. V., 302
- Eadie, G., 199–200, 211–212  
 Echigoya, E., 370  
 Eckert, C. A., 193, 207  
 Eckert, C. F., 141–142  
 Edwards, J. O., 78, 80, 103, 206–207
- Edwards, M. E., 439  
 Edwards, M. F., 517  
 Eibl, D., 517  
 Eibl, R., 517  
 Einstein, A., 87, 419  
 Eisenklam, P., 359, 367  
 Ekerdt, J. G., 535  
 Eldib, I. A., 151  
 Eldridge, J. M., 259  
 Emmett, P. H., 103, 160, 179, 439–440  
 Emond, H. H., 142  
 Enders, J. F., 499, 517  
 Ergun, S., 419, 429, 440  
 Eschard, F., 53  
 Espejo-Alcaraz, O., 366  
 Esteves, P., 185  
 Evans, M. G., 101, 104  
 Evans, R. B., III 439  
 Eyring, H., 98, 101, 104
- Fair, J. R., 220  
 Fan, L. T., 357, 359  
 Fareed, S., 517  
 Farrauto, R. J., 152, 179, 449, 535  
 Favela, E., 520, 522  
 Fel'dblyum, V. Sh., 147  
 Feng, H. Y., 67  
 Fernandez-Sempere, J., 366  
 Ferranti, F., 215  
 Ferrero, J. C., 151  
 Fidalgo, L., 150, 299  
 Firouzabadi, H., 58  
 Fischer, E., 198  
 Fisher, C. H., 232, 259  
 Flickinger, M. C., 517  
 Floriano, M. A., 209  
 Fogler, H. S., 535  
 Font-Montesinos, R., 366  
 Ford, R. A., 207  
 Foutch, G. L., 60  
 Franck, J., 191, 207  
 Franco, J., 143  
 Freiss, S. L., 53  
 Frey, H. M., 264  
 Fridman, R. A., 186  
 Froment, G. F., 186, 419, 421, 425, 440, 535  
 Frost, A. A., 67, 139–142  
 Fugitt, R. E., 145  
 Furrow, S. D. 59, 113  
 Furuoya, I., 370  
 Furusawa, T., 329
- Gabelica, Z., 184  
 Gao, W., 499, 517  
 Garagin, S. G., 144  
 Garcia Lopez, M. C., 143  
 Gardiner, W. C., Jr., 103  
 Garralda, M. A., 150, 299

- Garver, J. C., 182, 439  
 Gaspillo, P. A. D., 57  
 Gates, B. C., 535  
 Gato, S., 57  
 Gavriliiv, A. P., 54  
 Geankoplis, C. J., 408, 440  
 Gershenson, Yu. M. 114  
 Gesser, H. D., 142  
 Gevert, B. S. 148  
 Ghose, T. K. 213  
 Gibilaro, L. G., 351, 359  
 Gilani, S. L., 519  
 Gilkeson, M. M., 442, 444  
 Gill, R., 208  
 Giraud, A., 53  
 Glasstone, S., 103, 104  
 Glebov, L. S., 186  
 Glindkamp, A., 517  
 Glover, R. E., 369  
 Golber, P. L., 259  
 Goldfinger, P., 103  
 Gollapalli, N. R., 207  
 Golodets, G. I., 184, 186  
 Golubeva, N. N., 331  
 Gonzalez, A. C., 58, 61, 63, 106  
 Gonzalez, J. L., 259  
 Gooch, D. B., 259  
 Goodman, D. R., 439  
 Gopalakrishnan, M. 54  
 Gopalan, R., 266  
 Gordeeva, S. B., 301  
 Gordon, A. J., 207  
 Gordon, M. D., 333  
 Gore, P. H., 297  
 Goring, R. L., 392  
 Gostikin, V. P., 296  
 Goto, S., 265  
 Gould, E. S., 103  
 Gowenlock, B. G., 80, 103  
 Goyal, S. K., 333  
 Grace, J. R., 438, 440  
 Granger, P., 185  
 Greene, E. F., 103  
 Grigor'eva, E. N., 150  
 Grinberg, M. Ya., 147  
 Grunwald, E., 206–207  
 Guardia, M. J., 517  
 Guggenheim, E. A., 46–48, 53, 64–65,  
     67–68, 70–71, 103, 143, 207, 210  
 Guldberg, C. M., 206–207  
 Gupta, V. P., 442  
 Gurel, A., 517  
 Gurumurthy, R., 54  
 Guseinov, E. M., 296  
 Hafez, A. M., 209  
 Hagan, G., 378  
 Haldane, J. B. S., 200  
 Hambor, J. E., 517  
 Hammes, G. G., 80, 103  
 Hammett, L. P., 204–207, 214–215, 532  
 Hanes, C. S., 199–200, 212  
 Hanley, T. R., 365  
 Hansson, J., 206–207  
 Harnby, N., 517  
 Harned, H. S., 191, 207  
 Harrel, C. L. 298  
 Harriot, P. 516  
 Harrison, D., 439–440  
 Hatfield, J. D., 142, 269  
 Havewala, N. B., 212  
 Hawkins, J. E., 145  
 Hawks, R., 360  
 Hayes, P. C., 183  
 Hayes, R. E., 535  
 Hedden, K., 439  
 Hellin, M., 53, 121, 142  
 Helm, C. D., 179  
 Henkel, S., 517  
 Hensler, C. J., 333  
 Herguido, J., 521  
 Herraez, M.A., 259  
 Herzfeld, K. F., 84, 89–91, 103  
 Heydarzadeh, H. D., 519  
 Hicks, J. S., 396–398, 439–440  
 Hilton, M. G., 517  
 Himmelblau, D. M., 337, 343, 359  
 Hine, J. S., 194, 204–205, 207  
 Hinshelwood, C. N., 42, 53, 59, 65, 98, 104,  
     163, 181, 390, 457, 461, 516  
 Hinton, J. F., 192, 206–207  
 Hirschfelder, J., 82, 103  
 Hitzmann, B., 517  
 Hlavacek, V., 440  
 Hochfeld, W. L., 462, 516  
 Hofmann, H., 440  
 Hofstee, B. H. J., 199–200, 211  
 Holden, D., 208  
 Hong, H., 499, 517  
 Hong, M., 517  
 Hong, Z., 185  
 Hopkins, M. J., 348, 359, 367  
 Horman, I., 68  
 Horvath, M., 271, 303  
 Hougen, O. A., 160, 163–164, 166–170,  
     179, 181–182, 185, 187–188, 214, 390,  
     393–394, 398, 430, 440, 442, 527  
 Houser, T. J., 109  
 Houston, P. L., 535  
 Hsu, Y.-C., 147  
 Hu, W.-S., 517  
 Huang, T.-K., 517  
 Hückel, E., 191, 197, 207–208  
 Hughes, R. R., 368, 493, 516, 518  
 Huntington, R. L., 421  
 Huntsman, W. P., 261, 264  
 Hurley, M. D., 145  
 Hussain, M., 517  
 Hutchings, J., 440  
 Huybrechts, G., 296  
 Ibaraki, T., 264  
 Ibaraki, Y., 517  
 Ijadi-Maghsoodi, S., 105–106, 260  
 Inkley, F. A., 173, 179  
 Innes, W. B., 179  
 Inukai, T., 231, 259  
 Ito, K., 264  
 Iwasaki, M., 370  
 Izzo, B., 298  
 Jacob, S. M., 15  
 Jaffé, H. H., 207  
 Jafvert, C. T., 210  
 Jakob, M., 421, 440  
 Jaluria, Y., 362  
 Jeffreys, G. V., 437, 440  
 Jencks, W. P., 198, 207  
 Jenney, T. M., 259  
 Jenson, V. G., 437, 440  
 Jing, D., 517  
 Johnson, C. D., 206–207  
 Johnston, E. H., 103  
 Johnston, H. S., 103–104  
 Jones, A. W., 148  
 Jones, R. W., 259  
 Jonnalagadda, S. B., 66, 107, 207  
 Jonsson, K. A., 148  
 Jost, W., 103  
 Jung, G., 103  
 Jungers, J. C., 53, 121, 142  
 Kadlec, R. H., 299, 336  
 Kaiser, E. W., 145  
 Kakuda, T., 149  
 Kalechits, I. V., 150  
 Kalil, J., 440  
 Kalinkina, L. I., 331  
 Kaliya, M. L. 296  
 Kallenbach, R., 379, 439  
 Kallos, M. S., 517  
 Kao, H. S.-P., 439  
 Karbstein, H., 70  
 Kargi, F., 458, 489, 516–517  
 Karpenko, I. M., 446  
 Kato, K., 300  
 Kaufler, F., 137, 142  
 Kehoe, D. E., 517  
 Kembal, C., 146  
 Kembowski, Z., 360  
 Kerr, G. T., 227, 259  
 Kettenring, K. N., 414, 440  
 Khan, M. M. T., 105  
 Kieran, P., 146, 517  
 Kilpatrick, M., 47, 53  
 Kim, Y., 517  
 Kim, Y. K., 142, 269

- Kim, Y.-S., 517  
 Kindler, K., 206  
 King, E. L., 80, 103  
 Kiperman, S., 331  
 Kirk, R. S., 182, 439, 442–443  
 Kirkpatrick, S. D., 162  
 Kisarov, V. M., 331  
 Kisileva, T. S., 260  
 Kittrell, J. R., 45, 53  
 Kladko, M., 257–259, 308–309, 319, 328  
 Klapper, H., 57, 70  
 Klein, M. T., 298  
 Kliger, G. A., 186  
 Klingelhoefer, W. C., 115  
 Knudsen, C. W., 439  
 Knudsen, M., 160, 376–377, 381, 393, 410, 440–442, 528  
 Koch, S., 65  
 Kochubei, V. F., 54  
 Kohler, G., 499, 517  
 Kojima, T., 231, 259  
 Kolloff, A., 65  
 Koltunov, V. S., 111  
 Komlosi, A., 66, 302  
 Kondratiev, V. N., 104  
 Korobkov, V. Yu., 150, 181  
 Kosorotov, V. I., 302  
 Kozeny, J., 419  
 Kozhevnikov, I. V., 104  
 Kramers, H., 325, 328, 339, 359  
 Krawetz, R., 517  
 Kuchaev, V. L., 263  
 Kudryashova, L. V., 296  
 Kul'kova, N. V., 181  
 Kumar, J., 299  
 Kunii, D., 359, 375, 408, 421, 439–440  
 Kuntz, R. R., 113  
 Kuo, J. C. W., 15  
 Kustin, K., 69  
 Kwong, S. S., 421  
 Laidler, K. J., 92, 103–104, 194, 207, 209, 212, 535  
 Lang, W. H., 15  
 Langmuir, I., 156–160, 163, 165, 179–180, 199, 390, 461  
 Lapidus, L., 437, 440  
 Lazzeri, L., 69  
 Le Prince, P., 53  
 Leclercq, G., 185  
 Leclercq, L., 185  
 Ledakowicz, S., 109  
 Lefedova, O. V., 296  
 Leffler, J. E., 207  
 Lengyel, I., 271, 303  
 Letort, M., 103  
 Leung, K.-T., 499, 517  
 Leva, M., 421, 440  
 Leveen, L., 517  
 Levenspiel, O., 53, 238–240, 244–245, 250–251, 253, 255–256, 259, 274, 276–277, 281–286, 294, 325, 327–328, 337, 343, 345–347, 352, 355–359, 368, 375, 439–440, 535  
 Levush, S. S., 270  
 Lewis, E. S., 53, 80, 103, 207, 471  
 Lewis, G. N., 9  
 Lewis, W. K., 471, 516  
 Li, X., 517  
 Liang, S. C., 180  
 Liao, B.-Q., 499, 517  
 Liebhafsky, H. A., 79, 103  
 Lightfoot, E. N., 423, 439–440, 471, 516  
 Lim, H. C., 516–517, 523–525  
 Limido, G. E., 53  
 Lin, H., 499, 517  
 Lin, J., 517  
 Lin, K. F., 332  
 Lin, M. C., 65  
 Lind, S. C., 84, 103  
 Lindemann, F. A., 65, 89, 97–98, 104, 198  
 Lineweaver, H., 199, 211–212, 460  
 Lipshitz, S. D., 330  
 Liu, C., 214  
 Liu, M. C., 65, 517  
 Liu, S., 227, 259, 517  
 Liu, X., 65  
 Livingston, R., 44, 53, 192  
 Llobura, A., 214  
 Lock, L. T., 517  
 Los, G., 360  
 Lowe, K. C., 517  
 Lowry, T. M., 194  
 Lucetta Barnard, M., 212  
 Luckraft, D. A., 295  
 Luss, D., 391, 439–440  
 Luus, R. L., 296  
 Lyu, M. Y., 362  
 MacLoughlin, P. F., 517  
 Macosko, C. W., 330  
 Madhusudhan, V., 148  
 Maeda, M., 57  
 Mahajani, S. M., 266, 303, 361  
 Malfoy, P., 185  
 Malone, D. M., 517  
 Manderfield, E. L., 440  
 Mann, U., 328, 535  
 Marcali, K., 333  
 Marchenko, V. I., 111  
 Mardaleishvili, R. E., 181  
 Margerison, D., 44–45, 53  
 Marinas, J. M., 214  
 Markin, E. M., 114  
 Marshall, T. H., 518  
 Marshall, W. R., 421  
 Martell, A. E., 105  
 Martin, A. M., 520  
 Martin, H. D., 262  
 Martin, Y., 517  
 Marvel, C. S., 67  
 Mason, D. R., 259  
 Mason, E. A., 439  
 Massoth, F. E., 148  
 Mathur, G. P., 187–188, 448–449  
 Matouq, M. H., 265  
 Matthew, S. P., 183  
 Matveev, K. I., 104  
 Mauter, M., 517  
 Maxted, E. B., 179  
 Maymo, J. A., 398, 440  
 McCabe, W. L., 440, 471, 516  
 McClure, R., 212  
 McCracken, D. J., 58, 106  
 McDaniel, D. H., 207  
 McDonald, K. A., 517  
 McIlvried, H. G., 450  
 Mearns, A. M., 18  
 Meenhorst, P. L., 360  
 Meisen, A., 56  
 Melius, C. F., 65  
 Melville, H. W., 80, 103  
 Mendez, I., 517  
 Menéndez, M. A., 521  
 Meng, F., 499, 517  
 Meng, G., 517  
 Menten, M. L., 199, 207, 212, 214, 300, 460–461  
 Merchuk, J. C., 517  
 Messmer, J. H., 395, 439  
 Metzner, A. B., 440  
 Mezaki, R., 53  
 Michaelis, L., 199, 207, 212, 213–214, 262, 300, 460–461, 518, 529  
 Michelsen, M. L., 348, 359  
 Miller, D. N., 442–443  
 Milstein, C., 499, 517  
 Mischke, R. A., 365  
 Mittal, S., 56  
 Mixon, F. O., 359  
 Miyauchi, T., 329  
 Modell, M., 15, 20, 306, 327  
 Moelwyn-Hughes, E. A., 53, 104  
 Mohammed, A., 79, 103  
 Mohd, S., 517  
 Moin, F. B., 54, 270  
 Monge, M., 517  
 Monod, J., 519  
 Monzón, A., 521  
 Moore, J. W., 71, 93, 103–104, 136–137, 139–142, 194, 207, 535  
 Moorgat, G.K., 65  
 Morales, M. F., 212  
 Morland, P.T., 183  
 Morris, J. C., 103  
 Mosely, R. B., 207  
 Moss, F. D., 259

- Motsarev, G. V., 302  
 Mousavi, M. F., 58  
 Mukhida, K., 517  
 Mukhopadhyay, S.N., 213
- Nagy, J.B., 184  
 Najafpour, G. D., 519  
 Nashimura, H., 329  
 Nath, S., 299  
 Nechitailo, A. E., 296  
 Neeb, P., 65  
 Newberger, M. R., 299, 336  
 Newman, M. S., 207  
 Neyens, A., 37–38, 53  
 Ni, Y., 60  
 Nicoll, F., 62  
 Nielsen, J., 456, 516  
 Nienow, A. W., 517  
 Nigam, P. C., 333  
 Niyaz Khan, M., 149, 300  
 North, A. M., 190, 207  
 Nowicki, L., 109  
 Nusselt, W., 407
- O'Brien, G. J., 333  
 Occam, W., 82–83  
 Ogg, R. A., 77, 103  
 Okongwu, O. N., 296  
 Oldenburg, C. C., 179  
 Oldshue, J. Y., 517  
 Ollis, D. F., 453, 457, 516–517  
 Olson, R. W., 410, 440  
 Orcutt, J. C., 359  
 Oref, I., 294, 328  
 Osokin, Yu. G. 147  
 Østergaard, K., 348, 359  
 Ostrogovich, G., 60, 69  
 Otero, C., 149  
 Otterstedt, J.-E., 148  
 Ouellet, L., 212  
 Owen, B. B., 191, 207  
 Özdamar, T. H., 330
- Paek, K.-Y., 517  
 Palyutkin, G. M., 301  
 Pan, Z., 67  
 Pan'kovoi, B. E., 263  
 Panda, T., 489, 516  
 Pannetier, G., 132–133, 142  
 Papoutsakis, E. T., 517  
 Parker, A., 207  
 Parker, A. L., 368, 493, 516, 518  
 Pasquon, I., 357, 359  
 Patel, R. C., 535  
 Patwardham, A. A., 144  
 Pavlenko, N.V., 184, 186  
 Pearson, R. G., 67, 71, 93, 103, 104,  
     136–137, 139–142, 194, 207, 535  
 Pease, R. N., 177, 179
- Pelzer, H., 101, 104  
 Penney, W. R., 220  
 Perkowski, J., 109  
 Perlmutter, D. D., 320, 328  
 Perry, R. H., 7, 162, 440  
 Petersen, E. E., 407, 439–440  
 Peterson, R. S., 368  
 Peterson, T. I., 45, 53  
 Petrov, G. N., 301  
 Petrovic, L. J., 408, 440  
 Pigford, R. L., 439  
 Pinkus, A. G., 266  
 Pinsky, M. L., 108  
 Piret, E. L., 259, 294, 469, 531  
 Plank, C. L., 179  
 Platt, A. E., 266, 294  
 Plowman, K. M., 200, 207  
 Plummer, W. B., 419  
 Pogorski, L. A., 421, 440  
 Poiseuille, J. L., 378  
 Polanyi, M., 84, 101, 103–104  
 Poling, B. E., 7, 16  
 Porta, G., 66, 302  
 Portner, R., 517  
 Power, J. B., 517  
 Prater, C. D., 439  
 Prausnitz, J. M., 7, 16  
 Price, R. H., 447–448  
 Prince, A. J., 124–125, 142  
 Prodan, E. 146, 271, 296  
 Prokhorov, V. A., 331  
 Pulz, O. 517  
 Pyle, D. L., 438, 440
- Rabinowitch, E., 191, 207  
 Ragatz, R. A., 527  
 Rahman, M. 517  
 Ramaswami, D., 440  
 Rancourt, D. E., 517  
 Randall, M., 9  
 Rase, H. F., 139, 168, 179, 182  
 Ratchford, W. P., 232, 259  
 Rawlings, J. B., 535  
 Raymond, L. R., 440  
 Reardon, K. F., 517  
 Reed, J., 519–520, 523  
 Rehbock, C., 517  
 Reickers, D., 517  
 Reid, R. C., 16, 20  
 Rekoske, J. E., 535  
 Resnick, R., 360  
 Restelli, E. F., 180  
 Reynolds, O., 407–408, 412, 414, 419–421,  
     423, 434, 530  
 Reynolds, W. C., 306, 327  
 Riccetti, R. E., 409, 440  
 Rice, F. O., 89–91, 103  
 Rideal, E. K., 165, 170  
 Rizvi, A. F., 68
- Robbins, F. C., 499, 517  
 Roberts, G. W., 394, 439, 535  
 Robinson, P. J., 295  
 Rodebush, W. H., 115  
 Roig Muntaner, A., 63, 142  
 Roper, G. H., 260  
 Roseveare, W. E., 53  
 Rosing, H., 360  
 Ross, J., 103  
 Rothfeld, L. B., 173, 179, 439  
 Rotinov, A., 63  
 Rowe, P. N., 438, 440  
 Rubino, A. S., 69  
 Rudd, D. F., 535  
 Rylander, P. 446
- Saad, E. F., 297  
 Sabo, D. S., 328  
 Sajjadi, S., 266  
 Saliya, P. P. S., 209  
 Salvador, F., 259  
 Sanchez, M., 143  
 Santamaría, J. M., 521  
 Sathiyanarayanan, K., 54  
 Satterfield, C. N., 375, 378, 390–391, 394,  
     408, 439–441, 446–447, 535  
 Savage, P. E., 262, 270  
 Sayre, E. S., 517  
 Scheper, T., 517  
 Schiewetz, R. B., 447–448  
 Schilson, R. E., 439  
 Schmidt, E., 407, 411–412, 414–415, 417,  
     530  
 Schmidt, L. D., 535  
 Schubert, H., 70  
 Schuler, R. W., 440  
 Schumacher, H. J., 55, 58, 61, 63–64,  
     105–106, 115, 259, 261  
 Schwemer, W. C., 139–142  
 Scott, C. B., 207  
 Scott, D. S., 439  
 Semenov, N. N., 82, 103  
 Sen Gupta, A., 409, 440  
 Sen, A., 517  
 Sen'ko, O. V., 150  
 Seth, G., 517  
 Sevick, P., 269  
 Shacham, M., 329  
 Shamsipur, M., 58  
 Shapatina, E. N., 263  
 Sharma, M. M., 144, 266, 303, 361  
 Sharma, V., 56  
 Shashkova, I. L. 146, 271, 296  
 Sheppard, A. J., 359, 367  
 Sherwood, T. K., 407, 440, 530  
 Shevchuk, V. U., 270  
 Shin, H. S., 516–517, 523–525  
 Shirasaki, T., 370  
 Shukla, A. A., 517

- Shuler, M. L., 458, 489, 516–517  
 Sikora, L. J., 368, 493, 516–518  
 Silkina, N. N., 260  
 Silvestri, A. J., 15  
 Simons, J. B., 359  
 Sin-Chou, H., 181  
 Sinclair, A., 517  
 Sinisterra, J. V., 214  
 Sinke, G. C., 7  
 Sivasamban, M. A., 148  
 Skrabal, A., 195, 207  
 Smith, J. C., 440, 516  
 Smith, J. M., 15, 67, 94, 155, 306, 327, 378, 420–421, 423, 437, 439–440, 445  
 Smith, W. H. B., 209  
 Smith, W. K., 305, 359  
 Smorodinskaya, Zh. Ya., 181  
 Snider, E. H., 145  
 Souchay, P., 132–133, 142  
 Sridhar, T., 266, 303, 361  
 Srivasta, P. K., 112  
 Srivastava, R. D., 333  
 Staricco, E. H., 151  
 Stedman, G., 66, 302  
 Stephanopoulos, G. N., 456, 516  
 Sterrett, J. S., 450  
 Stewart, W. E., 423, 439–440, 471, 516  
 Storch, H. H., 259  
 Strachan, E., 180  
 Strauss, M. J., 68  
 Strickland-Constable, R. F., 14–15  
 Stul', B. Ya., 302  
 Stull, D. R., 7  
 Sturtevant, J. M., 53  
 Su, W. W., 517  
 Sueyoshi, H., 370  
 Sullivan, J. M., 260  
 Sumkina, V. G., 301  
 Sunavala, P. D., 17, 20  
 Swain, C. G., 57, 136–137, 142, 206–207  
 Szepe, S., 245, 259  
 Taft, R. W., Jr., 206–207  
 Taiani, J. T., 517  
 Taiwo, K., 70  
 Tajbl, D. J., 359  
 Takaç, S., 330  
 Takashima, K., 55  
 Taraban'ko, V. E. 104  
 Taylor, H. S., 157, 177, 179–180  
 Teller, E., 157, 160, 179  
 Temkin, M. I., 181, 263  
 Thiele, E. W., 380, 382–383, 385–386, 388, 390–394, 396, 398–403, 406, 417, 439, 442, 444  
 Thodus, G., 187–188, 408–409, 440, 448–449  
 Thomas, C. L., 179, 449, 535  
 Thomas, C. R., 517  
 Thomas, J. M., 179  
 Thomas, W. J., 179  
 Thömmes, J., 517  
 Thomson, S. J., 179  
 Thornton, T. D., 262, 270  
 Thurner, F., 328  
 Thyrión, F. C. 145  
 Tichacek, L. J., 357, 359  
 Tinkler, J. D., 439–440  
 Tipper, C. F. H., 53, 93, 103–104, 535  
 Tiscareño Lechuga, F., 15, 53, 535  
 Tobey, S. W., 71  
 Tokue, I., 149  
 Tolman, R. C., 81, 96, 103–104  
 Tong, C. H., 68  
 Torzecki, J., 360  
 Trambouze, P. J., 294  
 Tremper, J., 489, 516  
 Treviño, A., 535  
 Treybal, R. E., 471, 516  
 Tripol'skii, A. I. 184, 186  
 Tsvetkovskii, I. B., 301  
 Turner, J. C. R., 275, 294, 535  
 Tuumlets, A. V., 68  
 Twigg, M. V., 9  
 Tzaanakakis, E., 517  
 Ubide, C., 150, 299  
 Underberg, J. H., 360  
 Upadhyay, S. K., 112  
 Urbandk, T., 262  
 Ushakov, A. A., 302  
 Vaidyeswasan, R., 148  
 Valentine, R. L., 210  
 Van Heerden, C., 325, 328  
 Van Ness, H. C., 15, 306, 327  
 Van Gijn, R., 360  
 Van't Riet, K., 489, 516  
 van't Hoff, J. H., 8–9, 125  
 Vardar-Sukan, F., 517  
 Varela, A., 143  
 Vázquez, M., 520  
 Verbiest, J. J., 184  
 Vermette, P., 517  
 Villadsen, J. 479, 516  
 Villani, A., 69  
 Villet, R. H., 440  
 Viscut, 211 (No initials given)  
 Waage, P., 123, 142  
 Walas, S. M., 220, 259, 535  
 Wall, L. A., 103  
 Walles, W. E., 266, 294  
 Wallington, T. J., 145  
 Wan, S. W., 449  
 Wang, D. I. C., 517  
 Wang, S., 60  
 Wang, X., 60  
 Wang, Y., 265  
 Warnock, J. N., 500, 516–517  
 Wassermann, A., 226, 259  
 Watanabe, A., 149  
 Waters, D. N., 297  
 Watkins, S. B., 15  
 Watson, C. C., 53  
 Watson, K. M., 160, 163–164, 167–170, 179, 181–182, 185  
 Watts, H. P., 264  
 Wayne, R. P., 73, 80, 103–104, 192, 207  
 Weathers, P. J., 517  
 Weaver, E. E. C., 442, 444  
 Webb, G., 179  
 Weber, A. P., 259  
 Weekman, V. W., Jr., 391–392, 439  
 Weetall, H. H., 212  
 Wehner, J. F., 355, 359, 440  
 Weissberger, A., 53, 103  
 Weisz, P. B., 380, 396–398, 439–440  
 Weller, K. R., 517  
 Weller, T. H., 499, 517  
 Wells, P. R., 206  
 Wendel, M., 440  
 Wenner, R. R., 18  
 Westerterp, K. R., 325, 328, 359  
 Whalley, E., 209  
 Wheeler, A., 380, 386, 400–402, 406, 439–440  
 Whitaker, D. R., 359  
 White, D., 368  
 White, J. L., 362  
 White, M. L., 113  
 Whitehouse, A. M., 259  
 Whitman, W. G., 471, 516–517  
 Whitmire, M. T., 209  
 Wicke, E., 379–380, 439  
 Wigner, E., 101, 104  
 Wilhelm, R. H., 355, 359, 440  
 Wilson, E. J., 408, 440, 517  
 Wilson, P. D. G., 517  
 Winkler, M. A., 517  
 Winstein, S., 206–207  
 Wise, J. J., 15  
 Wolf, D., 368  
 Wood, W. C., 207  
 Woodside, W., 395, 439  
 Wu, J., 517  
 Wu, L. L., 332  
 Wu, R. J., 108  
 Wynne-Jones, W. F. K., 104, 208  
 Wyslouzil, B. E., 517  
 Yamasaki, K., 149  
 Yang, H. 145  
 Yang, H.-C., 147  
 Yang, K., 145, 166, 168, 179, 375  
 Yang, K. H., 187  
 Yang, W.-C. 439

- Yanovskii, M. I., 144  
Yeh, C. T., 108  
Yesil-Celiktas, O., 517  
Yoshida, F., 413, 415, 440  
Zachara, J. M., 214  
Zajcew, M., 446–447
- Zaleski, T., 359  
Zare, H., 519  
Zeldovitch, Ya. B., 380, 439  
Zemany, P. D., 103  
Zhao, L., 499, 517  
Zharkov, V. V., 301  
Zhong, J.-J., 517
- Zhou, W., 517  
Zhu, W., 362  
Ziglio, M., 55  
Ziman, R. A., 144  
Ziv, M., 517  
Zuman, P., 535



# Subject Index

---

- Absolute reaction rate theory (see Transition state theory)
- Absolute specificity, 198
- Acetic acid from methylacetoxypropionate, 232–234
- Acetylene production, 18
- Acid-base catalysis, 193–197
- form of rate constant, 194
  - general acid, 194
  - general base, 194
  - specific acid, 194–196
  - specific base, 194–196
  - weak acid, 196–197
  - weak base, 196–197
- Acrolein, reaction with butadiene, 132–133
- Activated adsorption (see Adsorption, chemical and chemisorption)
- Activated chemisorption, 154–155
- Activated complex, 98–103
- Activated complex theory (see Transition state theory)
- Activated molecules (see also energized molecules), 97
- Activation energy,
- apparent, 392–393, 398
  - bond strengths and estimation of, 82
  - catalyst geometry and, 454–455
  - collision theory, 95–96
  - defining equation, 24
  - determination of, 51
  - effectiveness factors and measurements of, 393, 462
  - external mass transfer and, 484
  - for diffusion, 393
  - for heterogeneous catalytic reactions, 164
  - for pore-mouth poisoned catalysts, 401–402
  - precision of, 53
- requirement for reaction, 95–96
- shifts at low effectiveness factor, 393
- thermodynamic limitations on, 124–125
- transition state theory, 98–102
- Activation volume, 192–193
- Active center (see also Intermediates and Active sites), 83
- Active sites of enzymes, 198
- Activity (thermodynamic),
- definition, 4
  - effect of pressure on (for condensed phases), 12
  - equilibrium constant and, 9, 10
  - fugacity and, 11
- Activity coefficients of ions, 191–192, 196–197
- Adiabatic operation,
- batch reactor, 308–310
  - CSTR, 318–319, 375–376
  - CSTR's in series, 313
  - definition, 224
  - fixed bed reactor, 425, 428–432
  - limitations on, 305
  - plug flow reactor, 314–315, 318, 324
- Adsorption (see also Adsorption isotherm), 153–160, 178
- activated chemisorption, 154–155
  - activation energy for, 154
  - bonding forces, 156
  - chemical, 154–156
  - coverage, 154–158
  - definition, 153–154
  - dissociative, 154, 159, 168–170, 185
  - enthalpy effect, 156
  - equilibrium constant for, 156, 159, 164, 166–170
  - extent of, 154–158
  - heterogeneous catalysis and, 155–156
- hydrogen on zinc oxide, 180
- isotherms, 156–165
- measurement of, 154–155
- measurement of surface areas by, 158
- monolayer, 156–158, 178
- nitrogen on alumina, 179
- nitrogen on silica gel, 180
- nonactivated chemisorption, 154
- physical, 154–157, 160
- rate of adsorption, 154–156
- rate of desorption, 158
- reversibility, 156
- specificity, 155
- temperature effect, 156
- Adsorption equilibrium constant, 170
- Adsorption isotherm (see also BET adsorption isotherm and Langmuir adsorption isotherm), types, 156, 157
- Adsorption term, 166
- Advancement (see Extent of reaction)
- Aeration of waste treatment bioreactors, 497
- material balances, 497–499
  - process control of bioreactors, 497
  - shock loading, 497
  - sludge age, 498
- Aging of catalysts, 178
- Agitation, 219–220
- Airlift bioreactors, 506
- Algebraic analysis of CSTR cascade, 246–249
- Aluminum chloride, 231–232
- Ammonia,
- decomposition, 65, 181
  - oxidation, 153, 162–163, 262–263, 371
  - reactions with ethylene oxide, 287–289
  - reaction with nitrochlorobenzene, 333–334
  - synthesis, 153, 221

Analysis of kinetics results (see Data analysis, see also Experimentation)  
 Analytical chemistry  
     criteria for use in kinetic studies, 32–34  
     methods, 32  
     physical properties, 49–51  
     uncertainties, 52–53  
 Anchorage dependent cell lines, 500  
 Arrhenius number, 396, 399  
 Arrhenius plot, 51, 393, 444–445  
 Arsenious acid, oxidation of, 79  
 Ascorbic acid, oxidation of, 105  
 Autocatalytic reactions, 214, 227, 238, 266–267, 290–294, 452, 454, 466, 473, 479, 481, 486, 488, 492, 493  
 Autothermal reactors, 309, 317–320, 330  
 Average residence time, 338  
 Axial dispersion, 228–229, 345, 347, 414, 415  
 Axial dispersion model, 344–349  
  
 Backmix reactor (see CSTR)  
 Base catalysis (see Acid-base catalysis)  
 Batch reactor,  
     adiabatic operation, 308–311  
     advantages and disadvantages, 218  
     agitation, 219  
     assumptions for design analysis, 307–308  
     configuration, 217–219  
     constant pressure, 226, 307  
     design analysis for, 225–228, 307–310  
     design equations, 307–310  
     energy balance, 307–310  
     heat transfer in, 219  
     high pressure, 219  
     material balance, 225–228  
     nonisothermal, 307–309  
     nonproductive periods, 218–219, 228  
     physical characteristics, 219  
     size, comparisons of, 256  
     uses, 218  
 Battery of CSTR's (see CSTR's in series)  
 Bed porosity, 408, 532  
 Bench scale experiments, 217  
 Benzene,  
     from cumene, 182, 379  
     nitration, 131–132  
 Benzhydryl bromide hydrolysis, 68  
 Benzoquinone, reaction with  
     cyclopentadiene, 226, 245–247, 249  
 Benzoyl chloride, methanolysis of, 50  
 Benzyl alcohol, reaction with  
     chlorophenylsilane, 151  
 Benzyl chloride, reaction with nitric acid, 131–132  
 BET adsorption isotherm, 160, 171, 179  
 Bimodal pore size distribution, 172–173  
 Bimolecular reaction, 73, 78, 94  
 Binder for catalyst, 174–175

Biochemical transformations,  
     applications, 451, 453, 473, 493, 499–500, 507–508, 512, 522–523  
     batch fermentation, time course, 468, 521  
     early examples, 451  
     effects of volume changes in aqueous medium, 465, 467  
     time for completion of a batch culture, 469  
     trajectory of biochemical reaction during batch reaction, 468, 521  
 Biomass specific rates (see q-rates), 464  
 Bioreactors,  
     advantages of batch operation, 473  
     agitation by gas bubbles, 452  
     agitation by mechanical devices, 472  
     batch and semibatch operation, 473  
     batch reactor, 465, 468, 474, 481  
     chemostat, 467, 522–523  
     definition, 451–452  
     design principles/products, 452–453  
     differences from chemical reactors, 481  
     disadvantages of batch operation, 473  
     effect of  $K_S$  on time necessary to achieve a specified conversion, 474  
     modes of operation in the design of a bioreactor, 472–473, 522–523  
     nonproductive periods for batch operation, 455  
     photobioreactors, 512–513  
     strategies for optimization of fed batch reactors, 474  
 Biotic phase, 472  
 Blake-Kozeny equation, 419  
 Bodenstein approximation (see Steady state approximation)  
 Bond energies and mechanisms, 78, 85–86  
 Boundary conditions,  
     cylindrical pore model, 381  
     dispersion model, 344  
     effective diffusivity model, 387  
     nonisothermal catalyst pellet, 396  
     pseudo homogeneous model, 427  
     two-dimensional model, 437  
 Branched chain reactions, 84–86, 91–93  
 Bromination of m-xylene, 37–38  
 Bromine,  
     reaction with hydrogen, 84–86  
     reaction with lactose, 291  
 Bromophenol blue reaction with hydroxide ions, 209  
 Brønsted acidity, 193  
 Brønsted-Bjerrum equation, 191  
 Bulk density, 418  
 Bulk diffusion, 376–378, 391  
 Burke-Plummer equation, 419  
 Butadiene,  
     from butene, 449–450  
     reaction with acrolein, 64–65, 132–133  
     reaction with ethylene, 315–316  
     reaction with methyl acrylate, 231–232  
 Butanol,  
     from isobutene, 442  
     reaction with 2,6-toluene diisocyanate, 141–142, 301–302  
 Butene,  
     dehydrogenation, 144, 186–187, 449–450  
     isomerization, 16  
 Cage effect, 190–191  
 Calorimetry, 68  
 Capillary condensation, 173  
 Carberry reactor, 359  
 Carbon dioxide, reaction with hydrogen, 187  
 Carbon monoxide, reaction with chlorine, 27, 263–264  
 Carrier for catalyst or microorganisms, 174–177, 500, 502, 505  
 Carrying capacity-logistic model, 475  
 Cascade of stirred tank reactors (see CSTR's in series)  
 Cascades of chemostats/Batteries of CSTBRs,  
     advantages, 488–489  
     graphical solutions, 491–493, 522–523  
     material balances, 489–493, 521–523  
     use of multiple feed streams (cross flow), 488–489, 520–522  
 Case studies, 308, 449–450  
 Catalysis (see also Catalyst; Acid-base catalysis; Homogeneous catalysis; Enzyme catalysis; Heterogeneous catalysis; and Biocatalysis)  
 Catalyst,  
     activation, 175  
     activity, 175–178, 373, 449  
     aging, 178  
     binder, 174, 175  
     carrier, 174–177  
     changes in activity, 177–178  
     commercial, 176–177  
     deactivation, 178, 305, 373–374, 425, 428–429, 434, 436  
     definition, 152, 193  
     diluent, 176  
     drying, 175  
     dual function, 176–177  
     effectiveness (see also Effectiveness factor), 371, 375, 380–401  
     extender, 175  
     fabrication, 174–177  
     formulation, 175–177  
     fouling, 174, 176, 178  
     geometry, 172, 374, 376, 378, 381, 383, 387, 390–391  
     handling of solid catalysts, 372  
     impregnation, 174–177

- impurities, 175, 178  
 industrial, 153, 174–175, 178  
 influence on equilibrium composition, 152  
 lifetime, 174, 373  
 loss of activity on poisoning, 152, 174, 177–178, 399–402  
 mechanical properties, 174, 502  
 in packed bed reactors, 371, 386, 407, 414, 418–421, 425, 429–437  
 pelleted, 424–425, 427, 429  
 physical characterization of, 171–173  
 poisoning, 152, 174, 177–178, 399–402  
 pore size distribution, 172–173  
 pore structure, 172–173  
 porosity, 171–172  
 preparation, 174–177  
 promoter, 175–177  
 reaction rate expressions (see Surface reactions)  
 regeneration, 176, 178, 373–374  
 selectivity, 178, 375, 397  
 shape, 176–177  
 size, 176–177  
 stabilizer, 177  
 support, 174–177  
 surface area, 172, 174, 178, 372, 384, 417  
 void volume, 171–172, 381, 408, 422, 425  
 Catalytic force, 152  
 Catalytic oxidation of naphthalene, 374  
 Catalytic processes, 153  
 Categories of major products from animal cell culture, 499  
 monoclonal antibodies, 499  
 recombinant glycosylated proteins, 499  
 viral vaccines, 499  
 Causes of cell damage in bioreactors, 502  
 Cell growth (modes),  
     increase in average mass of individual cells, 453  
     increase in number of cells, 453  
 CFSTR (see CSTR, CSTBR)  
 Chain carrier, 83–84, 87, 89, 91–92  
 Chain length, 83–84, 87, 90  
 Chain reactions, 83–93  
     branched chain, 84, 91–93  
     characteristics of, 87  
     explosions, 87, 91–93  
     hydrogen plus bromine, 84–86  
     identification of, 87  
     inhibitors, 91, 152, 177  
     ozone decomposition, 87–88  
     Rice-Herzfeld mechanisms, 89–91  
     straight chain, 84, 86, 92  
 Characteristic dimensions of different types of cells, 501  
 Chemical adsorption (see Adsorption, chemical)  
 Chemical analysis (see Analytical methods)  
 Chemical formulae for biochemicals, 462  
 Chemical kinetics (see also Reaction rate),  
     comparison with thermodynamics, 1  
     definition, 1  
 Chemical potential, 4, 5  
 Chemical shift, 68  
 Chemisorption (see Adsorption, chemical)  
 Chemostat (see also CSTBR), 461, 467, 480  
     advantages, 481  
     disadvantages, 481  
     use in studies of biochemical reaction kinetics, 482  
     use in studies of substrate allocation to various metabolic pathways, 482  
 Chilton-Colburn relation, 407, 414–415  
 Chlorine, reactions,  
     with carbon monoxide, 27, 263, 264  
     with 2-ethylhexene-1, 260–261  
     with hydrogen, 115, 116  
 Chlorophenylsilane, reaction with benzyl alcohol, 151  
 Closed boundary, 344  
 Closed sequence reactions (see Chain reactions)  
 Coefficients (see Stoichiometric coefficients)  
 Collision frequency,  
     bimolecular, 94–96  
     termolecular, 96  
 Collision theory,  
     accuracy of, 95–96  
     bimolecular collision frequency, 94–96  
     effectiveness of collisions for reaction, 94–95  
     energy requirement for reaction, 94–96, 98  
     for gases, 94–96  
     for liquid solutions, 189–191  
     rate expression, 94–96  
     steric factor, 95–96  
     termolecular collision frequency, 96  
 Combinations of reactors, 254–255  
 Combined diffusivity, 377–379, 393, 404  
 Comparative rate studies, 131–133  
 Competitive-consecutive reactions (see also Series-parallel reactions), 137–142  
 Competitive inhibition, 141  
 Competitive reactions (see Parallel reactions)  
 Computers (see Machine computation)  
 Concentration difference, bulk fluid-catalyst surface, 406–413  
 Concentration profile,  
     catalyst pore, 172, 381  
     spherical pellet, 381–382, 385–388  
 Concurrent reactions (see Parallel reactions)  
 Conductivity measurements, 50  
 Consecutive reactions (see also Series reactions),  
     batch reactor analysis, 278–280  
     CSTR analysis, 280–282  
     data interpretation for, 135–137  
     design strategy for, 278–283  
     diffusion limited, 404–406  
     effectiveness factors and, 404–406  
     first-order, 133–136  
     intraparticle mass transfer effects, 404–406  
     mathematical characterization of, 133–137  
     maximum concentration of intermediate, 134–135, 278–283  
     other than first-order, 135–142  
     plug flow reactor analysis, 278–280  
     temperature effect, 326–327  
 Contact catalysis (see Heterogeneous catalysis)  
 Contact time, 186, 224, 261, 370, 438  
 Contact time measurements, 370, 438  
 Continuous flow reactors (see also CSTBR; CSTR; Fixed bed reactor; Fluidized bed reactor; Moving bed reactor; PFR; Plug flow reactor; Slurry reactor; and Trickle bed reactor),  
     advantages, 217–221  
 Continuous flow stirred tank reactor (see CSTR)  
 Continuous flow tubular reactor (see Plug flow reactor)  
 Continuous stirred tank reactor (see CSTR)  
 Control of reactors, 322–324  
 Convergence, 226, 231, 353  
 Conversion (see also Extent of reaction; Fraction conversion),  
     by dispersion model, 355–357  
     by segregated flow model, 354–355  
     by stirred tanks in series mode!, 357–358  
     and yield, 273  
 Conversion rate (see also Reaction rate), 22–23  
 Cottonseed oil hydrogenation, 151  
 Cracking catalyst, 178, 379, 384, 400, 440  
 Cracking reactions, 178, 374, 379, 384, 389  
 C-star (see CSTR)  
 CSTBR (single),  
     concentration factor, 486, 523  
     cell separation and recycle enhances productivity, 486  
     operation with cell separation and recycle, 486–487, 522–523  
 CSTR,  
     adiabatic operation, 313, 318, 324–325  
     advantages and disadvantages, 219–221  
     assumptions, 234, 307  
     design of individual CSTR, 234–236, 311–314

- CSTR (Continued)**
- design equation, 235–236
  - dilution effect on rate, 220
  - energy balance, 311–314
  - F(t) curve, 341–343
  - heat transfer in, 220
  - material balance, 235–236
  - mixing in, 220
  - multiple CSTR cascade (see CSTR's in series)
  - nonisothermal, 311–314
  - nonsteady state analysis, 239–241
  - optimum temperature for reversible reaction, 325, 326
  - physical configuration, 218–220
  - relative volumetric efficiency, 239–240
  - residence time, 237
  - response to pulse stimulus, 341–342
  - response to step stimulus, 341–342
  - size requirements relative to PFR, 237–240
  - space time, 236–237
  - stability analysis, 320–324
  - use in kinetics studies, 236
  - volume requirements, 237–240
- CSTR cascades,**
- adiabatic cascade, 313
  - algebraic analysis, 246–249
  - argument for equal size reactors, 244–245, 249
  - combination with plug flow reactors, 254–255
  - graphical analysis, 242–246
  - heat transfer requirements, 311–313
  - minimization of cascade volume, 244–246
  - order of tank sizes, 254–255
  - overall yield in, 275–277
  - relative costs, 250–252
  - size comparison with plug flow reactor, 249–251
  - transient analysis, 253
- Culture of plant cells and tissues, 506–511**
- advantages, 507
  - constraints on this technology, 506, 508
  - disadvantages, 509
  - general categories of plant culture, 508
  - production of secondary metabolites, 511
  - productivity considerations, 510
- Cumene cracking, 379, 384, 389**
- Curvature of data plots, 40–41**
- Cyclohexadiene reaction with propylene, 296**
- Cyclohexane dehydrogenation, 442, 444**
- Cyclohexanol reaction with acetic acid, 58, 106**
- Cyclohexene,**
  - from ethylene and butadiene, 314–316
  - hydrogenation, 447–448
- Cyclopentadiene reaction with benzoquinone, 226–228, 245–248, 252**
- Cylindrical pore model (see also Effectiveness factor), 172–173, 383–385, 391–393, 399–402, 404–406**
- Data, sources of thermochemical data, 7**
- Data analysis (see also Differential methods; Differential methods of data analysis for consecutive reactions; Experimentation; and Integral methods),**
- enzyme kinetics, 198–200
  - surface reactions, 169–170
- Deactivation,**
- catalyst, 164–175, 177–178
  - enzyme, 201–202
- Debye-Hückel theory, 191–192**
- Decomposition (see also Pyrolysis), 5-methyl-2-oxazolidinime, 266–267**
- Degradation of phenolic compounds in a cascade of two CSTBRs, 521**
- Dehydration of propanol, 6**
- Dehydrogenation of,**
- butene, 144
  - cyclohexane, 442, 444
  - ethane, 18
  - ethylbenzene, 153
- Denitrification of wastewaters in a packed bed, 518**
- Depolymerization of dimeric dihydroxyacetone, 211**
- Design chart,**
- comparison of CSTR cascade volume and PFR volume, 249–251
  - comparison of single CSTR and PFR volumes, 239–240
  - dispersion model, 355–357
  - series-parallel reactions, 283–287
- Design equations,**
- batch reactor, 225–228
  - comparison of, 256
  - CSTR, 234–239
  - plug flow reactor, 228–234
  - recycle reactor, 253–254
- Design strategy,**
- autocatalytic reactions, 271, 290–294
  - parallel reactions, 274–278
  - series-parallel reactions, 283–289
  - series reactions, 278–283
- Desorption (see Adsorption)**
- Desorption isotherm method for pore size distribution, 172–174**
- Detailed balancing, 81**
- Determination of maximum feed flow rate for reaction in a chemostat, 520, 522–523**
- Development of shear stresses in the presence of velocity gradients, 501**
- Deviations from ideal flow conditions, 337–359**
- Dextrose production, 212–213**
- dF(t) (see also F(t) curve), 337–340**
- Diauxic growth, 457**
- Diels-Alder reaction, 132–133, 226–227, 231–232, 237, 247–249, 252, 315**
- Diethylsulfate reaction with sulfuric acid, 121–122**
- Differential methods of data analysis (see also Data analysis),**
- for consecutive reactions, 135–137
  - initial rate studies, 38–39, 120–122
  - least squares approach, 36, 45, 51
  - manipulation of concentration-time data, 35–38
  - procedure, 35–38
  - reversible reactions, 120–123
  - stoichiometric feed ratio, 36
  - use of, 37–38
- Differential yield of intermediate, diffusional limitations on, 404–406**
- Diffusion (see also Diffusivity),**
- bulk, 376–377
  - in heterogeneous catalysts, 160–161, 172
  - influence on rate (see Effectiveness factor)
  - Knudsen, 376–377, 379–380, 393
  - ordinary, 376–377
  - across poisoned pore mouth, 400–402
  - pore geometry and, 378–379
  - in porous catalysts, 376–380
  - and reaction in porous catalysts (see also Effectiveness factor), 380–406
  - surface, 376, 379
- Diffusion controlled reaction, 408–413**
- Diffusivity (see also Diffusion),**
- bulk, 376–377
  - combined, 378–379, 392–393, 402, 405–406, 441
  - effective, 378–379, 387–390
  - Knudsen, 376–377, 379–380, 393
  - pseudo binary, 411
- Dihydroxyacetone depolymerization, 211**
- Dilatometry, 47–48, 69**
- Dilution rate,**
- definition, 479
  - washout phenomena, 483, 522–523
- Disguised kinetics, 392–393, 408–410**
- Dispersion in fixed beds, 419–420**
- Dispersion model, 355–357, 361, 366, 368–369**
- assumptions, 344–348
  - F(t) curve, 345–346
  - material balance, 355
  - response to pulse stimulus, 346
  - response to step stimulus, 345

- Dispersion parameter,  
definition, 355  
estimation of, 346–349
- Disposable bioreactors (single use), 501, 513–516  
advantages, 513  
sizes, 513
- Dissociative adsorption (see Adsorption, dissociative)
- Drift factor, 412, 414–415
- Driving force term, 166–167
- Drying of catalysts, 175
- Dual function catalyst, 176–177
- Eadie plot, 199–200
- Effective diffusivity,  
definition, 376–379  
effectiveness factor and, 387–390
- Effective thermal conductivity,  
catalyst, 394–397  
fixed bed reactor, 421–429
- Effectiveness factor, 380–402  
asymptotic forms, 390–391  
cylindrical pore model, 381–387, 399–402, 404–406  
definition, 380  
determination of, 383–385  
effective diffusivity model, 387–389, 391, 294–299  
endothermic reactions, 397–398  
exothermic reactions, 395–399  
first-order reaction, 380–390, 392–393, 395–399  
flat plate, 390, 394  
greater than unity, 395–396  
Hougen-Watson kinetics, 393–394  
interpretation of, 381–383  
isothermal catalyst, 382–394  
multiple steady states, 398  
naphthalene oxidation, 374  
nonequimolar counterdiffusion, 391  
nonisothermal pellet, 395–399  
pellet geometry and, 390–391  
poisoned catalyst, 399–402  
pore model, 381–387, 392, 399–402, 404–406  
reversible reaction, 394  
second-order reaction, 385–387  
selectivity considerations, 403–406  
shifts in reaction order, 392–393, 408–410  
zero-order reaction, 385–387, 390–391
- Effectiveness factor plot,  
first-order reaction, 382–383, 386, 389–390  
nonequimolar counterdiffusion, 391–392  
second-order, 386–388  
spherical catalyst, 389–390  
zero-order, 386, 390
- Einstein's law of photochemical equivalence, 87
- Electrical measurements in rate studies, 34
- Electromeric effects, 203
- Electron donor substituents, 206
- Electron withdrawal, 206
- Electrostatic effects, 191–192
- Elementary reaction (see Mechanistic equation)
- Elimination of time as an independent variable, 126–127, 129–132, 138–140
- Endogenous metabolism, 458–459
- Endothermic reaction,  
definition, 6  
effectiveness factor for, 398
- Energized molecules, 97–98
- Energy of activation (see Activation energy)
- Energy balance,  
batch reactor, 307–310  
CSTR, 311–313  
fixed bed reactor, 422–423, 427–429  
general, 222–224, 305–307  
plug flow reactor, 314–317  
porous catalyst, 396–398  
semibatch reactor, 319–320  
stability analysis and, 320–324  
steady state, 306–307  
tubular reactor, 314–317
- Energy transformation function, 396–397
- Energy loss curves, 320–324
- Energy transformed by reaction, 320–324
- Energy requirement for reaction, 95–96, 98
- Enthalpy,  
of activation, 102  
of adsorption, 154, 156, 160, 164  
of formation, 6, 7  
of reaction, 20, 306, 309, 321  
standard enthalpy change, 5–6, 8, 15, 330, 331
- Entropy,  
of activation, 102–103  
standard entropy change, 5
- Enzymatic hydrolysis of lactose, 518
- Enzyme catalysis,  
data analysis, 198–200  
deactivation of enzyme, 201–202  
environmental effects, 201–202  
Haldane relation, 200  
inhibition effects, 201  
mechanisms, 198–200  
rate expressions for, 198–199  
specificity, 198  
temperature effect, 201
- Enzyme kinetics (see Enzyme catalysis)
- Equilibrium,  
criteria for chemical reaction, 4, 7–8  
standard states for calculation of, 5
- Equilibrium approximation, 74–78
- Equilibrium composition (see Equilibrium yield)
- Equilibrium constant,  
for adsorption, 158, 164–165, 170  
estimates of, 202–206  
heterogeneous reactions, 12  
pressure effect, 8–9  
relation to species activities, 9  
relation to standard Gibbs free energy change, 7–8  
temperature effect, 8, 11
- Equilibrium yield,  
calculation of, 9–12  
effect of catalysts, 12  
excess reactants, 12  
inerts, 12  
pressure, 11–12  
temperature, 11
- Equivalent particle diameter, 379, 407, 419
- Ergun equation, 419, 429
- Ethane dehydrogenation, 18
- Ethanol via hydration of ethylene, 10–11
- Ethyl magnesium bromide, reaction with pinacolin, 68
- Ethylene,  
from ethane, 18  
hydration of, 10, 11  
hydrogenation, 398–399, 444–445  
oxidation, 449  
reaction with butadiene, 314–316
- Ethylene bromide, reaction with potassium iodide, 41–42
- Ethylhexene chlorination, 260–261
- Excess concentration technique, 48–49, 131–132, 141–142
- Exothermic reaction,  
definition, 6  
energy transformation curve, 320–324  
reversible, 324–326
- Experimentation (see also Data analysis)  
determination of effective diffusivity, 376–379
- F(t) curve determination, 340–341
- isolation method, 49–49
- planning for, 31, 44–45
- precautions, 29–32
- residence time determination, 338–340
- techniques and apparatus, 32–34
- temperature control, 30
- tests for mass transfer limitations, 161–162
- void volume determination, 171–173
- Explosion limits, 92–93
- Explosions, 91–93
- Extender, catalyst, 175
- Extent of reaction,  
concept, 2, 3  
fraction conversion and, 3  
per unit volume, 23, 26, 117, 119

- External mass transfer, 406–413  
 External surface concentrations, elimination of, 409–413  
 estimation of, 409–413  
 Extinction temperature, 323–324  
 Eyring's theory (see Transition state theory)
- $F(t)$  curve, 337–352  
 CSTR, 340–343  
 definition, 337–338  
 determination of, 338–340  
 dispersion model, 344–349  
 laminar flow reactor, 342–343  
 plug flow reactor, 340  
 probabilistic interpretation, 340–341  
 stirred tanks in series model, 349–352  
 tubular reactor, 340–341  
 Families of reactions, 82  
 Fatty oils, hydrogenation of, 446–447  
 Fed batch operation of stirred tank (see also extended culture), 477–480, 523–526  
 Fick's first law, 344, 376–377, 387  
 First law of thermodynamics (see Energy balance)  
 First-order reactions, consecutive, 133–135  
 in CSTR, 245–246  
 in CSTR cascade, 246–247  
 effectiveness factor for, 380–390, 392–393, 395–399, 404–406  
 examples, 26  
 Guggenheim's method for data analysis, 46–48  
 mathematics of, 25  
 parallel, 125–127  
 precision of rate constants, 52–53  
 reversible, 117–118, 120  
 surface reaction, 164–165  
 Fixed bed reactor (see also Trickle bed reactor),  
 adiabatic operation, 425, 428–434  
 advantages of, 372  
 catalyst regeneration, 373–375, 449  
 configurations, 371  
 control of bed temperature, 371–372  
 description, 371–373  
 design of, 418–437  
 disadvantages of, 372–373  
 dispersion in, 419–420  
 energy balance, 421–423, 427–429  
 flow in, 372–373  
 heat transfer in, 372, 419–425, 427–429  
 homogeneous models, 425–437  
 mass transfer in, 406–408, 410–413, 445–446  
 material balance, 425–428  
 models, 418–419, 423–437  
 multiple steady states, 429–430  
 one-dimensional model, 418–419, 422, 425–436  
 packing, 176, 372  
 pressure drop, 373, 419, 533–535  
 pseudo homogeneous models, 425–437  
 thermal losses, 434–436  
 two-dimensional model, 418, 421–424, 425–427, 436–437  
 velocity profile, 427  
 Flow, in fluidized beds, 374–375, 437–439  
 through packed beds (see nonideal flow models), 371–373, 419–420  
 Fluidized bed reactor, advantages, 374–375  
 description, 374–375  
 design, 437–439  
 disadvantages, 374–375  
 heat transfer correlation, 409, 414–415  
 mass transfer in, 408–409, 445–446  
 models, 438–439  
 uses, 374  
 Formation, heat of, 6  
 Fouling of catalysts, 174, 176, 178  
 Fraction conversion, definition, 3  
 relation to extent of reaction, 3  
 Fractional life method of data analysis, 45–46  
 Fractional-order reactions, 27, 79, 87–88  
 Franck–Rabinowitch effect, 191  
 Free energy (see Gibbs free energy)  
 Free energy diagram for reaction, 98–100  
 Free energy of activation, 102, 202–204  
 rate constants and, 204–206  
 Free energy relations, 202–207  
 Free radicals (see also Chain reactions; Intermediates), mechanism, 109, 112  
 polymerization, 69, 87, 91  
 recombination, 191  
 Frequency factor (see also pre-exponential factor), 24  
 Frequency response diagram, 338  
 Friction factor, 231, 419  
 Fugacity, 9, 11  
 Fugacity coefficient chart, 527  
 Gel formation in catalyst preparation, 175  
 Gibbs free energy (see also Chemical potential), calculation of standard free energy change, 6–7, 10  
 equilibrium constant and, 7, 10–11  
 equilibrium criteria and, 7  
 of formation, 5, 6  
 pressure effect, 7  
 standard change on reaction, 5, 6  
 temperature effect, 6  
 Global reaction rate, 416–418  
 Glucoamylase use in dextrose production, 212  
 Glucose mutarotation, 210  
 Graphical analysis of CSTR cascade, 242–246  
 Graphical determination of  $V_R/F_{A0}$ , 234–239  
 Group contributions, 203–204  
 Group specificity, 198  
 Growth cycle of microorganisms, acceleration phase, 453  
 balanced growth, 454, 462  
 cryptic growth, 458  
 death phase (decline phase), 453, 459  
 deceleration phase, 453–454, 458  
 doubling time, 458, 462  
 exponential growth phase, 453–455, 458, 462  
 growth media considerations, 455  
 inhibition, 454  
 inoculation, 453  
 lag phase, 453, 455–456  
 logarithmic phase of growth (see exponential growth)  
 limits on growth, 454  
 maximum stationary phase, 453–454, 458  
 rate laws and mathematical descriptions, 455–459  
 Guggenheim's method of data analysis, 46–48  
 Hairy root culture, 509–510  
 Haldane relation, 200  
 Half-life method of data analysis, 45–47  
 Hammett equation, 204–206, 214–215  
 Hammett substituent constants, 203–206  
 Hanes plot, 199–200, 212  
 Hard sphere theory (see Collision theory of gases)  
 Heat of adsorption, 154, 160, 164  
 Heat of formation, 6, 7  
 Heat of reaction, 5, 7, 10  
 Heat transfer, batch reactor, 219, 307–310  
 bulk fluid to external catalyst surface, 413–416  
 to containing wall, 420–421  
 CSTR, 311–312  
 fixed bed reactor, 371–372, 420–425, 434–436  
 limitations on rate, 413–418  
 plug flow reactor, 314–318  
 in porous catalyst, 394–397  
 semibatch reactor, 319–320  
 Heat transfer coefficient, definition, 307  
 particle-bulk fluid, 408, 414–416

- Helium-mercury method for void volume determination, 171
- Henry's Law, 470
- Heterogeneous catalysis, diffusion and (see also Effectiveness factor), 160–163
- mass transfer and, 160–163
- rate expressions, 163–169
- rate limiting step, 162–163
- steps in process (see also Surface reaction), 160–161
- Heterogeneous model of fixed bed reactor, 418–419
- Heterogeneous reaction, thermodynamics of, 12
- Heterogeneous reaction system, 223–224
- High pressure batch reactor, 12, 219
- Hirschfelder rules, 82
- Hofstee plot, 199–200, 211
- Holding time, 223–224, 226–227, 307–310
- Homogeneous catalysis (see also Acid-base catalysis; Enzyme catalysis), 153, 193–202
- Homogeneous model (see Pseudo homogeneous model)
- Homogeneous reaction system, 223–224
- Hougen-Watson kinetics, effectiveness factor for, 393–394
- rate expressions for, 163–169
- Human stem cells, 503–506
- culture of, 504–506
- definition, 504–506
- human embryonic stem cells, 505
- induced pluripotent stem cells (iPSCs), 505
- pluripotent stem cells, 505
- regenerative capabilities, 504
- three dimensional culture, 505
- Hydration of isobutene, 47–48, 442
- Hydrodesulfurization, 373, 440
- Hydrogen, adsorption on zinc oxide, 180
- reaction with bromine, 84–86
- reaction with carbon dioxide, 165, 187
- reaction with chlorine, 83, 115–116
- reaction with nitric oxide, 76
- Hydrogen ion, 193–197
- Hydrogen peroxide, reaction with iodide ions, 208
- reaction with sodium thiosulfate, 332–333
- Hydrogenation of, acetylene, 444
- cottonseed oil, 151
- cyclohexene, 447–448
- edible oils, 153
- ethylene, 398–399, 444
- fats, 153
- fatty oils, 446–447
- linoleic acid, 151
- nitrobenzene, 446
- propionaldehyde, 168–169
- Hydrolysis, benzhydryl bromide, 68
- catalytic, 194
- ethyl esters, 206
- p-nitrophenyl trimethylacetate, 518
- Hydroquinone, 112–113
- Hydroxide ion, as a catalyst, 193–196
- reaction with bromophenol blue, 209
- reaction with nitrourethane ion, 208
- Hydroxybutyric acid, conversion to lactone, 268
- Hysteresis and stability analysis, 323–324
- Ideal reactors (see Batch reactor; CSTBR; CSTR; PFR; Plug flow reactor, PFBR)
- Ignition of reaction, 217, 323–324
- Immobilized enzymes, 213, 262, 368, 452, 518
- Impact of viscosity enhancers on cell damage, 502
- Imperfect pulse method to get dispersion parameter, 347
- Impregnation of catalysts, 175
- Impulse stimulus, 338–339, 347
- Impurity effects, 30
- Independent reactions, determination of, 12–14
- Inducers, 490, 511
- Induction period, 67, 87, 91
- Inductive effects, 203
- Inhibition, enzyme, 201
- Inhibitors, 57, 87, 91, 152, 177, 179, 201, 211, 262, 274, 457
- Initial conditions, dispersion model, 344
- Initial rate studies, 38–39, 54–55, 60, 110, 118, 120, 169–170, 181–183, 185–188, 199
- Initiation reaction, 83, 85–87, 89, 113
- Initiators, 69, 87, 91
- Innoculation, 453
- Instantaneous fractional yield, 275–276
- Integral methods (see also Data analysis; Experimentation), fractional life methods, 45–46
- general procedure, 39–41
- graphical procedure, 39–43
- Guggenheim's method, 46–48
- numerical procedures, 44–45
- reversible reactions, 117–123
- use of, 42–50, 117–123
- Integration, numerical, 47, 140, 278, 310
- Interaction energies, 202–204
- Intermediates, 78–80, 85–88, 92, 103, 106, 110, 113, 157, 182, 190, 193
- Intermittant addition of reactants, 218
- Intermolecular forces, 154, 156, 189–190
- Interpretation of kinetic data (see Data analysis)
- Interstage cooling, 325
- Intraparticle heat and mass transfer (see Effectiveness factor)
- Intrinsic rate, 23, 123, 381, 383, 403, 416–417
- Iodide ion, oxidation by hydrogen peroxide, 208
- Ionic strength, 189, 191–192, 196–197
- Ionization constants, 204–205
- Irreversible reaction, definition, 3
- Isobutene, hydration of, 47–48, 442
- Isolation method, 30, 481, 507–509
- Isomerization of xylene, 294
- Isopropyl benzene (see Cumene cracking)
- Isothermal operation, definition, 224
- Isotopic substitution, 80
- j Factor, for heat transfer, 408–409, 414–415
- for mass transfer, 408–409, 412–413
- Joule-Thompson expansion, 20–21
- Kinetic expression (see Rate expression)
- Kinetic term, 166–167
- Kinetic theory of gases (see Collision theory)
- Kinetics (see Chemical kinetics)
- Kinetics of cell growth in a well stirred batch reactor, 453–456
- Kinetics of formation of xanthan gum, 519
- Knudsen diffusion, 160, 376–381, 392, 410
- Kolmogorev, 502
- Laboratory studies (see Experimentation)
- Lactalbumin degradation, 519
- Lactoglobulin degradation, 519
- Lactose, hydrolysis, 262, 368, 518
- reaction with bromine, 291
- Lag phase, factors influencing length, 457
- Dean Hinshelwood Model, 457
- Laminar flow reactor, 330, 342–343, 352, 358, 360, 363, 419
- Langmuir adsorption isotherm, 156–160
- assumptions, 157, 159, 165
- derivation of, 158–160
- dissociative adsorption, 159
- Hougen-Watson models and, 163–170
- multicomponent, 158–159
- single component, 157–158
- Langmuir-Hinshelwood rate expression (see Hougen-Watson kinetics)
- Law of definite proportions, 2
- Least squares analysis, 36, 45, 51
- Lewis and Randall rule, 9

- Limitations on rate, mass transfer, 174, 217, 374–375, 406–413
- Limiting forms of rate expression, 409–410
- Limiting reagent, 3
- Limiting substrate, 460
- Lindemann mechanism, 65, 97–98, 198
- Linear free energy relations, 202–206
- Linearity of data, 31
- Lineweaver-Burk plot, 199–200, 211
- Linoleic acid, 151
- Liquid distribution in trickle bed reactor, 373
- Lock and key hypothesis, 198
- Logistic model of batch bioreactor, 475–477
- carrying capacity, 475–477
  - 2-parameter model, 476–477
- Long chain approximation, 87, 106–107, 109
- Long interval method, 44
- Longitudinal dispersion, 352, 355, 357, 361–362, 365–366, 368, 420, 429–431
- Longitudinal dispersion model (see Dispersion model)
- Longitudinal Peclet number, 420, 429
- Luedeking-Piret Model, 469
- Lysis of cells, 458
- Machine computation, 151, 217, 310, 418–419, 429, 436, 449, 491
- Mammalian cell culture, 503
- advantages, 503
  - disadvantages, 503
  - fabrication of three-dimensional mammalian tissues, 504
  - fed batch operation, 503–504, 523–526
  - protein post-translational modification, 503
  - sources of failure, 503
- Mass balance (see Material balance)
- Mass transfer (see also Diffusion),
- bulk fluid to catalyst surface, 161–163, 406–413
  - comparison of fixed and fluidized bed reactors, 445–446
  - intraparticle, 161–163, 376–380
  - limitations on rate (see also Effectiveness factor), 161–163, 406–413, 416–418
  - in porous catalysts, 161–163, 376–380
- Mass transfer coefficient, 471–472
- Material balance,
- batch reactor, 225
  - CSTR, 234–237, 239–240
  - fixed bed reactor, 260, 371–374, 407, 410
  - general, 222–223
  - plug flow reactor, 228–234
  - semi batch reactor, 256–259
  - tubular reactor, 228–234
- Mathematical characterization of rate expressions,
- consecutive, 133–138
  - irreversible, 25–29
  - parallel, 125–133
  - reversible, 117–123
- Maximization of autocatalytic rate, 290–294
- Maximum concentration of intermediate, series-parallel reaction, 283–287
- series reaction, 278–280
- Maximum yield of intermediate, diffusional limitations on, 404–406
- Mean residence time (see Residence time)
- Mechanism (see also Chain reactions: Free radicals), 72–94
- alternatives for same reaction, 73–74, 79–83
  - criteria for testing, 75
  - definition, 1, 72
  - derivation of rate expression from, 74–80
  - determination of, 73–74, 76–83
  - enzyme catalysis, 197–201
  - guidelines for determination of, 78–80
  - heterogeneous catalysis (see Surface reaction)
  - reversible reactions and, 78–79
  - Rice-Herzfeld, 89–91
  - steps in, 73–74
- Mechanistic equation, 74–75
- Mercury penetration method, 171–173
- Metabolic engineering, 456
- Metabolites,
- primary, 458
  - secondary, 458
- Methanolysis of benzoyl chloride, 50
- Methylacetoxypropionate pyrolysis, 232–234
- Methyl acrylate, from
- methylacetoxypropionate, 232–234
  - reaction with butadiene, 231–232, 236–237
- Methyl methacrylate polymerization, 112
- Methyl-2-oxazolidinone decomposition, 266–267
- Michaelis constant, 212
- Michaelis-Menten equation, 199, 212, 214
- Microscopic reversibility, 78–79, 81, 144, 155
- Minimization of CSTR cascade volume, 244–245, 249–251
- Minimum combustion temperature, 323
- Minimum ignition temperature, 323
- Mixed flow models, 343–352
- Mixing,
- characteristics of stirred tank, 234–235
  - effect on product yields, 283–289
- Models,
- fixed bed reactor, 418–437
  - fluidized bed reactor, 370–372, 374–375, 408–409, 414, 437–439
  - nonideal flow, 343–352
- pore structure, 172–173
- Molecular diffusion (see Diffusion)
- Molecular weight distribution, 289–291
- Molecularity, 73–74, 78, 88
- Monod rate law, 461
- analysis of kinetic data, 460
  - double reciprocal plot, 460
  - empirical relation, 461
  - kinetic parameters  $K_S$  and  $\mu_{\max}$ , 460
  - kinetic trajectories of species concentrations via Monod rate law, 519
- limiting form, 459, 461
- normalization with respect to quantity of biomass present, 460
- quenching a biochemical reaction, 467
- underlying rationalization, 461
- use of chemostat to generate kinetic data, 461
- Montmorillonite catalyst, 180
- Moving bed reactor, 371, 373
- Multiple CSTR's (see CSTR's in series)
- Multiple reactions (see
- Competitive-consecutive reactions;
  - Consecutive reactions. Multiple substitution reactions; Parallel reactions; Series-parallel reactions; and Simultaneous reactions)
- Multiple steady states, 329, 430
- Multiple substitution reactions (see also Competitive-consecutive reactions; Series-parallel reactions), 283–289
- Multitube reactors, 427
- Mutarotation of glucose, 210–211
- Nickel tetracarbonyl decomposition, 15
- Nitric acid, from ammonia oxidation, 153, 262–263
- Nitric oxide reaction with hydrogen, 76
- Nitrobenzene, hydrogenation, 131–132, 446
- Nitroethane, reaction with pyridine, 67
- Nitrogen, adsorption on silica gel, 180
- Nitrogen dioxide, 26, 54, 77
- Nitrogen pentoxide, mechanism for decomposition, 75, 77, 105
- Nitrogen tetraoxide, 124–125
- Nitrourethane ion, reaction with hydroxide ion, 208
- Nitrous oxide decomposition, 59, 185
- NMR (nuclear magnetic resonance), 57, 68, 70
- Nonactivated chemisorption, 154
- Noncompetitive inhibition, 201
- Non-equimolar counter-diffusion, effectiveness factors and, 391, 414–415
- Non-ideal flow models, 343–358
- Non-ideal reactors, conversion in, 352–358
- Non-isothermal effectiveness factors, 394–399

- Non-isothermal reactors, 305  
 Non-productive periods in batch reactor, 256  
 Non-steady state analysis,  
   CSTR, 239–241  
   CSTR cascade, 253  
 Numerical procedures,  
   data analysis, 44–45  
   use of, 47–48  
 Nusselt number, 407  
 Occam's razor, 82–83  
 Oleic acid, 83  
 One-dimensional model of fixed bed  
   reactor, 418, 422, 426–436  
 Open boundary, 344  
 Open sequence reactions, 83  
 Opposing reactions (see Reversible  
   reactions)  
 Optimization,  
   of intermediate concentration, 278–281  
   size ratio for two reactor cascade,  
     244–245, 249–252  
   temperature profile (see Temperature)  
 Optimization approaches,  
   minimize length of lag phase, 454  
   of chemostat productivity, 484  
   transition from batch to fed batch, 455  
   use of supplementary feeds, 455  
 Order (see also First-order reactions;  
   Second-order reactions),  
   changes in, 79, 97–98  
   definition, 24–25  
   fractional, 27, 79  
   heterogeneous catalytic reactions,  
     163–164  
   inverse, 79  
   mechanism and, 79  
   molecularity and, 73  
   negative, 79  
   noninteger, 27, 79  
   properties, 24  
   pseudo, 24, 48–49  
   shifts at low effectiveness factor, 391–392  
   stoichiometric coefficients and, 25, 79–80  
   thermodynamic consistency and,  
     123–125  
   under mass transfer control, 409–410  
 Ortho-para hydrogen conversion, 441  
 Overall fractional yield, 275  
 Oxidation,  
   ammonia, 262–263, 376  
   ascorbic acid, 105  
   ethylene, 153, 449  
   iodide ion, 208  
   sulfur dioxide, 153, 187–188, 376, 410,  
     424, 430–436, 441, 448–449  
 Oxidative dehydrogenation of butene,  
   449–450  
 Ozone decomposition, 87–88, 105  
 Packed bed reactor (see Fixed bed reactor)  
 Paclitaxel, 506  
 Parallel combinations of reactors, 234,  
   254–256  
 Parallel reactions, 125–133  
   competitive, 125–133  
   design strategy for, 274–277  
   determination of rate expressions,  
     127–133  
   effectiveness factors and, 402–404  
   elimination of time as a variable, 274  
   first-order, 127  
   general order, 127–129  
   irreversible, 126–129  
   mathematical characterization of,  
     126–131  
   operating conditions for selectivity,  
     274–276  
   reversible, 127–128  
   simple, 127–130  
   single reactant, 274–276  
   temperature effect, 325–327  
 Partial oxidation (see Oxidation)  
 Particle diameter, equivalent, 407  
 Particle size, effect on rate, 383–384  
 Partition functions, 99, 102  
 Péclet number (see also Dispersion  
   parameter), 345, 347, 414, 420, 426,  
   429  
 Pelleted catalysts, 174–177  
 Perfusion operation of bioreactors, 494–495  
   advantages, 495  
   disadvantages, 495  
   use with permselective membranes, 494  
 pH, effect on rate, 193–197, 201–202  
 Philosopher's Stone, 152  
 Phosgene production, 263–264  
 Photochemical equivalence, 87  
 Physical adsorption (see Adsorption)  
 Physical characterization of catalysts,  
   170–173  
 Physical methods in experimental studies,  
   32–34  
 Physical property measurements,  
   extent of reaction and, 49–50, 60, 62–71,  
     120  
   use in data analysis, 49–50, 120  
 Pilot plant reactors, 217  
 Pinacolin, reaction with ethyl magnesium  
   bromide, 68  
 Pinene isomerization, 145  
 Piston flow reactor (see Plug flow reactor)  
 Plasmodesmata, 509  
 Plug flow reactor (see also tubular reactor),  
   adiabatic operation, 314–319, 324–325  
   advantages, 221  
   assumptions, 228–229, 314–316, 358  
   axial transport, 228–229  
   combinations with CSTR's, 254–255  
   design, 227–234, 314–317  
   design equations, 229–234  
   energy balance, 314–317  
   F(t) curve, 340  
   heat transfer, 221, 314–317  
   heterogeneous catalytic reactor (see Fixed  
     bed reactor)  
   idealizations, 228  
   material balance, 229–230  
   nonisothermal, 314–317  
   physical configuration, 218, 221  
   pressure drop in, 229, 231, 419, 434  
   radial temperature gradients, 228  
   residence time, 233–234  
   series-parallel combinations, 234  
   single CSTR, 237–240  
   size comparison with CSTR cascade,  
     249–251  
   space time, 230  
   validity of assumptions, 358–359  
   velocity gradients, 228  
 Poisoning of catalysts, 177–179, 372  
   effectiveness factors and, 399–402  
   homogeneous, 399–401  
   nonselective, 399–401  
   pore-mouth, 399, 401–402  
   selective, 399, 401–402  
   uniform, 399–401  
 Polar effects, 203  
 Polar substituent constants, 203–204  
 Polymerization, 93, 152–153, 278, 289–290  
 Pore,  
   average length, 172  
   average radius, 172  
   characteristic dimensions, 379–381  
   effect of geometry on diffusion, 378–379  
 Pore geometry, 376–379  
 Pore model for effectiveness factor,  
   381–387, 392  
 Pore-mouth poisoning, 399–402  
 Pore size distribution, 172–173, 175  
 Porosity,  
   catalyst pellet, 171–172, 442, 444  
   packed bed, 408, 410, 413, 417, 441–442  
   total, 422, 445  
 Potassium iodide, reaction with ethylene  
   bromide, 41  
 Potential energy surface, 98–101  
 Prandtl number, 414–415  
 Precipitation in catalyst preparation, 175  
 Precision of kinetic data, 52–53  
 Preexponential factor, defining equation, 24  
 Pressure,  
   effect on rate, 169–170  
   effect on reactions in liquids, 192–193  
 Pressure drop,  
   fixed bed reactor, 419, 434  
   tubular reactor, 231  
 Pressurized batch reactor, 288

- Pressure measurements in rate studies (see also Physical property measurements), 33–34, 38, 49–51
- Primary salt effect, 192, 196–197, 210
- Principle of microscopic reversibility (see also Microscopic Reversibility), 81, 153
- Probability method to evaluate dispersion parameter, 344–349  
F(t) curve and, 346–348
- Product distribution (see Selectivity)
- Productivity of a CSTBR, 484  
definition, 484  
need for robust operating conditions, 485  
optimization, 484  
relative productivities of chemostat and batch reactor, 485–486
- Promoter, catalyst, 175–177, 179
- Propagation reactions, 83–84, 87, 89
- Propanol, dehydration of, 5, 6
- Propionalde hydehydrogenation, 168–169
- Propylene,  
from cumene, 379–380  
reaction with cyclohexadiene, 296
- Protein degradation, 519
- Proton, 193–194
- Pseudo homogeneous model, 418, 420–436
- Pulse stimulus, 338–340  
response of dispersion model, 344–349
- Purification of reagents, 30
- Pyridine, reaction with nitroethane, 67
- Pyrolysis (see also Decomposition),  
acetone, 184–186  
acetonitrile, 106  
mechanisms, 89
- q-rates, 464–465  
biomass specific rates, 464–465  
variables influencing, 465
- Quantum yield, 87
- Quenching, 30, 33, 228
- Questions addressed in reactor design, 216–217, 226, 236, 243, 252
- Radial dispersion, 418, 426–427
- Radial Peclet number, 420, 434, 436
- Radial temperature gradient, 229
- Radical (see Free radical)
- Rate (see Reaction rate)
- Rate constant,  
for acid-base catalysis, 193–197  
definition, 25  
estimates of (see also Hammett equation), 204–206  
precision of, 52–53  
prediction of, 204–206  
relation to equilibrium constant, 124–125  
temperature dependence, 24, 51, 53  
units, 25
- Rate controlling step (see Rate limiting step)
- Rate determining step (see Rate limiting step)
- Rate equation (see Rate expression; see also Mathematical characterization of rate expressions),  
adsorption limiting, 167–169  
adsorption term, 166–167  
degeneration of form, 35–39, 48–49, 169–170  
desorption limiting, 167–170  
determination of (see Data analysis)  
driving force term, 166, 407  
enzyme catalysis, 198–200  
form, 24–25  
heterogeneous catalytic reactions, 160–169  
Hougen-Watson, 163–170  
integrated forms of, 25–29  
kinetic term, 166  
Langmuir-Hinshelwood (see also Hougen-Watson kinetics), 164  
limiting forms of, 408–410  
reversible reaction, 117–120, 122–123  
sources of data for, 217  
thermodynamic consistency, 123–125  
use in design calculations, 217  
Yang-Hougen form, 166, 177, 179
- Rate limiting step, heterogeneous catalysis and, 74–75, 78–80, 161–163
- Reaction coordinate, 98–102
- Reaction mechanism (see Mechanism)
- Reaction order (see Order)
- Reaction progress variable (see Extent of reaction; and Fraction conversion)
- Reaction rate constant,  
definition, 22–23  
effect of pH, 193–197  
effect of temperature, 24  
in heterogeneous systems, 23, 439  
intrinsic, 24, 123, 380–383, 402  
pseudo homogeneous, 425–428  
time dependence, 24  
units, 25  
variables influencing, 23–24
- Reaction rate constant (see Rate constant)
- Reaction specificity, 152, 197–198
- Reaction step (see Mechanistic equation)
- Reactor (see also Batch reactor; CSTR; CSTBR; Fixed bed reactor; Fluidized bed reactor; Moving bed reactor; PFR; Plug flow reactor; PFBR; Semibatch reactor; Slurry reactor; Trickle bed reactor),  
networks, 254–256  
types, 217–218, 220–222
- Reciprocal plot, 199, 201, 460
- Recombinant DNA techniques (rDNA), 499
- Recombination of free radicals, 27, 85, 87, 115, 187, 191
- Recycle ratio, 253–254
- Recycle reactors, 253–254
- Reference state for design calculations, 224
- Reforming reaction, 18
- Regeneration of catalyst, 176–178, 216, 373–374
- Relative rate constants for consecutive reactions, 135–137
- Relative rate studies for parallel reactions, 131, 132, 137
- Relaxation technique, 122–123
- Relaxation time, 122–123
- Reproducibility of data, 31–32
- Residence time,  
average (mean), 224, 337–341  
CSTR, 234, 236–238  
effect on polymer molecular weight, 289–291, 360  
experimental determination of, 338–339, 340–342  
plug flow reactor, 233–234
- Residence time distribution function (see also F(t) curve), 337–352
- Resistance measurements to monitor reaction, 67, 71
- Resonance effects, 206
- Reversible reaction, 117–126  
definition, 3  
determination of rate expression, 120–122  
effectiveness factor, 394  
energy transformation curve, 321, 323–326  
exothermic, 324, 327–328  
mathematical characterization, 126–130  
opposing first-order reactions, 126–128  
parallel, 126–127  
relaxation techniques and, 122–123  
second-order, 118–120
- Reynolds number, 162, 358, 408, 412, 414, 419–421, 423, 434
- Rhinoceros, 170
- Rice-Herzfeld mechanisms, 89–91
- Rideal mechanism, 165, 170
- Role of oxygen as a limiting substrate, 469
- Salt effect,  
primary, 192, 196–197, 210  
secondary, 189, 207, 209
- Saponification of phenylacetate, 114–115
- Schmidt number, 407, 411–412, 414–415,

- Secondary metabolites of plant culture, 508  
 Secondary salt effect, 189, 207, 209  
 Second-order reactions, classes, 26  
 competitive-consecutive, 138–142  
 in CSTR cascade, 247–249, 251  
 effectiveness factor, 385–386  
 examples, 26  
 mathematical characterization, 26  
 reversible, 119–123  
 surface reactions, 165–166  
 Segregated flow model, 354–357, 365, 367–369  
 Selective poisoning, 400–401  
 Selectivity (see also Consecutive reactions, Parallel reactions; and Series reactions), catalyst, 152  
 definition, 273  
 instantaneous, 274  
 intraparticle mass transfer and, 403–406  
 poisons, 154, 174, 177–178  
 temperature profiles for, 326–327  
 Semibatch reactor, 218, 221–222, 256–259  
 energy balance, 319–320  
 material balance, 257–258  
 quasi-autothermal operation, 319–320  
 uses, 256–257  
 Semiflow reactor (see Semibatch reactor)  
 Sensible heat effects in batch reactors, 308–310  
 Sequence of molecular events in aerobic biotransformations, 469–471  
 Series combinations of plug flow reactors, 234, 254–256  
 Series-parallel reactions (see also Competitive-consecutive reactions), batch reactor analysis, 285  
 CSTR analysis, 285–288  
 design strategy for, 283–284  
 plug flow reactor analysis, 285  
 temperature effect, 325–327  
 Series reactions (see Consecutive reactions)  
 Shaft work, 223, 306  
 Shear sensitivity considerations in culture of animal cells, 500–503  
 Shell and tube reactors, 221, 333, 371–372  
 Sherwood number, 407, 440  
 Short interval method, 44  
 Single use disposable reactors, 501, 513–516  
 advantages, 514–515  
 disadvantages, 514–515  
 polymeric sandwich construction, 514  
 presterilization, 514  
 wave-mixed bag, 514–515  
 Silica-alumina catalyst, 153, 178, 182, 379, 384, 440, 442  
 Silica gel, adsorption of nitrogen, 180  
 Simple reaction (see Mechanistic equation)  
 Simultaneous reactions (see also Consecutive reactions; Parallel reactions; and Series-parallel reactions), equilibrium treatment of, 12, 13, 14  
 number of independent, 13, 14  
 Single substrate reactions, 198–200  
 Sinusoidal stimulus, 338  
 Size comparisons, batch reactor, 256  
 CSTR and plug flow reactor, 238–240  
 CSTR cascade and plug flow reactor, 249–251  
 Size of plant cells, 506  
 Skeletal density, 444  
 Slope method, to get dispersion parameter, 348–349  
 to get number of stirred tanks in series, 351–352  
 Slug flow reactor (see also Plug flow reactor), 228  
 Slurry reactor, 371, 375  
 Sodium phenolate, reaction with phenylacetate, 114  
 Sodium thiosulfate, reaction with hydrogen peroxide, 332  
 Solid catalyzed reactions (see Heterogeneous catalysis)  
 Solvent effects, chemical, 189  
 physical, 189–190  
 Somatic fusion, 508  
 Space time, CSTR, 236  
 CSTR cascade, 243–251  
 definition, 224  
 mean residence time and, 223–224  
 plug flow reactor, 228–229  
 Space velocity, 225, 482  
 Specific acid catalysis, 193–196  
 Specific base catalysis, 193–196  
 Specific growth rates, 462  
 Specificity, enzymatic reaction (see also Selectivity), 198  
 Spectroscopy in kinetic studies, 34, 114, 360, 516  
 Squared terms, 98  
 Stability analysis, CSTR, 322–323  
 fixed bed reactor, 429–430  
 Stability poison, 178  
 Stabilizer, catalyst, 174–175, 177  
 Stable operating conditions, 320–324  
 Standard energy changes (see Enthalpy; Gibbs free energy)  
 Standard reaction conditions, 5, 6  
 Standard states, conventional, 4, 5  
 relation to pressure effects for reactions, 7  
 Stationary state approximation (see Steady state approximation)  
 Steady state approximation (for intermediates), 75, 77, 84–85, 87, 92, 113–114, 198–199, 292, 299  
 Steady state operation, 223, 235, 240–242, 253, 260–261, 264–265, 268–271, 288, 290, 295  
 Stearic acid, 151  
 Step function stimulus, response to, 338–339  
 dispersion model, 346–347  
 stirred tanks in series model, 350–352  
 Steps in heterogeneous catalysis, 161–163  
 Stereochemical specificity, 198  
 Stereochemistry, 198  
 Steric effects, 203, 206–207  
 Steric factor, 94–96, 98, 102–103  
 Sterilization of whey, 519  
 Sterilization of whey - kinetics, 518–519  
 Stimulus-response technique, 337, 339–340  
 Stirred tank reactor (see also Batch reactor; CSTBR; CTSR; and Semibatch reactor), 217, 221–222, 256–259, 309, 317, 319–320, 447  
 tracer response curves, 367  
 Stirred tanks in series model, 349, 357–358  
 conversion, 357–358  
 determination of model parameter, 350–351  
 F(t) curves, 350–351  
 response to step stimulus, 349–352  
 Stoichiometric coefficients, convention for, 2  
 definition, 2  
 matrix of, 13  
 Stoichiometric feed ratio, effect on form of rate expression, 36, 42, 117, 131, 169  
 Stoikinetic equation (see Mechanistic equation)  
 Structure and mechanism, 78–79, 80–81  
 Substituent constants, 204–206  
 Substituent groups; effect on rate constants, 202–206  
 Substrate, 198–201  
 Successive reactions (see Consecutive reactions)  
 Sulfur dioxide, oxidation, 153, 187–188, 221, 410–411, 415, 430, 448  
 Sulfuric acid, reaction with diethyl sulfate, 121–122  
 Support, catalyst, 153, 168, 173–175  
 Surface area of catalyst, 175–177  
 measurement, 160, 172, 177–178  
 Surface concentrations, 407, 182  
 Surface diffusion, 433, 439

- Surface reaction,  
adsorption controlling, 167–168  
adsorption equilibrium, 163–166  
bimolecular, 164–165  
data interpretation, 169–170  
desorption limiting, 168  
first-order, 164  
Hougen-Watson models, 163–169  
limiting forms, 164–165  
molecules on different types of sites,  
164–165  
nonequilibrium adsorption, 163  
rate expressions for, 164–169  
rate maxima, 165  
Rideal mechanism, 165  
second-order, 165  
temperature dependence, 164  
vacant sites involved in, 165, 185–186
- Taft equation, 206  
Tank reactor, 218–219  
Tank sizes, ordering in CSTR cascade,  
241–249, 255–256  
Taxol, 506  
Temperature, effects of,  
on enzymatic reactions, 201–202  
on rate constant, 51, 53  
on surface reactions, 164–166  
Temperature difference,  
bulk fluid-catalyst exterior, 413–416  
within catalyst pellet, 394–399  
Temperature gradient (see also Temperature  
difference; Temperature profile),  
radial, 228–229  
Temperature profile,  
minimization of reactor volume, 324–325  
selectivity considerations, 326–327  
thermodynamic considerations, 324–326  
Termination reactions, 83–87, 89, 91–92,  
107–109, 291  
Termolecular reactions, 96  
Tests,  
for autocatalytic behavior, 290–293  
for mass transfer limitations, 161–162  
Tetraborane decomposition, 108–109  
Tetraethyl lead, 152  
Theory of absolute reaction rates (see  
Transition state theory)  
Thermal conductivity,  
fixed bed, 421–425  
porous catalyst, 394–395  
Thermodynamic consistency, 123–125  
Thermodynamics (see Energy balance;  
Enthalpy; Entropy; Equilibrium  
constant; and Equilibrium yield),  
comparison with chemical kinetics, 1, 5
- limits imposed by, 1, 2  
of reactions, 4–15  
Thiele modulus,  
flat plate geometry, 390  
first-order reaction, 381–383, 387–391  
interpretation of, 382  
poisoned catalyst, 399–402  
reversible reaction, 394  
second-order reaction, 386, 391–392  
zero-order reaction, 386, 390, 444
- Thiophene, 146, 440
- Third-order reactions,  
classes, 26  
examples, 27, 302  
mathematical characterization of, 27
- Time ratio method,  
competitive-consecutive reactions,  
137–141  
consecutive reactions, 135–137
- 2, 6-Toluene diisocyanate, reaction with  
butanol, 141–142
- Tortuosity factor, 378–379, 389, 440,  
442–444
- Total porosity, 445
- Totipotency, 509
- Tracer, 233, 235, 339, 344–346, 352,  
359–360, 363, 367, 501
- Transfer function method for dispersion  
parameter, 347–348, 367
- Transformed root culture, 509
- Transformed shoot culture, 509
- Transient analysis of CSTR behavior,  
239–241
- Transient operation, 223
- Transition state, 98–102
- Transition state theory, 98–103  
activation energy, 100, 102  
basic hypothesis, 98–99, 101  
collision theory and, 98  
enthalpy of activation, 102  
entropy of activation, 102–103  
equilibrium hypothesis, 98–99, 101  
free energy of activation, 102  
linear free energy relations and, 202–206  
potential energy surface, 98–101  
pressure effect and, 192–193  
rate constant, 102  
reaction coordinate, 98–101  
reaction mechanism, 100  
reaction rate, 101–102  
thermodynamic functions, 102
- Trickle bed reactor (see also Fixed bed  
reactor), 373, 375, 408, 510
- Tube furnaces, 221
- Tubular reactor (see also Plug flow reactor,  
F(t) curve), 340–341
- Turnover number, 197  
Two-dimensional model, 420–428  
Two-film theory of Lewis and Whitman,  
471
- Two phase model, 438–439
- Uncompetitive inhibition, 201  
Uniformly accessible surface, 407, 409  
Unimolecular reactions, 65, 73, 76, 78, 89,  
96–98, 164, 169, 198, 200, 293, 295
- Unstable operating point, 322–323
- Vanadium pentoxide, 430, 448
- Variable volume systems, mathematics of,  
27–29, 257
- Variance method,  
to evaluate dispersion parameter,  
347–348, 351, 361, 368  
to evaluate number of stirred tanks, 351,  
368
- Velocity, effect on conversion in  
heterogeneous catalysis, 217, 229, 262
- Velocity profile,  
fixed bed reactor, 161–162, 229, 334,  
427  
tubular reactor, 289, 360
- Vinyl chloride production, 146, 546
- Vinyl phenylbutyrate polymerization, 67
- Void volume of catalyst, 171–172
- Volume change modulus, 391
- Volume of activation, 193, 209
- Volume of reactor, 224
- Volumetric expansion parameter,  
calculation, 28–29, 45, 229, 233, 238,  
431  
definition, 28, 29  
relation to species concentrations, 29
- Volumetric hourly space velocity, 225
- Wacker process, 153
- Washout of cells, 483
- Waste treatment applications of bioreactors,  
495–496  
activated sludge, 495  
sludge composition, 496  
treatment of wastewaters, 496–497
- Water gas, 9, 187
- Weak acid catalysis, 193–194, 197, 210
- Weak base catalysis, 193–194, 197, 210
- Weight hourly space velocity, 225
- Whey, 262, 451, 518
- Xylene,  
bromination, 37–38  
isomerization, 294

Yang-Hougen form of rate expression, 166, 179, 187  
Yield (see also Selectivity),  
batch reactor, 276–277  
comparison for CSTR and plug flow reactors, 276–283  
concentration-yield curves, 276–278  
conversion and, 273  
CSTR, 276–278

CSTR cascade, 276–277  
effects of manner of mixing, 283–287  
instantaneous fractional, 275  
overall fractional, 275  
plug flow reactor, 275, 287  
Yield coefficients, 462–464, 467  
instantaneous, 462–464  
sign convention, 462  
variables for manipulating yields, 464

Zeolites, 278, 379  
Zeolite A production, 227–228  
Zero-order reaction,  
effectiveness factor, 385–386, 390, 392, 454, 461  
in CSTR cascade, 297, 364  
Zinc oxide, adsorption of hydrogen, 180

